PART-1

GPO PRICE $ _____

OTS PRICE(S) $ _____

Hard copy (HC) $2.62

Microfiche (MF) $3.50

RE-ORDER NO. 65-347

8422-6013-TU-000

FINAL REPORT
SURVEYOR VERNIER THRUST
CHAMBER ASSEMBLY DEVELOPMENT
- PHASE III -

Prepared For

The Jet Propulsion Laboratory
California Institute of Technology

Under Contract No. 950596

26 February 1965

Prepared by Members of STL
Surveyor Vernier Thrust
Chamber Assembly Project

Approved: Rupert
R. C. Rupert
Associate
Project Manager

Approved: H. Shieber
H. Shieber
Project Manager

Approved: A. F. Grant
A. F. Grant
Associate Director
Mechanics Division

This work was performed for the Jet Propulsion Laboratory, California Institute of Technology, sponsored by the National Aeronautics and Space Administration under Contract NAS7-100.

TRW SPACE TECHNOLOGY LABORATORIES
Thompson Ramo Wooldridge Inc.
One Space Park · Redondo Beach, California

ABSTRACT

23900

The MIRA 150A thrust chamber assembly (TCA) Phase III program is reported in detail. The operation and performance characteristics of the variable thrust, bi-propellant rocket engine, and detailed description of the assembly and its component parts are documented. The test history is presented, including tests under all specified interface conditions and with expected extremes of environmental conditions. The integrated TCA having successfully completed its prequalification test program is shown to be ready for use in overall systems tests and ready for entry into a formal qualification test program.

CONTENTS

CONTENTS (Continued)

CONTENTS (Continued)

CONTENTS (Continued)

CONTENTS (Continued)

CONTENTS (Continued)

LIST OF FIGURES AND TABLES

CONTENTS (Continued)

CONTENTS (Continued)

CONTENTS (Continued)

CONTENTS (Continued)

CONTENTS (Continued)

CONTENTS (Continued)

CONTENTS (Continued)

CONTENTS (Continued)

CONTENTS (Continued)

CONTENTS (Continued)

CONTENTS (Continued)

CONTENTS (Continued)

1.0 INTRODUCTION

1.1 Purpose

The purpose of this report is to provide a description of the design, performance, development, and testing of the MIRA 150A Thrust Chamber Assembly (TCA) and its sub-assemblies and component parts. The time period covered is from 1 April 1964 to 30 January 1965.

1.2 Contractual Coverage

The effort reported on herein was accomplished under JPL Contract Number 950596, Modifications 10 through 16.

1.3 Background

The STL Surveyor Vernier TCA effort began formally on 18 April 1963 with a 14-week Phase I feasibility demonstration program. This portion of the development program was performed using company-built MIRA 500 hardware and demonstrated the following objectives:

1. Feasibility of an electrohydraulic servoactuator to attain high speed and reproducible variable thrust control.

2. Durability of an uncooled combustion chamber to withstand 300 seconds of operation at 125 psia chamber pressure with an ablative throat, and at 150 psia chamber pressure with a tungsten throat insert.

3. An engine vacuum specific impulse of 295 lbf sec/lbm at the 150 lb thrust level using a 73:1 expansion ratio nozzle.

In addition to fulfillment of the above objectives, the Phase I program included the design effort to incorporate the basic features of the MIRA 500 throttle mechanism (injector and flow control valves) into an integrated flight weight TCA design. This design, called the MIRA 150, was sized to comply with the interface requirements of the Surveyor spacecraft vernier propulsion system.

With the successful completion of Phase I, STL received on 25 July 1963 a six-month Phase II contract to fabricate and test developmental hardware of the MIRA 150 design. An additional two-month period was added to this program, called the Phase II Follow-on, to effect advance fabrication of prequalification version of the MIRA 150 TCA, called the MIRA 150A TCA, and demonstrated the ability of the MIRA 150A TCA to meet the following criteria:

1. Vacuum specific impulse of 292 lbf sec/lbm between 90 and 150 lbs thrust and 260 lbf sec/lbm between 30 and 90 lbs thrust, both with a 37.8:1 expansion ratio.

2. Mixture ratio control between 1.4 and 1.6.

3. Engine survivability under the most severe mission cycle thrust program.

4. Dynamic response capability, both start-stop and variable thrust, adequate to meet current spacecraft control requirements.

The Phase II program was brought to a successful conclusion by the end of March 1964, whereupon the Phase III effort described herein commenced.

1.4 Phase III Chronology

Phase III of the Surveyor Vernier TCA project formally (contractually) began on 23 March 1964. The planning for the technical effort for this phase was described in the Development Plan, STL Document 9730.4-64-1-43. A summary of the major milestones accomplished during Phase III is presented in Table 1.4-1. These milestones are divided into three categories — development and prequalification testing, fabrication/procurement and acceptance testing, and major documentation — for convenient identification.

The Phase III development effort as described by Task 17 of the contract ran from 1 April to 1 August 1964. During this period, major development activities centered around establishing the MIRA 150A configuration baseline. The injector design went through a series of four modifications before the design was frozen. Fixed area injector tests were performed on the selected injector design to provide some basis for evaluation of the possible use of the coaxial injector with a GFE throttle valve. An alternate power source was subjected to a thorough analysis and evaluation. This concept was rejected by JPL on 18 June 1964 in favor of a fuel-powered servoactuator concept with overboard dump of fuel return flow. During the four-month development period, TCA thermal control studies were performed to establish the type of passive thermal control surface best suited for the purpose. By 1 August 1964 all of the major Phase III planning and testing documentation had been delivered to JPL.

On 11 August 1964, the first major milestone of the prequalification test phase took place when a Phase III TCA was fired at the JPL Edwards Test Site. The prequalification test phase may be characterized as that effort devoted to evaluation of the TCA under the extreme limits of interface and environmental conditions and to gathering nominal performance data at sea level and at altitude on a number of different HEAs and TCAs to obtain the data needed for the Model Specification. From August on through 8 January 1965 prequalification tests were performed at either the JPL Edwards Test Site (ETS) or the STL Inglewood Rocket Test Site (IRTS). On 27 November 1964, a hot firing centrifuge test was performed at the STL Capistrano Test Site (CTS). This firing was the only test performed at this site.

Phase III TCA hardware final assembly began in full swing during the last week of September 1964 and progressed through 4 December 1964. At this time, a decision was reached by JPL to terminate assembly of TCAs, head end assemblies (HEAs), and combustion chamber and nozzle assemblies (CC & NAs). Hardware not assembled at that time was packaged in an "As Is" condition and sent to Bonded Stores.

Final Phase III activities were devoted to: (1) finishing certain testing underway, (2) preparing the Final Report, including reduction of the November and December test data presented therein, (3) preparing the remaining final documentation - parts list, outline and mounting drawings, fabrication drawings and most importantly, the model specification, (4) cleaning and packaging the hardware which were subjected to the final prequalification tests, as well as all remaining contractually procured hardware, and (5) preparing a tabulation of the disposition of all items procured on the contract.

Table 1.4-1

Phase III Milestone Summary

SURVEYOR VERNIER TCA PROJECT	1964 APR	MAY	JUNE	JULY	AUG	SEPT	OCT	NOV	DEC	1965 JAN	FEB	MAR	APR
Phase III Program Start Date	△												
Phase III Prequalification Test Start Date					▲								
Phase III Program End Date												▲	
DEVELOPMENT AND PREQUALIFICATION TESTING													
1st MIRA 150A HEA (Phase II) Firing		▲											
Injector Modification Tests			▲										
Fixed Area Injector Tests					▲								
Durability Tests						▲							
Deep Vacuum Cycling Tests							▲						
Dynamic Response Tests (Phase II Servoactuator)							▲						
Steady State Altitude Performance Tests								▲					
Temperature and Propellant Pressure Tests									▲				
Acceleration (Centrifuge) Test									▲				
Dynamic Response Tests (Phase III Servoactuator)									▲				
Performance Repeatability Tests									▲				
Pre-Firing Vibration Test									▲				
FABRICATION/PROCUREMENT AND ACCEPTANCE TESTING													
Fabricate 6 Phase II Follow-on HEAs				▲									
Fabricate 1st Phase III HEA							▲						
Fabricate 1st Phase III CC & NA (Sea Level)						▲							
Acceptance Test 1st Phase III Servoactuator							▲						
Acceptance Test 1st Phase II - Follow-on TCA								▲					
Acceptance Test 1st Phase III TCA								▲					
Receive 40 Phase III Filters									▲				
Receive 40 Phase III Bekel (Solenoid) Valves									▲				
Receive 40 Phase III Vinson (Solenoid) Valves									▲				
Receive 15 Phase III Servoactuators										▲			
Fabricate 5 Phase III HEAs										▲			
Fabricate 15 Sea Level Phase III CC & NAs										▲			
Fabricate 11 Altitude Phase III CC & NAs										▲			
DOCUMENTATION													
Reliability Program Plan		▲											
Quality Control Program Plan		▲											
Development Plan			▲										
Manufacturing Plan						▲							
Acceptance Test Specification			▲										
Prequalification Test Specification			▲										
Model Specification												▲	
Operation and Maintenance Instructions Report					▲								
Reliability Parts List										▲			
Final Hardware Parts List										▲			
Final Outline and Mounting Drawings										▲			
Final Fabrication Drawings										▲			
Development Final Report												▲	

2.0 SUMMARY

This document is the final report on the development program of a TCA for application to the Surveyor spacecraft vernier propulsion system. The program was conducted under contract to the Jet Propulsion Laboratory, JPL Contract No. 950596, first initiated in the first quarter of 1961.

The Thrust Chamber Assembly is designated MIRA 150A. It consists of two variable-area cavitating venturi flow control valves to control the propellant flow rates; a single coaxial, variable-area injector element to maintain propellant injection velocities; propellant shutoff valves; a servoactuator; and an ablative-cooled combustion chamber and nozzle assembly. The flow control valves and the injector element are mechanically linked and are positioned by the fuel-operated electrohydraulic servoactuator. The ablative-cooled combustion chamber employs a hard throat insert in an ablative-lined titanium case which is extended to become a radiation-cooled expansion skirt.

This final report describes the development since April 1964 of the above TCA components and of the integrated TCA. It also presents the overall performance and control capabilities of the TCA, and the associated test data and analytical effort.

The report is divided into the following main categories:

1. The introductory sections 1.0 and 2.0, in which background and chronology are given.

2. The technical description of the final design, section 3.0, in which:

   (1) The TCA and its major subassemblies and components are described in detail.

   (2) The TCA operation is explained.

   (3) Values for performance parameters are given.

   (4) Interfaces between the TCA and the spacecraft are defined.

   (5) Detailed test data is not included.

   Section 3 may be considered a TCA characteristics report.

3. The detailed review of the testing effort is given in sections 4.0, 5.0, and 6.0. Section 4.0 reports on the HEA calibration and on the series of tests specified in the acceptance test specification. These are:

   (1) Leak checking.

   (2) Ablative throat or streak test.

   (3) HEA acceptance firing test.

   (4) TCA vibration test.

   (5) TCA acceptance firing test.

   Section 5.0 reports on the testing done in Phase III that did not involve firings. This testing includes:

(1) Functional acceptance tests of servoactuators, filters, and pilot valves.

(2) Laboratory testing under deep vacuum conditions.

(3) Component evaluation testing.

(4) Servoactuator power system studies.

Section 6.0, the largest section in the report, covers in detail all the firing tests, including discussion of the test hardware, the test setups, the results and the derivation of the overall TCA performance parameters.

4. The theoretical effort, section 7.0, includes discussion of that work that was primarily analytical in nature, such as theoretical internal ballistics, the dynamic response analytical model, thermal analytical computations, and applicable fluid flow theory.

5. The remaining sections, 8.0, 9.0, 10.0, 11.0, and 12.0 cover other items such as special test equipment, reliability, quality control, and references.

The integrated TCA design is shown to have demonstrated operational characteristics satisfying the contractual requirements of JPL Contract No. 950596. Based upon the demonstrated capabilities of the TCA design and upon STL's development record in accomplishing program objectives within the time and cost constraints of the subject Contract, the STL MIRA 150A TCA is now considered ready to be used in ground based integrated spacecraft systems tests and ready to advance through qualification testing to prove operational readiness.

3.0 THRUST CHAMBER ASSEMBLY DESCRIPTION AND OPERATION

3.1 General

3.1.1 TCA Description and Operation

The MIRA 150A TCA is a throttleable, liquid bi-propellant rocket engine with a thrust capability of 150 lbs maximum to 30 lbs minimum; a 5:1 throttling range. The TCA was developed for use on the Surveyor spacecraft to provide thrust for velocity correction and for attitude control during mid-course trajectory and velocity attenuation during lunar landing maneuvers. In this spacecraft control application, two of the prime performance requirements are:

1. The TCA must be cpable of smooth and continuous throttling.

2. The TCA thrust response to spacecraft commands must be predictable and repeatable.

The MIRA 150A TCA complies with the above requirements through mechanization of two cavitating venturi flow control valves, a coaxial variable area injector and a precision electrohydraulic servoactuator. These and other major TCA functional components are described in the following paragraphs. The TCA is designed for long-term compatibility with propellants by extensive use of 17-4 PH stainless steel and Teflon sealing elements.

Table 3.1.1-1 presents a brief summary of TCA physical and performance characteristics; subsequent paragraphs, noted below, contain more detailed data.

Envelope:	Paragraph 3.1.2
Mass Properties:	Paragraph 3.1.3
Components and Sub-assemblies:	Paragraph 3.2
Spacecraft Interfaces:	Paragraph 3.3
Performance:	Paragraph 3.4

The MIRA 150A TCA is shown in Figure 3.1.1-2. Part (a) of this figure shows a cross section of the TCA. It is comprised of two major subassemblies, the Head End Assembly and the Combustion Chamber and Nozzle Assembly, as shown in Figure 3.1.1-3. An exploded view of the Head End Assembly is shown in Figure 3.1.1-4.

3.1.1.1 Major Functional Components

The major TCA functional components are briefly described in the following paragraphs. Detailed descriptions are contained in paragraph 3.2. A schematic diagram of the TCA is shown in Figure 3.1.1-5 and is included for use as a reference during the following discussion.

Table 3.1.1-1

MIRA 150A TCA Performance Summary

Thrust, lb	F	Minimum: 30 Maximum: 150
Chamber Pressure, psia	P_c	Minimum: 22 Maximum: 110
Specific Impulse, lbf-sec/lbm (nominal delivered)	I_{sp}	291 (at 150 lbs thrust) 259 (at 30 lbs thrust)
Expansion Ratio		32.8
Characteristic Length, in.	L*	17
Thrust Coefficient	C_f	1.74
Characteristic Velocity, ft/sec	C*	5400 (at 150 lbs thrust)
Service Life at Maximum Thrust, sec		300
TCA Weight, lb		8.3
Mixture Ratio, $\dot{M}_{OX}/\dot{M}_F$	MR	1.5
Oxidizer		90% Nitrogen Tetroxide 10% Nitric Oxide
Fuel		Monomethylhydrazine
Total Engine Length, in.		13.3
Exit Diameter, in.	D_e	5.725
Throat Diameter, in.	D_t	1.00
Feed System Pressure, psia		720

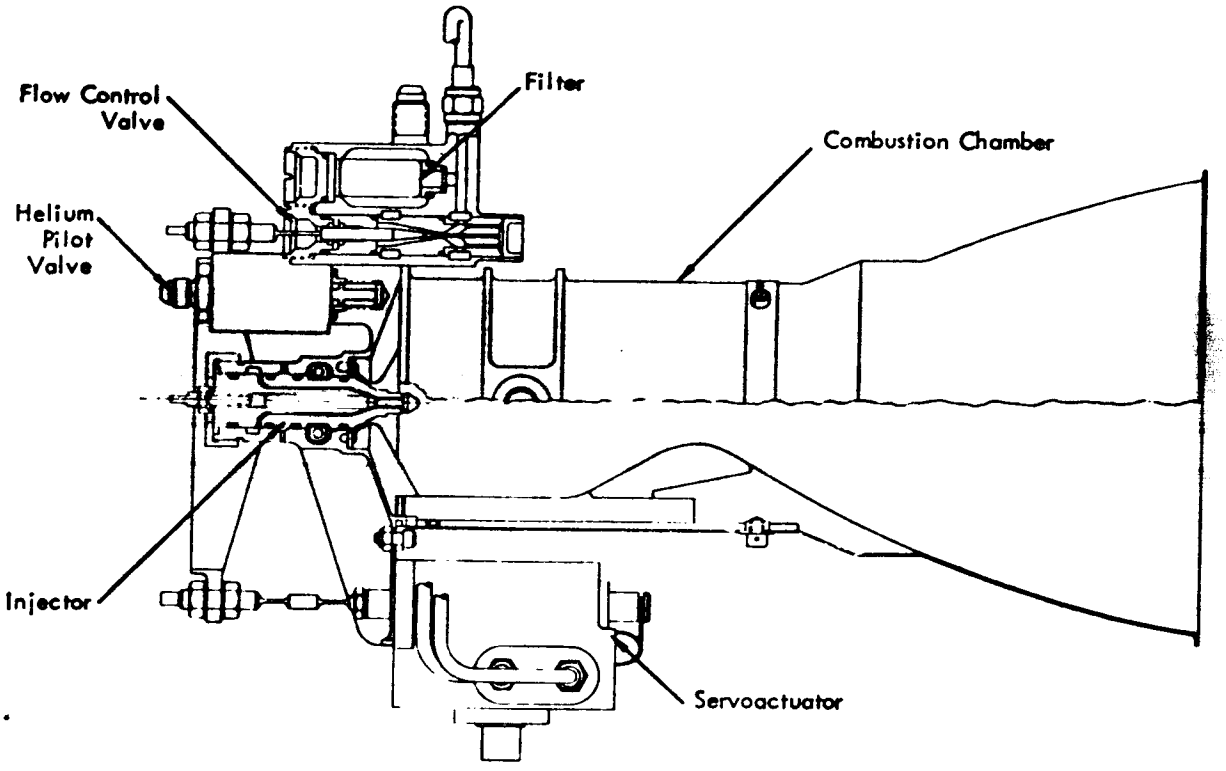

(a) Section View

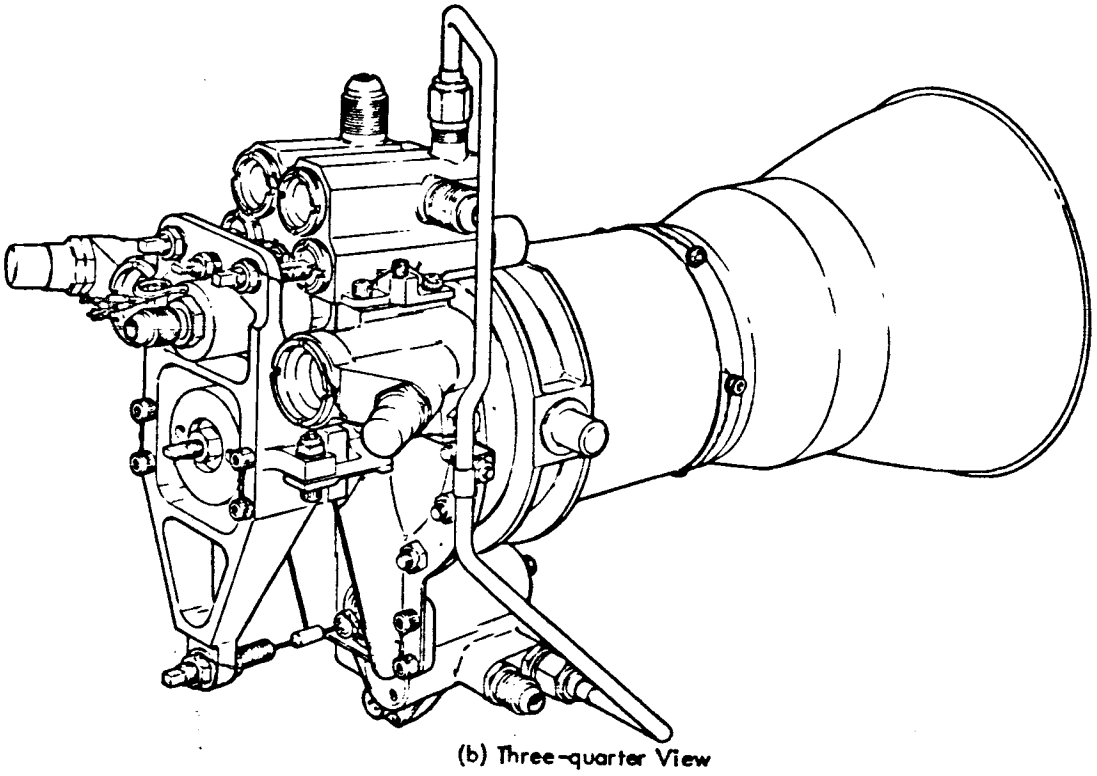

(b) Three-quarter View

Figure 3.1.1-2. MIRA 150A TCA

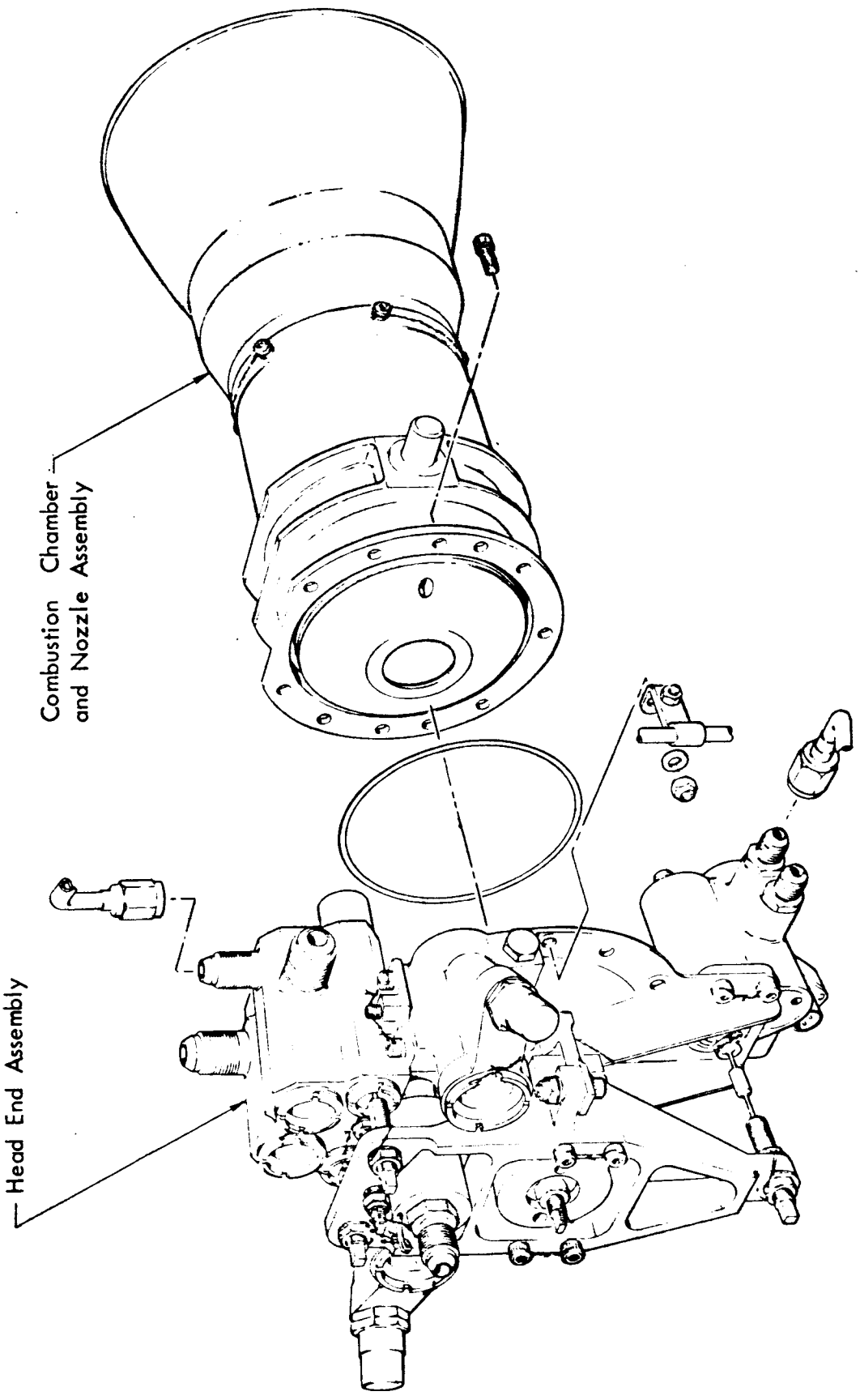

Figure 3.1.1-3. MIRA 150A PCA Major Subassemblies

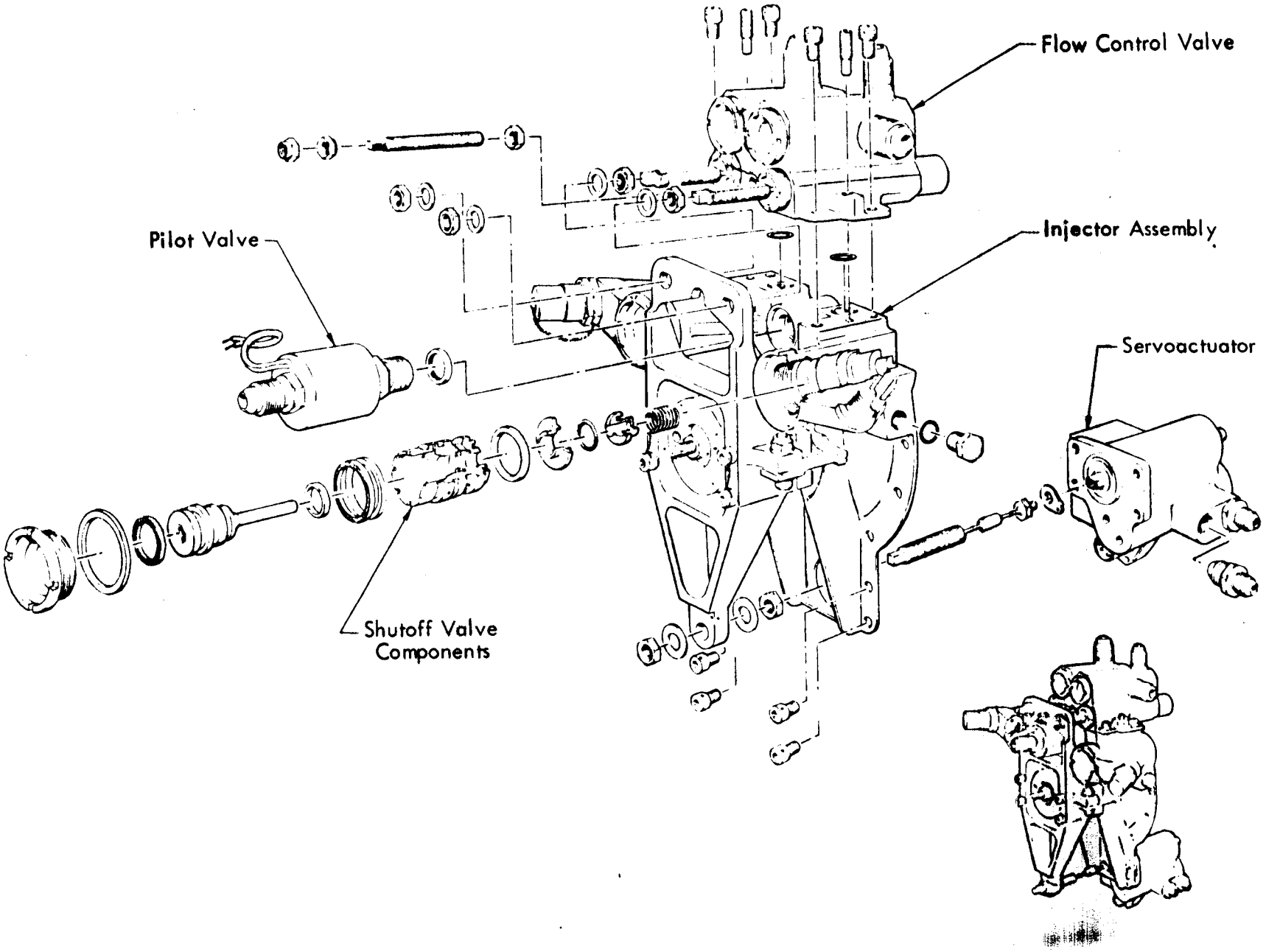

Figure 3.1.1-4. MIRA 150A HEA (Exploded View)

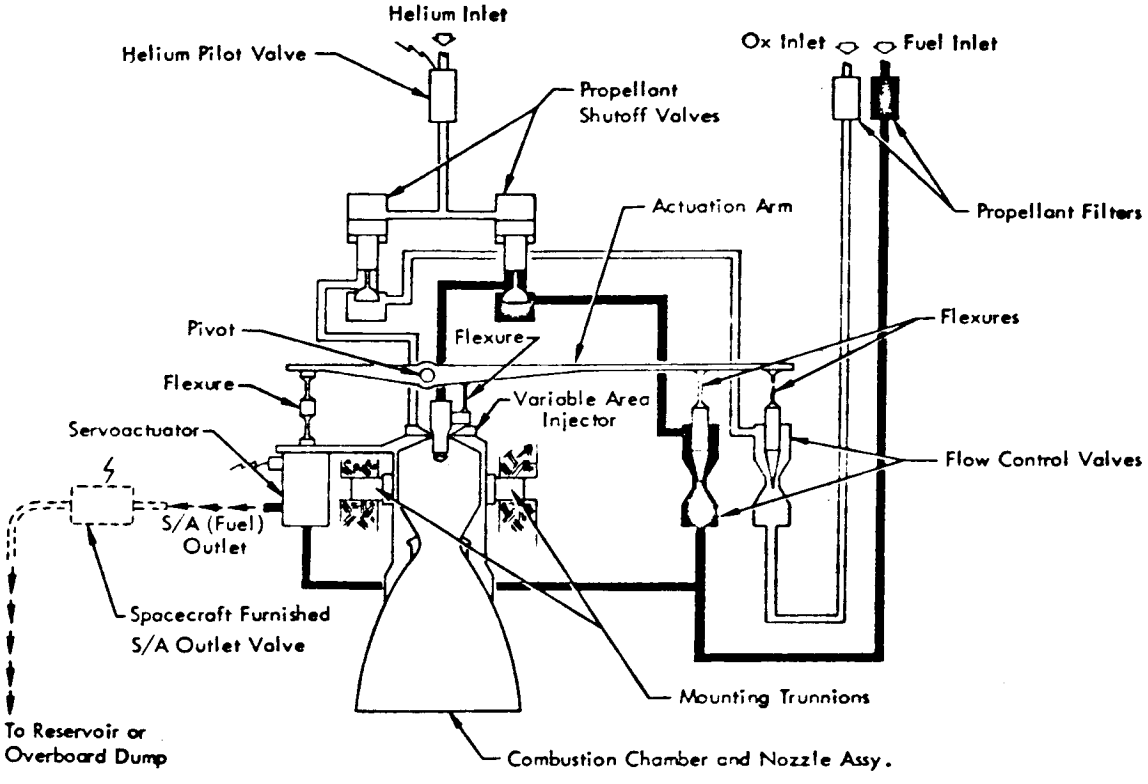

Figure 3.1.1-5. MIRA 150A TCA Schematic

Propellant Filters

A pair of 5 micron nominal (15 micron absolute) filters are contained within the TCA to provide filtration of supplied propellants. The filters are located immediately downstream of the propellant inlet ports and upstream of the flow control valves.

Flow Control Valves

Two cavitating venturi valves are used to control the flow rate and mixture ratio of the propellants to the injector. In the range of TCA pressures and flow rates, the rate of propellant flow through the valves is entirely a function of the position of the pintles relative to the venturi throats and thus insensitive to downstream pressure. Therefore, flow rate and mixture ratio are purely a function of the flow control valves and independent of injector opening. The total stroke of the flow control valve pintles (maximum to minimum thrust) is 0.155 inches.

Propellant Shutoff Valves

Two pilot-operated shutoff valves (normally closed) are used for start/stop control of propellant flow. The valves are actuated to the open position by application of helium pilot gas pressure. Valve closure and poppet seat sealing is achieved by a spring and propellant pressure. The valves are closely coupled to the injector in order to minimize downstream volume and, thus, minimize TCA start and stop times.

Helium Pilot Valve

A solenoid-operated, three-way valve supplies pilot gas to the propellant shutoff valves when energized with a DC signal. When de-energized, the pilot valve ports the pilot gas volumes of the shutoff valves to atmosphere.

Variable Area Injector

A coaxial, variable area injector provides the propellant velocities and patterns necessary to maintain combustion efficiency throughout the throttling range. At low propellant flows for minimum thrust the injector area is small and, therefore, the propellant velocities are maintained at the high value needed for efficient operation. The injector is configured such that a central pintle is stationary and area changes are obtained by rectilinear movement of the injector sleeve through a total stroke of 0.0067 inches during throttling from maximum to minimum thrust. Fuel flow is through the center of the injector around the fixed pintle. Oxidizer flow is on the outside, on the periphery of the movable sleeve.

Servoactuator

The servoactuator receives spacecraft electrical commands and resolves these into rectilinear motion (position) of its output shaft. The servoactuator has a built-in position feed-back and, therefore, an electrical command for a specific thrust is resolved into a specific shaft position. The output shaft is mechanically coupled to the injector and flow control valves through the flexures and actuation arm; thus, each servoactuator shaft position is translated into specific flow control valve and injector settings. The total stroke of the servoactuator output shaft is 0.174 inches. Fuel (MMH) is the servoactuator working fluid and is supplied from a connection downstream of the fuel filter and upstream of the fuel flow control valve.

Actuation Arm/Flexures

The actuation arm and flexures mechanically couple the servoactuator, injector and flow control valves. Flow control valve flexures are an integral part of each valve pintle. Injector and servoactuator flexures are separate parts. The actuation arm is pivoted on the head end body such that the lever arm from the pivot to each flexure is as follows (refer to Figure 3.1.1-5):

Servoactuator	2.466 inches to left of pivot
Injector Sleeve	0.095 inches to right of pivot
Flow Control Valves	2.195 inches to right of pivot

As the servoactuator shaft extends, the injector sleeve and flow control valve pintles retract. This motion reduces the flow area in the throats of the cavitating venturis and the orifice area in the injector. Reduction of flow area in the throats of the cavitating venturis reduces thrust, and reduction of orifice area injector maintains injectant velocities for the reduced flow.

Combustion Chamber and Nozzle Assembly

The Combustion Chamber and Nozzle Assembly (CC & NA) contains, directs and expands the gaseous products of combustion. Propellant combustion occurs in a 2.35 inch internal diameter ablative-cooled zone (silica-phenolic liners). Gases then converge to a 1.00 inch diameter hard throat of JTA graphite. Expansion of gases from the throat is through a silica-phenolic exit cone liner and radiation-cooled titanium skirt, with exhaust occuring at a diameter of 5.725 inches. The entire outer case of the Combustion Chamber Assembly is titanium with integral trunnions provided for spacecraft mounting of the TCA. The overall length of the CC & NA is 10.5 inches; other parameters are noted below and in paragraph 3.2.7.

Contraction Ratio (chamber area/throat area) = 5.5

Expansion Ratio (exit area/throat area) = 32.8

Characteristic Length (L*) = 17 inches

3.1.1.2 TCA Operation

The events involved in a typical TCA operational sequence are as follows:

Pre-Start

The TCA is placed in a ready condition by pressurizing the oxidizer, fuel and helium inlet ports to 720 psig (nominally) with their respective fluids. The pilot valve and servoactuator are not energized at this point. Since the fuel inlet to the servoactuator is upstream of the fuel shutoff valve, servoactuator null leakage occurs whenever the actuator is pressurized. Loss of fuel by null leakage can be avoided by use of a two-way (normally closed) solenoid valve connected to the servoactuator fuel outlet ports. (Such a component is, of course, required for use of the TCA on the spacecraft; however, STL was not required to design and develop this component.) In the pre-start condition, propellant pressure in the FCV causes the servoactuator output shaft to fully retract and, therefore, the "throttle position" is set at maximum thrust.

Start

To start the TCA, electrical commands are sinultaneously applied to the servoactuator and helium pilot valve (and actuator fuel outlet valve if used). Energizing the pilot valve produces actuation of the shutoff valves, and propellant now flows through the injector and ignites hypergolically in the combustion chamber. This sequence of events is shown graphically in Figure 3.1.1-6. The electrical signals to the servoactuator command the desired thrust. The servoactuator response is sufficiently faster than the pilot valve and shutoff valve combination such that the desired thrust setting will be in effect when ignition occurs. This, of course, assumes the delay of the null leakage dump valve is negligible.

Throttling

Throttling of the TCA is accomplished by electrically commanding the servoactuator to the desired thrust level(s). The electrical commands are resolved into specific output shaft positions. The actuation arm and flexures move the injector sleeve and flow control valves such that the commanded thrust level or profile is obtained.

Shutdown

TCA shutdown is achieved by removal of the electrical signals to the pilot valve and servoactuator (and its outlet valve if used). Power removal results in closure of the shutoff valves, shown graphically in Figure 3.1.1-6, and the TCA is restored to its pre-start condition.

3.1.2 Envelope

The TCA overall size and shape are delineated in Drawing No. 107062 and are illustrated in Figure 3.1.2-1.

3.1.3 Mass Properties

The mass properties of the 106570-1 TCA are given in Mass Properties Baseline Report 9730.4-64-3-6 and are summarized below.

Weight = 8.30 lb

Moment of Inertia About Trunnion Axis = 73.7 lb in.^{2}

Center of Gravity Location = Nominally on the trunnion axis at its intersection with the thrust axis (TCA centerline).

Minor design changes which have occurred since the baseline report was issued have not affected the figures given below.

An Engineering Technical Directive (ETD), MIRA-OF-001, entitled "Determination of Weight and Center of Gravity Location" was prepared. This ETD lists the procedures and equipment required to determine the weight and center of gravity location of the TCA devined by Drawing No. 106570-1.

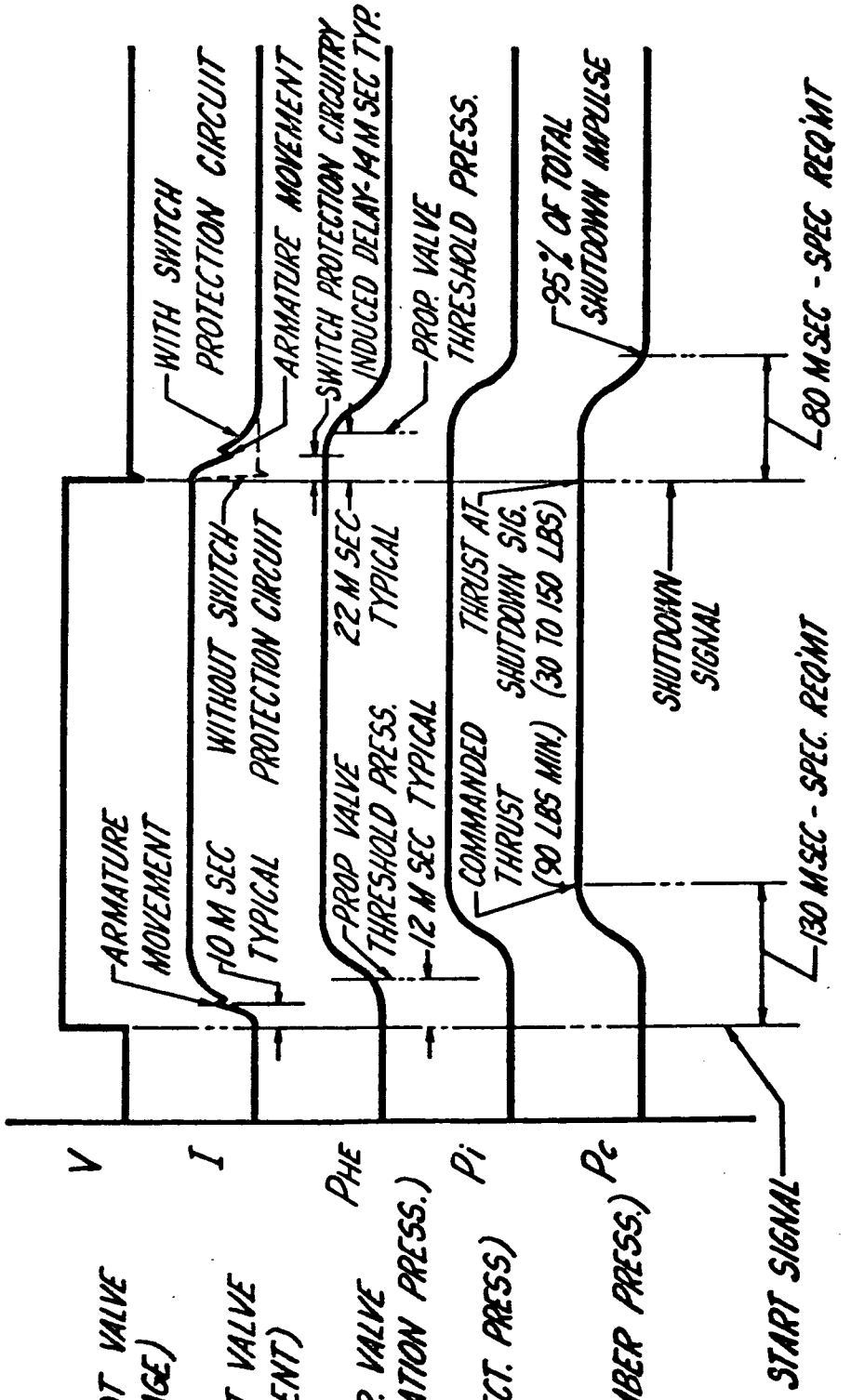

Figure 3.1.1-6. MIRA 150A TCA Start/Stop Response

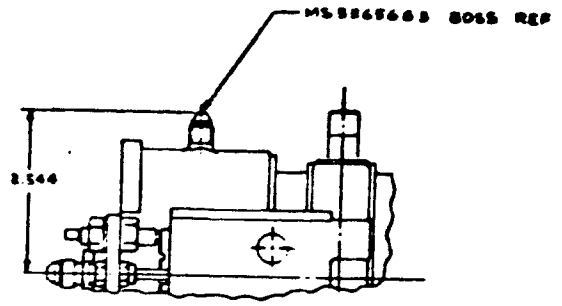

DETAIL A
FOR 106570-4 & -5

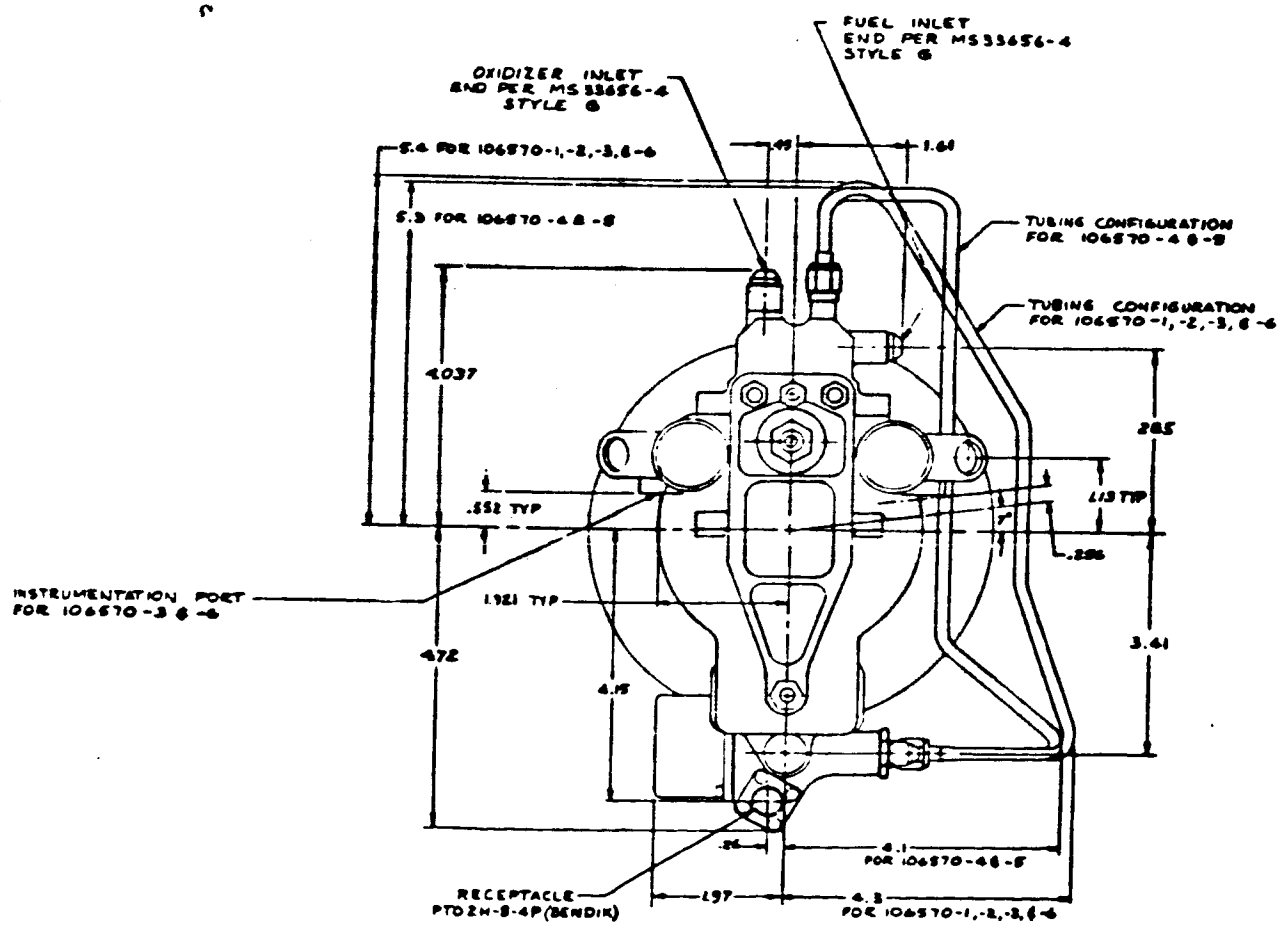

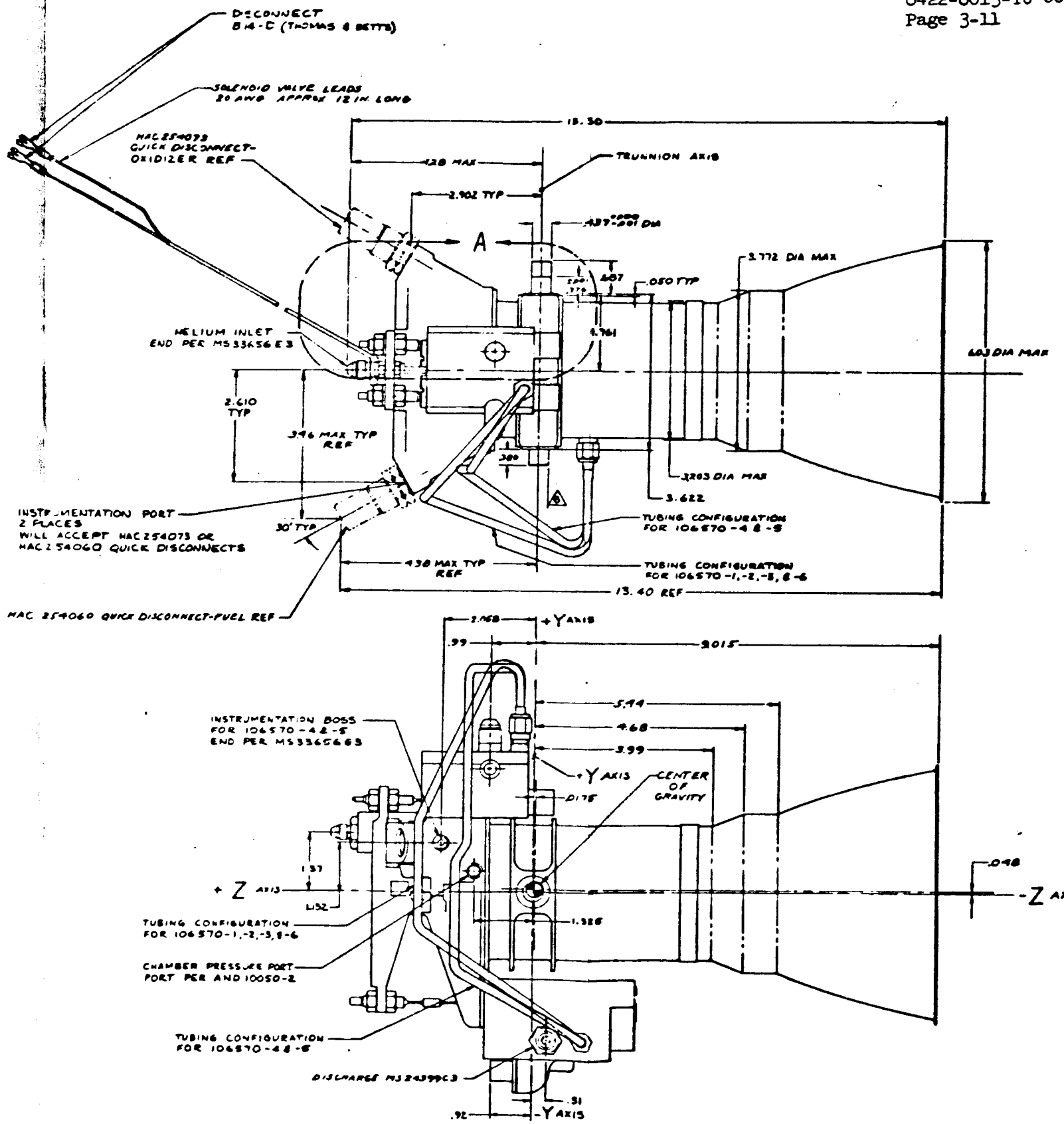

Figure 3.1.2-1. MIRA 150A Envelope

3.1.4 Parts List and Drawing Tree

The MIRA 150A TCA Drawing Tree, revised 15 January 1965, is given in Figure 3.1.4-1.

The MIRA 150A TCA Indentured Parts List, revised 15 January 1965, is presented in Table 3.1.4-2. This parts list contains parts manufactured by STL or purchased to STL specifications. Parts such as seals, lockwire, or fasteners, commercially available or covered by Military Standards, are not included in this indentured parts list.

The parts list and drawing tree contain not only Phase III final design part numbers but also the Phase II Follow-on part numbers, where appropriate.

3.1.5 Specification Tree

The MIRA 150A TCA Specification Tree, revised 30 September 1964, is presented in Figure 3.1.5-1. The specifications listed are as follows:

1. Specification No. SK1-7, Model Specification MIRA 150A Thrust Chamber Assembly.

2. Specification No. EQ1-94, Combustion Chamber Assembly.

3. Specification No. PK4-2, Packaging Specification, Surveyor Vernier Rocket Engine. This specification establishes requirements for the preservation, packaging, and packing of both the assembled TCA and the Combustion Chamber Assembly alone. The required shipping container as well as the package configuration is defined on STL Drawing No. C-302148, Surveyor Vernier TCA Shipping Container. The package identification is defined on STL Drawing No. 302444, Marking Drawing, Shipping Container Surveyor Engine.

4. Specification No. EQ1-95, Head End Assembly, although shown on the specification tree, this specification was not completed prior to phase out of the Surveyor Project. However, two specifications, containing technical content planned for inclusion in EQ1-95, are available — Specification No. EQ5-5A, Injector Assembly, and Specification No. EQ5-6A, Valve Assembly, Flow Control. These specifications cover Phase II Follow-on HEA parts defined on STL Drawing No. 105461, Head End Assembly. These parts were reworked to the Phase III configuration as noted in Paragraph 3.1.4.

5. Specification No. EQ2-25D, Solenoid Operated Three-Way Valve.

6. Specification No. EQ2-42, Servoactuator, Electrohydraulic.

7. Specification No. EQ1-73B, Filter, Propellant.

8. Material and process specifications applicable to the CC & NA parts are as follows:

   a. Specification No. MT3-9, Molding Compound, Chopped Silica Fabric Reinforced Phenolic. This specification establishes the requirements for the molding compound used in manufacture of the liner components.

   b. Specification No. PR10-9, Compression Molding of Chopped Silica Fabric Reinforced Phenolic Parts. This specification establishes requirements for molding the ablative molding compounds into the ablative liner components.

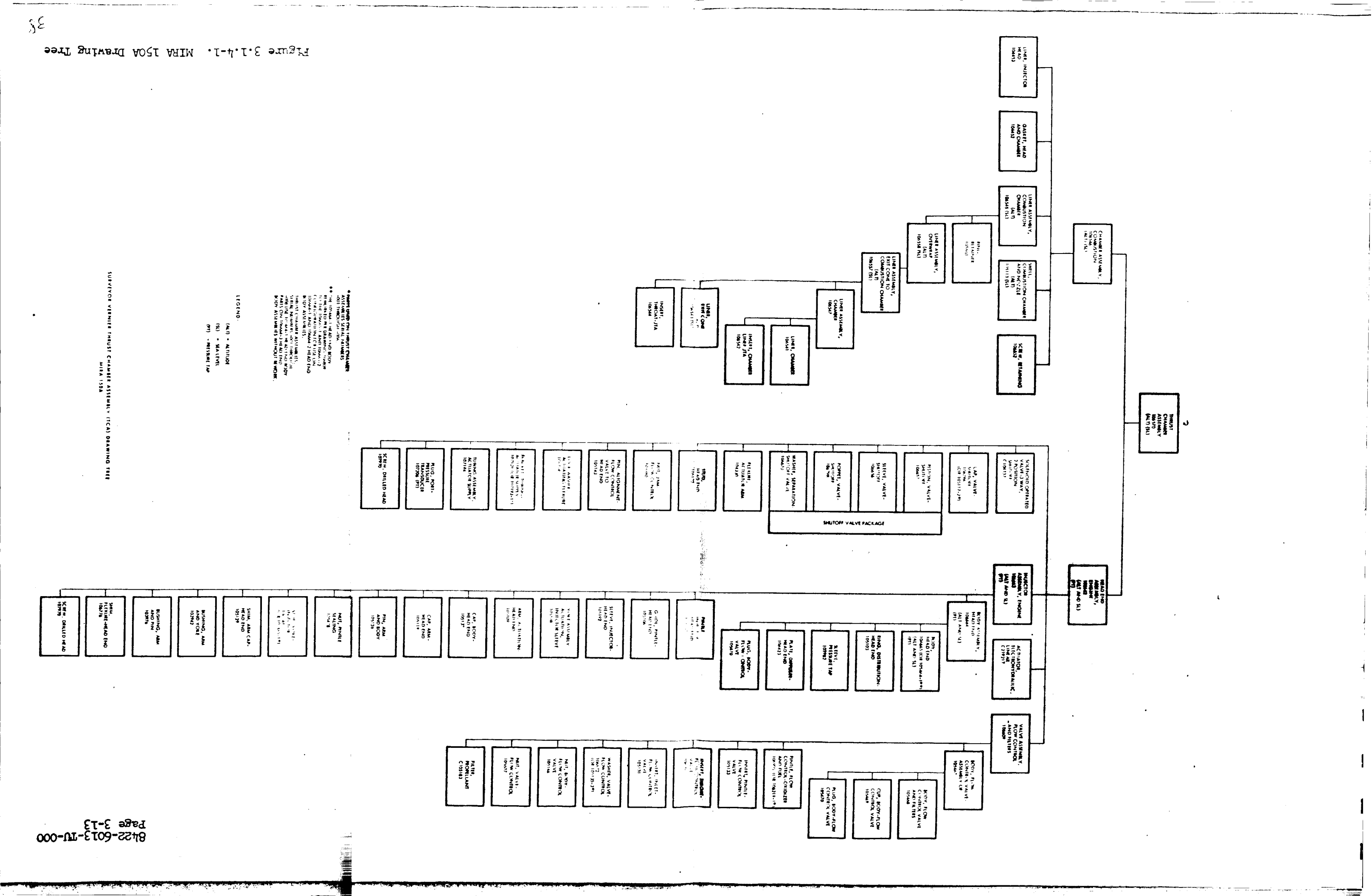

Figure 3.1.4-1. MIRA 150A Drawing Tree

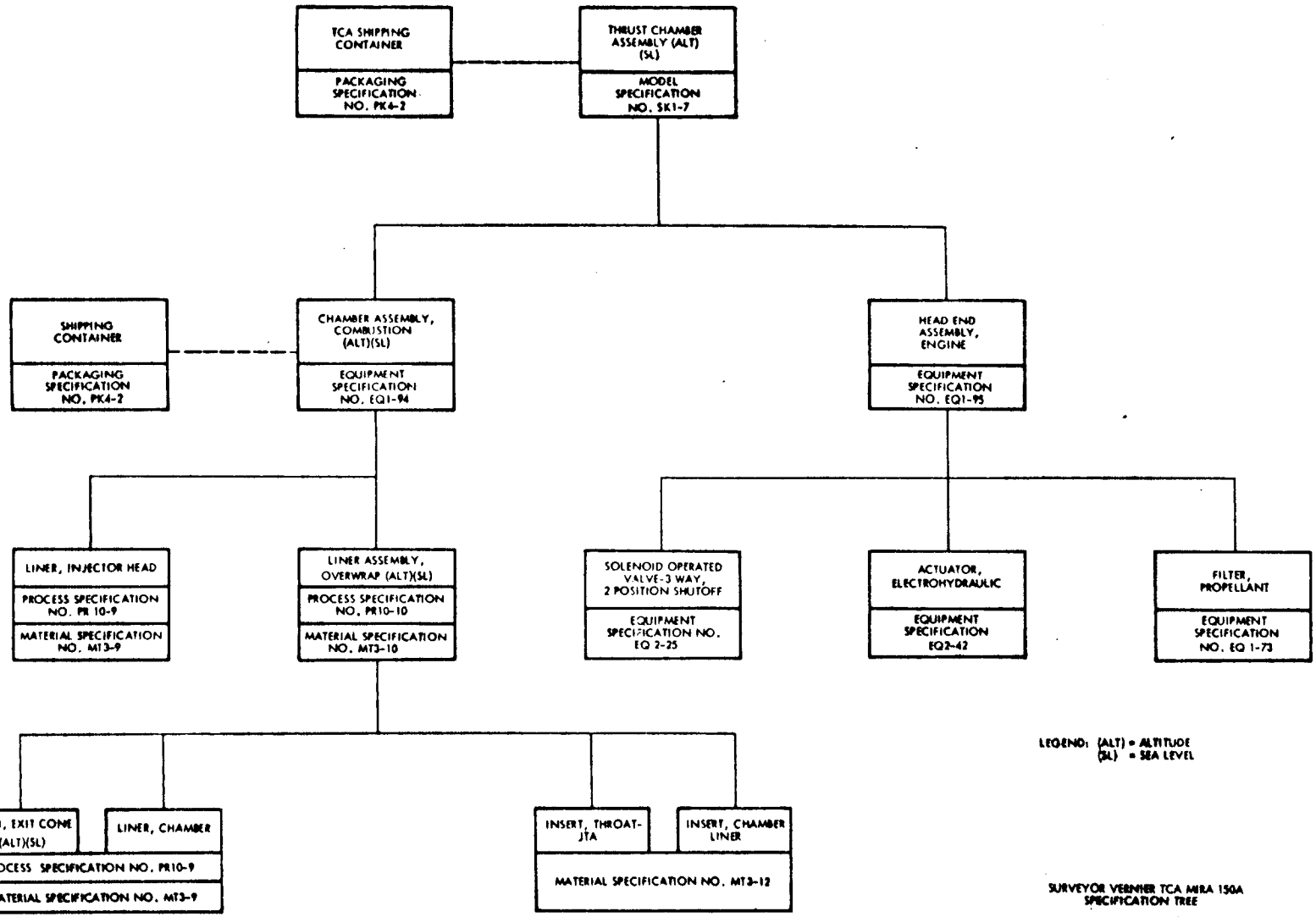

Figure 3.1.5-1. MIRA 150A Specification Tree

Table 3.1.4-2

Surveyor Vernier Thrust Chamber Assembly (TCA) Revised: 15 January 1965

MIRA 150A Indentured Parts List

106570-1	Thrust Chamber Assembly (Altitude)
106570-2	Thrust Chamber Assembly (Sea Level)
106570-3	Thrust Chamber Assembly (Sea Level with Pressure Tap)
106570-4	Thrust Chamber Assembly (Altitude)
106570-5	Thrust Chamber Assembly (Sea Level)
106570-6	Thrust Chamber Assembly (Altitude with Pressure Tap)
106546-1	Chamber Assembly, Combustion (Altitude)
106546-2	Chamber Assembly, Combustion (Sea Level)
104452-2	Gasket, Head and Chamber
104453-1	Liner, Injector Head
106552-1	Screw, Retaining
105113-3	Shell, Combustion Chamber and Nozzle (Altitude)
105113-4	Shell, Combustion Chamber and Nozzle (Sea Level)
106545-1	Liner Assembly, Combustion Chamber (Altitude)
106545-2	Liner Assembly, Combustion Chamber (Sea Level)
105603-2	Ring, Retainer
106558-1	Liner Assembly, Overwrap (Altitude)
106558-2	Liner Assembly, Overwrap (Sea Level)
106557-1	Liner Assembly, Exit Cone to Combustion Chamber (Altitude)
106557-2	Liner Assembly, Exit Cone to Combustion Chamber (Sea Level)
106547-1	Liner Assembly, Chamber
106541-1	Liner, Chamber
106542-1	Insert, Chamber Liner - JTA

Revised: 15 January 1965

106543-1	Liner, Exit Cone (Altitude)
106543-2	Liner, Exit Cone (Sea Level)
106544-1	Insert, Throat - JTA
106662-1	Head End Assembly, Engine
106662-2	Head End Assembly, Engine (with Pressure Tap)
* 106662-3	Head End Assembly, Engine
106663-1	Injector Assembly, Engine
106663-2	Injector Assembly, Engine (with Pressure Tap)
* 106663-3	Injector Assembly, Engine
106664-1	Body Assembly, Head End
106664-2	Body Assembly, Head End (with Pressure Tap)
* 106664-3	Body Assembly, Head End
106665-1	Body, Head End
106665-2	Body, Head End (with Pressure Tap)
* 105464-1	Body, Head End
** 106809-1	Rework, Body - Quick Disconnect Port
** 106809-2	Rework, Body - Quick Disconnect Port
** 106809-3	Rework, Body - Quick Disconnect Port
** 106809-4	Rework, Body - Quick Disconnect Port
** 105464-1	Body, Head End
105103-2	Ring, Distribution - Head End
106423-3	Plate, Diffuser - Head End
103982-1	Sleeve, Pressure Tap
105470-1	Plug, Body - Flow Control Valve

Revised: 15 January 1965

106748-1	Stop, Yoke - Injector
106748-2	Stop, Yoke - Injector
* 105465-1	Stop, Sleeve - Injector
105192-4	Sleeve, Injector - Head End
105106-1	Guide, Pintle - Head End
105107-4	Pintle, Injector - Head End
105137-1	Cap, Body - Head End
105108-1	Yoke Assembly, Actuation - Injector Sleeve
* 105109-2	Arm, Actuation - Head End
105109-3	Arm, Actuation - Head End
* 105119-2	Cap, Arm - Head End
105119-3	Cap, Arm - Head End
106776-1	Shim, Flexure - Head End
105129-2	Shim, Arm Cap - Head End
103942-2	Bushing, Arm and Yoke
103976-4	Bushing, Arm and Pin
105126-1	Pin, Arm and Body
105126-2	Pin, Arm and Body
105478-1	Nut, Pintle Sealing
107970-2	Screw, Drilled Head
C219217	Actuator, Electrohydraulic, Linear
C104337-1	Solenoid Operated Valve - 3 Way, 2 Position Shutoff
106609-1	Valve Assembly, Flow Control and Filters
* 106609-2	Valve Assembly, Flow Control and Filters

Revised: 15 January 1965

* 105467-2	Body, Flow Control, Valve - Assembly Of
105467-4	Body, Flow Control, Valve - Assembly Of
* 105468-2	Body, Flow Control Valve and Filters
105468-5	Body, Flow Control Valve and Filters
105469-2	Cup, Body - Flow Control Valve
105470-2	Plug, Body - Flow Control Valve
105131-2	Insert, Inlet - Flow Control Valve
106907-2	Insert, Throat - Flow Control Valve
105133-2	Insert, Pintle - Flow Control Valve
* 106219-1	Pintle, Flow Control - Oxidizer and Fuel
106905-1	Pintle, Flow Control - Oxidizer and Fuel
106905-2	Pintle, Flow Control - Oxidizer and Fuel
* 105135-3	Washer, Valve - Flow Control
106672-1	Washer, Valve - Flow Control
* 105607-2	Nut, Valve - Flow Control
105607-3	Nut, Valve - Flow Control
105146-3	Nut, Body - Flow Control Valve
C105183-1	Filter, Propellant
106798-1	Poppet, Valve - Shutoff
106656-1	Sleeve, Valve - Shutoff
106657-1	Piston, Valve - Shutoff
106670-1	Washer, Separation - Shutoff Valve
* 105117-2	Cap, Valve - Shutoff
106796-2	Cap, Valve - Shutoff

Revised: 15 January 1965

104330-1	Flexure, Actuator Arm
103980-1	Nut, Jam - Flow Control
105122-1	Stud, Head End
105143-1	Pin, Alignment - Flow Control Valve to Head End
106759-1	Lock Washer, Actuating Flexure
107928-1	Bracket, Tubing - Actuator Supply
* 107193-1	Clip, Tubing - Actuator Supply
107194-1	Tubing Assembly, Actuator Supply
107206-1	Plug, Port - Pressure Transducer
107970-1	Screw, Drilled Head

---

* Indicates part numbers for Thrust Chamber Assembly - Serial Numbers -001 through -006.

** Indicates that 105464-1 Head End Body parts are reworked per Drawing 106809 to the 106665-1 and 106665-2 configuration for use on 106664-1 and 106664-2 Head End Body Assemblies.

Thrust Chamber Assembly Serial Numbers -001 through -006 - use 105464-1 Head End Body parts on 106664-3 Head End Body Assemblies without rework.

c. Specification No. MT3-10, Silica Fabric Reinforced Phenolic Resin Tape and Broad Goods. This specification establishes requirements for the material used in overwrapping the molded liner component pieces.

d. Specification No. PR 10-10, Laminating and Wrapping of Silica Fabric Reinforced Phenolic Resin Tape and Broad Goods. This specification contains some of the requirements for the overwrapping operation.

e. Specification No. MT3-12, Graphite, Oxidation Resistant. This specification defines the requirements for the oxidation resistant graphite composite used in the throat insert, defined by Drawing No. 106544, and chamber liner insert, defined by Drawing No. 106542.

Specifications No. MT3-9 and No. PR10-9 apply to the following parts: Injector Head Liner, defined by Drawing No. 104453; Exit Cone Liner, defined by Drawing No. 106543; and Chamber Liner, defined by Drawing No. 106541. Specifications Nos. MT3-10 and PR10-10 apply to the Overwrap Liner Assembly, defined by Drawing No. 106558.

3.1.6 Log Book

The purpose of the "Quality Assurance Log Book" is to (1) provide a complete list of the parts and subassemblies constituting the particular TCA, (2) document any modifications to the TCA and components thereof, and (3) delineate the tests performed in the TCA or assemblies thereof. Thus, a permanent and current record is available for purposes of accountability and traceability of all raw materials and purchased components assembled into the TCA. Further, tests to which the TCA have been subjected are listed, and limited items of test data may be included in the log. The log then becomes a single gathering point for information related to assembly and testing of the engine so that, if required, more detailed information can be searched out from this point.

The basic log book contains 13 form-type pages which are supplemented by pertinent information such as component acceptance test reports, engine test data sheets, and oscillograph data as appropriate.

3.2 Components and Subassemblies

3.2.1 Flow Control Valve

Propellant flow control is accomplished by dual variable area cavitating venturi valves. The cavitating venturi valves separate any oscillations in the combustion or injection pressures from the feed system. The flow through the cavitating venturis is independent of downstream pressure and dependent only upon venturi inlet pressure and propellant density as shown in the following equation:

$$\dot{M} = C_D \, A \sqrt{2_g \, \rho \, (P_t - P_v)}$$

$\dot{M}$ = Mass Flow Rate

A = Venturi Throat Area

C_D = Discharge Coefficient

ρ = Propellant Density

P_t = Inlet Pressure

P_v = Vapor Pressure

Figure 3.2.1-1 shows the assembly drawing of the MIRA 150A flow control valve (FCV). An exploded view is shown in Figure 3.2.1-2. The pintle contour is a paraboloid resulting in a linear flow area with stroke. Figure 3.2.1-3 shows typical flow-stroke data from a throttled engine firing. Figure 3.2.1-4 shows typical mixture ratio data for a throttling run.

The cavitating venturi valve operation is based on the fact that as liquid flow through a venturi throat is increased by decreasing the pressure downstream of the throat, a point will be reached at which no further flow increase will be experienced with further decrease in the downstream pressure. The reason for this characteristic is that as the upstream pressure head is increasingly converted to fluid velocity, the throat static pressure finally reaches the vapor pressure of the liquid. At this point, some of the liquid vaporizes. Further lowering of the downstream pressure merely creates additional vapor (cavitation) at the throat, with the liquid flow rate remaining constant because the flow controlling pressure drop in this system is between the inlet pressure and the venturi throat pressure.

In a venturi with a well designed diffusing section downstream of the throat, cavitation will occur when the downstream pressure is about 85 percent of the upstream pressure; that is, a maximum of about 85 percent of the throat velocity head (which for low vapor pressure fluids is equivalent to the upstream pressure) can be recovered in the diffusing section of the venturi. Therefore, as long as the injector manifold pressure is less than this value of 85 percent of the upstream pressure, the propellant flow rate to the engine will be a function only of the tank pressure and the venturi throat area.

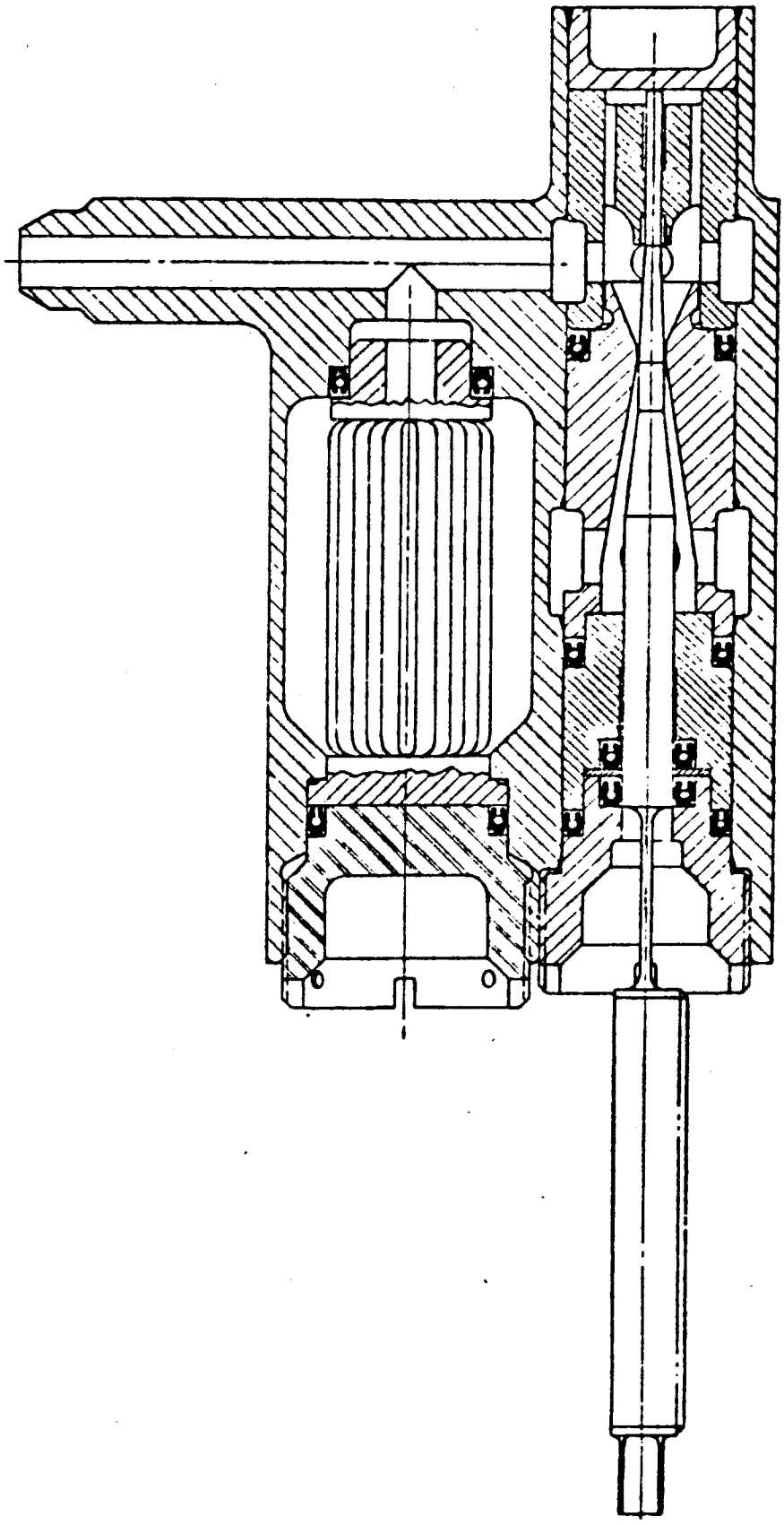

Figure 3.2.1-1. MIRA 150A Flow Control Valve Assembly

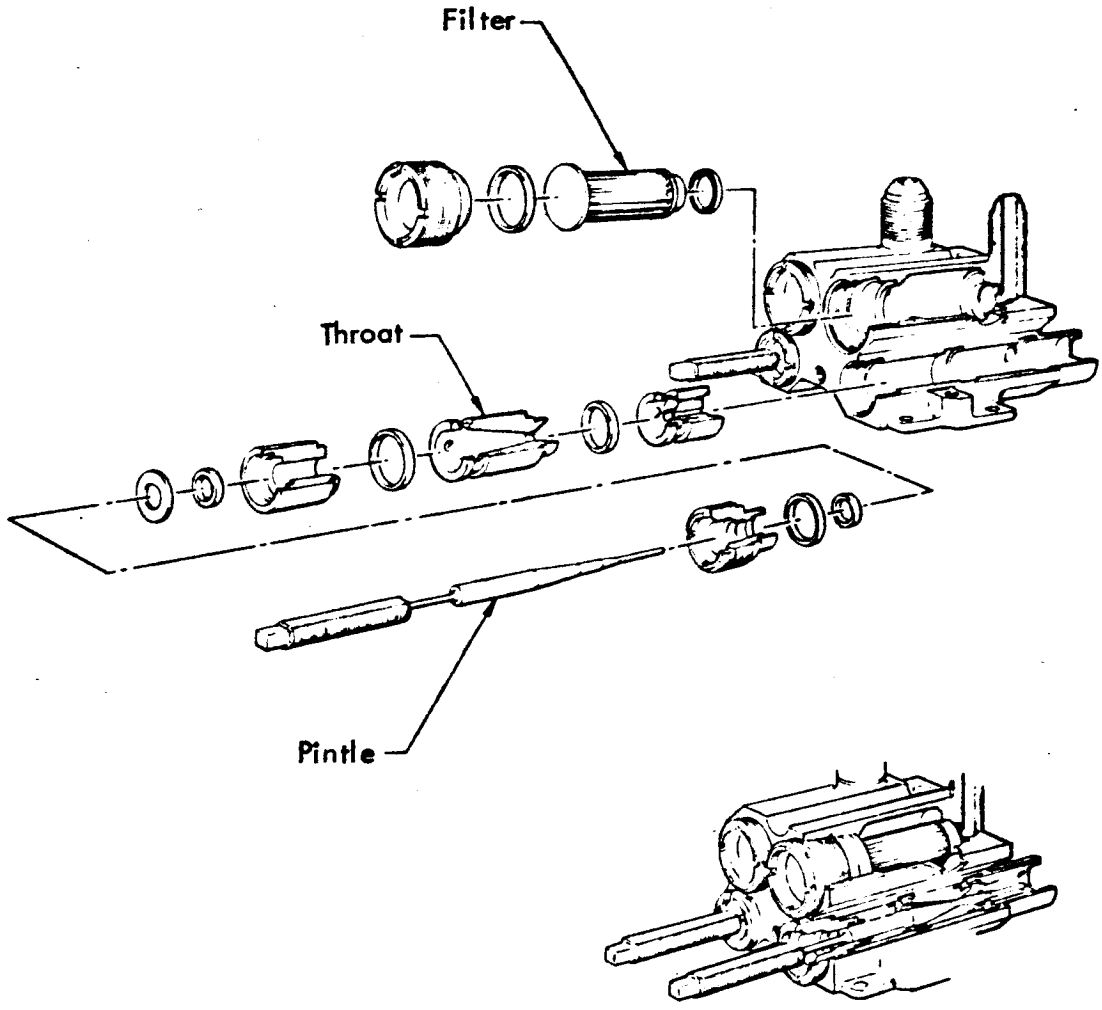

Figure 3.2.1-2. MIRA 150A Flow Control Valve Assembly (Exploded View)

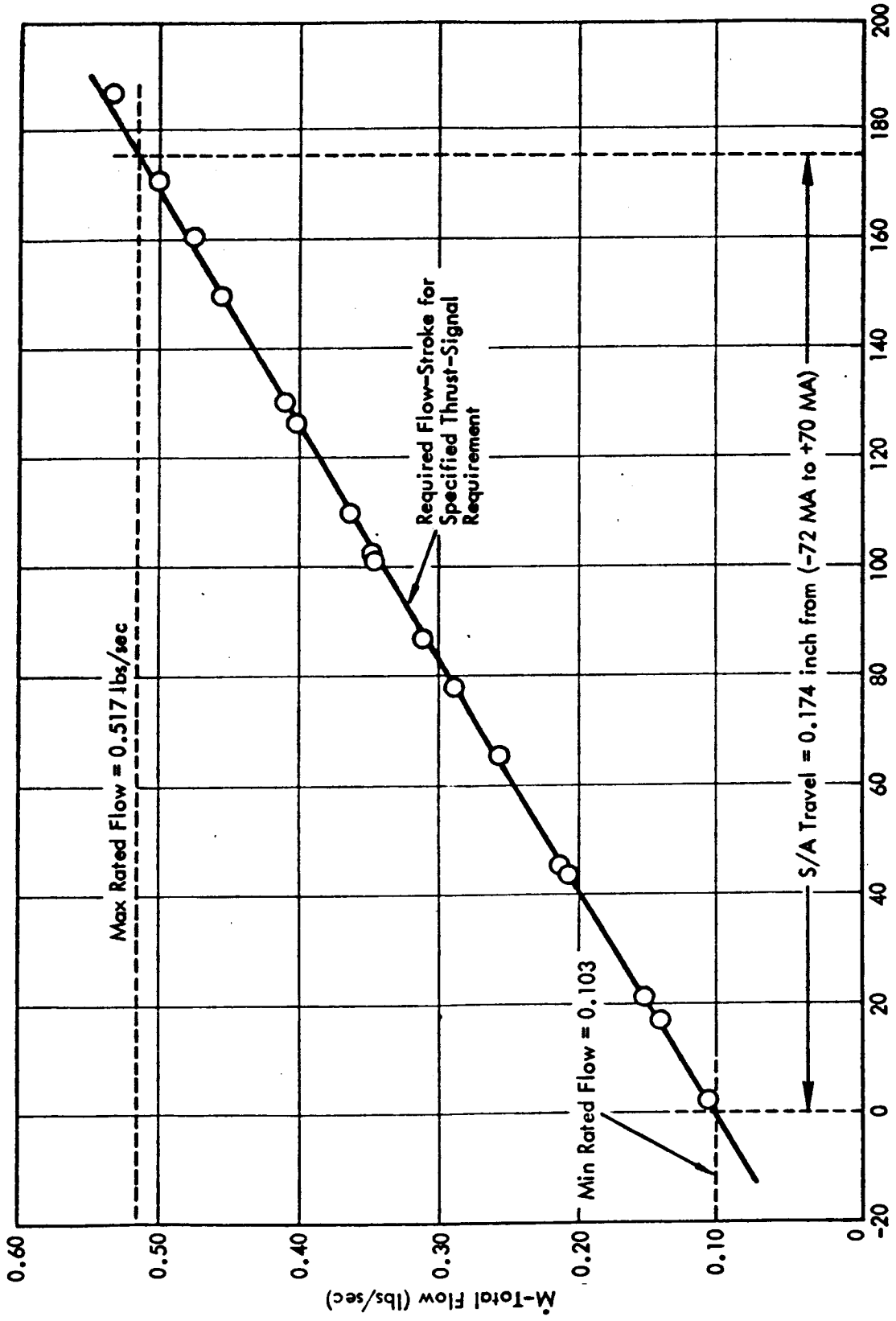

Figure 3.2.1-3. MIRA 150A Total Propellant Flow Versus Servoactuator Travel

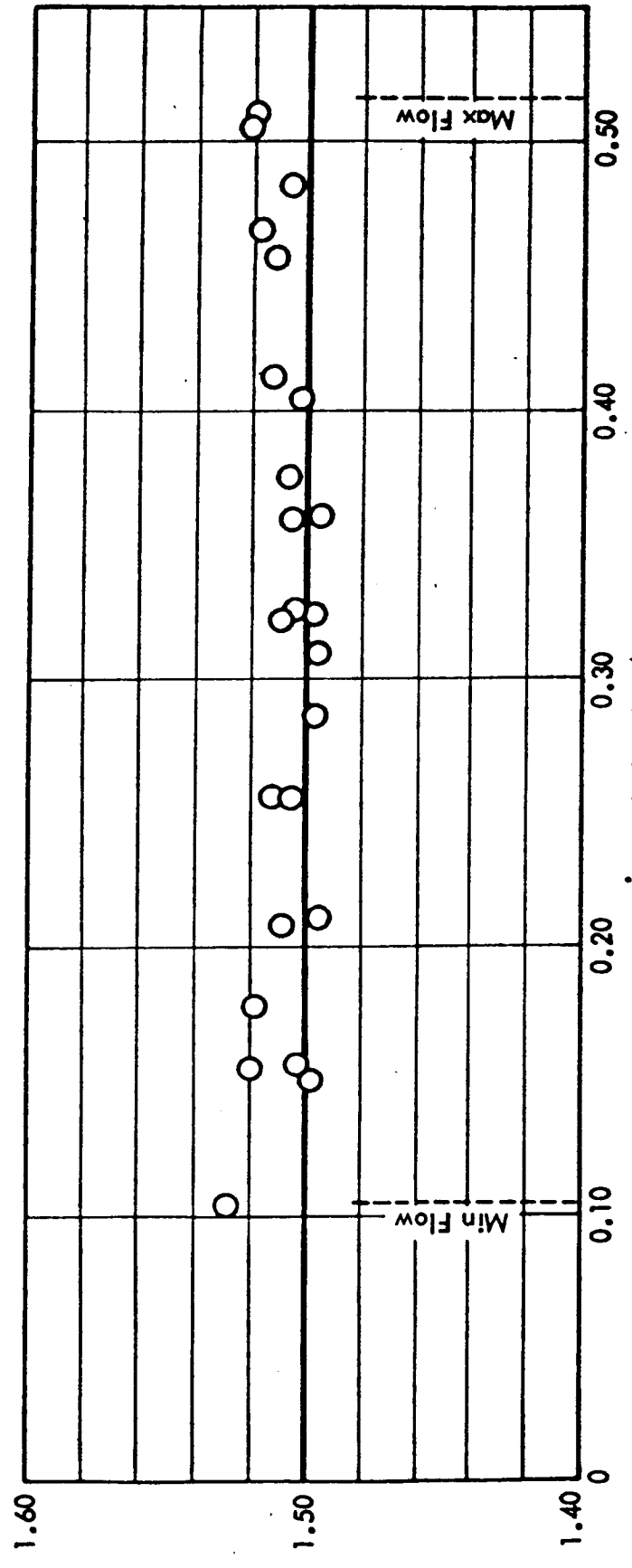

Figure 3.2.1-4. MIRA 150A Mixture Ratio Versus Total Flow Rate

Figure 3.2.1-5 shows the actual measured cavitating recovery pressure on the FCV during a water flow test. The scale also shows the equivalent oxidizer flow rates. This curve can be used to help predict the lowest possible tank pressure allowable for a given chamber pressure.

For example, a change in the FCV pintle contour could allow operation of the TCA at a chamber pressure of 110 psia with an oxidizer tank pressure of approximately 350 ± 20 psia. This would allow a pressure budget of the following approximate values:

Item	Nominal Pressure Drop, psi
Filters	15
Shutoff Valve	10
FCV	67
Other Passages	25
Injector	95
Total ΔP	212 psi

This 212 psi pressure drop plus a chamber pressure (P_c) of 110 psia gives 322 psia to the needed inlet pressure.

The 67 psi pressure drop for the FCV was derived assuming an inlet pressure to the FCV of 335 psia (i.e., 350 minus filter drop of 15) and an 80% recovery (see Figure 3.2.1-5) or 20% loss, thus, 67 psi drop (i.e., 0.20 x 335).

Further discussion of pressure budgets is given in paragraph 3.4.11.

The FCV pintle contours are paraboloids providing a linear flow area versus stroke over the throttling range. The true flow area is difficult to predict since the flow at the throat is not parallel to the centerline of the pintle nor parallel to the immediate parabolic surface. Though the later assumption is probably more valid, analysis shows that either assumption (flow parallel to centerline or to surface) results in a linear flow area versus stroke. A detailed analysis of the derivation of the proper shape of the paraboloids for the fuel and oxidizer is given in Appendix A. A closed form computer solution for the parabolic contour, and for the transformation to equivalent coordinates through which a machinists grinding tool must move to cut the contour is also available.

The flow discharge coefficient for both valves is assumed to be 0.92. Pintle contour tolerances are held to ± 0.0002 inches.

3.2.2 Propellant Filters

Filtration of propellants upon their entry into the TCA is necessary in order to avoid the detrimental effects of contamination which can cause: (1) jamming of moving parts, (2) seal leakage, and (3) disruption of established flow rates and combustion pattern. Fuel and oxidizer filters are provided within the TCA immediately upstream of the propellant flow control valves and permit the propellants to be filtered as soon as they enter the TCA. The two filters in each TCA are identical and interchangeable and provide the degree of filtration noted below:

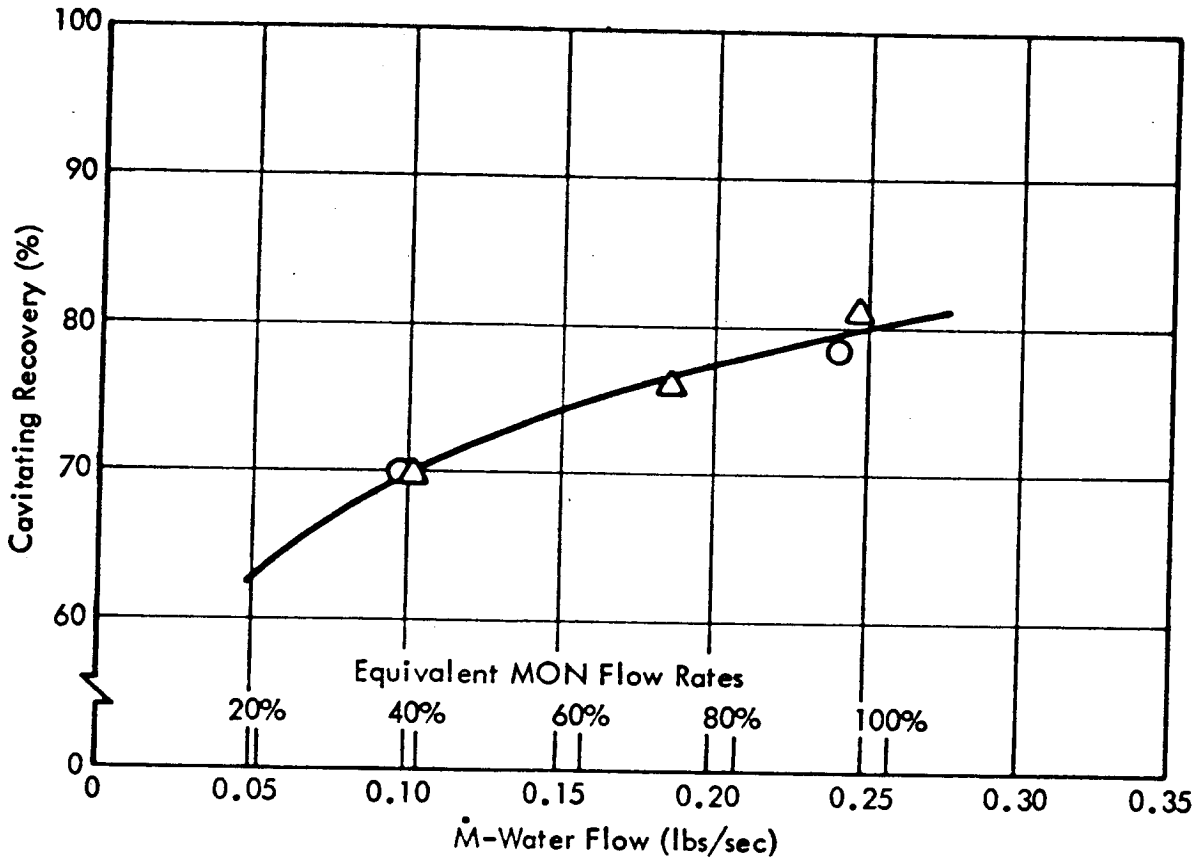

Figure 3.2.1-5. MIRA 150A Flow Control Valve Cavitating Recovery

98% filtration of particles 5 microns in minimum dimension.

100% filtration of particles 15 microns in minimum dimension.

100% filtration of fibers 1000 microns or greater in length.

The filters must meet the requirements delineated in STL Specification No. EQ 1-73B and Drawing No. C105183. The filter, shown in Figure 3.2.2-1 is constructed of Type 304 stainless steel wire mesh, pleated and welded to 304 stainless steel and rings and core. The closed end of the filter element contains a 10-32 tapped hole which is used to aid installation and removal. Flow direction is from outside to inside, and the pressure drop is 15 psi maximum for an oxidizer flow of 0.36 lb/sec or a fuel flow of 0.24 lb/sec.

Paragraph 5.1.2 discusses acceptance testing of the propellant filters and presents test data acquired during these tests.

3.2.3 Propellant Shutoff Valve

The TCA contains two propellant shutoff valves (SOVs) for start/stop control of fuel and oxidizer flow. The SOV outlet ports are closely coupled to the TCA injector in order to minimize TCA start/stop times. The SOVs are pilot operated by gaseous helium supplied at a nominal pressure of 720 psia from a common helium pilot valve (see paragraph 3.2.4).

Each SOV is comprised of a group of interchangeable component parts and utilizes the TCA head end body as a common valve body; the head end body contains all pilot gas and propellant porting. The SOV assembly and component parts are shown in Figures 3.2.3-1 (a) A picture of the parts that are inserted in the head end body is presented in Figure 3.2.3-1 (b).

All metallic parts are stainless steel. The seals (Bal-Seals) are made of Teflon with a stainless steel spring insert. The valve seat is sized to mate with a standard Teflon O-ring.

In the absence of pilot gas pressure, the SOV is closed with the poppet-to-seat seal maintained by a closure spring and propellant pressure. The spring will provide valve closure in the absence of propellant pressure. With the application of helium gas pressure, the valve piston moves downward (reference Figure 3.2.3-1 (a)) opening the poppet and compressing the closure spring. Upon removal of pilot gas pressure, the valve poppet is closed by propellant pressure and/or closure spring force. Pilot gas threshold pressures for opening and closing the valve are noted below.

1. Valve initially closed.
   Propellant Pressure = 720 psia
   Pilot gas opening threshold pressure = 400 psia:
   (i.e., valve will open when pilot gas pressure reaches approximately 400 psia).

2. Valve initially open.
   Propellant Pressure = 175 psia (corresponds to thrust of 100 lbs).
   Pilot gas closing threshold pressure = 150 psia:
   (i.e., valve will close when pilot gas pressure reaches approximately 150 psia

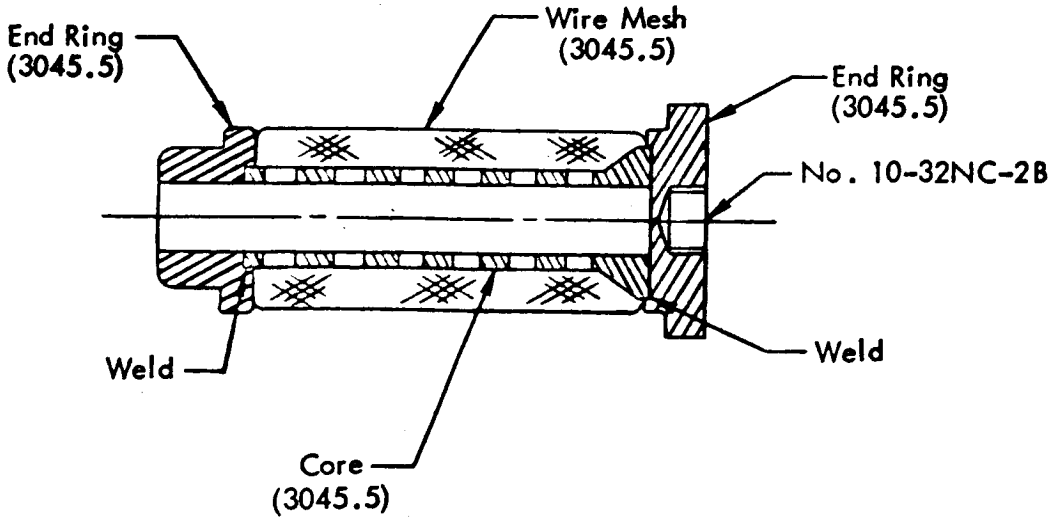

(a) Section View

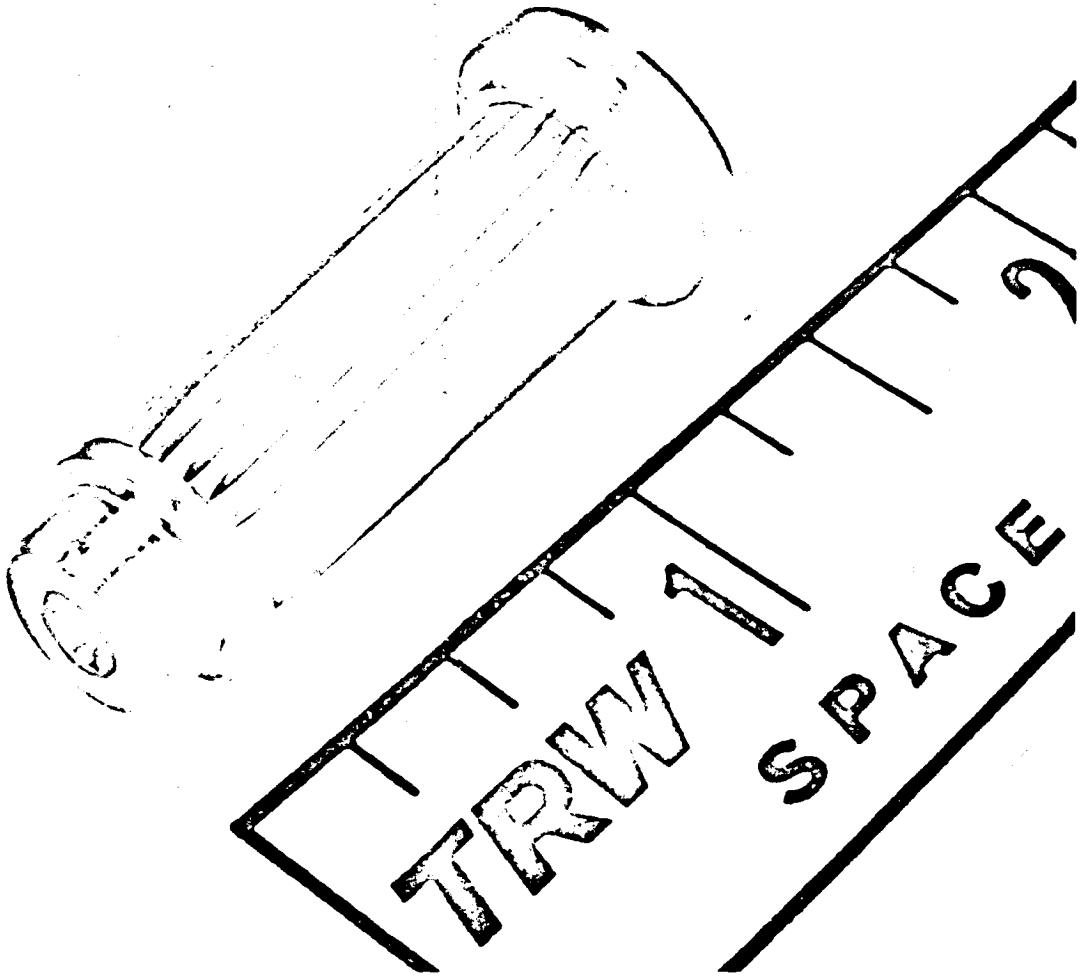

(b) Closeup Photograph

Figure 3.2.2-1. MIRA 150A Propellant Filter

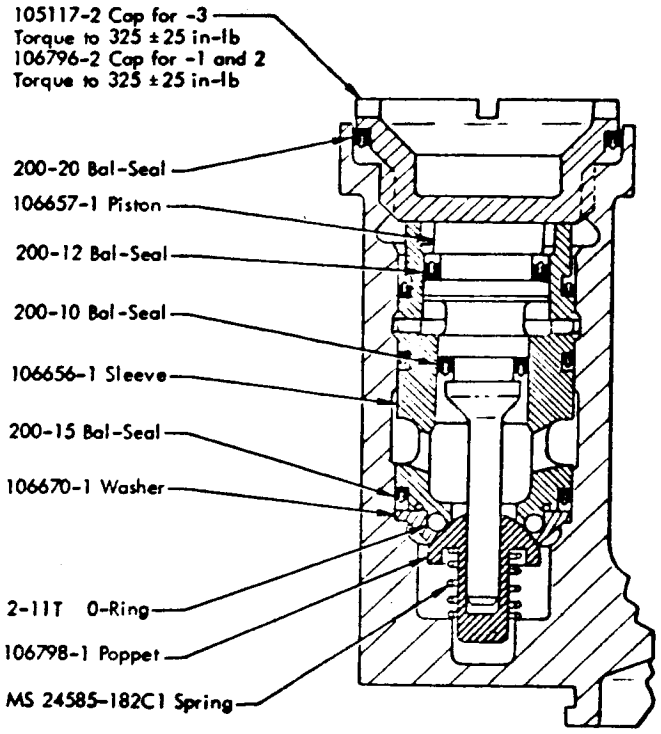

(a) Shutoff Valve Cross Section

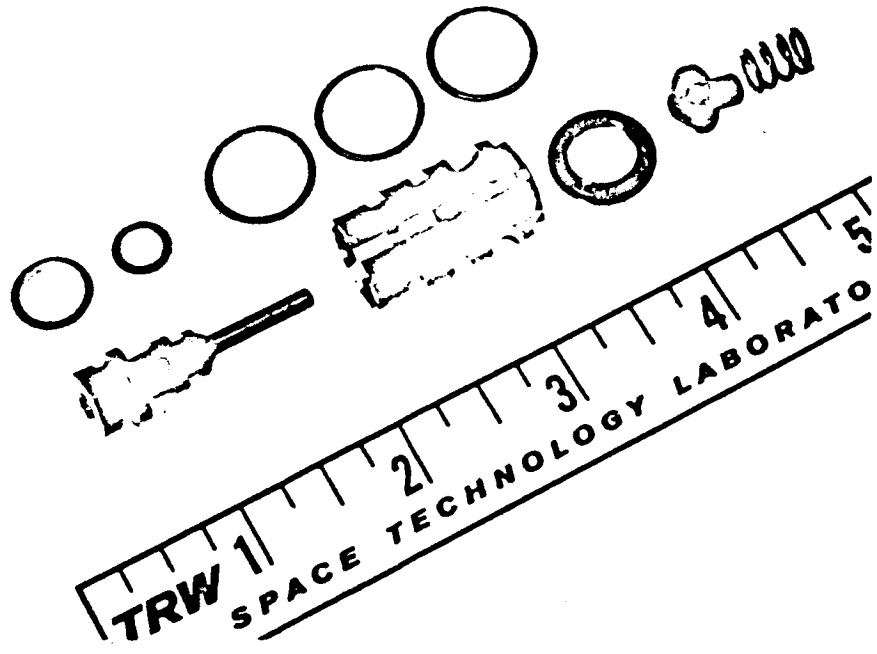

(b) Closeup Photograph of Shutoff Valve Kit Parts

Figure 3.2.3-1. MIRA 150A Propellant Shutoff Valve

It is noted that opening and closing threshold pressure may vary ± 50 psia from the values shown because of tolerances associated with spring force and seal friction.

The basic SOV design was developed during the Phase II effort and refinements were incorporated during Phase III. These refinements and the testing thereof are discussed in paragraph 5.3, SOV Component Evaluation Test Series. Environmental testing of the SOV is discussed in paragraph 5.2, Deep Vacuum Tests.

3.2.4 Helium Pilot Valve

The TCA contains a single, solenoid-operated, helium pilot valve for supplying and removing gaseous helium to and from the two propellant shutoff valves. The pilot valve is a three-way, two-position design, and its performance is an important factor in TCA start/stop operation. The pilot valve is attached to the TCA head end body such that its pilot (outlet) port is connected to the pilot gas inlet/outlet of both propellant shutoff valves.

Pilot valves were procured from two sources under STL Specification No. EQ 2-25D and Drawing No. C104337. During the early part of the Phase III effort, orders were placed with only one vendor. At that time, the possibility of delivery delinquencies appeared. Therefore, a second source was established and additional pilot valves were ordered. The two helium pilot valves are shown in Figures 3.2.4-1 and 3.2.4-2. The initial design, Part No. C104337-1 was finally chosen to become the component part of delivered TCAs and was used exclusively in the prequalification test program.

In operation, the inlet to the pilot valve is normally pressurized with gaseous helium at 720 ± 20 psia with a maximum possible inlet pressure of 850 psia. Inlet poppet closure is maintained by a spring to achieve a maximum allowable helium leakage of 10 scc/hr at 850 psia. With the valve de-energized and (inlet poppet closed), the vent and pilot ports are connected and the pilot gas portion of the propellant shutoff valves is now vented to atmosphere. Upon energizing the pilot valve solenoid, the armature moves thereby opening the inlet port and closing the vent port. Thus, with the pilot valve energized, the vent port is closed and the inlet port is connected to the pilot port with the result that propellant shutoff valves are actuated to the open position. With the pilot valve energized and the vent port closed, the maximum allowable leakage across the vent poppet is 10 scc/hr at 850 psia.

Electrical power for operation of the pilot valve is 15 watts maximum; voltage requirements are noted below.

Minimum Actuation Voltage:	16 vdc for one second (pull-in)
Minimum Hold-in Voltage:	13 vdc
Maximum Actuation Voltage:	23 vdc
Maximum Applied Voltage:	26 vdc for 5 minutes

The valve inlet port must be pressurized to approximately 400 psia in order to obtain valve actuation upon energizing the solenoid. Also, the pilot port must be capped or connected to a fixed volume to permit the armature to return to its unactuated position upon removal of power from the solenoids.

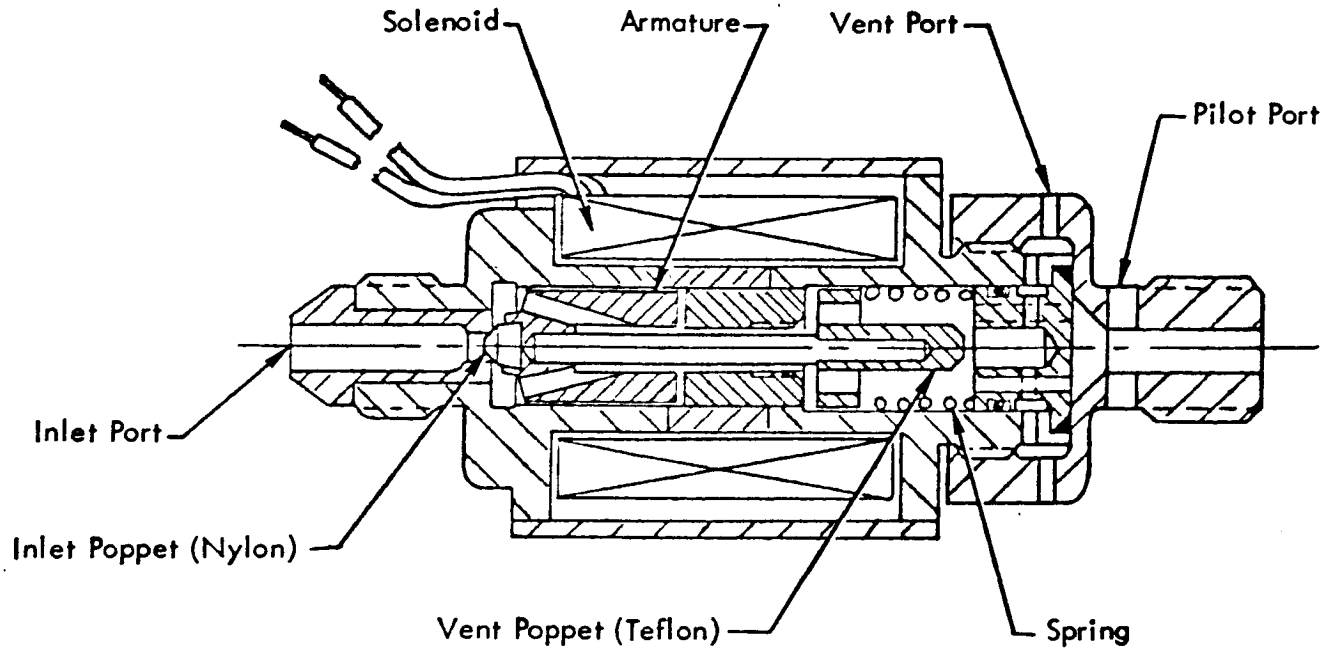

(a) Section View

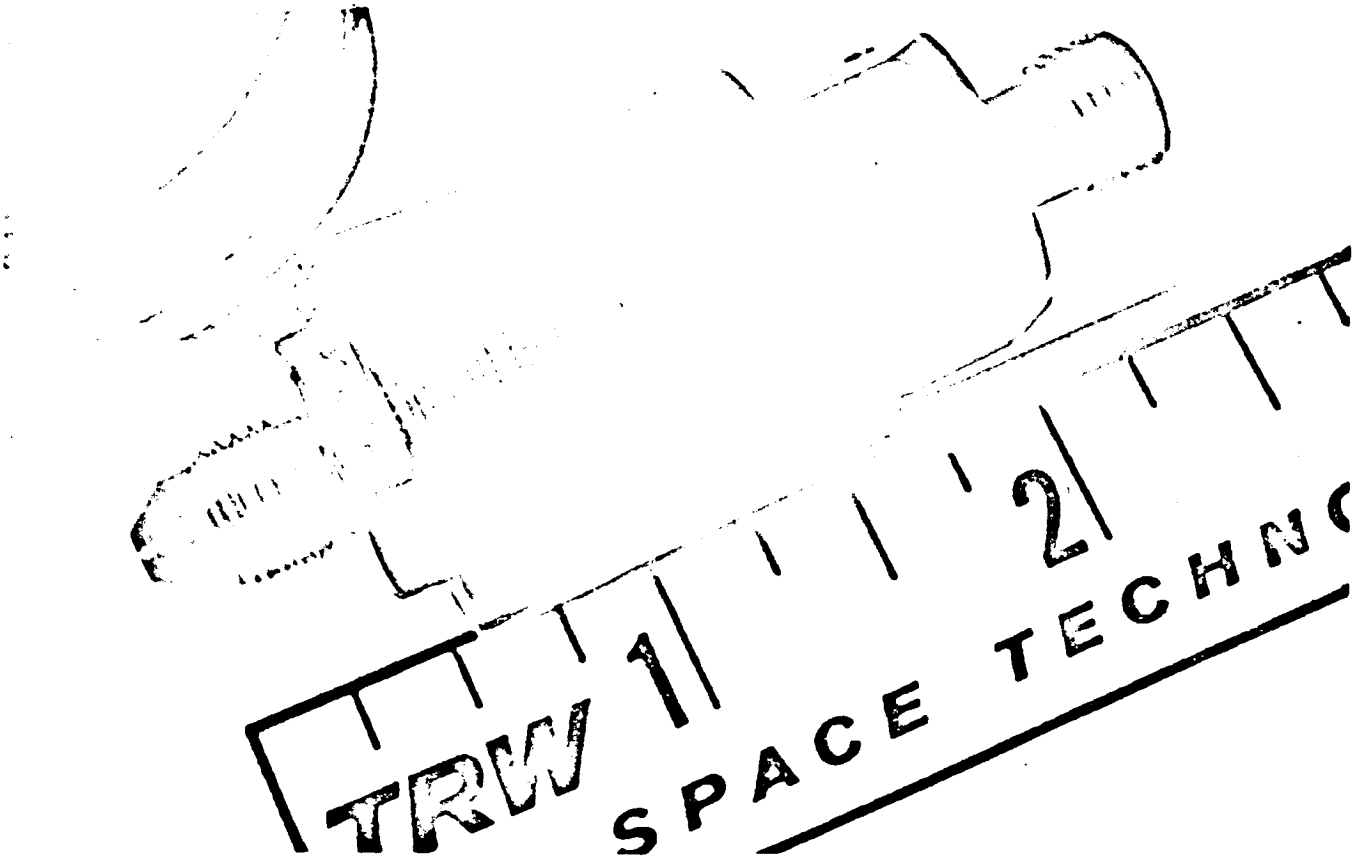

(b) Closeup Photograph

Figure 3.2.4-1. MIRA 150A Helium Pilot Valve
STL P/N C104337-1

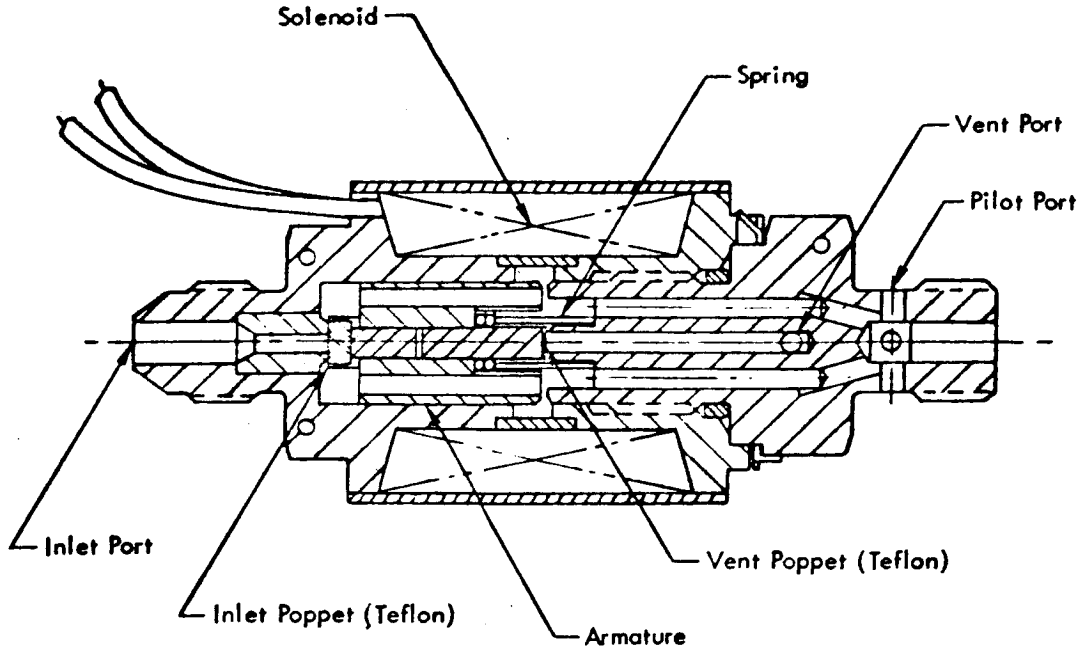

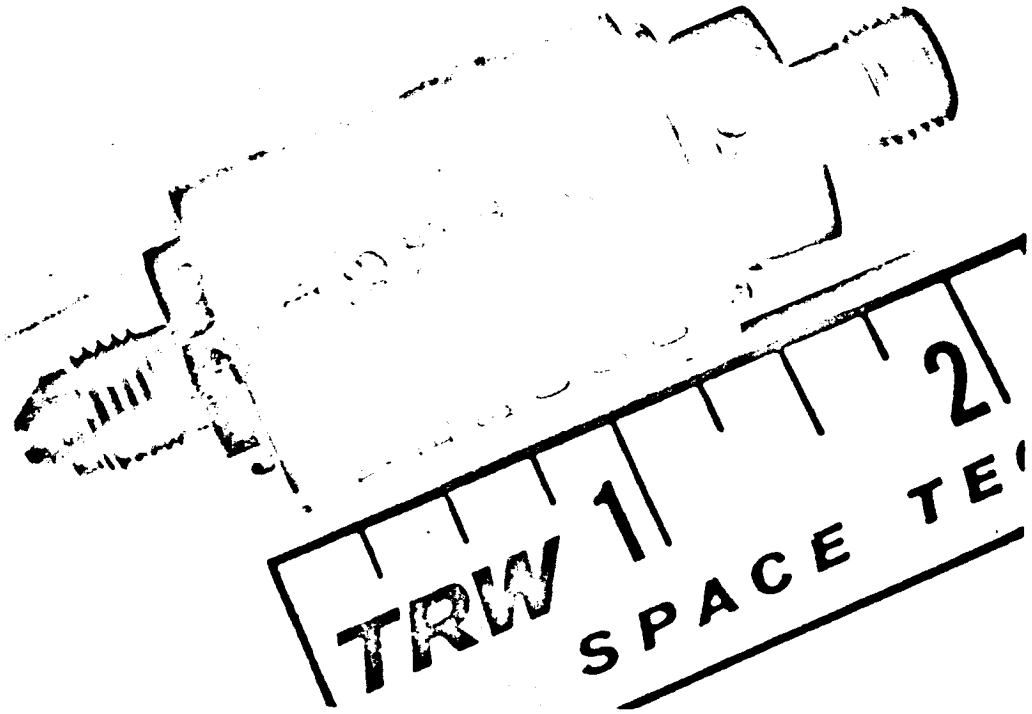

Figure 3.2.4-2. Alternate Helium Pilot Valve
STL P/N C104337-2

The magnetic circuit of the C104337-1 valve is high permeability iron coated with electroless nickel plate. The first lot of C104337-2 valves had a similar magnet circuit. On a second lot of C104337-2 valves, stainless steel replaced the nickel plated iron. The C104337-2 design used Teflon on both the inlet and vent poppets while the -1 design used Teflon on the vent poppet and nylon on the inlet poppet.

Paragraph 5.1.3 presents data from acceptance testing of the helium pilot valves. Pertinent environmental test data is in paragraph 5.2, Deep Vacuum Tests. Pilot valve cycle life data is contained in paragraph 6.4.3, Cycle Life.

3.2.5 Variable Area Injector

The HEA injector is a single element, coaxial type injector. The single moving injector element, the sleeve, is mechanically linked to the flow control (cavitating venturi) valves and to the servoactuator. Thus, as the propellant flow rate increases the injector orifice areas are simultaneously increased.

The injector has several unique characteristics:

1) The use of coaxial impinging sheets provides uniform circumferential propellant distribution in the combustion chamber.

2) The combustion zone is removed from the injection ports, minimizing coupling with the feed system.

3) The single moving injector element controls the injector gaps accurately to maintain the proper absolute and relative injection stream velocities over the entire throttling range.

4) Streaking and uneven heat flux to the chamber, faceplate and throat is minimized by the type of boundary layer generated.

5) The injector is not required to be a flow control mechanism - the cavitating venturi flow control valves have this function - thus the injector can be adjusted for optimum combustion efficiency. For example, the injector flow gaps can be set for wider tolerances than would be allowable if the injector controlled flow.

6) The injector geometry, impingement angles, pressure drops, flow rates and gaps are relatively easy to adjust and/or modify during developmental testing and calibration.

An exploded view of the injector is shown in Figure 3.2.5-1. A scaled injector cutaway drawing is shown in Figure 3.2.5-2.

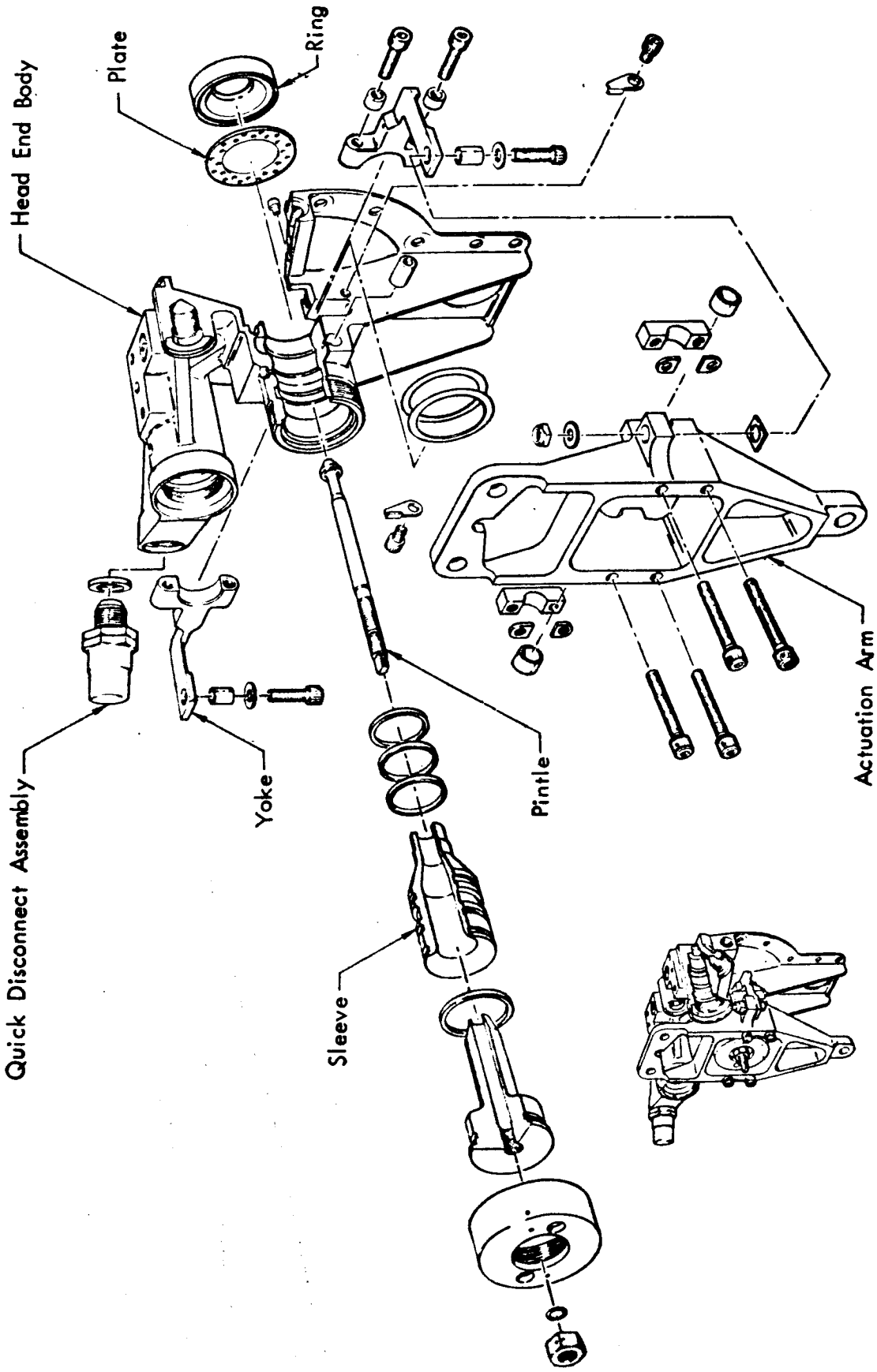

Figure 3.2.5-1. MIRA 150A Injector Assembly (Exploded View)

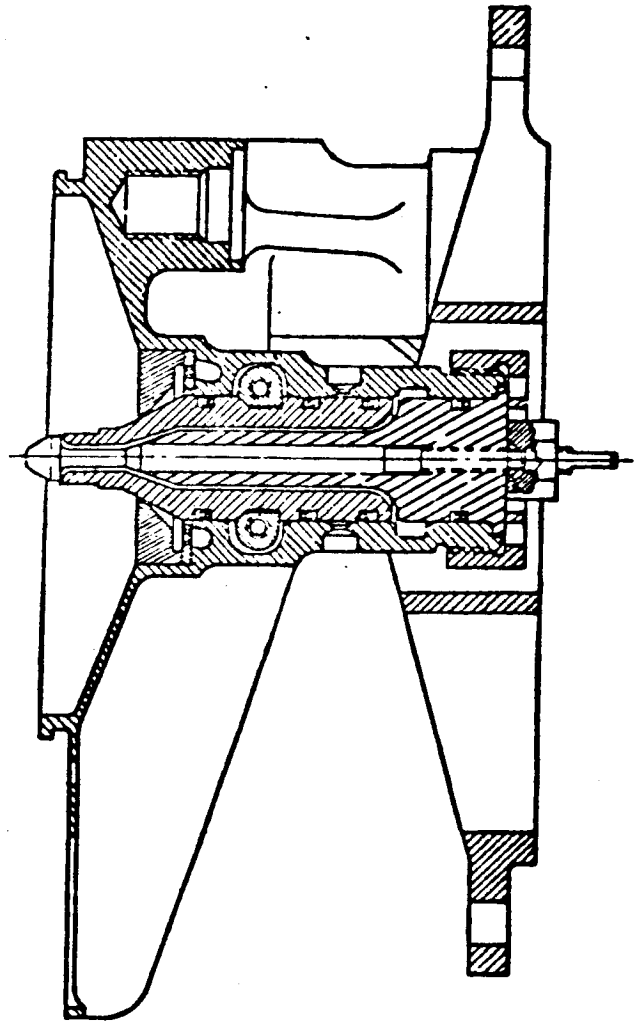

Figure 3.2.5-2. MIRA 150A Injector Assembly
(Section View)

As the flow of propellants is reduced linearly by the servoactuator, the fuel and oxidizer injector gaps are reduced simultaneously. The MIRA 150 injector orifice diameters, metering angles, and gaps are designed and adjusted to provide a nominal pressure drop for oxidizer and fuel as shown in Figure 3.2.5-3. The oxidizer to fuel momentum ratio, $\frac{\dot{M}_o v_o}{\dot{M}_f v_f}$, is kept approximately equal for the entire thrust range.

The injector sleeve stroke on the MIRA 150A is 0.0067 inches of travel from 30 to 150 lbs of thrust and the gap at the minimum thrust level (30 lbs) is approximately 0.0017 inches. Although this gap is quite small, the injector pressure drop at the low thrust level is relatively insensitive to fabrication tolerances.

Further discussion of pressure budgets is presented in paragraph 3.4.11.

Injector development and performance test data are discussed in paragraph 6.2.

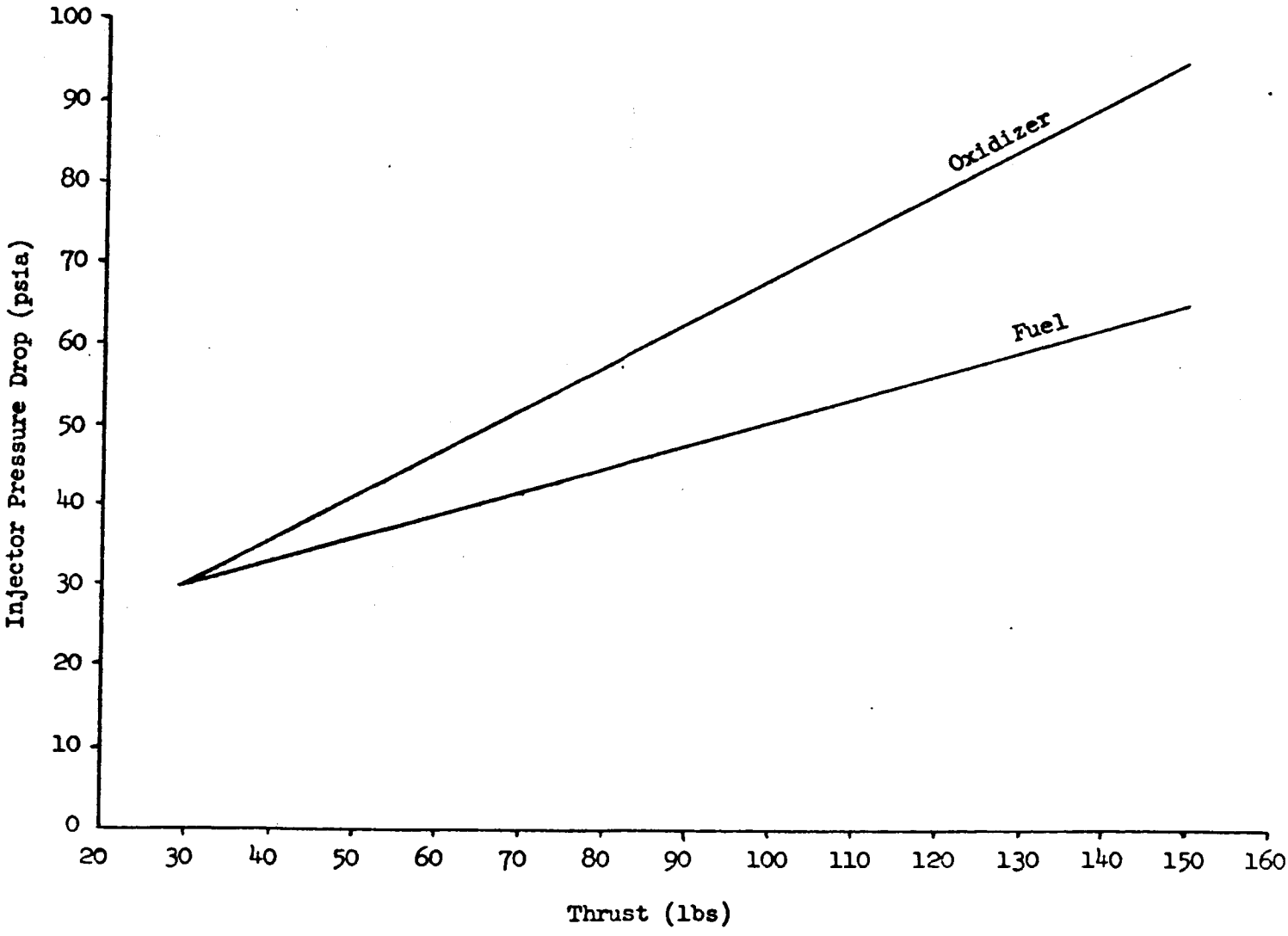

Figure 3.2.5-3. Typical Injector Pressure Drops

3.2.6 Electrohydraulic Servoactuator

The servoactuator converts thrust control electrical signals into output shaft position. It is powered with 720 psia fuel (MMH) from the spacecraft vernier engine fuel system. Two servoactuator designs are discussed herein - The Phase II Follow-on design and the Phase III design. Both designs are conceptually identical and operationally similar, but differ in stroke, electrical connector location, other minor design areas, and detailed performance.

The servoactuator design is shown in Figures 3.2.6-1, -2, -3, and -4. A schematic of the servoactuator is shown in Figure 3.2.6-1 and is applicable to both the Phase II Follow-on and the Phase III units. Figures 3.2.6-2, -3, and -4 apply only to the Phase III units.

The actuator consists of a double coil, torque motor which positions a single nozzle flapper fluid amplifier. Control pressure from the first stage amplifier positions a second-stage, three-way spool valve, which in turn supplies pressure to a balanced power piston which positions the load. A feedback spring mechanism is connected from the output shaft to the torque motor armature, insuring positioning accuracy. A pressure port filter, rated at 5 microns nominal, is installed to preclude inadvertent actuator contamination during handling and installation. In the TCA installation, the MMH flowing through this filter has already been filtered by the TCA filters described in paragraph 3.2.2. An additional internal servoactuator filter, rated at 2 microns nominal, protects the orifice and nozzle.

The differential command current signal to the two servoactuator torque motor coils varies from a nominal value of -72 ma at 150 lbs of thrust to +70 ma at 30 lbs of thrust. The permissible thrust to ΔI hysteresis and linearity envelope allows a small actuator over-travel. The ΔI signal is superimposed on a DC quiescent current of 45 ma per coil to insure correct current flow direction throughout the throttling range. A 400-cps differential current dither signal of 5 ma peak-to-peak is superimposed on the command ΔI signal to reduce actuator hysteresis and deadband.

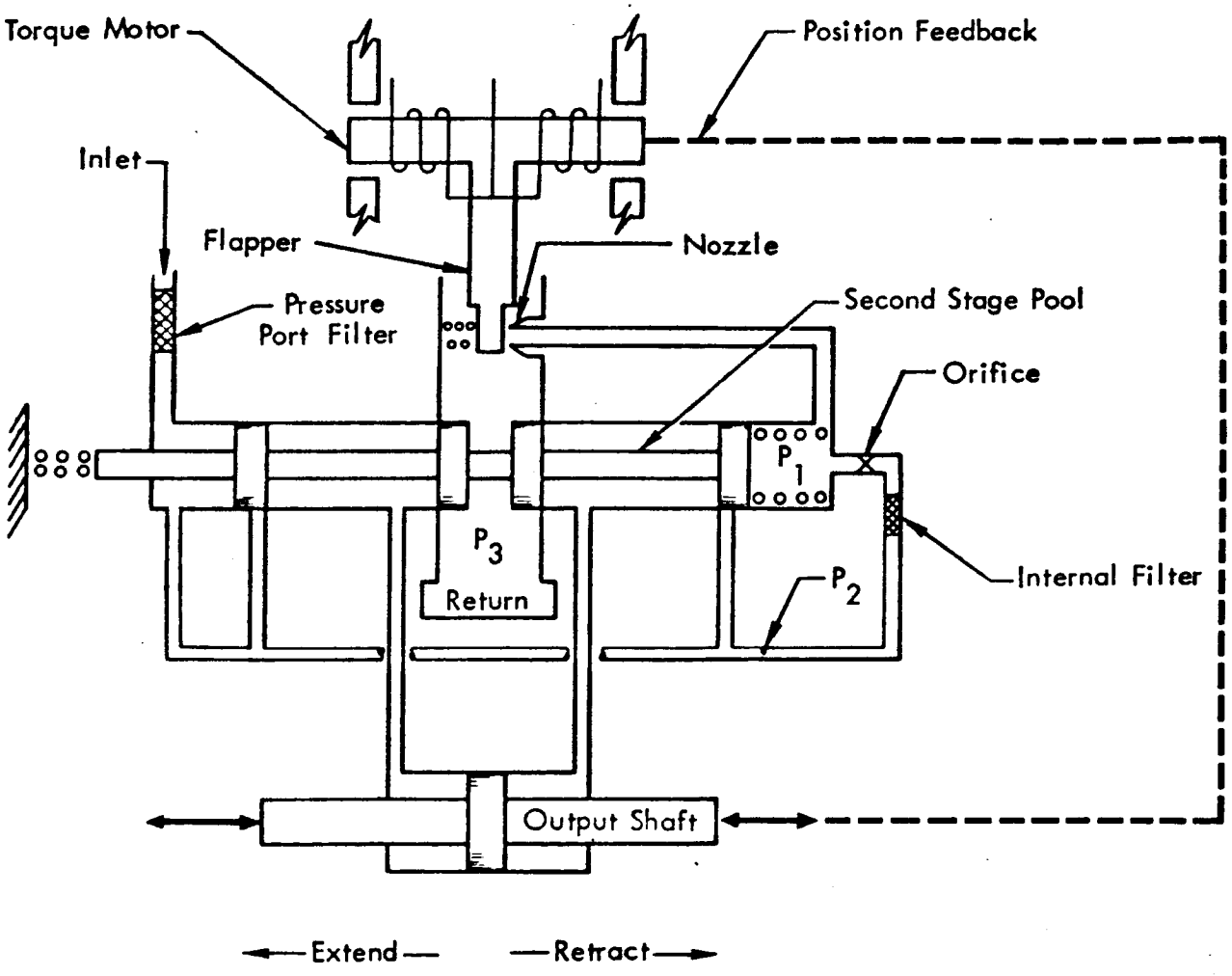

Figure 3.2.6-1. MIRA 150A Servoactuator Schematic

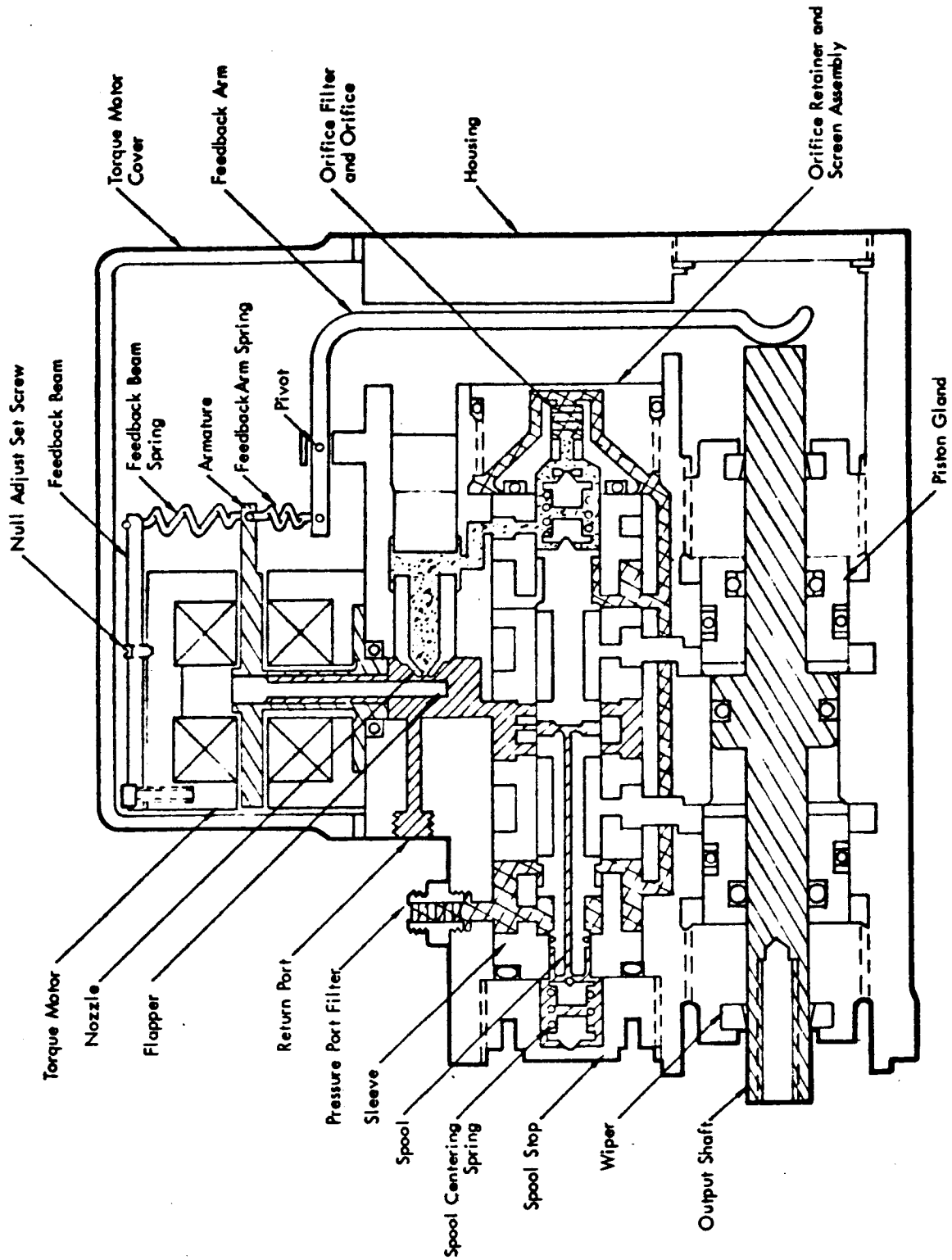

Figure 3.2.6-2. MIRA 150A Servoactuator Detailed Schematic

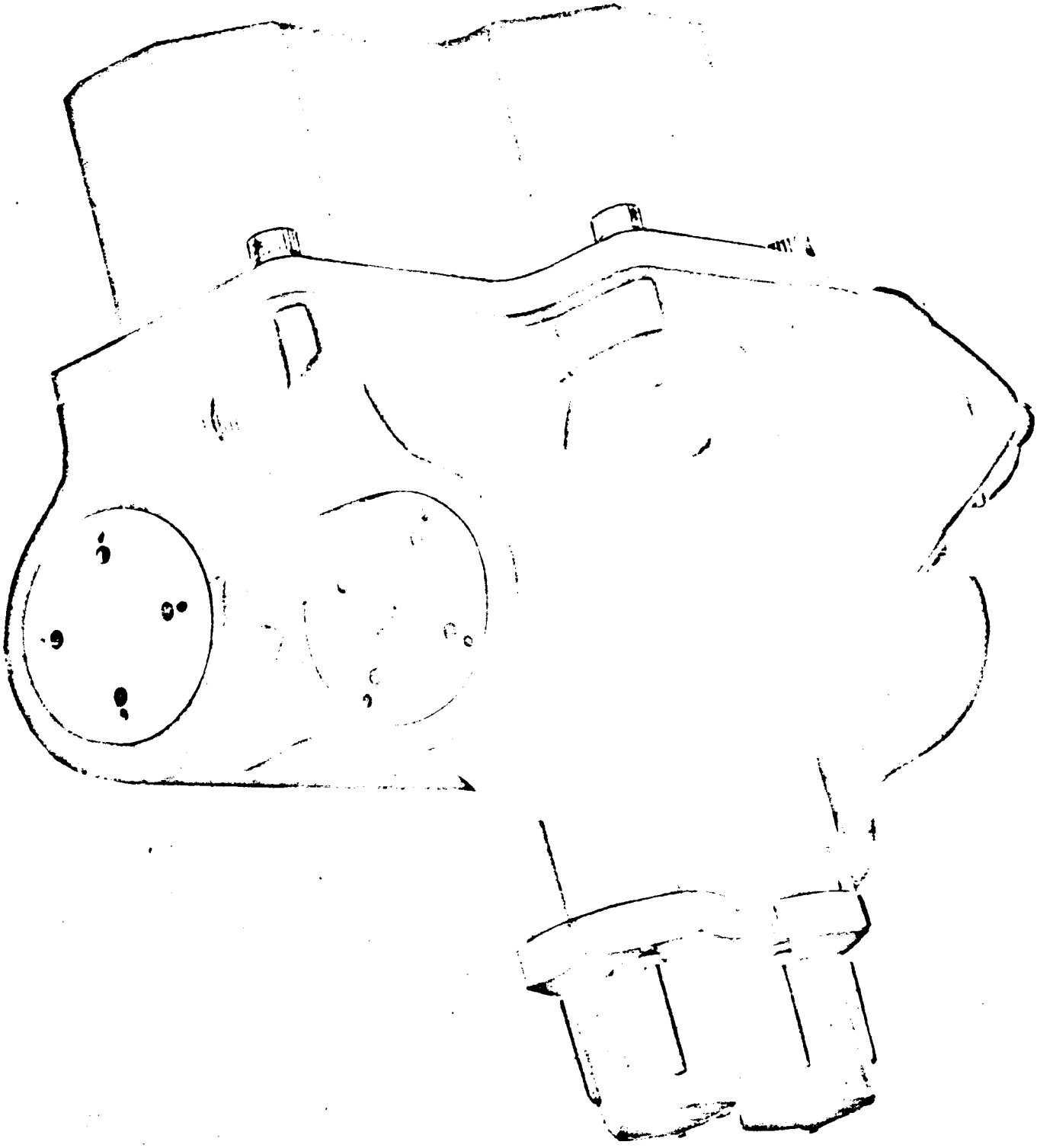

Figure 3.2.6-3. MIRA 150A Phase III Servoactuator

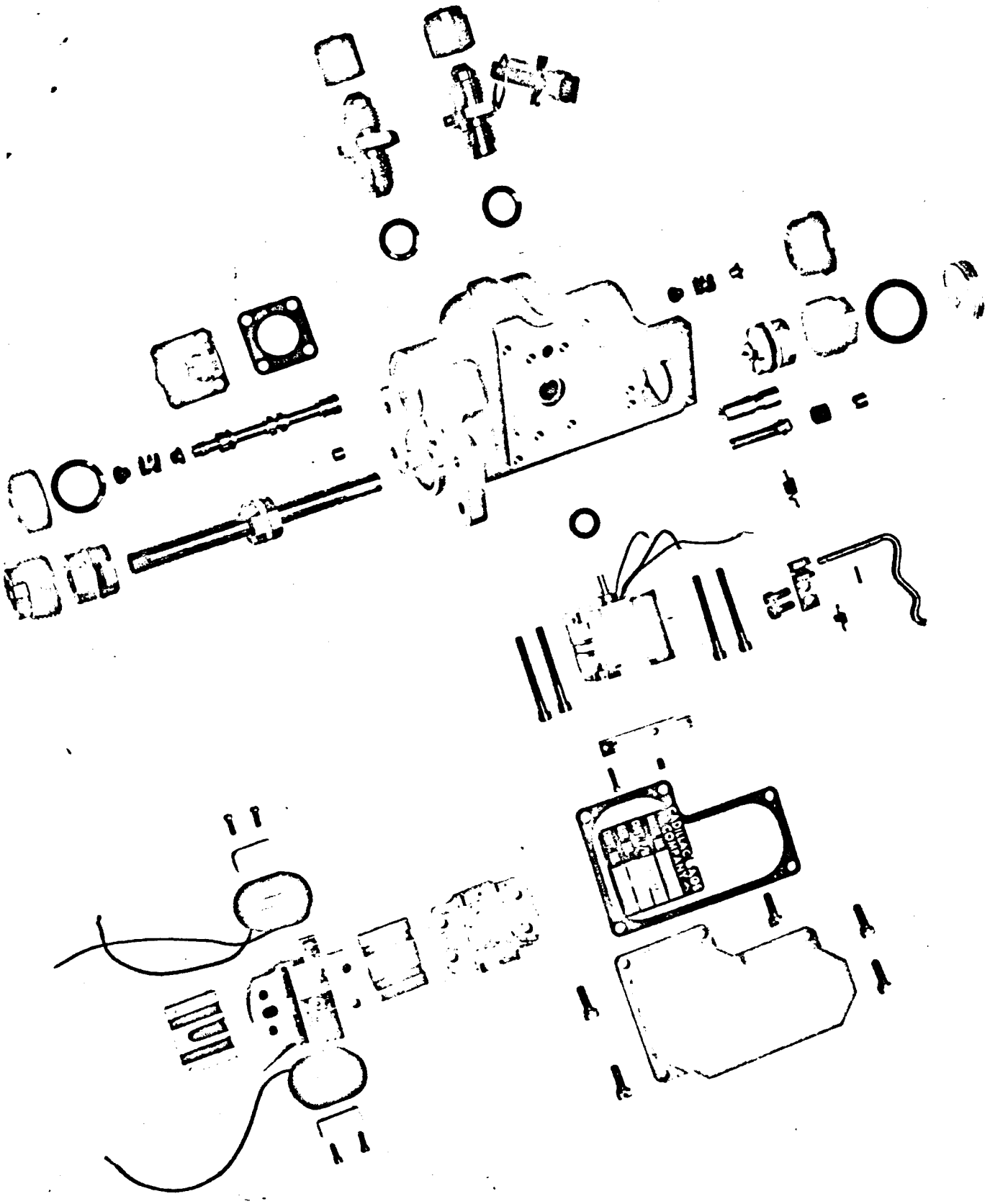

Figure 3.2.6-4. MIRA 150A Phase III Servoactuator (Disassembled)

A typical extend mode function is as follows (refer to Figure 3.2.6-1). A differential current signal to the torque motor moves the flapper away from the nozzle, increasing the effective nozzle area and allowing an increase in fluid flow through the nozzle. The nozzle control pressure, P_1, acting on the right hand side of the second stage spool decreases, because of the increase in effective nozzle area. The unbalanced second stage spool moves to the right until a force balance equilibrium is obtained, and ports fuel at high pressure, P_2, to the right side of the output piston. The left side of the output piston is ported to the low return pressure, P_3. The piston and output shaft assembly then extends to the left. As the desired position is approached, the feed back mechanism exerts a torque on the armature opposing the original commanded torque. When the desired position is reached, the feedback torque exactly balances the commanded torque and the flapper is then in the original or null position. This null position of the flapper results in increasing the nozzle pressure to its original or null value and returning the second stage spool to the center. Thus, for any steady state position of the output shaft, the flapper and second stage spool are always in the null or center position, except under one circumstance. This occurs when the torque motor receives a signal for an extreme position of the output shaft beyond the position its mechanical stops will allow. For example, a -80 ma signal to a servoactuator whose mechanical stops are set for a position corresponding to a signal of -75 ma will result in the flapper and second stage remaining away from the null or center position until the signal is changed to -75 ma or less (i.e., lower negative amperage or positive signal).

Dynamic throttling performance for the TCA for frequencies up to 10 cps are totally a function of the servoactuator dynamic response. Details on a mathematical model dealing with TCA dynamic performance are presented in STL Report 8422-6014-TV-000.

Table 3.2.6-5 lists servoactuator documentation and associated drawing numbers. Table 3.2.6-6 lists major servoactuator specification requirements when operating on MMH. Figures 3.2.6-7 and -8 support Table 3.2.6-6. Figure 3.2.6-9 graphically defines certain dynamic performance parameters

A passive resistance network was designed to allow a change in position gain of the Phase II Follow-on servoactuators to simulate the Phase III gain. This network allowed the input impedance to remain constant and also allowed the position of the extend stop to be altered by changing resistance values.

The formula for calculating the fuel dumped for a mission profile, shown below, is based on a piston area of 0.17 in^2, and a 100% stroke for -70 to +70 ma nominal signal range with no overshoot.

$$\text{Total Volume Flow} = V = 12t + (2)(f)(60)(x)(t)(.17)\ in.^3$$

$$= 12t + 20.4\ fxt,\ in.^3$$

V = Total Volume, $in.^3$

t = Time, min.

f = Frequency, cps

x = Actual Storke, in.

Total Weight Flow = Volume (V) times fuel density (ρ) = V(0.0316) lbs

This relationship is plotted in Figure 3.2.6-10 for the Phase III servoactuator. This figure can be used for determining fuel flow rates for any combination of stroke and frequency.

Calculation of typical (i.e., for typical mission profiles) fuel dump weights for Phase III servoactuators, using Figure 3.2.6-10, are given below.

Mode	Time (secs)	f (cps)	Stroke	$\dot{M}$ (lb/min)	Weight (lbs)	Weight - Three Actuators (lbs)
270-sec total duty cycle (4.5 minutes)	50	7	Stop-to-Stop	1.21	1.01	
	220	1	6.7% (10 lbs thrust)	.38	1.39	
				Totals	2.40	7.20
480-sec total duty cycle (8.0 minutes)	50	7	Stop-to-Stop	1.21	1.01	
	430	1	6.7%	.38	2.72	
				Totals	3.73	11.19

Table 3.2.6-5

Servoactuator Documentation

	Phase II Follow-on	Phase III
Part Number	C104312 B	C219217 A
Serial Numbers	C53747 to C53752	C55390 to C55407
Specification	EQ 2-23B Amended by 9354.4-149 9354.4-167	EQ 2-42
Specification Control Drawing	C104312, Revision B	C219217, Revision A
Acceptance Test Procedure	9354.4-140	9354.4-255
Quantity Procured	5	18

Table 3.2.6-6

Servoactuator Major Specification Requirements

A. Common to Both Phase II Follow-on and Phase III Units

Parameter	Required Value
Operating Differential Pressure	635 to 740 psia
Burst Pressure	1720 psia
Weight	1.7 lbs max, dry
Loading	15 to 25 lbs compressive, ± 4 to ± 10 lbs friction, 0.01 slugs max inertia
Input Signal	± 70 ma ΔI normal, ± 120 ma ΔI continuous overload
Dither Input Signal	5 ma peak-to-peak ΔI at 400 cps
Hysteresis	Less than 2.5 ma or 15% of any ΔI excursion, whichever is greater, and within envelope
Deadband	2.5 ma maximum
25% Stroke Step Response	
Rise Time	40 ma maximum
% Overshoot	23% maximum
Settling time	65 ma maximum
100% Stroke Step Response	
Rise Time	40 ma maximum
Frequency Response	
Amplitude Ratio	.97 min @ 5 cps, 15 ma peak-to-peak
Phase Lag	20° max @ 5 cps, 15 ma peak-to-peak
Static Shelf Life	2 years
Endurance	20,000 cycles minimum @ ± 70 ma, 1 cps sinusoidal input
Operating Altitude	100 hours in Cis-lunar space
Operating Temperature	0 - 100°F
Storage Relative Humidity	3 to 95% throughout a temperature range of 32 to 100°F for 2 years
Null Leakage	12 $in.^3$/min maximum

Table 3.2.6-6 (Continued)

B. Different for Phase II Follow-on and Phase III

Parameter	Required Value	
	Phase II Follow-on	Phase III
Proof Pressure	1050 psia	1035 psia (1035 psig at sea level)
Nominal Stroke	0.253 stop-to-stop 0.233 at ± 72 ma ΔI	0.1836 stop-to-stop 0.174 from 30 to 150 lbs thrust 0.172 at ± 70 ma ΔI
Quiescent Current	42.5 ± 2.1 ma/coil	45 ± 2.1 ma/coil
Coil Impedance	400 ± 20 ohms/coil DC	400 ± 20 ohms/coil DC 625 ohms/coil max at 400 cps
Dielectric Strength	2 ma max current at 500 VDC, pin to ground	5 megohms min at 125 VDC, pin to ground
Linearity	per Figure 3.2.6-7	per Figure 3.2.6-8

3.2.7 Combustion Chamber and Nozzle Assembly Description and Operation

The combustion chamber and nozzle assembly (CC & NA) is that portion of the TCA that contains, directs and expands the gaseous products of combustion. A cross section view of the CC & NA is shown in Figure 3.2.7-1 and an exploded view is presented in Figure 3.2.7-2.

The CC & NA is composed of six major parts; a combustion chamber liner, an exit cone liner, a throat insert, a convergent section insert, an injector head liner, and a metal case. These six major parts are fabricated from three different materials; a silica-phenolic ablative material, JTA graphite, and Titanium 6 Al-4V alloy.

The injector head liner, combustion chamber liner, and exit cone liner are machined as detailed parts from silica-phenolic billets. The raw stock billets are molded from ½" x ½" squares of pre-impregnated silica-phenolic material in a closed metal die and pressure cured at 2000 psig minimum for 4 hours at 310°F. The billets are then post-cured in a circulating air oven for 24 hours at 310°F. The uncured ablative material molding compound is composed of 23 to 27% resin solids and 2 to 5% volatiles by weight. The remaining material is 98%, or better, pure silica reinforcement material. The resulting molded billet has a minimum specific gravity of 1.77, an average Barcol hardness of 70, and less than 0.5% by weight of uncured material. The raw material billets are radiographically inspected before machining into detailed parts.

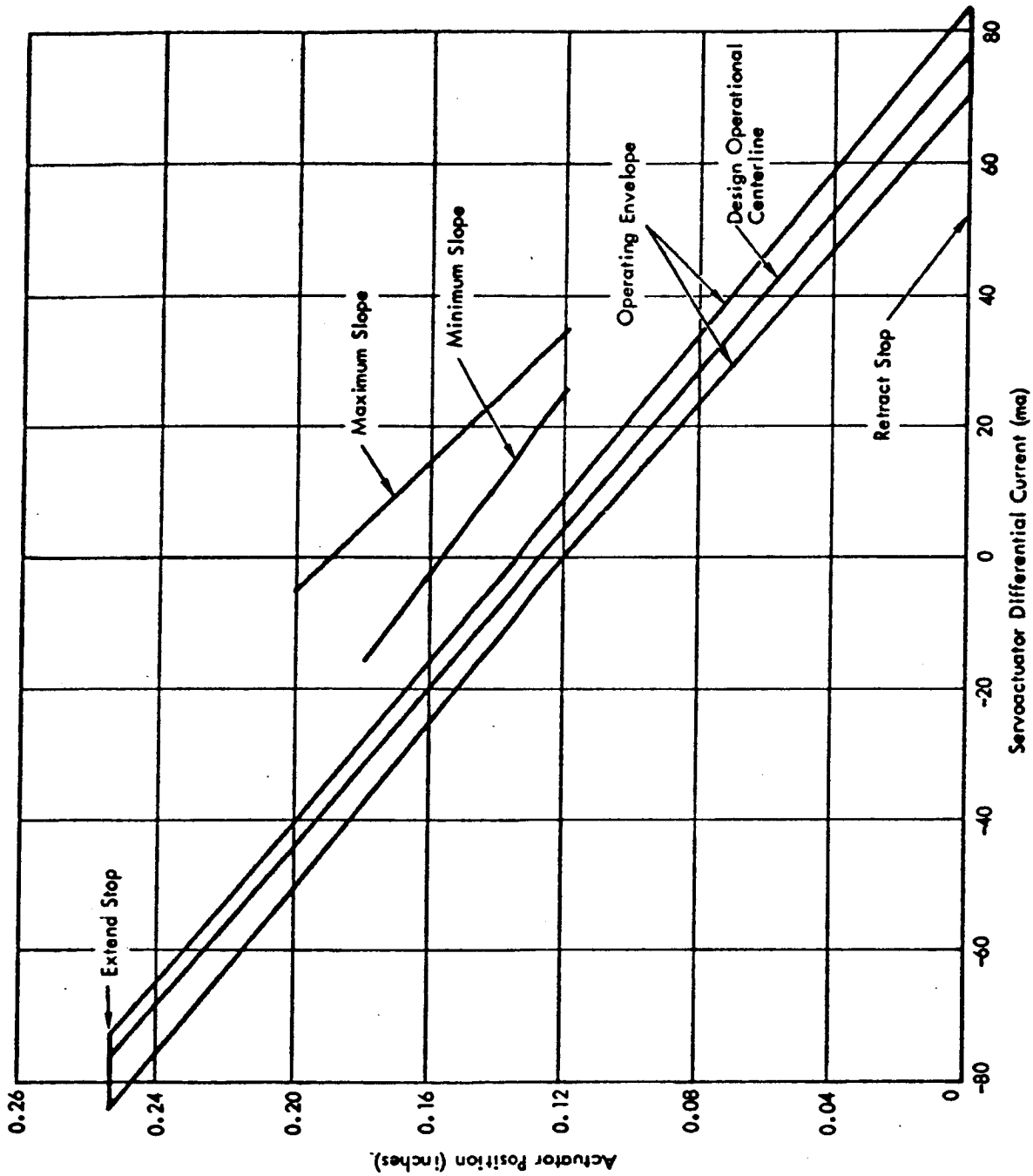

Figure 3.2.6-7. Phase II Follow-on Servoactuator Linearity Requirements

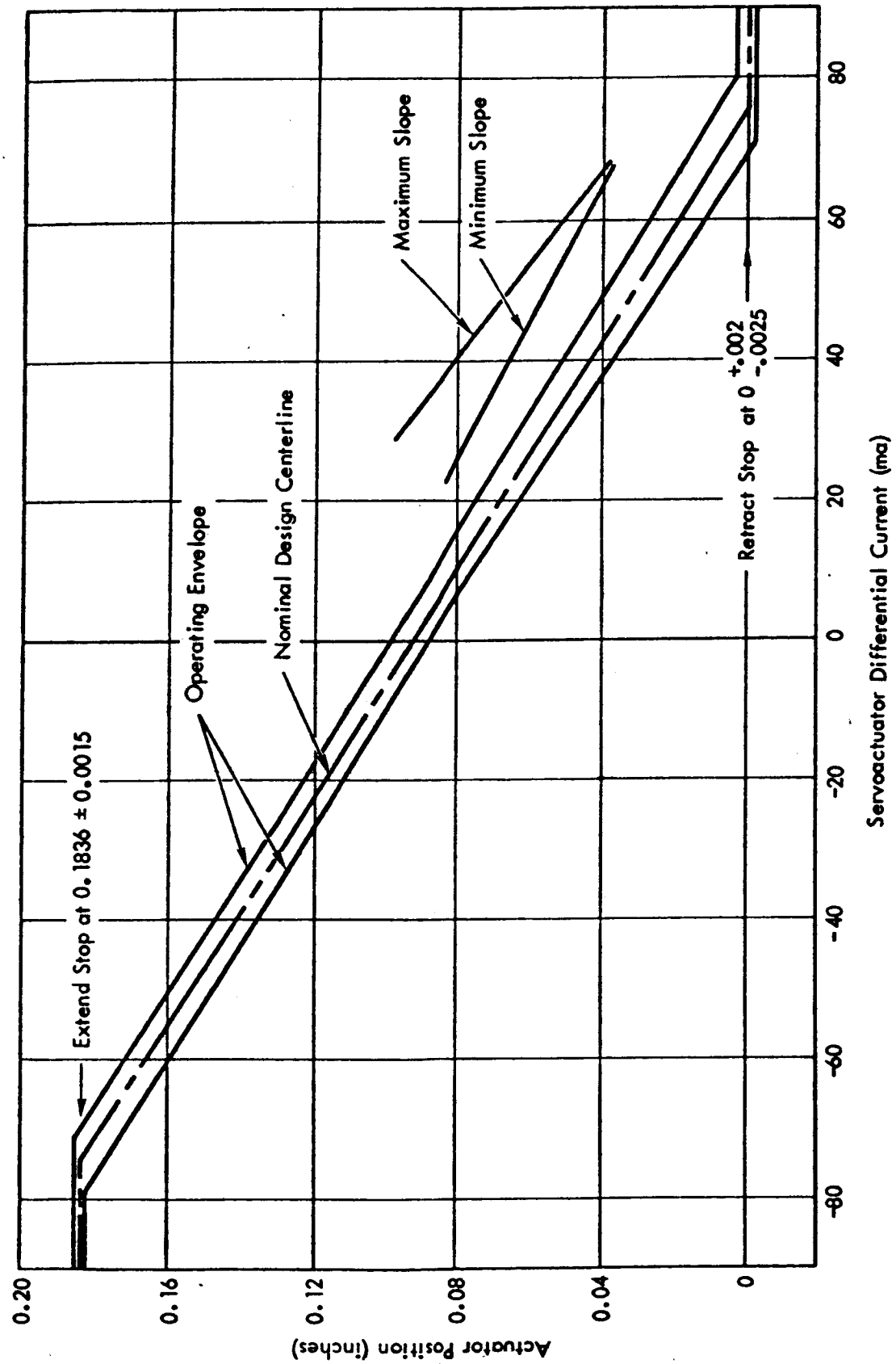

Figure 3.2.6-8. Phase III Servoactuator Linearity Requirements

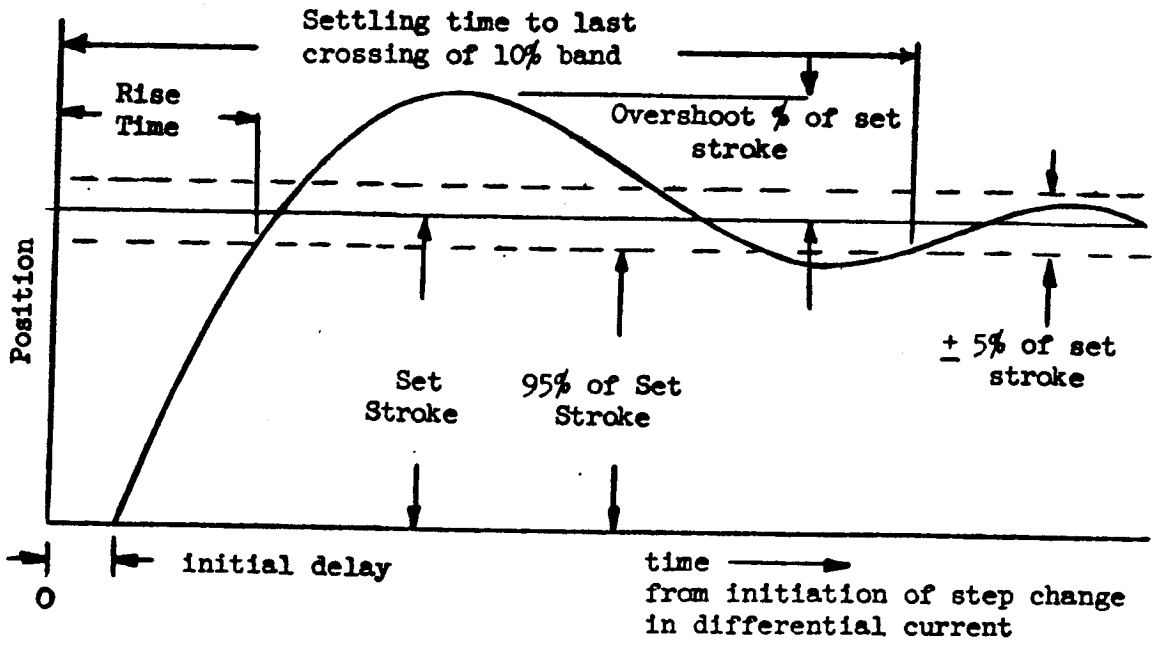

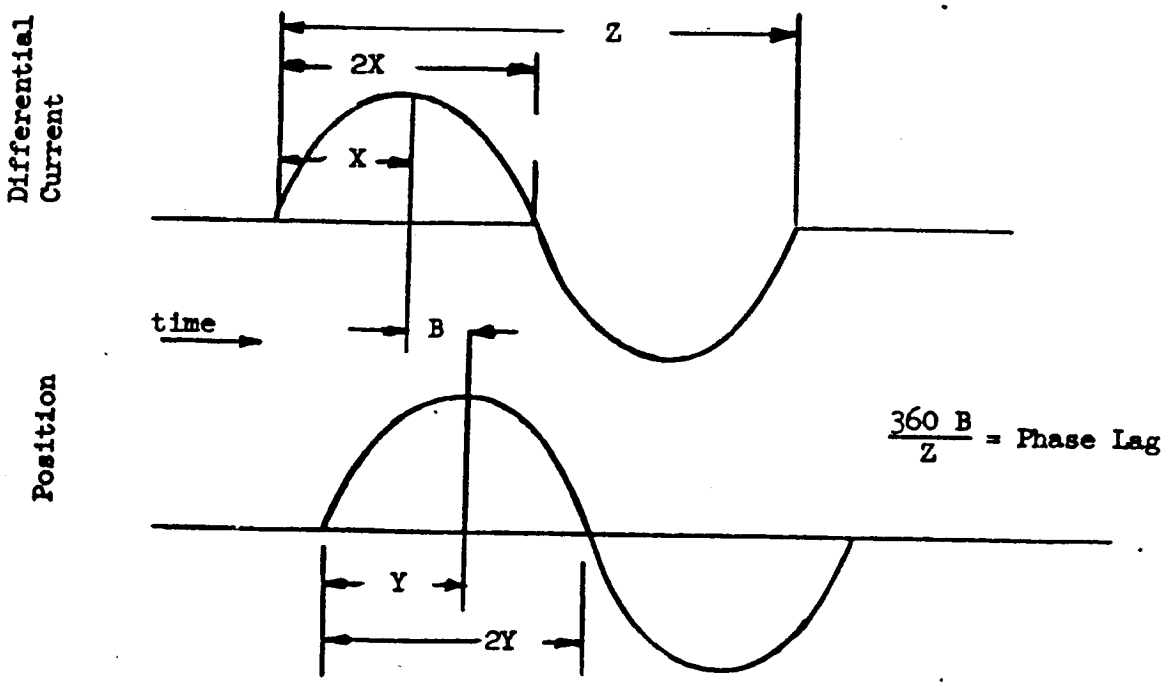

Figure 3.2.6-9. Servoactuator Step Response Definitions

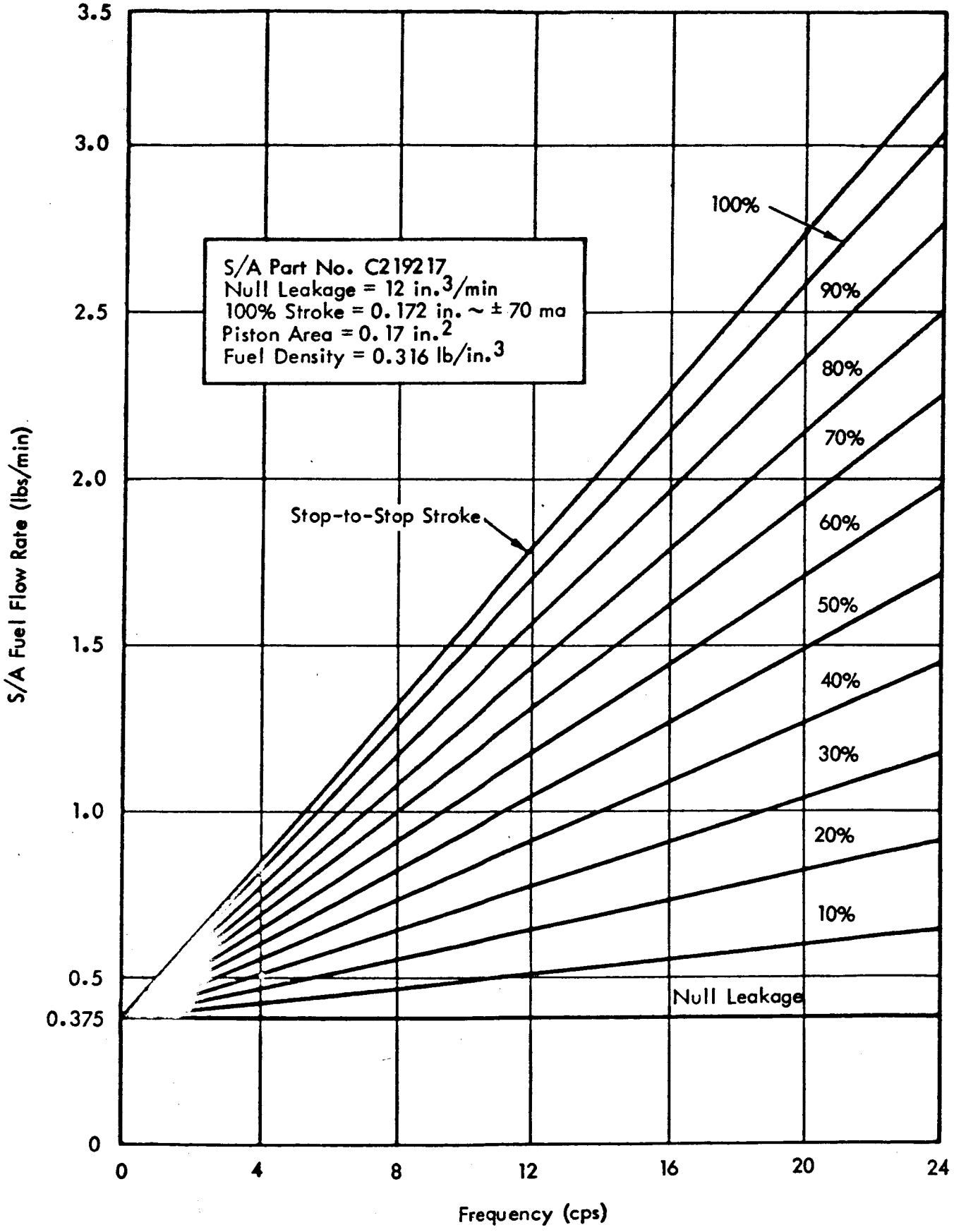

Figure 3.2.6-10. Phase III Servoactuator Fuel Flow Rates

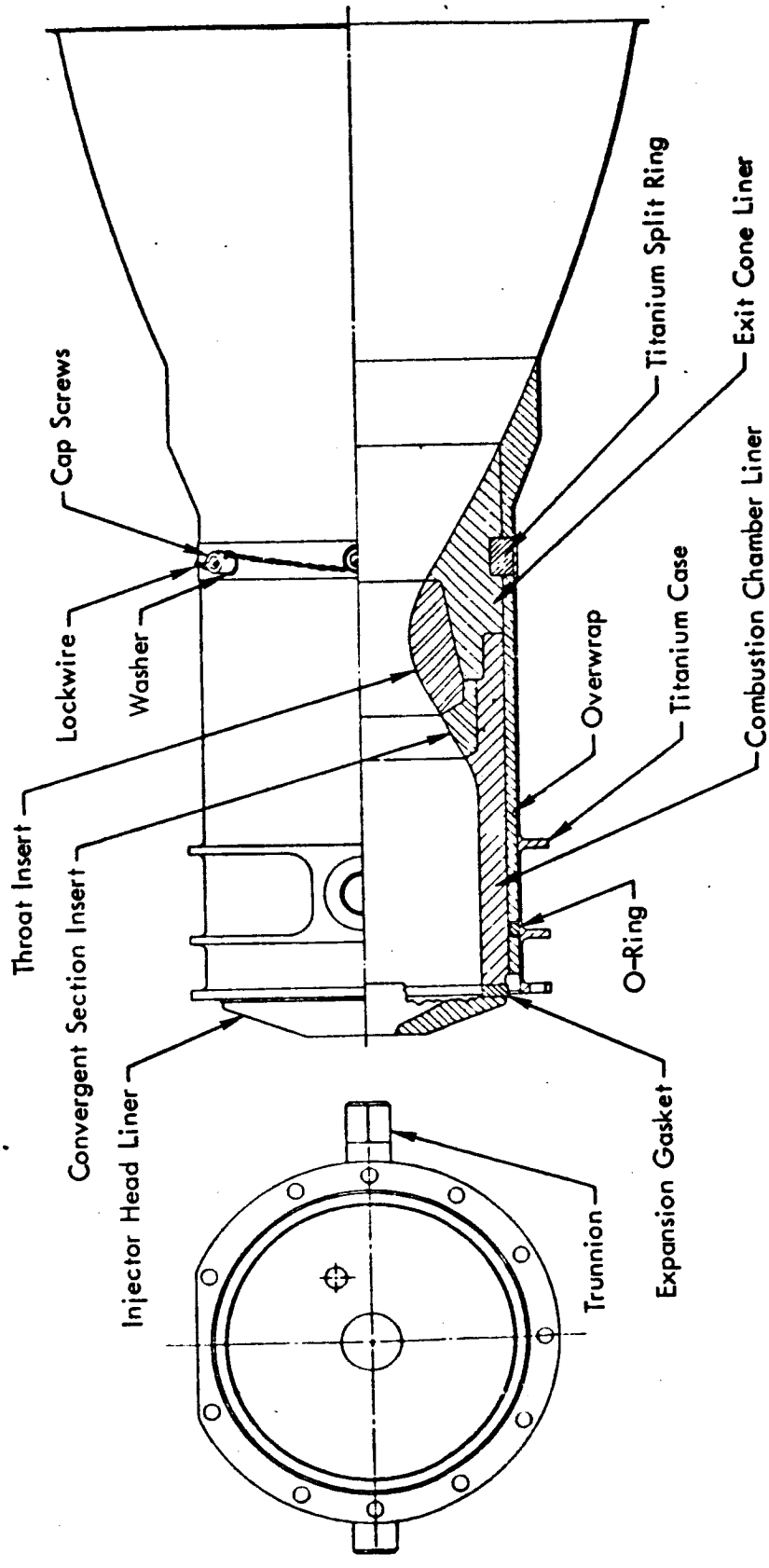

Figure 3.2.7-1. MIRA 150A Combustion Chamber

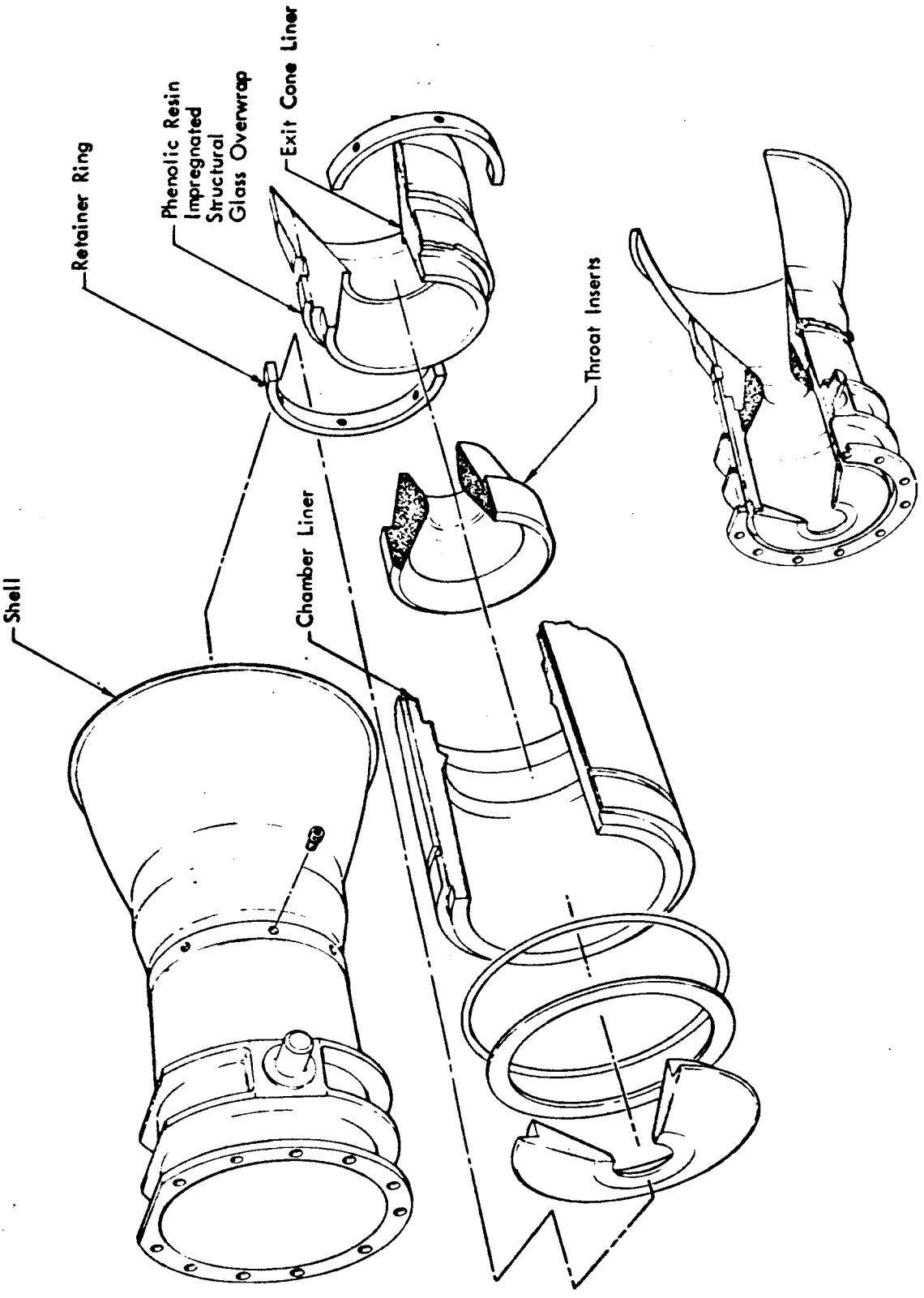

Figure 3.2.7-2. MIRA 150A Combustion Chamber and Nozzle Assembly (Exploded View)

The nozzle throat insert and convergent section insert are machined as detailed parts from JTA graphite billets. JTA graphite is chemically composed of 48% carbon, 35% zirconium, 8% boron, and 9% silicon by weight. During the hot press molding process, graphitization is accomplished at approximately 2500°C. Radiographic analysis of a finished billet shows carbon, zirconium diboride, and silicon carbide as the chemical products present. The finished billet has a minimum specific gravity of 3.0 and is radiographically inspected before machining into detailed parts.

A unique feature of JTA is its oxidation resistance at high temperature. This characteristic is provided by a surface coating of oxides (e.g. $Si\ O_2$) that forms during the high temperature use and which wets and coheres to the basic JTA substrate. Thus, the characteristic is a function of the use temperature and of the shear forces and boundary layer conditions which could strip the molten surface coating away.

The metal case is machined to its final configuration from solid bar stock material composed of 90% titanium - 6% aluminum - 4% vanadium by weight (Ti-6Al-4V) alloy. The metal case retains the ablative liner assembly, provides trunnions for mounting to the spacecraft, and is the unlined aft portion of the nozzle divergent section from an area ratio of 13.5 to 32.8.

Upon completion of the machining of the detailed parts, the nozzle insert and convergent section insert are bonded into the combustion chamber liner and exit cone liner using a high temperature adhesive. The ablative liner assembly is then overwrapped with a silica-phenolic broadgoods cloth. The uncured silica-phenolic material used for this operation is composed of 29 to 33% resin solids and 3 to 7% volatiles by weight. The remaining material is 98%, or better, pure silica reinforcement material. Following the overwrap process, the part is pressure cured at a minimum pressure of 200 psig for 6 hours at 310°F followed by a post-cure cycle of 24 hours at 310°F in an air circulating oven. The resulting cured overwrap material has a minimum specific gravity of 1.70, an average minimum Barcol hardness of 70, and less than 0.5 percent uncured material by weight. Following the post-cure cycle, the ablative liner assembly is radiographically inspected to assure conformance with specified requirements.

The completed ablative liner assembly after machining to final configuration is assembled to the remaining portions of the CC & NA (see Figure 3.2.7-2). The CC & NA is pressure checked as a component at 110 ± 5 psig in accordance with Engineering Test Directive ETD MIRA-2F-001 before it is installed on an HEA injector.

The CC & NA has the following nominal physical characteristics:

Overall Length: 10.090 inches

Largest Diameter: 6.000 inches

Internal Diameter: 2.350 inches

Throat Diameter: 1.000 inch

Exit Diameter: 5.275 inches

Contraction Ratio: 5.5

Ablative/Radiation Skirt Interface Area Ratio: 13.5

Characteristic Length: 17 inches

Weight: 2.6 lbs

The CC & NA has the following operational characteristics:

1. Throat erosion is zero and case temperatures will not exceed 2000°F during or following operation under operating conditions of 100,000 feet altitude vacuum environment, 1.6 mixture ratio, 100°F propellant temperatures, maximum thrust of 150 pounds for a total of 300 seconds consisting of three starts with a maximum single firing of 180 seconds.

2. The total weight loss of the CC & NA as a result of an accumulated 300-second firing under the operating conditions described above will not exceed 7.8 percent of the pre-fired weight.

Additional information on the CC & NA development is given in paragraphs 3.4.9, 3.4.10, and 6.4.

3.3 TCA/Spacecraft Interfaces

The paragraphs herein define the mechanical, electrical, pneumatic/hydraulic, and thermal control interfaces. Drawing No. 107062 or Figure 3.1.2-1 may be used as a reference for the dimensional relationships of the various interfaces.

3.3.1 Mechanical

TCA mounting provisions conform in general to Hughes Aircraft Company (HAC) Drawing No. 276594, Rev. A, dated 20 April 1964. The TCA is designed to be mounted on the spacecraft using trunnions which are an integral part of the TCA combustion chamber and nozzle assembly. The mounting trunnions are normal to the TCA thrust axis and their centerline passes through the TCA center of gravity.

During attachment of the TCA to the spacecraft, nozzle centerline alignment may be achieved by using a special alignment tool, P/N XT106429, designed for this purpose. Installation procedure and use of the alignment tool is described in STL Document No. 9730.4-64-54, Informal Operating and Maintenance Instructions, revised 14 September 1964.

3.3.2 Electrical

The TCA contains two items which must be electrically connected to the spacecraft; the helium pilot valve and the electrohydraulic servoactuator. The electrical interfaces conform in general to HAC Drawing No. 276594, Revision A, dated 20 April 1964. Electrical power for these items is required only during operation of the TCA.

3.3.2.1 Helium Pilot Valve

The helium pilot valve is a DC solenoid-operated device. It is electrically connected to the spacecraft by two wires, each fitted with a wristlock disconnect connector, Thomas and Betts P/N B-14D. The pilot valve is not polarity sensitive and thus, either wire may be grounded. The mating spacecraft connector is also a Thomas and Betts P/N B-14D.

Maximum input power is 15 watts and the minimum pilot valve coil resistance is 45 ohms. Input voltage requirements are as follows:

Minimum Actuation Voltage:	16 VDC for one second (pull-in) followed by 13 VDC continuously (holding)
Maximum Actuation Voltage:	23 VDC
Maximum Applied Voltage:	26 VDC for 5 minutes

3.3.2.2 Electrohydraulic Servoactuator

The servoactuator (S/A) is a dry-coil torque motor device. It is electrically connected to the spacecraft through an electrical receptacle (Bendix P/N PTO 2H-8-4P) located on the servoactuator. Polarity of the electrical connection is important. The mating spacecraft connector is a MS 3116 and must be wired in accordance with the following schematic:

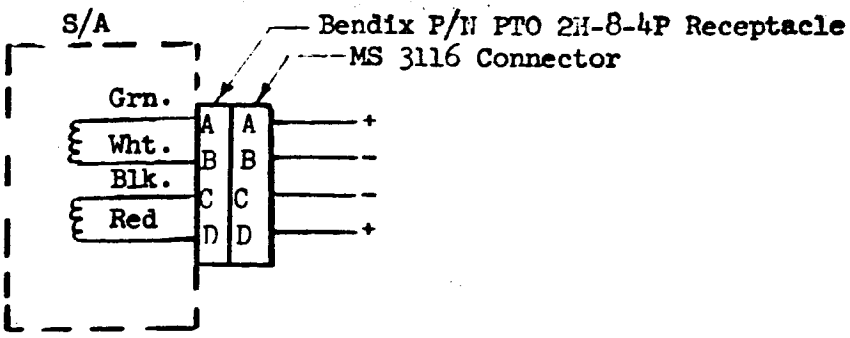

Current Input	S/A Output Shaft Position
AB = CD	Mid-position (Mid Thrust)
AB > CD	Extends (Min Thrust)
CD > AB	Retracts (Max Thrust)

Pertinent servoactuator electrical interface values are as follows:

Differential Signal Current:	± 70 ma (Normal)
	± 120 ma (Overload Capability)
Quiescent Current:	45 ± 2.1 ma/coil
Coil Impedance (maximum):	625 ohms/coil at 400 cps 400 ohms/coil DC
Dither Differential Signal Current:	5 ma peak-to-peak at 400 cps

3.3.3 Pneumatic/Hydraulic

The TCA is designed to operate from a pressure regulated feed system of pilot gas and propellants. The TCA is also equipped with fittings/ports for servoactuator fluid outlet, pressure instrumentation, and connection to ground supply propellants. The following paragraphs define each of the pneumatic/hydraulic interfaces.

3.3.3.1 Pilot Gas

Helium pilot gas is supplied to the TCA by connection to the MS 33656E3 inlet fitting on the helium pilot valve. The pressure at the interface is 720 ± 20 psia during operation of the TCA. The maximum static system pressure is 850 psia. Pilot gas temperature range is 0°F to 100°F. Flow requirements are small; each actuation of the pilot valve uses approximately 0.3 in^3 of pilot gas. A 3/16-inch nominal diameter supply line is adequate.

3.3.3.2 Propellants

The propellants consist of the fuel, monomethylhydrazine (MMH) per MIL-P-27404, and the oxidizer, which is a mixture of 90% by weight of nitrogen tetroxide (N_2O_4) per MIL-P-26539A and 10% by weight of nitric oxide (NO). Propellants are supplied to the TCA by connection to the two MS 33656-4 fittings on the flow control valve body. The fuel inlet fitting is parallel to the centerline of the TCA mounting trunnions, and the oxidizer inlet fitting is normal to the centerline of the trunnions. The propellant pressure at the inlet fittings is 720 ± 20 psia during TCA operation. The maximum static system pressure is 850 psia. Propellant temperature range is 0°F to 100°F. Propellant flow at maximum thrust are:

Fuel: .21 lb/sec

Oxidizer: .31 lb/sec

(For I_{sp} of 291 sec, MR = 1.5)

Refer to paragraph 3.5 for additional propellant details.

3.3.3.3 Servoactuator Outlet

The servoactuator (S/A) working fluid is fuel (MMH). This fluid is supplied to the S/A inlet port by a feed line connected to a fitting on the flow control valve body, upstream of the propellant shutoff valves. The S/A fuel feed line is an integral part of the TCA, and therefore, whenever fuel is supplied to the TCA, the S/A is pressurized. The S/A outlet port must be connected to a normally closed dump valve in order to avoid fuel loss due to null leakage. To activate the S/A, the dump valve must be opened to route the S/A outlet fluid overboard or to a collection tank. The outlet connection on the S/A is MS 24299C3. The outlet valve used should not impose a pressure drop in excess of 20 psi with a fuel flow of 0.0493 lb/sec. The S/A outlet dump valve was not developed during Phase II, since this valve was considered a spacecraft propulsion system component.

3.3.3.4 Pressure Instrumentation Connections

All TCAs have a port for instrumenting combustion chamber pressure. This port conforms to AND 10050-2 and must be either plugged or connected to pressure instrumentation.

TCAs 106570-4 and -5 have provisions for instrumenting fuel and oxidizer injection pressures. These instrumentation bosses conform to MS33656-G3 and must be either capped or connected to pressure instrumentation.

3.3.3.5 Ground Supply Connection

The flight TCAs have provisions for connection to ground supply propellants or purge equipment. A ground supply boss is located on each shutoff valve. These ground supply bosses are ported to the upstream side of the fuel and oxidizer SOVs and must be either plugged or fitted with the quick disconnect fittings listed below.

Fuel Quick Disconnect: HAC P/N 254060 (or equivalent)

Oxidizer Quick Disconnect: HAC P/N 254073 (or equivalent)

3.3.4 Thermal Control

Considerable thermal interface analysis and materials testing was performed during Phase III; however, the thermal design was not finalized because spacecraft thermal interface requirements were not provided. Thus, the TCA in its present form does not include surface finishes compatible with the Surveyor spacecraft passive thermal control requirements.

In accordance with paragraph 3.4.5 of JPL Specification SAM-50255-DSN-C, the temperature of the inactive TCA will be controlled during flight within the temperature range of $0^{\circ}F$ to $125^{\circ}F$. In compliance with this requirement, several meetings between STL and HAC were held to discuss TCA thermal control design requirements, surface processing methods, coating patterns, etc. In early STL/HAC thermal interface discussions, the TCA passive temperature control was conceptually configured as an overall coating of vacuum deposited aluminum (VDA) with 3 to 10 in^2 of black on some of the forward facing surfaces of the TCA. Subsequently, gold plating was suggested by STL as being superior to VDA, since gold is more resistant to atmospheric conditions, more easily cleaned, and is operable at higher temperature because no organic subcoating is used. In addition, a "Cap" to enclose the HEA was proposed and analyzed. Ultimately it was decided to pursue the STL design approach utilizing the HEA cap to passively control the temperature of the TCA while leaving all exposed surfaces below the HEA-to-CC & NA split line to be gold finished to provide low values of absorptance and emittance.

An analysis of the MIRA 150A using a cap for thermal control is presented in Appendix B. Recommendations resulting from this analysis were as follows:

1. A cap should be used over the HEA for thermal control.

2. The cap should be aluminum with a liquid bright gold finish.

3. The external surface of the CC & NA should have a gold finish.

The thermal properties of various sample surfaces representative of the TCA surfaces were determined. These included various gold finishes and several titanium surfaces representative of the uncoated case and nozzle before and after firing. Details of this analysis are presented in Appendix C.

3.4 TCA Performance

The MIRA 150A TCA steady-state and transient performance characteristics presented herein are based on static test data provided by the Phase III prequalification testing. The supporting data for this information may be found in Section 6.0.

3.4.1 Specific Impulse

Table 3.4.1-1 provides nominal and 3-sigma deviation estimates of specific impulse at three different thrust levels. The requirements of JPL Specification SAM-50255-DSN-C are provided for comparison. Figure 3.4.1-2 shows vacuum specific impulse as a function of vacuum thrust and operating mixture ratio. Further details may be found in paragraph 6.8.5.

Table 3.4.1-1

MIRA 150A Specific Impulse Variability at Standard Inlet Conditions*

	I_{sp} (seconds)			
	Measured Values		SAM-50255-DSN-C	
	Nominal	± 3-Sigma Deviation	Nominal	± 3-Sigma Limit
Minimum Thrust (30 lbs)	258.7	12.5	260	7
Midrange Thrust (90 lbs)	287.6	5.2	290	5
Maximum Thrust (150 lbs)	291.3	3.3	290	5

*NOTE: Standard inlet conditions are defined as 720 psia TCA propellant inlet pressure and 70°F propellant inlet temperature.

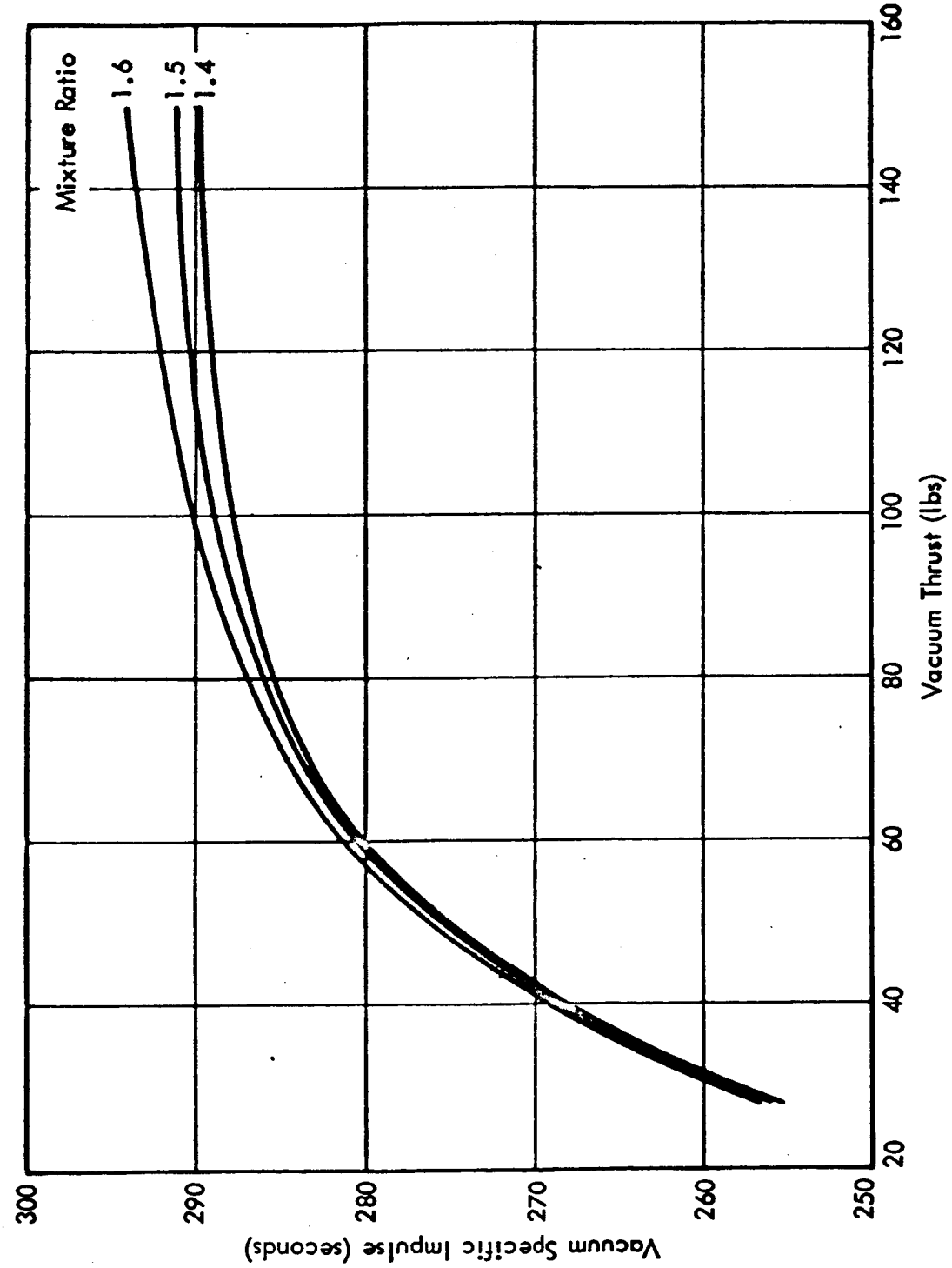

Figure 3.4.1-2. MIRA 150A Vacuum Specific Impulse Versus Vacuum Thrust and Mixture Ratio

3.4.2 Characteristic Exhaust Velocity

Table 3.4.2-1 provides nominal and 3-sigma deviation estimates of characteristic exhaust velocity at three thrust levels. Figure 3.4.2-2 shows characteristic exhaust velocity versus nozzle stagnation pressure and mixture ratio. Further details may be found in paragraph 6.8.5.

Table 3.4.2-1

MIRA 150A Characteristic Velocity Variability
at Standard Inlet Conditions

	C* Measured Values (fps)	
	Nominal	± 3-Sigma Deviation
Minimum Thrust (30 lbs)	4826	180
Midrange Thrust (90 lbs)	5286	99
Maximum Thrust (150 lbs)	5328	101

3.4.3 Thrust Coefficient

Table 3.4.3-1 provides nominal and 3-sigma deviation estimates for thrust coefficient at standard inlet conditions. Figure 3.4.3-2 shows vacuum thrust coefficient versus nozzle stagnation pressure and mixture ratio. Further details may be found in paragraph 6.8.5.

Table 3.4.3-1

MIRA 150A Vacuum Thrust Coefficient Variability
at Standard Inlet Conditions

	C_F Measured Values	
	Nominal	± 3-Sigma Deviation
Minimum Thrust (30 lbs)	1.711	0.074
Midrange Thrust (90 lbs)	1.752	0.035
Maximum Thrust (150 lbs)	1.763	0.042

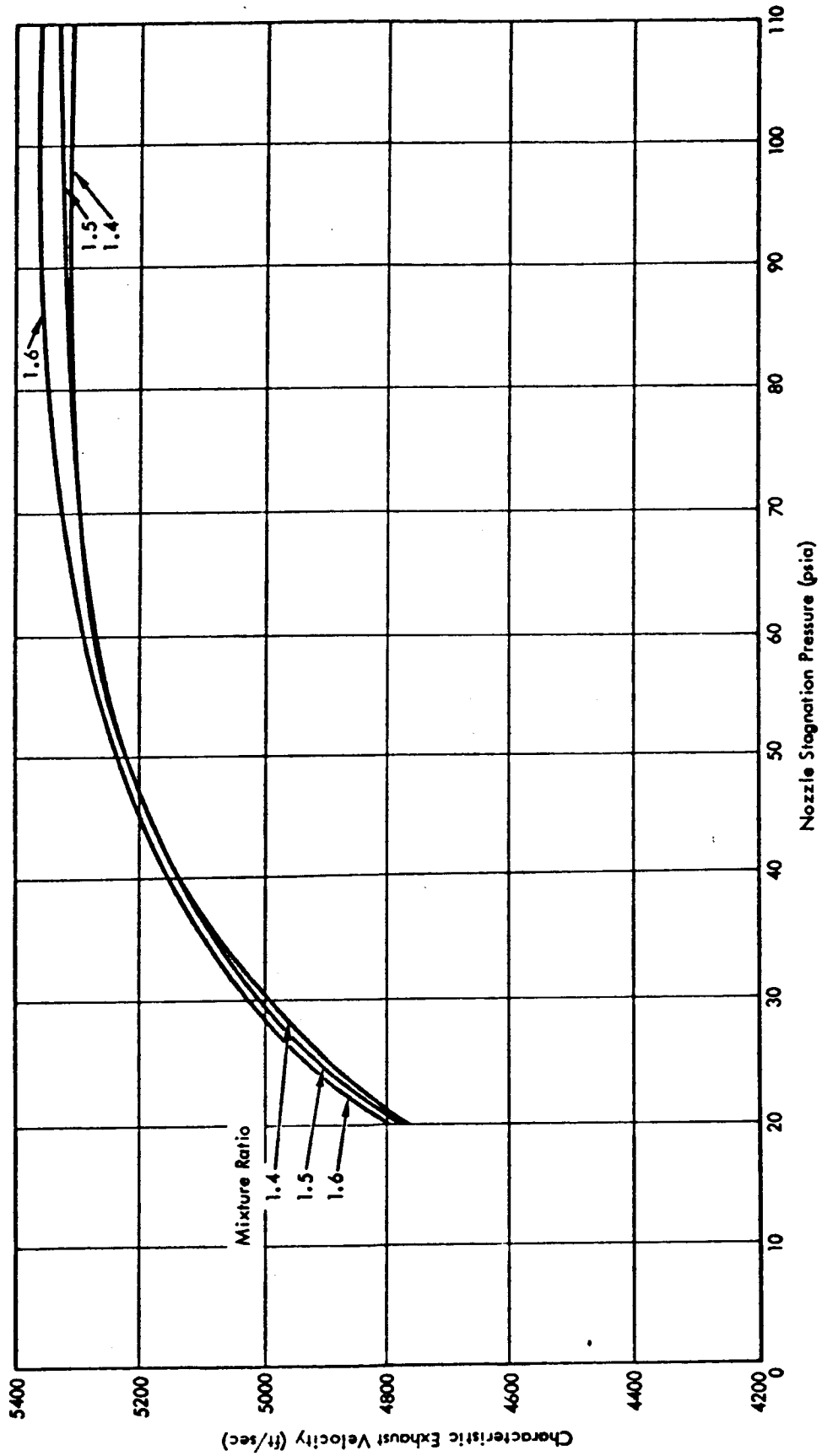

Figure 3.4.2-2. MIRA 150A Characteristic Exhaust Velocity Versus Nozzle Stagnation Pressure and Mixture Ratio

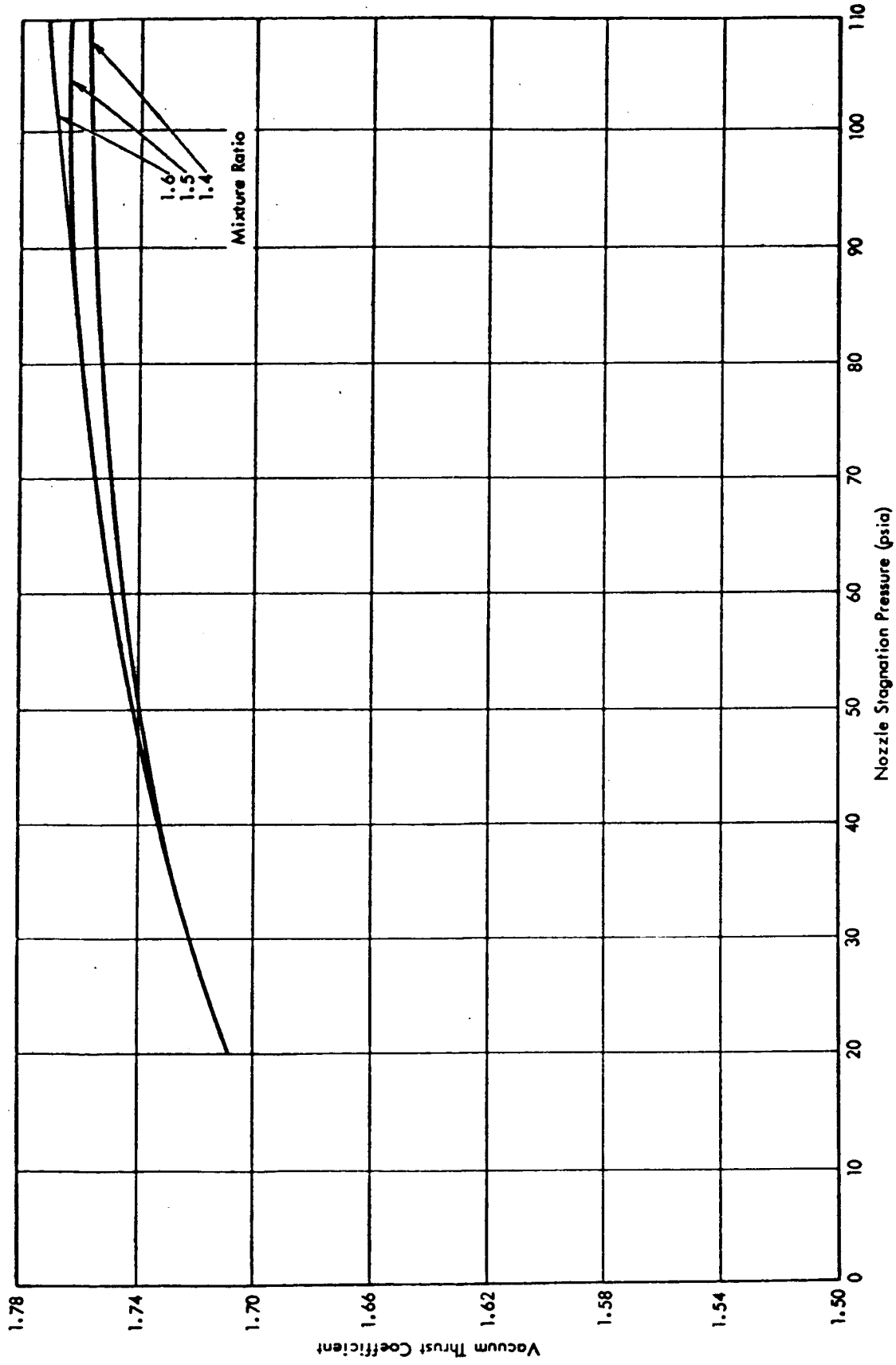

Figure 3.4.3-2. MIRA 150A Vacuum Thrust Coefficient Versus Nozzle Stagnation Pressure & Mixture Ratio

3.4.4 Mixture Ratio

The nominal and allowable limits of mixture ratio at standard inlet conditions are 1.50 + 0.03 for any thrust level. These values are the acceptance test limits, and any TCA found outside this range during acceptance testing will be recalibrated and readjusted as needed to meet these limits. Further details may be found in paragraph 6.8.4.

Figure 3.4.4-1 provides propellant temperature effects over the 0°F to 100°F specification range. The information presented in Figure 3.4.4-1 is based on a perfectly adjusted nominal mixture ratio at standard inlet conditions of 1.50. Any deviation because of the "imperfectness" of the HEA (e.g., the allowable of + 0.03) would be added to that shown. Further details may be found in paragraphs 6.5.1 and 6.5.2.

3.4.5 Chamber Pressure

Table 3.4.5-1 provides nominal and 3-sigma deviation estimates of chamber pressure at three thrust levels. Figure 3.4.6-5 may be used to determine nominal chamber pressure as a function of vacuum thrust. Further details may be found in paragraphs 6.8.5 and 6.8.7.

Table 3.4.5-1

MIRA 150A Head End Chamber Pressure Variability
at Standard Inlet Conditions

Vacuum Thrust (lbs)	P_c Measured Values (psia)	
	Nominal	± 3-Sigma Deviation
30	22.4	1.3
90	65.2	1.1
150	108.2	2.4

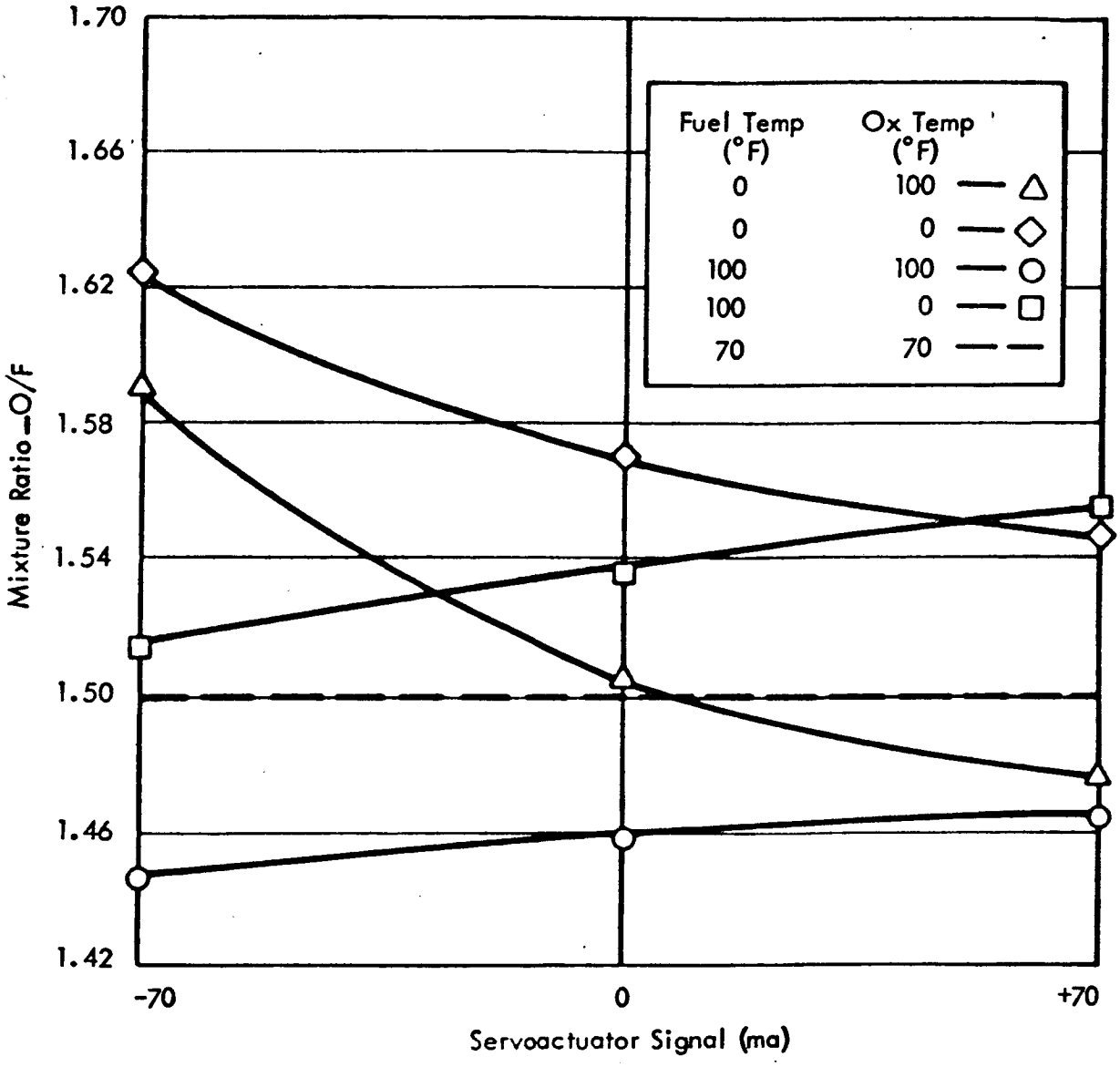

Figure 3.4.4-1. MIRA 150A Mixture Ratio Versus Propellant Temperature for Various S/A Signals

3.4.6 Thrust

Table 3.4.6-1 presents nominal and 3-sigma deviation estimates of thrust at five different servoactuator signal levels under standard inlet conditions. Figure 3.4.6-2 shows the nominal thrust versus signal curve with the SAM-50255-DSN-C limits superimposed. Figure 3.4.6-3 provides the influence of TCA inlet pressure on thrust. Figure 3.4.6-4 shows the effect of inlet temperature variations on thrust over the specification range of $0^{\circ}F$ to $100^{\circ}F$. Figure 3.4.6-5 is a plot of vacuum thrust versus head-end chamber pressure.

Further details may be found in paragraphs 6.5.3, 6.8.6, and 6.8.7.

Table 3.4.6-1

MIRA 150A Vacuum Thrust Variation
at Standard Inlet Conditions

Signal Level (ma)	Measured Values: Nominal Thrust (lbs)	Measured Values: ± 3-Sigma Deviation (lbs)
-80	26.4	6.2
-70	29.0	8.6
0	95.5	4.2
+70	154.6	2.9
+80	160.8	3.0

3.4.7 Startup and Shutdown Transients

The TCA startup and shutdown transient data provided herein is based on altitude firings at the JPL/ETS facility and sea level firings at the IRTS. Sea level and altitude transients summaries are presented separately.

3.4.7.1 Sea Level Startup and Shutdown Transients

Table 3.4.7-1 presents estimates of nominal and 3-sigma deviation for startup times; and Table 3.4.7-2 presents startup impulse estimates at different startup thrust levels for sea level firings. Specification SAM-50255-DSN-C specifies a maximum startup time of 0.130 seconds.

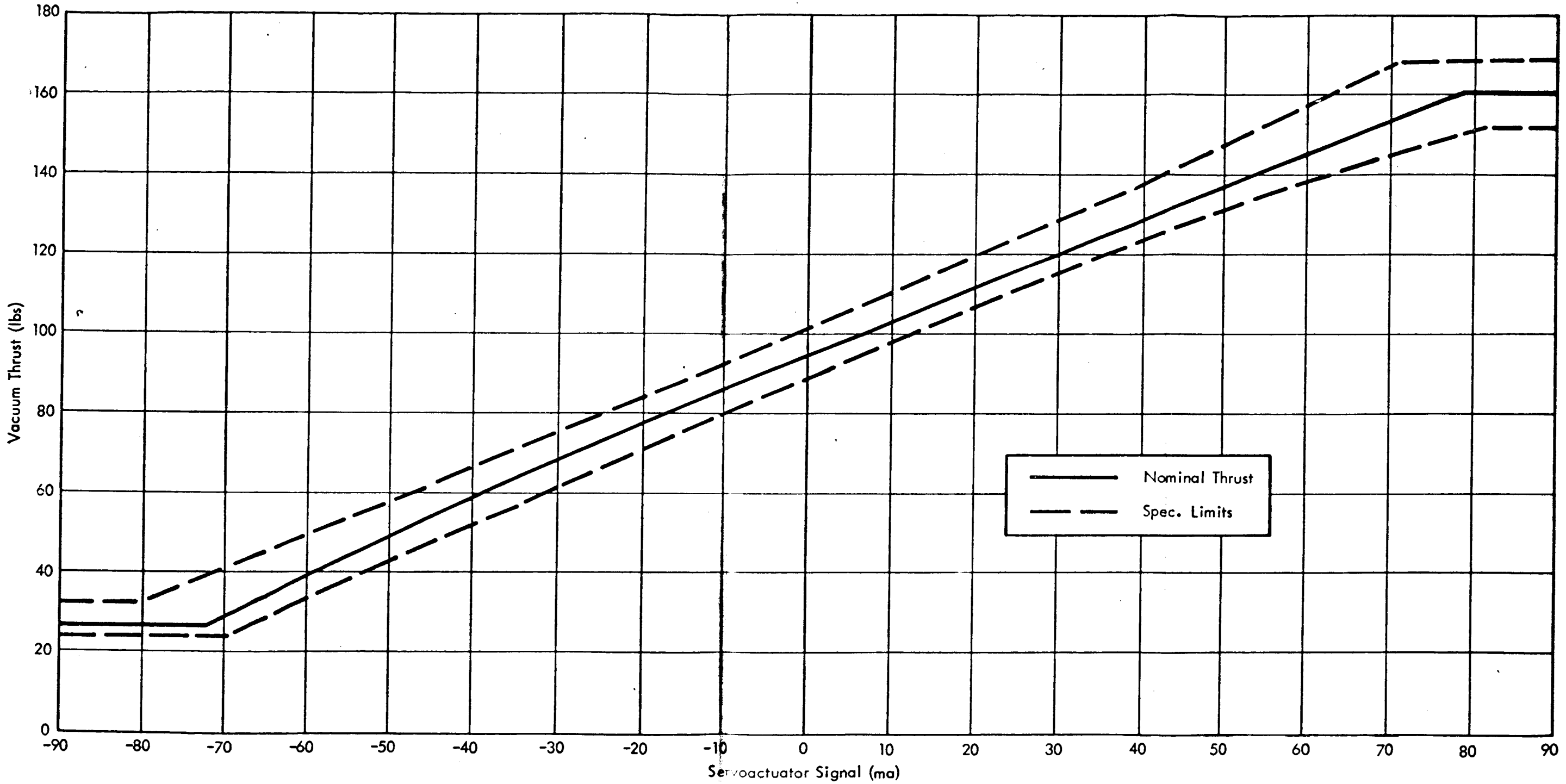

Figure 3.4.6-2. MIRA [illegible]OA Vacuum Thrust (At Standard Conditions) Versus Servoactuator Signal

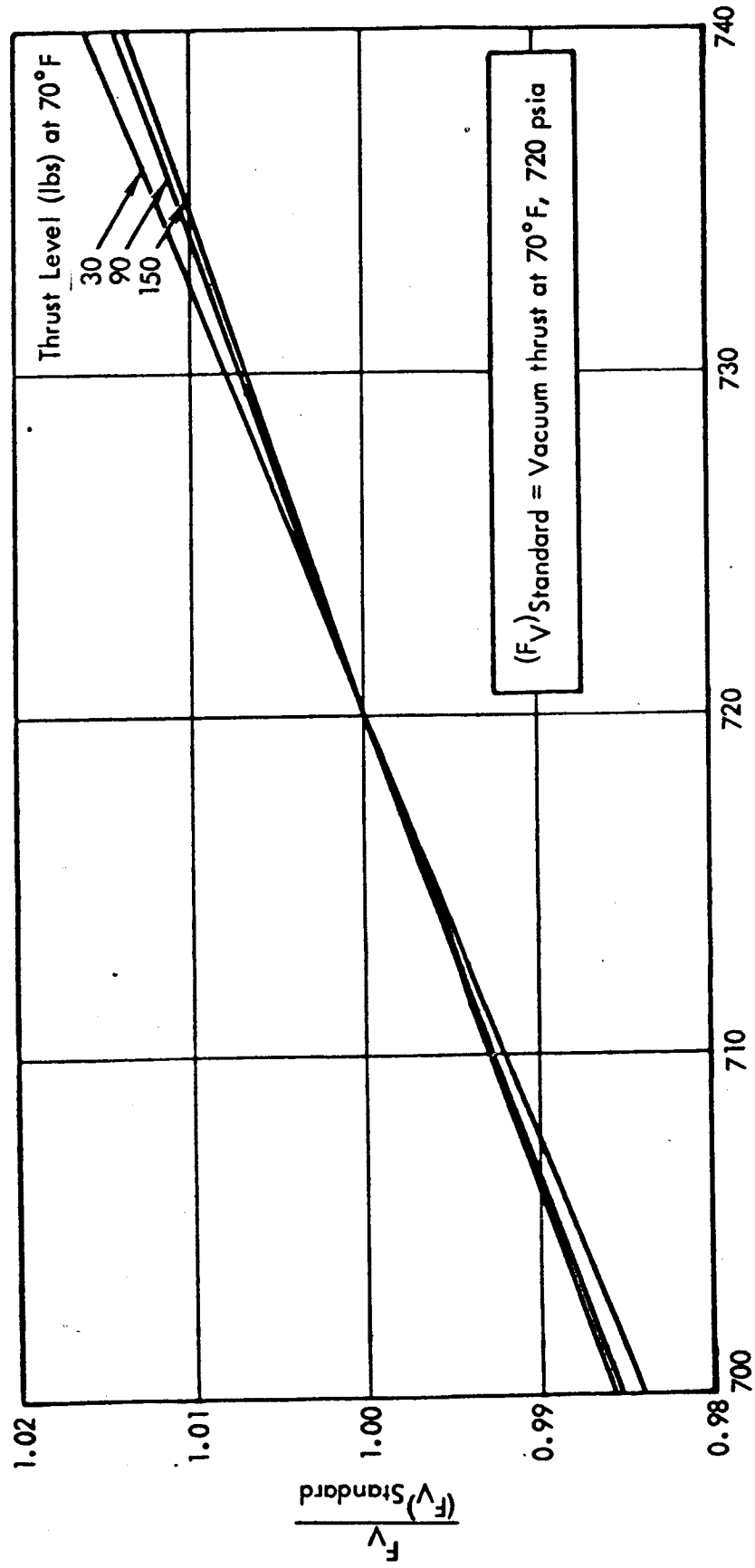

Figure 3.4.6-3. MIRA 150A Vacuum Thrust Variations Versus Propellant Inlet Pressure

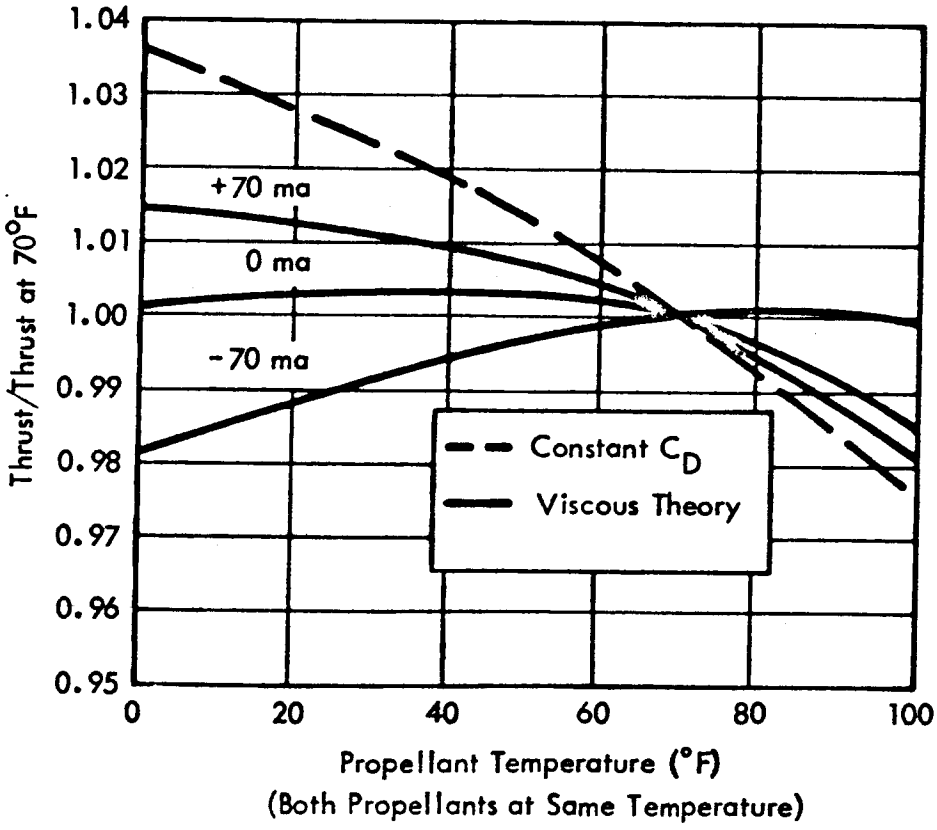

Figure 3.4.6-4. MIRA 150A Vacuum Thrust Variation Versus Propellant Inlet Temperatures (For Various S/A Signals)

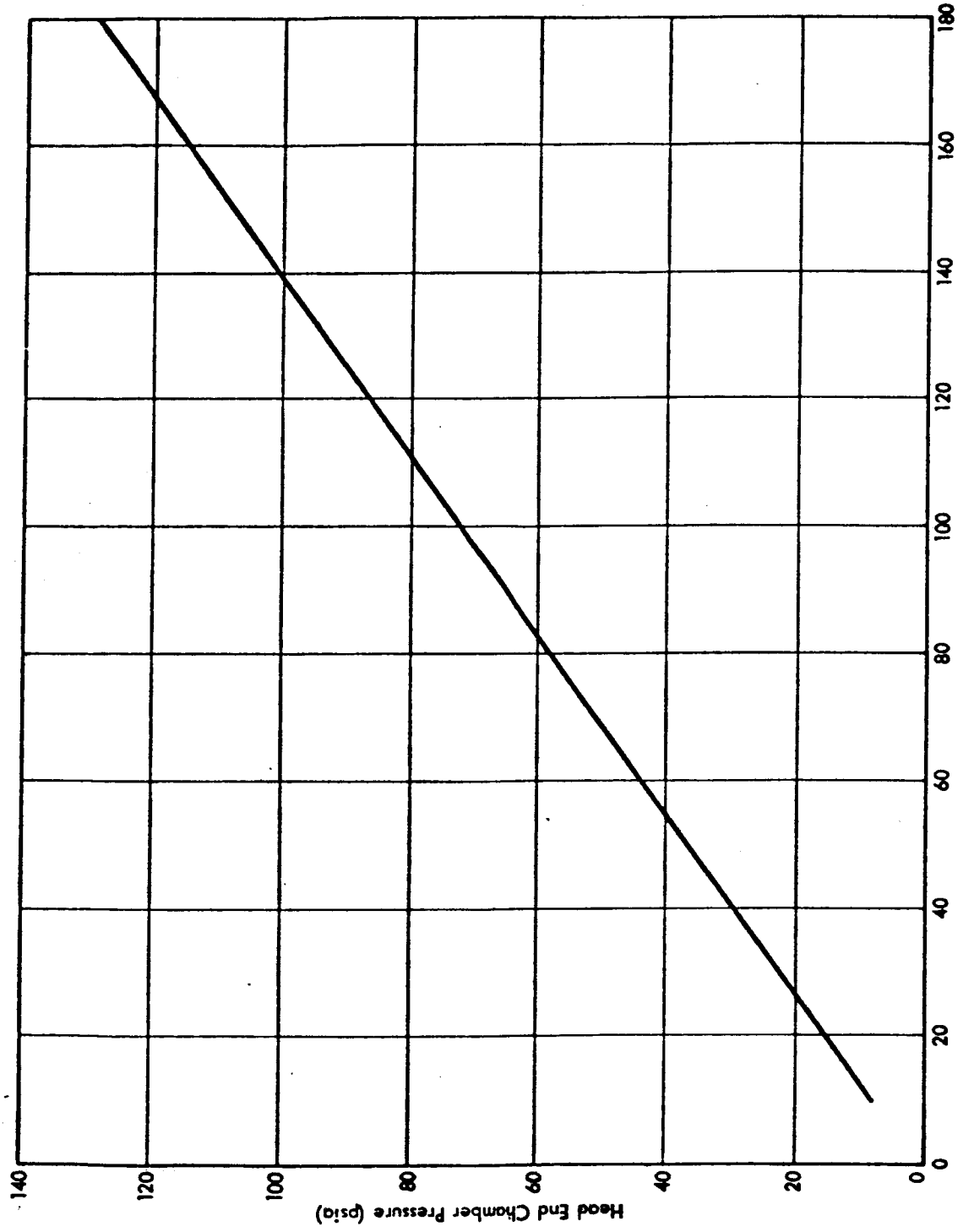

Figure 3.4.6-5. MIRA 150A Vacuum Thrust Versus Head End Chamber Pressure

Table 3.4.7-1

MIRA 150A Sea Level Startup
Time Estimates

	Startup Time Measured Values (seconds)	
	Nominal	± 3-Sigma Deviation
Minimum Thrust (30 lbs)	(1)	(1)
Midrange Thrust (90 lbs)	0.069	± 0.036
Maximum Thrust (150 lbs)	0.026	+ 0.048 - 0.026

NOTE: (1) Sufficient data was not available for a reliable estimate.

Table 3.4.7-2

MIRA 150A Sea Level Startup
Impulse Estimates

	Startup Impulse Measured Values(1) (lb-sec)	
	Nominal	± 3-Sigma Deviation
Minimum Thrust (30 lbs)	(2)	(2)
Midrange Thrust (90 lbs)	1.9	± 1.4
Maximum Thrust (150 lbs)	0.87	± 0.31

NOTES: (1) These estimates are based on chamber pressure integrals converted to vacuum impulse by $I_{vac} = C_{f_{vac}} \cdot A_t \int P_c \, dt$.

(2) Sufficient data was not available for a reliable estimate.

Table 3.4.7-3 presents estimates of shutdown times; Table 3.4.7-4 provides shutdown impulse estimates under sea level conditions. Further details may be found in paragraphs 6.9.2 and 6.9.3.

Table 3.4.7-3

MIRA 150A Sea Level Shutdown
Time Estimates

	Shutdown Time Measured Values (seconds)	
	Nominal	± 3-Sigma Deviation
Minimum Thrust (30 lbs)	(1)	(1)
Midrange Thrust (90 lbs)	0.035	± 0.030
Maximum Thrust (150 lbs)	0.028(2)	± 0.003 (2)

NOTES: (1) Sufficient data was not available for a reliable estimate.

(2) Estimate based on data from only one HEA.

Table 3.4.7-4

MIRA 150A Sea Level Shutdown
Impulse Estimates

	Shutdown Impulse Measured Values (lb-sec)(1)	
	Nominal	± 3-Sigma Deviation
Minimum Thrust (30 lbs)	(2)	(2)
Midrange Thrust (90 lbs)	2.8	± 2.5
Maximum Thrust (150 lbs)	3.9(3)	± 0.3(3)

NOTES: (1) Impulse values based on chamber pressure integrals converted to vacuum impulse.

(2) Sufficient data was not available for a reliable estimate.

(3) Estimates based on data from only one HEA.

3.4.7.2 Vacuum Startup and Shutdown Transients

Table 3.4.7-5 provides estimates of startup times; Table 3.4.7-6 gives startup impulse estimates for vacuum conditions. Tables 3.4.7-7 and 3.4.7-8 provide estimates of shutdown times and shutdown impulse at vacuum. Further details may be found in paragraphs 6.9.1 and 6.9.3.

Table 3.4.7-5

MIRA 150A Altitude Startup
Time Estimates

	Startup Time Measured Values (seconds)	
	Nominal	± 3-Sigma Deviation
Minimum Thrust (30 lbs)	0.275	(1)
Midrange Thrust (90 lbs)	0.104	± 0.013
Maximum Thrust (150 lbs)	0.077	± 0.012

NOTE: (1) Sufficient data was not available for a reliable estimate.

Table 3.4.7-6

MIRA 150A Altitude Startup
Impulse Estimates

	Startup Impulse Measured Values (seconds)	
	Nominal	± 3-Sigma Deviation
Minimum Thrust (30 lbs)	3.4	(1)
Midrange Thrust (90 lbs)	3.1	± 1.2
Maximum Thrust (150 lbs)	3.1	± 2.6

NOTE: (1) Sufficient data was not available for a reliable estimate.

Table 3.4.7-7

MIRA 150A Altitude Shutdown
Time Estimates

	Shutdown Time (seconds)		
	Measured Values		SAM-50255-DSN-C
	Nominal	± 3-Sigma Deviation	Requirement
Minimum Thrust (30 lbs)	0.179	+ 0.280 - 0.179	0.200 max
Midrange Thrust (60-100 lbs)	0.165	± 0.122	0.200 max
Maximum Thrust (150 lbs)	0.123	± 0.056	0.200 max

Table 3.4.7-8

MIRA 150A Altitude Shutdown
Impulse Estimates

	Shutdown Time (lb-sec)		
	Measured Values		SAM-50255-DSN-C
	Nominal	± 3-Sigma Deviation	Requirement
Minimum Thrust (30 lbs)	3.2	± 2.9	None
Midrange Thrust (60-100 lbs)	3.3	± 2.4	± 1.0 (variation)
Maximum Thrust (150 lbs)	5.6	± 1.1	None

3.4.8 Thrust Dynamic Response

This paragraph summarizes the MIRA 150A dynamic throttling characteristics. Table 3.4.8-1 provides step response information. Figures 3.4.8-2 and -3 show typical chamber pressure response characteristics to large step servoactuator position changes. Table 3.4.8-4 summarizes loop width and 5-cps response characteristics. Typical sinusoidal response as a function of frequency is shown in Figure 3.4.8-5. Hysteresis loop characteristics are shown in Figure 3.4.8-6.

Paragraph 6.9 presents additional details on TCA thrust-to-signal dynamic response test firing information. At frequencies below 10 cps, the thrust-to-signal dynamic response is almost totally a function of the servoactuator response. Thus, additional information that deals with dynamic response is available in paragraphs 3.2.6, 5.1.1.2, and 7.3.

Table 3.4.8-1

MIRA 150A Step Response
Characteristics

		Measured Values		SAM-50255-DSN-C
		Nominal	± 3-Sigma Deviation	Requirement
Large Steps(1)				
Rise Time(4)	(seconds)	0.038	0.023	0.065
Overshoot(4)	(%)	0	0(2)	25
Small Steps(3)				
Rise Time(4)	(seconds)	0.014	0.008	0.065
Overshoot(4)	(%)	19	10	25

NOTES:
(1) A large step is defined as step signal inputs from +70 to -80 ma and -70 to +80 ma.
(2) The output spool reaches the mechanical stops preventing any overshoot in response to ±80 ma signals.
(3) A small step is defined as any 35 ma amplitude step signal between -70 and +70 ma.
(4) Rise time and overshoot are defined in Figure 3.2.6-7; for purposes here, the ordinate callout of position in 3.2.6-7 may be assumed to be equivalent to thrust.

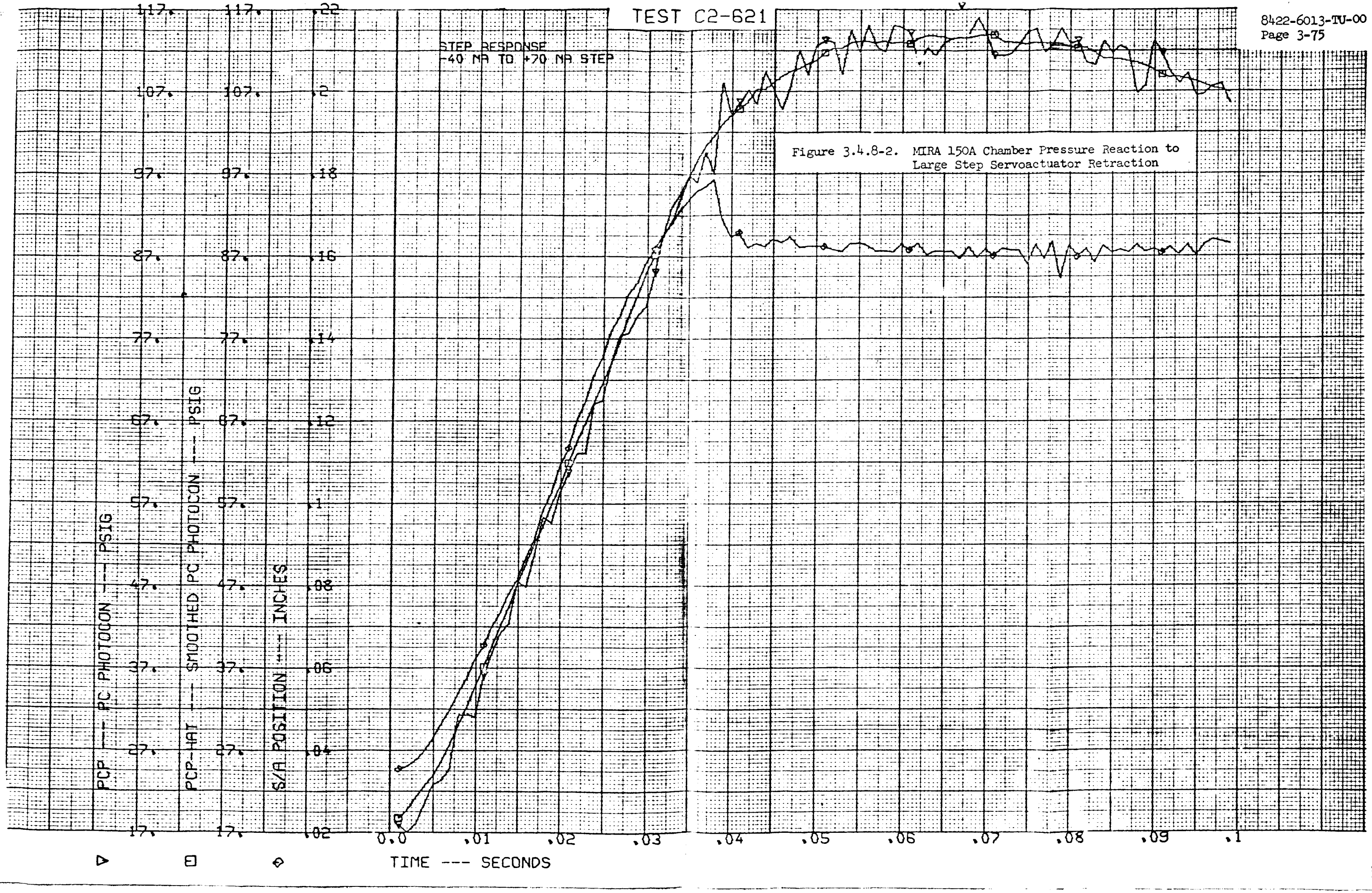

Figure 3.4.8-2. MIRA 150A Chamber Pressure Reaction to Large Step Servoactuator Retraction

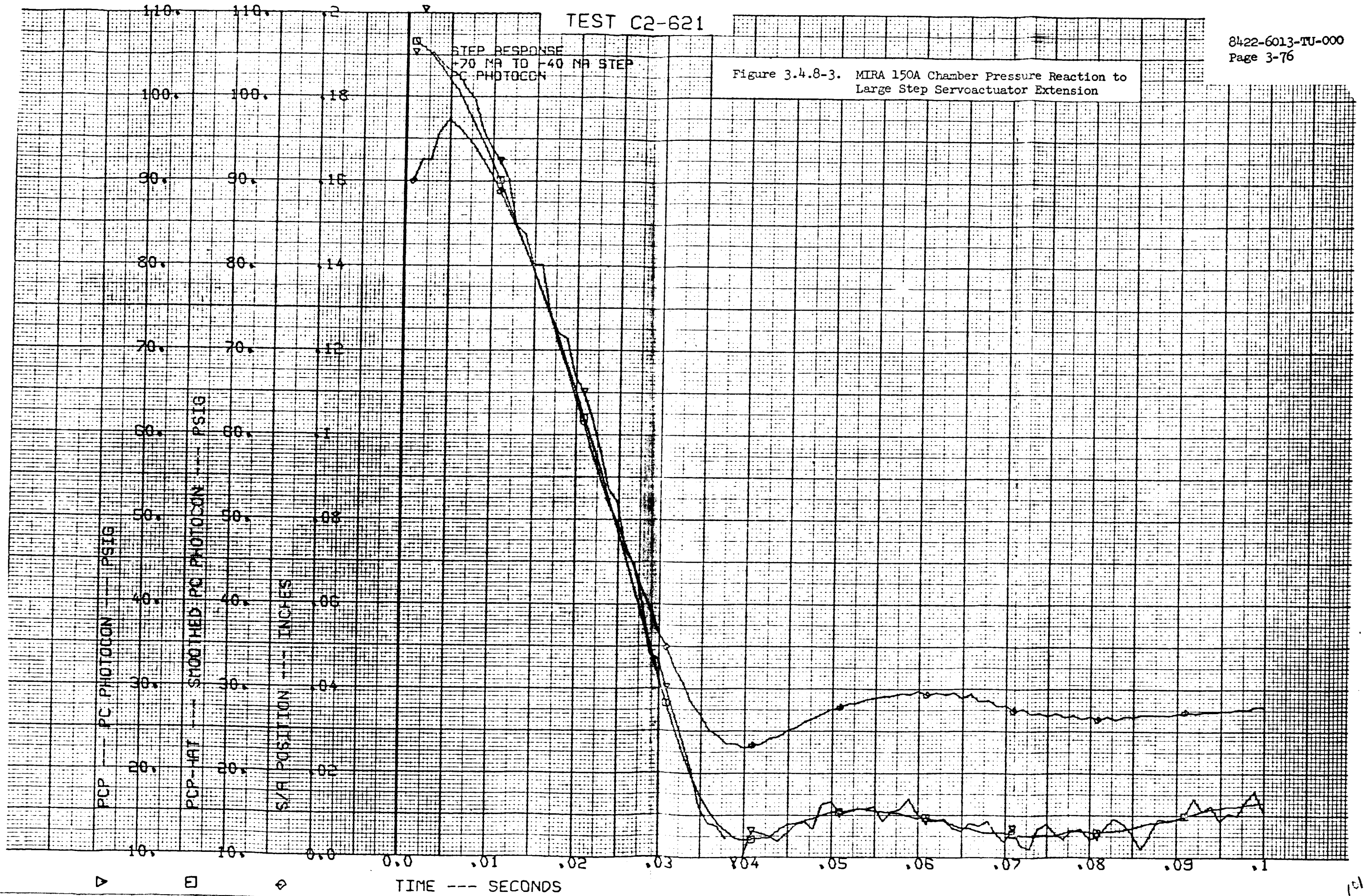

Figure 3.4.8-3. MIRA 150A Chamber Pressure Reaction to Large Step Servoactuator Extension

Figure 3.4.8-6. MIRA 150A Hysteresis Loop for Full Servoactuator Signal Excursion

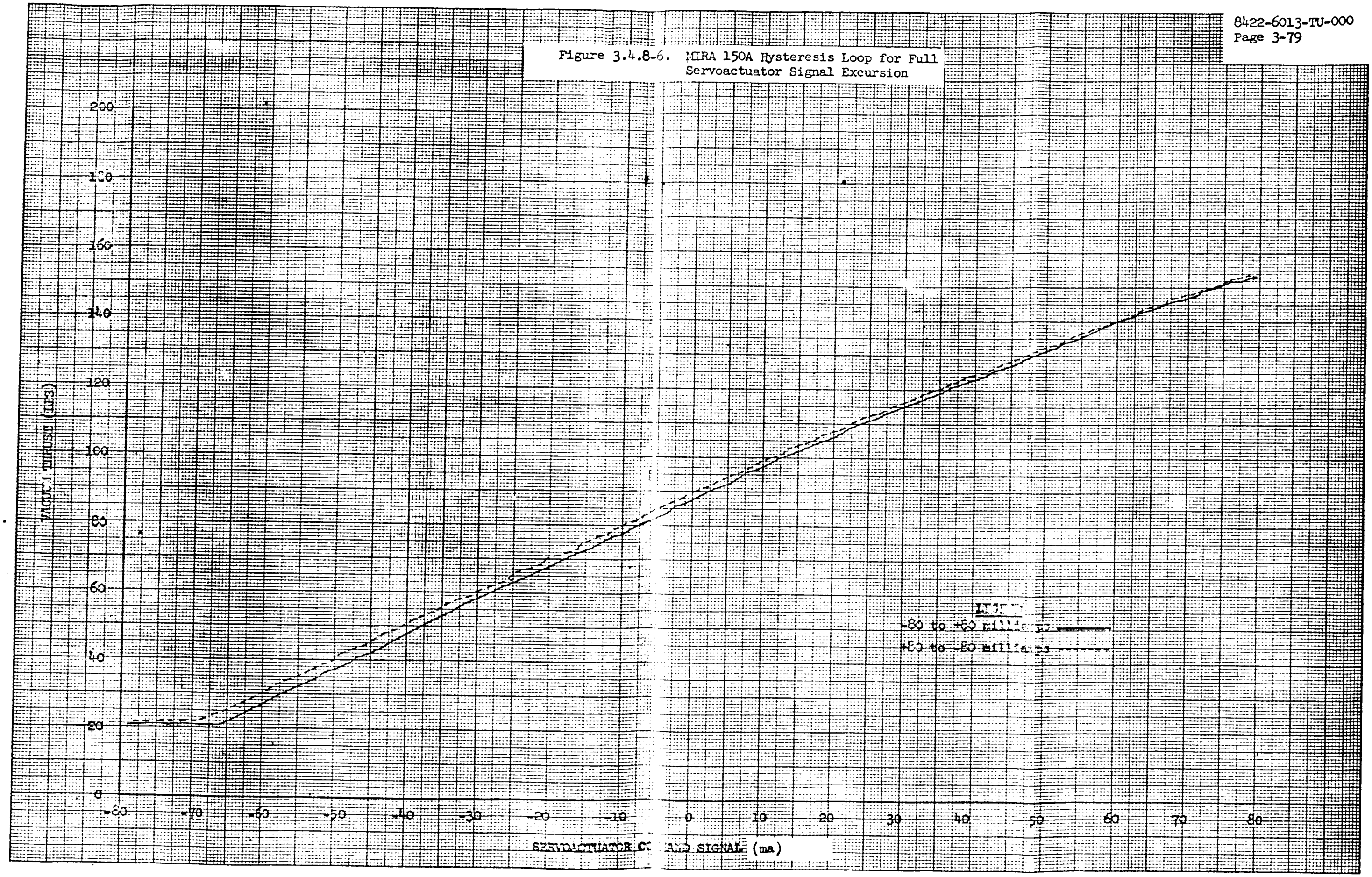

Table 3.4.8-4

MIRA 150A Loop Width
And 5-cps Sinusoidal
Response Characteristics

	Measured Values		SAM-50255-DSN-C
	Nominal	± 3-Sigma Deviation	Requirement
Loop Width(1) (%)	1.8	1.4	15 max
Phase Lag(2) (degrees)			
-62.5 ± 7.5 ma Signal	17.4	11.8	28 max
0 ± 7.5 ma Signal	17.4	8.7	28 max
+62.5 ± 7.5 ma Signal	14.2	13.4	28 max
Amplitude Ratio(3)			
-62.5 ± 7.5 ma Signal	1.01	0.20	0.95 min
0 ± 7.5 ma Signal	1.02	0.12	0.95 min
-62.5 ± 7.5 ma Signal	1.01	0.19	0.95 min

NOTES: (1) Percentage loop width is defined from a plot of thrust versus servo-actuator signal current in which the width of the plotted hysteresis loop is divided by the command current excursion times 100.

(2) Phase lag is defined in Figure 3.2.6-7.

(3) Amplitude ratio is defined as the peak-to-peak thrust attained under dynamic signal excursions conditions divided by the peak-to-peak thrust attained by the same signal excursions under steady state conditions.

3.4.9 TCA Operational Temperatures

Temperature profiles of the TCA external surfaces were obtained during Phase III development and prequalification testing. Figure 3.4.9-1 shows the thermocouple locations on the TCA altitude configuration. Figures 3.4.9-2 through 3.4.9-4 show typical surface temperatures as a function of time for maximum thrust, minimum thrust, and variable thrust conditions, respectively. These plots were derived from altitude test firings in which the test cell pressure was approximately 0.16 psia (100,000ft pressure altitude) and the test cell walls were uncooled and painted white. The temperature of the cell walls during the firings was approximately 100°F.

During the test firings, view factors for radiation cooling of the external surfaces were not simulated to represent the actual spacecraft condition. The differences between actual test conditions and spacecraft conditions in effect on surface temperatures are: (1) small but unconservative for conductive and convective heat transfer considerations, and (2) somewhat greater and conservative for radiation considerations. In general, the TCA surfaces would run cooler in the spacecraft environment than in the altitude test firings.

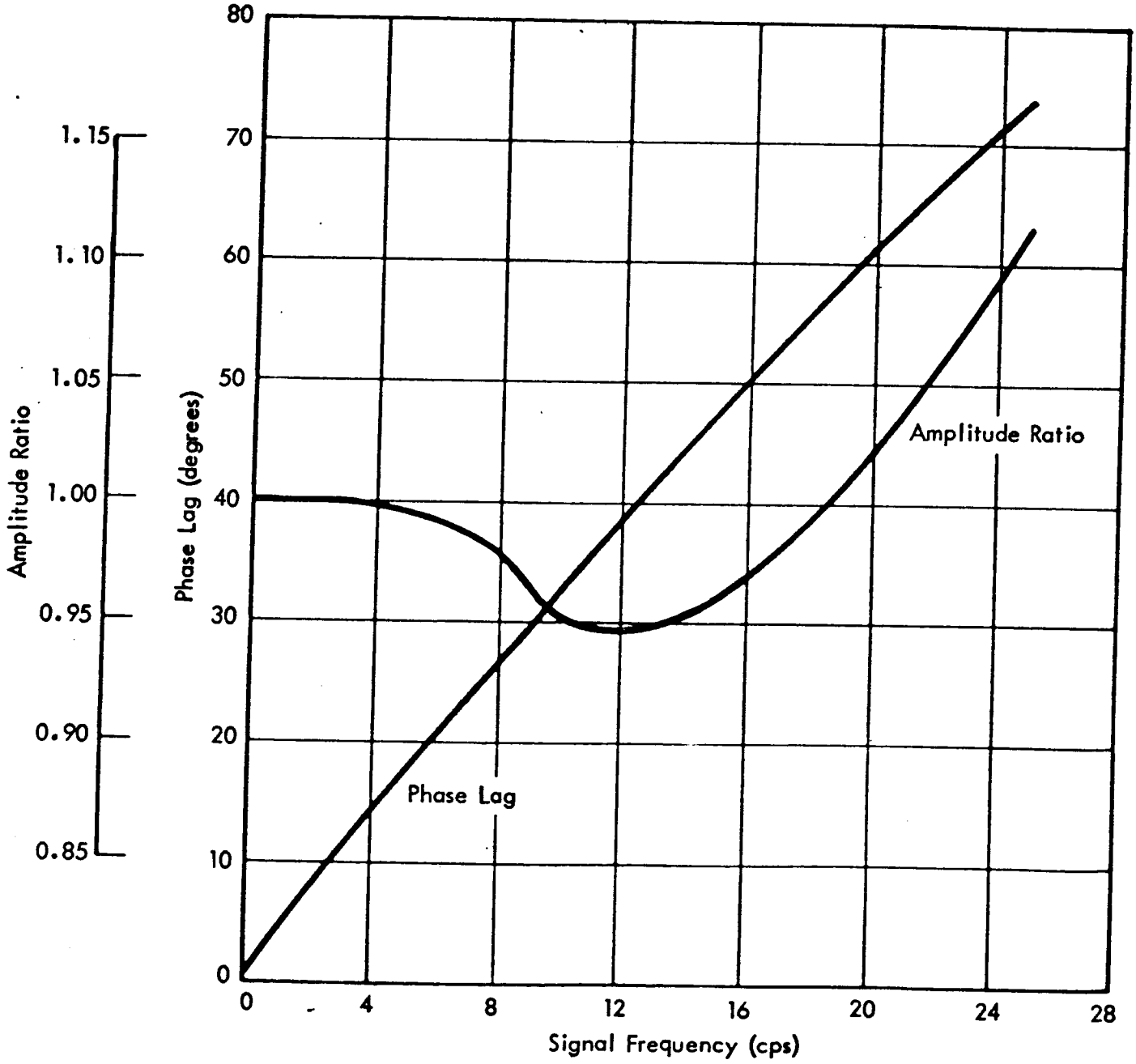

Figure 3.4.8-5. MIRA 150A Sinusoidal Response Characteristics for All ± 7.5 ma Amplitude Signals within a -70 to +70 ma Range

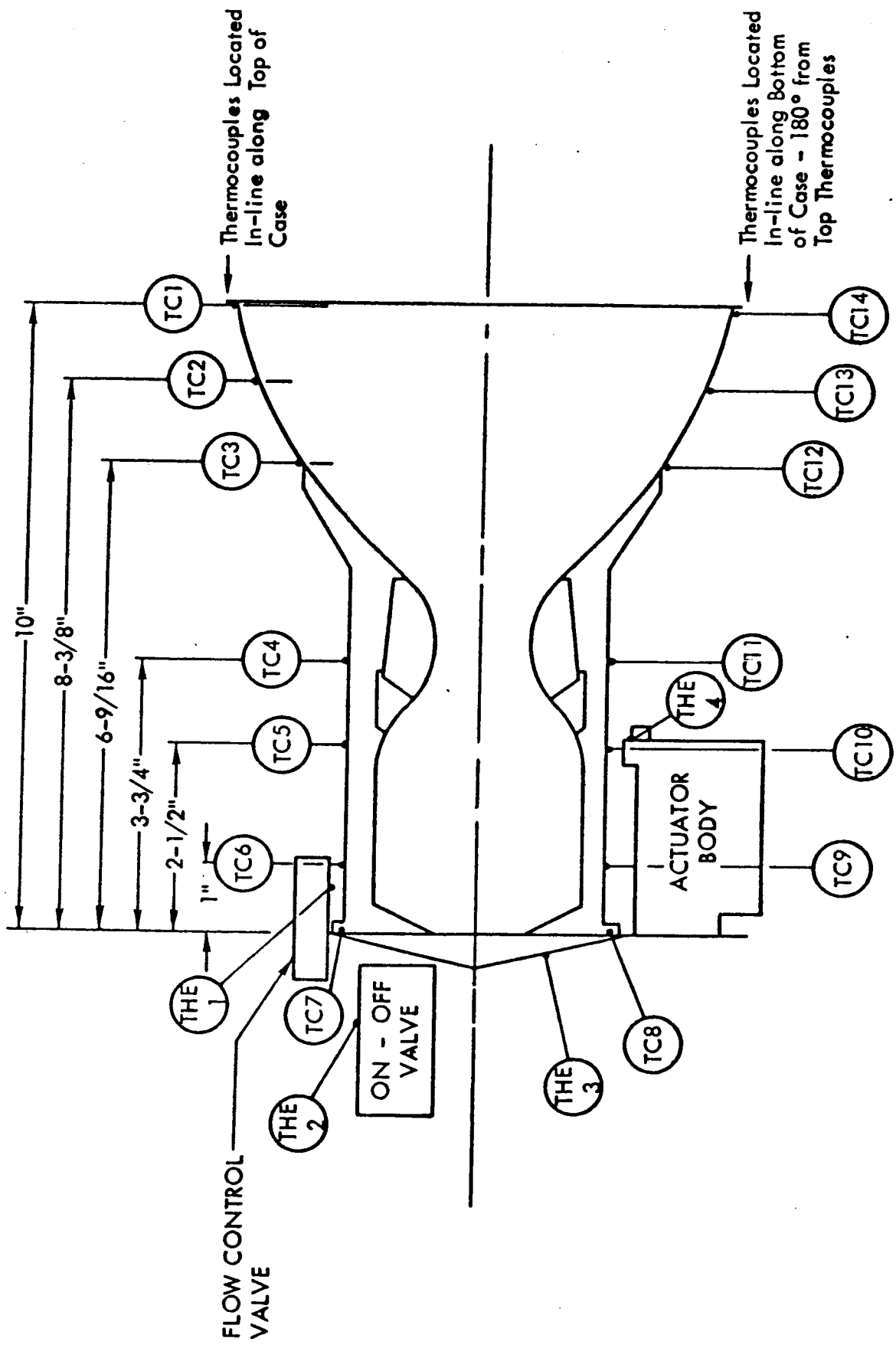

Figure 3.4.9-1. MIRA 150A Thermocouple Locations

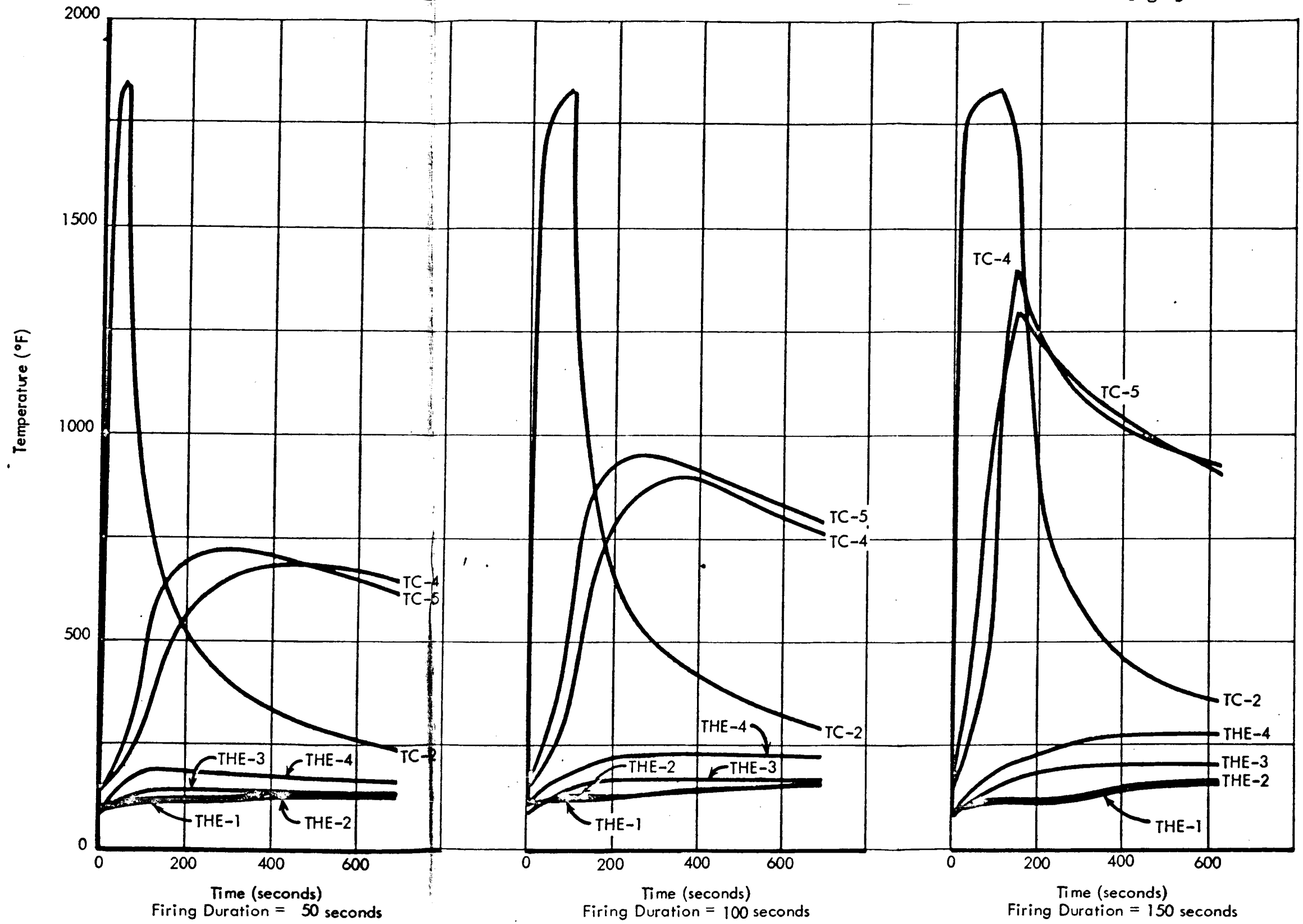

Figure 3.4.9-2. Typical TCA External Surface Temperatures
Maximum Thrust Conditions Altitude Environment

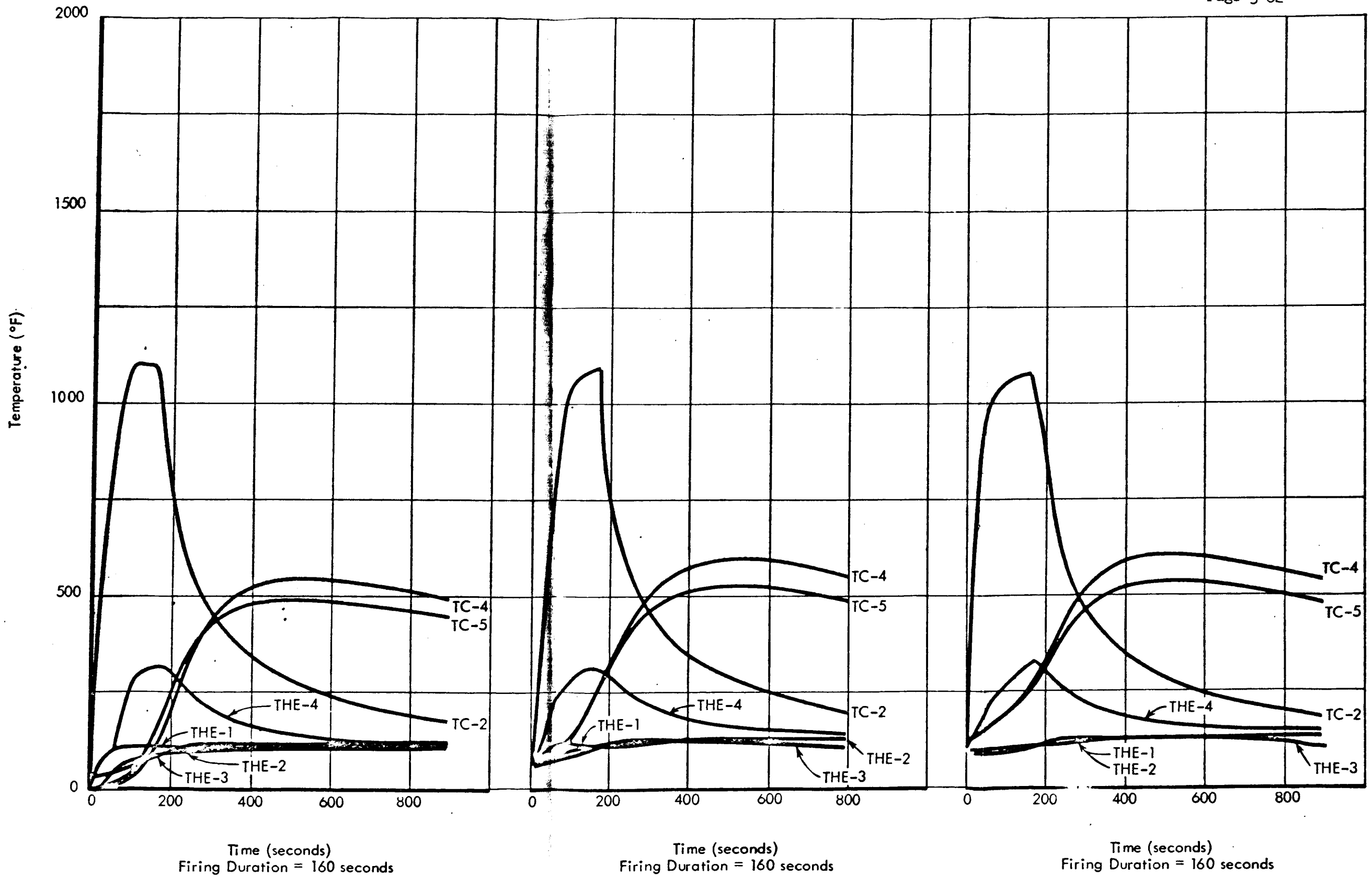

Figure 3.4.9-3. Typical TCA External Surface Temperatures
Minimum Thrust Conditions Altitude Environment

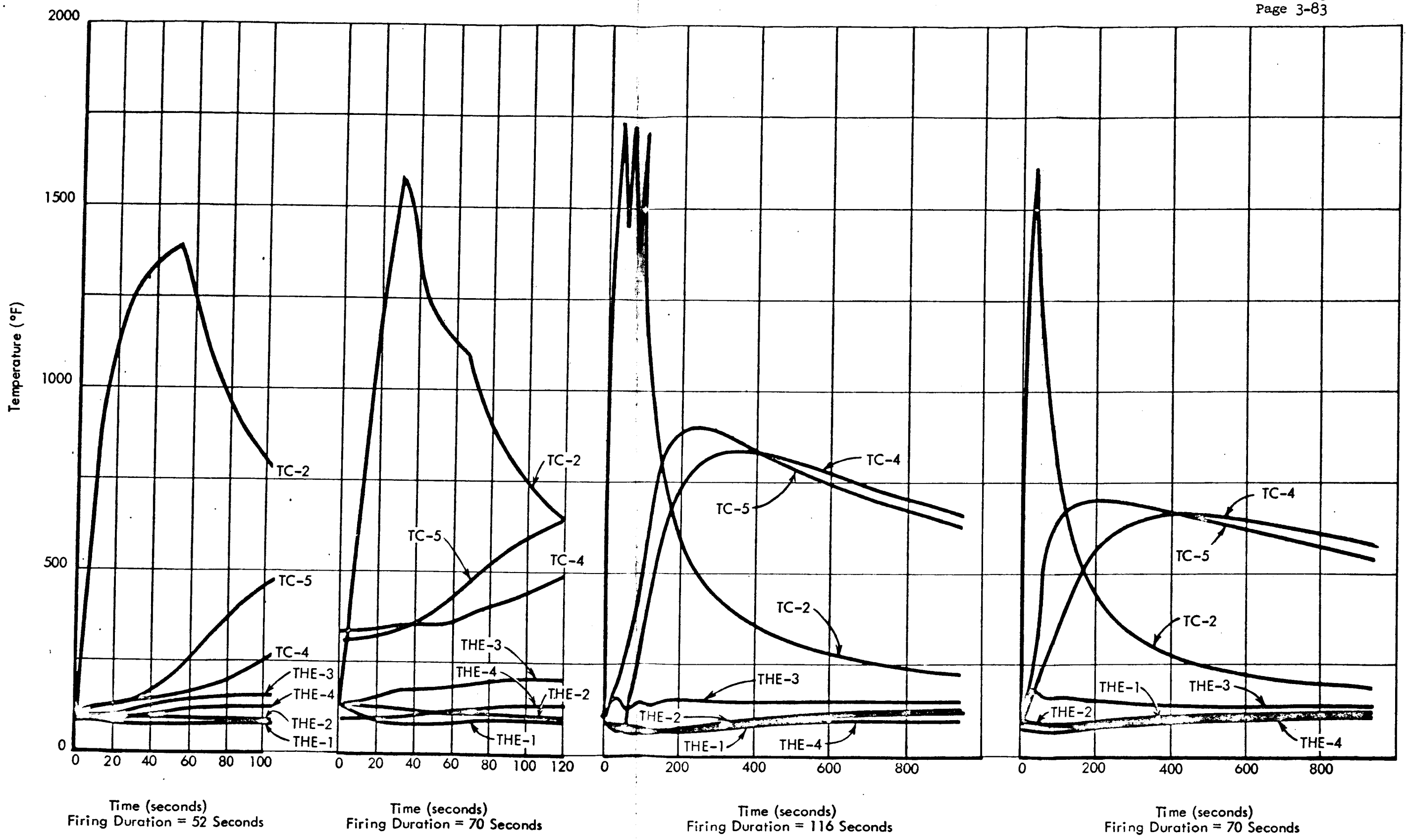

Figure 3.4.3-4. Typical TCA External Surface Temperatures
During Stable Thrust Conditions Altitude Environment

3.4.10 CC & NA Charring, Erosion, and Weight Loss

The testing performed during Phase III did not include individual tests whose primary objective was the determination of any CC & NA liner charring, erosion, or weight loss. Data applicable for these determinations was derived from tests performed for other purposes, such as durability and overall TCA performance tests under extreme operating conditions. (Refer to paragraph 6.4 for details.)

Typically char depth and pattern are not highly reproducible parameters being functions not only of the injector and chamber design and the unit-to-unit variability but are also a function of the firing duration, chamber pressure, and the environmental conditions influencing the CC & NA external heat transfer.

Based on the data obtained from several CC & NAs used on altitude firings, the predicted char depth of the ablative liner as a function of firing duration for a typical variable thrust program is shown in Figure 3.4.10-1.

CC & NAs tested at sea level were fired for no less than 300 seconds duration, and thus no data on duration versus char depth or weight loss are available. Figure 3.4.10-2 shows a comparison of typically sectioned CC & NA liners that had: (1) 300 seconds at maximum thrust, (2) 315 seconds of variable thrust, (3) 480 seconds at minimum thrust, and (4) 57 seconds at maximum thrust. The variability of the char pattern in the combustion chamber is readily seen in these photographs. The buttercup char pattern is directly relatable to the 12-hole distributor ring used in the oxidizer propellant manifold. It is also of interest to note that the minimum thrust firing is more severe on the head end liner than a maximum thrust firing. This occurs primarily because the combustion zone moves back toward the head end liner as the TCA is throttled back. Charring completely through the liner, especially at station 2 (shown in Figure 3.4.10-1), is typical for most test duty cycles used. The estimated nominal mission profile, per JPL Specification SAM-50255-DSN-C has a duration of 162 seconds; thus the test cycles used represent a considerable overstress condition.

The total chamber liner weight loss following a typical 300-second maximum thrust multi-start firing does not exceed 7.8% of the prefiring CC & NA weight —— nominally 2.6 lbs. The CC & NA percentage weight loss varies approximately linearly with firing time.

The MIRA 150A TCA rarely experiences any nozzle throat erosion with a HEA that has satisfied acceptance criteria. Based on experience with 30 CC & NAs in more than 10,000 seconds of total firing time there have been only three instances of JTA graphite throat erosion. In each of the three cases, the calculated thrust vector deviation, based on throat area centroid shift calculations, was within design specification criteria. (Refer to paragraph 6.4 for details.)

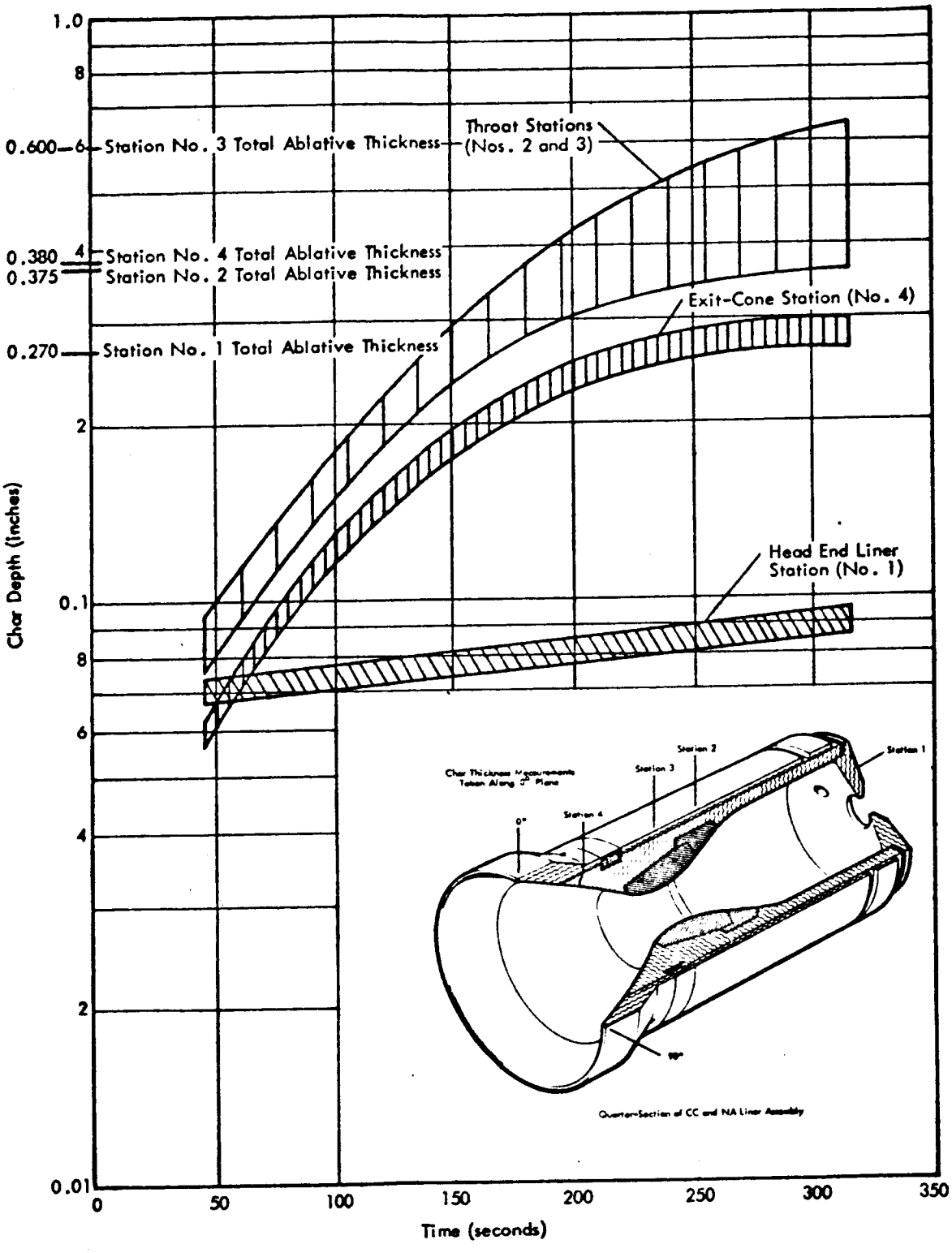

Figure 3.4.10-1. Predicted Char Depth as a Function of Firing Duration at Typical Variable Thrust Conditions (Altitude Environment)

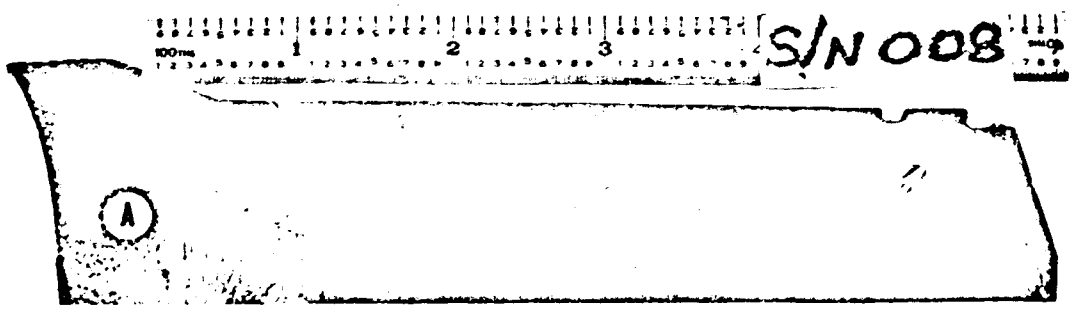

(a) 300-Second Firing at Max Thrust (3 Starts)

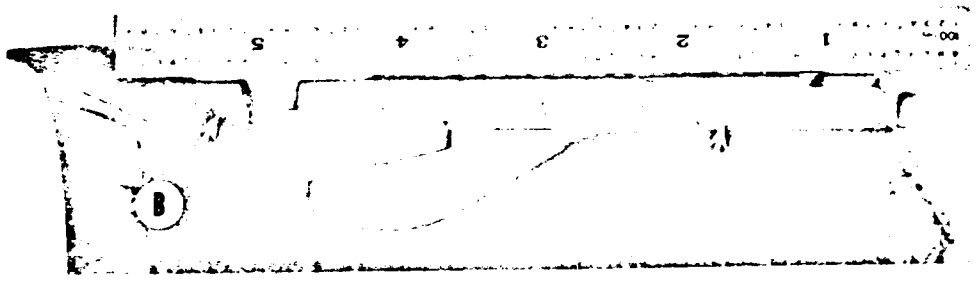

(b) 315-Second Firing at Variable Thrust (4 Starts)

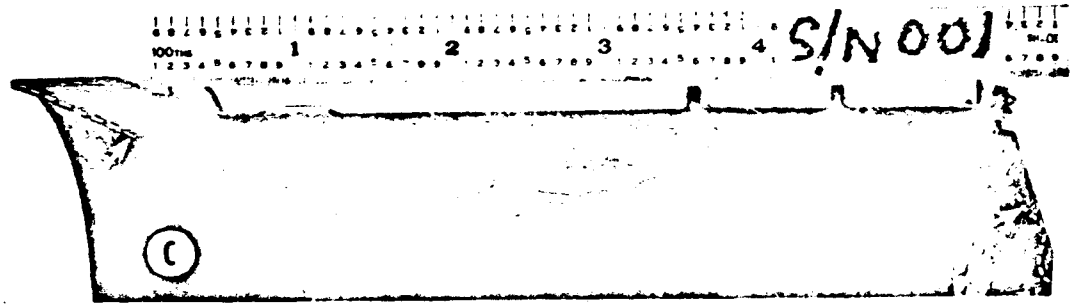

(c) 480-Second at Min Thrust (3 Starts)

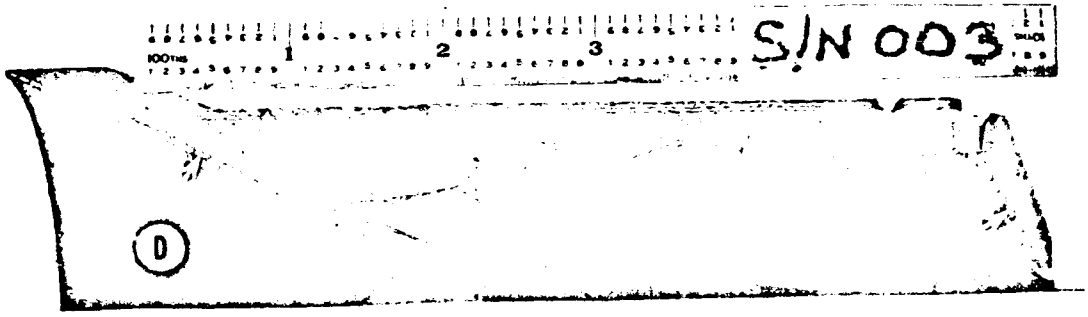

(d) 57-Second Firing at Max Thrust (1 Start)

Figure 3.4.10-2. Typical CC & NA Char Patterns (Dotted Line Represents Char Depth)

3.4.11 Pressure Schedule

This paragraph presents the nominal MIRA 150A propellant pressure schedule. Since the only pressures measured during a static firing are inlet pressures (P_{o_1} and P_{f_1}), injection pressures (P_{o_5} and P_{f_5}), and combustion chamber pressure (P_c), the remaining pressure drop information was extrapolated from water flow data. Figure 3.4.11-1 shows various TCA propellant pressures as a function of TCA thrust level. Figure 3.4.11-2 shows the pressure measurement locations.

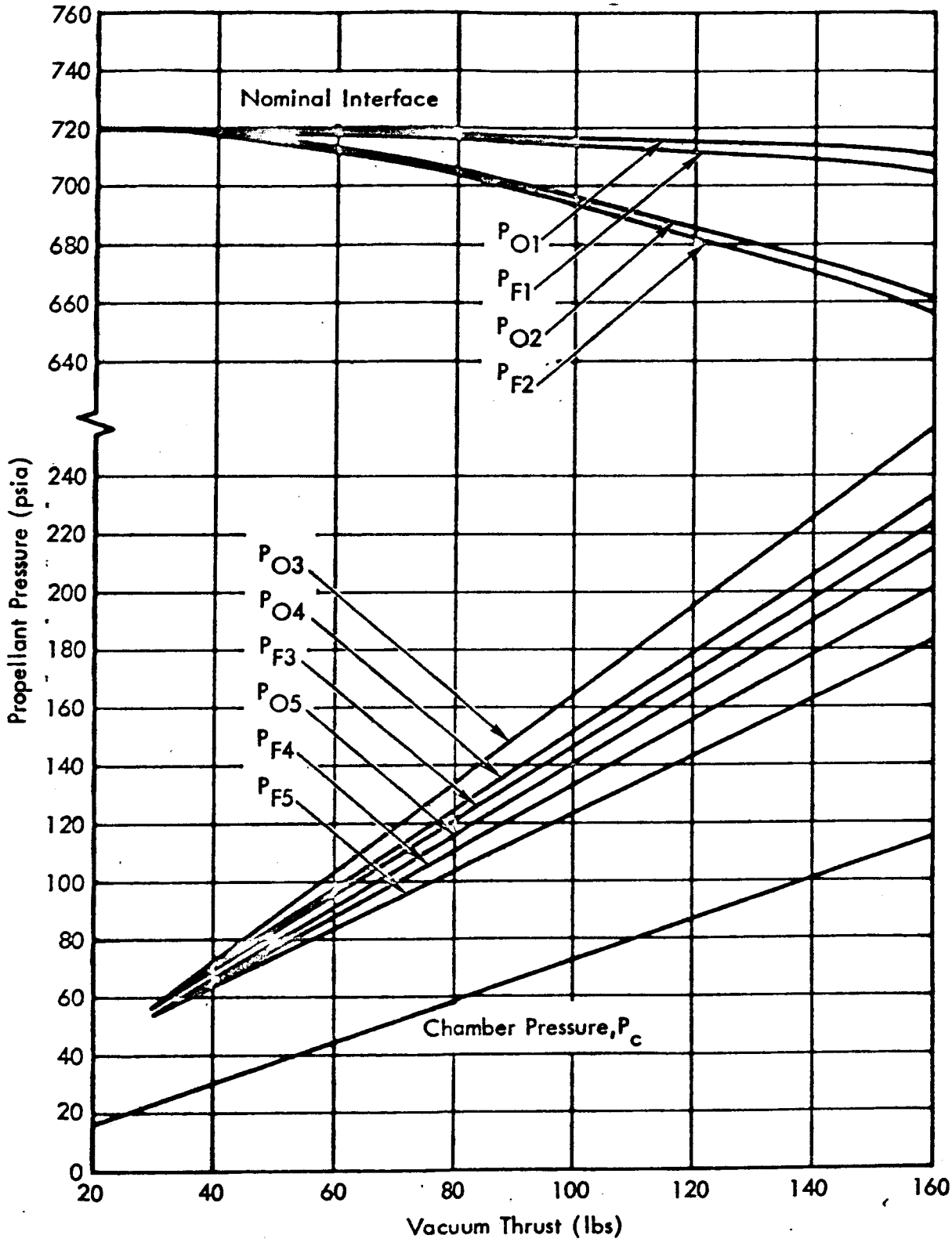

Figure 3.4.11-1. MIRA 150A Propellant Pressure Schedule

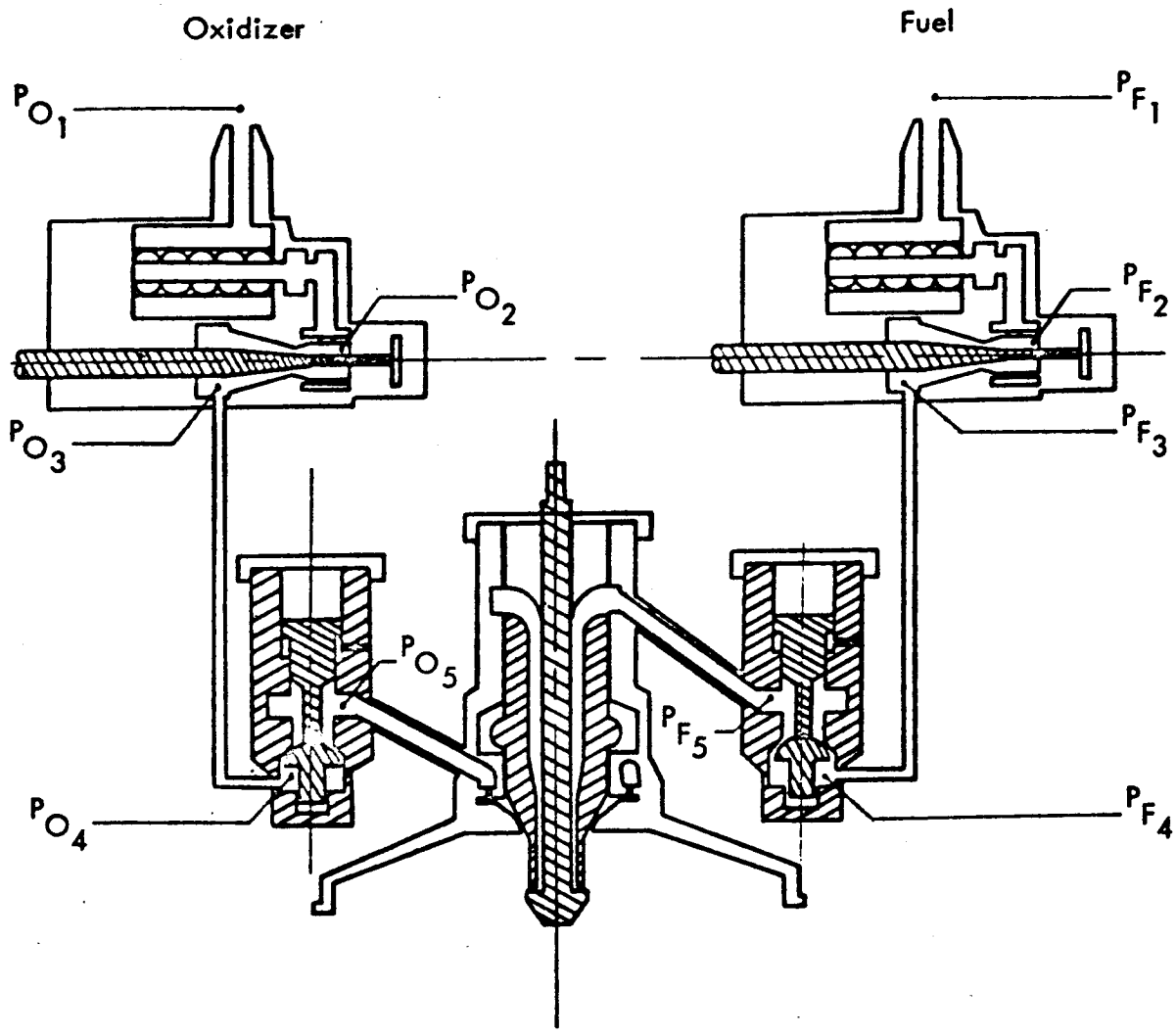

Figure 3.4.11-2. Pressure Measurement Locations

3.5 Propellants

The bipropellant MIRA 150A TCA uses a fuel and oxidizer having the characteristics described herein.

Fuel - Monomethylhydrazine (MMH) conforming to MIL-P-27404.

Oxidizer - MON 90/10, which is a mixture of 90% by weight of nitrogen tetroxide (N_2O_4) per MIL-P-26593A and 10% by weight of nitric oxide (NO).

Table 3.5-1 and Figures 3.5-2 through -7 present physical properties of MMH and MON 90/10. Freezing and boiling points are given in Table 3.5-1; Figures 3.5-2 and -3 provide density versus temperature relationships; Figures 3.5-4 and 3.5-5 give vapor pressure - temperature data; and viscosity versus temperature data is shown in Figures 3.5-6 and -7.

Table 3.5-1. Propellant Freezing and Boiling Points

	MMH	MON 90/10
Freezing point at standard atmospheric conditions.	-62°F	-10°F
Boiling point at standard atmospheric conditions.	+189.5°F	54.0°F

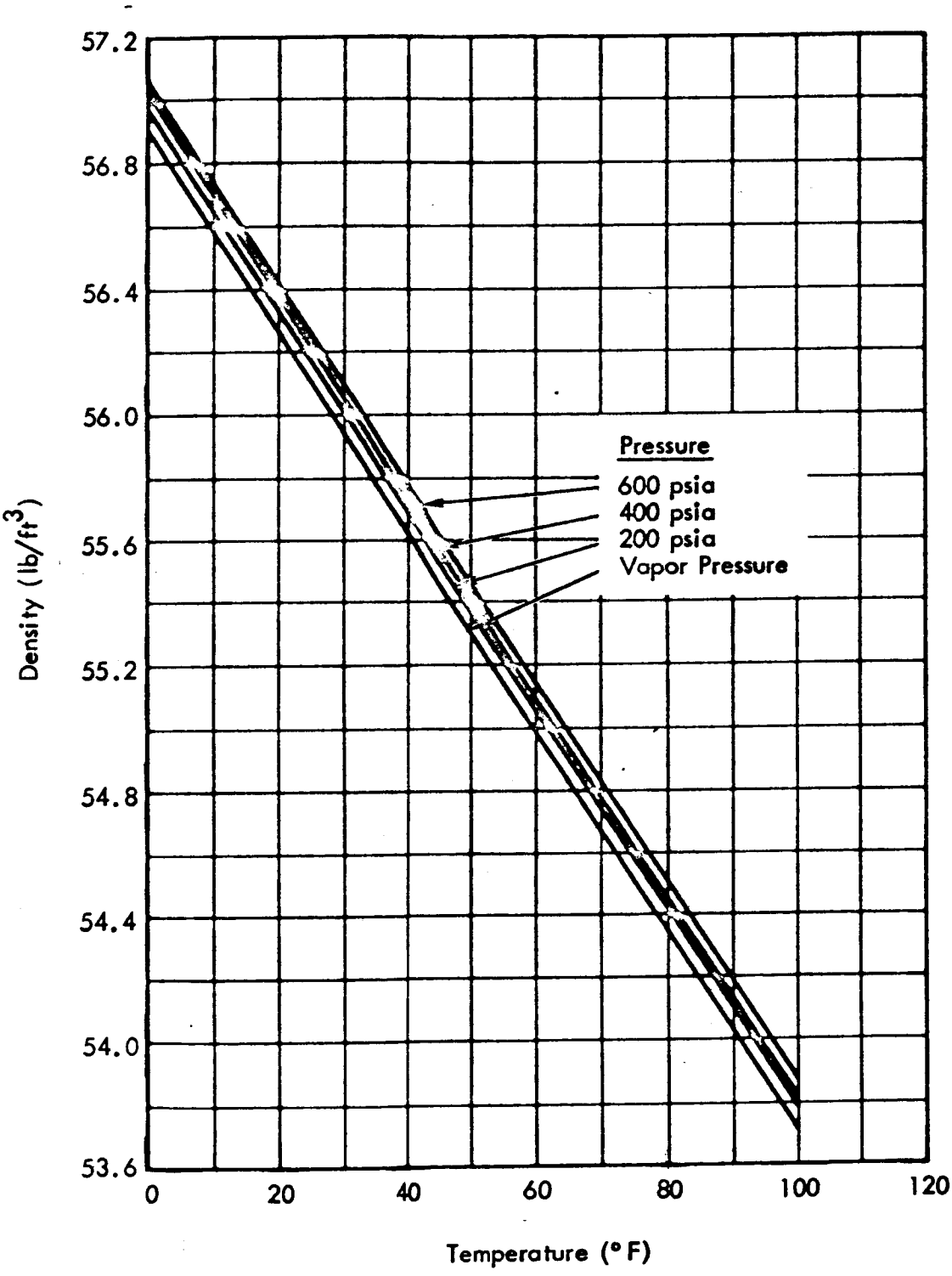

Figure 3.5-2. Density of Monomethylhydrazine (MMH)

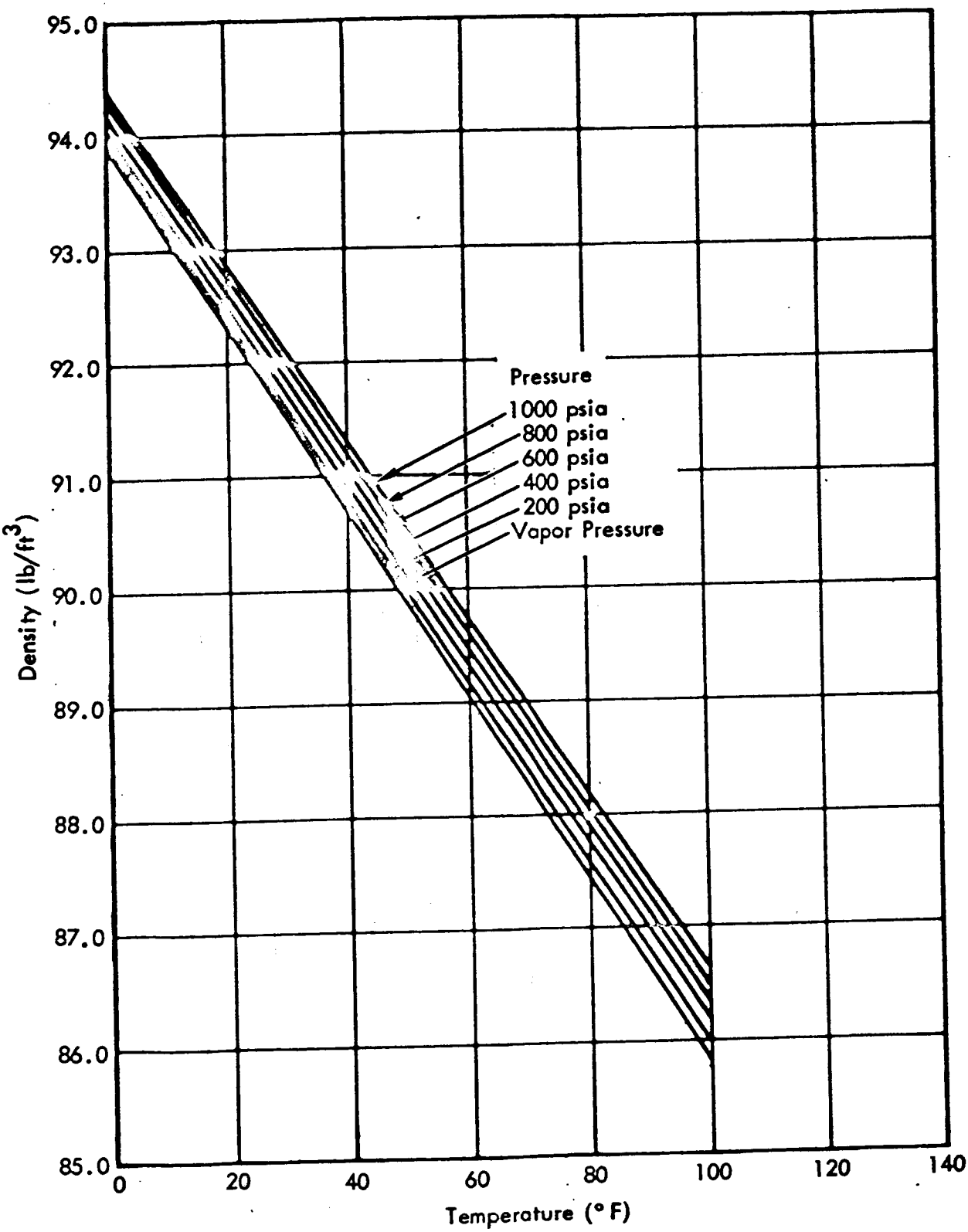

Figure 3.5-3. Density of Mixed Oxides of Nitrogen (MON) (90% N_2O_4 and 10% NO by Weight)

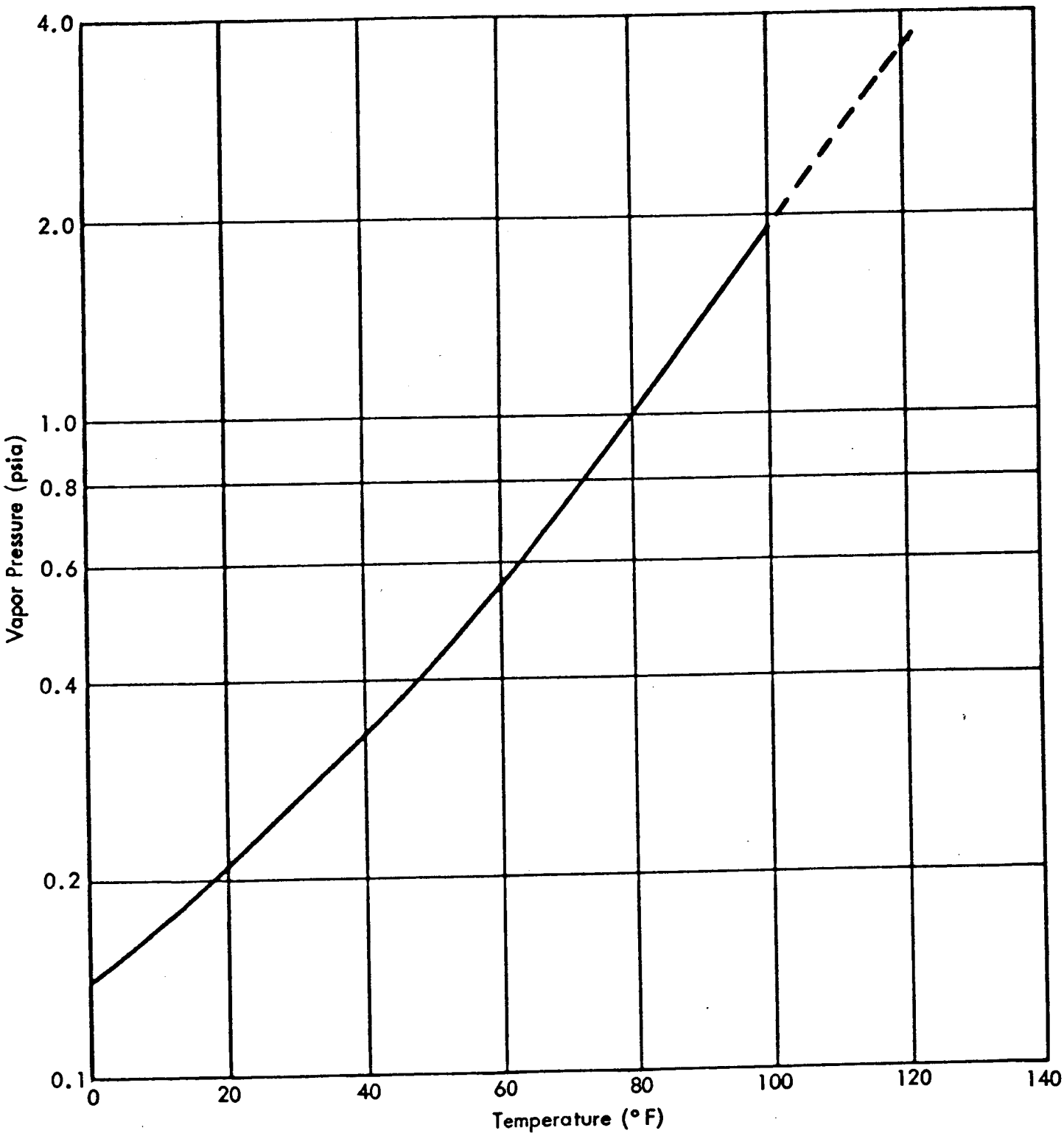

Figure 3.5-4. Vapor Pressure of Monomethylhydrazine (MMH)

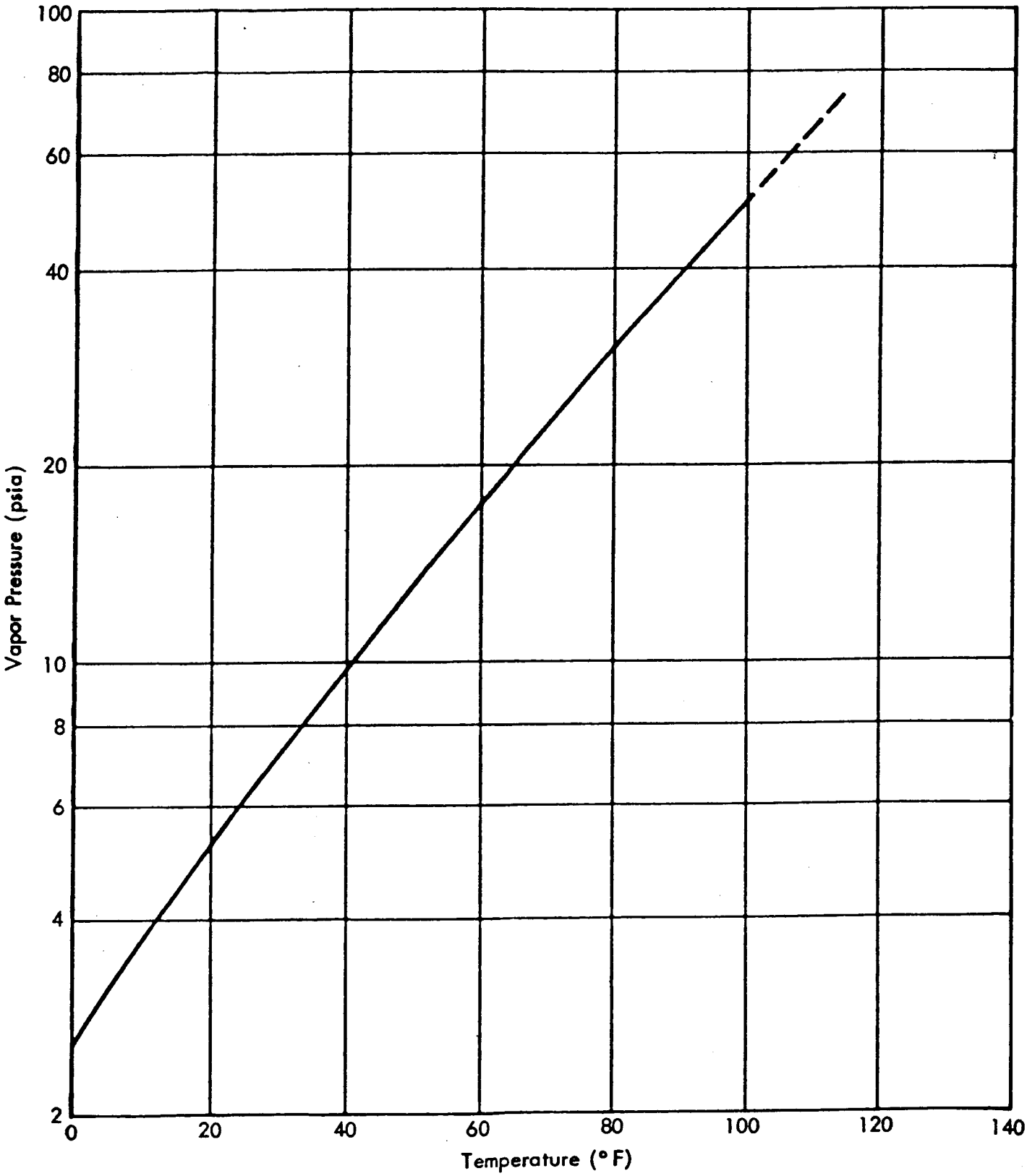

Figure 3.5-5. Vapor Pressure of Mixed Oxides of Nitrogen (MON)

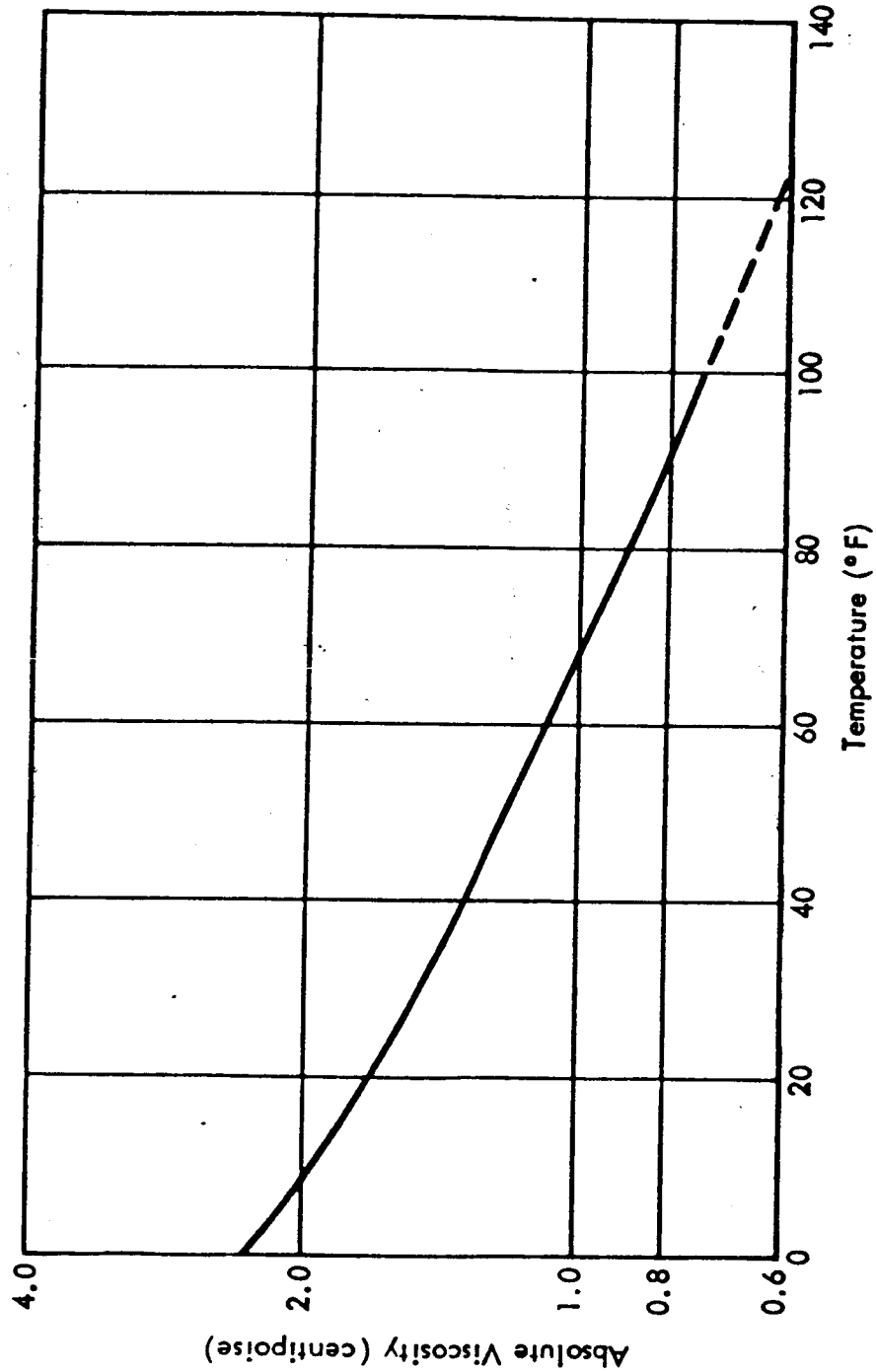

Figure 3.5-6. Absolute Viscosity of Monomethylhydrazine (MMH)

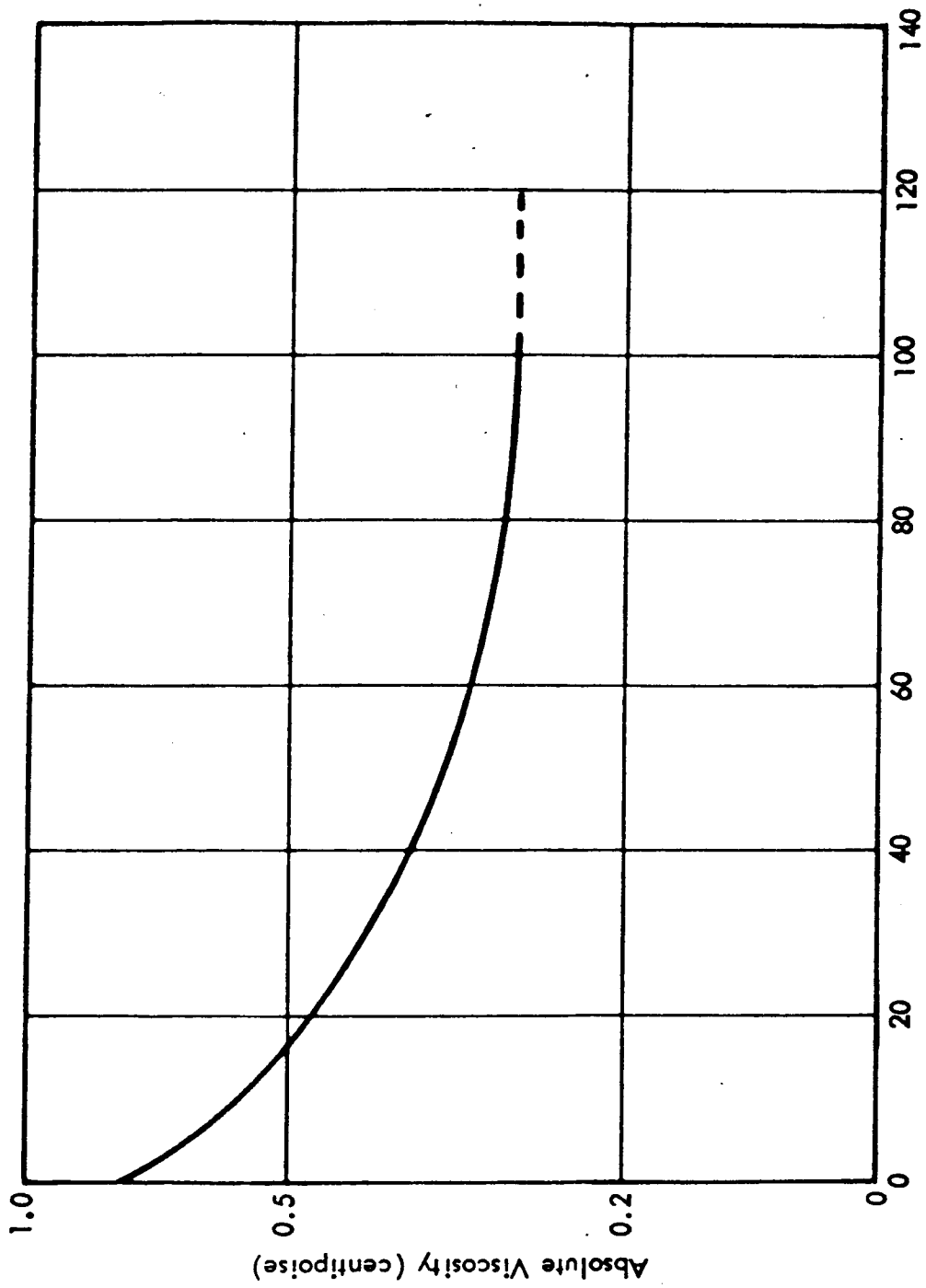

Figure 3.5-7. Absolute Viscosity of Mixed Oxides of Nitrogen (MON)

4.0 FINAL ASSEMBLY AND ACCEPTANCE TESTING

This section discusses program activities associated with the final assembly and acceptance testing of the TCA.

Acceptance testing of STL-fabricated assemblies was initiated at the HEA level and included tests and operational checkout during and after final assembly of the TCA. The major steps in the final assembly of the HEA and TCA are listed in Table 4-1. Figure 4-2 depicts the acceptance test sequence as defined by Acceptance Test Specification TS3-01B. The final assembly and acceptance test procedures developed during the Surveyor program are considered to be a substantial contribution to state-of-the-art techniques of assuring operational adequacy for a delivered variable thrust rocket engine. In particular, these procedures applied in conjunction with associated special test equipment permit:

1. The HEA to be adjusted after final assembly to achieve the desired flow rate/pressure drop/input signal relationships to produce within specification performance characteristics,

2. The HEA to be hot-fired on a substitute combustion chamber employing a soft throat such that the erosion pattern of the soft throat establishes the subsequent minimum life of the flight weight chamber.

Item 1. above is made possible because the MIRA 150A injector, being a coaxial tube design, permits orifice sizing to be accomplished after final assembly, merely by adjusting the axial location of the coaxial elements. The as-assembled coaxial tube injector characteristics are readily adjusted to acceptable values in the calibration procedure. Thus, in-process fabrication controls are considerably less stringent and manufacturing yield is higher than would be experienced without the adjustability feature and without the HEA calibration technique.

The calibration procedure in which the coaxial tube injector is adjusted to its final configuration requires the use of in-process test equipment, called the HEA Calibration Stand. This stand is essentially a water-flow bench, on which the water flow characteristics of a master HEA have been measured and recorded. All final assembled MIRA 150A HEAs are adjusted on this stand to match the water-flow characteristics of the master unit. Details of this equipment are presented in section 8.0.

Item 2. requires an ablative test firing, or "streak test", as part of the routine acceptance testing on every HEA. This streak test, with specified, quantitative accept/reject criteria, is a means of evaluating the compatibility of an injector with a particular chamber geometry. The test employs an erodable nozzle throat to record the effect of the combustion pattern. This part of the HEA acceptance test is run at an overstress condition, namely, maximum thrust for 200 seconds when the nominal mission cycle is equivalent to mid-thrust for 162 seconds.

These two techniques of calibrating and streak testing are interrelated in that it is possible to adjust the coaxial tube injector for optimum streak test results, just as it is possible to adjust it for optimum combustion efficiency. Thus, if an assembled HEA produces an unsatisfactory throat erosion characteristic in its streak test, this characteristic can be modified by coaxial tube injector adjustment. However, the most important reason for the use of a streak test as an HEA acceptance criterion is that a reproducible and quantitative correlation between the durability of a streak test throat and the flight chamber has been developed. Data to corroborate acceptance test criteria by prequalification test results of flight chambers is available on HEAs -001, -004, -008 and -010; refer to paragraph 4.4 for streak test results and paragraph 6.6 for prequalification test results on these four HEAs. Thus,

Table 4-1

Major Items in HEA and TCA
Final Assembly and Acceptance Testing Operational Flow

Item No.	Description of Operation	Remarks
1.	Partially assembly head end assembly, i.e., excluding the S/A, solenoid pilot valve, lockwires, and adjustments.	
2.	Perform total immersion leak check.	ETD MIRA-IF-001 is applicable.
3.	Continue head end partial assembly, still excluding S/A and throttling torquing and lockwiring those items to be adjusted later during calibration.	
4.	Perform partial HEA calibration, i.e., adjust and fix into proper position the FCV pintles and injector pintle and sleeve.	ETD MIRA-IF-002 is applicable.
5.	Install S/A on HEA with HEA remaining on calibration stand.	
6.	Complete all HEA adjustments (specifically S/A adjustments).	ETD MIRA-IF-002 is applicable.
7.	Complete torquing of jam nuts at specified values, and finish lockwire of HEA.	
8.	Run HEA calibration formally.	ETD MIRA-IF-002 is applicable. At this point HEA P/N 106662 is complete; i.e., HEA calibration is considered part of the assembly operation and is not part of acceptance testing.
9.	Leak check.	This is first formal operation under Acceptance Test Specification requirements. ETD-MIRA-IF-001 is applicable.
10.	Perform 200-second streak test firing.	
11.	Perform 130-second HEA acceptance test firing.	
12.	Flush and dry.	
13.	Assemble HEA to CC & NA including proper torque on screws; however, do not lockwire screws joining HEA and CC & NA.	The CC & NA (P/N 106546) has already been leak checked per ETD MIRA-2F-001.
14.	Perform leak check.	ETD-MIRA-OA-001 is applicable.
15.	Lockwire HEA and CC & NA joint fasteners.	TCA assembly (P/N 106570) is considered complete when this item is completed.
16.	Determine weight and balance on TCA.	Preliminary ETD-MIRA-OF-001 is applicable.
17.	Subject TCA to vibration test.	
18.	Perform leak check.	ETD-MIRA-OA-001 is applicable.
19.	Perform 12-second TCA acceptance test firing.	
20.	Flush and dry.	
21.	Perform final pressure decay leak check	ETD-MIRA-OA-002 is applicable.
22.	Perform final cleaning.	At this point, assuming all acceptance test criteria are met, the TCA is considered a deliverable or useable TCA.
23.	Package.	
24.	Store or ship	

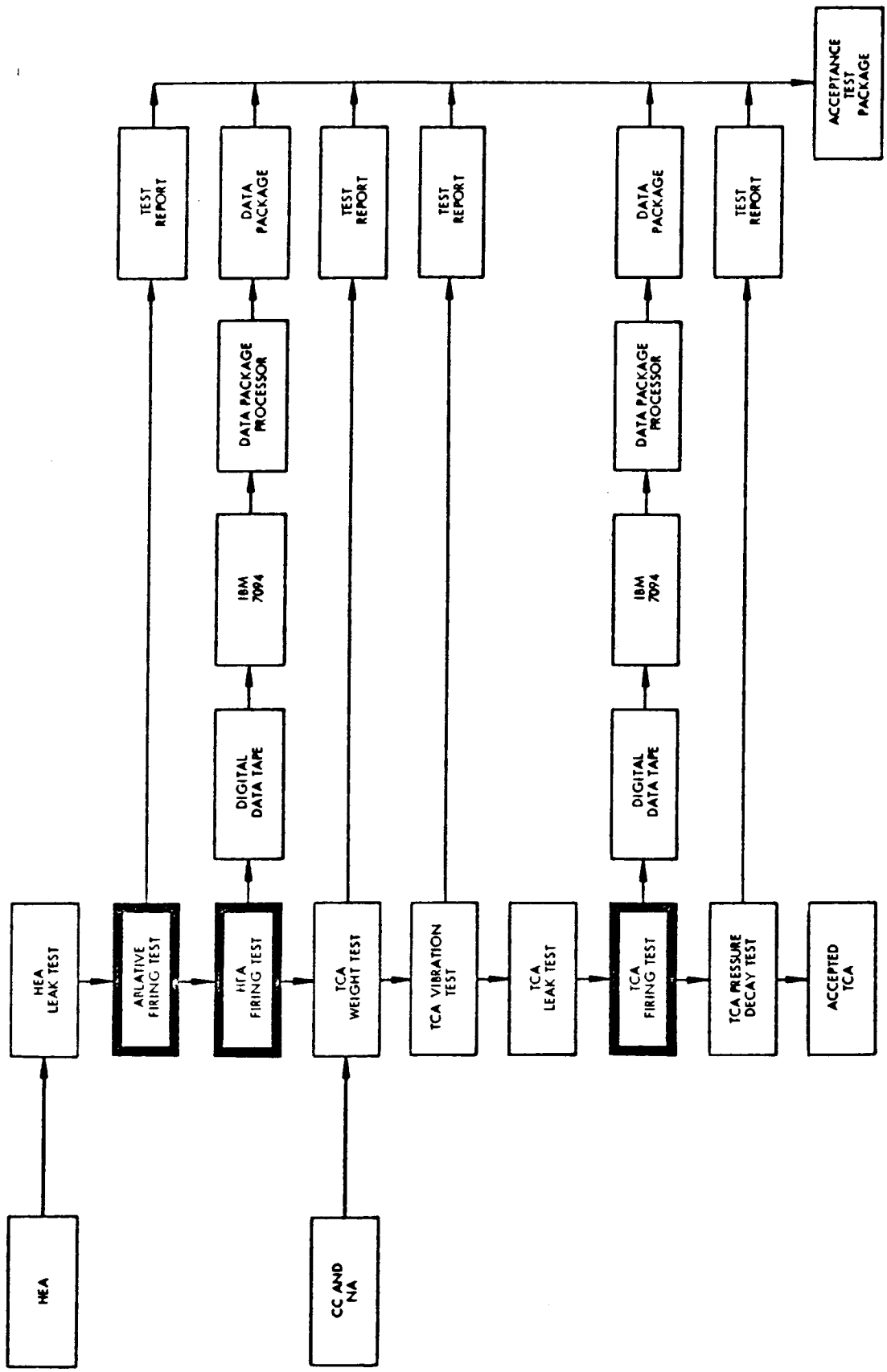

Figure 4-2. Acceptance Test Sequence

it is possible to predict with confidence the durability of the flight chamber based upon the streak test characteristics of the HEA during its acceptance test.

4.1 Leak Checking

Fluid leakage in excess of stipulated amounts can adversely affect operation of the TCA. Therefore, leak checking techniques were developed and implemented in the TCA fabrication and acceptance test operations.

4.1.1 Potential Leakage Paths

Possible leakage paths and the allowable rates and affects associated with such leakage are discussed below.

External Leakage

No external leakage of propellants is allowed other than the small external leakage appearing as wetting of the output shaft of the servoactuator. Leakage other than this could: (1) damage adjacent spacecraft equipment, (2) be hazardous to personnel during spacecraft operations, (3) affect mixture ratio and flow, and (4) waste the spacecraft propellant supply.

Potential external propellant leakage paths associated with the flow control valve are from: (1) the propellant inlet supply fittings, (2) the servoactuator fuel supply line fitting, (3) the filter retention nuts, (4) the flow control valve insert retention nuts, and (5) the face seals between the valve body and the head end body.

Potential external propellant leakage associated with the injector, possible only during the firing mode, is limited to oxidizer or fuel leakage across the injector sleeve seal and fuel leakage across the pintle guide seal and/or pintle O-ring.

External fuel leakage associated with the servoactuator includes those sealing elements of: (1) the torque motor cover gasket, (2) the feedback cap gasket, (3) the spool stop O-ring, (4) the piston outside gland ID and/or OD O-rings, and (5) the inlet and/or return port fittings.

Internal Leakage

Internal propellant leakage is possible across the filter outlet seals, and, if small, would have no adverse affect on TCA operation; however, if large, this leakage would result in inadequate filtration and possible TCA malfunction. Internal propellant leakage could also occur across the flow control valve throat inserts. Similarly, this leakage, if small, would have no adverse affect on TCA operation but, if large, could affect TCA mixture ratio and flow control performance.

In the nonactuated state, internal propellant leakage across the shutoff valve poppet seat and/or bottom sleeve seal would emerge as unacceptable external leakage at the injector. In the actuated state, shutoff valve leakage across the small piston seal and/or center sleeve seal would emerge as unacceptable external leakage at the shutoff valve vent.

Internal leakage of fuel is possible across the sealing elements in the servoactuator at: (1) the torque motor flapper O-ring, (2) the orifice retainer face seal and/or O-ring, (3) the piston inside gland ID or OD O-rings, (4) the piston O-ring, and (5) across the spool (i.e., null leakage). Allowable spool null leakage is 12 $in.^3/min$ at 700 psig. Other servoactuator internal fuel leakages are allowable only to the extent that they do not produce excessive external leakage or impair performance of the servoactuator.

Internal helium leakage in the shutoff valves is possible across the large piston seal and/or top sleeve seal (which would emerge as external leakage at the shutoff valve vent) and across the shutoff valve cap. This leakage if small would be tolerable, but if large, could prevent the shutoff valves from actuating and/or waste spacecraft helium supply.

With the helium pilot valve in the nonactuated state, internal helium leakage can occur across the inlet poppet/seat. In the actuated state, internal helium leakage can occur through the valve case or across the outlet poppet/seal. In both cases, the leakage would emerge externally at the valve vent ports. This leakage, plus any from across the face seal between the pilot valve and head end body, would waste the spacecraft helium supply; excessive outlet poppet seat leakage could prevent shutoff valve actuation. Internal helium leakage is limited to 10 scc/hr at 850 psig.

CC & NA Leakage

Leakage of combustion gases in the CC & NA can occur: (1) between the ablative liner and shell, (2) between the ablative liner and hard throat, and (3) at the CC & NA/HEA joint. This leakage is limited to minor amounts that will not: (1) erode the ablative liner materials and destroy the joint integrity, (2) cause structural failure of the titanium shell because of overheating, and (3) result in structural failure of the head end body/chamber shell flange.

4.1.2 Test Techniques and Equipment

Four Engineering Test Directives (ETD) were prepared specifically for conducting leakage tests on the TCA and its major subassemblies. These ETDs are listed below.

ETD No.	ETD Title
ETD-MIRA-2F-001	Combustion Chamber and Nozzle Assembly Leak Check
ETD-MIRA-1F-001	Head End Assembly Leak Check
ETD-MIRA-0A-001	TCA Leak Test
ETD-MIRA-0A-002	TCA Pressure Decay Test

In addition, a portion of the following component acceptance test procedures for the helium pilot valve and servoactuator is devoted to leak checks on these items:

ETD-MIRA-3R1-001	Acceptance Test Procedure Solenoid-Operated Three-Way Valve
STL Document No. 9354.4-255	Acceptance Test Procedure, Surveyor TCA Electro-hydraulic Servoactuator

4.1.2.1 Component Level Leakage Tests

During component acceptance testing of the helium pilot valve, external and internal leakage are measured quantitatively with a helium leak detector (mass spectrometer). Leak measurements are made with the valve energized and de-energized, using helium test gas at 850 psig.

Component level leak checking of the servoactuator is performed during its acceptance test. External leakage is checked by pressurizing the unit with fuel to proof pressure (1035 psia) and visually checking for leakage other than normal wetting of the output shaft. The null leakage is quantitatively measured by pressurizing the servoactuator with fuel to 700 psig and collecting the "null flow" in a graduated cylinder over a one-minute period. Internal leakage cannot be measured directly, but is assessed by the foregoing checks and servoactuator performance measurements.

4.1.2.2 Combustion Chamber and Nozzle Assembly Leak Check

A leak test is performed prior to attaching the CC & NA to the HEA. The CC & NA is tested while on a special test setup that seals off the chamber head end and plugs the throat. The CC & NA is pressurized with nitrogen at 110 psig and leakage is qualitatively checked by applying Leak-Tec to the potential leak paths and visually checking for bubble formation.

4.1.2.3 Head End Assembly Leakage Tests

The HEA is subjected to two types of leakage tests. The first test is an immersion test and is performed before the servoactuator and helium pilot valve are installed on the HEA (the head end body fluid attach points being plugged or capped). The HEA is attached to a chamber face cap fixture which seals the injector face and provides a fitting for test gas pressurization. The leak check is performed with nitrogen gas pressurization. The leak check is performed with nitrogen gas by pressurizing the propellant inlets to 500 psig and the sealed injector face to 125 psig and then immersing the assembly in water. Leakage is detected by emmission of bubbles and corrective rework, if required, is implemented before proceeding with further assembly and test.

The second technique of HEA leak checking is performed with the pilot valve installed on the HEA. The pilot valve is pressurized to 720 psig with nitrogen and then energized. Leakage is checked (with Leak-Tec) at the pilot valve and its attach point and at the SOV vents and SOV caps. The pilot valve is depressurized and the propellant inlet ports are pressurized with nitrogen to 500 psig. The test gas fitting on the chamber face cap fixture is connected to a water-filled inverted graduate. Leakage across the SOV poppets is then measured by observing the change in water level in the graduate as a function of time.

4.1.2.4 TCA Leakage Test

The TCA leakage test provides a check on all external leakage paths of the TCA and is performed during the acceptance test sequence. For this test, the combustion chamber is fitted with a throat plug having an integral fluid fitting. In the first phase of the test, the propellant inlet ports and the pilot valve are pressurized with nitrogen to 720 psig and the throat plug fitting is connected to a water-filled inverted graduate. Using Leak-Tec, the potential leak paths of the TCA are qualitatively checked, except for leakage across the SOV poppets which is quantitatively measured by displacement

versus time of the water in the inverted graduate. Next, the throat plug fitting is pressurized with nitrogen to 110 psig and the potential leak paths of the TCA are qualitatively checked again using Leak-Tec.

4.1.2.5 TCA Pressure Decay Test

The TCA pressure decay test provides a quantitative measure of the total TCA external leakage. Maximum leakage of gaseous helium of 10 scc/hr is allowed when the TCA is pressurized to 500 psig. In this pressure decay method the propellant inlet ports are pressurized to 720 psig and then closed off with a resultant total fixed volume of the propellant passages and test equipment of 10 $in.^3$. Test acceptance is based on a maximum allowable pressure decay of 10 psi/hour. The helium pilot valve is also pressurized to 720 psig and then closed off, with a second test system also having a total volume of 10 in^3, in order to perform a similar pressure decay test. The pressure decay tests are run over a time period of 8 hours minimum.

4.1.3 Test Results

The results of the component leakage tests (conducted during component acceptance testing) are contained in paragraphs 5.1.1 (servoactuator) and 5.1.3 (helium pilot valve). Data are not tabulated here for: (1) CC & NA Leak Check, (2) HEA Leakage Tests, and (3) TCA Leakage Test, which are in-process type tests used in the production cycle to assure leak-free items for subsequent operations (i.e., assembly, calibration, firing). The TCA pressure decay test was conducted on three TCAs (2 Phase IIs and 1 Phase III); test results are given below.

Test Specimen	Test Date	Initial Pressure (psig)	Final Pressure (psig)	Test Duration (hrs)	Pressure Decay (psi/hr) Actual	Allowable
MIRA 150A-001	10/1/64					
Propellant Passages		720	345	5	75	10
Pilot Valve		720	718	8	0.25	10
MIRA 150A-005	10/7/64					
Propellant Passages		737	723	16	0.88	10
Pilot Valve		737	735	16	0.13	10
MIRA 150A-007	11/11/64					
Propellant Passages		720	723*	10	0	10
Pilot Valve		720	725*	10	0	10

*Small increase in test specimen temperature caused pressure rise.

The above data show that the propellant passages of MIRA 150A-001 did not meet the test requirement, and propellant leakage could therefore be expected. However, subsequent pressurization of this TCA with propellants did not result in propellant leakage and, therefore, the allowable helium leakage requirement was shown to be conservative. MIRA 150A-005 and -007 (which met pressure decay requirements) of course did not exhibit propellant leakage.

4.1.4 Discussion of Test Results

The several in-process type leak check procedures proved to be very useful in detecting leak problems and, thus, enabled remedial action to be performed prior to subjecting the particular item to operation. The following paragraphs discuss the reasons for the leaks found, the leakage criteria, and the influence the leakage had on TCA design.

4.1.4.1 Leakage Causes

Investigation of the causes for leaks revealed that leakage was generally attributable to one or more of the following:

1. Contamination (i.e., foreign material on sealing surfaces)
2. Defective sealing elements (i.e., scratches, cuts, etc.)
3. Improper assembly (e.g., shearing of seals)
4. Inadequate sealing surface (i.e., rough or scratched bores, seal grooves).

During the course of the Phase III program, leakage problems were resolved by an iterative process of; (1) leak checking/detection, (2) isolation of leak cause, (3) change in material, design or assembly technique, and (4) final leak checking.

Leakage attributable to contamination was resolved by increased attention to cleanliness procedures and requirements and by elimination or improved processing of micro-sealed surfaces.

Defective sealing elements resulted in a few leakage problems. Some Bal-seals and Omniseals were found to have small scratches or imperfections on the sealing lips which resulted in leakage after assembly. These defective parts were not detected in Receiving Inspection, since when received these items were classified in the small hardware category (i.e., nuts, bolts, etc.). As a result of this problem, assembly technicians began to visually inspect every seal with a 5-power eye loupe prior to using the seal in a TCA assembly.

Improper installation of seals, subsequently resulting in leaks, was generally confined to: (1) excessive seal stretching when the seal was pulled over a land, and (2) shearing of seal lips upon assembly into a bore. The stretching problem was resolved by incorporating a procedure of heating the Teflon seals to 400 to 500°F and installing in the hot condition using a tapered-type installation tool. Shearing of seal lips was eliminated by using a "sizing" procedure on a seal before insertion in a bore. The "sizing" consisted of depressing the seal lips in a cylindrical tool whose I.D. is slightly less than the seal O.D.

The need for very smooth metal surfaces in contact with sealing elements was recognized in Phase II testing, and as a result surface improvements were incorporated into the Phase III TCAs (see paragraph 4.1.4.3).

4.1.4.2 Leakage Criteria

Leak testing has shown that, for the TCA to exhibit zero external propellant leakage, it is not necessary to comply with the 10 scc/hr helium leakage requirement at 500 psig (see paragraph 4.1.3). Though compliance with this helium leakage requirement assures zero propellant leakage, 10 psi/hr pressure decay can be exceeded without subsequent propellant leaks.

For example on MIRA 150A-001, TCA leak checking of the HEA revealed a total SOV poppet leakage of 70 scc/hr of helium at 500 psig. An additional check using water at 700 psig was conducted, and after one hour there were no visible leaks. The TCA was subsequently, pressurized with propellants at 720 psig, and there were no visible leaks.

Complete evaluation of the leakage criteria and determination of an allowable helium leakage that is equivalent to zero propellant leakage was not made. Indications are that propellant leakage will not be encountered if the item exhibits a helium leakage of 100 scc/hr at 500 psig. Qualitative leak checking(using Leak-Tec) of paths such as SOV vent holes, flow control valve pintles, etc., indicated that a bubble formation of approximately one bubble per second (using nitrogen at 720 psig) is acceptable to the extent that the path will not leak propellants.

The need for a leak-free CC & NA is also not believed to be mandatory, since within-specification firings have been performed on chambers which did leak prior to firing.

4.1.4.3 Design Considerations

To achieve a leak-free seal between a metal surface and a sealing element the smoothness of the metal surface is very important. Thermal effects on Teflon seals cause the surface finish to be even more important when sealing is to be accomplished at low temperatures. Experience gained with TCA S/N-001 through -006 resulted in refinement of surface finishes on the Phase III TCAs S/N-007 and subsequent. This is shown in the following table:

Seal Application	Surface Finish of Metal Parts (RMS per MIL-STD-10)	
	HEA S/N 001 thru 006	HEA S/N 007 and Subsequent
Dynamic Sealing of Propellants	8-16	4
Static Sealing of Propellants	16-32	8

In addition to surface finish refinements, surface processing methods were also improved for Phase III TCAs. The use of micro-seal (a dry film lubricant) was minimized in Phase III units, and this material was used only in those areas where galling is a definite possibility because of extremely small clearances (e.g., in the flow control valves and injector). Where microseal was used, the surface was subsequently highly burnished in order to avoid flaking of material which could buildup on seals and cause leaks.

It is important to note that in conducting in-process type leak checks, significantly fewer leaks were encountered with Phase III TCAs than with Phase II units (HEAs-001 thru 006). There were no failure reports due to leakage against a Phase III TCA.

4.2 HEA Calibration

The Head End Assembly Calibration Stand, described more fully in section 8.0, was developed for the purpose of measuring and adjusting HEA flow and pressure drop characteristics during fabrication. The goal was to achieve complete HEA calibration with water flow thereby minimizing the number of static firings required to prepare a TCA for delivery.

In addition to serving as a calibration tool, the HEA stand also proved most useful in diagnosing and correcting fabrication and design problems.

The experience and data obtained with this stand during the Phase III is summarized herein. By the end of the program, a total of five Phase II HEAs (S/N-001,-002,-004, -005, and -006) and five Phase III HEAs (S/N-007 through -011) were calibrated on the stand at least once and subsequently static tested at the Inglewood Rocket Test Site (IRTS). Detailed test data is provided in Figures E-1 through E-8 of Appendix E. In developing the final calibration procedure, a matching technique was used. This procedure consisted of first calibrating a standard HEA by means of static firing. Without changing any settings the standard HEA was then completely characterized on the stand with water flow. Subsequent HEAs were then matched to the standard HEA.

Experience gained with this testing demonstrated the feasibility of using a water flow calibration technique to measure primary HEA performance parameters and to allow their proper adjustment without injector gap setting without resorting to a static firing. Even in early testing, before the calibration technique was fully developed, firing data from water calibrated HEAs indicated that in many instances no resettings were required.

The HEA Calibration Stand alcohol subsystem, required to simulate the servoactuator hydraulic supply, was not completed until late in Phase III. As a result, only limited data are available on the servoactuator setting operations performed during a complete HEA calibration.

Table 4.2-1 provides a summary of the HEA calibration data for HEAs S/N-008 and -009, the only two HEAs that underwent a complete calibration. Table 4.2-2 provides the static firing data from tests conducted on these two HEAs without readjustments between water calibration and firing. Figures 4.2-3 and 4.2-4 provide a comparison of these data.

Table 4.2-1

MIRA 150A HEA Calibration Data

HEA S/N	Servoactuator Signal (ma)	Pinlet (psig)	$\dot{M}_{ox}$* Water Flow (lbs/sec)	$\dot{M}_{f}$* Water Flow (lbs/sec)	Mixture Ratio (o/f)	Δ Pox (psi)	Δ Pf (psi)
008	-80.6	722	0.0528	0.0458	1.154	30	25
	-70.4	720	0.0611	0.0528	1.158	34	28
	-48.4	718	0.0903	0.0778	1.160	46	34
	-25.4	716	0.1305	0.1125	1.160	61	42
	- 0.4	714	0.1652	0.1445	1.144	71	47
	+24.8	715	0.2013	0.1721	1.171	83	52
	+47.8	714	0.2318	0.1986	1.167	92	57
	+70.2	714	0.2595	0.2222	1.167	100	62
	+80.4	714	0.2722	0.2332	1.168	104	64
009	-80.6	722	0.0501	0.0426	1.175	33	21
	-70.6	720	0.0528	0.0456	1.158	35	23
	-45.4	718	0.0973	0.0834	1.166	52	33
	-25.4	716	0.1292	0.1111	1.163	64	39
	- 0.3	714	0.1666	0.1444	1.155	75	46
	+24.9	712	0.2055	0.1763	1.165	86	53
	+45.1	710	0.2348	0.2012	1.167	94	57
	+70.2	710	0.2694	0.2320	1.162	103	64
	+80.2	711	0.2780	0.2388	1.164	106	66

*Indicated water flow in lbs/sec obtained by converting from gal/min measured on HEA Calibration Stand.

Table 4.2-2

MIRA 150A HEA Performance Data

HEA S/N	Servoactuator Signal (Ma)	$\dot{M}_{ox}$ (1) (lbs/sec)	$\dot{M}_{f}$ (1) (lbs/sec)	Mixture Ratio (o/f)	Pch (psia)	C* (fps)
008	-80.0	0.0641	0.0428	1.499	21.0	4938
	-50.4	0.1033	0.0692	1.494	34.8	5077
	-35.6	0.1326	0.0879	1.509	45.5	5192
	- 0.6	0.1975	0.1318	1.499	69.8	5332
	+35.4	0.2585	0.1727	1.497	92.1	5382
	+71.0	0.3132	0.2113	1.482	111.9	5378
	+78.6	0.3243	0.2205	1.470	115.8	5359
009	-79.4	0.0628	0.040	1.554	19.9	4807
	-49.6	0.0998	0.0655	1.524	32.4	4904
	-34.4	0.1305	0.0857	1.522	44.5	5139
	+ 0.6	0.1992	0.1326	1.502	70.3	5300
	+35.8	0.2663	0.1770	1.505	93.9	5304
	+71.4	0.3240	0.2180	1.486	115.0	5314
	+81.4	0.3327	0.2223	1.496	117.8	5315

(1) Data corrected to standard inlet conditions.

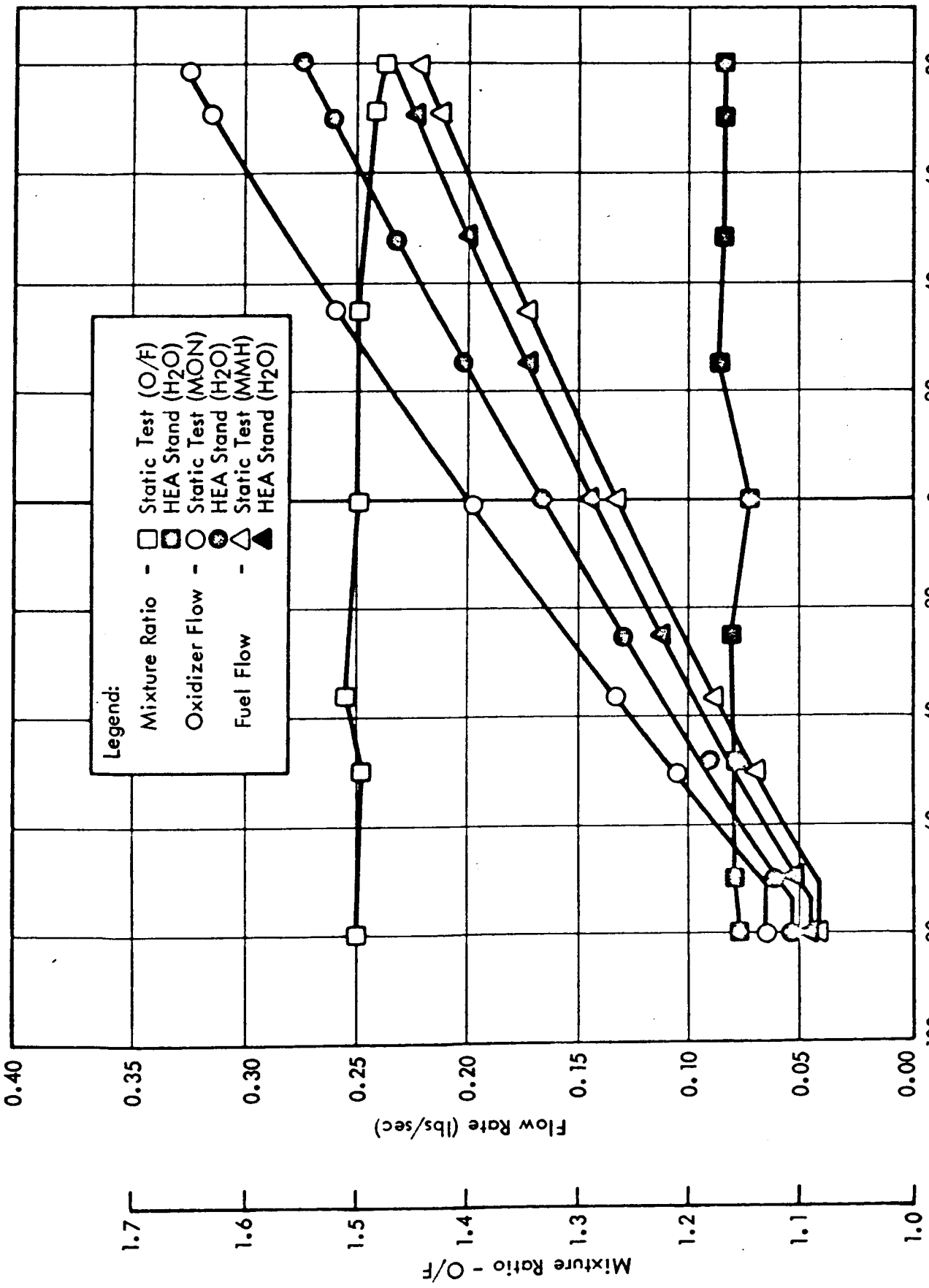

Figure 4.2-3. Comparison between Water Calibration and Static Firing Data for HEA S/N 150A-008

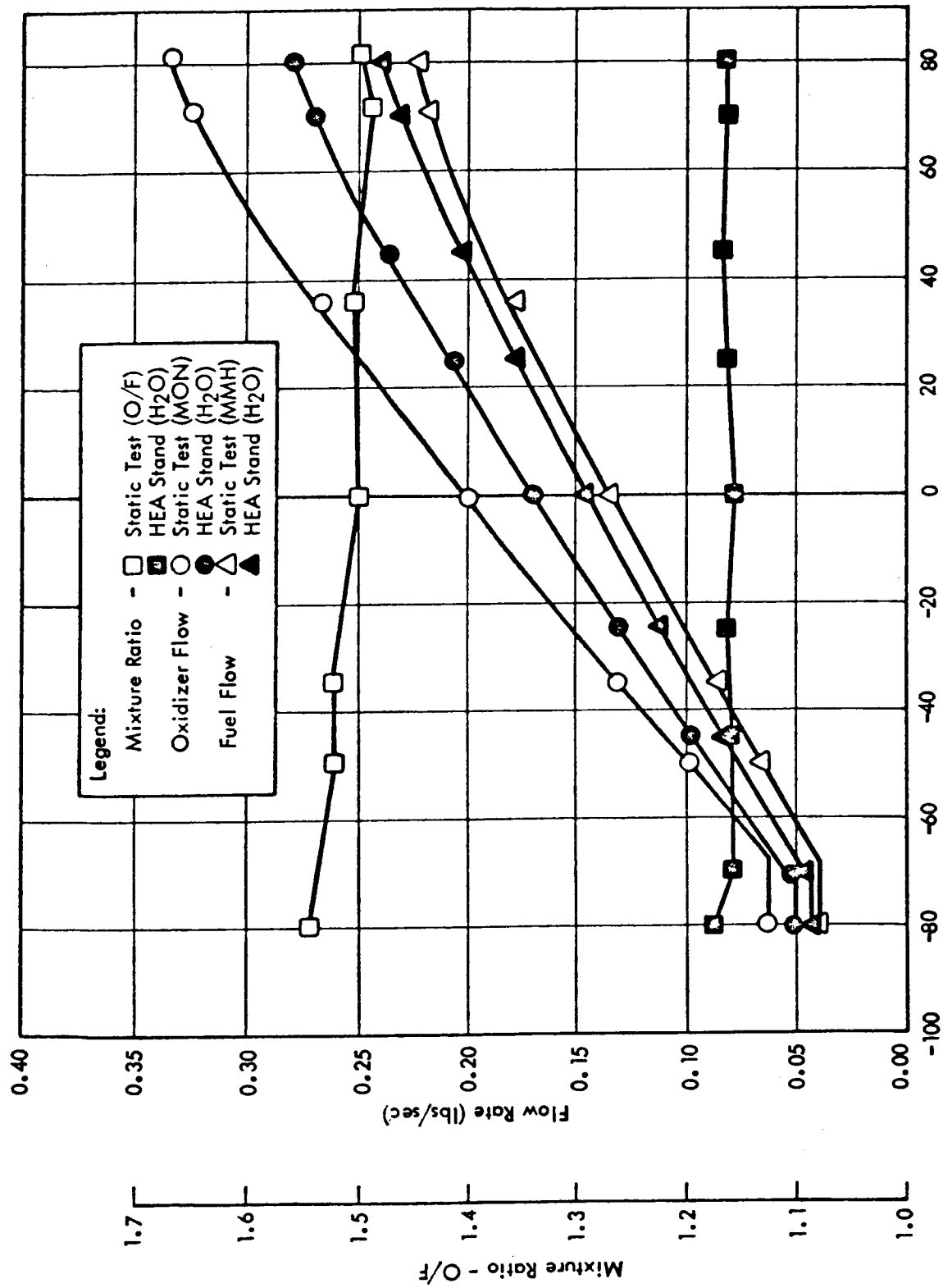

Figure 4.2-4. Comparison between Water Calibration and Static Firing Data for HEA S/N 150A-009

4.3 HEA Ablative Throat Test

HEA ablative throat tests were conducted in accordance with STL Acceptance Test Specification TS3-01B. This test followed the HEA calibration (paragraph 4.2) and was conducted prior to the HEA performance test (paragraph 4.4).

The test consisted of a 200-second maximum thrust sea level static firing with the HEA mated to a water-cooled combustion chamber (Part No. 106694) that incorporates an ablative throat insert.

The objectives of the test were to demonstrate that: (1) the combustion characteristics of the HEA and the resultant heat transfer to the chamber were acceptable, and (2) that there was no nonuniform distribution of propellants in the injector spray pattern.

Objective (1) is determined by the change in throat area as evidenced by chamber pressure changes under the constant propellant flow rate conditions of the test. Any decrease in chamber pressure indicates an increase in throat area. Any throat area increase is cause for rejection.

Objective (2), propellant distribution uniformity is measured in terms of maintenance of throat symmetry. This is determined by change in the initial throat radius and the shape of the throat after firing. Any increase in radius (using the original throat center and radius as reference) is cause for rejection. The resultant post-test allowable out of roundness is determined first by locating the maximum post-test throat diameter, D_{max}, and the diameter at right angles to it, $D_{\perp}$, then measuring the two, and finally computing $\frac{D_{max} - D_{\perp}}{D_{initial}}$. If this ratio is greater than 0.05, the HEA is not accepted without rework and/or retest.

The piece-to-piece reproducibility of the ablative throat insert material must be maintained at a high level. Therefore, the ablative throat material is procured to the same material specification used for the liners in the flight CC & NA.

During Phase III, a total of nine different Phase II and Phase III HEAs were tested with ablative throats in accordance with the Acceptance Test Specification TS3-01B. The results of these tests are summarized in Table 4.3-1. Typical ablative throats after firing are shown in Figure 4.3-2. These photographs show inlet and exit views of throats tested on two different HEAs, one being acceptable and the other being not acceptable. Circles are drawn to show the original diameter of the throat before firing. A mark is placed at the bottom of each throat insert indexed to the oxidizer inlet passage.

Of the nine HEAs tested, three failed to pass the acceptance criteria. Each of the three nonacceptable tests were run at abnormal fuel injection pressure drops, ΔP_F, as discussed in paragraph 6.2.2. Two of the failed HEAs (S/N-009 and -010) were later re-tested at normal fuel injection pressure drops and successfully passed the acceptance criteria for the ablative throat test. The third failed HEA was not available for retesting.

Table 4.3-1

MIRA 150A HEA Ablative Throat Acceptance Tests

Conditions for All Tests:

200 seconds at maximum thrust

Nominal P_c = 110 psia, M.R. = 1.5 ($\dot{M}_o/\dot{M}_f$)

Flow rates constant within ± 2%

Initial throat diameter, $D_{initial}$, = 1.00 in.

Acceptance Criteria: (Specification TS3-01B)

A. No increase in throat area

B. No increase in throat radius

C. $\frac{D_{max} - D_{\perp}}{D_{initial}} \leq 5\%$

HEA S/N	ΔP_F (psi)	Area Change (%)	D_{max} (in)	$D_{\perp}$ (in)	$\frac{D_{max} - D_{\perp}}{D_{initial}} \times 100$ (%)	Accept or Reject
001 Phase II	59	+7.6	0.90	0.88	2	Accept
002 Phase II	71	+4.3	0.90	0.90	0	Accept
004 Phase II	62	+6.1	0.88	0.86	2	Accept
005 Phase II	71	-8.4	0.89	0.85	4	Accept
007 Phase III	85**	-7.4	0.92	0.86	6*	Reject, C > 5%
008 Phase III	62	-9.3	0.90	0.86	4	Accept
009 Phase III	76**	+5.0	0.94	0.88	6*	Reject, C > 5%
009 (Repeat)	63	-14.5	0.88	0.84	4	Accept
010 Phase III	82**	+0.9*	1.02*	0.91	11*	Reject A&B increased, C>5%
010 (Repeat)	60	+11.6	0.88	0.84	4	Accept
011 Phase III	59	+9.8	0.89	0.86	3	Accept

*Nonacceptable value.

**Abnormal ΔP_F - see paragraph 6.2.2 for discussion.

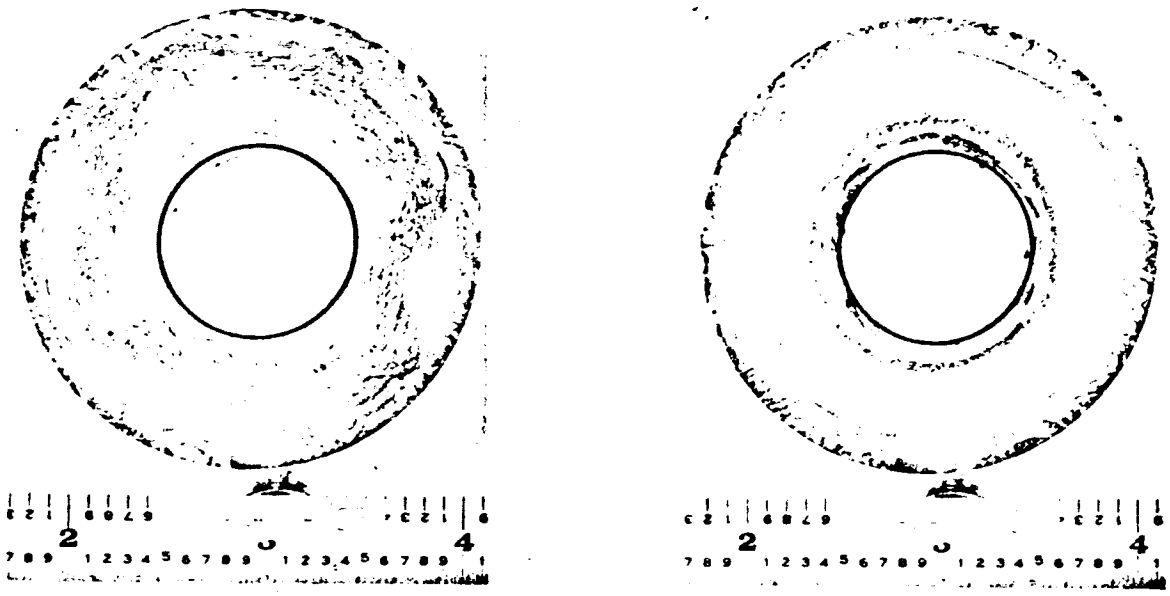

Inlet Exit

150A S/N 008 - Acceptable

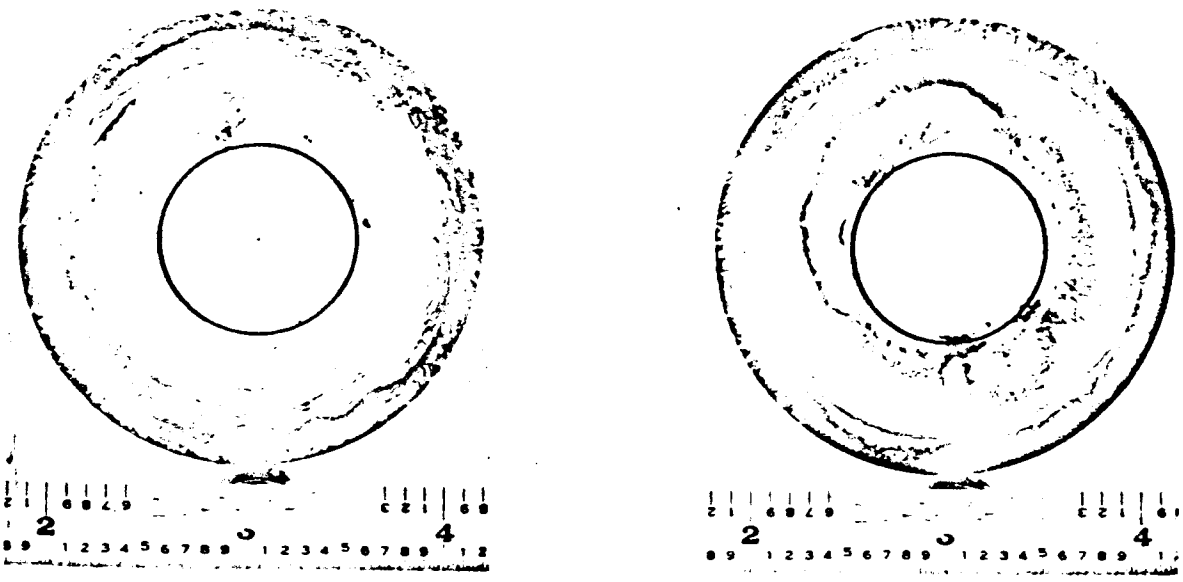

Inlet Exit

150A S/N 010 - Not Acceptable

Figure 4.3-2. Typical Ablative Throats After Acceptance Firing

4.4 HEA Performance Test

The HEA performance test, defined by STL Acceptance Test Specification TS3-01B, is normally conducted immediately after the HEA ablative throat test described in paragraph 4.3, and prior to the TCA vibration test discussed in paragraph 4.5. The objective of the test is to demonstrate the acceptability of the HEA steady-state and dynamic performance characteristics. This thrust cycle was modified during the course of Phase III by adding several large steps near the end of the cycle for dynamic response analysis.

The test consists of a 130-second, sea level static firing with the HEA mated to a water-cooled CC & NA. The thrust cycle used for these firings is prerecorded on magnetic tape and is given in Table 4.4-1. Primary performance parameters determined by this test include characteristic velocity, chamber pressure, propellant flow rates, mixture ratio, thrust versus servoactuator signal, 5-cps signal dynamic response, large step signal-thrust response, thrust-signal hysteresis loop width, and startup and shutdown transients.

During Phase III, a total of eight HEA performance firings were completed with seven different Phase II and Phase III HEAs. The detailed test data is presented in Tables D-2-20 and D-2-21 of Appendix D-2 and also in paragraph 6.7. Table 4.4-2 presents a typical summary of data acquired during this test and entered in the TCA Log Book (see paragraph 3.1.6).

The characteristic velocity data obtained early in the acceptance test program were somewhat lower than the more recent data. As a result of investigation of a characteristic velocity data bias between the JPL/ETS and IRTS test sites with HEA S/N 001, a data reduction and measurement discrepancy were discovered which had resulted in erroneously lowering the reported characteristic velocity data during the earlier testing.

Table 4.4-1

AT-1 Thrust Cycle (Modified)

Command, (± .5)		Time From Startup, (± .1)
0	Step	-10.0
0	Startup	0.0
+35	Step	5.0
+70	Step	10.0
+35	Step	15.0
0	Step	20.0
-35	Step	25.0
-80	Step	30.0
-50	Step	35.0
-35	Step	40.0
0	Step	45.0
+7.5	Step	50.0
-7.5	Step	52.0
0	Step	54.0
0 ± 7.5	Sinusoidal, 5 cps	54.2
0	Step	59.0
+70	Step	60.0
+55.0	Step	62.0
+62.5	Step	64.0
+62.5 ± 7.5	Sinusoidal, 5 cps	64.2
+62.5	Step	69.0
-47.5	Step	70.0
-32.5	Step	[illegible]
-40.0	Step	74.0
-40.0 ± 7.5	Sinusoidal, 5 cps	74.2
-40.0	Step	79.0
+80.0	Step	80.0
-40.0	Step	82.0
-40.0 to +70.0	Ramp	84.0 - 94.0
+70.0 to -40.0	Ramp	94.0 -104.0
0	Step	104.0
0 to + 15.0	Ramp	105.0 - 107.0
+15 to 0	Ramp	107.0 - 109.0
0	Step	109.0
-80	Step	112.0
+70	Step	113.0
-70	Step	118.0
+70	Step	118.1
-70	Step	118.6
+70	Step	118.8
-70	Step	119.8
+70	Step	120.3
-70	Step	122.8
+70	Step	123.8
-62.5	Step	128.8
0	Step	129.0
0	Shutdown	130.0

Table 4.4-2

HEA Acceptance Test Firing Log

Test HEA Acceptance Test Document TS3-01 Date 15 September 1964

HEA Serial No. 150A-007 Rev. No. B

Date Performed 3 November 1964 Input Tape No. AT-1M Output Tape No. 162

Test No. C2-621 Test Engineer B. Wallace Inspector No. 32

Parameter	Signal Level	Required	Measured	Accept	Reject
I_{sp}	+ 70 MA	285 sec	291	X	
I_{sp}	+ 35	283.7	289.7	X	
I_{sp}	0	282.5	289.3	X	
I_{sp}	- 35	270.5	277	X	
I_{sp}	- 50	262	267	X	
Mixture Ratio (Std)	+ 70	1.5 ± 0.03	1.470	X	
	+ 35	1.5 ± 0.03	1.474	X	
	0	1.5 ± 0.03	1.484	X	
	- 35	1.5 ± 0.03	1.497	X	
	- 80	1.5 ± 0.03	1.494	X	
Thrust Envelope	- 40 to + 70	per Spec		X	
Phase Lag	60 ± 7.5	28°	15	X	
	0 ± 7.5	28°	16	X	
	- 45 ± 7.5	28°	13	X	
Step Response Time	- 40 to +80MA	< 0.065 sec.	0.048	X	
	+ 80 to -40MA	< 0.065	0.036	X	
Start Impulse	0 MA	1.9 ± 1.4	2.0	X	
Thrust Buildup Time	0 MA	< 0.130	0.076	X	
Shutdown Impulse	0 MA	2.8 ± 1.4	4.2	X	
Shutdown Time	0 MA	< 0.065	0.04	X	

These discrepancies affected the HEA performance data reported for IRTS Runs C2-548 through C2-585 conducted as part of acceptance testing. JPL/ETS and IRTS test data after Run C2-585 were not affected.

Table 4.4-3 summarizes the results of the HEA performance tests. It may be noted that the acceptance criteria defined by Acceptance Test Specification TS3-01B were not entirely met during some of the firings. HEA 150A-004 failed the specific impulse criteria when tested with N_2O_4. Subsequent tests at IRTS and JPL/ETS showed a significant performance improvement when MON was used as the oxidizer and would have resulted in acceptable performance for HEA 150A-004.

Both HEA 150A-004 and 150A-005 fell below certain portions of the thrust-signal acceptance envelope. The use of MON as the oxidizer would have brought HEA 150A-004 within acceptance limits. Correcting for the previously mentioned C* error would bring the 150A-005 thrust-signal curve within the allowable envelope. Only two HEAs (S/Ns 005 and 007) passed the 1.50 ± 0.03 standard mixture ratio criteria. The specification tolerance was tightened from a previous value of 1.50 ± 0.05 after it was discovered that the mixture ratio variability with temperature was greater than expected (see paragraph 6.5). Since all of these HEAs were calibrated to the earlier limits, many of them did not meet the newer criteria. However, only HEA 150A-004 could not have been recalibrated to meet specification requirements. Rework of the flow control valve would have been required on S/N 004.

Both HEA 150A-001 and -005 failed the step response requirement when tested with Phase II Follow-on servoactuators. No HEA has failed this criteria when tested with the improved Phase III servoactuator. HEA 150A-002 exceeded the startup impulse upper limit by only 0.1 lb-seconds, and probably could have been brought within specification limits by substitution of a different helium pilot pilot valve or new shutoff valve parts. HEA 150A-005 failed both the shutdown time and impulse criteria because of sluggish helium pilot valve operation. Subsequent investigation revealed severe valve corrosion caused by inadequate surface plating. A helium pilot valve design improvement corrected this situation. No HEAs failed the phase lag or startup time requirements.

Table 4.4-3

HEA Performance Acceptance Test Summary

HEA S/N	Steady-State Performance			Dynamic Response Performance					
	I_{sp} (1)	Mixture Ratio (1)	Thrust Envelope	Step Response (1)	Phase Lag (1)	Startup Time	Startup Impulse (1)	Shutdown Time (1)	Shutdown Impulse (1)
150A-001	Pass	Fail	Pass	Fail	Pass	Pass	Pass	(1)	(1)
150A-002	Pass	Fail	Pass	Pass	Pass	Pass	Fail	Pass	Pass
150A-004	Fail	Fail	Fail	Pass	Pass	(2)	(2)	Pass	Pass
150A-005	Pass	Pass	Fail	Fail	Pass	Pass	Pass	Fail	Fail
150A-007	Pass	Pass	Pass	Pass	Pass	Pass	Pass	Pass	Pass
150A-008	Pass	Fail	Pass	Pass	Pass	Pass	Pass	Pass	Pass
150A-009	Pass	Fail	Pass	(2)	(2)	(2)	(2)	(2)	(2)

NOTES: (1) For required value see Table 4.4-2.

(2) Data not reduced.

4.5 TCA Vibration Test

The TCA vibration test was conducted in accordance with STL Acceptance Test Specification TS3-01B and was then followed by a leak check and a final TCA acceptance firing test (paragraph 4.6) in the acceptance test series. The vibration test setup is illustrated in Figures 4.5-1 and 4.5-2 showing the TCA installed on the shaker.

During the vibration test, the servoactuator control cavities were filled with alcohol and the external ports were capped. The TCA propellant passages were filled with water and pressurized to 300 ± 20 psig by means of a regulated gaseous nitrogen pressure source. A control accelerometer was mounted on the test fixture and the output was recorded on an X-Y plotter. No other instrumentation was required.

The vibration spectrum is illustrated in Figure 4.5-3. It consisted of two variable frequency sine wave sweeps of three minutes duration each along each of three mutually perpendicular axes (along the thrust axis, the trunnion axis, and the axis perpendicular to the first two). During and after the vibration test visual inspections were made for evidence of structural damage or leakage. At the completion of the vibration test, a thorough leak check was performed prior to subjecting the TCA to the final acceptance firing.

During Phase III, a total of four different TCAs were subjected to the vibration test. These included TCA S/Ns 001, 002, 005 and 007. No post-vibration difficulties were encountered with TCA S/N 001. This unit successfully completed the prequalification test program without hardware replacement or calibration readjustments (see paragraphs 6.6 and 6.9). After the vibration test, TCA S/N 002 exhibited a fuel leak in the torque motor static seal of the Phase II Follow-on servoactuator. Design changes were initiated for all Phase III servoactuators to correct this failure mode (reference paragraph 6.12.1.2).

Following the vibration test of TCA S/N 005, both the flow control valve pintle jam nuts and the servoactuator jam nuts were found to be loose resulting in a TCA performance shift during the TCA acceptance firing test (see paragraph 4.6). This problem was traced to inadequate torque in tightening these nuts, and resulted in a fabrication procedural change to preclude a recurrence.

Problems were also encountered during vibration testing of TCA S/N 007. The post-vibration firing (discussed in paragraph 4.6) exhibited a significant chamber pressure shift downward for a given servoactuator signal. The difficulty was traced to a servoactuator null shift. It was found that the torque motor cover screws were loose. A design change incorporating more stringent torque and lockwire requirements was immediately accomplished (reference paragraph 6.12.2). The null shift had also been noted on other Phase III servoactuators which had not been subjected to vibration. This problem was traced to spring design deficiencies (further detail is given in paragraph 6.12.2). A servoactuator spring design change was incorporated. Design verification of this change was demonstrated in Prequalification Test -011 wherein TCA S/N 008 was successfully subjected to "qualification" vibration levels that were well in excess of the acceptance test levels. (See paragraph 6.10.2 for discussion of this test.)

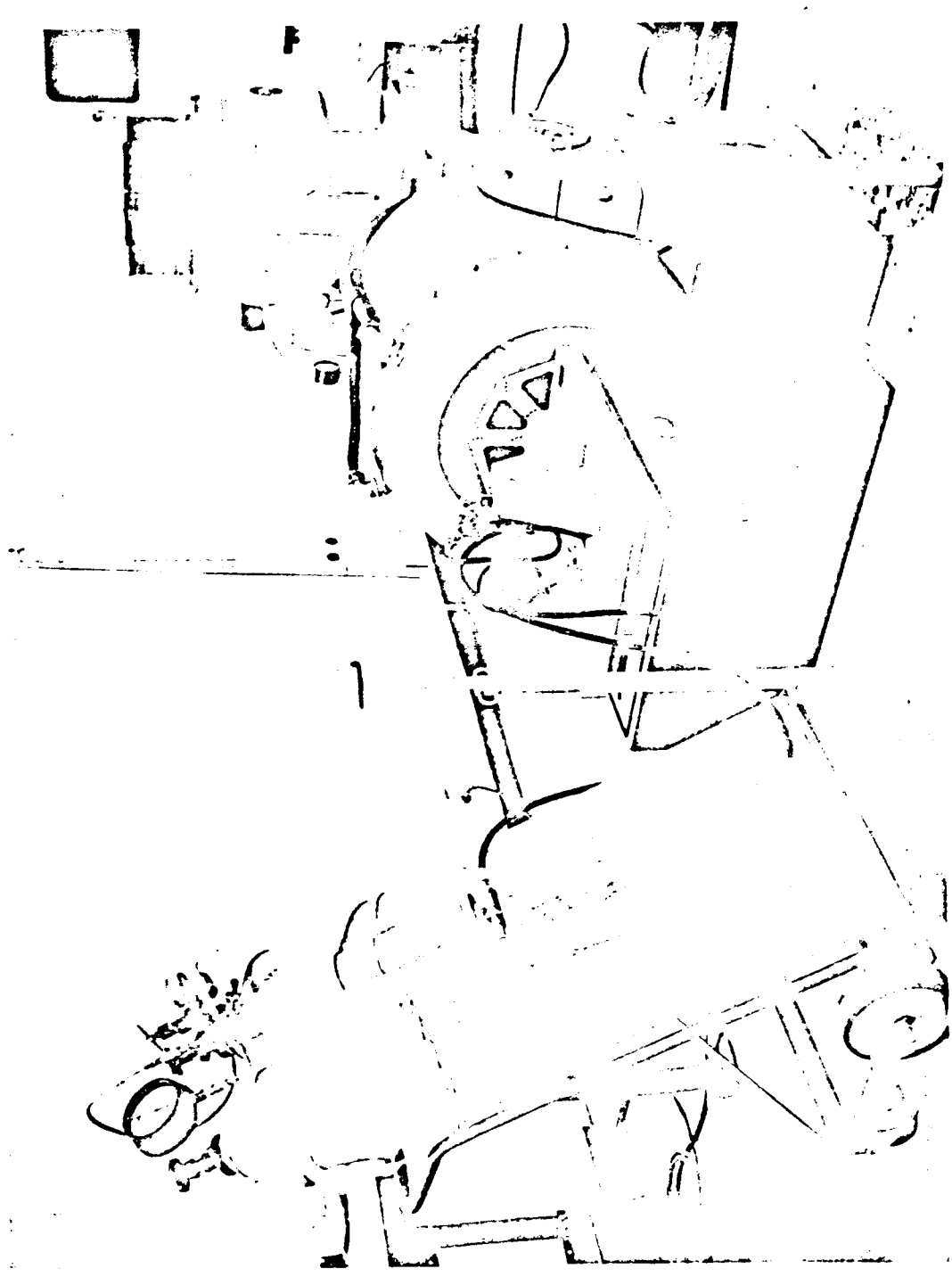

Figure 4.5-1. Acceptance Vibration Test Setup

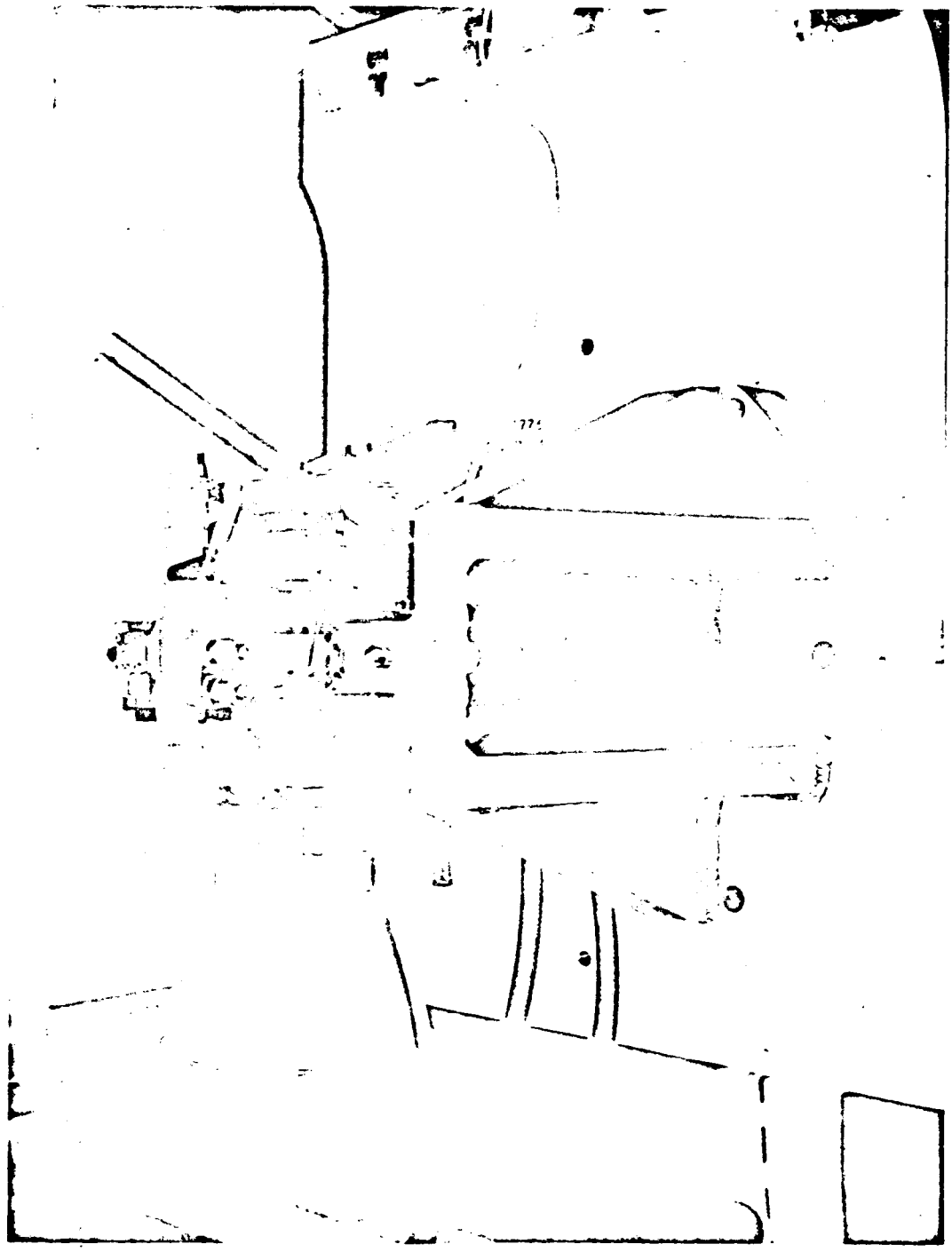

Figure 4.5-2. Acceptance Vibration Test Setup - Closeup

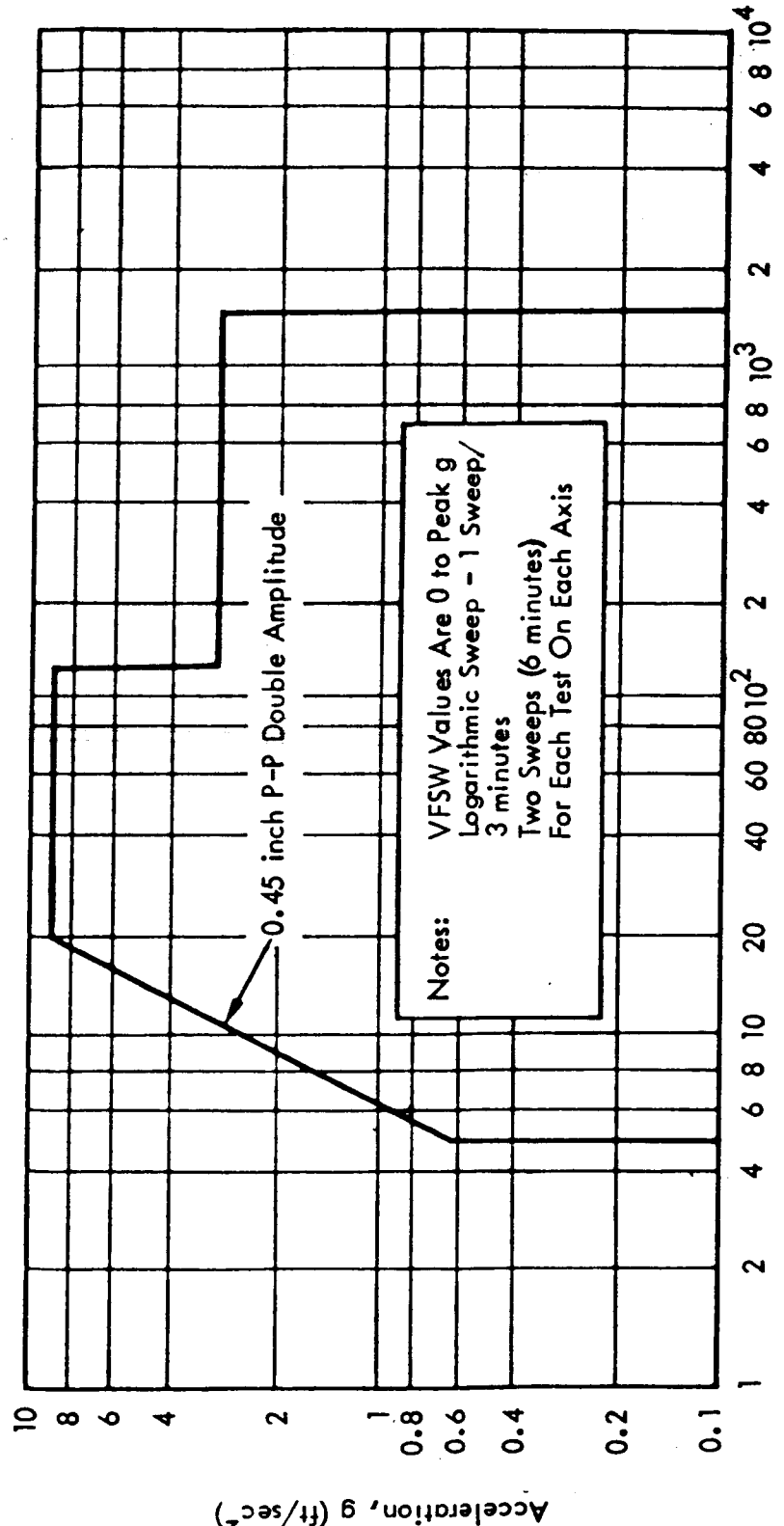

Figure 4.5-3. Acceptance Test Vibration Levels

4.6 TCA Acceptance Firing Test

The TCA acceptance firing test, conducted in accordance with STL Acceptance Test Specification TS3-01B, was performed immediately after the TCA vibration test (paragraph 4.5) in the acceptance test series. The test consisted of a 12-second programmed hot firing test at sea level on the complete TCA. The thrust-time profile used is shown in Table 4.6-1.

The objective was to verify HEA performance after the TCA vibration test and to check on the quality of the CC & NA.

Three complete TCAs were subjected to the TCA acceptance test. Tests on two of the TCAs (S/Ns 005 and 007) were invalid because of loose adjustment screws on the HEA and servoactuator. Remedial action was initiated as outlined in paragraph 4.5.

The TCA acceptance firing test on TCA S/N 001 was successfully completed on 23 September 1964. Relationships among characteristic velocity, mixture ratio, chamber pressure, specific impulse, thrust, and servoactuator command are presented in Figures 4.6-2, 4.6-3, and 4.6-4. Data from the previbration HEA performance test are also shown in these figures to present a direct comparison of HEA performance characteristics before and after vibration. These data, plus the phase lag between signal and actuator position for the 5-cps servoactuator signal, showed acceptable post-vibration HEA performance. Both the test data and the post-firing inspection verified the acceptability of the CC & NA (S/N 003). Thus, TCA S/N 001 passed all the TCA acceptance requirements of STL Specification TS3-01B.

Table 4.6-1

AT-2 Thrust Cycle Profile

Command (milliamps ± .5)		Time From Startup (sec ± .1)
0	Step	-10.0
0	Startup	0.0
+70	Step	3.0
-80	Step	5.0
-50	Step	7.0
0	Step	9.0
0 ± 7.5	Sinusoidal, 5 cps	9.5
0	Step	11.5
0	Shutdown	12.0

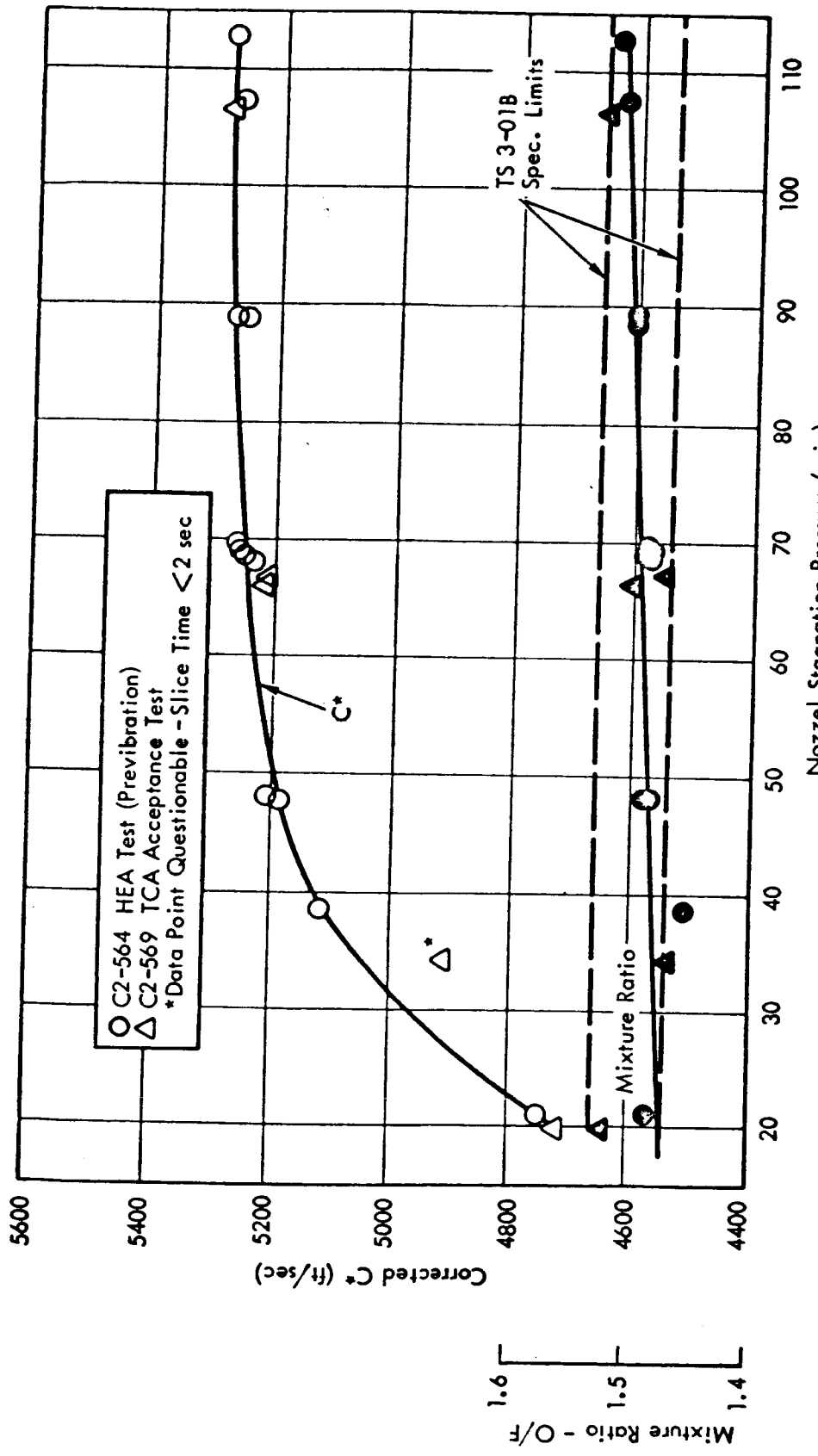

Figure 4.6-2. TCA Acceptance Test Data on C* and MR for MIRA 150A S/N 001

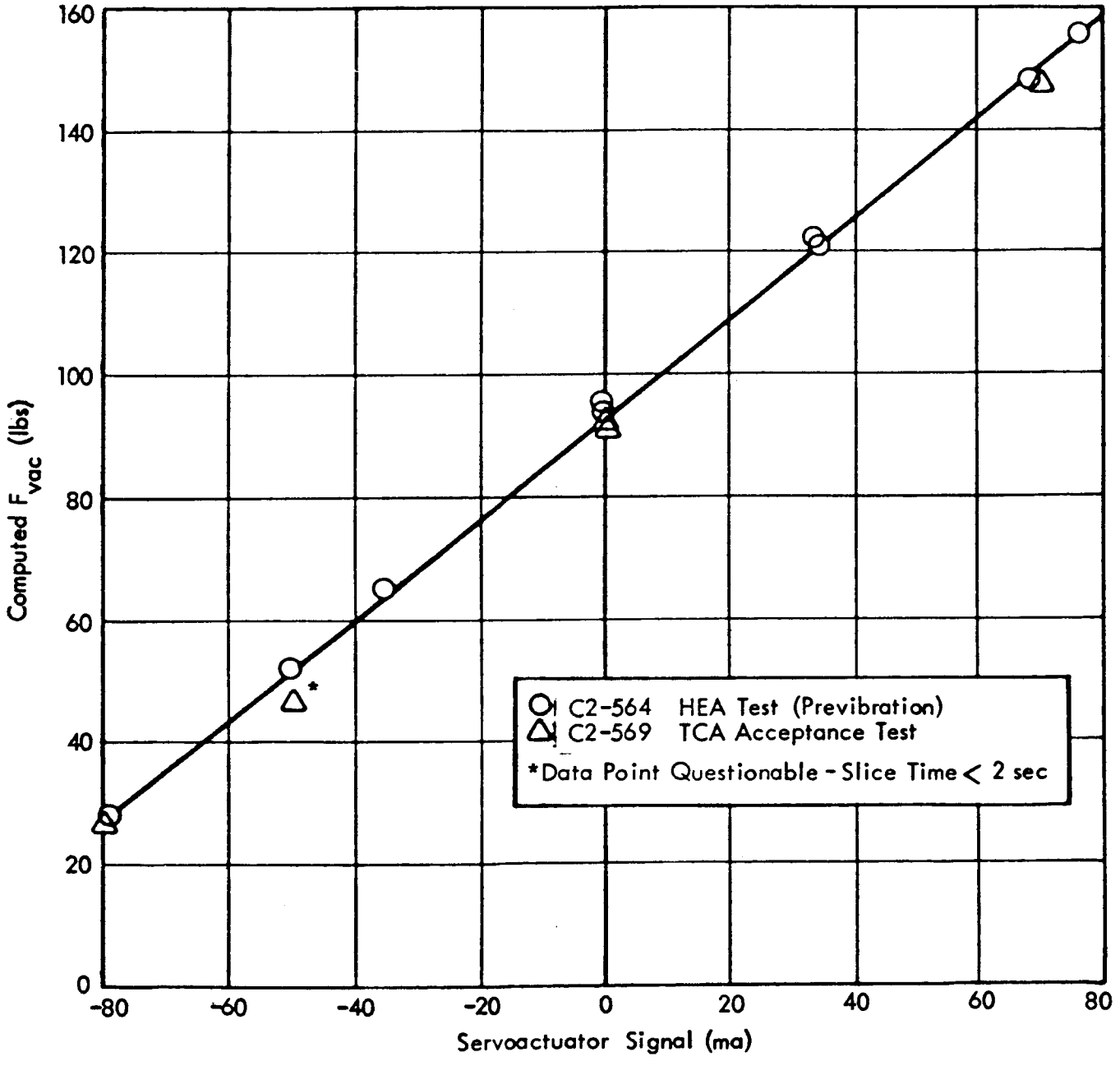

Figure 4.6-3. TCA Acceptance Test Thrust Data for MIRA 150A S/N 001

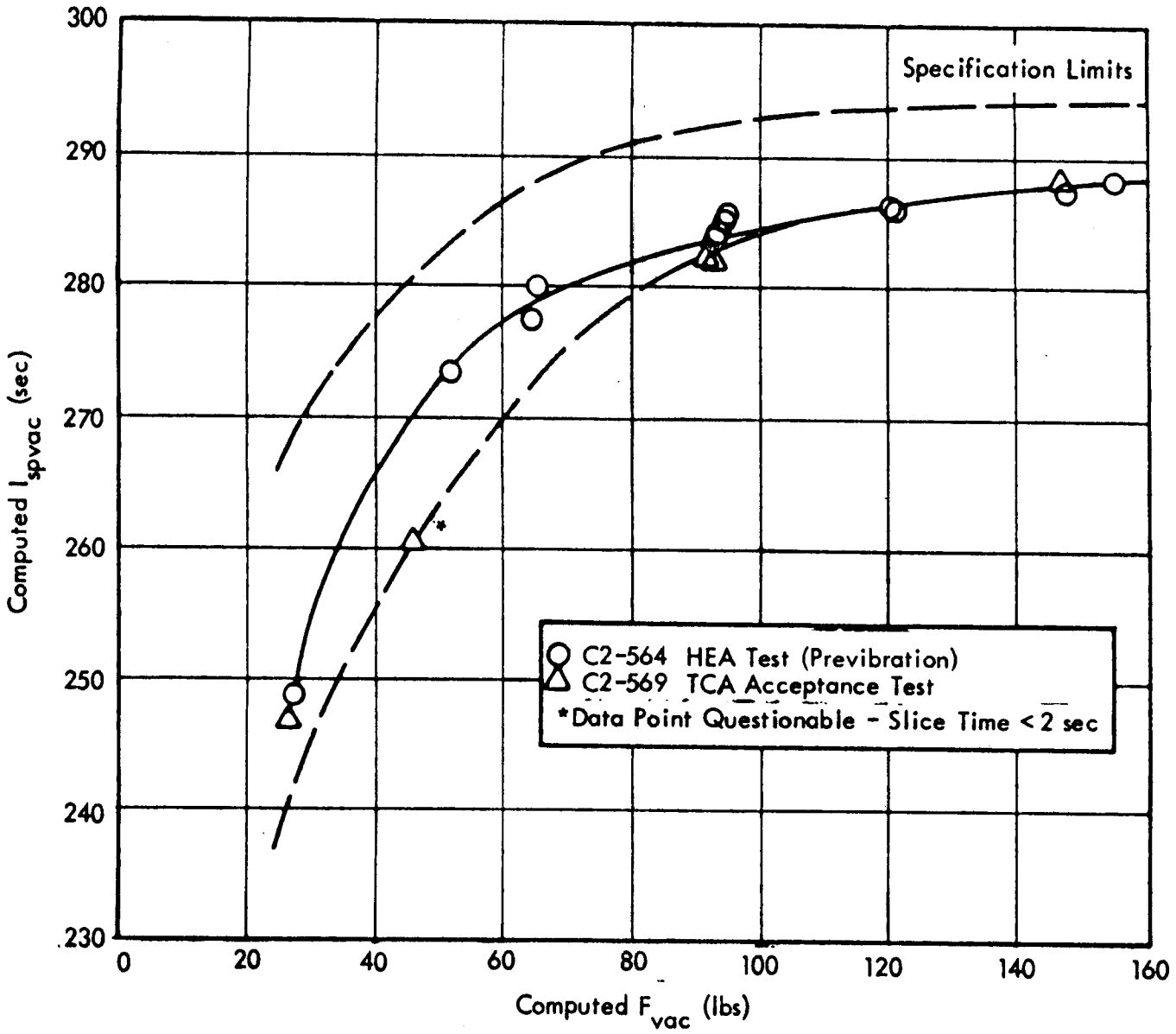

Figure 4.6-4. TCA Acceptance Test Data on I_{sp} for MIRA 150A S/N 001

5.0 NONFIRING DEVELOPMENTAL EFFORT

Nonfiring testing accomplished during Phase III included component functional acceptance testing, other component evaluations and vacuum tests in the laboratory. Also, effort was expended in design studies that were involved with the servoactuator and related power systems. These areas of effort are discussed in this section.

5.1 Component Subassemblies - Functional Acceptance Testing

As part of STL company standard practice, all incoming parts were subjected to receiving inspection. In addition, component subassemblies delivered by vendors as complete units were functionally acceptance tested in an "As Received" condition in accordance with the applicable procurement specification and associated acceptance test procedural document. The three component subassemblies receiving acceptance tests were the electrohydraulic servoactuator, the helium pilot valve, and the propellant filter. These subassemblies are listed below with their corresponding acceptance testing procedures and specifications.

Subassembly	Specification No.	Accept. Test Doc. No.
Electrohydraulic Servoactuator	EQ 2-42	9354.4-255
Helium Pilot Valve (Solenoid-Operated, Three-Way Valve)	EQ 2-25	ETD-MIRA-3R1-001
Propellant Filter	EQ 1-73	ETD-MIRA-4R1-001

5.1.1 Servoactuator

The servoactuator (S/A) was acceptance tested in accordance with STL Document No. 9354.4-255. In Addition to the S/A acceptance test results discussed below; S/A experience of any unusual nature occurring after acceptance is discussed in paragraph 6.12.

5.1.1.1 Test Setup

Required S/A acceptance test measurement tolerances are given in Table 5.1.1-1. The servoactuator MMH test stand is shown in Figures 5.1.1-2 and -3. The stand includes a complete MMH recycling pressurization and supply system capable of supplying fuel at the required flows and pressures. A servoactuator load fixture was designed and constructed to simulate TCA induced loads. These loads consisted of a pressure area load simulated by a spring and a superimposed friction load simulated with an electromagnetic friction brake.

The Surveyor servoamplifier design schematic was used as a basis for the construction of laboratory test servoamplifiers. These amplifiers incorporate dither oscillators to simulate the spacecraft-imposed dither signal.

5.1.1.2 Servoactuator Acceptance Test Results

5.1.1.2.1 Phase II Follow-on Servoactuators - Acceptance tests were conducted on all six Phase II Follow-on servoactuators. Table 5.1.1-4 summarizes the internal leakage tests. Because these units were procured only for HEA and TCA development test purposes (rather than on deliverable TCAs), all units were found usable for subsequent testing. TCA dynamic response data was not obtained using any of these six S/As.

Table 5.1.1-1

Instrumentation Measurement Tolerances

Current	± 0.5 milliamperes
Displacement	± 2.3 milli-inches
Force	± 3.0 lbs
Resistance	± 0.4 ohms
Inductance	± 10 millihenries
Pressure	± 10 psi

Phase III Servoactuators

Acceptance tests were conducted on seven of the 18 Phase III servoactuators. Results are given in Table 5.1.1-5. Figure 5.1.1-6 illustrates a typical Phase III hysteresis curve.

Based on experience with earlier units, servoactuator S/Ns C55394, C55395, C55398, and C55390 were somewhat modified prior to delivery and acceptance.

Unit C55398 passed all tests.

Unit C55394 passed all tests with the exception of linearity and phase lag. The actuator failed the linearity requirement because the retract stop was reached at -69.5 ma instead of the -70 ma required. Phase lag at 5 cps was 22.5° at -60 ma, instead of the allowable 20° maximum.

Unit C55395 passed all requirements with the exception of amplitude ratio, which was as low as 0.95 compared to the 0.97 minimum specification value.

Unit C55390 passed all tests except frequency response. Amplitude ratio was as low as 0.91 and phase lags as large as 27°.

Units C55394 and C55395 were marginal in performance but were accepted after review of the test data. Actuator C55390 would have allowed the TCA to meet all systems requirements with the exception of amplitude ratio, which was 4% low. This actuator was also accepted by Material Review Board (MRB) action.

The remaining 14 Phase III units were not acceptance-tested at STL but received similar testing at the vendor's plant.

5.1.2 Propellant Filter

Acceptance testing of propellant filters procured to STL Specification EQ 1-73B, consisted of functional testing in accordance with ETD-MIRA-4R1-001 plus visual and mechanical inspection.

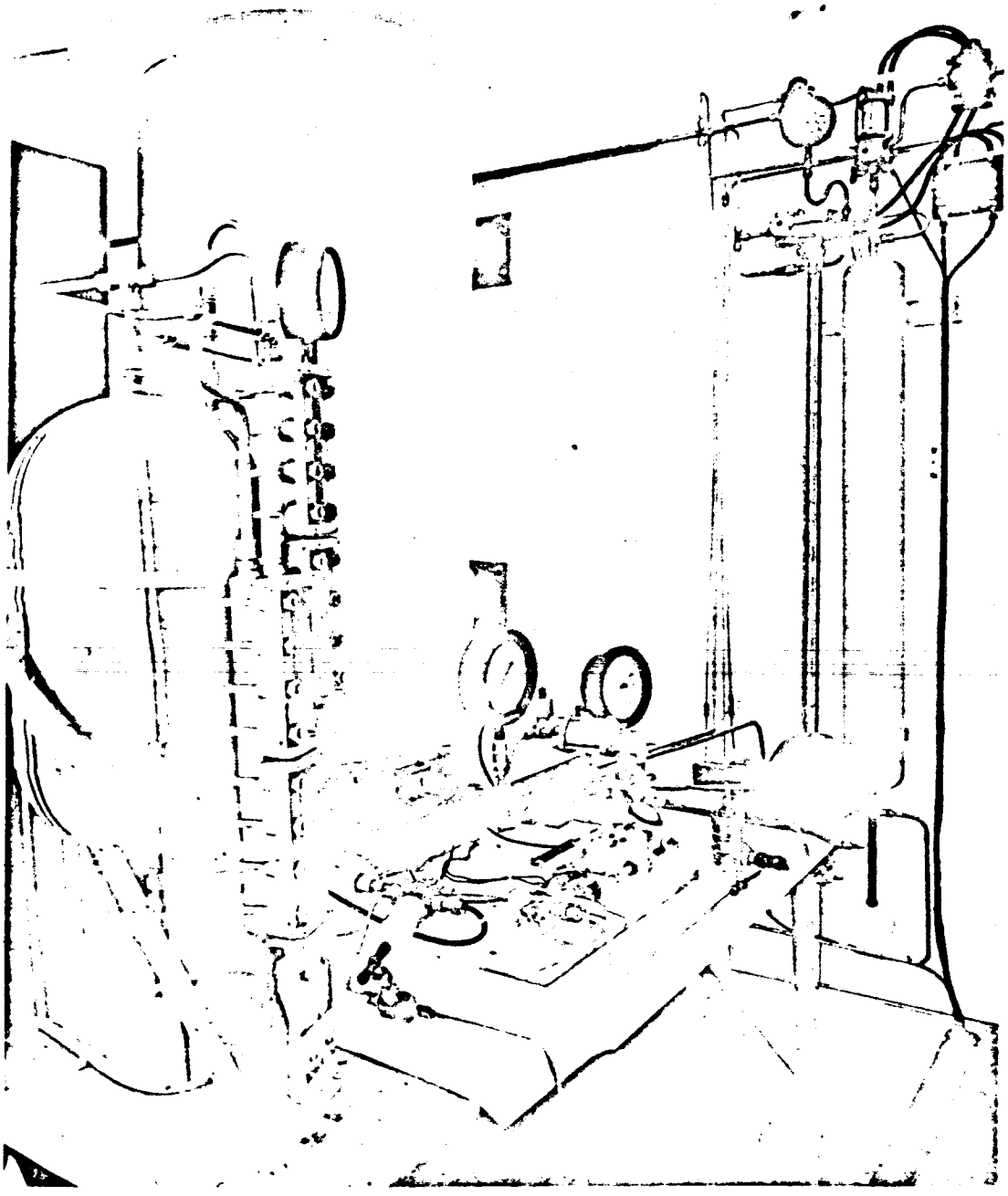

Figure 5.1.1-2. Servoactuator Test Stand

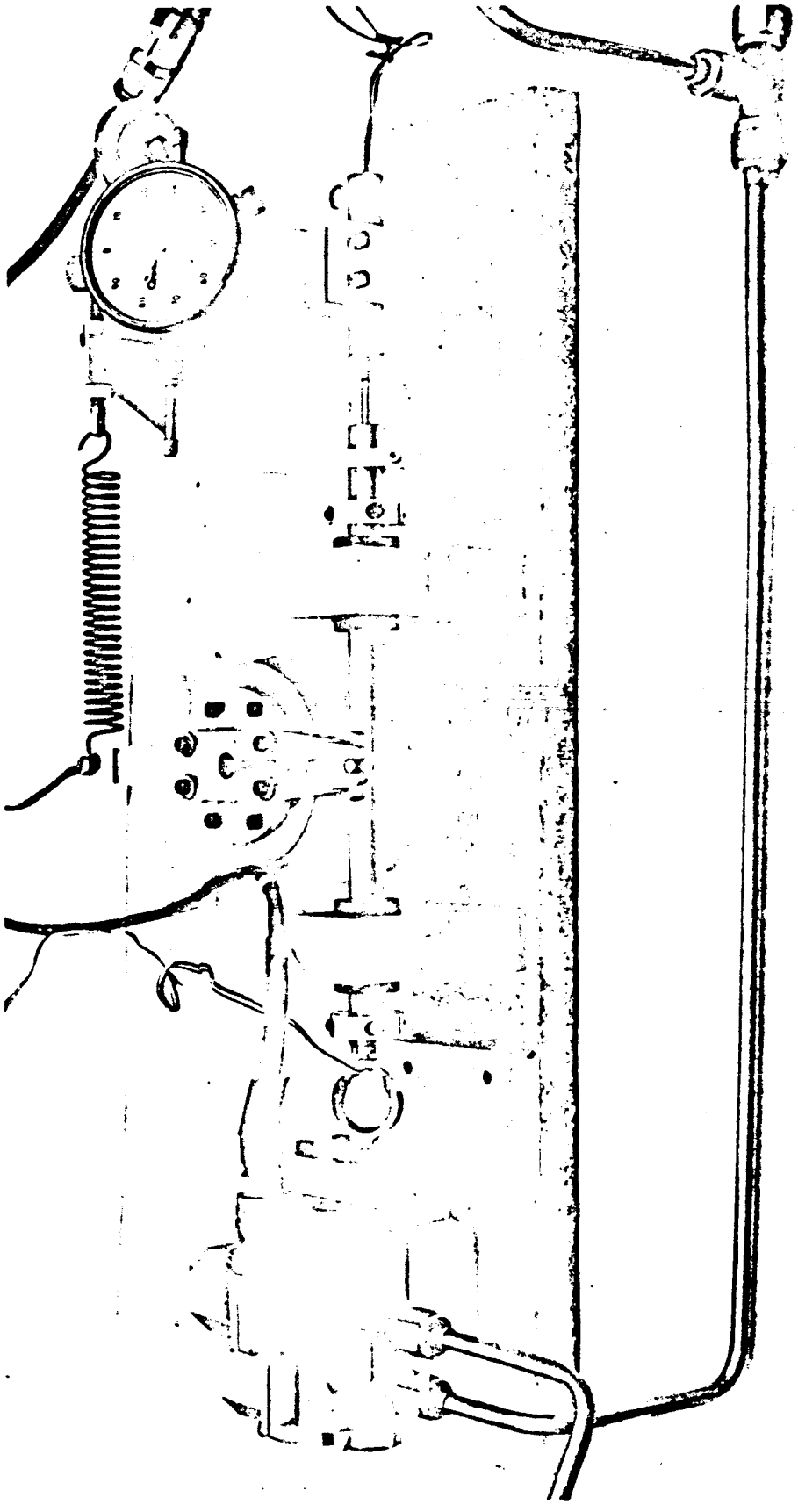

Figure 5.1.1-3. Servoactuator Test Stand Load Fixture

Table 5.1.1-4

Acceptance Test Results
Phase II Follow-on Servoactuators

	Requirement	Dimensions	Dielectric Strength (microamps)	Coil Resistance (ohms)	Proof Pressure (psia)	External Leakage (ml/min)	Coil Inductance (millihenry)	Internal Leakage (ml/min)	Hysteresis (ma)	Linearity	Deadband at mean ΔI (ma)			Step Response - max/mean: 25% Stroke (8 Steps) Rise Time (milliseconds)	Step Response - max/mean: 25% Stroke (8 Steps) Overshoot (%)	Step Response - max/mean: 25% Stroke (8 Steps) Settling Time (milliseconds)	Step Response - max/mean: Stroke 100% Rise Time (milliseconds)	Frequency Response 5 cps, 15 ma, Peak-to-Peak: Amplitude Ratio at mean ΔI			Frequency Response 5 cps, 15 ma, Peak-to-Peak: Phase Lag at mean ΔI		
	Specification Value (EQ 2-23B)	Per STL Drawing C1043128	Current less than 500	400 ± 2b per Coil	Proof at 1050 ± 10	None Allowed at Proof Pressure	1000 Maximum per Coil	197 Maximum	Less Than Linearity Envelope	Within Envelope	2.5 Maximum at -60	2.5 Maximum at 0	2.5 Maximum at +60	40 Maximum	23 Maximum	65 Maximum	40 Maximum	0.97 Minimum at -60	0.97 Minimum at 0	0.97 Minimum at + 60	20 Maximum at -60	20 Maximum at 0	20 Maximum at +60
S/N	C53747	Pass	Pass	385/385	Pass	None	1.49/1.5	187	Pass (5 ma)	Out by - 3 ma	0.5	0.5	0.5	25/18.8	32/23.1	120/73.1	65/52.5	1.0	1.0	1.0	9.0	18.0	9.0
S/N	C53748	Pass	Pass	380/390	Pass	None	1.45/1.5	184	Pass (2.7 ma)	Pass	1.0	1.0	1.0	18/15.3	29/20.8	75/57.8	40/35	1.0	1.0	1.0	9.0	9.0	9.0
S/N	C53749	Pass	Pass	387/387	Pass	None	30/30	154	Pass (3 ma)	Out by +1.5 ma	0.4	0.4	0.5	50/17.4	48/28.5	90/63.9	35/32.5	1.0	1.0	1.0	9.5	18.0	9.0
S/N	C53750	Stroke out of tolerance	Pass	385/383	Pass	None	20/20	134	Pass (2.5 ma)	Out by -9 ma	0.7	0.5	0.5	26/18.4	42/22.4	65/51.6	90/60	1.0	1.0	1.05	27.0	18.0	27.0
S/N	C53751	Stroke out of tolerance	Pass	393/391	Pass	None	1.5/1.5	236	Pass*	Out*	0.5	0.4	0.5	25/15.5	49/27.6	90/58.8	40/37.5	1.0	1.0	1.0	9.0	18.5	9.2
S/N	C53752	Stroke out of tolerance	Pass	401.5/395	Pass	None	2.6/2.6	173	Pass (4 ma)	Pass	0.6	0.6	0.5	15/12.6	44/35.1	200/141.8	35/34	1.167	1.13	1.0	0	0	0
	Averages	--	Pass	--	Pass	None	--	178	Pass	--	0.55	0.57	0.58	26.5/16.3	40.7/26.3	106.7/75.3	50.8/41.9	1.03	1.02	1.01	10.6	13.6	10.5

* Curve not available

Table 5.1.1-5

Phase III Servoactuator Acceptance Test Results

Requirement	Dimensions	Dielectric Strength (microamps)	Coil Resistance (ohms)	Proof Pressure (psig)	External Leakage	Coil Impedance (ohms)	Internal Leakage (ml/min)	Hysteresis (ma) (Maximum recorded hysteresis)	Linearity
Specification Value (EQ 2-42 or 9354.4-255)	Per STL Drawing C219217	Current less than 500	400 ± 20 per Coil	Proof at 1035 ± 10	None Allowed at Proof Pressure	625 per Coil Maximum	197 Maximum	Less than Spec Linearity	+70 stops -70; Within spec Linearity Envelope
S/N C55390	Pass	Pass	405/407	Pass	Pass	408/380	137	Pass (2.5 ma)	Pass
S/N C55391	Pass	Pass	401/403	Pass	Pass	474/435	113	Pass (2.5 ma)	Fail(null shift)
S/N C55392	Pass	Pass	404/407	Pass	Pass		83	Pass (2.8 ma)	Fail(null shift)
S/N C55393	Pass	Pass	403/403	Pass	Pass	600/564	93	Pass (2.2 ma)	Pass
S/N C55394	Pass	Pass	402/402	Pass	Pass	625/691	112	Pass (2.8 ma)	Fail
S/N C55395	Pass	Pass	399/399	Pass	Pass	574/566	76	Pass (4.5 ma)	Pass
S/N C55398	Pass	Pass	405/404	Pass	Pass	625/613	82	Pass (3.6 ma)	Pass
S/N C55390**	Pass	Pass	403/406	Pass	Pass	461/451	101	Pass (3.1 ma)	Pass

Requirement				Step Response - max/mean 25% stroke (8 steps)			100% Stroke	Frequency Response 5 cps, 15 ma, Peak-to-Peak						Stop-to-Stop Stroke (inches)	Remarks
	Deadband	at mean I	(ma)	Rise Time (milliseconds)	Overshoot (%)	Settling Time (milliseconds)	Rise Time (milliseconds)	Amplitude	Ratio at mean I		Phase Lag	at mean I	(degrees)		
Specification Value (EQ 2-42 or 9354.4-255)	2.5 Maximum at -60	2.5 Maximum at 0	2.5 Maximum at +60	40 Maximum	23 Maximum	65 Maximum	40 Maximum	.97 Minimum at -60	.97 Minimum at 0	.97 Minimum at +60	20 Maximum at -60	20 Maximum at 0	20 Maximum at _60		
S/N C55390	1.5	1.0	0.5	10/10	25/16.6	65/46.9	35/33	1.14	1.11	1.12	22.5	18.0	9.0	.1865	*
S/N C55391	0.8	0.8	0.8	12/10.2	19.5/16.4	25/21.1	40/40	1.0	1.0	1.0	13.8	13.8	9.2	.183	*
S/N C55392														.184	*
S/N C55393	1.0	0.5	0.5	15/11.9	16/11.3	25/22.5	40/37.5	1.0	1.03	1.0	13.8	18.0	9.1	.183	*
S/N C55394	1.5	1.0	0.6	14/11	18/9.9	27/18.6	40/37.5	1.0	1.0	1.0	22.5	13.5	13.5	.182	Used as is
S/N C55395	2.5	1.0	2.5	18/13.6	18/12.7	40/30	40/30	0.96	1.0	0.95	16.2	16.2	13.5	.183	Used as is
S/N C55398	1.5	1.5	1.8	15/13.3	23/7.6	30/19.8	35/25	0.98	1.0	1.0	18.0	18.0	14.2	.1805	
S/N C55390**	1.0	1.0	1.0	12/10.8	17/9.5	35/22.2	32/31	0.91	0.92	0.95	27.0	23.0	18.0	.185	Used as is

*Returned to vendor for retrofit of springs and installation of torque motor screw lockwire.

** Second Acceptance test on this unit.

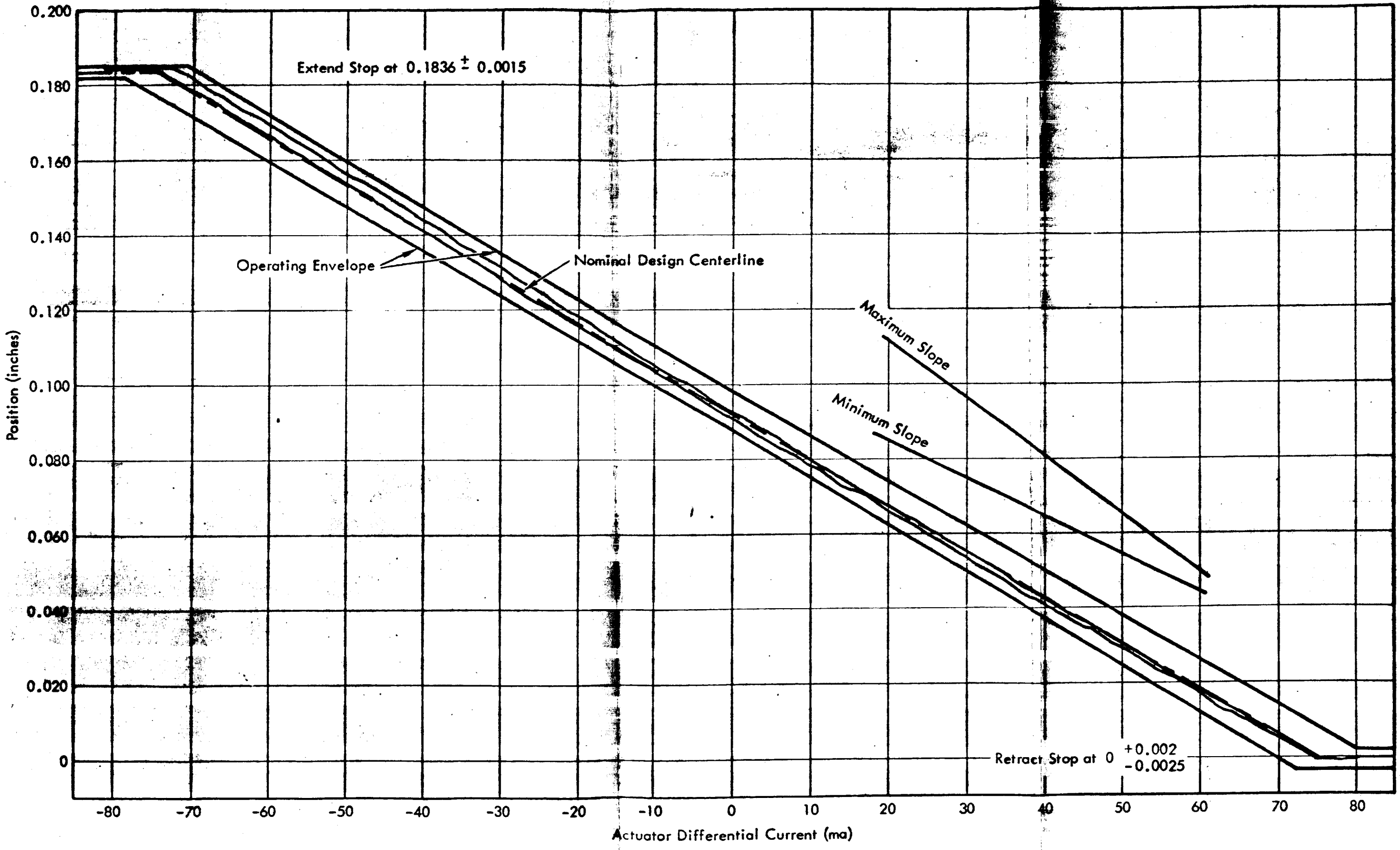

Figure 5.1.1-6. Typical Phase III Actuator Hysteresis Curve

The functional parameters checked by acceptance testing were:

1. Nominal Filtration Rating
2. Pressure Drop Versus Flow

In performing these tests, the maximum allowable tolerances on test condition measurements were:

1. Pressure: ± 1%
2. Flow: ± 2%

A bubble point test was used to evaluate the nominal filtration rate. In this test, the filter element in a test fixture is submerged in alcohol and nitrogen gas is slowly applied to the filter outlet. For the nominal 5-micron filter to be acceptable, the initial bubble emission must occur at a pressure greater than 11 inches of water and the entire surface must emit bubbles at a pressure of less than 30 inches of water. These requirements are shown graphically in Figure 5.1.2-1.

The pressure drop versus flow test was conducted in accordance with ETD-MIRA-4R1-001. Water was used as the test fluid, and with appropriate density and flow corrections, acceptance criteria was established as a pressure drop of 13 psi maximum at water flow of 2 gpm. Figure 5.1.2-2 shows the nominal pressure drop versus flow for water (acceptance test fluid), and for oxidizer and fuel. Two filters failed to pass this acceptance test (S/Ns 36 and 38). These filters were subsequently accepted by MRB action.

Data from acceptance testing of 27 filters is shown in Table 5.1.2-3.

5.1.3 Helium Pilot Valve

Acceptance testing of helium pilot valves consisted of visual and mechanical examinations and functional testing of each valve in accordance with ETD-MIRA-3R1-001 to check for compliance with EG 2-25 specification requirements.

As noted in paragraph 3.2.4, two designs of helium pilot valves were evaluated, differentiated here by the part numbers C104337-1 and C104337-2.

Among other configurational differences the two designs differed in the materials used in the magnetic circuit (including the case) and in the poppets. The magnetic circuit of the C104337-1 valve is electroless nickel plate over high permeability iron. The plating process is proprietory to the vendor and was developed for use in propellant systems. The inlet poppet is nylon whereas the vent poppet is Teflon. Teflon is used on the vent poppet because of problems which occurred during Phase II testing involving propellant contamination in this area of the pilot valve. Inlet poppet contamination problems have never occurred. The C104337-2 valve use Teflon on both the inlet and vent poppets.

The first lot of C104337-2 valves received also used electroless nickel plate over high permeability iron in the magnetic circuit. However, the plating process (apparently not identical to that used by the other vendor) was inadequate, and the valves rusted from exposure to atmospheric and rocket test stand moisture. These valves were removed from service, and a second lot was ordered with appropriate design changes.

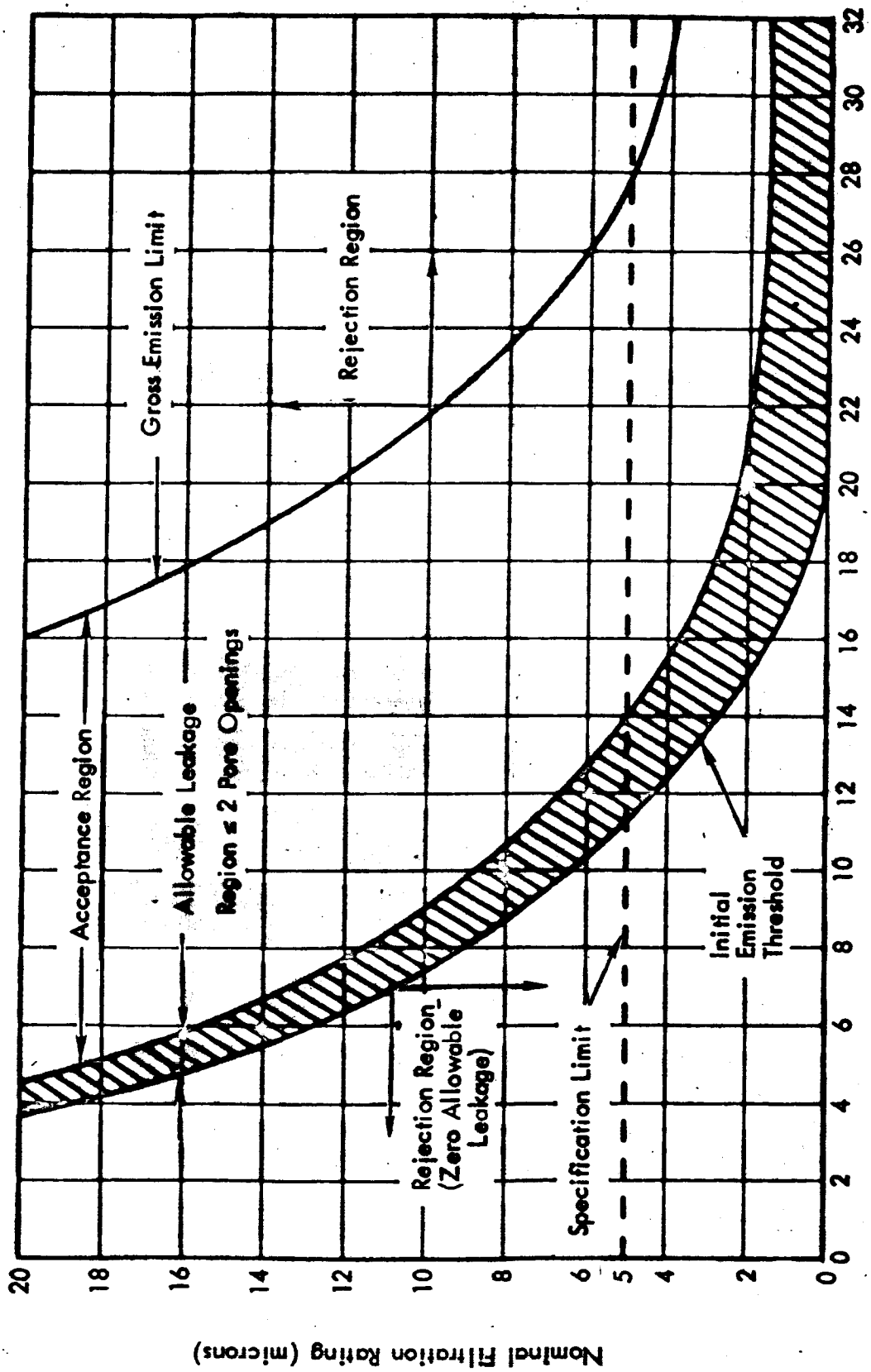

Figure 5.1.2-1. Bubble Point Curve

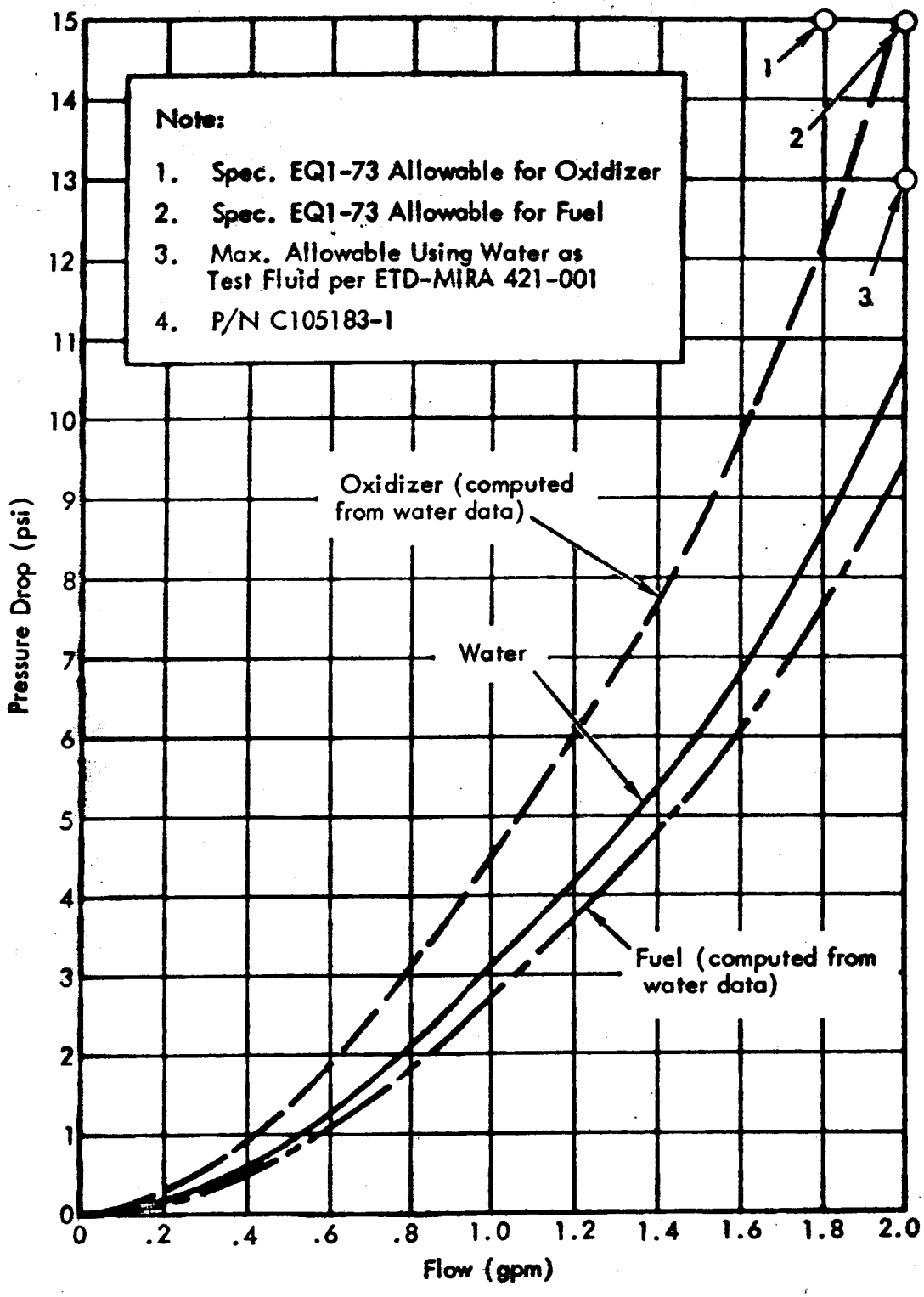

Figure 5.1.2-2. Filter Pressure Drop Versus Flow

Table 5.1.2-3

Filter Acceptance Test Data

Filter Serial No.	Bubble Point Pressure		Pressure Drop		
	Initial Emission ($in.H_2O$)	Gross Emission ($in.H_2O$)	For Water Flow of 2 gpm (psi)	For Fuel Flow(1) of .24 lb/sec (psi)	For Ox Flow(1) of .36 lb/sec (psi)
Accept. Test Reqm't	Greater than 11	Less than 30	Less than 13	None	None
1	13	26	10.5	8.8	12.2
2	15	25	11.4	9.6	13.3
3	19	26	12.0	10.1	14.0
5	19	27	9.4	7.9	10.9
6	12	27	9.7	8.2	11.3
7	20	28	9.6	8.1	11.2
8	13	27	9.5	8.0	11.1
9	20	28	10.1	8.5	11.8
10	20	27	9.4	7.9	10.9
11	21	27	9.2	7.7	10.7
12	17	27	9.8	8.2	11.4
13	16	28	9.5	8.0	11.1
14	13	27	9.6	8.1	11.2
15	20	28	9.3	7.8	10.8
16	20	28	9.4	7.9	10.9
17	17	27	10.5	8.8	12.2
18	20	27	10.1	8.5	11.8
19	19	28	12.5	10.5	14.6
22	20	24	10.7	9.0	12.5
23	10	24	10.5	8.8	12.2
24	19	24	12.5	10.5	14.6
26	16	23	11.3	9.5	13.2
28	19	27	11.3	9.5	13.2
30	20	23	10.7	9.0	12.5
36	11	24	15.5	13.0	18.1
37	13	22	11.3	9.5	13.2
38	19	26	15.4	12.9	18.0

NOTE: (1) Fuel and Ox ΔP's computed from water flow data.

The second lot of C104337-2 valves received used 446 stainless steel for the magnetic circuit. Unfortunately, these stainless steel valves were delivered too late in the program for TCA usage; therefore, the -1 valves were used exclusively on all hardware scheduled for delivery or for use in the prequalification test program.

The specific items checked during functional acceptance testing were:

1. Dielectric (500 volts for one minute with no breakdown).
2. Coil Resistance (45 ohms minimum).
3. Proof Pressure (1000 psig).
4. Leakage (zero external; internal, 10 scc/hr of helium at 850 psig).
5. Response Time (armature movement at 0.020 sec for 16 VDC and 0.012 sec for 16 vdc and 0.012 sec for 23 vdc; 0.025 sec for pilot pressure increase to 200 psig and decrease to 100 psig with 700 psig applied).

In performing these tests, the maximum allowable tolerances on test condition movements were:

Current:	± 1%
Voltage:	± 1%
Resistance:	± 1%
Pressure:	± 1%
Flow:	± 2%
Time:	± 2%

The dielectric test was conducted by applying a potential of 500 volts rms for one minute between each valve lead wire, in turn, and the valve case. Insulation breakdown was defined as a current flow in excess of two milliamperes.

The coil resistance test consisted of measuring the resistance of the valve solenoid, using a Wheatstone bridge circuit.

The proof pressure test was conducted by applying a pressure of 1000 psig to each valve in the energized condition and checking for any detrimental effect during the following five-minute period.

External and internal leakage tests were performed using a helium leak detector. Leakage was checked using helium at 850 psig. Internal leakage measurements were performed for both the inlet poppet and the vent poppet with the maximum allowable leakage for either being 10 scc/hr.

Response time tests were conducted using a test setup that simulated TCA pilot gas porting and volume. Tests were conducted by pressurizing the valve inlet with helium at 700 psig. Valve response was measured both with and without the use of switch protection circuitry shown below:

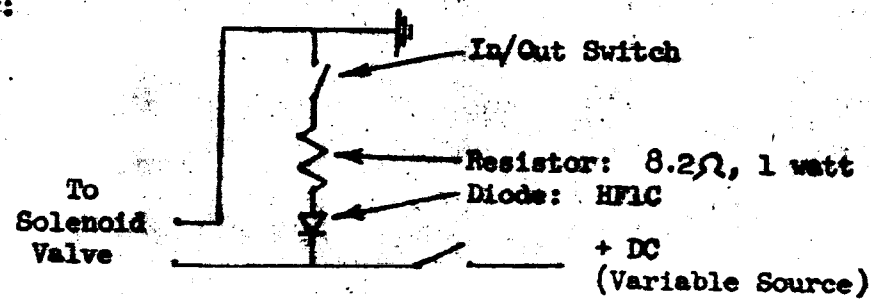

This circuit simulated that used in the Surveyor spacecraft. Pilot valve opening and closing (energize and de-energize) response times were measured for the following two signal conditions:

(1) 16 vdc pull-in for a one-second duration followed by a 13 vdc holding signal.

(2) 23 vdc.

Table 5.1.3-1 presents data from acceptance testing of the 28 C104337-1 design valves. The de-energize response time data shown were obtained with the simulated spacecraft switch protection circuitry (diode and resistor) connected. The observed effect of this switch protection circuitry was to delay valve armature movement upon de-energizing the valve by approximately nine to ten milliseconds, but had no affect on energize response times. Thus, the response data shown for the energized condition is applicable for both use and nonuse of the switch protection circuitry.

When <u>de-energizing</u> a valve <u>without</u> switch protection circuitry, the response time, ta, was observed to be typically 0.5 to 1.0 milliseconds for the voltage range of 13 to 23 vdc. Analysis of test data also showed that upon de-energizing a valve, the time interval between t_a and t_{200} and between t_a and t_{100} (i.e., $t_{200} - t_a$ and $t_{100} - t_a$) was not affected by switch protection circuitry. In other words, the switch protection circuitry delays the beginning of armature movement but has no affect (within the accuracy of instrumentation and analysis) on armature travel time and pressure decay time. Thus, de-energize response times <u>without</u> switch protection circuitry may be readily computed from the data given.

The response time pilot pressures presented were selected because: (1) the propellant shutoff valve opening threshold pressure is equal to approximately 400 psig pilot pressure at a propellant pressure of 740 psig, and (2) the propellant shutoff valve closing threshold pressure is equal to approximately 150 psig pilot pressure at a propellant pressure of 175 psig.

Figures 5.1.3-2 and -3 show the nominal energize and de-energize response times for the C104337-1 valve.

Late delivery of the -2 design stainless steel valves resulted in acceptance testing of only two of these valves. Table 5.1.3-4 contains these data.

All valves tested passed the acceptance requirements for dielectric strength, coil resistance, proof pressure, external leakage, and internal leakage, and response time, with one exception. Valve P/N C104337-1, S/N 001, did not meet the energize response time requirements. This valve was subsequently accepted through MRB action.

Table 5.1.3-1

Acceptance Test Data - Valve C104337-1

VALVE S/N	ENERGIZE RESPONSE TIME (1) 16 vdc Applied t_a (msec)	t_{350} (msec)	t_{450} (msec)	23 vdc Applied t_a (msec)	t_{350} (msec)	t_{450} (msec)	DE-ENERGIZE RESPONSE TIME (1) 13 vdc Removed t_a (msec)	t_{200} (msec)	t_{100} (msec)	23 vdc Removed t_a (msec)	t_{200} (msec)	t_{100} (msec)	Coil Resistance (ohms)	Internal Leakage (2) Energized (scc/hr)	De-energized (scc/hr)
Specification Value	20	25 (5)		12	-	-	-	-	34 (6)	-	-	-	45	10	10
001	24	28.5	29.8	11	15.3	16.5	11	19.5	25.5	11.2	20	26	54.8	.002	.0002
002	13	16.8	17.8	6.8	10.8	11.8	11.5	20.2	26	13	20.5	25.5	55.6	.002	.05
003	14.2	18.3	19.3	9.5	13	14	11.8	20	26.5	12.2	20.5	26.8	55.1	.001	.008
004	18	21.8	22.8	9	13	14	10	20.2	24.5	11.8	19.5	24.8	55.2	.004	.01
005	12.8	17	18	9.2	13.5	14.5	9.5	17.8	22.8	10	18.5	24	55.1	.004	.002
006	14.2	18.3	19.3	9	12.8	13.8	9.2	17.2	22.5	10.5	18.2	24.2	55.6	.002	.04
007	11.2	15.3	16.3	7.5	10.8	11.8	8	18	24	9.8	19.5	25.5	55.2	.003	.05
008	20	24	25.3	9.8	13.8	14.8	8.5	18	24.8	9.8	18.5	25	54.6	.002	.007
009	15.8	20.5	21.5	9.8	13.8	15	10.8	19.5	26.2	11.2	21	27.2	55.1	.0008	.004
010	13.2	17.3	18.5	7.5	11.8	13	10	18.8	24.2	11.8	20.2	25.5	55.3	.0002	.0006
011	13.5	17.5	18.8	8.2	12	13	7.8	17.5	24.2	9.8	19	25.2	55.0	.0008	.003
012	14	17.8	19	8.8	12.5	13.5	9	18.2	24.5	11	19.2	25.2	55.7	.003	.005
013	16.2	20.3	21.3	8.2	12.3	13.3	9.2	17.2	22.5	10.8	18.8	23.8	55.2	.016	.05
014	12	16	17	8.2	12	13	11.5	20	25.8	12	20	25.2	55.0	.02	.003
015	12.8	16.8	17.8	7	10.5	11.5	9.5	18.2	24.8	11.2	19.2	24.2	55.9	.002	.09
016	11.8	15.5	16.5	8.5	12.3	13.3	10.8	19.2	25.2	11.2	19.6	25	54.9	.006	.01
017	14.8	19	20.3	8.2	12.5	13.5	9.8	19.5	25.5	11	20.5	26	55.1	5.0	.006
018	16.2	20.3	21.3	9.8	13.8	14.8	8.2	17	22.8	8.8	17.2	22.2	55.2	.02	.007
[illegible]	13.8	17.[illegible]	18.8	8.2	11.8	12.[illegible]	8.8	[illegible]	23.5	9.2	17.8	23.2	55.3	.005	.004
020	13.2	17.3	18.3	8	11.8	13	6.8	16.2	21.8	8	17	22.5	55.6	.007	.02
021	9.8	13.8	14.8	6	10	11.3	9	18.8	24.2	10.2	20	26.8	55.1	.002	.05
022	14	18.5	19.8	7.8	12	13.5	10.8	20	25.5	10	20.5	26	55.8	.0004	.004
023	12	16.5	17.5	8.2	12.3	13.3	8.8	17.2	23.2	9.8	18.5	23.8	55.6	.002	.002
024	13.5	18	19	8.5	12.8	13.8	10.5	19.2	25.2	11	20	26	55.9	.0009	.01
025	15.8	20.3	21.3	9.2	13.5	14.5	10.5	18.5	24.2	11.8	19.8	25	55.6	.003	.009
026	13.2	17.8	18.8	8.2	12.3	13.3	9.5	20.5	27	10.8	19.8	25	55.7	.001	.007
027	11	14.7	16	7.2	11.3	12.3	10	18.8	24.8	11.2	19.5	25	55.5	.002	.003
028	11	14.8	16	7.2	10.8	12	10.5	19.2	25.8	12.5	21.2	26.5	55.2	.001	.002
$\bar{x}$ (3)	14.1	18.2	19.3	8.4	12.3	13.4	9.7	18.7	24.6	10.8	19.4	25.0			
σ (4)	±2.9	±3.0	±3.1	±1.1	±1.2	±1.2	±1.2	±1.2	±1.3	±1.1	±1.1	±1.2			

NOTES: (1) Response time data acquired using helium at 700 psig. Valve attached to test block which simulates TCA pilot gas porting and volume.
t_a = time from application/removal of voltage until valve armature moves.
t_{xxx} = time from application/removal of voltage until pilot pressure = xxx psig.

(2) Internal leakage measured with helium at 850 psig. (Helium leak detector used.)

(3) $\bar{x}$ (arithmetical average) $= \frac{1}{N} \sum_{1}^{N} x_i$

(4) (standard deviation) $= \left[\frac{1}{N-1} \sum_{1}^{N} (x_i - \bar{x})^2 \right]^{\frac{1}{2}}$

(5) Spec. value energize response time of 25 msec is for t_{200} (i.e. time for pressure to reach 200 psig).

(6) Spec. value de-energize response time is for condition without switch protection circuitry and is 25 msec. The value shown (34 msec) assumes a switch protection circuitry delay of 9 msec.

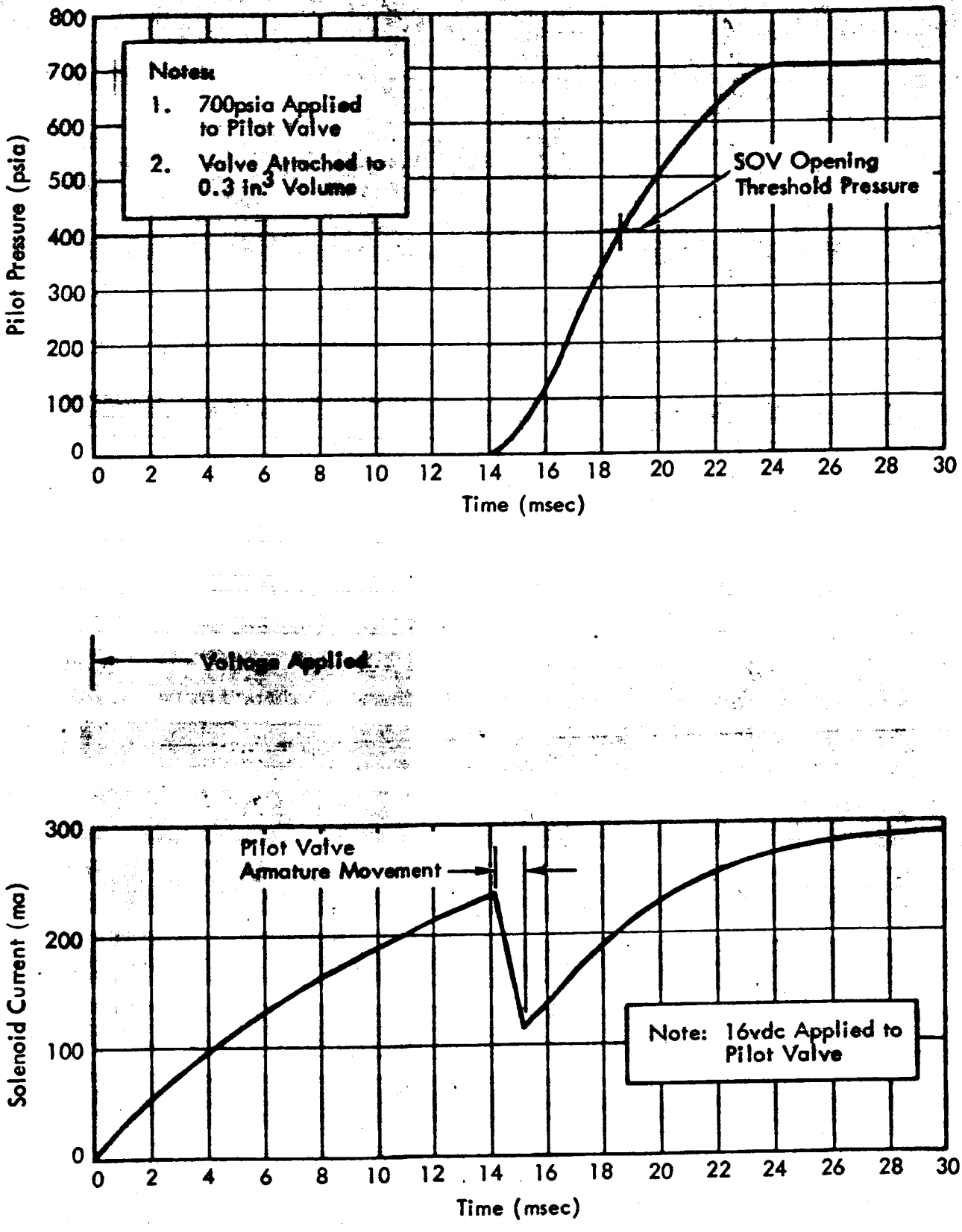

Figure 5.1.3-2. Nominal Energize Response Time for Helium Pilot Valve P/N C104337-1

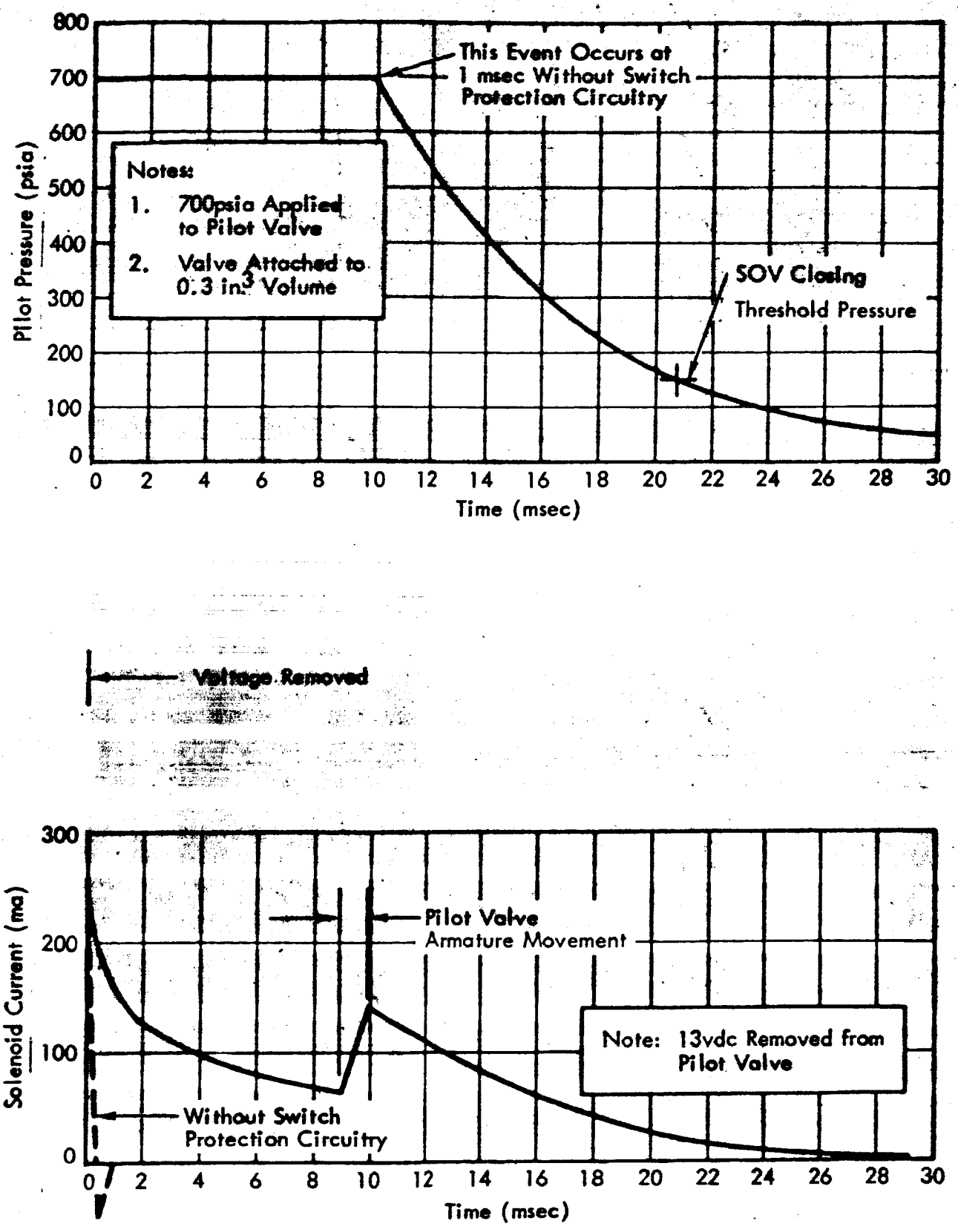

Figure 5.1.3-3. Nominal De-Energize Response Time for Helium Pilot Valve P/N C104337-1 (with Switch Protection Circuitry)

Table 5.1.3-4(1)

Acceptance Test Data - Part Number C-104337-2

Serial Number	16 vdc Applied			23 vdc Applied			18 vdc Removed			23 vdc Removed			Resistance (ohms)	Internal Leakage	
	t_a (msec)	t_{350} (msec)	t_{450} (msec)	t_a (msec)	t_{350} (msec)	t_{450} (msec)	t_a (msec)	t_{200} (msec)	t_{100} (msec)	t_a (msec)	t_{200} (msec)	t_{100} (msec)		Energized (scc/hr)	De-energized (scc/hr)
1010	10	15.5	17	7	12.8	14.2	17.5	27.2	33.8	20.2	30	36	46.4	0.0002	0.05
1012	15	22.9	25.1	10	15.3	18.6	9.8	18.8	24.5	10.8	19.4	24.8	47.8	0.004	0.92

(1) The footnotes and specification values noted for Table 5.1.3-2 are also applicable here.

5.2 Deep Vacuum Tests

Three deep vacuum tests were conducted during July and August 1964. The primary objective of these tests was to determine the effect of space environment on the function of the HEA moving parts; for example, to see if actuation friction levels increased, or if leaks developed.

These tests were performed at a point in time when all assembled and operational MIRA 150A HEAs were being utilized for high priority firing tests; therefore, a MIRA 150 HEA (Part No. 103950 and S/N 002) was selected as the basic vacuum test specimen. At the outset of this vacuum testing with the MIRA 150, it was planned to conduct subsequent tests with MIRA 150A HEA hardware; however, it was felt that the MIRA 150 HEA testing would indicate potential problem areas and provide definition of test equipment and instrumentation requirements.

The paragraphs which follow discuss the three vacuum tests.

5.2.1 Head End Assembly Vacuum Test

5.2.1.1 Test Specimen and Test Setup

The test specimen was MIRA 150 HEA S/N 002. The test setup is shown schematically in Figures 5.2.1-1 and -2; a photograph of the setup is presented in Figure 5.2.1-3.

For this test, water was used as a substitute for both fuel and oxidizer and gaseous nitrogen was used as the pilot gas in place of helium. The servoactuator was supplied with Brayco 910 (a fuel-simulating fluid) fluid from a hydraulic power supply developed for actuator testing. To collect and drain the water flowing through the HEA (when actuated), a pump tank was attached in place of the CC & NA.

5.2.1.2 Instrumentation

Servoactuator instrumentation, shown photographically in Figure 5.2.1-4, consisted of a rectilinear potentiometer for position readout and a load link for output shaft force measurement. The load link was fabricated from aluminum and employed four foil-type strain gages in a bridge arrangement containing four active arms. Pilot valve actuation current was monitored by an oscilloscope connected across a one-ohm shunt. Actuation of the oxidizer shutoff valve was detected with a pressure transducer attached to the oxidizer injection pressure tap.

Thermocouples were attached to the test specimen to verify the 125°F temperature maintained during vacuum storage by means of a pair of heat lamps.

The specific HEA performance parameters of interest in the test were:

1. Friction loads as measured at the actuator end of the HEA actuation arm (load link instrumentation).
2. Servoactuator hysteresis deadband and linearity (shaft position instrumentation).
3. Pilot valve actuation (current instrumentation).
4. Shutoff valve actuation (injection pressure instrumentation).

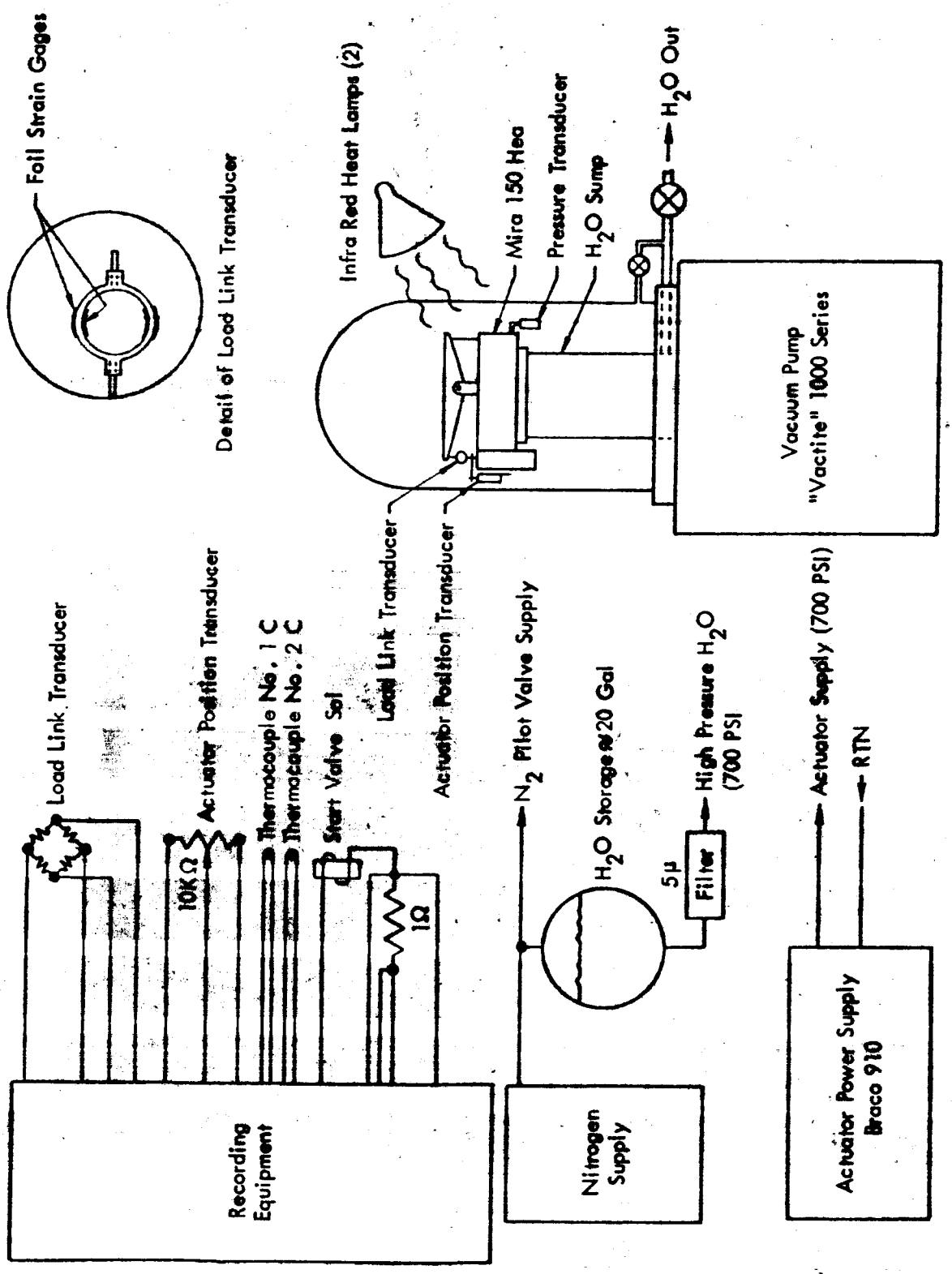

Figure 5.2.1-1. Equipment Setup Schematic - HEA Vacuum Test

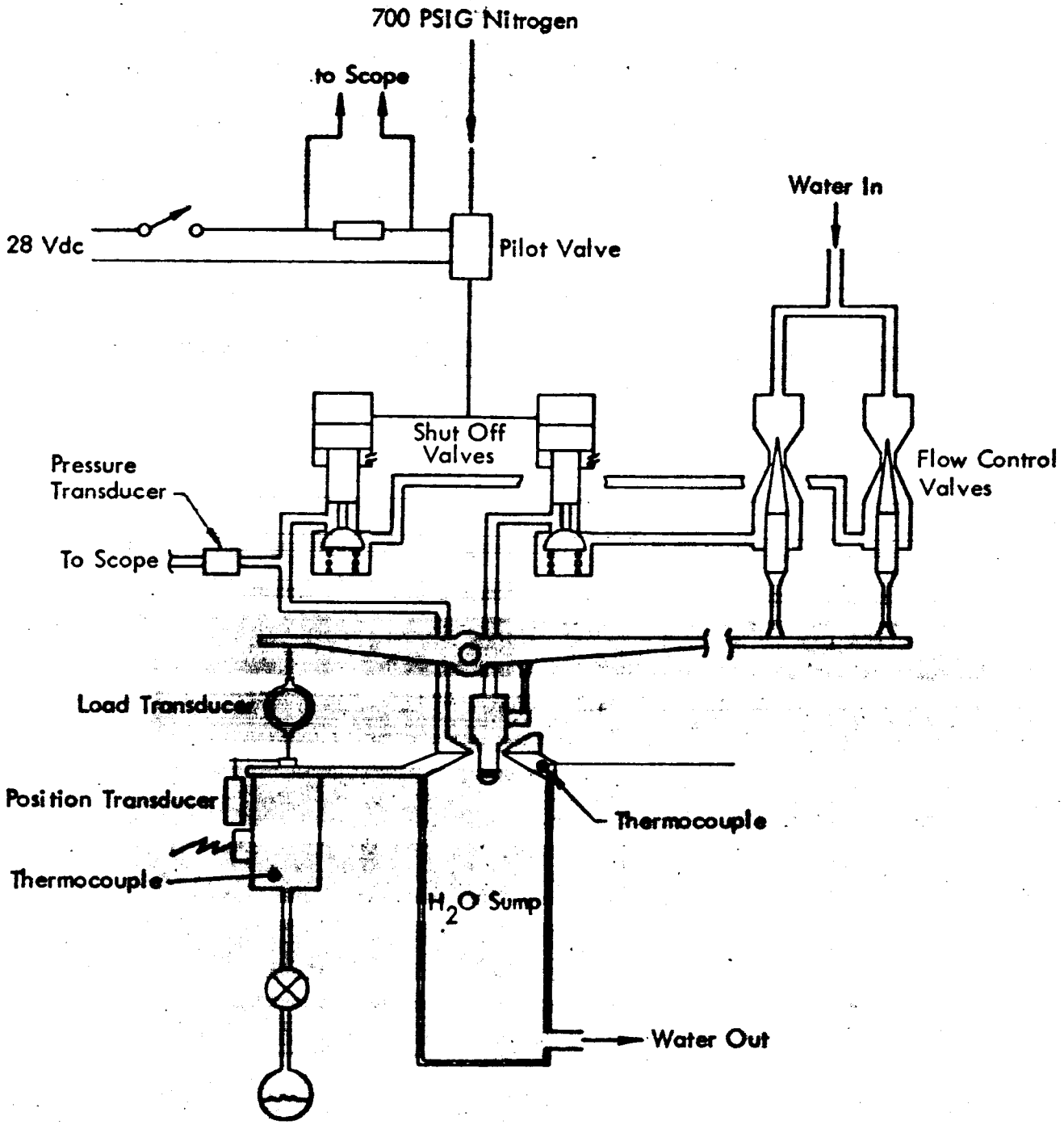

Figure 5.2.1-2. HEA Vacuum Test Setup - Schematic

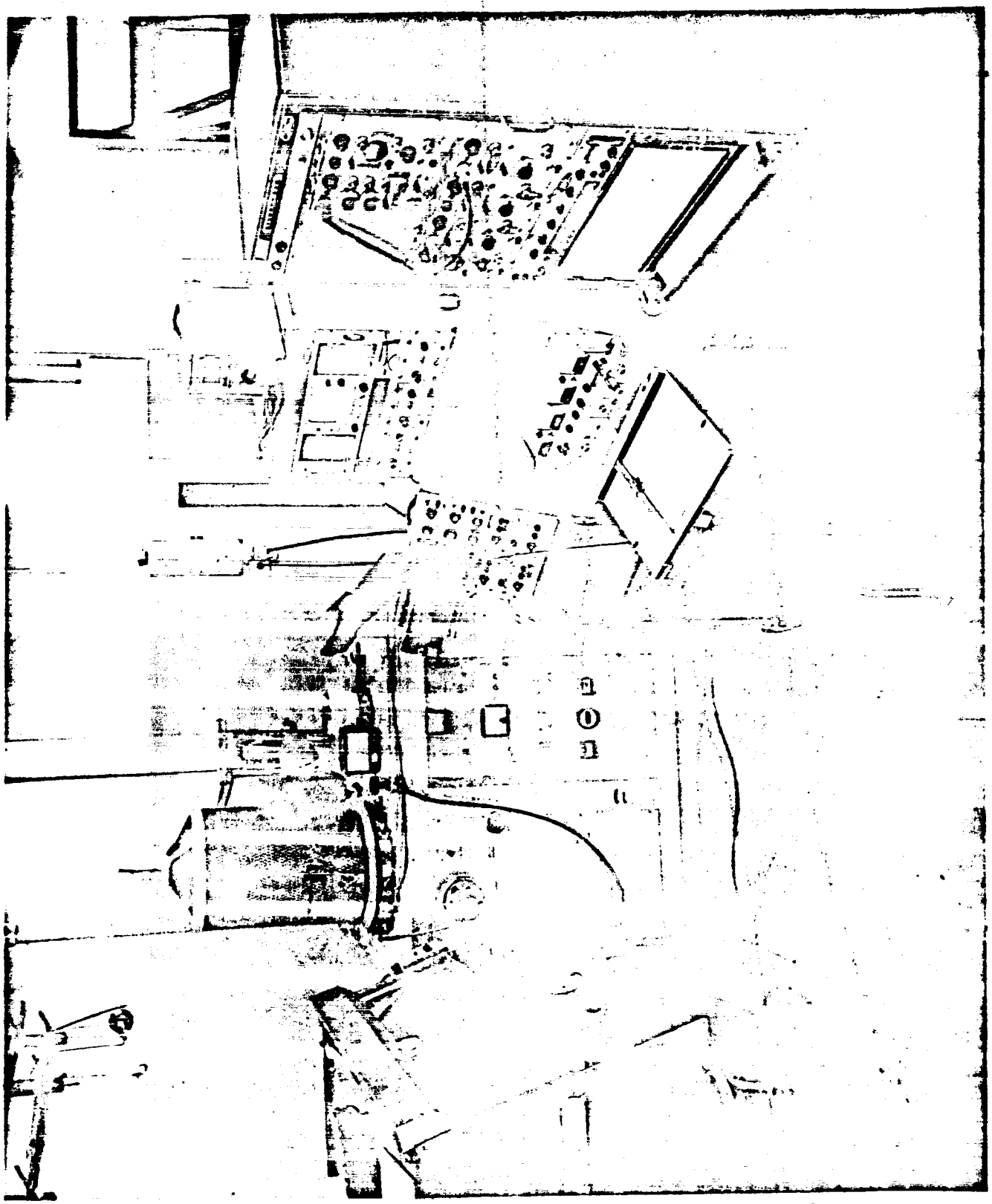

Figure 5.2.1-3. HEA Vacuum Test

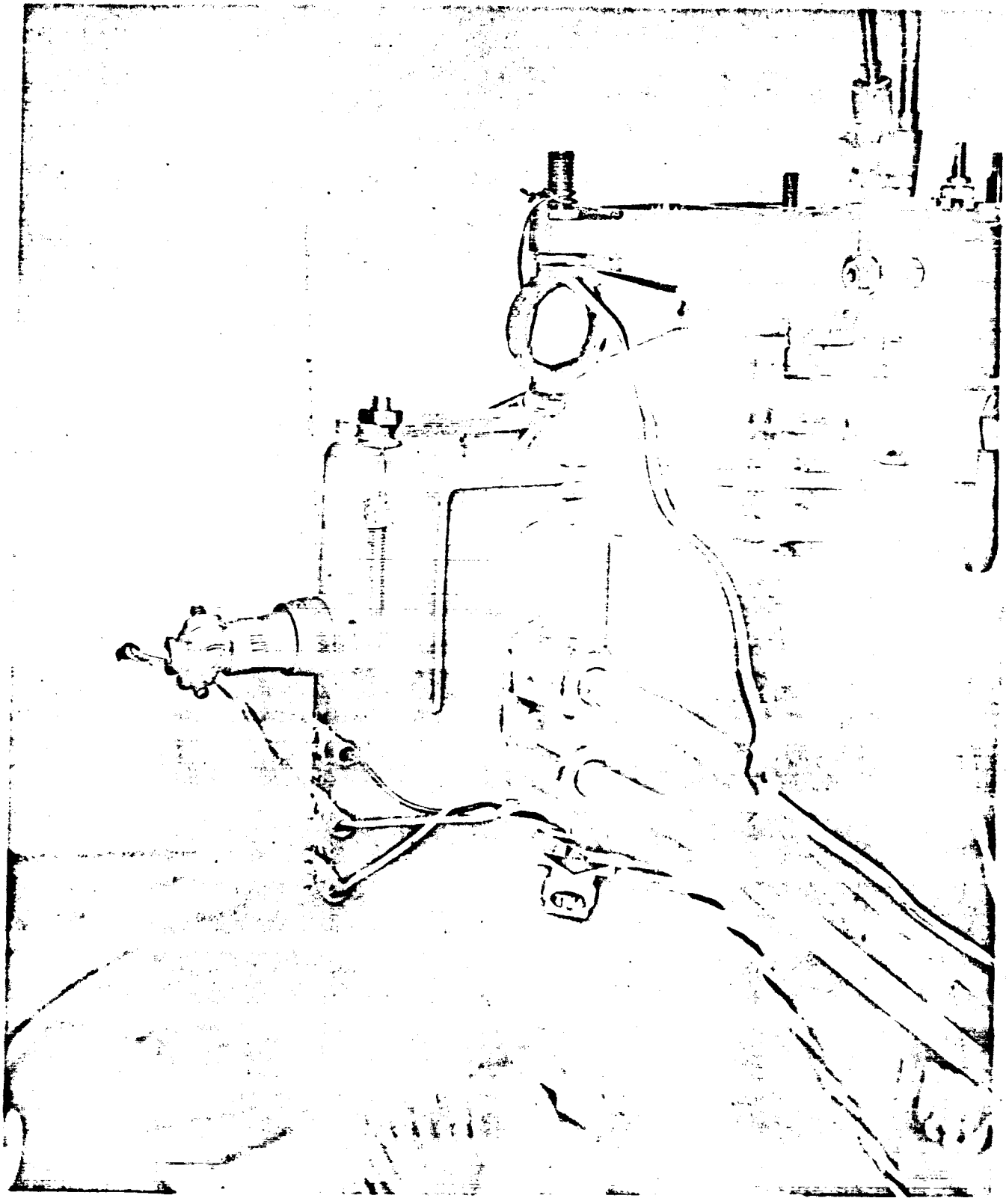

Figure 5.2.1-4. HEA Vacuum Test Actuator Shaft Position and Load Instrumentation

5.2.1.3 Test Procedure

Prior to subjecting the test specimen to the vacuum environment, the above performance parameters were measured to provide reference values. The friction loads were measured both with and without water flow, and the water was then purged from the HEA with dry gaseous nitrogen.

The dry, unpressurized HEA was next exposed to a vacuum environment, and following a pump-down period of four and one half days the HEA was soaked for approximately 100 hours at a mean pressure of 4×10^{-7} torr. During this time, the specimen temperature was maintained at 125°F, except for brief cycles from 80°F to 160°F to expedite out-gassing.

Following the 100-hour soak, fluid pressures were slowly applied to the HEA in order to fill the various volumes without causing a pressure surge which might break loose any cold welds and this mask sticking or friction changes. The aforementioned performance parameters were then measured and recorded; these data are presented in paragraph 5.2.1.4.

Following the performance measurements, the HEA was again subjected to the vacuum environment; however, this time the test specimen was pressurized with the various working fluids (i.e., water, Brayco 910 and nitrogen). In the pressurized condition it was only possible to achieve a vacuum of 6×10^{-5} torr (apparently because of test specimen leakage); the HEA was soaked at this pressure for approximately 100 hours. After 100-hour soak in the pressurized condition, the HEA performance parameters were again measured and recorded; these data are also presented in paragraph 5.2.1.4 .

5.2.1.4 Test Data

Figure 5.2.1-5 shows a plot of bell jar pressure versus time for the unpressurized and pressurized vacuum storage test runs.

Upon pressurizing the servoactuator after the 100-hour dry vacuum storage, fluid (Brayco 910) leakage was detected by the output shaft; however, after cycling the servoactuator at 0.05 cps and an amplitude less than full travel, the leakage stopped and a 100-second actuation (throttling) run was conducted with full shaft excursion. Because of an inadvertent grounding of the trigger signal, the pilot valve solenoid current and oxidizer injection pressure were not recorded during the first HEA start. However, normal water flow occurred during this start; in subsequent starts current and pressure recordings were successfully obtained.

Servoactuator hysteresis plots taken after both vacuum storage tests revealed no gain changes or null shifts. The actuator fluid leakage which occurred at the conclusion of the dry storage test stopped with shaft motion and no further leakage was encountered. This action suggests that the leakage was due to shrinkage of the shaft seal causing it to pull away from the shaft and that wetting and/or fluid pressure restored the seal. Pilot valve current rise and oxidizer injection pressure build-up are shown in Figure 5.2.1-6. Pilot valve armature movement as noted by the cusp in the current trace did not indicate any vacuum environmental effect. The oxidizer injection pressure trace for the post dry storage test was attenuated, since the flow setting at startup for this test was different than for the control test and post wet storage test.

Started Roughing

Time (milliseconds)

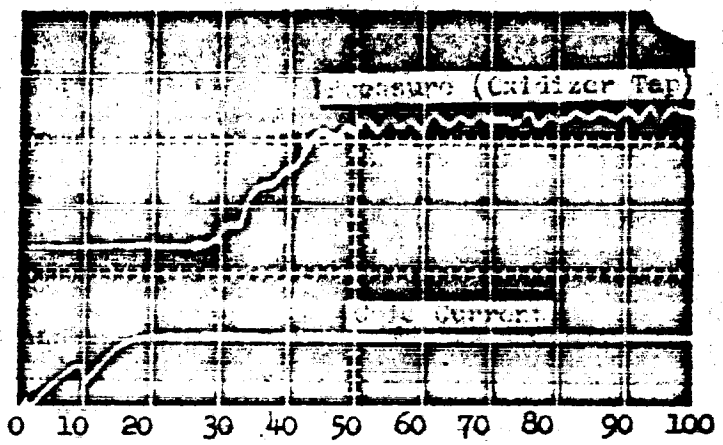

(a) Initial Control Test

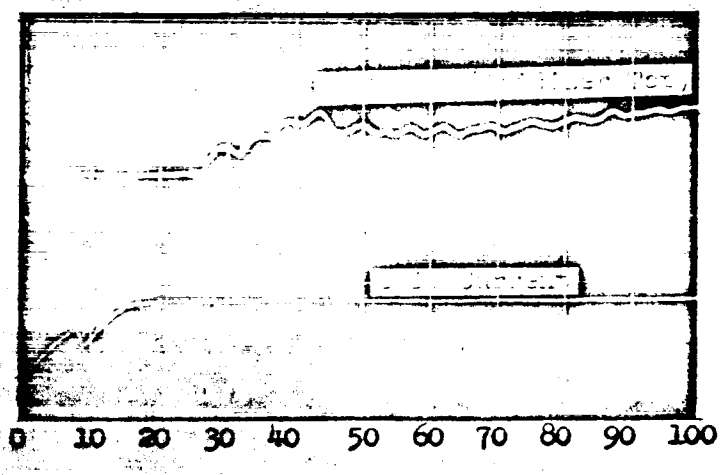

(b) Post Dry Storage Test

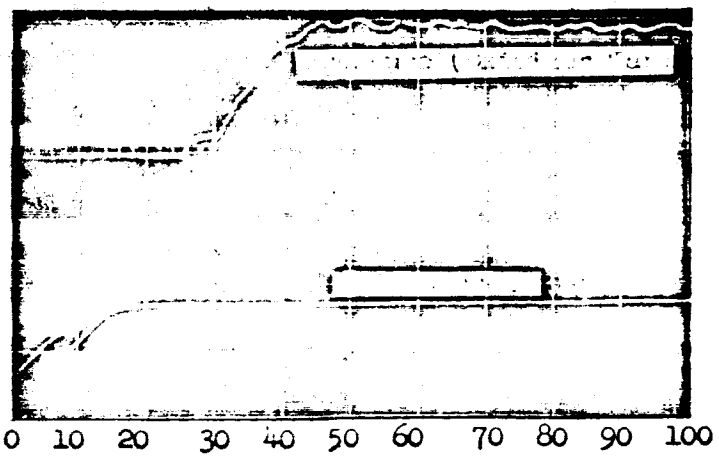

(c) Post Wet Storage Test

Scales:

Sweep Speed 10 ms/cm
Pressure 25 lb/cm
Current 200 ma/cm

Figure 5.2.1-6. HEA Vacuum Test Startup Data

Figure 5.2.1-7 shows the total compressive load on the servoactuator versus actuator shaft position. These loads do not include any friction within the actuator itself. The "Flow Condition" in Figure 5.2.1-7 is with the shutoff valves open and water flowing through the HEA. The "No-Flow Condition" is with the shutoff valves closed and, thus, the flow control valve pintles are working against the static water pressure. The difference in water pressure between flow and no-flow conditions results in a reduced actuator loading of approximately 20 lbs for this flow condition. The post wet storage total load curve is shifted approximately 6 lbs higher than either of the other two curves possibly because of a drift in the load readout instrumentation or a shift in the strain gage excitation level.

The friction load is equal to one-half of the difference in loading that occurs during a shaft direction reversal. Table 5.2.1-8 shows the friction load data derived from Figure 5.2.1-7. Changes in actuator loading resulting from changes in friction are negligible when compared to the 100-lb stall load rating of the servoactuator. The exact reason for the observed increase in friction loads is not clear; however, it may possibly be attributed to measurement technique and accuracy and variations in seal friction. Cold welding was not observed nor expected. A review of available data on cold welding indicates pressures less than 1×10^{-7} torr are necessary to produce cold welding.

Table 5.2.1-8

Friction Loads at S/A Shaft

Condition	NO FLOW CONDITION (SOVs Closed)		FLOW CONDITION (SOVs Open)	
	S/A Shaft Retract Load (lb)	S/A Shaft Extend Load (lb)	S/A Shaft Retract Load (lb)	S/A Shaft Extend Load (lb)
Pre-Storage	3.5	3.5	3	4
Post Dry Storage	5	6.5	3.5	6
Post Wet Storage	4.5	6.5	3.5	3.5

5.2.2 Shutoff Subsystem Vacuum Test

Immediately following the HEA vacuum test discussed in Paragraph 5.1.1, a similar vacuum test was conducted on the shutoff subsystem. The test objective here was to determine if shutoff subsystem performance would be affected by vacuum storage in the pressure region where cold welding phenomenon occurs (less than 1×10^{-7} torr).

5.2.2.1 Test Setup Description

The shutoff subsystem functionally consisted of the shutoff valves and the helium pilot valve. The test article was the same head end body, shutoff valves, and helium pilot valve used in the previous test (described in Paragraph 5.2.1) but with the FCV, and servoactuator removed. The injector elements also remained, fixed in the full-open position. The shutoff valves used were of the Phase II design, except that Microseal

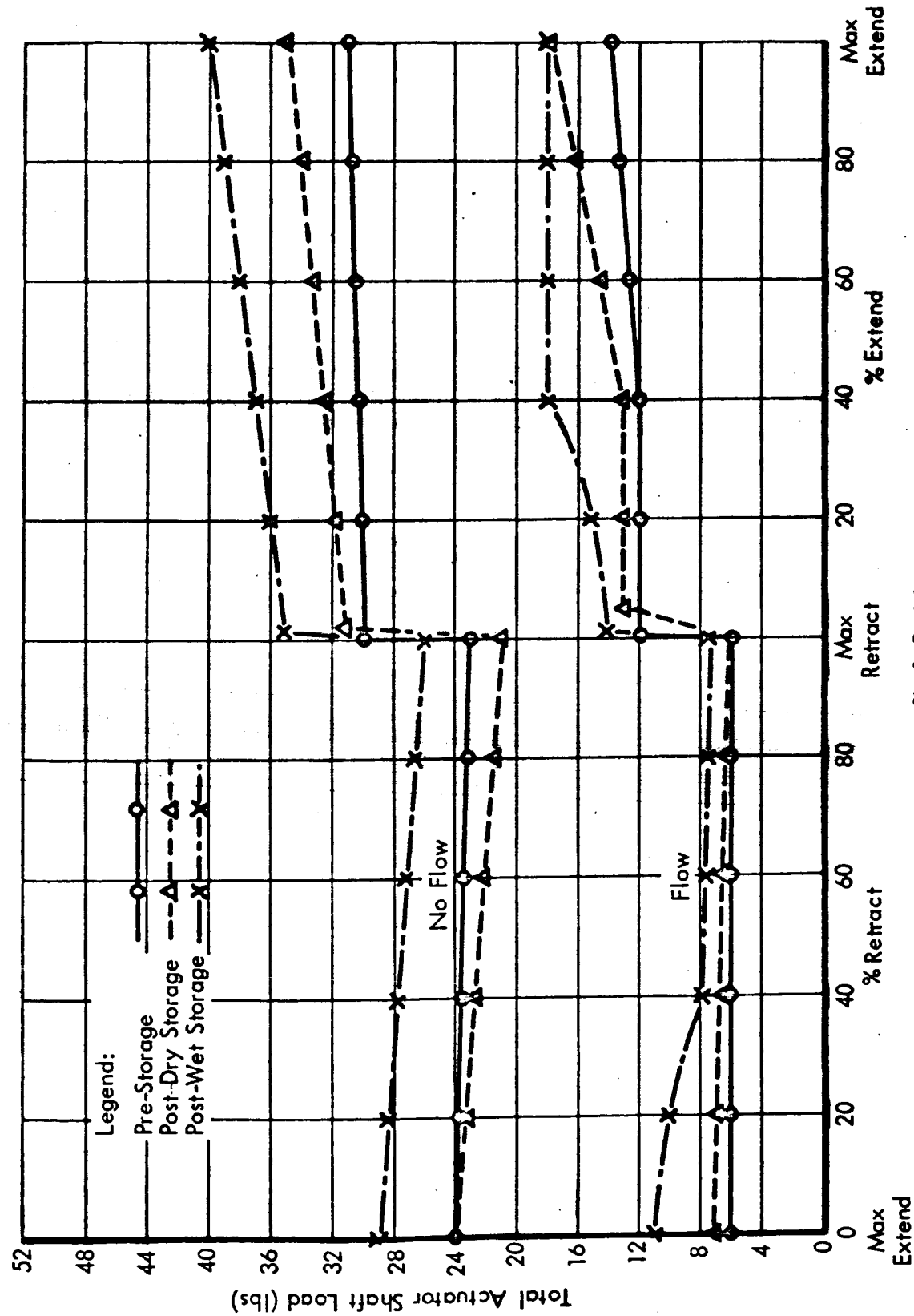

Figure 5.2.1-7. Actuator Shaft Loading Before and After Vacuum Test

was not used on the metal parts and Bal-Seals were used for static and dynamic seals. The helium pilot valve was P/N C 104337-1 (S/N 005).

The test setup, shown schematically in Figure 5.2.2-1, used helium for the pilot gas and water in lieu of propellants. Heat lamps were used to maintain a test specimen nominal temperature of 125°F.

5.2.2.2 Instrumentation

Test instrumentation was provided to measure and record the following performance parameters as functions of time:

1. Fuel and oxidizer injection pressures
2. Pilot valve solenoid current
3. Pilot valve solenoid voltage

Additionally, test specimen temperature was monitored to verify the 125°F temperature requirement.

5.2.2.3 Test Procedure

The test article was pressurized and the performance parameters were measured at (room) ambient conditions to establish reference values prior to vacuum storage. Following these initial control tests and with the system still pressurized, vacuum pumpdown was started. A pressure level of 2×10^{-8} torr was readily obtained, and the test specimen was soaked at this pressure for 168 hours. Throughout the vacuum storage, the pilot valve inlet pressure was 700 psig, the inlets to the SOVs were pressurized to 740 psig and the test specimen temperature was maintained at 125°F. It is noted that during the vacuum storage the water sump outlet was valved to the vacuum chamber such that the downstream portion of the SOVs was exposed to the vacuum environment.

At the conclusion of the 168-hour vacuum storage, the water sump outlet was valved to (room) ambient pressure. The pilot valve was then energized and de-energized several times with the aforementioned performance parameters being recorded during each actuation. The actuation signal was 16 VDC and the switch protection circuitry (see Paragraph 5.1.3) was connected to the pilot valve.

5.2.2.4 Test Data

Table 5.2.2-2 presents pre-vacuum storage and post-vacuum storage data on energize response times of the pilot valve and SOVs.

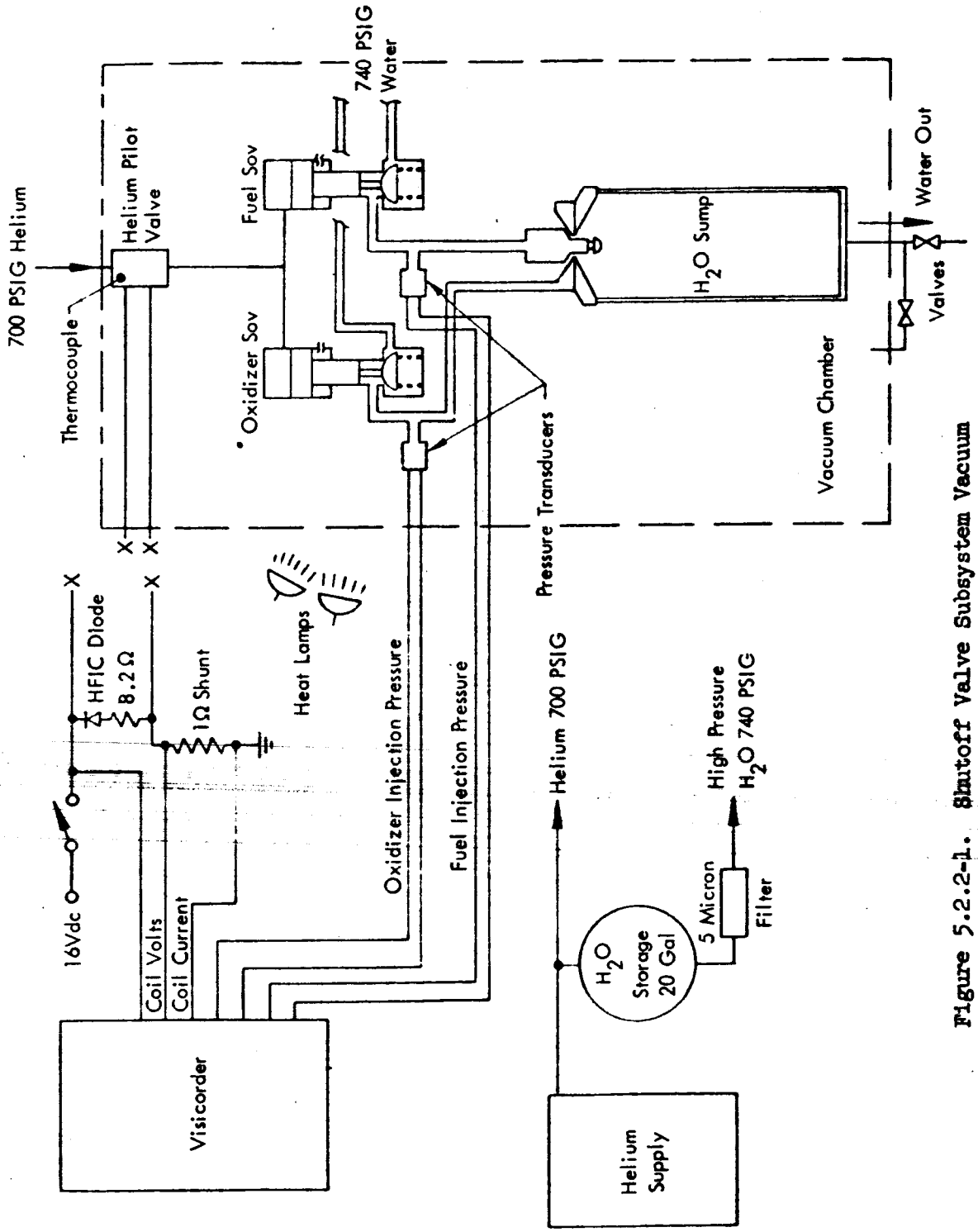

Figure 5.2.2-1. Shutoff Valve Subsystem Vacuum Test Setup - Schematic

Table 5.2.2-2

Shutoff Subsystem Energize Response Times

	Pre-Storage Energize Response Time (msec)	Post-Storage Energize Response Time 1 st Actuation (msec)	Post-Storage Energize Response Time 2 nd Actuation (msec)
Helium Pilot Valve	11	57	13
Shutoff Valves	13 (11 + 2)	61 (57 + 4)	15 (13 + 2)

NOTE: The energize response time is defined as the interval of time from closure of the pilot valve switch until movement of the particular valve is detected. Pilot valve movement is noted by a cusp in the solenoid current trace which indicates armature movement (see Figure 5.1.3-2). SOV movement is detected by a change in injection pressure downstream of the SOV poppet.

The first actuation of the pilot valve following the vacuum storage displayed a large delay in response time, perhaps caused by the start of cold welding. In subsequent actuations, the response time was approximately equal to the initial value; the small differences could be attributed to instrumentation and data reduction inaccuracy and to the fact that input power to the valve was less than that during control tests because of the temperature difference.

Cold welding or sticking of the SOVs was not indicated. The two-millisecond increase in time interval between pilot valve armature movement and SOV movement (i.e. 13-11=2 msec versus 61-57=4 msec) can be attributed to instrumentation and data reduction inaccuracy. The de-energize response times are not tabulated, since the oscillograph tapes did not indicate a difference between pre-storage and post-storage values.

To verify the apparent vacuum environmental affect on the pilot valve response, a third vacuum test, discussed in the paragraph 5.2.3, was performed.

5.2.3 Pilot Valve Vacuum Test

A third vacuum test was conducted in order to further assess the effect of a vacuum environment on performance of the helium pilot valve.

5.2.3.1 Test Setup Description

The same test setup was used for this test as was used in the previous vacuum test, except that two additional helium pilot valves were added as test specimens. The added pilot valves (P/N C104337-1) were S/N 016 and 017. For this test they were secured to a metal block within the vacuum chamber. The pilot ports of the added valves were capped and the vent ports were open to the vacuum chamber. Further, the inlets of these two valves were connected such that during vacuum storage the inlets could be either pressurized with pilot gas or exposed to the vacuum.

5.2.3.2 Instrumentation

Instrumentation for this test was the same as the previous vacuum test (see Paragraph 5.2.2.2) with the exception that current and voltage instrumentation were added for the two additional pilot valves.

5.2.3.3 Test Procedure

Prior to vacuum storage, the performance parameters were measured for each of the three pilot valves and two SOVs.

After initial control tests to establish test specimen reference values, vacuum pumpdown was started. Throughout the pumpdown and vacuum storage, the shutoff subsystem was pressurized as in the previous test whereas the two added pilot valves were internally as well as externally exposed to the vacuum environment. The test specimens were soaked at 2×10^{-8} torr and 125°F for 144 hours. At the conclusion of the 144-hour vacuum storage, the inlets to the two separate pilot valves were pressurized with helium. Each of the three pilot valves was then actuated twice by a 16 vdc signal and the various response times recorded.

5.2.3.4 Test Data

Table 5.2.3-1 presents the energize response time data of the three pilot valves. The SOV energize response time was not obtained because of an error in instrumentation wiring.

Table 5.2.3-1

Pilot Valve Energize Response Times

Pilot Valve Serial Number	Pre-Storage Energize Response Time (msec)	Post-Storage Energize Response Time 1st Actuation (msec)	Post-Storage Energize Response Time 2nd Actuation (msec)
005*	11	14	11
016	12	13	10
017	14	16	17

* Same valve used in previous test.

The post-storage actuation of the pilot valves did not indicate the sticking that had apparently occurred in the previous test. The small variations in energize response time can be attributed to instrumentation and readout in-accuracy, temperature differences and valve repeatability. The de-energize response times were, as before, unaffected.

As a result of this test, it was concluded that the pilot valve is not affected by vacuum environment. The previous indication of sticking with the S/N 005 valve may possibly have been caused by dirt between the armature and the bore.

5.3 SOV Component Evaluation Test Series

In Paragraph 3.2.3 it is stated that refinements to the SOV were incorporated during Phase III. Testing of these refinements is discussed in this paragraph. Table 5.3-1 outlines the parts of the shutoff valve package and the corresponding part numbers for the Phase II and Phase III designs. The SOV design features that were refined for the Phase III design are briefly described below:

1. Seals - The Phase II SOV used Omniseals. This seal is a spring-loaded Teflon configuration and sealing is achieved by single ridges on the O.D. and I.D. peripheries. The Phase III SOV uses Bal-Seals throughout. The Bal-Seal is also a spring-loaded Teflon configuration; however, it provided superior sealing because of uniform spring loading and two sealing ridges each on the O.D. and I.D. peripheries.

2. Microseal - Microseal is a dry film lubricant applied by a high velocity spraying process and was used on the Phase II SOV sleeve and piston to avoid galling and seizure. Action of the piston seals caused the Microseal to wear and flake off. The subsequent buildup of this material on the piston seals resulted in leakage. Microseal was not used in the Phase III SOV, since adequate piston to sleeve clearance presented no problem of galling or seizure.

3. Surface Finish - Critical area surface finishes of 8 and 16 microinches rms (per MIL-STD-10) in the Phase II SOV were replaced in the Phase III SOV with finishes of 4 and 8. The better finishes improved sealing, decreased friction, and enhanced seal life.

4. Poppet and Seat - The same basic poppet and seat design concept is used in Phase II and III SOVs. However, in the Phase II SOV, the poppet to seat contact diameter is 0.38 inches whereas the Phase III SOV a smaller Teflon O-ring seat is 0.31 inches. The smaller contact diameter of the Phase III SOV lowers the pilot gas pressure at which the SOV opens and enables the SOV to be used in a lower pressure system (e.g., 370 psia system instead of 720 psia).

5. Tolerances - The Phase III SOV incorporates smaller dimensional tolerances than those used in the Phase II configuration. The reduced tolerances improve performance repeatability and enhance component part interchangeability.

The SOV component evaluation test series was comprised of three separate tests which are discussed in the following paragraphs.

5.3.1 Seal Comparison Test

The objective of this test was to make a comparative evaluation of the performance characteristics of Omniseals versus Bal-Seals. The test specimens were a pair of Phase II SOVs with one valve assembly equipped entirely with Omniseals and the second valve assembly equipped with Omniseals for the static elements (i.e., sleeve seals) and Bal-Seals for the dynamic elements (i.e., piston seals). Each SOV was installed in a test block containing a cavity identical to the SOV cavity in the Phase II HEA. The two SOVs were pressurized with N_2O_4 at 700 psig. Valve actuation was accomplished by supplying the SOVs with 700 psig helium (through a tee connection) from a helium pilot valve.

Table 5.3-1

Shutoff Valve Package Refinements -
Part Number Changes

Item	Phase II Design	Phase III Design P/N
Sleeve	103947	106656
Piston	103948	106657
Poppet	103946	106798
Separation Washer	None	106670
Poppet Spring	MS 24585-182C1	MS 24585-182C1 (no change)
O-Ring Seat	Parker O-Ring 2-110T	Parker O-Ring 2-11T
Sleeve Seals	Omniseal R10105-015 A1N	Bal Seal 200-15
Piston Seal (small)	Omniseal R105J-.242 A1Q	Bal Seal 200-10
Piston Seal (large)	Omniseal R105J-.370 A1Q	Bal Seal 200-12

The test consisted of concurrent cycling of the SOVs and periodically measuring the fluid leakage from the vent of each SOV. The method of measuring leakage did not afford quantitative data; however, the test revealed that qualitatively the Bal-Seals were superior to the Omniseals in this application. From the start of the test the valve assembly completely equipped with Omniseals exhibited some leakage of N_2O_4 during actuation. This leakage was sporadic throughout the cycling period and became severe after 400 cycles. On the other test article using Bal-Seals there was no initial N_2O_4 leakage, but some did develop gradually with wear and became severe after 600 cycles. Static leakage, leakage of N_2O_4 during nonactuation - was undetected for either test aritcle after 1000 cycles of operation.

5.3.2 SOV Seal Life Test No. 1

The objectives of this test were to evaluate SOV life and galling or seizure resulting from not using Microseal. The test specimens were a pair of Phase II SOVs incorporating the design deviations noted below.

1. Microseal was not used.
2. All seals were Bal-Seals.
3. Surface finish in critical areas was 4 and 8 microinches rms.

The two SOVs were installed in the same test blocks used in the seal comparison test (described in paragraph 5.3.1). The SOVs were pressurized with N_2O_4 at 700 psig. Actuation was accomplished with 700 psig helium via a tee-connection from a helium pilot valve.

For this test, the SOVs were cycles for 2000 actuations with periodic interruptions for quantitative leakage measurements. The specific leakage paths which were periodically checked are identified in Figure 5.3.2-1. The leakage rates as a function of total actuations are tabulated in Table 5.3.2-2. Upon completion of 2000 actuations, the SOVs

were disassembled and visually examined. The seals were quite clean as compared to seals run in Microsealed bores, and there were no indications of galling or seizure. Visual inspection did not reveal the cause of helium leakage in Valve No. 1 (Path 1-2), but it is noted that this leakage would have been detected in HEA leak checks and corrective action taken.

Figure 5.3.2-1

SOV Leakage Paths

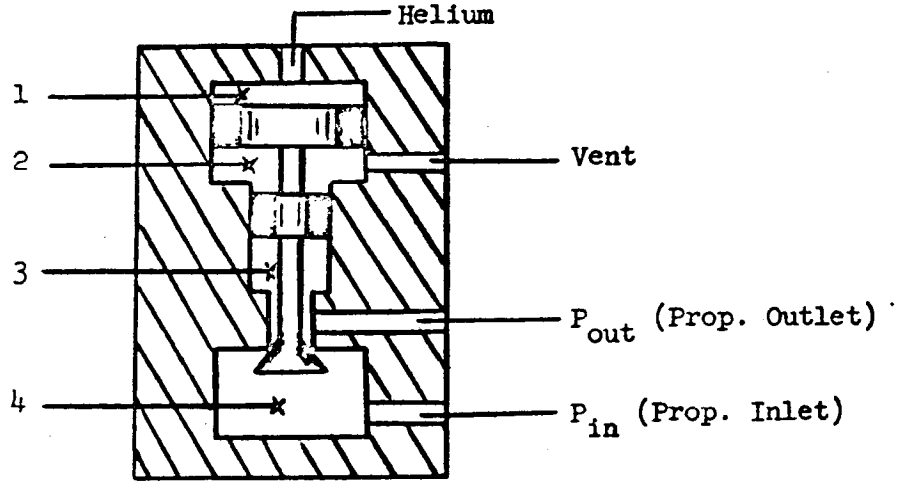

Leakage Path	Leakage Type	Pressure Conditions (psig) H_e	VENT	P_{out}	P_{in}
1 - 2	Helium	700	0	0	0
3 - 2	N_2O_4	700	0	250	250
4 - 3	N_2O_4	0	0	0	700

* Leakage from 4-3 checked with helium before testing and after 2000 valve actuations. All other leakage paths checked before testing and after each 200 valve actuations.

Table 5.3.2-2

Leakage Versus Actuations - SOV Seal Life Test No. 1

Number of Valve Actuations	Leakage Path and Type							
	1 - 2 Helium (scc/min)		3 - 2 N_2O_4 (scc/min)		4 - 3 N_2O_4 (scc/min)		4 - 3 Helium (scc/min)	
	Valve #1	Valve #2	Valve #1	Valve #2	Valve #1	Valve #2	Valve #1	Valve #2
0	23	0	0	0	0	0	0	0
200	67	.7	0	0	0	0	-	-
400	60	.3	0	0	0	0	-	-
600	40	0	0	0	0	0	-	-
800	60	0	0	0	0	0	-	-
1000	20	0	0	0	0	0	-	-
1200	30	0	0	0	0	0	-	-
1400	30	0	0	0	0	0	-	-
1600	30	0	0	0	0	0	-	-
1800	20	0	0	0	0	0	-	-
2000	30	0	0	0	0	0	.05	.06

Zero (0) leakage is defined as not detectable during an observation period of approximately one minute.

5.3.3 SOV Seal Life Test No. II

The objectives and conduct of this test was the same as in SOV Seal Life Test No. I. The identical SOV pistons were used in this test as in Test No. I but all other SOV parts were new. Here again, Microseal was not used and all seals were Bal-Seals.

The results of this test are presented in Table 5.3.3-1; the leakage path definitions of Figure 5.3.2-1 also apply. No leakage of N_2O_4 developed after 2000 cycles. The valves were disassembled and visually inspected. Here again, the seals were very clean and there were no indications of galling or seizure.

Table 5.3.3-1

Leakage Vs. Actuations - SOV Seal Life Test No. 2

Number of Valve Actuations	Leakage Path & Type					
	1 - 2 Helium (CC/Min)		3 - 2 N_2O_4 (CC/Min) (a)		4 - 3 Helium (CC/Min) (b)	
	Valve #3	Valve #4	Valve #3	Valve #4	Valve #3	Valve #4
0	3.3	1.3	0	0	0	0
400	2.0	.9	0	0	-	-
800	1.5	.8	0	0	0	0
1200	1.0	1.2	0	0	-	-
1600	1.3	1.2	0	0	0	0
2000	3.6	1.0	0	0	0	0

(a) Zero leakage is defined as not detectable during an observation period of approximately 2 minutes.

(b) Zero leakage is defined as not detectable during an observation period of approximately 10 minutes.

5.3.4 Additional Data

The poppet seat design of the Phase III SOV was not evaluated by a specific test series. The basic poppet and seat configuration, consisting of a Teflon O-ring seat and speherical radius poppet, is used in both the Phase II and III SOVs and was well tested. However, the reduced poppet seat contact diameter used in the Phase III results in the bottom sleeve static seal (Bal-Seal 200-15) being exposed to system pressure and functioning as a primary seal. In the Phase II SOV design, the bottom sleeve seal was actually a secondary element since primary sealing was performed by compression of the O-ring seal between the sleeve and a step in the SOV port.

The Phase III SOVs have been installed in nine MIRA 150A HEAs (S/Ns 001, 002, 004, 005, 007, 008, 009, 010, and 011) and have undergone leak tests and operational use. The performance of the design has been satisfactory. The few leaks associated with the poppet seat or lower seal that were encountered were traceable to installation of defective parts, dirt, or inadequate surface finish. These leaks would have been detected during HEA acceptance testing and would have resulted in replacement parts being installed on the TCA prior to its delivery.

5.4 Servoactuator Evaluations

Two short developmental tests were performed on the servoactuator alone. One was a test for performance at the expected minimum, in-flight temperature, i.e., near 0°F. The other test was to determine performance at various inlet fuel (MMH) pressure levels down to 350 psia. This latter test was accomplished to support a spacecraft system evaluation of a possible low pressure propellant feed system and to support the servoactuator power system evaluation study discussed in paragraph 5.5.

The servoactuator low temperature test was performed on a Phase II Follow-On unit, S/N C53751. Hysteresis, deadband, step response, and frequency response characteristics were measured at ambient temperature in accordance with STL Acceptance Test Procedure 9354.4-140. The actuator and fuel were then cooled to 0-15°F, and the servoactuator characteristics were again measured. No change in performance occurred.

The low pressure tests were conducted on two Phase II Follow-On servoactuators, S/N C53747 and C53748, to determine the following performance parameters at three pressures 700, 500 and 350 psi:

1. Null Leakage
2. 100% Stroke Rise Time
3. 25% Stroke % Overshoot
4. 25% Stroke Settling Time
5. 5 cps 10% Stroke Phase Lag

These tests were conducted under imposed loads corresponding to those imposed by the FCV loading. The compressive loads assumed were 12 lbs at 350 psia MMH pressure, 19 lbs at 500 psia, and 25 lbs at 700 psia.

Test results are shown in Figure 5.4-1. Null leakage and phase lags were within STL specification limits for all differential pressures from 350 to 750 psi. Step response rise times and settling times were generally over the required limits specified in the component specification.

In view of these results, it was concluded that the performance parameters can be altered to result in a S/A design that would meet all performance requirements at the 350 psi ΔP condition. However, the effect of low differential pressure on reliability is unknown.

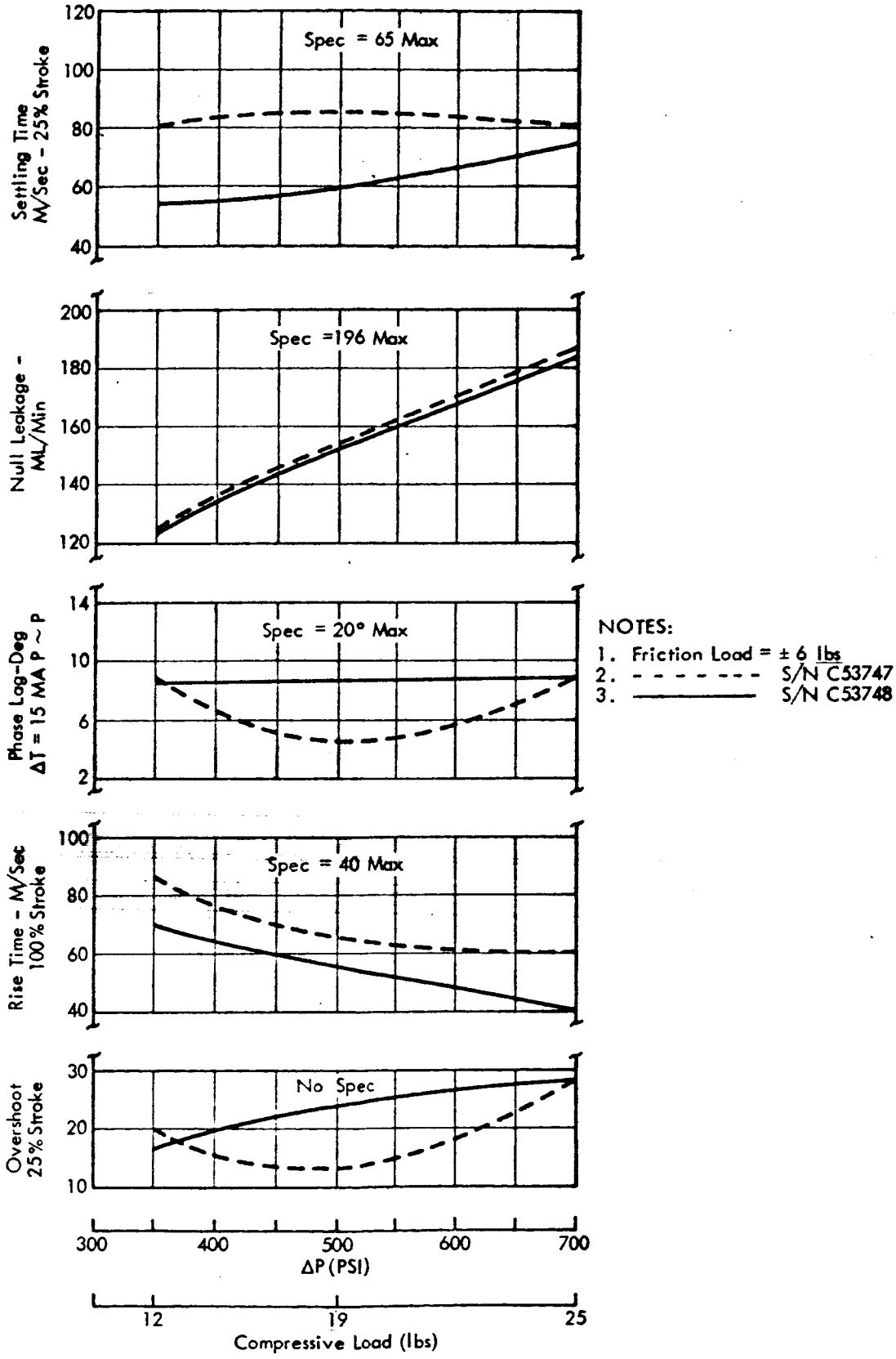

Figure 5.4-1. Servoactuator MMH Low Pressure Tests

5.5 Servoactuator Power Systems Evaluations

Prior to final selection of the servoactuator power system using MMH with overboard dump (see section 3.0), several other possible power systems were evaluated. Of the alternate approaches the most extensive effort was expended on a separate hydraulic power supply (HPS).

5.5.1 Alternate Systems Considered

Six different servoactuator power systems were considered. They are shown schematically in Figure 5.5.1-1.

Scheme	Description
I	Battery driven, separate hydraulic power unit (HPU), using oil.
II	Low pressure drop, fuel-driven servoactuator with regulator bypass.
III	High pressure, fuel-driven servoactuator with overboard MMH dump.
IV	Electromechanical servoactuator.
V	Helium motor-driven hydraulic power supply, using MMH as hydraulic fluid.
VI	Electropneumatic servoactuator using helium.

The evaluation results are summarized in Table 5.5.1-2. As a result of the evaluation, STL recommended System I, the electric motor-driven hydraulic power supply for the following reasons:

1. Existence of a highly reliable, readily adaptable, qualified, missile type hydraulic power unit now used on the second stage of the MINUTEMAN Wing VI missile.
2. High system reliability.
3. Competitive overall weight for spacecraft vernier engine system.
4. Short development and qualification test periods.
5. Sealed hydraulic system resulting in lowest possibility of actuator contamination.
6. Excellent ground functional checkout capability.
7. System dynamics uncoupled from the propellant feed system.
8. Allows man rating the propellant tanks because of reduction in feed system pressure requirements.

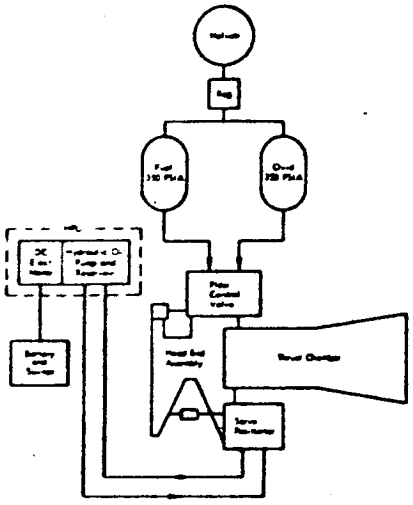

Hydraulic Power Unit - Electric Motor Drive

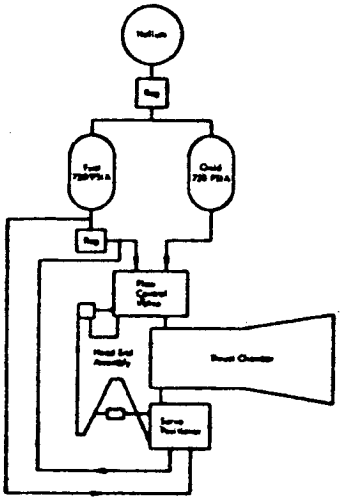

Low ΔP Servo Positioner

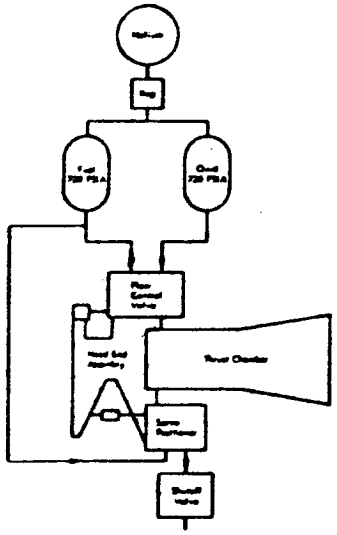

High ΔP Servo Positioner - Overboard Dump

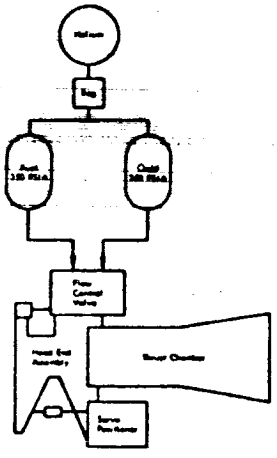

Electro-Mechanical Servoactuator

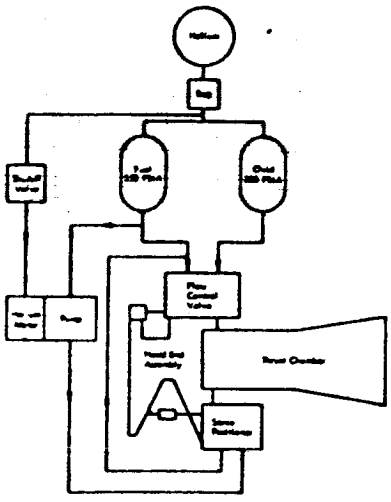

Helium Driven Fuel Power Supply

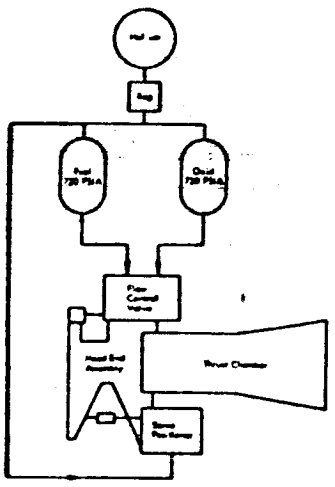

Electro - Pneumatic Servo Positioner

Figure 5.5.1-1. Alternate Servoactuator Power Systems

Table 5.5.1-2

Servoactuator Alternate Power Schemes
Comparison

Scheme	I Battery-Driven Separate HPS	II Low P MMH S/A P.R. Bypass	III MMH S/A Overboard Dump	IV Electromechanical S/A	V Helium Motor-Driven HPS Using MMH	VI Electropneumatic Helium S/A
STL components	1. HPU (Mod of Existing). 2. Battery & switch. 3. Alter S/A for oil.	1. Low P S/A. 2. Pressure. regulator.	1. On-off valve.	1. Servoactuator. 2. Battery & Switch 3. Power amplifier.	1. He driven motor. 2. MMH pump. 3. He solenoid valve.	1. Servoactuator
HAC components to alter develop	1. Lighten He bottle. 2. Redesign Prop. tanks. 3. Redesign He P.R. 4. Redesign relief valve. 5. Hydraulic lines. 6. Thermal control. 7. HPS mounting and wiring. 8. GSE & telemetry.	1. Redesign He bottle. 2. Thermal control.	1. Dump manifold and valve. 2. Thermal control. 3. Valve wiring. 4. Redesign He bottle.	1. Wiring. 2. Thermal control. 3. Battery mounting. 4. Redesign He bottle. 5. GSE & telemetry. 6. Redesign regulator.	1. He lines. 2. Redesign He bottle. 3. Wiring. 4. Thermal control. 5. Redesign regulator. 6. GSE & telemetry.	1. Redesign He bottle 2. He lines. 3. Redesign regulator. 4. Redesign relief valve.
Spacecraft vernier engine system weight, lbs (no propellants)	98.26 assuming optimized 370 psia feed system design.	98.38 assuming 720 psia feed system.	105.13 assuming 8 lb fuel dumped and 720 psia feed system.	113 (rough estimate)	97.76 assuming present He tank, titanium prop. tanks, and 370 psia feed system.	109.5 (rough estimate)
Expected component qualification program completion date	1 March 1965	1 July 1965	15 March 1965	May 1966 with twice required deadband & phase lag.	August 1965	Approx. 2 years
Primary development considerations	1. S/A redesign low. 2. Exercise of control system simple. 3. System uncoupled from prop. feed system. 4. Allows man rating prop. tanks. 5. Provides for HPS spacecraft. 6. No S/A purge required for defueling 7. No fuel dumped.	1. Minimum changes to spacecraft. 2. Least change to spacecraft.	Highest confidence for qual. completion on time.	System uncoupled from prop. feed system.	No battery or DC motor required compared to Scheme I.	High reliability

9. Excellent spacecraft growth potential with regard to use of the HPS for other uses (e.g., to drive equipment to be used after the spacecraft reaches the moons surface).

10. Low development risk.

5.5.2 Hydraulic Power Supply

A development program was initiated to develop a completely closed HPS using hydraulic oil as the power fluid. The HPS was comprised of a hydraulic power unit (discussed in paragraph 5.5.2.2) and associated hydraulic lines and fittings. One HPS was designed to provide power to the servoactuators of all three TCAs on board the spacecraft.

The spacecraft location chosen for the HPS was near the helium tank, somewhat outboard of the main spacecraft frame. This location was chosen to satisfy thermal control, weight and balance, and hydraulic line routing and length considerations.

Two system detail design alternatives were considered. One alternative was to package the battery and switch in a separate container, requiring the HPU to undergo modifications needed for operation in a hard vacuum environment. The second alternative was to package the HPU, battery, and switch in a sealed container which would be pressurized with inert gas at a moderate pressure. Figures 5.5.2-1 and -2 show two packaging arrangements for the second alternative, assuming 20 battery cells.

The MMH servoactuator design (see paragraph 3.2.6) was reviewed for use with hydraulic oil. Items requiring design changes for the change in fluid media were:

- Seal materials (compatibility).
- Orifice and nozzle sizes.
- Feedback spring rates.
- Spool centering springs.

These required changes were considered minor and easy to incorporate in the existing MMH servoactuator design.

During the course of the HPS program, purchase requisitions were submitted to procure 5 HPUs including a special test HPU, to permit hard vacuum starts to be made during spacecraft systems tests, and one mass mockup unit. In addition, the loan of two MINUTEMAN units was negotiated. One HPU and three pressure transducers were received from vendors, and the two loan HPU units were received.

Before testing was started on HPS components a decision was made to develop Scheme III (see Figure 5.5.1-1).

A detailed discussion follows on the major constituents of the HPS and its predicted performance.

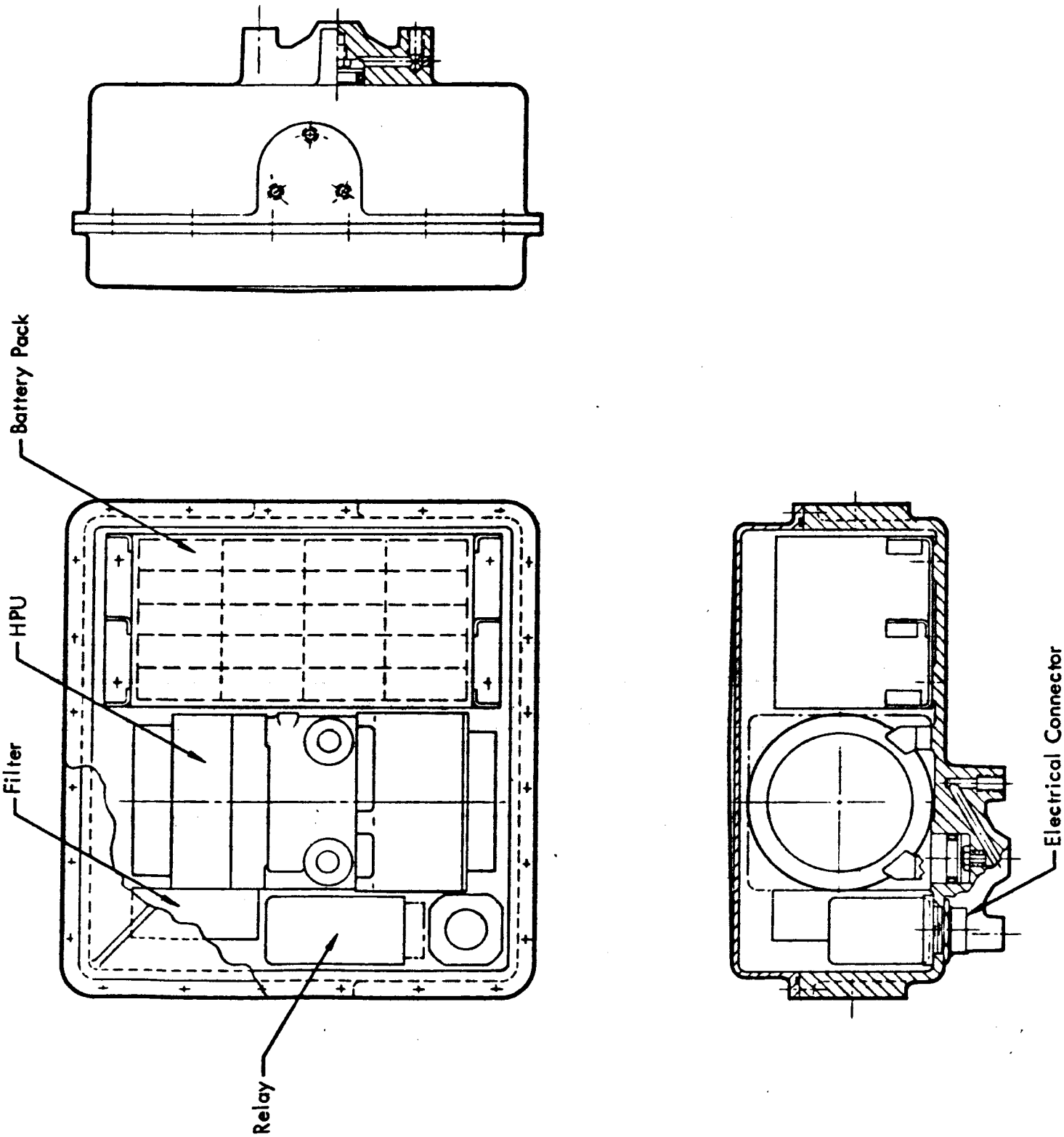

Figure 5.5.2-1. HPS Package-Alternate A

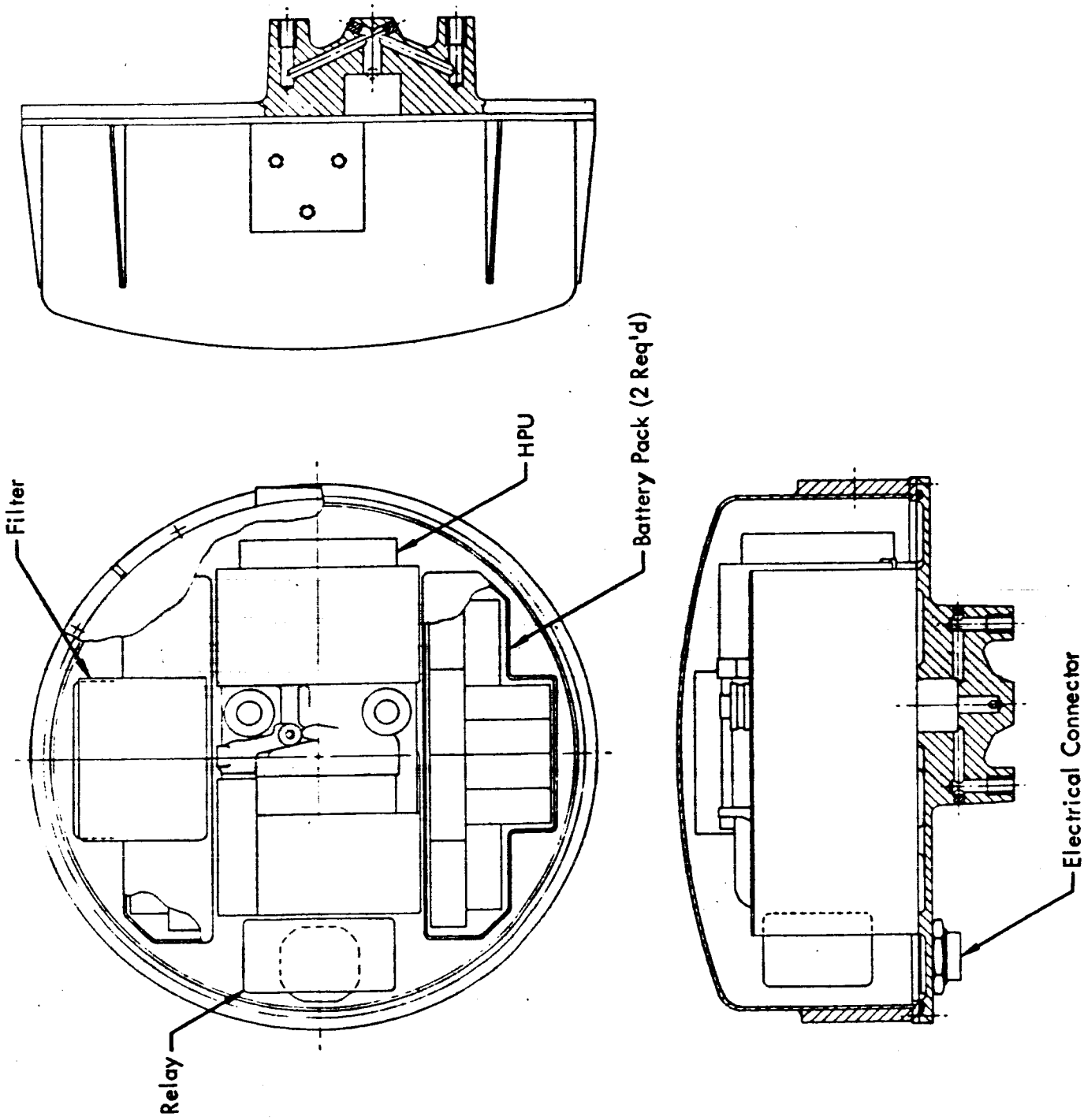

Figure 5.5.3-2. HPS Package-Alternate B

5.5.2.1 Hydraulic Power Unit (HPU)

Vickers Aerospace Division, vendor of the second stage Wing VI MINUTEMAN HPU, was chosen to make the minor modifications to this HPU for use with the MIRA 150A. The modified HPU was given Part No. EA1513711-2 and it is schematically represented in Figure 5.5.2-3. Figure 5.5.2-4 shows the actual MINUTEMAN HPU.

The modified HPU consists of the following components:

- Variable-delivery, pressure compensated hydraulic pump.
- DC, explosion-proof, pump-drive electric motor.
- Self-pressurizing reservoir.
- Pressure transducer.
- Hydraulic oil filter.
- Radio noise filter.
- Check valve.
- Manifold.
- Fill and bleed disconnects.

The displacement of the pump is varied by controlling the angle of the cam plate by use of the compensator. The compensator is a three-way valve which senses system pressure and ports fluid to the stroke control piston to change pump flow, maintaining system pressure between required limits.

The welded steel bellows reservoir acts as a compression spring to maintain a minimum system pressure for storage purposes and to facilitate pump startup. Following the initial startup command, the reservoir is pressurized by system pressure.

Radio frequency interference (RFI) requirements were given in Hughes Aircraft Company Specification No. 226100, "Electromagnetic Interference Specification." Low ripple voltages and essentially no commutator arcing result from a minimum number of armature turns and a maximum number of commutator bars in the motor. This motor design keeps the armature reactance voltage and commutator bar-to-bar voltage at a minimum. The radio noise filter utilizes the inherent inductance of the motor field windings as inductive elements of symmetrical filter networks. The motor compensating field windings are divided equally between the positive and negative circuits in a four pole configuration. Conducted and radiated RF energy is thus kept below specification requirements using a light weight radio noise filter.

5.5.2.1.1 Considerations for Space Environment Operation - If the pump-drive, DC motor were to operate satisfactorily in a deep vacuum environment without the packaging and pressurization noted earlier, modifications from the original MINUTEMAN design would be required. A study was performed, investigating the feasibility of such modifications.

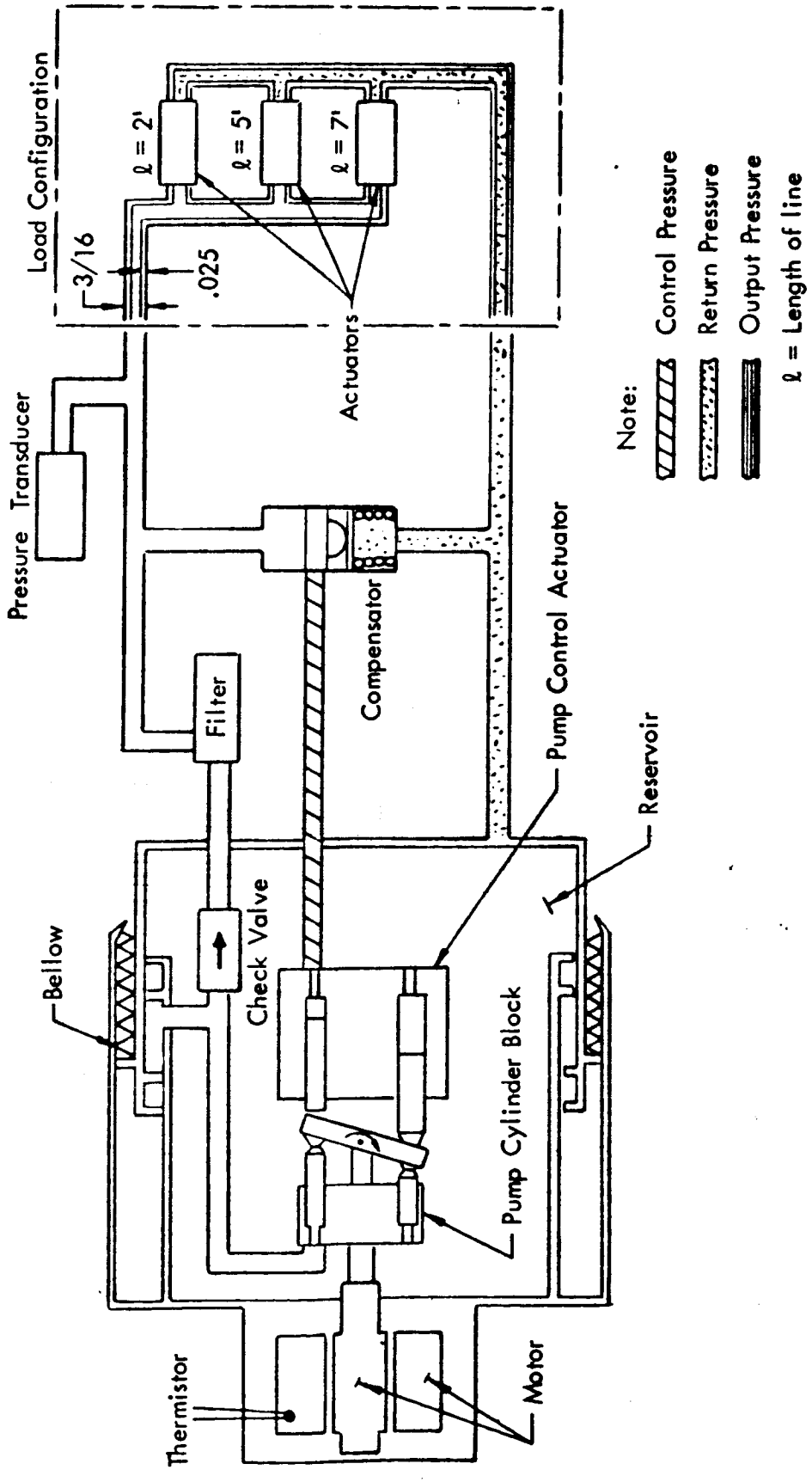

Figure 5.5.2-3. Hydraulic Power Unit Schematic

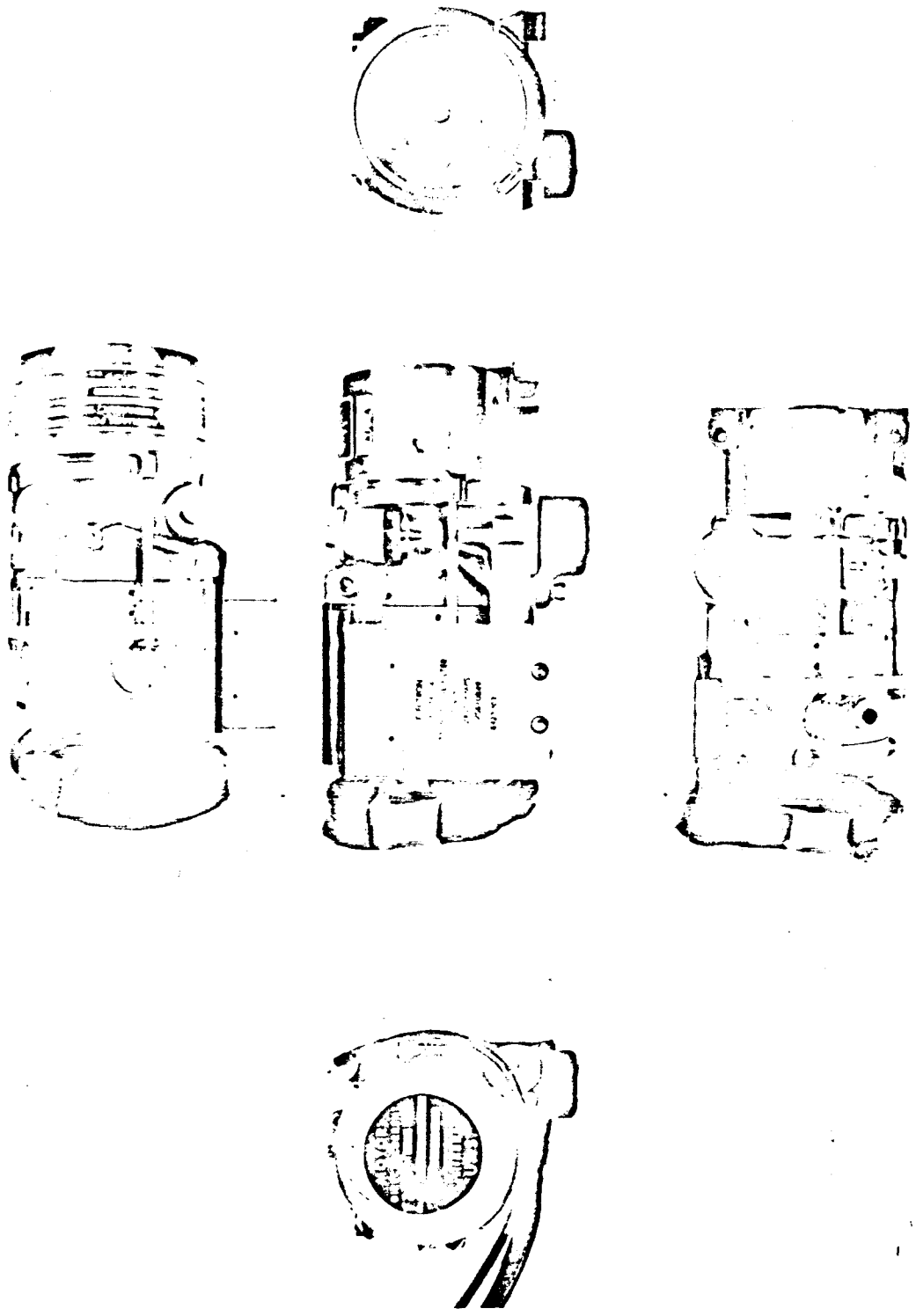

Figure 5.5.2-4. Hydraulic Power Supply Pictorial Views

On the proposed design the motor and pump have a common shaft allowing good heat conduction. The partially sealed bearings combined with the explosion-proof motor sealing were estimated to result in pressures at the bearings of about 10^{-6} torr when the HPU is exposed to 10^{-11} torr. Proposed plugging of the shaft seal drain port would further improve this motor internal pressure situation. In a vacuum, the DC motor brush material deposition must supplant the ambient oxidation film and provide a lubricant film on the commutator of low enough resistance to minimize voltage drop, but sufficiently high to prevent undue brush short-circuiting and wear out. A possible brush material for use in deep vacuum was estimated to consist of electrographitic carbon, copper, silver and additives to control filming rate. This material would have to operate at temperatures not to exceed 550°F. A change to the brush spring rate probably would also be required.

The order of sublimation of materials of the HPU were considered to be: oil, lubricant, insulation of armature and field, highly polymerized resins of the mechanical insulation, brush impregnants, and lastly, metals. Of the 2.23 lbs of motor weight, it was estimated that 5% would sublimate in three years under deep vacuum environment.

Other anticipated changes required to convert the existing Vickers HPU from Model No. EA1513-530-2 to Model No. EA1513-711-2, are summarized below. These changes would permit the HPU to operate within the performance requirements and environmental conditions defined for the Surveyor application.

Reservoir - Change spring preload on bellows to simulate the existance of sea level atmospheric pressure under outer space conditions.

Manifold - Revise shaft seal leakage drain holes to permit plugging after seal leakage check.

Seals - Change all O-ring seals to a material capable of withstanding the required temperature cycle.

Pressure Transducer - Change operating pressure range from 0-700 psia to 0-1000 psia.

5.5.2.1.2 Predicted Performance of HPU - A special test was performed by the vendor prior to subcontract award to insure that the Vickers MINUTEMAN HPU would meet the pressure-flow requirements. Test data, shown in Table 5.5.2-5, confirmed that the unit would meet the requirements subsequent to slight modifications. Considerable effort was expended in an analysis of the HPU predicted performance and its compatibility with system requirements and servoactuator characteristics.

These studies confirmed the earlier opinion that minor modifications to the existing HPU, plus development of the batteries and the packaging, would provide an HPU that was: (1) fully capable of powering the servoactuators, and (2) adaptable to the required spacecraft installation.

A preliminary draft of an equipment specification for the HPU was prepared. This unreleased document was given the specification number, EQ 2-40. Some of the primary performance requirements are excerpted in Table 5.5.2-6.

Table 5.5.2-5

MINUTEMAN HPU Performance

Notes: 1. Motor brushes: M46 type with 1 hour run-in.

2. Flowmeter calibrations: 352 cps = .70 gpm
454 cps = .90 gpm
475 cps = .95 gpm
504 cps =1.00 gpm

3. HPU Model 442-2.

4. MIL-H-5606 oil.

5. Surveyor maximum required flow = .79 gpm at 750 psi ΔP.

ΔP (psi)	P_{in} (psig)	P_{out} (psig)	Flow (gpm)	Shaft Torque (in.-lb)	Shaft (rpm)	Motor Voltage (volts)	Current (amps)	Oil Temp. (^{o}F)	Remarks
421	47	468	.95	3.04	11,179	24	24.5	85	Motor yoke-setting poing.
741	79	820	.71	3.49	11,127	24	28.6	86	Motor cold.
750	70	820	.60	3.22	11,275	24.5	26.2	91	Motor hot.
750	70	820	.70	3.44	11,084	24	28.4	89	Motor hot.
750	70	820	.90	4.05	10,470	24	32.9	91	Maximum available flow at 750 psi ΔP, motor hot.

Table 5.5.2-6

Selected HPU Performance Requirements
(From EQ 2-40)

Operating Fluid	MIL-H-5606 hydraulic oil
Voltage, vdc	
Nominal Operating	22 to 30
Overload Rating - for 0.010 seconds	40
Operating Pressures, psia	
Nominal differential operating pressure	750
Maximum inlet pressure	90
Pressure versus flow demonstration requirement	See Figure 5.5.2-7
Flow Rates, gpm	
Minimum operating flow rate	0.156
Maximum flow rate	0.790
Flow demonstration	See Figure 5.5.2-8
Flow Response	
Demonstration requirement	See Figure 5.5.2-9
Maximum Time, seconds	
(1) From 63% of full flow to minimum flow	0.015
(2) From minimum flow to 63% of demanded full flow.	0.015
Startup time, seconds (from voltage application to achievement of 0.160 gpm)	0.090

5.5.2.2 Battery

The battery and switch requirements for powering the HPU during the mission cycle were analyzed in detail, resulting in the selection of a secondary type battery.

Battery development activity was suspended in the middle of June 1964.

5.5.2.2.1 Requirements - Preliminary battery design requirements were derived based on the 8.5 - minute duty cycle shown in Table 5.5.2-10. This duty cycle was considered to be very conservative. The total power requirements derived from the duty cycle (Table 5.5.2-10) in conjunction with Figures 5.5.2-11 and -12 are given below for alternate average battery voltages.

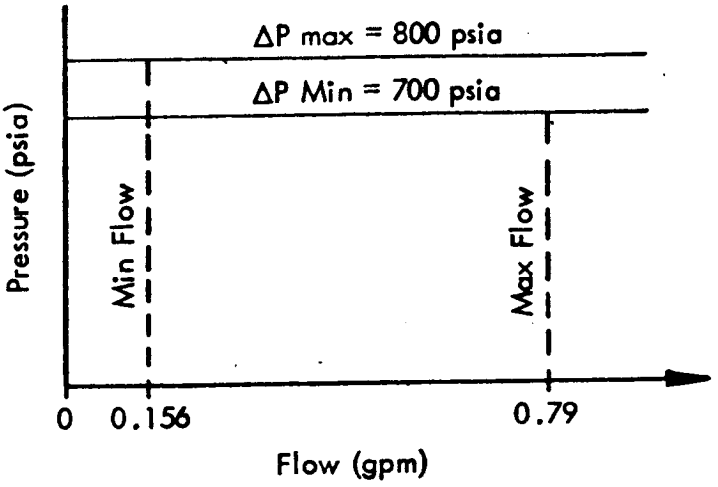

Figure 5.5.2-7. HPS Pressure Flow Relationship

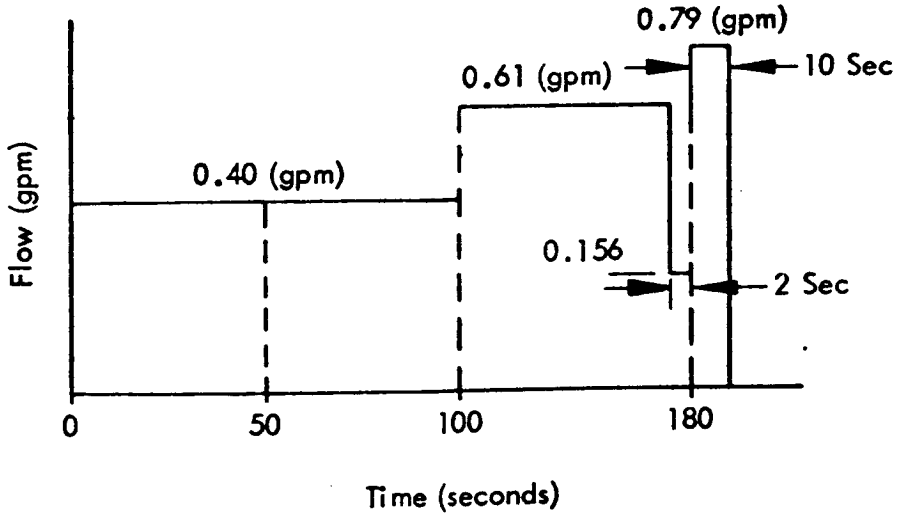

Figure 5.5.2-8. Flow Time Demonstration

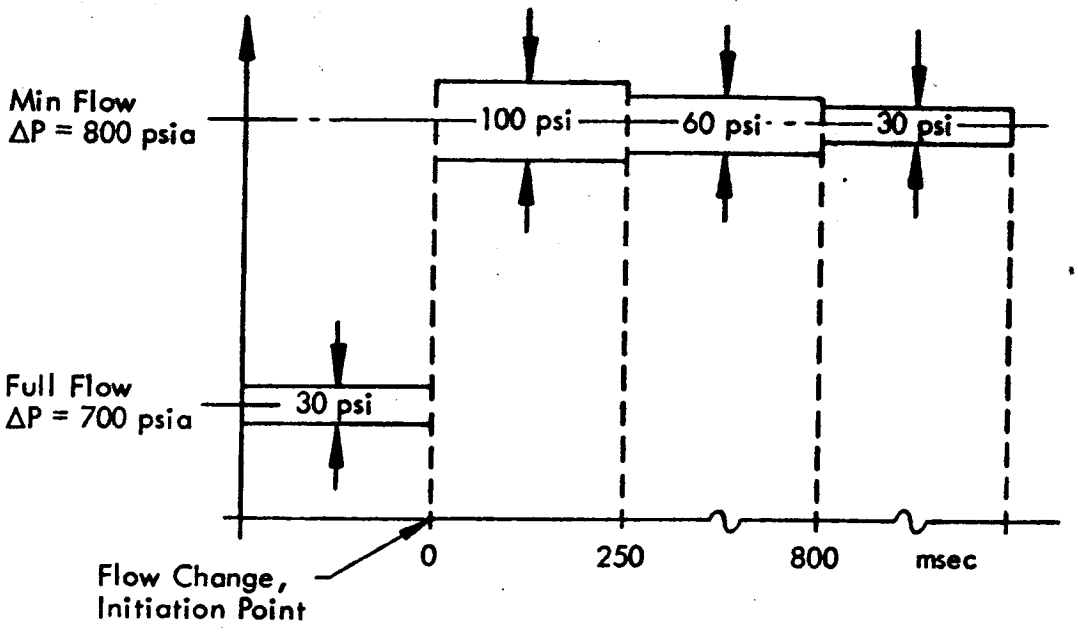

Pressure Versus Time (Max-Min Flow)

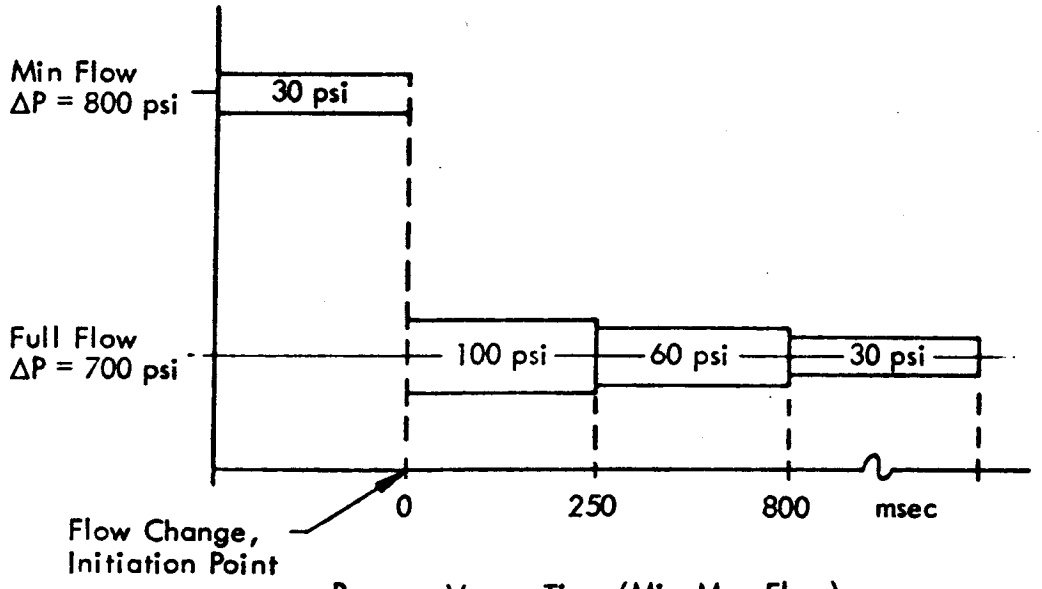

Pressure Versus Time (Min-Max Flow)

Figure 5.5.2-9. Dynamic Response Demonstration

Design Voltage	22 vdc	24 vdc	28 vdc	30 vdc
Watt hours over mission cycle	70.3	74.1	79.8	82.7

In addition to the approximately 80 watt-hour power requirement, other technical requirements established for the battery were:

1. To survive after the lunar landing without liquid leakage or explosion for 5 days at 300°F followed by 15 days at -300°F.

2. To be capable of at least 30 days stand time when wet at 20°F to 100°F prior to launch - recharging permitted during this period.

3. To be capable of operating during launch and in any attitude in space.

4. To be capable of supplying motor current requirements during the start transient, (assuming a start voltage of 24 vdc the motor current requirements for start was 90 amperes, decaying to the steady state requirement in approximately 0.3 seconds

Table 5.5.2-10

Battery Duty Cycle

Starts	Load Curve Shown in Figure 5.5.2-11	Time (sec)
#1	A	30
#2	A	60
#3	B	20
#4	B	20
#5	B	20
	A	10
	B	10
	A	30
	B	10
	A	280
	B	10
	A	10
Totals	A	420
	B	90

Battery usage to occur as follows:

1) Turn on #1 to occur near beginning of 100-hour period.

2) Turn on #2 to occur near middle of 100-hour period.

3) Turn on #3, #4, and #5 to occur near end of 100-hour period.

Total mission time = 100 hours.

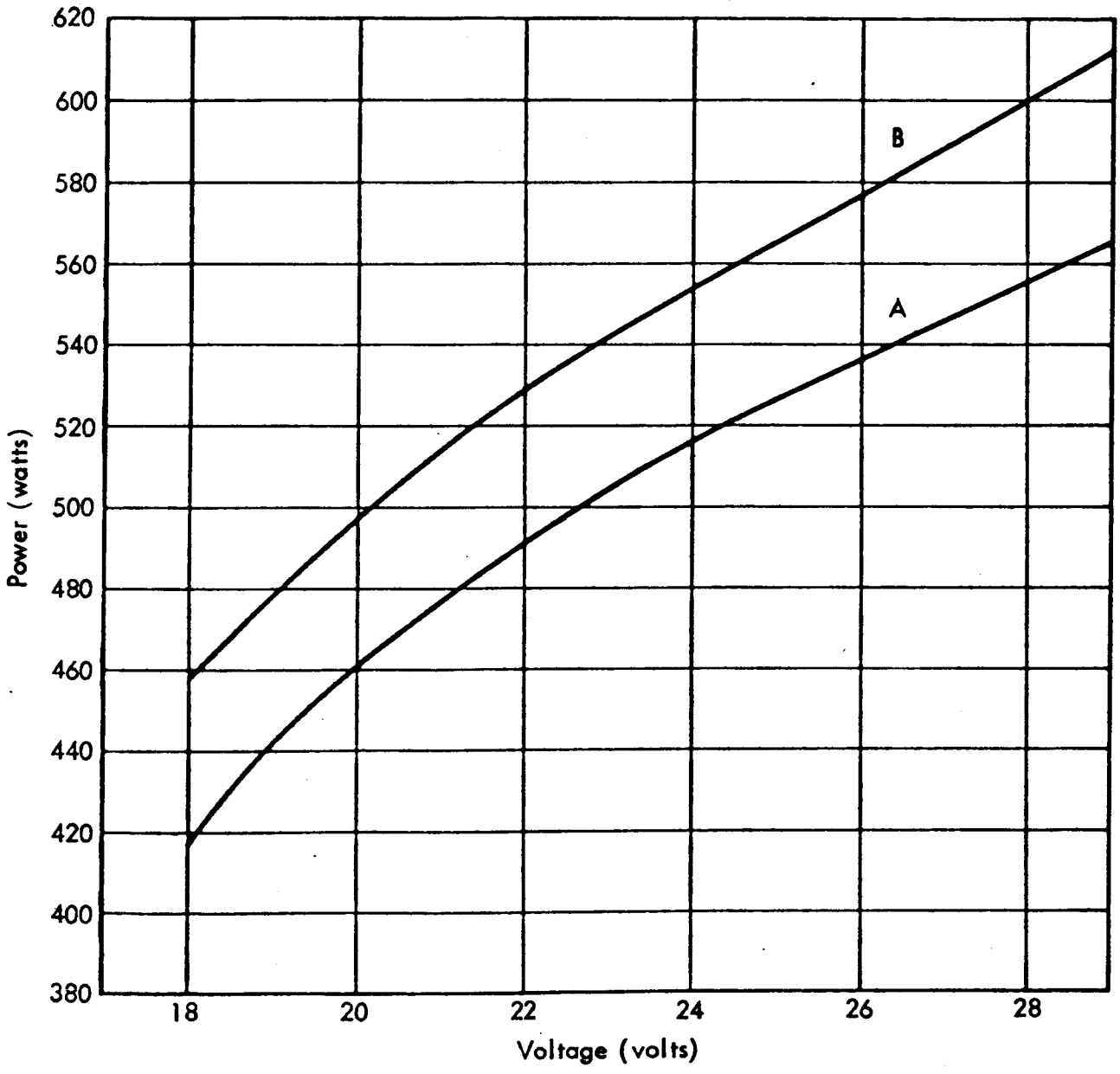

Figure 5.5.2-11. Motor Power Versus Voltage

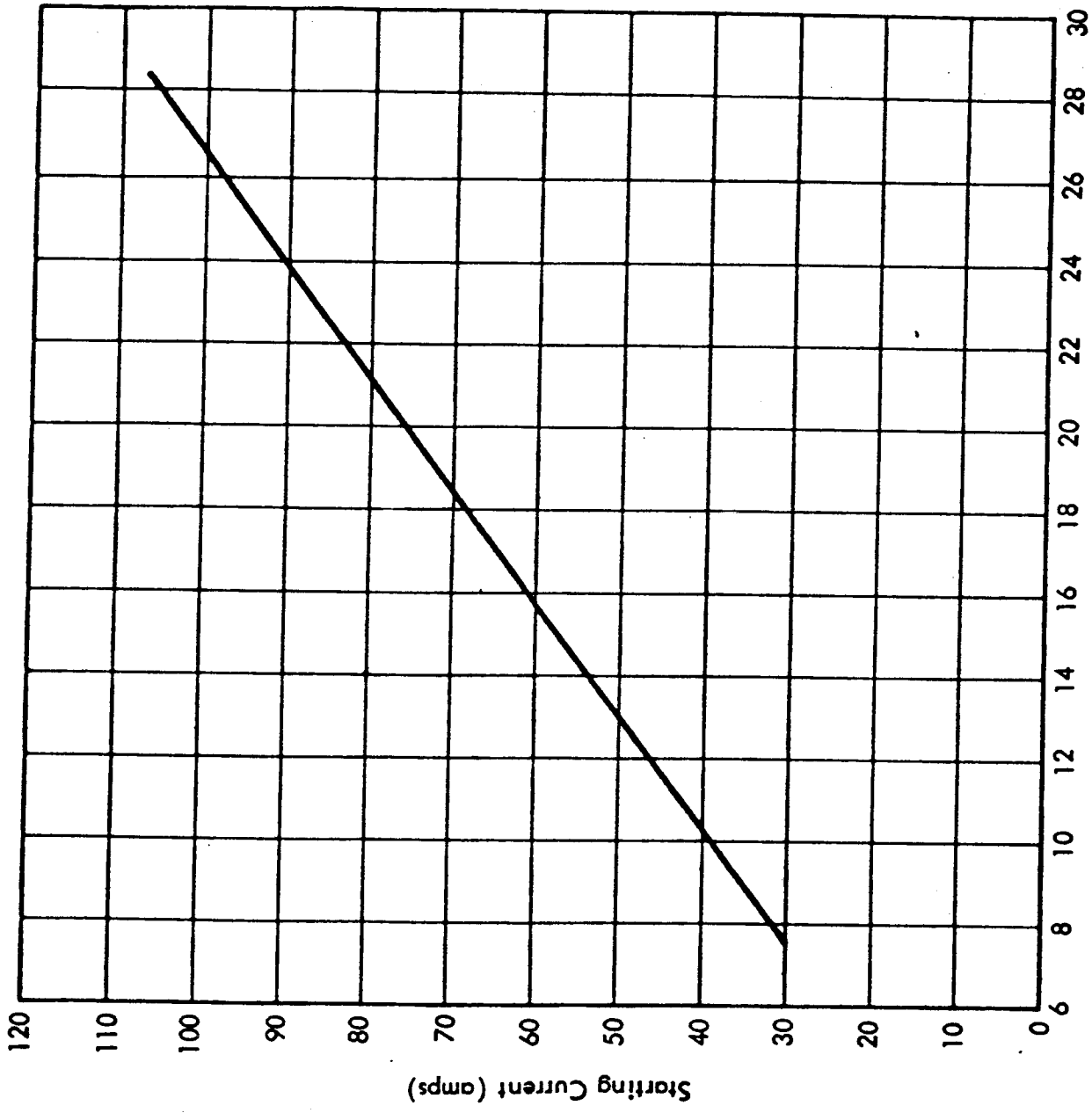

Figure 5.5.2-12. Motor Starting Current Versus Voltage

A summary of the battery requirements was given to vendors to obtain their recommendations. Since there was not time to develop a new battery for this application, a choice was to be made of batteries or cells presently in production. The following is a summary of vendor recommendations:

(1) Electric Storage Battery - The ESB Type 224 battery was recommended. It was in production and was to be used on Surveyor Test Spacecraft T-2. The cells have a six-month stand life and are capable of 10 cycles of operation. Twenty cells, the number needed, would weigh four pounds and could probably be packaged for a total weight of 5.0 lbs. The ESB Type 241 battery weighing 6.8 lbs might also be useable.

(2) Eagle-Picher - Eagle-Picher recommended using Type 515 cells in a MAR 4196 container. This battery was similar to one of the batteries that was supplied to STL for the Polaris STV Program. This battery weighed 6.0 lbs.

(3) Yardney Electric - Yardney Electric had no suitable battery in production. However, they recommended using 17 Type HR-3 cells in a titanium case estimating a maximum weight of 6.0 lbs. Delivery of this battery was estimated at 3-4 months, cells alone in 4-5 weeks.

6.0 TEST FIRING EFFORT

The hot firing tests conducted during Phase III are outlined in this section. The results of these tests are discussed to the extent needed to substantiate the performance set forth in paragraph 3.4.

6.1 Combustion Chamber and Nozzle Assembly Final Selection Tests

As related in the Phase II Final Report (STL Document 9730.4-64-36), the two-piece JTA nozzle throat insert had been chosen by the end of Phase II as the primary throat configuration for the MIRA 150A CC & NA. A secondary design, still under consideration at that time, was the tantalum-tungsten alloy throat insert.

As planned in paragraph 3.1.2 of the Phase III Development Test Plan (STL Document 9730.4-64-1-43), a series of final selection tests were performed using three sea level chambers with coated tungsten throat inserts, three sea level chambers with 90% tantalum-10% tungsten throats, and nine sea level chambers with JTA graphite throats (eight of which were of the final configuration). The specific test objectives for these final selection tests were to:

1. Determine the reproducibility of service life of the JTA insert design by testing with several MIRA 150 injectors.
2. Determine the effect of a silica-tape overwrap on the service life of the ablative liners.
3. Determine the effect of a JTA graphite convergent section upstream of the throat on the durability of the throat inserts.
4. Compare service life limits of the candidate nozzle materials.
5. Determine the valve of an oxidation protective coating on tantalum-tungsten.

The test conditions for the final selection test series were the following:

Propellants:	NTO or 90-10 MON, and MMH
Mixture Ratio:	1.5 ± 0.05
Starting Chamber Pressure:	125 ± 5 psia (0.920 inch diameter throat) 104 ± 5 psia (1.00 inch diameter throat)
Combustion Efficiency, C*:	5400 ft/sec ± 1%
Firing Schedule:	15 seconds at maximum P_c followed by a cool down to ambient temperature, 50 seconds at maximum P_c followed by a cool down to ambient temperature, and a final 235-second firing at maximum P_c.
Environmental Conditions:	Ambient sea level conditions with ambient propellant temperatures and prestart chamber temperature. No thermal blanket used on chambers.

The results of the final design selection tests are summarized in Table 6.1-1. The significant conclusions drawn from these tests are as follows:

1. The primary throat design (i.e., two-piece JTA insert) is more than adequate for the intended use. (Full duration firings were successfully completed on eight chambers employing this throat design. Two MIRA 150 injectors were used in this series, neither producing any throat erosion following 300 seconds of operation. One JTA throat was fired for a total of 1141 seconds and resulted in only an 11% throat area increase. Another JTA graphite throat was tested at the maximum MIRA 150A chamber pressure of 110 psia for a total of 688 seconds without throat erosion.)

2. The silica-tape overwrap used to hold the multi-piece composite together, provides structural integrity to the entire assembly.

3. The JTA graphite nozzle convergent section extends the service life of a refractory throat insert. (The JTA convergent section does not erode and disturb the boundary layer that provides long throat life.)

4. Oxidation protective coating is not essential to provide long service life of a tantalum tungsten throat insert.

5. The tantalum tungsten insert provided the longest service life of the throats tested. (A total of 2266 seconds was achieved with no change in throat insert dimensions.)

Based upon these test results, the two-piece JTA graphite throat design was selected for advanced development directed toward final qualification because it is adequately erosion resistant and lighter weight and easier to fabricate than the Ta-W alloy design.

Table 6.1-1

Summary Final Design Selection Tests

CC & NA I.D. No.	Description	STL Dwg. No.	Throat Area Increase (%)	Total Duration (sec)	Remarks
TG-003	100-mil thick tungsten shell throat insert coated with Durak MGF oxidation protective coating and backed with molded graphite. (0.920 inch diameter throat).	105945	0	301	Three firings-15, 50, & 236 seconds at P_c = 90 psia.
TG-004	100-mil thick tungsten shell throat insert coated with Durak MGF oxidation protective coating and backed with molded graphite. Chamber overwrapped with silica-tape 0.100 inch thick on the radius (0.920 inch diameter throat).	105945 with overwrap.	12% increase in final 10 seconds	740	Throat failed at 730 seconds. Four firings-15,50,237 & 438 seconds.
TG-005	100-mil thick tungsten shell throat insert coated with Durak MGF oxidation protective coating and backed with molded graphite. JTA graphite convergent section. Chamber overwrapped with silica-tape 0.100 inch thick on the radius (0.920 inch diameter throat).	105945 with overwrap and JTA upstream.	0	468	Ablative liner failed. Case overheated. Four firings 15,50,335, & 168 seconds.
TTG-001	100-mil thick tantalum-tungsten (87.5 - 12.5%) shell throat insert coated with Durak MGF oxidation protective coating and backed with molded graphite. Chamber overwrapped with silica-tape 0.100 inch thick on the radius (0.920 inch diameter throat).	105945 with Ta-W insert and overwrap.	0	1001	Ablative liner failed. Case overheated. Four firings 15,50,234 & 702 secs. duration.
TTG-002	100-mil thick tantalum-tungsten (87.5 - 12.5%) shell throat insert coated with Durak MGF oxidation protective coating and backed with molded graphite. JTA graphite convergent section. Chamber overwrapped with silica-tape 0.100 inch thick on the radius (0.920 inch diameter throat).	105945 with Ta-W insert, JTA upstream, and overwrap.	10% increase in final 13 seconds of last firing.	1717	Throat failed at 1704 sec. Five firings, 15-50, 235,735 & 682 seconds.
TTG-004	100-mil thick tantalum-tungsten (87.5 - 12.5%) shell throat insert uncoated and backed with molded graphite. JTA graphite convergent section. Chamber overwrapped with silica-tape 0.100 inch thick on the radius (0.920 inch diameter throat).	105945 with uncoated Ta-W insert, JTA upstream, and overwrap.	0	2266	Throat and chamber still in good condition. Six firings 15,51,236, 826, 929, & 299 seconds.
JTA-006 Thru JTA-012	JTA graphite throat insert with a JTA graphite convergent section (2-pieces). Chamber overwrapped with silica-tape 0.100 inches thick on the radius (1.00 inch diameter throats).	106546-2	0	300 per CC & NA	Seven CC & NAs successfully survived maximum thrust durability test.
JTA-013	Same as JTA-006 through JTA-012.	106546-2	0	688	Ablative liner finally failed. Case overheated. Five firings-15,50,237, 300, & 88 seconds.
JTA-014	JTA graphite throat insert extending back down entire convergent section (one-piece). Chamber overwrapped with silica-tape 0.100 inch thick on the radius (0.920 inch diameter throat).	106546-2, except one-piece JTA insert.	11% increase during last 820 seconds of final firing, appearing over 60% of the perifery.	1141	Four firings-15,50,235, & 841 seconds. No deep gouges resulted.

6.2 Injector Modification Tests

During the course of the Phase III development program there were two occasions when the basic injector design was modified and tested.

The first such effort took place in May - June 1964 and led to injector design modifications that became part of the final MIRA 150A design. This effort is discussed in paragraph 6.2.1.

The other effort was primarily one of testing and characterizing the current injector design under unusual test conditions. It also included evaluation of some design features that are different from those on the MIRA 150A. This effort is discussed in paragraph 6.2.2.

6.2.1 Mod 1 to Mod 4 Injector Development

Early in Phase III the initial injector design for the MIRA 150A was found to exhibit excessive throat erosion on streak testing. The injector development program described herein was undertaken to arrive at an injector design that would exhibit acceptable throat erosion when tested at full thrust on standard streak test throat inserts.

6.2.1.1 Background

The MIRA 150 injector was satisfactory from the standpoint of low throat erosion after the propellants were reversed from oxidizer center to fuel center. In that design the total injector sleeve stroke from 0 lb to 150 lbs of thrust was approximately 0.0050 inch. Thus, at the 20% thrust level (i.e., 30 lb), the gap on the fuel and oxidizer injection control point was approximately 0.0010 inch. The sensitivity of this small dimension to manufacturing tolerances made it difficult to control reproducibly the injection pressure drop at the low thrust levels. These small gaps also increased the danger of completely closing the injector gap and stopping flow, thereby introducing high pressures into the injection ports and seals. The initial MIRA 150A injector was designed with a smaller injector pintle and sleeve to reduce the effective diameter at which propellant injection velocity is controlled. The injector sleeve travel and gaps were therefore increased proportionally. The injector sleeve stroke on the MIRA 150A HEA is designed for 0.0084 inch of travel from 0 lb to 150 lbs of thrust. Therefore, the gap at a minimum thrust is approximately 0.0017 inch. This gap is still quite small; nevertheless it makes the injector pressure drop at the low thrust level considerably less sensitive than on the MIRA 150 HEA.

The above-mentioned injector design change (resulting in the MIRA 150 HEA becoming MIRA 150A HEA) completely altered the geometry of the injector although the general impingement angles, ramps and steps were still very similar. Unfortunately, the design change resulted in unforeseen rough combustion. Throat erosion during 200-second streak tests increased from essentially zero to over 35%. The initial MIRA 150A screamed (i.e., emitted a high pitch sound) at full thrust with various injection pressure ratios. Screaming did not exist at low thrust levels. The appearance of the erosion and char pattern of the streak sample was completely different from that exhibited by the MIRA 150 injector. Whereas the streak sample on the MIRA 150 injector had a sharply defined 12-leaf char pattern with absolutely no char upstream of this distinct char pattern, the initial MIRA 150A injector (unmodified design) had no virgin material visible after 200 seconds. The unmodified 150A injector produced characteristic velocities at the high thrust level in the range of 5400 to 5500 ft/sec uncorrected. Low thrust level performance was above

5000 ft/sec with readjusted injector pressure drops. This HEA had a 108-hole distributor ring, and all streak samples tested on this design (Runs C2-237 and C2-250) resulted in an eroded oval throat aligned to the inlet of the oxidizer manifold. It was apparent from these tests that a higher pressure drop was required across the distributor ring. A 24-hole, 0.021-inch hole diameter, distributor ring was then selected and tested. This ring resulted in a 7.5-psig pressure drop at 100% flow. This change eliminated the high erosion at the 1 and 7 o'clock positions.

After preliminary tests (water-cooled and streak) were performed on two of the initial design MIRA 150A HEAs, S/Ns 001 and 002; four modifications were made to the injector geometry on HEAs S/Ns 001 through 005. These design changes are discussed in paragraph 6.2.1.2, and the test results are presented in paragraph 6.2.1.3.

6.2.1.2 Design Modification Descriptions

The four injector modifications evaluated are shown in Figure 6.2.1-1.

Mod No. 1 - The first modification involved reboring the sleeve I.D. from 0.148 in. to 0.175 in. The modification was incorporated on all HEAs after it was shown that the fuel velocities and dynamic pressures in the pintle-sleeve passage were excessive (effective fuel pressure drop was approximately 10 to 15 psi) and probably resulted in poor fuel distribution. The velocity in the fuel flow passage could not be reduced beyond a certain limit; otherwise, the radius of curvature of the fuel passage at the injection zone would be reduced to a point which introduces losses and unstable flows. This modification is shown in the upper left hand corner of Figure 6.2.1-1.

Mod No. 2 - The second mocification involved adding a 10^{o} ramp extension on the injectro sleeve. It was incorporated in an effort to move the propellant impingement zone away from the pintle and sleeve thereby reducing combustion reoughness (which was believed to be contributing to the excessive erosion). This modification is shown in the upper right hand corner of Figure 6.2.1-1.

Mod No. 3 - Modification No. 3 (shown in the lower left corner of Figure 6.2.1-1) was made by press fitting an extended oxidizer ramp onto the injector. This modification was designed to move the impingement zone away from the fuel injection point and still maintain a 90^{o} impingement angle. The ramp was designed to prevent oxidizer from overlapping at the fuel injection point as it probably did on Mod No. 2. The distance from the end of the ramp and the fuel injection plane was also significantly reduced. Testing of this modification was done with a rebored sleeve (Mod No. 1) and a 108-hole distribution ring.

Mod No. 4 - Modification No. 4 involved a simultaneous 0.200-inch lengthening of the injector pintle, increasing the diameter of the oxidizer upstream ramp, and lengthening the downstream oxidizer step. This modification was first tested on HEA 150A-005 with a 24-hole distributor ring and with a rebored sleeve (Mod No. 1). It is shown in the lower right hand corner of Figure 6.2.1-1.

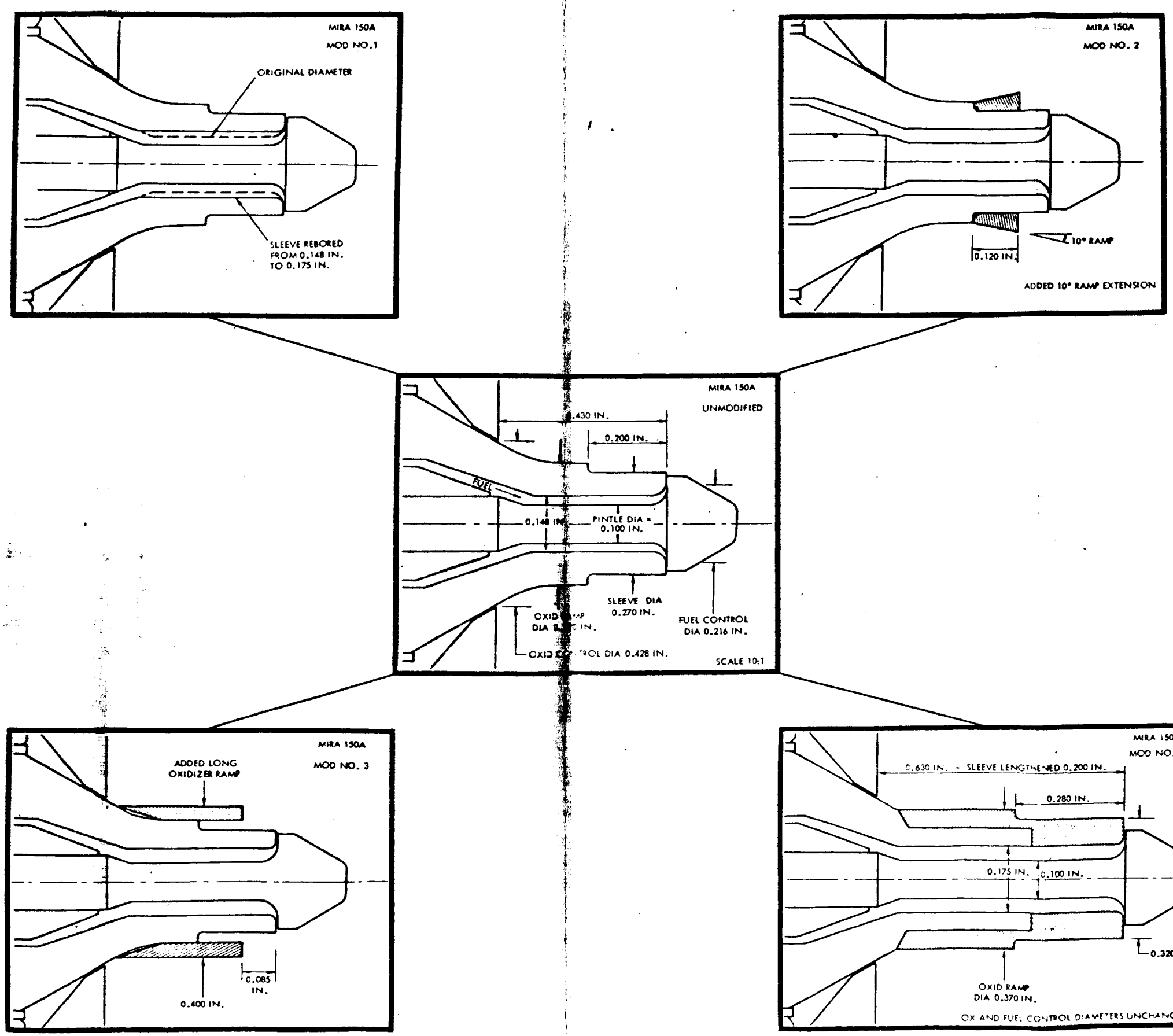

Figure 6.2.1-1. MIRA 150A HEA Modifications

6.2.1.3 Test Results

A total of 228 firings were conducted during this injector modification effort. Of these firings, two were done with JTA throat inserts, 13 were done with ablative streak test throat inserts, and the remaining 213 firings were done with completely water-cooled chambers including the throat section. The following HEAs were test fired: 150A-001, -002, -003, -004, -005, and 150-003.

Table 6.2.1-2 summarized the tests performed on these HEAs. A summary of the individual streak tests performed during this series is presented in Table 6.2.1-3. Seven streak samples selected from those listed in Table 6.2.1-3 are pictured in Figures 6.2.1-4 through 6.2.1-10. They are viewed from the upstream end.

The characteristic velocity, C_u^*, listed in Table 6.2.1-2 is an average of the uncorrected values obtained on water-cooled chambers during that test series. There is normally an 80 to 120 ft/sec C* correction which is added to the tabulated figure. This correction includes pressure correction, throat growth, and water-cooling correction. The $\Delta C^*_{H_2O}$ shown in the fifth column of Table 6.2.1-2 is the correction for heat removed from the chamber by the water-cooled combustion chamber. The sixth column, P_{ch}, indicates the roughness in chamber pressure as measured by the downstream transducer. Whenever a streak test was performed during the test series shown in Table 6.2.1-2, said test is identified in the Comments column.

Table 6.2.1-3, the streak test summary, lists the run number, HEA number, injector modification, and mixture ratio. The listed C_u^* and $\Delta C^*_{H_2O}$ are measured on the water-cooled run which preceded the streak test. In all cases no HEA adjustments were made between the streak test and the preceding water-cooled test. P_{ci}/P_{cf} indicates the initial and final chamber pressures. The injector pressure drops tabulated for the oxidizer and fuel indicate the pressure drop between the pressures measured just below the shutoff valve and the chamber pressure. Of this pressure drop, approximately 20 to 30 psia is irreversible at full flow and does not contribute to injection velocity. The roughness indicates in the P_{cd} column were obtained from the Photocon transducer used for the water-cooled run just prior to the streak test.

The only effect Mod 1 appeared to have on HEA operation was to lower the heat flux correction, $\Delta C^*_{H_2O}$ from 40-42 ft/sec to about 35-40 ft/sec. Characteristic velocity was not significantly affected but streak test throat erosion was still unsatisfactory.

Mod 2 probably gave the most interesting set of test results of all the modifications; however, the streak tests were unsuccessful. Testing on Mod No. 2 alone resulted in high C*'s (5400 ft/sec uncorrected) as indicated by Test Series 4 of Table 6.2.1-2. The injector when reworked to include both Mod No. 1 and No. 2 produced the lowest C* (5000 ft/sec or less), lowest heat flux, and smoothest Photocon traces of any TCA fired. Tests on HEAs with these modifications are shown in Test Series 5 and 10 of Table 6.2.1-2. No screaming was evident on either series of tests.

With Mod 3 the heat flux was low - 30 ft/sec but screaming was pronounced. The resulting characteristic velocity was low - 5200 ft/sec (uncorrected). The Mod 3 streak test failed; chamber pressure dropped from 109 to 75 psia in 200 seconds. The erosion pattern on the streak sample was oval and aligned to the inlet oxidizer port. (See Figure 6.2.1-7.) This was the only unsuccessful streak test that showed a sharp char border with about 1/4 inch of virgin material at the water-cooled ablative interface.

Table 6.2.1-2

HEA Injector Test Summary
May - June 1964

Order Of Test	HEA	Mod #	C_u^*	$\Delta C^*_{H_2O}$	P_{ch}	P_{cd}		Comments
1.	150A-001	None-108 DR	5400	40	3/3	8/17	T	Streak test C2-237 performed. Excessive erosion.
2.	150A-002	None-108 DR	5400	40	3/4	5/15	T	Streak Test C2-250 performed. Excessive erosion.
3.	150A-001	Mod #1, 108 DR	5350	36	4/3	7/12	T	No streak test performed.
4.	150A-002	Mod #2-108 DR	5400	38	1/2	2/6	P	Streak Test C2-276 performed. Excessive erosion.
5.	150A-001	Mod #1, Mod #2 108 DR	5000	34	4/7	3/5	P	No streak test performed.
6.	150-003	Std-12 DR	5400	30	5/12	3/6	P	Streak Test C1-202 performed. Little erosion.
7.	150A-002	Mod #1-12 DR	5370	35	3/5	7/14	P	Streak Test C2-249 performed. Excessive erosion.
8.	150A-003	Mod #1, Mod #3 108 DR	5150	28	4/7	5/7	P	Streak Test C2-221 performed. Excessive erosion.
9.	150A-002	Mod #1-12 DR	5200	28	2/3	7/12	P	No streak test performed.
10.	150A-001	Mod #1, Mod #1 108 DR	4900	26	3/4	3/6	P	Streak Test C1-227 performed. Excessive erosion.
11.	150A-005	Mod #1, Mod #4 24 DR	5300	24	3/5	4/8	P	Streak Tests C1-239, C1-242, and C1-243 performed. Little erosion.
12.	150A-004	Mod #B-24 DR	5350	29			P	Streak Test C2-325 performed. Little erosion.
13.	150A-005	Mod #1 Mod #4-24 DR	5350	24	3/3	3/4	P	Streak Test C1-239 performed. Little erosion. JPA Test C1-257 performed. Little erosion.

NOTES: C_u^* - Uncorrected value.

$\Delta C^*_{H_2O}$ - C* correction due to heat removed from chamber by water-cooled chamber.

P_{ch} - Head end chamber pressure roughness mean and maximum in % of chamber pressure.

P_{cd} - Aft end chamber roughness mean and maximum in % of chamber pressure.

T,P - Taber, Photocon transducers.

DR - Distributer ring. Number indicates number of holes in ring.

Table 6.2.1-3

HEA Injector Streak Test Summary

Run No.	HEA	Mod #	MR	C_u*	$C^*_{H_2O}$	P_{ci}/P_{cf}	P_{ox}-P_f	P_{cd}	Post Streak Test Figure No.	Throat, Test Duration (seconds), and Condition of Throat
C2-237	150A-001	None-108 DR	1.43	5516	39.2	113/88	93-62	8/18	6.2-4	Refrasil, 200, Failed.
C2-250	150A-002	None-108 DR	1.54	5383	53.6	115/76	73-82	5/12	-----	Refrasil, 200, Failed.
C2-276	150A-002	Mod #1, Mod #2 108 DR	1.48	5364	38.6	109/75	73-68	3/4	6.2-5	Refrasil, 200, Failed.
C1-202	150-003	Std-12 DR	1.47	5415	31.4	114/129	85-66	5/9	-----	Refrasil, 200, Good.
C2-249	150A-002	Mod #1-12 DR	1.53	5288	33.3	114/68	58-48	15/15	6.2-6	Refrasil, 200, Failed.
C1-221	150A-003	Mod #1, Mod #3 108 DR	1.47	5127	26.8	104/75	67-65	4/7	6.2-7	Refrasil, 200, Failed.
C1-227	150A-001	Mod #1, Mod #2 108 DR	1.53	4868	25.4	101/63	133-74	4/4	6.2-8	Refrasil, 200, Failed
C1-239	150A-005	Mod #1, Mod #4 24 DR	1.52	5220	25.2	110/121	100-116	4/4	6.2-9	Refrasil, 200, Good.
C1-242	150A-005	Mod #1, Mod #4 24 DR	1.51	5250	23.7	107/125	87-93	4/4	6.2-10	Refrasil, 200, Good.
C1-243	150A-005	Mod #1, Mod #4 24 DR	1.54	5250	23.7	107/131	84-86	4/4	-----	Refrasil, 200, Good.
C1-257	150A-005	Mod #1, Mod #4 24 DR	1.52	5350	24.8	111/111	90-125	3/3	-----	JTA, 302, Good (three starts).
C2-325	150B-004	Mod #B-24 DR	1.52	5350	28.6	109/108	79-80	---	-----	Refrasil, 300, Good.
C1-289	150A-005	Mod #1, Mod #4 24 DR	1.47	5370	----	111/118	96-75	3/3	-----	Refrasil, 160, Good.

NOTES: $C^*_{H_2O}$ - Uncorrected value of water-cooled run prior to streak test, except on JTA or TTG runs.

P_{ci}/P_{cf} - Initial and final pressure.

P_{cd} - Numbers indicate Photocon roughness measurement (mean/max) on water-cooled run prior to streak test.

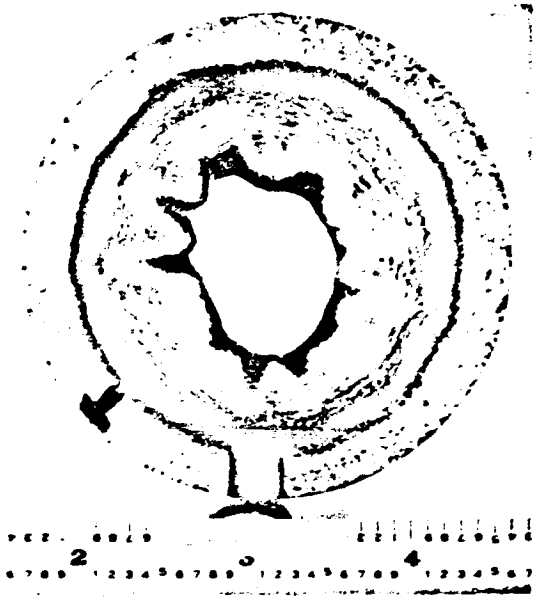

Figure 6.2.1-4. Run C2-237
Streak Test

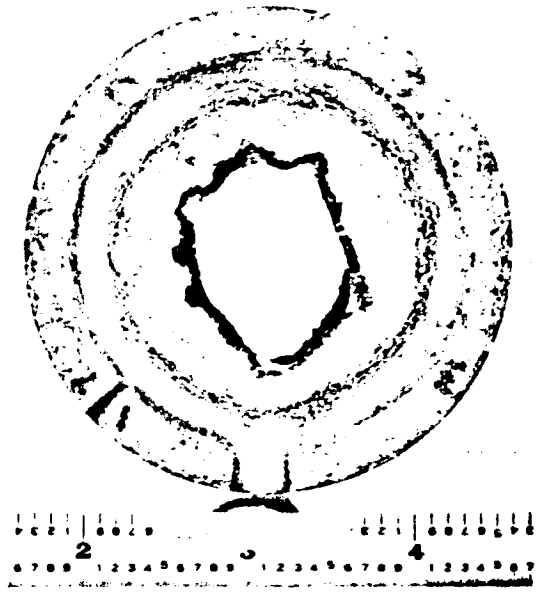

Figure 6.2.1-5. Run C2-276
Streak Test

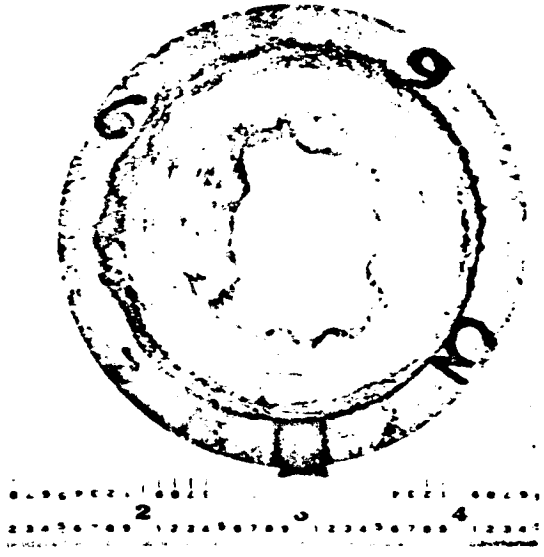

Figure 6.2.1-6. Run C2-299
Streak Test

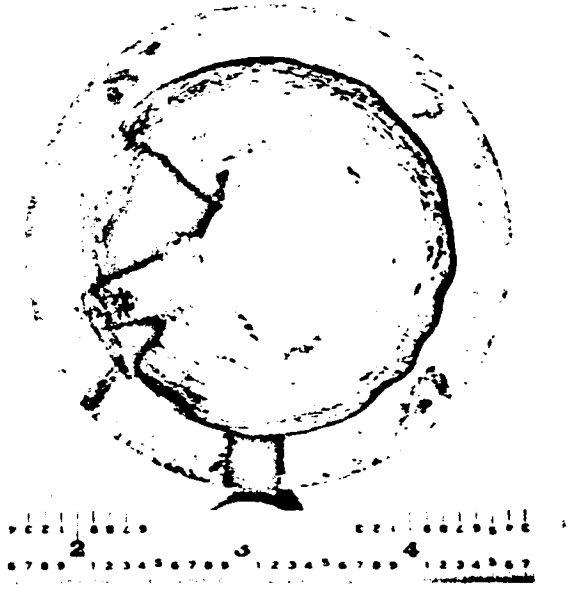

Figure 6.2.1-7. Run C1-221
Streak Test

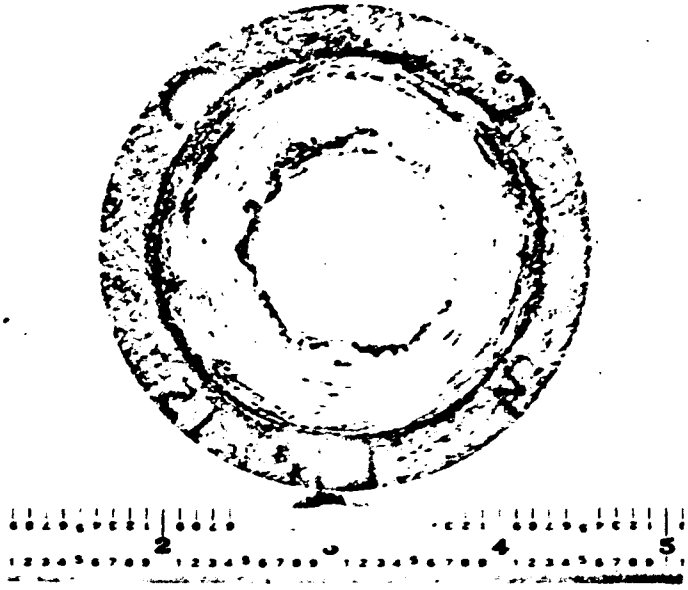

Figure 6.2.1-8. Run C1-227
Streak Test

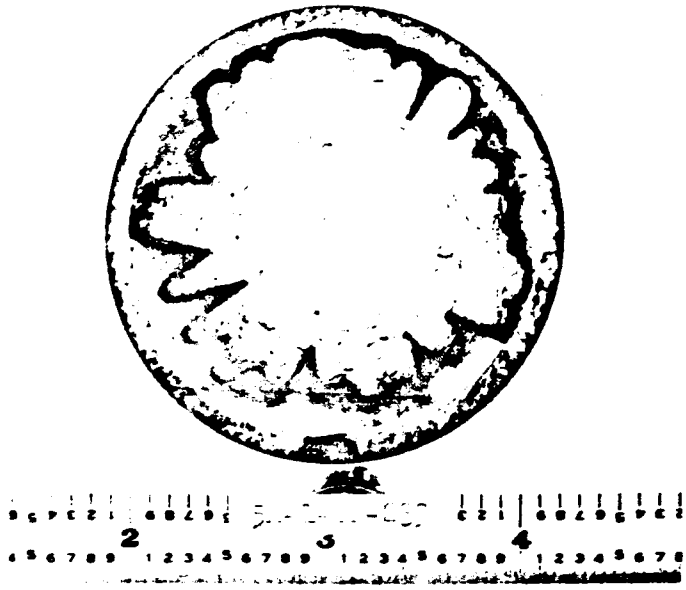

Figure 6.2.1-9. Run C1-239
Streak Test

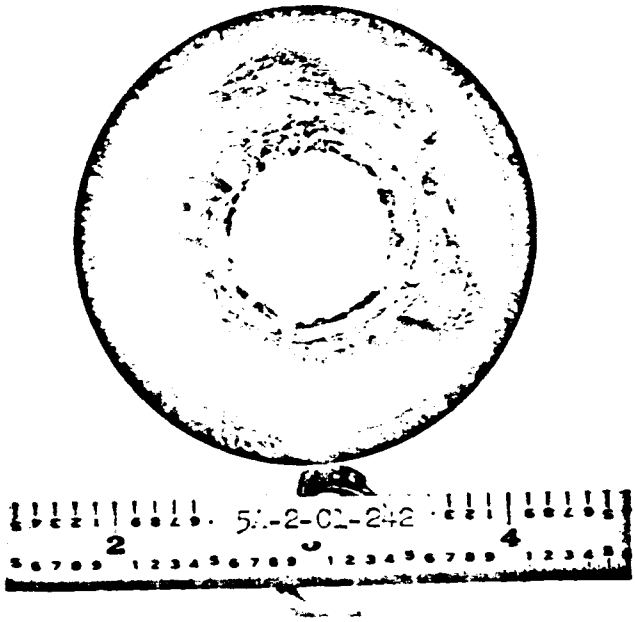

Figure 6.2.1-10. Run C1-242
Streak Test

For Mod 4, three streak samples and a JTA chamber were tested with complete success. The initial tests demonstrated a characteristic velocity of about 5250 ft/sec at the high thrust level. Later testing, during the same series, demonstrated characteristic velocities of 5350 ft/sec at maximum thrust. The test on the JTA chamber (with no erosion) was run for three separate runs with a C* of 5420 ft/sec on all runs. The water-cooled runs prior to the JTA test showed uncorrected C*'s of 5360, 5354, and 5337 ft/sec. This TCA did not scream at any thrust level or injector pressure drop. With the Mod No. 4 injector design, a sharply defined char pattern was also distinctly evident after a 50-second run with a JTA throat insert in an ablative chamber. Heat fluxes were the lowest experienced over the entire range of pressure drop ratios. The patternator tests showed oxidizer flow varied from plus 15-20% high on one side to minus 15-20% low on the other side.

6.2.1.4 Test Conclusions

The following conclusions were reached based on the test data and earlier data obtained from testing the MIRA 150 HEA:

1. Characteristic velocity (ft/sec) is not the controlling parameter on throat erosion.

2. Combustion roughness measured at either the head end or the downstream end of the chamber with Taber or Photocon transducers does not correlate with throat erosion.

3. Injector pressure drops (absolute or relative) do not have a significant affect on throat erosion, using an otherwise good injector.

4. Low heat flux is a necessary but not sufficient criterion for low throat erosion.

5. Injector geometry is the primary parameter controlling erosion. Roughness, injection pressure drop, and characteristic velocity are controllable parameters which can affect erosion within limits on a poor (high erosion causing) injector.

6. A direct measurement of throat erosion using a streak test sample is the best method of predicting the throat erosion characteristic of an injector.

The Mod 4 design provided smooth combustion, eliminated throat erosion and maintained high performance. All Phase II HEAs (S/Ns 001 through 006) were modified to the Mod 4 injector configuration by fabrication of new injector sleeves of the size and shape achieved experimentally by the two-piece arrangement shown in Figure 6.2.1-1. This Mod 4 design thus became the standard injector configuration on the MIRA 150A; all Phase III HEAs (S/Ns 007 and subsequent) were fabricated with the Mod 4 shape and size.

6.2.2 Bi-Stable Combustion Investigation

The objective of the bi-stable combustion investigation was to determine the cause(s) of observed operating differences between Phase II and Phase III HEAs such as greater than usual streak test erosion with Phase III HEAs than with Phase II HEAs. As a result of this investigation, it was determined that: (1) two possible combustion modes existed, (2) the mode causing higher heat transfer could be triggered only at sea level, and (3) the CC & NA could tolerate the more severe mode.

6.2.2.1 Background

The basic design difference between Phase II and Phase III HEAs was the addition of quick disconnect ports to the injector body. This change necessitated relocation of the injection pressure taps and propellant passages. No change was made to the basic injector element configuration.

Initial streak testing of the first Phase III HEA (S/N 007), resulted in an erosion and char pattern noticeably different from that of Phase II HEAs. Overall erosion was greater, the erosion pattern was less uniform, and the throat insert appeared "hotter" than in previous streak tests. Another unusual characteristic of this HEA was an occasional 20 psi increase in the pressure drop between the fuel injection manifold and chamber head end. This anomaly correlated with an increase in heat transfer to the water-cooled chamber and an increase in combustion noise. Initial tests on the next Phase III HEA (S/N 008) showed none of these characteristics, while the third and fourth Phase III HEAs (S/N 009 and 010) exhibited all of the anomalies of S/N 007. It was then evident that a bi-stable combustion condition existed which had not been experienced during testing of Phase II HEAs.

An investigation was initiated to determine any differences between the Phase II and Phase III 150A HEAs which might explain the combustion characteristics mentioned above. A reinspection of all major parts of the Phase III units was conducted. The sleeve (Part No. 105192), pintle (Part No. 105107), pintle guide (Part No. 105106), and body (Part Nos. 106809 and 105464) were reinspected to original prints. In addition to reinspection, the parts from Phase III HEA 150A-007 were compared to the parts from Phase II HEA 150A-006 at high magnification on an optical comparator in an attempt to identify differences that might explain the change in performance. After a thorough investigation of Phase III and Phase II parts, the differences noted between the two injectors were: (1) the method of applying Micro Seal treatment to the 106664 Body Assembly on the Phase III unit, (2) the method of staking in the distribution ring (Part No. 105103-2), and (3) the aforementioned additions of quick disconnect ports and relocation of injector pressure ports on the Phase III design. The third item results in a slight increase in propellant volume upstream of the shutoff valves.

A series of engine firing tests were performed concurrently with the reinspection of parts mentioned above. Comparative tests under identical conditions were made on three Phase II 150A HEAs and five Phase III HEAs, and also on the MIRA 150 HEA-003, which has a significantly different basic injector element. Figure 6.2.2-1 shows the injector configuration of the MIRA 150 HEA and the modifications to the basic 150A element which were tested in this investigation. These modifications are described in paragraph 6.2.2.2, and the results are discussed in paragraph 6.2.2.4.

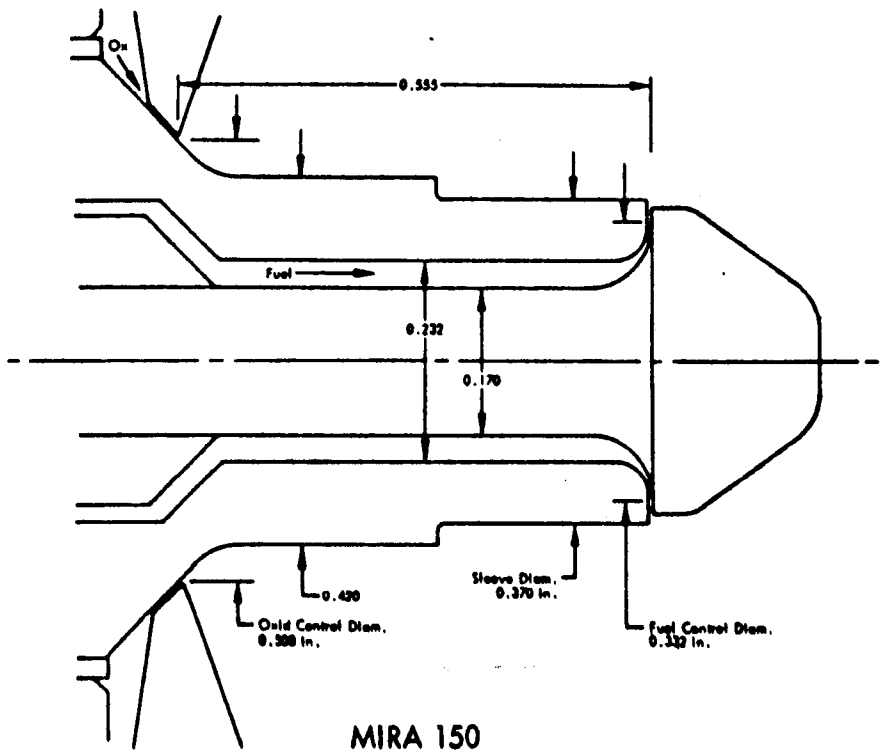

MIRA 150

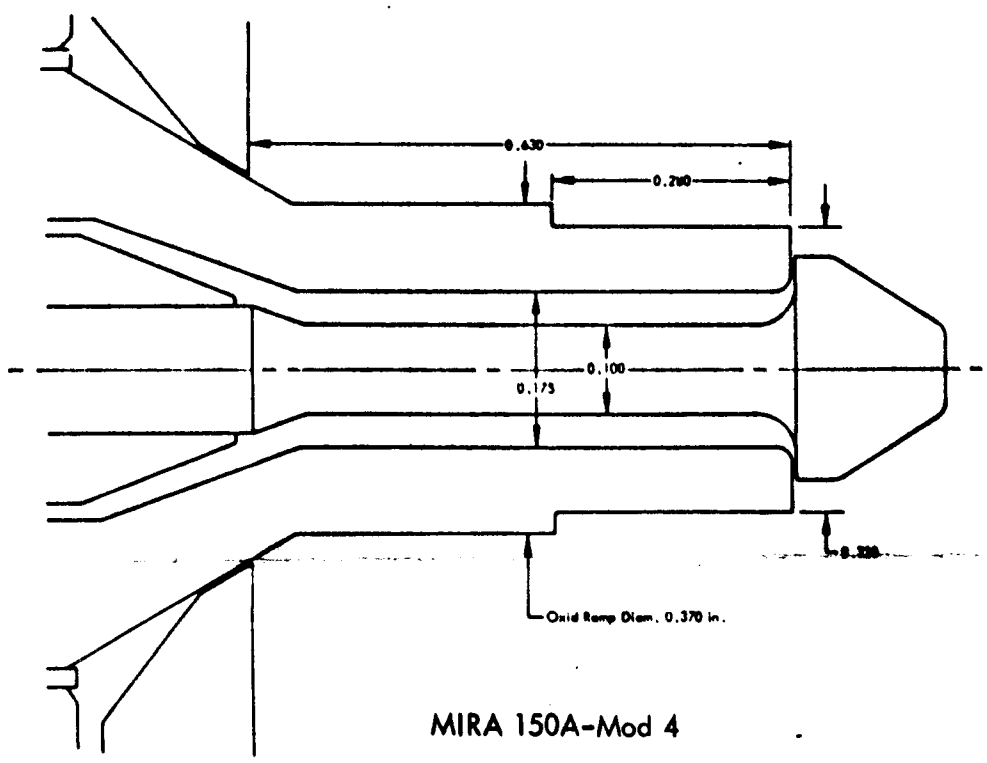

MIRA 150A-Mod 4

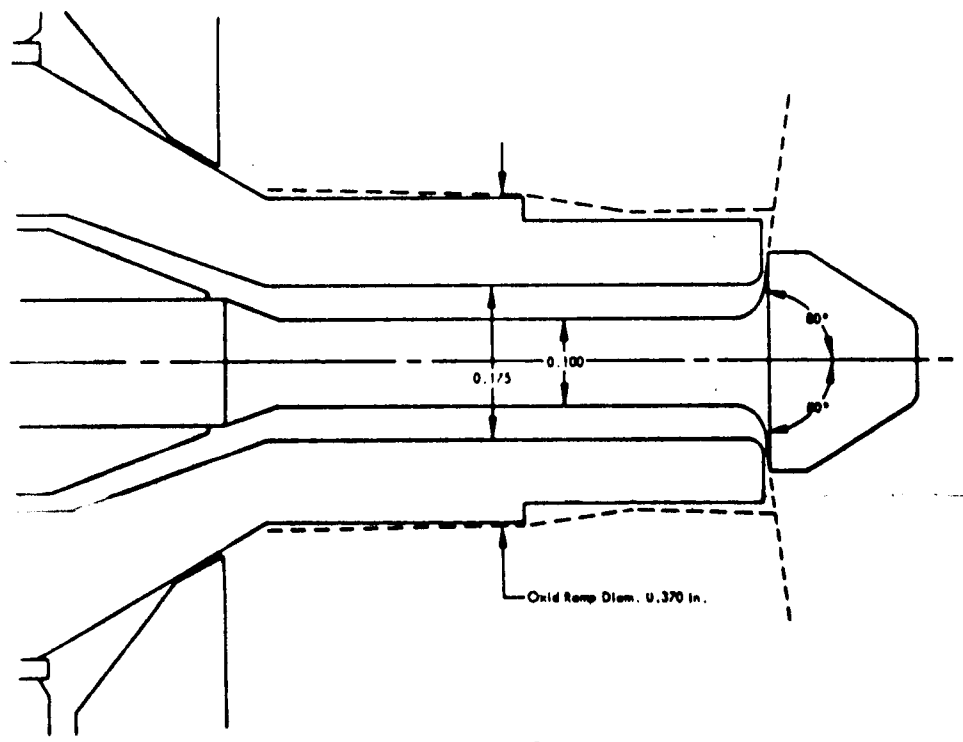

MIRA 150A-80° Pintle

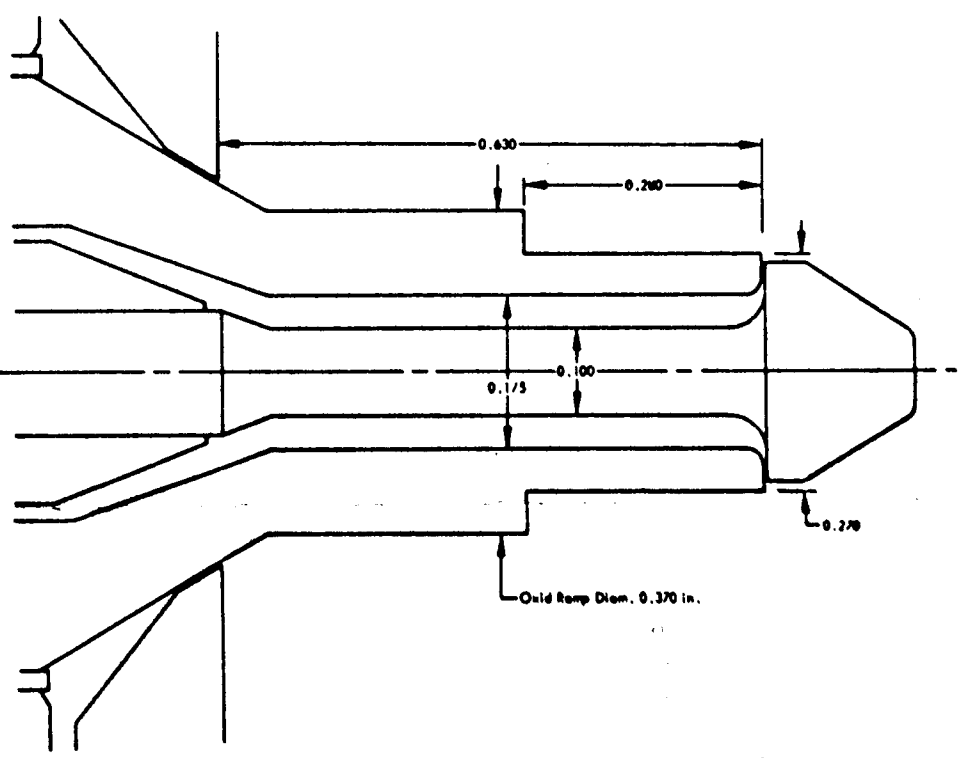

MIRA 150A-Cutdown Sleeve

Figure 6.2.2-i. HEA Injector Modifications and Configurations

6.2.2.2 Injector Configurations and Modifications

The injector configurations and modifications (to the basic condigurations) which were tested during this combustion investigation are shown in Figure 6.2.2-1.

The basic configurations were:

- Phase II 150A HEA - This configuration was the standard Phase II design. HEAs S/Ns 004, 005, and 006 were tested under this configuration.
- Phase III 150A HEA - HEAs S/Ns 007, 008, 009, 010, and 011 were tested under this configuration as standard Phase III HEAs. Basic change from the Phase II design was the addition of quick disconnect ports, as discussed in paragraph 6.2.2.1.
- 150 HEA - HEA S/N 003 tested was one of the original MIRA 150 HEAs. This design has a larger diameter sleeve and pintle compared to the MIRA 150A HEAs.

Injector modifications for these tests were limited to changes which could be readily performed on existing HEAs by remachining of parts already fabricated.

The modifications tested were:

- "Roughened" Sleeve - The surface of the injector sleeve on 150A HEA S/N 010 was roughened using #400 emery paper while the HEA was on the test stand between Runs C2-664 and C2-665. This was done to alter the oxidizer flow boundary layer conditions. The roughened sleeve was left in the HEA while other modifications were being investigated.
- 80° Pintle - A fuel pintle (Part No. 105107) was reground from 90° to 80° as shown in Figure 6.2.2-1 to change the propellant impingement angle in an attempt to eliminate injection pressure drop shifts by relocating the combustion flame front. This pintle was installed on HEA S/N 010 for Runs C2-696 through C2-698. This HEA already had the "roughened" sleeve modification mentioned above.
- Reduced Diameter Sleeve Tip - This modification was tested on 150A HEA S/N 009 during Runs C2-681 through C2-684. The tip of the sleeve, (Part No. 105192) was machined to a smaller diameter, as shown in Figure 6.2.2-1.

In addition to these modifications, the fuel pintle from Phase II HEA S/N 006 was installed in Phase III HEA S/N 010 for Runs C2-699 through C2-708. Although Phase II and Phase III HEAs both use the same pintle design, this exchange was performed to ascertain that no change in fabrication techniques had occurred between the times the Phase II and Phase III pintles were produced that might have affected the flow characteristics of the injector. Each of these basic configuration and modifications were subjected to an identical series of test conditions as described in paragraph 6.2.2.3. The results of these tests are given in paragraph 6.2.2.4.

6.2.2.3 Test Setup and Conditions

After inspection of HEA detail parts showed no significant change in injector configuration between the Phase II and Phase III HEAs, a review of the test setup at the Inglewood Test Site was made to determine whether the Phase III HEAs had been tested under different conditions which might explain the change in combustion characteristics.

The Phase III HEA tests, except those for dynamic response and start-stop transient response, were run without the nitrogen gas purge lines which were usually connected to injection pressure taps. Earlier, purging had been used as a safety precaution to prevent accidental accumulation of propellants in the combustion chamber when the HEAs were fired on the IRTS horizontal test stand, C-1. Since the Phase III HEAs were to be fired only on the IRTS vertical stand, C-2, where propellants would drain from the chamber, it was decided to eliminate purge volumes to enable the acquisition of valid response data on all runs.

The elimination of purging had two effects on run conditions: (1) successive firings without purging may result in varying amounts of residual propellants in the injector passages, which could cause an oxidizer or fuel lead on startup; (2) the fill volumes between the shutoff valves and the metering gaps are decreased by two-thirds, which causes shorter start transient times and rapid chamber pressure rise on startup. Both of these conditions were considered as possible causes of the bi-stable combustion experienced in initial testing of Phase III HEAs.

Figure 6.2.2-2 shows the relative locations of the fuel and oxidizer passages downstream of the shutoff valves. Vertical mounting of the HEA creates a trapped fuel volume between the shutoff valve and the pintle guide, while the oxidizer passages drain freely. In addition, the low vapor pressure of the mixed oxides of nitrogen (MON) compared to monomethylhydrazine (MMH) causes rapid boil-off of the oxidizer compared to the fuel. Both of these conditions tend to cause a fuel lead on ignition when the injector passages are not purged prior to starting.

To investigate the effects of the above conditions, tests were conducted both with and without the purge volumes attached. Additional tests were made with the purge volumes disconnected and the propellant passages completely free of trapped propellant by purging the injector with nitrogen and then removing the purge lines immediately prior to firing.

Phase III HEAs, which had the quick disconnects ports upstream of the shutoff valves, were tested with and without the additional volumes of these ports filled with propellants (attained by bleeding) or plugged with Teflon rods.

Instrumentation used for all tests is listed in Table 6.2.2-3. The results are listed in Table 6.2.2-4 and described in paragraph 6.2.2.4.

The test conditions for each of the HEAs fired during this investigation are summarized as follows:

1. Empty Passages Downstream of Shutoff Valve - This condition was attained when the HEA was first installed on the test stand or by purging through the injection pressure ports. Purge line volumes then were or were not removed before the firing.

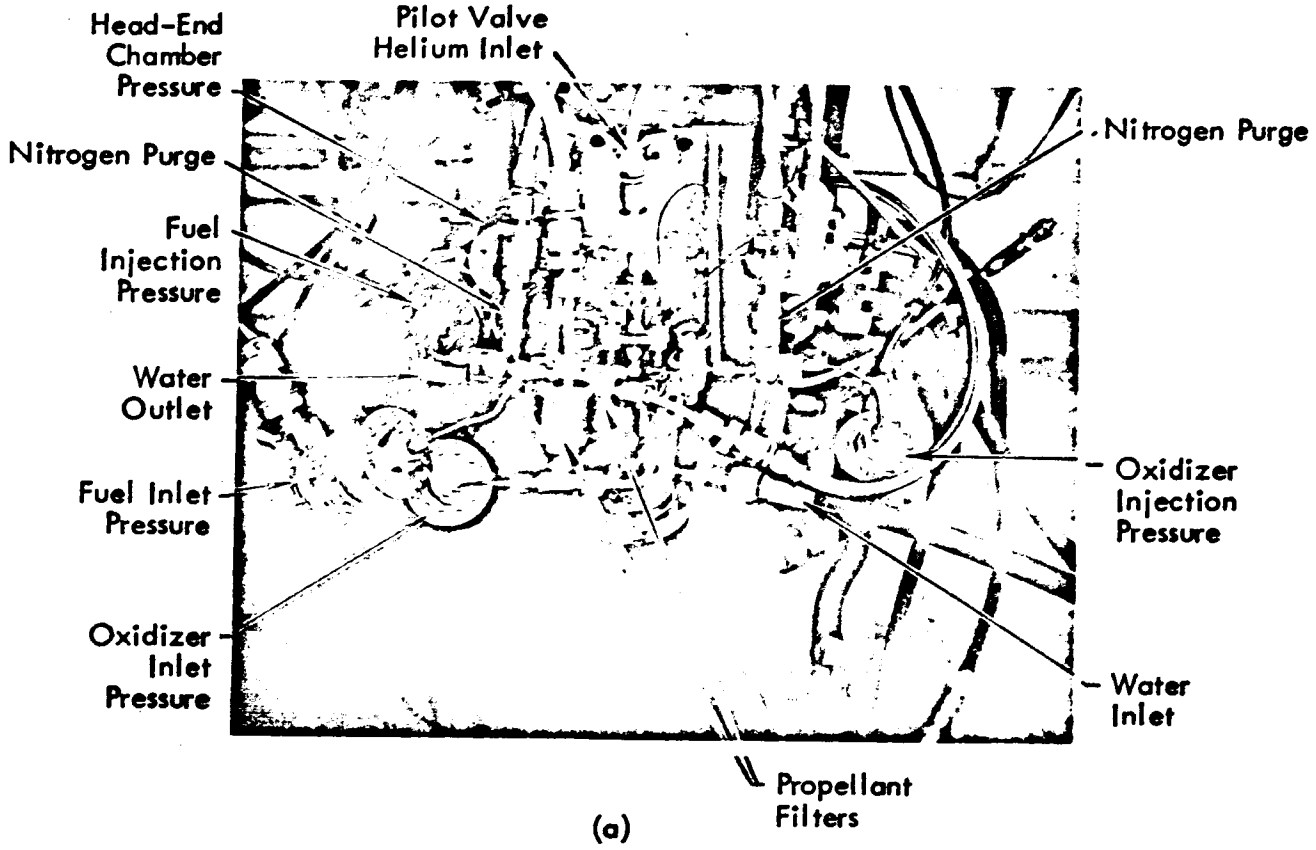

(a)

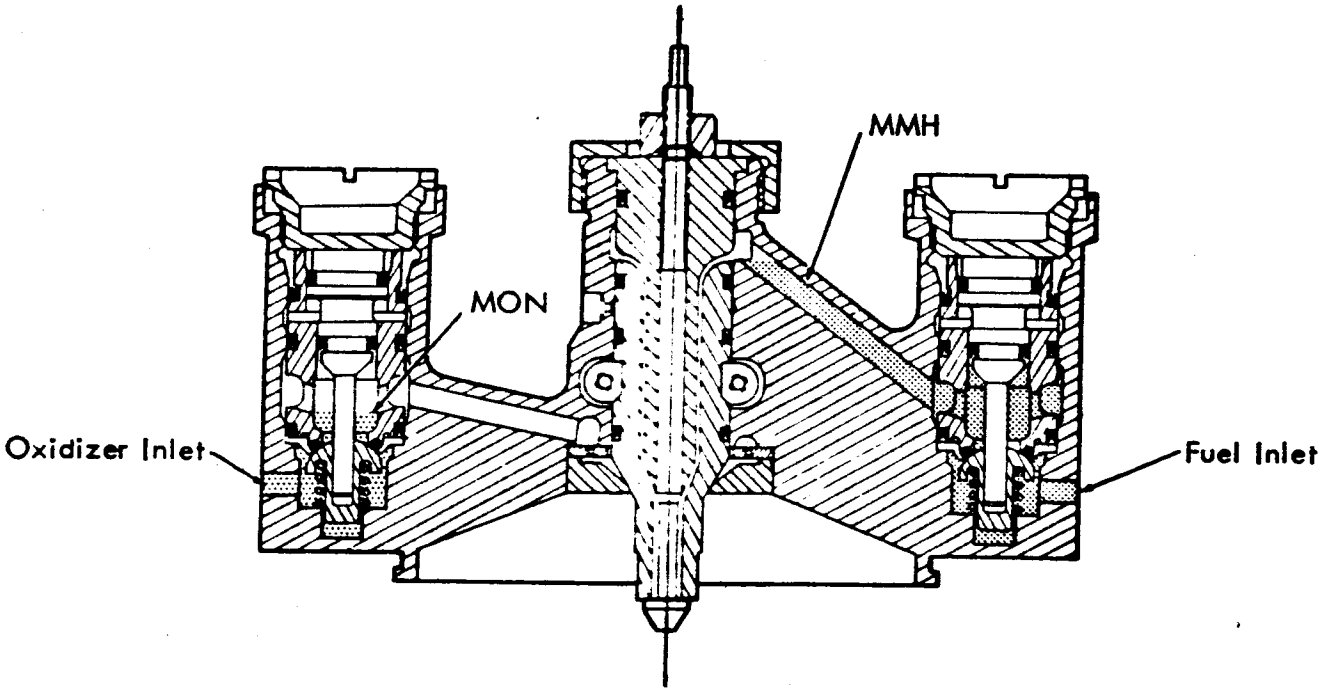

(b) Partially Filled Propellant Passages

Figure 6.2.2-2. Test Setup

Table 6.2.2-3

Instrumentation Requirements

Symbol	Parameter	Instrument Type	Range
P_{CH}	Chamber Pressure 1	Taber	0 - 150 psia
P_{CD-1}	Chamber Pressure 2	Taber	0 - 150 psia
P_{CD-2}	Chamber Pressure 3	Photocon	0 - 150 psia
POUV	Inlet Venturi Pressure, Oxidizer	Taber	0 - 1000 psia
PFUV	Inlet Venturi Pressure, Fuel	Taber	0 - 1000 psia
FMF	Fuel Flowrate	Rotating Vane	.03 - .3 lb/sec
FMO	Oxidizer Flowrate	Rotating Vane	.05 - .5 lb/sec
ISA	Actuator Signal	Ammeter	± 100 Mamps
LSA	Actuator Position	Potentimeter	+ 0.12 Inch
FMW	Cooling Water Flowrate	Rotating Vane	0 - 10 lb/sec
TWD	Cooling Water Temperature Rise	Thermocouples	0 - 50°F
TF	Fuel Temperature	Thermocouples	0 - 100°F
TO	Oxidizer Temperature	Thermocouples	0 - 100°F
SSV	Start Signal	Relay	0 - 1 Volt
*P_{if}	Injection Pressure Fuel	Taber	0 - 250 psia
*P_{io}	Injection Pressure Oxidizer	Taber	0 - 250 psia

*Optional Instrumentation

Table 6.2.2-4

Bi-Stable Combustion Test Summary

HEA	Empty Passages		Partially Filled Passages		Throttling		ΔC*	Heat Flux-$\dot{Q}$
Type and S/N	Bi-Stable Combustion Attained	Number Starts	Bi-Stable Combustion Attained	Number Starts	Bi-Stable Combustion Attained	Number Steps to Max Thrust	ft/sec Increase	% Increase
150-003	0	1	0	20	0	12	---	---
Phase II 150A								
004	0	1	5	8	0	21	120	17
005	0	1	3	4	---	--	80	10
006	0	2	2	4	---	--	0(3)	0(3)
TOTAL	0	4	10	16	0	21		
Phase III 150A								
007	1(1)	4	3	4	0	5	0(4)	7
008	0	9	7	12	0	16	60	7
009	0	2	2	3	---	--	60	7
009(5)	0	2	6	7	0	15	100	20(5)
010 (7)	0	25	31	82	60(2)	116	60	14
011	0	1	4	6	0	2	-90(6)	-7(6)
TOTAL	1(1)	43	53	114	60(2)	154		
Phase II and III TOTAL	1(1)	47	63	130	60(2)	175		

NOTES: (1) Data questionable because fuel system bypass valve was accidently left open on this run.

(2) Bi-stable combustion initiated during throttling occurred only on HEA S/N 010 with "roughened" sleeve described in paragraph 6.2.2.2. This HEA was not throttled prior to this modification.

(3) HEA S/N 006 showed no increase in C* or heat flux. This injector was later found to have a helium leak into the oxidizer passage, which would have affected distribution.

(Notes 4, 5, 6, and 7 explained on next page.)

Table 6.2.2-4 (Continued)

NOTES: (4) HEA S/N 007 did not increase in C*, possibly because of poor oxidizer flow distribution as verified by observation of water flows. However, heat flux did increase.

(5) HEA S/N 009 with reduced diameter sleeve tip modification described in paragraph 6.2.2.2.

(6) Minus sign indicates reduced heat flux and C*. This occurred only on 150A S/N 011. Water flows of this HEA showed extremely nonuniform distribution.

(7) Includes both standard and 80° pintle modification.

2. Partially Filled Passages Downstream of Shutoff Valve - This condition occurred when an injector was repeatedly fired on the test stand and not purged prior to restarts.

3. Throttling - To achieve this condition, HEAs of each configuration were step throttled from minimum to maximum thrust to check for initiation of the bi-stable combustion mode.

6.2.2.4 Test Results

A total of 98 firings were performed on nine different HEAs. HEAs of the three basic configurations described in paragraph 6.2.2.2 were tested. Most of these tests included multiple starts and/or variable thrust operation of the HEA. Twenty-three streak test ablative throat inserts and four ablatively cooled CC & NAs were tested in addition to the majority of the firings that were made using a water-cooled combustion chamber.

A summary of the test results are presented in Table 6.2.2-4. The table lists the number of times the bi-stable combustion mode was attained compared to the number of times the particular test conditions were imposed. Tests results are listed separately for each test condition on each HEA tested, and are also subtotaled for each configuration. The right hand columns of the table show the change in C* performance and chamber heat flux measured when the bi-stable combustion conditions existed.

Typical effects of bi-stable combustion on HEA measured parameters are shown in Figure 6.2.2-5. Exceptions to some of these norms are discussed in the notes below Table 6.2.2-4. In general, bi-stable combustion resulted in increased C* performance, higher heat flux, and an increase of about 20 psia in fuel injection pressure drop.

High speed oscillograph traces of the tests, such as the one reproduced in Figure 6.2.2-6, showed that the chamber pressure fluxuations measured by a Photocon transducer increased in amplitude from $\pm$ 5% of the mean pressure peak-to-peak under normal conditions to $\pm$ 10% peak-to-peak under bi-stable combustion conditions. The oscillograph traces also showed a significant fuel injection pressure lead on ignition when the injector passages downstream of the shutoff valve were partially filled with propellants, as described in paragraph 6.2.2.3. Photocon measurements of chamber pressure frequencies indicated a shift from 2000-3000 cps at normal conditions to a consistent 1500 cps at the bi-stable combustion conditions. This 1500 cps frequency was occassionally audible during TCA firings.

The Handbook of Astronautical Engineering (H. H. Knoelle, Editor-in-Chief; McGraw Hill 1961), page 20-66, described an "Entropy Wave" mode caused by a sudden mixture ratio shift at the injector resulting in a pressure wave traveling to a zone near the throat, changing in pressure at the sonic nozzle, and propagating back to the injector, thereby causing a further change in mixture ratio. The fuel lead on ignition resulting from residual fuel in the injector passages was a possible cause of such a mixture ratio shift. Inserting the actual combustion chamber dimensions in the equations presented in the above reference results in a calculated frequency of 1525 cps, which is very consistent with the measured frequency of 1500 cps. It was also possible that local mixture ratio variations caused by nonuniform flow distribution may have initiated an "Entropy Wave." This was a possible explanation for the fact that the bi-stable combustion mode was initiated by throttling HEA S/N 010 after the sleeve was roughened.

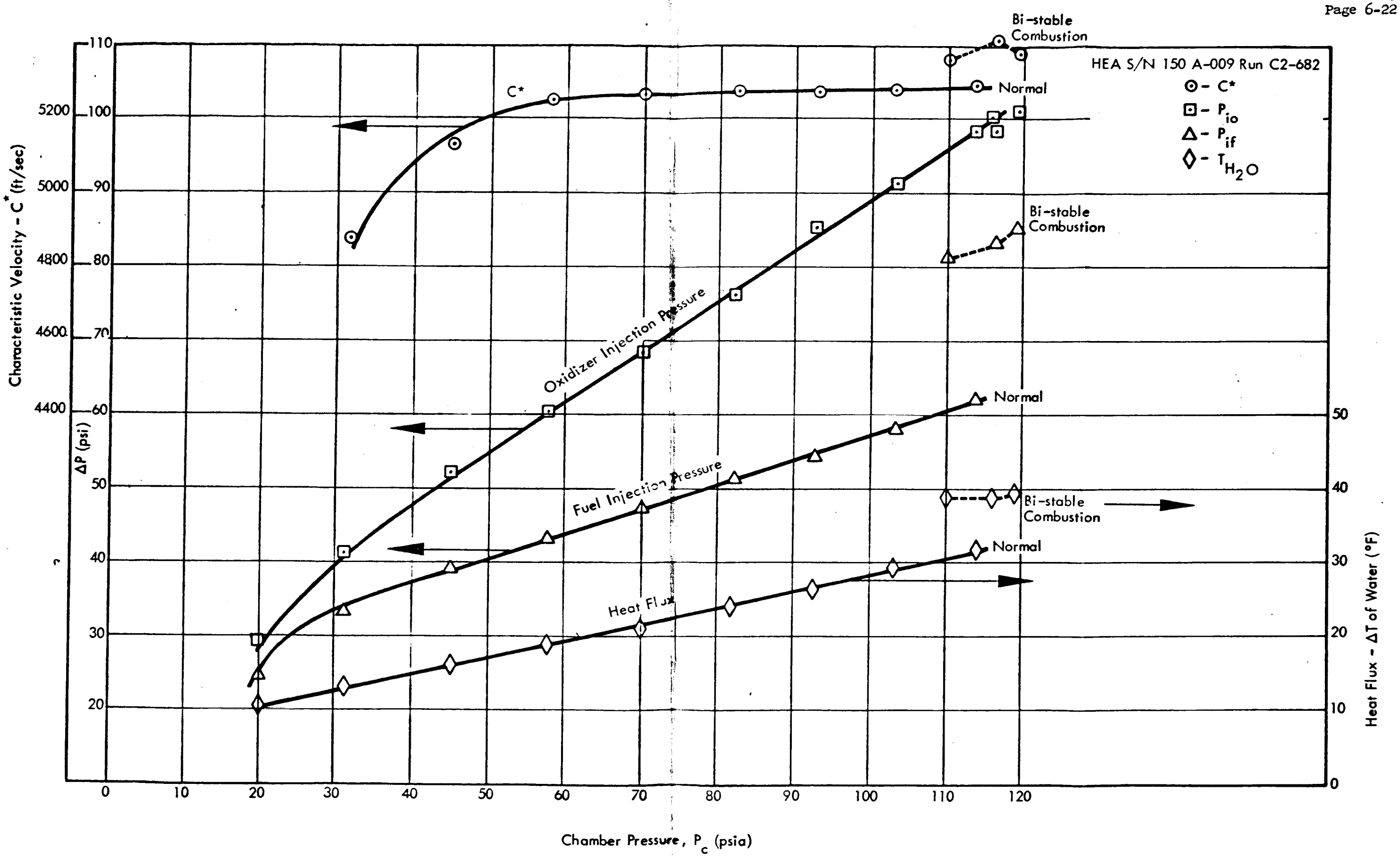

Figure 6.2.2-5. Injector Parameters as Affected by Bi-Stable Combustion

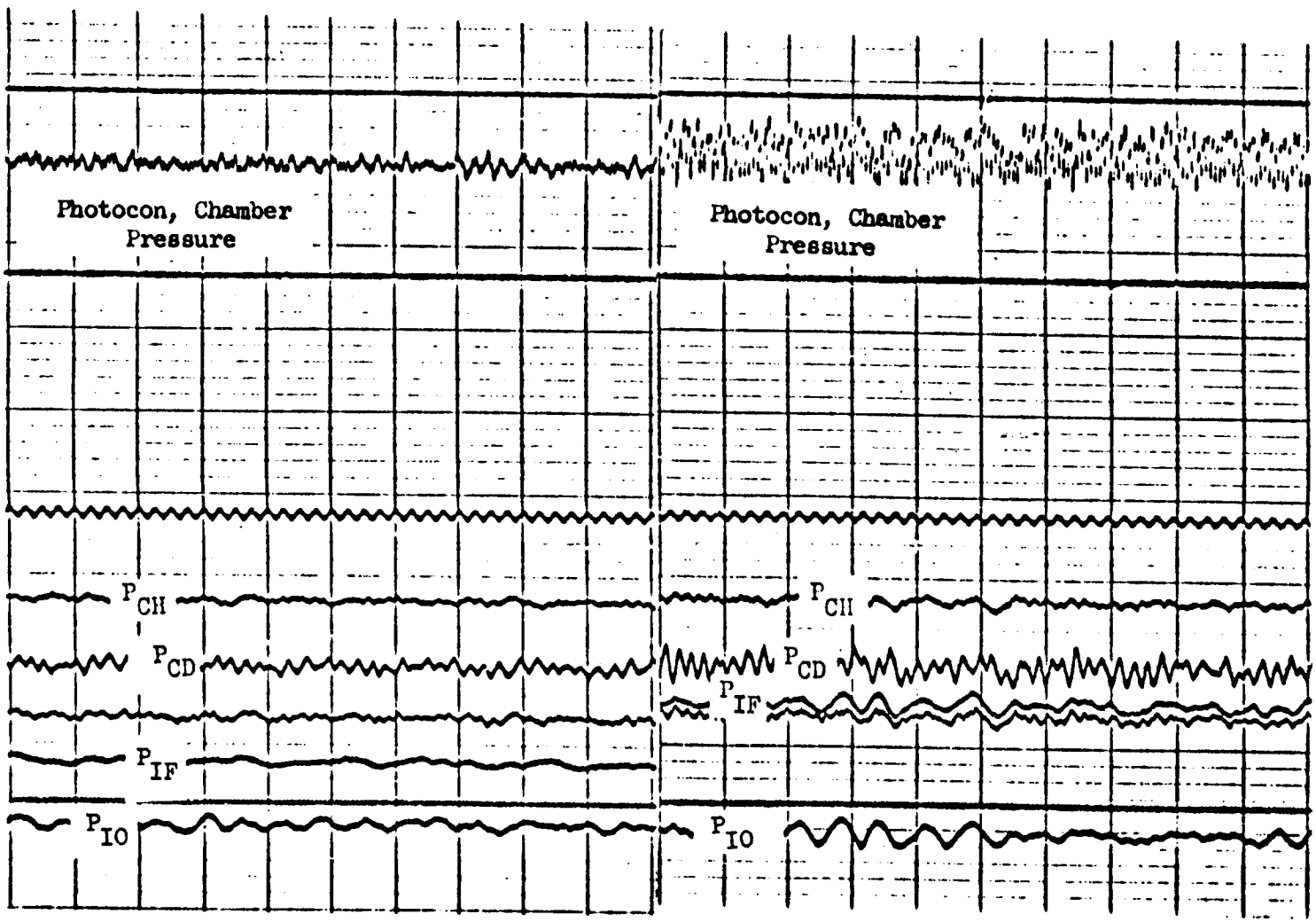

Figure 6.2.2-6. Oscillograph Traces for Bi-Stable and Normal Conditions

Streak test ablative throat inserts and injector face plate liners tested on 150A HEA S/N 010 at both normal and bi-stable combustion conditions are shown in Figure 6.2.2-7. The only difference in test conditions for these two firings was purging of the fuel passages before Run C2-673. Purge lines were then removed before the firing. Both test samples showed that the injector distribution pattern was not perfectly centered, causing more charring on one of the throat. However, the streak test at normal combustion conditions was acceptable by the criteria described in paragraph 4.3, while the streak sample at bi-stable combustion conditions had more erosion and a serious streak at one point. Both the ablative throat and face plate liner from the test operated at the bi-stable combustion conditions (Figure 6.2.2-7) showed the characteristic white glass flow associated with higher temperatures at the chamber wall.

On all HEAs tested, the streak test nozzles operated under bi-stable combustion conditions showed more erosion and a less uniform pattern than those run under normal conditions.

Three of the four CC & NAs tested during this investigation were run at the bi-stable combustion conditions: CC & NA S/N 004 on HEA S/N 007, Run C2-620; CC & NA S/N 009 on HEA S/N 006, Run C2-515; and CC & NA S/N 014 on HEA S/N 010, Run C2-694. These chambers had a noticeable amount of throat erosion after the 300-second, full-thrust durability tests; however, the thrust vector deviation which would have been caused by this erosion did not exceed the required limits. Paragraph 6.4.2.2 discusses this subject more fully.

The results of all tests discussed under this investigation have shown that the bi-stable combustion condition is attained only when the injector passages are partly filled, which occurs when the injector is not purged or exposed to vacuum between firings. Altitude testing experienced at JPL/ETS indicated that residual propellants are expulsed during the shutdown transient, as described in paragraph 6.9.1.2.

6.2.2.5 Conclusions

The following conclusions were derived from the test results presented in paragraph 6.2.2.4:

1. Bi-stable combustion conditions would not have occurred under actual mission conditions where a vacuum environment would assure empty injector manifold passages between restarts of the TCA.

2. Bi-stable combustion conditions did not result in unacceptable durability of the CC & NA.

3. The geometry of the injector element (sleeve tip and pintle) is the critical parameter in control of combustion characteristics.

4. The use of ablative streak test nozzles is the most consistent quantitative method of determining both the overall and localized erosion characteristics of an injector.

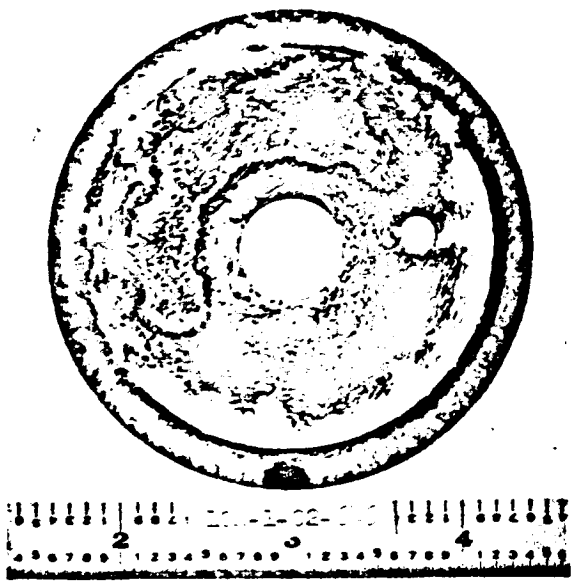

Face Plate Liner

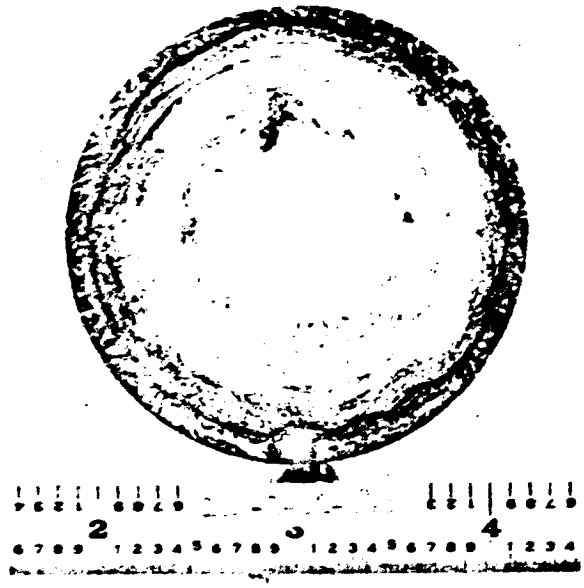

Nozzle Insert

Run C2-646: Streak Test - Bi-Stable Combustion Condition
C* = 5420 ft/sec, M.R. = 1.54, ΔP_f = 82 psia

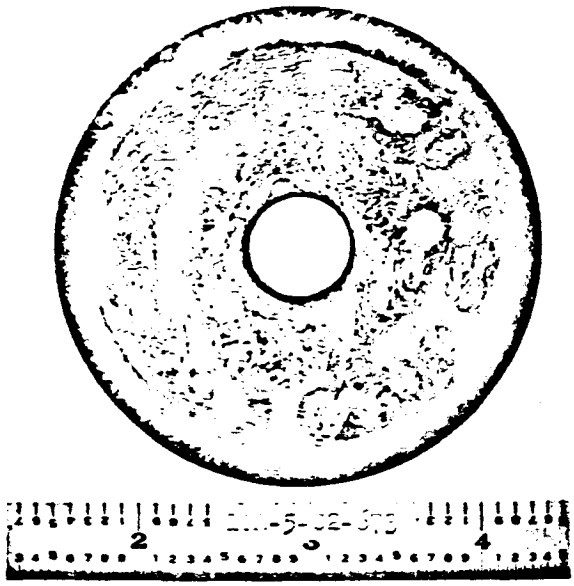

Face Plate Liner

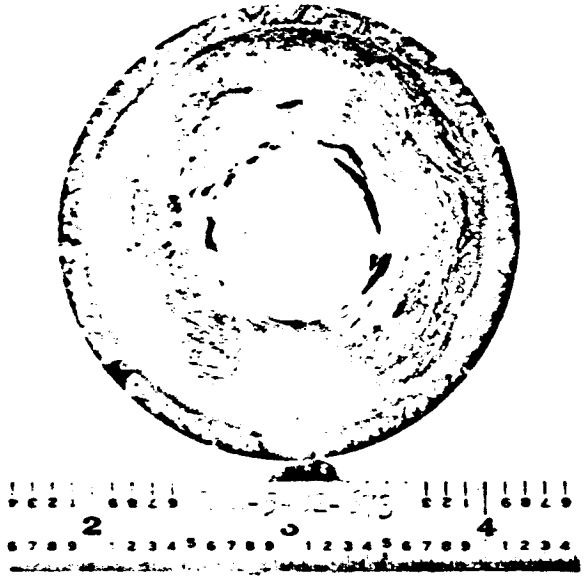

Nozzle Insert

Run C2-673: Streak Test - Normal Combustion Condition
C* = 5375 ft/sec, M.R. = 1.52, ΔP_f - 60 psi

Figure 6.2.2-7. Ablative Streak Tests

6.3 Fixed Area Injector Tests

A series of static firings were conducted on MIRA 150* HEA S/N 002 with the injector sleeve locked in position. The purpose of these tests was to demonstrate the operation and performance of the MIRA 150 Design in a fixed area injector configuration.

One test series had the sleeve position set for optimum performance at maximum thrust. During a second test series the sleeve position was set for optimum low thrust performance.

Performance is depicted in Figure 6.3-1. Additional tabulated data from these runs are presented in Table D-2-21 of Appendix D-2.

These data indicated that the MIRA 150 injector with the injector sleeve fixed is capable of being employed for limited range throttling as a fixed area injector.

*Details of this Phase II type injector configuration are discussed in the Phase II Final Report (STL Document No. 9730.4-64-36).

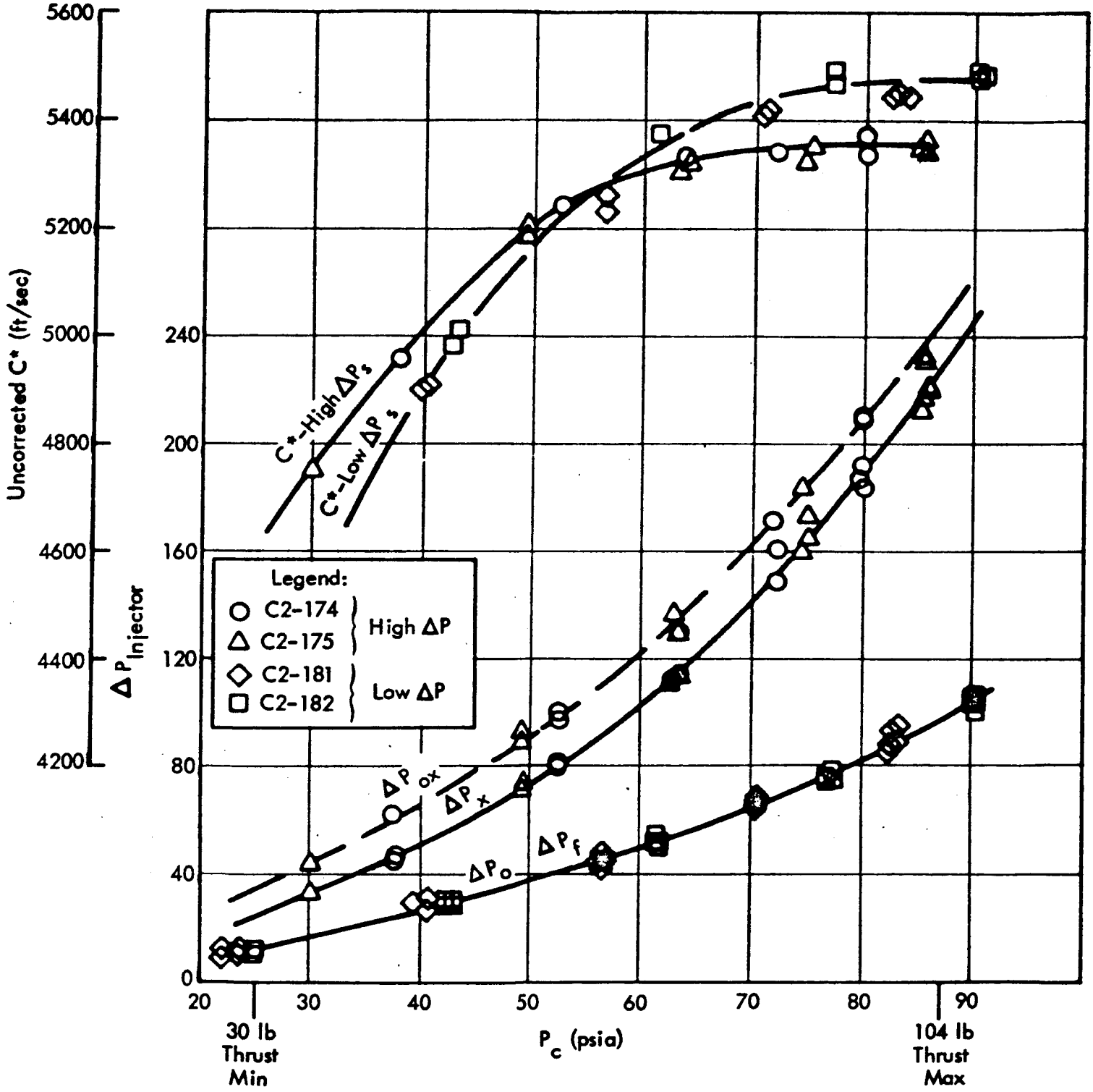

Figure 6.3-1. MIRA 150 HEA Fixed Area Injector Tests

6.4 Service Life Tests

The MIRA 150A TCA service life capability may be considered from two points of view - one involving primarily cumulate firing time and the other involving the number of cycles of operation.

The former consideration is most applicable to the CC & NA. First, because it contains the ablative liner that chars progressively with total cumulate firing time. Secondly, because it contains JTA in the throat that (theoretically at least) must give up to its surface as a function of time at elevated temperature molten Si O_2 to serve as a protective layer. (It is recognized that char and erosion rates of ablative liners are also dependent on the number of starts and cool-downs, and the liner temperature at restart. However, in the context of the MIRA 150A CC & NA performance where restarts should never exceed six, this startup influence is quite small.)

The latter consideration (i.e., cycles of operation) is most applicable to the HEA and especially to the following component subassemblies of the HEA: Servoactuator, helium pilot valve, shutoff valve, flow control valve, and injector.

Paragraphs 6.4.1 and 6.4.2 discuss the CC & NA durability (or service life aspects). Paragraph 6.4.3 deals with the HEA cycle life aspects.

6.4.1 Applicable CC & NA Service Life Tests

6.4.1.1 Sea Level Durability Tests

During Phase III, a total of 18 CC & NAs incorporating ablative liner assemblies and JTA nozzles of the final design were tested under sea level conditions at IRTS. The first eight of these 18 tests served to verify the choice of the final design of the ablative liner and two-piece JTA nozzle throat insert. The next ten sea level durability tests successfully demonstrated the two categories of service life specified in JPL Specification SAM-50255-DSN-C that required 300 seconds at maximum thrust and 480 seconds at minimum thrust with the mixture ratio at 1.6. Anomalous behavior resulted on one chamber (S/N 014) where the chamber burned through after 255 seconds of maximum thrust. Only three CC & NAs exhibited any detectable throat erosion and what was measured would not have resulted in excessive thrust vector deviation or any risk of continued firing. These three CC & NAs (S/N 004, 009, and 014, also the CC & NA on which the burn through occurred) were tested either with HEA S/N 006 that had a helium leak causing unacceptable combustion characteristics, or with HEAs that were operating in the bi-stable mode discussed in paragraph 6.2.2. Such performance would not occur under spacecraft operational conditions.

6.4.1.1.1 Test Article and Set-Up - In early Phase III CC & NA durability testing, eight CC & NAs with liner assemblies identical to that specified on STL Drawing 106546-2 were tested under maximum thrust conditions. The metal case used on these tests was stainless steel (80 mils thick) instead of the flight weight titanium case. These eight tests (identified as CC & NAs JTA-006 through 013) are also discussed in paragraph 6.1.

Later in Phase III, ten more durability tests were performed in accordance with paragraph 3.1.3.1.2 of the Development Test Plan. These tests were performed with complete CC & NAs (case included) that conformed to STL Drawing 106546-2.

A typical test setup for a sea level TCA firing is shown in Figures 6.7.1-1 and -2, except that an ablative-cooled CC & NA was used in place of the water-cooled chamber shown in the figures. The CC & NAs tested during the early stages of Phase III (JTA-006 through JTA-013) were not insulated from the test cell environment. The later Phase III sea level tests were conducted with insulated CC & NAs. A schematic of the sea level CC & NA thermocouple locations is shown in Figure 6.4.2-1.

6.4.1.1.2 Test Objectives - The eight early durability tests discussed in paragraph 6.1 were maximum thrust firings conducted to verify the choice of the final design by testing under the following conditions:

Propellants	N_2O_4 + 10% NO or N_2O_4 MMH
Mixture Ratio ($_{ox}$/Fuel):	1.5 ± 0.1
Chamber Pressure:	104 psia ± 5 psia
C^* (Corrected):	5400 ft/sec ± 1.0%
Firing Schedule:	15 seconds at max P_c followed by a cooldown to ambient temperature, 50 seconds at max P_c followed by a cooldown to ambient temperature, and a final 235 second firing at max P_c.

The purpose of the later ten sea level durability tests was to demonstrate the following two categories of minimum service life on the selected final design using MON and MMH at a 1.6 mixture ratio.

- Maximum Thrust Duration: 300 seconds in 3 increments (15, 50, and 235 seconds) at maximum thrust with complete cool-downs to ambient temperature between firings.
- Minimum Thrust Duration: 480 seconds in 3 increments (15 seconds at maximum thrust followed by 50 and 415-second firings at minimum thrust) with complete cool-downs to ambient temperature between firings.

6.4.1.1.3 Test Matrix - The test matrix for the ten durability tests performed in accordance with paragraph 3.1.3.1.2 of the Development Test Plan is shown in Table 6.4.1-1.

Table 6.4.1-1

Sea Level CC & NA Service Life Test Matrix

CC & NA Serial Number	Test Type Max. Thrust	Test Type Min. Thrust	HEA Serial Number	Initial Chamber Temperature (°F)	Propellant Temperature (°F)
010	X		006	Ambient	Ambient
009	X		006	125	Ambient
011		X	006	Ambient	Ambient
013	X		005	0	100
001	X		005	125	100
012		X	005	0	100
004	X		007	Ambient	Ambient
003	X		002	Ambient	Ambient
014	X		014	Ambient	Ambient
002	X		008	Ambient	Ambient

6.4.1.1.4 Test Results - The test results of the Phase III sea level CC & NA durability tests are presented in Table 6.4.1-2.

6.4.1.2 Other Applicable CC & NA Tests

Table 6.4.1-3 summarizes the other applicable CC & NA service life tests performed during Phase III. These tests are described in other paragraphs of this report; the applicable paragraphs are referenced in the last column of this table.

Considered herein are 13 CC & NAs (including seven flight expansion ratio chambers) tested at altitude at JPL/ETS. The results in terms of char, erosion, external TCA surface temperature, and weight loss are reported in paragraph 6.4.2. In every case the CC & NAs performed acceptably.

Table 6.4.1-2

Sea Level Durability Test Results

CC & NA P/N & S/N	HEA S/N	Run No.	Test Ref(1)	Chamber Pressure (psia)	Total Flow Rate (lbs/sec)	Throat Erosion (%)	Liner Wt Loss (grams)	Thrust Level	Firing Duration (seconds)	Total Duration (seconds)	Total Number of Starts	Measured C* (ft/sec)	Mixture Ratio (O/F)	Fuel Temp(2) (°F)	Oxidizer Temp(2) (°F)	Initial Chamber Temp(°F)	Max. Case Temp. TC-4 (°F)	Max. Case Temp. TC-5 (°F)	Remarks
JTA-006	150-003	C_1-153A		107.3	0.501	0		Max.	15			5325	1.543	59	55	68	269	269	
		B		107.3	0.501	0		Max.	50			5320	1.546	59	55	113	404	413	
		C		108.5	0.508	0		Max.	236	301	3	5305	1.493	58	55	123	537	654	
JTA-007	150-003	C_1-154A		107.1	0.505	0		Max.	15			5321	1.529	56	51	77	251	208	
		B		107.8	0.509	0		Max.	50			5308	1.509	56	48	95	404	463	
		C		107.4	0.505	0		Max.	237	302	3	5332	1.533	56	51	95	598	691	
JTA-008	150-003	C_1-155A		106.4	0.495	0		Max.	15			5388	1.577	57	54	68	265	275	
		B		106.0	0.492	0		Max.	50			5399	1.619	56	51	70	430	460	
		C		104.6	0.485	0		Max.	236	301	3	5404	1.699	56	50	76	600	610	
JTA-009	150-003	C_1-160A		107.4	0.496	0		Max.	15			5398	1.585	57	55	59	245	235	
		B		109.0	0.504	0		Max.	50			5395	1.592	55	54	68	400	400	
		C		107.0	0.498	0		Max.	15			5356	1.512	59	53				
		D		106.4	0.498	0		Max.	20			5331	1.467	57	50	77	260	256	
		C_1-165		108.2	0.500	0		Max.	204	304	5	5409	1.551	60	58	79	595	595	
JTA-010	150-002	C_2-216A		106.3	0.502	0		Max.	15			5295	1.550	59	58	59	246	251	
		B		109.5	0.505	0		Max.	50			5419	1.524	59	58	121	422	449	
		C		108.5	0.502	0		Max.	239	304	3	5409	1.533	59	57	102	790	836	
JTA-011	150-002	C_2-215A		109.1	0.500	0		Max.	15			5447	1.563	54	54	68	251	253	
		B		109.3	0.500	0		Max.	50			5454	1.559	55	55	64	422	431	
		C		109.0	0.502	0		Max.	235	300	3	5420	1.527	59	59	104	778	846	
JTA-012	150-002	C_2-222A		109.7	0.517	0		Max.	15			5317	1.572	56	56	55	251	269	Propellants: N_2O_4 and MMH
		B		110.1	0.518	0		Max.	50			5331	1.567	56	56	86	443	449	
		C		108.5	0.516	0		Max.	235	300	3	5268	1.568	55	56	113	735	803	
JTA-013	150A-005	C_1-257A		111.9	0.525	0		Max.	15			5326	1.535	63	62	70	247	239	Propellants: N_2O_4 and MMH
		B		111.3	0.523	0		Max.	50			5321	1.536	64	63	130	386	368	
		C		110.7	0.520	0		Max.	235			5322	1.529	62	62	86	546	510	Ablative liner
	150A-003	C_2-369		109.0	0.516	0		Max.	300			5284	1.517	69	67	77	829	786	failed and case overheated.
		C_2-372		109.9	0.514	0		Max.	88	688	5	5349	1.508	64	64	73	1032	1053	
106546-2	150A-005	C_2-612A	3.1.3.1.2	106.6	0.5088	0		Max.	15			5252	1.622	100	95	128	367	395	
001		B		105.6	0.5027	0		Max.	50			5263	1.593	98	97	137	555	658	
		C		107.6	0.5080	0		Max.	235	300	3	5313	1.597	98	97	126	846	1299	
106546-2	150A-005	C_2-623A	5.2.5			0		Variable	52			5278	1.496	65	65	68	506	563	Thrust-time Tape
002		B				0		Variable	70			5278	1.509	65	65	67	580	605	PQ-1A & PQ-1B
	150A-008	C_2-633	3.1.3.1.2	108.6	0.5140	0	53.1	Max.	235	357	3	5310	1.610	49	47	85	1640	1593	

Table 6.4.1-2 (Continued)

CC & HA P/N & S/N	HEA S/N	Run No.	Test Ref.(1)	Chamber Pressure (psia)	Total Flow Rate (lbs/sec)	Throat Erosion (%)	Liner Wt Loss (grams)	Thrust Level	Firing Duration (seconds)	Total Duration (seconds)	Total Number of Starts	Measured C* (ft/sec)	Mixture Ratio (O/F)	Fuel Temp(2) (°F)	Oxidizer Temp(2) (°F)	Initial Chamber Temp(°F)	Max. Case Temp. TC-4 (°F)	Max. Case Temp. TC-5 (°F)	Remarks
106546-2	150A-002	C_2-626A	3.3.1.2	108.6	0.5110	0		Max.	15			5322	1.617	61	59	67	375	403	Slight bulge in chamber case noted after last firing.
003		B		108.6	0.5130	0		Max.	50			5300	1.620	62	55	146	641	697	
		C		108.7	0.5116	0		Max.	235	300	3	5319	1.619	63	58	134	1704	1641	
106546-2	150A-007	C_2-628A	3.3.1.2	106.2	0.5094	0		Max.	15			5207	1.431	59	58	64	332	375	
004		B		110.0	0.5174	0		Max.	50			5309	1.532	60	59	106	593	697	
		C		108.2	0.5038	9.58		Max.	235	300	3	5365	1.565	58	58	104	1394	1394	
106546-2	150A-006	C_2-515A	3.3.1.2	110.4	0.516	0		Max.	15			5330	1.562	66	62	120	390	412	
009		B		112.0	0.536	0		Max.	50			5330	1.669	66	62	125	600	690	
		C		110.3	0.539	0.96	64.4	Max.	235	300	3	5310	1.664	66	62	125	1570	1680	
106546-2	150A-006	C_2-522A	3.3.1.2	109.7	0.533	0		Max.	15			5139	1.648	68	68	80	215	205	
010		B		109.1	0.529	0		Max.	50			5148	1.622	68	70	130	535	622	
		C		109.3	0.529	0		Max.	235	300	3	5159	1.631	67	66	140	1290	1470	
106546-2	150A-006	C_2-525A	3.3.1.2	110.1	0.532	0		Max.	15			5181	1.632	60	59	77	190	200	
011		B		28.1	0.146	0		Min.	50			4832	1.612	68	63	150	370	420	
		C		28.5	0.146	0	46.1	Min.	415	480	3	4858	1.607	66	62	140	875	1180	
106546-2	150A-002	C_2-572A	2.2.5			0		Variable	52			5123	1.496	74	70	77	458	563	
012		B				0		Variable	70			5000	1.480	74	70	121	458	541	
		C				0		Variable	93			5150	1.487	74	70	99	756	842	
	150A-005	C_2-610	3.3.1.2	30.7	0.1593	0		Min.	415	630	4	4824	1.653	89	93	0	714	1097	
106546-2	150A-005	C_2-611A	3.3.1.2	105.4	0.5034	0		Max.	15			5261	1.618	93	94	0	379	403	
013		B		103.9	0.4979	0		Max.	50			5240	1.599	103	104	87	554	596	
		C		106.1	0.5070	0		Max.	235	300	3	5257	1.619	91	91	128	1084	1199	
106546-2	150A-010	C_2-694A	3.3.1.2	114.0	0.5322	0		Max.	15			5398	1.614	44	47	50	412	475	HEA operated in bi-stable mode chamber burned through side.
014		B		112.6	0.5281	0		Max.	50			5350	1.614	46	48	114	641	820	
		C		113.0	0.5303	3.54		Max.	190	255	3	5370	1.543	59	55	56	1715	1703	

NOTES: (1) Numbers refer to paragraphs of the Development Test Plan.

(2) Propellants: MON and MMH unless otherwise noted.

Table 6.4.1-3

Other Applicable CC & NA Service Life Tests

CC & NA Serial Number	Test Designation	CC & NA Type	Test Matrix (Ref)	Test Objectives, Summary, Configurations, Setup, Conditions, and Results (Ref)
002	5.2.11(1)	Altitude	6.6	6.6.3
003	PQT-001	Altitude	6.6	6.6.4
005	PQT-002, 003, 004A	Altitude	6.6	6.6.4
005	PQT-004B	Altitude	6.6	6.6.6
010	PQT-005	Altitude	6.6	6.6.11
008	PQT-007	Altitude	6.6	6.6.7
001	PQT-008	Altitude	6.6	6.6.8
007	PQT-011	Altitude	---	6.10.2
006	5.2.1(1)	Sea Level	6.5	6.5(2)
008	5.2.2(1)	Sea Level	6.5	6.5(2)
005	5.2.3(1)	Sea Level	6.5	6.5(2)
007	5.2.4(1)	Sea Level	6.5	6.5(2)
002 & 012	5.2.5(1)	Sea Level	(2)	(3)

(1) Development Test Plan paragraph number describing the test.

(2) The test objectives, summary, conditions, and results are described in paragraph 6.5. The test setup was identical to that used in the CC & NA sea level durability tests (paragraph 6.4.1.1.1).

(3) Test 5.2.5 was to have been the last test in the propellant temperature-pressure extremes tests with all conditions at mean values. It was never completed. The sea level CC & NA Serial Numbers 002 and 012 were used partially in test 5.2.5 and partially on the CC & NA durability tests.

6.4.1.2.1 Test Results - The CC & NA test results from the tests listed in Table 6.4.1-3 are presented in Table 6.4.1-4.

Table 6.4.1-4

Other Applicable Phase III CC & NA Service Life Tests

CC & NA P/N & S/N	HEA S/N	Run No.	Test Ref.	Throat Erosion ($)	Liner Wt Loss (grams)	Thrust Time(1) Type	Firing Duration (seconds)	Total Duration (seconds)	Total Number of Starts	Environment	Fuel(2) Temp (°F)	Oxidizer(2) Temp (°F)	Initial Chamber Temp(°F)	Maximum External Surface Temperatures(3) (°F) TC-1	TC-2	TC-3	TC-4	TC-5	TC-7	THE-1	THE-2	THE-3	THE-4	Char Depth, (inches) STA.1	STA.2	STA.3	STA.4	Remarks
106546-1 001	008	DY-38	PQT-008	0		PQ-8	160			Altitude	98	97	0	1075	1125	875	540	485	165	119	113	105	324					
		DY-39		0		PQ-8	160				100	102	50	1025	1085	890	590	520	170	129	127	120	318					
		DY-40		0	27.9	PQ-8	160	480	3		98	96	130	1010	1075	890	600	530	175	132	134	124	35	0.150	0.080	0.120	0.050	
106546-1 002	004	DY-20	5.2.11(4)	0		PQ-1A	52			Altitude	70	69	100	1370	1390	950	270	475	135	92	95	155	125					
		DY-21		0		PQ-1B	70				69	69	310	1560	1580	1035	490	635	160	140	140	205	133					
		DY-22		0		PQ-1C	40				65	61	50	1580	1625	1060	655	705	130	104	109	158	83					
		DY-23		0		PQ-1C	116				66	63	100	1700	1730	1310	840	910	170	131	133	172	102					
		DY-24		0	63.1	PQ-1B	70	348	5		65	62	120	1570	1610	1010	660	710	150	115	123	186	109	0.090	0.375	0.600	0.230	
106546-1 003	001	DY-25	PQT-001	0		PQ-3	45	45	1	Altitude	69	73	100	1572	1699	1211	554	578	100	112	118	164	137	0.070	0.080	0.090	0.060	Chamber leaked during leak check. Replaced with S/N 005
														1518	1694	1264	528	549	125	105	107	168	110					
						PQ-4	45			Altitude	69	70	76	1621	1839	1430	624	687	151	114	123	212	124					
106546-1 005	001	DY-26	PQT-002	0		PQ-5	45				68	70	90	1556	1733	1328	624	683	148	110	119	191	120					
		DY-27	PQT-003	0		PQ-3	45				66	68	90	1732	1757	1652	978	985	116	52	50	178	146	0.090	0.375	0.600	0.280	
		DY-28	PQT-004A	0													662	716										
		DY-33	PQT-004B	0	77.5	PQ-6	180	315	4		-6	2	-3				668	735						0.150	0.350	0.310	0.010	
106546-1 006	001	HC-001	Centrifuge	0		AT-1	130			Sea Level	53	52	68				572	668										
		HC-002	Checkout	0		AT-1	130	260	2		53	52	70				778	905										
106546-1 007	008	C_2-709A	PQT-011	0		PQ-7A	50			Sea Level	53	49	64															
		B		0		PQ-7A	100				53	49	93				926	1116										
		C		0		PQ-7A	150	300	3		53	54	82	1700	1840	1550	690	720	160	140	135	137	182					
106546-1 008	008	DY-35	PQT-007	0		PQ-7A	50			Altitude	100	100	130	1680	1825	1675	910	960	210	157	165	162	222					Slight bulge in case noted after final firing.
		DY-36		0		PQ-7A	100				99	97	130	1706	1854	1523	1784	1314	243	166	171	194	273	0.060	0.375	0.600	0.380	
		DY-37		0	82.4	PQ-7A	150	300	3		96	98	150	1382	1516	1055	486	480	113	81	80	189	77					
106546-1 010	010	DY-47	PQT-005	0		PQ-3	45			Altitude	50	51	53															
		DY-48A		0		PQ-4	45				62	62	74															
		DY-48B		0		PQ-5	45				68	65		1493	1643	1295	758	746	153	110	108	214	121	0.060	0.300	0.350	0.220	Runs DY-48 A, B, and C were run with approximately 10 second intervals between runs
		DY-48C		0	44.3	PQ-3	45	130	4		69	68					350	476										
106546-2 005	005	C_2-606A	5.2.3(4)	0		PQ-3	45			Sea Level	18	18	0				493	562										
		B		0		PQ-4	45				10	16	105				489	582										
		C		0		PQ-5	45				8	11	60				518	602										
		D		0		PQ-3	45				9	14	130				1190	1390										
		E		0		PQ-6	180	360	5		6	5	140				334	392										
106546-2 005	005	C_2-605A	5.2.1(4)	0		PQ-3	45			Sea Level	13	29	15				480	470										
		B		0		PQ-4	45				7	21	60				574	570										
		C		0		PQ-5	45				6	18	115				615	605										
		D		0		PQ-3	45				7	8	150				872	790										
		E		0		PQ-6	180	360	5		5	2	110				412	450										
106546-2 005	005	C_2-504A	5.2.4(4)	0		PQ-1A	52			Sea Level	94	93	10				495	506										
007		B		0		PQ-1B	70				100	98	90				670	725										
		C		0		PQ-1C	116				102	102	150				565	618										
		D		0		PQ-1A	52				102	102	120				596	610										
		E		0		PQ-1B	70	360	5		96	98	150				482	494										
106546-2 005	005	C_2-600A	5.2.2(4)	0		PQ-3	45			Sea Level	93	85	120				498	517										
008		B		0		PQ-4	45				97	92	115				456	481										
		C		0		PQ-5	45				98	94	130				525	547										
		C_2-603A		0		PQ-3	45				95	93	140				636	675										
		B		0		PQ-6	180	360	5		100	104	109															

NOTES: (1) Thrust signal-time profiles are as follow:

PQ-1: Table 6.6.3-2
PQ-3: Table 6.6.4-1, Profile 1
PQ-4: Table 6.6.4-1, Profile 2
PQ-5: Table 6.6.4-1, Profile 3
PQ-6: Table 6.6.6-1
PQ-7: Fixed at max. thrust
PQ-8: Fixed at min. thrust
AT-1: Table 6.6.1-3

NOTES: (2) Propellants: MON and MMH

(3) Maximum temperatures shown occurred during soak back period, except for TC-1, 2, and 3 where maximum values were attained during the run. Only TC-4 and TC-5 were used on CC & NA 106546-2 (S/N 005, 006, 007, and 007).

(4) The numbers correspond to paragraphs of the Development Test Plan.

6.4.2 Applicable CC & NA Service Life Test Results

6.4.2.1 External Surface Temperatures

Temperature profiles of the MIRA 150A TCA external surfaces were obtained on both sea level and altitude firings. Temperature measurements were not acquired on the HEA during sea level firings because of the difficulty of thermally insulating the injector from the convective cooling environment inherent in the test cell. Such insulation is necessary to make the temperature meaningful as related to the operational condition. Some of the CC & NAs fired at sea level were thermally insulated from the test cell environment with one-half inch thick silica batting. Figures 6.4.2-1 and -2 show the thermocouple locations on the sea level and altitude configurations.

Figures 6.4.2-3 through 6.4.2-5 show CC & NA surface temperatures obtained under sea level conditions with use of the thermal blanket for Runs C2-522 (maximum thrust), C2-525 (minimum thrust), and C2-604 (variable thrust conditions). In Figure 6.4.2-3, the surface temperature profiles of a CC & NA tested under sea level conditions without the thermal blanket (Run C1-155C) is also shown for a 235-second firing. The case temperatures are approximately 600°F lower for the uninsulated case where convective cooling is apparently appreciable.

Figures 6.4.2-6 through 6.4.2-8 show typical surface temperatures obtained at JPL/ETS under altitude conditions for maximum thrust firings (Runs DY-35, -36, and -37), minimum thrust firings (Runs DY-38, -39, and -40), and variable thrust firings (Runs DY-20 through DY-24).

Figures 6.4.2-3 and 6.4.2-6 show that at maximum thrust the simulated altitude environmental conditions result in approximately 300°F higher surface temperatures at Stations 4 and 5 than with the insulated chamber in a sea level test. This can be seen by comparing Run C2-522B with Run DY-35. Figures 6.4.2-5 and 6.4.2-8 (Runs C2-604C and DY-23) show approximately 200°F higher surface temperatures at Stations 4 and 5 for the altitude conditions than for the insulated sea level test under variable thrust conditions.

Comparing Runs DY-27 (maximum thrust) on Figure 6.4.2-6 with Run DY-39 (minimum thrust) on Figure 6.4.2-7, the surface temperatures were higher for maximum thrust conditions at all stations, except THE-4. Station THE-4 was approximately 50°F hotter during the minimum thrust firing than during the maximum thrust firing. This may have been caused by more local convective heat transfer surrounding THE-4, since the test cell pressure was about five times higher because water was injected into the test cell to cool the facility butterfly valve during the maximum thrust firing.

Also of interest is the tendency for surface temperatures at Stations 4 and 5 to rise more rapidly and to reach higher values under the same firing conditions as the liner becomes more charred. This can be seen by a comparison of the three successive 160-second firings shown in Figure 6.4.2-7.

Selected theoretical temperature profiles, extracted from those given in paragraph 7.5.3 for corresponding stations are shown as dotted lines in Figure 6.4.2-8. Agreement is good between predicted and measured temperatures at an expansion area ratio of 24 in the radiation portion of the nozzle skirt, TC-2. Larger variations between predicted and measured temperatures occur at the other combustion chamber stations. Less accurate prediction of these temperatures may be attributed to lack of knowledge on the gas film heat transfer coefficient. The heat transfer prediction is especially difficult in a chamber such as the MIRA 150A where there is appreciable film cooling.

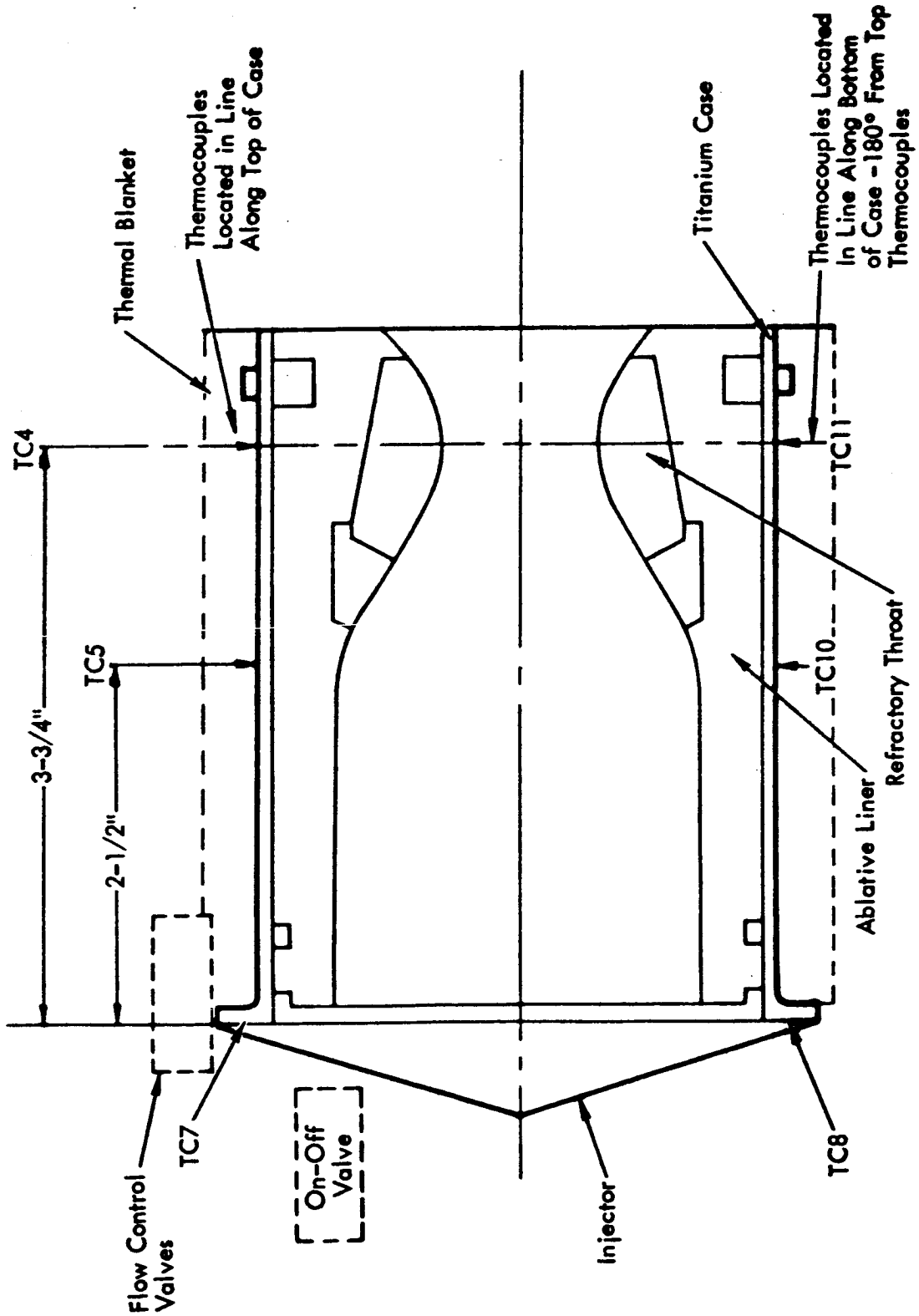

Figure 6.4.2-1. Thermocouple Locations on MIRA 150A Sea Level CC & NA

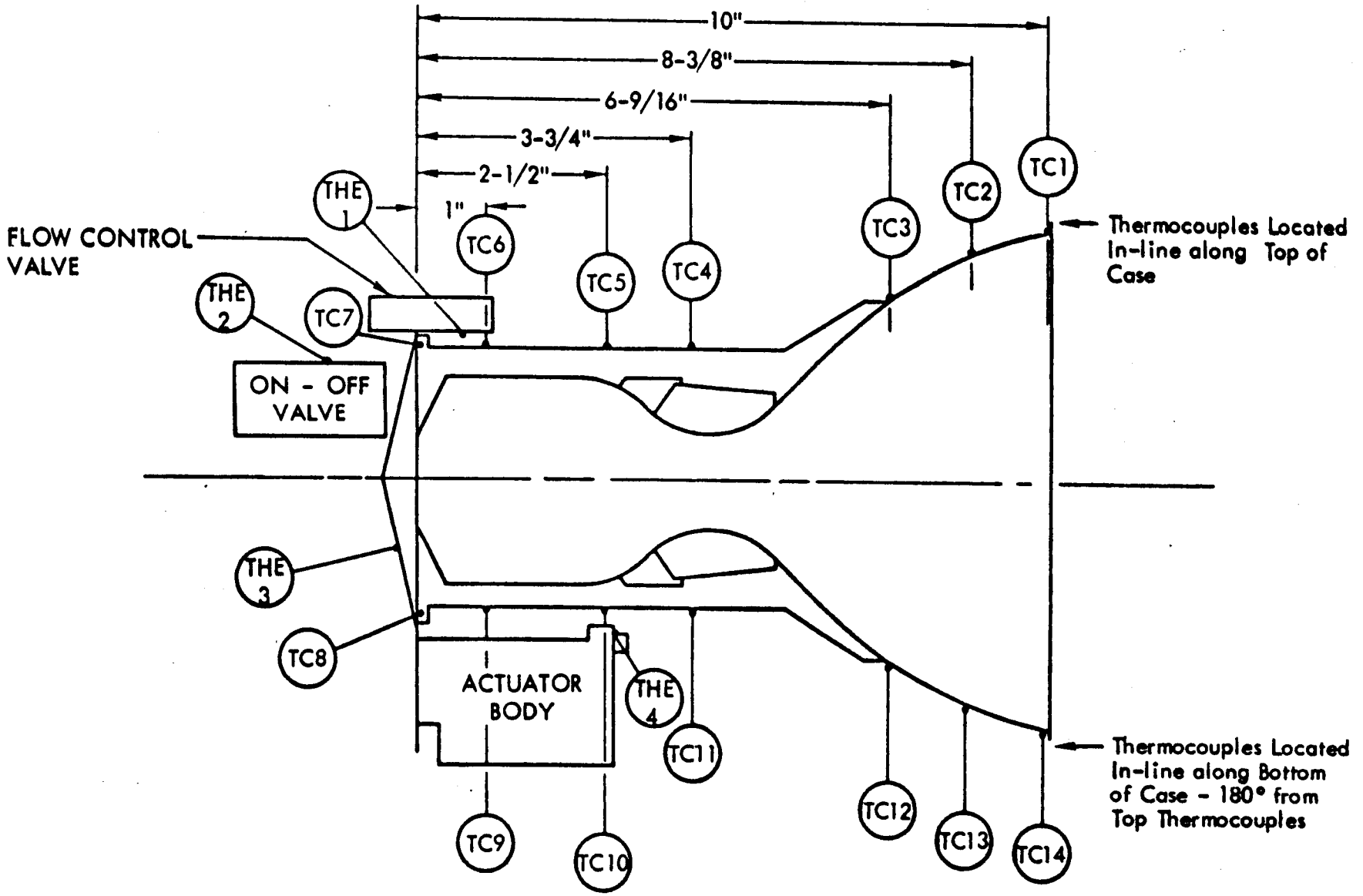

Figure 6.4.2-2. MIRA 150A Thermocouple Locations

Figure 6.4.2-3. MIRA 150A CC & NA Surface Temperature Profiles Maximum Thrust at Sea Level Conditions with Insulated Case

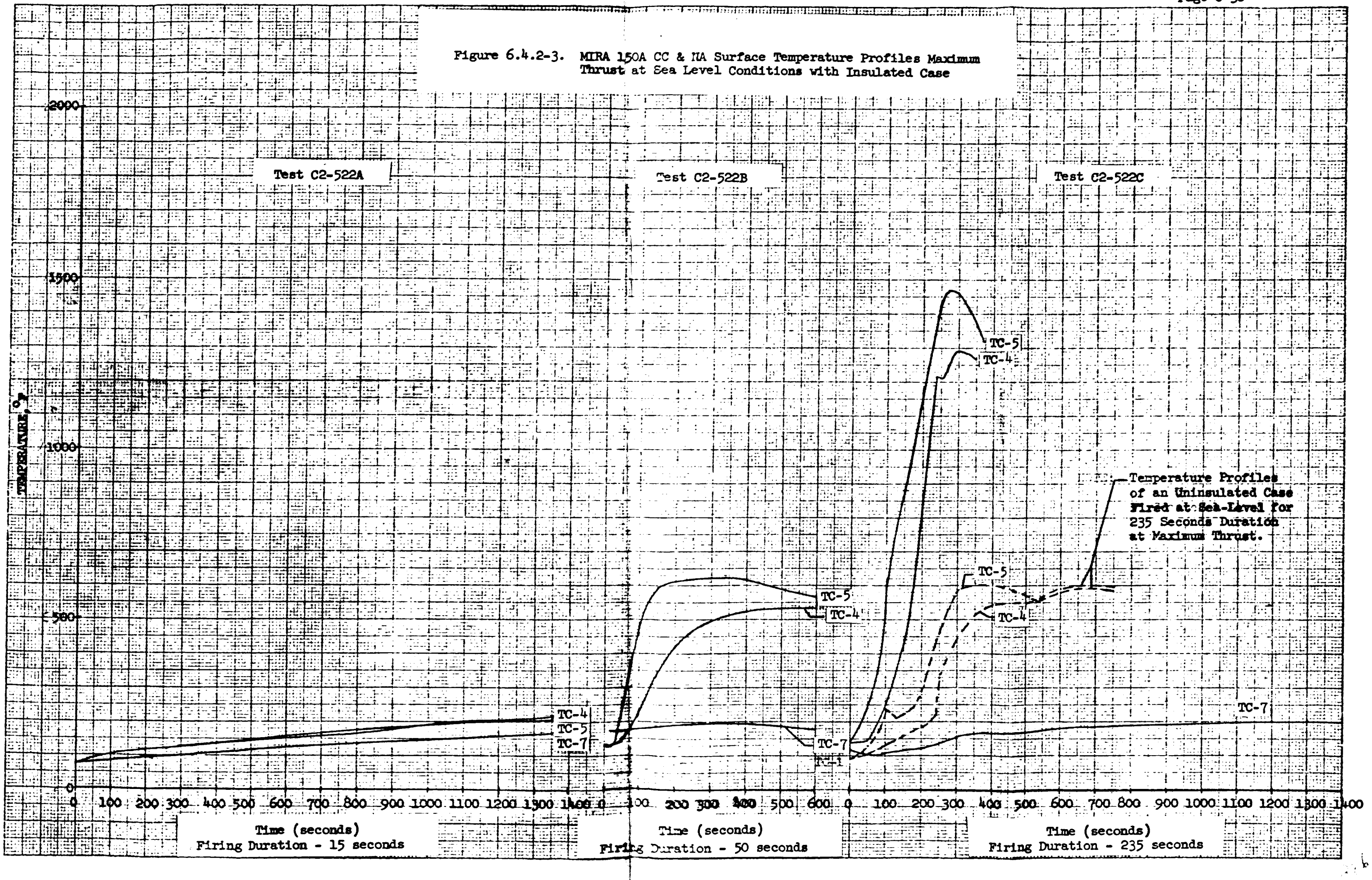

Figure 6.4.2-4. MIRA 150A CC & NA Surface Temperature Profiles Minimum Thrust at Sea Level Conditions Insulated Case

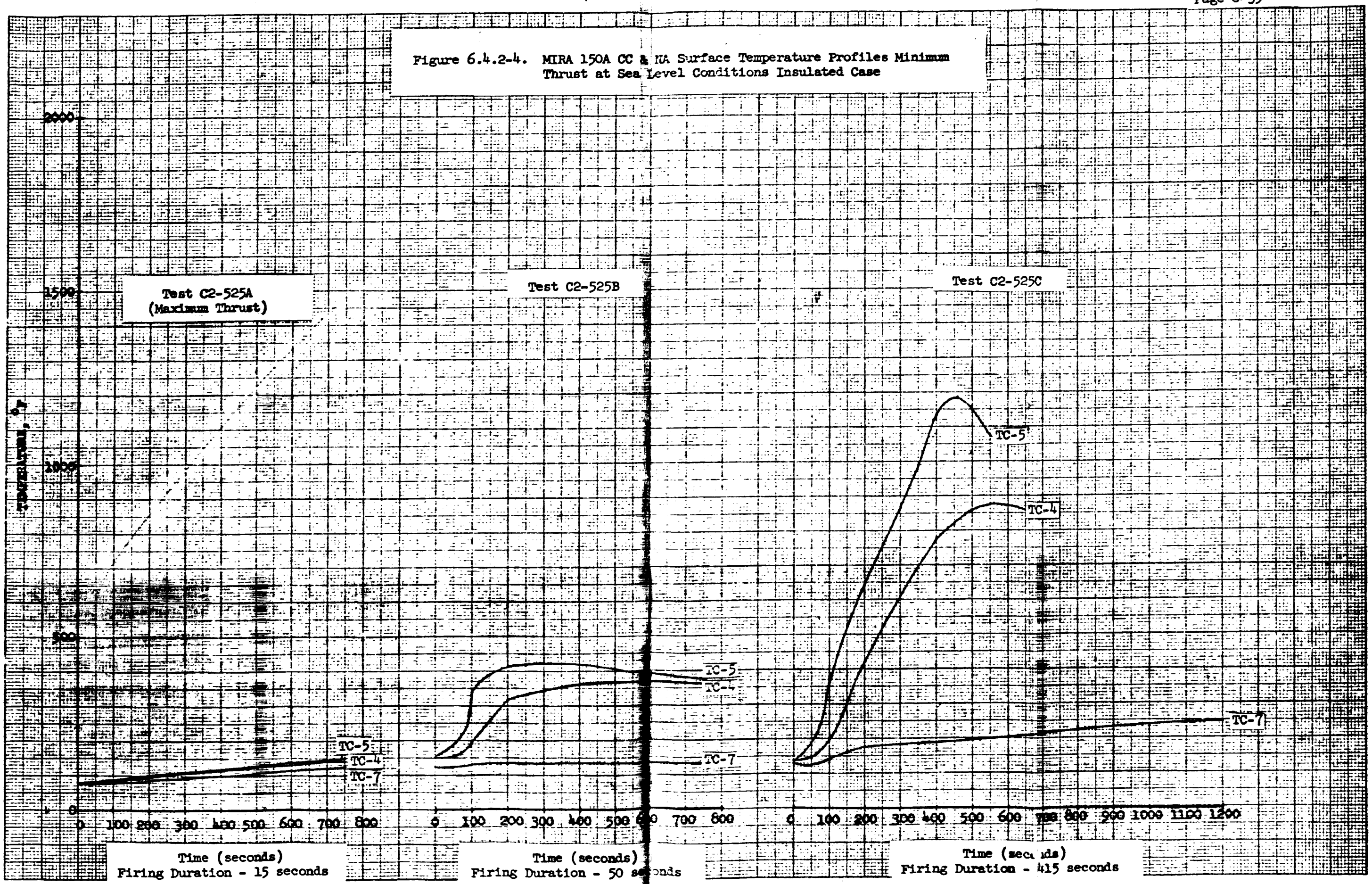

Figure 6.4.2-5. MIRA 150A CC & NA Surface Temperature Profiles Variable Thrust at Sea Level Conditions Insulated Case

Test C2-604A Thrust-Time Profile PQ-1A*	Test C2-604B Thrust-Time Profile PQ-1B*	Test C2-604C Thrust-Time Profile PQ-1C*	Test C2-604D Thrust-Time Profile PQ-1A*	Test C2-604E Thrust-Time Profile PQ-1B*

*See Table 6.6.3-2 for Thrust-Signal-Time Profiles Used

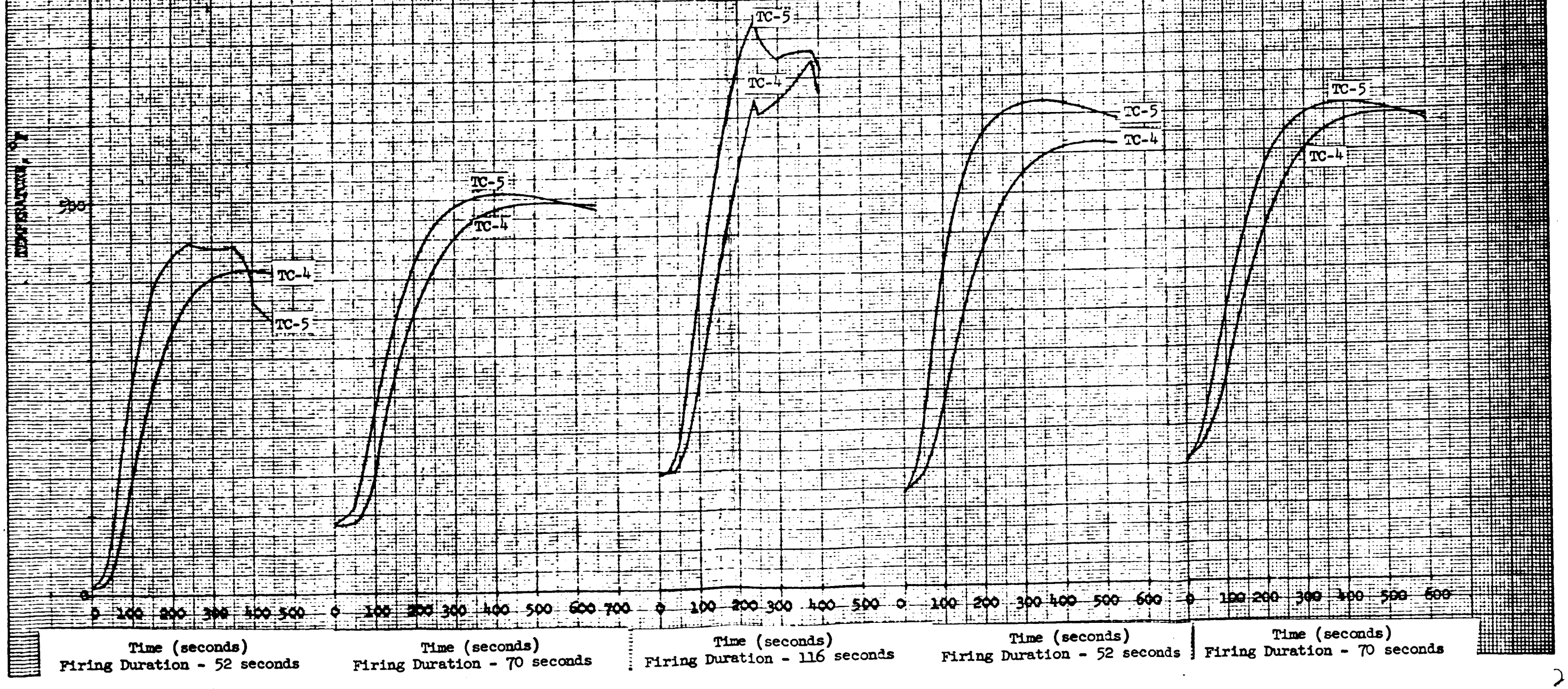

Figure 6.4.2-6. MIRA 150A TCA Surface Temperature Profiles
Maximum Thrust at Altitude

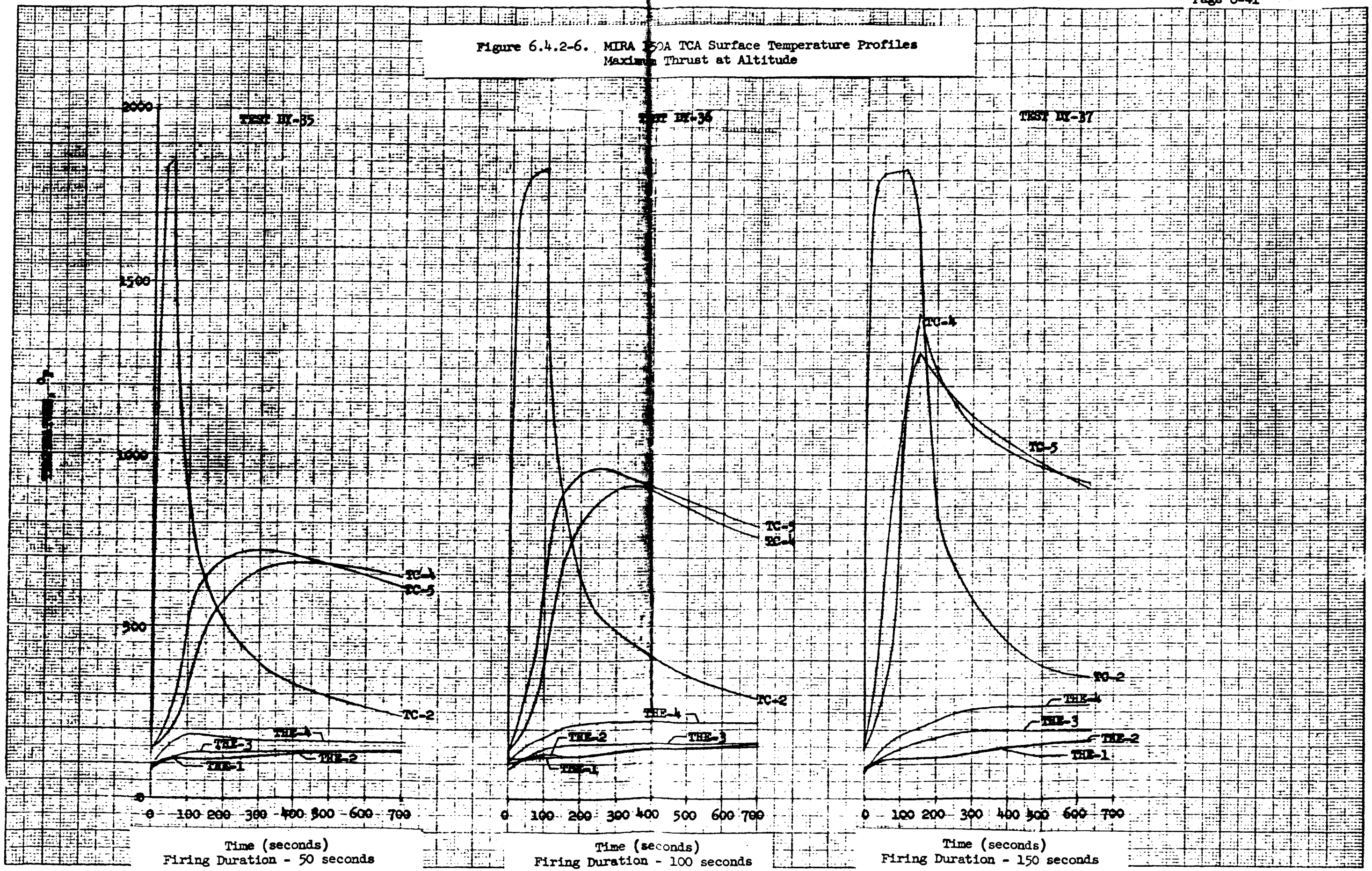

Figure 6.4.2-7. MIRA 150A TCA Surface Temperature Profiles
Minimum Thrust at Altitude

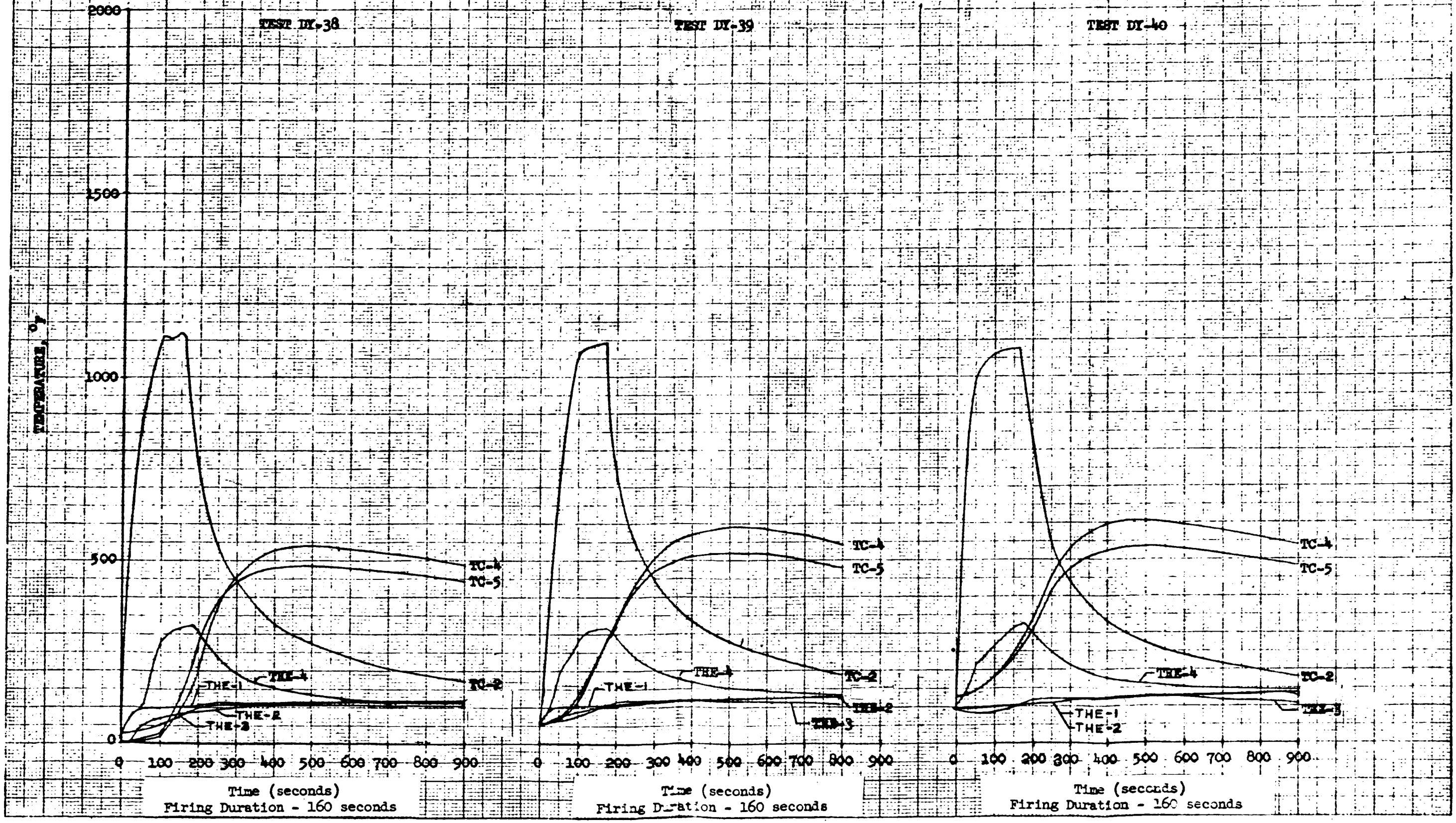

Figure 6.4.2-8. MIRA 15CA TCA Surface Temperature Profiles
Variable Thrust At Altitude

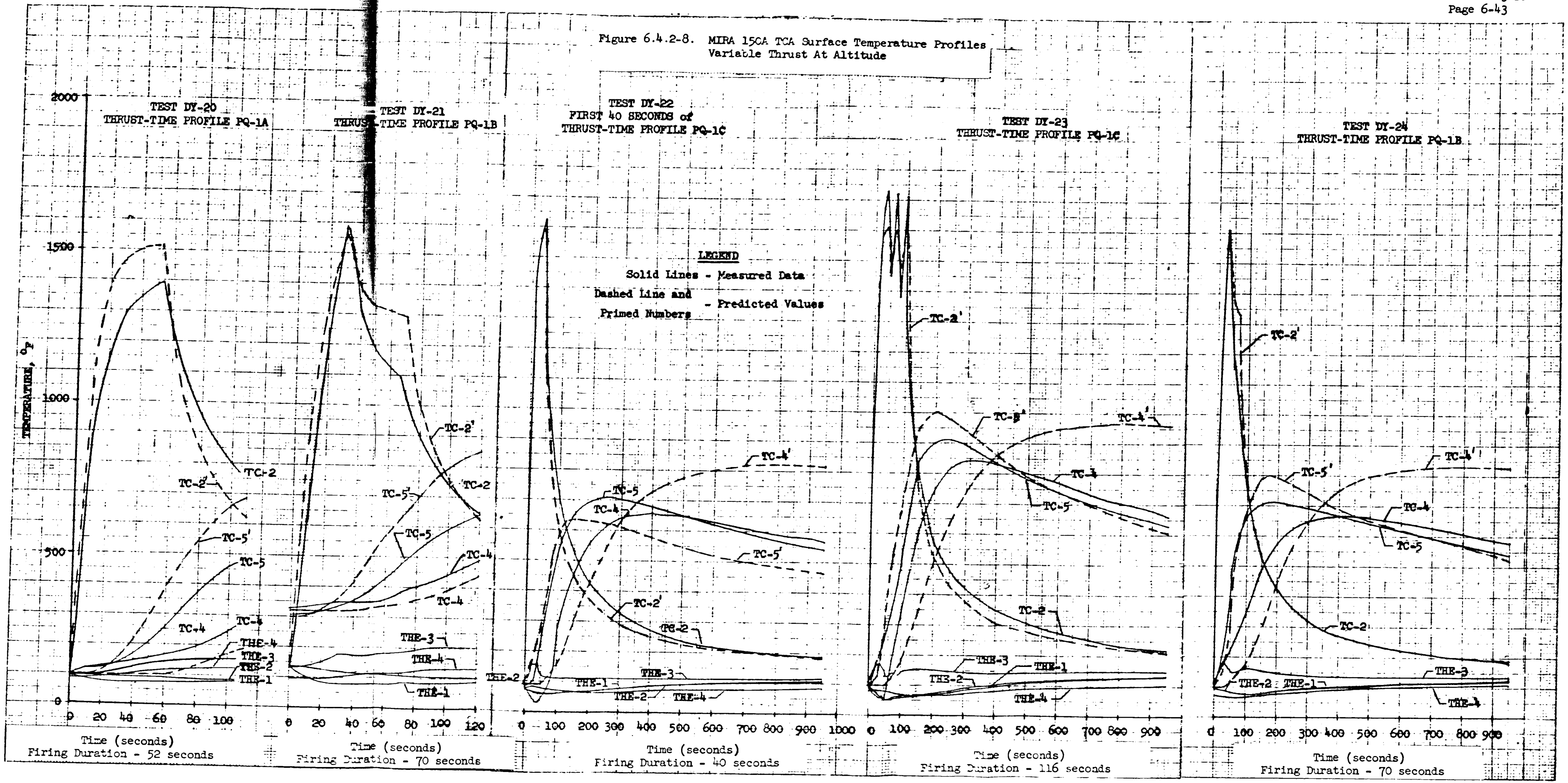

6.4.2.2 Nozzle Erosion

During Phase III, a total of 10,000 seconds of firing time was accumulated on 30 CC & NAs incorporating JTA graphite nozzle inserts. During these tests, only three CC & NAs exhibited throat erosion. The erosion in each instance occurred during the sea level maximum thrust durability tests. The three eroded sea level chambers (P/N 106546-2) had Serial Numbers 004, 009, and 014 and were tested on HEAs S/Ns 007, 006, and 010 respectively. Figures 6.4.2-9 through 6.4.2-15 are post firing photos of the CC & NAs showing the nozzle erosion and their corresponding streak test nozzles.

CC & NA S/N 004 was tested on HEA 150A-007, the first Phase III production HEA. The streak test nozzle shown in Figure 6.4.2-10 was used in the ablation throat acceptance test of this HEA (see paragraph 4.3); the HEA failed this test. Evidence of a bi-stable combustion condition existing with HEA 007 was apparent on Runs C2-619, a water-cooled chamber firing, and C2-620, a streak test firing (see paragraph 6.2.2 for further details). A maximum thrust durability test was performance on a CC & NA S/N 004 to experimentally determine the corresponding erosion on a JTA graphite nozzle that is characteristic of an HEA that had failed the streak test.

CC & NA S/N 009 was tested on HEA 150A-006. The injector body of HEA 006 had been reworked by welding a sleeve in the oxidizer shutoff valve body to correct an unacceptable machined dimension. The weld was faulty allowing a helium gas leak past the sleeve into the oxidizer manifold. The flow of helium caused abnormal oxidizer injector pressures and a more erosive environment.

CC & NA S/N 014 was test fired on HEA 150A-010. During preliminary checkout and streak test firings, it was noted that HEA 010 operated in a bi-stable mode (see paragraph 6.2.2). As with HEA 007, a maximum thrust durability test on a CC & NA was performed to determine the effect of the bi-stable mode of operation on chamber durability.

Figures 6.4.2-16, -17, and -18 show the chamber pressure versus time curves for the final firings of CC & NA S/Ns 004 (Run C2-628C), 009 (Run C2-515C), and 014 (Run C2-694C). Erosion of the JTA graphite nozzles occurred during the final 235-second duration firing in all three cases.

On CC & NA S/N 004, the throat area increase following the final firing was 9.6% with a throat area centroid shift of 0.035 inch. If the throat erosion pattern is assumed to have occurred on an altitude type chamber and the exit diameter remained concentric with the centerline of the TCA, a nozzle area centroid shift of 0.035 inch would correspond to a thrust vector deviation of 0.316 degree. A thrust vector deviation of 0.316 degree is within the allowable deviation of 0.35 degree as specified by JPL Specification SAM-50255-DSN-C.

The throat area increase on CC & NA S/N 009 following the final firing on HEA 006 was 0.96% with a throat area centroid shift of 0.010 inch. This corresponds to a thrust vector deviation of 0.091 degree assuming the erosion occurred on an altitude type CC & NA. This was again within the allowable thrust vector deviation.

The steps in chamber pressure data on CC & NA S/N 014, shown in Figure 6.4.2-18, represents an attempt to trigger on HEA S/N 010 the mode of operation that produces the erosive environment. After 190 seconds of firing, the CC & NA burned through the case upstream of the JTA graphite insert. The burn-through was coincident with a streak area or point of propellant impingement on the ablative wall. At the time the final firing was stopped, the nozzle throat area had increased 8.54%. The throat

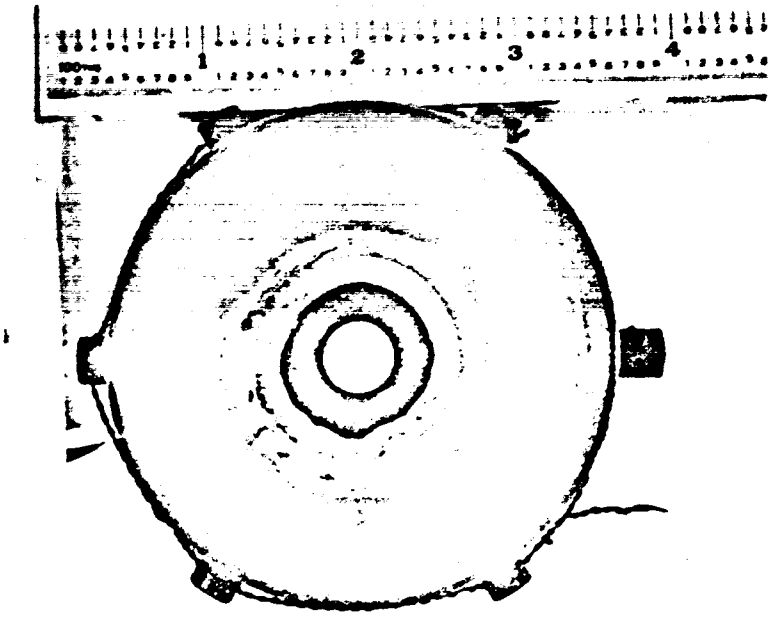

Figure 6.4.2-9. CC & NA S/N 004 Maximum Thrust Durability Test C2-682 on HEA 150A-007

Figure 6.4.2-10. Pretest Streak Nozzle Number 7A-1-C2-620 on HEA 150A-007

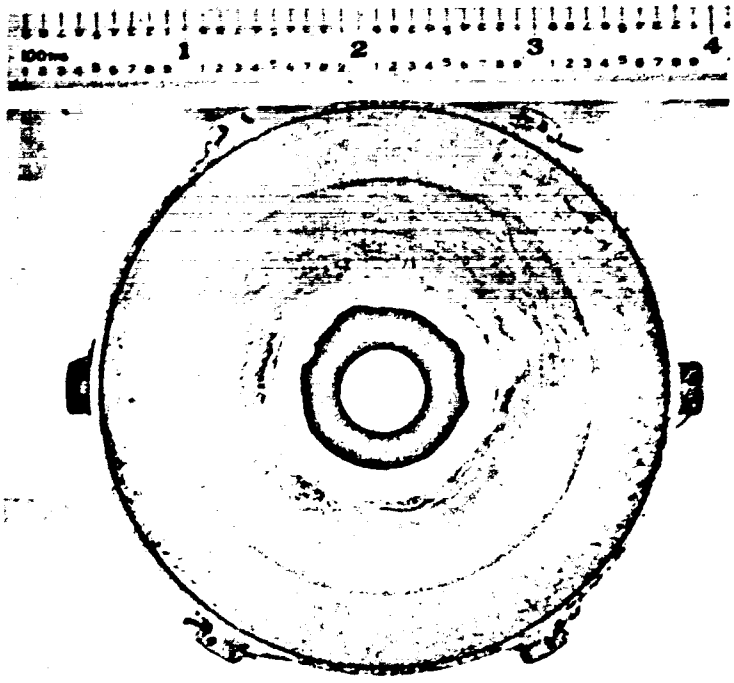

Figure 6.4.2-11. CC & NA S/N 009 Maximum Thrust Durability Test C2-515 on HEA 150A-006

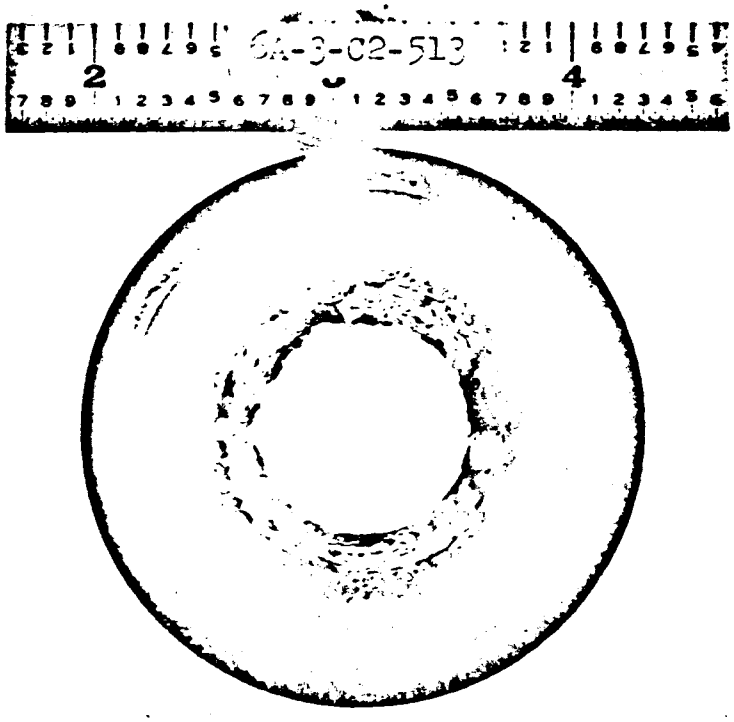

Figure 6.4.2-12. Pretest Streak Nozzle Number 6A-3-C2-513 on HEA 150A-006

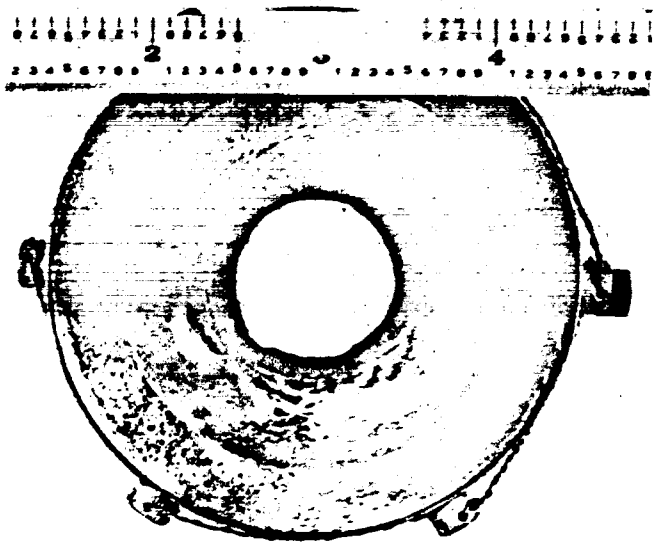

Figure 6.4.2-13. CC & NA S/N 014 Maximum Durability Test C2-694 on HEA Number 150A-010

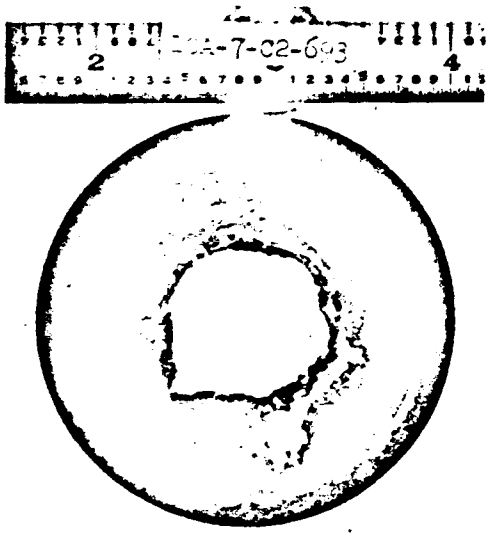

Figure 6.4.2-14. Pretest Streak Nozzle Number 10A-7-C2-693 on HEA Number 150A-010

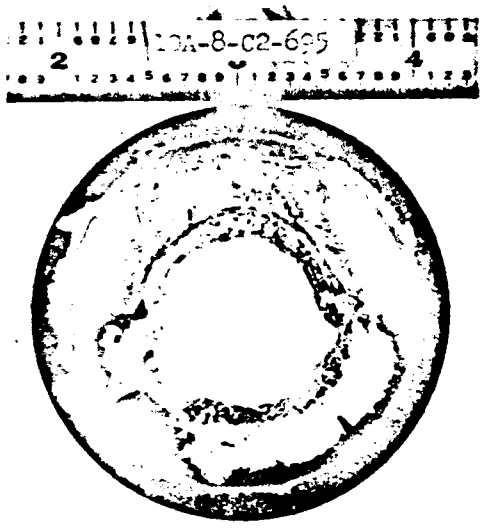

Figure 6.4.2-15. Post-Test Streak Nozzle Number 10A-8-C2-695 on HEA Number 150A-010

Figures 6.4.2-16 Through -18. Chamber Pressure as a Function of Firing Time Final Firings of Maximum Thrust Durability Tests

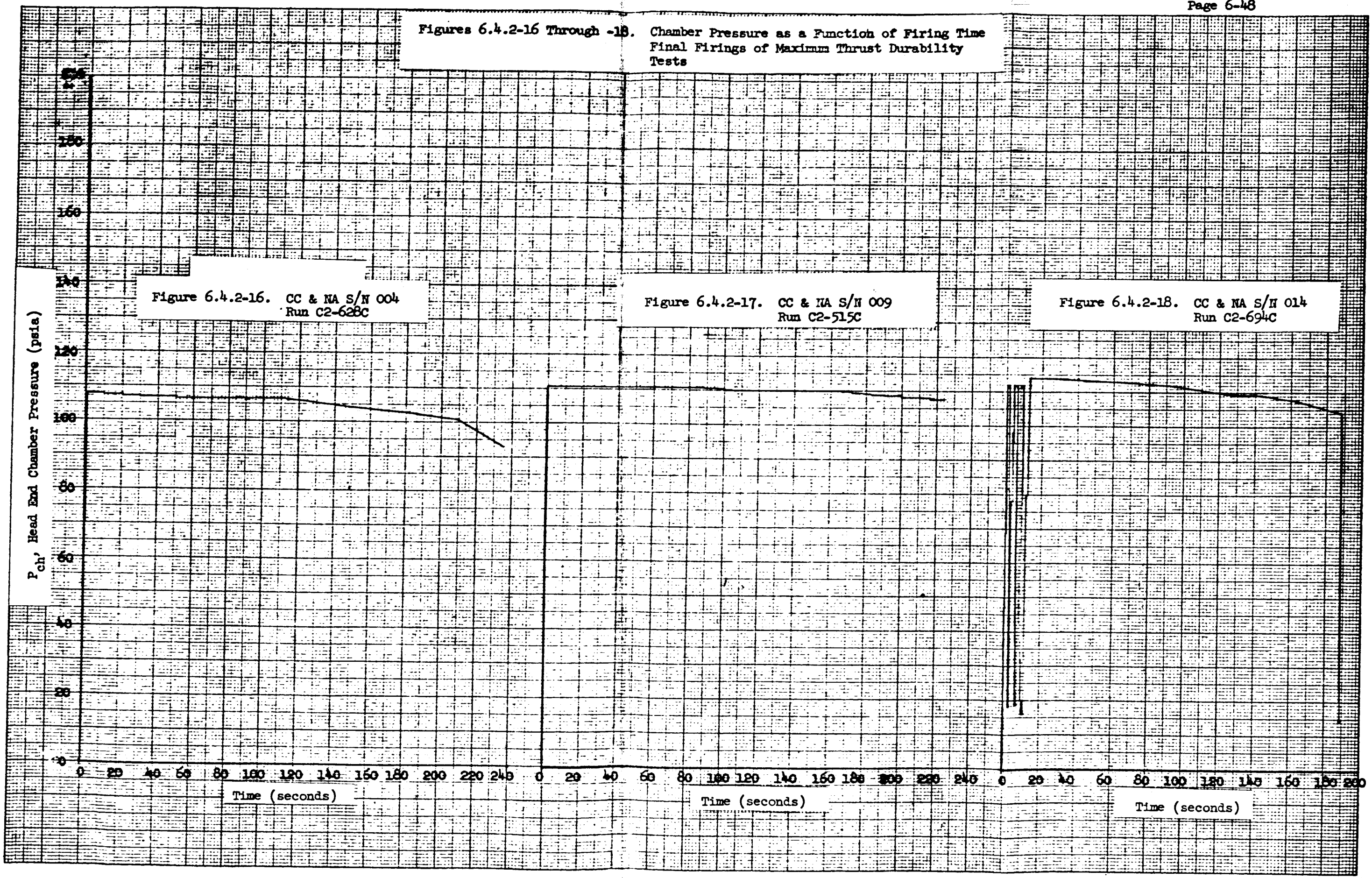

Figure 6.4.2-16. CC & NA S/N 004 Run C2-628C

Figure 6.4.2-17. CC & NA S/N 009 Run C2-515C

Figure 6.4.2-18. CC & NA S/N 014 Run C2-694C

area centroid shift was 0.020 inch which corresponds to a thrust vector deviation on an operational CC & NA of 0.181 degree; again an acceptable deviation.

Tests on the Thrust Vector Deviation Stand, designed and built to measure the angle of thrust deviation from the centerline of the TCA, were not accomplished. Therefore, the assumptions used in the geometric analysis of thrust vector deviation on CC & NA S/Ns 004, 009, and 014 were not proved experimentally. A discussion of this stand is included in section 8.0 (Special Test Equipment) and also in Appendix G.

The three tests cited above did show that HEAs that fail the acceptance streak test described in paragraph 4.3 do indeed cause more than normal erosion of an operational CC & NA throat. However, the resultant erosion is not of such a magnitude that unacceptable thrust vector deviation is expected to result.

It is noted that had the TCAs been operated at the nominal mission cycle of 162 seconds at an average thrust near 85 lbs (per JPL Specification SAM-50255-DSN-C) rather than the overstress conditions used in the above tests, the erosion would probably have been barely detectable.

6.4.2.3 Char Depth

Determination of CC & NA liner char depth was not a primary objective of Phase III testing. Test data suitable for char depth determinations was derived from tests performed for other purposes, such as durability and overall TCA performance tests under extreme operating conditions.

An isometric cutaway view of a typical CC & NA liner assembly is shown in Figure 6.4.2-19. This figure defines the axial location of the char depth measurements. These measurements were taken at the zero degree section which coincides with the plane that passes mid-way between the oxidizer and fuel flow control valves.

Figure 6.4.2-20 shows the effect of firing duration on char depth. The char depth data was obtained from three CC & NAs tested at simulated altitude curing: (1) 45-second PQT-001 (Run CY-25), (2) 180-second PQT-005 (Runs DY-47 and -48), and (3) 315-second total duration Test Series PQT-002, -003, -004A, and -004B (Runs DY-26, -27, -28, and -33). Cutaway views of the CC & NAs used to obtain the char depth for Figure 6.4.2-20 are shown in Figures 6.4.2-21, -22, and -23. The CC & NAs tested during PQT-001 and PQT-005 were the only ones fired for durations less than 300 seconds. All of the CC & NAs tested at sea level were completely charred in the zones of interest. Further, since the sea level tests were conducted under a less severe heat transfer environment than the operational one, sea level char depth data was excluded.

Table 6.4.2-24 summarizes the measured char depth data at four average thrust levels. The data were obtained from the following tests performed in the JPL/ETS altitude cell: (1) 480-second, minimum thrust PQT-008 (Runs DY-38, -39, and -40), (2) 315-second, variable thrust Test Series PQT-002, -003, -004A, and -004B (Runs DY-26, -27, -28, and -33), (3) 300-second, maximum thrust PQT-007 (Runs DY-35, -36, and -37) and (4) 348-second, initial dynamic throttling test (Runs DY-20 through DY-24). Cutaway views of the CC & NAs used to obtain the char depth for Table 6.4.2-24 are shown in Figures 6.4.2-23, -25, -26, and -27.

A line of white dots has been added to the cutaway CC & NA views to clarify the char to uncharred material interface.

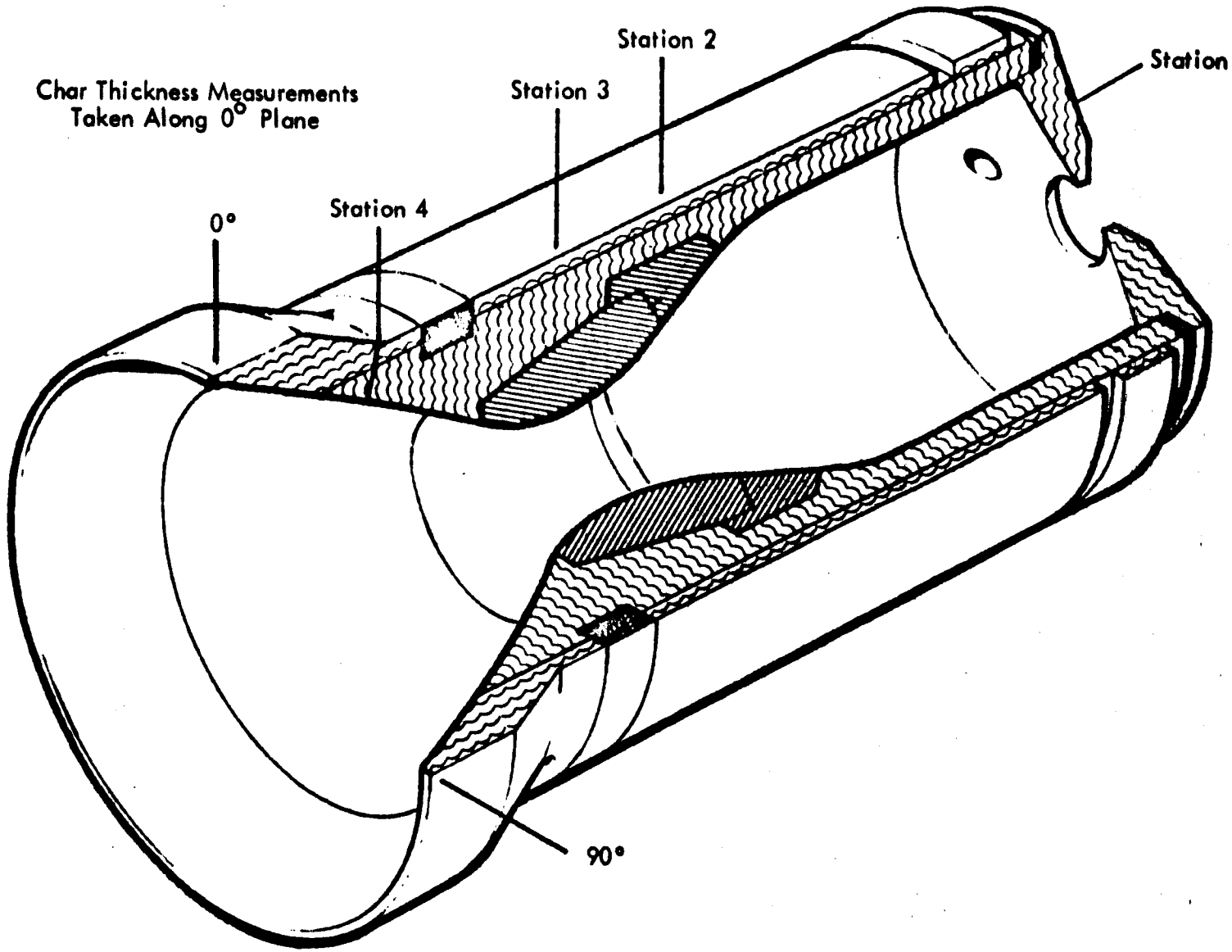

Figure 6.4.2-19. Quarter-Section of Surveyor CC & NA Liner Assembly

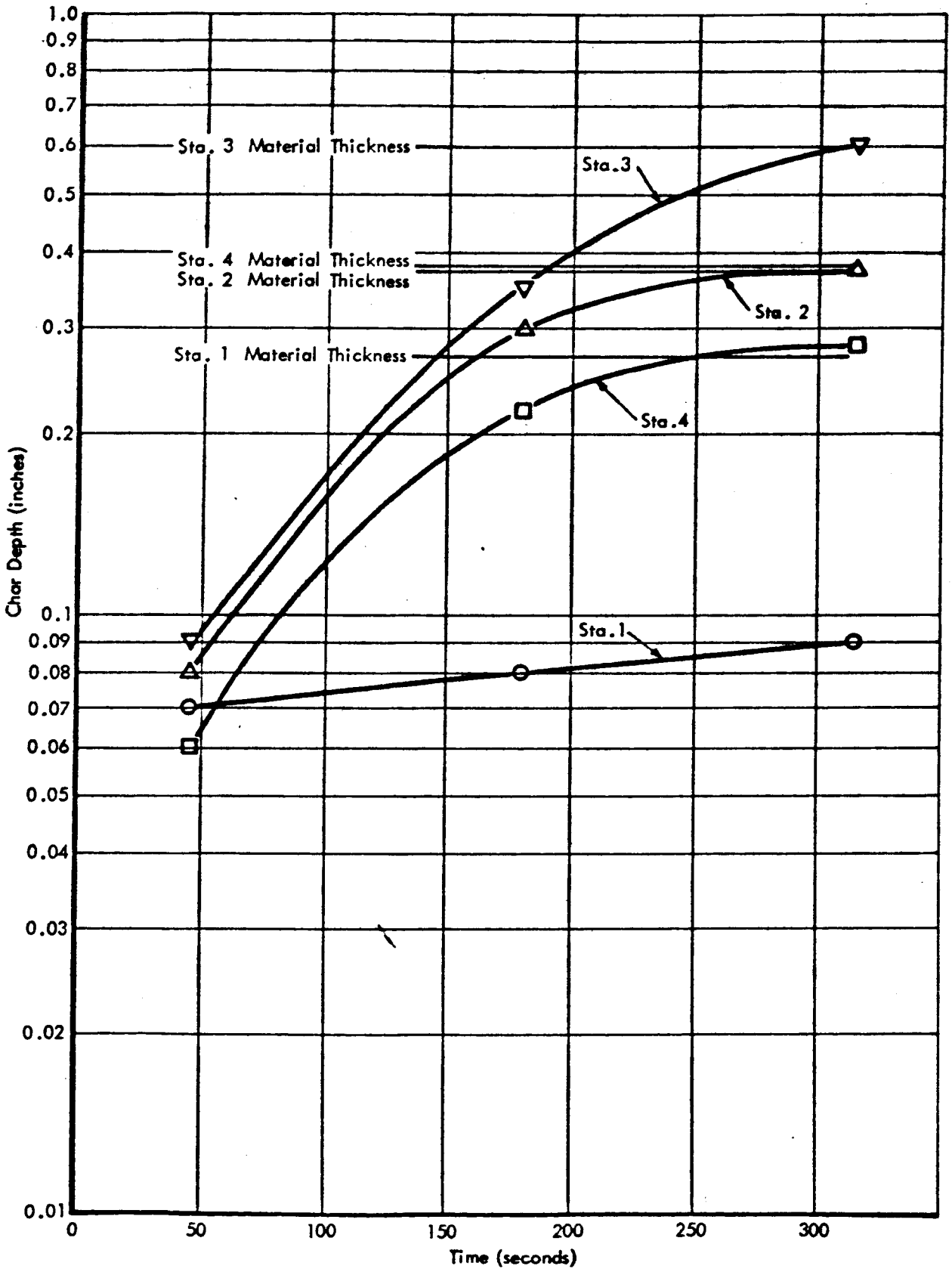

Figure 6.4.2-20. Char Depth as a Function of Firing Duration Variable Thrust at Altitude Conditions (Stations per Figure 6.4.2-19)

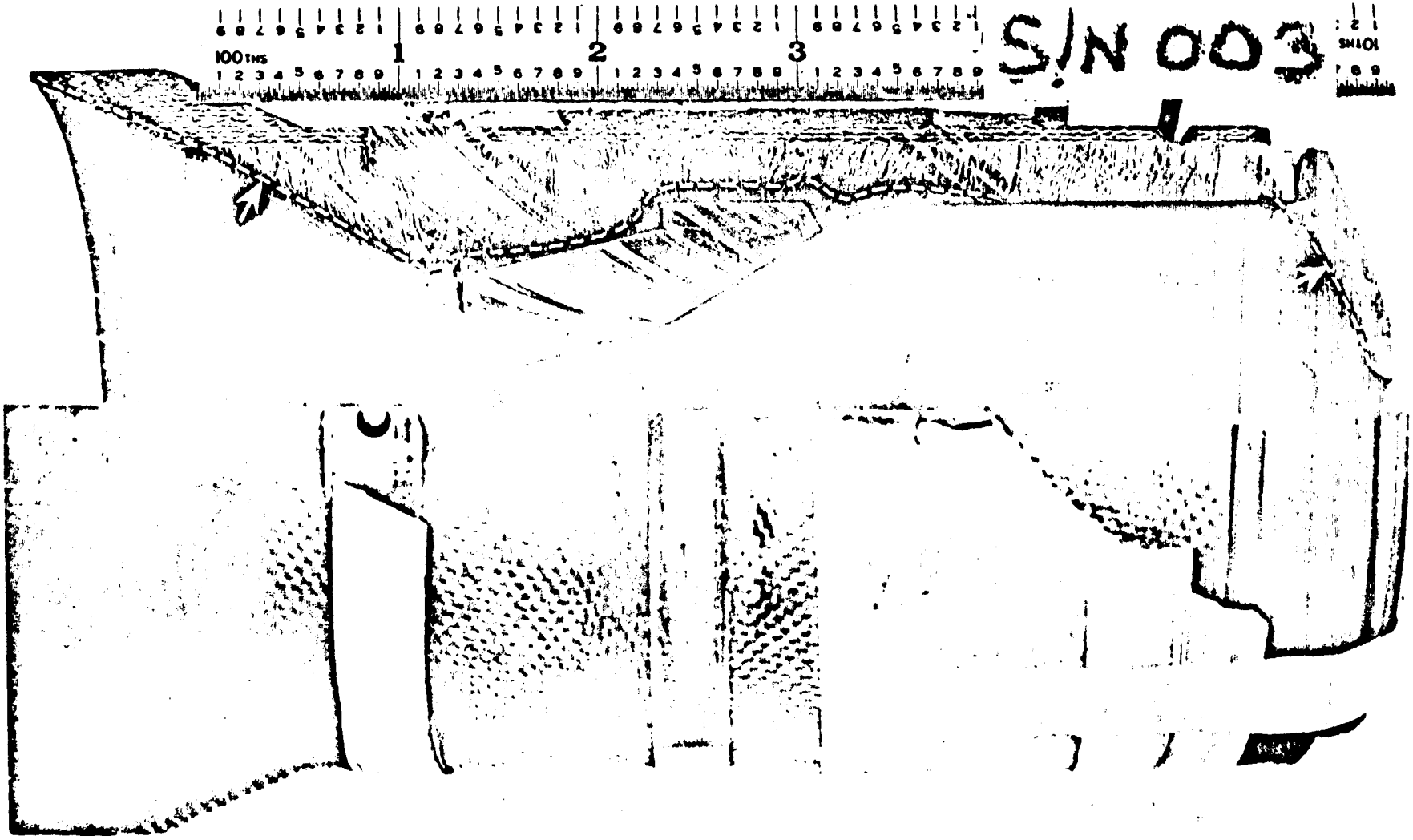

Figure 6.4.2-21. Cross-Section of CC & NA S/N 003 Fired on PQT-001 for 45-second Duration

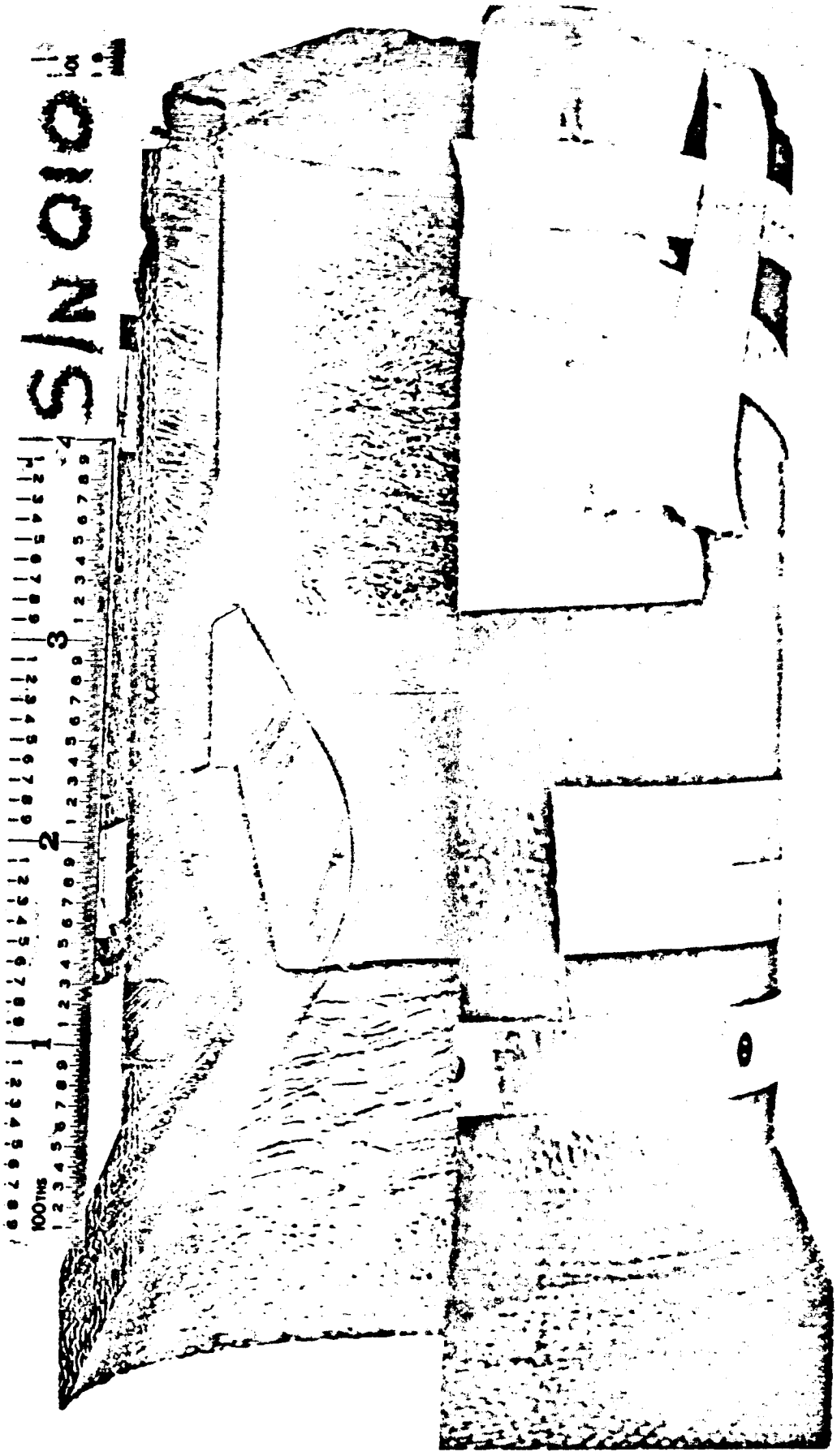

Figure 6.4.2-22. Cross-Section of CC & MA S/N 010 Fired on PQM-005 for 180-second Duration

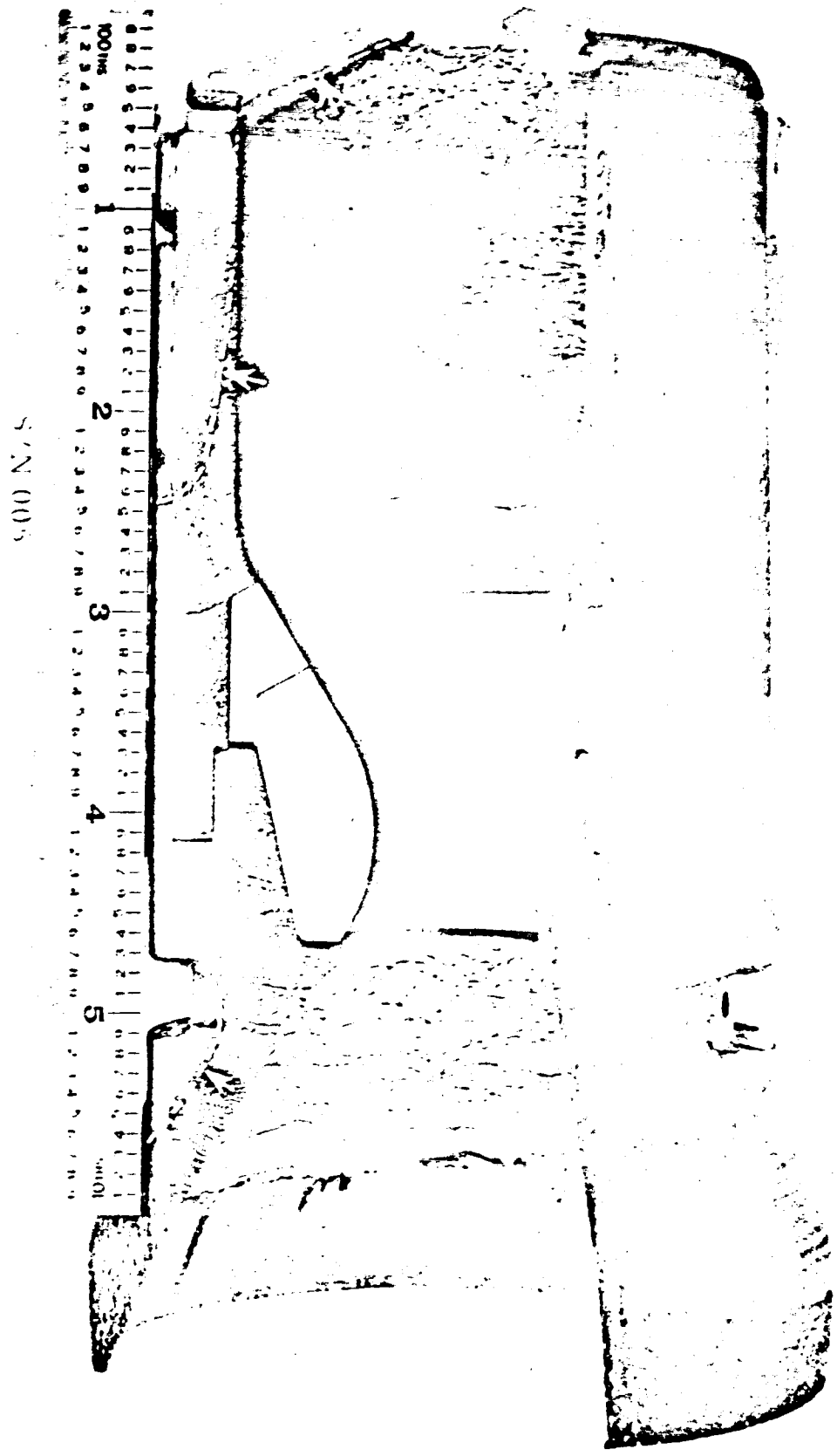

Figure 6.4.2-23. Cross-Section of CC & NA S/N 005 Fired on PQT-002, -003, -004A and -004B for 315-second Duration

Table 6.4.2-24

Char Depth to Thrust Level Relationship

Station No. (per Figure 6.4.2-19)	Maximum Ablative Material Thickness (inches)	Average Thrust (lbs)	Total Firing Duration (sec)	Measured Char Depth (inches)
1	.270	32	480	.150
		81	348	.090
		96	315	.090
		152	300	.060
2	.375	32	480	.080
		81	348	.375
		96	315	.375
		152	300	.375
3	.600	32	480	.120
		81	348	.600
		96	315	.600
		152	300	.600
4	.380	32	480	.050
		81	348	.230
		96	315	.280
		152	300	.380

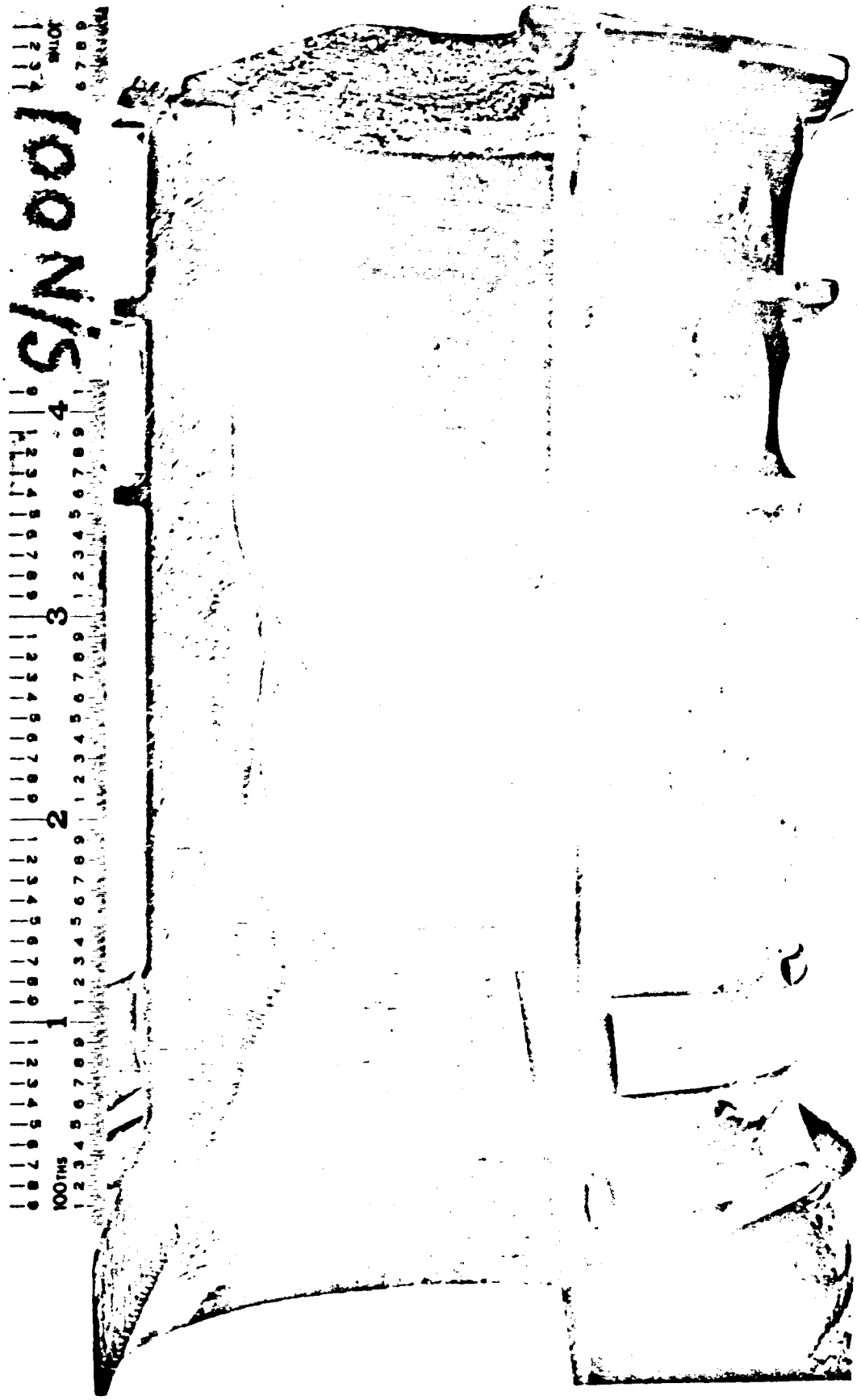

Figure 6.4.2-25. Cross-Section of CC & NA S/N 001
Fired on PQT-008 for 480-second
Duration at Minimum Thrust

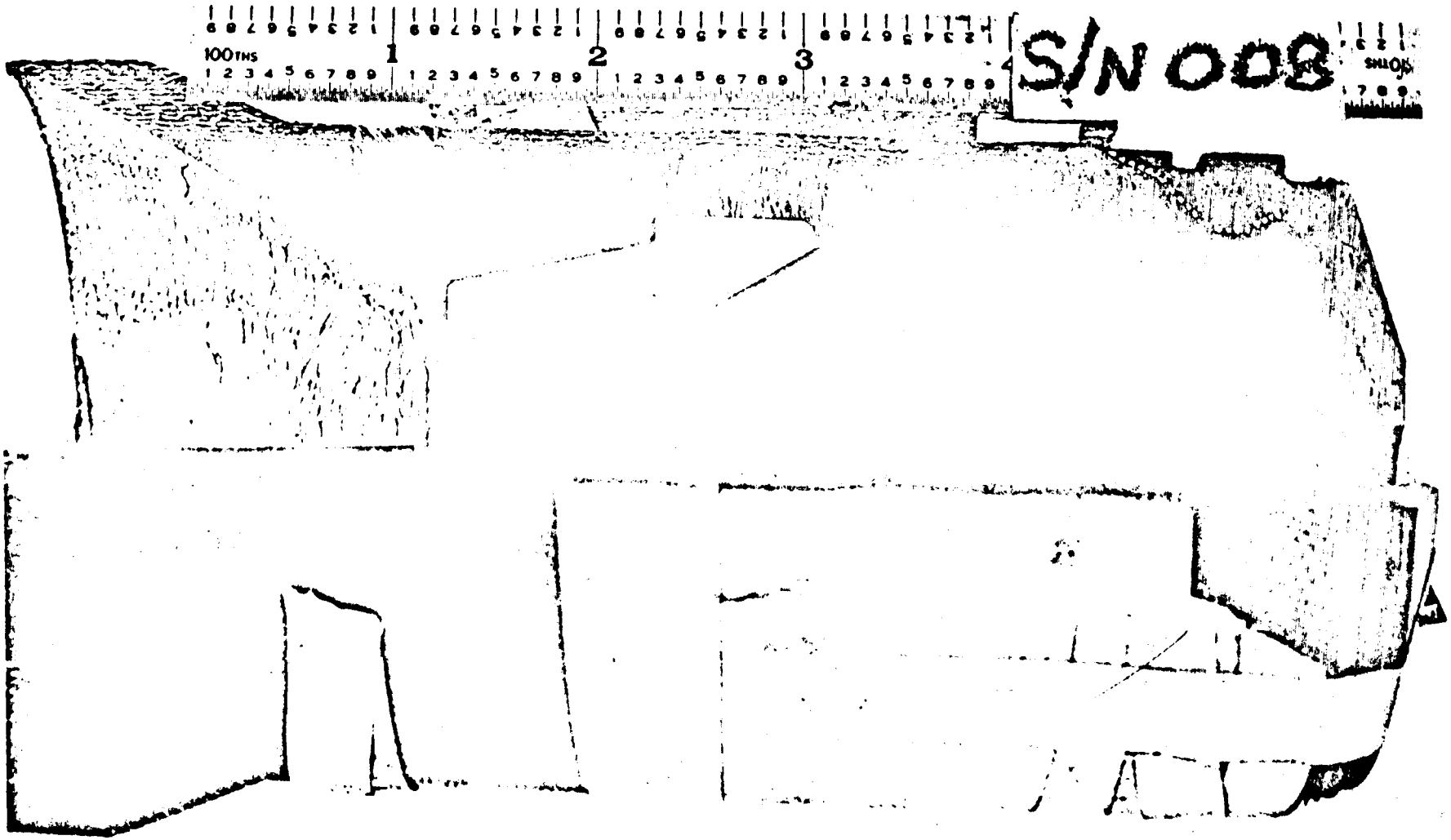

Figure 6.4.2-26. Cross-Section of CC & NA S/N 008 Fired on PQT-007 for 300-second Duration at Maximum Thrust

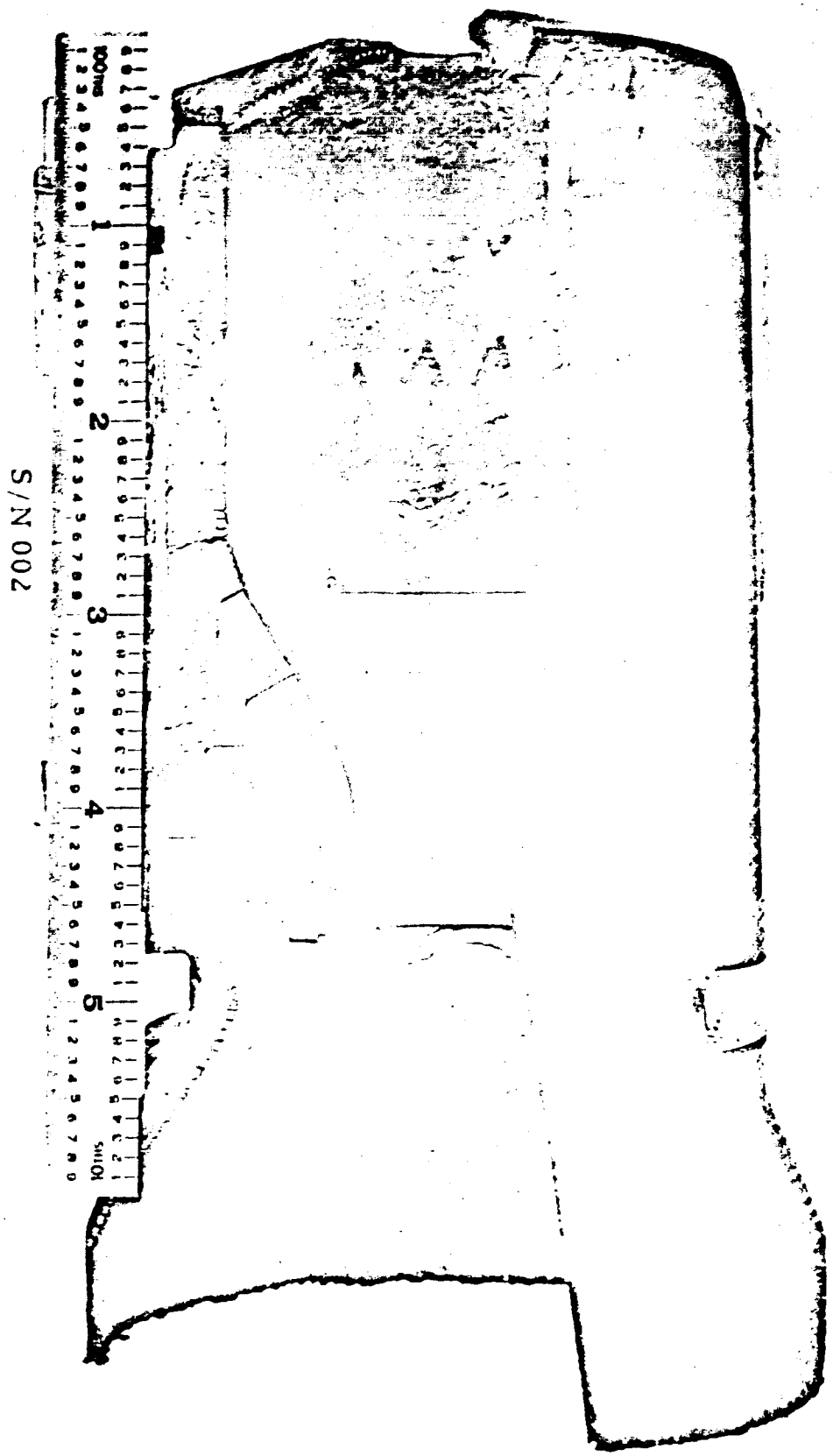

Figure 6.4.2-27. Cross-Section of CC & NA S/N 002 Fired for 348-second Duration at Variable Thrust

The head end liner (Station 1) chars more at minimum thrust than at other levels. This is caused by a shifting of the combustion zone towards the head end liner when the TCA is at minimum chamber pressure.

The 81 and 96-pound average thrust levels were calculated by integrating the thrust-time plots and dividing by the total firing time. The 32 and 152-pound average thrust levels were obtained by fixed thrust level firings at minimum and maximum levels.

6.4.2.4 CC & NA Ablative Liner Weight Loss

Data acquired from two CC & NAs tested with variable thrust-time profiles under altitude conditions at JPL/ETS (180-second PQT-005 Runs DY-47 and 48 and 315-second Test Series PQT-002, -003, -004A, and -004B Runs DY-26, -27, -28, and -33) showed a direct linear relationship between firing times and weight loss increases. The CC & NAs lost 45 grams during PQT-005 and 78 grams during the 35-second test series. Figure 6.4.2-28 shows the effect of thrust level on chamber liner weight loss under both sea level and altitude conditions. The data on altitude conditions shown in Figure 6.4.2-28 were obtained from the same four CC & NAs cited as used for Table 6.4.2-24. The sea level data in Figure 6.4.2-28 were obtained from Runs C2-525, C2-515, and C2-623. The dashed lines shown represent estimated weight loss values as a function of average thrust level for a 300-second duration firing, and are based on a linear relationship between firing time and weight loss. It is assumed that the weight loss is all from the polymeric material in the chamber liner. The weight of the CC & NA prior to test is nominally 2.60 pounds. Data from Figure 6.4.2-28 indicates that the MIRA 150A CC & NA weight loss will not exceed approximately 7.8% of its prefire weight for thrust levels and firing durations typical of those used in Phase III testing.

6.4.2.5 CC & NA Gas Leakage

Even though test data show that the present CC & NA design is adequate in all respects for Surveyor application, most CC & NAs did not exhibit zero gas leakage on pressure checking.

When the cause of the leakage was traced to a damaged O-ring between the ablative liner and titanium shell, the leak was repairable. On other occasions, replacement of the O-ring seal did not stop the gas leakage. When leakage occurred on firing, it could be detected at the following places: between the ablative liner and titanium case, at the radiation skirt to ablative exit cone interface, around the ablative liner retaining pins, and between the ablative liner and JTA nozzle insert.

When the leakage became a regularly detected characteristic during the CC & NA leak check procedure, several units were disassembled and the ablative liner assemblies leak checked separately. These ablative liners themselves were found to be leaking nitrogen gas at pressures as low as 30 psig. An attempt was made to pressure impregnate the ablative liner assembly with a high temperature resin. Upon leak checking the liners following resin impregnation, the leaks through the ablative liner were reduced but still present. These CC & NAs were re-assembled and subsequently tested without failure.

Delaminations between the ablative inner liners and silica overwrap were present to some degree on the majority of CC & NAs tested. They were never proven to be the cause of gas leakage through the ablative chamber wall.

Following a firing, the leakage rate generally became worse. Experience showed that a CC & NA that exhibited detectable leakage did not have a shortened service life and did not effect the performance of the TCA.

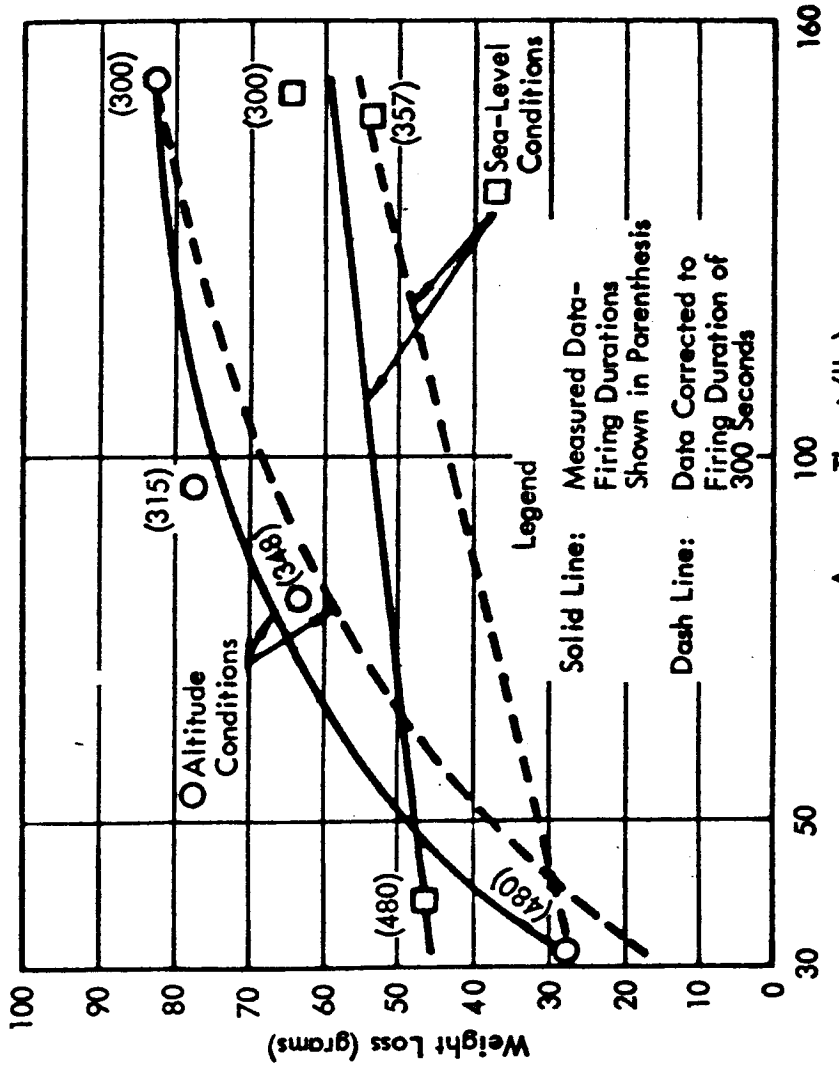

Figure 6.4.2-28. Ablative Liner Weight Loss as a Function of Thrust Level

Gross leakage led to CC & NA replacement during prequalification testing on CC & NA S/N 003. The chamber had been fired for 12 second during acceptance testing and 45 seconds during PQT-001. Leak checking of S/N 003 at JPL/ETS following PQT-001 disclosed a severe gas leak between the ablative liner and titanium shell. The CC & NA was disassembled and the ablative liner alone was leak checked. The main leakage occurred through a crack in the ablative liner. The crack was believed to have been caused by the 135-psig leak check procedure performed on the partially charred chamber at JPL/ETS.

Altitude CC & NA S/N 008 and sea level CC & NA S/N 003 successfully completed maximum thrust durability firings, but the titanium shells were slightly bulged. CC & NA S/N 007 successfully withstood a maximum thrust durability test at sea level, but showed extensive gas leakage from the ablative liner retaining pins.

Thus, it was shown that gas leaks in the CC & NA do not lead to burn-throughs or degraded performance. On the other hand, a "zero leakage" CC & NA would enhance confidence in the CC & NA design. The possible solutions to the leakage problems are listed below. These solutions were considered but neven implemented.

1. Overwrap the ablative liner assembly before the internal machining is started, thereby reducing damage to the inner ablative liners during the overwrap process.

2. Increase the overwrap thickness and allow no overwrap delaminations.

3. Move the head end O-ring seal down near the titanium split ring, and allow the combustion gases to pressurize the annulus between the shell and ablative liner assembly. (This change would require the use of a type of seal other than a rubber O-ring, since the temperatures in the split ring area reach 1500°F during the required demonstration testing.)

6.4.3 Cycle Life

Tests whose principal objective involved cycle life determination of HEA components were conducted on the helium pilot valve and propellant shutoff valve. In addition, "trouble-free" HEA firings serve as an indicator of cycle life of the entire HEA ("trouble-free" meaning total run time without a hardware change or malfunction).

The cycle life potential of the propellant shutoff valve, as tested on the component level, is indicated in paragraph 5.3 wherein the results of a successful 2000 cycle life test are discussed. The JPL Specification SAM-50255-DSN-C SOV cycle life requirement of 250 cycles after TCA delivery is, therefore, well within the capability of the present propellant shutoff valve design.

The helium pilot valve cycle life after TCA delivery is specified in JPL Specification SAM-50255-DSN-C as 250 cycles. A simple test was conducted on one pilot valve to check for poppet/seat durability. Valve S/N 023 was processed through the pilot valve acceptance testing, installed in MIRA 150A-007 and processed through the TS3-013 acceptance tests. Therefore, the valve underwent all predelivery actuations. The valve was then cycled 125 times with a 700 psig inlet pressure and 125 times with a 740 psig inlet pressure (250 cycles total). The inlet and vent poppet/seat

leakage was then checked with a helium leak detector and the values compared to those obtained in pilot valve acceptance tests. These data are shown below.

	Inlet Poppet/Seat Leakage (scc/hr)	Vent Poppet/Seat Leakage (scc/hr)
Valve Acceptance Test Values	0.002	0.002
After Pre-Delivery Actuations plus additional 250 cycles	0.05	0.10
Maximum Allowable	10.0	10.0

In addition to the above cycle life test, a qualitative evaluation of poppet/seat life was conducted by the valve manufacturer wherein a pair of valves were cycled approximately 1500 times each. The pair of valves were then disassembled; examination of the poppets and seats revealed that they were still in good condition and capable of many more actuations.

Cycle life testing at the component level was not conducted on any TCA components other than the two discussed above. Other TCA components or subassemblies and the HEA per se were not given any specific cycle life testing. However, in the development and prequalification testing complete HEAs underwent various test firings of considerable total duration during which no hardware changes occurred or were required. This testing testifies to the general service cycle life capability of the HEA. For example, HEA S/N 005 underwent a series of tests with no parts replacements nor malfunctions extending over 2934 seconds in 38 starts with test durations ranging from 26 to 415 seconds, thrust levels from minimum to maximum, and with 65% of the total time under conditions of step or dynamic throttling. Similarly, HEA S/N 010 underwent 1845 seconds of testing, in 23 starts with test durations ranging from 70 to 275 seconds. These HEAs were in every way complete, e.g., including servoactuators.

Based on test data of the above type, various HEAs demonstrated a capability of three repetitions of the "operating sequence" including a "nominal mission thrust-time profile," as given in paragraph 3.6.2 and 3.6.3 of JPL Specification SAM-50255-DSN-C.

271

6.5 Extreme Propellant Temperature and Inlet Pressure Tests

The MIRA 150A TCA is designed to operate over a propellant temperature range of 0°F to 100°F and the following inlet pressure range:

Nominal Thrust, lbs	30	90	150
Oxidizer Pressure, psia	719 ± 20	715 ± 20	707 ± 20
Fuel Pressure, psia	720 ± 20	717 ± 20	712 ± 20

The Surveyor propellant tanks are pressurized to 720 ± 20 psia by a common regulator. Thus at any one time, there will be no significant pressure differential between inlet fuel and oxidizer. The propellant temperatures can vary independently and the TCA must operate at any combination of fuel and oxidizer temperatures between 0° and 100°F. Therefore, a series of tests were run to evaluate the effect of propellant temperature and inlet pressure on mixture ratio, propellant flow rates and resultant performance.

The test series specified in paragraph 3.6.2.3 of the Development Test Plan was designed to cover the possible matrix of propellant and TCA inlet conditions. These tests were conducted at sea level conditions with HEA 150A-005 coupled to a water-cooled combustion chamber. Each test consisted of a ten-step throttle run. In addition, the test series described in paragraph 5.2 of the Development Test Plan was performed with temperature conditioned propellants and two levels of inlet pressure. For this series, flight-type, ablative-cooled combustion chambers were employed. Table 6.5-1 summarizes the conditions for these tests.

Table 6.5-1

Development Test Summary

Development Test Plan Para. Number	Test Number	Fuel Temp. (°F)	Oxid. Temp. (°F)	Propellant (psia)	CC & NA Chamber Temp. (°F)
3.1.3.1.2 -4	C2-612ABC	100	100	As Req'd*	Ambient
-5	611ABC	100	100	As Req'd*	Ambient
-6	610	100	100	As Req'd*	Ambient
3.6.2.3 -1	C2-592AB	Ambient	Ambient	740	Water cooled
-2	C2-592C	Ambient	Ambient	700	Water cooled
-3	C2-593A	100	100	720	Water cooled
-4	C2-599A	0	0	720	Water cooled
-5	C2-592D	Ambient	Ambient	720	Water cooled
-6	C2-599B	0	0	720	Water cooled
-7	C2-593B	100	100	720	Water cooled
-8	C2-597AB	100	0	720	Water cooled
-9	C2-594AB	0	100	720	Water cooled
5.2.1	C2-605ABCDE	0	0	740	0
5.2.2	C2-600ABC	100	100	740	125
	C2-603AB	100	100	740	125
5.2.3	C2-606ABCDE	0	0	700	0
5.2.4	C2-604ABCDE	100	100	700	0

*As required to achieve a 1.6 mixture ratio.

272

6.5.1 Effect of Temperature and Inlet Pressure on Mixture Ratio and Flowrates with Constant Venturi Discharge Coefficients

As described in paragraph 3.2, the MIRA 150A flow control valve employs dual, variable-area cavitating venturis to control the propellant flow, with the flowrate through a cavitating venturi defined by Equation 1.

$$\dot{M} = C_D \; A \sqrt{2g \; \rho \; (P_t - P_v)} \qquad (1)$$

Where: $\dot{M}$ = Mass Flowrate

A = Venturi Throat Area

C_D = Discharge Coefficient

ρ = Propellant Density

P_t = Inlet Pressure

P_v = Vapor Pressure

The flow control valve pintles for the MIRA 150A were designed with average discharge coefficients of 0.92. Previous testing at room temperature showed that the variation in discharge coefficient had little effect on mixture ratio and an average C_D was satisfactory. The predicted variation in mixture ratio with propellant temperature based on constant C_D is shown in Figure 6.5.1-1. The variation in flow rate and mixture ratio noted is solely based on variations in vapor pressure and propellant densities as expressed in Equations (2) and (3).

$$\dot{M}_{ST} = \dot{M}_T \sqrt{\frac{\rho_{ST} \; (P_t - P_v)_{ST}}{\rho_T \; (P_t - P_v)_T}} \qquad (2)$$

Where: ST = Standard conditions for constant C_D

T = Conditions during the test

and:

$$MR_{ST} = \left(\frac{\dot{M}_{OX}}{\dot{M}_F} \right)_{ST} \qquad (3)$$

Where: MR_{ST} = Mixture Ratio at standard conditions

The FCV pintles are parabolic in shape to provide a linear relation between flow and position. Equation (4) used for the pintle design is shown below.

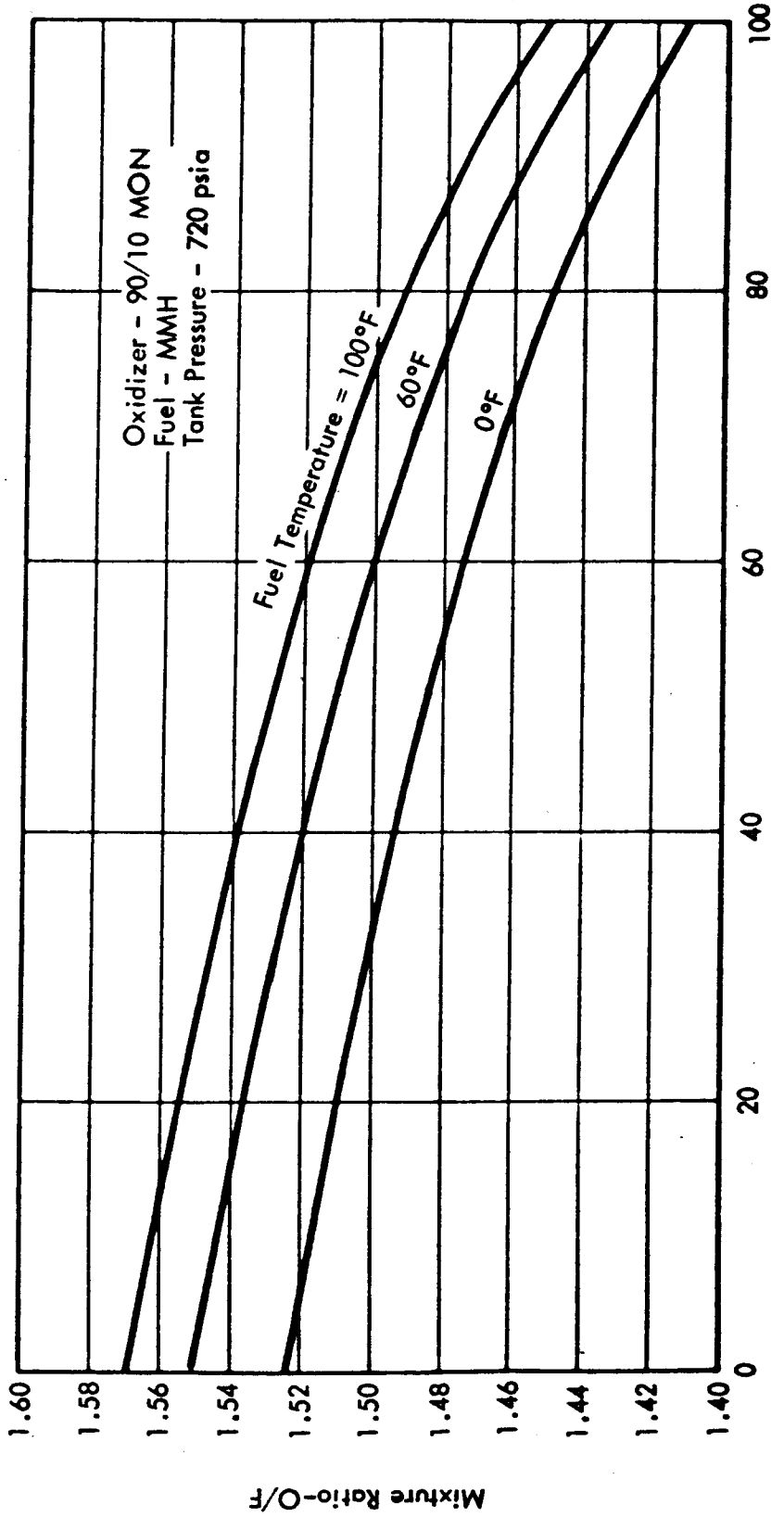

Figure 6.5.1-1. Mixture Ratio Versus Propellant Temperature for Venturi Constant C_D

$$\frac{A_{ox}}{A_F} = \frac{K_{ox}\ L_{ox}}{K_F\ L_F} \sqrt{\frac{\rho_F\ (P_t - P_v)_F}{\rho_{ox}\ (P_t - P_v)_{ox}}} \qquad (4)$$

Where: $\frac{K_{ox}\ L_{ox}}{K_F\ L_F}$ = Design mixture ratio of 1.50.

L = Position of venturi pintle in inches.

K = Rate of change of standard flow rate with position in lb/sec/in.

The actual mixture ratio obtained at standard conditions for pintles designed in Equation (4) is obtained from Equation (5).

$$MR = \frac{\dot{M}_{ox}}{\dot{M}_F} = \frac{C_{D_{ox}}\ K_{ox}\ L_{ox}}{C_{D_F}\ K_F\ L_F} \qquad (5)$$

In Equation (5) it may be assumed that $L_{ox} = L_F$; i.e., the pintle position relative to the throat of both the oxidizer and fuel pintle are identical, thus, the projected zero intercepts are identical.

In paragraph 7.5, it is shown that the discharge coefficients are neither equal nor constant but vary with temperature and flow rate (or pintle position).

Figure 6.5.1-2(a) presents the mixture ratio at standard conditions predicted by the use of Equation (5) with L_{ox} equal to L_F and discharge coefficients that vary with flow rate. (Details on this aspect are found in paragraph 7.5, and the C_D to servo-actuator signal relationships used in deriving Figure 6.5.1-2(a) are those given in Figure 7.5-3.) This mixture ratio deviates appreciably from the design goal of 1.50 $\pm$ 0.10. Note that temperature extremes were <u>not</u> considered.

It is possible to adjust the pintles so as to reduce relatively the oxidizer area (or increase the fuel area) by a constant amount over the entire throttle range. The effect of such an offset is shown in Equation (6).

$$MR = \frac{\dot{M}_{ox}}{\dot{M}_F} = \frac{C_{D_{ox}}\ K_{ox}\ L_{ox}}{C_{D_F}\ K_F\ L_F} = \frac{C_{D_{ox}}\ K_{ox}\ (L_F - \delta)}{C_{D_F}\ K_F\ L_F} \qquad (6)$$

Where: δ = relative adjustment of oxidizer pintle

The effect on mixture ratio of adjusting one pintle is much more pronounced at low thrust than at high thrust. Thus, the relative adjustment of one pintle can compensate for the increase of mixture ratio with decreasing flow rate shown in Figure 6.5.1-2(a). In Figure 6.5.1-2(b), the effect of adjusting the oxidizer pintle to provide a mixture ratio of 1.510 at low flow is shown. It is seen that it is possible to produce a relatively flat mixture ratio over the entire throttle range. As the flow control valve pintle positions are set during actual flow tests, the mixture ratio is maintained relatively constant over the entire throttle range. This is further shown by test data presented in Figure 6.5.2-2 for HEA 150A-005.

215

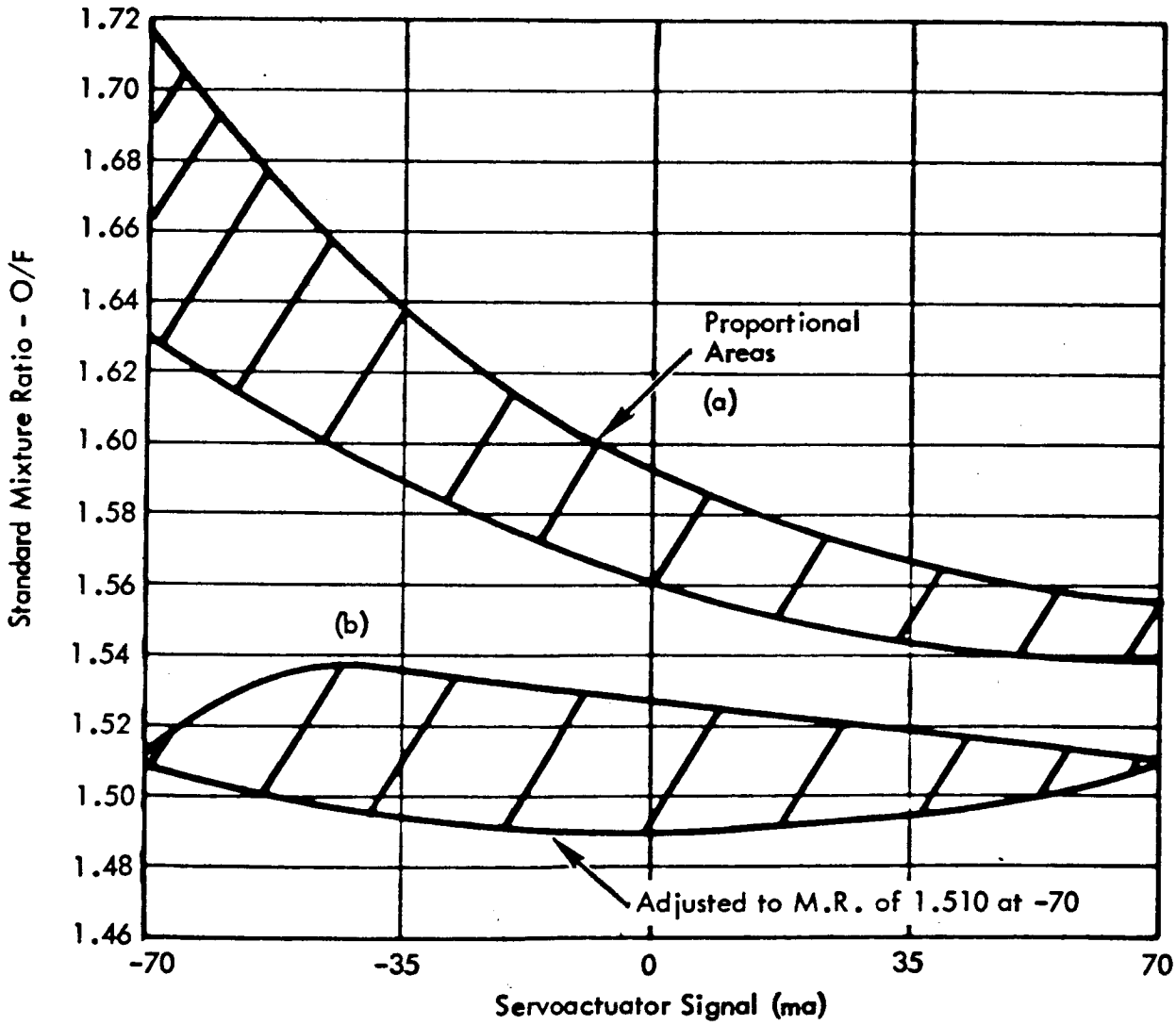

Figure 6.5.1-2. Viscous Effect on Ambient Temperature Mixture Ratio

6.5.2 Test Results and Discussion

The results of the extreme temperature and inlet pressure tests are shown graphically in Figures 6.5.2-1 through -6. The detailed tabular data from which these figures are prepared appear in Table D-2- of Appendix D-2. From the results of these tests, it is apparent that the simple standard MR formula shown by Equation (3) does not adequately represent the venturi flow over a wide temperature range.

In Figures 6.5.2-7, -8, -9, and -10, the bands of the standard mixture ratios predicted by the viscous discharge coefficient theory (discussed in paragraph 7.5) are compared with the "As Measured" experimental data obtained during the different extreme temperature tests on HEA 150A-005. The data is standardized to the temperatures shown. Also for comparison, is shown the standard mixture ratio obtained on the ambient temperature tests (Run C2-592). The boundaries of the theoretical curves shown have been corrected to correspond to the measured ambient temperature mixture ratio for HEA 150A-005. As the mixture ratio varies appreciably between the fuel temperature range of $0^{\circ}F$ and $-20^{\circ}F$, both boundaries are shown in Figure 6.5.2-10.

The standard mixture ratio value varied appreciably between the low temperature test (Figure 6.5.2-9) and the high temperature test (Figure 6.5.2-7). As the basic Equation (1) for mass flow rate must be satisfied, the discharge coefficients in the venturi must be considered to be varying with temperature.

Comparing the theory with the experimental data it is seen that the upper boundary of the theoretical curves corresponding to the high range of L_{eq}/D seems to fit the experimental data best, particularly at the low temperatures. (L_{eq} and D are defined and discussed in paragraph 7.5.)

In Figures 6.5.2-11, -12, and -13, the predicted standard and actual mixture ratios are plotted as a function of the S/A signal level and propellant temperature for the high L_{eq}/D condition. The curves are constructed for a FCV with a "nominal" mixture ratio of 1.50 over the entire throttle range. Allowing a mixture ratio variation of $\pm$ 0.03 at standard conditions for the FCV, the expected boundary of actual mixture ratio as a function of S/A signal under the expected temperature and pressure extremes is shown in Figure 6.5.2-14.

6.5.3 Effect of Propellant Temperature and Tank Pressure on Thrust

Extremes in propellant supply pressure and propellant temperature result in a thrust change. Supply pressure affects flow rate directly and therefore causes a change in thrust. Propellant temperature variations indirectly affect flow rate and thrust by temperature-induced changes in density, vapor pressure, and discharge coefficient.

The quantitative effect on thrust of extremes in propellant supply pressure and temperature are given in Table 6.5.3-1. These values were computed using the following assumptions:

1. Thrust is proportional to propellant flow rate (specific impulse is constant).

2. Propellant supply pressure and temperature are independant variables.

3. Nominal thrust at any commanded level occurs at a propellant supply pressure and temperature of 720 psig and $70^{\circ}F$, respectively.

277

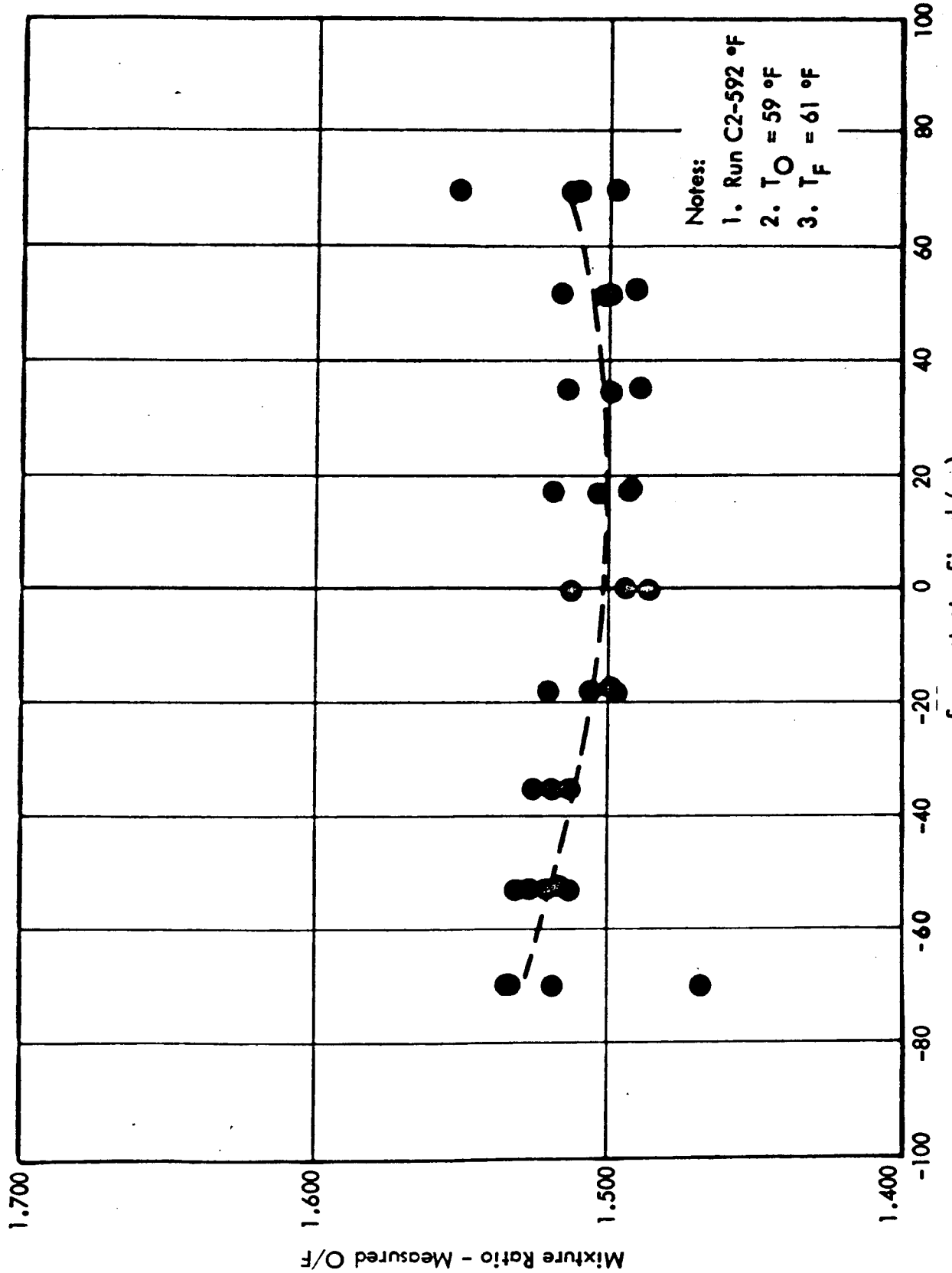

Figure 6.5.2-1. Measured Mixture Ratio Versus Servoactuator Signal Ambient Temperature Propellants

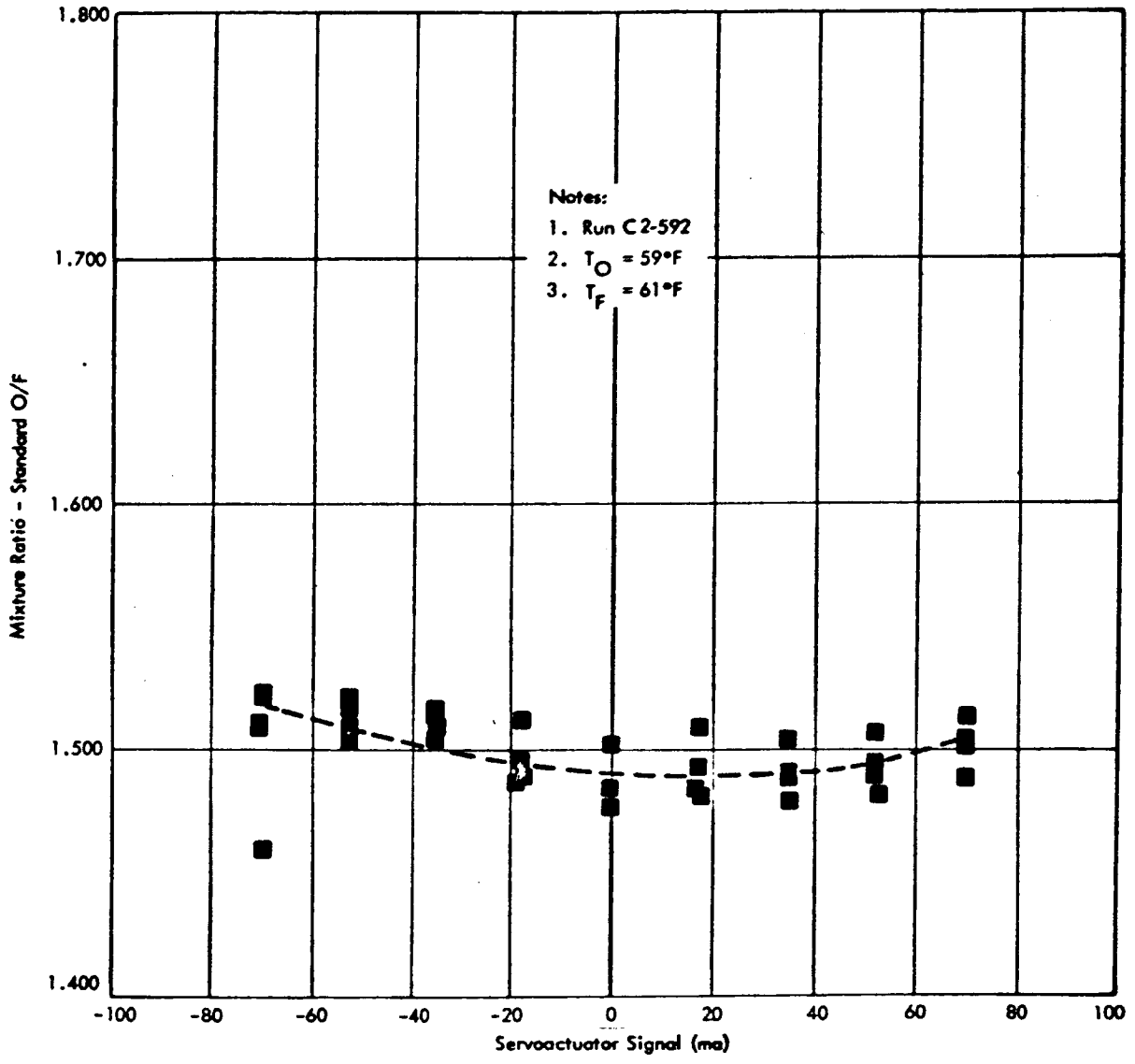

Figure 6.5.2-2. Standard Mixture Ratio Versus Servoactuator Signal Ambient Temperature Propellants

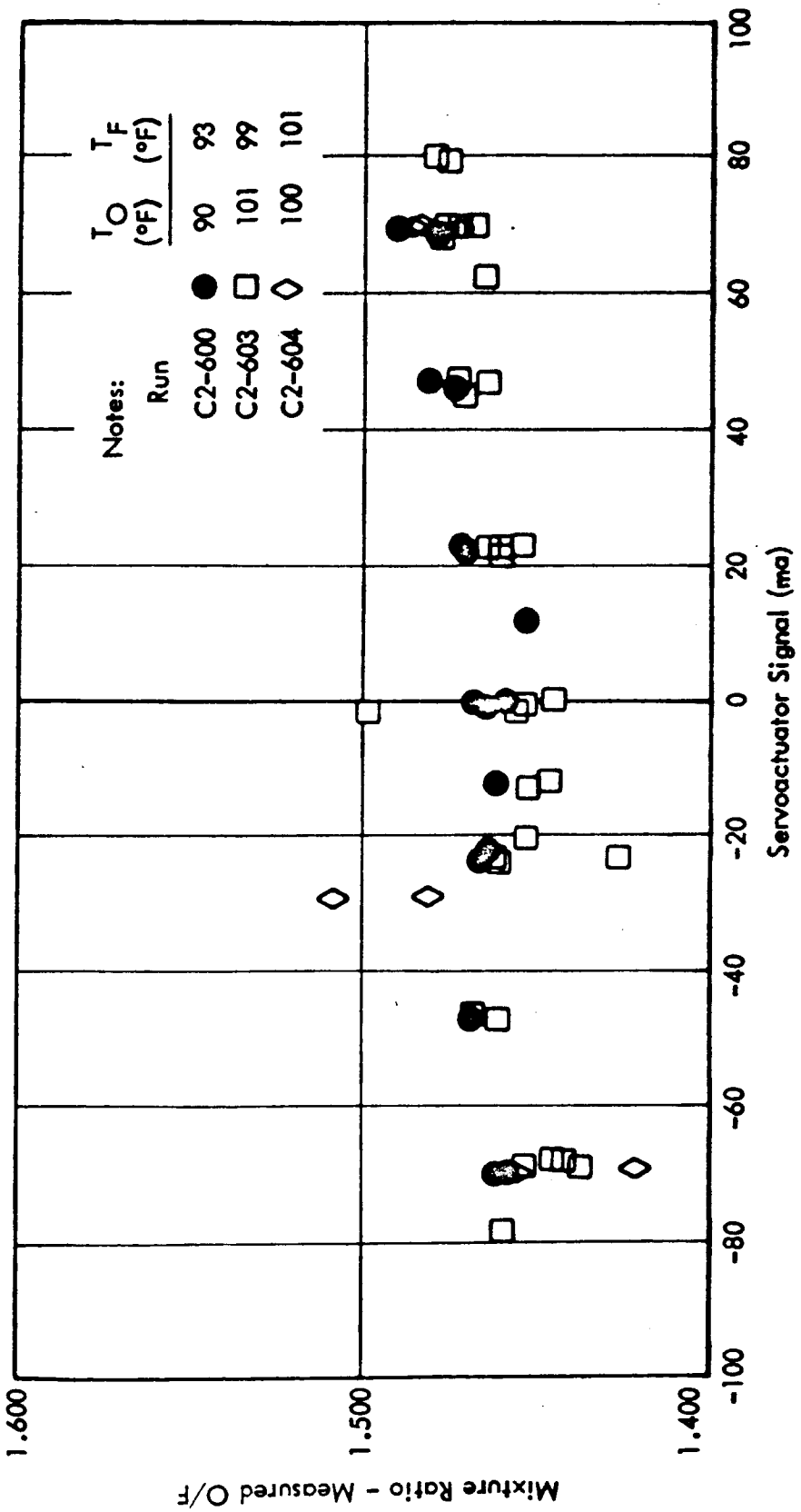

Figure 6.5.2-3. Measured Mixture Ratio Versus Servoactuator Signal High Temperature Propellants

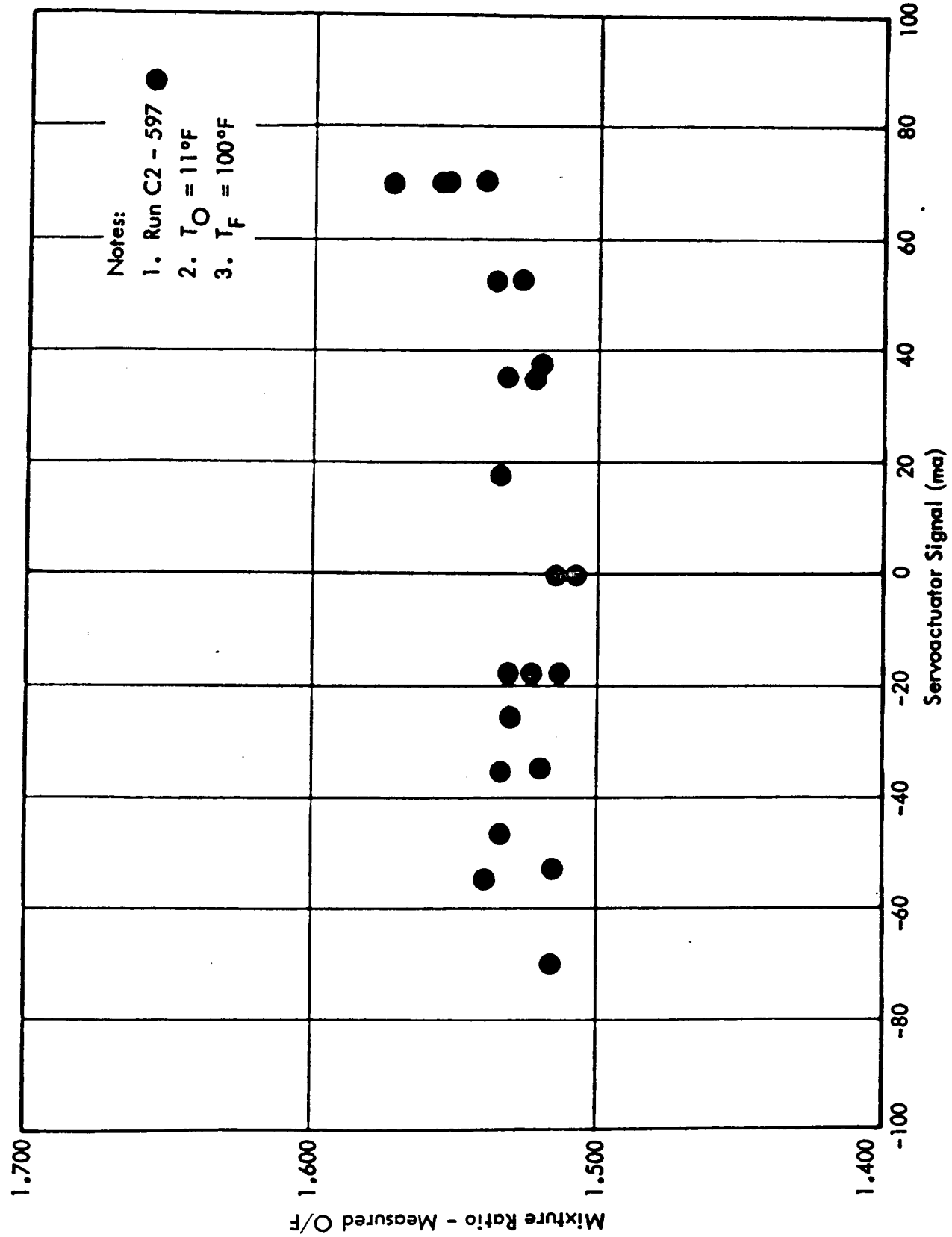

Figure 6.5.2-4. Measured Mixture Ratio Versus Servoactuator Signal-Low Temperature Oxidizer, High Temperature Fuel

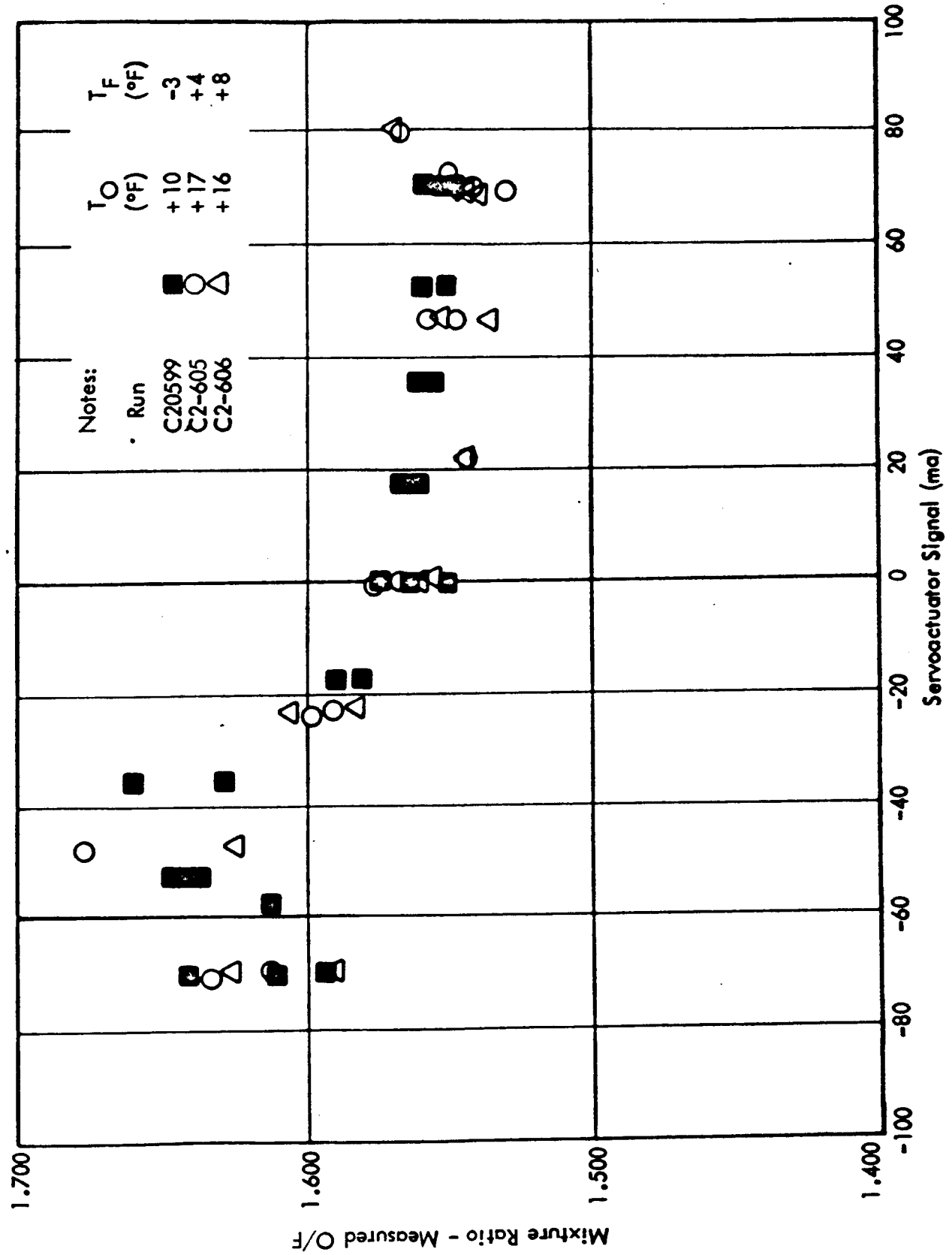

Figure 6.5.2-5. Measured Mixture Ratio Versus Servoactuator Signal - Low Temperature Propellants

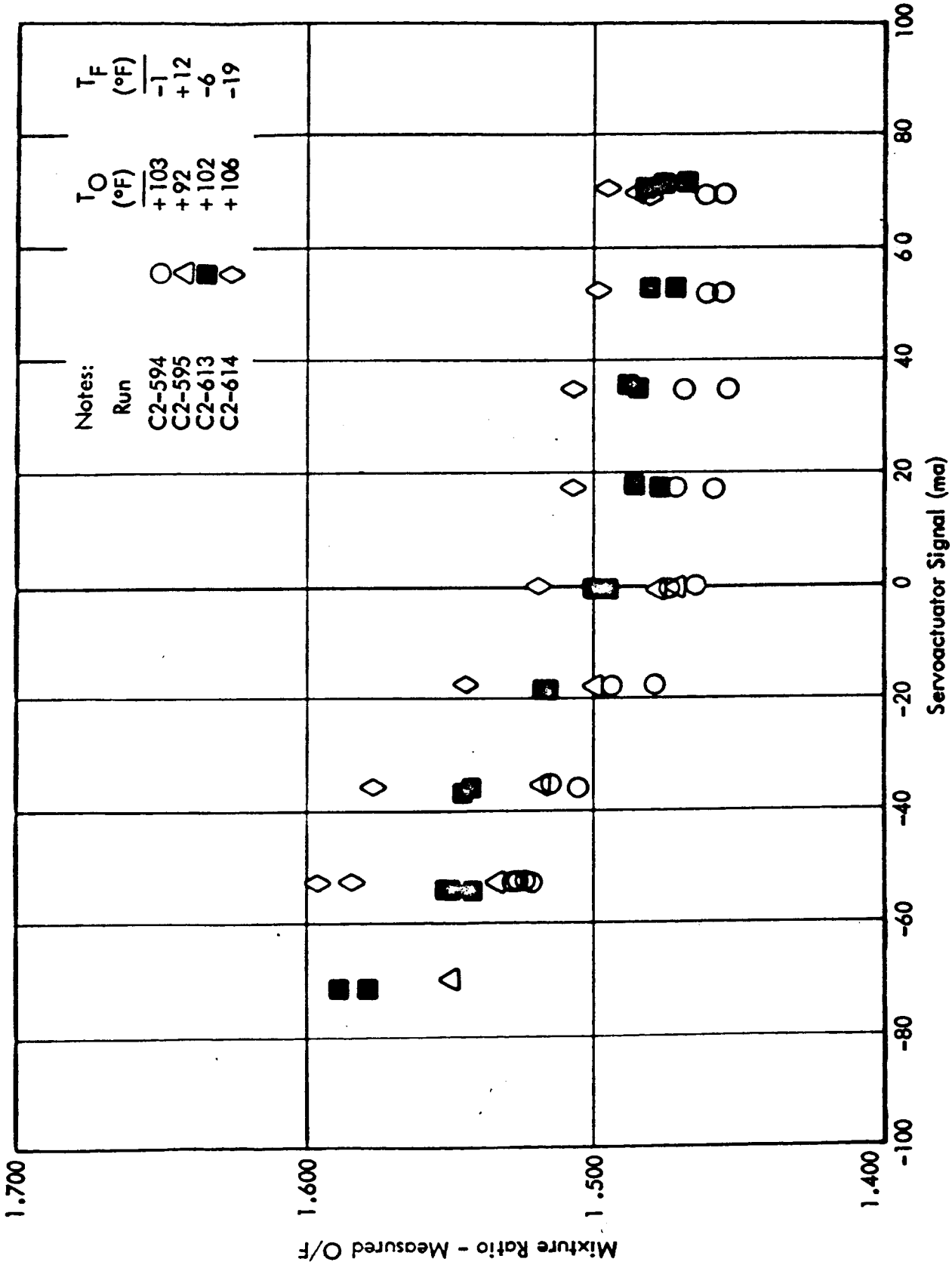

Figure 6.5.2-6. Measured Mixture Ratio Versus Servoactuator Signal High Temperature Oxidizer, Low Temperature Fuel

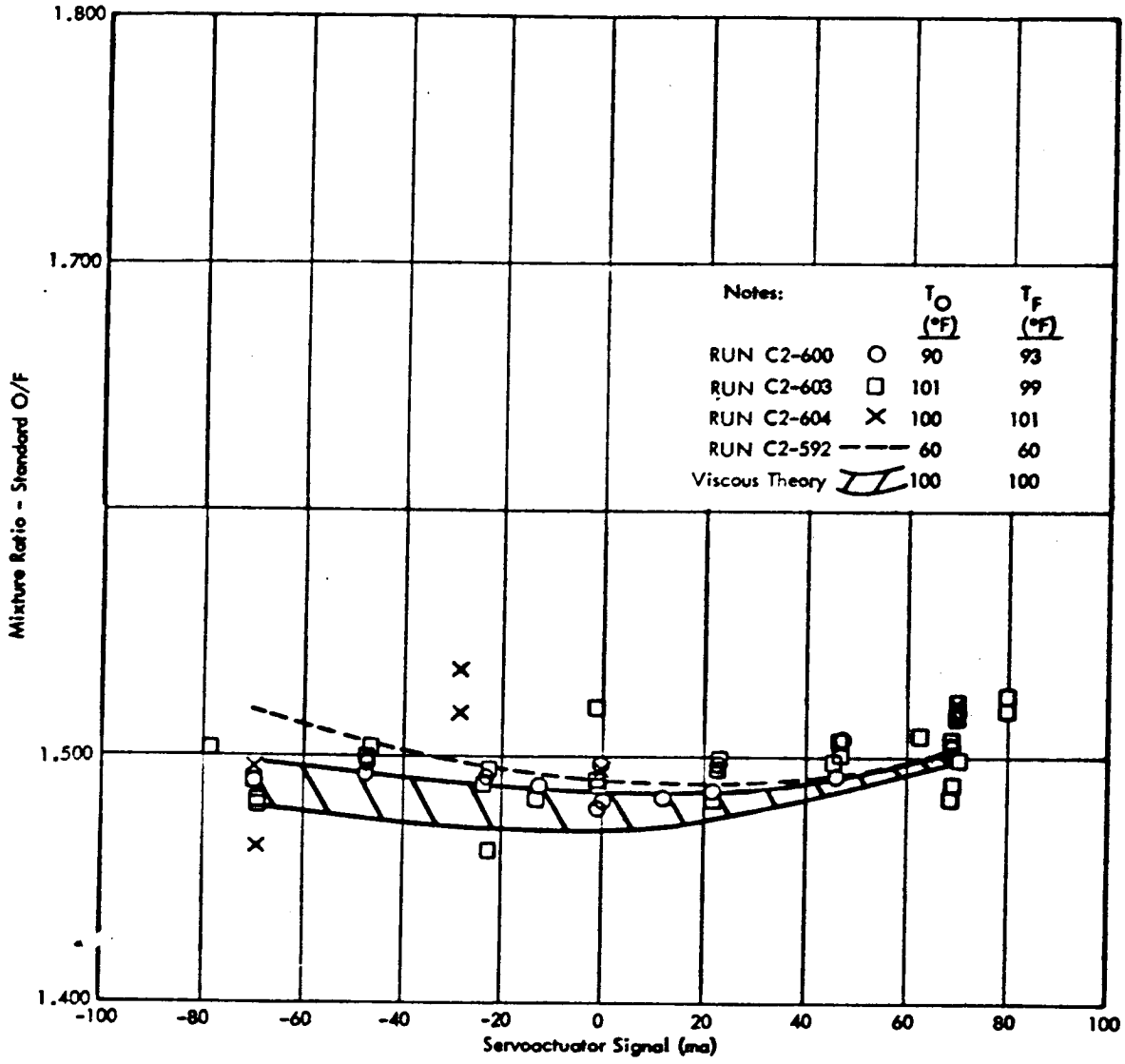

Figure 6.5.2-7. Standard Mixture Ratio Versus S/A Signal-High Temperature Propellants

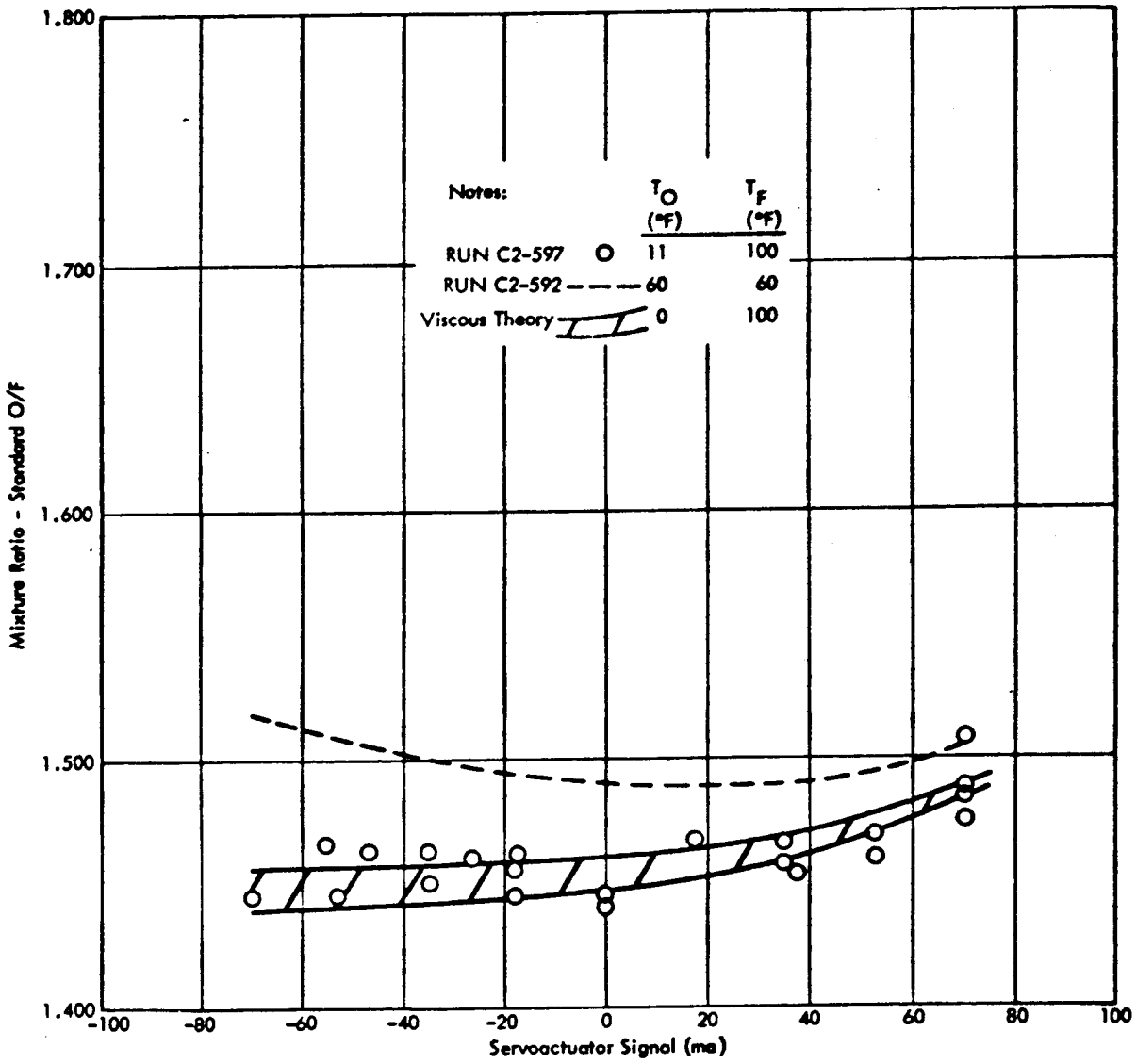

Figure 6.5.2-8. Standard Mixture Ratio Versus S/A Signal - Low Temperature Oxidizer, High Temperature Fuel

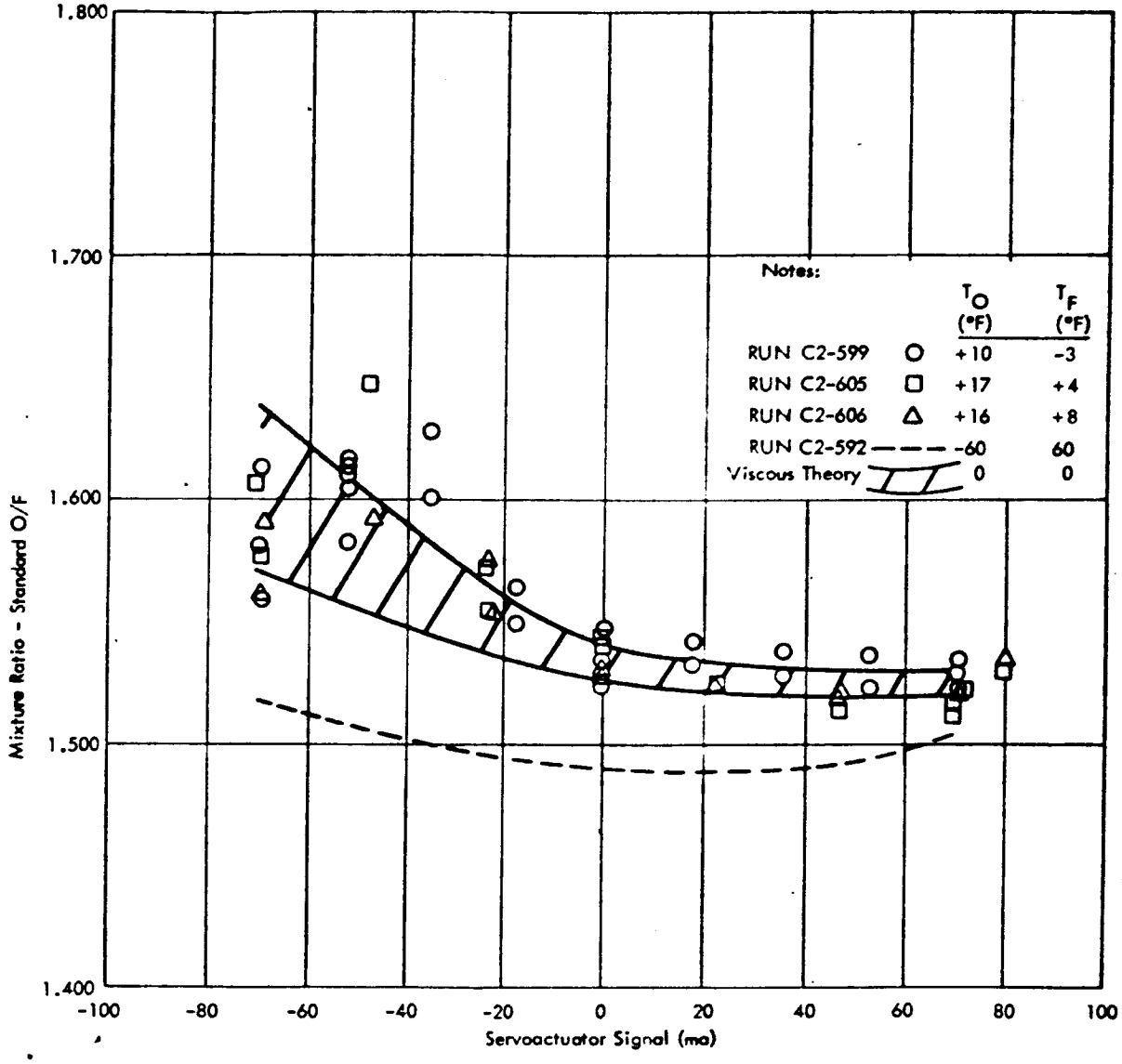

Figure 6.5.2-9. Standard Mixture Ratio Versus Servoactuator Signal Low Temperature Propellants

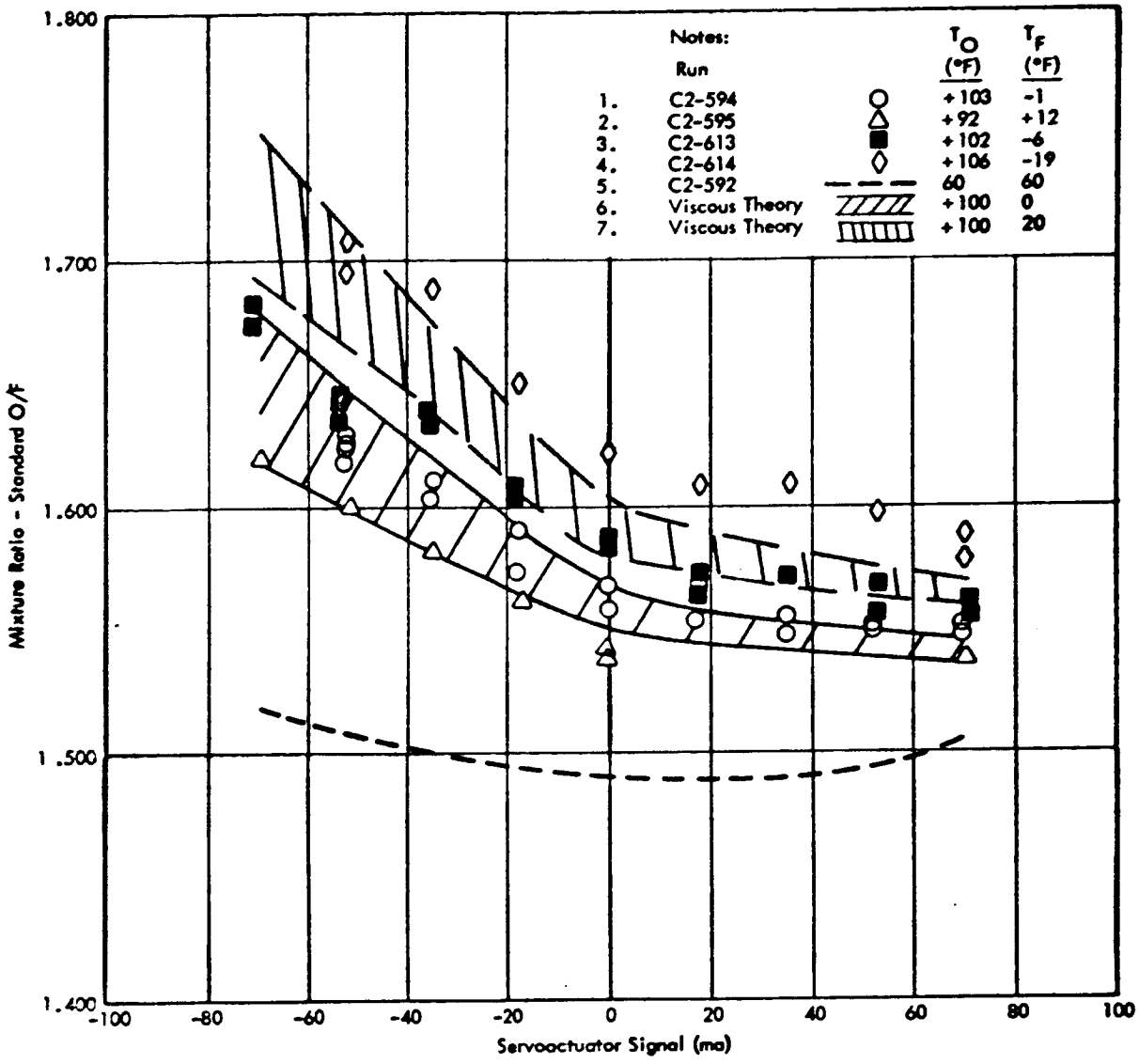

Figure 6.5.2-10. Standard Mixture Ratio Versus S/A Signal-High Temperature Oxidizer, Low Fuel

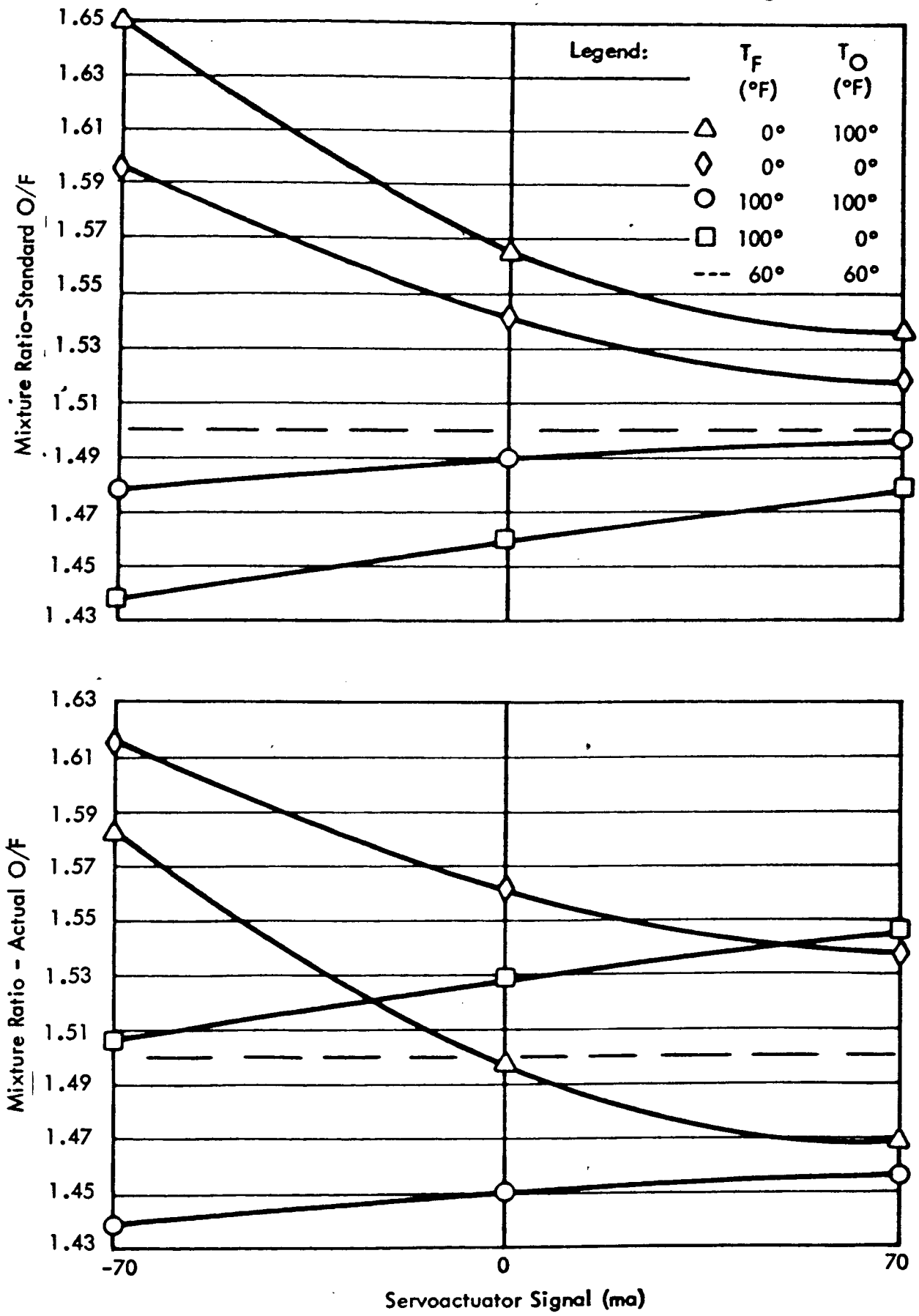

Figure 6.5.2-11. Standard and Actual Mixture Ratio Versus S/A Signal

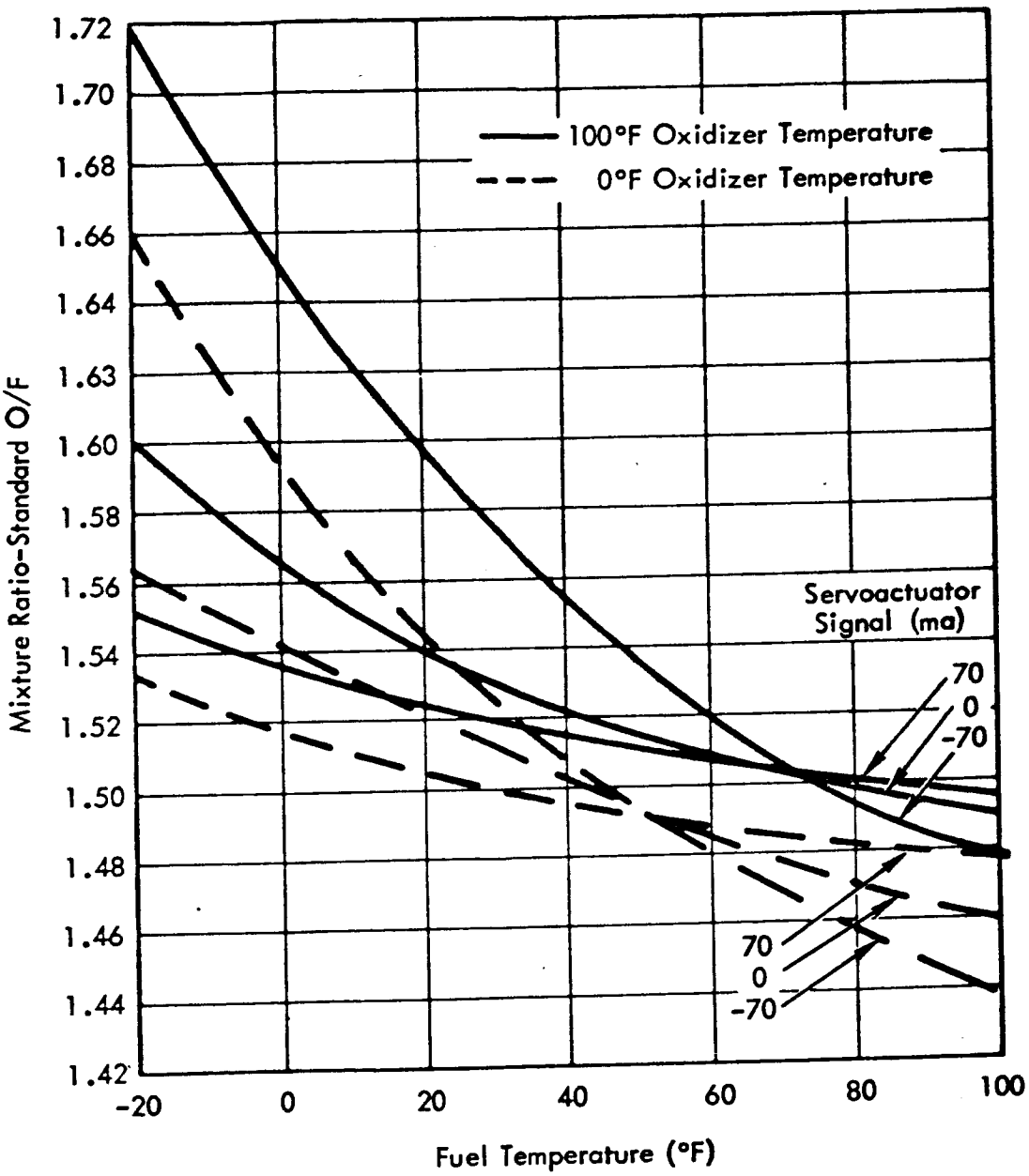

Figure 6.5.2-12. Standard Mixture Ratio Versus Propellant Temperature for High $L_{eq/D}$

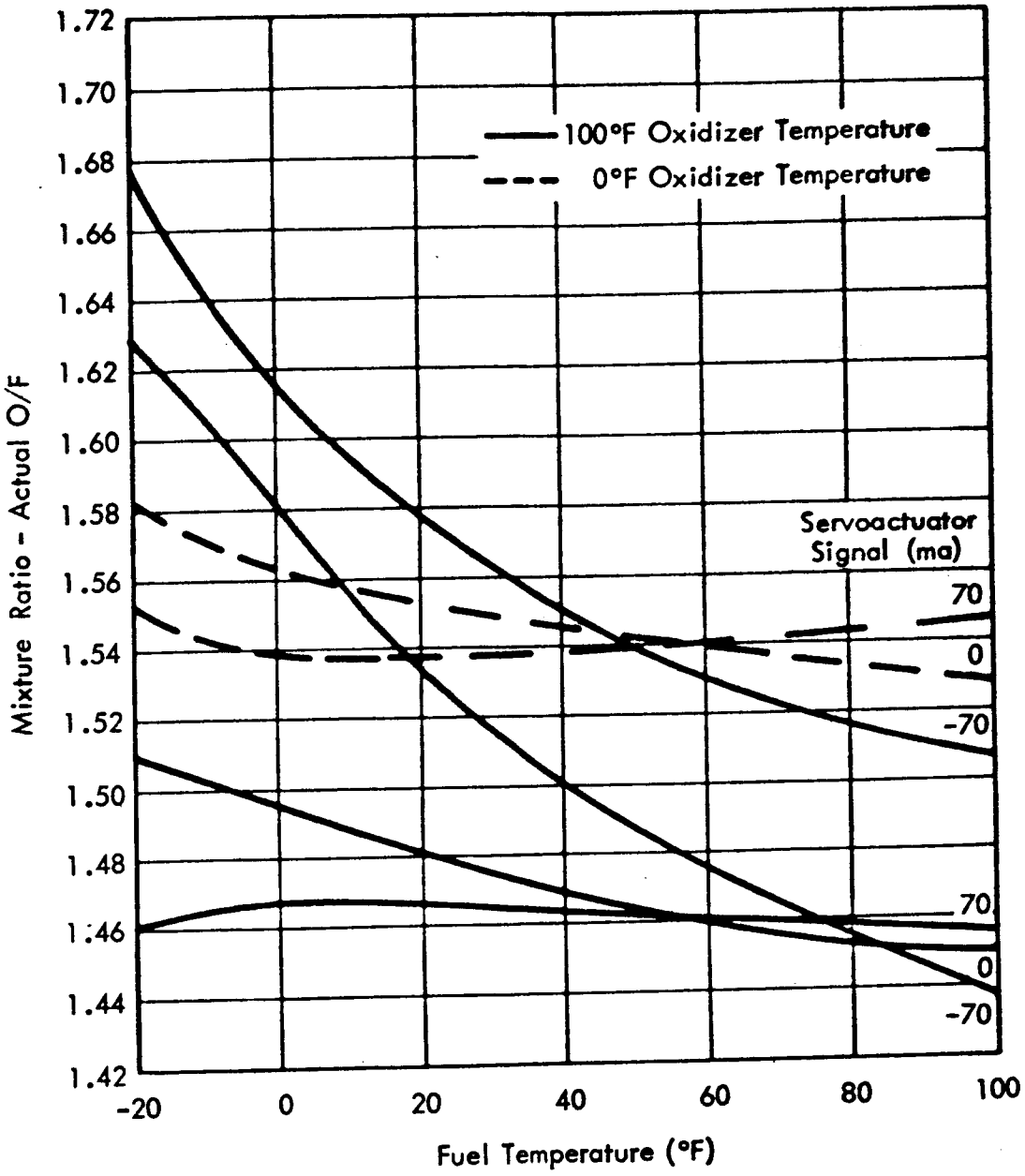

Figure 6.5.2-13. Actual Mixture Ratio Versus Propellant Temperature

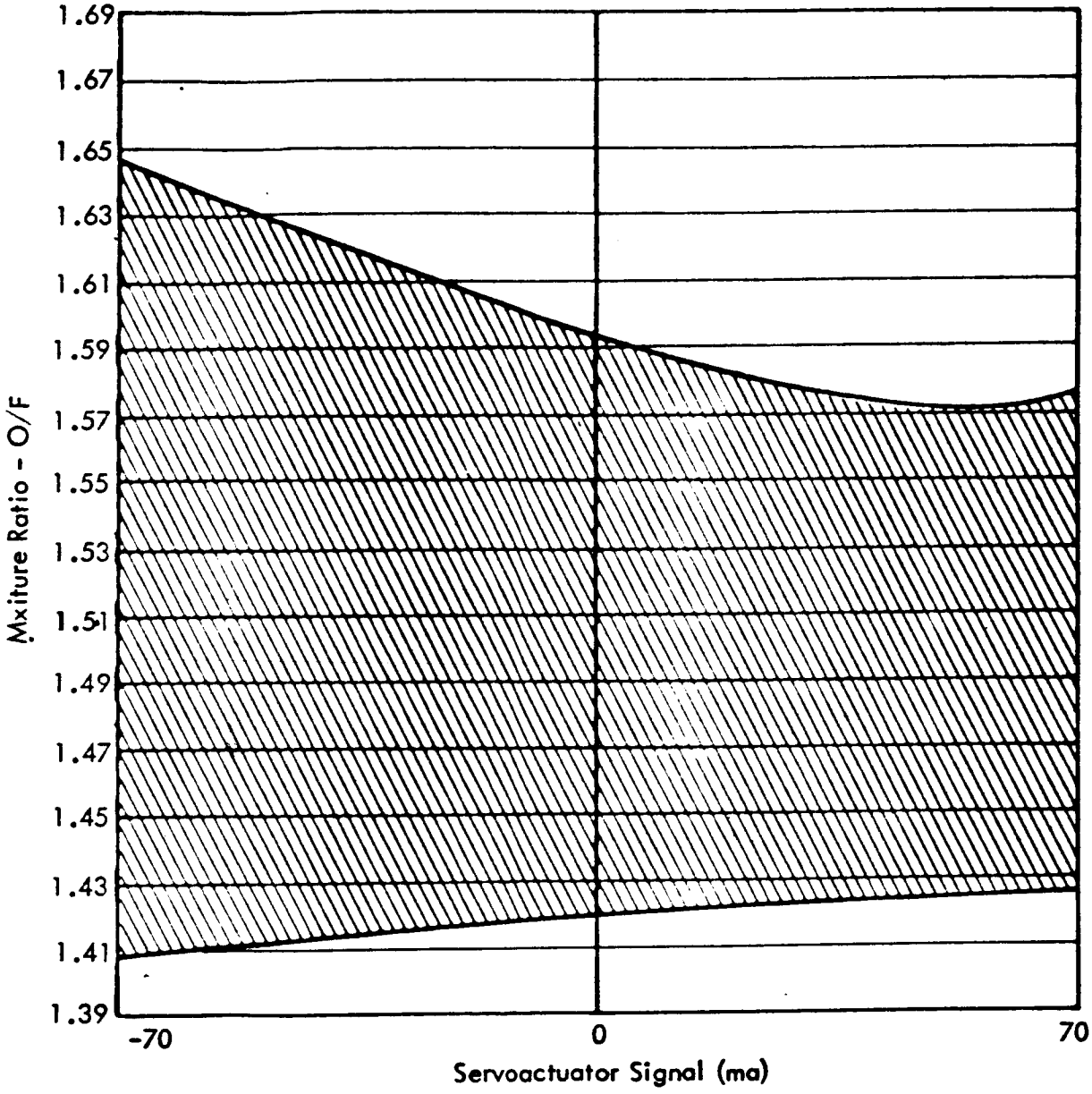

Figure 6.5.2-14. Boundary of Mixture Ratio as a Function of S/A Signal

Table 6.5.3-1

Propellant Pressure and Temperature Effect on Thrust

Commanded Thrust (S/A Signal) (ma)	Specification Thrust Boundary (Per JPL Spec. SAM-50255-DSN-C) Max (lbs)	Min (lbs)	Propellant Supply Pressure Effect (740 to 700 psig) on Commanded Thrust (%)	Propellant Temperature Effect (0 to 100°F) on Commanded Thrust (%)	Combined Pressure and Temperature Effect on Commanded Thrust (%)	Allowable Thrust Boundary for Acceptance (Commanded Thrust at 720 psia and 70°F) Max (lbs)	Min (lbs)
+70 (Max Thrust)	168	145	± 1.4	+ 1.4 - 1.8	+ 2.8 - 3.2	164	150
0 (Mid-Thrust)	101	89	± 1.4	+ 0.35 - 1.4	+ 1.75 - 2.8	99	91.8
-70 (Min Thrust)	41.5	20	± 1.4	+ 0.05 - 1.9	+ 1.45 - 3.3	41	22

4. The viscous theory discharge coefficient (discussed in paragraph 7.5) is applicable.

5. Propellant supply pressure extremes are 740 psig maximum and 700 psig minimum.

6. Propellant temperature extremes are 100°F maximum and 0°F minimum.

Supply pressure effects are computed using Equation (2) in paragraph 6.5.1. For this calculation, propellant temperature was assumed constant (at 70°F), and therefore density and vapor pressure were assumed constant. As shown in Table 6.5.3-1, supply pressure extremes result in a ± 1.4% effect on commanded thrust.

Propellant temperature effects were computed using Equation (4) in paragraph 7.5. This calculation provided the "viscous theory" thrust ratio versus temperature curves given in Figure 6.5.3-2. Although not used in assessing temperature effects here, the "constant C_D" thrust ratio versus temperature curve is also shown in Figure 6.5.3-2. The curves in Figure 6.5.3-2 were computed assuming a constant propellant supply pressure of 720 psig. The effect of temperature on commanded thrust varies from +1.4% to -1.9%, as shown in Table 6.5.3-1.

The last column in Table 6.5.3-1, entitled "Allowable Thrust Boundary for Acceptance" gives maximum and minimum values of thrust for S/A signals of -70, 0, and +70 ma (corresponding to minimum, mid, and maximum thrust, respectively). These thrust boundaries were computed using the combined effect of extremes in propellant supply pressure and temperature, and assuming that acceptance firings were conducted at (or corrected to) 720 psig supply pressure and 70°F propellant temperature. The "Allowable Thrust Boundary for Acceptance" is assumed to be centered within the "Specification Thrust Boundary."

The "Allowable ... Boundary" limits are those within which unit to unit variation is allowable on acceptance testing at standard temperature and pressure (70°F and 720 psia). This hardware variability is allowable in conjunction with the added variability from propellant temperature and supply pressure extremes which results in overall variability that complies with the design specification (JPL SAM-50255-DSN-C) thrust to signal boundary.

Table 6.5.3-3 presents the results of test firings conducted on four Phase III TCAs and one Phase II TCA (S/N 004).

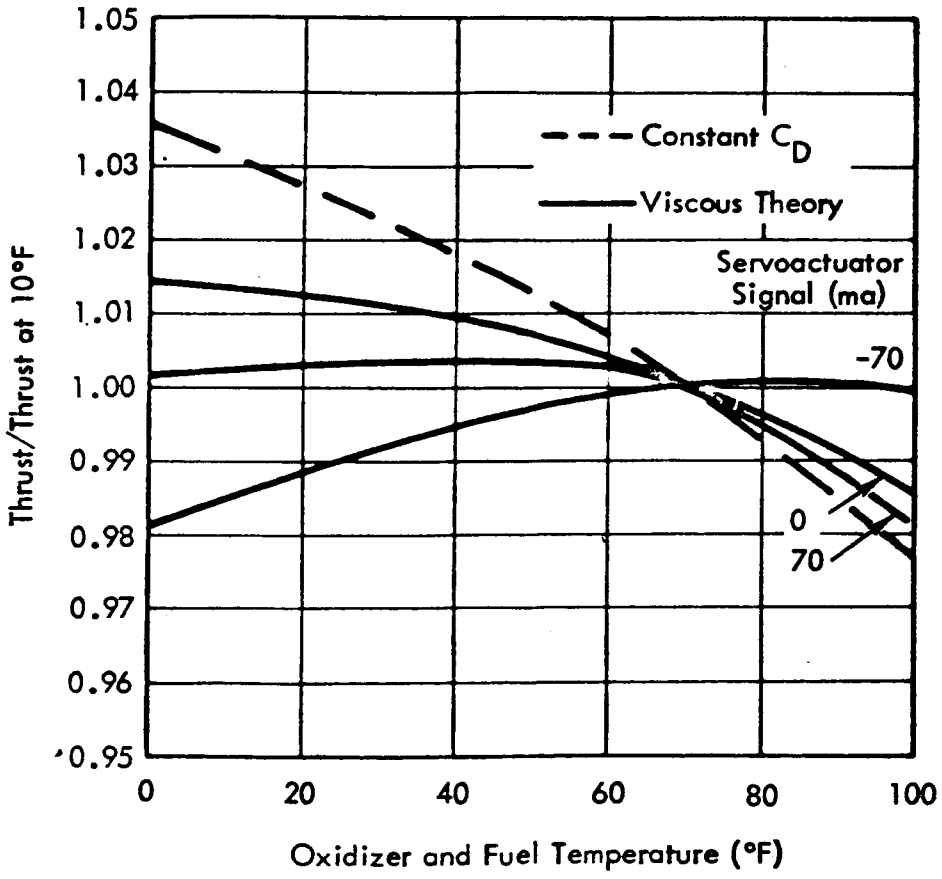

Figure 6.5.3-2. Variation of Thrust with Propellant Temperature

Table 6.5.3-3

Actual Thrust Versus Commanded Thrust for Phase III TCAs

	Thrust (lb)* at Standard Conditions for S/A Signal (ma) of			Acceptable
	+70	0	-70	
Allowable - per Table 6.5.3-1	150 to 164	91.8 to 99	22 to 41	-----
TCA S/N 004	154.2	96.0	28.8	Yes
TCA S/N 007	155.0	94.1	28.2	Yes
TCA S/N 008	153.3	95.0	27.7	Yes
TCA S/N 009	157.1	95.0	26.6	Yes
TCA S/N 011	154.0	97.6	33.6	Yes

*Standard conditions are defined as propellant pressure of 720 psig and propellant temperature of 70°F.

6.6 Altitude Steady-State Performance Tests

All steady-state performance testing associated with the Development and Prequalification Test Program conducted at the JPL Edwards Test Station under simulated altitude conditions (plus one sea level checkout test and one sea level test for photographic purposes) is discussed in this section. Additional steady-state data from tests conducted at STL's Inglewood Rocket Test Site are discussed in other subsections of 6.0. The results of individual tests are discussed here; however, the discussion of combined data from all tests used to determine the steady-state performance characteristics of the MIRA 150A are given in Paragraph 6.8. Transient data is discussed in Paragraph 6.9.

The TCA test program conducted at JPL/ETS consisted of 32 firings (DY-18 through DY-49) for a total of 35 TCA starts and a run duration of 2,405 seconds. This program was conducted in accordance with the Development Test Plan (STL Document Number 9730.4-64-1-43) and Prequalification Test Specification TS3-02B. Table 6.6-1 provides a summary of the total test matrix, and the following paragraphs discuss the detailed test results. Three test series were run prior to initiation of the formal prequalification test program. These tests were a checkout run of the data acquisition system (per Paragraph 5.2.8 of the Development Test Plan) and two additional altitude tests (per paragraph 5.2.9 and 5.2.11 of the plan) to verify the readiness of the MIRA 150A to enter the formal prequalification test program.

6.6.1 Initial Checkout Test

6.6.1.1 Test Objectives

The primary test objectives of the initial checkout test (Run DY-18) were to:

1. Perform an initial checkout firing at JPL/ETS under sea level conditions.
2. Obtain sea level performance data.
3. Obtain acoustic data.

6.6.1.2 Test Summary

With the exception of obtaining acoustic measurements, the primary test objectives were achieved. At JPL direction, the acoustic measurements were deleted prior to the firing. This sea level test was conducted according to paragraph 5.2.8 of the Development Test Plan except that a 130-second AT-1 thrust cycle was substituted for the cycle originally planned. The test article consisted of HEA S/N 004 coupled to a sea level, water-cooled combustion chamber.

6.6.1.3 TCA Configuration

The HEA tested was MIRA 150A-004, built to the basic Phase II configuration (STL Drawing No. 105461-1, A-1) and included the following major parts:

Component	P/N	S/N
Helium Pilot Valve	C104337-1	004
Servoactuator	C104312-1	C53748
Injector Assembly	105462-1A1	004
Shutoff Valve Piston	103948-3B1	N/A
Shutoff Valve Sleeve	103947-3B1	N/A
Shutoff Valve Poppet	103946-1A	N/A
Flow Control Valve	105466-1A2	004

Table 6.6-1

JPL/ETS Test Program Matrix

(All runs were a simulated pressure altitude except DY-18 and DY-34)

PQT or Development Test Number	JPL Run Number	Primary Objectives	HEA S/N	CC & NA S/N	Thrust Time Profile — Fixed,	Step,	Dynamic	Reference	Chamber Temp. (°F)	Propellant Temp. (°F)	Mixture Ratio - O/F	Duration & Starts (Seconds and Nos.)
5.2.8	DY-18	Initial checkout at sea level.	004	(H_2O cooled)		X	X	Table 6.6.1-3 (AT-1)	Ambient	Ambient	1.5	130-1 start
5.2.9	DY-19	Altitude performance prior to Prequal. testing.	004	(H_2O cooled)		X		Table 6.6.4-1 (Profile 1)	Ambient	Ambient	1.5	45-1 start
5.2.11	DY-20 Thru DY-24	Altitude performance and dynamic throttling prior to prequal. testing.	004	002		X	X	Table 6.6.3-2 (PQ-1)	Ambient	Ambient	1.5	340-5 starts
PQT-001	DY-25	Altitude performance as a function of mixture ratio and thrust.	001	003		X		Table 6.6.4-1 (Profile 1)	Ambient	Ambient	1.5	45-1 start
PQT-002	DY-26		001	005		X		Table 6.6.4-1 (Profile 2)	Ambient	Ambient	1.4	45-1 start
PQT-003	DY-27		001	005		X		Table 6.6.4-1 (Profile 3)	Ambient	Ambient	1.6	45-1 start
PQT-004A	DY-28		001	005		X		Table 6.6.4-1 (Profile 1)	Ambient	Ambient	1.5	45-1 start
PQT-004.5	DY-29 Thru DY-32	Startup & shutdown transients and correlation between H_2O - cooled and ablative-cooled chambers at altitude.	001	(H_2O cooled)		X		Table 6.6.4-1	Ambient	Ambient	1.4, 1.5, and 1.6	180-4 starts
PQT-004B	DY-33	Minimum temperature effect on performance.	001	005		X	X	Table 6.6.6-1	0	0	1.5	180-1 start
PQT-005	DY-47 Thru DY-49	Altitude performance repeatability.	010	010 (H_2O cooled on Run DY-49)		X	X	Table 6.6.4-1 and 6.6.6-1	Ambient	Ambient	1.5	364-6 starts
PQT-007	DY-35 Thru DY-37	Durability at Max thrust, M.R., and temperature.	008	008	X			None	125	100	1.6	300-3 starts

Table 6.6-1 (Continued)

PQT or Development Test Number	JPL Run Number	Primary Objectives	HEA S/N	CC & NA S/N	Thrust Time Profile Fixed, Step, Dynamic		Reference	Chamber Temp. (^{o}F)	Propellant Temp. (^{o}F)	Mixture Ratio - O/F	Duration & Starts (Seconds and Nos.)
PQT-008	DY-38 Thru DY-40	Durability at Min thrust and Max M.R. and propellant temperature.	008	001	X		None	0(DY-38 only) & ambient.	100	1.6	480-3 starts
PQT-010	DY-41 Thru DY-43	Dynamic throttling.	004	(H_2O cooled)	X	X	Table 6.6.3-2 (PQ-1)	Ambient	Ambient	1.5	238-3 starts
PQT-009.5	DY-44 Thru DY-46	Dynamic throttling at Min temperature.	004	(H_2O cooled)	X	X	Table 6.6.3-2 (PQ-1)	0 (S/A only)	0	1.5	238-3 starts
None	DY-34	Sea level photo coverage.	001	011	X	X	Table 6.6.1-3 (AT-1)	Ambient	Ambient	1.5	130-1 start
Program Total											2,405-35 starts

This HEA was functionally different from the basic Phase III configuration (STL Drawing No. 106662) in the following major respects:

1. Servoactuator response, linearity, hysteresis, and gain characteristics were different. (A Phase II servoactuator was used in place of a Phase III servoactuator.)

2. Leakage characteristics were different through various static and dynamic seals, because of differences in seal design. (Bal seals are used exclusively on the Phase III HEA while some Omniseals were used on the Phase II HEA.)

3. Propellant flow rate versus stroke was slightly different between the Phase II HEA and the Phase III HEA, because of changes in flow control valve pintle and insert design.

4. No quick-disconnect bosses or fittings were available on the Phase II configuration precluding propellant bleeding at the shutoff valves. This difference affects the initial startup transient.

However, since the major parts of the HEA 004 injector assembly (pintle P/N 105107-4, sleeve P/N 105192-4, guide P/N 105106, and plate P/N 106423-3) are dimensionally identical to their Phase III counterparts, it may be stated that the two HEAs are identical from the standpoint of combustion characteristics (C*, I_{sp}, etc.). The CC & NA tested consisted of a sea level, water-cooled combustion chamber (P/N 106372).

6.6.1.4 Test Setup and Test Conditions

The TCA was installed in a thrust fixture (P/N X-104433) which was rigidly mounted to the altitude chamber door. The test installation is illustrated in Figures 6.6.1-1 and 6.6.1-2. The TCA was tested under sea level ambient conditions with sufficient measurements to determine sea level steady-state and transient performance characteristics. However, because of the additional fluid volumes imposed by the use of injection pressure measurements, none of the transient data are considered valid. An unmodified* AT-1 thrust program cycle (Table 6.6.1-3) was used resulting in a 130-second test duration.

6.6.1.5 Test Results

The initial checkout run (DY-18) was successfully completed on 11 September 1964 satisfying the requirements of Development Test Plan paragraph 5.2.8. Detailed steady-state performance data for this test are summarized in Table D-1-1 of Appendix D-1. With the exception of a slightly high mixture ratio at the maximum thrust step (1.557 at standard conditions), measured performance characteristics were within acceptance test specification limits. Corrected C* data varied from 5276 fps at a 108-psia chamber pressure to 5048 fps at a 20-psia chamber pressure. Because of the differences between Phase II and Phase III servoactuators and the flow control valves (discussed in 6.6.1.3), these data are not representative of Phase III thrust-signal characteristics.

*This AT-1 thrust-time profile was later modified by additional stepping during the last 20 seconds. Refer to paragraph 4.5.

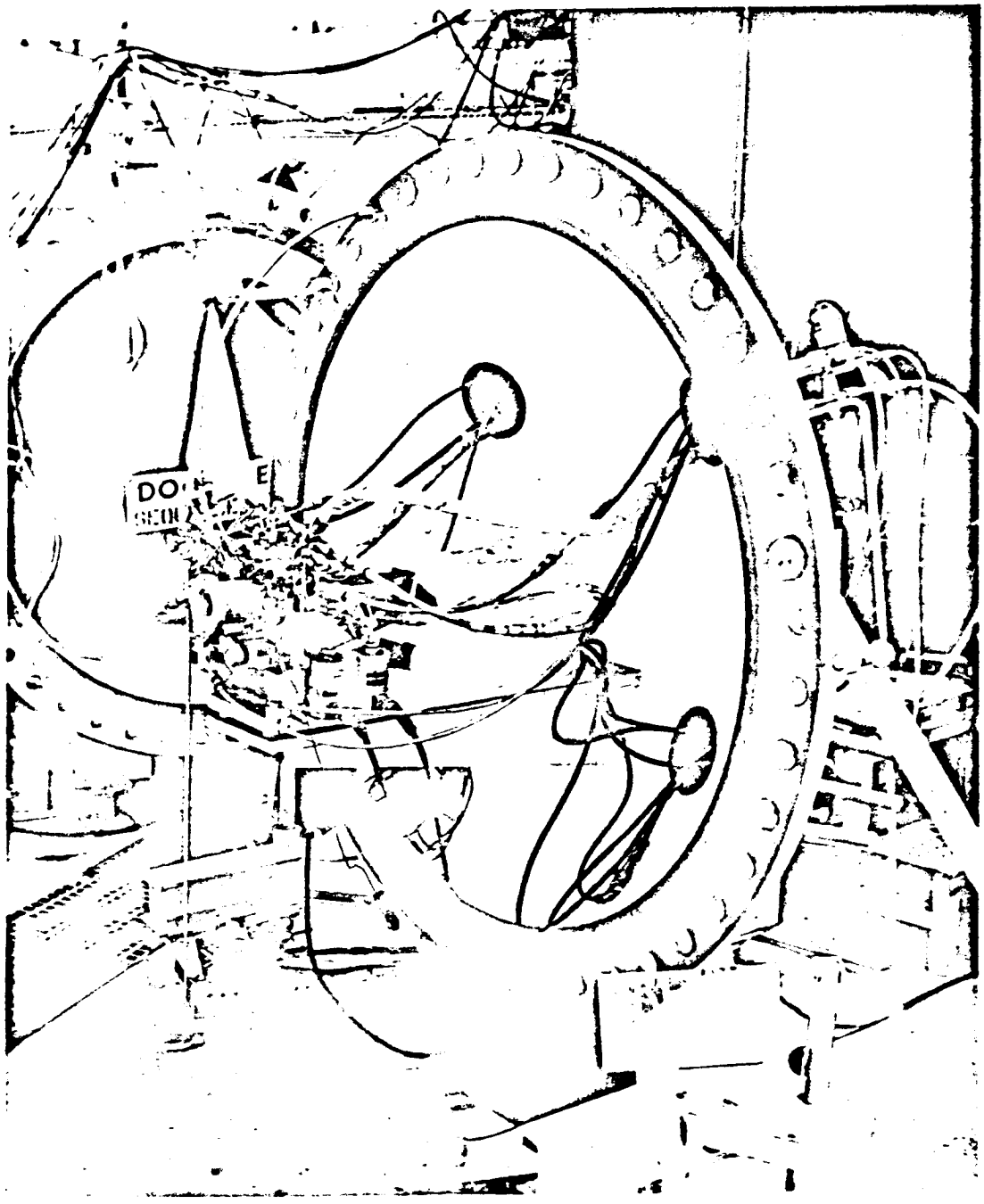

Figure 6.6.1-1. Initial Checkout Test Setup (Run DY-18)

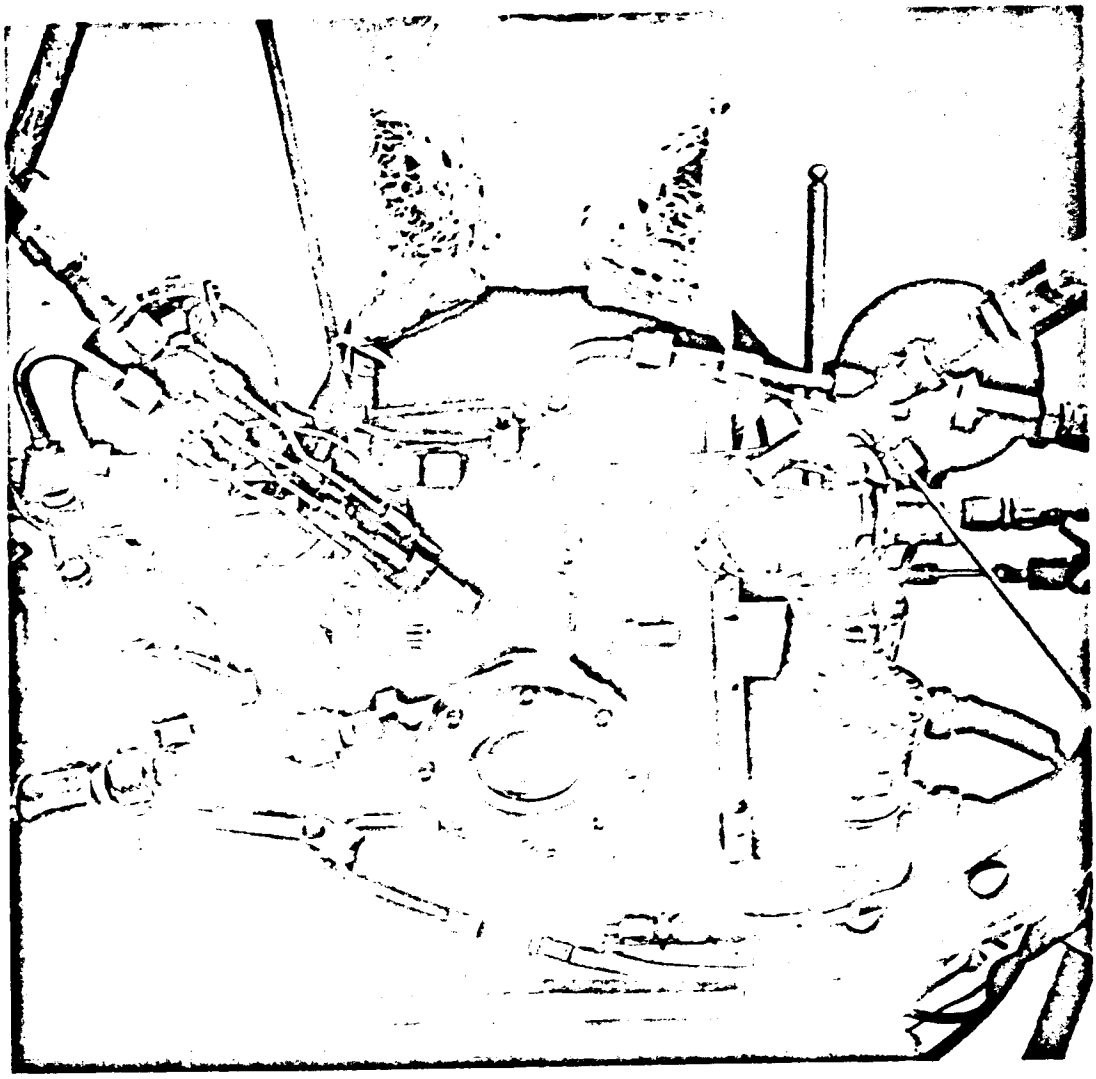

Figure 6.6.1-2. Initial Checkout Test Setup Closeup (Run DY-18)

Table 6.6.1-3

Thrust Cycle AT-1 - Unmodified

Command (± 0.5 ma)		Time From Startup (± 0.1 sec)
0	Startup	0.0
+35	Step	5.0
+70	Step	10.0
+35	Step	15.0
0	Step	20.0
-35	Step	25.0
-80	Step	30.0
-50	Step	35.0
-35	Step	40.0
0	Step	45.0
+7.5	Step	50.0
-7.5	Step	52.0
0	Step	54.0
0 ± 7.5	Sinusoidal, 5 cps	54.2
0	Step	59.0
+70	Step	60.0
+55.0	Step	62.0
+62.5	Step	64.0
+62.5 ± 7.5	Sinusoidal, 5 cps	64.2
+62.5	Step	69.0
-47.5	Step	70.0
-32.5	Step	72.0
-40.0	Step	74.0
-40.0 ± 7.5	Sinusoidal, 5 cps	74.2
-40.0	Step	79.0
+80.0	Step	80.0
-40.0	Step	82.0
-40.0 to + 70.0	Ramp	84.0 - 94.0
+70.0 to - 40.0	Ramp	94.0 - 104.0
0	Step	104.0
0 to + 15.0	Ramp	105.0 - 107.0
+ 15 to 0	Ramp	107.0 - 109.0
0	Step	109.0
0	Shutdown	130.0

6.6.2 Initial Altitude Test

6.6.2.1 Test Objectives

The primary test objectives of the first altitude test (Run DY-19) were to:

1. Determine altitude performance of the TCA with a water-cooled CC & NA.

2. Determine altitude startup and shutdown characteristics.

6.6.2.2 Test Summary

This test was successfully conducted under altitude conditions according to paragraph 5.2.9 of the Development Test Plan except that a 45-second, step-thrust cycle (PQ-3) was substituted for the cycle originally planned. All major objectives were achieved. The test article consisted of HEA S/N 004 coupled with a water-cooled combustion chamber and radiation cooled skirt.

6.6.2.3 TCA Configuration

The HEA was identical to that described in paragraph 6.6.1.3. The CC & NA consisted of a water-cooled combustion chamber (P/N 106372) and a radiation-cooled altitude expansion cone (P/N 106831).

6.6.2.4 Test Setup and Test Conditions

The TCA was installed as described in paragraph 6.6.1.4; the test setup is shown in Figure 6.6.2-1. The TCA was fired under simulated altitude conditions using a thrust cycle planned for part of the PQT series and given by Profile 1 in Table 6.6.4-1 (see paragraph 6.6.4) with the cell pressure varying between approximately 0.03 to 0.14 psia depending on the TCA thrust level. The TCA was at test cell ambient temperature conditions prior to firing; the propellants were maintained near 70°F by water cooling the propellant tanks. Prime performance measurements included thrust, Photocon and Taber measured chamber pressures, propellant and cooling water flow rates, and servo-actuator signal and position.

6.6.2.5 Test Results

The initial altitude test (DY-19) was successfully completed on 16 September 1964 satisfying the requirements of paragraph 5.2.9 of the Development Test Plan. Detailed steady-state performance data for this test are summarized in Table D-101 and Figures D-1-2 through D-1-5 of Appendix D-1. It may be seen from Figure D-1-2 that the specific impulse data falls within the limits of JPL Specification SAM-50255-DSN-C which are superimposed on the data plot. The standard mixture ratio was slightly high at maximum thrust (1.547 at 151.7 lbs compared to a 1.50 $\pm$ 0.03 allowable range).

Figure 6.6.2-1. Initial Altitude Test Setup (Run DY-19)

6.6.3 Initial Altitude Dynamic Throttling Test

6.6.3.1 Test Objectives

The primary test objectives of the initial altitude dynamic firings were to:

1. Determine TCA dynamic throttling characteristics.
2. Determine altitude performance of the TCA with a flight-weight CC & NA.
3. Demonstrate TCA durability under throttling conditions.
4. Obtain TCA reliability data.

6.6.3.2 Test Summary

The initial altitude dynamic throttling test series (Runs DY-20 through DY-24) were conducted in compliance with the requirements of paragraphs 5.2.11 of the Development Test Plan. This test was only partially successful in achieving the primary objectives, because of facility problems and measurement response limitations. Although transient response data are not considered to be valid because of these problems, some satisfactory steady-state data were obtained.

6.6.3.3 TCA Configuration

The HEA was identical to that described in paragraph 6.6.1.3. The CC & NA was a Phase II (P/N 106546-1) altitude CC & NA, S/N 002, which is functionally identical to the Phase III CC & NA with the exception of the trunnion location which influences CG and mounting provisions only.

6.6.3.4 Test Setup and Test Condition

The test setup is illustrated in Figure 6.6.3-1. The TCA was fired under altitude conditions with the propellants held near 70°F. The original plan was to conduct the first two firings, Profiles A and B of thrust cycle PQ-1 (see Table 6.6.3-2), vacuum soak the TCA for at least 48 hours, complete Profile C of PQ-1, and then repeat Profiles A & B of PQ-1.

Because of JPL facility problems during the third start (Run DY-22), the firing was terminated after approximately 40 seconds. As a result, the actual sequence consisted of: (1) the first two firings (Run DY-20 and DY-21) according to plan, (2) a vacuum soak of approximately 70 hours duration, (3) the first 40 seconds of Profile C of PQ-1 (Run DY-22), (4) a complete 115.8-second firing per Profile C of PQ-1 (Run DY-23), and (5) a repeat of Profile A of the PQ-1 cycle (Run DY-24).

In addition to the prime performance measurements mentioned in paragraph 6.6.2.3, a number of TCA external surface temperatures were measured at the locations shown in Figure 6.4.2-2.

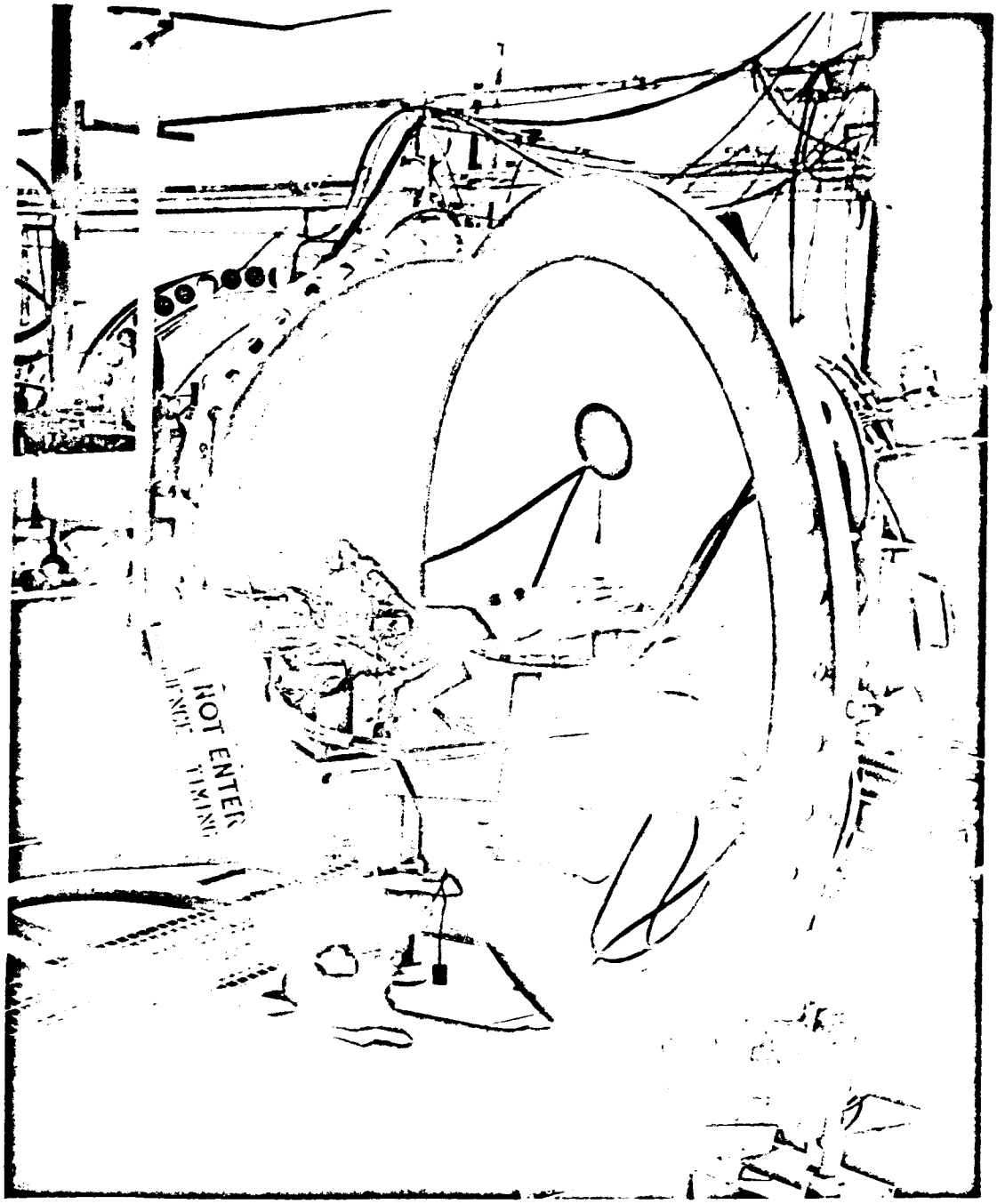

Figure 6.6.3-1. Test Setup for Initial Altitude Dynamic Throttling Test (Runs DY-20 Through DY-24)

Table 6.6.3-2

Thrust Cycle PQ-1

Command (± 0.5 ma)		Time from Startup (± 0.1 sec)
	Profile A	
0	Step	-10.0
0	Startup	0.0
0 ± 7.5	Sinusoidal, ½ cps	1.0
0 ± 7.5	Sinusoidal, 2 cps	2.0
0 ± 7.5	Sinusoidal, 5 cps	12.0
0 ± 7.5	Simusoidal, 7 cps	14.0
0 ± 7.5	Sinusoidal, 10 cps	16.0
0 ± 7.5	Sinusoidal, 15 cps	18.0
0 ± 7.5	Sinusoidal, 20 cps	19.0
0 ± 7.5	Sinusoidal, 25 cps	20.0
0	Step	20.8
0 to + 7.5	Ramp	21.0 - 22.5
+ 7.5 to - 7.5	Ramp	22.5 - 25.5
- 7.5 to 0	Ramp	25.5 - 27.0
+ 7.5	Step	27.0
- 7.5	Step	29.0
0	Step	31.0
0	Shutdown	52.0
	(Tape Change and Calibrate)	
	Profile B	
-29	Step	-10.0
-29	Startup	0.0
0	Step	9.8
0 ± 70	Sinusoidal, 5 cps	10.0
0	Step	20.0
+ 70	Step	20.2
- 62.5	Step	30.0
- 62.5 ± 7.5	Sinusoidal, ½ cps	31.0
- 62.5 ± 7.5	Sinusoidal, 2 cps	39.0
- 62.5 ± 7.5	Simusoidal, 5 cps	42.0
- 62.5 ± 7.5	Sinusoidal, 7 cps	44.0
- 62.5 ± 7.5	Sinusoidal, 10 cps	46.0
- 62.5 ± 7.5	Sinusoidal, 15 cps	48.0
- 62.5 ± 7.5	Sinusoidal, 20 cps	49.0
- 62.5 ± 7.5	Sinusoidal, 25 cps	50.0
- 62.5	Step	51.0
- 62.5 to - 55.0	Ramp	52.0 - 53.5
- 55.0 to - 70.0	Ramp	53.5 - 56.5
- 70.0 to - 62.5	Ramp	56.5 - 58.0
- 55.0	Step	58.0
- 70	Step	60.0
- 70	Shutdown	70.0

Table 6.6.3-2 (Continued)

Command (± 0.5 ma)		Time from Startup (± 0.1 sec)
	(Tape Change and Calibrate) Profile C	
+ 62.5	Step	-10.0
+ 62.5	Startup	0.0
+ 62.5 ± 7.5	Sinusoidal, ½ cps	1.0
+ 62.5 ± 7.5	Sinusoidal, 2 cps	9.0
+ 62.5 ± 7.5	Sinusoidal, 5 cps	12.0
+ 62.5 ± 7.5	Sinusoidal, 7 cps	14.0
+ 62.5 ± 7.5	Sinusoidal, 10 cps	16.0
+ 62.5 ± 7.5	Sinusoidal, 15 cps	18.0
+ 62.5 ± 7.5	Sinusoidal, 20 cps	19.0
+ 62.5 ± 7.5	Sinusoidal, 25 cps	20.0
+ 62.5	Step	21.0
+ 62.5 to + 70.0	Ramp	22.0 - 23.5
+ 70.0 to + 55.0	Ramp	23.5 - 26.5
+ 55.0 to + 62.5	Ramp	26.5 - 28.0
+ 70.0	Step	28.0
+ 55.0	Step	30.0
+ 70.0	Step	32.0
- 80.0	Step	40.0
- 80.0 to + 80.0	Ramp	41.0 - 61.0
+ 80.0	Step	61.0
+ 80.0 to - 80.0	Ramp	62.0 - 82.0
- 80.0	Step	82.0
+ 70.0	Step	83.0
- 70.0	Step	88.0
+ 70.0	Step	88.1
- 70.0	Step	88.6
+ 70.0	Step	88.8
- 70.0	Step	89.8
+ 70.0	Step	90.3
- 70.0	Step	92.8
+ 70.0	Step	93.8
- 62.5	Step	98.8
- 62.5 ± 7.5	Sinusoidal, ½ cps	99.8
- 62.5 ± 7.5	Sinusoidal, 5 cps	102.8
- 62.5	Step	104.8
- 70.0	Step	105.8
- 70.0	Shutdown	115.8

6.6.3.5 Test Results

Runs DY-20 through DY-24 were completed during the 18 through 21 September 1964 time period, satisfying the requirements of paragraph 5.2.11 of the Development Test Plan. Since the PQ-1 thrust cycle was designed primarily for dynamic response determination, only a limited amount of steady-state data were available from these firings. Only data time slices of 4 seconds or longer are reported in Table D-1-1 and Figure D-1-6 through D-1-9 of Appendix D-1. The vacuum specific impulse was again within specification limits; also, the mixture ratio was slightly high at maximum thrust.

The post-fire condition of the CC & NA was excellent after undergoing five starts and a total firing duration of 348 seconds. (For a more detailed discussion of CC & NA performance and TCA temperatures, refer to paragraph 6.4.)

6.6.4 PQT-001, -002, -003, and -004A

6.6.4.1 Test Objectives

The primary test objectives of PQT-001, -002, -003, and -004A were to:

1. Determine TCA vacuum performance characteristics over the full specification thrust and mixture ratio range.
2. Determine test-to-test TCA vacuum performance reproducibility.
3. Acquire additional data on TCA reliability.

6.6.4.2 Test Summary

The test requirements of PQT-001, -002, -003, and -004A given in paragraph 7.2 of the prequalification test specification (TS3-02B) and the primary test objectives were successfully achieved during Runs DY-25 through DY-28. These firings were conducted under altitude conditions with HEA 150A S/N 001 and two different flight-weight altitude CC & NAs S/Ns 003 and 005.

6.6.4.3 TCA Configuration

HEA 150A-001 was built to the basic Phase II configuration (STL Drawing No. 105461-1, A1) and then fitted with several Phase III design features. The HEA major parts and components are listed below.

Component	P/N	S/N
Helium Pilot Valve	C104337-1	022
Servoactuator	C104312-1	C53750
Injector Assembly	105462-1A1	001
Shutoff Valve Piston	106657-1	N/A
Shutoff Valve Sleeve	106656-1A1	N/A
Shutoff Valve Poppet	106798-1A1	N/A
Flow Control Valve	105466-2A2	001

The same comments with respect to the major functional differences between this configuration and the Phase III configuration discussed in paragraph 6.6.1.3 apply here, except that the following items had been reworked to the Phase III configuration prior to initiation of PQT-001 (DY-25):

1. 106657-1 shutoff valve piston replaced 103943-3B1.
2. 106656-1A1 shutoff valve sleeve replaced 103947-3.
3. 106798-1A1 shutoff valve poppet replaced 103946-1A.
4. 106219-1A and 106905-2A flow control valve pintles were installed.
5. 106907-2 flow control valve throat inserts were installed.
6. 106423-1 injector diffuser plate replaced 103966-3C1.
7. 200-12, 200-10, and 200-15 Bal seals replaced R105J-370A1Q, R105J-242A1Q, and R10105-015A1N Omniseals, respectively.

As a result of this rework, HEA 150A-001 shutoff valve operation, flow rate versus valve stroke, and combustion characteristics were all considered identical to the Phase III configuration.

Altitude CC & NA (P/N 106546-1A4) S/N 003 was used on PQT-001, but was replaced by CC & NA (P/N 106546-1A6) S/N 005 for PQT-002 through PQT-004A. CC & NA S/N 005 was later used for PQT-004B (see paragraph 6.6.6).

6.6.4.4 Test Setup and Test Conditions

The test setup and test conditions were as described in detail in paragraphs 7.2.2 through 7.2.6 of the prequalification test specification (TS3-023). Propellant supply tank pressures were varied off-nominal to obtain 1.4 and 1.6 operating mixture ratios during Runs DY-26 and DY-27 while maintaining total propellant flow rate approximately constant. The thrust signal-time programs used are given in Table 6.6.4-1 - Profile No. 1 for PQT-001 and -004A, Profile No. 2 for PQT-002, and Profile No. 3 for PQT-003.

6.6.4.5 Test Results

PQT-001 through -004A were successfully completed by Runs DY-25 through DY-28 from 12 through 20 October 1964 satisfying the requirements of the prequalification test specification. During PQT-001 and -004A, the propellant tank pressures were set at the nominal 720 psia to achieve a target mixture ratio of 1.5. For PQT-002, the fuel pressure was set at 770 psia and the oxidizer at 674 psia for a 1.4 mixture ratio. In a similar fashion, the oxidizer pressure was set at 760 psia and the fuel at 663 psia to target a 1.6 mixture ratio during PQT-003.

No HEA hardware changes or resettings were made during this series. After PQT-001 (Run DY-25), a TCA leak check performed with gaseous nitrogen and soap solution revealed that CC & NA S/N 003 leaked at the liner retaining pins, and at the aft interface between the ablative liner and titanium expansion cone. CC & NA S/N 003 was subsequently removed prior to Run DY-26 and replaced by CC & NA S/N 005. Since both of these CC & NAs were of identical configuration except for trunnion locations, the performance results were not affected.

Table 6.6.4-1

PQT-001 Through -004A, -004.5, and -005
Step Thrust Cycles

Command (± 0.5 ma)		Time from Startup (± 0.1 sec)
	Profile No. 1	
0	Step	-10.0
0	Startup	0.0
+ 23	Step	5.0
+ 47	Step	10.0
+ 70	Step	15.0
0	Step	20.0
- 23	Step	25.0
- 47	Step	30.0
- 70	Step	35.0
- 12	Step	40.0
- 12	Shutdown	45.0
	Profile No. 2	
0	Step	-10.0
0	Startup	0.0
+ 23	Step	5.0
+ 47	Step	10.0
+ 70	Step	15.0
0	Step	20.0
- 23	Step	25.0
- 47	Step	30.0
- 70	Step	35.0
+ 12	Step	40.0
+ 12	Shutdown	45.0
	Profile No. 3	
0	Step	-10.0
0	Startup	0.0
+ 23	Step	5.0
+ 47	Step	10.0
+ 70	Step	15.0
0	Step	20.0
- 23	Step	25.0
- 47	Step	30.0
- 70	Step	35.0
- 35	Step	40.0
- 35	Shutdown	45.0

Detailed performance data for the test series is provided in Table D-1-1 and Figures D-1-10 through D-1-28 of Appendix D-1. It may be noted from Figures D-1-11, D-1-16, D-1-21, and D-1-25 that all of the vacuum specific impulse data falls within the performance limits established by JPL Specification SAM-50255-DSN-C. Further discussion of performance variation with mixture ratio is given in paragraph 6.8 wherein data from PQT-001 through PQT-004A firings are combined with the results of similar tests such as PQT-004.5.

6.6.5 PQT-004.5

6.6.5.1 Test Objectives

The primary test objectives of PQT-004.5 were to:

1. Verify performance corrections for water-cooled CC & NA firings.
2. Determine TCA startup and shutdown characteristics with high response chamber pressure measurements.
3. Confirm performance variation with mixture ratio.

6.6.5.2 Test Summary

The test requirements of PQT-004.5 are given in paragraph 7.3 of the prequalification test specification (TS3-023) and the above test objectives were successfully achieved during Runs DY-29 through DY-32. These firings were conducted under altitude conditions using HEA 150A S/N 001 coupled to a water-cooled combustion chamber and radiation-cooled nozzle divergent section.

6.6.5.3 TCA Configuration

The HEA tested was identical to that described in paragraph 6.6.4.3. The CC & NA consisted of a water-cooled combustion chamber (P/N 106372) connected to a radiation-cooled nozzle divergent section (P/N 106831).

6.6.5.4 Test Setup and Test Conditions

The test setup and test conditions were as described in detail in paragraphs 7.3.2 through 7.3.5 of the prequalification test specification. The actual test setup used was similar to that illustrated in Figure 6.6.2-1. These tests were essentially identical to PQT-001 through PQT-004A (Runs DY-25 through DY-28), with the exception that a water-cooled chamber was substituted for the flight-weight chamber. No alterations in HEA hardware or settings were made.

6.6.5.5 Test Results

PQT-004.5 was successfully completed by Runs DY-29 through DY-32 from 22 through 26 October 1964 satisfying the requirements of the prequalification test specification. The tank pressures were again varied (see paragraph 6.6.4.5) to achieve a 1.5 mixture ratio during Runs DY-29 and DY-32, a 1.4 mixture ratio during Run DY-32, and a 1.6 mixture ratio during Run DY-31.

Detailed performance data for each of these tests is provided in Table D-1-1 and Figures D-1-29 through D-1-48 of Appendix D-1. These test results are pooled with other data (especially from PQT-001 through -004A from paragraph 6.6.4.5) and discussed in detail in paragraph 6.8.

6.6.6 PQT-004B

6.6.6.1 Test Objectives

The primary test objectives of PQT-004B were to:

1. Demonstrate TCA start capability at low ($0^{\circ}F$) temperature.
2. Determine the influence of low temperature on TCA steady-state and dynamic performance characteristics.

6.6.6.2 Test Summary

The test requirements of PQT-004B given in paragraph 7.2 of the prequalification test specification and the above test objectives were partially achieved during Run DY-33. The test was only a partial success because of an error in test procedure which comprised the steady-state data accuracy. However, the transient data were obtained and are discussed in paragraph 6.8. This test was conducted with HEA S/N 150A-001 and flight-weight CC & NA S/N 005 under altitude and low temperature environmental conditions.

6.6.6.3 TCA Configuration

The HEA was identical to that used for PQT-001 through PQT-004.5 (see paragraph 6.6.4.3). CC & NA S/N 005 which had previously been fired for 135 seconds total during PQT-002 through -004A (Runs DY-26 through DY-28) was used for this test.

6.6.6.4 Test Setup and Test Conditions

The test setup and test conditions are described in detail in paragraphs 7.2.2 through 7.2.5 of the prequalification test specification. The thrust signal versus time used is given in Table 6.6.6-1. The test setup was identical to that used for PQT-001 through PQT-004A with the exception that the propellant and TCA temperature conditioning equipment described in section 8 was employed to achieve nominal $0^{\circ}F$ temperatures. This conditioning equipment is illustrated in Figures 6.6.6-2 through 6.6.6-4.

6.6.6.5 Test Results

PQT-004B was completed by Run DY-33 on 11 November 1964 satisfying the requirements of the prequalification test specification. At TCA ignition, the fuel temperature was $-4^{\circ}F$ and the oxidizer $+4^{\circ}F$. These values increased slightly to $-2^{\circ}F$ and $+10^{\circ}F$, respectively, by the end of the firing. Immediately prior to firing, TCA temperatures varied from a minimum of $5^{\circ}F$ on the combustion chamber to a maximum of $45^{\circ}F$ on the nozzle exit cone. The transient data from this test is discussed in paragraph 6.9.

The detailed steady-state data for this test are provided in Table D-1-1 and Figures D-1-49 through D-1-53 of Appendix D-1. Unfortunately, the accuracy of these data are comprised by the fact that the propellant bleed valves located immediately upstream of the TCA inlets were left open during the entire firing. Since the flowmeters were upstream of this point, the measured flows included the bleed rates as well as the true TCA flow rates. An attempt was made to correct for the bleed flows by observing the rates immediately before and after the firing, and assuming that they varied with the square root of the TCA inlet pressures during the firing.

Table 6.6.6-1

PQT-004B, -005 Thrust Cycle

Command (± 0.5 ma)		Time from Startup (± 0.1 sec)
+ 70	Step	-10.0
+ 70	Startup	0.0
+ 47	Step	5.0
+ 23	Step	10.0
0	Step	15.0
- 23	Step	20.0
- 47	Step	25.0
- 70	Step	30.0
- 47	Step	35.0
- 23	Step	40.0
0	Step	45.0
+ 23	Step	50.0
+ 47	Step	55.0
+ 70	Step	60.0
+ 47	Step	65.0
+ 23	Step	70.0
0	Step	75.0
- 62.5	Step	78.0
- 62.5 ± 7.5	Sinusoidal, 5 cps	80.0
- 62.5	Step	84.0
0	Step	84.0
0 ± 7.5	Sinusoidal, 5 cps	85.0
0	Step	88.0
+ 62.5	Step	89.0
+ 62.5 ± 7.5	Sinusoidal, 5 cps	90.0
+ 62.5	Step	93.0
+ 70	Step	94.0
- 80	Step	99.0
- 70	Step	104.0
+ 80	Step	107.0
+ 70	Step	112.0
- 70	Step	115.0
- 70 to + 70	Ramp	120.0 - 140.0
+ 70 to - 70	Ramp	140.0 to 160.0
- 70	Step	160.0
+ 80	Step	163.0
+ 62.5	Step	168.0
+ 62.5 ± 7.5	Sinusoidal, 5 cps	173.0
+ 62.5	Step	176.0
- 12	Step	177.0
- 12	Shutdown	180.0

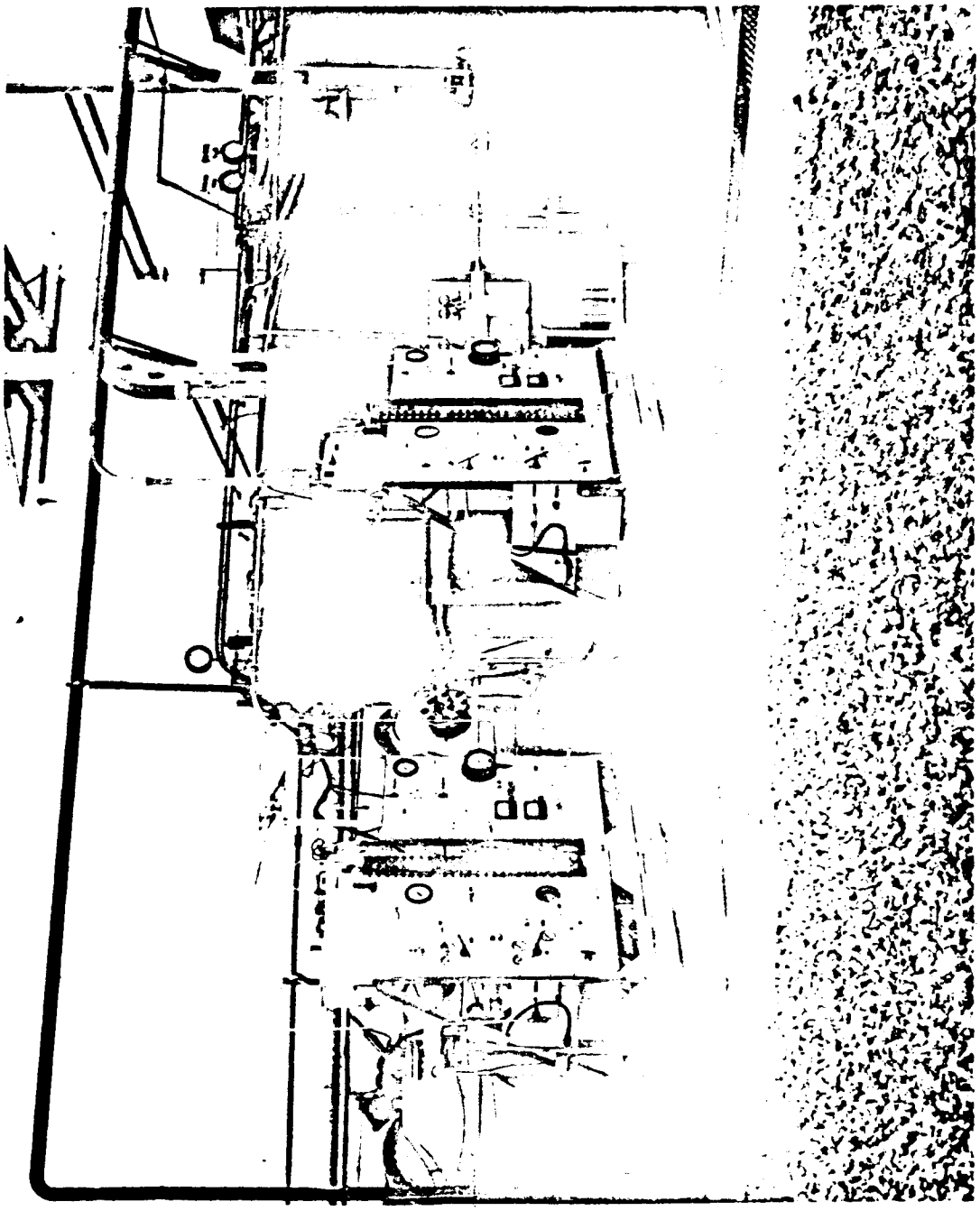

Figure 6.6.6-2. Propellant Temperature Conditioning Equipment as Used on PQT-004B (Run DY-33)

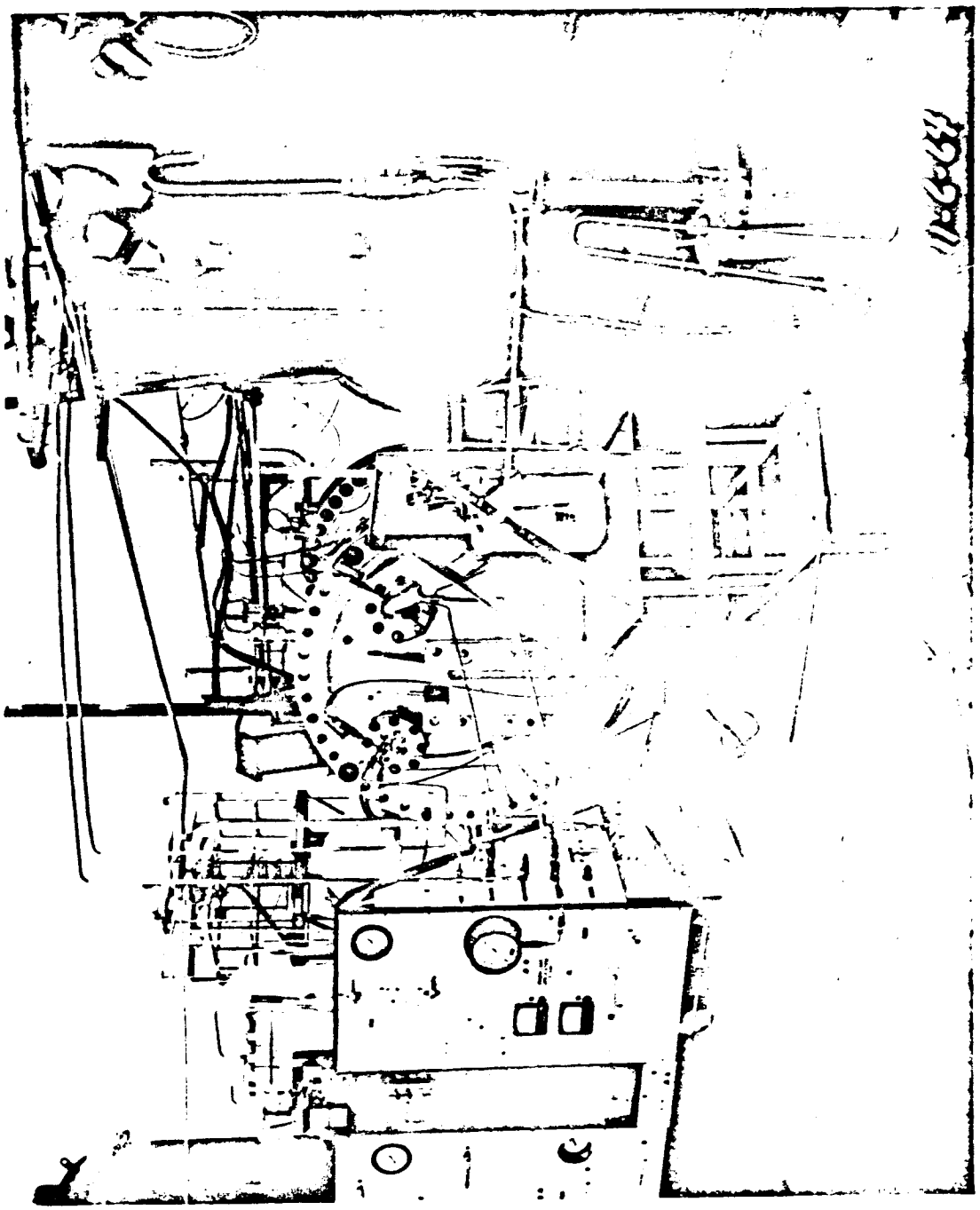

Figure 6.6.6-3. Chamber Temperature Conditioning Equipment for PQT-004B (Run DY-33)

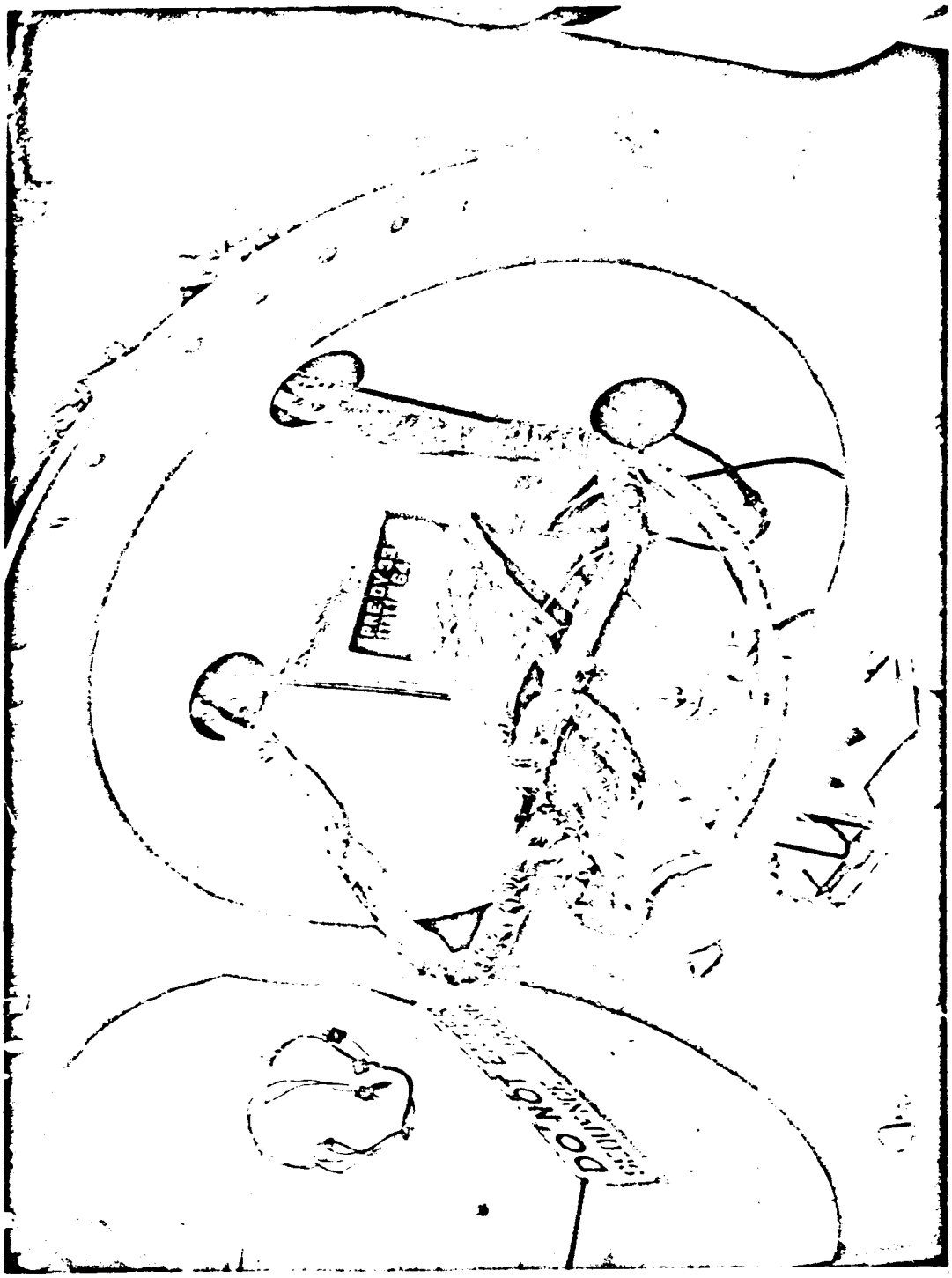

Figure 6.6.6-4. PQT-004B (Run DY-33) Test Setup (With Temperature Conditioning Equipment)

By this technique specific impulse values of approximately 292 seconds at maximum, 291 seconds at mid-range, and 244 seconds at minimum thrust levels were obtained. Except for the minimum thrust point, these values compare favorably with typical values of 292, 288, and 260 seconds at the same respective thrust levels determined from PQT-001 through -004A and -004.5. Mixture ratio data also appeared fairly normal with the exception of a 1.75 value obtained at minimum thrust. It is evident that for a given absolute error in estimating the bleed flow rates, the percentage error in performance determination becomes greater as total flow rates diminish near minimum thrust.

The post-run hardware condition was excellent. This test demonstrated the capability of the TCA to start and operate under minimum temperature conditions.

6.6.7 PQT-007

6.6.7.1 Test Objectives

The primary test objectives of PQT-007 were to:

1. Demonstrate TCA endurance capability at maximum specification values of mixture ratio, thrust, and temperature.

2. Acquire additional data on TCA reliability.

6.6.7.2 Test Summary

The test requirements of PQT-007 given in paragraph 7.5 of the prequalification test specification (TS3-02B) and the above test objectives were successfully achieved by Runs DY-35 through DY-37. These firings were conducted under altitude conditions with HEA 150A S/N 008 and CC & NA S/N 008. This test consisted of three starts of 50, 100, and 150 second durations with a 1.6 mixture ratio, maximum thrust, and 100°F propellant temperatures.

6.6.7.3 TCA Configuration

HEA 150A-008 was the second to be fabricated to the Phase III design (STL Drawing No. 106662-2, B3). The only major deviation from this configuration was the use of a Phase II servoactuator (P/N C104312). The major components used on this HEA are listed below.

Helium Pilot Valve	C104337-1B3	024
Servoactuator	C104312B	C53751
Injector Assembly	106663-2A6	002
Shutoff Valve Piston	106657-1A1	003 & 004
Shutoff Valve Sleeve	106656-1A1	007 & 009
Shutoff Valve Poppet	106798-1A1	009 & 010
Flow Control Valve	106609-1A	002

Phase III altitude CC & NA P/N 106546-1 S/N 008 was used for these firings.

6.6.7.4 Test Setup and Test Conditions

The test setup is defined in detail in paragraphs 7.5.2 through 7.5.4 of the prequalification test specification. The test setup was identical to PQT-004B (Run DY-33) including the propellant conditioning equipment with the exception that heat lamps were placed in the altitude cell to raise the TCA temperatures to the desired levels prior to each test. Figure 6.6.7-1 illustrates the TCA test setup.

Propellant temperatures measured in the propellant feed lines were maintained at 100 ± 5°F during these firings. TCA pre run temperatures varied from 80°F minimum on the HEA to 250°F maximum on the CC & NA. All tests were conducted under altitude conditions. Propellant tank pressures were varied to target a 1.6 mixture ratio.

6.6.7.5 Test Results

PQT-007 was successfully completed by Runs DY-35 through DY-37 on 1 through 2 December 1964 satisfying the requirements of paragraph 7.5 of the prequalification test specification. Since these firings were designed primarily for CC & NA durability demonstration at one fixed thrust level, only limited steady-state data is available from these firings. Table D-1-1 of Appendix D-1 presents the data obtained.

A quick review of the performance data revealed that the specific impulse values obtained (291.3 to 293.5 seconds) were well within the experience of the previous altitude firings. Mixture ratios ranged from 1.565 to 1.625. One point of interest noted during these firings is that the throat area appears to be thermally expanding by approximately 0.6 percent. This is deduced by the observation that C_f increased by 0.6 percent and C* decreased by a like amount over the duration of each firing, while I_{sp} remained essentially constant. Since C* and C_f are both computed from a constant throat area determined by prerun measurements, the observed shifts in these two performance parameters must be attributed to an actual throat change during the firing. Post test measurements of the throat indicated no erosion had occurred, therefore any throat area change was from thermal expansion.

Although the CC & NA successfully survived the required duration, there was evidence of localized overheating in the combustion zone upstream of the nozzle throat in the form of a noticeable bulge in the titanium shell at that point.

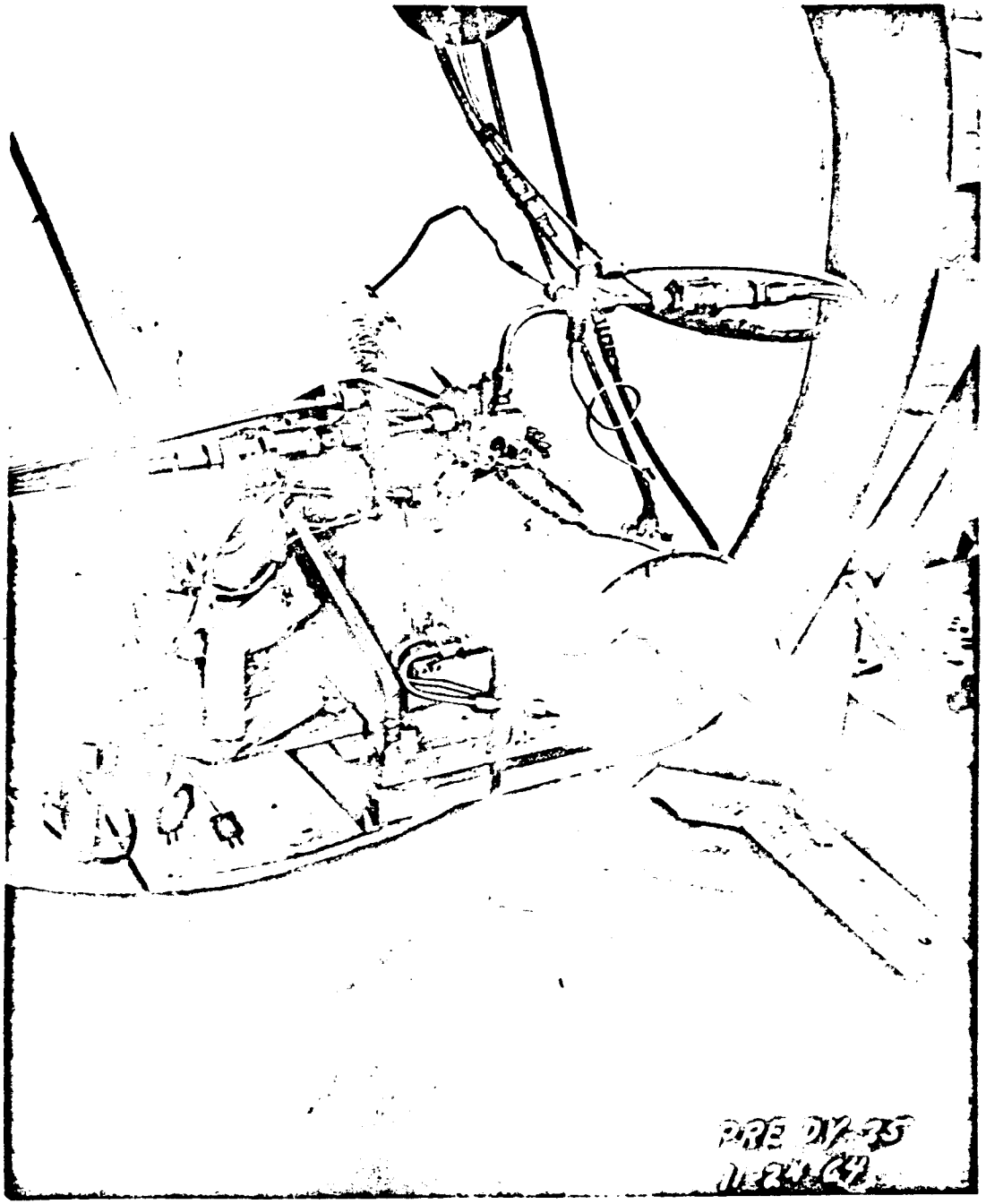

Figure 6.6.7-1. PQT-007 Test Setup
(Run DY-35)

6.6.8 PQT-008

6.6.8.1 Test Objectives

The primary test objectives of PQT-008 were to:

1. Demonstrate TCA endurance capability at maximum specification mixture ratio and temperature, and at minimum thrust.

2. Acquire additional data on TCA reliability.

6.6.8.2 Test Summary

The test requirements of PQT-008 given in paragraphs 7.5.2 through 7.5.4 of the prequalification test specification (TS3-02B) and the above test objectives were successfully achieved by Runs DY-38 through DY-40. These firings were conducted under altitude conditions using HEA 150A S/N 008 and CC & NA S/N 001 with a 1.6 MR, 100°F propellant temperatures, and minimum thrust for 480 seconds.

6.6.8.3 TCA Configuration

HEA S/N 150A-008 used for this test was previously described in paragraph 6.6.7.2. The HEA was assembled with altitude CC & NA S/N 001 (P/N 106546-1A4).

6.6.8.4 Test Setup and Test Conditions

The test setup was as described in detail in paragraphs 7.5.2 through 7.5.4 of the prequalification test specification. Prior to the first run (DY-38), the TCA was conditioned to temperatures ranging from -30°F to 28°F with the propellant temperatures maintained at 100 ± 5°F during the firing. For the next two runs (DY-39 and -40), the propellants were again conditioned to maximum temperature (100 ± 5°F), but no attempt was made to condition the TCA. Propellant tank pressures were adjusted to target a 1.6 mixture ratio. Each of the three firings were performed at minimum thrust for a duration of 160 seconds for a total of 480 seconds.

6.6.8.5 Test Results

PQT-008 was successfully completed by Runs DY-38, -39, and -40 on 4 through 7 December 1984 satisfying the requirements of the prequalification test specification. The amount of steady-state data available was minimal because only one thrust level was tested. Detailed performance data are reported in Table D-1-1 of Appendix D-1.

Difficulties were encountered in attempting to target the 1.6 mixture ratio on these firings. During Run DY-38 mixture ratios ranged from 1.70 to 1.73. Tank pressures were readjusted prior to Run DY-39 resulting in a 1.55 to 1.57 mixture ratio range. The tank pressures were again readjusted in an effort to raise mixture ratio, but a lower 1.52 to 1.55 mixture ratio range resulted. Post-test disassembly of the flow control valve inlet filters showed evidence of foreign material and partial blockage which could explain the mixture ratio shifts.

Another item of note during these firings was the variation in vacuum specific impulse during each test. Performance data slices were obtained at 5-10, 75-80, and 155-160 seconds after ignition. Typical values of I_{sp} at these times were 249.6, 259.3, and 260.4 seconds, respectively. The latter value agrees closely with minimum thrust performance obtained during previous altitude firings wherein minimum thrust steps were preceded by periods of operation at midrange and maximum thrust levels.

The apparent explanation for this performance increase with time is the thermal losses from the combustion gases to the initially cold CC & NA result in a relatively long period of time required to achieve equilibrium heat transfer condition and performance. At higher thrust levels this phenomenon has also been observed, but the time required to reach steady-state was much shorter due to the higher heat transfer rates. Since the typical Surveyor mission profile provided in JPL Specification SAM-50255-DSN-C indicates a period of midrange and maximum thrust operation prior to minimum thrust operation, it is likely that the low initial performance levels experienced during these firings would not be experienced in flight.

6.6.9 PQT-010

6.6.9.1 Test Objective

The primary objective of PQT-010 was to determine the TCA dynamic throttling characteristics at ambient temperature using a Phase III servoactuator.

6.6.9.2 Test Summary

The test requirements of PQT-010 given in paragraph 7.6 of the prequalification test specification (TS3-02B) and the above test objective were successfully achieved by Runs DY-41 through DY-43.

Although this was primarily a dynamic response test, limited steady-state data were also obtained. The item tested was Phase II HEA S/N 004 fitted with a radiation-cooled expansion skirt.

6.6.9.3 TCA Configuration

Phase II HEA S/N 150A-004 used in this test was previously described in paragraph 6.6.1.3, except for the following retrofit and rework items:

1. Servoactuator P/N C219217, (S/N C55394) replaced P/N C105312-1, (S/N C53348).
2. Piston P/N 106657-1, Sleeve P/N 106656-1A1, and Poppet P/N 106798-1, replaced P/N 103948-3B1, P/N 103947-3B1, and P/N 103946-1A, respectively, in the shutoff valves.
3. Bal Seals P/N 200-20, P/N 200-12, 200-10, and 200-15 Bal replaced omniseals R10105-020 A1N, R105J-370A1Q, and R10105-015A1N, respectively.
4. Inserts P/N 105133-2 and P/N 1060907-2 replaced inserts P/N 105133-1A2 and 105131-1, respectively, in the flow control valves.

These retrofit items were accomplished with the objective of making HEA 150A-004 functionally identical to a Phase III HEA, especially with respect to throttling characteristics. A water-cooled combustion chamber (P/N 106372) and a radiation-cooled skirt (P/N 106831) were mounted on the HEA for these firings.

6.6.9.4 Test Setup and Test Conditions

The test setup for PQT-010 is described in paragraphs 7.6.2 through 7.6.5 of the prequalification test specification and is illustrated in Figure 6.6.9-1. The TCA was fired at altitude with propellant tank pressures set at the nominal 720 psia.

The thrust signal-time program used was the PQ-1 program given in Table 6.6.3-2.

6.6.9.5 Test Results

PQT-010 was successfully completed by Runs DY-41 through DY-43 on 10 through 11 December 1964 in accordance with paragraph 7.6 of the prequalification test specification. Steady-state performance data were again limited because of the dynamic thrust cycle used. This thrust cycle was run in a somewhat reversed order with the 115.8-second duration portion (Profile C of PQ-1) being used first on Run DY-41 and the 52 and 70-second segments (Profiles A and B of PQ-1) following on Runs DY-42 and DY-43.

The detailed steady-state data are presented in Table D-1-1 and Figures D-1-54 through D-1-59 of Appendix D-1. Specific impulse values obtained ranged from 291.6 seconds at 154.8 lbs vacuum thrust to 255.5 seconds at 27.5 lbs vacuum thrust. These values are well within JPL Specification SAM-50255-DSN-C, and agree favorably with previous altitude tests. Mixture ratio varied from 1.476 at minimum thrust to 1.535 at maximum thrust, again well within prescribed limits.

6.6.10 PQT-009.5

6.6.10.1 Test Objective

The primary objective of PQT-009.5 was to determine the TCA dynamic throttling characteristics at minimum (0°F) temperature using a Phase III servoactuator.

6.6.10.2 Test Summary

The test requirements of PQT-009.5 given in paragraph 7.6 of the prequalification test specification (TS3-02B) and the above test objective were successfully achieved by Runs DY-44 through DY-46. These firings were conducted under altitude conditions with HEA 150A S/N 00- and a water-cooled CC & NA. The test item was identical to that used for PQT-010. The test conditions were altered by conditioning the servoactuator and propellants to minimum temperature (0°F nominal).

6.6.10.3 TCA Configuration

The TCA configuration was identical to that defined for PQT-010 (see paragraph 6.6.9.3).

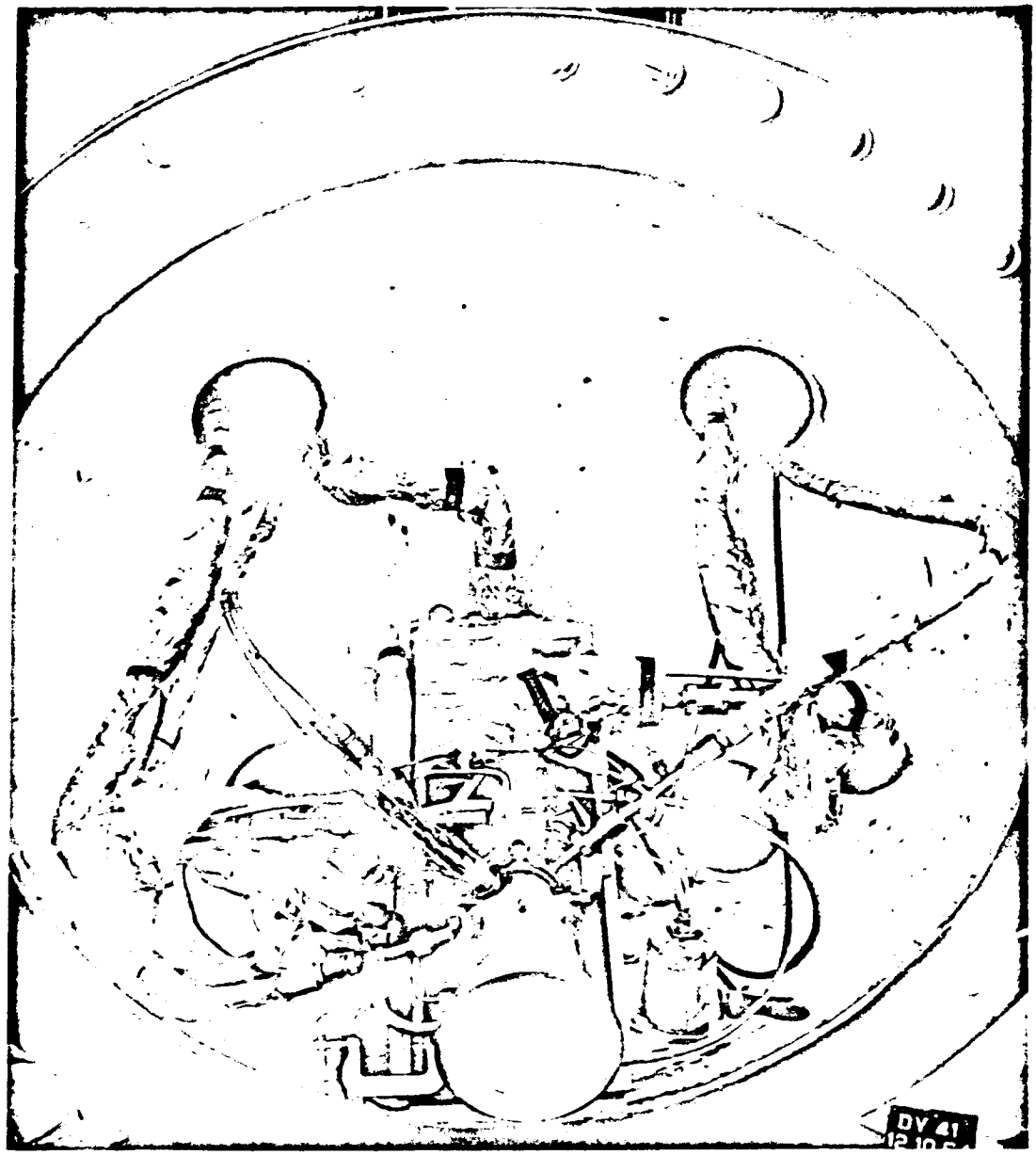

Figure 6.6.9-1. PQT-010 Test Setup

6.6.10.4 Test Setup and Test Conditions

The test setup was identical to that described in paragraph 6.6.9.4 except propellant and TCA conditioning equipment were used. Figure 6.6.10-1 illustrates the method for cooling the servoactuator by blowing vaporized liquid nitrogen over the exterior surfaces. During this test series, the propellant temperatures varied from -20°F to +14°F and servoactuator temperature varied from 16°F to 33°F. Propellant tank pressures were set at the 720 psia nominal level. The thrust signal-time program used is given in Table 6.6.3-2.

6.6.10.5 Test Results

PQT-009.5 was successfully completed by Runs DY-44 through DY-46 on 15 through 16 December 1964 satisfying the test requirements of the prequalification test specification. Only limited steady-state performance data are available because of the dynamic thrust cycle used.

The detailed data are provided in Table D-1-1 and Figures D-1-60 through D-1-64 of Appendix D-1. Specific impulse values at maximum thrust varied from 290.2 to 293.2 seconds and were comparable to the values obtained from PQT-010 (Runs DY-41 through DY-43). However, at 23 lbs thrust the performance was slightly lower than PQT-010 varying from 247.8 to 253.6 seconds. This may be explained by the lower flow rates and higher mixture ratios which resulted from the lower propellant temperatures.

Mixture ratios obtained during these firings were higher than predicted values based solely on the propellant vapor pressure and density changes, especially at the lower thrust levels. A 1.733 mixture ratio at 23.6 lbs thrust was obtained on Run DY-45. Correcting this value to standard conditions (720 psia and 70°F) yields a 1.678 mixture ratio compared to a 1.480 standard mixture ratio at 25.6 lbs thrust measured during Run DY-43, the ambient temperature firing. It is concluded that the increase in fuel viscosity at low temperature results in a boundary layer growth at the flow control valve throat, thereby lowering the discharge coefficient, C_D. The net result is a decrease in fuel flow rate with decreasing temperature. Paragraph 6.5 discusses the temperature extreme tests conducted at IRTS, and describes this phenomenon in detail.

6.6.11 PQT-005

6.6.11.1 Test Objectives

The primary objectives of PQT-005 were to:

1. Determine the test-to-test TCA vacuum performance reproducibility; and, determine TCA-to-TCA vacuum performance reproducibility.

2. Demonstrate TCA endurance capability.

3. Acquire additional data on TCA reliability.

6.6.11.2 Test Summary

The test requirements of PQT-005 given in paragraph 7.4 of the prequalification test specification (TS3-02B) and the above test objectives were partially achieved by Runs DY-47 through DY-49. Runs DY-47 and -48 were conducted under altitude conditions with HEA 150A S/N 010 and CC & NA S/N 010. For Run DY-49, a water-cooled combustion chamber and radiation-cooled skirt were used. These tests were for the most part unsuccessful in accomplishing their major objectives because a metal chip caught in the fuel side of the injector degraded the injection pattern and resultant performance.

Figure 6.6.10-1. Test Setup for Cooling Servoactuator on PQT-009.5

6.6.11.3 TCA Configuration

Phase III HEA S/N 010 (P/N 106662-2B3) used for these tests had the following major components:

Component	P/N	S/N
Injector Assembly	106663-2A	004
Flow Control Valve	106609-1B1	004
Helium Pilot Valve	C104337-1B3	026
Shutoff Valve	106662-2B3	010
Servoactuator	C219217	C55394

Flight-weight altitude CC & NA S/N 010 (P/N 106545-1A) was used during Runs DY-47 and DY-48. This chamber was replaced by a water-cooled combustion chamber (P/N 106372) with a radiation-cooled skirt (P/N 106831) for Run DY-49.

6.6.11.4 Test Setup and Test Conditions

The test setup is described in detail in paragraphs 7.4.2 through 7.4.5 of the prequalification test specification. The three runs were all conducted under altitude conditions and near standard propellant temperatures and pressures (70°F and 720 psia). The thrust-time profile used was essentially the same as used on PQT-001, -002, -003, -004A, and -004B successively plus an added four-second long firing just before -004B. Thus, the thrust signal-time program used was Profiles No. 1, 2, 3, and 1 (repeated) of Table 6.6.4-1 followed by a four-second firing at mid-thrust, and concluded with a 180-second firing per Table 6.6.6-1.

The four-second firing was inserted to assure filled propellant passages down to the shutoff valves prior to the next restart. This was done to obtain applicable startup data on the 180-second run that followed.

6.6.11.5 Test Results

PQT-005 was completed by Runs DY-47 through DY-49 on 18 through 21 December 1964 satisfying the requirements of paragraph 7.4 of the prequalification test specification. With the exception of mixture ratio and startup and shutdown performance characteristics determination, these firings were unsuccessful in obtaining valid altitude performance data or in demonstrating CC & NA durability under nominal performance conditions.

Table D-1-1 and Figures D-1-65 through D-1-76 of Appendix D-1 present detailed steady-state performance data for these firings. A review of the vacuum specific impulse data indicated highly nonreproducible performance values during these tests. For example, during Run DY-49 specific impulse varied from 273.4 to 283.3 seconds at maximum thrust. Similar relatively large performance variations were noted for Runs DY-47 and DY-48A, B, and C. A post-test visual inspection of the CC & NA after the testing revealed approximately a 60 degree sector over which the CC & NA temperatures were significantly lower than the surrounding area. This pattern may be clearly seen in the nozzle shown in Figure 6.6.11-1.

Immediately after Run DY-49, the TCA was removed from the test stand and shipped directly to IRTS. There a HEA performance test was conducted at sea level with a water-cooled CC & NA (refer to Run C2-685 discussed in paragraph 6.7.5). This test substantiated the abnormally low and erratic performance experienced at JPL/ETS. An injector water flow visual check was subsequently performed and revealed a void in the fuel flow pattern equivalent to approximately 60 degrees of the total circumference of the fuel injector gap.

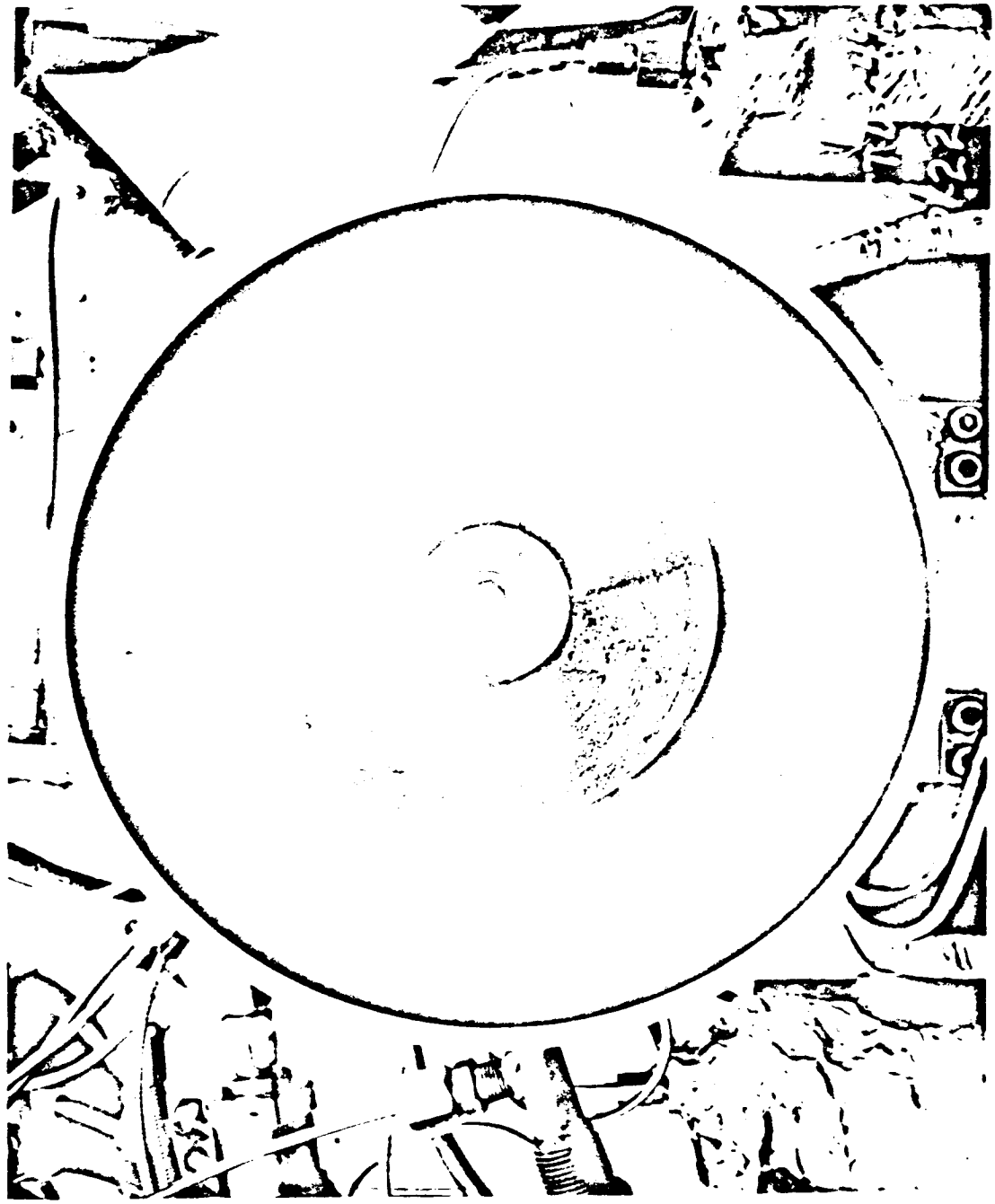

Figure 6.6.11-1. Post-Test Aft View of CC & NA After FQT-005

Disassembly of the injector fuel pintle resulted in the discovery of a small metal chip (approximately 0.020 inches across) located in the annulus between the pintle and sleeve near the fuel injection gap. The chip was removed, and another HEA performance test was conducted (refer to Run C2-686 discussed in paragraph 6.7). Performance data obtained from this test was essentially normal compared to other HEAs.

The conclusion reached is that the metal chip in the injector disturbed the fuel injection pattern sufficiently to impair TCA combustion efficiency during PQT-005. These tests dramatically demonstrated the need for stringent cleanliness and inspection procedures during TCA fabrication, assembly, handling, and testing.

6.6.12 Photo Coverage Test

The sole purpose of this test (Run DY-34) was to obtain photographic coverage of a sea level firing. Instrumentation was kept to a minimum, and no steady-state data reduction was attempted. HEA S/N 001 and sea level CC & NA S/N 011 were used.

6.7 IRTS Steady-State Performance Tests

The MIRA 150A steady-state performance data obtained from the STL Inglewood Rocket Test Site (IRTS) is presented in this paragraph. Rather than include all available data (which would have added to the volume of this paragraph without contributing significantly to its value) representative data from different HEAs were selected.

Test data deliberately eliminated from this sample fell in one or more of the following categories:

1. N_2O_4 was used rather than MON as the oxidizer.
2. Downstream pressure rather than head end chamber pressure was used to compute performance. This alternate measurement was made on all tests prior to Run C2-587. (Head end chamber pressure must be used in order to establish a correlation between ablative-cooled and water-cooled CC & NA firings, since downstream chamber pressure is not measured during the latter.)
3. The test was conducted under temperature extremes. (These data are reported in paragraph 6.5).
4. The HEA was operating in the out-of-specification, high injection pressure mode. (This bi-stable operation is described in paragraph 6.2.2).
5. The HEA was not previously calibrated.
6. Known instrumentation problems made the test data unreliable.

On this basis a total of 16 sea level firings on six different HEAs were selected. The performance data obtained from the IRTS were not in general as repeatable as that acquired at the JPL/ETS under vacuum conditions. The following factors account for the difference:

1. The microsadic digital acquisition system at JPL/ETS is more accurate and has better precision than the IRTS analog system. Even strip chart reading errors become significant in the low thrust range with the latter.
2. The sea level combustion chamber data may not always be valid at chamber pressures from 20 to 26 psia because choked flow may not be achieved. (Theoretically, at a ratio of ambient pressure (P_o) to chamber pressure (P_c) less than $\left(\frac{2}{\gamma+1}\right)^{\frac{\gamma}{\gamma-1}}$, the flow will not be sonic at the throat. If P_o is 14.7 psia, γ= 1.24 (per Table 7.1.2-1), P_c must be at least 26.4 psia for choked flow. However, the actual value of P_c below which throat flow is not sonic is affected by the actual γ, the nozzle shape in the throat region, and the fact that the low P_c value may be achieved by slowly decreasing P_c from higher values. The lack of perturbations in some internal ballistic parameters such as C^* at chamber pressures as low 19 psi indicates flow may actually be sonic at this pressure on some sea level tests).
3. During most of the JPL/ETS performance tests, end-to-end or transducer calibrations were accomplished before and after each test. Transducer calibrations are performed less frequently at the IRTS.

4. Difficulties with the patch panel were often experienced at the IRTS resulting in short-term drift in the measurements. A new and superior patch system was subsequently installed and used on all tests after Run C2-661.

Rather than grouping the test data by test number or test objectives as was done in paragraph 6.6 (where the firings were conducted in accordance with the prequalification test specification), the IRTS data are organized herein according to HEA serial number.

6.7.1 HEA 150A S/N 005 - Runs C2-591, C2-592, and C2-596

6.7.1.1 Test Objectives

The primary objective of Runs C2-591 and C2-596 was to establish sea level performance at as near standard inlet conditions as possible. Run Test C2-592C was conducted as part of the testing described by paragraph 3.6.2.3 of the development test plan. This test was designed to establish performance variation with inlet pressures varying from 700-740 psia at ambient temperature.

6.7.1.2 TCA Configuration

HEA MIRA 150A-005 was built to the basic Phase II configuration (Drawing No. 105461-1A1) plus several Phase III retrofit parts. The following major components were installed on the HEA for the three firings:

Component	P/N	S/N
Helium Pilot Valve	C104337-1	019
Servoactuator	C104312-1	C53747
Injector Assembly	105462-1A1	005
Shutoff Valve Piston	106657-1A1	N.A.
Shutoff Valve Sleeve	106656-1A1	N.A.
Shutoff Valve Poppet	106798-1A1	N.A.
Flow Control Valve	105466-2	N.A.

The following Phase III parts were retrofitted:

1. Piston P/N 106657-1A1, Sleeve P/N 106656-1A1, and Poppet P/N 106798-1A1 replaced P/N 103948-3B1, P/N 103947-3, P/N 103946-1A, respectively, in the shutoff valves.

2. Bal Seals P/N 200-20, 200-12, 200-10, and 200-15 replaced omniseals R10105-020A1N, R105J-370AIQ, R105J-242IQ, and R10105-015A1N, respectively.

3. Pintle P/N 106905-2, Insert 105133-2, Insert 106907-2, Insert 105131-2A3 replaced P/N 105116-3, 105133-1, 105132-3A1, and 105131-1A3, respectively, in the flow control valve.

A water-cooled sea level CC & NA (P/N 106372) was used for these tests.

6.7.1.3 Test Setup and Test Conditions

The typical HEA water-cooled test setup used at the IRTS is illustrated in Figures 6.7.1-1 and 6.7.1-2. The HEA is rigidly mounted on a test fixture. Thrust measurements were not made on the fixture. Typical measurements include propellant and cooling water flow rates, head end and nozzle end chamber pressures, injection pressures, propellant inlet pressures, cooling water and propellant temperatures, servoactuator and helium pilot valve electrical signals, and servoactuator position.

Figure 6.7.1-1. Typical HEA Performance Test Setup at the IRTS (Left Quarter View)

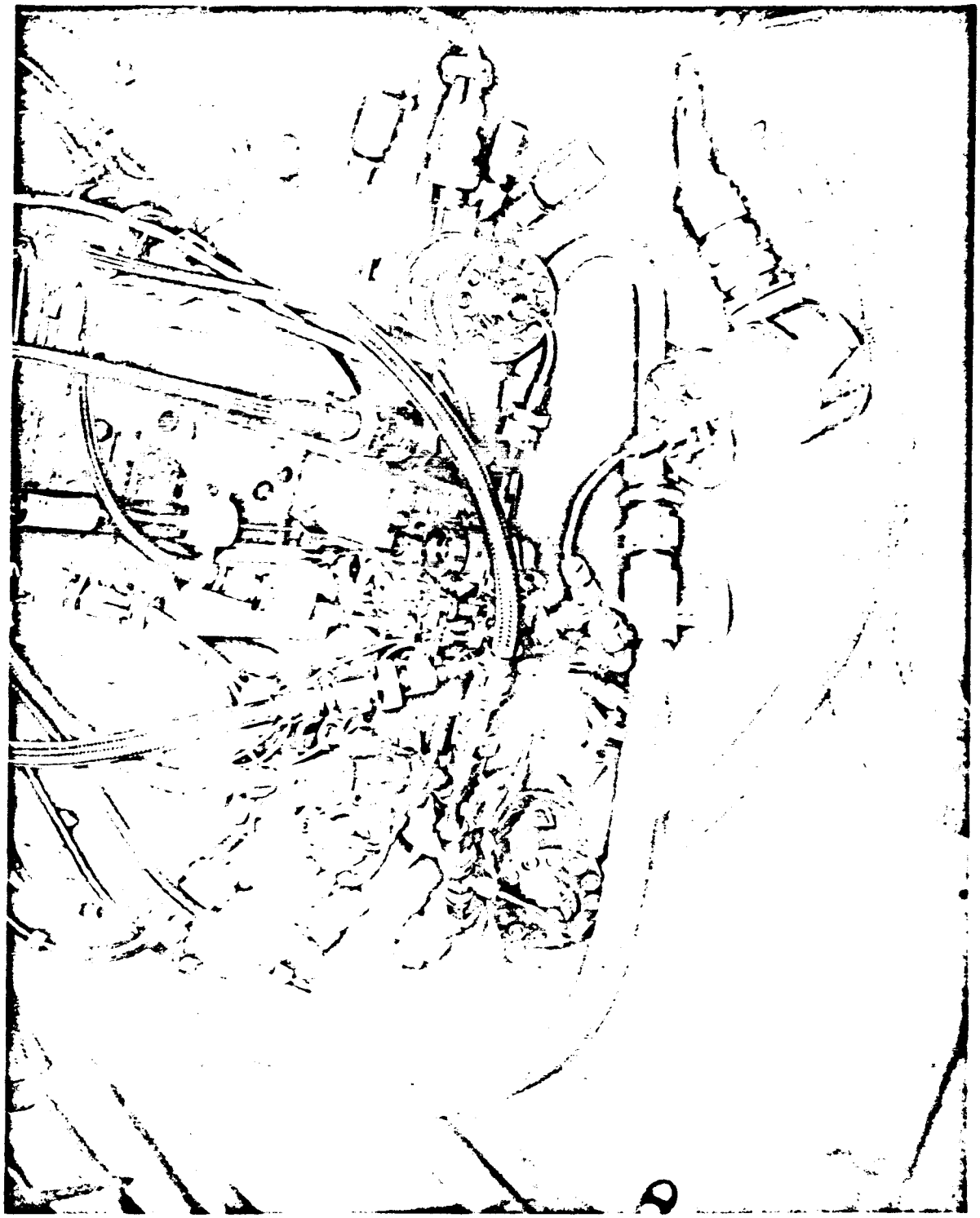

Figure 6.7.1-2. Typical HEA Performance Test Setup at the IRTS (Right Quarter View)

The three tests were all conducted under sea level ambient pressure and temperature conditions. No attempt was made to temperature condition the HEA or propellants. For all three tests the manual switch on the tape programmer control unit was used to achieve step throttling.

6.7.1.4 Test Results

Detailed test data from these firings are reported in Table D-2-1 and Figures D-2-2 through D-2-4 of Appendix D-2. Mixture ratio values at standard inlet conditions (720 psia and 70°F) ranged from 1.459 to 1.523 over the full thrust range. Characteristic velocity varied from 4928 fps at minimum thrust to 5408 fps at mid-range thrust after applying the water cooling correction factors. The shape of the characteristic velocity versus nozzle stagnation pressure curve (Figure D-2-3) is somewhat unusual, since the maximum value was achieved at 75 psia chamber pressure, and then decreased by approximately 130 fps at 110 psia chamber pressure. The reason is unknown for this departure from the normal characteristic of slightly increasing C* values with increasing chamber pressure above 66 psia. Other performance characteristics appeared normal.

6.7.2 HEA 150A S/N 007 - Run C2-618 and C2-621

6.7.2.1 Test Objectives

Run C2-618 was conducted as a performance verification test prior to the formal acceptance firing. Test C2-621 was conducted as an HEA performance acceptance firing.

6.7.2.2 TCA Configuration

HEA 150A-007 was the first unit fabricated to the Phase III configuration (Drawing No. 105662-2B3). The following major components were installed on the HEA during these firings:

Component	P/N	S/N
Helium Pilot Valve	C104337-1B3	023
Servoactuator	C219217-A	C55390
Injector Assembly	106609-1B1	001
Shutoff Valve Piston	106657-1A1	001 & 002
Shutoff Valve Sleeve	106656-1A1	003 & 006
Shutoff Valve Poppet	106798-1A1	007 & 008
Flow Control Valve	106609-1B1	001

A sea level, water-cooled CC & NA was used for these tests.

6.7.2.3 Test Setup and Test Conditions

The test setup was identical to that described in paragraph 6.7.1.3. The HEA was fired under sea level ambient pressure and temperature conditions. Propellant tank pressures were set at the nominal 720 psia. The manual step switch was used to achieve throttling during Run C2-618, and an AT-1 acceptance test thrust program tape (see Table 4.4-1) was used for Run C2-621.

6.7.2.4 Test Results

Detailed test data are provided in Table D-2-1 and Figures D-2-5 through D-2-7 of Appendix D-2. Standard mixture ratio ranged from 1.487 to 1.515 during the acceptance firing (Acceptance Test Specification TS3-01B limits are 1.50 ± 0.03). Characteristic velocity values ranged from 5026 fps at 33.9 psia chamber pressure to 5351 fps at 113 psia chamber pressure. These performance values are comparable to the JPL/ETS test data reported in paragraph 6.6.

6.7.3 HEA 150A S/N 008 - Runs C2-680, C2-709, and C2-710

6.7.3.1 Test Objectives

The primary objectives of these tests were to:

1. Demonstrate the capability of the TCA to meet specification requirements after simulated missile boost phase vibration.

2. Acquire additional data on TCA reliability.

6.7.3.2 TCA Configuration

The configuration of HEA S/N 150A-008 is described in paragraph 6.6.7.3, with the exception that Phase III Servoactuator P/N C219217A (S/N C55398) replaced Phase II servoactuator P/N 104312B (S/N C53751). A water-cooled CC & NA was used during Runs C2-680 and C2-710. Altitude CC & NA P/N 106546-1 (S/N 007) was installed for Run C2-709.

6.7.3.3 Test Setup and Test Conditions

The test setup was identical to that described in paragraph 6.7.1.3. Runs C2-680 and C2-710 were performed under sea level ambient pressure conditions using the AT-1 thrust cycle. For Run C2-709 the propellant tank pressures were adjusted to target a 1.6 mixture ratio and the thrust level was fixed at the minimum level.

The three runs were conducted as a portion of the PQT-011 vibration test sequence described in paragraph 7.7 of the prequalification test specification, and are discussed further in paragraph 6.10.2. The specific purpose of Runs C2-680 and C2-710 was to determine whether vibration had any influence on HEA performance characteristics. Run C2-680 was conducted prior to the vibration test described in paragraph 6.10.2, and Runs C2-709 and -710 were conducted after exposure to the vibration environments. Run C2-709 was a 300-second, post-vibration, CC & NA durability test conducted in three starts of 15, 50, and 235 seconds duration.

6.7.3.4 Test Results

Table D-2-1 and Figures D-2-8 through D-2-10 of Appendix D-2 provide detailed test data.

Figures 6.7.3-1 through 6.7.3-3 provide a comparison of the pre-vibration and post-vibration performance characteristics of the HEA. The minor performance differences indicated therein are considered to be within the normal data scatter and are not significant. The vibration levels imposed had no effect on HEA performance.

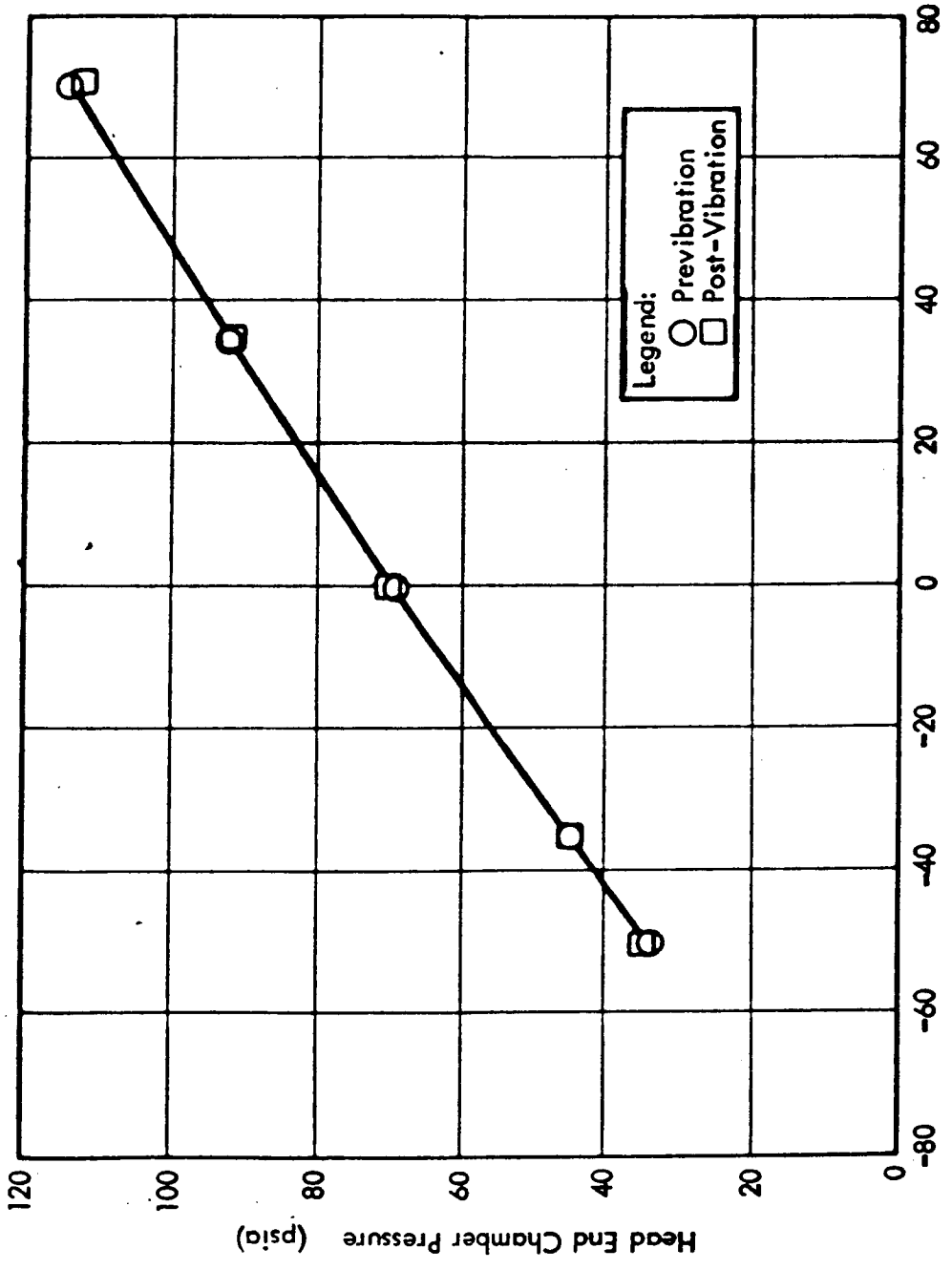

Figure 6.7.3-1. Chamber Pressure Data for Previbration and Post-Vibration Firings Using HEA S/N 150A-008

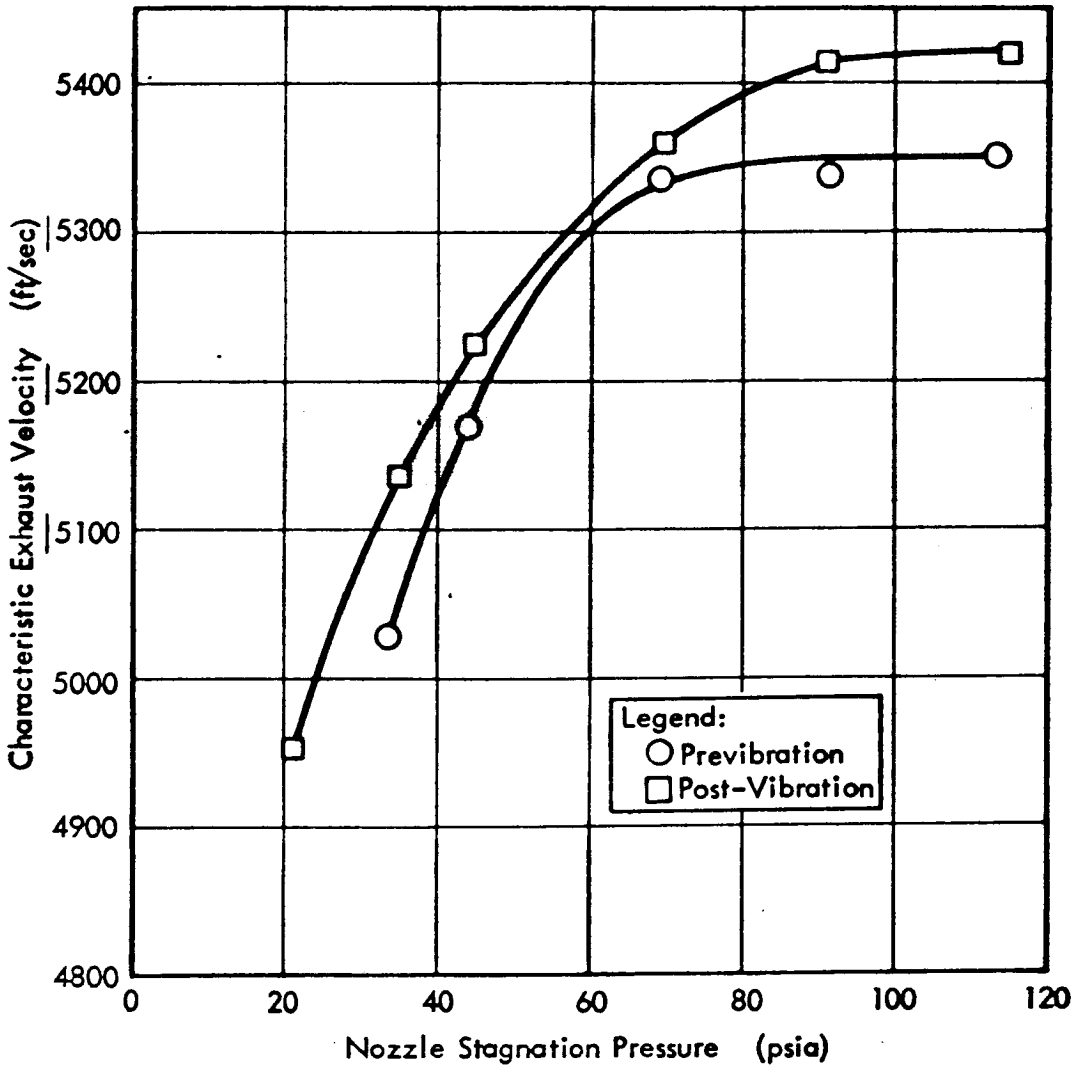

Figure 6.7.3-2. Characteristic Exhaust Velocity Data for Previbration and Post-Vibration Firings Using HEA S/N 150A-008

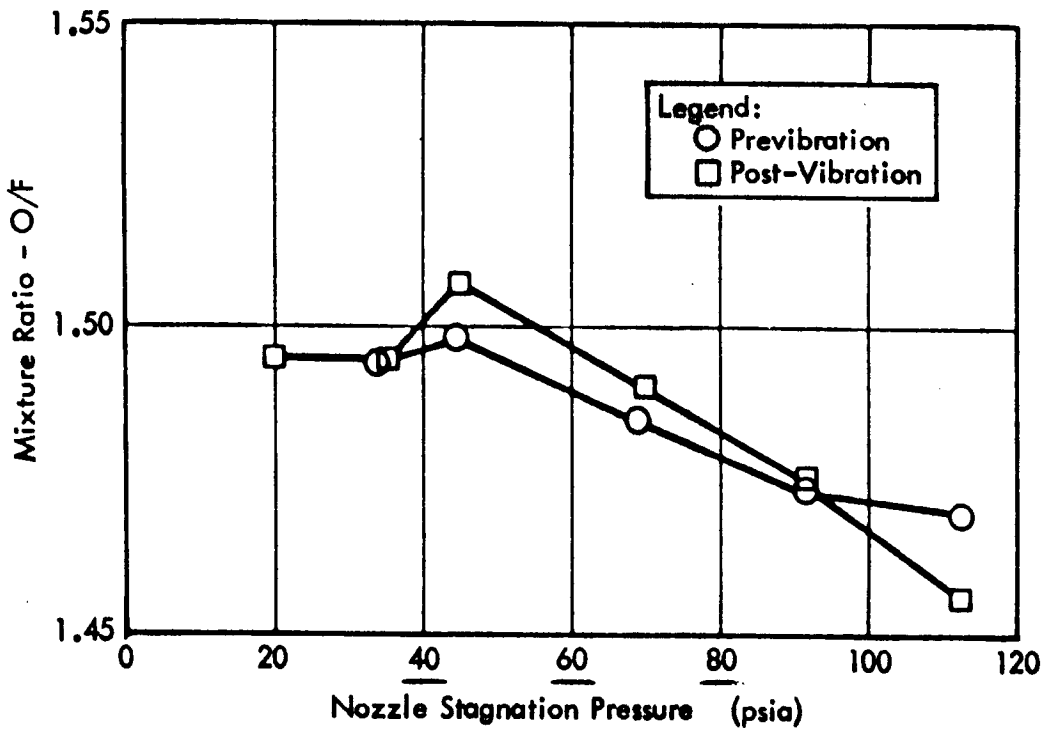

Figure 6.7.3-3. Standard Mixture Ratio Data for Previbration and Post-Vibration Firings Using HEA S/N 150A-008

The post-test condition of the CC & NA after Run C2-709 (the post-vibration CC & NA durability test) was satisfactory. The CC & NA condition is discussed in detail in paragraph 6.4.1.

6.7.4 HEA 150A S/N 009 - Runs C2-682 and C2-683

6.7.4.1 Test Objectives

Run C2-682 was conducted to check HEA performance acceptance test. Run C2-683 was an HEA acceptance test conducted in accordance with the acceptance test specification (TS3-01B).

6.7.4.2 TCA Configuration

HEA 150A-009 was fabricated to the Phase III configuration (Drawing No. 106662-2B3). The following major components were installed on the HEA during these firings:

Component	P/N	S/N
Helium Pilot Valve	C104337-1B3	025
Servoactuator	C219217A	C55390
Injector Assembly	106663-2A	003
Shutoff Valve Piston	106657-1A1	005 & 006
Shutoff Valve Sleeve	106656-1A1	010 & 011
Shutoff Valve Poppet	106798-1A1	013 & 014
Flow Control Valve	106609-1A	003

A water-cooled CC & NA was used for both the firings.

6.7.4.3 Test Setup and Test Conditions

The test setup was identical to that described in paragraph 6.7.1.3. The HEA was operated under sea level ambient pressure and temperature conditions. Propellant tank pressures were set at the nominal 720 psia level. Throttling was controlled by a manual step switch during Run C2-682 and by the AT-1 thrust profile for Run C2-683.

6.7.4.4 Test Results

Detailed test data are provided in Table D-2-1 and Figures D-2-11 through D-2-13 of Appendix D-2. Standard mixture ratio varied from 1.478 to 1.560 compared to an allowable variation of 1.470 to 1.530. Although the 1.560 value is above the specification maximum, it occurred only at the minimum thrust level; the mixture ratio at all other thrust levels was well within prescribed limits.

This HEA could easily have been readjusted to bring the low thrust mixture ratio within specification limits without seriously affecting the values at the higher thrust levels. This is attributed to the fact that for a 5% change in mixture ratio at minimum thrust, only a 1% change would be experienced at maximum thrust because of the five to one throttling range.

Characteristic velocity data were well within previous experience varying from 4848 fps at minimum thrust to 5326 fps at maximum thrust.

6.7.5 HEA 150A S/N 010 - Runs C2-685, C2-686, and C2-689

6.7.5.1 Test Objective

The primary test objective of Runs C2-685, C2-686, and C2-689 was to investigate the cause of the abnormal TCA performance experienced during the PQT-005 test series at the JPL/ETS (refer to paragraph 6.6.11).

6.7.5.2 TCA Configuration

The configuration of HEA S/N 010 is described in paragraph 6.6.11.3. For the subject IRTS runs, it was mated to a water-cooled CC & NA.

6.7.5.3 Test Setup and Test Conditions

The test setup is described in paragraph 6.7.1.3. All three runs were conducted under sea level ambient pressure and temperature conditions using a manual step switch for throttle control.

6.7.5.4 Test Results

Detailed test results for Runs C2-685, and C2-689A are provided in Table D-2-1 and Figures D-2-14 through D-2-16 of Appendix D-2. Run C2-685 was conducted immediately after the last PQT-005 firing (Run DY-49) at the JPL/ETS without altering the HEA. The characteristic velocity was lower than normal as well as being erratic.

After Run C2-685 an injector water flow pattern check was conducted. Although the oxidizer flow appeared normal, the fuel injection pattern exhibited a 60° void around the circumference of the fuel gap. A metal chip 0.020 inches across was subsequently found lodged near the fuel injection gap between the pintle and sleeve. The fuel pintle was removed and the chip taken out. Run C2-686 was then conducted resulting in normal HEA performance. Since the fuel injection pressure drop was low on this test, a readjustment was made prior to Run C2-689A. The performance data before and after the chip removal is shown in Figure 6.7.5-1.

6.7.6 HEA 150A S/N 011 - Run C2-676

6.7.6.1 Test Objective

Run C2-676 was conducted primarily as an HEA performance checkout firing with a water-cooled CC & NA.

6.7.6.2 TCA Configuration

HEA S/N 150A-011 was fabricated to the Phase III configuration (Drawing No. 106662-2), and was assembled with the following major components:

Component	P/N	S/N
Helium Pilot Valve	C104337-1B3	015
Servoactuator	C219217A	C55395
Injector Assembly	106663-2B1	005
Shutoff Valve Piston	106657-1A1	009 & 010
Shutoff Valve Sleeve	106656-1A1	005 & 008
Shutoff Valve Poppet	106798-1A1	017 & 018
Flow Control Valve	106609-1B1	005

A water-cooled CC & NA was used for this test.

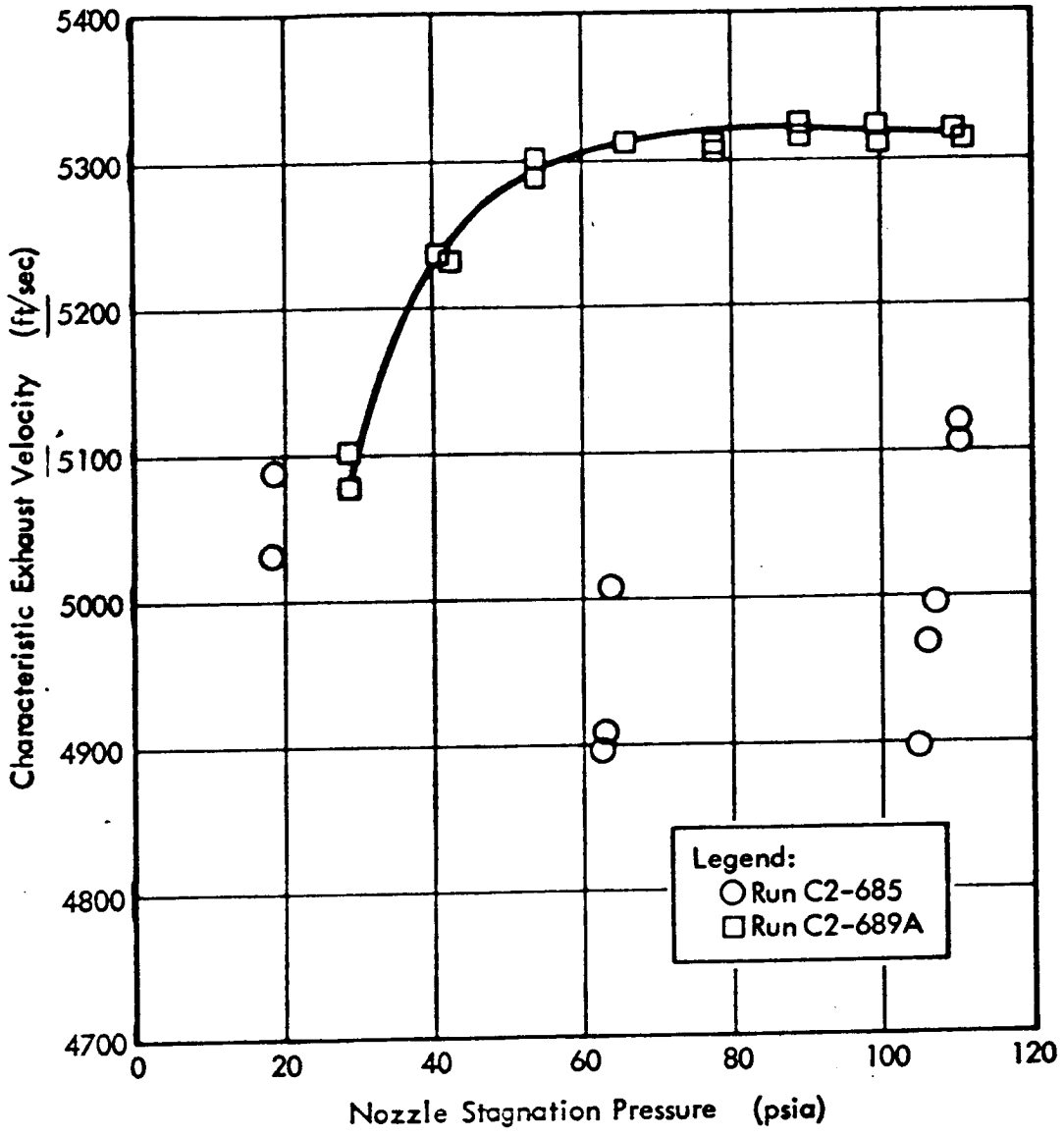

Figure 6.7.5-1. Characteristic Exhaust Velocity Data for Runs C2-685 and C2-689A Using HEA S/N 150A-010

6.7.6.3 Test Setup and Test Conditions

The test setup was identical to that described in paragraph 6.7.1.3. Run C2-676 was conducted under sea level ambient pressure and temperature conditions with the propellant tank pressure set at nominal 720 psia. A manual step switch was used to control throttling.

6.7.6.4 Test Results

Detailed test data are provided in Table D-2-1 and Figures D-2-17 through D-2-19 of Appendix D-2. Standard mixture ratio varied from 1.444 at 101.8 psia chamber pressure to 1.487 at 50.1 psia chamber pressure. Readjustment to raise the 1.444 to 1.470 at the high thrust level would result in a mixture ratio greater than 1.530 at the low thrust end. Thus, the HEA could not have been readjusted to meet the 1.50 $\pm$ 0.03 requirement. Characteristic velocity varied from 4810 fps at minimum thrust to 5333 fps at maximum thrust, thus meeting minimum performance requirements.

6.8 Combined Results of Altitude and Sea Level Steady-State Performance

In the two previous paragraphs (6.6 and 6.7) the data on steady-state performance were presented. These data were derived from firings at the IRTS and JPL/ETS. The objectives, test setup, test article, and test results were described on an individual test or test series basis. In this section such data from paragraphs 6.6 and 6.7, as is applicable, is combined to present overall TCA steady-state performance characteristics. The following paragraphs are organized on the basis of performance parameters.

6.8.1 Specific Impulse Comparison of Water-Cooled Versus Albatively Cooled Chamber Test Data

Comparative performance plots of vacuum specific impulse versus vacuum thrust for the tests using both ablatively cooled chambers (PQT 001 through 004A at the JPL/ETS) and water-cooled chambers (PQT 004.5 at the JPL/ETS) are given in Figures 6.8.1-1 through -3. Mixture ratios of 1.4, 1.5, and 1.6 are considered. The performance measurements illustrated by these three figures indicate an excellent correlation between the ablatively cooled and the corrected, water-cooled I_{sp} data, thus verifying the heat transfer term employed for correcting water-cooled performance in the STL data reduction computer program.

6.8.2 Characteristic Exhaust Velocity Comparison - Ablatively Cooled Versus Water-Cooled Chamber Test Data

Since the water-cooled performance corrections contain a combustion chamber throat growth term which does not enter into the I_{sp} correction, the C* data for ablatively cooled and water-cooled chamber tests were compared in Figures 6.8.2-1 through 6.8.2-3 to determine the validity of the throat area correction. These figures show a positive bias in C* resulting in higher values for the water-cooled data. As a result of these data, a revision was made to the Surveyor data reduction program to reduce the magnitude of the throat growth term eliminating all significant differences between ablatively cooled and water-cooled test C* data. All data reported in Appendix D-1 contain the revised water-cooled corrections.

6.8.3 Characteristic Exhaust Velocity Comparison - IRTS Versus JPL/ETS Test Data

Characteristic velocity data from all of the firings reported in paragraph 6.7, except for Runs C2-685, C2-686, and C2-689, were used for statistical estimates of C*. These three firings were eliminated because of the abnormal performance characteristics of HEA S/N 150A-010 discussed in paragraph 6.7.5. Based on IRTS data only, the estimates presented in Table 6.8.3-1 were obtained. These data were statistically compared with the JPL/ETS data and it was determined that there was no difference at the 90% confidence level in the mean values obtained. The variances were also tested at the same confidence level, and it was determined that a significant difference existed only at the 30-lb thrust level. With the exception of the variances at minimum thrust, the JPL/ETS and IRTS data were then pooled. The results of a study of the combined data are presented in paragraph 6.8.5.

Two major reasons are offered to explain the greater characteristic velocity variation at minimum thrust observed at the IRTS. Considerable discrepancy has been discovered in comparing strip chart determined flow at low flow rates with flowmeter frequencies determined from counters or oscillograph records. The bulk of the performance data was based on the strip chart readings. Also, at low thrust the nozzle is operating in the region where it may unchoke, resulting in nonrepeatable chamber pressure. The JPL/ETS data are therefore more representative in the low thrust region.

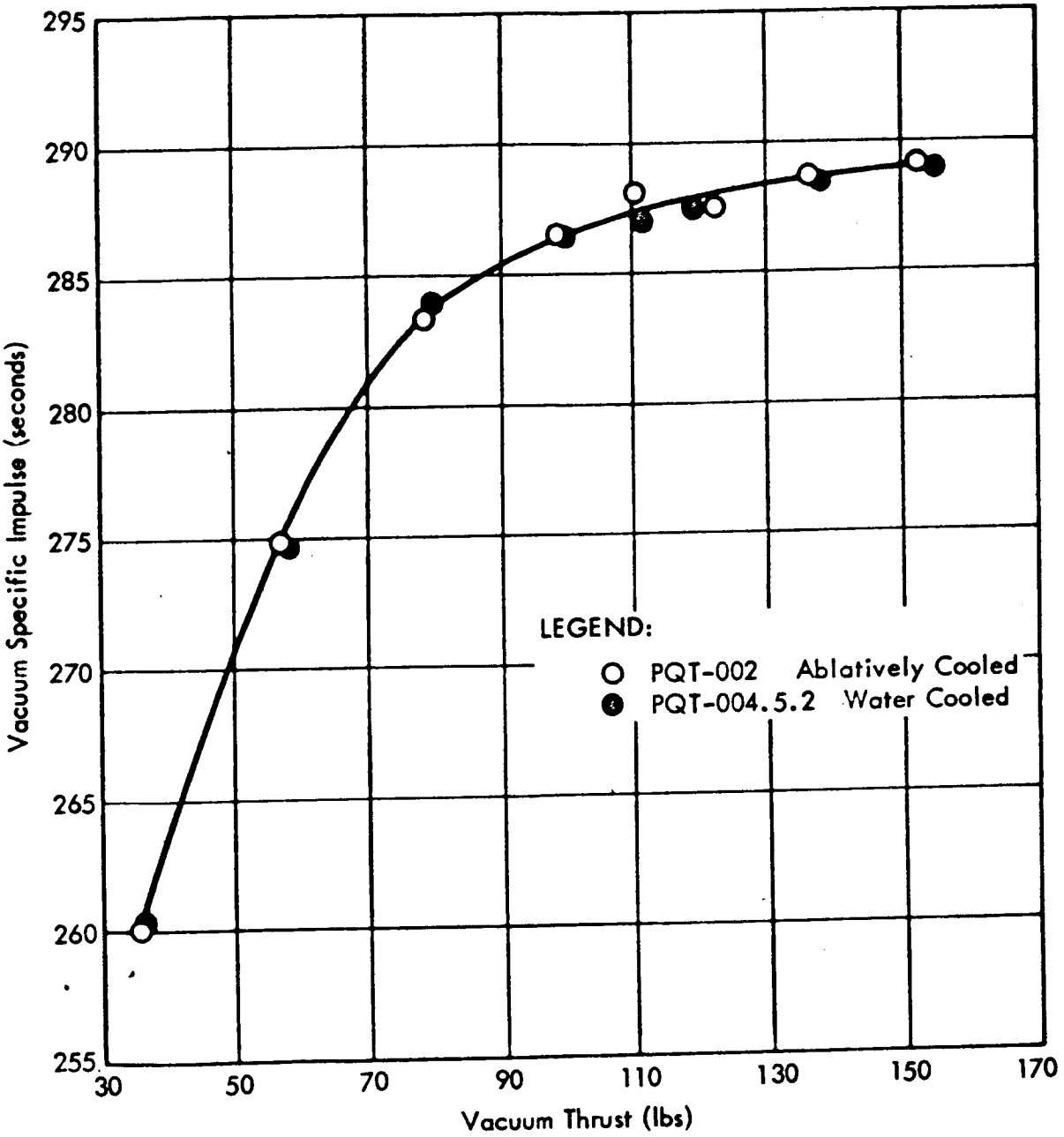

Figure 6.8.1-1. Vacuum Specific Impulse Versus Vacuum Thrust for Ablative and Water-Cooled Firings at 1.4 Mixture Ratio

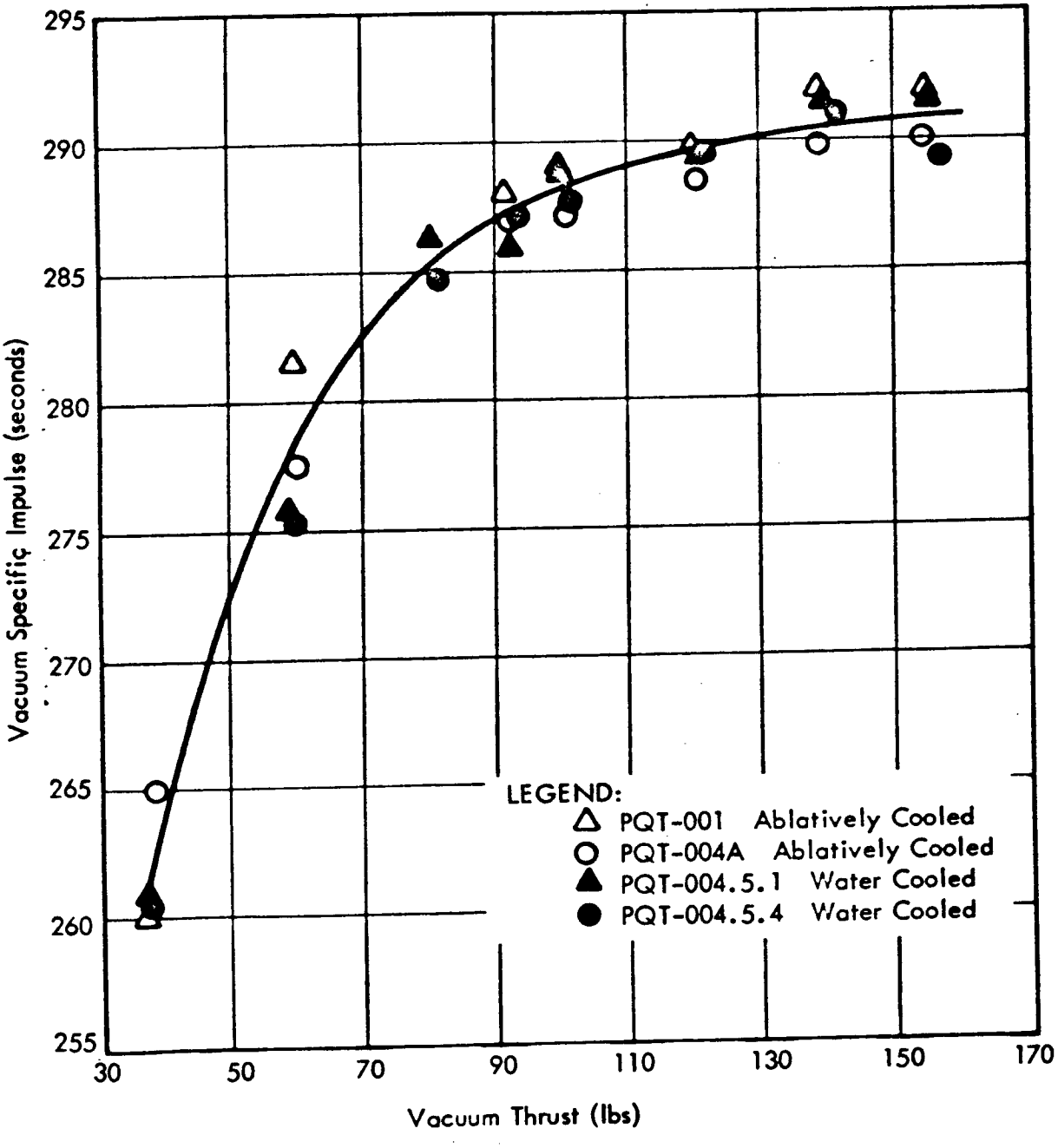

Figure 6.8.1-2. Vacuum Specific Impulse Versus Vacuum Thrust for Ablative and Water-Cooled Firings at 1.5 Mixture Ratio

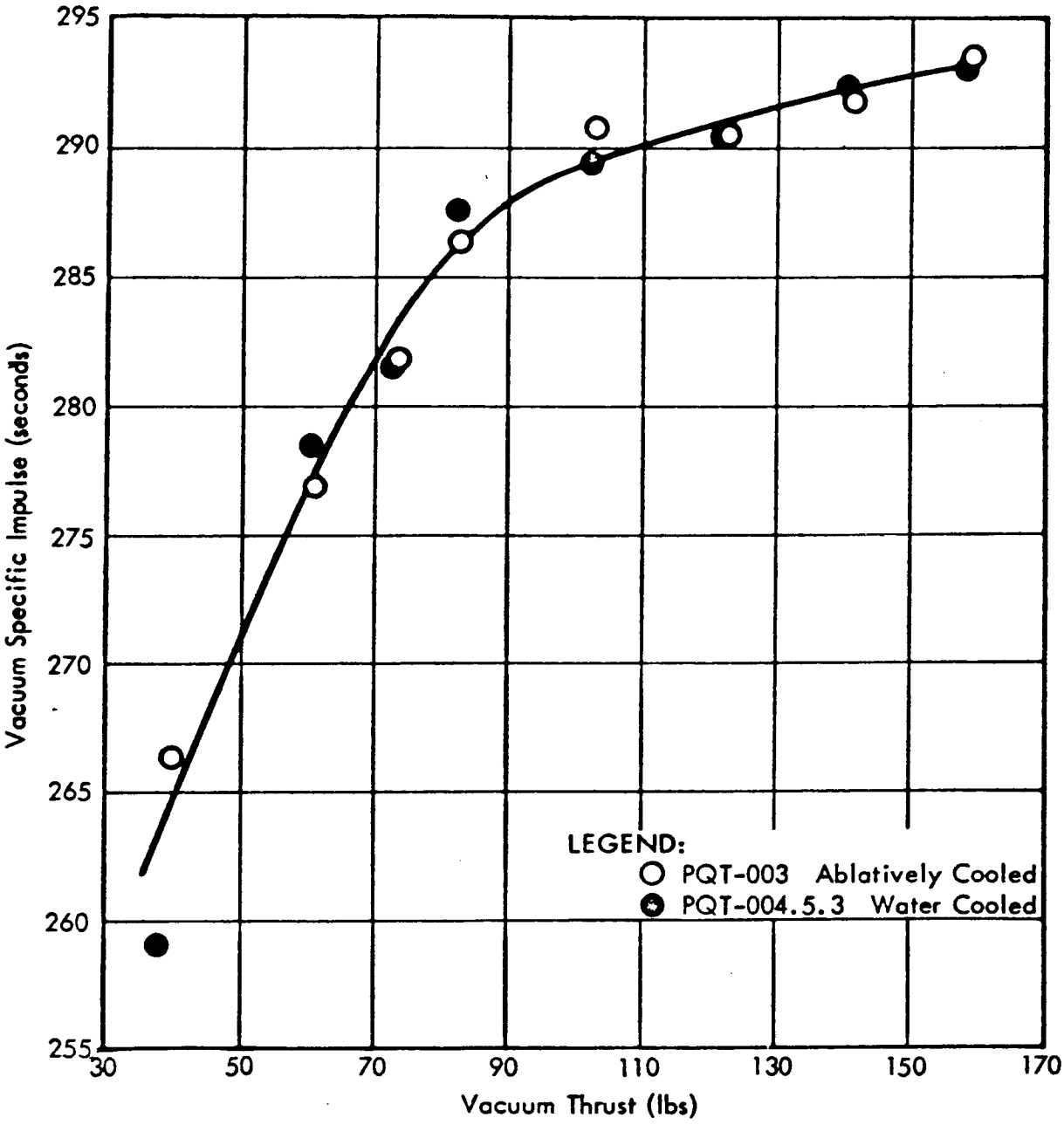

Figure 6.8.1-3. Vacuum Specific Impulse Versus Vacuum Thrust for Ablative and Water-Cooled Firings at 1.6 Mixture Ratio

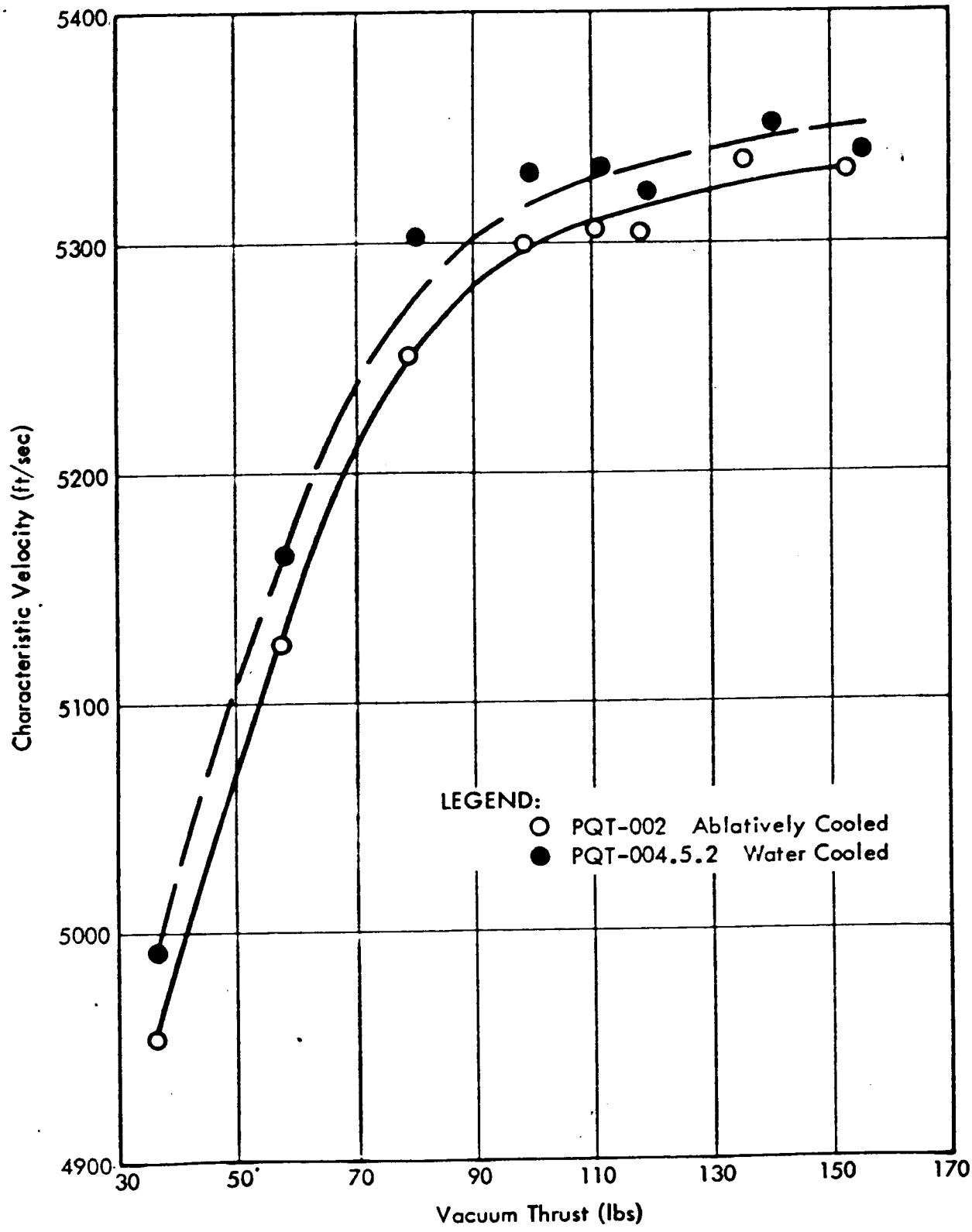

Figure 6.3.2-1. Characteristic Velocity Versus Vacuum Thrust for Ablative and Water-Cooled Firings at 1.4 Mixture Ratio

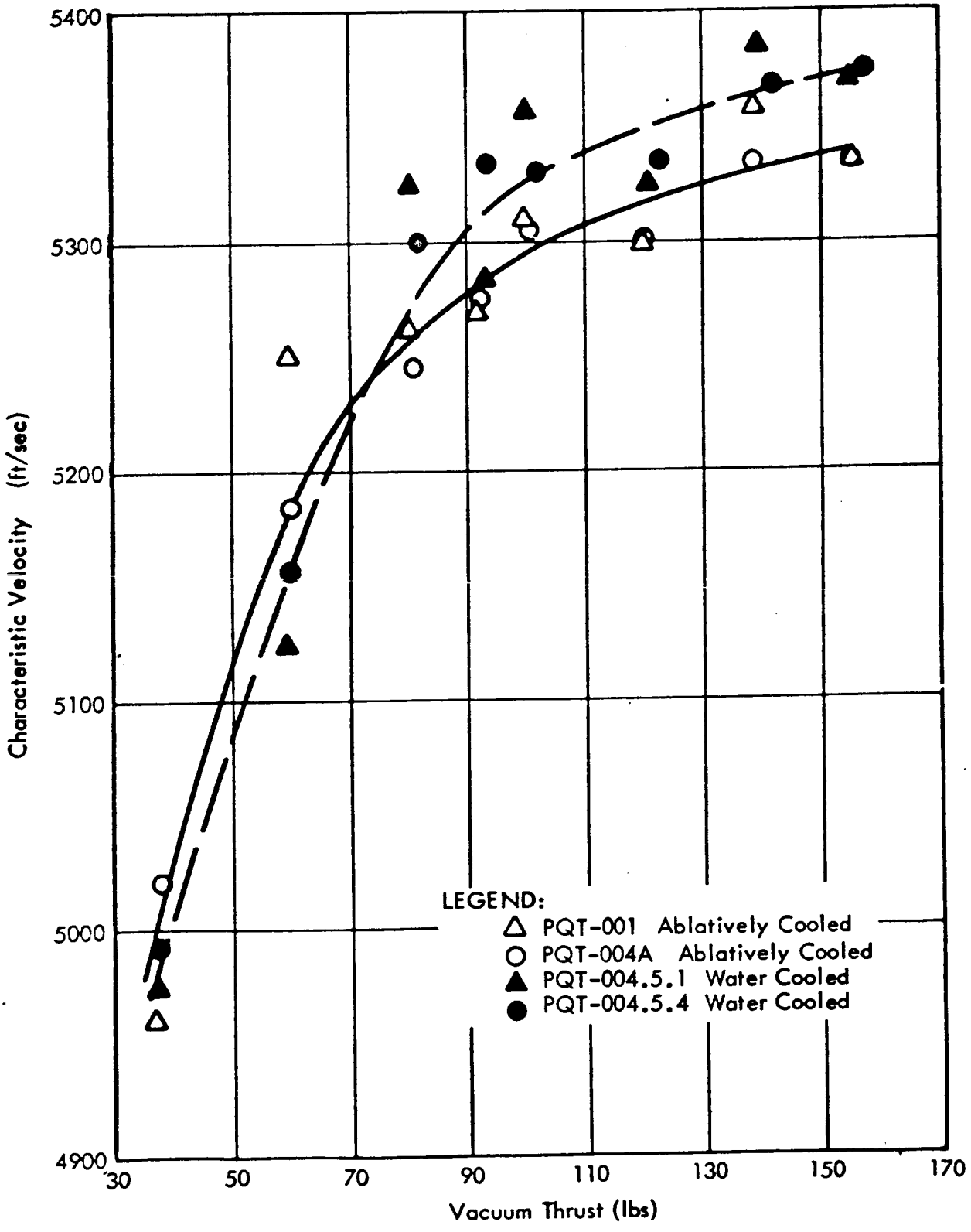

Figure 6.8.2-2. Characteristic Velocity Versus Vacuum Thrust for Ablative and Water-Cooled Firings at 1.5 Mixture Ratio

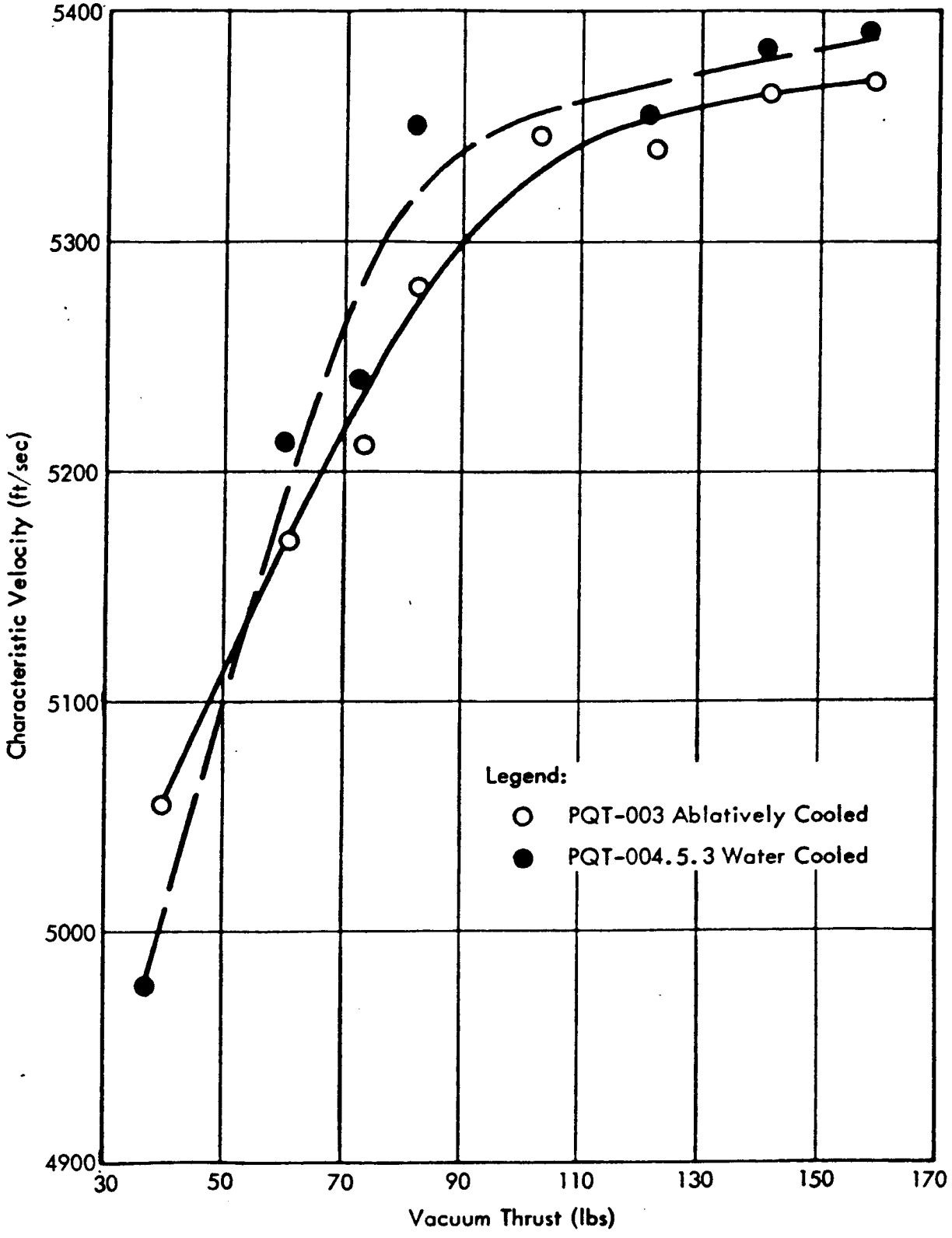

Figure 6.8.2-3. Characteristic Velocity Versus Vacuum Thrust for Ablative and Water-Cooled Firings at 1.6 Mixture Ratio

Table 6.8.3-1

TCA IRTS Characteristic Velocity Data Summary

Vacuum Thrust Level (lbs)	Characteristic Velocity (fps)	
	Mean	± 3-Sigma Deviation
30	4826	460
90	5286	114
150	5328	105

6.8.4 Mixture Ratio Comparison - IRTS Versus JPL/ETS Test Data

Mixture ratio data at standard inlet conditions were summarized for both the JPL/ETS and IRTS tests. Table 6.8.4-1 presents the results of the statistical analysis performed. The analysis showed that there was a significant difference in the mean and the 3-sigma values obtained from the JPL/ETS as compared to the IRTS data. In particular, the 3-sigma mixture ratio deviations determined from IRTS data were two to three times greater than the JPL/ETS deviations.

A number of factors contributed to these larger variations. The problem encountered in determining the flow rates from the IRTS strip charts was previously mentioned in paragraph 6.8.3. Several of the HEAs used in the IRTS data summary being tested before adequate experience had been gained in calibration and, thus they were not properly calibrated for mixture ratio. With the exception of HEA 150A-011, all of the Phase III HEAs tested could have been readily recalibrated to yield a 1.50 ± 0.03 standard mixture ratio over the total throttling range by means of a simple flow control valve pintle adjustment. The best possible mixture ratio setting on HEA 150A-011 would have ranged from 1.47 at maximum thrust to 1.54 at minimum thrust, and a flow control valve pintle replacement would have been required to meet the 1.50 ± 0.03.

Based on the experience gained during the IRTS testing, it was decided to set the acceptance test mixture ratio limits at the 1.50 ± 0.03 level with the expectation that the recalibration and possible rework rate would be acceptable. With the basic STL design, adapted to adjustability and accurate calibration, final hardware scrappage would not be required. For example, in a case such as HEA S/N 011, noted above, where readjustment alone would not suffice, the flow control valve pintles could be matched in sets to achieve the desired flow characteristic (i.e., oversized and undersized pintles could be paired).

The influence of temperature and pressure on mixture ratio is discussed in paragraph 6.5.

6.8.5 Characteristic Exhaust Velocity, Specific Impulse, and Thrust Coefficient Relationship to Mixture Ratio, Chamber Pressure and Thrust

After combining performance data from simulated pressure altitude Runs DY-25 through DY-32 (PQT-001, -002, -003, -004A, and -004.5), a multiple regression analysis was conducted to determine the variation in TCA performance with mixture ratio and nozzle stagnation pressure. The regressed parameters included characteristics velocity efficiency (η_{C^*}) and thrust coefficient efficiency (η_{C_f}) which were computed based

Table 6.8.4-1

MIRA 150A Mixture Ratio Data at Standard Inlet Conditions

Test Site	Thrust Level (lbs)	Mixture Ratio Mean	± 3-Sigma Deviation
IRTS	30	1.502	0.115
	90	1.481	0.064
	150	1.475	0.061
JPL/ETS	30	1.477	0.042
	90	1.506	0.024
	150	1.541	0.038

on the frozen flow theoretical data presented in paragraph 7.1.3. Specific impulse efficiency ($\eta_{I_{sp}}$) was then computed from the product, $\eta_{C^*} \times \eta_{C_f}$. These efficiencies are plotted versus nozzle stagnation pressure and mixture ratio in Figures 6.8.5-1 through 6.8.5-3. The partial derivatives, $\frac{\delta C_f}{\delta MR}$, $\frac{\delta C^*}{\delta MR}$, and $\frac{\delta I_{sp}}{\delta MR}$ were next computed and plotted as a function of nozzle stagnation pressure. These data are shown in Figures 6.8.5-4 through 6.8.5-6.

The present analytical engine performance model used in the Surveyor data reduction program is based on frozen flow theory, and assumes performance efficiencies do not change in extrapolating TCA test data from one set of mixture ratio and chamber pressure conditions to another. It is evident from the data presented herein that this assumption is not completely valid over the entire chamber pressure range. For example, Figure 6.8.5-3 shows that there is a considerable variation in $\eta_{I_{sp}}$ with nozzle stagnation pressure below approximately 60 psia, with a much reduced variation above 60 psia. Conversely the mixture ratio influence is relatively small in the range above 60 psia with a more significant influence between an MR of 1.4 to 1.6 at higher pressures. However, since a majority of the MIRA 150A static firings were conducted within a 1.50 ± 0.04 mixture ratio range, with chamber pressures within a few psi of the nominal thrust-to-signal envelope, performance data extrapolated to "standard" (720 psia and 70°F) and to "rated" 1.5 mixture ratio conditions are within at least 0.5% of the true values for most cases.

After performing the regression analysis, all valid vacuum performance data were corrected to a 1.5 mixture ratio, and mean value and standard deviation estimates were obtained for I_{sp}, C*, and C_f. The test data used in this analysis included the following runs:

1. DY-19 through DY-21 (see paragraphs 6.6.2 and 6.6.3).
2. DY-23 through DY-32 (see paragraphs 6.6.3, 6.6.4, and 6.6.5 on PQT-001, -002, -003, -004A, and -004.5).
3. DY-35 through DY-46 (see paragraphs 6.6.7, 6.6.8, 6.6.9, and 6.6.10 on PQT-007, -008, -010, and -009.5).

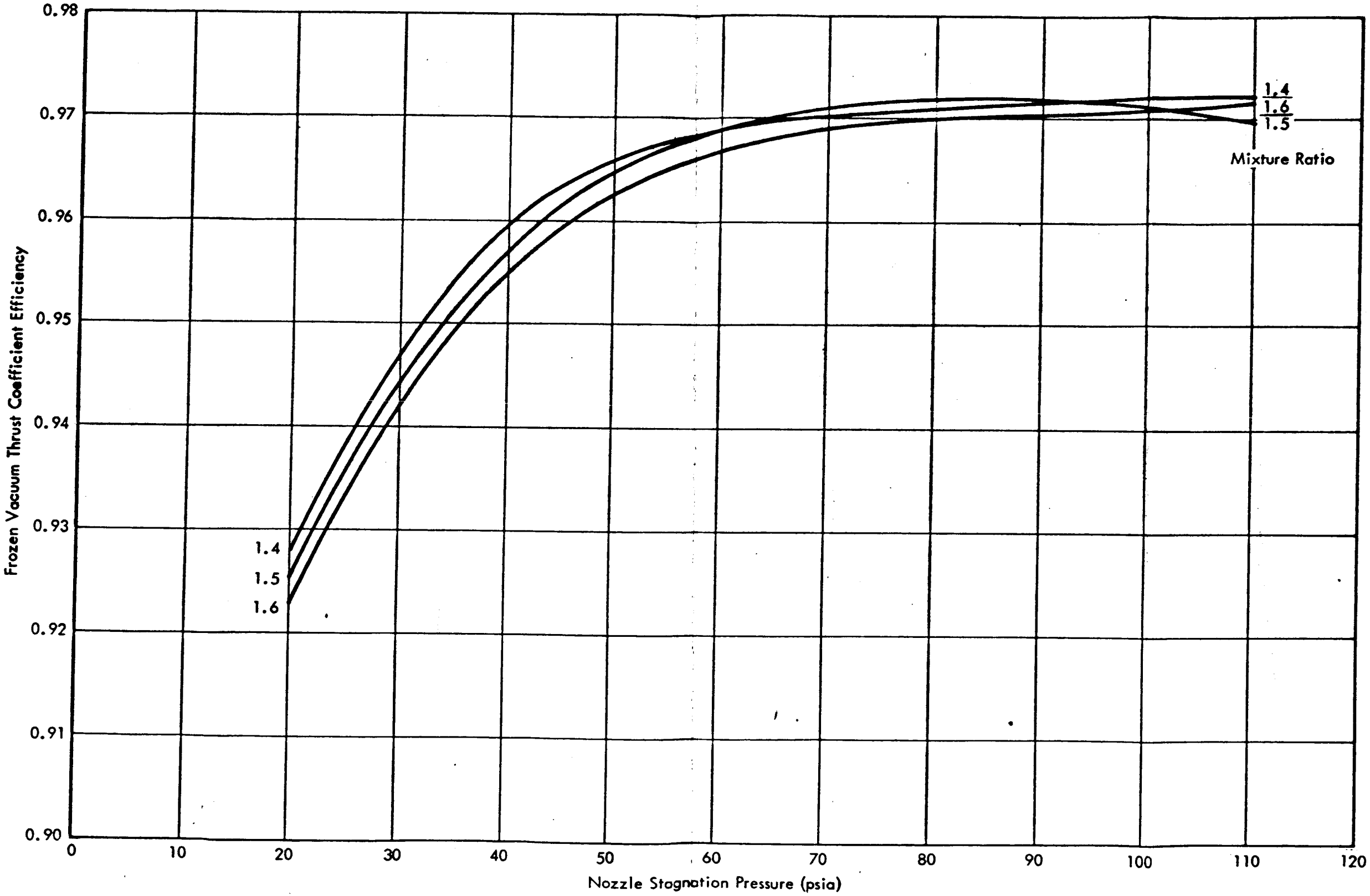

Figure 6.8.5-1. Thrust Coefficient Efficiency

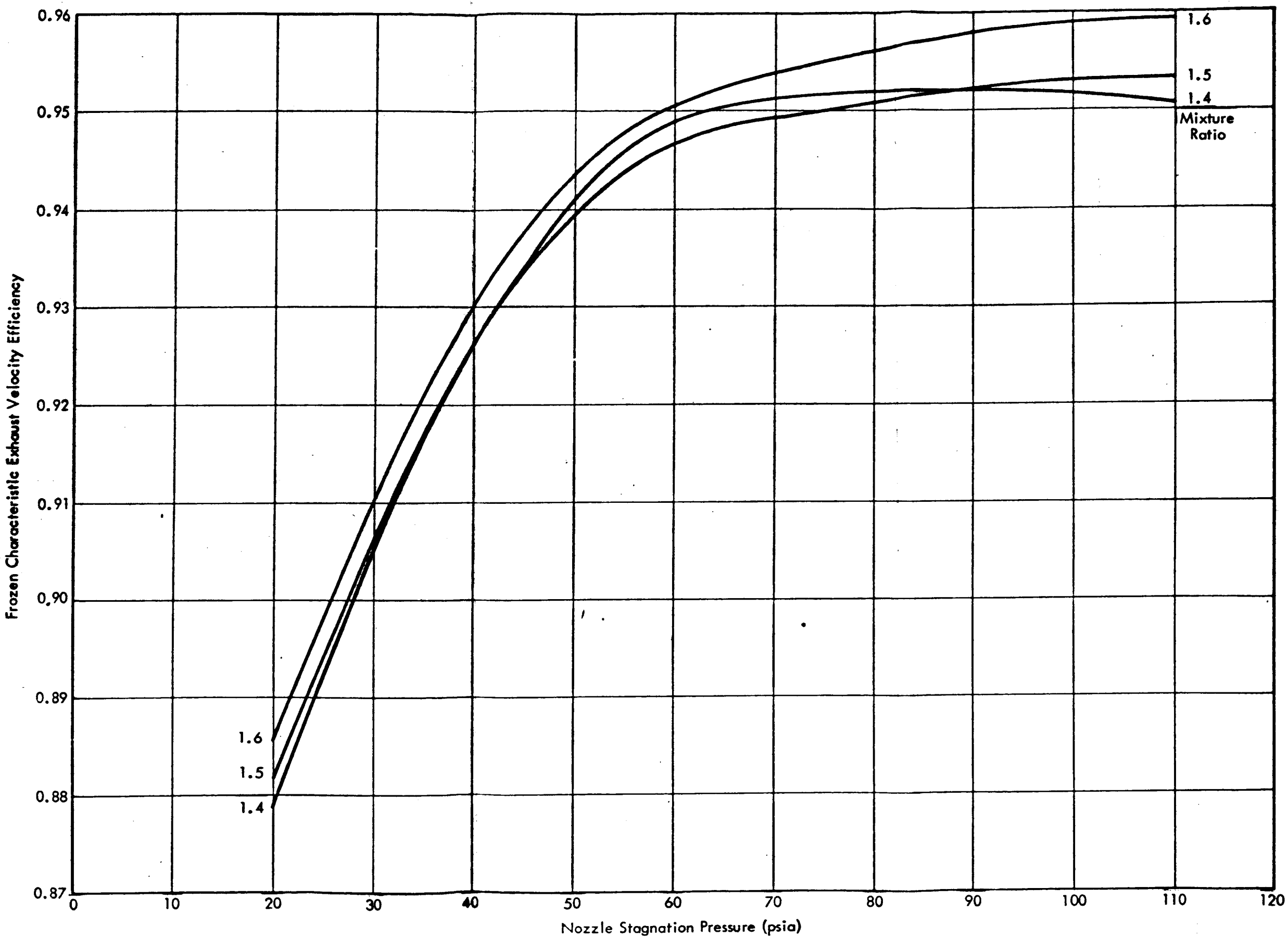

Figure 6.8.5-2. C^* Efficiency

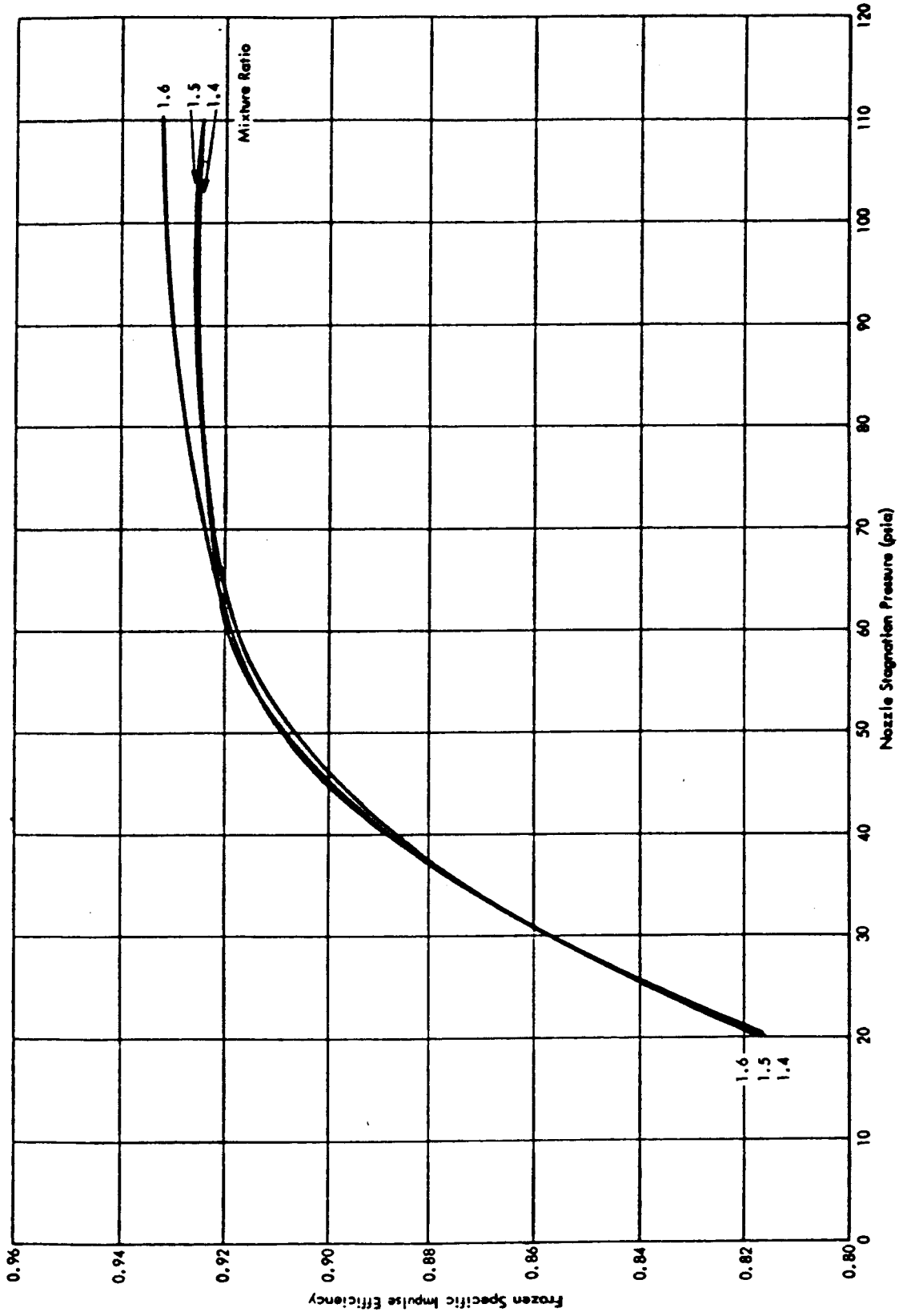

Figure 6.8.5-3. Specific Impulse Efficiency

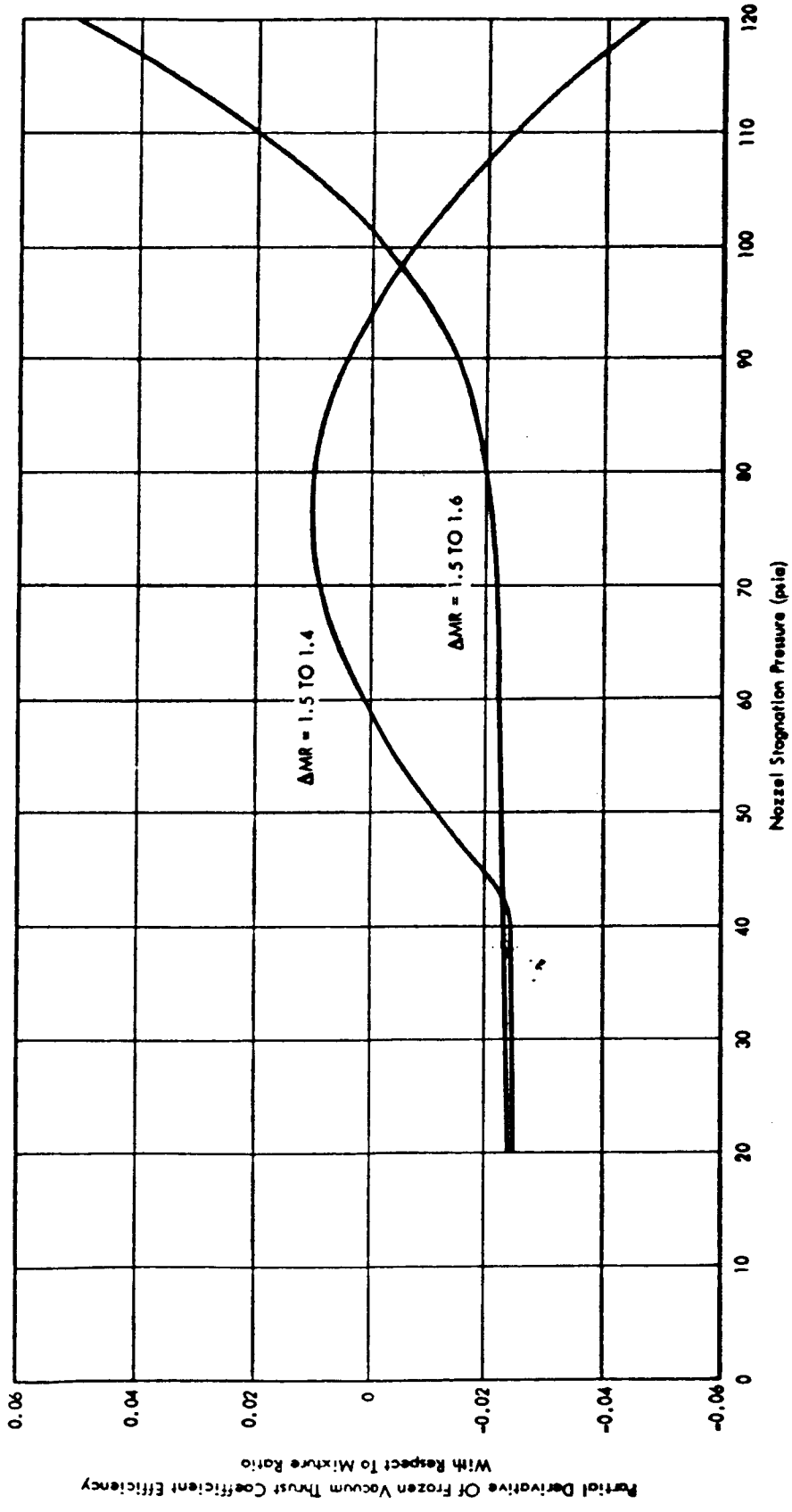

Figure 6.8.5-4. Partial Derivative of η_{CF} with Respect to Mixture Ratio

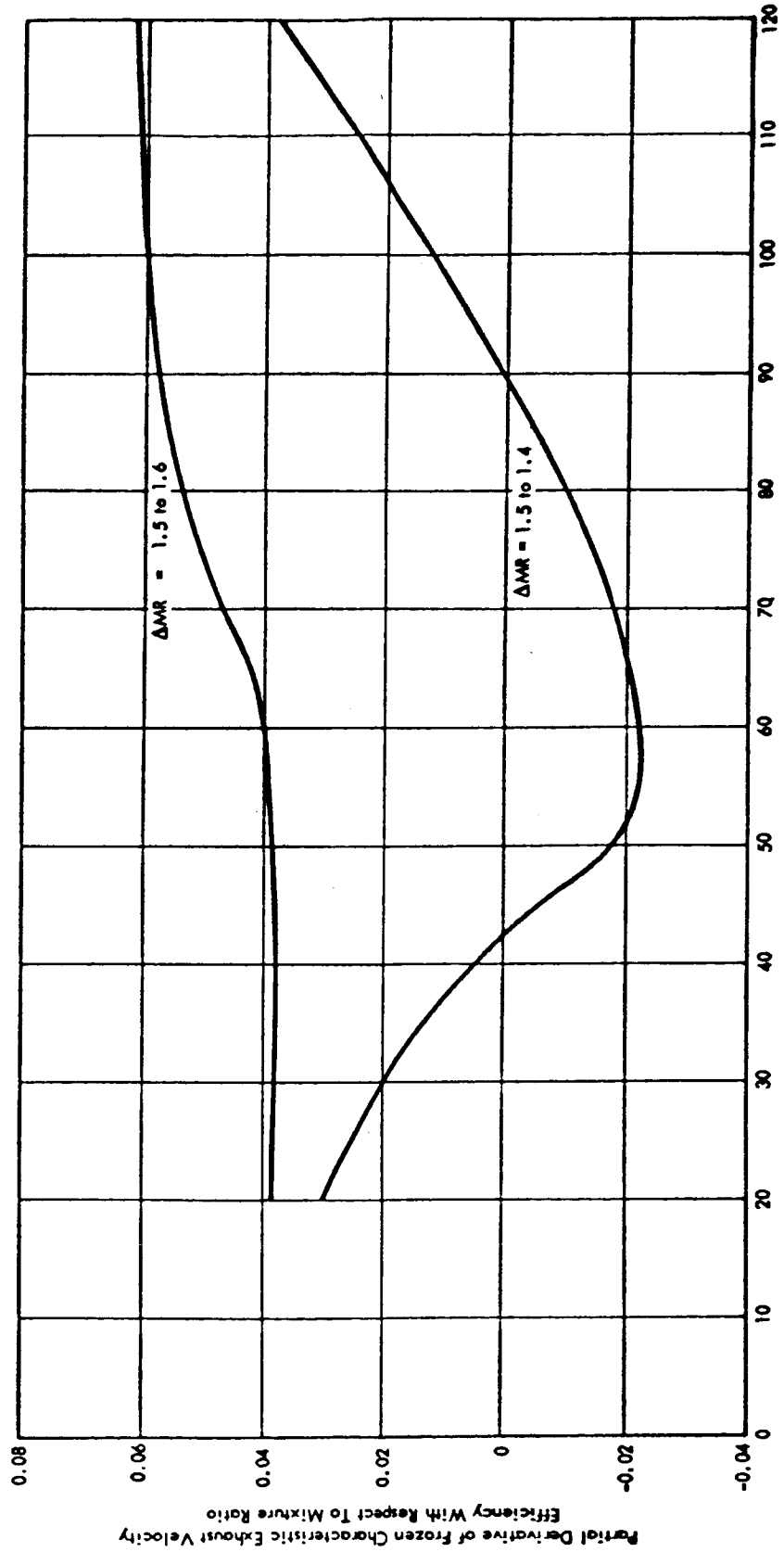

Figure 6.8.5-5. Partial Derivative of η_{C^*} with Respect to Mixture Ratio

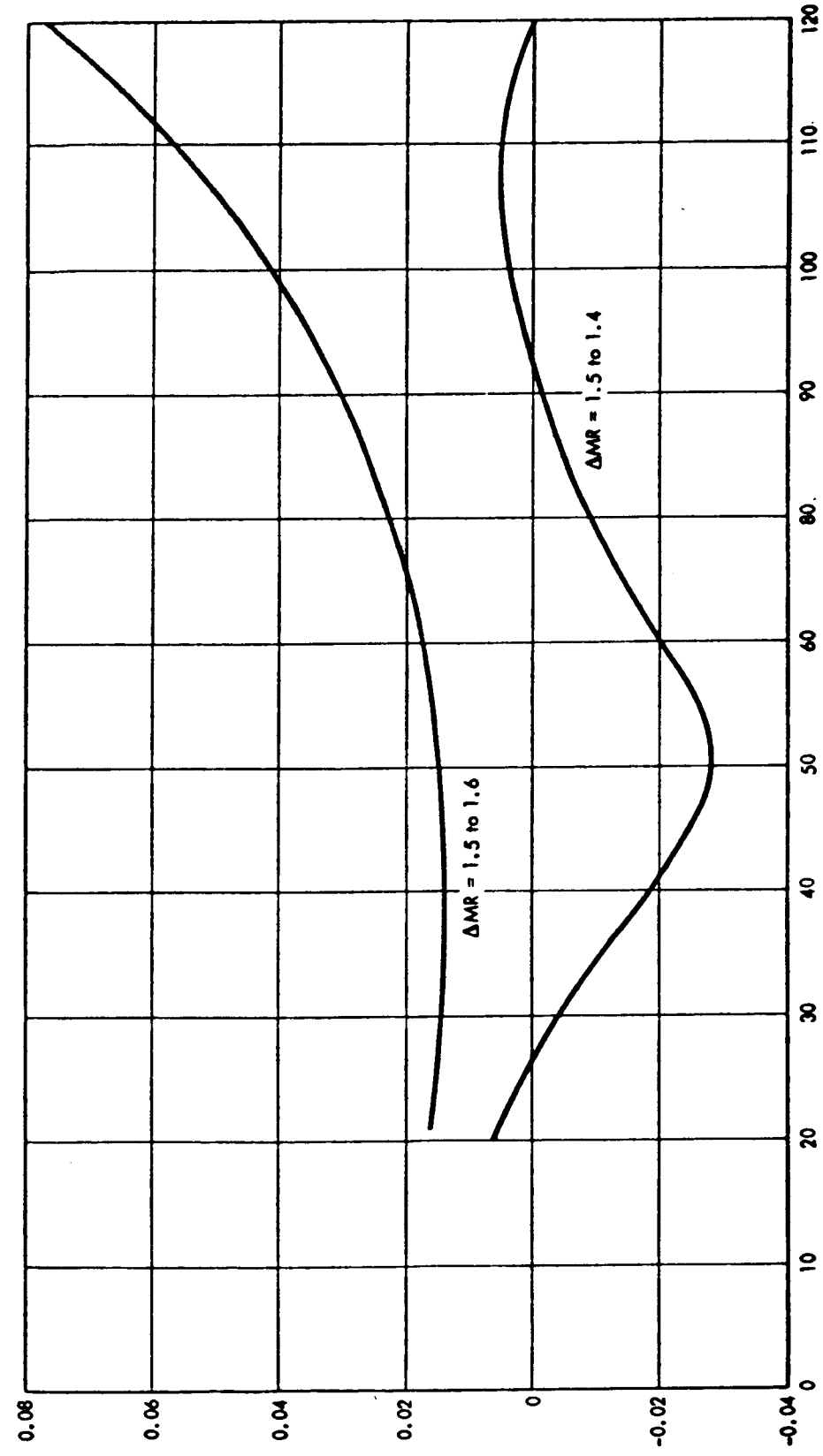

Figure 6.8.5-6. Partial Derivative of $\eta_{I_{sp}}$ With Respect to Mixture Ratio

The remaining data were deleted because of their questionable validity (see discussions under the appropriate individual test paragraphs). Table 6.8.5-7 provides the statistical performance estimates derived from these data plotted in Figures 6.8.5-8 through 6.8.5-10. The C* estimates also include data from IRTS firings conducted at sea level (see paragraph 6.7). Before merging the JPL/ETS and IRTS data, statistical tests were performed to determine whether the means and variances were the same. The tests were all positive with the exception that the C* variance obtained from IRTS data was significantly greater than that obtained from JPL/ETS data at the minimum thrust level. After computing the mean performance values at a 1.5 mixture ratio, the previously derived partial derivatives (Figures 6.8.5-4 through 6.8.5-6) were applied to compute the performance variation as a function of mixture ratio, thrust and nozzle stagnation pressure. The resulting variations are shown in Figures 6.8.5-11 through 6.8.5-13.

6.8.6 Thrust to Servoactuator Signal Relationship

Data from five static tests (four at IRTS —— C2-621, C2-676, C2-680, C2-683 and one at ETS —— PQT-010) using five different HEAs (S/Ns 150A-004, -007, -008, -009, and -011) and four different Phase III servoactuators (S/Ns C55390, C55394, C55393, and C55398) were selected as a basis for this analysis. Tests with other than Phase III servoactuators would not be valid for use here.

Measured thrust extrapolated to standard vacuum conditions was used for PQT-010 conducted at altitude. The remaining tests were conducted at sea level without thrust measurements; it was therefore necessary to compute thrust from measured chamber pressure and the vacuum thrust coefficient curve previously presented in Figure 6.8.5-10. The resulting thrust-signal servoactuator curves were then plotted and the values read off at the points of interest. Data at low pressures from the four IRTS tests were used despite the risk associated with possible unchoked flow. An indication that throat flow was sonic is the fact that the C* values on these runs, at the low chamber pressures corresponding to the minimum stop and -70 ma signals, ranged from 4810 to 4960. This is within the standard $\bar{X} + 3$ range for C* (reference paragraph 3.4.2). The instrumentation error and any zero shift of chamber pressure is more significant at the low pressure levels than at higher pressures; this would contribute to the higher 3 sigma deviation at the low chamber pressure levels.

The retract stop on the servoactuator (S/N C55394) used during PQT-010 had been set too low, thus limiting the maximum thrust. This low setting was detected during the component acceptance test (see paragraph 5.1.1 - Table 5.1.1-10) which indicated that the stop was set at approximately +69 milliamperes differential current equivalent, and was rejected on this basis. MRB action boughtoff the unit because the Surveyor test program at that time required that firings be expedited with available hardware. During acceptance of deliverable hardware, this servoactuator would have received a null setting readjustment. Therefore, in order to include the data from PQT-010 without invalidating the sample, the thrust versus servoactuator signal curve was first readjusted to represent this servoactuator null adjustment.

Table 6.8.5-7

MIRA 150A Vacuum Performance Estimates at 1.5 Mixture Ratio

	Measured Value		SAM-50255-DSN-C Requirements	
	Mean	+3-Sigma Variation	Mean	+3-Sigma Limit
A. Specific Impulse (seconds)				
1. Minimum Thrust (30 lbs)	258.7	12.5	260	7
2. Midrange Thrust (90 lbs)	287.6	5.2	290	5
3. Maximum Thrust (150 lbs)	291.3	3.3	290	5
B. Characteristic Velocity (ft/sec)				
1. Minimum Thrust (30 lbs)	4826*	180	N.R.**	N.R.
2. Midrange Thrust (90 lbs)	5286*	99*	N.R.	N.R.
3. Maximum Thrust (150 lbs)	5328*	101*	N.R.	N.R.
C. Thrust Coefficient				
1. Minimum Thrust (30 lbs)	1.711	0.074	N.R.	N.R.
2. Midrange Thrust (90 lbs)	1.752	0.035	N.R.	N.R.
3. Maximum Thrust (150 lbs)	1.763	0.042	N.R.	N.R.

*Pooled estimate from both JPL/ETS and IRTS data.

**N.R. designates no specification requirements.

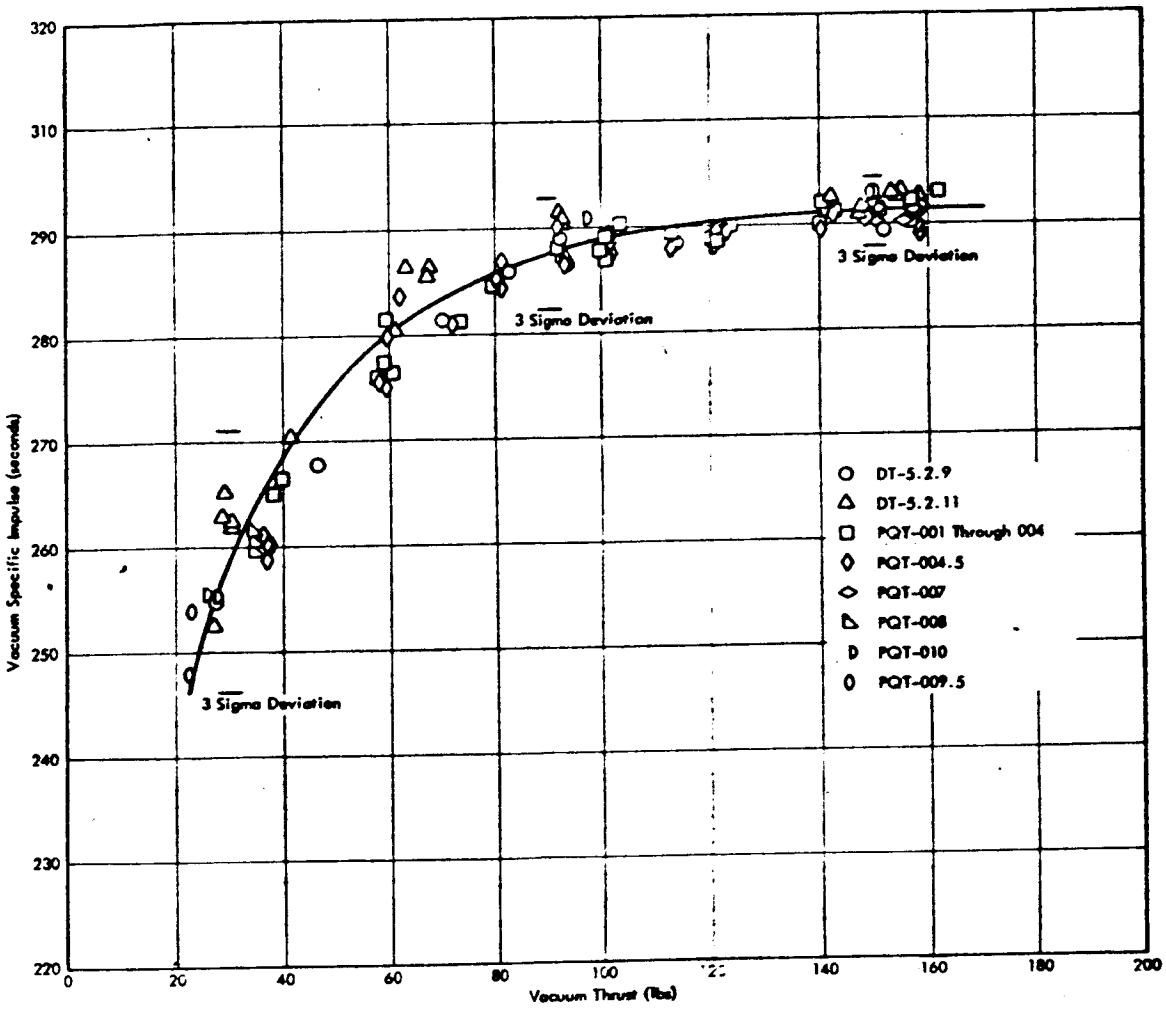

Figure 6.8.5-8. MIRA 150A TCA Vacuum Specific Impulse Versus Thrust at 1.5 Mixture Ratio

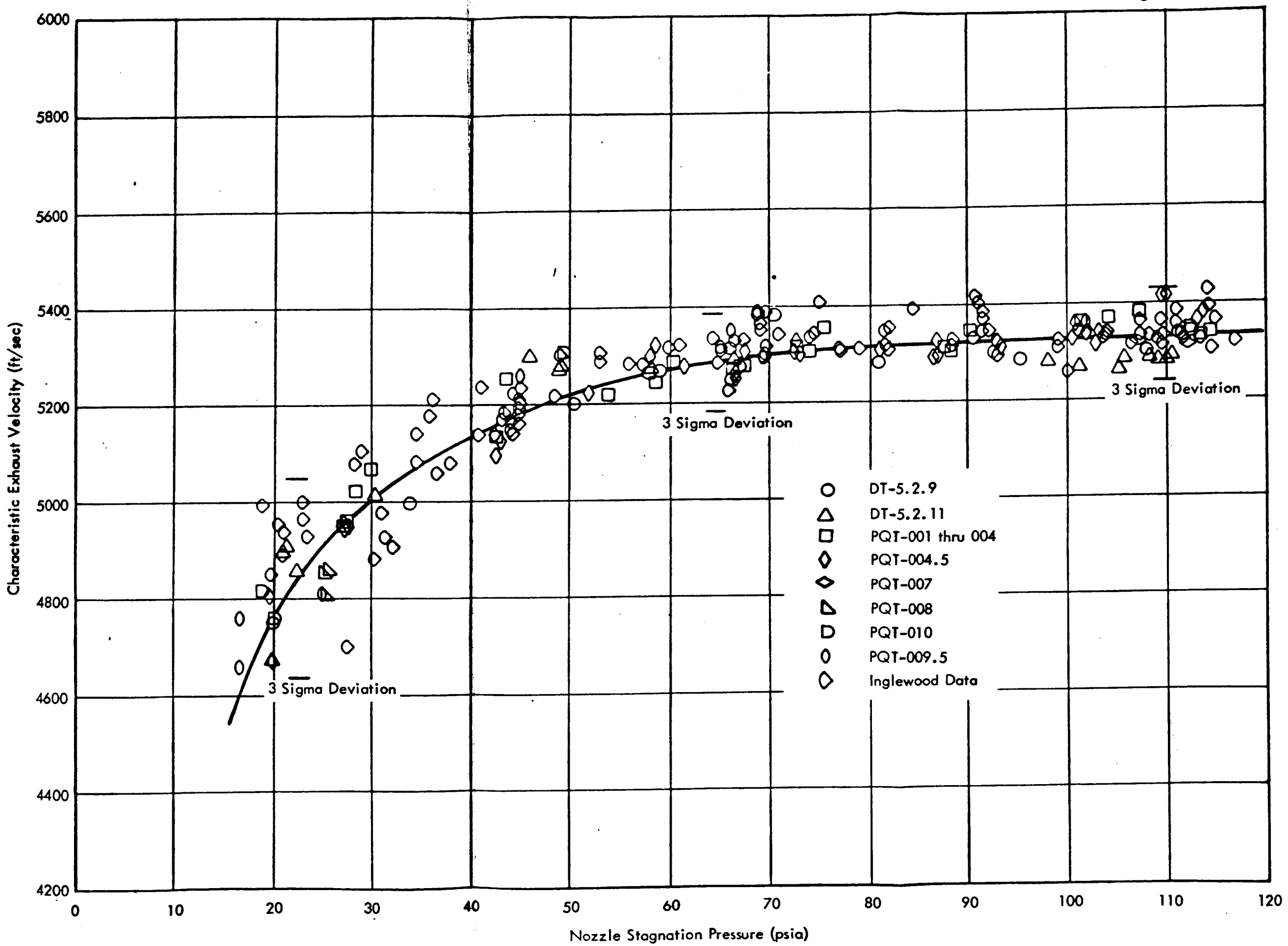

Figure 6.8.5-9. MIRA 150A TCA Characteristics Velocity Versus Nozzle Stagnation Pressure at 1.5 Mixture Ratio

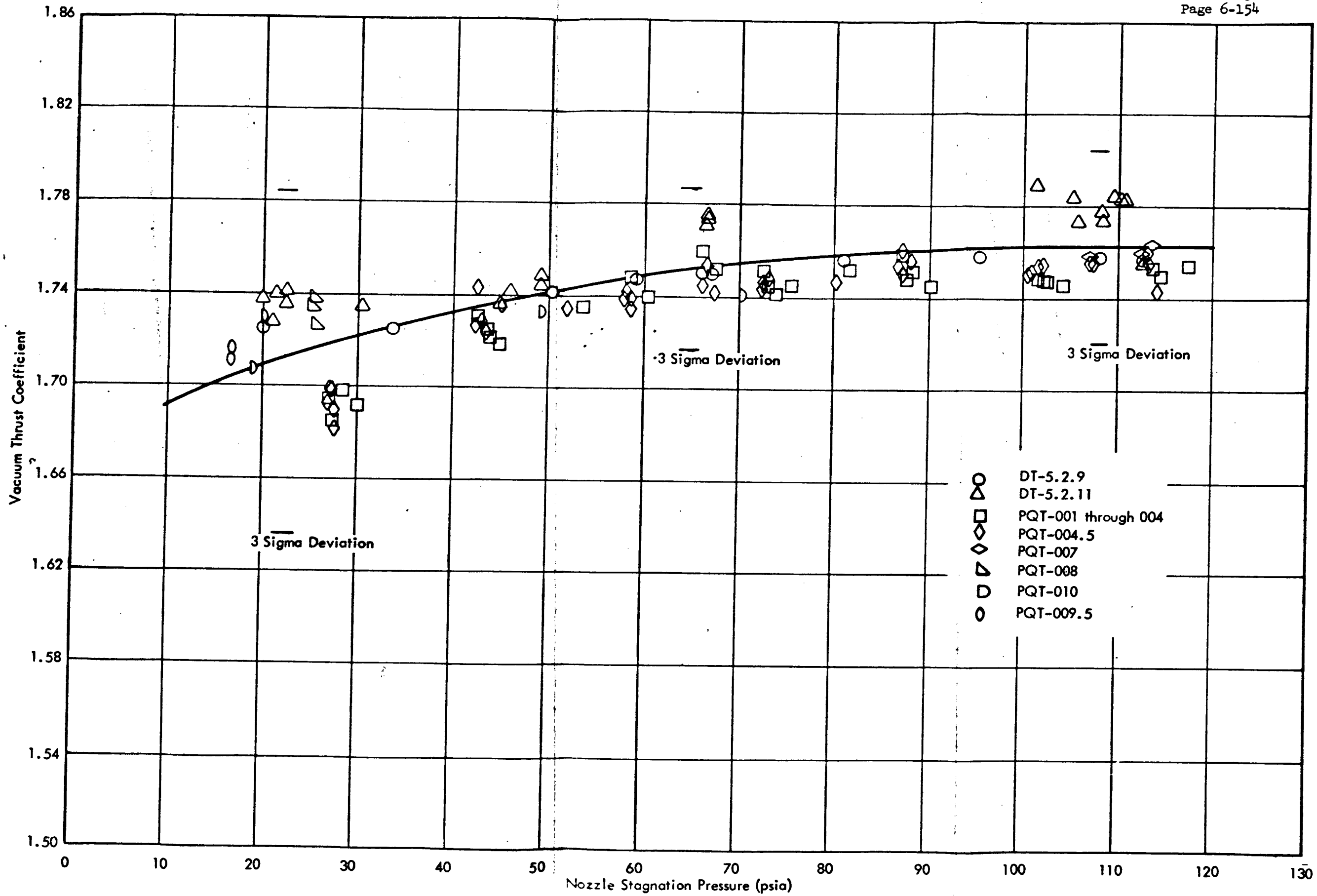

Figure 6.8.5-19. MIRA 15:A TCA Vacuum Thrust Coefficient Versus Nozzle Stagnation Pressure at 1.5 Mixture Ratio

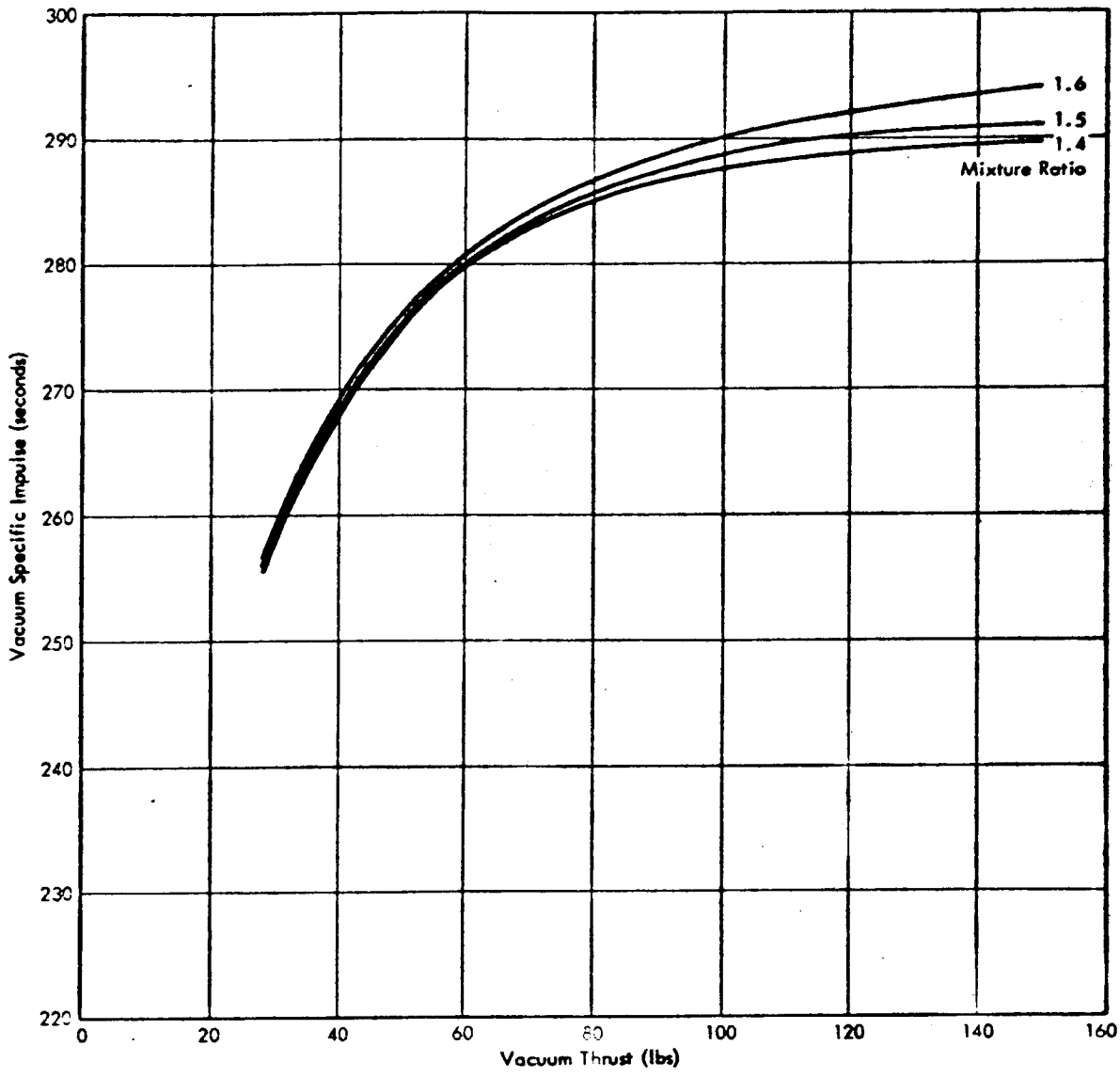

Figure 6.8.5-11. MIRA 150A TCA Vacuum Specific Impulse Versus Thrust and Mixture Ratio

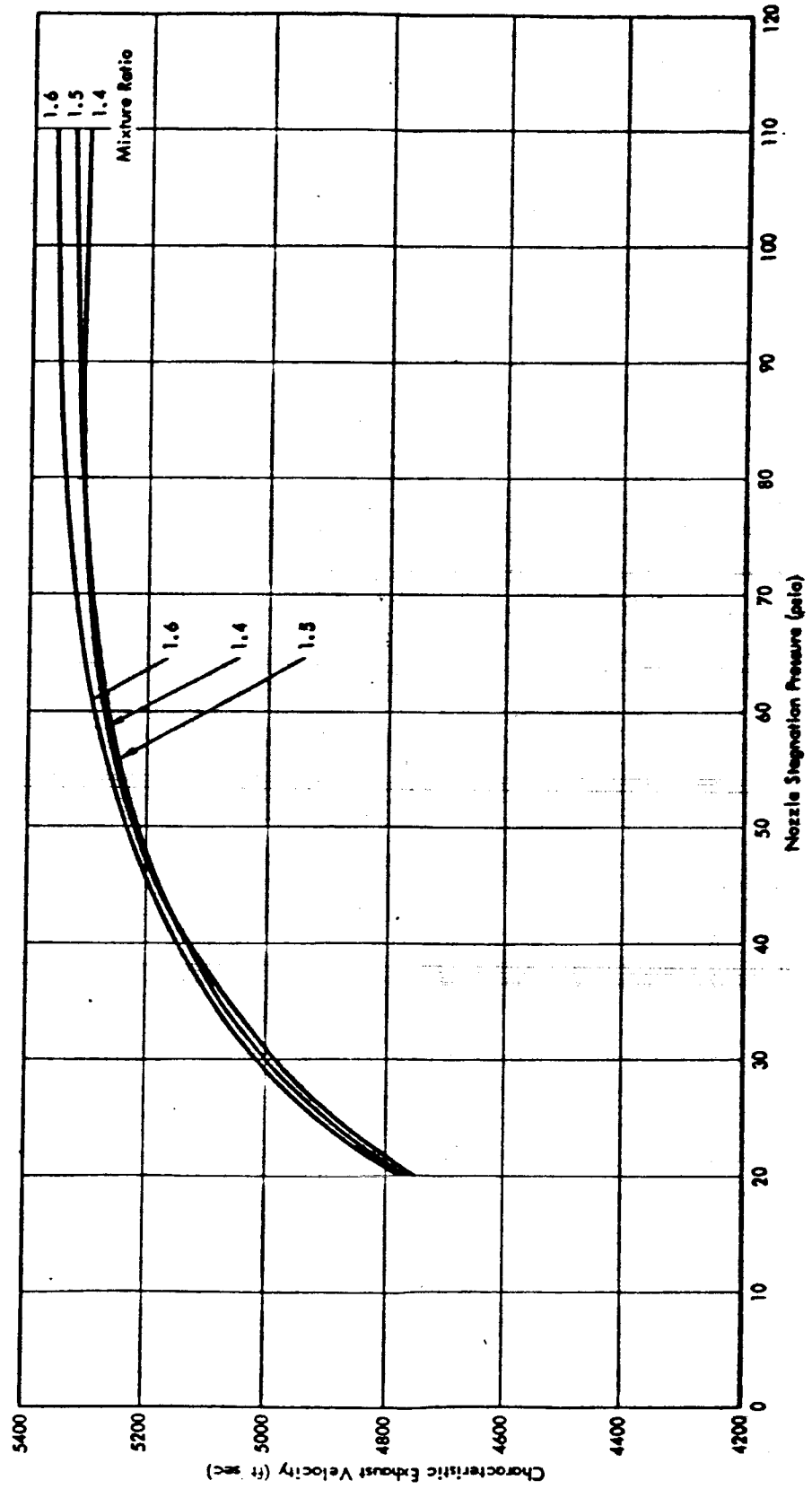

Figure 6.8.5-12. MIRA 150A TCA Characteristic Velocity Versus Nozzle Stagnation Pressure and Mixture Ratio

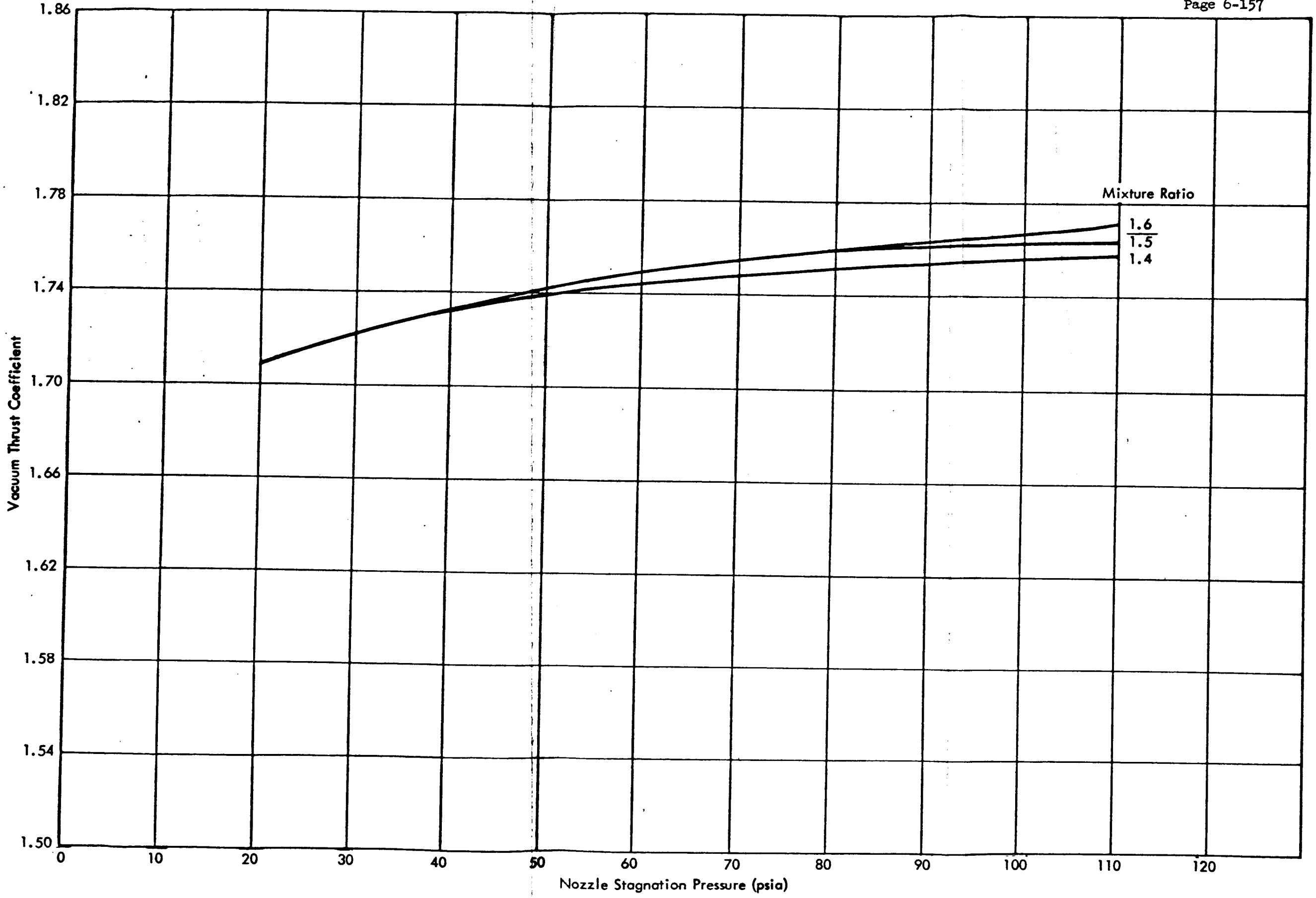

Figure 6.8.5-13. MIRA 150A TCA Vacuum Thrust Coefficient Versus Nozzle Stagnation Pressure and Mixture Ratio

All thrust data were then corrected to standard inlet conditions (720 psia, 70°F), as summarized in Table 6.8.6-1. The mean and 3-sigma limit estimates based on these data were computed and are also provided in this table. The temperature (0 - 100°F range) and pressure (700 - 740 psia range) effects summarized in Table 6.5.3-1 (paragraph 6.5) were next applied by selecting the worst possible combinations of TCA-to-TCA variation, temperature, and pressure. (NOTE: This worst-on-worst combination of 3-sigma deviation levels of independent variables is very conservative compared to computation of a true overall 3-sigma deviation, but is required by JPL Specification SAM-50255-DSN-C.) The resultant thrust-signal servoactuator envelope is defined by the following eight straight line segments:

Upper Limit (lb)	Differential Current (milliamp)
33	-80 and less
101	0
168	+70 and greater

Lower Limit Vacuum Thrust	Differential Current (milliamp)
20	-70 and less
89	0
153	+80 and greater

6.8.7 Thrust-to-Chamber Pressure Relationship

Head end chamber pressure as a function of vacuum thrust is shown in Figure 6.8.7-1 with the mean and 3-sigma limit estimates provided in Table 6.8.7-2. These results are based on the 27 altitude firings at the JPL/ETS discussed in paragraphs 6.6.2 through 6.6.5 and 6.6.7 through 6.6.10.

Table 6.8.7-2

MIRA 150A Chamber Pressure - Vacuum Thrust Relationship

Vacuum Thrust (lbs)	Head End Chamber Pressure (psia)	
	Mean	± 3-Sigma Deviation
30	22.4	1.3
90	65.2	1.1
150	108.2	2.4

Table 6.8.6-1

MIRA 150A Thrust Servoactuator Signal Data
at Standard Inlet Conditions

Head End S/N	150A-004	150A-007	150A-008	150A-009	150A-011	Mean	± 3-Sigma Deviation
Servoactuator S/N	C55394	C55390	C55398	C55390	C55395		
Test Number	PQT-010	C2-621	C2-680	C2-683	C2-676		
Thrust (lbs) at:							
Min Stop	28.2*	-----	24.5	26.4	-----	26.4	6.2
-70 ma	28.8*	28.2	27.7	26.6	33.6	29.0	8.6
0 ma	96.0*	94.1	95.0	95.0	97.6	95.5	4.2
+70 ma	154.2*	155.0	153.3	157.1	154.0	154.6	2.9
Max Stop	160.8*	-----	159.9	161.7	-----	160.8	3.0

*These data have been adjusted for a change in servoactuator null setting.

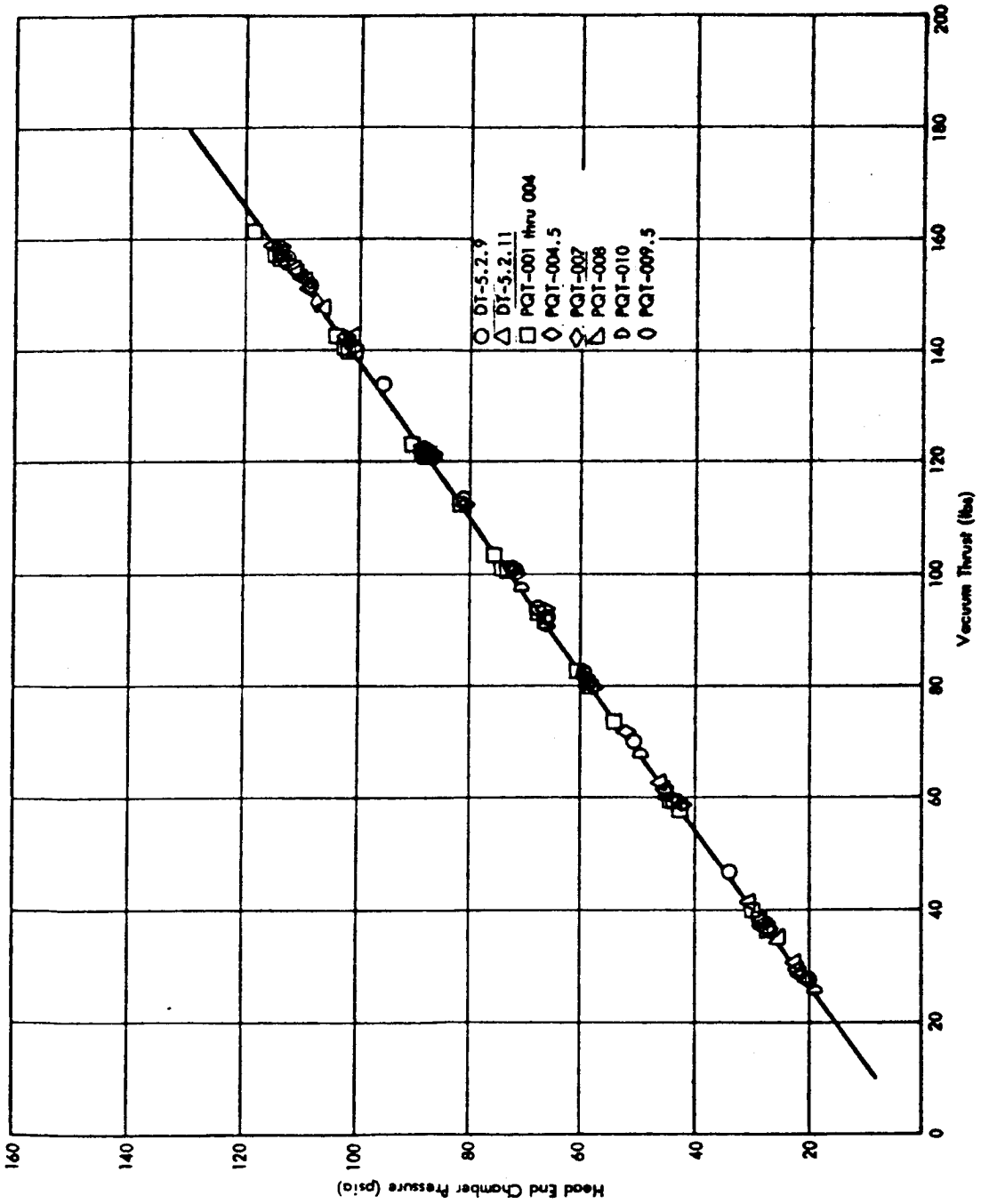

Figure 6.8.7-1. MIRA 150A Head End Chamber Pressure - Vacuum Thrust Data

This work was performed for the Jet Propulsion Laboratory, California Institute of Technology, sponsored by the National Aeronautics and Space Administration under Contract NAS7-100.

6.9 Dynamic Response Performance Tests

Dynamic response data from the JPL/ETS altitude test program are outlined in paragraph 6.9.1. Dynamic response information on typical sea level firings at the IRTS is presented in paragraph 6.9.2. Paragraph 6.9.3 presents a discussion of the applicable combined data on startup, shutdown and variable thrust transient performance.

The detailed discussion of dynamic response parameters that follows will require an understanding of the following definitions:

1. Startup Time - The time interval between TCA receipt of startup signal and attainment of 95% of the initially commanded thrust level.

2. Shutdown Time - For altitude firings, shutdown time is the time interval from shutdown signal (removal of the signal from the electronic switch that controls the helium pilot valves) until 95% of the total shutdown impulse has been generated. For sea level firings, shutdown time is the time interval from shutdown signal until the chamber pressure decays to 30 psia.

3. Startup Impulse - The area under the thrust-time curve over the startup time interval.

4. Shutdown Impulse - For altitude firings, shutdown impulse is the area under the thrust-time curve over the time interval from shutdown signal to the time at which thrust has decayed to 0 lb. For sea level firings, shutdown impulse is the area under the thrust-time curve over the shutdown time interval.

5. Step Response Overshoot - The maximum percentage by which the TCA-delivered thrust increment exceeds the commanded thrust increment in response to a step change in thrust signal level.

6. Step Response - The time interval between a step change in thrust signal level and the initial attainment of the commanded thrust level.

7. Phase Lag - The time interval between a sinusoidally varying thrust command signal and the resultant delivered thrust divided by the period of one full command cycle; the quotient to be multiplied by 360 degrees and the resultant product expressed in degrees phase lag.

8. Amplitude Ratio - The peak-to-peak thrust amplitude delivered in response to a sinusoidally varying thrust command signal divided by the thrust amplitude change in response to the same amplitude change in steady-state thrust signal levels.

9. Loop Width - Loop width is the maximum width of the thrust-signal control loop (expressed in milliamps) for complete and continuous thrust excursions at rates well below system dynamic lags.

6.9.1 Altitude Dynamic Performance Tests

Test Objectives, TCA configuration, test setup, and test conditions during the altitude test program conducted at the JPL/ETS are presented in paragraph 6.6. The test discussion contained herein will be limited to a presentation of the transient test results.

6.9.1.1 Initial Checkout Test

The transient data obtained from Run DY-18, the initial checkout test, were of little value for the following reasons:

1. The test was not conducted in the altitude cell; thus, the startup and shutdown transients were not comparable to altitude conditions.

2. Injection pressure measurements were made adding to the effective injector fluid volumes, and significantly degrading both throttling response and startup and shutdown times.

3. Propellants were not bled at the shutoff valves resulting in a slow thrust buildup.

4. The servoactuator used (P/N C104312B, S/N C53748) was of the Phase II Follow-on configuration rather than the appropriate Phase III flight configuration.

Detailed test data are provided in Table D-1-77 of Appendix D-1; these data are useful for reference only.

6.9.1.2 Initial Altitude Test

The initial altitude test, Run DY-19, provided limited data characterizing MIRA 150A TCA altitude dynamic performance. The chamber pressure at the nozzle end was measured by a Model 351 Photocon pressure gage with a manufacturer's stated response of 10,000 cps.*

Detailed response data based on the Photocon gage are provided in Table D-1-77 of Appendix D-1. Figures 6.9.1-1 and 6.9.1-2 provide copies of the original oscillograph data showing the startup and shutdown transients. During startup the Photocon pressure data indicated several ignition spikes, the largest of which was approximately 115% of the final steady-state level and lasted for 3 milliseconds from initial buildup to final decay. Under sea level ambient conditions, similar Photocon measurements revealed no ignition spikes (see paragraph 6.9.2). The low ambient pressure (approximately 0.05 psia) experienced during the altitude startup has a definite influence on the injector priming and ignition characteristics. Because of the relatively high vapor pressures of the propellants (.75 psia for MMH and 23 psia for MON at 70°F), it is conceivable that the propellants flash vaporized upon opening of the shutoff valves, entered the combustion chamber in the vapor phase, and ignited before the injector passages were fully primed with liquid.

The combustion chamber shell is capable of at least a 1000 psi overpressure at room temperature without structural failure and thus a momentary pressure of approximately 125 psia (115% of 109) is not a structural problem. A total of 20 altitude starts were accomplished with flight weight CC & NAs without failure; thus, it is concluded that TCA reliability is not compromised by the small chamber pressure spikes seen by the Photocon.

*CPL conducted a shock tube test with one of the gages used and obtained a measured response of from 3500 - 4000 cps. Even accepting the lower response values, the Photocon gage is considered adequate for determination of all normal MIRA 150A transients excluding high frequency combustion noise.

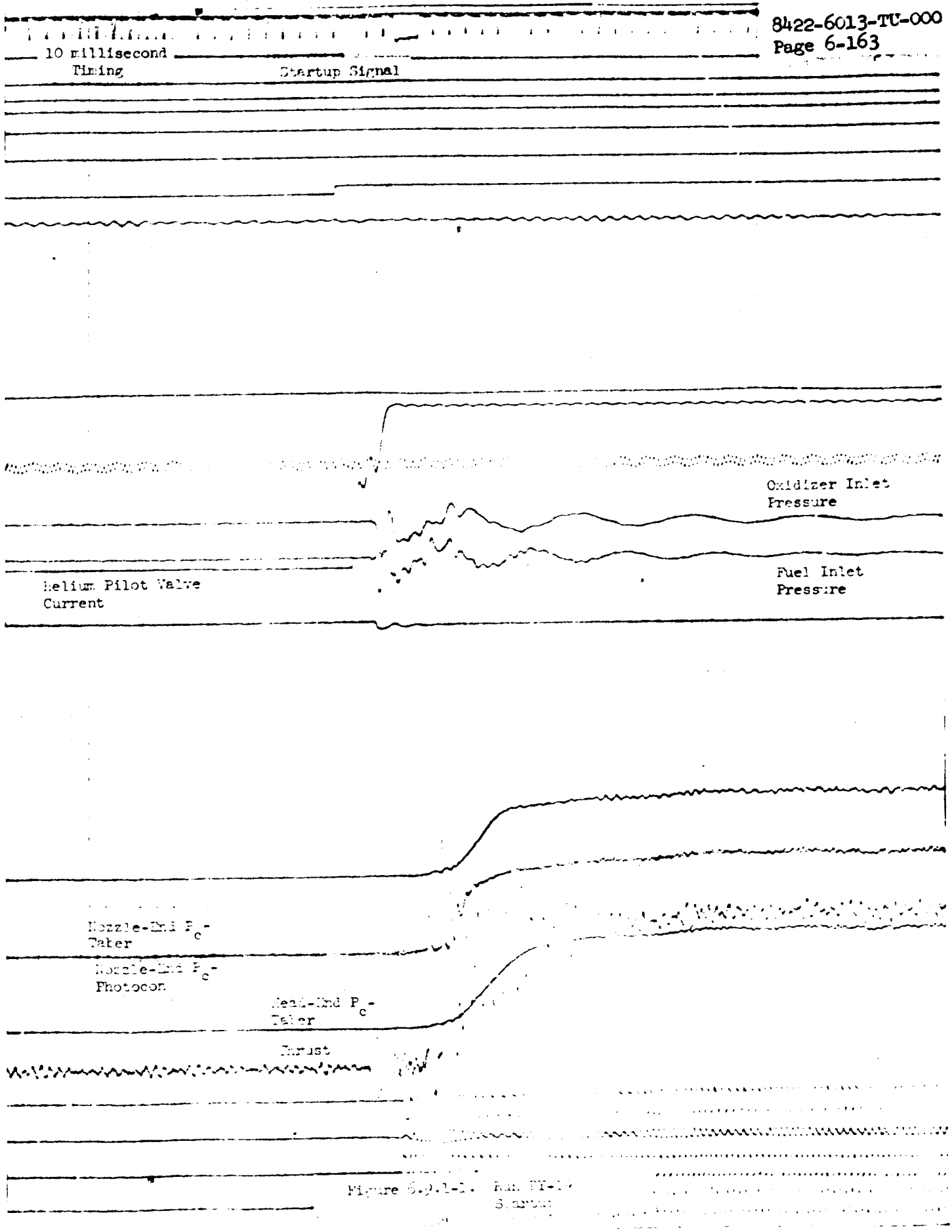

Figure 6.9.1-2. Run PI-1
Startup

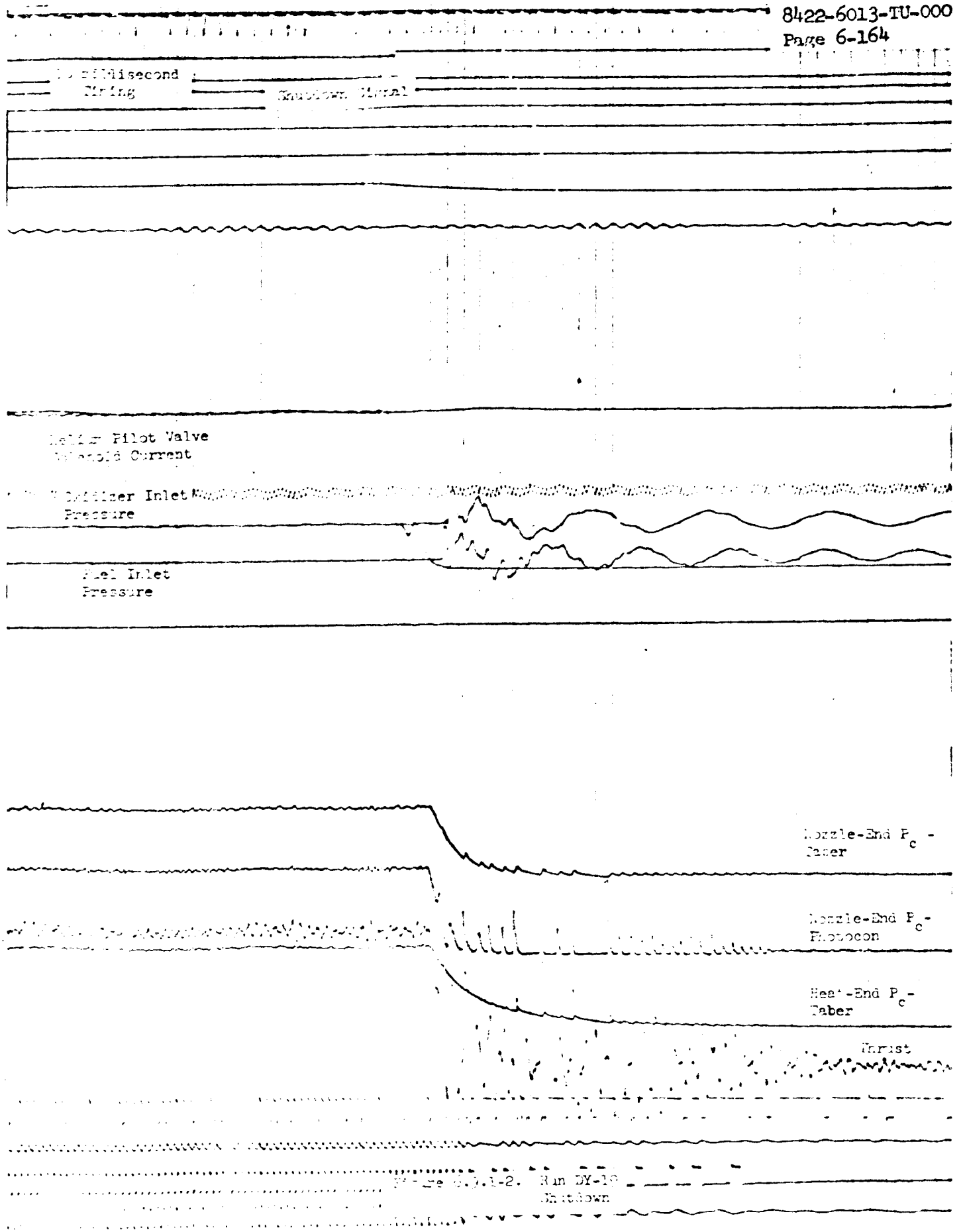

Figure 6.7.1-2. Run DY-10 Shutdown

Table 6.9.1-3 summarizes the startup sequence for Run DY-19. The unusually long start-up time of 0.174 seconds and large startup impulse of 8.5 lb-sec is characteristic of a Phase II type HEA like S/N 004 which had no provision for filling all propellant passages down to the shutoff valves prior to a firing. During a subsequent start, the startup condition would be typical of the flight configuration if the propellants were not removed. Relatively slow thrust buildup results in all cases on an initial firing conducted immediately after TCA installation. Vacuum filling of the propellant passages and bleeding at the quick disconnect ports on the Phase III HEAs will be required for any flight installation.

During shutdown (see Figure 6.9.1-2), somewhat unusual characteristics were noted compared to the sea level firings at the IRTS. On all of the latter tests, the Photocon pressure data indicated a rapid and smooth thrust decay with typical shutdown times ranging from 0.020 - 0.040 second. During Run DY-19, after the initial chamber pressure spikes occurred over a 0.190-second time interval. The cell pressure at the time of shutdown apparently had a significant influence on the propellants trapped in the injector downstream of the propellant shutoff valves. These trapped liquids probably vaporized rapidly, entered the combustion chamber, and then reignited. As the chamber pressure increased and exceeded the propellant vapor pressures, the vaporization ceased until the chamber pressure once more decayed. This cycle is repeated until all of the trapped propellants were exhausted. Table 6.9.1-4 summarizes the shutdown sequence.

Servoactuator signal response data are also provided in Table D-1-77, although they do not truly represent the flight configuration since a Phase II servoactuator was used. Thrust rise time in response to step commands ranged from 0.013 to 0.034 second, readily satisfying the 0.065-second maximum allowable requirement of JPL Specification SAM-50255-DSN-C.

Table 6.9.1-3

TCA Startup Sequence During
Altitude Test DY-19 (Nontypical Startup Conditions)

Event Description	Time (seconds)
Helium pilot valve receives startup signal.	0.000
Helium pilot valve starts to open.	0.004
Helium pilot valve fully open; Propellant Valves start to open.	0.014
First chamber pressure rise indicated.	0.045
Maximum ignition pressure spike followed by rapid chamber pressure rise.	0.055
Chamber pressure and thrust achieve 95% of commanded level.	0.174

6.9.1.3 Initial Altitude Dynamic Throttling Tests

Although the initial altitude dynamic throttling tests (Runs DY-20 through DY-24) were conducted with Thrust Cycle PQ-1 (see Table 6.6.3-2) which was designed to obtain transient response data, the information obtained was of limited usefulness because of facility instrumentation problems. A 60-cps noise of approximately 2.5 ma peak-to-peak amplitude was inadvertently superimposed on the servoactuator command signal influencing the servoactuator response characteristics. Further, during Runs DY-20 through DY-23 the servoactuator command and position signals were amplified by differential amplifiers with only a 100-cps response which compromised the data accuracy. These test setup problems were corrected for later firings. Detailed test results for the initial altitude test are presented in Table D-1-77 of Appendix D-1.

Table 6.9.1-4

MIRA 150A Shutdown Sequence
During Altitude Test DY-19

Event Description	Time (seconds)
Helium pilot valve receives shutdown signal.	0.000
Helium pilot valve starts to close.	0.005
Helium pilot valve fully closed.	0.016
Propellant valves start to close; chamber pressure decay initiated.	0.024
Major chamber pressure decay completed; first reignition spike indicated.	0.035
95% of total shutdown impulse accumulated.	0.160
Last reignition spike occurs.	0.230

6.9.1.4 PQT-001, -002, -003, and -004A

Since PQT-001, -002, -003, and -004A (Runs DY-25 through DY-28) were conducted primarily to obtain steady-state performance information, only limited transient data are available. These data are presented in Table D-1-77 of Appendix D-1. Start and shutdown transients are not reported for PQT-002 (Run DY-26), because helium pilot valve current and voltage signals were inadvertently not recorded making accurate determination of TCA receipt of startup and shutdown commands impossible.

Prior to each of these firings, the feed lines and TCA were drained of propellants and were not bled or vacuum filled prior to startup. The resultant startup transients were therefore not representative of the flight condition wherein propellants are vacuum filled down to the shutoff valve seats.

This test series did serve to show the lack of high response of a Taber gage. The start-up transient during Run DY-25 as represented by the thrust measurement is shown in Figure 6.9.1-5, and as shown by the Taber gage at the head end in Figure 6.9.1-6. The response of the head end Taber gage is obviously inferior as indicated by the long rise time relative to thrust, and by the lack of any ignition pressure spike. The long tubing between the transducer and the TCA (see Figure 6.6.7-1) and the small internal passage (0.058 inch diameter) between the TCA chamber pressure tap and the combustion chamber are contributing reasons. JPL determined by shock tube tests that this installation results in a measurement response of 30 cps at best. Therefore, on the remainder of the transient data, only thrust and/or Photocon chamber pressure data were considered.

Based on measured thrust, the TCA startup times for PQT-001, -002, -003, and -004A were all less than the 0.130-second maximum allowed by JPL Specification SAM-50255-DSN-C in spite of the fact that propellants were not bled at the shutoff valves. Shutdown times ranged from 0.180 to 0.190 second, meeting the 0.200-second JPL specification maximum allowable time. Servoactuator step response times ranged from 0.014 to 0.050 second, all within the JPL specification upper limit of 0.065 second.

6.9.1.5 PQT-004.5

Since all four firings on PQT-004.5 (Runs DY-29 through DY-32) were conducted with a water-cooled combustion chamber, high response Photocon gage chamber pressure measurements were available to evaluate transient response. The detailed response data of PQT-004.5 are provided in Table D-1-77 of Appendix D-1. Figures 6.9.1-7 and 6.9.1-8 provide comparison between thrust and Photocon chamber pressure data on TCA startup and shutdown during Run DY-32. (The zero references on the time axes of these two plots do <u>not</u> correspond to the startup or shutdown signal times - these signals are not shown).

The thrust measurement was found to have two major shortcomings in the determination of TCA transients. First, because of the thrust stand natural frequency of approximately 150 - 185 cps, the chamber pressure spikes during startup and shutdown were not accurately represented by thrust. A significant phase lag and amplitude distortion may be seen by a careful review of Figures 6.9.1-7 and 6.9.1-8. Considerable thrust undershoot or overshoot may be detected, typical of an underdamped spring-mass system.

The second problem is associated with the accurate determination of proper limits of integration for purposes of startup and shutdown impulse computation. Because of the thrust stand oscillations, highly accurate definition of startup and shutdown times was nearly impossible. However, the impulse values based on thrust and Photocon chamber pressure over any given time interval were found to agree within nine percent or better. This relatively small error gave confidence in the Photocon data which was used whenever available for transient response determination for all tests reported in paragraph 6.9.

Figure 6.9.1-5. Run DY-25 Thrust Startup Transient

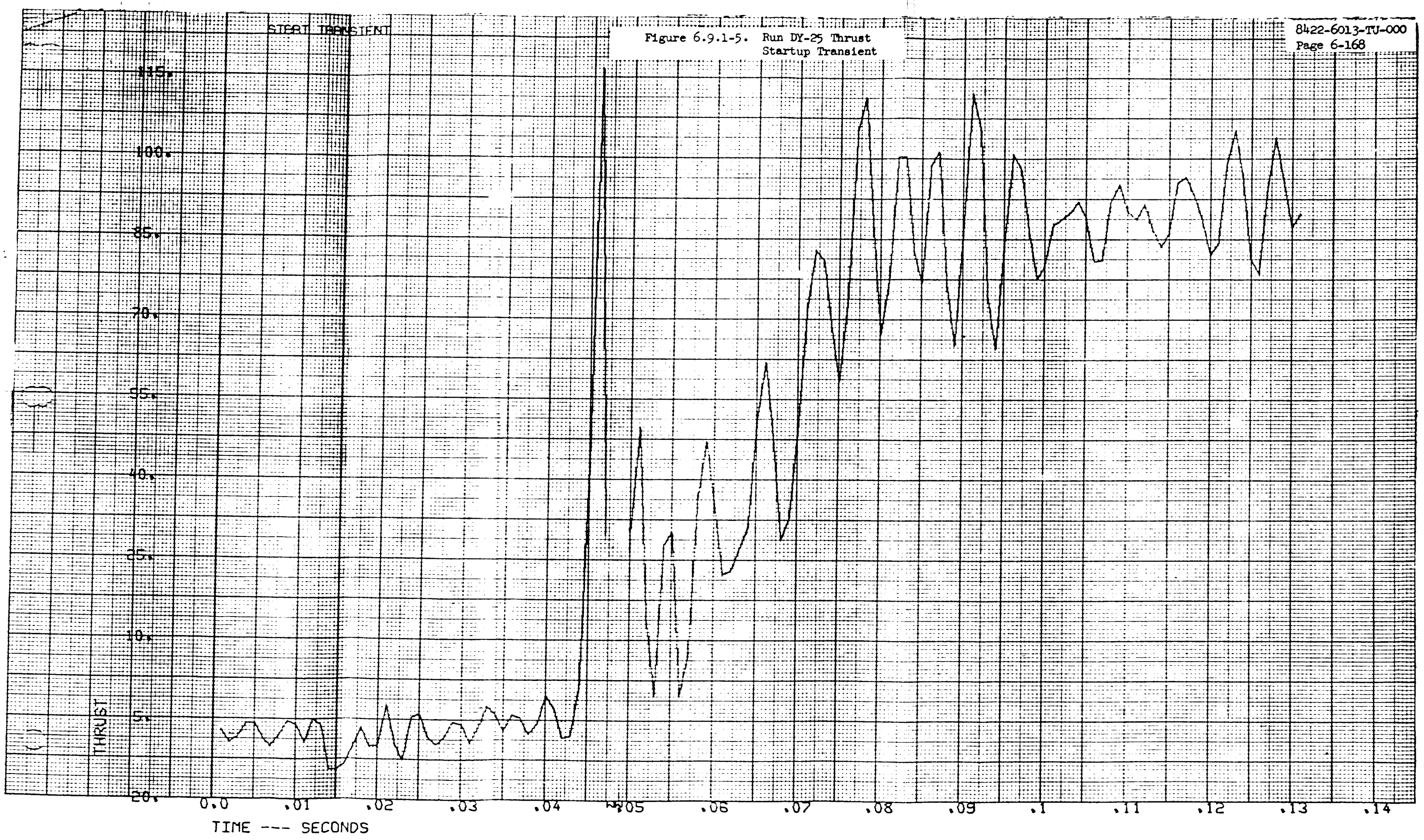

Figure 6.9.1-6. Run DY-25 Head End Chamber Pressure Startup Transient

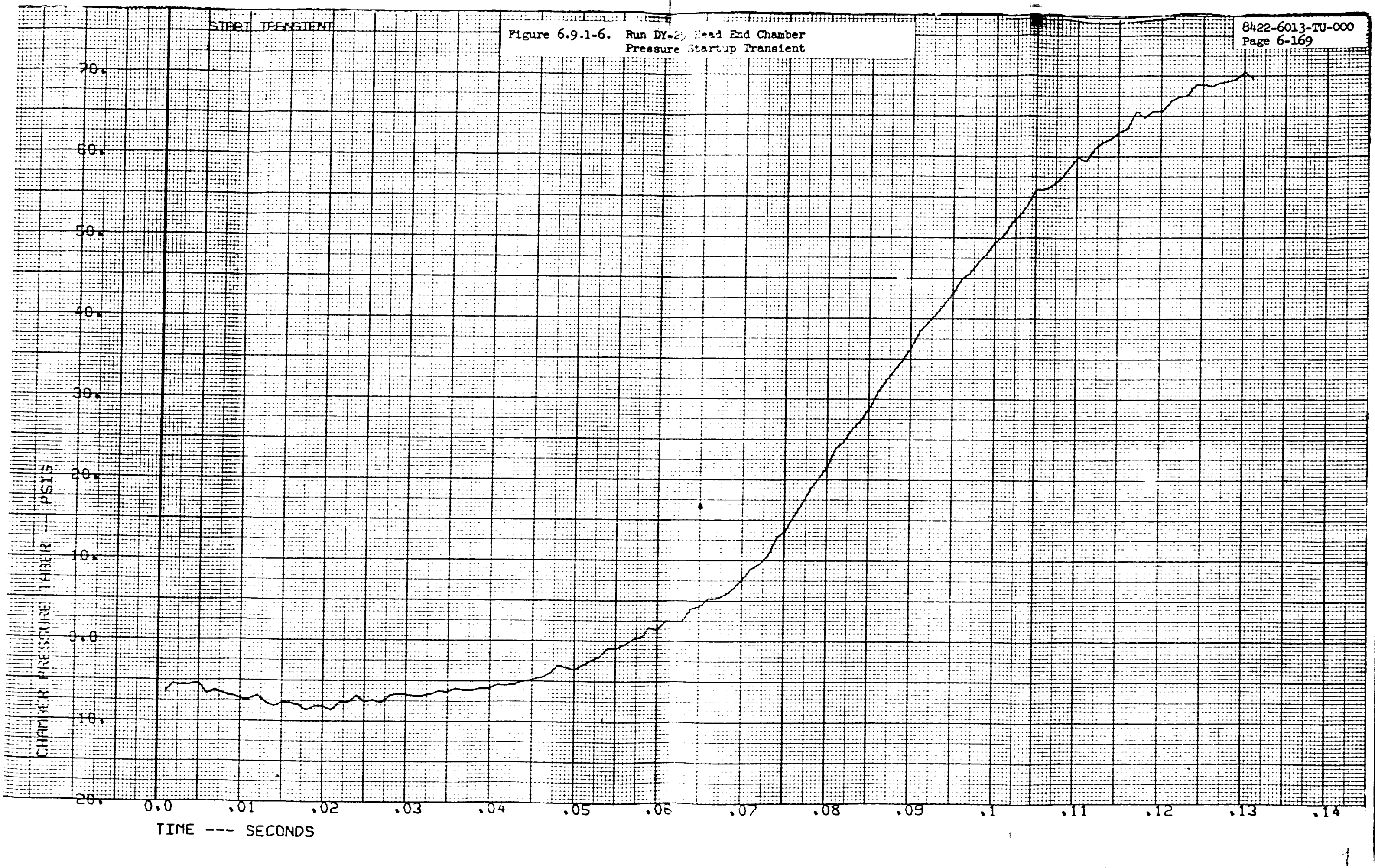

Figure 6.9.1-7. Comparison Between Thrust and Photocon Chamber Pressure During Startup Transient of Run DY-32

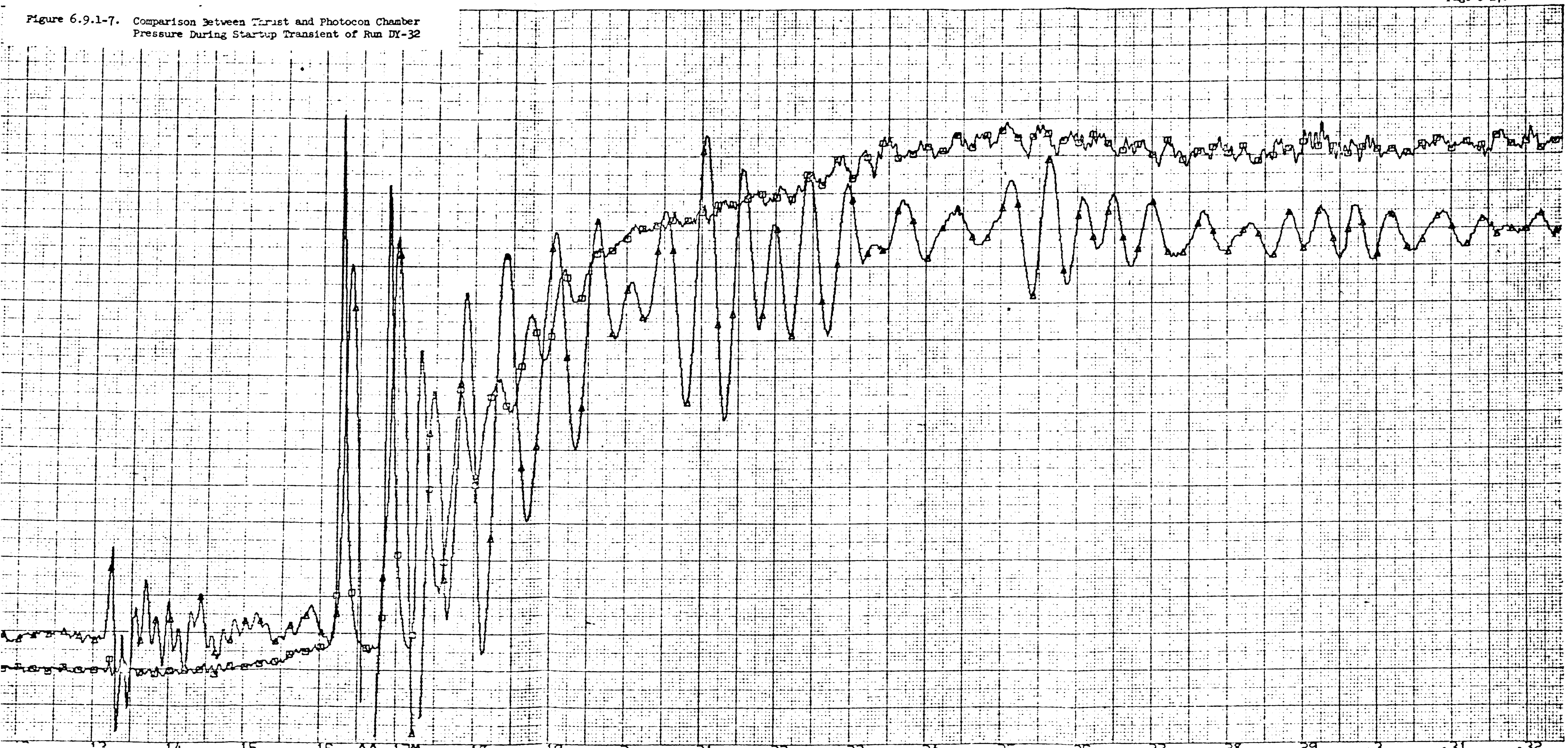

DY-32 MAX SAMPLE --- 5000 SPS

START UP TRANSIENT

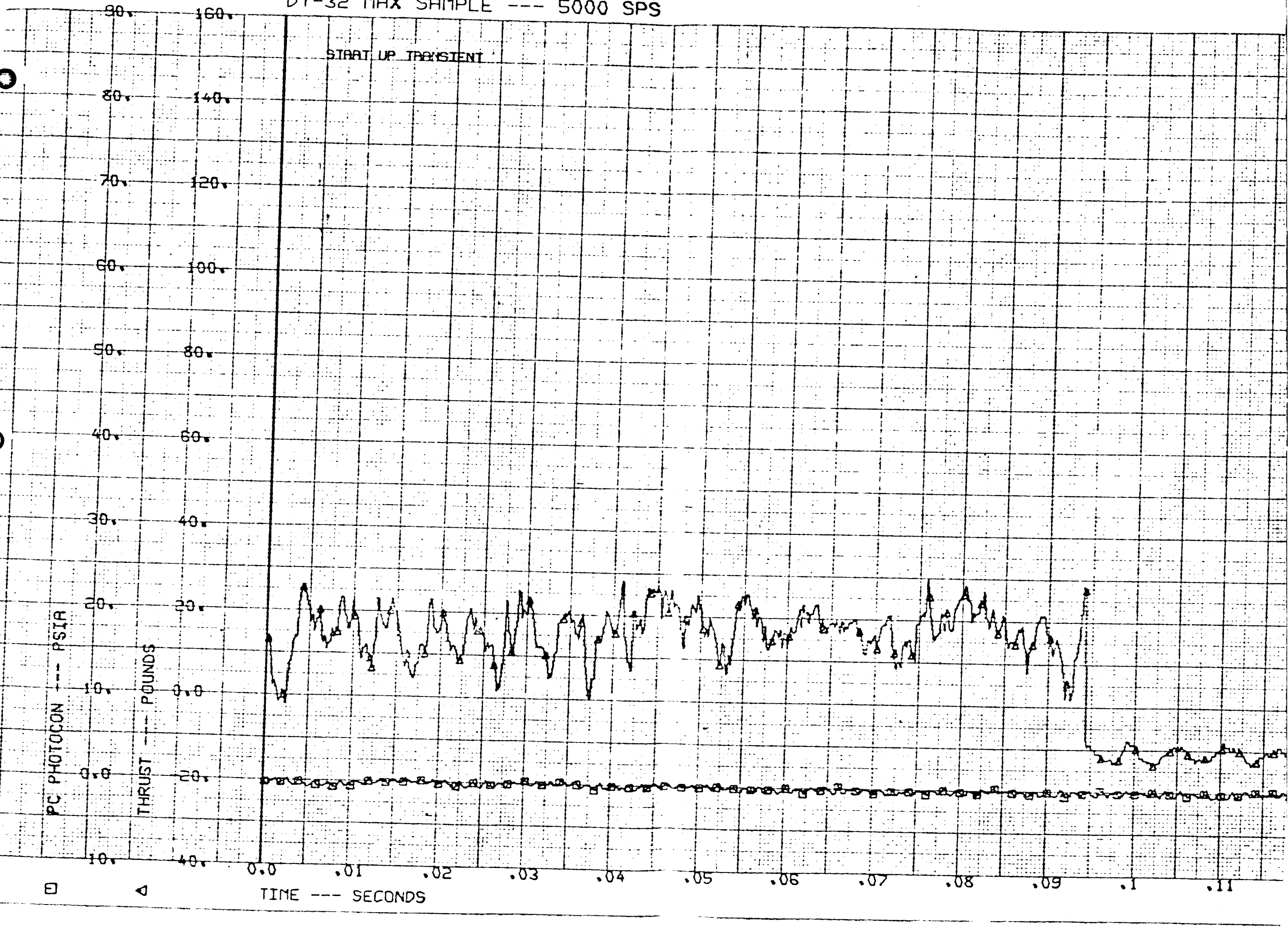

Figure 6.9.1-8. Comparison Between Thrust and Photocon Chamber Pressure During Shutdown Transient of Run DY-32

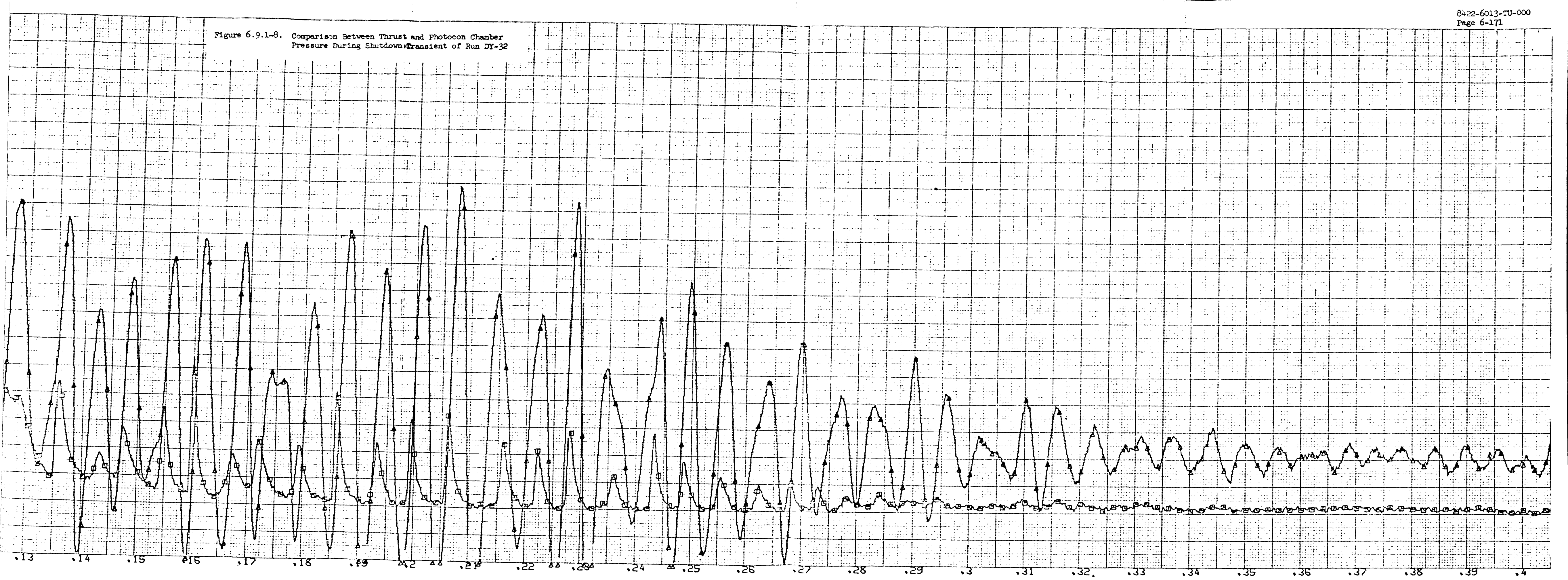

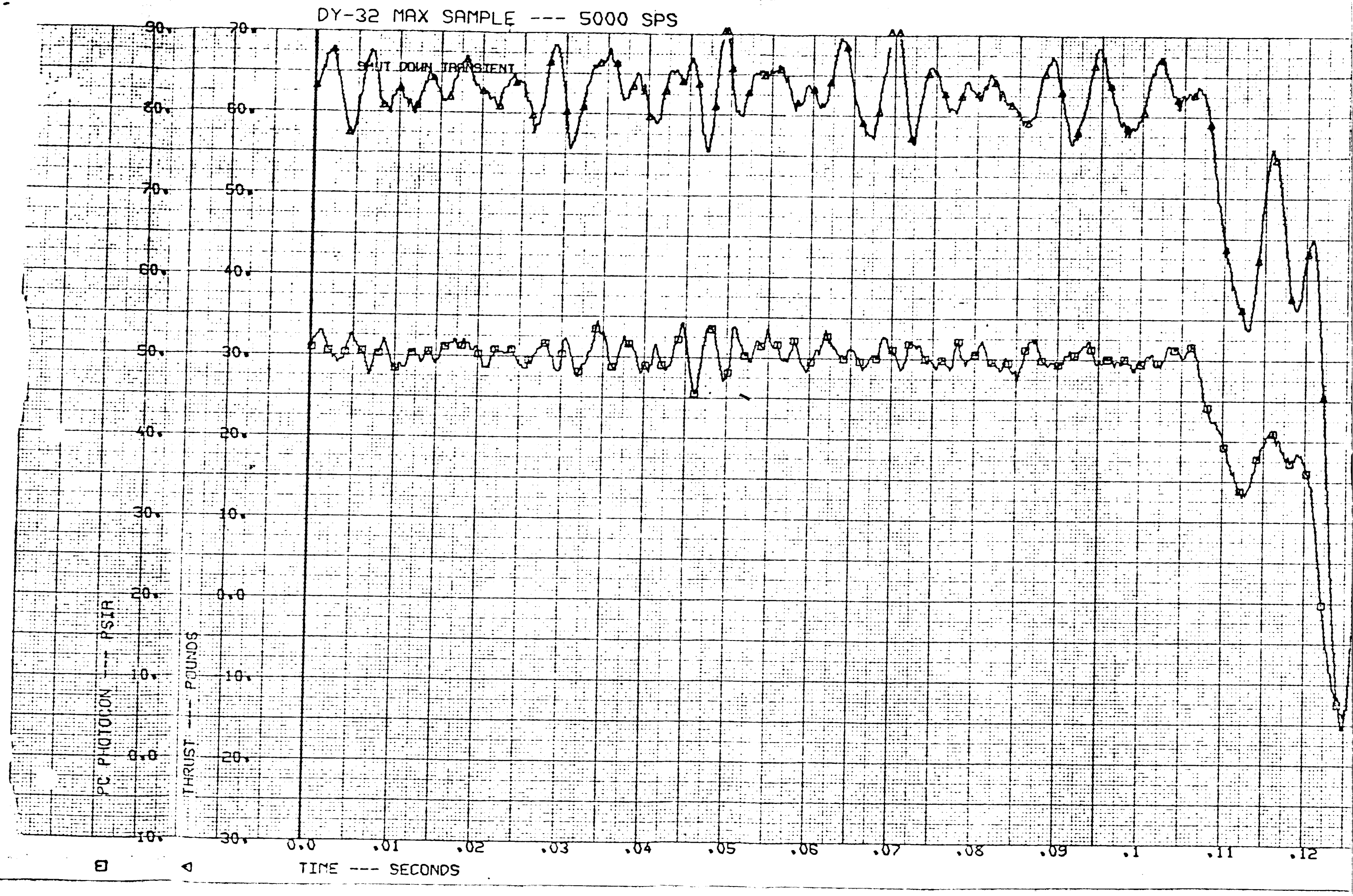
DY-32 MAX SAMPLE --- 5000 SPS
SHUT DOWN TRANSIENT
PC PHOTOCON --- PSIA
THRUST --- POUNDS
TIME --- SECONDS
90.
80.
70.
60.
50.
40.
30.
20.
10.
0.0
70.
60.
50.
40.
30.
20.
10.
0.0
10.
20.
30.
0.0
.01
.02
.03
.04
.05
.06
.07
.08
.09
.1
.11
.12

Thrust response to servoactuator step commands ranged from 0.012 to 0.053 seconds, meeting the 0.065-second maximum requirement. Since propellants were drained from the feed lines prior to all tests, with the exception of Run DY-32, the validity of the start transients during Runs DY-29 through DY-31 is questionable. Startup impulse values ranged from 2.1 to 4.1 lb-sec with startup times varying from 0.102 to 0.125 second. Shutdown impulse values ranged from 2.4 to 3.4 lb-sec with a slight variation with shutdown thrust level indicated. Shutdown times ranged from 0.095 to 0.187 second meeting the 0.200-second specification maximum requirement.

6.9.1.6 PQT-004B

Since PQT-004B (Run DY-33) was conducted with a flight weight CC & NA with only a head end pressure measurement, all response data were based on measured thrust. The major significance of this firing was the demonstration of the capability of the MIRA 150A TCA to achieve a normal startup at the specification minimum TCA and propellant temperatures of 0°F. The startup transient observed during this firing was comparable to the previous startup (Run DY-32) at ambient temperature. Shutdown was normal. The detailed transient data are provided in Table D-1-77 of Appendix D-1.

Anomalous servoactuator behavior was detected. In every instance when the servoactuator received a positive step command while resting against the extend position mechanical stop (minimum thrust), the resultant step response exceeded the specification limit of 0.065 second. In three of these cases, the servoactuator output stage failed to move for periods of 0.015, 01094, and 0.102 second after receipt of a signal even though there were indications from fuel pressure data that the first two stages had functioned. Excessive phase lag was also noted in response to 5 cps sinusoidal commands with values of 31 to 38 degrees obtained as compared to a maximum allowable specification requirement of 28 degrees.

In the investigation of this performance failure, all previous test history with the servoactuator (P/N C104312B, S/N C53750) was carefully reviewed. During component acceptance testing, excessive step response times of up to 0.090 second and phase lags of 27 degrees at 5 cps were experienced. This unit had been submitted to MRB and subsequently bought off. During the acceptance firing of HEA 150A-001 (see Test C2-564 in paragraph 4.4), step response of 0.075 second and 5-cps phase lags of 27 degrees were experienced.

A sea level firing (Run DY-34 - see paragraph 6.6.12) at ambient temperature was conducted at the JPL/ETS immediately after Run DY-33. The response data from this test (see Table D-1-77 of Appendix D-1) again showed an excessive phase lag of 36 degrees and a step response of 0.071 second. After completion of TCA testing, the servoactuator was given component level tests and then disassembled and inspected. No evidence of distortion, wear, or galling was found. It was concluded that the out-of-specification performance was not caused by low temperature, since it had been experienced prior to Run DY-33. However, the investigation failed to uncover the exact cause of this performance. (For further details on this servoactuator, see paragraph 6.12.1). During a formal production program this servoactuator would have been rejected and not used for TCA testing or delivery.

6.9.1.7 PQT-007

No throttling data are available from PQT-007, because the three firings (Runs DY-35, -36, and -37) were all conducted at fixed maximum thrust. All available data are provided in Table D-1-77 of Appendix D-1.

Run DY-36 was the only firing of this series of three starts not preceded by propellant drainback. The startup time was 0.073 second compared to 0.128 and 0.105 second during Runs DY-35 and DY-37, respectively. A considerable difference in startup impulse between Run DY-36 and the other two firings was also noted. Shutdown impulse values ranged from 5.4 to 6.0 lb-sec corresponding to a shutdown time range of from 0.104 to 0.135 second.

6.9.1.8 PQT-008

PQT-008 was conducted at a minimum fixed thrust level limiting the amount of transient operating information. Detailed data for these firings (Runs DY-38 through DY-40) are provided in Table D-1-77 of Appendix D-1. Run DY-38 was conducted after draining and refilling of the propellant feed lines resulting in a somewhat slower startup compared to Runs DY-39 and DY-40. Startup times were 0.261 and 0.290 second during the latter two firings.

Shutdown characteristics differed somewhat from those at the higher thrust levels. Figure 6.9.1-9 shows the shutdown of Run DY-40 at a thrust level of 32 lbs. Pressure spikes are not present for this low thrust shutdown. Rather, chamber pressure tailoff is smooth and lasts for a longer time period than for shutdown at higher chamber pressures. This different combustion transient characteristic may be attributed to the smaller injector gap settings at minimum thrust resulting in the trapped propellants entering the chamber at a steadier rate and reacting more smoothly.

Another significant difference is the time required for closing the propellant shutoff valves. The valve closure times may be roughly estimated by noting the time at which the water hammer is sensed by the propellant inlet pressure transducers. By this determination technique, the oxidizer and fuel shutoff valve closing times were 0.048 and 0.029 second, respectively, during the minimum thrust shutdown on Run DY-40, compared to 0.019 and 0.015 second, respectively, during the mid-thrust shutdown on Run DY-32 (see Figure 6.9.1-2).

This increase in the required shutoff valve closing time with decreasing shutoff thrust levels may be readily explained by considering the principles of the valve operation. The propellant shutoff valves are opened pneumatically. A spring returns the poppet to the closed position, and while propellant is flowing, the propellant pressures also generate a closing force. These propellant pressures vary as shown in Figure 3.4.11-1. The total force tending to close the poppet therefore varies directly with thrust level, and causes an inverse valve closing time relationship with thrust.

6.9.1.9 PQT-009.5 and -010

PQT-009.5 and PQT-010 test series (Runs DY-41 through DY-46) were identical in all respects with the exception that PQT-009.5 was conducted with the servoactuator and propellants conditioned to the specification minimum temperature ($0^{\circ}F$), and PQT-010 was conducted at ambient temperature conditions. The use of a water-cooled combustion chamber for these tests permitted a Photocon chamber pressure measurement to be made. Photocon pressure and servoactuator signal data were used in the thrust transient analysis. Table D-1-77 of Appendix D-1 provides some of the detailed transient data. Further discussion of these test results is presented in paragraph 6.9.3.

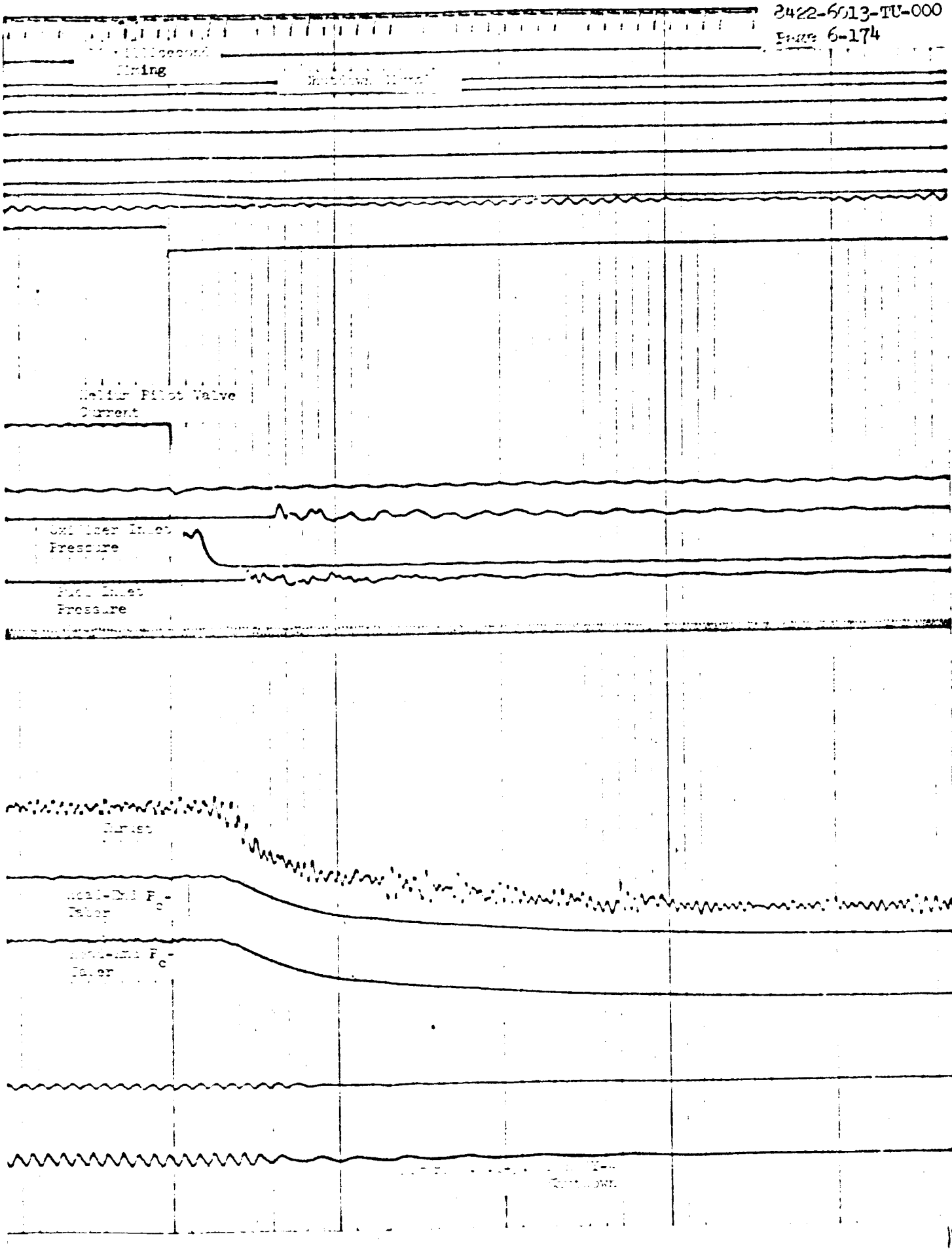
Firing
Pilot Valve
Current
Pressure
Pressure

6.9.1.10 PQT-005

Detailed test data on PQT-005 (Runs DY-47, -48, and -49) are provided in Table D-1-77 of Appendix D-1. Runs DY-47 and DY-48 were conducted with a flight weight CC & NA, and Run DY-49 employed a water-cooled combustion chamber. Thrust data were used on Runs DY-47 and DY-48, and Photocon chamber pressure data were used on the latter firing.

Startup, shutdown, and throttling transients were comparable to previous test results. Servoactuator response times again exceeded 0.065 second for steps initiated from the mechanical stop positions on the servoactuator.

6.9.2 Sea Level Dynamic Performance Tests

Detailed sea level transient data are reported in Table D-2-20 of Appendix D-2. The tests in this table include HEA performance firings conducted in accordance with Acceptance Test Specification TS3-01B (paragraph 4.4), and miscellaneous other firings conducted at the IRTS. Photocon chamber pressure data were used for dynamic analysis of all of these tests. Chamber pressure was converted to equivalent thrust by applying the vacuum thrust coefficients reported in paragraph 6.8.

Figures 6.9.2-1 through 6.9.2-5 show acceptance test data from Phase III HEA 150A-007 fired at sea level. These data are typical of sea level dynamic response data on startup and shutdown chamber pressure, step thrust response increase and decrease, and chamber pressure to signal linearity. A comparison of Figures 6.9.2-1 and 6.9.2-2 with Figures 6.9.1-7 and 6.9.1-8 (in the previous section) indicates differences between sea level and altitude transients. These differences are discussed in detail in paragraph 6.9.1.2.

Although the sea level startup and shutdown transients are not accurate representation of TCA behavior at altitude, the sea level data are useful quality control information. For example, Run C2-568 with HEA 150A-005 resulted in a 0.154 second shutdown time and a 16.4 lb-sec shutdown impulse; both were well outside the normal data spread. It was subsequently discovered that corrosion and dirt had caused sluggish operation of the helium pilot valve.

No significant difference between altitude and sea level throttling dynamics was detected.

6.9.3 Combined Sea Level and Altitude Transient Data Discussion

6.9.3.1 Altitude Startup and Shutdown Transients

This paragraph presents the statistical summary of the startup and shutdown transient data discussed in paragraph 6.9.1. The following data were eliminated from the sample:

1. All startup transient data from firings preceded by propellant drain-back (includes Runs DY-19, DY-20, DY-25 through DY-31, DY-33 through DY-35, DY-37, DY-38, DY-41, and DY-44 through DY-48A).

2. All shutdown transients where thrust stand oscillations were sufficiently severe to preclude an accurate determination of shutdown time, and where no Photocon chamber pressure data were available (includes Runs DY-20 through DY-28, DY-33, DY-34, DY-47, and DY-48).

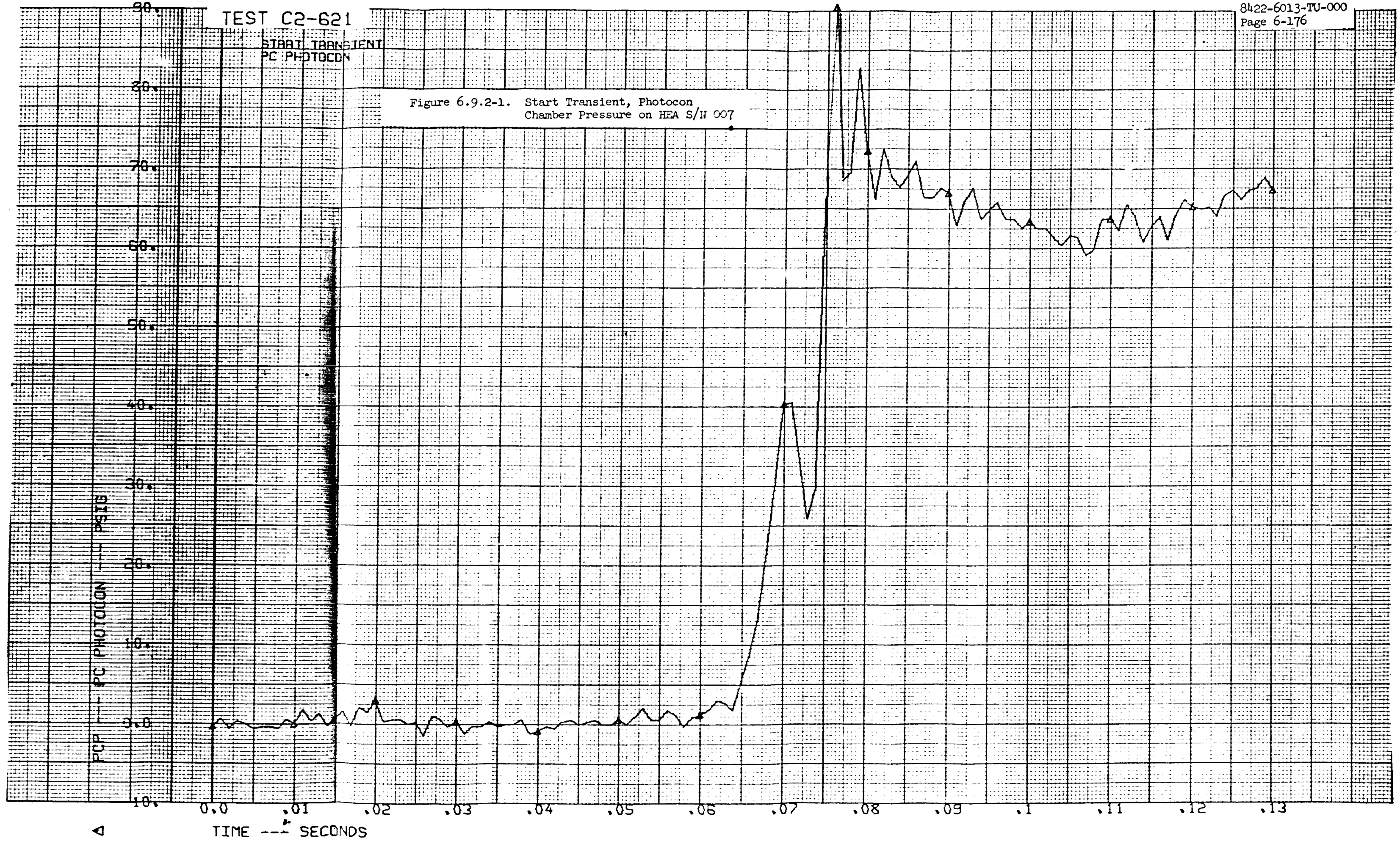

Figure 6.9.2-1. Start Transient, Photocon Chamber Pressure on HEA S/N 007

Figure 6.9.2-2. Stop Transient, Photocon Chamber Pressure on HEA S/N 007

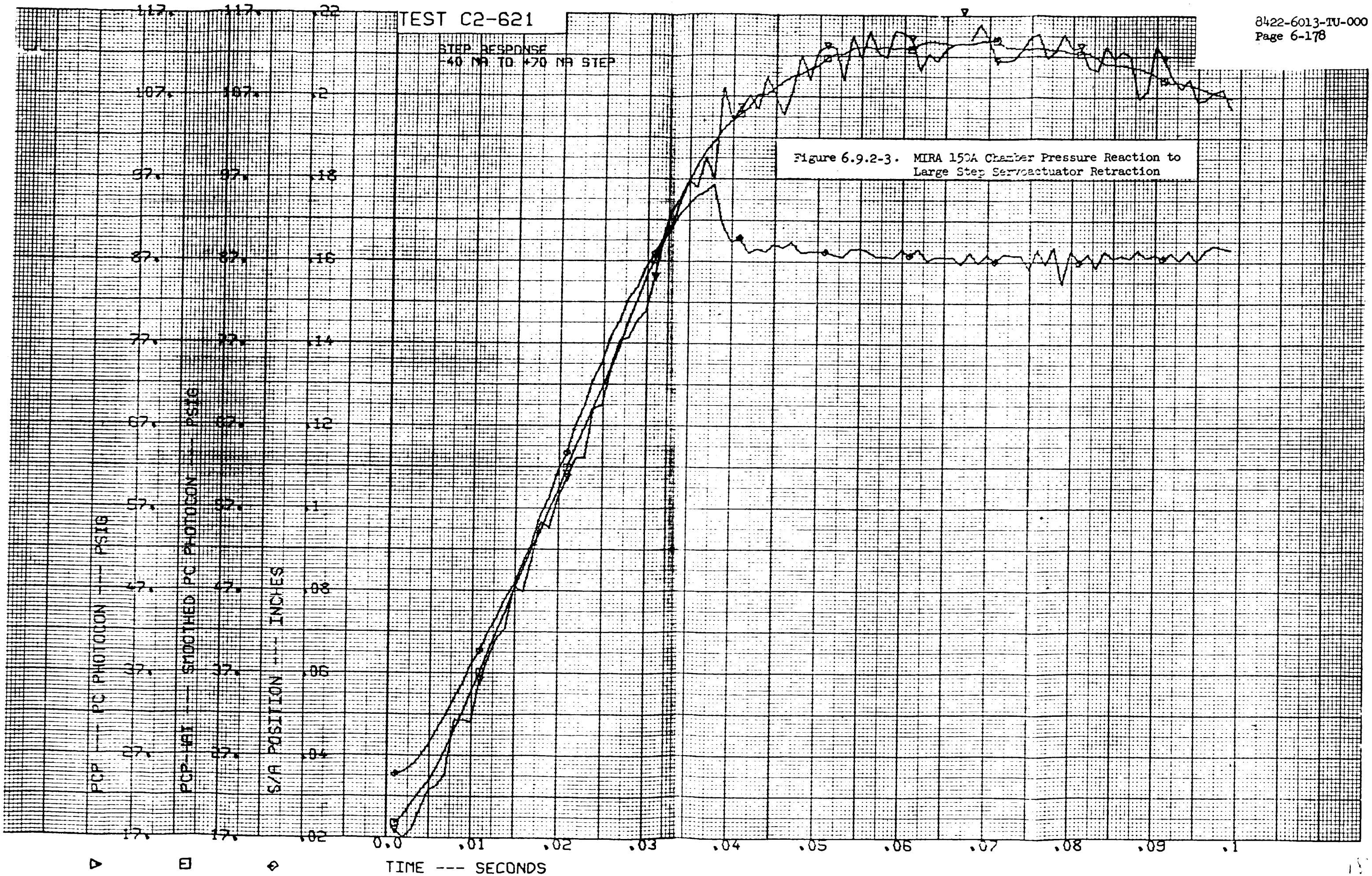

Figure 6.9.2-3. MIRA 150A Chamber Pressure Reaction to Large Step Servoactuator Retraction

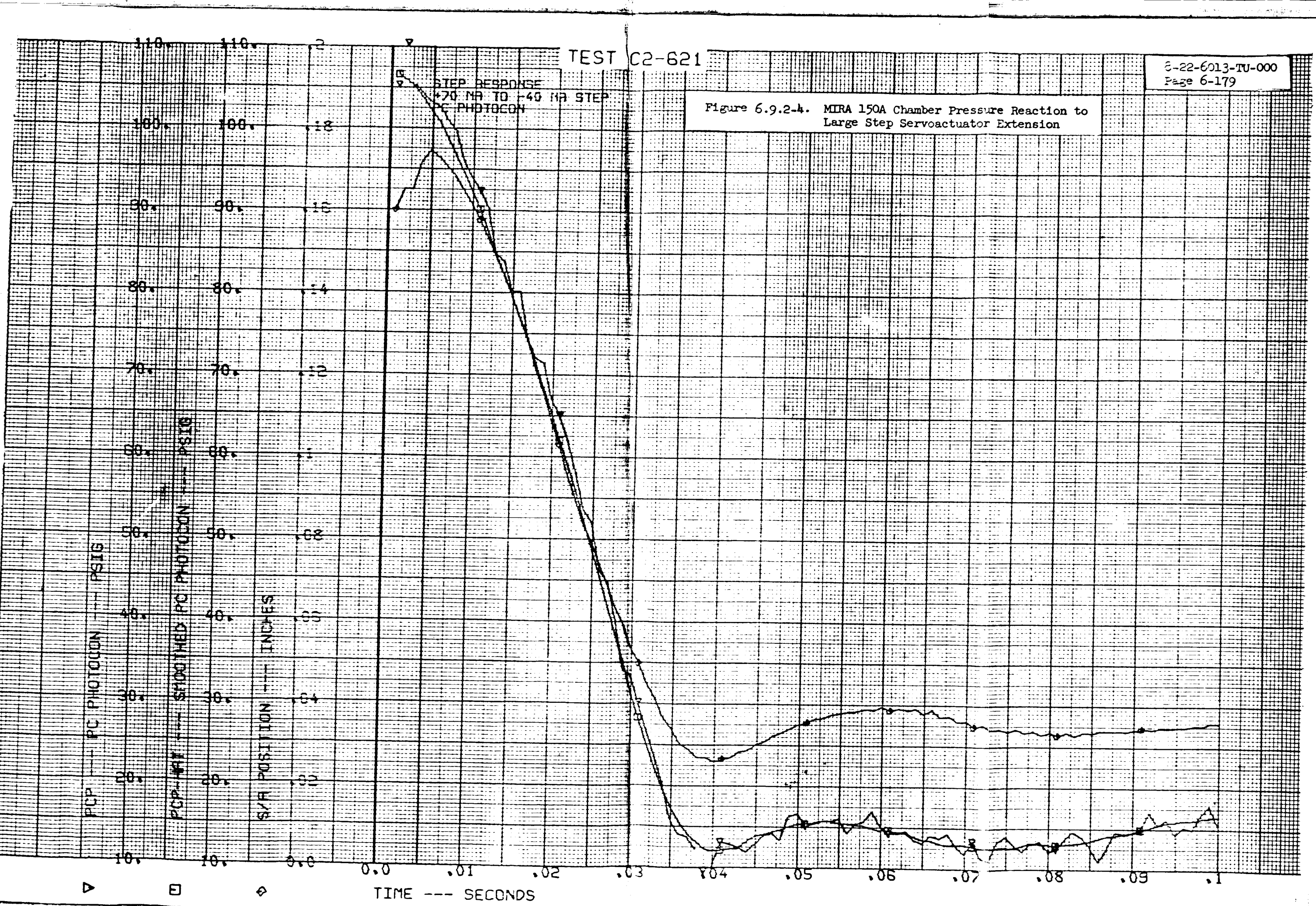

Figure 6.9.2-4. MIRA 150A Chamber Pressure Reaction to Large Step Servoactuator Extension

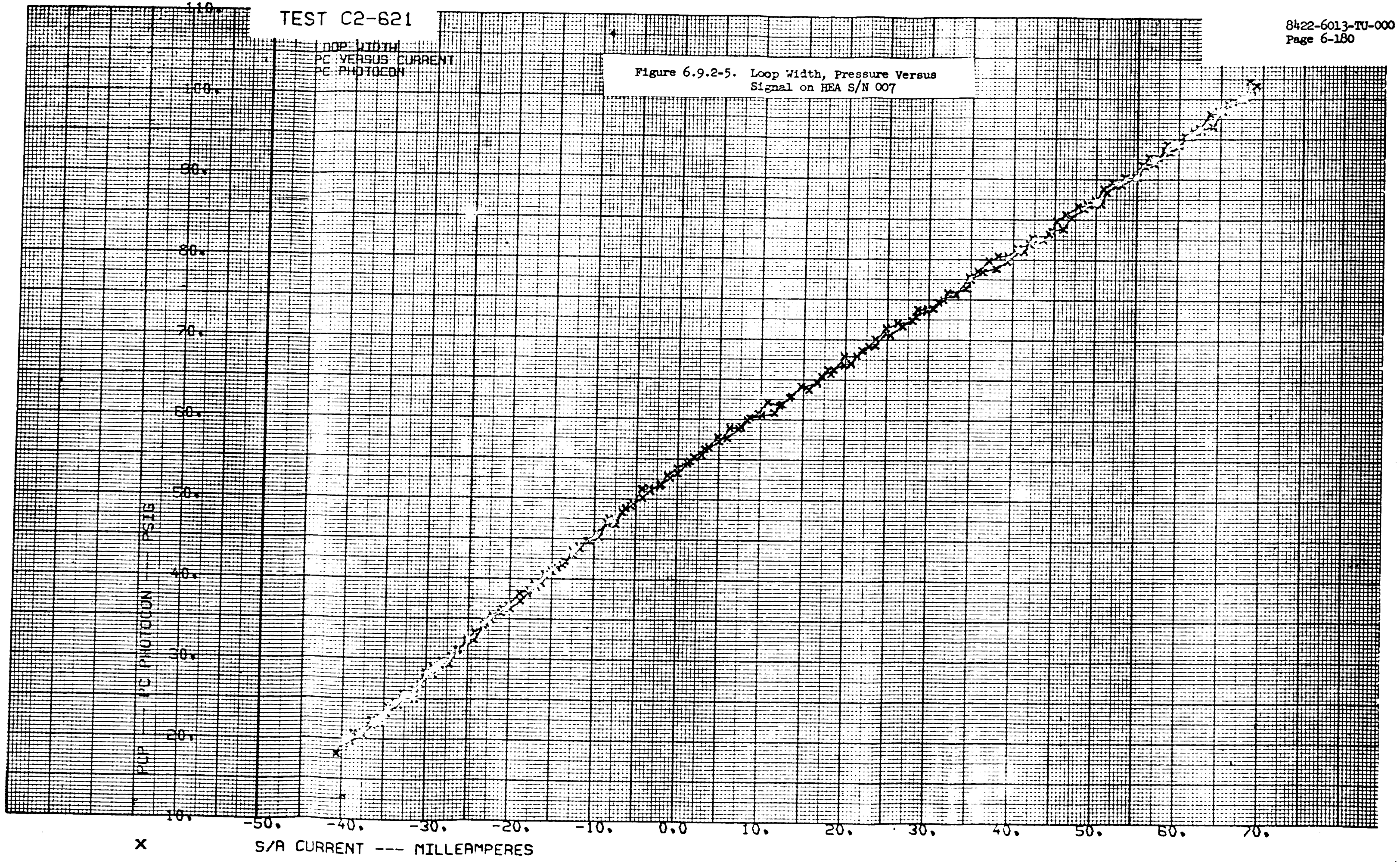

Figure 6.9.2-5. Loop Width, Pressure Versus Signal on HEA S/N 007

The remaining data were then grouped according to the approximate startup and shutdown thrust levels (minimum, mid-range, or maximum), and the mean and 3-sigma deviation estimates were computed. These estimates of startup time and impulse, and shutdown time and impulse are provided in Tables 6.9.3-1 through 6.9.3-4. In some instances, the sample size was not sufficient to obtain reliable estimates. In other cases, only one TCA was used for an estimate, and the TCA-to-TCA variability could not be determined. In general, sample sizes were small and additional test data would be required to obtain more accurate limits.

JPL Specification SAM-50255-DSN-C requires that startup times not exceed 0.130 second for all thrust levels of 90 lbs or above. Table 6.9.3-1 indicates this requirement would be met by the 0.117 second maximum estimate at 90 lbs thrust as well as by the reduced time of 0.089 second at the 150-lb thrust level. The JPL specification also requires a 0.200-second maximum shutdown time and a 2 lb-sec maximum shutdown impulse variation.

Table 6.9.3-1

TCA Altitude Startup
Time Estimates

	Sample Size	Nominal Value (second)	3-sigma Deviation
Minimum Thrust (30 lbs)	2	0.275	*
Midrange Thrust (90 lbs)	3	0.104	±0.013
Maximum Thrust (150 lbs)	5	0.077	±0.012

*Sample size insufficient for reliable estimate.

Table 6.9.3-2

TCA Altitude Startup
Impulse Estimates

	Sample Size	Nominal Value (lb-sec)	3-sigma Deviation
Minimum Thrust (30 lbs)	2	3.4	*
Midrange Thrust (90 lbs)	3	3.1	± 1.2
Maximum Thrust (150 lbs)	5	3.1	± 2.6

*Sample size insufficient for reliable estimate.

Table 6.9.3-3

TCA Altitude Shutdown
Time Estimates

	Sample Size	Nominal Value (second)	3-sigma Deviation
Minimum Thrust (30 lbs)	7	0.179	+0.280 -0.179
Midrange Thrust (60-100 lbs)	7	0.165	±0.122
Maximum Thrust (150 lbs)	3	0.123*	±0.056*

*Estimates based on data from one TCA only.

Table 6.9.3-4

TCA Altitude Shutdown
Impulse Estimates

	Sample Size	Nominal Value (second)	3-sigma Deviation
Minimum Thrust (30 lbs)	7	3.2	± 2.9
Midrange Thrust (60-100 lbs)	7	3.3	± 2.4
Maximum Thrust (150 lbs)	3	5.6*	± 1.1*

*Estimates based on data from only one TCA.

Table 6.9.3-3 indicates the shutdown time requirement will not be met, except at maximum thrust. The measured ± 2.4 lb-sec shutdown impulse variation also exceeds the ± 1 lb-sec specification requirement. The part of this impulse variability which is attributable to TCA-to-TCA variation is estimated to be ± 1.9 lb-sec. For use on a single spacecraft, reliability would be enhanced by matching TCAs with approximately equal shutdown impulse values. Helium pilot valve data provided in paragraph 5.1.3 indicate that approximately ± 0.31 lb-sec (80 lb thrust multiplied by ± 3.9 milliseconds variation in valve closing times) of the total impulse variation is caused by helium pilot valve functioning time. The remainder is caused by shutdown thrust level (60-100 lbs range), propellant valve closing time, and transient combustion variability.

6.9.3.2 Sea Level Startup and Shutdown Transients

All of the sea level data provided in Table D-2-20 of Appendix D-2 with the exception of Run C2-568 shutdown (helium pilot valve malfunction) were used to derive the statistical data provided in Tables 6.9.3-5 through 6.9.3-8. Because the MIRA 150A nozzle may not achieve choked flow at minimum thrust under sea level conditions, no minimum thrust transient data are available.

Table 6.9.3-5

TCA Sea Level Startup
Time Estimates

	Sample Size	Nominal Value (second)	3-sigma Deviation
Minimum Thrust (30 lbs)	*	*	*
Midrange Thrust (90 lbs)	8	0.069	± 0.036
Maximum Thrust (150 lbs)	4	0.026	+ 0.048 - 0.026

*Data not available.

Table 6.9.3-6

MIRA 150A Sea Level Startup
Impulse Estimates

	Sample Size	Nominal Value (second)	3-sigma Deviation
Minimum Thrust (30 lbs)	*	*	*
Midrange Thrust (90 lbs)	9	1.9	± 1.4
Maximum Thrust (150 lbs)	4	0.87	± 0.31

*Data not available.

Table 6.9.3-7

TCA Sea Level Shutdown
Time Estimates

	Sample Size	Nominal Value (second)	3-sigma Deviation
Minimum Thrust (30 lbs)	(1)	(1)	(1)
Midrange Thrust (90 lbs)	8	0.035	± 0.030
Maximum Thrust (150 lbs)	3	0.028(2)	± 0.003(2)

NOTES: (1) Data not available.

(2) Estimates based on data from one HEA only.

Table 6.9.3-8

TCA Sea Level Shutdown
Impulse Estimates

	Sample Size	Nominal Value (second)	3-sigma Deviation
Minimum Thrust (30 lbs)	(1)	(1)	(1)
Midrange Thrust (90 lbs)	8	2.8	± 2.5
Maximum Thrust (150 lbs)	3	3.9(2)	± 0.3(2)

NOTES: (1) Data not available.

(2) Estimates based on data from one HEA only.

6.9.3.3 Throttling Dynamics

Only tests using a Phase III servoactuator were considered in determining TCA dynamic throttling characteristics. The primary tests providing these data are PQT-009.5 and PQT-010. Other applicable tests include Runs C2-621, C2-680, and C2-710 conducted at the IRTS.

Servoactuator acceptance test results reported in Table 5.1.1-10 should also be considered, because almost all TCA dynamic lags are attributed to the servoactuator for step and 5-cps sinusoidal response performance.

In comparing the data from PQT-009.5 and -010, no significant difference in step response was detected between the low temperature and ambient temperature tests. However, a significant difference in step response was noted when the servoactuator was commanded off the extend or retract mechanical stop positions. In these cases, there was an initial delay before the output stage started to move after receipt of the step command. After motion was initiated, the rise time was well within the 0.065 second requirement. Because of the time delay in starting movement of the servoactuator output shaft, these step responses were as long as 0.088 second total. For all intermediate signal levels, the maximum step response times did not exceed 0.038 second.

The reason for this initial time delay may be explained by a review of servoactuator operation. (Refer to paragraph 3.2.6.) For all command signals within the limits of the mechanical stops, the second stage spool and flapper are caused to return to the null or center position by the feedback spring once the output shaft reaches the commanded position. The limits on the mechanical stops are required to be outside the -70 to +70 milliamp range by Servoactuator Equipment Specification EQ2-23B. If a command signal exceeds that required to place the output spool against one of its stops, the feedback spring is unable to exert sufficient force to null out the torque motor force on the flapper, and both the flapper and second stage spool are driven to an extreme position. The initial time lag is that required for the flapper and second stage spool to travel the full stroke before the output stage can respond.

JPL Specification SAM-50255-DSN-C expresses response requirements in terms of step command signals of -70 to +80 and +70 to -80 milliamps. Under these conditions, a servoactuator that meets component acceptance test requirements would never be required to initiate a large step from a stop position, and would therefore not experience the response lags noted during these firings. The servoactuator used for these tests had the retract stop set at +69 milliamps and the extend stop set at -76 milliamps. Actual signal levels during the TCA firings ranged from -79 to +73 milliamps. The shape of the step response traces on the oscillograph records indicated no overshoots upon approaching the extreme positions, further confirming the fact that the servoactuator was hitting the mechanical stops.

Sinusoidal signal response data from PQT-009.5 and -010 firings are provided in Figures 6.9.3-9 through 6.9.3-12. Phase lag data (Figures 6.9.3-9 and -10) indicate no significant differences between the ambient and low temperature firings at comparable signal levels. Although more erratic, the amplitude ratio data (Figures 6.9.3-11 and -12) are also similar at the two temperature levels. Temperature apparently has no significant effect on servoactuator response in the $0^{\circ}F$ to $70^{\circ}F$ range.

Signal level did have a noticeable influence on TCA response characteristics, especially at the minimum thrust level. Phase lag at 5 cps for the 0 ± 7.5 and $+62.5 \pm 7.5$ signal levels did not exceed 23 degrees. At the -62.5 ± 7.5 signal level, the phase lage at 5 cps reached 34 degrees compared to a maximum allowable value of 28 degrees. The shape of the response curve at the low level was also somewhat unusual as indicated by Figure 6.9.3-13. The actual command signal levels were measured as -64.5 ± 8.5 milliamps, slightly lower than the -62.5 ± 7.5 intended level. These levels are shown on the thrust-signal hysteresis loop obtained from the large ramp signal input during Run DY-41 and plotted in Figure 6.9.3-14. This figure shows that the servoactuator was operating in the region having the largest loop width (approximately 4 milliamps at the -64.5 milliamp level), and was at the mechanical stop at the low end of the sinusoidal curve (at -73 milliamps). The behavior noted is attributed to this situation. The MIRA 150A TCA equipped with a Phase III servoactuator will meet the specification requirements of a 28-degree maximum phase lag and 0.95 minimum amplitude ratio in response to a 5-cps sinusoidally varying input signal of 15 milliamps peak-to-peak amplitude at all signal levels except those which cause the servoactuator to operate in the regions of the mechanical stops (+70 milliamps, or greater).

Large ramp signal response data for PQT-009.5 and PQT-010 are provided in Figures 6.9.3-14 and 6.9.3-15. The maximum loop width for these tests was approximately 4.5 milliamps occurring at the minimum thrust level. This is well within the maximum allowable 15% of the command current excursion (160 milliamps in this case) required by JPL Specification SAM-50255-DSN-C. The thrust-signal gain values also fell well within the 0.7 to 1.0 lb/ma specification limits. The downward shift in the thrust-signal curve during Run DY-46 was caused by a decrease in total propellant flow rate at low temperature. This phenomenon is explained in paragraph 6.5.

The summarized dynamic throttling characteristics of the MIRA 150A TCA are provided in Table 6.9.3-16.

On a 3-sigma deviation worst case basis, several of the demonstrated dynamic response characteristics did not meet the requirements of JPL Specification SAM-50255-DSN-C. Step response overshoot was 4% above the allowable 25%, the phase lag for 5-cps signals of -62.5 ± 7.5 milliamps amplitude was 1.2 degrees above the 28-degree limit, and the 3-sigma deviation estimates of amplitude ratio fell as much as 0.14 below the 0.95 minimum allowable. However, checkout of Phase III TCA and servoactuator acceptance testing (which would be conducted on all units prior to delivery) indicated that all of the specification requirements could be met with a tighter screening of component performance.

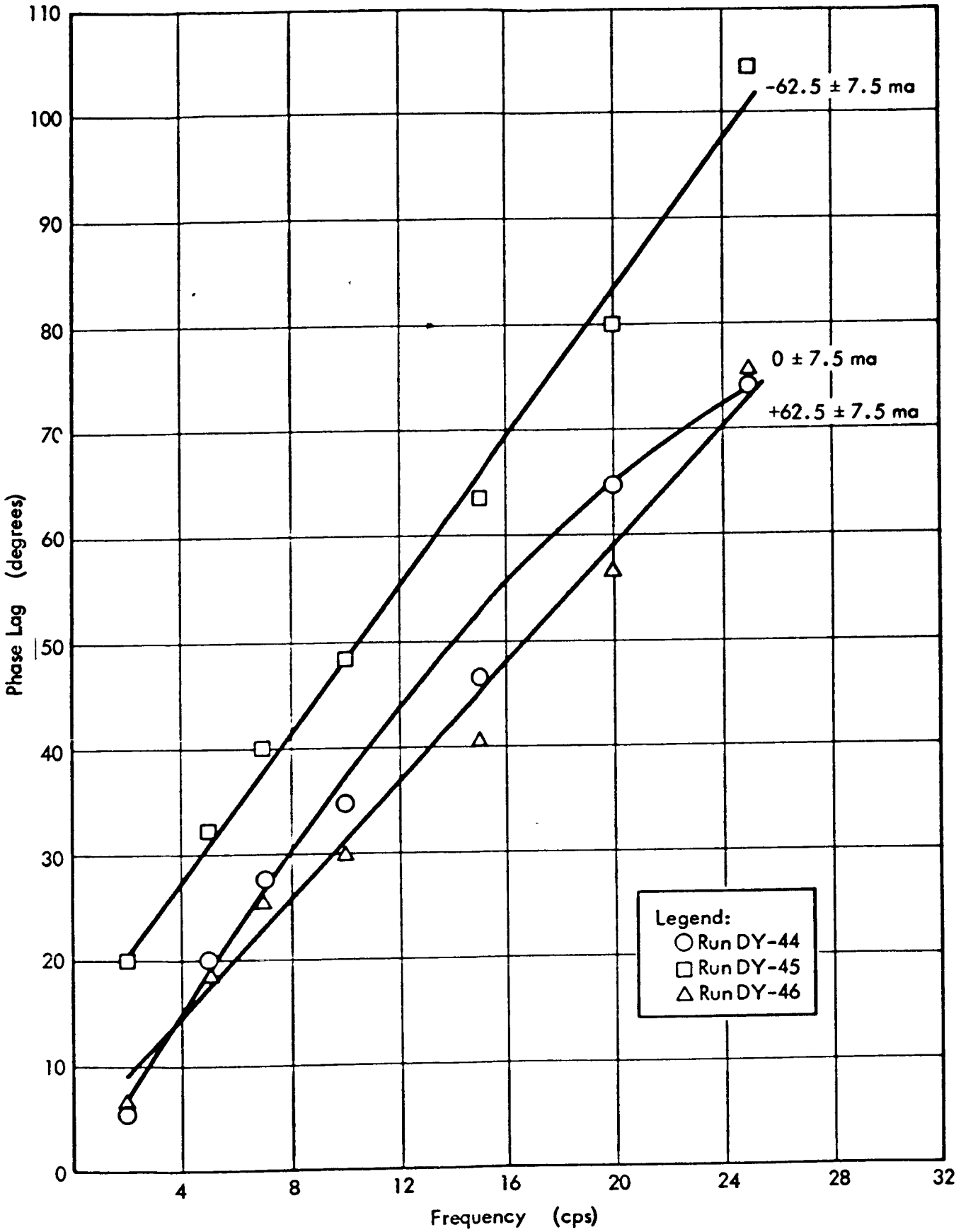

Figure 6.9.3-9. Phase Lag for PQT-009.5

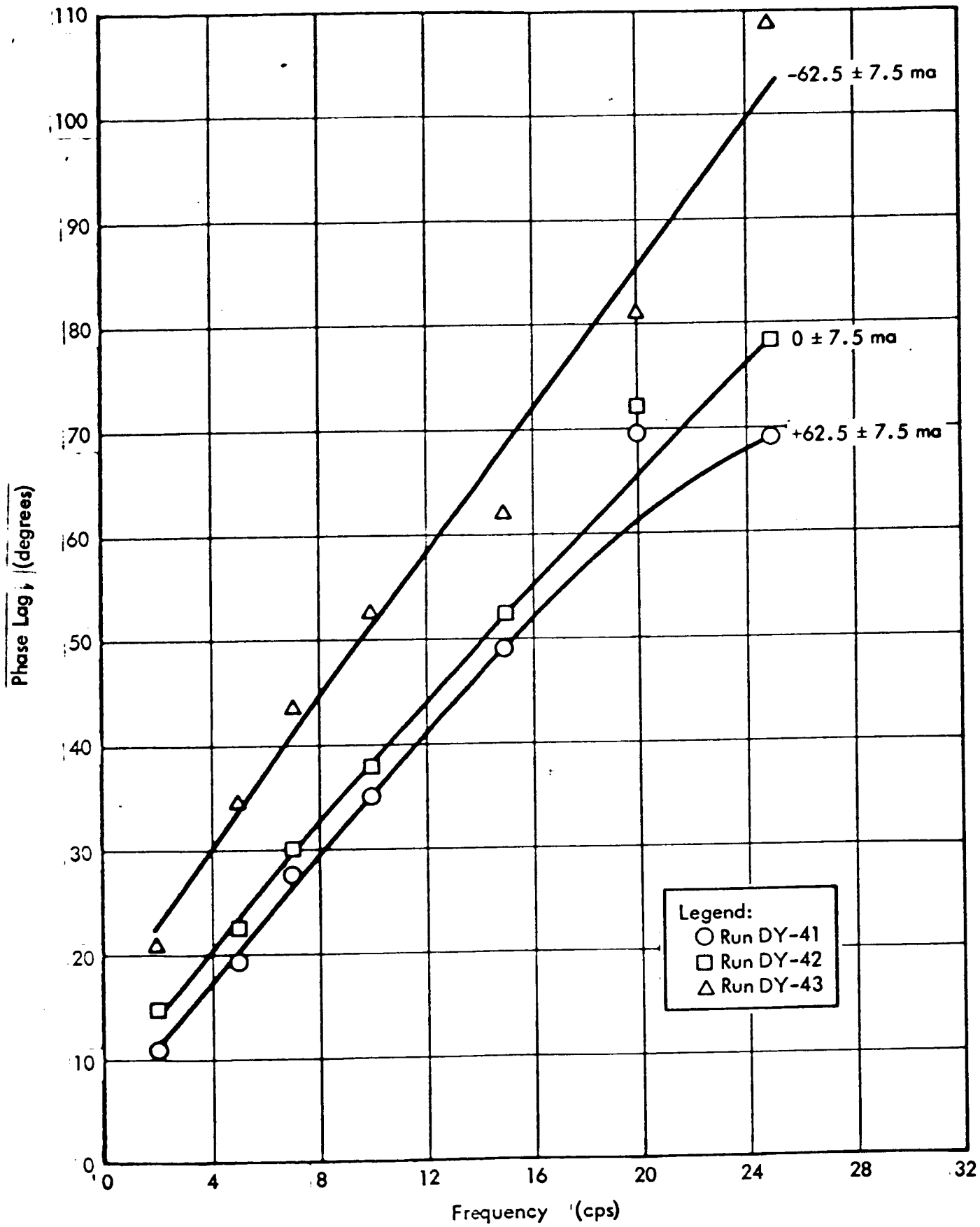

Figure 6.9.3-10. Phase Lag for PQT-010

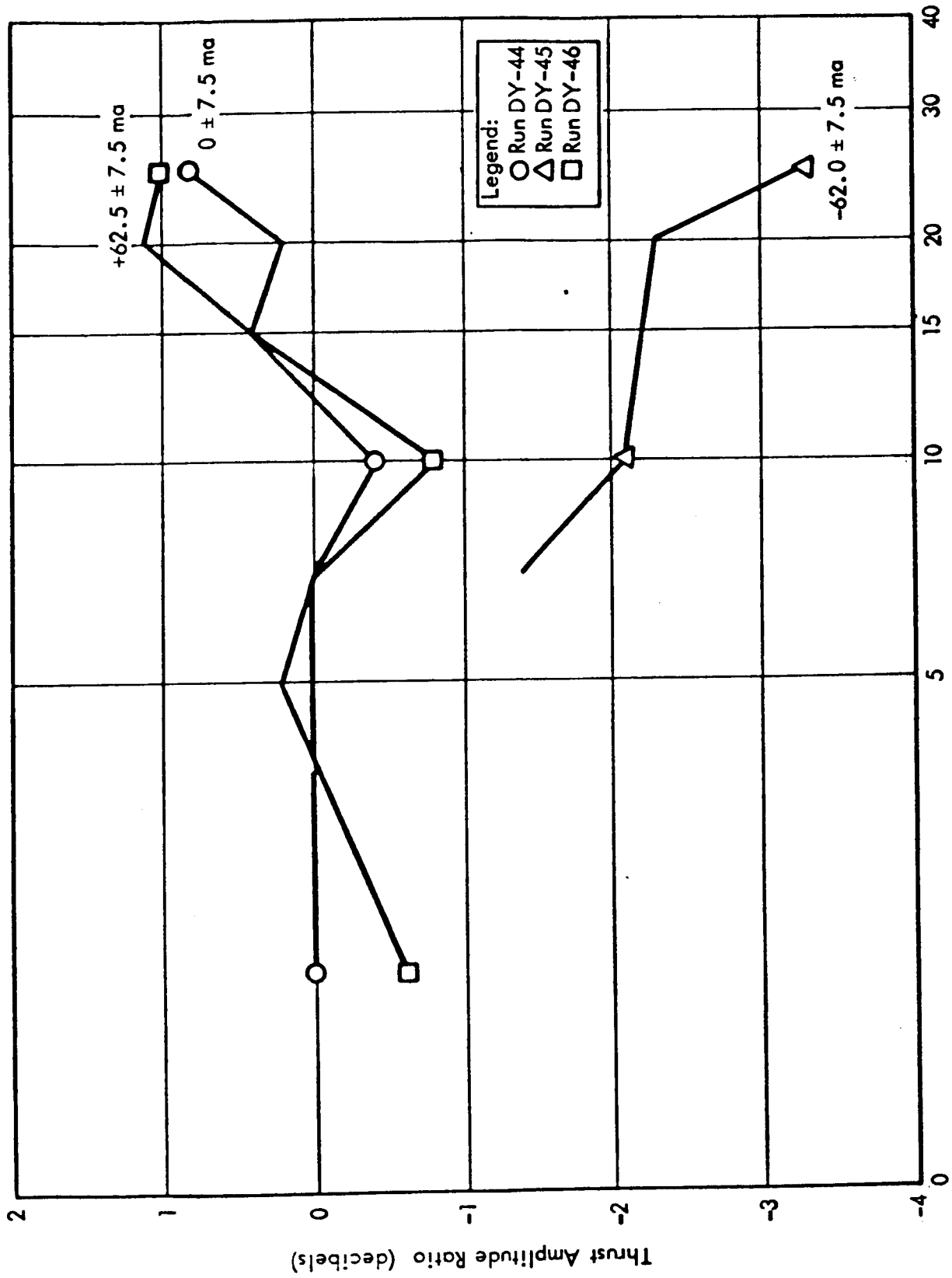

Figure 6.9.3-11. Amplitude Ratio for PQT-009.5

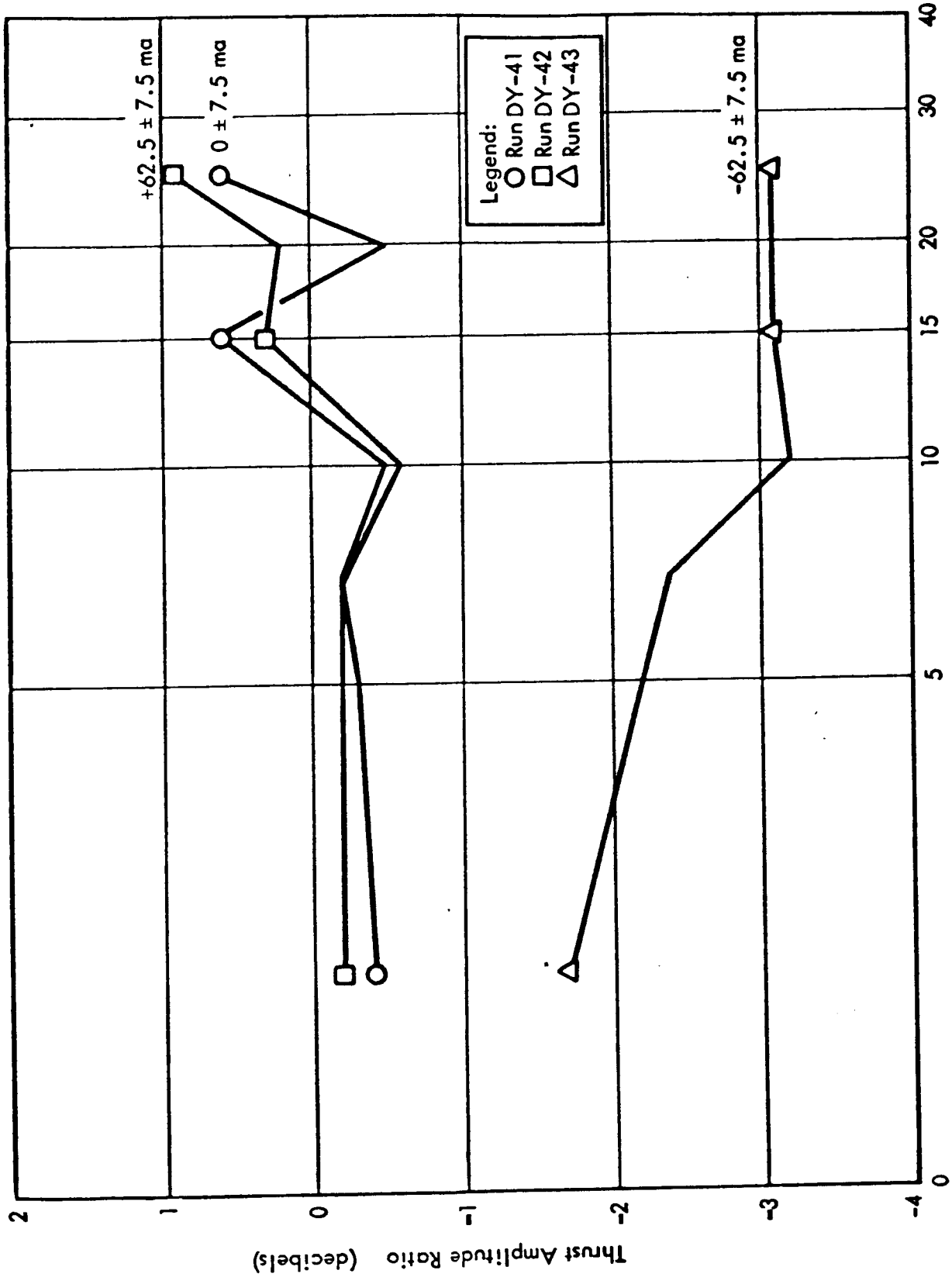

Figure 6.9.3-12. Amplitude Ratio for PQT-010

Figure 6.9.3-13. MIRA 150A TCA S/N 004 Anomalous Throttle Characteristics

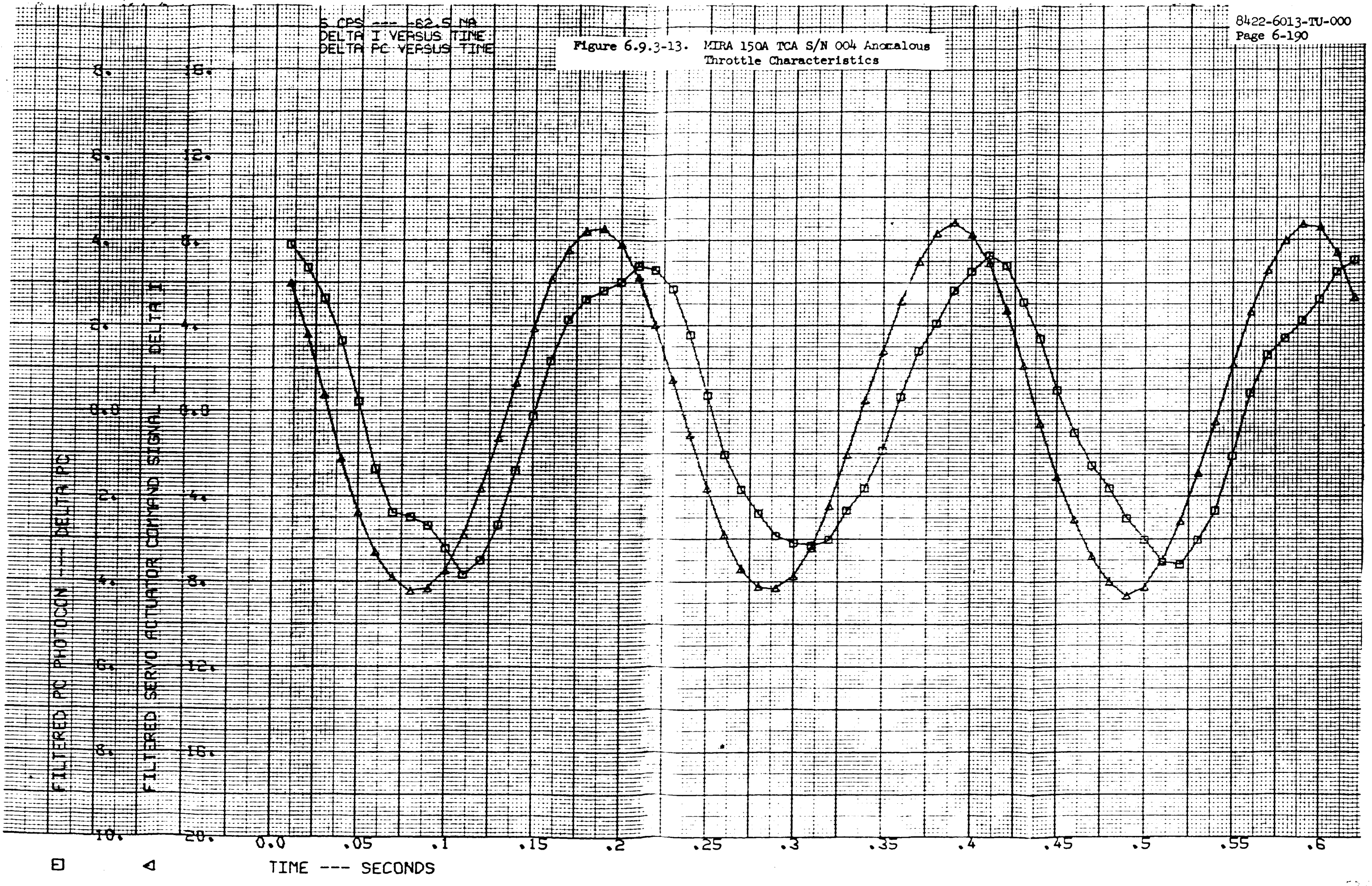

Figure 6.9.3-14. Hysteresis Loop - PQT-010

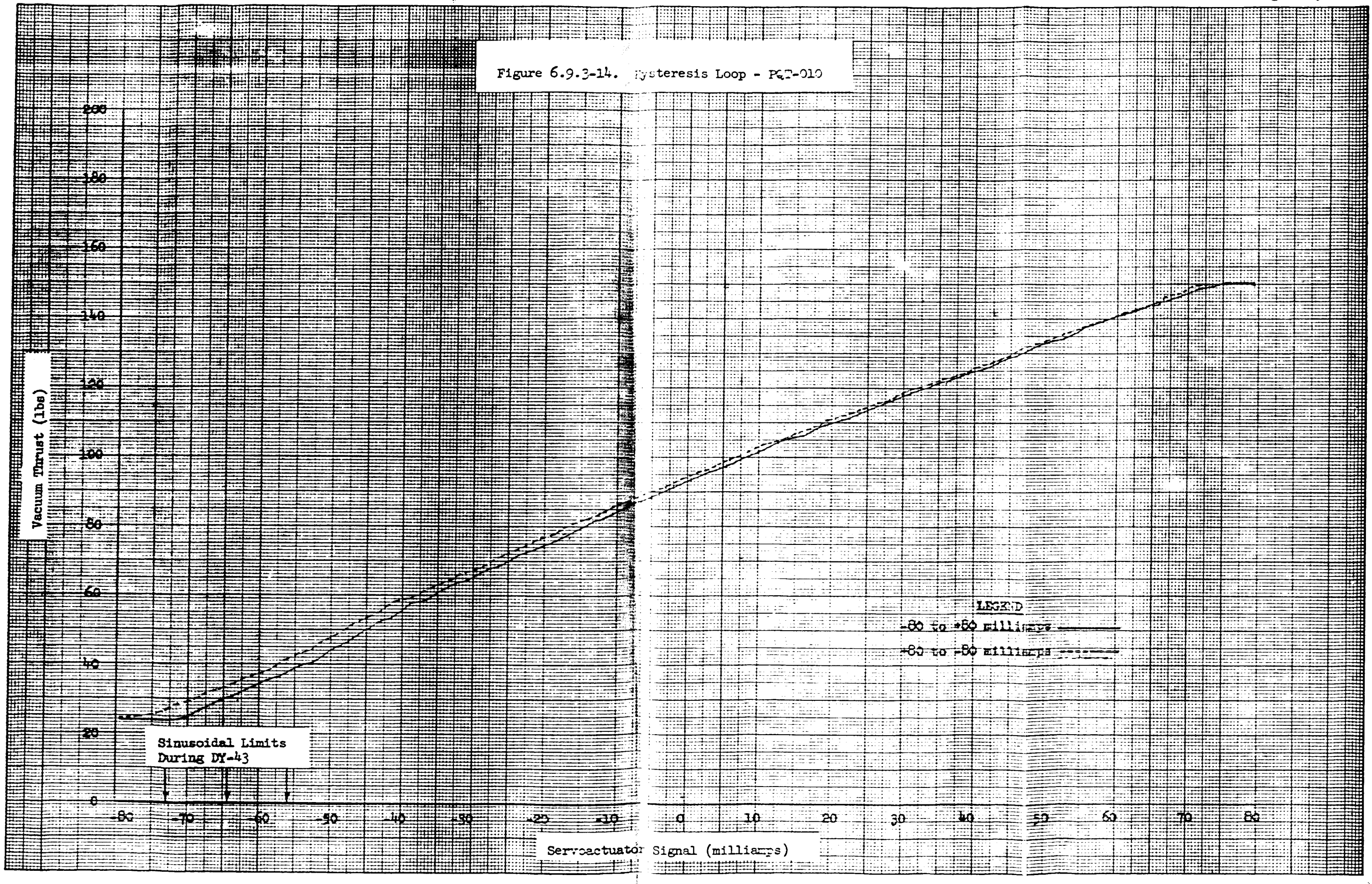

Figure 6.3.3-15. MIRA 150A Hysteresis Loop for Full Servoactuator Signal Excursion

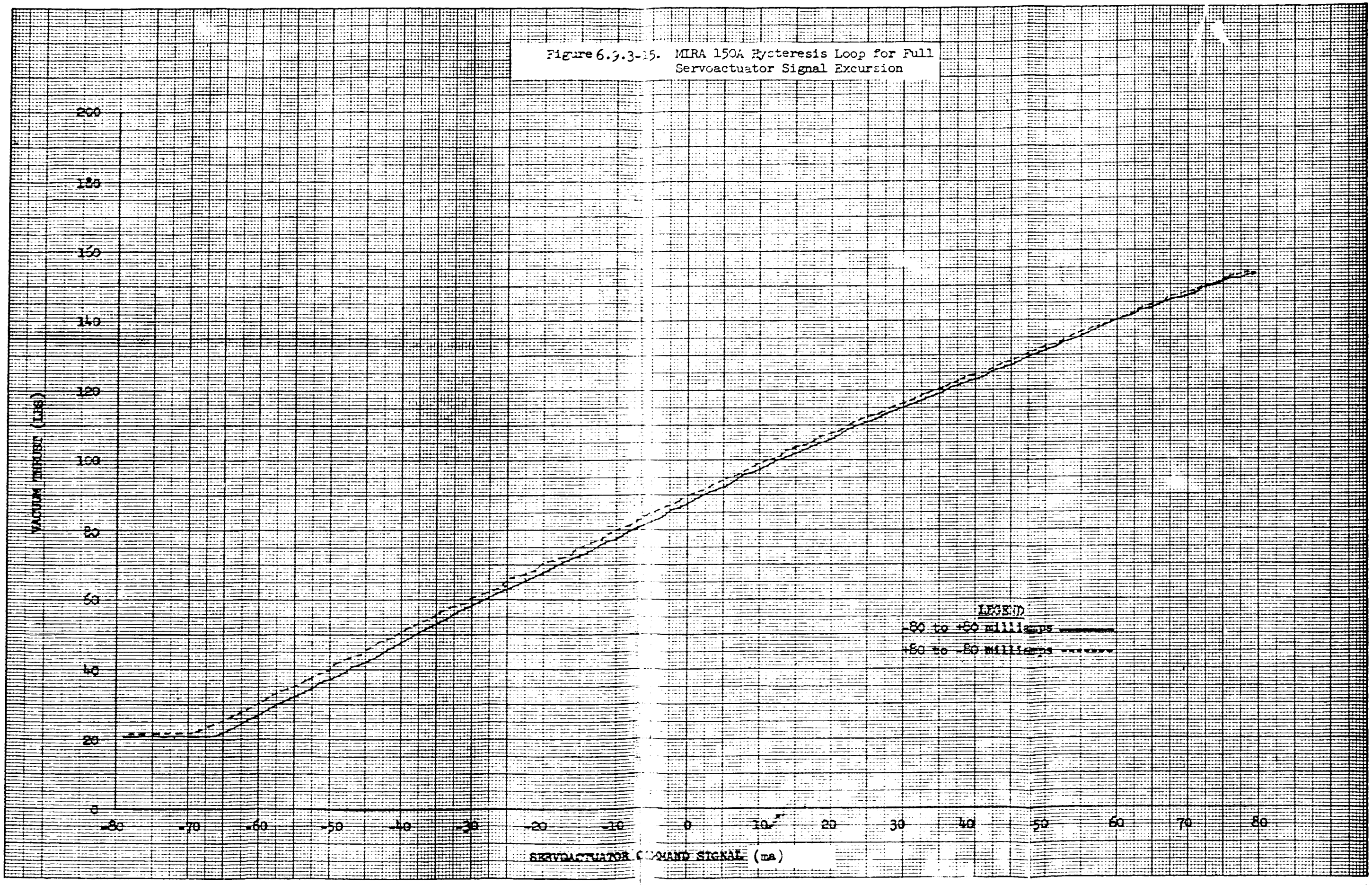

Table 6.9.3-16

MIRA 150A TCA Throttling Characteristics

Step Response (seconds):	Sample Size	Mean Value	3-sigma Deviation	Requirement SAM-50255-DSN-C
-80 to +80 ma (Stop-to-stop)	7	0.084	0.099 max	No Requirement
-70 to +80 or +70 to -80 ma	16	0.038	0.061 max	0.065 max
All 35 ma steps between -70 to +70 ma	9	0.014	0.022 max	0.065 max
Step Response Overshoot (%)	8	19	29 max	25 max
5-cps Phase Lag, (degrees):				
-62.5 ± 7.5 ma Signal Amplitude	7	17.4	29.2 max	28 max
0 ± 7.5 ma Signal Amplitude	9	17.4	26.1 max	28 max
+62.5 ± 7.5 ma Signal Amplitude	9	14.2	27.6 max	28 max
5-cps Amplitude Ratio:				
-62.5 ± 7.5 ma Signal Amplitude	6	1.01	0.81 min	0.95 min
0 ± 7.5 ma Signal Amplitude	8	1.02	0.90 min	0.95 min
+62.5 ± 7.5 ma Signal Amplitude	8	1.01	0.82 min	0.95 min
Loop Width (%)	9	1.8	3.2 max	15% or 2.5 ma max

Of the three TCAs tested with Phase III servoactuators, none failed the response requirements while operating within the specification limits (including low temperature). Out of seven different Phase III servoactuators acceptance tested (see Table 5.1.1-10), only one (S/N 55390 which had a 0.91 amplitude ratio and 27-degree phase lag at 5 cps) would have caused a TCA to fail response requirements. Other characteristics such as loop width, thrust-signal envelope, and rise time performance presented no problem even on a conservative 3-sigma deviation basis.

Thus, it is believed that the basic MIRA 150A TCA design will meet all transient performance requirements when: (1) proper care is taken on acceptance testing, (2) added experience has been gained in fabrication and testing, and (3) added test data (from a qualification test program for example) becomes available to add to the statistics.

6.10 Vibration and Acceleration Environmental Tests

Two tests were performed to determine the effects of high level vibration and acceleration external load environment.

The acceleration loads were imposed by centrifuge. The centrifuge tests were planned as a prelude to more extensive testing under a combined vibration and acceleration envrionment. These tests are discussed in paragraph 6.10.1.

One prefiring, high level vibration test was performed as described for PQT-011 in the prequalification test specification. This test is discussed in paragraph 6.10.2.

6.10.1 Centrifuge Tests

MIRA 150A TCA centrifuge tests at the STL Capistrano Test Site (CTS) were limited to two checkout firings, Runs HEPS-001 and HEPS-002. Additional acceleration tests which were scheduled as part of the prequalification test program were later deleted from Phase III. However, the centrifuge tests that were conducted demonstrated the capability of the MIRA 150A TCA to operate satisfactorily while under the simultaneous influence of 10g acceleration in the longitudinal axis (required by paragraph 3.7.5.2 of JPL Specification SAM-50255-DSN-C) plus the operational vibration characterized as white Gaussian at a level of 3g rms between 100 and 3000 cps along three orthogonal axes (required by paragraph 3.7.3.2 of JPL Specification SAM-50255-DSN-C).

6.10.1.1 Test Objectives

The primary objectives of the centrifuge tests, Runs HEPS-001 and HEPS-002, were to:

1. Perform initial checkout firings of the centrifuge stand.
2. Determine any changes in TCA operating characteristics when fired under flight acceleration and vibration conditions as compared to standard static firing conditions.

6.10.1.2 Test Summary

All major test objectives were achieved. The two tests on the centrifuge, one with and one without the centrifuge spinning, used the same TCA and were performed in immediate succession to enhance the validity of the comparison of the static and acceleration conditions.

6.10.1.3 TCA Configuration

The HEA tested was MIRA 150A-001 (STL P/N 10546-1-1A1) and included a Phase III servo-actuator (S/N C53750). The altitude CC & NA (P/N 10654-6-1) was S/N 006.

6.10.1.4 Test Setup and Test Conditions

The TCA was installed on the mounting bracket on the centrifuge stand as shown in Figure 6.10.1-1. The centrifuge is described in section 8 (Special Test Equipment). The same 130-second duration AT-1 thrust-time program (see Figure 6.10.1-2) was used for both firings. Sufficient instrumentation measurements were made to determine

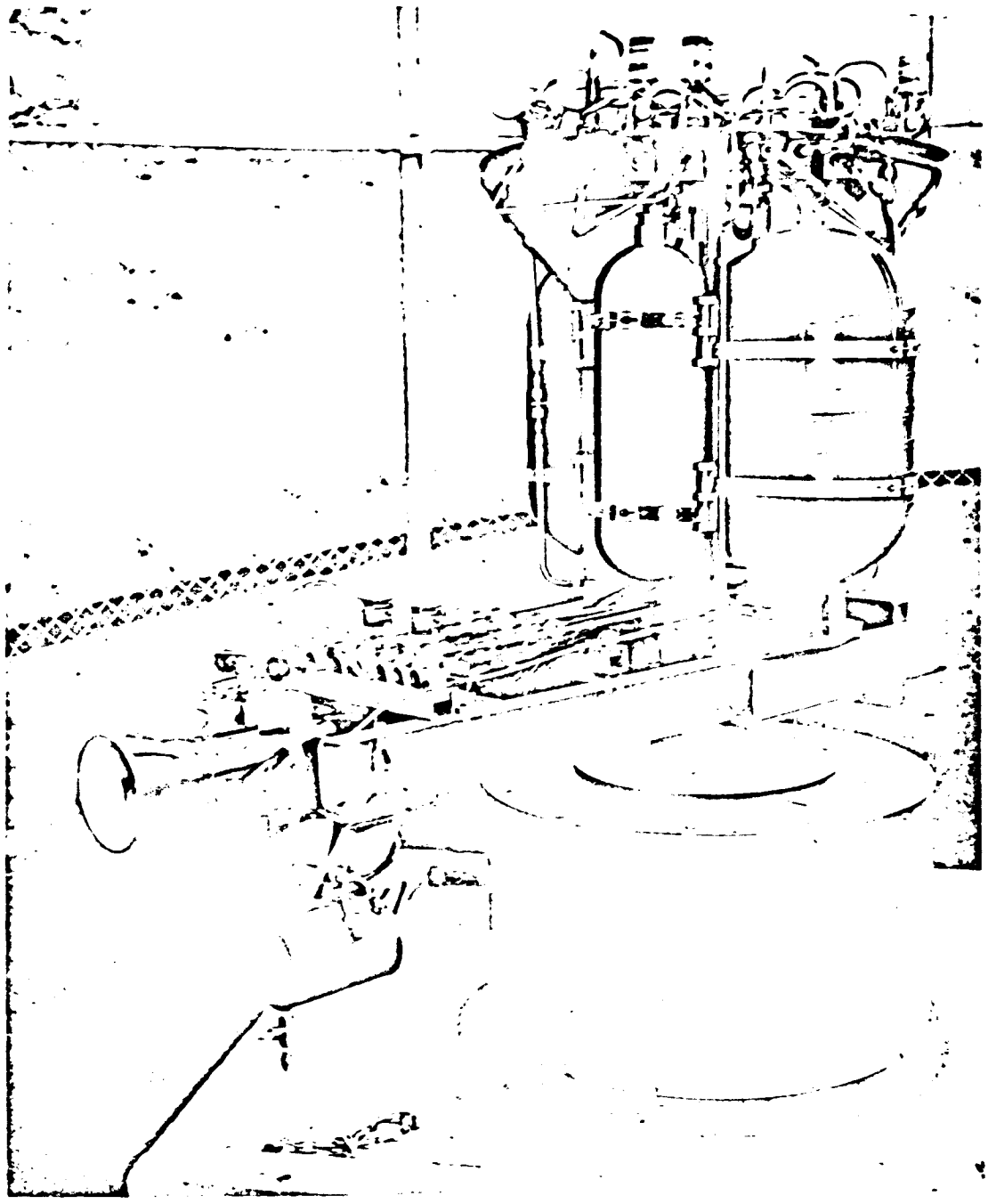

Figure 6.10.1-1. Centrifuge Test Setup

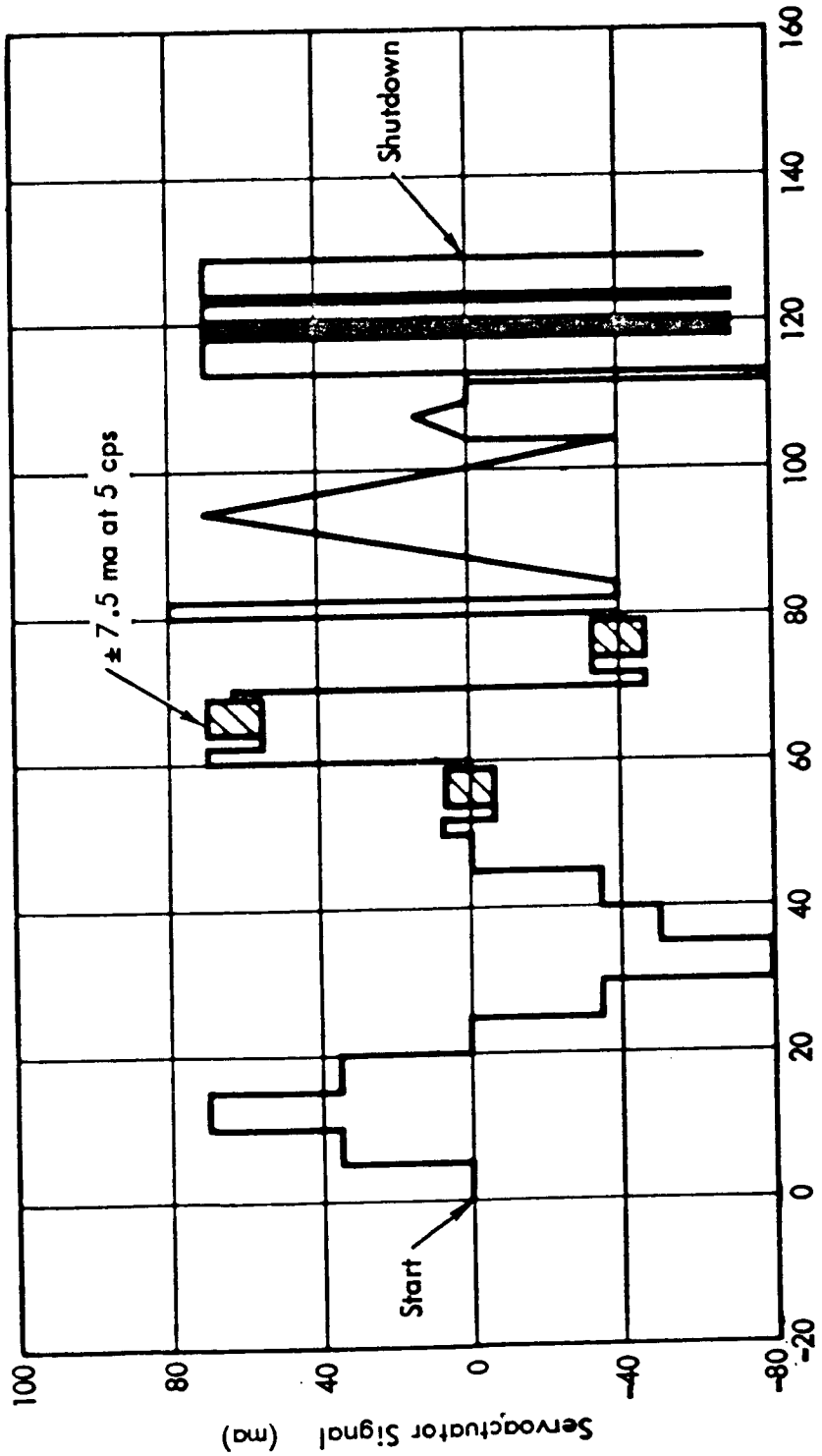

Figure 6.10.1-2. Thrust Cycle No. AT-1

steady-state and transient performance characteristics. Because additional propellant volumes were imposed by the use of injection pressure measurements, none of the transient data are considered valid. A triaxial accelerometer was mounted to the TCA (see Figure 6.10.1-3) for the nonspinning firing to determine the g level and frequency of the vibration environment self induced by the TCA during firing.

6.10.1.5 Test Results

The centrifuge checkout firings, Runs HEPS-001 and HEPS-002, were successfully completed on 27 November 1964. The data showed no significant change in TCA operating characteristics at 10g acceleration compared to static conditions. Figures 6.10.1-4, -5, and -6 compare the C*, mixture ratio, and injection pressures of the two firings. No derived data is available for values below 40 psia chamber pressure, because of an instrumentation setup error causing loss of oxidizer flow meter data at low flows; however, extrapolation of data at low levels is verified by all other measured values (fuel flow, injection pressure, etc.). Instrumentation failed on servoactuator signal and position. Detailed tabulated data from these runs is summarized in Table D-3-1 of Appendix D-3.

Measured self-induced vibration levels during static firings (see Figures 6.10.1-7, -8, and -9) indicate that the required value of 3g rms or greater white Gaussian over the frequency sepctrum of 100-300 cps was attained at all thrust levels. Unfiltered vibration data over the entire frequency spectrum indicated levels of from 20 to 50g rms.

6.10.2 PQT-011 —— Prefiring Vibration Test

6.10.2.1 Test Objectives

The primary objectives of this test were to:

1. Demonstrate the capability of the TCA to meet specified performance requirements after subjection to simulated spacecraft boost phase flight vibration.

2. Acquire additional data on TCA reliability.

6.10.2.2 Test Summary

This test was successfully completed according to paragraph 7.7 (PQT-011) of the prequalification test specification. The complete PQT-011 test series consisted of: (1) a previbration HEA calibration test (Run C2-680) accomplished according to the procedures of the acceptance test specification, (2) the vibration test described herein, (3) a postvibration TCA durability test (Run C2-709), and (4) a repeat of the HEA calibration test (Run C2-710). The results of the previbration and two postvibration static firing tests are discussed in paragraph 6.7.3. Detailed information on the vibration test may be found in STL Document Number 9522.3-272, "Test Report Surveyor Vernier Thrust Chamber Assembly Pre-Qualification Non-Operating Vibration Test," dated 1 February 1965.

6.10.2.3 TCA Configuration

The TCA tested was a complete Phase III flight-wiehgt configuration (MIRA 150A-008) and is described in paragraph 6.7.3.2.

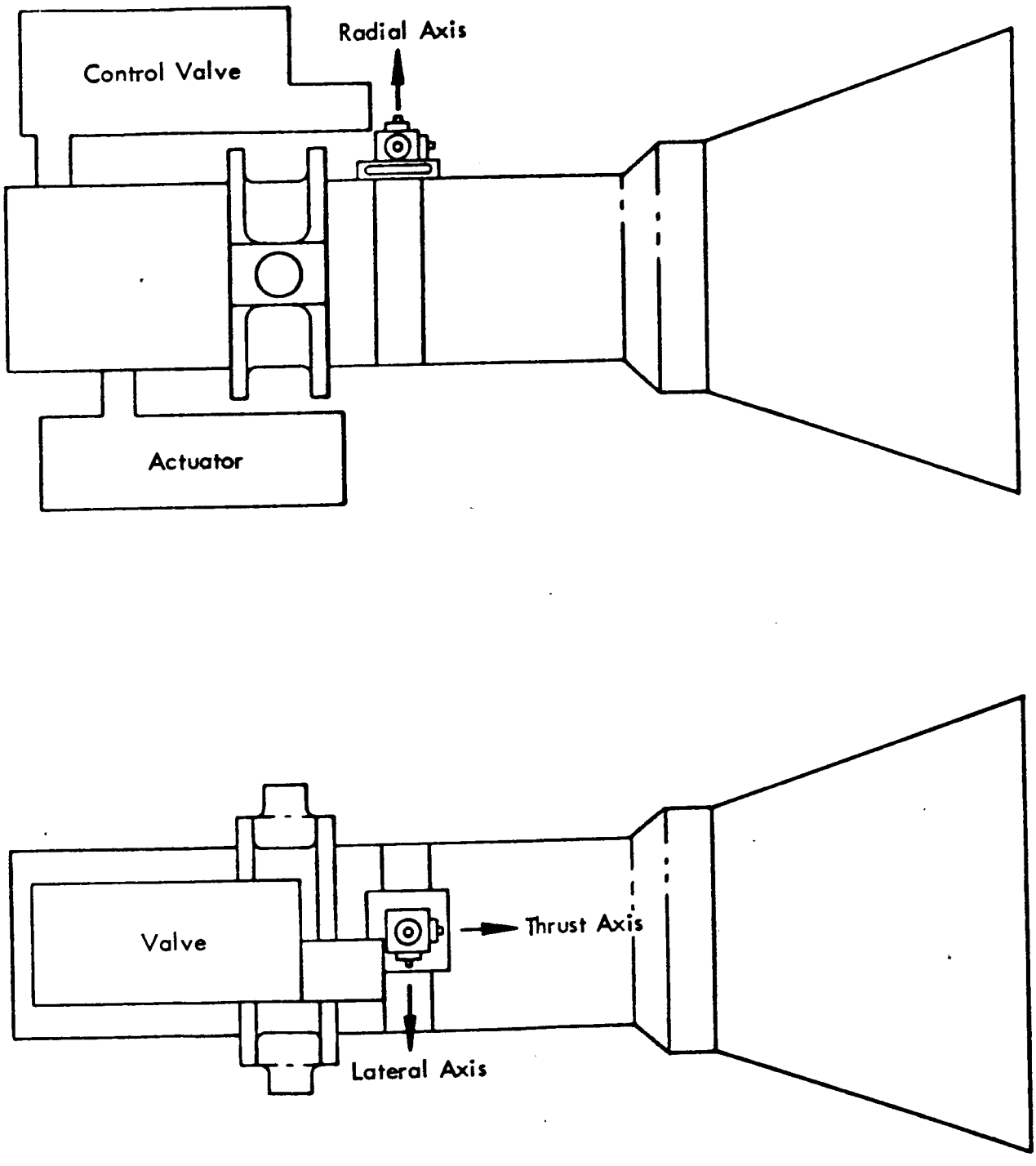

Figure 6.10.1-3. MIRA 150A TCA Centrifuge Test

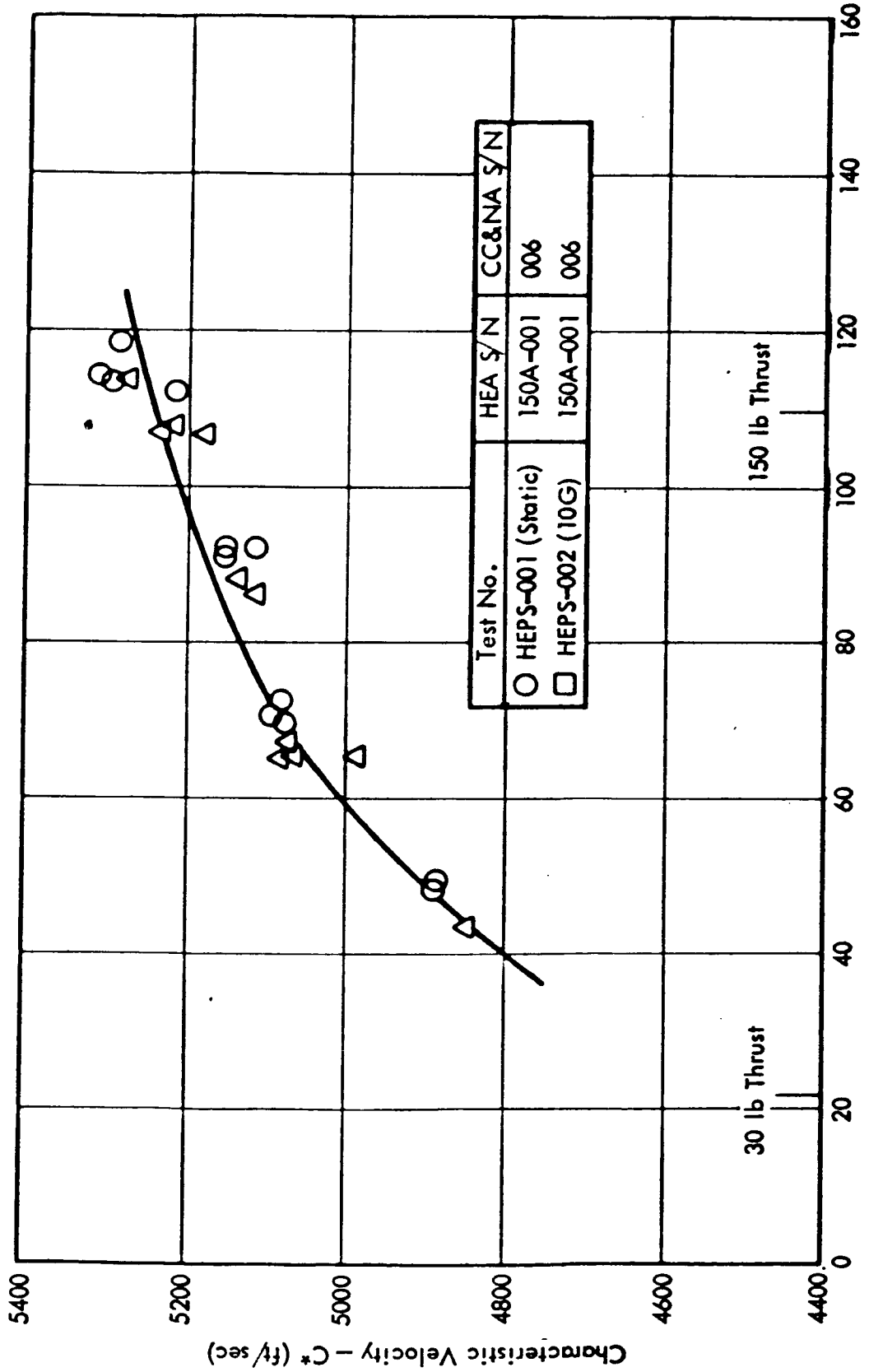

Figure 6.10.1-4. Centrifuge Test Data - C^* Versus P_c

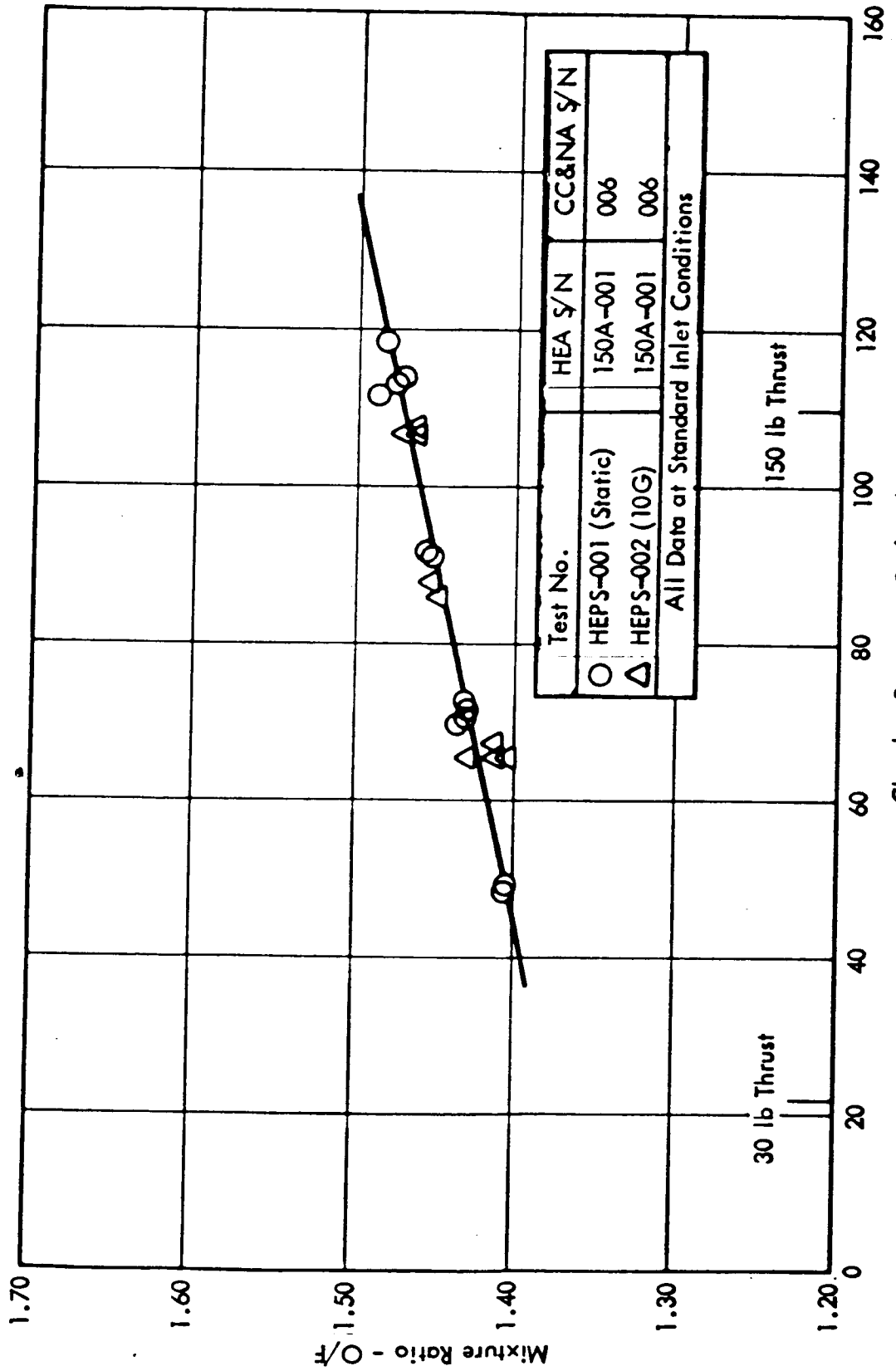

Figure 6.10.1-5. Centrifuge Test Data - MR Versus P_c

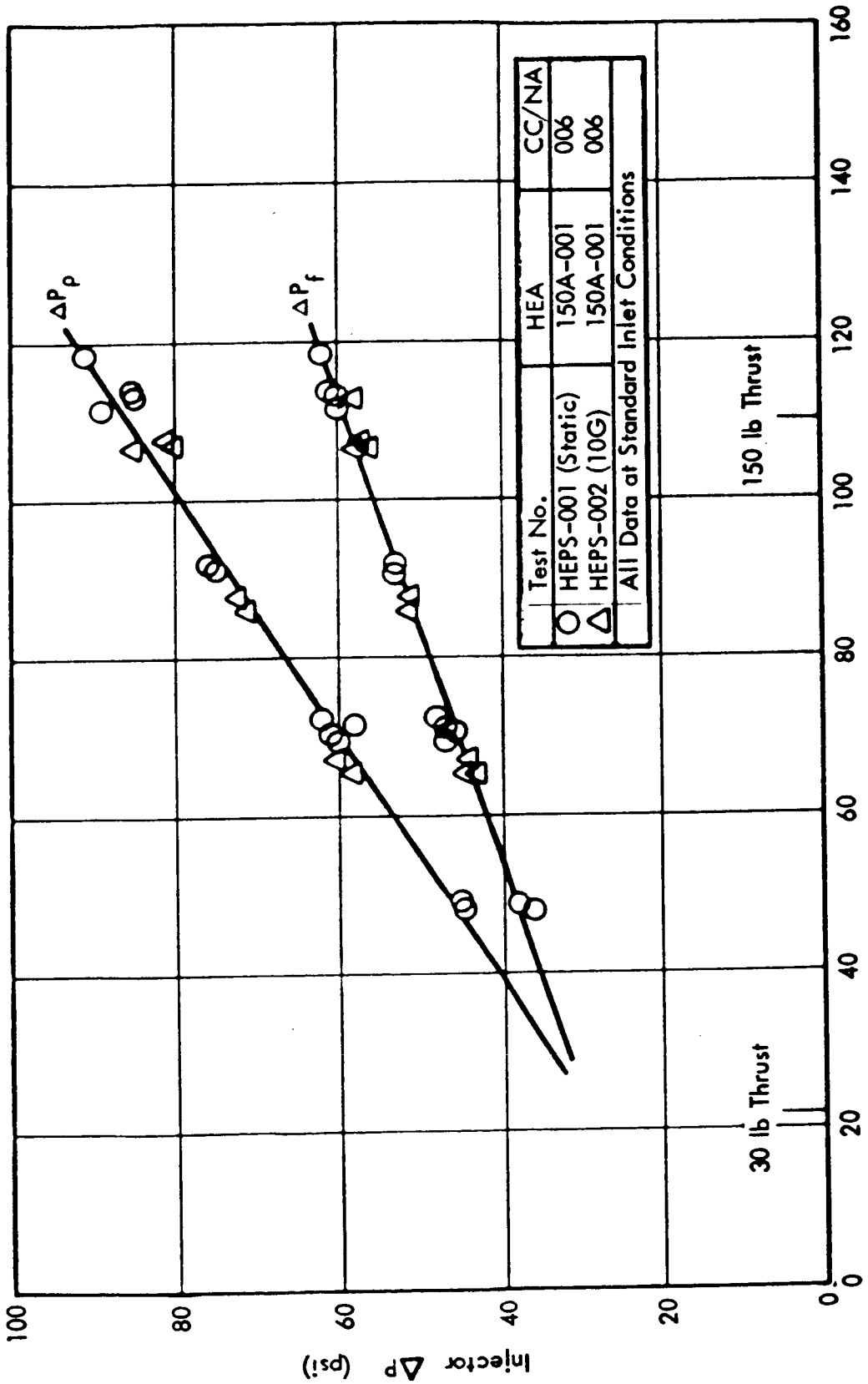

Figure 6.10.1-6. Centrifuge Test Data - Injector ΔP Versus P_c

Figure 6.10.1-7. Centrifuge Test Vibration Level - Thrust Axis (3000 cps Low Pass Filter)

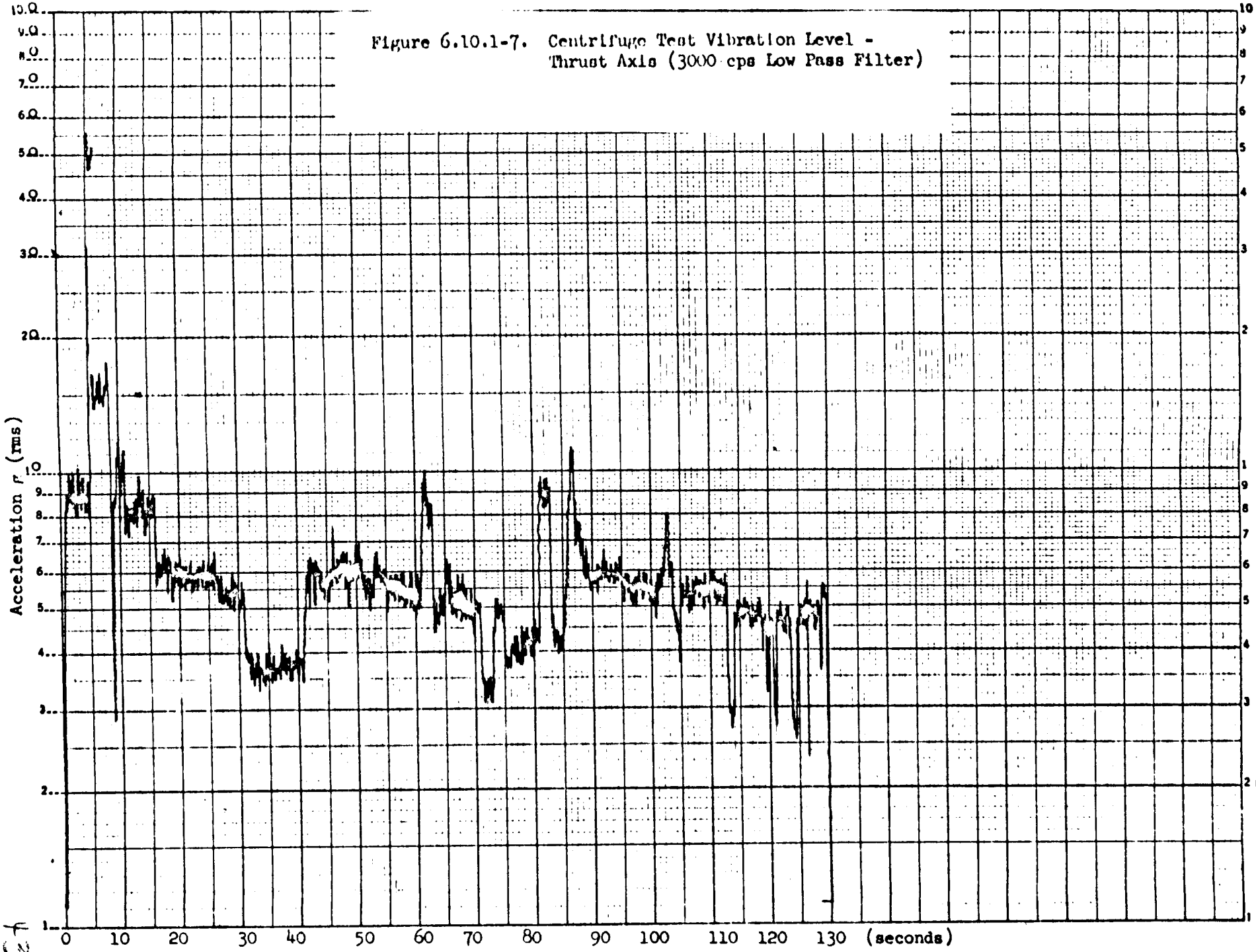

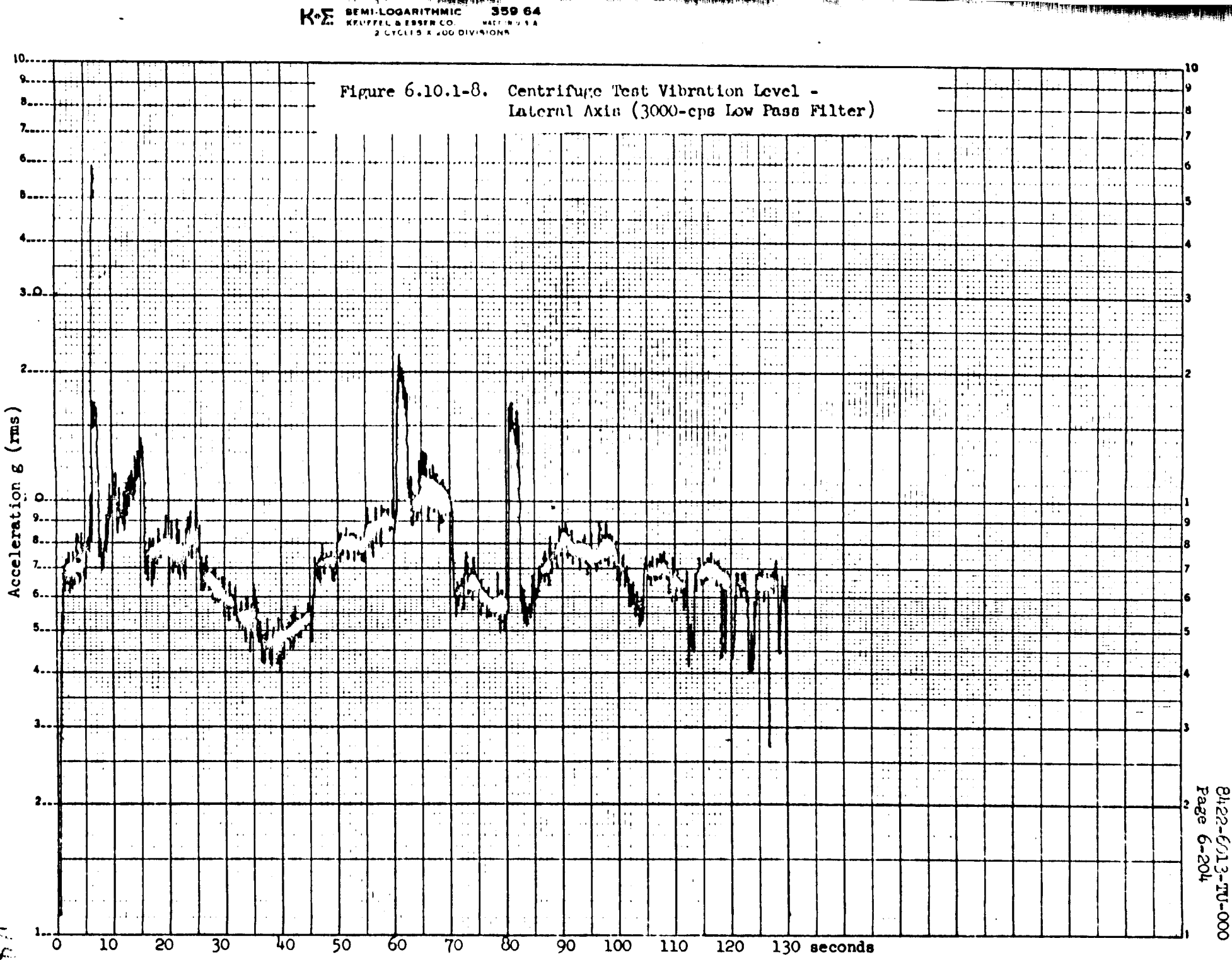

Figure 6.10.1-8. Centrifuge Test Vibration Level - Lateral Axis (3000-cps Low Pass Filter)

Figure 6.10.1-9. Centrifuge Test Vibration Level Radial Axis (3000-cps Low Pass Filter)

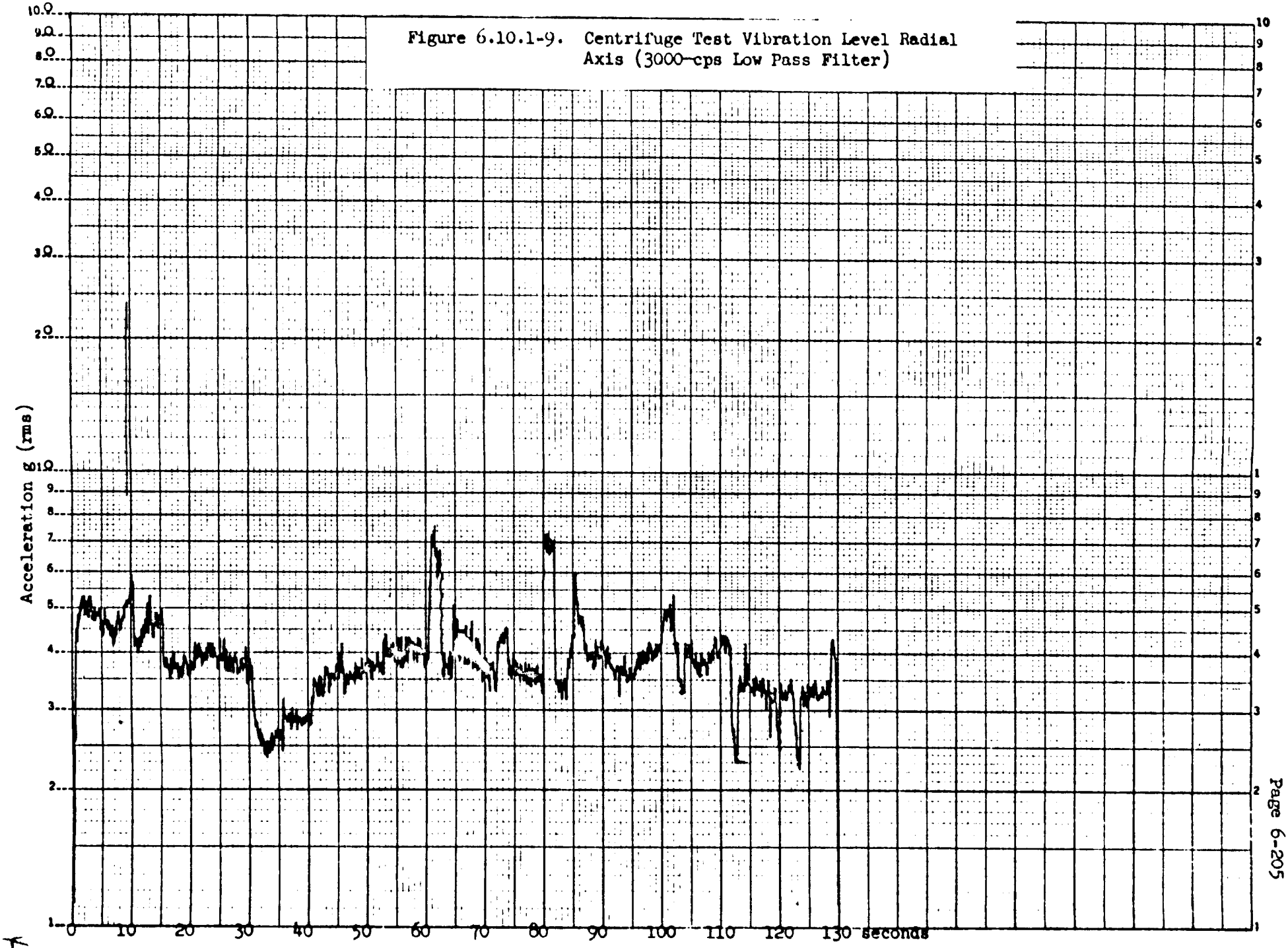

6.10.2.4 Test Setup and Test Conditions

The detailed test procedures followed are contained in paragraph 7.7 of the prequalification test specification. During the vibration test, the TCA propellant passages down to the shutoff valve seats were pressurized with water at 300 ± 20 psig. The servoactuator cavities were filled with alcohol, and the inlet and outlet ports were plugged. Figure 6.10.2-1 illustrates the overall test setup used.

Measurements were made of vibration input levels and the resultant responses at various key locations on the TCA components. The exact transducer locations for each of the three axes tested are illustrated in Figures 6.10.2-2 through 6.10.2-4. All transducers used were piezoelectric accelerometers which were calibrated for basic sensitivity amplitude linearity and frequency response by means of a combination optical and stroboscopic technique prior to the test.

The vibration input levels complied with the requirements of PQT-011 in the prequalification test specification, except the sinusoidal sweeps were initiated at 10 cps rather than at the specified 5 cps frequency, because of shaker servo control limitations at low frequency. Also, during the first sweep, intermittent loss of shaker servo control resulted in erratic vibration input. The actual inputs used are provided in Table 6.10.2-5. A typical combined random and sinusoidal input is illustrated by Figures 6.10.2-6 and 6.10.2-7.

Vibration was applied by a MB 10,000 force-pound exciter (Model C125), controlled at the TCA trunnion mounting point on the test fixture (i.e., accelerometer number 1 in Figure 6.10.2-2). Both the sine and random components of the complex wave were controlled to maintain the specified rms vibration level by use of separate servo systems coupled through a tracking filter with sine reject capability. Sinewave control was accomplished with a conventional Bruel and Kjaer servo control system.

6.10.2.5 Test Results

Typical results for each of the three orthogonal axes tested are provided in Appendix I. Included are plots of vibration input levels, both the sinusoidal and random, and the transmissibility plots for each of the transducer locations illustrated in Figures 6.10.2-2 through 6.10.2-4.

No TCA resonant frequencies were found in the low frequency range; thus, the test was not compromised by the 10-cps initiation or by the aforementioned loss of servo control on the first of the six vibration runs.

The transmissibility plots in Appendix I indicate that no TCA resonant frequencies occur below 250 cps. The highest resonant frequencies noted within the 10-1500 cps frequency band were in the range of 700 to 800 cps for the TCA throttle arm, nozzle exit, and the servoactuator. These all occurred along the Z-Z axis (parallel to the trunnions).

The highest transmissibility ratios (the ratio of measured output g to input g) were 19 at 800 cps on the nozzle exit, 21 at 760 cps on the servoactuator, and 22 at 365 cps on the nozzle exit. The first two ratios were noted during sweeps along the Z-Z axis, and the third along the Y-Y axis.

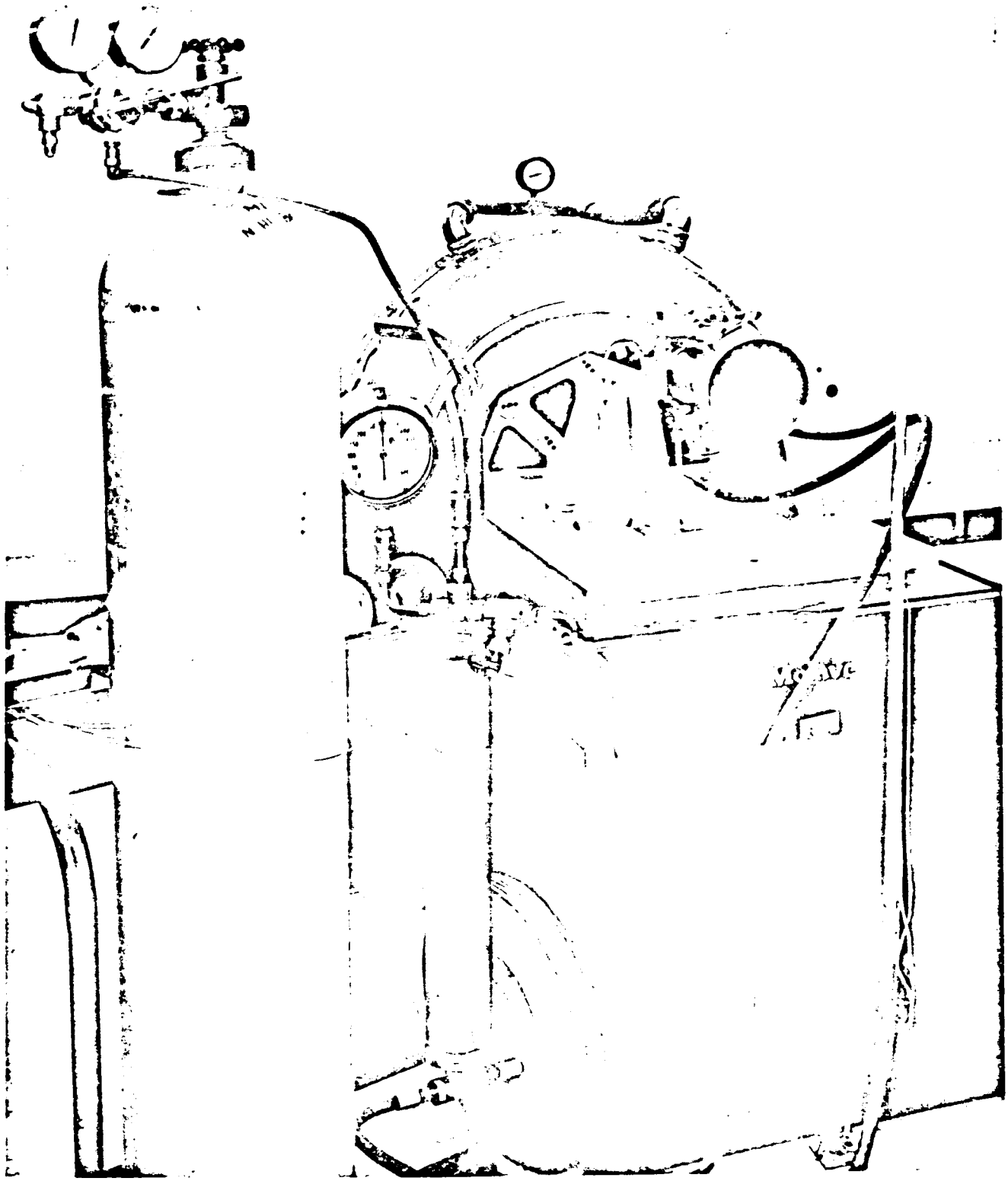

Figure 6.10.2-1. Longitudinal Vibration Test Configuration - Parallel to TCA Thrust (X-X) Axis

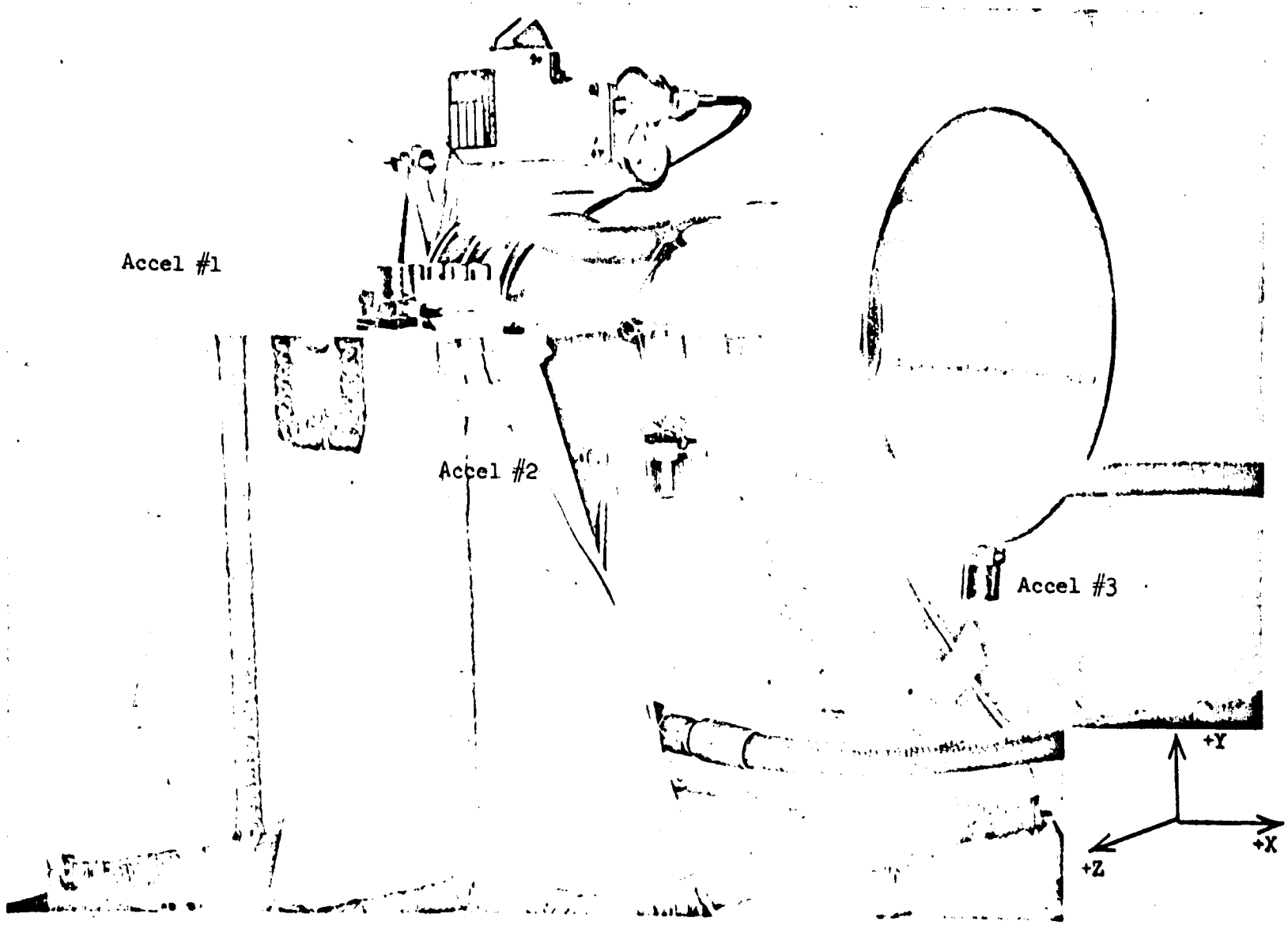

Figure 6.10.2-2. Lateral Vibration Test Configuration - Perpendicular to Trunnion (Y-Y) Axis

Accel No.	Identification	Sensitive Axis
1	Control	+Y
2	Nozzle Throat	-Y
3	Nozzle Exit	-Y
4 (not shown - located on backside)	Shaker Head	+Y

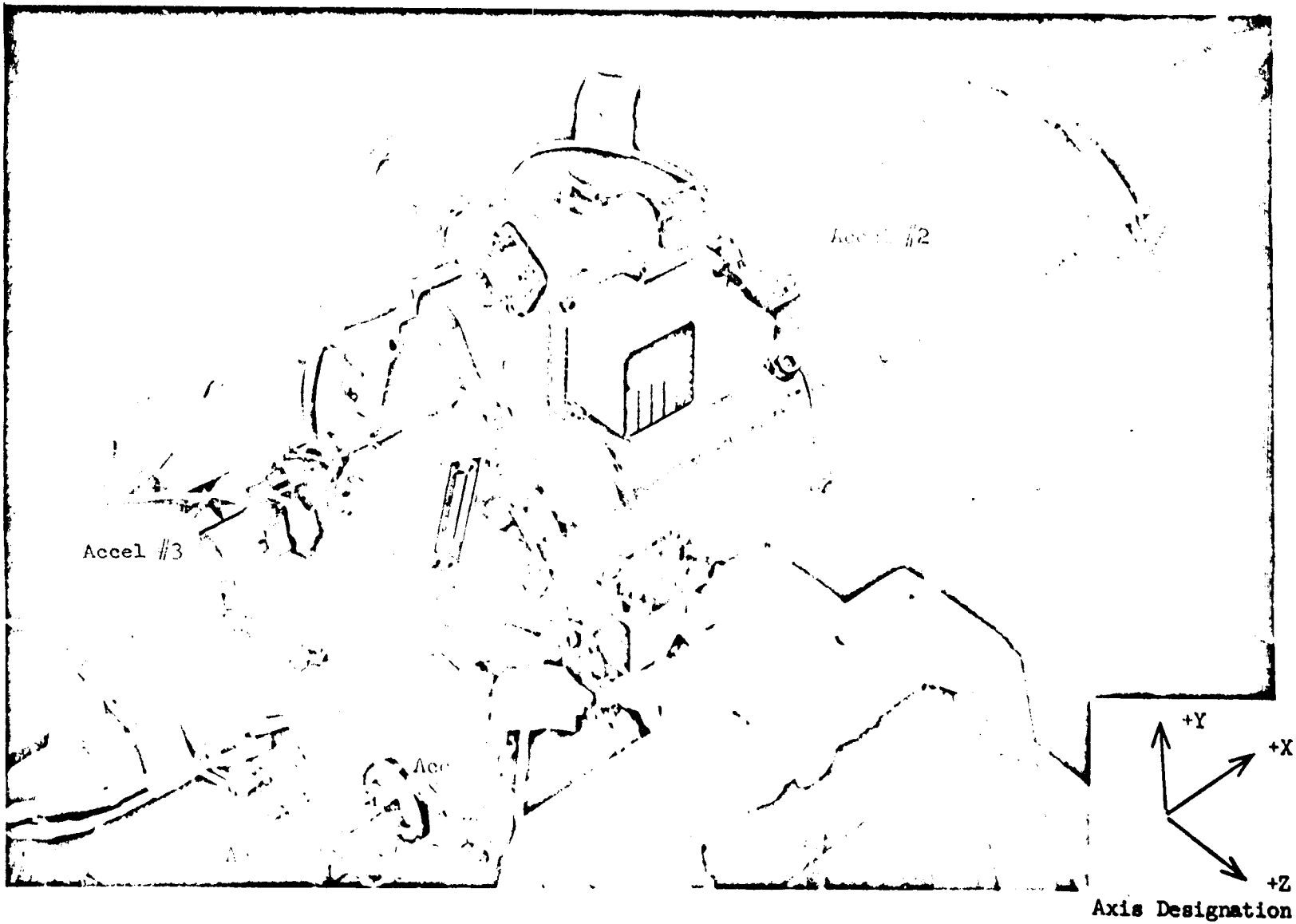

Figure 6.10.2-3. Longitudinal Vibration Test Configuration - Parallel to TCA Thrust (X-X) Axis

Accel No.	Identification	Sensitive Axis
1	Control	-X
2	Nozzle Throat	+X
3	Throttle Arm	-X
4	Servoactuator	+X
5	Oxidizer Shutoff Valve	-X

Figure 6.10.2-4. Lateral Vibration Test Configuration - Parallel to Trunnion (Z-Z) Axis

Accel No.	Identification	Sensitive Axis
1	Control	+Z
2	Nozzle Throat	+Z
3	Throttle Arm	+Z
4	Servoactuator	+Z
5	Nozzle Exit	+Z

Table 6.10.2-5

TCA Nonoperational Vibration Spectrum

Test No.	Input Directions	VIBRATION INPUT[1]				Duration per Axis (min)
		Sinusoidal	VFSW	Random - White Gaussian		
		Level (g-vector)	Frequency (cps)	Level (grms)	Bandwidth (cps	
1.	3[2]	8[3]	10 - 35	6.7	100 - 1500	2[4]
		18	35 - 150			
		6	150 - 1500			
2.	3[2]	8[3]	10 - 35	3.0	100 - 1500	10[5]
		18	35 - 150			
		6	150 - 1500			

NOTES: (1) The VFSW and Random Vibration inputs were combined.

(2) The three input axes were orthogonal with respect to TCA trunnion axis.

(3) Input levels at lower frequencies were limited to 0.4 inch double amplitude.

(4) The sinusoidal sweep rate was logarithmic and of 2 minutes duration for each axis.

(5) The sinusoidal sweep rate was logarithmic. Two 5-minute sweeps from 5 to 1500 to 5 cps were performed for a total test time of ten minutes for each axis.

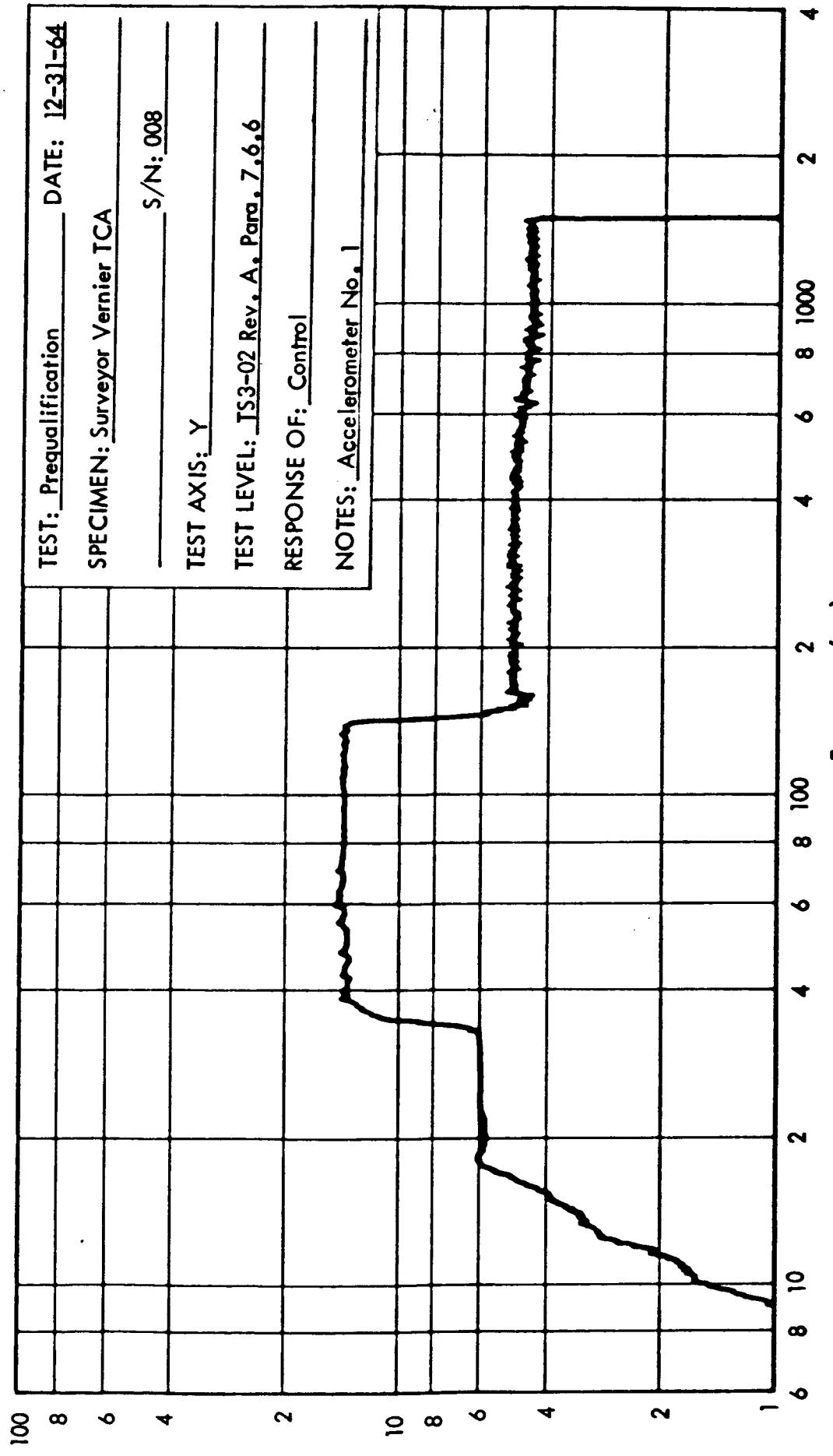

Figure 6.10.2-6. Response Plot

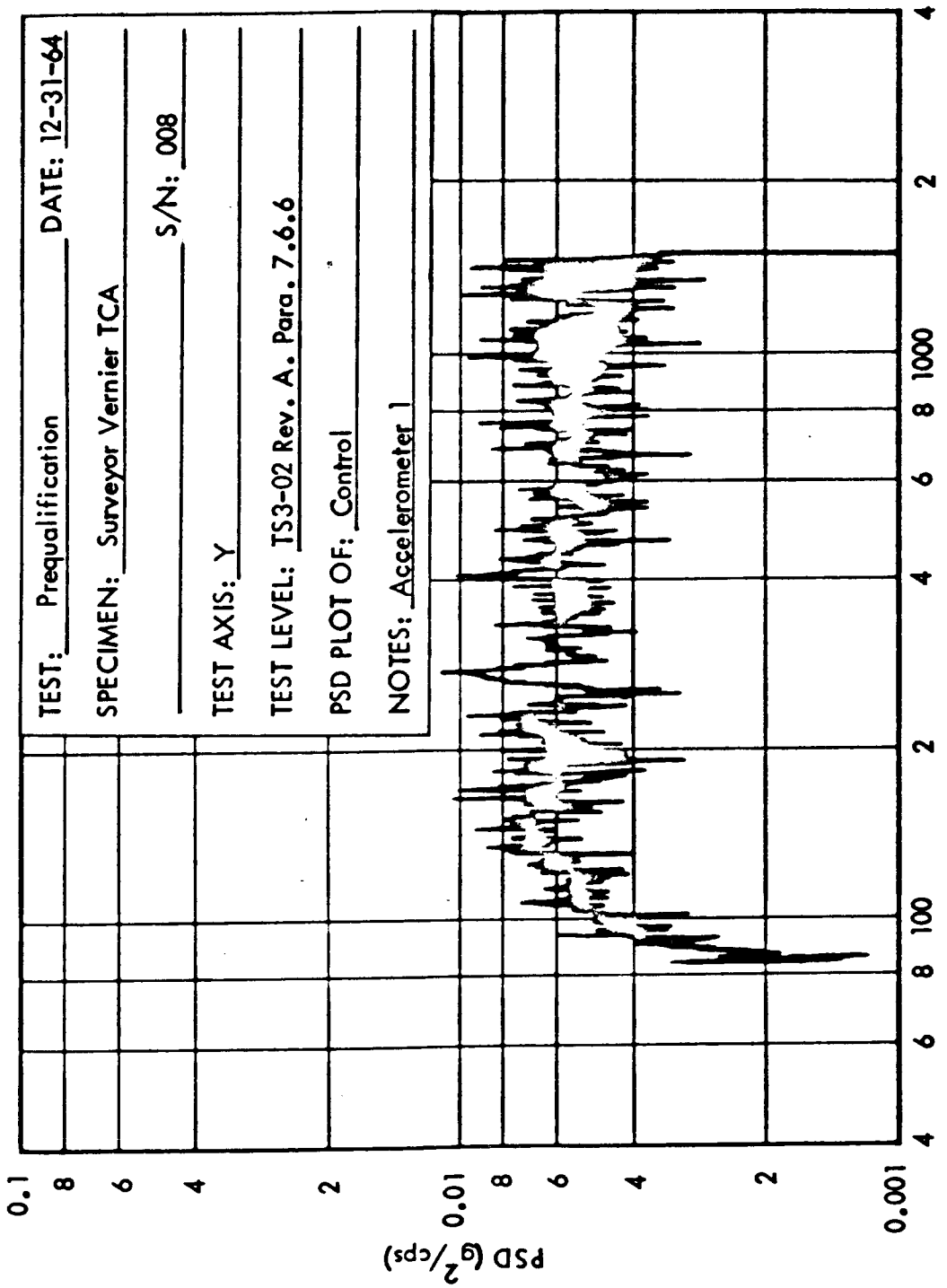

Figure 6.10.2-7. PSD Plot

No signs of liquid leakage or physical damage were noted upon visual inspection after each sweep. After the last sweep, no leakage was detected when the TCA was leak checked. The 300-second TCA maximum thrust durability test (Run C2-709) performed in 3 starts (50, 100, and 150 seconds) and then a repeat of the previbration HEA calibration test (Run C2-710) with a water-cooled CC & NA, were successfully completed after the vibration test. The static test results are provided in paragraph 6.7.3.

This test series demonstrated the capability of the MIRA 150A TCA to operate satisfactorily after exposure to simulated spacecraft boost phase flight vibration.

6.11 Extended Range Throttling Tests

A limited number of tests were made at the conclusion of Phase III testing to determine the capability of the MIRA 150A HEA to perform satisfactorily over a throttling range extended to 9:1 —— 20 lbs to 180 lbs vacuum thrust.

6.11.1 Test Objectives

The primary objectives of these tests were to:

1. Throttle the MIRA 150A design beyond the required 5:1 (30 lbs to 150 lbs vacuum thrust) range presently specified.

2. Obtain sea level performance data over a throttling range from 20 lbs to 180 lbs vacuum thrust.

6.11.2 Test Summary

All major test objectives were achieved by Run C2-714. This test was conducted under sea level conditions at the Inglewood Rocket Test Site.

6.11.3 TCA Configuration

The HEA used was MIRA 150A-004, including a Phase II servoactuator (S/N C53666) which was capable of providing a 0.240 in. stroke, compared to the 0.174 in. stroke required for Phase III servoactuators. A water-cooled CC & NA (P/N 106372) was used for these tests.

6.11.4 Test Setup and Test Conditions

The TCA was installed on the C-2 test stand and instrumented to measure all parameters required to determine steady-state and transient performance characteristics. A Phase II servoactuator was used (without the resistive network required to reduce the servoactuator stroke for Phase III performance) to provide sufficient stroke for a 9:1 throttling range. Engine throttling was accomplished by use of a manual stepping switch preset to provide step signals to the servoactuator giving nine thrust levels.

6.11.5 Test Results

Run C2-714 was successfully completed on 12 January 1965. Figure 6.11.5-1 summarizes C*, mixture ratio, and injector pressure drops measured over the throttling range. Detail tabulated data are presented in Table D-2-23 of Appendix D-2. C* values are not plotted at the 20-lb vacuum thrust level, because the nozzle became unchoked at sea level at the low chamber pressures.

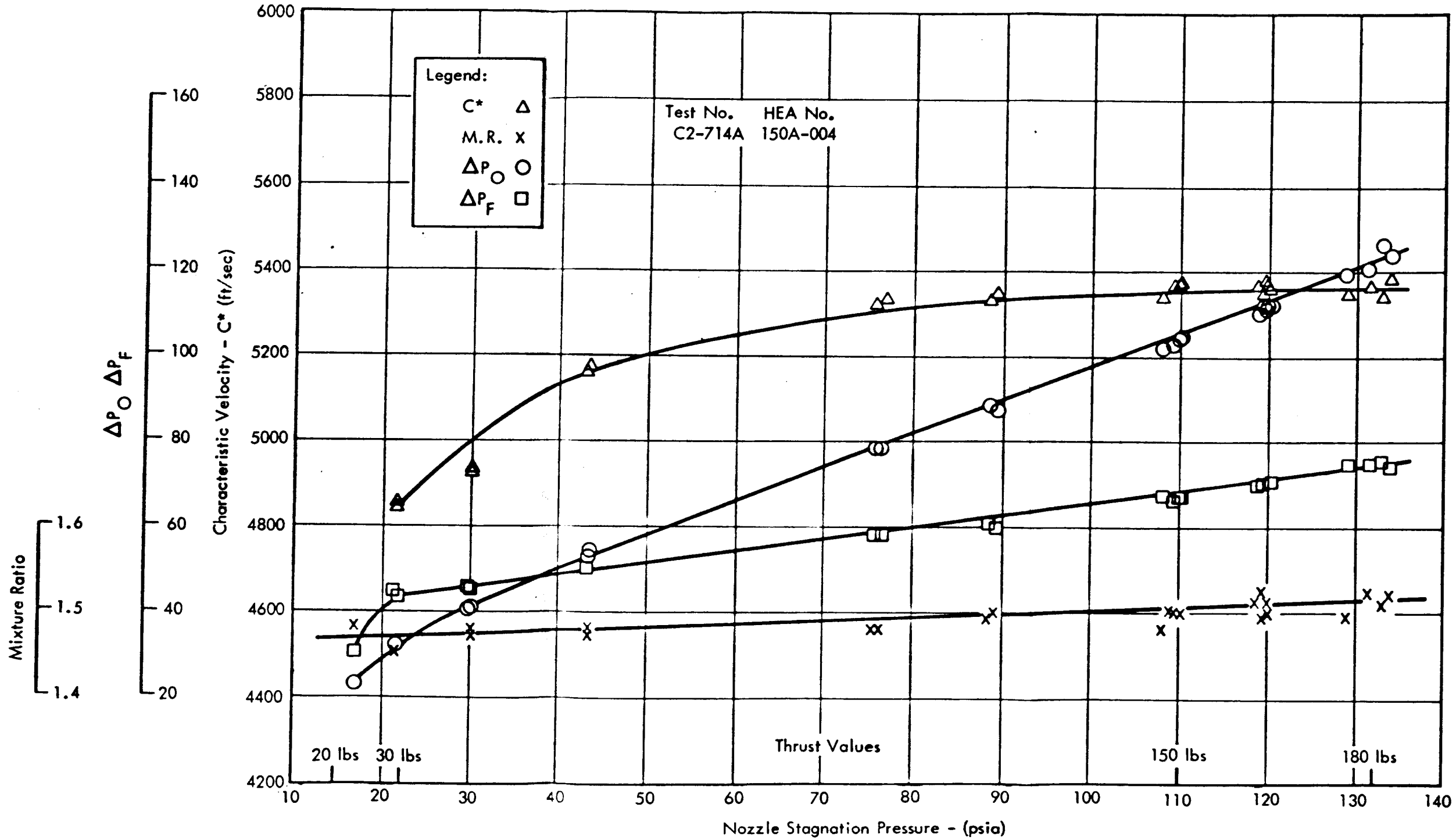

Figure 6.11.5-1. Extended Range Throttling Performance

6.12 Summary of Servoactuator Anomalies

During the course of the testing discussed elsewhere in this report, there were occurrences of anomalous performance and malfunctions of the servoactuators. Details of these occurrences are gathered in this paragraph. Also outlined herein are the corrective actions taken to evolve the satisfactorily performing, reliable final design.

For details about servoactuator design, performance, and acceptance testing, see paragraphs 3.2.6 and 5.1.1.

6.12.1 Phase II Follow-on Units

Six servoactuators were ordered and received as part of the Phase II Follow-on Program. All six servoactuators were used during Phase III testing; these servoactuators had serial numbers C53747 through C53752.

6.12.1.1 Failures and Anomalies

Three units (S/Ns C53747, C53748, and C53749) developed severe fuel leakage past the torque motor static seals. These units were retired from service after the leakage was detected. Unit C53748 was used successfully at the JPL/ETS for tests there prior to leaking.

Unit C53752 experienced a null shift and leakage through the output shaft dynamic seal and nozzle and was returned to the vendor for rework. After rework the unit was used in IRTS firings and in time developed a leak through the spool stop O-ring static seal. It was retired from service.

Unit C53750 showed intermittent, excessive initial step response delay times in leaving the extreme stop positions during the minimum temperature test (PQT-004B) at the JPL/ETS. Initial delays of up to 0.103 second resulted in step response rise times as high as 0.160 second. This was accompanied by excessive position slew rates. This performance characteristic occurred intermittently during later tests at the IRTS and the centrifuge tests at CTS. (For further details on dynamic performance refer to paragraph 6.9.)

In an effort to ascertain the cause of the anomalous behavior of Unit C53950 the following steps were taken:

1. Using this servoactuator on HEA S/N 001, the friction force required to move the crossarm without propellant pressure to the TCA was determined.

2. The servoactuator-to-crossarm flexure was replaced with a load ring. Then, 500 psi fuel pressure was applied to the TCA and servoactuator (with actuator dump line open); full stroke ramp inputs of ±80 ma at 0.03, 0.1, 0.5, and 1.0 cps were imposed and the loads were measured on the load ring.

3. The servoactuator was installed alone on the actuator test stand and pressurized to 700 psia without the resistive (stroke reducing) network. A sinusoidal differential current input of ±80 ma at 0.03 and 1.0 cps was then imposed, and the load, position, and signal were measured.

4. With the same setup as described in (3) above, step inputs of ±80 ma were imposed, and the load and position were measured.

Analysis of the data from (1) through (4) above revealed no malfunctions; performance was normal.

Unit C53750 was next partially disassembled; all parts appeared to be in excellent condition. Thus, the causes of the anomalous performance on Phase II Follow-on Unit C53750 remain unknown.

Analysis of the performance cited above and of the acceptance test data, plus restudy of the Phase II design showed the following major inadequacies of the Phase II Follow-on servoactuator:

- Inadequate linearity.
- Excessive step response rise time, overshoot, and setting time.
- Excessive internal leakage.
- Leakage of torque motor static seal.
- Leakage through the output shaft dynamic seal. (This was caused by metal particles that got by the shaft wiper during stroke retract because the shaft wrench flats were too long making the wiper ineffective.)
- Electrical zero shift and nozzle leakage. (This was caused by inadequate nozzle press fit.)

6.12.1.2 Design Changes Instituted for Phase III Servoactuators

The following changes were required for Phase III servoactuators to eliminate the inadequacies noted in paragraph 6.12.1.1:

1. Overall actuator linearity was improved by more rigid inspection controls on torque motor linearity.
2. Step response was improved by altering the second stage porting.
3. Internal leakage tendencies were reduced by tighter quality control during second stage assembly and matching.
4. Torque motor static seal leakage was corrected by a design improvement using an ethylene-propylene O-ring.
5. Leakage through the output shaft was corrected by shortening the wrench flats on the shaft to make the wiper effective.
6. Nozzle leakage and nozzle zero position shift were corrected by new nozzle press fit dimensions.

6.12.2 Phase III Servoactuators

Only seven of the 18 Phase III units ordered (S/Ns C55390 through C55395 and C55398) were tested at STL. Some anomalies occurred.

Actuator S/N C55390 developed a severe random null shift during firing of HEA S/N 007. The actuator was removed and returned to the vendor. Disassembly of the unit revealed that the four long-lock torque motor mounting screws had loosened (possibly during vibration) allowing the flapper to shift with respect to the first stage nozzle. All Phase III servoactuator torque motor mounting screws were then changed to be lockwired to alleviate the possibility of this malfunction reoccurring.

Units S/N C55391, C55392, and C55393 were received from the manufacturer and performed as expected during acceptance tests. However, these units experienced null shifts during subsequent HEA testing. Investigation in some depth indicated that the second stage spool centering springs could be overstressed during conditions of maximum error signal causing spring length changes. As a result, both centering springs, the feedback beam spring and the feedback arm spring were redesigned to preclude changes in performance caused by occurrence of maximum stress conditions. These actuators were returned to the vendor for rework and subsequent units had the spring redesign features. After rework, these three units passed the normal tests to which they are subjected by the vendor prior to delivery and were again delivered. By this time STL no longer was performing acceptance tests. Further, these units were not tested on an HEA subsequent to rework.

7.0 THEORETICAL ANALYSIS

Significant theoretical effort on the Phase III program centered around the six subjects listed below.

1. TCA Passive Thermal Control Analysis - See paragraph 3.3.4 and Appendix B.
2. Theoretical Thermochemical and Ballistic Properties.
3. Exhaust Plume Temperature and Pressure Profiles.
4. Dynamic Response Analytical Model.
5. TCA Predicted Firing Temperatures.
6. Venturi Discharge Coefficients.

The last five items will be discussed in this section.

7.1 Theoretical Thermochemical and Internal Ballistic Properties

7.1.1 Chemical Composition of Exhaust Products

Assuming frozen flow conditions, the theoretical gas composition in the combustion chamber and at the nozzle exit plane are identical; these data for a mixture ratio, M.R., of 1.5 and mid-range chamber pressure, P_c, of 66 psi are provided in Table 7.1.1-1.

7.1.2 Specific Heat Ratio and Molecular Weight

The specific heat ratio, γ, is defined as

$$\gamma = \frac{\Sigma X_i \quad C_{pi}}{(\Sigma X_i \quad C_{pi}) - R}$$ when:

1. $\Sigma X_i \; C_{pi}$ is evaluated at the temperature of the combustion products in the chamber, T_c, or at the exit plane, T_e.
2. R has the value of 1.987 when X_i is expressed in mole fraction and C_{pi} is in cal/mole^{o}K.

The average molecular weight is defined by $MW = \Sigma X_i \; MW_i$ where:
MW_i is the molecular weight of the i-th combustion gas constituent.

The heat capacity ratios (γ_c is γ at T_c and γ_e is γ at T_e) and the average molecular weight at M.R. = 1.5 and P_c = 66 psia are given in Table 7.1.2-1 along with some other properties.

Table 7.1.1-1

Theoretical Gas Composition
(Expressed as mole fraction for MON/MMH at MR = 1.5 and P_c = 66 psia)

Gas	Mole Fraction	Additional Gases of Low Concentration
N_2	0.30240	Mole fraction 10^{-5} to 10^{-6}
		N, NH, NH_3
H_2O	0.28489	
H_2	0.20444	Mole fraction 10^{-6} to 10^{-8}
		CN, HCN, H_2CO, HNCO, NH_2, N_2O, NO
CO	0.14118	
CO_2	0.02800	Mole fraction 10^{-8} to 10^{-10}
		CH_2, CH_3
H	0.02517	
OH	0.01129	Mole fraction 10^{-10} to 10^{-15}
		C, CH, CH_4, HCCH, NCCN, O_3, H^+, O^+, e^-
NO	0.00129	
O	0.00084	Mole fraction less than 10^{-15}
O_2	0.00047	C_2, C_3, C_4, C_5, C_3O_2, C_4N_2, H_2O_2,
		$H_2C{=}CH_2$, N_2O_3, N_2H_4, N_2O_4, N_2O_5,
HCO	0.00001	$H_2C\!-\!O\!-\!CH_2$, C^+

Table 7.1.2-1

Various Thermochemical Properties
(MR = 1.5 and P_c = 66 psia)

$\gamma_c = 1.243$

$\gamma_e = 1.337$

$MW = 19.49$

$T_c = 5237\ ^oR$

C^*(frozen) = 5564 ft/sec

I_{sp}(frozen) = 311.3 sec at $\epsilon = 32.8$

C_F (frozen) = 1.8003 at $\epsilon = 32.8$

$T_e = 1328\ ^oR$

$P_c/P_e = 520$

7.1.3 Theoretical Internal Ballistic Properties

Equilibrium, frozen, and kinetic theoretical performance calculations were made. The results of these calculations are given in Figures 7.1.3-1 through -3. These figures show theoretical characteristic exhaust velocity, thrust coefficient, and specific impulse of the TCA as a function of chamber pressure. The equilibrium and frozen performance calculations were made using STL's IBM 7094 Rocket Chemistry Program. This program considers all possible reaction products and calculates the adiabatic chamber conditions and the equilibrium or frozen isotropic nozzle expansion using JANAF thermal functions (free energies, enthalpies, and heat capacities). Reaction rates are not considered; thermodynamic characteristics alone are considered. Extensive comparisons of the results of these calculations with similar calculations performed by associate contractors during the Air Force ballistic missile programs has established the overall accuracy of the program. The kinetic calculations were performed using STL's Nonequilibrium Performance Program. Assuming that equilibrium conditions exist in the combustion chamber, this program calculates the nonequilibrium nozzle expansion accounting for the effects of finite rate chemical reactions occurring between combustion products. The program considers the 12 chemical species: H_2O, CO_2, H_2, CO, N_2, O_2, NO, H, O, N, and C, and the 24 chemical reactions given in Table 7.1.3-4. It has been shown that these 12 chemical species and 24 chemical reactions are the only ones of importance in currently used space storable propellants containing the elements carbon, oxygen, hydrogen, and nitrogen when complete combustion occurs in the chamber. Examination of Figures 7.1.3-1 through 7.1.3-3 shows that even with complete combustion there is an appreciable kinetic performance loss associated with the lack of complete recombination in the Surveyor nozzle. The calculations show that the theoretical kinetic performance estimates for Surveyor are closer to the frozen flow performance estimates than to the equilibrium flow performance estimates.

For purposes of the data reduction program (STL Document 8422-6007-TU-000, R02) the frozen flow theoretical performance was assumed and these data are provided in Figures 7.1.3-5 through -7. Data are included in these figures on characteristic exhaust velocity, mixture ratio, thrust coefficient, and chamber pressure interrelationships (Figures 7.1.3-5 and -6) plus combustion gas temperature (Figure 7.1.3-7). The information shown in Figures 7.1.3-5 through -7 is tabularly presented in Tables 7.1.3-8, -9 and -10.

Analytical relations were derived to express the vacuum thrust coefficient as a function of nozzle stagnation pressure, mixture ratio, and nozzle expansion ratio. These relations, shown graphically in Figure 7.1.3-6 and presented in Table 7.1.3-11, are also used in the Surveyor Data Reduction Program.

Data similar to that shown in Figures 7.1.3-5, -6, and -7 and in Tables 7.1.3-8, -9, -10, and -11 for MMH and N_2O_4 (a propellant combination used on the program for a brief period) are provided in Appendix F.

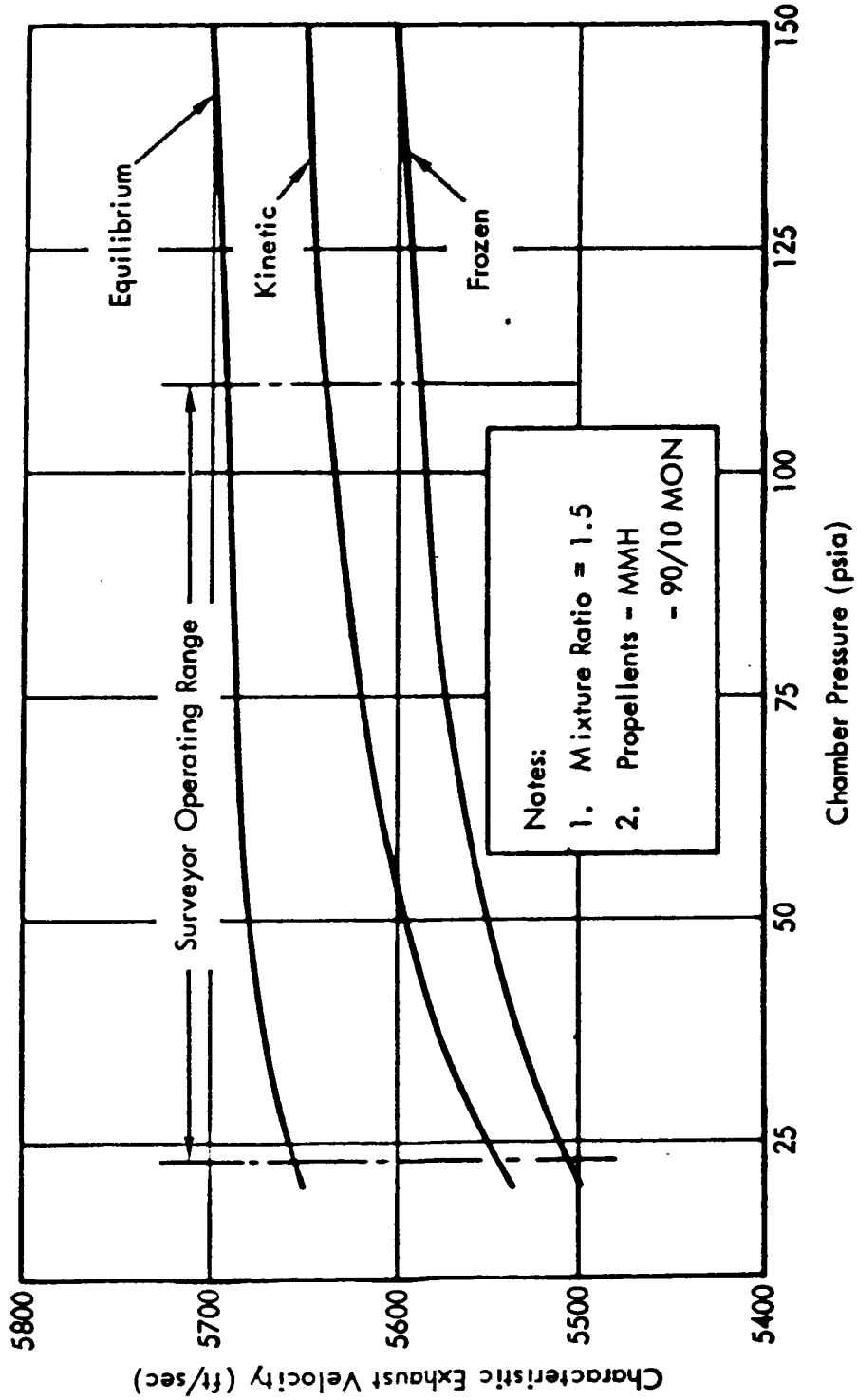

Figure 7.1.3-1. Theoretical Characteristic Exhaust Velocities Versus Chamber Pressure

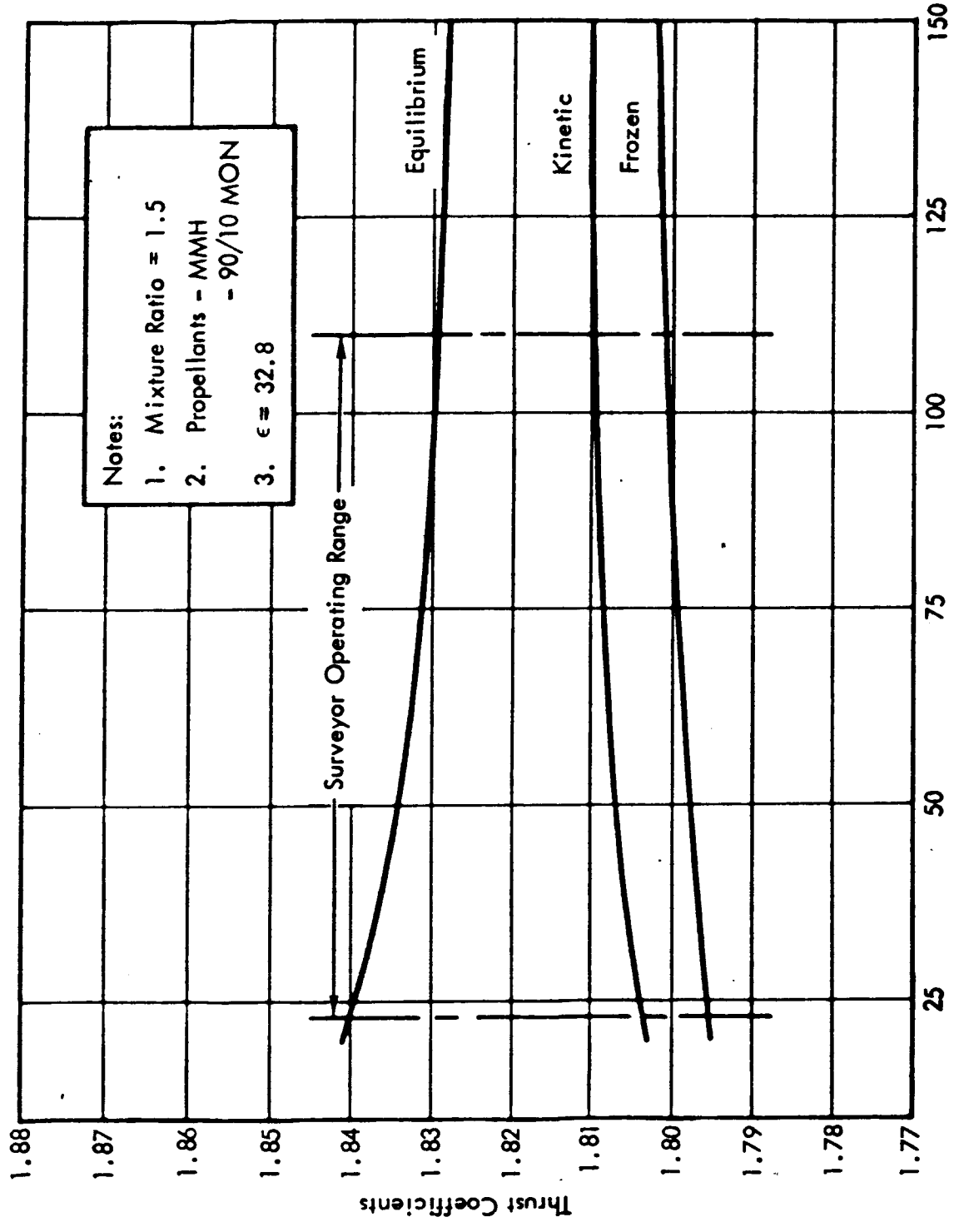

Figure 7.1.3-2. Theoretical Thrust Coefficients Versus Chamber Pressure

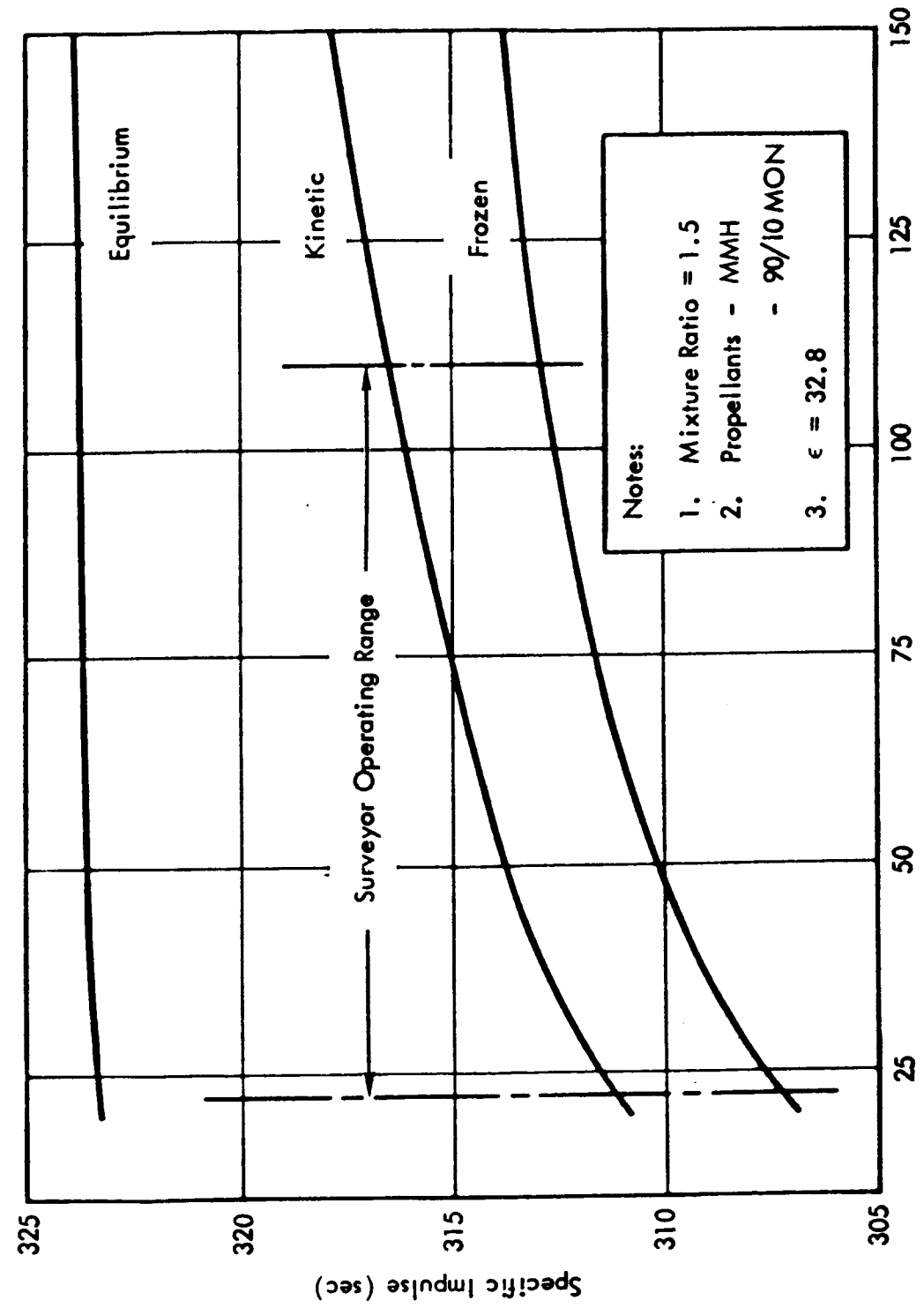

Figure 7.1.3-3. Theoretical Specific Impulse Versus Chamber Pressure

Table 7.1.3-4

Assumed Chemical Reactions

Reaction Number	Reaction	k_r	Reference
1	$N_2 + M \rightleftarrows N + N + M$	$2 \times 10^{18}\ T^{-1}$	Byron, S., quoted by Wray, K. L., Avco Research Report 104 (1961)
2	$O_2 + M \rightleftarrows O + O + M$	$2 \times 10^{18}\ T^{-1}$	Wray, K. L., and Teare, J. D., Avco Research Report 95 (1961)
3	$NO + M \rightleftarrows N + O + M$	$2 \times 10^{18}\ T^{-1}$	Wray, K. L., and Teare, J. D., Avco Research Report 95 (1961)
4	$CO + M \rightleftarrows C + O + M$	$2 \times 10^{18}\ T^{-1}$	Wray, K. L., and Teare, J. D., Avco Research Report 95 (1961)
5	$CO_2 + M \rightleftarrows CO + O + M$	$3 \times 10^{20} T^{-1} - 11393/T$	Avramenko, L. I., and Kolesnikova, R. V., Izvest. Akad. Nauk. S.S.S.R., Otdel. Khim. Nauk., 1562, (1959)
6	$H_2O + M \rightleftarrows OH + H + M$	$3 \times 10^{19}\ T^{-1}$	Bulewicz, E. M., and Sugden, T.M., Trans. Far. Soc., 54, 1855, (1958)
7	$H_2 + M \rightleftarrows H + H + M$	$2 \times 10^{18}\ T^{-1}$	Rink, J. P., J Chem. Phys., 36, 262, (1962)
8	$H + M \rightleftarrows O + H + M$	$2 \times 10^{18}\ T^{-1}$	Wray, K. L, and Teare, J. D., Avco Research Report 95 (1961)
9 [a]	$N_2 + O \rightleftarrows NO + N$	$1.5 \times 10^{16} T^{-1}$	Phillips, L. F., and Schiff, H. I., J. Chem. Phys., 36, 1509, (1962)
10	$N_2 + O_2 \rightleftarrows NO + NO$	$2.7 \times 10^{13} \exp(-53{,}800/T)$	Ralston, A., and Wilf, H. S., Mathematical Method for Digital Computers, 1960
11	$NO + O \rightleftarrows N + O_2$	$1.011 \times 10^{11} T^{-0.5} \exp(-3120/T)$	Vincenti, W. G., Stanford University Department of Aeronautical Engineering Report 101 (1961)
12	$CO + O \rightleftarrows C + O_2$	$2.48 \times 10^{13} \exp(-990/T)$	Avramenko, L. I., and Lorentso, R. V., Zhur. Fiz. Khim., 24, 207, (1950)
13	$CO_2 + O \rightleftarrows CO + O_2$	$3.58 \times 10^{15}\ T^{-1}$	Avramenko, L. I. and Kolesnikova, R. V., Izvest. Akad. Nauk., S.S.S.R., Otdel. Khim. Nauk., 1562 (1959)
14	$CO + N \rightleftarrows C + NO$	$1.44 \times 10^{16}\ T^{-1}$	Avramenko, L. I., and Lorentso, R. V., Zhur, R Fiz. Khim., 24, 207, (1950)
15	$CO + NO \rightleftarrows CO_2 + C$	$2.11 \times 10^{15}\ T^{-1}$	Avramenko, L. I., and Kolesnikova, R. V., Izvest. Akad. Nauk., S.S.S.R., Otdel. Khim. Nauk., 1562 (1959)
16	$CO + CO \rightleftarrows CO_2 + C$	$2.11 \times 10^{16}\ T^{-1}$	Avramenko, L. I., and Lorentso, R. V., Zhur. Fiz. Khim., 24, 207, (1950)
17	$H + O_2 \rightleftarrows OH + O$	$3.3 \times 10^{16}\ T^{-1}$	Kaufman, F., and Del Greco, F. P., Ninth International Symposium on Combustion (1963)
18	$H + NO \rightleftarrows OH + N$	$4.01 \times 10^{23}\ T^{-1}$	Kaufman, F., and Del Greco, F. P., Ninth International Symposium on Combustion (1963)
19	$H + CO \rightleftarrows OH + C$	$1 \times 10^{14} \exp(-13{,}000/T)$	Porter, A. E., Heimel, S., and Butler, J. N., Eighth International Symposium on Combustion (1962)
20	$H_2 + O \rightleftarrows OH + H$	$5.7 \times 10^{12} \exp(-2900/T)$	Kaufman, F., and Del Greco, F. P., Ninth International Symposium on Combustion (1963)
21	$H + CO_2 \rightleftarrows OH + CO$	$1 \times 10^{13} \exp(-5000/T)$	Westenberg, A. A., and Fristrom, R. M., J. Phys. Chem. 65, 591, (1961)
22	$H + H_2O \rightleftarrows H_2 + OH$	$1.35 \times 10^{13}\ T^{-1}$	Kaufman, F., and Del Greco. F. P., Ninth International Symposium on Combustion (1963)
23	$H_2O + O \rightleftarrows OH + OH$	$4.5 \times 10^{15}\ T^{-1}$	Kaufman, F., and Del Greco, F. P., Ninth International Symposium on Combustion, (1963)
24	$H_2 + O_2 \rightleftarrows OH + OH$	$2.7 \times 10^{16} \exp(-53{,}800/T)$	Kaufman, F., and Kelso, J. P., J. Chem. Phys., 23. 1072, (1955)

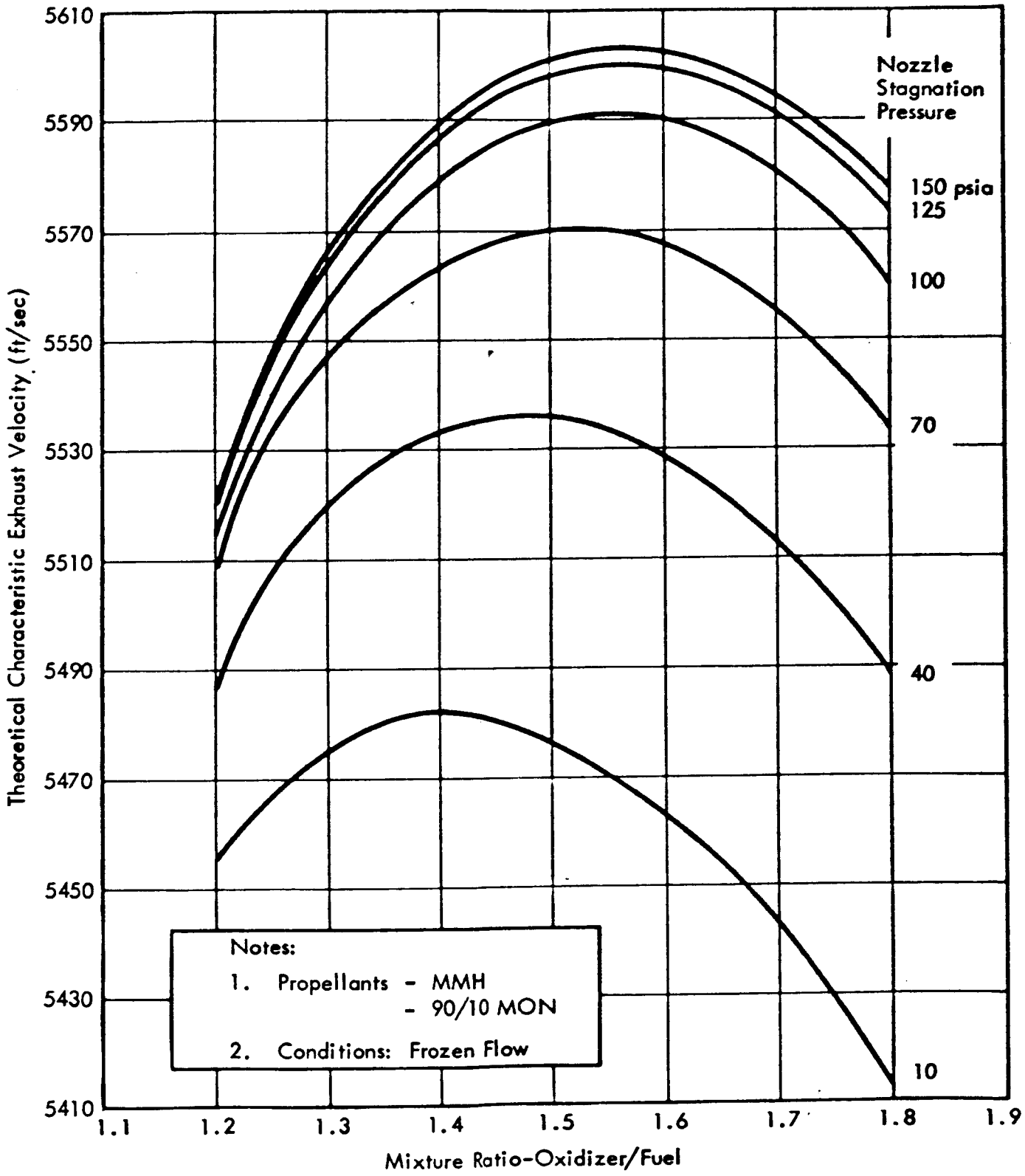

Figure 7.1.3-5. Theoretical Characteristic Velocity Versus Mixture Ratio

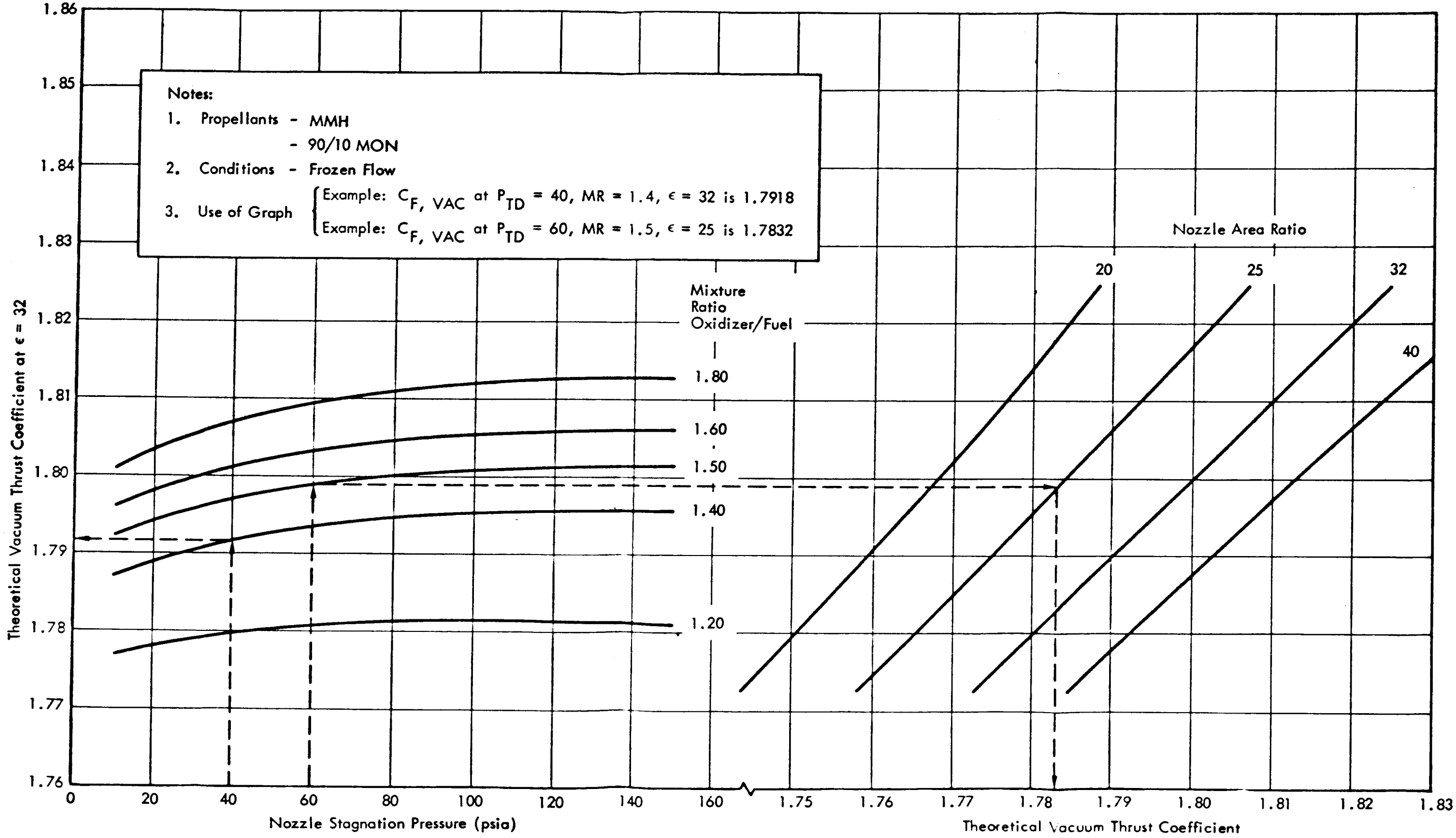

Figure 7.1.3-6. Theoretical Vacuum Thrust Coefficient Versus Nozzle Stagnation Pressure

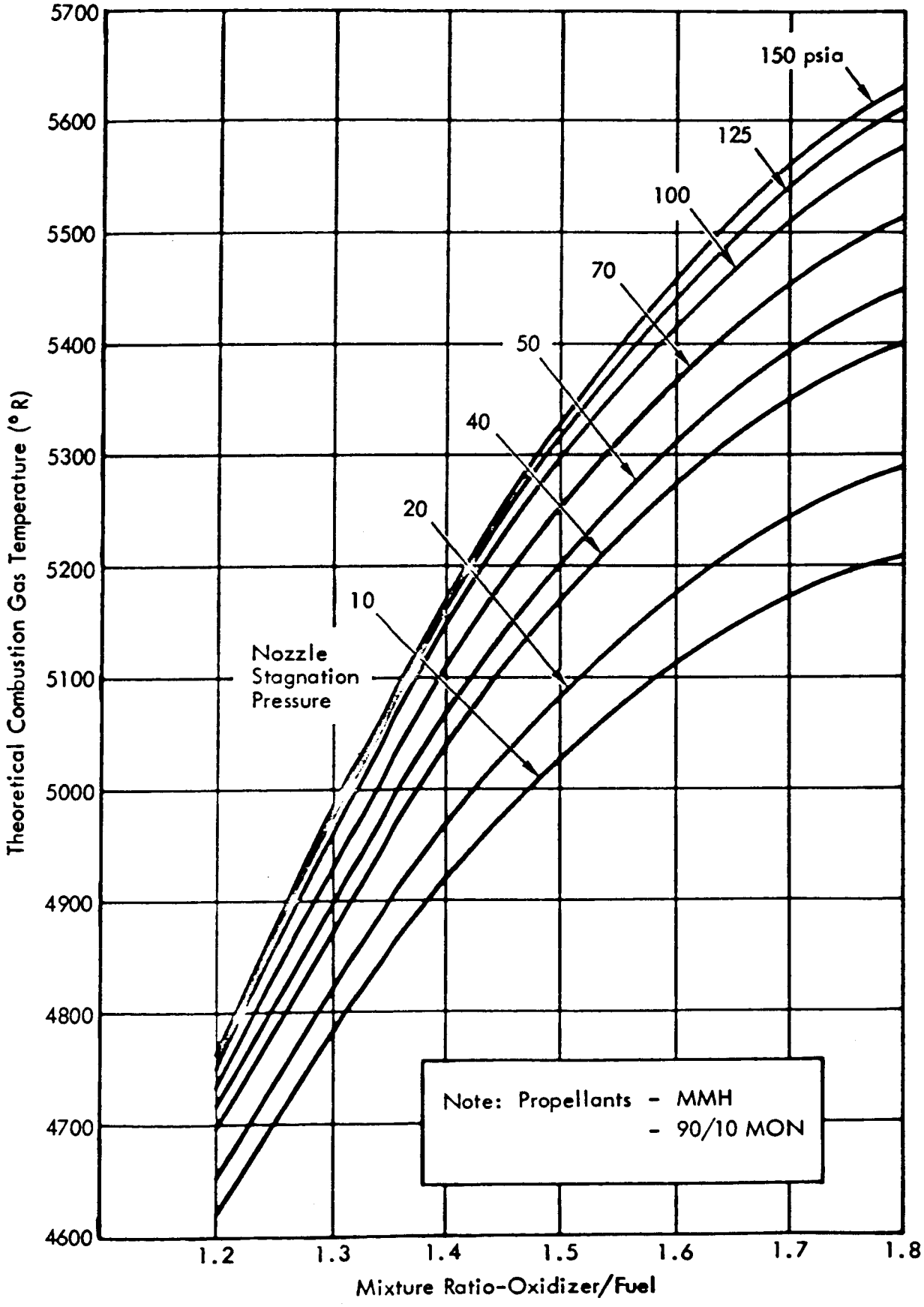

Figure 7.1.3-7. Theoretical Combustion Gas Temperature Versus Mixture Ratio

Table 7.1.3-8

Theoretical Characteristic Exhaust Velocity

Propellants: MMH - MON (90% N_2O_4 - 10% NO by weight)
Conditions: Frozen Flow

Nozzle Stagnation Pressure (psia)	Mixture Ratio Oxidizer/Fuel	Characteristic Exhaust Velocity (ft/sec)
20	1.20	5467
	1.40	5502
	1.50	5500
	1.60	5488
	1.80	5443
50	1.20	5495
	1.40	5546
	1.50	5550
	1.60	5543
	1.80	5506
150	1.20	5521
	1.40	5589
	1.50	5602
	1.60	5602
	1.80	5577

Table 7.1.3-9

Theoretical Vacuum Thrust Coefficient

Propellants: MMH - MON (90% N_2O_4 - 10% NO by weight)
Conditions: Frozen Flow

Nozzle Stagnation Pressure (psia)	Mixture Ratio Oxidizer/Fuel	Nozzle Area Ratio	Vacuum Thrust Coefficient
20	1.20	15.746	1.7312
		25.619	1.7652
		34.072	1.7823
		41.707	1.7932
20	1.40	16.208	1.7427
		26.485	1.7781
		35.320	1.7958
		43.320	1.8072
20	1.50	16.391	1.7471
		26.829	1.7832
		35.815	1.8012
		43.962	1.8127
20	1.60	16.544	1.7508
		27.119	1.7874
		36.234	1.8056
		44.505	1.8174
20	1.80	16.776	1.7563
		27.562	1.7936
		36.876	1.8123
		45.338	1.8243
50	1.20	15.813	1.7328
		25.745	1.7671
		34.256	1.7842
		41.946	1.7952
50	1.40	16.324	1.7456
		26.704	1.7814
		35.637	1.7993
		43.734	1.8108
50	1.50	16.529	1.7506
		27.091	1.7871
		36.195	1.8054
		44.457	1.8171
50	1.60	16.702	1.7548
		27.419	1.7919
		36.670	1.8104
		45.073	1.8223
50	1.80	16.965	1.7609
		27.922	1.7989
		37.400	1.8179
		46.021	1.8301
150	1.20	15.874	1.7344
		25.861	1.7688
		34.424	1.7860
		42.166	1.7971
150	1.40	16.442	1.7486
		26.927	1.7848
		35.960	1.8029
		44.154	1.8145
150	1.50	16.675	1.7543
		27.368	1.7913
		36.598	1.8098
		44.981	1.8217
150	1.60	16.875	1.7591
		27.748	1.7968
		37.148	1.8156
		45.695	1.8277
150	1.80	17.182	1.7662
		28.336	1.8049
		38.003	1.8243
		46.807	1.8368

Table 7.1.3-10

Theoretical Combustion Gas Temperature

Propellants: MMH - MON (90% N_2O_4 - 10% NO by weight)

Nozzle Stagnation Pressure (psia)	Mixture Ratio Oxidizer/Fuel	Combustion Gas Temperature ($^{\circ}R$)
20	1.20	4651
	1.40	4971
	1.50	5086
	1.60	5175
	1.80	5291
50	1.20	4709
	1.40	5070
	1.50	5203
	1.60	5309
	1.80	5450
150	1.20	4763
	1.40	5171
	1.50	5328
	1.60	5457
	1.80	5634

Table 7.1.3-11

Theoretical Vacuum Thrust Coefficient

Propellants: MMH - MON (90% N_2O_4 - 10% NO by weight)

(Applicable for $20 < P_{TD} < 150$, $1.20 < MR < 1.80$, $20 < \epsilon < 40$)

$$C_{F,VAC} = C_{F,VAC}(P_{TD}, MR, \epsilon)$$

$$C_{F,VAC}(P_{TD}, 1.5, 32.0) = -5.7671 \times 10^{-7} P_{TD}^2 + 1.5108 \times 10^{-4} P_{TD} + 1.7916$$

For $1.2 \leq MR < 1.4$

$$\left(\frac{\delta C_{F,VAC}}{\delta MR}\right) = -4.6470 \times 10^{-7} P_{TD}^2 + 1.8376 \times 10^{-4} P_{TD} + 0.0508$$

For $1.4 < MR < 1.5$

$$\left(\frac{\delta C_{F,VAC}}{\delta MR}\right) = -4.1396 \times 10^{-7} P_{TD}^2 - 1.8306 \times 10^{-5} P_{TD} + 0.0523$$

For $1.5 \leq MR < 1.6$

$$\left(\frac{\delta C_{F,VAC}}{\delta MR}\right) = -8.9646 \times 10^{-7} P_{TD}^2 + 2.0895 \times 10^{-4} P_{TD} + 0.0344$$

For $1.6 \leq MR < 1.8$

$$\left(\frac{\delta C_{F,VAC}}{\delta MR}\right) = -6.3323 \times 10^{-7} P_{TD}^2 + 1.6479 \times 10^{-4} P_{TD} + 0.0274$$

For $\epsilon \leq 32$

$$\left(\frac{\delta C_{F,VAC}}{\delta \epsilon}\right) = 7.739 \times 10^{-2} C_{F,VAC}^2(P_{TD}, 1.5, 32.0) - 0.2662\, C_{F,VAC}(P_{TD}, 1.5, 32.0) + 0.2311$$

For $\epsilon > 32$

$$\left(\frac{\delta C_{F,VAC}}{\delta \epsilon}\right) = 6.027 \times 10^{-2} C_{F,VAC}^2(P_{TD}, 1.5, 32.0) - 0.2102\, C_{F,VAC}(P_{TD}, 1.5, 32.0) + 0.1848$$

$$C_{F,VAC} = C_{F,VAC}(P_{TD}, 1.5, 32.0) + \left(\frac{\delta C_{F,VAC}}{\delta MR}\right)(MR - 1.50) + \left(\frac{\delta C_{F,VAC}}{\delta \epsilon}\right)(\epsilon - 32.0)$$

7.2 Exhaust Plume Temperature and Pressure

The exhaust plume for the MIRA 150A nozzle was calculated for vacuum conditions. A perfect gas isentropic expansion from a uniform parallel flow at the nozzle exit was assumed, and the flow field was calculated by the method of characteristics. At a nominal mixture ratio of 1.5 and at an area ratio of 32.8 the average kinetic specific heat ratio for a chamber pressure of 110 psia (maximum thrust) and 66 psia (mid-range thrust) is 1.3275 and 1.3307, respectively. An average kinetic specific heat ratio of 1.329 was chosen for the exhaust plume calculation. Therefore, the flow field shown in Figures 7.2-1 and 7.2-2 represents the estimated exhaust plume characteristic applicable to both maximum and mid-range thrust levels.

7.3 Dynamic Response Analytical Model

A mathematical model for the throttling capability of the MIRA 150A was derived and verified. The servoactuator was shown to be the only component with significant dynamics at low frequency. The model of the actuator was simulated on the analog computer and verification achieved by matching the simulation results with the 25% and 100% step response test data, and the 15 ma and 30 ma peak-to-peak frequency response test data of two Phase III servoactuators —— S/Ns C55391 and C55393. The final model contained the following nonlinearities:

1. Spool velocity deadband caused by Coulomb friction.
2. Flow deadband caused by spool overlap.
3. Asymmetrical piston flow coefficients due to asymmetrical porting to piston.
4. Flow limit due to saturation of pressure drop.
5. Spool and piston position limit caused by physical stops.
6. Loading effects including preload, Coulomb friction, and spring forces.
7. Asymmetrical torque motor gain.

Figure 7.3-1 illustrates the final analytical model. A detailed description of the model is given in STL Document 8422-6014-TU-000.

7.4 Predicted Firing Temperatures of the CC & NA

During Phase III, thermal analyses were performed on the CC & NA to predict the external surface temperatures under various duty cycle conditions.

7.4.1 Computer Programs

The following STL computer programs were used in connection with these analyses.

7.4.1.1 Bartz Turbulent Boundary Layer and Heat Transfer Program

This program solved the equations governing turbulent boundary layer growth and heat transfer in axisymmetric nozzles. The integral momentum and energy equations for the turbulent boundary layer were solved simultaneously using semi-empirical relations for skin friction and heat transfer coefficients. The nozzle wall heat transfer coefficient calculated by this program was used as input to the Thermal Analyzer Program.

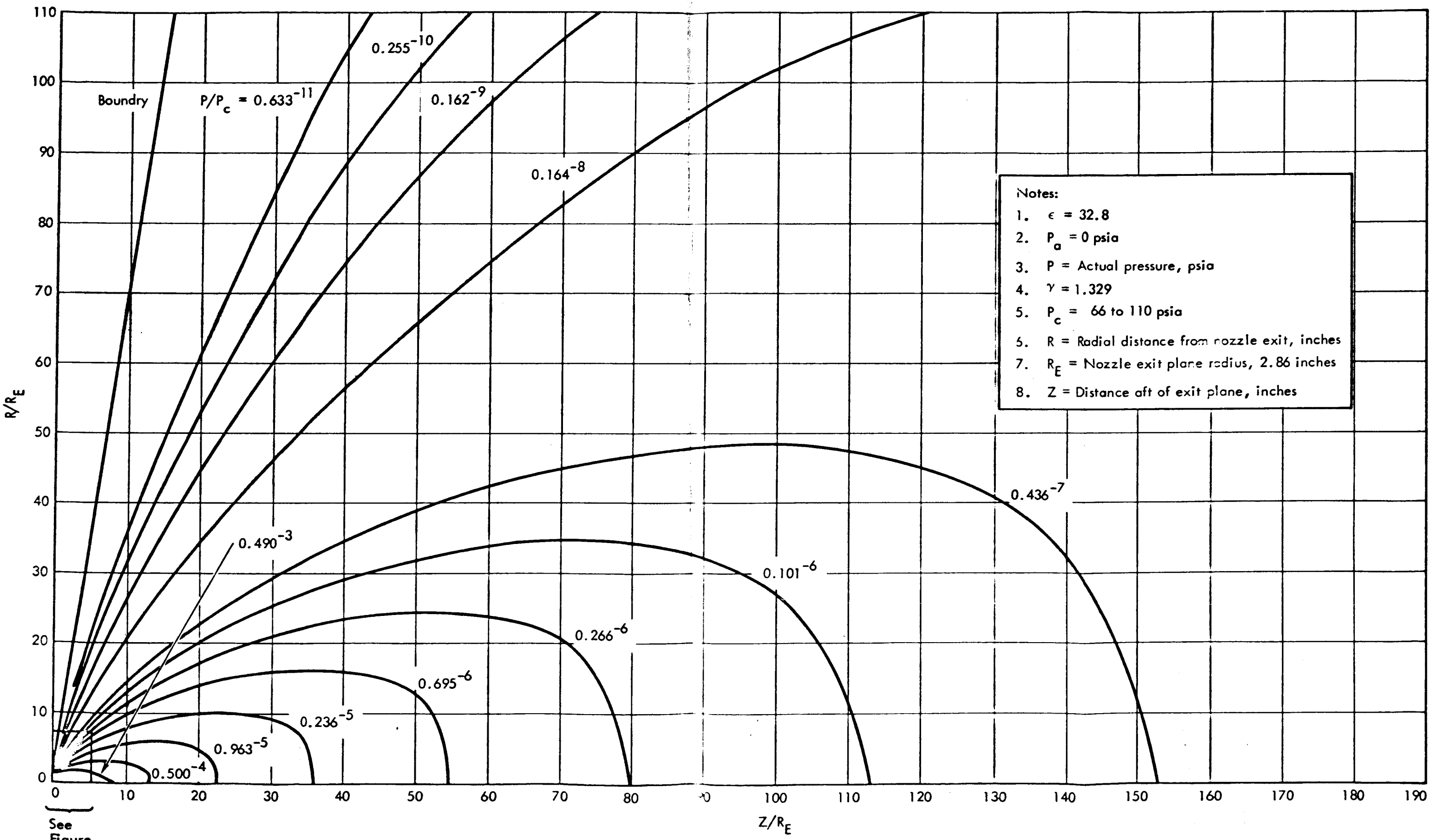

Figure 7.2-1. Exhaust Plume Pressure Profile

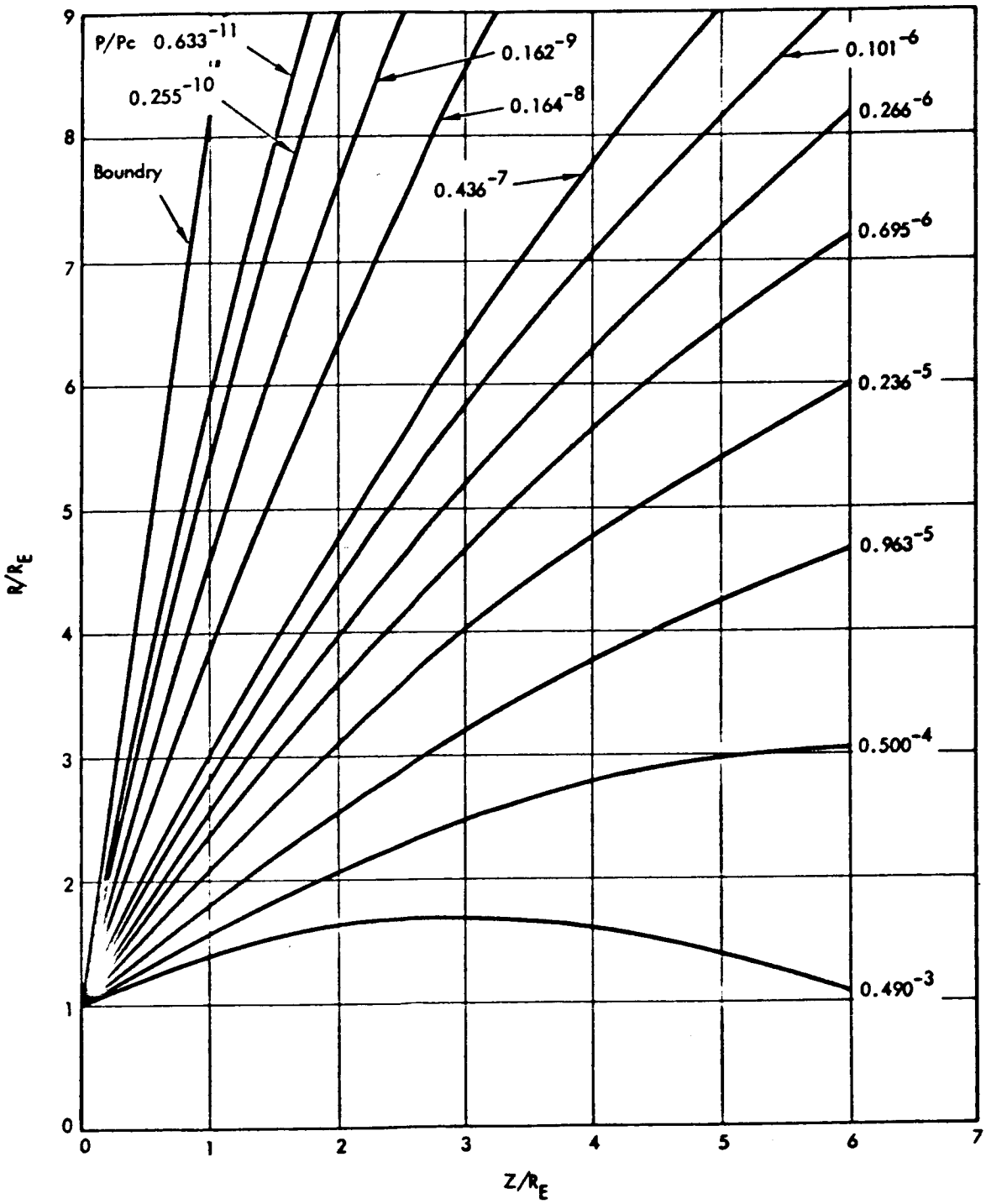

Figure 7.2-2. Exhaust Plume Profile - Near Exit Plane

Coefficients

K_{I_R}	= 0.0555 lb/ma	$Q_{a_{max}}$	= 0.8955 in^3/sec
K_{I_E}	= 0.0546 lb/ma	$Q_{a_{min}}$	= 0.8305 in^3/sec
K_f	= 44.1 lb/in	D_{x_s}	= 0.029 in/sec
K	= 0.0095 in/lb	$D_{\dot{x}_s}$	= 0.58 x 10^{-3}
τ	= 0.00413 sec	$X_{s\ max}$	= 0.01 in
K_{QE}	= 190 in^2/sec	$X_{a\ min}$	= 0.086 in
K_{QR}	= 137.5 in^2/sec	$X_{a\ max}$	= 0.0918 in
A_p	= 0.17 in^2	F_L	= 20 lbs
P_s	= 700 psi	F_c	= 5 lbs
A_s	= 0.049 in^2	K_a	= 14.75 lb/in
T_{min}	= 30 lbs	K_T	= 698 lb/in

Note: $X_s = 0$ when $X_s = \pm X_{s\ max}$
$X_a = 0$ when $X_a = \pm X_{a\ max}$

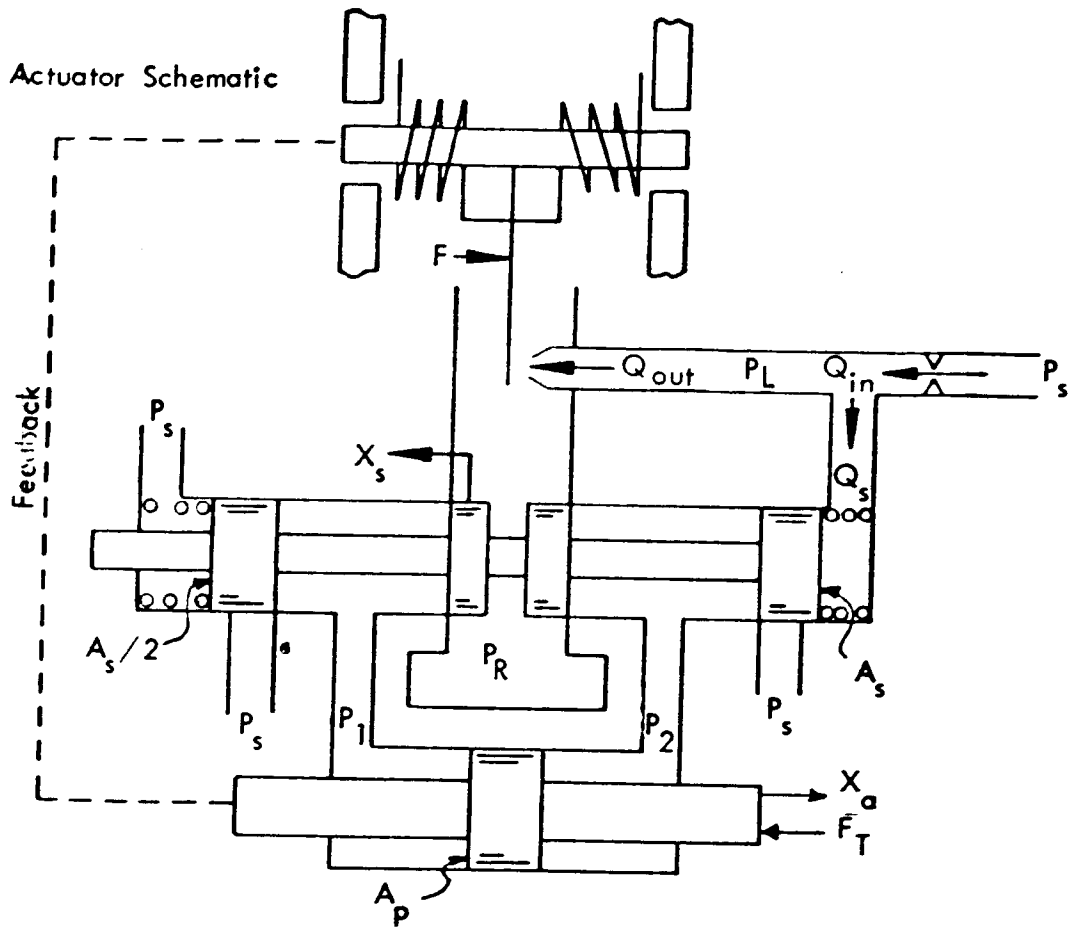

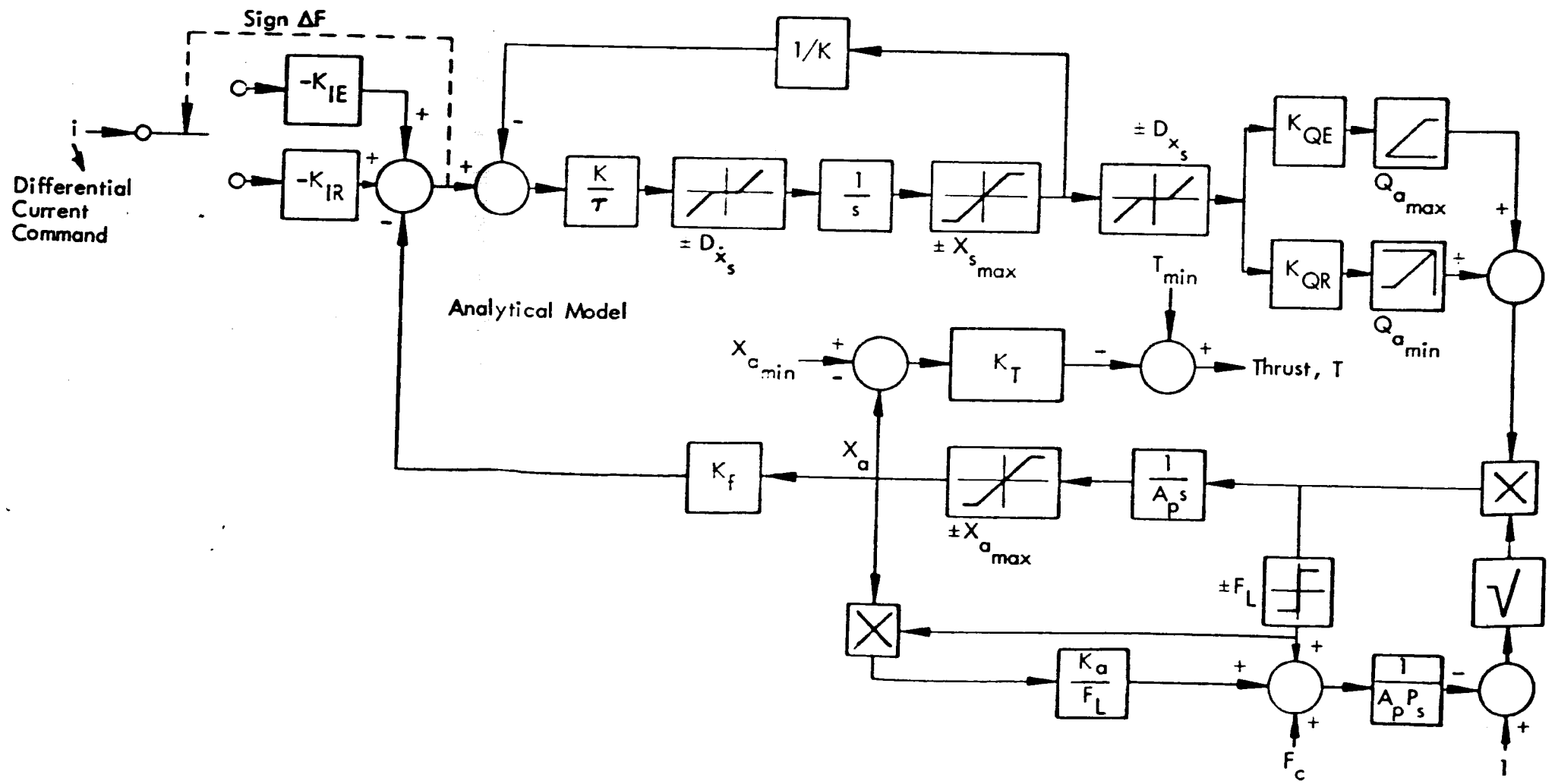

Legend

A_p	- Piston Area
A_s	- Spool Area
$D_{\dot{x}_s}$	- Spool Velocity Deadzone
D_{x_s}	- Spool Overlap Deadzone
F_c	- Load Force Coulomb Friction
F_L	- Constant Load Force
F_T	- Total Load Force
K	- Spool Valve Static Gain
K_a	- Load Force Spring Constant, Actuator Flexure Spring Constant
K_f	- Actuator Feedback Constant
K_T	- Actuator Position to Thrust Gain
K_{QE}, K_{QR}	- Piston Flow Gain in Extend and Retract Direction
K_{IE}, K_{IR}	- Flapper Valve Force Gain in Extend and Retract Direction
P_1, P_2	- High and Low Load Pressures on Piston
P_L	- Spool Load Pressure
P_s	- Supply Pressure
P_R	- Return Pressure
Q_a	- Volumetric Flow to Piston
Q_s	- Volumetric Flow to Spool
Q_{in}	- Flow to Actuator Upper Stage
Q_{out}	- Flow Out Flapper Nozzle
T	- Engine Thrust
X_a	- Actuator Position
X_s	- Spool Position
τ	- Spool Valve Time Constant
i	- Differential Current Command

Figure 7.3-1. MIRA 150A Dynamic Analytical Model

7.4.1.2 Geometrical View Factor Program

This program computed the geometrical view factors between the elemental sections of a given body for use in the solution of radiation heat transfer problems. The geometrical view factors obtained were used in the Thermal Analyzer Program for those surface nodes where radiation interchange must be considered.

7.4.1.3 Charring Ablation Program

This program solved the one-dimensional heat transfer equations for the transient behavior of decomposing materials that yield gaseous products and leave a porous solid matrix. The program output consisted of temperature and density distributions as a function of time, surface recession rate, and pyrolytic gas flow rate. Input parameters consisted of the material's thermophysical properties, Arrhenius decomposition constants, recession rate constants, and system geometry. Head input can be specified at both inner and outer boundaries of the material composite as being convective, radiative, or an arbitrary function of time.

7.4.1.4 Thermal Analyzer Program

This program used the results of the above three programs and solved the electrical network analog of the TCAs heat transfer characteristics. The output of the program resulted in a temperature-time history at each of the specified nodes.

7.4.2 Predicted Temperature for Mid-Course Correction Firing

A thermal analysis of the Surveyor TCA during and immediately after the 50-second, half-thrust firing for the mid-course correction was performed to predict the temperature history of the combustion chamber shell and nozzle extension.

The combustion chamber used for the analysis was defined by STL Drawing No. 106546-1. Twelve stations were analyzed along the TCA as shown in Figure 7.4-1. One dimensional analysis considering radial conduction only was performed at the combustion chamber and nozzle throat. For the nozzle expansion cone (both the ablative-cooled portions and radiation-cooled extension), a two dimensional thermal model was set up. This model considered axial conduction along the 0.020 inch thick titanium shell and radial conduction through the ablative liner. A complex thermal radiation network was set up whereby each station along the expansion cone was allowed to view each of the other stations through its appropriate geometric view factor. Multiple reflections were considered in the thermal radiation calculations. It was also assumed that both the emitted and reflected radiation were diffuse. Each of the internal stations on the expansion cone were allowed to view space through the nozzle exit plane. The stations on the outside of the nozzle extension were also allowed to view space (geometric view factor taken as 1.0). The sink temperature for space was taken as 0°R. Emissivities used in the analysis were summarized in the following table:

Sta. No.	Description
1	Chamber
2	Throat
3	0.4 Inches from Throat
4	1.2
5	2.0
6	2.55
7	2.8
8	3.2
9	3.9
10	4.6
11	5.2
12	6.0 Inches from Throat

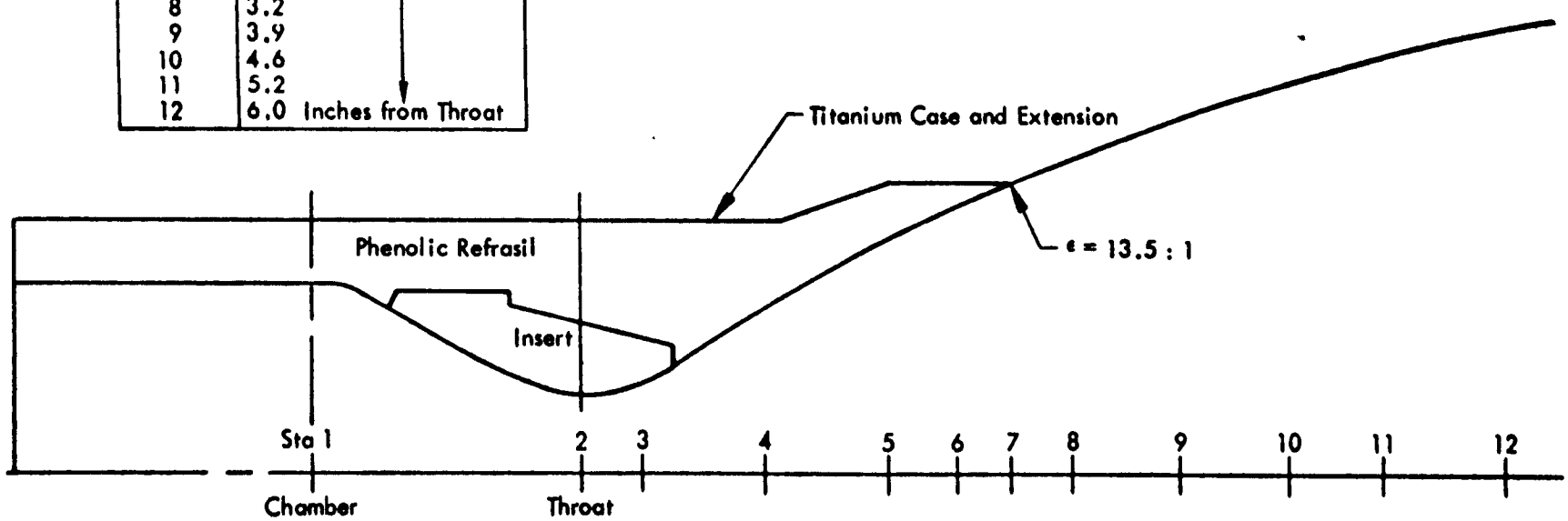

Figure 7.4-1. Schematic of MIRA 150A Combustion Chamber for Analysis

Summary of Emissivities Used in Analysis

Component	Emissivity
Combustion Chamber Shell	0.05
External Nozzle Extension	0.5
Internal Nozzle Extension	0.7
Internal Ablative Expansion Cone	0.55

The convective heat input was calculated by the Bartz method. The total temperature (combustion chamber flame temperature) was corrected for variation in C* efficiency (η_{C^*}). The η_{C^*} used for the analysis was 94.5%, and the corrected flame temperature was 4688°R.

The thermal analysis was performed for a 1800-second period which consisted of a 50-second firing at half thrust followed by a 1750-second cooldown. The results of the thermal analysis are presented in Figures 7.4-2 through -5. Figures 7.4-2 and 7.4-3 present the first 100 seconds of the analysis, while Figures 7.4-4 and 7.4-5 present the total 1800-second analysis.

7.4.3 Predicted Temperatures for a Full Duration Firing

A thermal analysis was performed on the CC & NA (defined by STL Drawing No. 106546-1) for a full duration, 5-start, variable thrust firing. The thrust-time profiles used as an input to the Thermal Analyzer Program are described in Table 6.6.3-2. The thrust-time profile inputs were used in the following sequence: (1) 52 seconds of PQ-1 profile A, (2) 70 seconds of PQ-1-B, followed by a 72-hour vacuum soak, (3) the first 40 seconds of PQ-1-C, (4) 116 seconds of PQ-1-C, and (5) 70 seconds of PQ-1-B. Seven stations were analyzed along the CC & NA axis.

The same assumptions were used for this thermal analysis as was used on the mid-course correction thermal analysis with the following exceptions:

1. The emissivity on the nozzle extension was 0.25.
2. The environmental sink temperature for the TCA was 100°F.
3. The sink temperature seen by the nozzle exit area during firing was 1000°F; at the end of the firing this temperature was reduced to 100°F and maintained constant during the heat soak back period.

The results of the thermal analysis are presented in Figures 7.4-6 through 7.4-10.

The experimental data obtained under the same operating conditions were generated at JPL/ETS during five test firings —— Runs DY-20 through DY-24. A comparison of the experimental results and theoretical predictions is presented in paragraph 6.4.

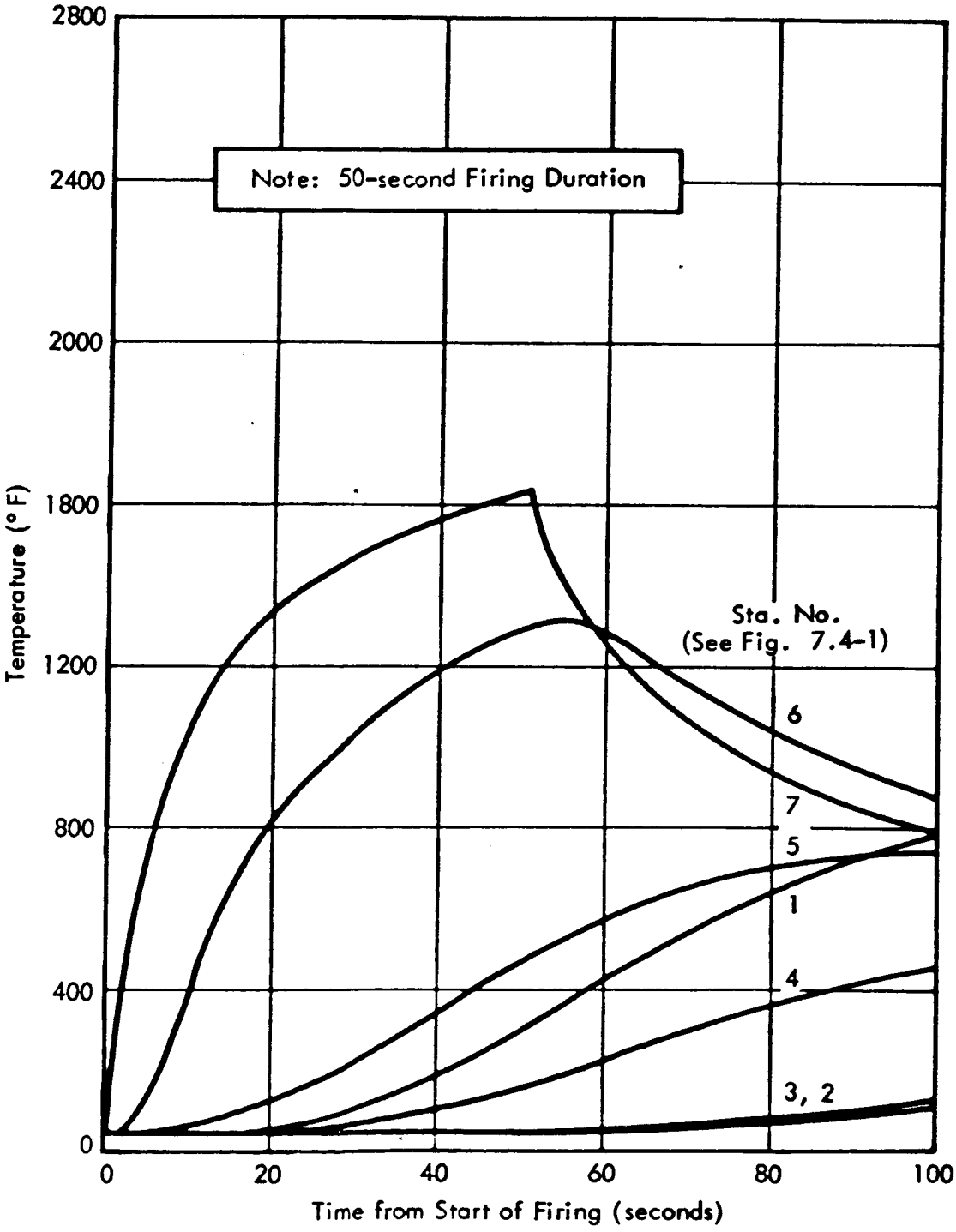

Figure 7.4-2. Predicted Surface Temperatures of Combustion Chamber Shell

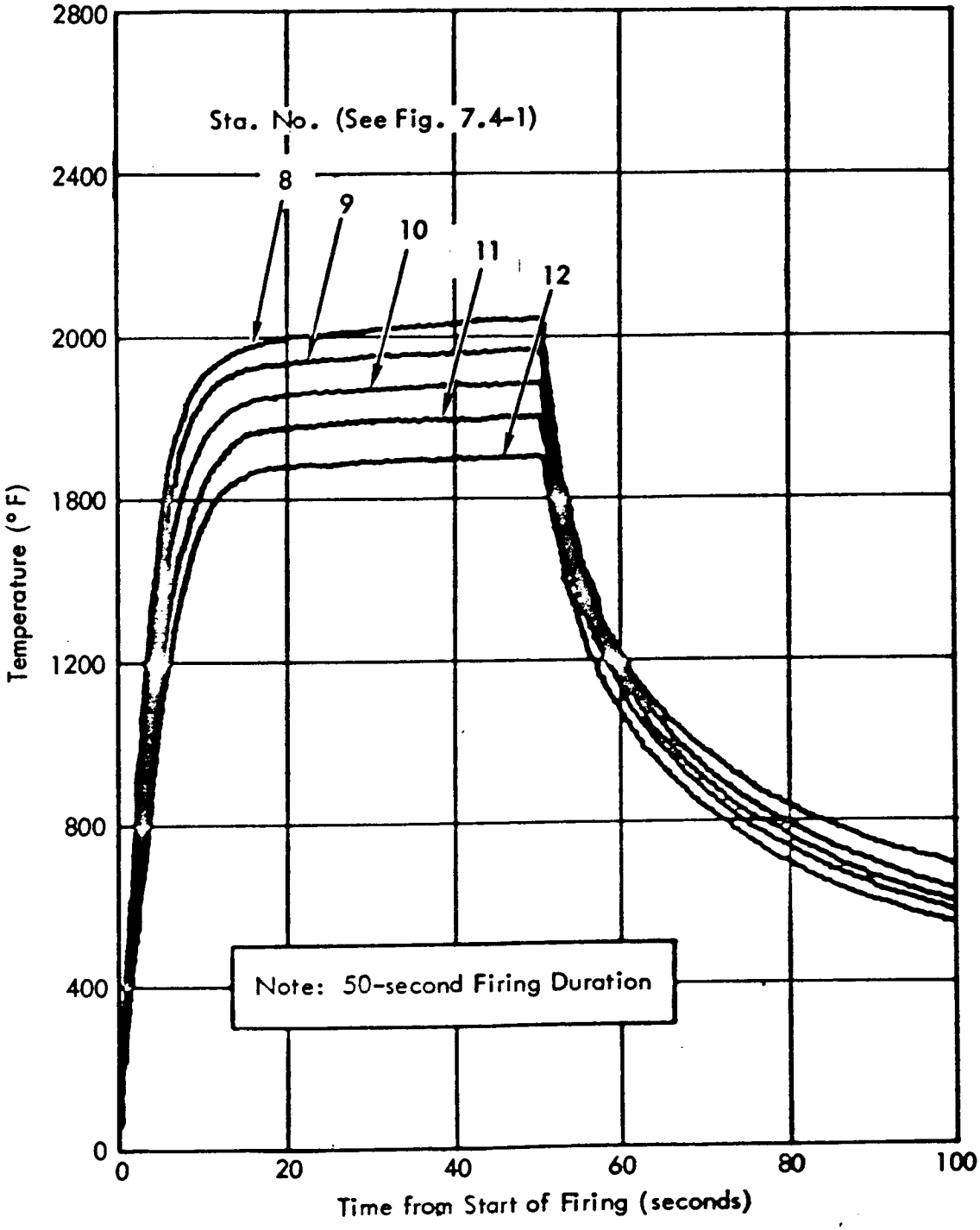

Figure 7.4-3. Predicted Surface Temperatures of Nozzle Extension

Figure 7.4-4. Predicted Surface Temperatures of Surveyor Combustion Chamber Shell (50-second Firing with 1750-second Cooldown Period)

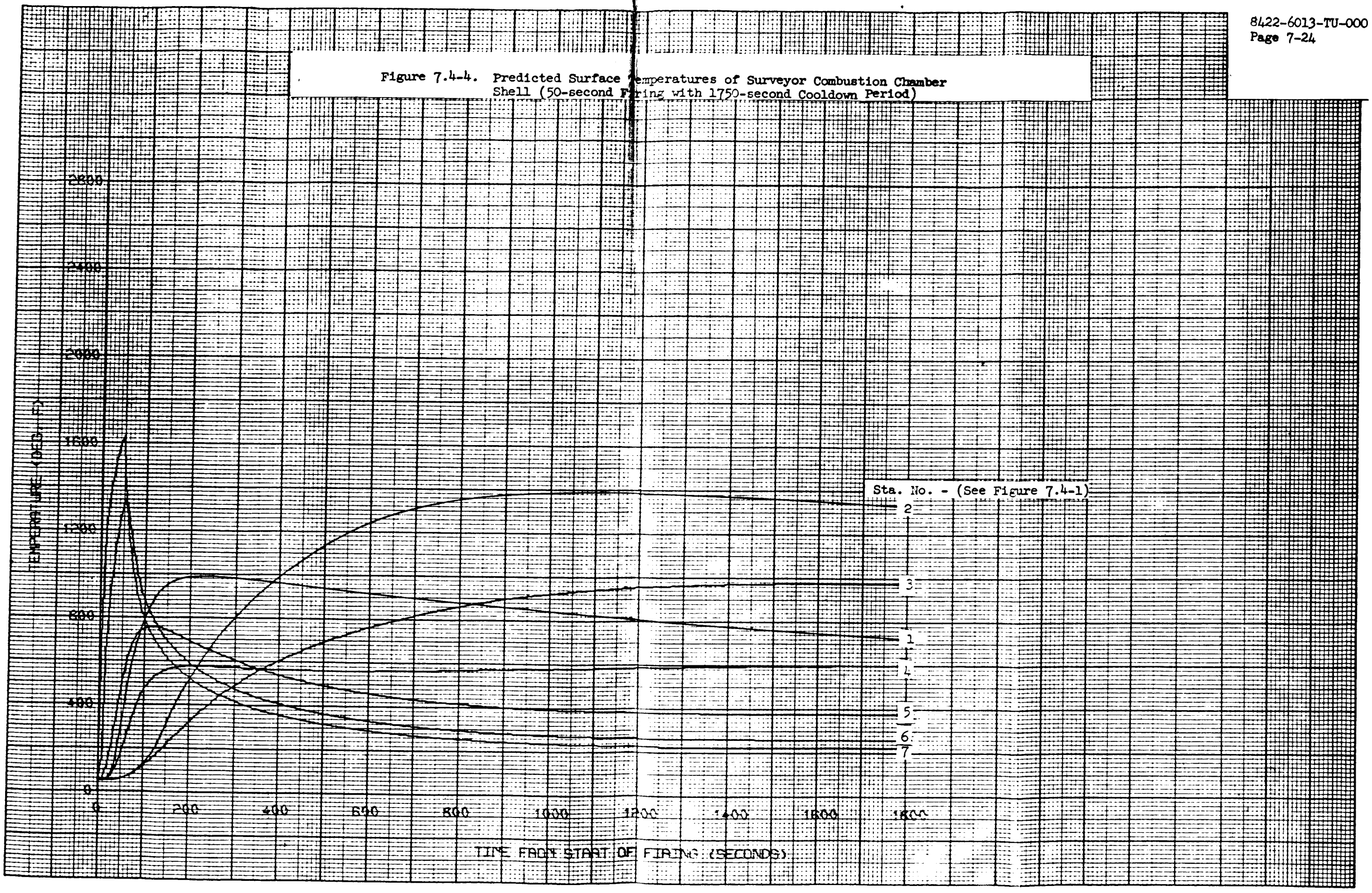

Figure 7.4-5. Predicted Surface Temperatures of Surveyor Nozzle Extension (50-second Firing with 1750-second Cooldown Period)

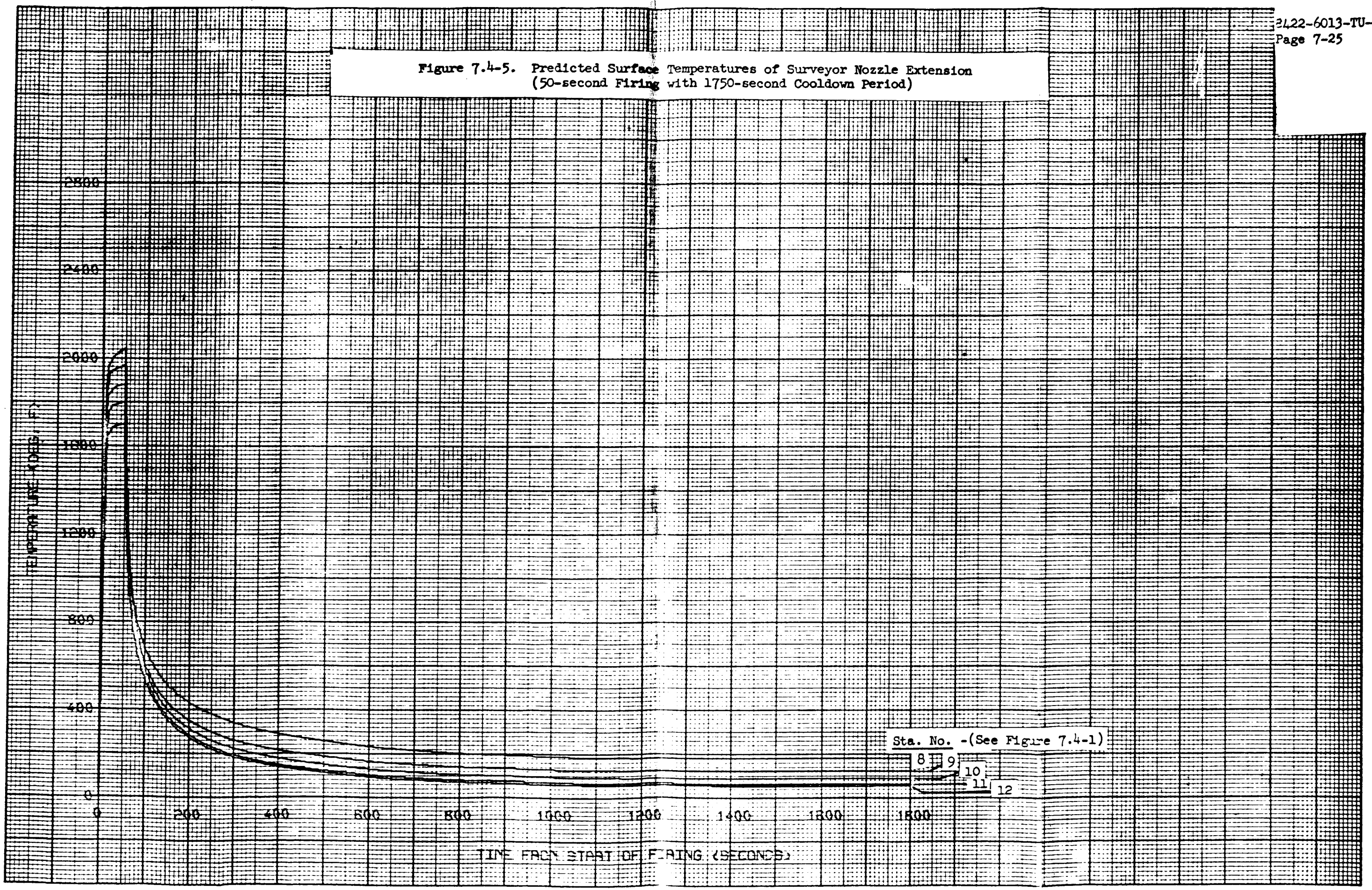

Figure 7.4-6. Predicted Temperature History of Surveyor Titanium Shell Thrust-Time Profile PQ-1A

Curve No.	Area Ratio
1	15.7
2	20.1
3	24.3
4	28.4
5	31.7

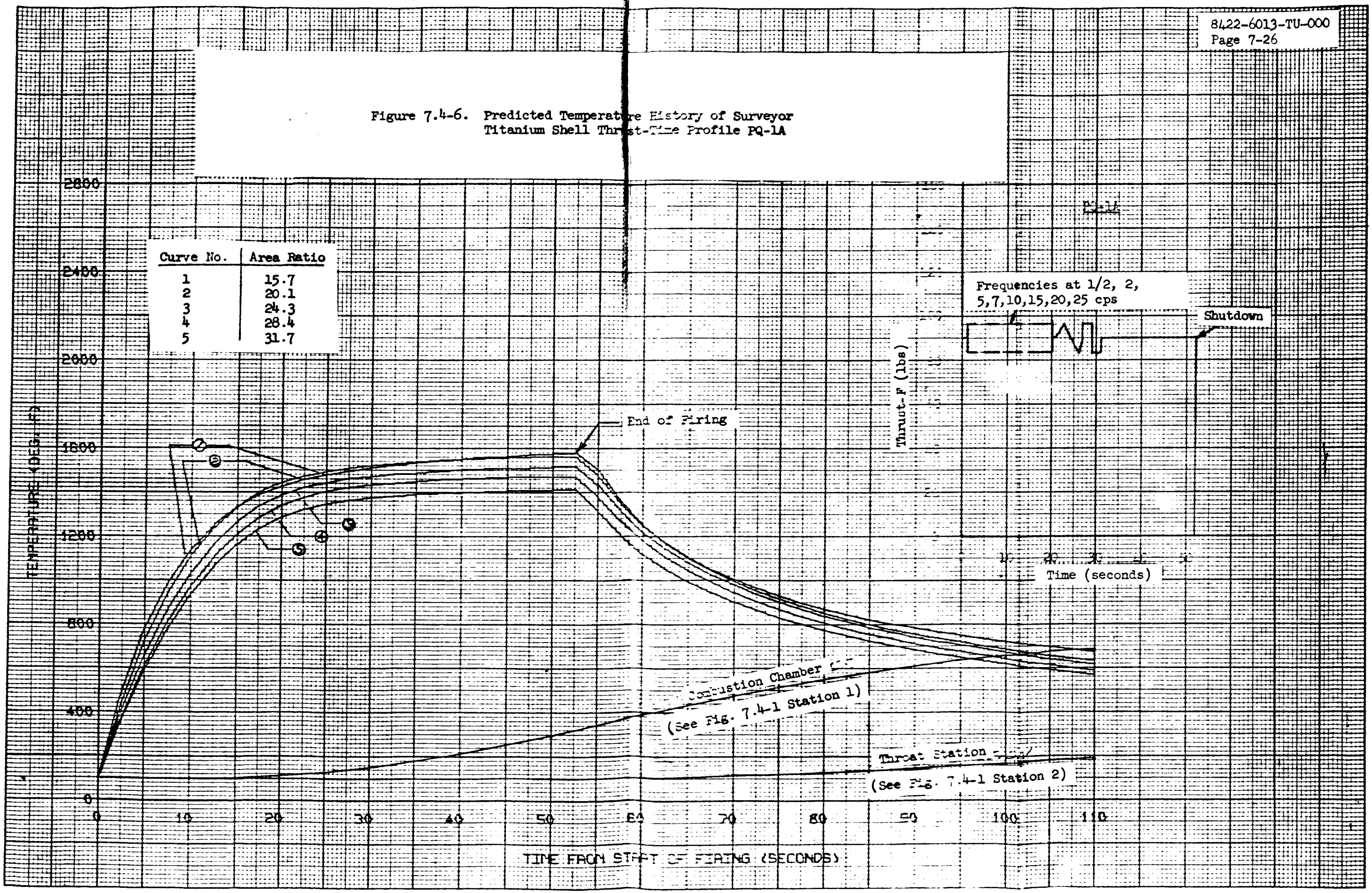

Figure 7.4-7. Predicted Surface Temperatures of Surveyor Titanium Shell Thrust-Time Profile PQ-1B

Curve No.	Area Ratio
1	15.7
2	20.1
3	24.3
4	28.4
5	31.7

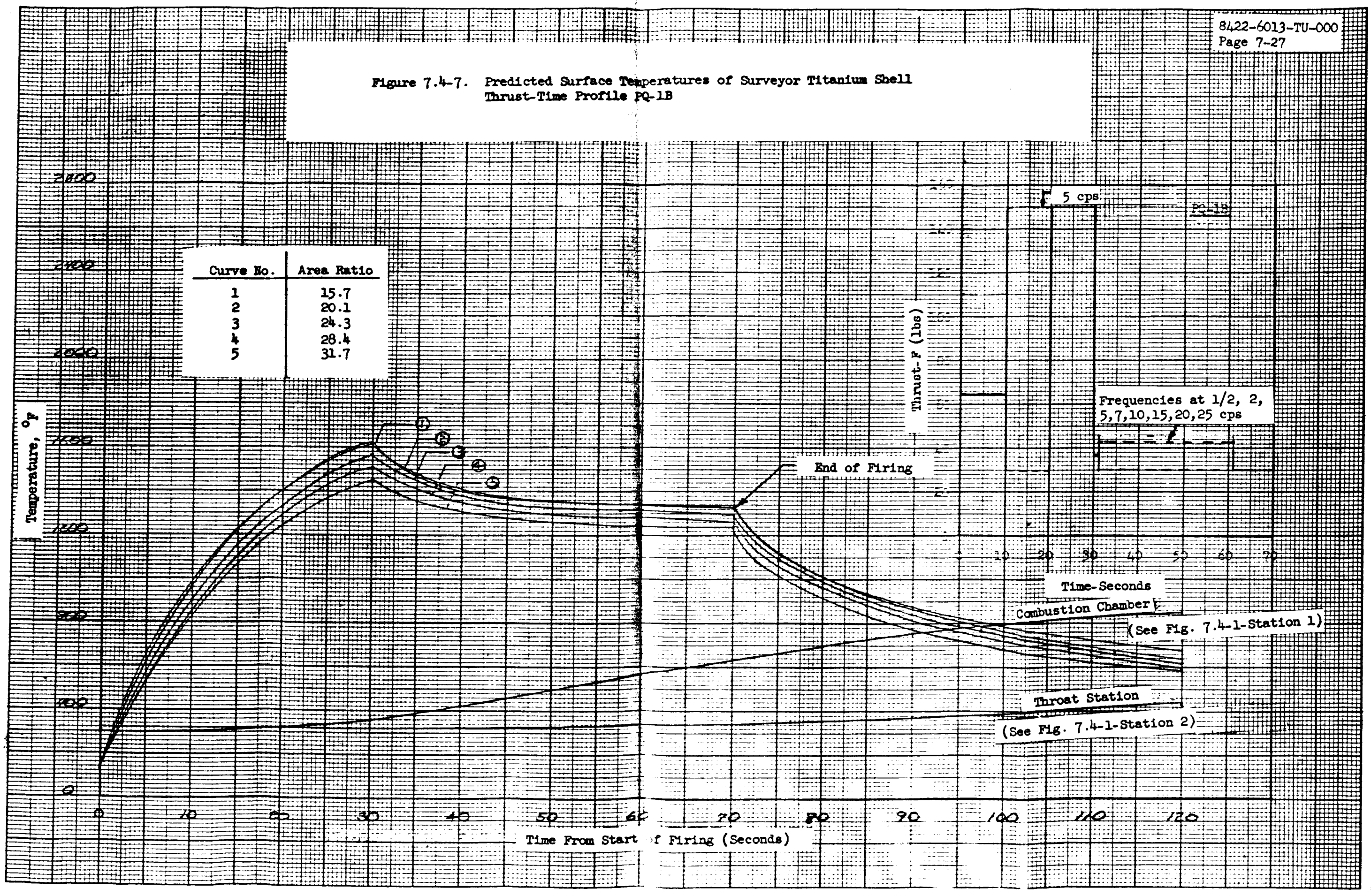

Figure 7.4-8. Predicted Surface Temperatures of Surveyor Titanium Shell
First 40 Seconds of Thrust-Time Profile PQ-1C

Curve No.	Area Ratio
1	15.7
2	20.1
3	24.3
4	28.4
5	31.7

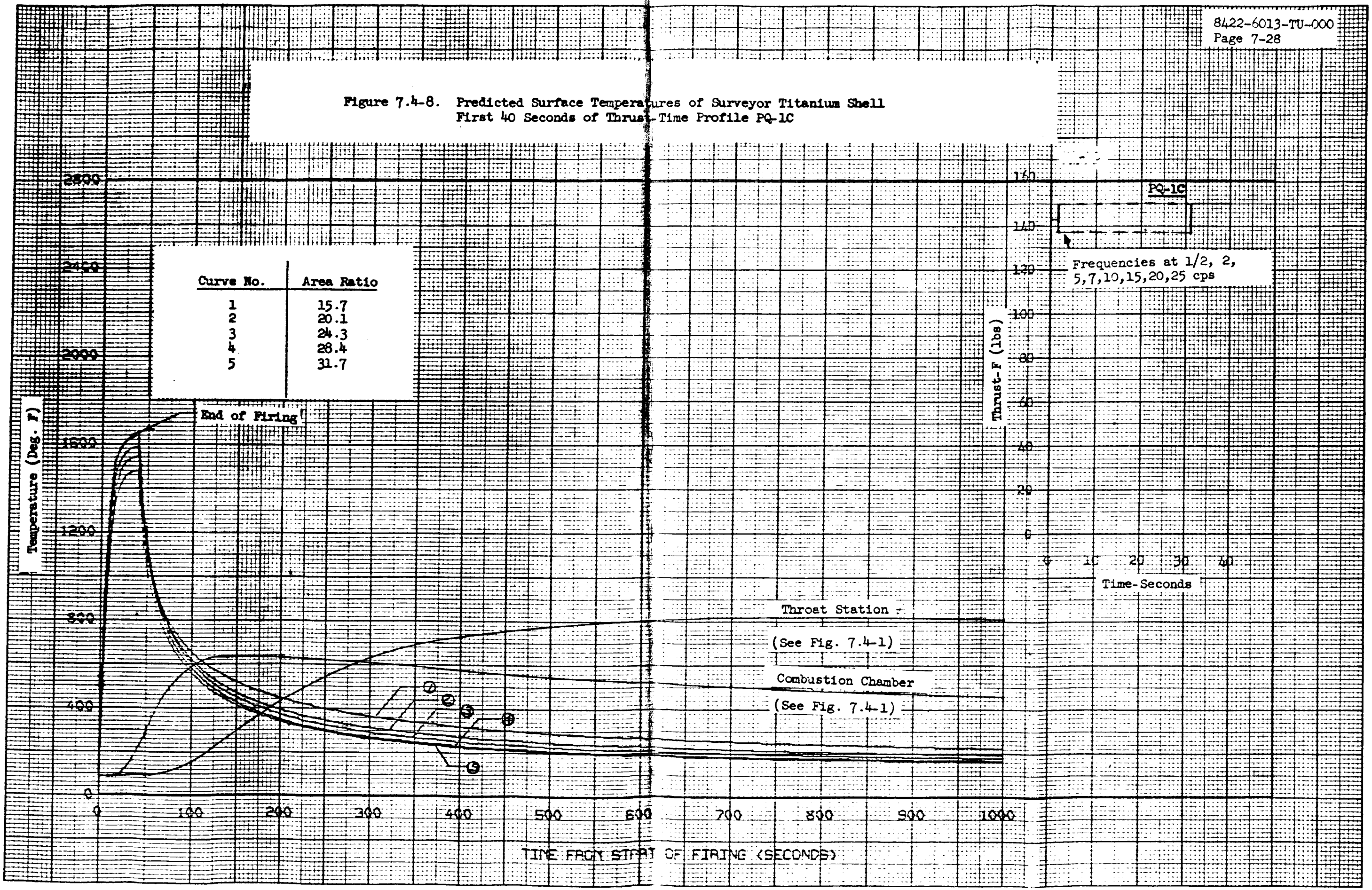

Figure 7.4-9. Predicted Surface Temperatures of Surveyor Titanium Shell Thrust-Time Profile PQ-1B

Curve No.	Area Ratio
1	15.7
2	20.1
3	24.3
4	28.4
5	31.7

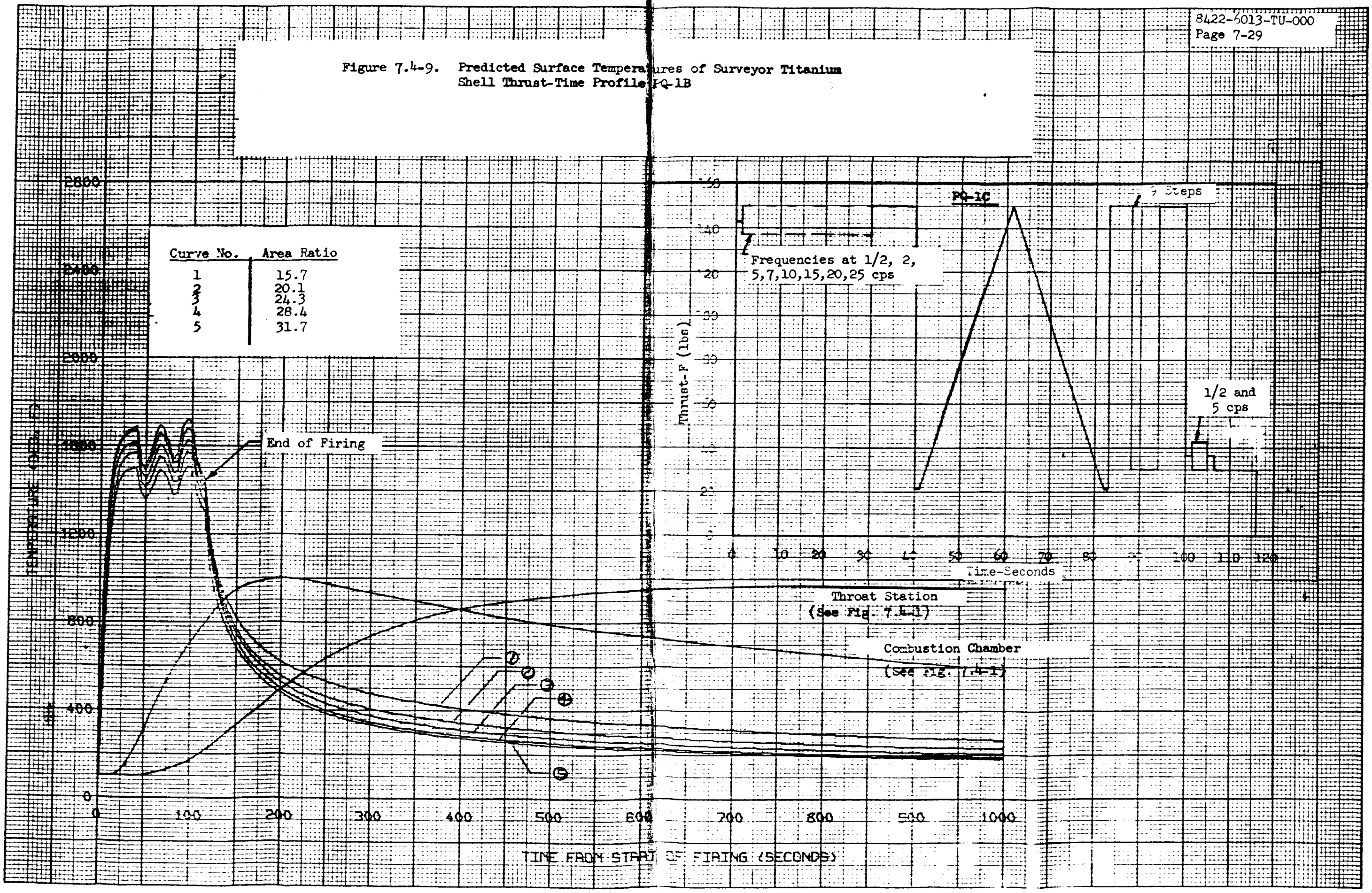

Figure 7.4-10. Predicted Surface Temperatures of Surveyor Titanium Shell Thrust-Time Profile PQ-1B

Curve No.	Area Ratio
1	15.7
2	20.1
3	24.3
4	28.4
5	31.7

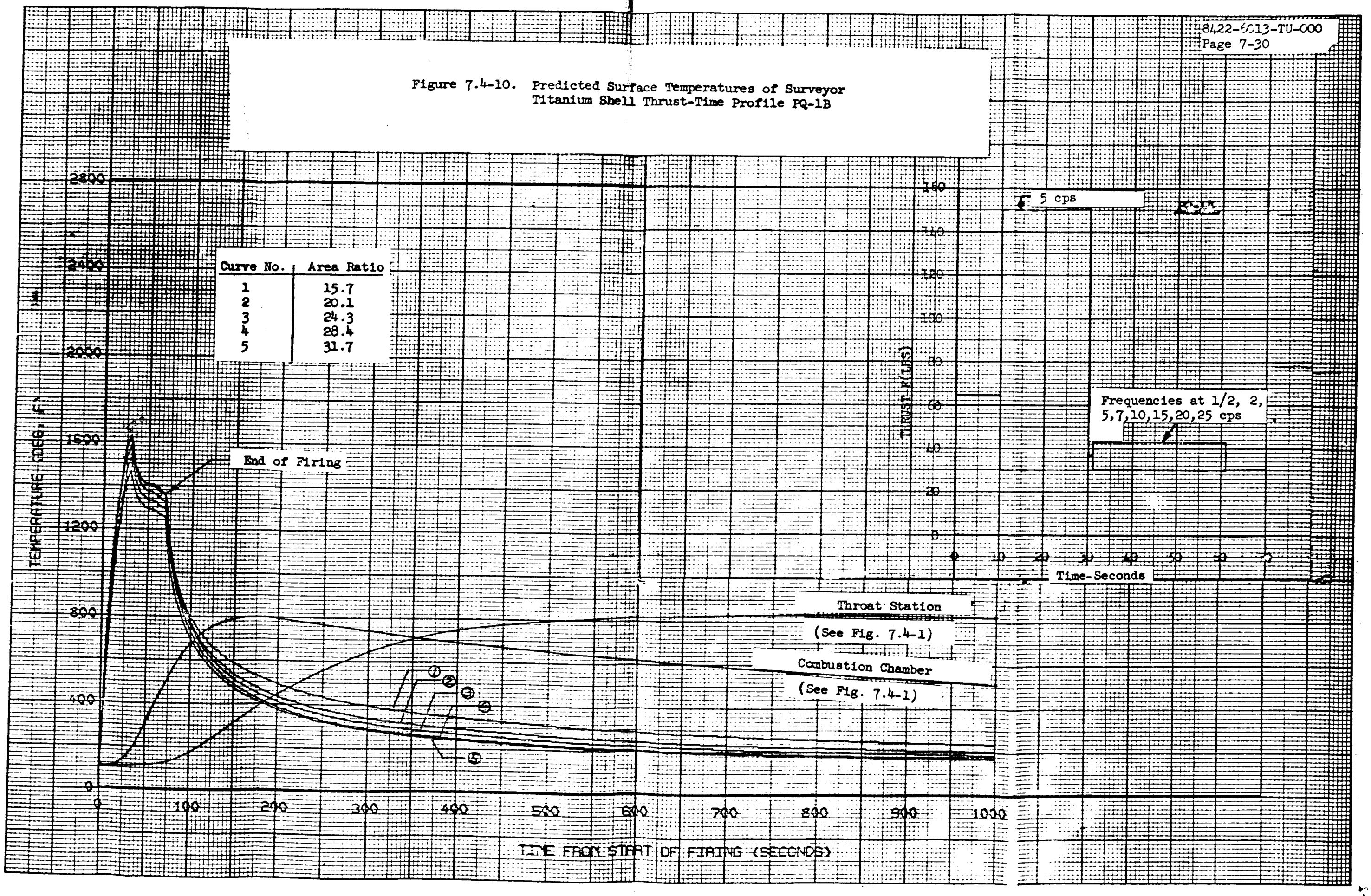

7.5 Theory of Venturi Discharge Coefficients

In the Rivas and Shapiro paper, "On the Theory of Discharge Coefficients for Rounded-Entrance Flowmeters and Venturis," a theory is presented for the prediction of discharge coefficients based on potential flow profile, friction, and boundary layer buildup in a converging nozzle. The theory is shown to correlate much of the available experimental data for rounded entry flowmeters (flowmeters with no Vena Contracta). Basically, the theory shows that two factors affect the discharge coefficient in the viscous flow regime —— the momentum boundary layer thickness and friction.

In order to evaluate the discharge coefficient, it is necessary to determine whether the flow in the throat of the venturi is laminar or turbulent. As the pressure gradient in the entrance section of the venturi becomes smaller, the boundary layer in the venturi should remain laminar for a longitudinal length equal to a length Reynolds number (Rey_L)* of 2×10^5. With careful contouring it is possible to maintain laminar flow up to values of Rey_L of 4×10^6. For the range of temperatures, flow areas, and fluids specified for the MIRA 150A Rey_L ranges from 10^5 to 10^6. Thus, flow through the venturi will be laminar through most of the flow range encountered in MIRA 150A testing.

Rivas and Shapiro show that the discharge coefficent of a venturi in the laminar region can be expressed in terms of a "mean apparent friction factor, f_{app}, and an equivalent length, L_{eq}. The mean apparent friction factor over a length, L, includes the effect of changes in momentum flux, as well as wall friction, on the pressure drop. The equivalent length is defined as the equivalent length of the actual cylindrical section (constant area) resulting in the same boundary layer growth as the contracting section (refer to Figure 7.5-1).

The discharge coefficient, C_D, is determined from the following formula:

$$C_D = \sqrt{\frac{1}{1 + 4 f_{app} \frac{L_{eq}}{D}}} \qquad (1)$$

Where: $D = (D_o - D_i)$ for an anmulus.

Rough approximations of the detailed potential flow and boundary layer solution indicate that the value of L_{eq}/D for the two TCA flow control valve venturis are between 1.0 and 2.0 at maximum thrust and 6.0 to 10.0 at minimum thrust. The uncertainty in the value of L_{eq}/D is caused by two factors:

1. The very simple boundary layer solution used. Detailed numerical integration and reiteration are required to improve the accuracy of the solutions according to Rivas and Shapiro.

2. The allowable tolerances on the length of the cylindrical section.

The value of f_{app} in the range of interest here has been both experimental and theoretically determined to be:

* $Rey_L = \frac{\rho V L}{\mu} = \frac{\dot{M} L}{\mu A} = Rey_D \frac{L}{D}$

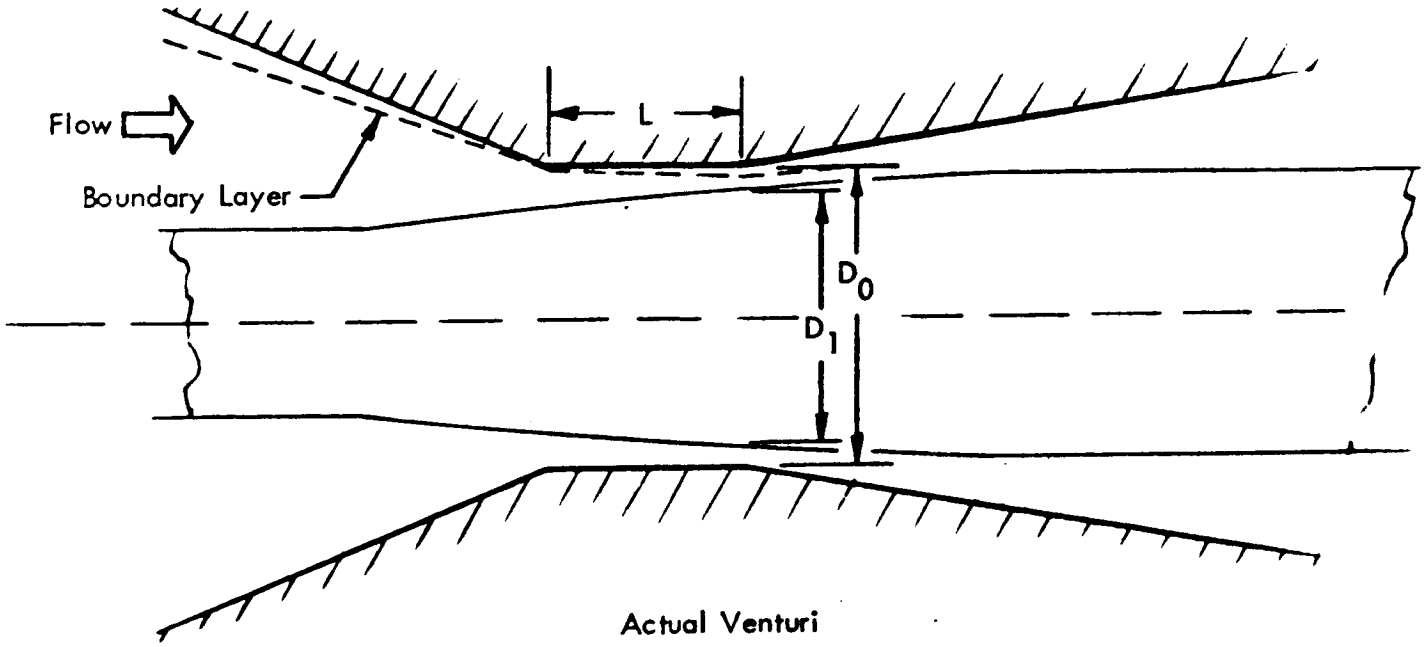

Actual Venturi

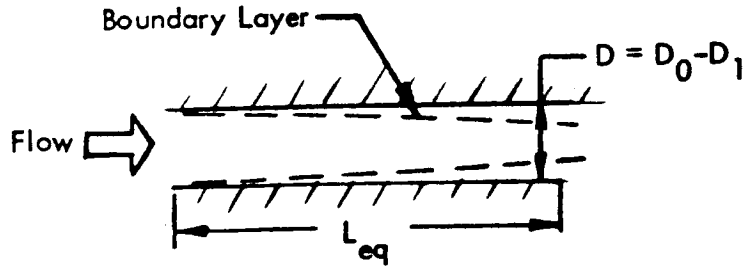

Equivalent Venturi

Figure 7.5-1. Boundary Layer in Actual and Equivalent Venturi

$$4f_{app}\ \frac{L_{eq}}{D} = 13.74\sqrt{\frac{(L_{eq}/D)}{Rey_D}} \qquad (2)$$

Combining equations (1) and (2), results in the following equation for C_D:

$$C_D = \sqrt{\frac{1}{1 + 13.74\sqrt{\frac{L_{eq}/D}{Rey_D}}}} \qquad (3)$$

Where: $Rey_D = \frac{D\dot{M}}{\mu A}$

and μ = Viscosity

Curves from the literature showing the venturi discharge coefficient as a function of L/D and Rey_D are shown in Figure 7.5-2. In Figure 7.5-3, the discharge coefficients for the two propellants, based on this theory, are shown both as a function of servo-actuator signal (i.e., equivalent position) and propellant temperature. The discharge coefficients are shown as a band rather than lines, because of the uncertainty of the value of L_{eq}/D. Although not incorporated in the standard data reduction program, equation (3) does express the discharge coefficient useable in the standard flowrate equation. No experimental evaluation of this relationship was attempted.

If equation (3) is combined with basic flow equation (1) and the definition of Reynolds number is inserted followed by normalizing to standard temperature and pressure, the standard flow rate equation results:

$$\dot{M}_{SV} = \dot{M}_{ST}\ C_{D_O}\sqrt{1 + \left(\frac{1 - C_{D_O}^2}{C_{D_O}^2}\right)\frac{\mu_T}{\mu_O}\frac{\dot{M}_{SV}}{\dot{M}_T}} \qquad (4)$$

Where: $\dot{M}_{SV}$ = Standard flowrate with varying C_D

$\dot{M}_{ST}$ = Standard flowrate with constant C_D

$\dot{M}_T$ = Flowrate at test conditions

C_{D_O} = Discharge coefficient at standard condition

μ_T = Absolute viscosity at test conditions

μ_O = Absolute viscosity at standard conditions.

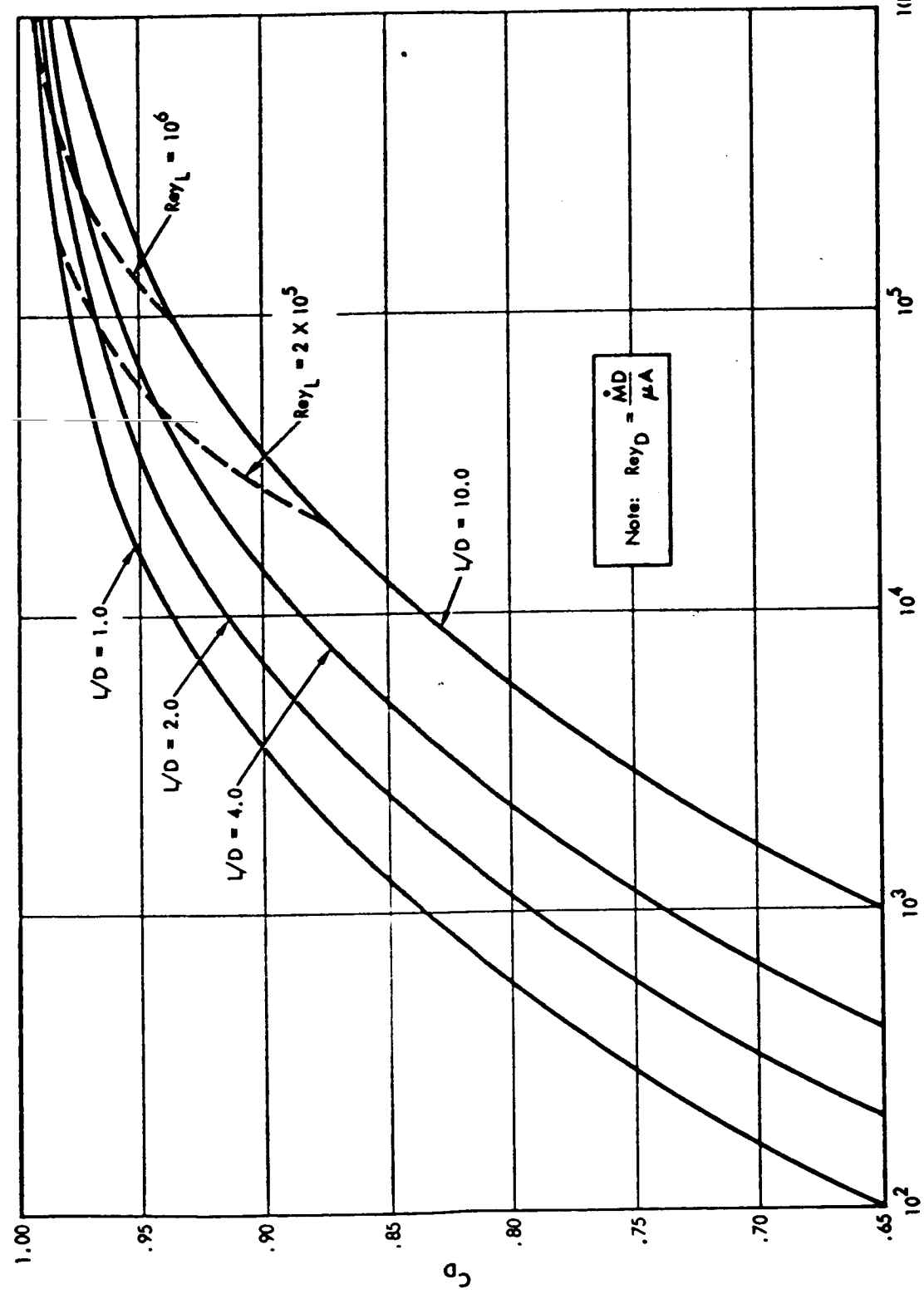

Figure 7.5-2. Discharge Coefficient Versus Diameter Reynolds Number - Rey_D

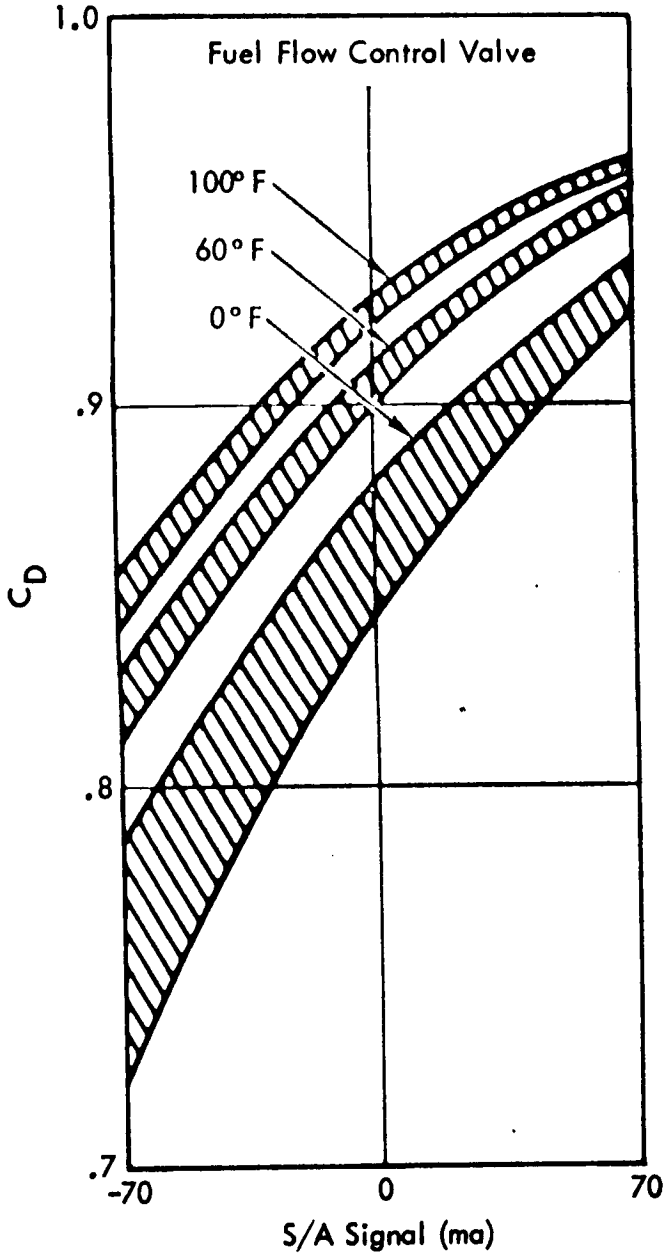

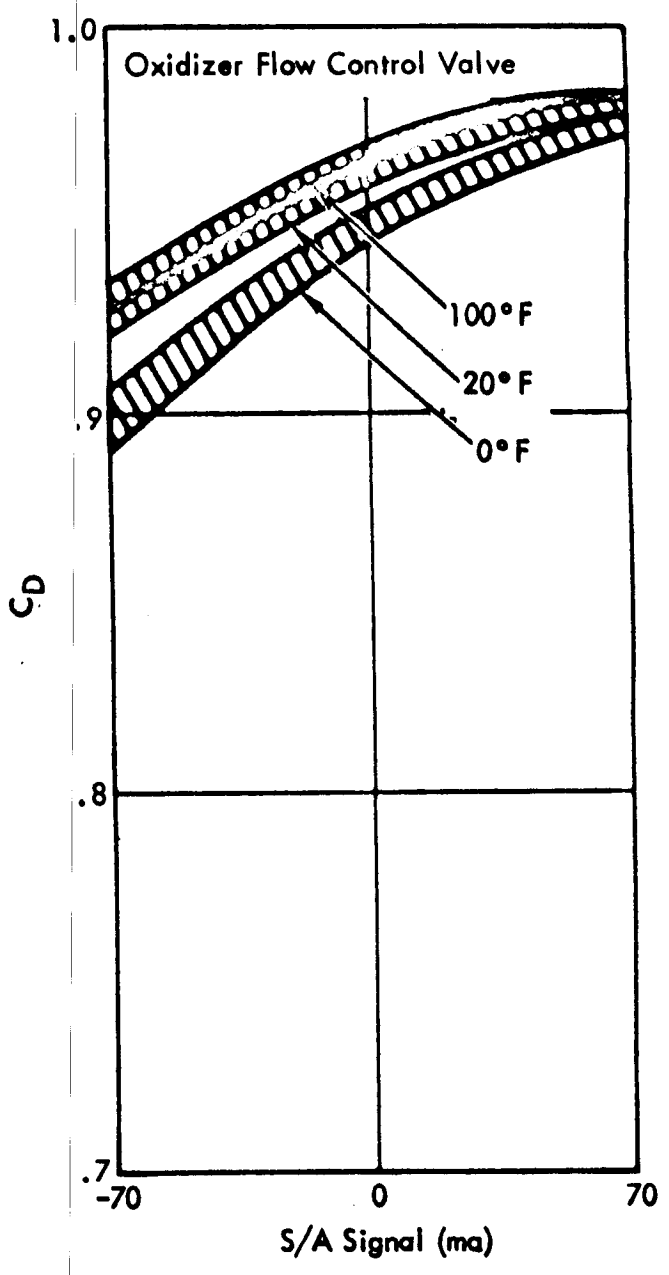

Figure 7.5-3. Discharge Coefficients for MIRA 150A Flow Control Valve

8.0 SPECIAL TEST EQUIPMENT

Eight items of Special Test Equipment were designed, constructed, and used during Phase III, with the exception that no actual engine firings were made on the Thrust Vector Deviation Measurement Stand. These eight items are discussed briefly below; more detailed data is provided in Appendix G.

8.1 Dynamic Tape Programmer

The Dynamic Tape Programmer, shown in Figure 8-1, includes a 14-channel FM tape transport and auxiliary equipment capable of providing prerecorded start-stop signals and a variable-thrust program input signal to the TCA for engine throttling tests. Response characteristics of the TCA may be simultaneously recorded on the same tape for computer printout and analysis.

8.2 Head End Assembly Calibration Stand

The Calibration Stand, shown in Figure 8-2, provides a servoactuator signal; high-pressure, distilled water and alcohol to simulate the propellants; and measuring equipment required for end-to-end calibration of flow rates versus servoactuator signal and for setting injector pressure drops and mixture ratio over the 5:1 throttling range.

8.3 Cleaning Set

The Cleaning Set, shown in Figure 8-3, consists of a console-mounted, dual evacuation system (for fuel and oxidizer) to remove residual propellants from the TCA. Each system includes a vacuum pump, LN_2 cooled condenser to trap propellants, and necessary valves and gages. In order to increase the rate of evacuation, an electric blanket capable of enclosing the TCA is part of the Cleaning Set.

8.4 Leak Check Console

The Leak Check Console, shown in Figure 8-4, contains pressure regulators, filters, gages, valves, a Freon 12 bottle and associated halogen leak detector "Leak-Tek" for gross leak indications, and an accurate pressure gage and thermometer for pressure-decay measurements.

8.5 Propellant Thermal Conditioning Units

The Propellant Thermal Conditioning Units, shown in Figures 8-5 and 8-6, are two identical, pallet-mounted, transportable units capable of maintaining oxidizer and fuel at any temperature from 0° to 100°F. Propellants are cooled or heated by heat exchangers immersed in the propellant tanks. The heating fluid is water, heated by electrical heaters. The cooling fluid is liquid nitrogen. Pumps are used to circulate propellants through insulated feed lines immediately prior to engine firings.

8.6 Thermal Conditioning Equipment

The TCA Thermal Conditioning Equipment provides prefiring TCA temperatures from 0° to 125°F as measured by thermocouples on the TCA. This is accomplished by directing cold nitrogen gas into a vented shroud enclosing the TCA for below ambient temperatures (shown in Figure 8-7) and by the use of three variable-current heat lamps for heating. The equipment can be used for both sea level and altitude chamber firings.

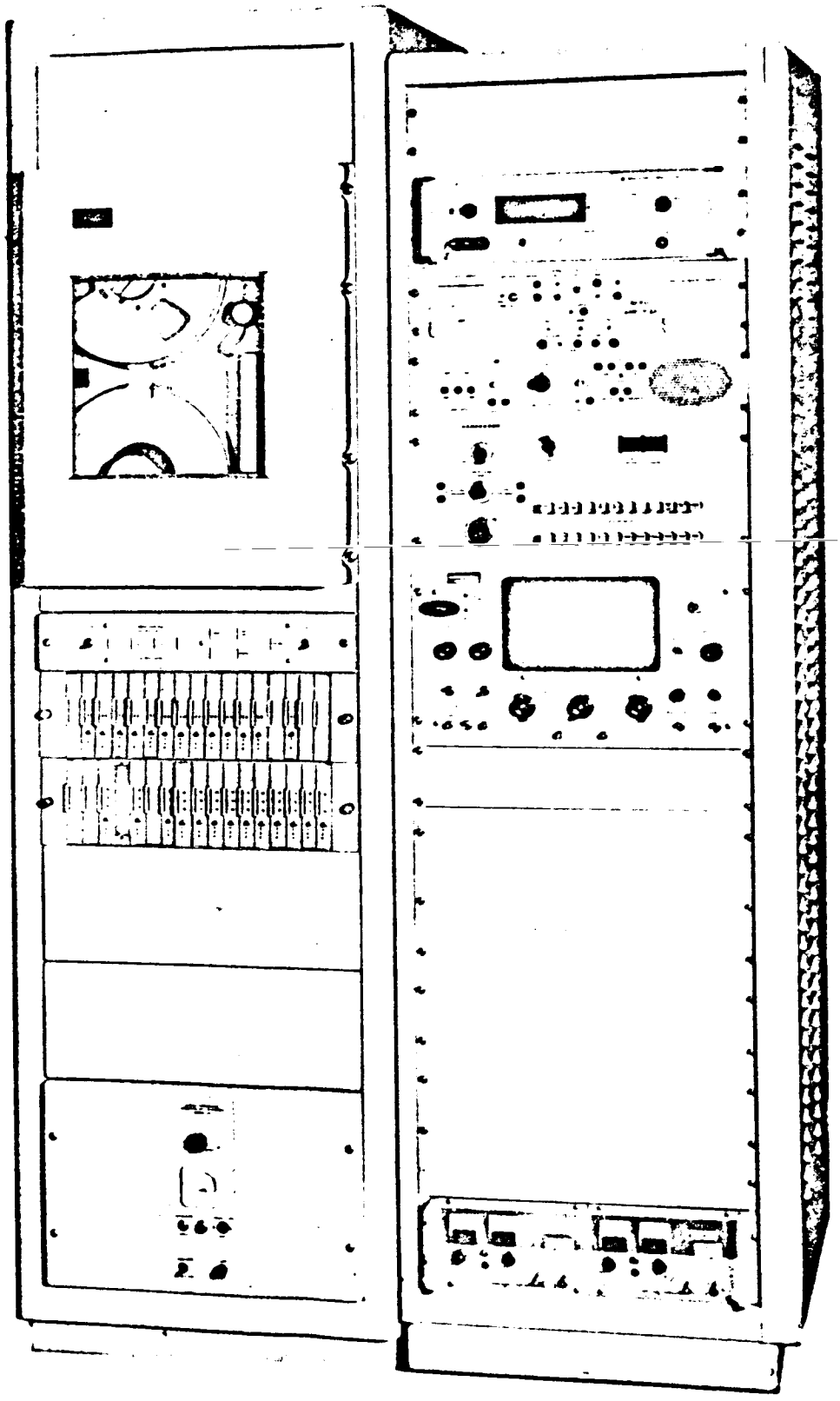

Figure 8-1. Dynamic Tape Programmer

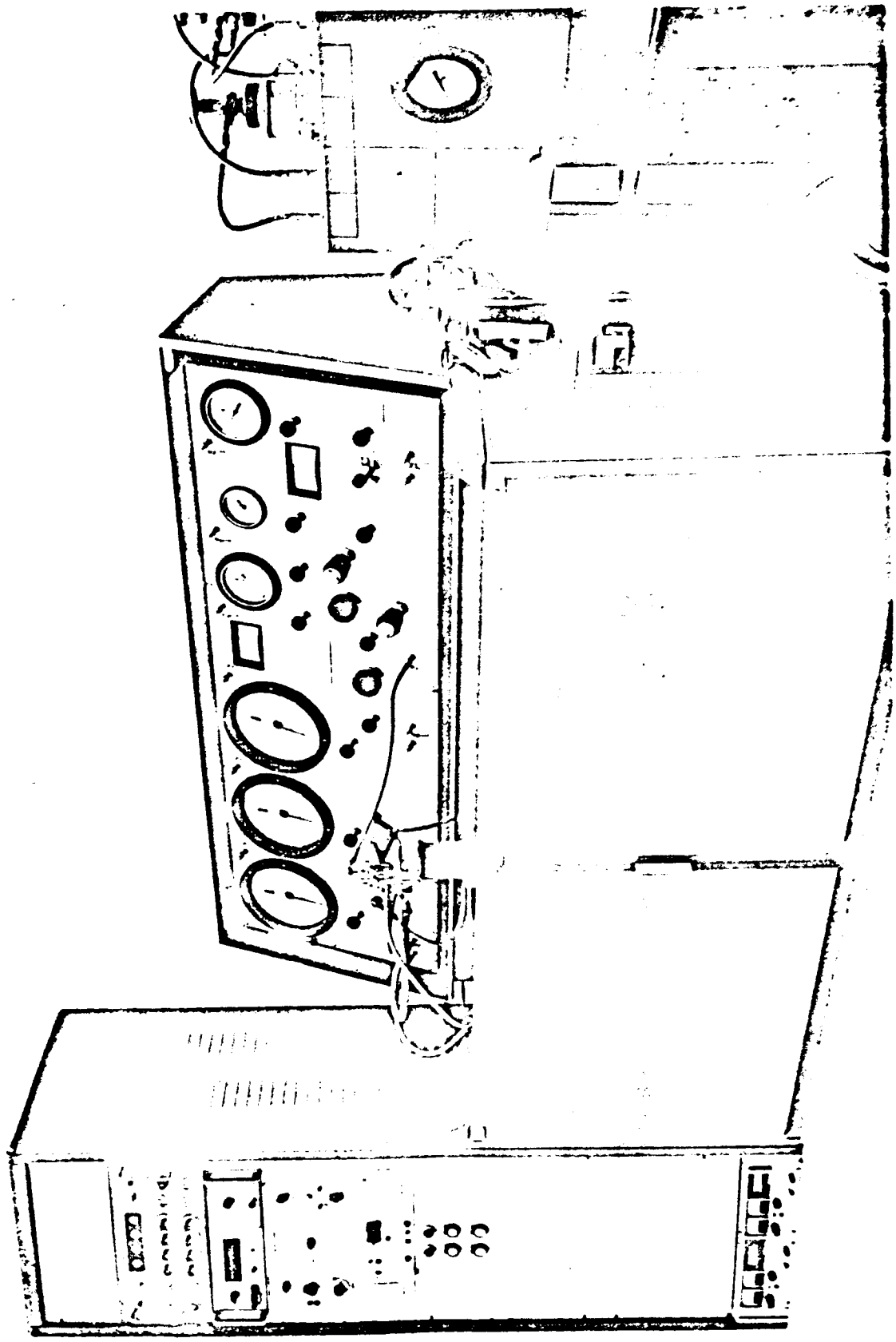

Figure 8-2. HEA Calibration Stand

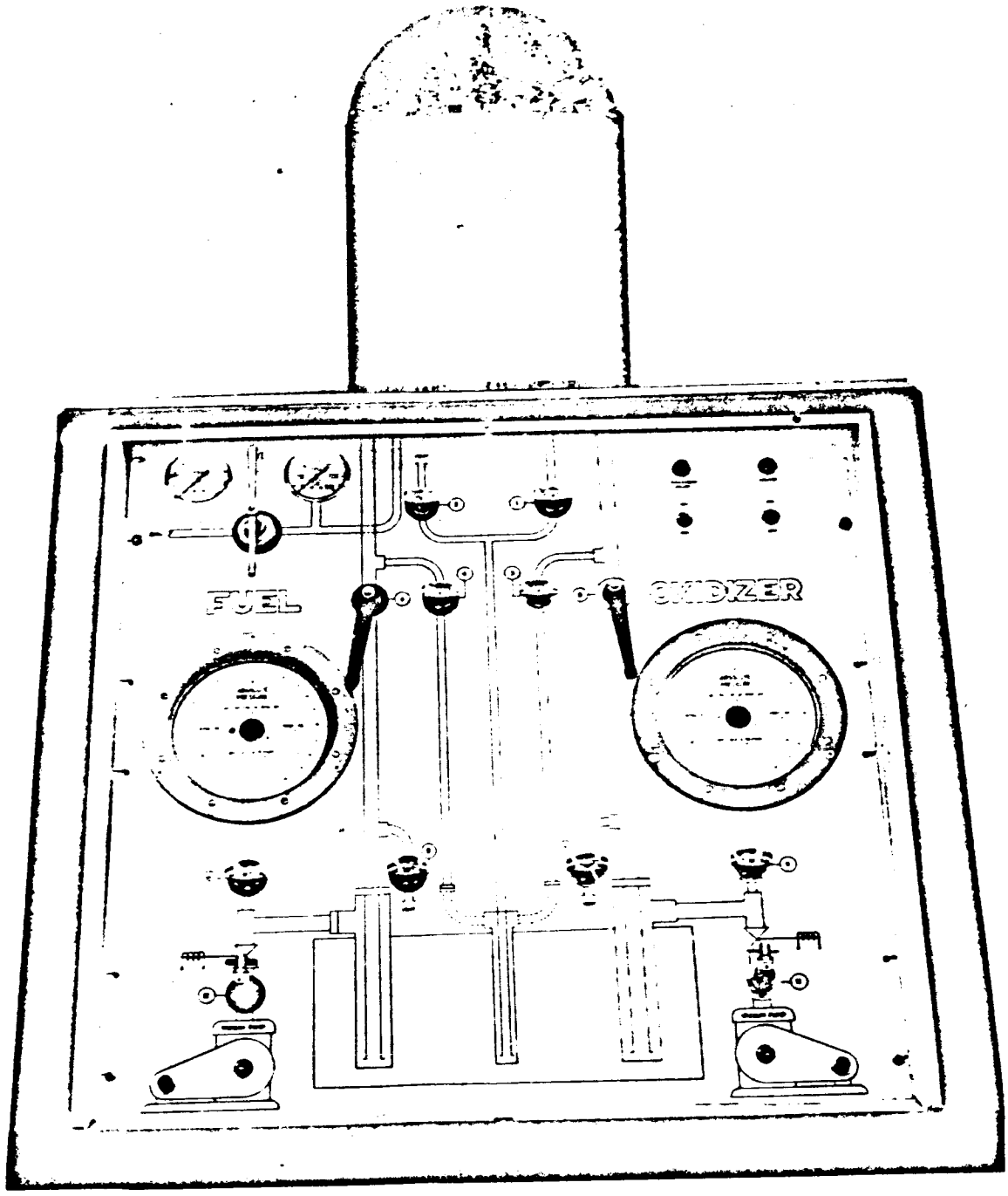

Figure 8-3. Cleaning Set

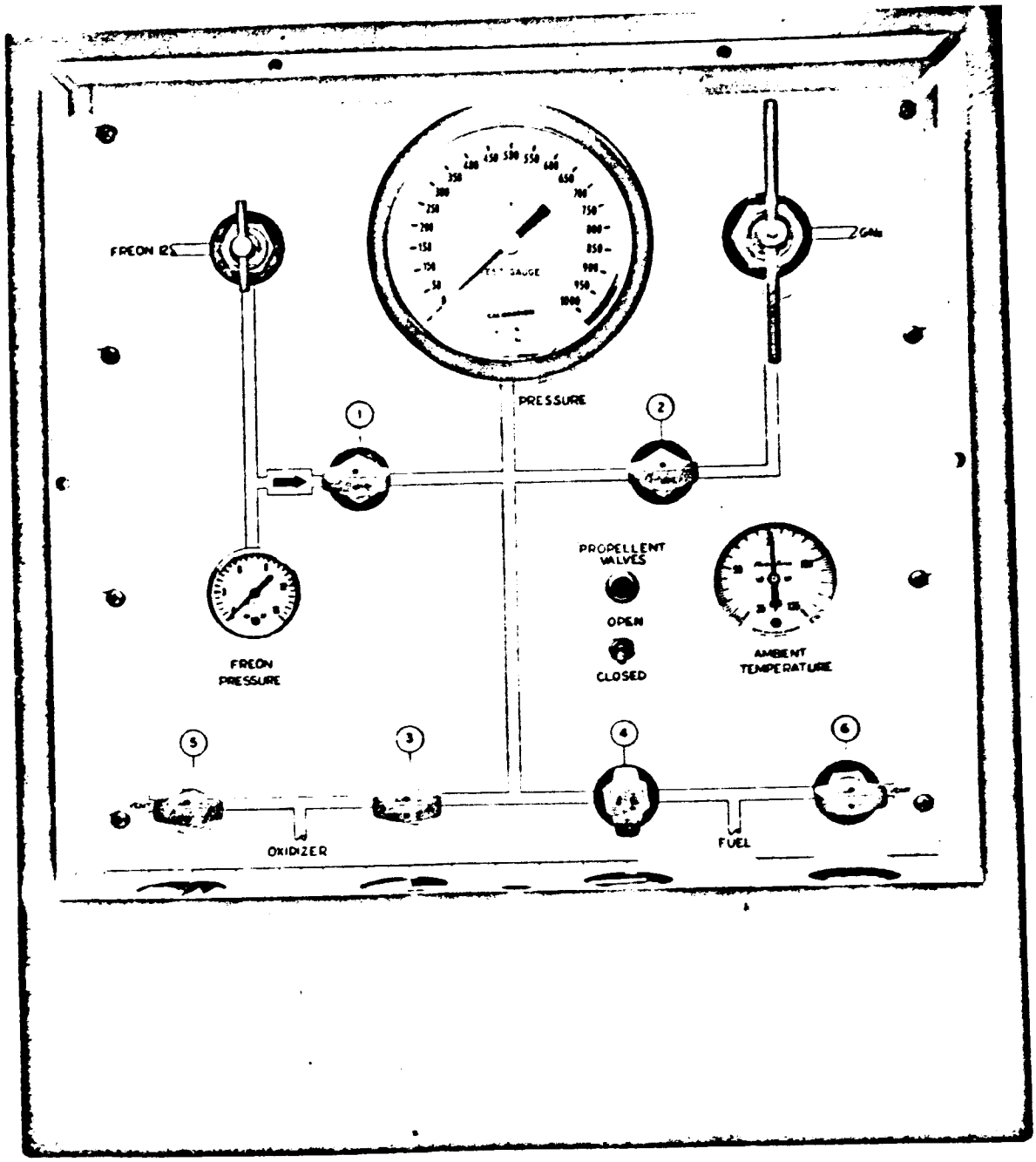

Figure 8-4. Leak Check Console

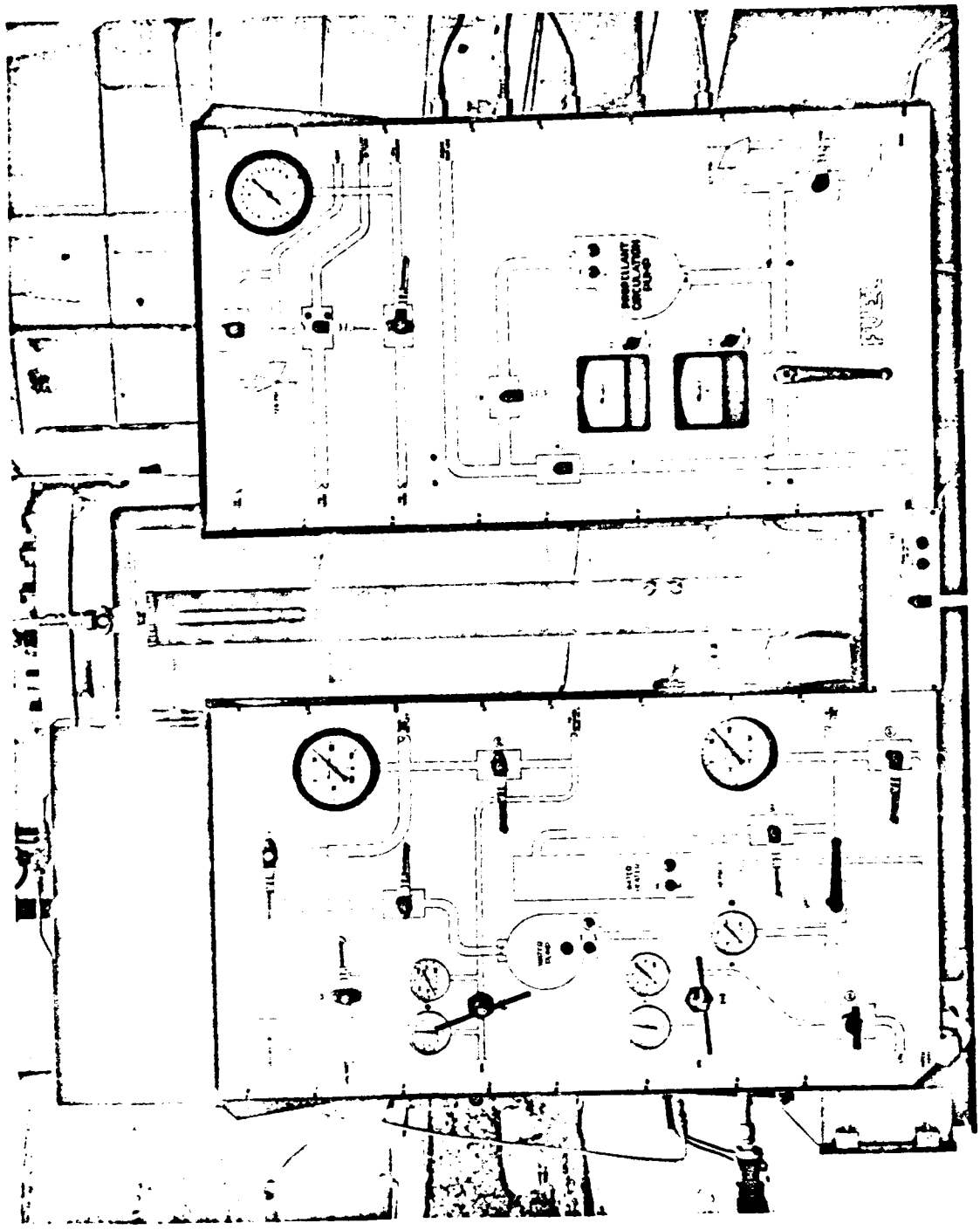

Figure 8-5. Fuel Thermal Conditioning Units - Front

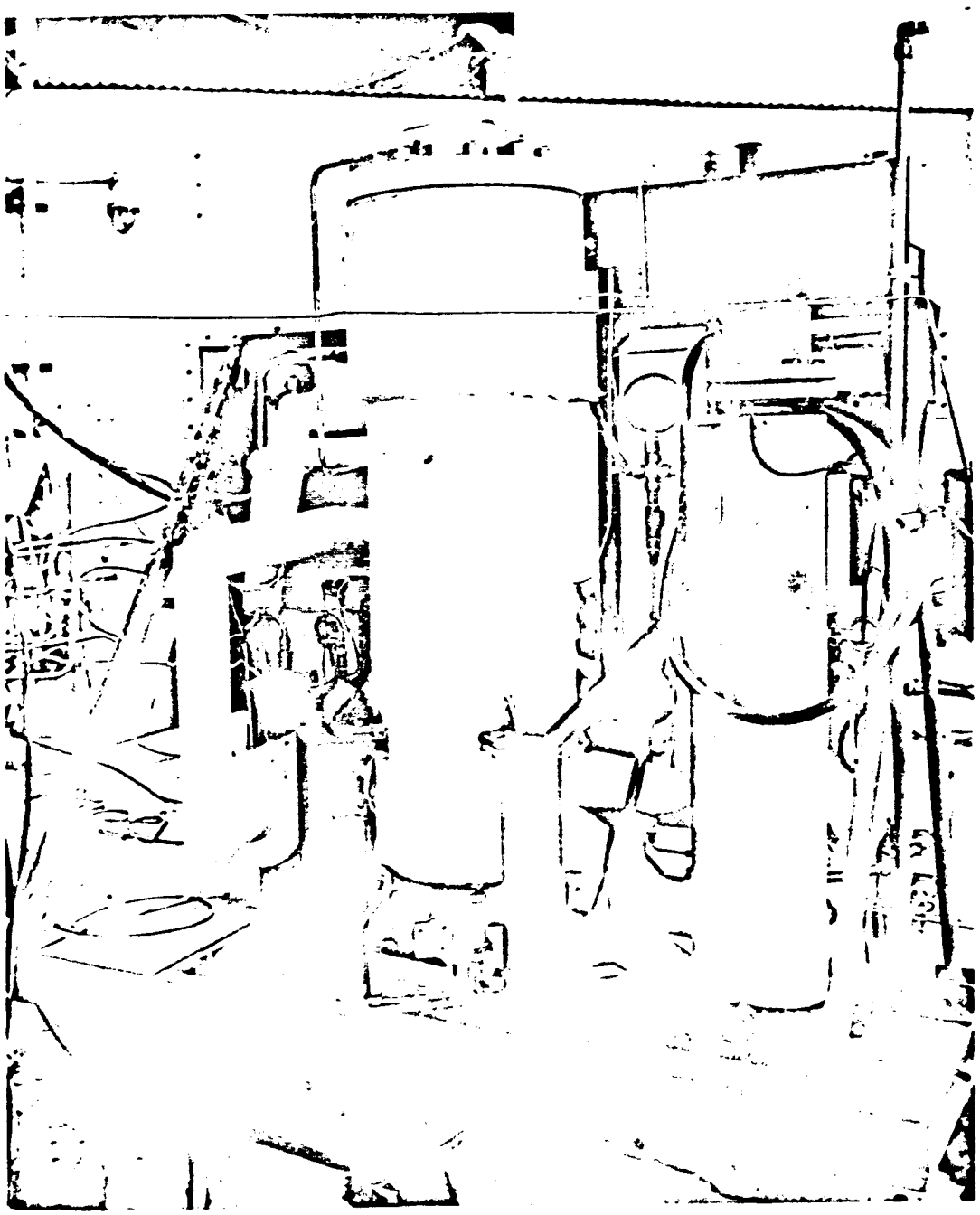

Figure 8-6. Fuel Thermal Conditioning Unit - Back Side

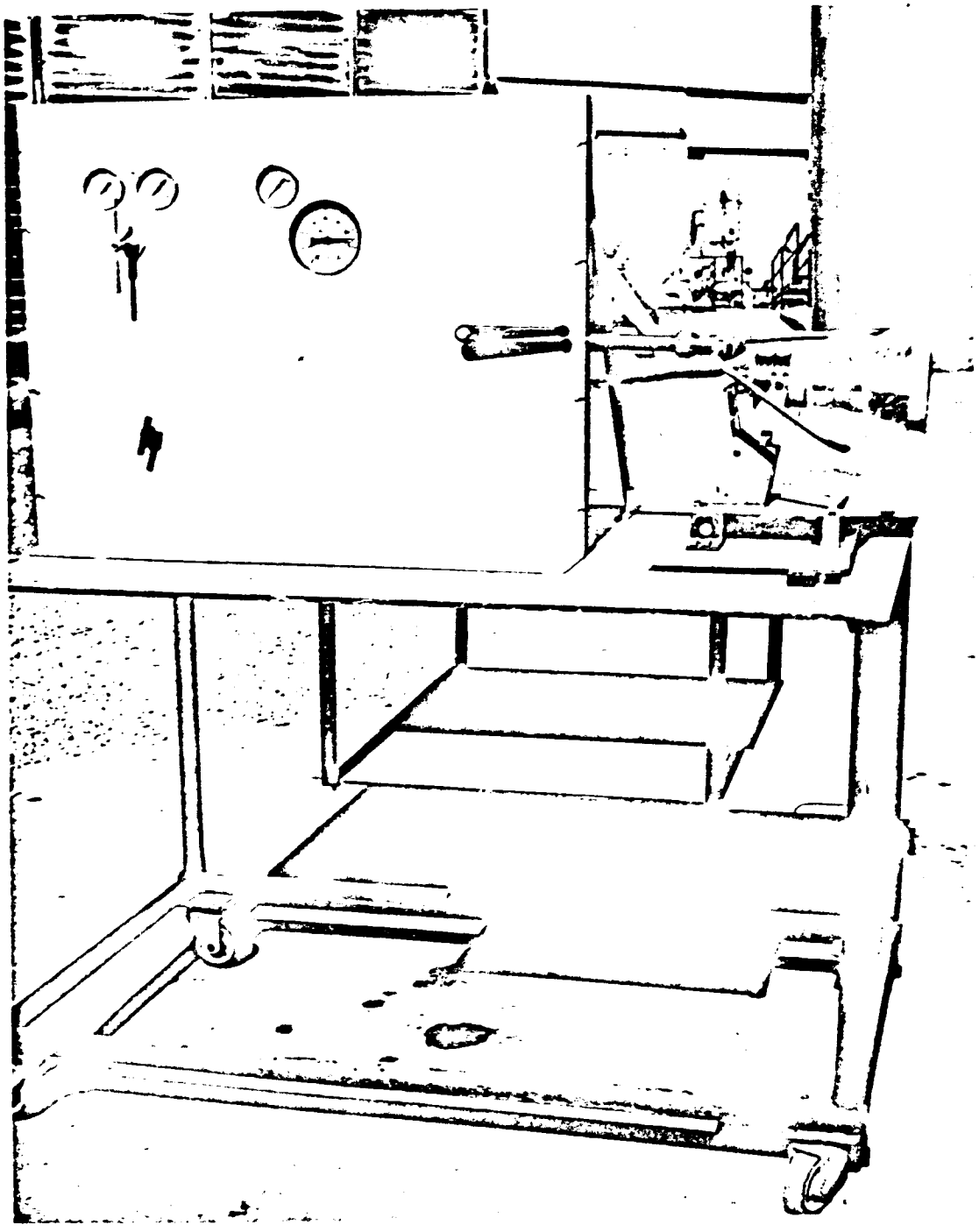

Figure 8-7. TCA Thermal Conditioning Equipment

8.7 Centrifuge

The Centrifuge, shown in Figures 8-8, -9, and -10, was installed at the STL Capistrano Test Site. The Centrifuge was used to determine TCA performance changes when the TCA was subjected to g forces simulating Surveyor main retro engine firing. The Centrifuge is powered by a variable speed electric drive motor and includes accommodations for mounting the TCA, counterweights, propellant and pressurization tanks and lines, flowmeters, and transducers. Shielded slip rings transmit command and instrumentation signals between the rotating stand and the Centrifuge control center.

8.8 Thrust Vector Deviation Measurement Stand

The Thrust Vector Deviation Measurement Stand, shown in Figure 8-11, is a gimbal-mounted, counter-balanced beam (with mounting provisions for the TCA) which rotates about the gimbal center when subjected to any side load component of thrust. Thrust vector deviation while firing is derived by measuring angular displacement of the beam using position potentiometers in two planes perpendicular to the thrust axis. Calibration of the pressurized stand correlates displacement with side forces.

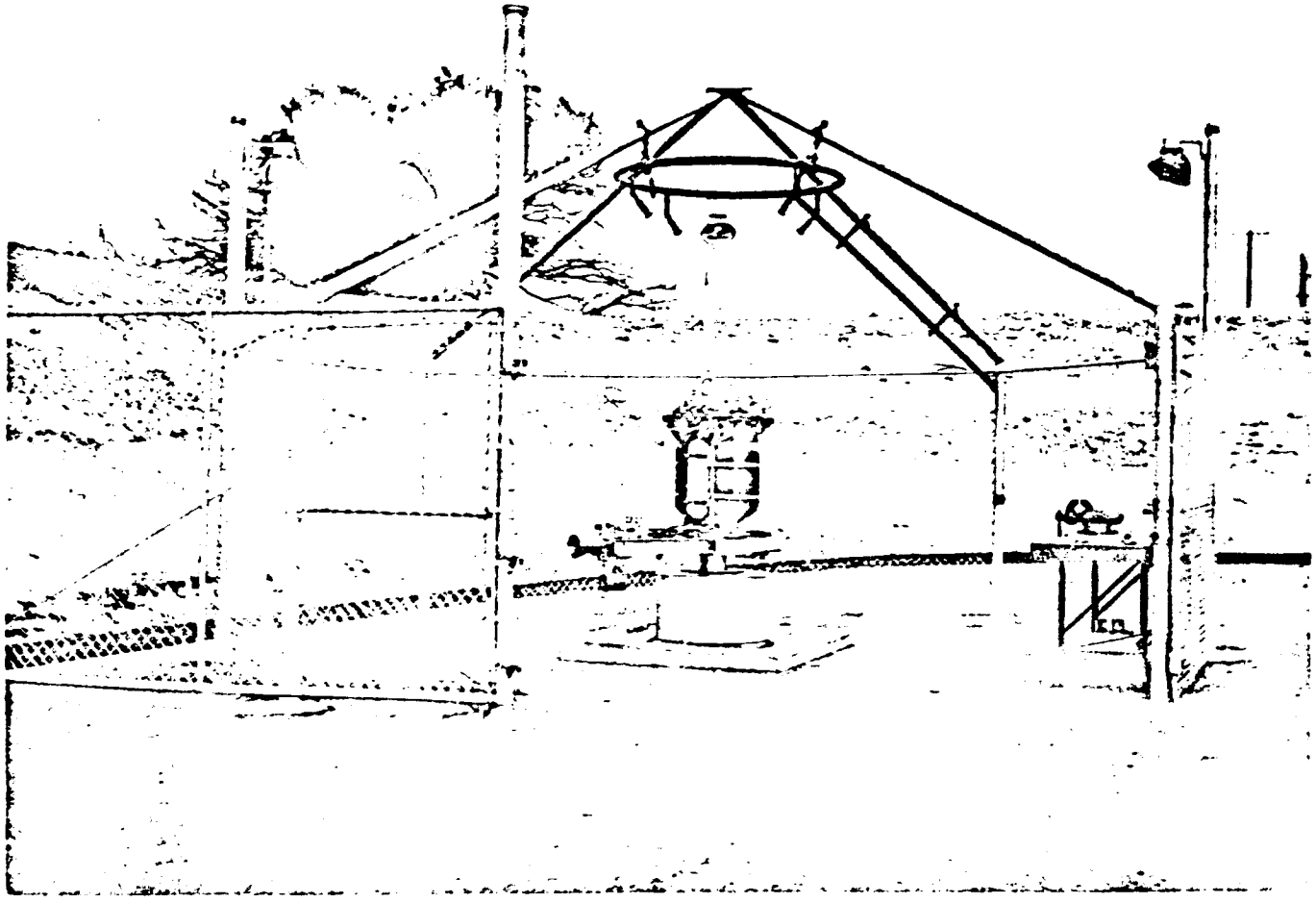

Figure 8-8. Centrifuge

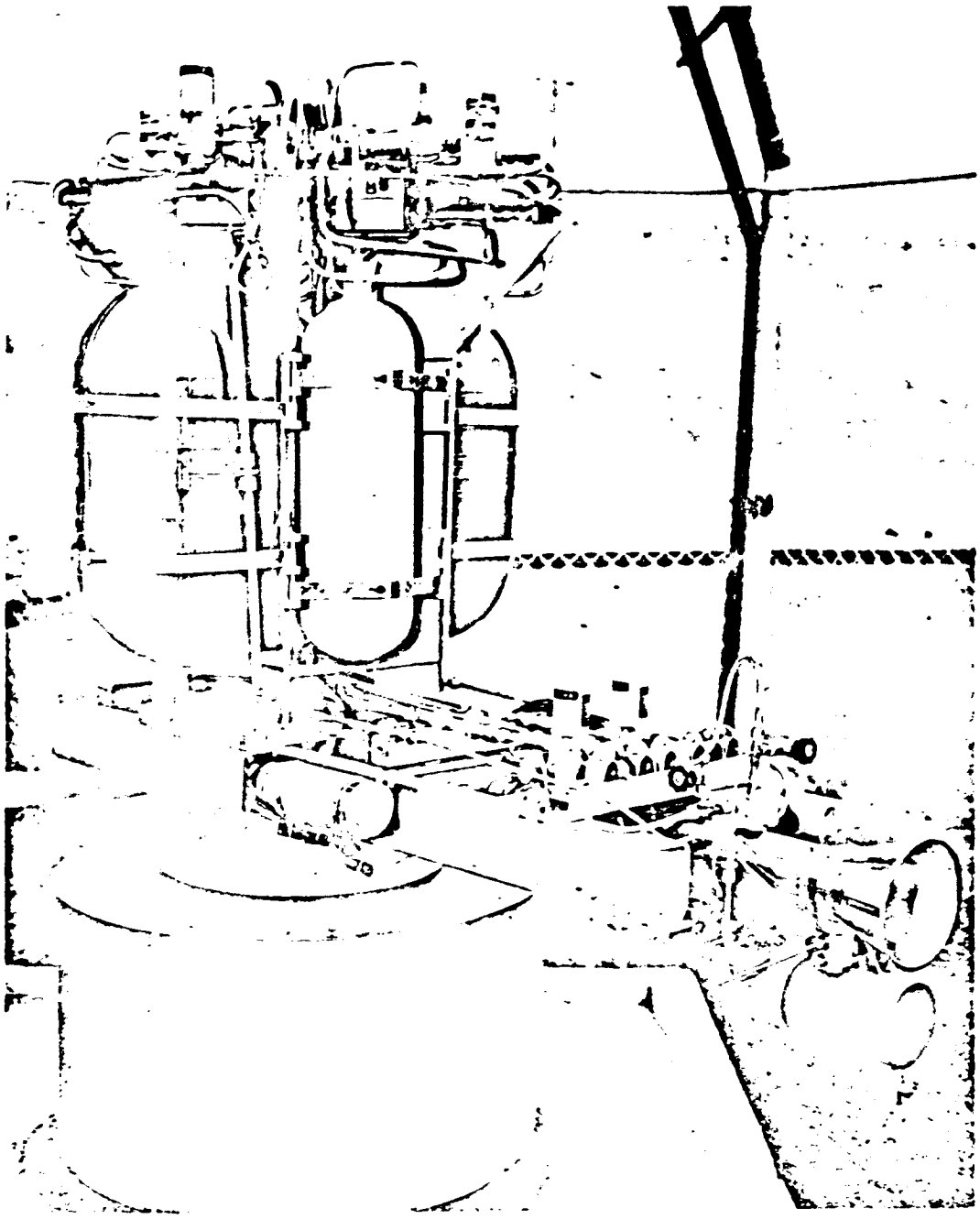

Figure 8-9. Centrifuge Closeup - TCA Installed

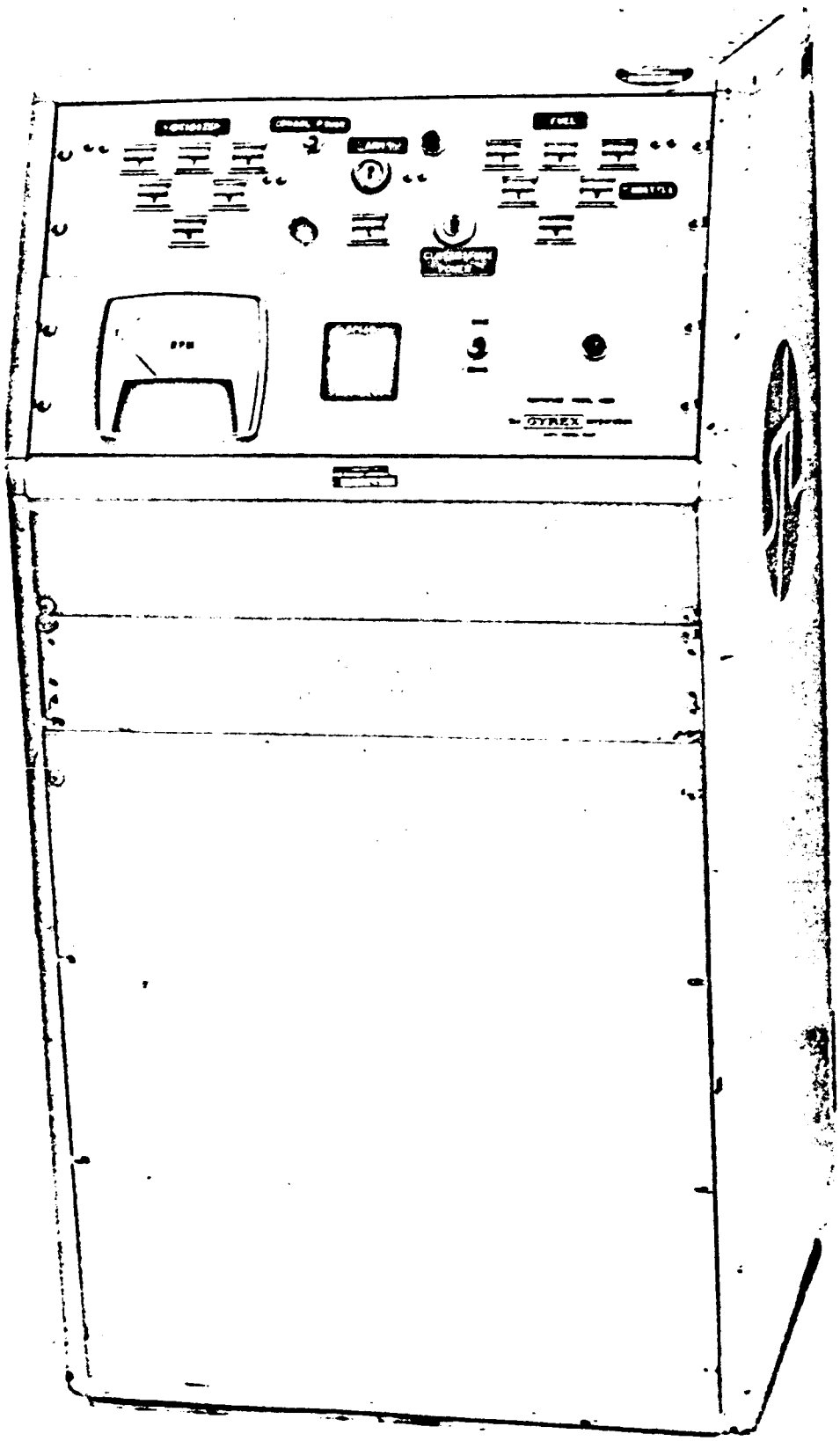

Figure 8-10. Centrifuge Electrical Console

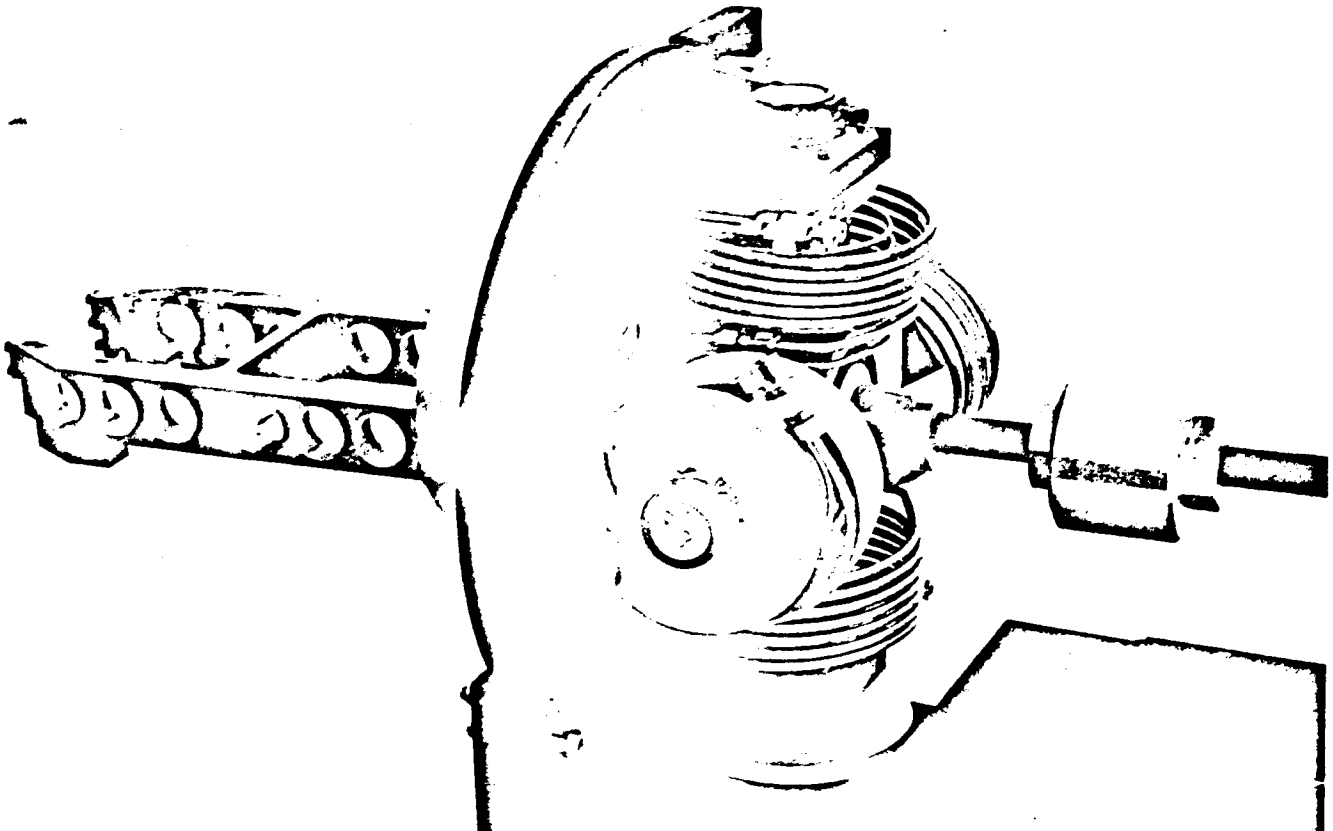

Figure 8-11. Thrust Vector Deviation Measurement Stand

9.0 RELIABILITY PROGRAM

This section presents the reliability program results and the final documentation required by Modification 14 (Phase III) to Contract No. 950596. The reliability program was carried out in accordance with Reliability Program Plan -8422-6006-TU-000, Revision A. With the documents presented herein, all documentation requirements of Phase III have been satisfied. Discussed in this section are: the Reliability Parts List, the Reliability Estimate, the Performance Reliability Analysis, and the Failure Report Summary.

9.1 Reliability Parts List

The Reliability Parts List is presented in Appendix H-1 and is current through November 1964. This list presents the estimated reliability of the TCA major components, including the number of tests performed on each and the number of failures experienced by each. The list, as scheduled in the Reliability Program Plan, has been presented in two stages - the first issue (preliminary) being presented in the July 1964 Surveyor Monthly Progress Report and the second issue being presented herein.

The list is summarized in Figure 9.1.1 wherein reliability information is limited to: (1) the component reliability goal (as established by an apportionment of the specified goal* for one TCA), (2) the current estimated reliability, and (3) the estimated 80% lower confidence limit.

The servoactuator reliability displayed in Figure 9.1-1 represents data from testing of Phase I and II servoactuators only. Data on the Phase III servoactuators were not available for inclusion in this presentation. These data have since become available and show Phase III units are far superior to the earlier versions.

---

*Based on the reliability measurement contained in the JPL Specification SAM-50255-DSN-C, to be obtained at the completion of qualification.

November 1963 through November 1964

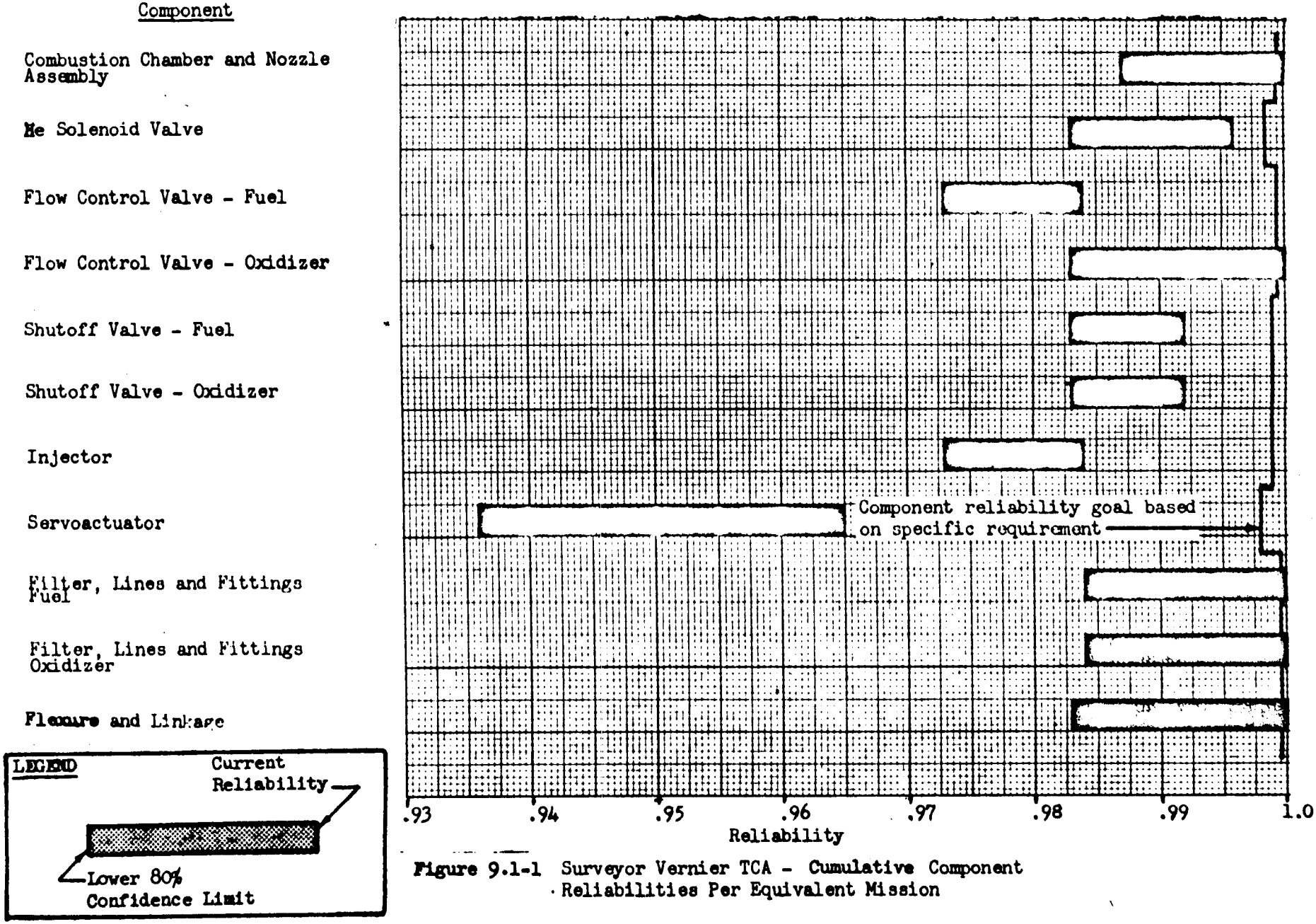

Figure 9.1-1 Surveyor Vernier TCA - Cumulative Component Reliabilities Per Equivalent Mission

9.2 Reliability Estimate

The complete TCA test firing history is presented in Table 9.2-1. The reliability estimate through November 1964 is based on the total number of firings not excluded for reliability purposes along with the number of firings which experienced a failure. The estimate prefiring is the reliability of one TCA for a firing of 45 seconds (average firing time) under various test site conditions. This estimate is not to be construed as a mission estimate. The mission estimate (based on a 186-second firing duration) with its 80% confidence limit is presented in the same table.

The reliability growth experienced during the entire Surveyor program is presented in Figures 9.2-2 and 9.2-3. Figure 9.2-2 shows the growth of the probability for a successful start of a single TCA. Figure 9.2-3 shows the growth of the probability of one TCA completing a successful mission. This curve is based on a mission time of 186 seconds, each mission having an average of 4.6 starts. This is more than twice the number of starts expected to occur during the actual mission. For this reason the reliability estimate obtained is considered conservative, whereas the reliability estimate on a per firing basis is high. The true, current reliability for a single TCA is somewhere between these two numbers.

These reliability estimates are for gross TCA performance and do not include the probability of operation within the specified parameter tolerance. This variation is taken up in the Reliability Performance Analysis in Appendix H-2.

The reliability goal is that specified in the JPL Specification SAM-50255-DSN-C for a single TCA completing a mission (the goal to be obtained at the completion of qualification).

9.3 Performance Reliability Analysis

The Surveyor Performance Reliability Analysis is presented in Appendix H-2. Due to the unavailability of data in sufficient quantities on all parameters, the analysis is based on a model using only three parameters; I_{sp}, M.R., C^*.

9.4 Failure Report Summary

The status of the failure reporting and analysis activities for the complete Surveyor TCA program is presented below:

Total number of failure reports received	91
Total number of failure modes	34
Total number of failure reports closed	89
Total number of failure modes closed	32
Number of failures under investigation	2
Number of failure modes under investigation	2

Table 9.2-1

TCA Firing Summary

(November 1963 through November 1964)

	Constant Thrust	Variable Thrust	All Firings
Number of Firings (TCA Starts)	795	326	1,085
Total Firing Time (seconds)	29,317	19,079	48,396
Number of Firings with Failure	5	9	14
Estimated TCA Reliability per Firing	---	---	.99183
80% Lower Confidence Limit	---	---	.9825
Estimated TCA Mission Reliability	---	---	.97528
80% Lower Confidence Limit	---	---	.9587
Specified Goal	---	---	.9930

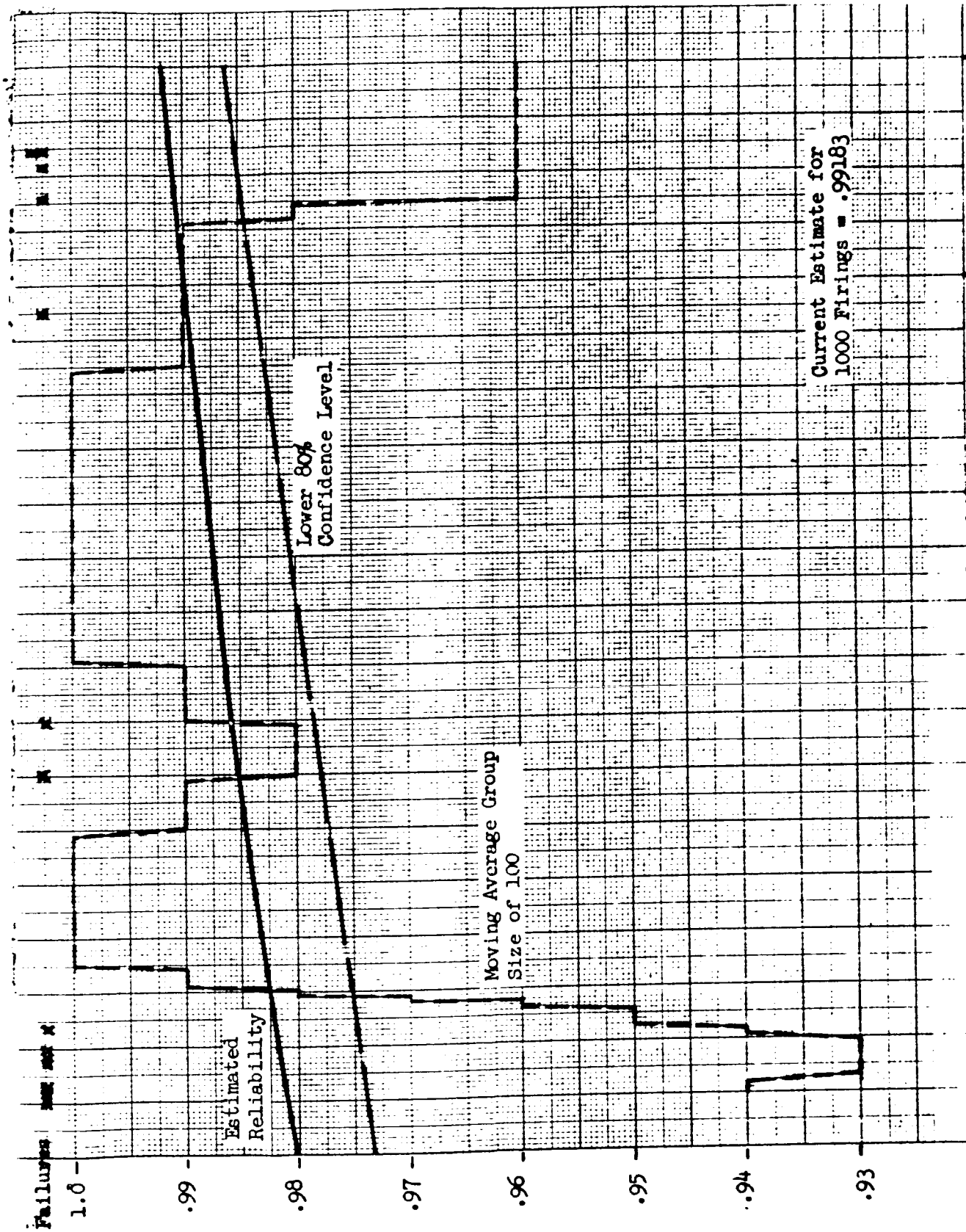

Figure 9.2-2. Engine Firing Reliability Growth Curve (For One TCA)

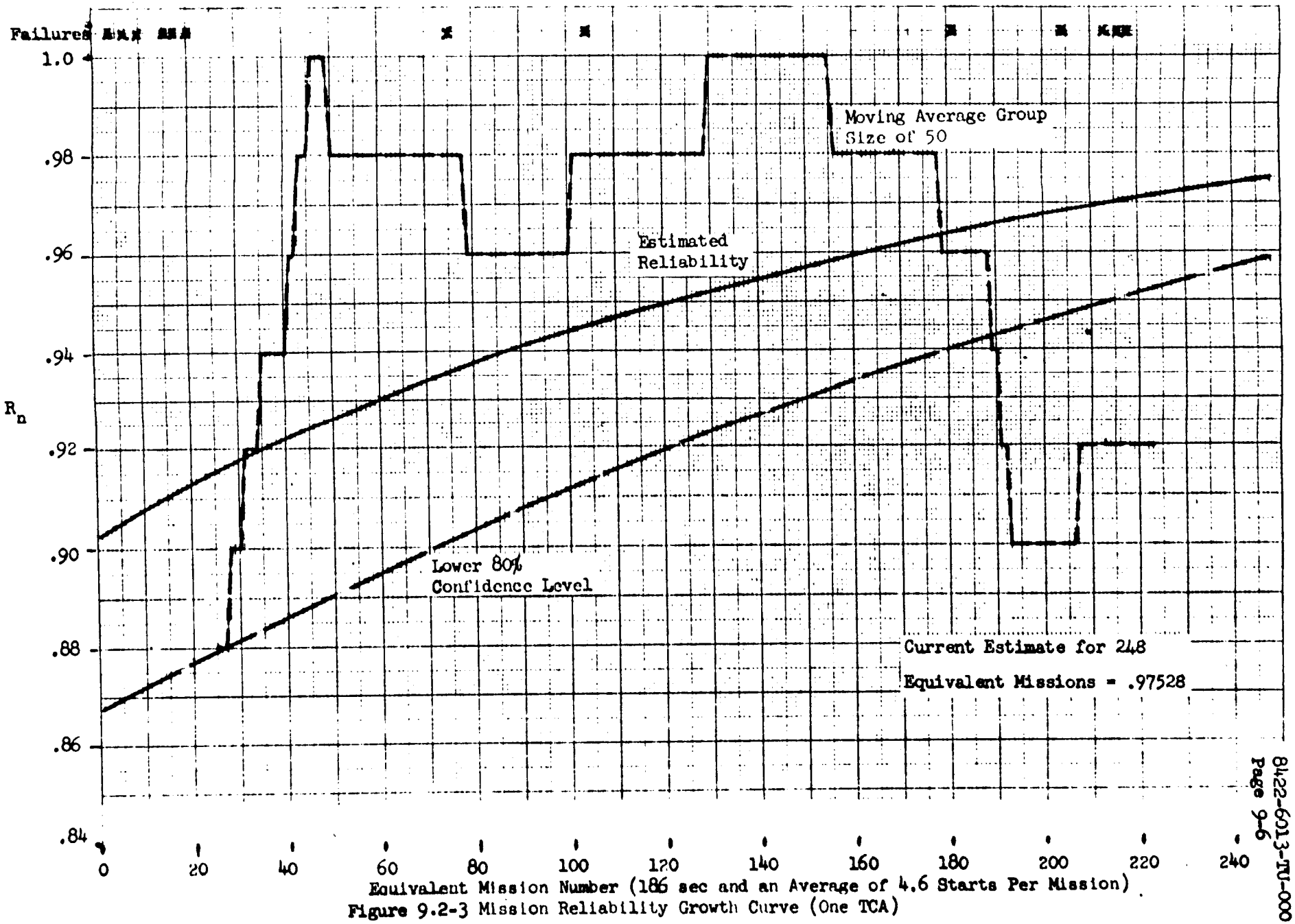

Figure 9.2-3 Mission Reliability Growth Curve (One TCA)

Figures 9.4-1 through 9.4-4 display the complete engine failure history. Figure 9.4-1 and 9.4-2 show the complete TCA total failures and mission failures, respectively. Figures 9.4-3 and -4 present the component total failure history and cumulative mission failures. These failures are classified as to whether they are critical, major, or minor. The three classifications are defined below.

Critical - Catastrophic type failure, rendering the TCA incapable of performing a successful mission.

Major - Out of tolerance performance or conditions that could abort or compromise a mission.

Minor - Failure other than critical or major that does not seriously affect TCA performance.

A complete failure summary is presented in Appendix H-3. This summary is arranged such that the failures experienced by each major component or subassembly are listed in chronological order. The components are presented in the following order: Injector Assembly, Combustion Chamber and Nozzle Assembly, Fuel Shutoff Valve; Oxidizer Shutoff Valve, Fuel Flow Control Valve, Oxidizer Flow Control Valve, Electrohydraulic Servoactuator, and Helium Pilot Valve. The corrective action statements reflect the status of each component as of 31 December 1964.

Two failure reports are still under investigation at the close of the Surveyor program. One report (No. 9375) dealt with the servoactuator sticking at minimum thrust; the other report (No. 10795) dealt with the Fuel Flow Control Valve Assembly leaking fuel during a test run.

Extensive testing of the servoactuator, in an effort to reproduce the failure, was unsuccessful.

Less than optimum seal clearances within the Fuel Flow Control Valve Assembly may have been responsible for the fuel leakage. The analysis conducted prior to the conclusion of the Surveyor program indicated that less seal clearance may be required to prevent leakage under conditions of differential temperature between the two propellants.

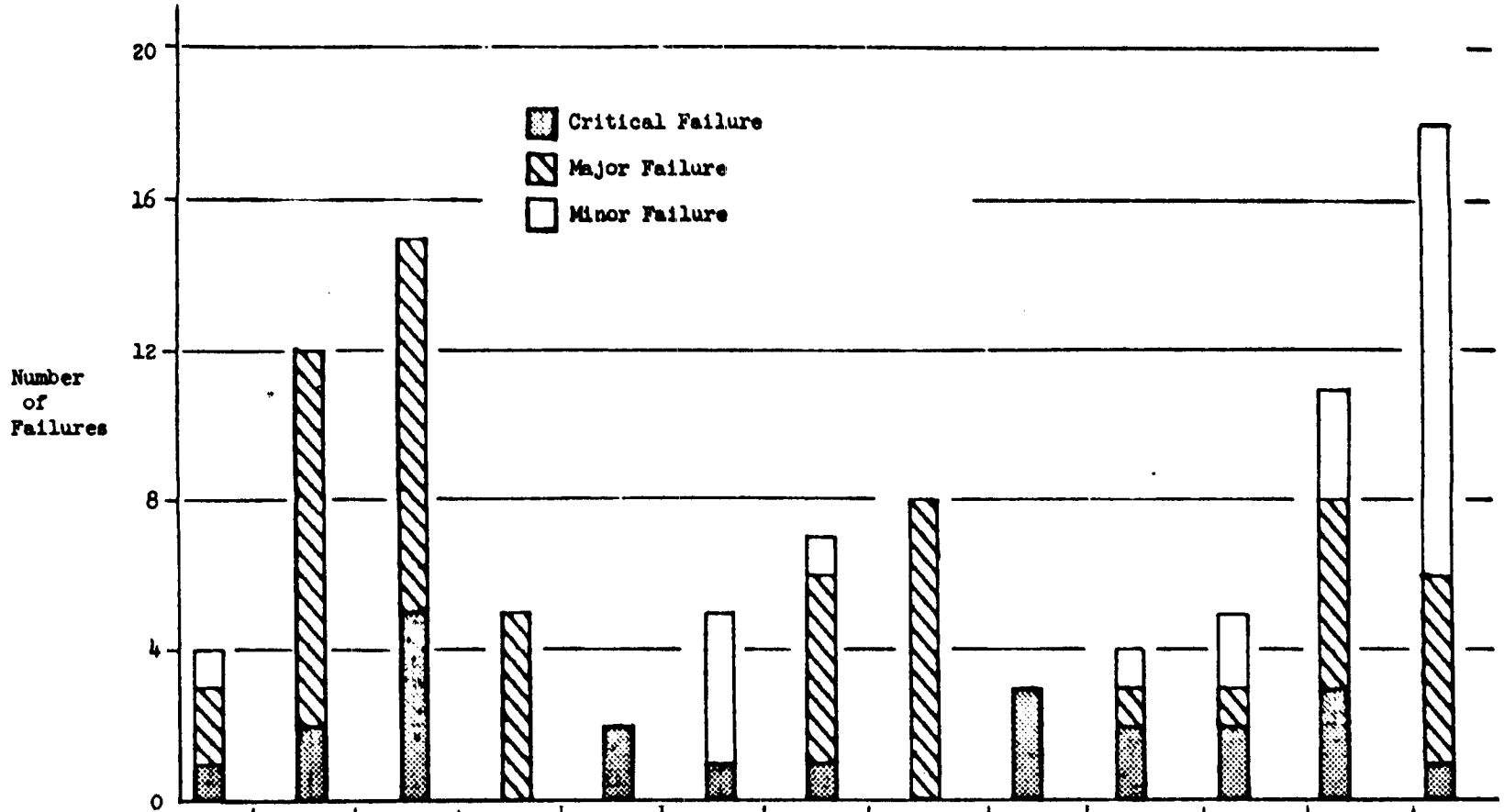

Month	Nov.	Dec.	Jan.	Feb.	March	April	May	June	July	August	Sept.	Oct.	Nov.
No. of Firings	61	38	68	63	107	66	60	181	156	84	46	90	44
Cum. No. of Firings	61	99	167	230	337	403	463	644	800	884	930	1020	1064
Time (Secs.)	1616	1921	2502	2564	5087	5957	2545	7265.5	3604	2703.7	2817.3	5264	4099
Cum. Time (3ecs.)	1616	3537	6039	8603	13690	19647	22192	29457.5	33061.5	35765.2	38581.5	43845.5	47944.5

Figure 9.4-1 Surveyor Vernier TCA
TCA Total Failure History

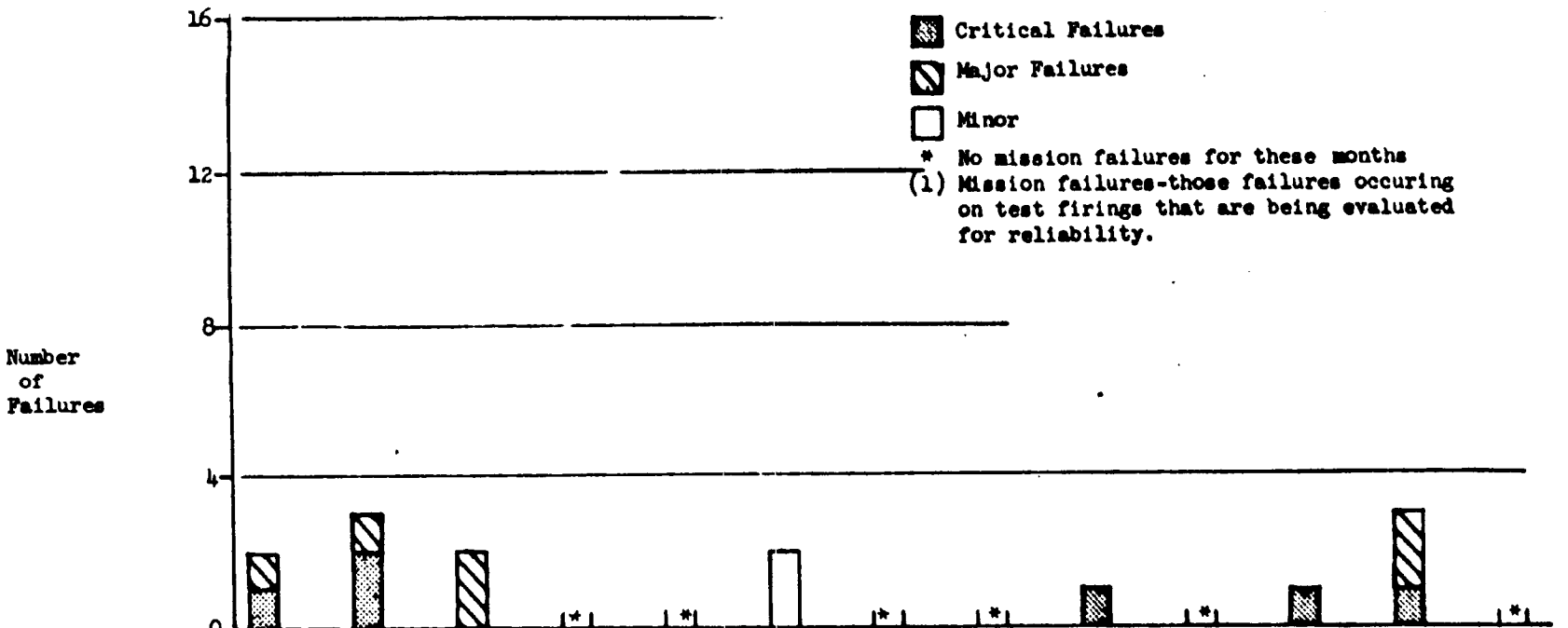

	Nov.	Dec.	Jan.	Feb.	March	April	May	June	July	August	Sept.	October	November
No. of Firings	61	38	68	63	107	66	60	181	156	84	46	90	44
Cum. No. of Firings	61	99	167	230	337	403	463	644	800	884	930	1020	1064
Time (Secs.)	1616	1921	2502	2564	5087	5957	2545	7265.5	3604	2703.7	2817.3	5264	4099
Cum. Time (Secs.)	1616	3537	6039	8603	13690	19647	22192	29457.5	33061.5	35765.2	38581.5	43845.5	47944.5

Figure 9.4-2 Surveyor Vernier TCA TCA Mission Failure(1) History

Figure 9.4-3 Surveyor Vernier TCA - Component Total Failure History

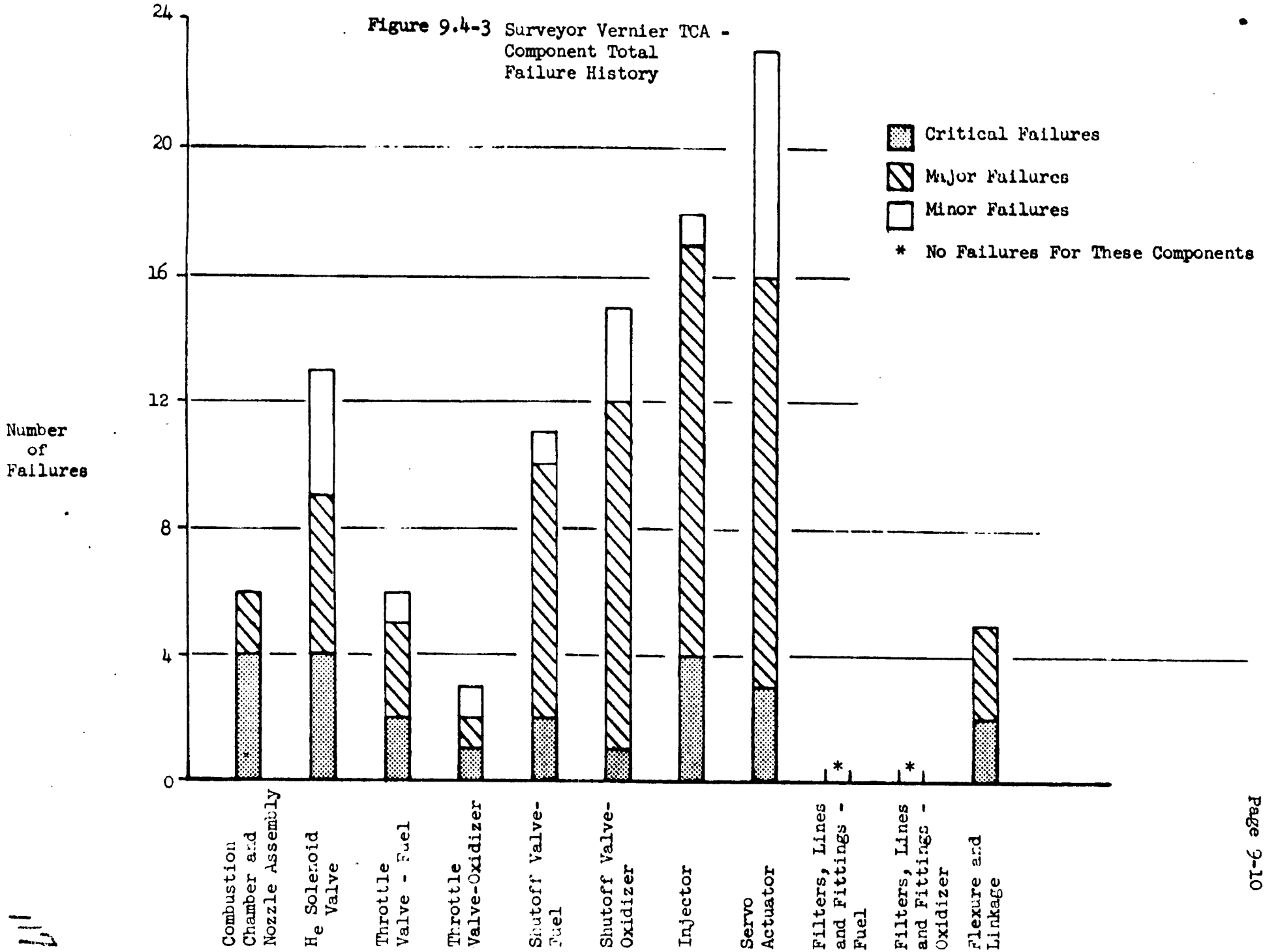

Figure 9.4-4 Surveyor Vernier TCA - Component Mission Failure[1] History

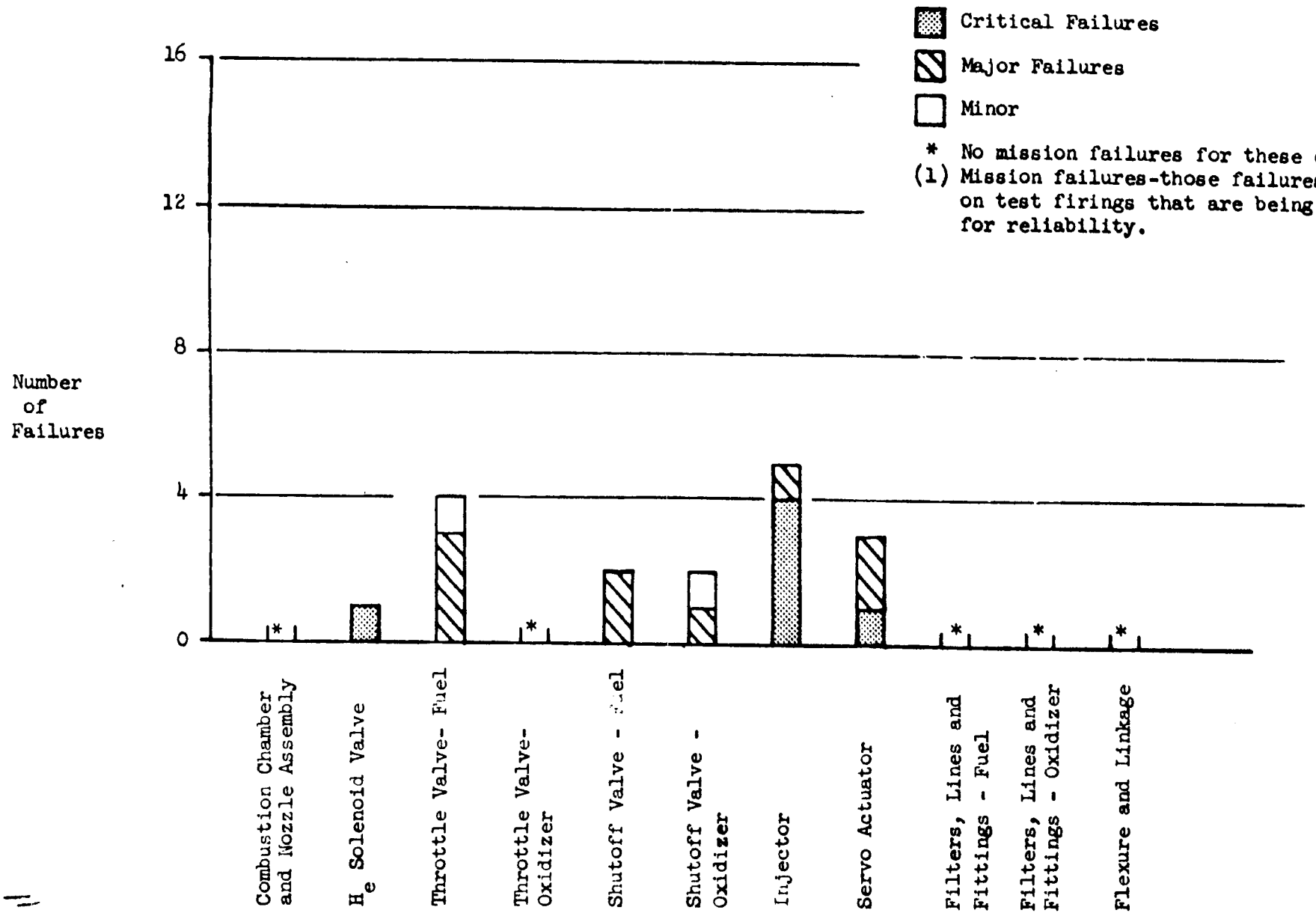

10.0 MANUFACTURING AND QUALITY CONTROL

The manufacturing operations and associated control techniques and applicable documentation used in fabrication and assembly of the MIRA 150A TCA are presented in detail in STL Surveyor Manufacturing Plan 9550.8-91. The fabrication and assembly experience gained in the manufacture of liquid and solid propellant development engines, the Lunar Excursion Module Descent Engine, and the Surveyor Phase II TCA was the basis for the Manufacturing Plan.

In the interests of cost control and accurate schedule, well understood and tested fabrication operations were employed almost exclusively. These included lathe, mill, surface and cylindrical grind, hone, bore, drill, tap and die, polish, electron beam weld, and passivation processes. In special situations where proprietary processes were employed or where a more advantageous price or delivery could be obtained, outside vendor facilities were employed. The Quality Assurance (QA) organization worked closely with the manufacturing group with the result that Quality Control functions were performed smoothly and efficienctly at various stages of fabrication.

Upon completion of fabrication of parts and subassemblies, the hardware was subjected to final inspection with referral for Material Review Board (MRB) action if it did not meet specified requirements. The form of the rejection was a Noncomforming Material Report (NCMR). The NCMR provided for engineering buy-off, rework, or scrap disposition of the parts. During fabrication of Phase III TCA parts, a total of 222 MRB actions occurred. Appropriate corrective action was taken following each MRB review. Table 10-1 shows quantities, categories, disposition and percentages of all Nonconforming Material Reports.

In addition to the Quality Control Inspection function and MRB activity discussed above, the Quality Assurance organization was involved in the following activities:

1. All outside suppliers were surveyed and approved by Vendor Quality Assurance prior to the placement of the first purchase order in accordance with STL Quality Procedure Number 30.12. Source surveillance inspection was used for eight Surveyor hardware fabricating vendors and for three suppliers of complete assemblies. The following list gives the suppliers names and the MIRA 150A hardware fabricated by them.

Grindley Manufacturing Co.	Pintles - Flexures
Schroeder Mgf. Co.	Yoke Assembly
U.S. Beryllium Co.	Actuator Arm
L.A. Gage Co.	Actuator Arm
PreMec Engineering	Head End Body
Fibreform Products	Head End Body
Altco	Sleeves, Pistons, Inserts
Haveg Reinhold	Ablative Billets
Reflective Laminates	Ablative Billets
Vinson Valve	Solenoid Valves
Eckel Valve	Solenoid Valves
Cadillac Gage Co.	Servoactuators

Table 10-1

NCMR Surveyor Phase III - 222 Total

Head End - 120 Total

Dimensional Rejects - 93 Total			Workmanship Rejects - 27 Total		
Use as is	50	41%	Use as is	13	11%
Return to Vendor	16	13%	Return to Vendor	1	1%
Scrap	13	11%	Scrap	4	4%
Rework	14	12%	Rework	9	9%

Combustion Chamber and Nozzle Assy. - 55 Total

Dimensional Rejects - 43 Total			Workmanship Rejects - 12 Total		
Use as is	35	64%	Use as is	6	11%
Return to Vendor	0		Return to Vendor	0	
Scrap	4	7%	Scrap	0	
Rework	4	7%	Rework	6	11%

Helium Pilot Valves - 42 Total

Use as is	35	83%
Return to Vendor	7	17%

Phase III Servoactuators - 5 Total

Return to Vendor	5

TOTAL NCR ALL CATEGORIES

	Use as is	RTV	Scrap	Rework
	139	29	21	33
Percent of Total	62%	13%	9%	15%

2. An instrument calibration and certification system, defined in STL Quality Assurance Procedure Numbers 3 and 4, was used throughout Phase III.

3. Prequalification firing tests performed at the IRTS and JPL/ETS were monitored by the QA test surveillance group.

4. Operating Instruction Number 48-3003-35, entitled "Documentation of Experimental and Developmental Hardware - Surveyor Phase II TCA," was written and implemented to maintain control of Phase II Follow-on HEAs during the accelerated hardware redesign period when six Phase II HEAs (S/N 001 - 006) were being updated (with injector modifications) at the same time the first Phase III units (S/N 007 and subsequent) were being readied for delivery.

11.0 SUMMARY OF NEW IDEAS AND CONCEPTS

Summarized below are new ideas and concepts originated during the design and development effort described in this report. This summary is intended to comply with the "Reporting of New Technology" clause in JPL Contract No. 950596.

The following four items may be included in the category of a new idea or concept:

1. The technique of matching flow performance of an HEA to a master unit in the calibration and adjustment of HEAs on the Head End Assembly Calibration Stand. Refer to section 4.0 and paragraph 4.2 for further details.

2. The ablative throat testing technique used during the acceptance testing series on an assembled HEA. Acceptability of the HEA under the criteria of this test assures the service life of the CC & NA. Refer to section 4.0 (paragraph 4.3 in particular) for details.

3. A prestressed ceramic nozzle throat insert design concept. A disclosure entitled, "Prestressed Ceramic Rocket Nozzle" and marked Docket No. 908 was forwarded to the STL Patent Office in May 1963 on STL Form 125A.

4. The Thrust Vector Deviation Measurement Stand designed to allow measurement of any rocket engine thrust vector deviations during firing in terms of angular displacement of the gimbal-mounted beam on which the engine is mounted. Further details can be found in paragraph 8.8. A disclosure entitled, "Rocket Engine Thrust Vector Deviation Measurement Device" and marked Docket No. 3073 was forwarded to the STL Patent Office in August 1964 on STL Form 125A.

12.0 REFERENCES

This section contains a list of all reports, specifications, and standards referenced in the report. The date and latest change of the documentation is shown herein and is not reported each time the document is referenced in the text of the report.

In addition, the symbols used in the report are identified herein for convenient reference.

12.1 Miscellaneous Documentation

Specifications

Military Specifications and Standards

MIL-P-26539A 5 April 1963	Military Specification Propellant, Nitrogen Tetroxide
MIL-P-27404 3 April 1962	Military Specification Propellant, Monomethylhydrazine
MIL-STD-10	Military Standard, Surface Roughness Waviness and Lay
MS 33656-G3	Military Standard, Connections, Ground Leakage Test, Pressurized Cabin, Aircraft
AND 10050-2	Air Force - Navy Aeronautical Design Standard, Bosses, Standard Dimensions for Gasket Seal Straight Thread

JPL/EAC Specifications

JPL SAM-50255-DSN-C 30 December 1964	Design Specification Surveyor Flight Equipment Thrust Chamber Assembly (MIRA 150A)
EAC No. 226100, Rev. A 24 January 1962	Electromagnetic Interference Specification Surveyor Spacecraft and Associated Support Equipment

STL Specifications

EQ 1-73B 12 February 1964	Filter, Propellant
EQ 1-94 25 January 1965	Combustion Chamber Assembly
EQ 2-23B 7 February 1964	Actuator, Servo Control, Electro-hydraulic (Phase II Follow-on)
EQ 2-25D 29 October 1964	Solenoid-Operated, Three-Way Valve (Phase III)

STL Specifications (Continued)

EQ 2-42 25 August 1964	Servoactuator, Electrohydraulic
EQ 5-5A 29 February 1964	Injector Assembly
EQ 5-6A 29 February 1964	Valve Assembly, Flow Control
PK 4-2 12 August 1964	Packaging Specification, Surveyor Vernier Rocket Engine
SK 1-7 26 February 1965	Model Specification, MIRA 150A Thrust Chamber Assembly
TS 3-01B 26 February 1965	Acceptance Test Specification Surveyor Vernier MIRA 150A Thrust Chamber Assembly
TS 3-02B 24 December 1964	Prequalification Test Specification Surveyor Vernier Thrust Chamber Assembly

STL Manufacturing and Process Specifications

MT 3-9 3 December 1963	Molding Compound, Chopped Silica Fabric Reinforced Phenolic
MT 3-10 13 April 1964	Silica Fabric Reinforced Phenolic Resin Tape and Broad Goods
MT 3-12 15 September 1964	Graphite, Oxidation Resistant
PR 10-9 3 December 1963	Compression Molding of Chopped Silica Fabric Reinforced Phenolic Parts
PR 10-10 20 April 1964	Laminating and Wrapping of Silica Fabric Reinforced Parts, Resin Tape and Broad Goods

STL Engineering Technical Directives

MIRA-0A-001 15 January 1965	TCA Leak Test
MIRA-0A-002 15 January 1965	TCA Pressure Decay Test

STL Engineering Technical Directives (Continued)

MIRA-0F-001 15 January 1965	Determination of Weight and Center of Gravity Location
MIRA-0T-001 15 January 1965	Flowmeter Calibration Procedure
MIRA-1F-001 15 January 1965	Head End Assembly Leak Check
MIRA-1F-002 15 January 1965	Head End Assembly Water Flow Calibration
MIRA-2F-001 15 January 1965	Combustion Chamber and Nozzle Assembly Leak Check
MIRA-3R1-001 15 January 1965	Solenoid-Operated, Three-Way Valve Acceptance Test
MIRA-4R1-001 15 January 1965	Propellant Filter Acceptance Test
MIRA-5T-001 15 January 1965	Electrical Control Console Calibration

STL Miscellaneous Reports

8422-6006-TU-000, Rev. A 19 June 1964	Reliability Program Plan
8422-6007-TU-000, R02 6 October 1964	Data Reduction and Analysis Procedures for Surveyor Vernier Thrust Chamber Assembly
8422-6014-TU-000 11 December 1964	Analytical Model for the Surveyor MIRA 150A Engine
9354.4-255 29 September 1964	Acceptance Test Procedure, Surveyor Thrust Chamber Assembly Electrohydraulic Servoactuator
9522.3-272 1 February 1965	Surveyor Vernier Thrust, Chamber Assembly Prequalification Nonoperating Vibration Test
9550.8-91 1 August 1964	Manufacturing Plan, Surveyor Vernier TCA, Qualification Program - Phase III MIRA 150A
9730.4-64-1-43 30 June 1964	Development Test Plan

STL Miscellaneous Reports (Continued)

9730.4-64-3-6 5 August 1964	Surveyor Vernier Thrust Chamber Assembly MIRA 150A Mass Properties Baseline Report (U)
9730.4-64-36 15 May 1964	Final Report - Feasibility (Phase I) and Development (Phase II) Surveyor Vernier Thrust Chamber Assembly
9730.4-64-54 14 September 1964	Informal Operating and Maintenance Instructions

Technical Papers

ASME Transactions 1956 Vol. 78, Part I, Page 489	On the Theory of Discharge Coefficients for Rounded-Entrance Flowmeters and Venturis

12.2 Symbols and Units

Symbol	Description	Units and/or Definitions
A_i	Injector Flow Area	$in.^2$
A_v	Venturi Throat Area	$in.^2$
C_D	Discharge Coefficient	None
C_f	Thrust Coefficient	None - $(\frac{F}{P_c \cdot A_t})$
C_P	Specific Heat at Constant Pressure	$cal/mol\,^oK$
C^*	Characteristic Velocity	ft/sec
D	Diameter	in.
ϵ	Expansion Ratio	None - $\frac{A_x}{A_t}$ $(\frac{\text{Exit Plane Area}}{\text{Throat Area}})$
ϵ_c	Contraction Ratio	None - $\frac{A_c}{A_t}$ $(\frac{\text{Chamber Area}}{\text{Throat Area}})$
F	Thrust	lbs
f	Frequency	cps
f_{app}	Mean Apparent Friction Factor	None
γ	Specific Heat Ratio	-
HAC	Hughes Aircraft Company	

Symbol	Description	Units and/or Definitions
I_{sp}	Specific Impulse	seconds (or lbf - sec/lbm)
L	Length	in.
L*	Characteristic Length	in. $\frac{V_c}{A_t}$ ($\frac{\text{Chamber Volume}}{\text{Throat Area}}$)
L_{eq}	Equivalent Length	in.
$\dot{M}$	Mass Flow Rate	lb/min
MR	Mixture Ratio	None - $\frac{\text{Oxidizer Flow}}{\text{Fuel Flow}}$
MW	Molecular Weight	None - lb/sec-ft
P_c	Chamber Pressure	psia
P_{inj}	Injector Pressure	psia
ΔP_{inj}	Injector Pressure Drop	psi
P_t	Feed System Inlet Pressure	psia
P_v	Vapor Pressure	psia
R	Radial Distance from Nozzle Exit	in.
R_E	Nozzle Exit Plane Radius	in.
Rey_D	Reynolds Number	
Rey_L	Length Reynolds Number	
ρ	Propellant Density	lbs/ft^3
S	Servoactuator Stroke	in.
STL	TRW/Space Technology Laboratories	--
t	Service Life or Time	seconds (or minutes)
V	Velocity of Injection Stream (V_O for oxidizer and V_F for fuel)	ft/sec
μ	Viscosity	lb/sec-ft

Symbol	Description	Units and/or Definitions
x	Actuator Stroke	in.
X_i	Mole Fraction	None
Z	Distance aft of Exit Plane	in.

APPENDICES

The nine appendices that are provided here are arranged as follows:

Appendices A, B, C, F, H, and I are part of Volume II and follow on the subsequent pages.

Appendices D, E, and G are provided in a separate Volume III because they consist totally of pages that are about 17 inches in length or greater. Thus, they have been bound separately.

APPENDIX A

DERIVATION OF FCV PARABOLIC SHAPE

No. of Pages: 5

APPENDIX A

DERIVATION OF FCV PARABOLIC SHAPE

The flow control valves (FCV) are designed to cavitate over the entire throttling range, thereby permitting propellant flow to be independent of conditions downstream of the valves. For the actuator stroke to be linear with thrust the flow-area through the FCVs must be linear with stroke assuming the following criteria were met: (1) the flow coefficient are constant, (2) there is no appreciable loss in total pressure up to the throat of the venturi, and (3) the specific impulse is independent of thrust level. Development tests have indicated that the flow coefficients do change. However, it is considered preferable to accept this slight nonlinearity in thrust rather than attempt to design the contour for variable flow coefficients. This procedure does not affect mixture ratio, since the flow coefficients of both valves normally vary in a similar manner. Since the characteristic velocity and thrust coefficient (and thus the specific impulse) do vary with thrust level, a further error in thrust-stroke linearity is introduced. However, because of the unpredictability of this error at the time the FCV pintle design had to be decided upon, it was not advisable to try and match valve contour to TCA performance.

A FCV pintle should have a parabolic contour if the area normal to the pintle center line is to increase linearly with stroke. However, this solution will result in a slight error in the stroke, since the flow through the valve is actually parallel to the pintle surface rather than parallel to the pintle centerline. With the flow assumed to be normal to the pintle centerline, the area-stroke curve is linear but the total stroke is slightly less than for the case where flow is parallel to the pintle surface. This effect becomes more pronounced as the flow control point moves further toward the vertex of the parabola.

The procedure outlined in this appendix computes the contour equation based on a flow area through the valve normal to the pintle surface. This area is represented as the surface of a truncated cone.

The following routine supplies the basic data necessary for the FCV sleeve and pintle contour calculations:

$\dot{M}_t = F/I_{sp}$

$\dot{M}_f = \dot{M}_t/(r + 1)$

$\dot{M}_o = \dot{M}_f\, r/(r + 1)$

$A = M_t/C_D \sqrt{\rho\, 2g\, (P_t - P_v)}$ — Where:

$\dot{M}_t$ = Total Mass Flow of Propellants

$\dot{M}_f$ = Total Mass Flow of Fuel

$\dot{M}_o$ = Total Mass Flow of Oxidizer

F = Thrust

I_{sp} = Specific Impulse

r = $\frac{\dot{M}_o}{\dot{M}_f}$, mixture ratio

g = Gravitational Constant

ρ = Propellant Density

C_D = Flow Coefficient

P_t = Inlet Pressure

P_v = Propellant Vapor Pressure

A = Throat Area or Flow Area at 100% Thrust

Figure A-1 shows the standard geometric nomenclature used in the analysis. The total stroke from 0% to 100% thrust is given by S_o. The throat radius and pintle diameter at zero thrust are given by H, X, and Y are the pintle contour corrdinates with X being measured from the pintle parabolic vertex. A transformation of coordinates allows the use of X' which is measured from the zero thrust position on the contour. G and H are the coordinates of the throat, and C is the gap between throat and the pintle measured normal to the pintle centerline. Two arbitrary dimensions must be chosen before the valve pintle contour can be computed; these dimensions are S_o (total stroke) and H (the throat radius). The total stroke is chosen to conform to the injector and actuator requirements. The throat diameter is determined by setting the throat area, A, equal to approximately twice the flow area as computed in the above equation. This insures that the flow will not be controlled by the rapidly changing pintle surface near the vertex of the parabola and that the throat diameter will not be too large resulting in small gaps and tight tolerances. Thus, the throat radius can be determined by:

$$H \cong \sqrt{2A/\pi} \qquad (1)$$

This value was rounded off and used on both the oxidizer and fuel FCVs. The following procedure derived the pintle contour coefficients:

$Y^2 = aX = a\,(X_o - X')$ where a and X_o are the coefficients to be determined when knowing S_o, H, and A. (2)

$dY/dX = a/2Y$ slope of pintle surface at any point (3)

$m = -2Y/a$ slope of line normal to surface (4)

With G and H as coordinates of the throat, the following equation establishes the relationship between G, H, X, Y, and a:

$$(Y-H) \,/\, (X-G) = -2Y/a \qquad (5)$$

Defining C as the distance between the throat and the pintle normal to the pintle centerline results in the two following equations:

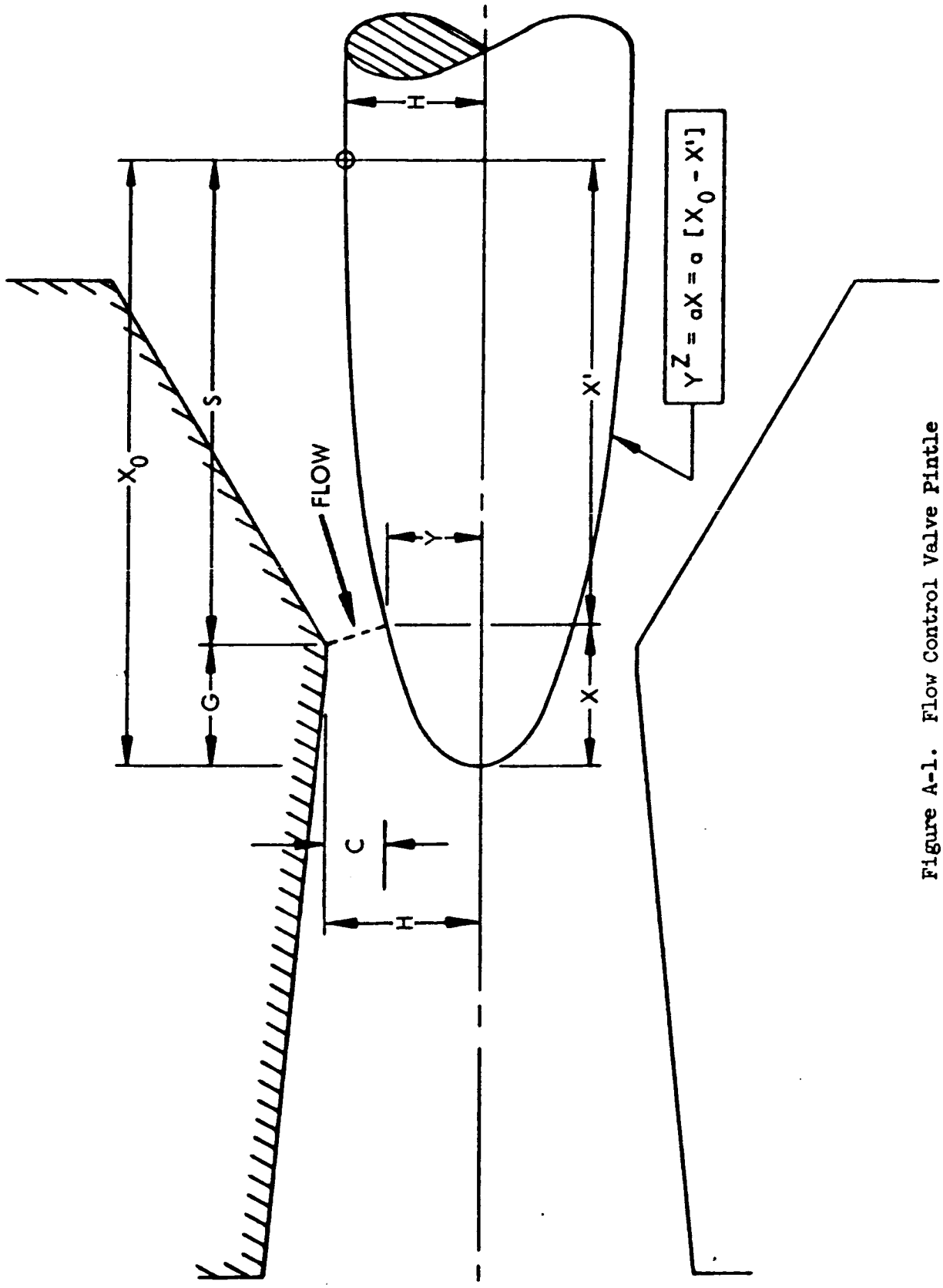

Figure A-1. Flow Control Valve Pintle and Throat Geometry

$$a = \frac{C}{S_o} (2H-C) \tag{6}$$

$$G = \frac{(H-C)^2}{a} \tag{7}$$

Equations (2) and (5) when combined yield:

$$Y^3 + \frac{a^2}{2} \left(1 - \frac{2G}{a}\right) Y + \frac{-a^2 H}{2} = 0 \tag{8}$$

The flow area is related by:

$$A = \pi \sqrt{(H-Y)^2 + (X-G)^2} \; (H+Y) \tag{9}$$

An approximate value for C is used in equations (6) and (7) and values for G can now be obtained, which in turn permits values of Y and X to be obtained from equation (8). The flow area is then obtained from equation (9) and compared with the desired flow area. By linear interpolation a new value for C is selected and the process iterated until the flow area is satisfactorily converged. Then the coefficient, a, in the parabolic equation is known, which is the same value when either X or X' is used. If the X' coordinate form of the quation is desired, then X_o is required and is simply defined as:

$$X_o = H^2/a$$

A computer routine is available for the above calculations and iterations.

APPENDIX B

MIRA 150A THERMAL CONTROL ANALYSIS

No. of Pages: 9

APPENDIX B

MIRA 150A THERMAL CONTROL ANALYSIS

Summary

A thermal analysis was conducted to determine the feasibility of using a "cap" over the head of the MIRA 150A TCA for passive thermal control. This study was general in nature because an exact definition of environment for the three locations of the TCAs on the spacecraft was not available. Two cap models were evaluated — a buffed aluminum cap, and an aluminum cap with a bright gold finish. Either cap will require some amount of black paint on the side faces to maintain the TCA within the proper temperature range. The areas that require painting and the temperature profiles of the TCA are presented herein.

An error analysis was made to determine the effects of potential variations of surface properties (α_s and ϵ_H) from their nominal values. It was found that the gold-coated cap was much less sensitive to variations in these properties than the buffed aluminum cap.

The changes in TCA temperature profile due to changes in the exit cone interior surface emissivity (because of mid-course firing) were evaluated. It was found that the exit cone temperature could change only about 15°F if the titanium emissivity varied from 0.20 to 0.80. The nominal value of emissivity for 6Al4V titanium is about 0.2 to 0.3. However, it was found that drastic changes in the temperature profile result as a function of the amount of exit cone area exposed to solar heating. For a TCA that has no solar heating of its exit cone, temperature as low as -160°F may be expected.

The concept of using a cap over the HEA was found to offer several advantages, the most important of which are: (1) more flexibility in maintaining the TCA within its temperature limitations if the thermal environment is revised at some point in the Surveyor program, (2) simplification of the manufacturing requirements, (3) a configuration that can be easily cleaned during spacecraft assembly and checkout, and (4) simplification in geometry (hence, better confidence level) in the thermal analysis.

Based on this analysis, it is therefore recommended that a gold-coated aluminum cap be used for thermal control of the MIRA 150A TCA. The weight of a 0.02-inch thick cap is about 0.15 pounds. Gold should also be used on the chamber walls to minimize TCA heat losses if the exit cone receives no solar heating.

Assumptions

The following assumptions were used in this study:

1. The top surface of the cap was fully exposed to the sun at all times.
2. The chamber cylindrical section and inside exit cone surface had an unobstructed view of space, i.e., the shape factor for emission was 1.0.
3. The exit cone external surface had a shape factor of 0.70 for emission to space.

4. The chamber was coated with a liquid bright gold (Reflective Laminates, Inc. No. 381 applied per RLI Process 1554, modified).

5. The exit cone was bare titanium.

6. Joint conductances of 0 and 10 BTU/hr-ft^2-$^\circ$F were used at the cap-to-TCA interface.

7. The nominal values of the thermal properties used are presented in Table B-I.

Table B-I

Thermal Properties Used in Analyses

Material	Thermal Conductivity
Titanium (6Al4V)	4.21 BTU/hr-ft-$^\circ$F
Fiberglass (Ablative Liner)	0.26
Aluminum	70.0

Material	Absorptivity, α_s	Emissivity, ϵ_H
Buffed Aluminum	0.17	0.04
Liquid Bright Gold	0.35	0.03
Black Paint	not used	0.85
Titanium (6Al4V)	0.55	0.20
Titanium (after mid-course firing)	0.55	0.20 - 0.80
Fiberglass Liner	not used	0.90

Analysis and Results

Analyses were performed to determine: (1) the temperature profiles of the MIRA 150A TCA, (2) the paint patterns required to maintain the TCA at proper operating temperatures, and (3) the effects of variations in the surface properties (α_s and ϵ_H). Two different caps were considered: (1) a "buffed" aluminum cap, and (2) a gold-coated aluminum cap.

For determining the temperature profile, the HEA was held at 100°F, and the temperature profiles were computed for the following conditions:

1. Fifty percent of the projected area of the exit cone exterior exposed to solar heating.

2. No solar heating of the exit cone.

3. Same as (2) with a higher emissivity for the exit cone's internal surface.

The results are shown in Figure B-1 where it can be seen that the temperature profile is very sensitive to the amount of solar heating experienced by the exit cone. The foregoing analysis was based on the understanding that the exit cone of one TCA will be completely shadowed and receive no solar heating. The variation in temperature due to changes of emissivity of the inside surface, due to mid-course firing, was minor. The reason for this is that about one half of the exit plane losses originate from the nozzle throat and nozzle internal insulation, both of which

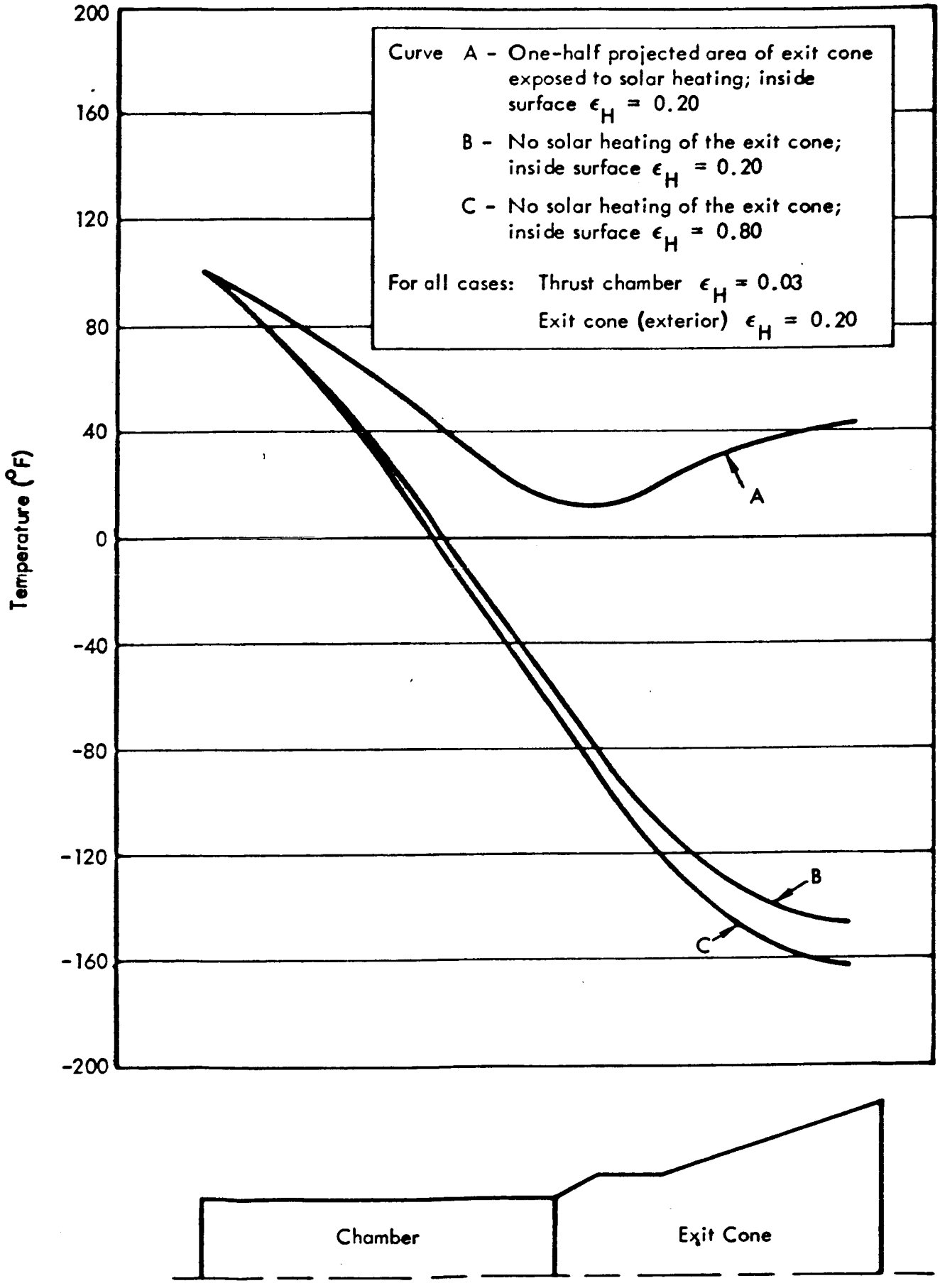

Figure B-1. Temperature Profiles of MIRA 150A

experience negligible changes in emissivity due to firings of a TCA. The heat losses from the various portions of the TCA are summarized in Table B-II for two of the temperature profiles from Figure B-1. This table indicates that the cap must supply from 4 to 7.3 BTU/hr to the HEA, depending on the amount of solar heating of the exit cone. That is, for the case represented by curve A in Figure B-1. there is sufficient solar heating of the exit cone that only 4 BTU/hr need be supplied to the head end from the cap. For curve B, where there is no solar heating of the exit cone, about 7.3 BTU/hr must be supplied to the head end by the cap. Thus, the paint pattern on the cap will have to be tailored for the thermal environment expected for each location on the Surveyor spacecraft.

Table B-II

Summary of TCA Heat Losses

Thermal Properties	Case 1 (Curve A)	Case 2 (Curve B)
Thrust Chamber, ϵ_H	0.03	0.03
Exit Cone (exterior), ϵ_H	0.20	0.20
Exit Cone (interior)		
Throat and Fiberglass liner, ϵ_H	0.90	0.90
Titanium, ϵ_H	0.20	0.20

Heat Losses	Case 1	Case 2
Thrust Chamber	1.26 BTU/hr	0.98 BTU/hr
Exit Cone (exterior)	7.00	1.58
Exit Cone (interior)		
Throat and Fiberglass liner	5.72	3.02
	5.01	1.73
Total	18.99 BTU/hr	7.31 BTU/hr
Solar Heating of Exit Cone	15.00	0
Net Heating from Cap	3.99	7.31 BTU/hr

The second protion of the calculations was made to determine the amount of black paint on the side faces of the cap necessary to provide the required energy to the HEA. The results are shown in Figure B-2 for both the buffed aluminum cap and the gold-coated cap. This calculation was based on the assumption that the inside surface of the cap and the components on the HEA have high emittance surfaces. It was also assumed that no gaps or holes existed in the cap. These curves can be adjusted to account for small openings in the top and side faces of the cap.

An evaluation of the sensitivity of the engine temperature to possible variations in surface properties (α_s and ϵ_H) was made for both cap designs. The variations of the properties used in this study are noted below.

	α_s	ϵ_H
Liquid Bright Gold	$0.35 \pm .035$	$0.03 \pm .01$
Buffed Aluminum	$0.17 \begin{matrix} + .02 \\ - .03 \end{matrix}$	$0.04 \pm .01$
Black Paint	Not used	$0.85 \pm .05$

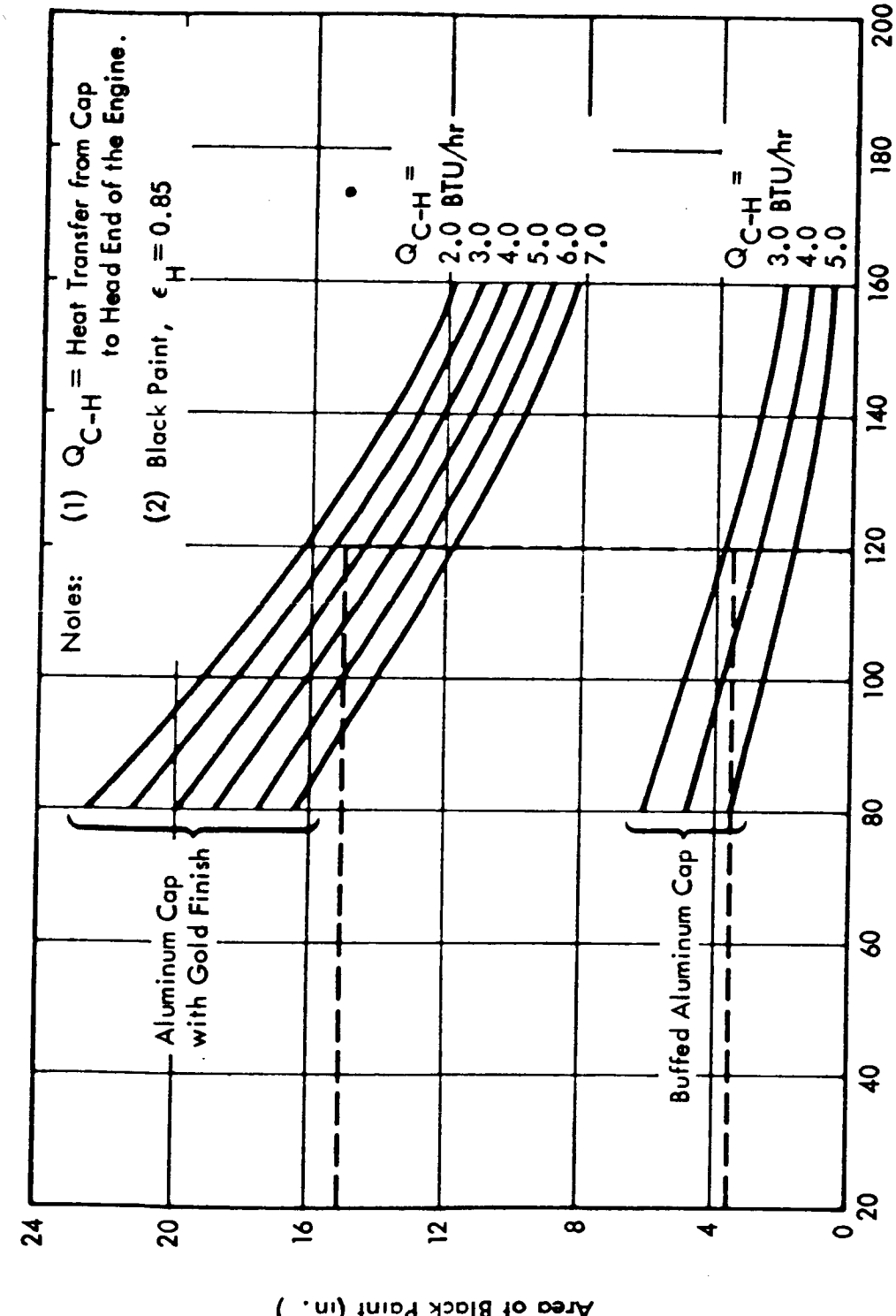

Figure B-2. Paint Area for Sides of Cap

These are the type of variations that may result due to errors in the experimental measurements of the properties, variations from one application to another, aging, etc.

The results of this evaluation are presented in Figure B-3 where it can be seen that the buffed aluminum cap is more sensitive to variation in α_s and ϵ_H than the gold cap. This is because there is about twice as much solar energy absorbed by the gold cap, and therefore about twice as much energy is reradiated by the black paint on the sides. Since the variation of the black paint ϵ_H is much smaller, percentage-wise, than the highly reflective surfaces, this has the effect of reducing the error in the amount of heat exchanged with the HEA.

An analysis of the potential variations of the joint conductance between the cap and the TCA was made, and the results are presented in Figure B-4. The joint conductance of 10 BTU/hr-ft^2-^{o}F is considered an upper limit for this type of interface, and the value of zero, of course, represents the lower limit. It can be seen that the joint conductance is not a significant variable; however, if necessary, it could be made to approach zero joint conductance by proper design of the cap surfaces which are in contact with the TCA.

Recommendations

Based on this study, it is recommended that:

1. A cap be used over the HEA for thermal control.
2. The cap be aluminum with a bright gold finish.
3. Gold surface treatment be used on the combustion chamber walls.

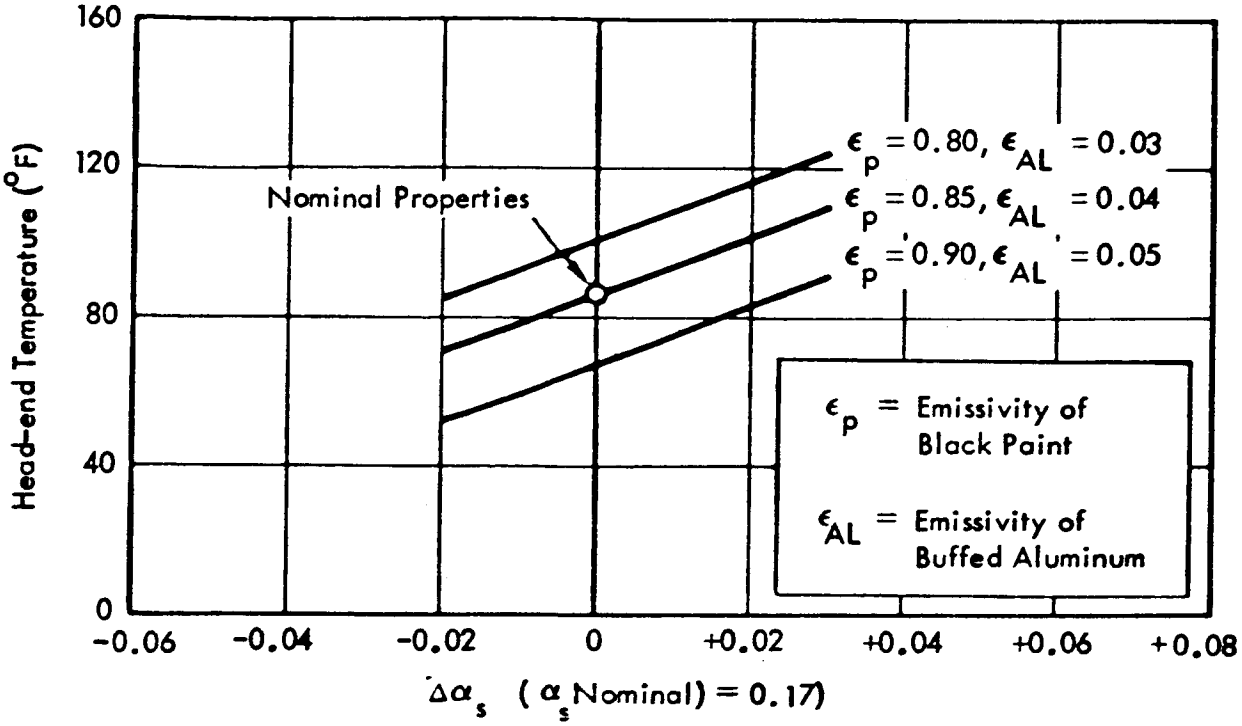

a Buffed Aluminum Cap

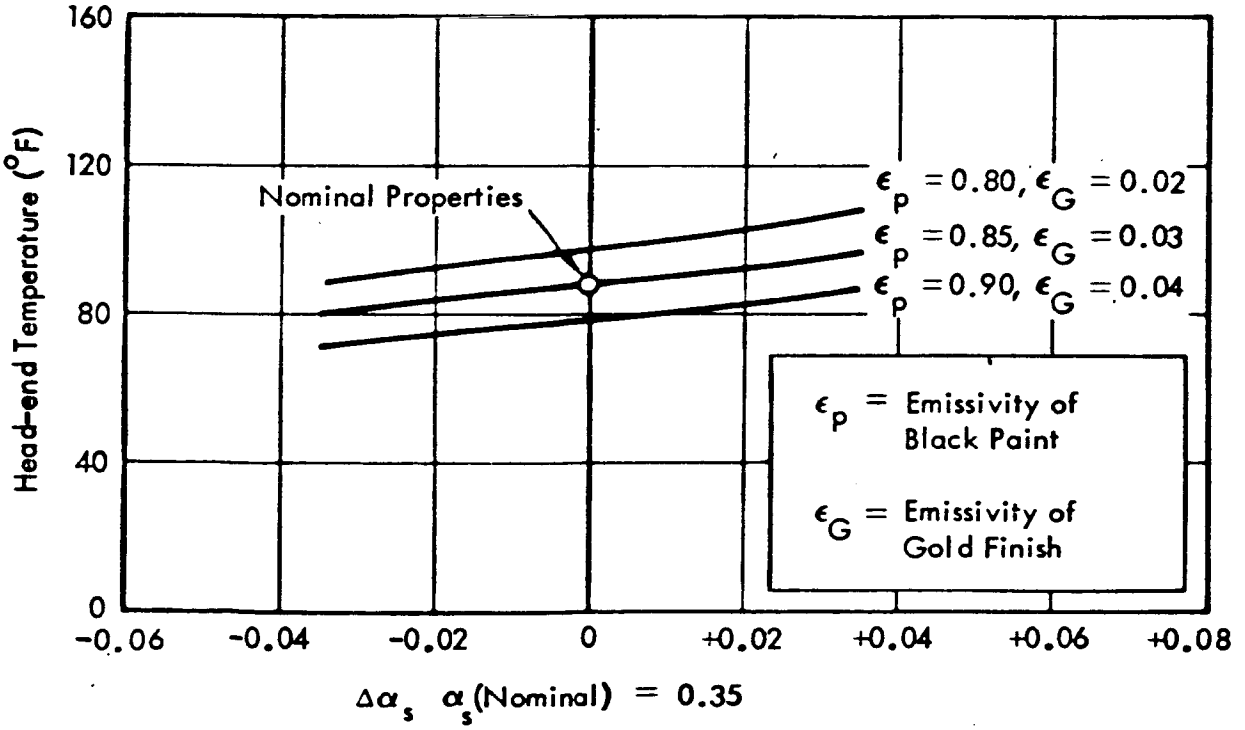

b Aluminum Cap with Gold Finish

Figure B-3. Error Analysis of Surface Properties

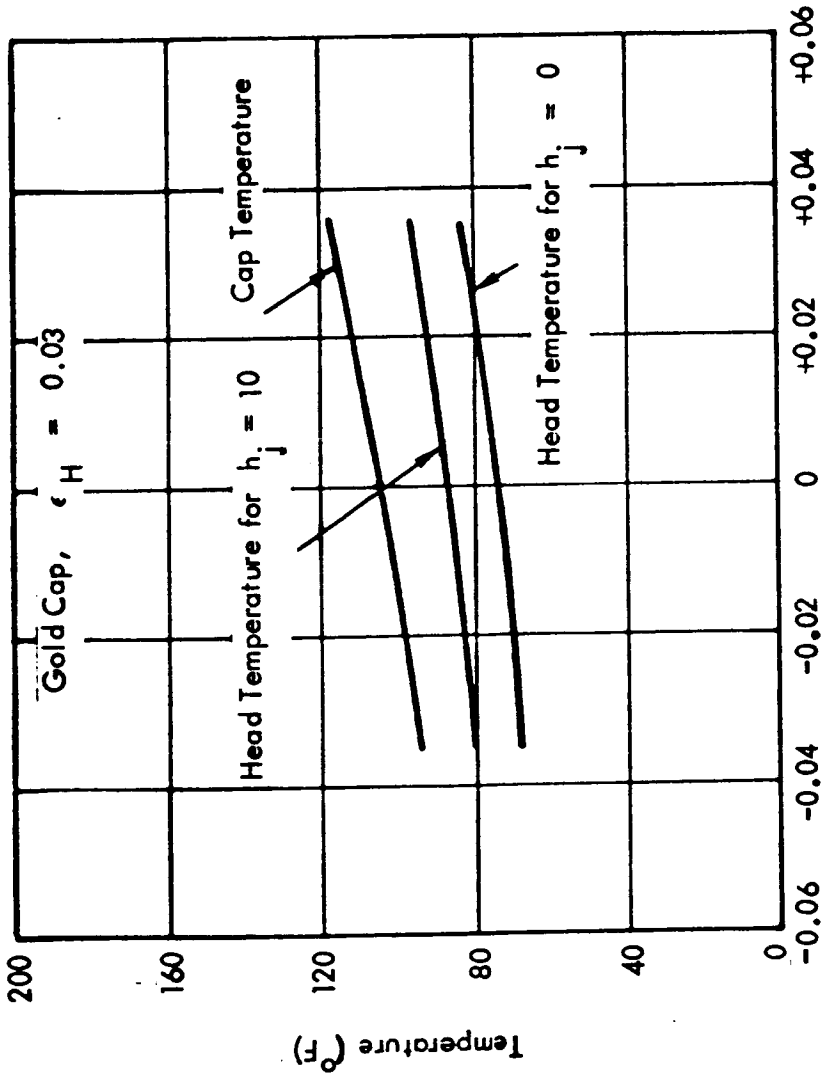

Figure B-4. Effect of Joint Conductance on Cap and Head End Temperatures

APPENDIX C

THERMAL PROPERTIES OF VARIOUS SURFACES

No. of Pages: 3

APPENDIX C

THERMAL PROPERTIES OF VARIOUS SURFACES

Two series of determinations of thermal properties of various surfaces were conducted - Series A and Series B. A discussion of each series follows:

Series A - The spectral reflectance of five samples of gold on titanium were measured. Measurements in the wave length region of 0.32 to 2.0 microns were made with a Beckman DK-2A instrument with a STL integrating sphere attachment. A paraboloid reflectometer was utilized for data at wave lengths between 2.0 microns and 26.0 microns.

A descirption of the samples tested with corresponding values of solar absorptance, α_s, and room temperature (80°F) normal and hemispherical emittance, ϵ_N and ϵ_H, are shown in Table C-I.

Table C-I

Sample Descriptions and Values of Solar Abosrptance, α_s, Normal and Hemispherical Room Temperature Emittance

Sample No.	Sample Description	Solar Absorptance, α_s	Normal Emittance, ϵ_N	Hemispherical Emittance, ϵ_H
1.	Gold, liquid bright, RLI (Reflective Laminates, Inc.) No. 381, two coats. Applied per RLI 1544 process, except maximum cure temperature was 675°F + 10°F for 60 minutes. Total dry film thickness 3 to 5 millionths of an inch. Substrate-titanium 6AL4V, 400-600 grit wet polish.	0.35	0.02	0.03
2.	Same as sample 1, except jewelers rouge polish also used on substrate.	0.37	0.02	0.03
3.	Same as sample 2.	0.40	0.02+	0.03+
4.	Same as sample 2, except tripoli polish also used on substrate.	0.42	0.02+	0.03+
5.	Same as sample 4.	0.42	0.02+	0.03+

Values of solar absorptance were obtained from the spectral reflectance data by summing the average reflectance in each of 25 wave length bands corresponding to four percent energy increments of the solar spectrum, obtaining the average solar reflectance, ρ_s, and then subtracting this value from unity. The normal emittance values were determined by multiplying the average reflectance in the various wave

length bands by the percentage of energy emitted by a Planckian radiator at 80°F in the same spectral bands, summing the resulting products, and then subtracting the sum from unity. Values of hemispherical emittance, ϵ_H, were determined by applying the theoretical values for the ratio of hemispherical to normal emittance found in Figures 13 through 15 of "Heat and Mass Transfer," by E. R. G. Eckert and R. M. Drake, Jr. (McGraw-Hill Book Company, Inc., New York, 1959).

Series B - The thermal radiation properties of a number of titanium specimens were measured. Table C-II contains a descirption of the test specimens and a summary of the test results. Samples 5 and 6 were exposed to TCA combustion products during a test firing in vacuum with the hemispherical emittance, ϵ_H, being the only property of interest. The solar absorptance, α_s, as well as the hemispherical emittance of four other titanium samples of varying surface finishes were determined. The values of emittance in Table C-II are room temperature data and provide only an indication of their properties at high temperatures.

The same measurement equipment used in Series A was used here.

Samples 5 and 6 were nonuniform in appearance. A "spot-check" of the emittance of the samples showed the values of normal emittance to vary widely over small areas on the material. The values shown in Table C-II may not, therefore, be representative of the case as a whole. They should, however, provide an indication of what values of α_s and ϵ_H can be expected.

Table C-II

Thermal Properties of Titanium Surfaces

Sample Description	Solar Absorptance, α_s	Hemispherical Emittance, ϵ_H
1. Titanium, 6Al-4V, 5 RMS Machine Finish.	.50	.17
2. Titanium, 6Al-4V, 8 RMS Machine Finish.	.50	.17
3. Titanium, 6Al-4V, 16 RMS Machine Finish.	.50	.18
4. Titanium, 6Al-4V, 12 RMS Machine Finish.	.50	.18
5. Titanium Portion of TCA Case After Firing (Sample #1).	---	.49
6. Titanium Portion of TCA Case After Firing (Sample #2).	---	.28

APPENDIX F

THEORETICAL THERMOCHEMICAL DATA ON MMH AND N_2O_4

No. of Pages: 10

APPENDIX F

THEORETICAL THERMOCHEMICAL DATA ON MMH AND N_2O_4

For a short period during the development effort in Phase III the propellants planned for flight use on Surveyor were MMH and N_2O_4 instead of MMH and MON which were used for most of the testing. Included here for information only is thermochemical data on MMH and N_2O_4. Similar data for MMH and MON are included in paragraph 7.1 of the main body of the report.

Figure F-1

THEORETICAL CHARACTERISTIC EXHAUST VELOCITY

Propellants: N_2O_4 - MMH

Conditions: Frozen Flow

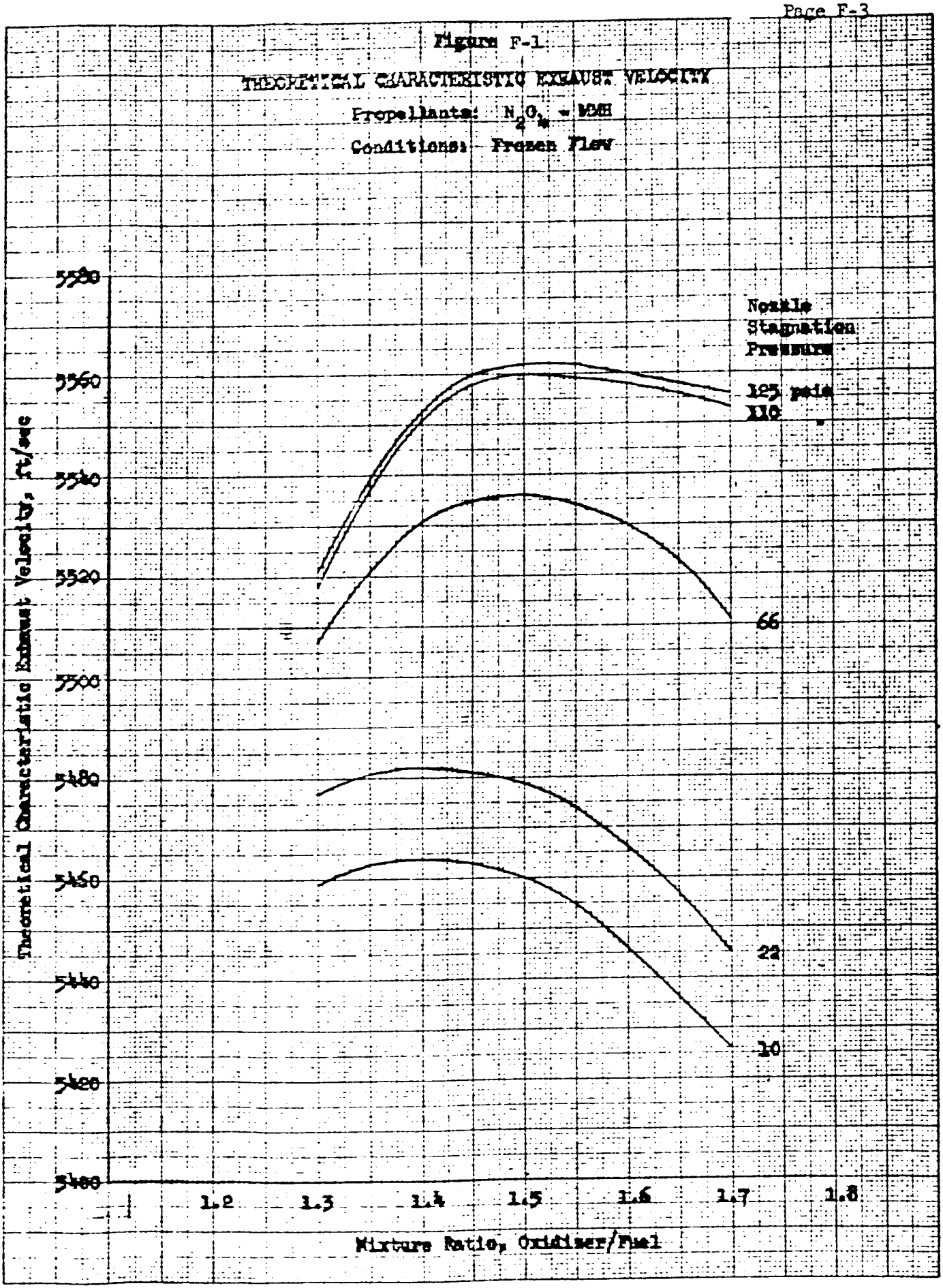

Figure F-2

THEORETICAL VACUUM THRUST COEFFICIENT

Propellants: N_2O_4 - MMH

Conditions: Frozen Flow

Use of Graph { Example: $C_{F,VAC}$ at P_{STD} = 60, MR = 1.3, ϵ = 32 is 1.7870
Example: $C_{F,VAC}$ at P_{STD} = 60, MR = 1.3, ϵ = 25 is 1.7839

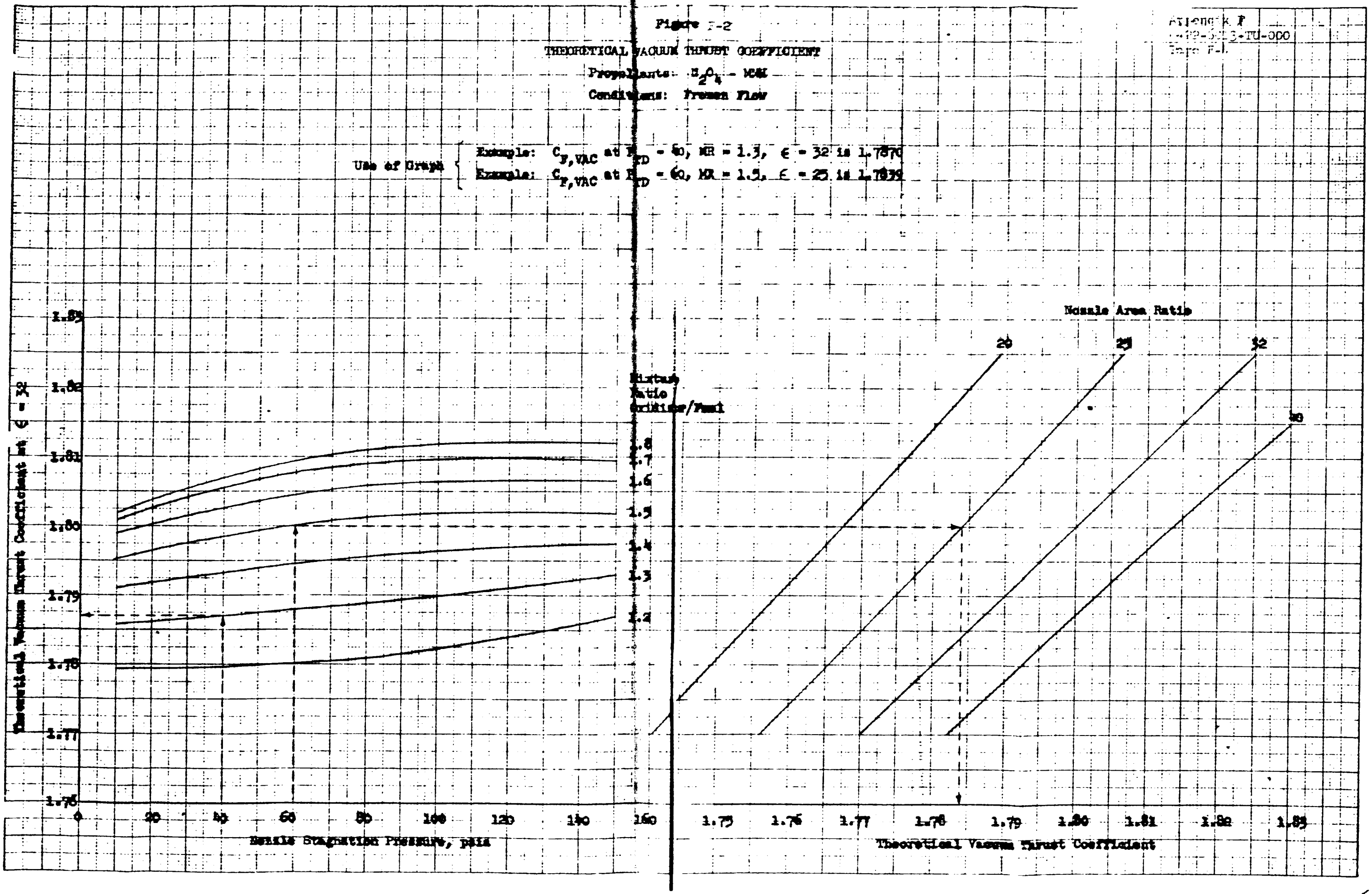

Figure F-3

THEORETICAL COMBUSTION GAS TEMPERATURE

Propellants: N_2O_4 - MMH

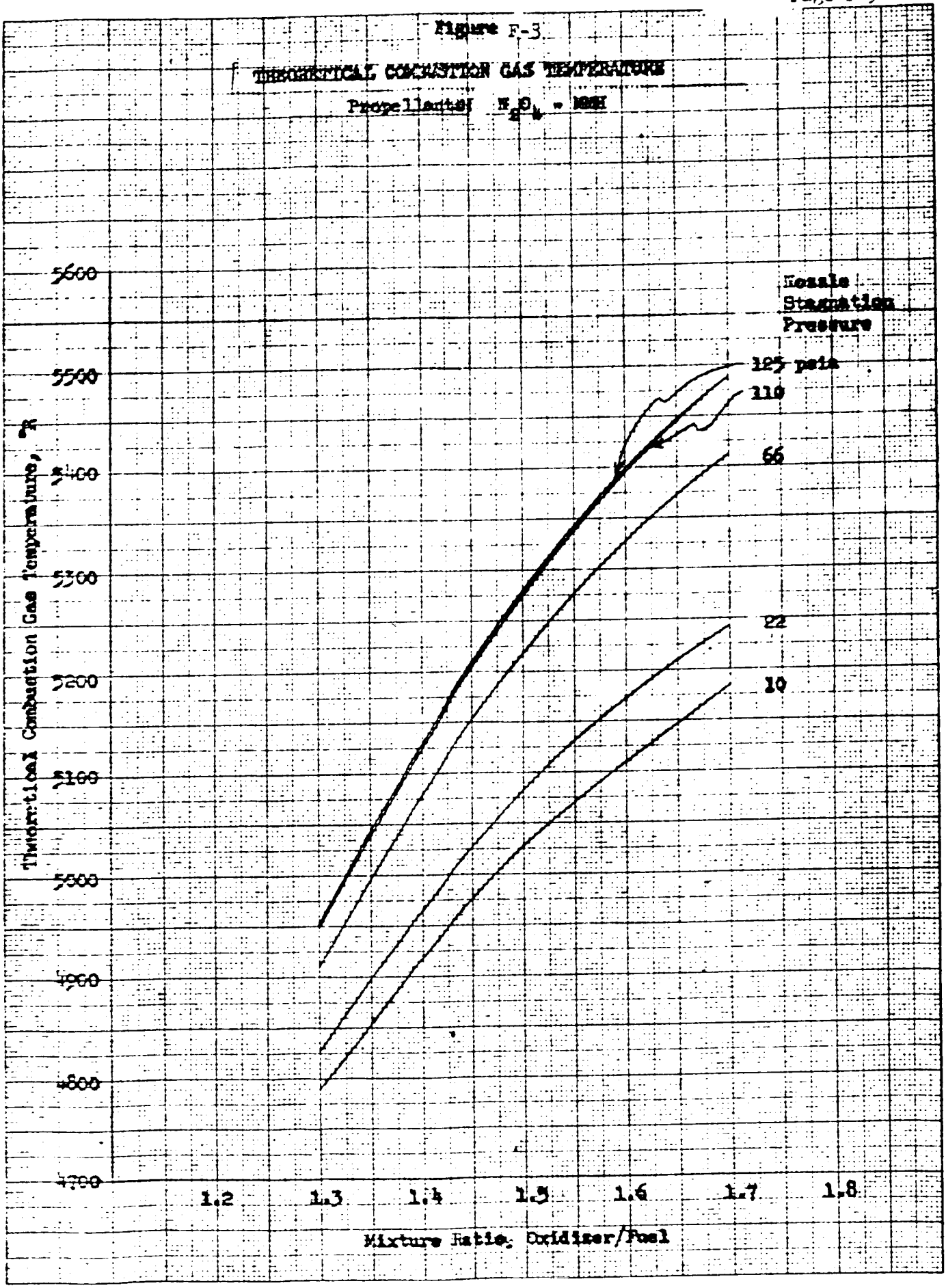

TABLE F-4

THEORETICAL CHARACTERISTIC EXHAUST VELOCITY

Propellants: N_2O_4 - MMH
Conditions: Frozen Flow

Nozzle Stagnation Pressure, psia	Mixture Ratio, Oxidizer/Fuel	Characteristic Exhaust Velocity, ft/sec
22	1.40	5482
	1.50	5479
	1.60	5466
66	1.40	5531
	1.50	5536
	1.60	5530
110	1.40	5551
	1.50	5560
	1.60	5558

TABLE F-5

THEORETICAL VACUUM THRUST COEFFICIENT

Propellants: N_2O_4 - MMH

Conditions: Frozen Flow

Nozzle Stagnation Pressure, psia	Mixture Ratio Oxidizer/Fuel	Nozzle Area Ratio	Vacuum Thrust Coefficient
22	1.40	16.300	1.7447
		21.729	1.7665
		26.657	1.7804
		31.241	1.7905
		35.567	1.7983
		39.687	1.8046
		43.639	1.8098
22	1.50	16.492	1.7494
		22.007	1.7715
		27.019	1.7857
		31.684	1.7960
		36.089	1.8039
		40.287	1.8103
		44.315	1.8156
22	1.60	16.653	1.7533
		22.242	1.7757
		27.324	1.7901
		32.058	1.8006
		36.530	1.8086
		40.795	1.8151
		44.888	1.8204
66	1.40	16.433	1.7481
		21.923	1.7701
		26.910	1.7843
		31.552	1.7945
		35.934	1.8023
		40.110	1.8087
		44.117	1.8140
66	1.50	16.653	1.7535
		22.242	1.7759
		27.325	1.7904
		32.060	1.8008
		36.533	1.8088
		40.800	1.8153
		44.895	1.8206

TABLE F-5 (CONT'D)

Nozzle Stagnation Pressure, psia	Mixture Ratio Oxidizer/Fuel	Nozzle Area Ratio	Vacuum Thrust Coefficient
66	1.60	16.839	1.7579
		22.513	1.7808
		27.679	1.7954
		32.494	1.8060
		37.046	1.8142
		41.388	1.8208
		45.559	1.8263
110	1.40	16.487	1.7494
		22.001	1.7715
		27.012	1.7858
		31.676	1.7960
		36.081	1.8039
		40.280	1.8103
		44.309	1.8156
110	1.50	16.720	1.7552
		22.341	1.7778
		27.454	1.7923
		32.218	1.8028
		36.720	1.8108
		41.014	1.8174
		45.138	1.8228
110	1.60	16.919	1.7599
		22.631	1.7829
		27.832	1.7977
		32.682	1.8084
		37.268	1.8166
		41.645	1.8232
		45.849	1.8288

TABLE F-6

THEORETICAL COMBUSTION GAS TEMPERATURE

Propellants: N_2O_4 - MMH

Nozzle Stagnation Pressure, psia	Mixture Ratio Oxidizer/Fuel	Combustion Gas Temperature ^oR
22	1.40	4965
	1.50	5082
	1.60	5172
66	1.40	5079
	1.50	5218
	1.60	5328
110	1.40	5125
	1.50	5275
	1.60	5396

TABLE F-7

THEORETICAL VACUUM THRUST COEFFICIENT

Propellants: N_2O_4 - MMH

Conditions: Frozen Flow

(Applicable for $20 < P_{TD} < 140$, $1.20 < MR < 1.8$, $20 < \epsilon < 40$)

$$C_{F,VAC} = C_{F,VAC}\ (P_{TD},\ MR,\ \epsilon)$$

$$C_{F,VAC}\ (P_{TD},\ 1.5,\ 32.0) = -0.5225 \times 10^{-6}\ P^2_{TD} + 1.2907 \times 10^{-4}\ P_{TD} + 1.7942$$

For MR 1.5

$$\left(\frac{\delta C_{F,VAC}}{\delta MR}\right) = -0.9237 \times 10^{-6}\ P^2_{TD} + 2.2815 \times 10^{-4}\ P_{TD} + 0.0120$$

For $MR \leq 1.5$

$$\left(\frac{\delta C_{F,VAC}}{\delta MR}\right) = -3.1626 \times 10^{-6}\ P^2_{TD} + 4.7716 \times 10^{-4}\ P_{TD} + 0.0492$$

For $\epsilon > 32$

$$\left(\frac{\delta C_{F,VAC}}{\delta \epsilon}\right) = 0.1250\ C^2_{F,VAC}\ (P_{TD},\ 1.5,\ 32.0) - 0.4393\ C_{F,VAC}\ (P_{TD},\ 15.,\ 32.0) + 0.3874$$

For $\epsilon \leq 32$

$$\left(\frac{\delta C_{F,VAC}}{\delta \epsilon}\right) = 3.5750 \times 10^{-2}\ C^2_{F,VAC}\ (P_{TD},\ 1.5,\ 32.0) - 0.1198\ C_{F,VAC}\ (P_{TD},\ 1.5,\ 32.0) + 0.1026$$

$$C_{F,VAC} = C_{F,VAC}\ (P_{TD},\ 1.5,\ 32.0) + \left(\frac{\delta C_{F,VAC}}{\delta MR}\right)(MR - 1.50) + \left(\frac{\delta C_{F,VAC}}{\delta \epsilon}\right)(\epsilon - 32.0)$$

APPENDIX H-1

RELIABILITY PARTS LIST - FINAL

No. of Pages: 11

APPENDIX H-1

RELIABILITY PARTS LIST - FINAL

The Reliability Parts List is presented for the combined accumulative testing on all three of the Surveyor Vernier TCAs: MIRA's 150, 180, and 150A. The 150A has three model designations: 150A-F (Flight weight), 150A-SL (Sea Level), 150A-SL-PT (Sea Level with Port-transducer).

Explorations of the Reliability Parts List column headings are presented below.

Part Number	-	All part numbers having the same descriptions are listed together.
Second Column	-	The particular head end designation to which the part belongs.
Order of Assembly	-	As presented in the engineering indentured parts list.
Part Description	-	As presented in the engineering indentured parts list.
Manufacturer's No.	-	Federal Supply Code for manufacturers.
Reliability Goal	-	Represents the apportioned reliability. A complete apportionment is listed for first and second order of assembly part numbers. A partial list appears for the third order.
Number of Tests	-	This column does not include tests during which an excluded failure occurred.
Cumulative Operating Time/Cycle	-	Time units are seconds. The figures do not include the time/cycles accumulated during a test in which an excluded failure occurred.
Number of Failures	-	The "total" column does not include the excluded failures. The "Exempt" column includes exclusions that are specified each month in the progress report under "Tabulation and Scoring of Test Data".
Estimated Reliability	-	Per Test = $\frac{\text{Successes}}{\text{No. of Tests}}$
		Per Mission = $\frac{(\text{Successes})\ (\text{Mission Time})^*}{\text{Cumulative Time}}$

The variations in the times and the number of tests are due to the excluded tests being subtracted from the total time and tests.

* Mission time used is 186 seconds.

SURVEYOR VERNIER ENGINE - Thrust Chamber Assembly

RELIABILITY PARTS LIST

Part Number		Order of Assembly	Part Description	Manufacturer's Number	Quantity Per Engine	Reliab. Goal	No. of Tests	Cumulative Operating Time	Cycles	No. of Failures Total	No. Exempt	No. of Parts Tested	Estimated Reliability Per Test	Per Mission	Failure Report Reference No.
103940-1	150	X	Thrust Chamber Assembly	11982* (STL)	1	.993	88	16380		4	2	4	.95454	.95454	
103940-1	150F	X			1		5	416			1	3	1.0	1.0	
105100-1	180A	X			1		1	46				1	1.0	1.0	
106662-2	150A-SL	X			1		61	7820		1	11	10	.98361	.97619	
106662-1	150A-F	X			1		10	657.8				4	1.0	1.0	
104452-2	150		Gasket, Head and Chamber		1		88	16380				4	1.0	1.0	
104452-2	150F				1		5	416				4	1.0	1.0	
104452-2	180A				1		1	46				1	1.0	1.0	
104452-2	150A-SL				1		61	7820				10	1.0	1.0	
104452-2	150A-F				1		10	657.8				4	1.0	1.0	
104453-3	150		Liner, Injector Head		1		88	16380				4	1.0	1.0	
104453-3	150F				1		5	416				4	1.0	1.0	
104453-1	180A				1		1	46				1	1.0	1.0	
104453-1	150A-SL				1		61	7820				10	1.0	1.0	
104453-1	150A-F				1		10	657.8				4	1.0	1.0	
105605-1	150		Chamber Assembly, Combustion		1	$.9^{(3)}_{47}$	88	16380			1	4	1.0	1.0	8887
105605-1	150F				1		5	416			1	4	1.0	1.0	8886, 9399
105605-1	180A				1		1	46				1	1.0	1.0	
106546-2	150A-SL				1		61	7820				44	1.0	1.0	
106546-1	150A-F				1		10	657.8				4	1.0	1.0	
105113-1	150		Shell, Combustion Chamber and Nozzle		1		88	16380				4	1.0	1.0	
105113-1	150F				1		5	416				4	1.0	1.0	
105113-1	180A				1		1	46				1	1.0	1.0	
105113-4	150A-SL				1		61	7820				10	1.0	1.0	
105113-3	150A-F				1		10	657.8				4	1.0	1.0	
105604-1	150		Liner Assembly, Combustion Chamber		1		88	16380				4	1.0	1.0	
105604-1	150F				1		5	416				4	1.0	1.0	
105604-1	180A				1		1	46				1	1.0	1.0	
106545-2	150A-SL				1		61	7820				10	1.0	1.0	
106545-1	150A-F				1		10	657.8				4	1.0	1.0	
106552-1	150A-SL		Screw, Retaining		6		61	7820				60	1.0	1.0	
106552-1	150A-F				6		10	657.8				24	1.0	1.0	
105601-1	150		Liner, Combustion Chamber		1		88	16380				4	1.0	1.0	
105601-1	150F				1		5	416				4	1.0	1.0	
105601-1	180A				1		1	46				1	1.0	1.0	
106541-1	150A-SL				1		61	7820				10	1.0	1.0	
106541-1	150A-F				1		10	657.8				4	1.0	1.0	

* All manufacturing numbers are the same except as noted.

SURVEYOR VERNIER ENGINE - Thrust Chamber Assembly

RELIABILITY PARTS LIST

Part Number		Order of Assembly							Part Description	Manufacturer's Number	Quantity Per Engine	Reliab. Goal	No. of Tests	Cumulative Operating Time	Cumulative Operating Cycles	No. of Failures Total	No. of Failures No. Exempt	No. of Parts Tested	Estimated Reliability Per Test	Estimated Reliability Per Mission	Failure Report Reference No.
105602-1	150				X				Liner Exit Cone		1		88	16380				4	1.0	1.0	
105602-1	150F				X						1		5	416				4	1.0	1.0	
105602-1	180A				X						1		1	46				1	1.0	1.0	
106543-2	150A-SL						X				1		61	7820				10	1.0	1.0	
106543-1	150A-F						X				1		10	657.8				4	1.0	1.0	
105603-1	150					X			Ring, Retainer		1		88	16380				4	1.0	1.0	
105603-1	150F					X					1		5	416				4	1.0	1.0	
105603-1	180A					X					1		1	46				1	1.0	1.0	
105603-2	150A-SL					X					1		61	7820				10	1.0	1.0	
105603-2	150A-F					X					1		10	657.8				4	1.0	1.0	
105145-2	150					X			Throat-Combustion Chamber Assembly		1		88	16380				4	1.0	1.0	
105145-2	150F					X					1		5	416				4	1.0	1.0	
105145-2	180A					X					1		1	46				1	1.0	1.0	
106558-2	150A-SL					X			Liner Assembly, Overwrap		1		61	7820				10	1.0	1.0	
106558-1	150A-F					X					1		10	657.8				4	1.0	1.0	
105144-1	150					X			Liner, Throat		1		88	16380				4	1.0	1.0	
105144-1	150F					X					1		5	416				4	1.0	1.0	
105144-1	180A					X					1		1	46				1	1.0	1.0	
106557-2	150A-SL					X			Liner Assembly, Exit Cone to		1		61	7820				10	1.0	1.0	
106557-1	150A-F					X			Combustion Chamber		1		10	657.8				4	1.0	1.0	
C105825-2	150						X		Forging, Tungsten		1		88	16380				4	1.0	1.0	
C105825-2	150F						X				1		5	416				4	1.0	1.0	
C105825-2	180A						X				1		1	46				1	1.0	1.0	
106547-1	150A-SL						X		Liner Assembly, Chamber		1		61	7820				10	1.0	1.0	
106547-1	150A-f						X				1		10	657.8				4	1.0	1.0	
106542-1	150A-SL							X	Insert, Chamber Liner JTA		1		61	7820				10	1.0	1.0	
106542-1	150A-f							X			1		10	657.8				4	1.0	1.0	
106544-1	150A-SL						X		Insert, Throat JTA		1		61	7820				10	1.0	1.0	
106544-1	150A-F						X				1		10	657.8				4	1.0	1.0	
103950-1	150	X							Head End Assembly, Engine		1		415	26577		11	16	4	.97357	.92673	
103950-1	150F	X									1		17	1274				4	1.0	1.0	
105110-1	180A	X									1		7	108				1	1.0	1.0	
106662-1	150A-SL	X									1		608	18964.7		6	41	10	.99003	.94682	
106662-1	150A-F	X									1		17	1020.8			1	4	1.0	1.0	

SURVEYOR VERNIER ENGINE - Thrust Chamber Assembly

RELIABILITY PARTS LIST

Part Number		Order of Assembly	Part Description	Manufacturer's Number	Quantity Per Engine	Reliab. Goal	No. of Tests	Cumulative Operating Time	Cumulative Operating Cycles	No. of Failures Total	No. of Failures No. Exempt	No. of Parts Tested	Estimated Reliability Per Test	Estimated Reliability Per Mission	Failure Report Reference No.
103952-1	150	X	Guide, Pintle - Head End		1		415	26577				4	1.0	1.0	
103952-1	150F	X			1		17	1274				3	1.0	1.0	
105106-1	180A	X			1		7	108				1	1.0	1.0	
105106-1	150A-SL	X			1		596	18050.7				10	1.0	1.0	
105106-1	150A-F	X			1		17	1020.8				4	1.0	1.0	
103953-1	150	X	Pintle, Injector - Head End		1		415	26577				4	1.0	1.0	
103953-1	150F	X			1		17	1274				3	1.0	1.0	
105107-1	180A	X			1		7	108				1	1.0	1.0	
105107-1	150A-SL	X			1		596	18050.7				10	1.0	1.0	
105107-1	150A-F	X			1		17	1020.8				4	1.0	1.0	
103943-1	150	X	Yoke Assembly, Acuation, Injector		1		415	26577				4	1.0	1.0	
103943-1	150F	X	Sl		1		17	1274				3	1.0	1.0	
105108-1	180A	X			1		7	108				1	1.0	1.0	
105108-1	150A-SL	X			1		596	18050.7				10	1.0	1.0	
105108-1	150A-F	X			1		17	1020.8				4	1.0	1.0	
103958-1	150	X	Arm, Head End		1		415	26577				4	1.0	1.0	
103958-1	150F	X			1		17	1274				3	1.0	1.0	
105109-1	180A	X			1		7	108				1	1.0	1.0	
105109-3	150A-SL	X			1		596	18050.7				10	1.0	1.0	
105109-3	150A-F	X			1		17	1020.8				4	1.0	1.0	
103942-3	150	X	Bushing, Arm and Yoke		2		415	26577				8	1.0	1.0	
103942-3	150F	X			2		17	1274				6	1.0	1.0	
103942-2	180A	X			2		7	108				2	1.0	1.0	
103942-2	150A-SL	X			2		596	18050.7				20	1.0	1.0	
103942-2	150A-F	X			2		17	1020.8				8	1.0	1.0	
103976-1	150	X	Bushing, Arm and Pin		2		415	26577				8	1.0	1.0	
103976-1	150F	X			2		17	1274				6	1.0	1.0	
103976-3	180A	X			2		7	108				2	1.0	1.0	
103976-3	150A-SL	X			2		596	18050.7				20	1.0	1.0	
103976-3	150A-F	X			2		17	1020.8				8	1.0	1.0	
103779-1	150	X	Pin, Arm and Body		2		415	26577				8	1.0	1.0	
103779-1	150F	X			2		17	1274				6	1.0	1.0	
105126-1	180A	X			2		7	108				2	1.0	1.0	
105126-1	150A-SL	X			2		596	18050.7				20	1.0	1.0	
105126-1	150A-F	X			2		17	1020.8				8	1.0	1.0	
105137-1	180A	X	Cap, Body - Head End		1		7	108				1	1.0	1.0	
105137-1	150A-SL	X			1		596	18050.7				10	1.0	1.0	
105137-1	150A-F	X			1		17	1020.8				4	1.0	1.0	

SURVEYOR VERNIER ENGINE - Thrust Chamber Assembly

RELIABILITY PARTS LIST

Part Number		Order of Assembly	Part Description	Manufacturer's Number	Quantity Per Engine	Reliab. Goal	No. of Tests	Cumulative Operating Time	Cycles	No. of Failures Total	No. Exempt	No. of Parts Tested	Estimated Reliability Per Test	Per Mission	Failure Report Reference No.
	150	X	Seals, Omniseals		4		415	26577		1			.99759	.99301	8819
	150F	X			4		17	1274				6	1.0	1.0	
	150A-SL	X			4		596	18050.7		1		20	.99832	.98969	10792
105119-1	180A	X	Cap, Arm - Head End		1		7	108					1.0	1.0	
105119-3	150A-SL	X			1		596	18050.7				10	1.0	1.0	
105119-3	150A-F	X			1		17	1020.8					1.0	1.0	
103129-1	180A	X	Shim, Arm Cap - Head End		1		7	108					1.0	1.0	
105129-1	150A-SL	X			1		596	18050.7				10	1.0	1.0	
105129-1	150A-F	X			1		17	1020.8					1.0	1.0	
105478-1	180A	X	Nut, Pintle Sealing		1		7	108					1.0	1.0	
105478-1	150A-SL	X			1		596	18050.7				10	1.0	1.0	
105478-1	150A-F	X			1		17	1020.8					1.0	1.0	
106748-1	150A-SL	X	Stop, Yoke - Injector		1		596	18050.7				10	1.0	1.0	
106748-1	150A-F	X			1		17	1020.8				4	1.0	1.0	
106748-2	150A-SL	X	Stop, Yoke - Injector		1		596	18050.7				10	1.0	1.0	
106748-2	150A-F	X			1		17	1020.8				4	1.0	1.0	
106745-1	150A-SL	X	Filter Assembly - Dust		1		596	18050.7				10	1.0	1.0	
106745-1	150A-F	X			1		17	1020.8				4	1.0	1.0	
106746-1	150A-SL	X	Filter - Dust		1		596	18050.7				10	1.0	1.0	
106746-1	150A-F	X			1		17	1020.8				4	1.0	1.0	
106747-1	150A-SL	X	Ring, Screen Retainer		1		596	18050.7				10	1.0	1.0	
106747-1	150A-F	X			1		17	1020.8				4	1.0	1.0	
106743-1	150A-SL	X	Cover, Dust Injector		1		596	18050.7				10	1.0	1.0	
106743-1	150A-F	X			1		17	1020.8				4	1.0	1.0	
106744-1	150A-SL	X	Spring, Cover - Injector		1		596	18050.7				10	1.0	1.0	
106744-1	150A-F	X			1		17	1020.8				4	1.0	1.0	
106776-1	150A-SL	X	Shim, Flexure - Head End		1		596	18050.7				10	1.0	1.0	
106776-1	150A-F	X			1		17	1020.8				4	1.0	1.0	
105122-1	180A	X	Stud-Head End		1		7	108				1	1.0	1.0	
105122-1	150A-SL	X			1		596	18050.7				10	1.0	1.0	
105122-1	150A-F	X			1		17	1020.8				4	1.0	1.0	

SURVEYOR VERNIER ENGINE - Thrust Chamber Assembly

RELIABILITY PARTS LIST

Part Number		Order of Assembly	Part Description	Manufacturer's Number	Quantity Per Engine	Reliab. Goal	No. of Tests	Cumulative Operating Time	Cycles	No. of Failures Total	No. Exempt	No. of Parts Tested	Estimated Reliability Per Test	Per Mission	Failure Report Reference No.
103960-1	150	X	Valve Assembly, Flow Control		1	$.9^{(3)}_{20}$	413	26542		3	2	4	.99275	.97902	8856,8857,9334,9387,
103960-1	150F	X			1		17	1274				3	1.0	1.0	9394
105115-1	180A	X			1		7	108				1	1.0	1.0	
106609-1	150A-SL	X			1		608	18964.7		1		10	.99836	.99020	10795
106609-1	150A-F	X			1		17	1020.8				4	1.0	1.0	
103967-1	150		Body - Flow Control Valve Assembly		1		415	26577				4	1.0	1.0	
103967-1	150F				1		17	1274				3	1.0	1.0	
105111-1	180A				1		7	108				1	1.0	1.0	
105467-3	150A-SL				1		608	18964.7				10	1.0	1.0	
105467-3	150A-F				1		17	1020.8				4	1.0	1.0	
103962-1	150	X	Body-Flow Control Valve		1		415	26577				4	1.0	1.0	
103962-1	150F	X			1		17	1274				3	1.0	1.0	
105112-1	180A	X			1		7	108				1	1.0	1.0	
105468-3	150A-SL	X			1		608	18964.7				10	1.0	1.0	
105468-3	150A-F	X			1		17	1020.8				4	1.0	1.0	
103959-1	150	X	Plug-Flow Control Valve		1		415	26577				4	1.0	1.0	
103959-1	150F	X			1		17	1274				3	1.0	1.0	
105470-2	150A-SL	X			1		608	18964.7				10	1.0	1.0	
105470-2	150A-F	X			1		17	1020.8				4	1.0	1.0	
103956-1	150	X	Sleeve-Flow Control Valve		1		415	26577				4	1.0	1.0	
103956-1	150F	X			1		17	1274				3	1.0	1.0	
105130-1	180A	X	Cup, Body-Flow Control Valve		2		7	108				2	1.0	1.0	
105469-2	150A-SL	X			2		608	18964.7				20	1.0	1.0	
105469-2	150A-F	X			2		17	1020.8				8	1.0	1.0	
103954-1	150	X	Pintle, Valve-Flow Control		2		415	26577				8	1.0	1.0	
103954-1	150F	X			2		17	1274				6	1.0	1.0	
105116-1	180A	X			2		7	108				2	1.0	1.0	
106608-3	150A-SL	X			2		608	18964.7				24	1.0	1.0	
106608-3	150A-F	X			2		17	1020.8				8	1.0	1.0	
103954-2	150	X	Pintle, Valve-Flow Control		2		415	26577				8	1.0	1.0	
103954-2	150F	X			2		17	1274				6	1.0	1.0	
105116-2	180A	X			2		7	108				2	1.0	1.0	
106608-4	150A-SL	X			2		608	18964.7				24	1.0	1.0	
106608-4	150A-F	X			2		17	1020.8				8	1.0	1.0	
103957-1	150	X	Nut, Valve-Flow Control		2		415	26577				8	1.0	1.0	
103957-1	150F	X			2		17	1274				6	1.0	1.0	
105136-1	180A	X			2		7	108				2	1.0	1.0	
105607-3	150A-SL	X			2		608	18964.7				0	1.0	1.0	
105607-3	150A-F	X			2		17	1020.8				8	1.0	1.0	

SURVEYOR VERNIER ENGINE - Thrust Chamber Assembly

RELIABILITY PARTS LIST

Part Number		Order of Assembly	Part Description	Manufacturer's Number	Quantity Per Engine	Reliab. Goal	No. of Tests	Cumulative Operating Time	Cycles	No. of Failures Total	No. Exempt	No. of Parts Tested	Estimated Reliability Per Test	Per Mission	Failure Report Reference No.
	150	X	Seals - Omniseals	Reid Enterprises	5		415	26577		2		20	.99518	.96601	8857,8856
	150F	X			5		17	1274				15	1.0	1.0	
	180A	X			5		7	108				5	1.0	1.0	
	150A-SI	X			5		608	18964.7		1		50	.99836	.99020	10795
	150A-F	X			5		17	1020.8				20	1.0	1.0	
103961-1	150	X	Washer Valve-Flow Control		2		415	26577				8	1.0	1.0	
103961-1	150F	X			2		17	1274				6	1.0	1.0	
105135-1	180A	X			2		7	108				2	1.0	1.0	
106672-1	150A-SI	X			2		608	18964.7				20	1.0	1.0	
106672-1	150A-F	X			2		17	1020.8				8	1.0	1.0	
103956-1	150	X	Insert, Inlet-Flow Control Valve		2		415	26577				8	1.0	1.0	
103956-1	150F	X			2		17	1274				6	1.0	1.0	
105131-1	180A	X			2		7	108				2	1.0	1.0	
105131-2	150A-SI	X			2		608	18964.7				28	1.0	1.0	
105131-2	150A-F	X			2		17	1020.8				8	1.0	1.0	
103957-1	150	X	Insert, Throat-Flow Control Valve		2		415	26577				8	1.0	1.0	
103957-1	150F	X			2		17	1274				6	1.0	1.0	
105132-1,2	180A	X			2		7	108				2	1.0	1.0	
105132-4	150A-SI	X			2		608	18964.7				28	1.0	1.0	
105132-4	150A-F	X			2		17	1020.8				8	1.0	1.0	
103959-1	150	X	Insert, Pintle-Flow Control Valve		2		415	26577				8	1.0	1.0	
103959-1	150F	X			2		17	1274				6	1.0	1.0	
105133-1	180A	X			2		7	108				2	1.0	1.0	
105133-1	150A-SI	X			2		608	18964.7				26	1.0	1.0	
105133-1	150A-F	X			2		17	1020.8				8	1.0	1.0	
105146-3	150A-SI	X	Nut, Body-Flow Control Valve		2		608	18964.7				20	1.0	1.0	
105146-3	150A-F	X			2		17	1020.8				8	1.0	1.0	
103946-1	150	X	Poppet, Valve Shutoff		2		412	26507				8	1.0	1.0	
103946-1	150F	X			2		17	1274				6	1.0	1.0	
103946-1	180A	X			2		7	108				2	1.0	1.0	
106798-1	150A-SI	X			2		593	18679.7				26	1.0	1.0	
106798-1	150A-F	X			2		17	1020.8				8	1.0	1.0	
103947-3	150	X	Sleeve, Valve Shutoff		2	.99860	412	26507		3	2	13	.99875	.97903	9395,9400,9358,8852,
103947-3	150F	X			2		17	1274				6	1.0	1.0	8812
103947-3	180A	X			2		7	108				2	1.0	1.0	
106656-1	150A-SI	X			2		593	18679.7		1	15	26	.99834	.99001	9383,9381,8862,9370,
106656-1	150A-F	X			2		17	1020.8				8	1.0	1.0	9367,10791,9369,9358, 9351,8863,9382,9384, 9366,9385,9360,10796

SURVEYOR VERNIER ENGINE - Thrust Chamber Assembly

RELIABILITY PARTS LIST

Part Number		Order of Assembly	Part Description	Manufacturer's Number	Quantity Per Engine	Reliab. Goal	No. of Tests	Cumulative Operating Time	Cumulative Operating Cycles	No. of Failures Total	No. of Failures No. Exempt	No. of Parts Tested	Estimated Reliability Per Test	Estimated Reliability Per Mission	Failure Report Reference No.
C104337-1	150		Valve, Solenoid Operated	Eckel	1	$.9^{(3)}_{09}$	414	[illegible]577	414	1	1	4	.99758	.99515*	8820,8861
C104337-1	180A			(BF63C-1)	1		7	108	7			1	1.0	1.0	
C104337-1	150A-SL			Adel	1		601	[illegible]95.7	601	1	7	10	.99834	.99667*	9357,9361,9362,9389,
C104337-1	150A-F			(71135)	1		17	1020.8	17			4	1.0	1.0	10036,10918,11526, 9390
C105183-1	150A-SL		Filter, Propellant	FE1304	2	.99961	608	[illegible]4.7				20	1.0	1.0	
C105183-1	150A-F				2		17	1020.8				8	1.0	1.0	
C219217-1	150		Servo Actuator	Hyd.Research	1	.99790	56	[illegible]33		3	8	4	.94043	.85000	9331,9332,9333,9335,
C219217-1	150F			(300500-1)	1		15	10.9				3	1.0	1.0	8818,8870,8859,8815,
C219217-1	180A			Cad.Gage	1		7	108				1	1.0	1.0	8868,8876,8858
C219217-1	150A-SL			(22003)	1		205	[illegible]72.7			7	6	1.0	1.0	10797,9354,9374,9355
C219217-1	150A-F				1		16	640.8			1	4	1.0	1.0	

*Because H_e Solenoid Valve is more sensitive to cycles than to time, mission reliability is computed on that basis.

APPENDIX H-2

SURVEYOR VERNIER THRUST CHAMBER ASSEMBLY

PERFORMANCE RELIABILITY ANSLYSIS

No. of Pages: 27

FORWARD

The analysis contained in this report was performed to meet the need for a mission reliability evaluation of the SURVEYOR Vernier Engine Thrust Chamber Assembly with respect to its critical performance parameters. Sufficient performance parameter data were not available to fully utilize all aspects of the reliability model. The model was designed to accommodate data that would have added by the Qualification Program to that currently available.

TABLE OF CONTENTS

17

INTRODUCTION

Performance Reliability is defined for the SURVEYOR Vernier Engine Thrust Chamber Assembly as the probability, for a specified SURVEYOR mission, that each of the critical TCA parameters will have a value that is within the parameter specification limits. When this analysis was initiated the following procedure was planned. Firstly to define a sequence of mission events and the parameters involved together with their design specification limits. Secondly, a determination was to be made of a frequency function for each of the parameters, treated as variables. If a frequency function appeared to be non-normal a transformation would be sought such that the properties of the normal distribution could be utilized for such statistics as tolerance intervals. Thirdly, a determination of dependence (or independence) between parameters was to be made. If dependence between two parameters existed a bivariate distribution would have to be determined. Because of a restriction on time and data the approach above was curtailed. The probability of success of all events of the mission, defined below, could not be calculated. Data was sufficient for three parameters: mixture ratio, specific impulse, and characteristic velocity. Correlation studies could not be made and so independence was assumed between parameters (as variables). The probability of a mission success is then based on the three above parameters. Normality was verified graphically by fractile plots. Two statistics (besides mean & variance) were calculated for each parameter with the exception of characteristic velocity (C*). The first one is the probability, under the assumptions of normality, sample mean $\bar{X}$ = true mean μ and sample variance S^2 = true variance σ^2,

that each parameter is within its specified limits. Since C* does not have design limits specified, the statistic is not calculated for it. The second statistic is more conservative and is the same probability as the first but determined under the condition that $\bar{X} \pm KS$ will contain the area under the normal curve that represents this probability, the probability statement made at 80% confidence and also $\bar{X} \pm KS$ is contained in the specification limits. $\bar{X}$ is the sample mean, S the sample standard deviation, and K a positive constant. $\bar{X} \pm KS$ is commonly known as a tolerance interval. Finally, these two statistics are combined in the model of the following sections to form two cases. For this exercise independence of events is assumed.

SUMMARY OF RESULTS

In the table below

P_R = the probability that the mixture ratio value for one engine during one continuous firing is within its required limits.

$P_{I\,1}$ = the probability that the specific impulse value for one engine during one continuous firing is within its required limits defined at 90-158 lbs. thrust.

$P_{I\,2}$ = the same as $P_{I\,1}$ except defined for 70-85 lbs. thrust.

$P_{I\,2}$ = the same as $P_{I\,1}$ except defined for 30-150 lbs. thrust.

$P_{I\,3}$ = the same as $P_{I\,1}$ except defined for 100-150 lbs. thrust.

$P_{I\,4}$ = the same as $P_{I\,1}$ except defined for 30-50 lbs. thrust.

$P_{I\,5}$ = the same as $P_{I\,1}$ except defined for 30-60 lbs. thrust.

These estimates are based on the assumptions that the sample mean $\bar{X}$ is equal to the true mean μ, the sample variance, S^2, is equal to the true variance σ^2, and the variables are distributed normally. An estimate of this type is not made for the characteristic velocity (C*) since its required limits are not yet specified. From these estimates, probability estimates for three engines, $P_R{}^3$ and $P_{Ij}{}^3$ ($j = 1,2,3,4,5$) is calculated. These values are then entered into the mission event model given in the next section to obtain an estimate $\hat{P}(S)$ of P(S) the probability of mission success. A more conservative estimate is obtained for P(S) if we substitute for P_R & P_I $P_R{}^*$ & $P_{I\,1}{}^*$ the probability values under the normal distribution for 80% tolerance intervals. $P_R{}^{*3}$ & $P_{Ij}{}^{*3}$ ($j = 1,2,3,4,5$) are

calculated again leading to P* (S), another estimate of P(S). As mentioned in the Introduction, specified limits for C* are not available. However tolerance limits containing 0.999 of the population at 80% confidence were calculated and are symbolized by $\bar{X} \pm KS$ in the table.

TABLE OF RESULTS

Method of Point Estimates		Method of Tolerance Interval	
P_R	0.99995	P_R*	0.99982
P_R3	0.99985	P_R*3	0.99946
$P_{I\ 1}$	0.99883	$P_{I\ 1}$*	0.99315
$P_{I\ 13}$	0.99649	$P_{I\ 1}$*3	0.97959
$P_{I\ 2}$	0.99883	$P_{I\ 2}$*	0.99315
$P_{I\ 23}$	0.99649	$P_{I\ 2}$*3	0.97959
$P_{I\ 3}$	0.99883	$P_{I\ 3}$*	0.99315
$P_{I\ 33}$	0.99646	$P_{I\ 3}$*3	0.97959
$P_{I\ 4}$	0.99995	$P_{I\ 4}$*	0.99984
$P_{I\ 43}$	0.99985	$P_{I\ 4}$*3	0.99952
$P_{I\ 5}$	0.99995	$P_{I\ 5}$*	0.99984
$P_{I\ 53}$	0.99985	$P_{I\ 5}$*3	0.99952
P(S)	0.9848	P*(S)	0.9170

For C*: $\bar{X} \pm KS$ = 5267.6 ± 413.88 sec. will contain 0.999 of the population at 80% confidence.

TCA RELIABILITY PERFORMANCE ANALYSIS
EVENT MODEL

Prior to any analytic attack on the problem, a review of critical performance parameters affecting reliability was made that resulted in a list of parameters to be used as inputs to define mission success events. If a particular parameter is treated as a variable and variability limits specified, then a sub-event of the event of success is defined. A description was made of events and their sequence necessary to complete a successful mission. However, at this writing insufficient data exists for some parameters so that exercising the model in its entirety is not possible. A list of events that make up the model for a successful mission for one TCA is presented below together with a status of the data required.

a. Start Time Event No. 1 - Event consisting of sub-events following the initiation of an electrical signal to the helium pilot valve such that 90% of the selected thrust is accomplished in less than 130 msecs.

Data: Samples of elapsed time to perform sub-events from a sample space similar to that expected in a mission configuration. Data is unavailable at this time.

b. Continuous Operation Event No. 1 - A success event occurs in this case if each event of any set of values of the critical steady-state parameter lies within its required interval. The parameters (or variables in this case) are: thrust, vacuum specific impulse (I_{sp}) at the indicated thrust range, mixture ratio (vacuum conditions), corrected characteristic velocity (C*) at the indicated thrust range.

Data: Samples of the above variables at proper environment and specified chamber type. (All

the TCA test results will be corrected to standard inlet conditions for homogeneity of data.) Data to date is sufficient only on vacuum specific impulse (I_{sp}) 90-158 lbs. thrust, mixture ratio, and corrected characteristic velocity (C*).

c. Shutdown Time Event - Event consisting of the removal of electrical signal from the switch which controls the helium pilot valve until 95% of the total shutdown impulse has been generated, all accomplished in less than 80 msecs.

Data: Samples of elapsed time to perform this event from a sample space similar to that expected in a mission configuration. Data is unavailable at this time.

d. Start Time Event No. 2 - Same as a. above.

Data: Same as a. above.

e,f,g,h,&i. Continuous Operation Events No. 2, 3, 4, 5, & 6

Same as b. above with different steady-state thrust levels, and therefore different ranges for I_{sp}

Data: Same as b. above.

j. This event occurs if the thrust levels T_e, T_f, T_g, T_h, & T_i of events e, f, g, h, & i form a complete and continuous thrust excursion and the width of all thrust vs. servoactuator control current loops is less than 2.5 ma or 15.0 percent of the control current excursion, whichever is greater.

Data: Cal-Comp plots of thrust loops. Data not available at this time.

k. This event occurs if the servoactuator control current during e, f, g, h, & i is a monotonic function of time and the slope of the thrust-servoactuator current curve thereby created, is between 0.7 lb/ma and 1.0 lb/ma.

Data: Cal-Comp plots of thrust loops. Data not available at this time.

It is assumed in this model that the TCA is of the ablative type. Therefore, data from ablative type testing is used unless data from other types, via statistical analysis, can be combined with the ablative results. Also, Edwards test site data is used because the configuration at that site has juxtaposition with respect to the expected final configuration. The data are based upon a reduction to standard inlet conditions of 720 psia venturi inlet pressures and 70° F propellant temperatures.

I. Mixture Ratio

A. Estimates of μ, σ^2: Unbiased estimates of the population variance, σ^2, were calculated separately from 21 acceptance tests at Inglewood Test Site and JPL Edwards Test Site. The data from Inglewood are from water-cooled test chambers and the data from Edwards are from water-cooled and ablative type chambers. Each test generates a sample by "slicing" of the data and sample number or number of slices ranged from 1 to 26 over the 21 samples. Besides the 21 estimates of population variance, the means of the 21 samples were calculated. However, the data appears to indicate that the mixture ratio mean value is the result of a "setting" made for each test and varies from test to test as a function of human as well as mechanical variability. The mixture ratio variable within samples is considered to be a random variable. Therefore, variances were pooled but not sample means. The mean of the mixture ratio is assumed to be 1.5. Even though the mean obtained from pooling all 21 sample means is $\bar{X} = 1.501185$, it is not a verification of the assumption that $\mu = 1.5$. The data of the ablative TCA test at Edwards is partitioned by order of magnitude of variance estimates into two sets, A & A' where the elements of A are S_i, $i = 1, 2, 3, 4$. And the elements of A' are S_i', $i = 1, 2, 3$. Estimates of the population variance were made from the elements of A & A' using $S^2 = \sum_{i=1}^{K} f_i S_i^2 \Big/ \sum_{i=1}^{K} f_i$

for K samples with f_i the degrees of freedom of the computation for S_i.

The results were

$S^2 = 0.000661$ for A

& $S'^2 = 0.001930$ for A',

Where $\sum N_i = 32$, $K = 4$ for A

& $\sum N_i' = 24$, $K = 3$ for A',

Let $F = \frac{S^2}{S'^2} = \frac{.000661}{.001930} = 0.342$

An F ratio test at the .01 level of significance yields an acceptance region of $0.340 < F < 3.21$. The value of F "falls in too close" at the high level of significance so that the two estimates of σ^2 are considered to be from two populations. However, a sample of 5 tests of 45 slices total yielded a variance estimate of $S^2 = .000560$ for <u>water cooled</u> TCA units at Edwards Test Site. By pooling this estimate we obtain $S^2 = .000602$ with 68 degrees of freedom. Based on its much larger number of sample points we take $S^2 = .000602$ as the variance estimate of the mixture ratio parameter rather than $S^2 = .001930$.

$S^2 = 0.000602$ yields

$S = 0.0246$ as an estimate of the standard deviation.

B. Assumption of Normality

The assumption that the variable of mixture ratio is normally distributed has some verification when one observes the plots of the fractiles approximating the distribution function. Figure 0 shows data points from a sample of 19 mixture ratio measurements of the ablative type chamber and Figure 1 shows a fractile diagram for water-cooled chamber results from the Inglewood Test Site with a sample of N = 26.

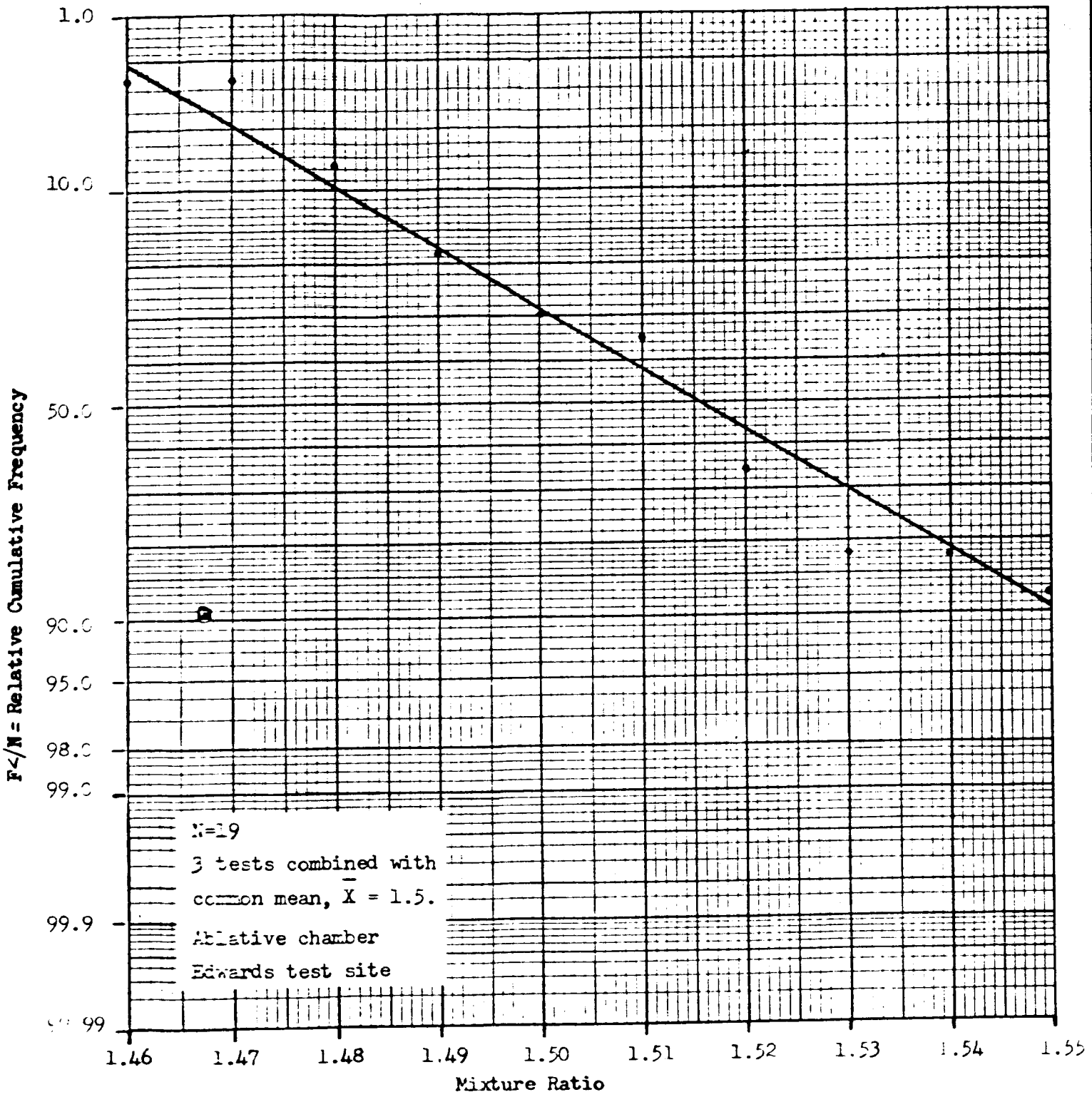

Figure 0: Fractile plot for mixture ratio sample

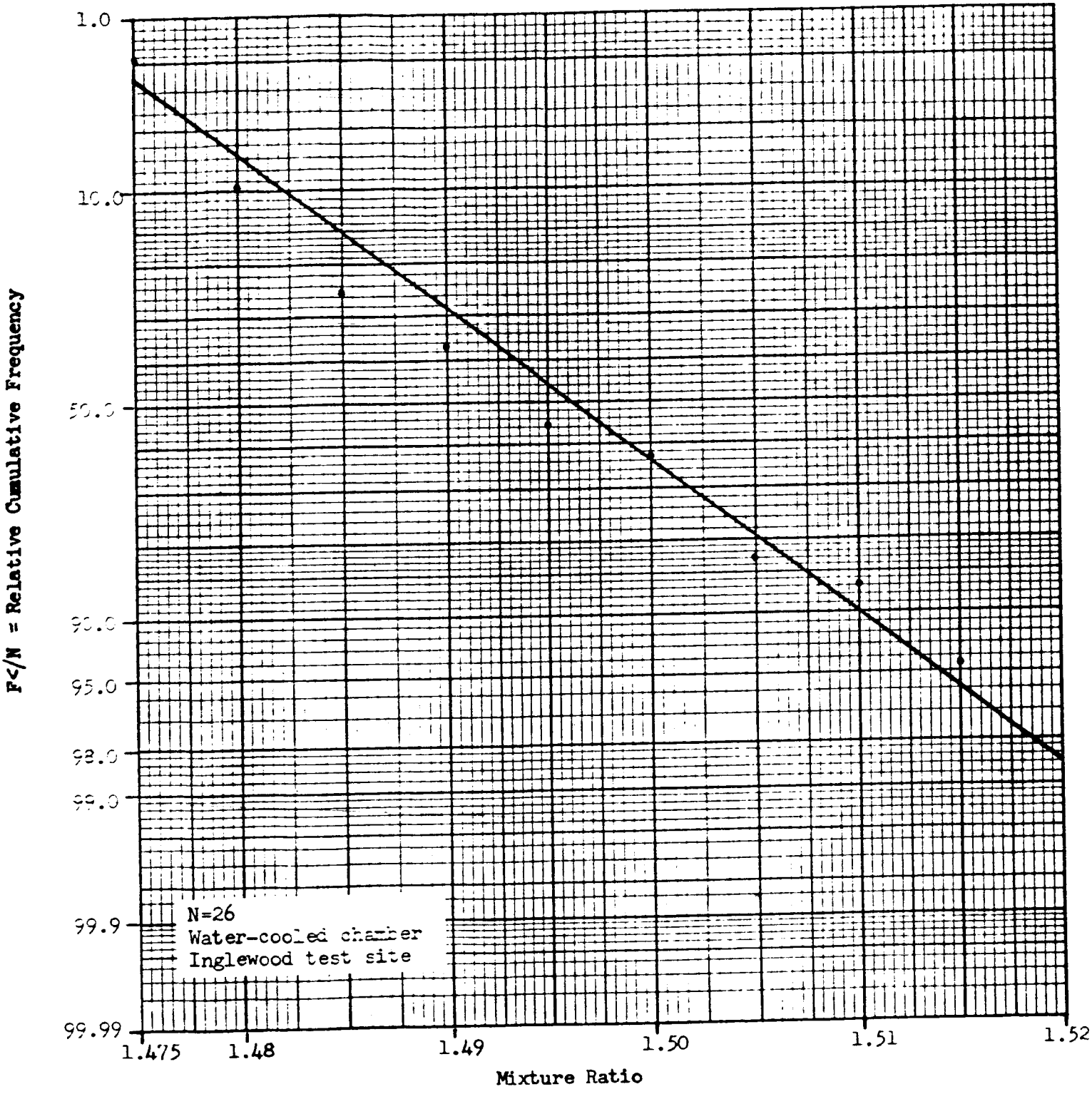

Figure 1: Fractile plot for mixture ratio sample

C. Calculation of Statistics from Mixture Ratio Data

We assume the normal density function $\Phi(X)$, for mixture ratio and calculate, $\hat{P}_R$, the estimate of steady-state probability P_R, or the probability at any point in time during the operation of one TCA that the value of mixture ratio will be in the interval $[1.4, 1.6]$ which represents the current specification limits. $\therefore X \in [1.4, 1.6]$ defines a successful event where X is a value of mixture ratio. Taking $\hat{\mu} = 1.5$ & $\hat{\sigma} = 0.0246$

yields $\hat{P}_R = \int_{\frac{1.4-1.5}{.0246}}^{\frac{1.6-1.5}{.0246}} \Phi(X)\, dX = 0.99995$

With the mean, μ, of the population of mixture ratio values assumed known S^2 will vary from sample to sample. So, consider the problem of finding a value K such that $\mu \pm KS$ will contain at least $1-\alpha$ of the population with 100P% confidence, $0 < \alpha < 1$, $0 < P < 1$. $\mu \pm KS$ are the sample tolerance limits. From theory we know $K = j_{1-\frac{\alpha}{2}} \sqrt{\frac{f}{\chi^2_{1-P}}}$ where f is the degrees of freedom & $j_{1-\frac{\alpha}{2}}$ is defined by $\int_{\mu - j_{1-\frac{\alpha}{2}}\sigma}^{\mu + j_{1-\frac{\alpha}{2}}\sigma} \Phi(X) = 1 - \alpha$

From, χ^2 tables with $1-\alpha = 0.999,82$ $f = 68$

& $P = 0.80$ $K = 4.06$

or $KS = 4.06 \times .0246$

$= 0.10$

Or there is 80% confidence that at least 0.99982 of the population is contained in $1.5 \pm .10$.

Implicit, in the use of either of these statistics as the probability of success for proper mixture ratio is the

assumption that these estimates of the probability of success hold over a finite time interval of TCA operation.

II. Specific Impulse (I_{sp}), (90-150# thrust range)

A. Estimate of μ, σ^2:

I_{sp} data utilized was as follows:

5 samples (tests with slices) of water-cooled chamber firings at Inglewood,

5 samples of water-cooled chamber firings at ETS &

7 samples of ablative chamber firings at ETS.

There is no significant difference in means between abalative - ETS & water-cooled - ETS with means of $\bar{X}$ = 290.56 sec. & $\bar{X}$ = 289.15 sec. respectively from sample sizes of 27 & 22 respectively. There is a significant difference between the data from these configuration-sites & the water-cooled tests at Inglewood. The latter is excluded since ablative - ETS data is to be preferred. The pooled value of estimated mean from ETS is $\bar{X}$ = 289.97 sec. The data with respect to variance estimation partitions itself again at Edwards. The ETS ablative results generate one estimate (by the partitioning per order of magnitude) of $S^2 = 2.36$, $df = 10$. This is the maximum S^2 generated of all data and therefore is taken as an estimate since ablative - ETS is considered the most likely environment; also the estimate is conservative. In addition, the water-cooled chamber tests at Edwards are partitioned into two sets of variance, the maximum being $S^2 = 2.95$ with $df = 10$. This is not significantly different from the above ablative

estimate so that the two are pooled using again

$$s^2 = \sum_{i=1}^{2} f_i S_i^2 \Big/ \sum_{i=1}^{2} f_i \quad \text{yielding, (with df = 20)}$$

$s^2 = 2.63$. The sample size for ablative - ETS is 13 and for water-cooled - ETS it is 13.

$s^2 = 2.63$ implies $S = 1.54$

B. Assumption of Normality Graphical Verification

The fractile diagram approximating the distribution is shown in Figures 2, 3 & 4 for ablative - ETS at sample N = 30, water-cooled Inglewood at sample N = 63 and water-cooled Edwards at sample N = 24 respectively.

C. Calculation of Statistics from I_{sp} Data

The specification for I_{sp} is 290 ± 5 sec., at 90-158 lbs. thrust Following the procedure of the mixture ratio exercise we obtain from tables of the normal distribution

$$\hat{P}_{I\,1} = \int_{\frac{285-289.97}{1.54}}^{\frac{295-289.97}{1.54}} \Phi(x)\,dx = \int_{-3.227}^{3.266} \Phi(x)dx = 0.99883$$

To calculate a value of K such that $\bar{X} \pm K$ contains at least $1 - \alpha$ of the population (this time μ is considered unknown) with 100P% confidence we can show that $K = J_{(1-\frac{\alpha}{2})}\sqrt{\frac{f}{\chi^2_{1-P}}\left(1 + \frac{1}{2(f+1)}\right)}$

With $1 - \alpha = .99315$, K = 3.24 at 80% confidence or

KS = 3.24 x 1.54 ≈ 4.99

That is to say, there is 80% confidence that at least .99315 of the population is contained in 289.97 ± 4.99 (284.98, 294.96)

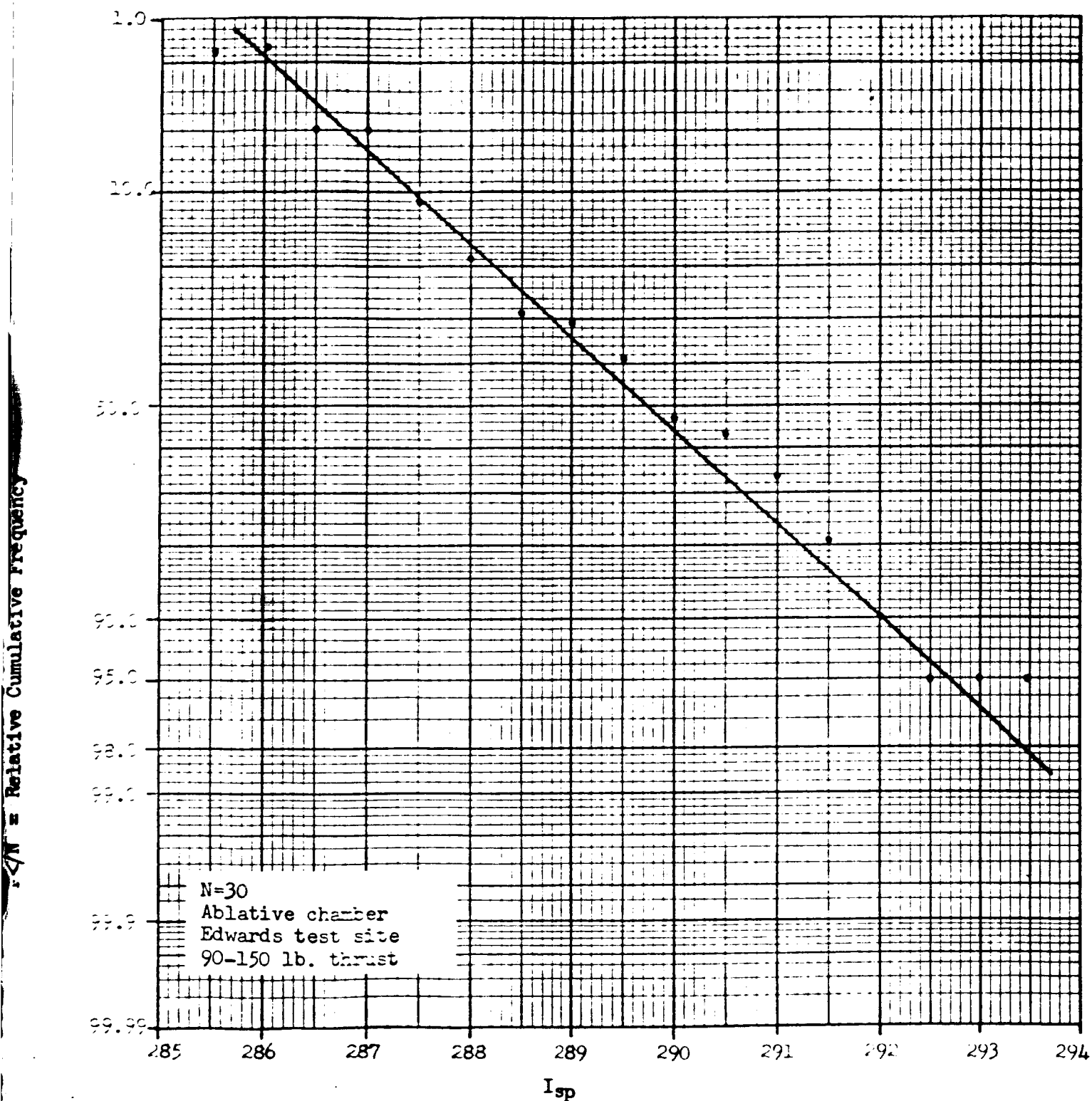

Figure 2 : Fractile plot for I_{sp} sample

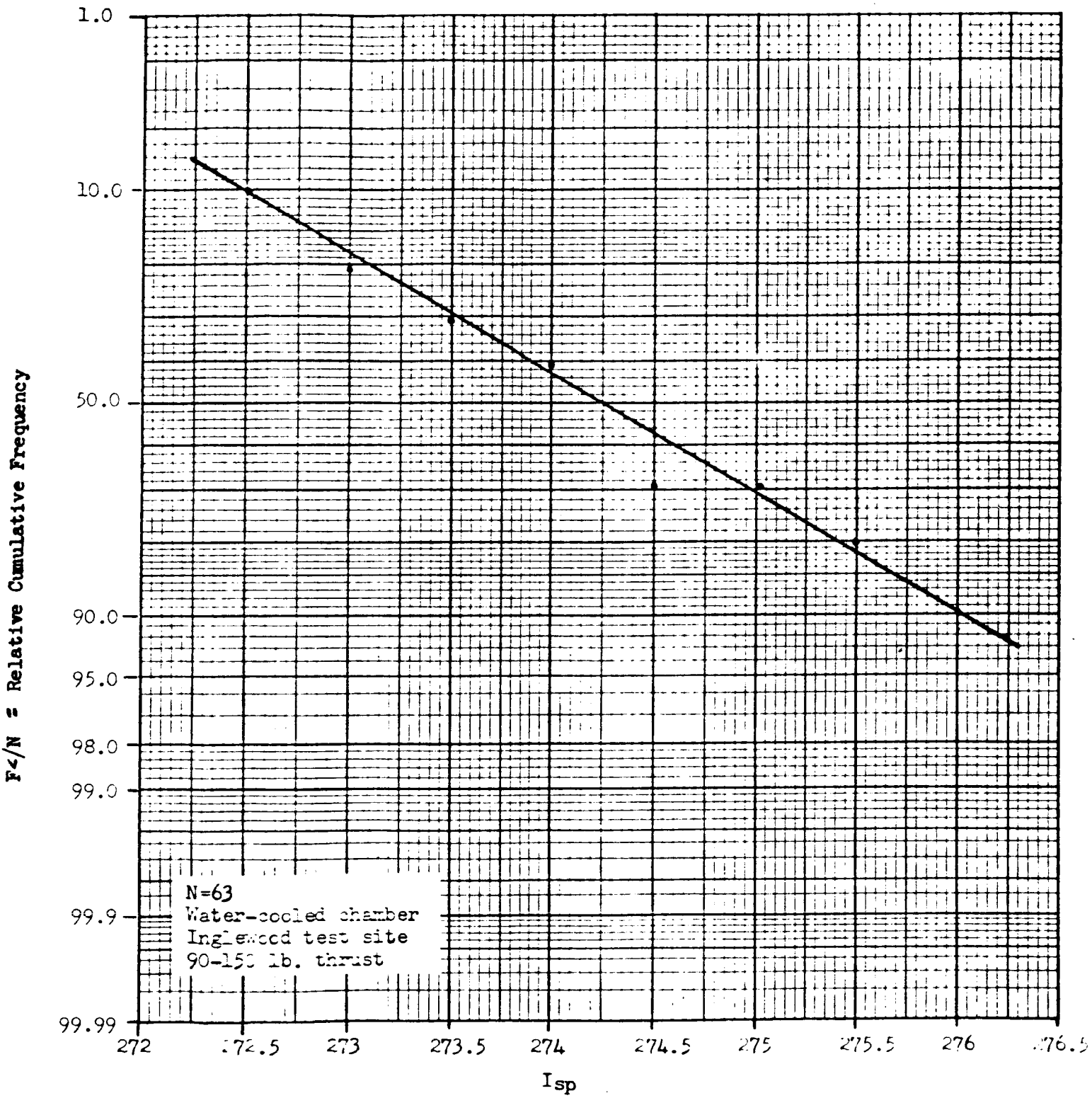

Figure 3: Fractile plot for I_{sp} sample

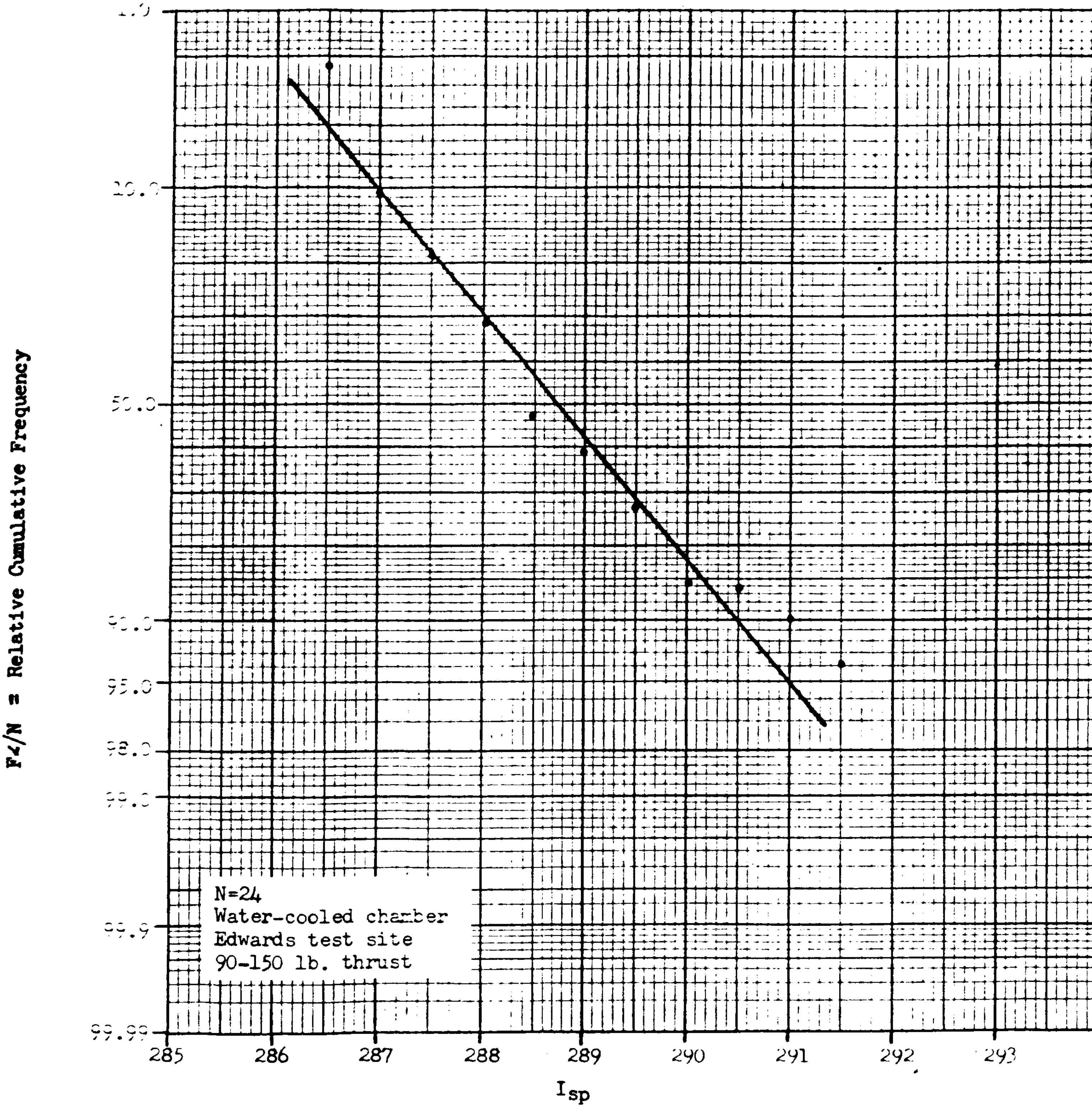

Figure 4: Fractile plot for I_{sp} sample

III. Characteristic Velocity (C*)

A. Estimate of μ, σ^2: Samples from ablative - ETS & watercooled Edwards indicate no significant differences. The pooled mean is $\bar{X} = 5267.798$ ft/sec. All Edwards data (ablative & water-cooled) yield a pooled variance estimate, $S^2 = 13,366.406$, df = 72. implying S = 115.61.

B. Assumption of Normality

A single-parameter transformation to the normal distribution of the ablative water-cooled Edwards variates was attempted without success. In lieu of further research at this time, Figure 5 shows a fractile diagram from 100 samples of C* for the water-cooled TCA at Inglewood which is somewhat normal.

C. Calculation of Statistics from C* Data

Specification limits have not as yet been established for C*. Also, at this writing it is not certain that C* is critical. However, we shall calculate a tolerance interval at 80% confidence such that .999 of the population is contained in the interval, $\bar{X} \pm KS$. The result is K = 3.58 implying 5267.55 ± 413.88 contains.999 of the population at 80% confidence.

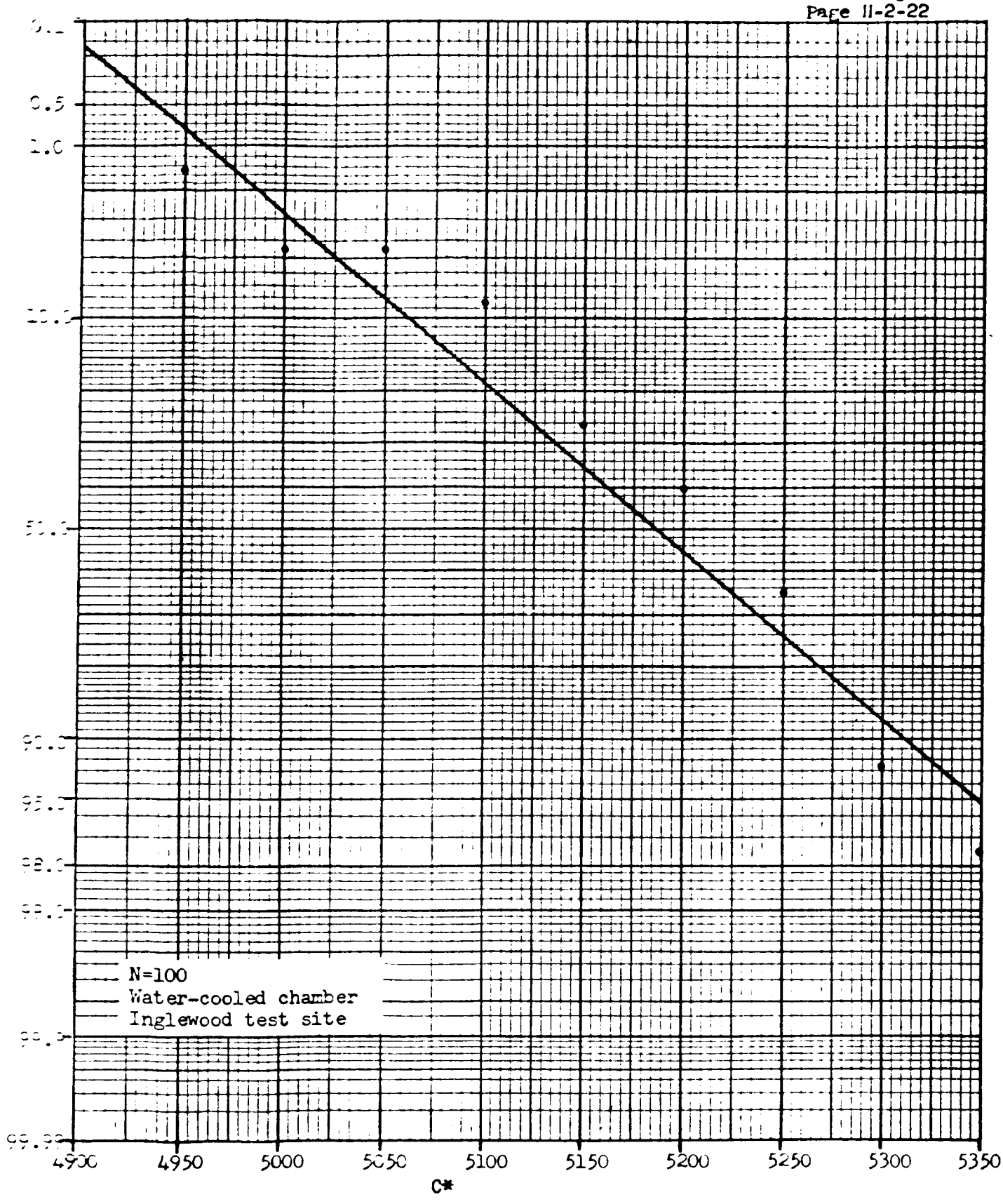

F(X) = Relative Cumulative Frequency

0.5
1.0
50.0
90.0
95.0
98.0
99.0
99.99

N=100
Water-cooled chamber
Inglewood test site

4900 4950 5000 5050 5100 5150 5200 5250 5300 5350

C*

Figure 5: Fractile plot for C* sample

Probability of Mission Success Based on the Available Data

As mentioned above, because of the insufficient data only the continuous operation events are considered here for mixture ratio and I_{sp} variation. C* is not included because requirements do not exist for it. Let E_1 =Event of continuous operation #1 (see (b)p. 5) JPL Spec. SAM-50255 DSN-B lists the thrust range at 70 to 85 lbs. The I_{sp} calculations were made from the best data available at 90 - 158 lbs. Therefore, we assume that the variation of I_{sp} around some $X \in [70,85]$ can be measured by $S = 1.54$. SAM-50255 also lists the requirement for I_{sp} at 260 $\pm$ 7 secs at 30 lbs. thrust & 290 $\pm$ 5 sec. at 90 - 158 lbs. thrust. A curvalinear band through these points and all intermediate points is given, but the accuracy in reading off points is not very good. Because of this fact and since the I_{sp} required interval for [70, 85] is very close to the I_{sp} interval for [90, 158], we assume the requirement of $X \pm 5$ $X \approx 290$. With $S = 1.54$ we can then say that the probability of the correct I_{sp} at some value of thrust in (70, 85) is 0.99883 as obtained above under the assumption that the sample mean $\bar{X} = \mu$ (population mean) and $S^2 = \sigma^2$. . Under this last assumption the probability of correct mixture ratio is 0.99995 as calculated above. Then since there are three engines $P(E_1) = .99995^3 \times .99883^3$

$= .99985 \times .99649$

$= .99634$.

SAM-50255 lists the duration of E_1 as 40 seconds (nominal) to 200 secs (max.). It must be pointed out again that $P(E_1)$ was arrived at by assuming that the event of I_{sp} and mixture ratio being within their limits at the beginning of the time interval

of the event assumes that they will be in control at any other point of time of the event besides the initial point. After shutdown and start again five continuous fixed thrust events follow in succession. We shall make the above assumption for each of them. This implies that I_{sp} and mixture ratio are most likely to shift out of specification where the thrust is varied. Before considering these events, consider calculating $P(E_1)$ with the propabilities obtained in generating 80% confidence tolerance limits for I_{sp} and mixture ratio. This yields

$$P(E_1) = 0.99982^3 \times 0.99315^3$$
$$= .99946 \times .97959$$
$$= .97906$$

Let E_2 = Event of continuous operation #2. SAM-50255 lists the thrust range/chamber at 30-150 lbs. Since we cannot predict the exact thrust setting, we shall assume the I_{sp} calculation above for this wide range and obtain (since the mixture ratio probabilities remain the same).

$$P(E_2) = P(E_1) = 0.99634 \text{ for } \bar{X} = \mu \text{ , } S^2 = \sigma^2$$

& $P(E_2) = P(E_1) = 0.97906$ for unknown population at the 80% confidence tolerance interval

Let E_3 = Event of continuous operation #3. Range of thrust is given as 100-150 lbs. which is contained in 90-150 lbs. such that

$$P(E_3) = P(E_1) = 0.99634$$

& 0.97906 for the two calculations.

Let E_4 = Event of continuous operation #4. Thrust range is given by SAM-50255 to be 30 to 50 lbs. In this case assume S = 1.54 for I_{sp} from the data available for 90-158 lbs. thrust. Also assume operation will be at the lower end point of 30 lbs. The requirement at this point is I_{sp} = 260 ± 7 secs. Assume (because of lack of data) that $\bar{X}$ = 260. We obtain from normal tables

$$P_{I\,4} = \int_{\frac{253-260}{1.54}}^{\frac{267-260}{1.54}} \Phi(X)\,dX = \int_{-4.05}^{4.05} \Phi(X)\,dX$$

= 0.99995. With the mixture ratio probability of $.99995^3 = .99985$ we obtain $P(E_4) = .99985 \times 0.99985$

$= .9997$ with $\mu = \bar{X}^2$, $\sigma^2 = s^2$

For 80% confidence on I_{sp} at 30-50 lbs.

K = 4.55 and $1 - \alpha$ = 0.99984

or 99.98% of the population is contained in

$$260 \pm 4.55 \times 1.54$$

$$= 260 \pm 7.00$$

With this

$$P(E_4) = .99982^3 \times .99984^3$$

$$= .99946 \times .99952$$

$$= .99898$$

Let E_5 = Event of continuous operation #5. Here again the thrust range is 100 to 150 lbs.

Therefore $P(E_5) = P(E_3) = P(E_1) = 0.99634$

& 0.97906 from the two calculations

Let E_6 = Event of continuous operation #6, where the thrust range is 30 to 60 lbs. Therefore E_6 is close to E_4 which has operation defined over 30-60 lbs. thrust,

Therefore $P(E_6) = P(E_4) = .99985 \times 0.99985$

$= 0.9997$

$P\{$ Mission Success (assuming all other events have $P = 1)\}$

$= \prod_{i=1}^{6} P(E_i) = .99634^4 \times .9997^2$

$= .98544 \times 0.99940$

$= 0.9848$ for $\bar{X} = \mu,\ S^2 = \sigma^2$

& $P\{$ Mission Success$\} = .97906^4 \times .99898^2$

$= .91883 \times .99796$

$= 0.9170$ from the second type of statistics

This last estimate is of course more pessimistic since it is calculated from tolerance intervals around each parameter from each engine.

REFERENCE

Hald, A., Statistical Theory with Engineering Applications; John Wiley and Sons, Inc., New York, 1952, Section 11.10, Tolerance Limits.

APPENDIX H-3

SURVEYOR VERNIER FAILURE

REPORT SUMMARY

No. of Pages: 20

Severity Code
CR - Critical
MA - Major
MI - Minor

SURVEYOR VERNIER THRUST CHAMBER ASSEMBLY
FAILURE REPORT SUMMARY
INJECTOR ASSEMBLY - ENGINE

Failure Date and Report No.	Unit: I. D. Number and Responsible Engr.	Unit: Part Name and Number	Unit: Mfgr. and Serial No.	Sev.	Failure Description and Cause	Corrective Action Taken
12/6/63 8819	13-24-15-00 R. Johnson	Locknut 103955-2	STL	CR	Propellant (fuel) leak past locknut threads (sealing type) at pintle guide, resulting in small fire (throttling run). Sealing threads failed to prevent fuel from leaking to external areas.	Sealing threads inadequate to prevent fuel leakage. Nut replaced with "O" ring type and pintle machined to seal with same. Drawing X-105447 (nut), 12/9/63. EO 10395341 (Pintle) 12/30/63.
12/15/63 8877	13-26-00-00 E. Fitzpatrick	Flexure 104330	STL	MI	Flexure broke during installation of servo-actuator due to mishandling during installation.	Caution personnel on handling and installation procedures.
1/16/64 8872	13-26-00-00 E. Fitzpatrick	Flexure 104330	STL	CR	Flexure broke as a result of the fuel venturi pintle freezing. This is a secondary failure due to the pintle. Overstressed due to freezing of fuel pintle.	None - secondary failure.
1/19/64 8875	13-26-00-00 E. Ftizpatrick	Flexure 104330	STL	CR	Flexure broke when the servo-actuator (Cad. Gage S/N 50666) ran out of fuel and went into high frequency vibrations. Overstressed due to high frequency vibrations.	Prevent running of actuator when fuel supply low. When no fuel is supplied, the actuator exhibits violent vibrations in the output shaft.
1/20/64 8878	13-26-00-00 E. Fitzpatrick	Flexure 104330	STL	MI	Flexure bent during installation. Mishandling of flexure.	Caution personnel on handling and installation procedures.
2/13/64 9397	13-26-00-00 E. Fitzpatrick	Flexure 104330	STL	MA	Flexure broke when air was run through servo-actuator (Cad. Gage S/N 50666) and went into high frequency vibrations. Overstressed due to high frequency vibrations.	Bleed fuel line before actuation (secondary malfunction).
4/7/64 9387	13-02-01-00 E. Fitzpatrick	Sleeve-Injector Head End 103951-1	STL 002	MA	Uneven oxidizer flow caused by pits in sleeve. Normal wear and tear - 6000 secs. accumulative hot firing.	Used beyond expected life. No corrective action necessary.

Failure Date and Report No.	Unit: I. D. Number and Responsible Engr.	Unit: Part Name and Number	Unit: Mfgr. and Serial No.	Sev.	Failure Description and Cause	Corrective Action Taken
7/4/64 9353	13-24-07-00 E. Fitzpatrick	Omniseal R105J-.560	Reid	MA	Fuel leak from around sleeve. Microseal collecting on seal surfaces.	Burnish microseal parts to remove excess lubricant. Burnishing note added to assembly drwg.
7/25/64 9356	13-24-07-00 E. Fitzpatrick	Omniseal R105J-.560	Reid	MA	Propellant leak, fuel past omniseal out through vent hole	Same as above
9/3/64 9372	13-00-00-00 E. Fitzpatrick	Head End Assembly 105461	STL 006	MA	Helium leak from solenoid port into oxidizer manifold (injector). Faulty drilling of helium passage.	Reweld part to fix passage. Incorp leak check of this passage in Acceptance test.
9/25/64 9365	13-00-00-00 E. Fitzpatrick	Head End Assembly 105461	STL 002	CR	Lost fuel flow after 30 sec. of Run 1A. Engine shutdown manually. During Run 1B there were intermittent start-stop pulses. Injector fuel gap had closed as ox continued to flow.	Set lower pressure drop (layer gap) at minimum thrust (> 50 psi)
10/14/64 10792	13-00-00-00 E. Fitzpatrick	Head End Assembly 105461	STL 005	MA	Fuel leak past fuel injector pintle "O" ring. During Run C2-590. Both "O" ring and lock nut were replaced.	Replace O-ring and retorque nut. "O" did not center on shaft prior to tightening. Can't happen on flight engine.
10/15/64 10793	13-00-00-00 E. Fitzpatrick	Head End Assembly 105461	STL 005	CR	During throttle run when in thrust position, engine shutdown (lost fuel flow). T_{ox} = 100°F, T_f=0°F. Oxidizer continued to flow.	Set lower pressure drop (larger gap) at minimum thrust in future (less than 30 psi).
10/15/64 10794	13-00-00-00 E. Fitzpatrick	Head End Assembly 105461	STL 005	MA	Fuel leak passed fuel injector pintle "O" ring. During Run C2-594. T_{ox} = 100°F, T_f=0°F. "O" ring replaced prior to Run C2-591.	None required. This gradient cannot be obtained in space.
11/12/64 11191	13-00-00-00 B. Siegel	Head End Assembly	STL 007	MA	Shift downward in mixture ratio from approx. 1.5 to approx. 1.43. Ref. Run C2-621 and C2-627 thru 630.	Check instrumentation.

Severity Code

CR - Critical
MA - Major
MI - Minor

SURVEYOR VERNIER THRUST CHAMBER ASSEMBLY
FAILURE REPORT SUMMARY
INJECTOR ASSEMBLY - ENGINE (CONT'D)

Failure Date and Report No.	Unit: I. D. Number and Responsible Engr.	Unit: Part Name and Number	Unit: Mfgr. and Serial No.	Sev.	Failure Description and Cause	Corrective Action Taken
11/18/64 11192	13-00-00-00 B. Siegel	Head End Assembly 106662-2	STL 008	MI	Bent fuel venturi pintle due to error in actuator set-up at test site. Engine was driven past minimum flow position, bottoming pintle. Injector should be checked for other damage.	None required. Error in actuator setup method, did not follow prescribed procedure.
11/18/64 11194	13-00-00-00 B. Siegel	Head End Assembly 106662-2	STL 150A-009	MA	Fuel ΔP's shifted approx. 20 psi. Streak test indicated hot running engine with random erosion.	See F.R. 11195
11/18/64 9376	13-00-00-00 B. Siegel	Head End Assembly 106662-2	STL 150A-007	MA	Fuel ΔP's shifted approx. 20 psi. Streak test indicated hot running engine with random erosion.	See F.R. 11195.
11/23/64 11195	13-00-00-00 B. Siegel	Head End Assembly 106662-2	STL 150A-010	MA	Fuel ΔP's shifted approx. 20 psi. Streak test indicated hot running engine with random erosion.	None required, excessive fuel lead will not occur in Surveyor test profile.

Severity Code

CR - Critical
MA - Major
MI - Minor

SURVEYOR VERNIER THRUST CHAMBER ASSEMBLY
FAILURE REPORT SUMMARY
COMBUSTION CHAMBER ASSEMBLY

Failure Date and Report No.	Unit: I. D. Number and Responsible Engr.	Unit: Part Name and Number	Unit: Mfgr. and Serial No.	Sev.	Failure Description and Cause	Corrective Action Taken
1/8/64 8886	12-00-00-00 R. Henderson	Combustion Chamber and Nozzle Assy 103945	STL 001	CR	Burn-through of the titanium case in the area behind the throat. Char completely thru to case in area of high heat flux thus overheating titanium case. Too thin ablative material thickness in area behind throat.	Redesign combustion chamber to incorporate approx. 50% thicker ablative material in back of throat.
1/29/64 8887	12-00-00-00 R. Henderson	Combustion Chamber and Nozzle Assy. 103945	STL 001	MA	A hot spot occurred on the titanium shell in back of throat (1/4 in. diameter and located 3.55 in. downstream of flange) Crack or burnthrough of ablative liner and possible gas flow behind ablative material.	Redesign case and liner to increase ablative material thickness to prevent complete charring and flow of gases behind liner.
2/21/64 9399	01-00-00-00 R. Henderson	Faceplate Liner 104074-1	STL	MA	Liner was used on injector No. 003 and water cooled chamber. Liner was not tightly held as with flight weight chamber. Observed cracked liner after DY-15, 16, large fragment found outside. Fracture of faceplate liner. Liner not held securely as required and as is in flight weight configuration.	None required - secondary
2/5/64 8879	12-00-00-00 R. Henderson	Combustion Chamber and Nozzle Assy. 103945	STL 003	MA	Combustion chamber leaked on pressure test after vibration test. "O" ring lost its elastomeric quality due to hardening of the adhesive in the groove.	Combustion chamber has been redesigned to remove the "O" ring adhesive requirement.

Severity Code

CR - Critical
MA - Major
MI - Minor

SURVEYOR VERNIER THRUST CHAMBER ASSEMBLY
FAILURE REPORT SUMMARY
COMBUSTION CHAMBER ASSEMBLY (CONT'D)

Failure Date and Report No.	Unit: I. D. Number and Responsible Engr.	Unit: Part Name and Number	Unit: Mfgr. and Serial No.	Sev.	Failure Description and Cause	Corrective Action Taken
9/23/64 8888	12-00-00-00 R. Henderson	Combustion Chamber and Nozzle Assy. 106546-1	STL 006	CR	Gas leaks were detected at the retaining pins holding the ablative liner assembly in the titanium shell. The retaining pin holes in the shell cut the O-ring during the assembly operation.	Retaining pin holes will be properly de-burred. The bond between the case and liner will be eliminated to facilitate changing O-ring seals. Seal washers will be added under retaining pins. Ref. Design Change EQ A6.
10/13/64 11772	12-00-00-00 R. Henderson	Combustion Chamber and Nozzle Assy. 103945	STL 003	CR	During leak check between firings, nitrogen gas leaks were detected at the liner retaining pins, at the liner/skirt interface and around the throat insert. Retaining pin hole in case cut O-ring during final assembly. O-ring burned by spot-welding thermocouples to case. Ablative liner did not meet STL Spec. PR 0-10.	Retaining pin holes will be properly deburred. Bond eliminated to facilitate easy change of O-rings; thermocouples removed from area of seal. A failure analysis is being conducted on the ablative liner leaks. Changes authorized by E.O. A-6, Effective S/N 007 and subs.

Severity Code

CR - Critical
MA - Major
MI - Minor

SURVEYOR VERNIER THRUST CHAMBER ASSEMBLY
FAILURE REPORT SUMMARY
SHUT-OFF VALVE - FUEL

Failure Date and Report No.	Unit: I. D. Number and Responsible Engr.	Unit: Part Name and Number	Unit: Mfgr. and Serial No.	Sev.	Failure Description and Cause	Corrective Action Taken
12/18/63 8812	13-21-00-00 H. Hoffman	Sleeve, Valve 103947	STL	MA	Fuel shut-off valve leaking with pressure applied. Believed due to corrosion of aluminum parts. Reddish residue inside valve. Units flushed with water which is very corrosive with oxidizer.	Sleeve and piston are now stainless steel per drawings X-105194 and X-105193, dated 11/26/63. Omniseals replaced by Bal-seals and "micro-seal" eliminated. New P/N's 106656-1 sleeve, 106657-1 piston, 106798-1 poppet. Passivate per MIL STD 171.
5/6/64 9382	13-22-00-00 D. Webb	Piston 103947-3	STL 001-150A	CR	Fuel valve sticking.	Same as above.
5/18/64 9384	13-03-00-00 D. Webb	Omniseal R105-J- .242A1Q	Reid	CR	Fuel leak from propellant valve vent, also valve was closing slow.	Same as above.
5/25/64 9366	13-03-00-00 D. Webb	Omniseal R105-J- .242A1Q	Reid	CR	Fuel leak from shutoff valve vent hole.	Same as above.
6/16/64 9351	13-03-00-00 D. Webb	Omniseal R105-J- .242A1G	Reid	MA	Fuel leak from shutoff valve vent hole.	Same as above.
6/23/64 9368	13-03-00-00 D. Webb	Omniseal R105J- .242A1G	Reid	MA	Fuel leak from shutoff valve vent hole.	Same as above.
6/24/64 8863	13-03-00-00 D. Webb	Omniseal 105J-.370 A1Q	Reid	MA	Fuel leak from shutoff valve vent hole.	Same as above.
6/25/64 9369	13-03-00-00 D. Webb	Omniseal R105J- .242A1G	Reid	MA	Fuel leak from shutoff valve vent hole.	Same as above.

Severity Code

CR - Critical
MA - Major
MI - Minor

SURVEYOR VERNIER THRUST CHAMBER ASSEMBLY
FAILURE REPORT SUMMARY
SHUTOFF VALVE - FUEL (CONT'D)

Failure Date and Report No.	Unit: I. D. Number and Responsible Engr.	Unit: Part Name and Number	Unit: Mfgr. and Serial No.	Sev.	Failure Description and Cause	Corrective Action Taken
7/18/64 9385	13-20-00-00 R. D. Webb	Shut-off Valve-Fuel	STL 150A-002	CR	Valve was stuck in open position allowing raw fuel to run from engine during vents.Bulkhead valve was closed, 50 psig applied to run tank, then bulkhead valve reopened to slam shut on-off valve. Valve o.k. from then on.Procedural error-valve purged in reverse direction without activating piston.	Purge procedure changed to prevent purging without activation of piston. The new cleaning procedure specification will reflect the proper procedure of purging and flushing valves.
8/1/64 9360	13-20-00-00 R. D. Webb	Fuel Shut-Off Valve	STL	MI	Valve was stuck in open position allowing fuel to run from engine during vents-closed bulkhead valve, turned on N_2 purge for several secs. then reopened bulkhead. Valve had closed; valve OK from then on.	Purge procedure changed to prevent purging without activation of piston. The new cleaning procedure spec. will reflect the proper procedure of purging and flushing valves.

Severity Code

CR - Critical
MA - Major
MI - Minor

SURVEYOR VERNIER THRUST CHAMBER ASSEMBLY
FAILURE REPORT SUMMARY

SHUT-OFF VALVE - OXIDIZER

Failure Date and Report No.	Unit: I. D. Number and Responsible Engr.	Unit: Part Name and Number	Unit: Mfgr. and Serial No.	Sev.	Failure Description and Cause	Corrective Action Taken
11/22/63 8817	13-21-00-00 H. Hoffman	Sleeve, Valve (Shut-off) 103947	STL	MA	Oxidizer valve froze open - would not close after electrical signal was removed. Contamination and swelling of aluminum sleeve (from corrosion) caused seizure. Contamination due to corrosion of aluminum valve parts in the presence of ox. and H_2O.	All aluminum parts now made of stainless steel per drawings X-105193 (piston) and X-105194 (sleeve) dated 11/26/63.
11/30/63 8816	13-21-00-00 H. Hoffman	Sleeve, Valve (Shut-off) 103947	STL	MA	Same as above.	Same as above.
12/18/63 8867	13-22-00-00 H. Hoffman	Valve, Shut-off (Oxidizer) 71136	Adel 7011	MA	Valve inoperative-piston froze in sleeve. Valve failed on test stand not on HEA. Two others showed corrosion but did not fail (S/N 7007, 7016). Corrosion of aluminum parts in valve.	All future valves will be the STL design and will be made entirely of stainless steel.
12/26/63 8852	13-21-00-00 H. Hoffman	Sleeve, Valve (Shut-off) 103947	STL	MA	Oxidizer shut-off valve leaking during engine operation. Failure due to corrosion of aluminum material of sleeve and piston assembly. Valve cleaned after failure on Report 8817. Contamination due to corrosion of aluminum valve parts in the presence of ox. and H_2O.	All aluminum parts now made of stainless steel per drawings X-105193 (piston) and X-105194 (sleeve) dated 11/26/63.

Severity Code

CR - Critical
MA - Major
MI - Minor

SURVEYOR VERNIER THRUST CHAMBER ASSEMBLY
FAILURE REPORT SUMMARY
SHUT-OFF VALVE - OXIDIZER (CONT'D)

Failure Date and Report No.	Unit: I. D. Number and Responsible Engr.	Unit: Part Name and Number	Unit: Mfgr. and Serial No.	Sev.	Failure Description and Cause	Corrective Action Taken
1/4/64 8891	13-21-00-00 13-22-00-00 H. Hoffman	(Sleeve and Piston) On-off Valve (Oxidizer) 103947-1 103947-1	STL	MA	Leak test at 80 psig showed leak out vent hole with valve closed and pressure on down-stream side (in chamber). Leaked after cycling of valve also. Contamination due to corrosion of aluminum sleeve where mishandling damage occurred.	Sleeve and piston are now stainless steel per drawings X-105194 and X-105193, dated 11/26/63.
1/15/64 8894	13-22-00-00 H. Hoffman	Valve, Shut-off 71136	Adel 7012	MA	Oxidizer on-off valve leaked on pressure test allowing flow across seat into chamber. Replaced with spare valve. Contamination of valve-bottom seal on sleeve damaged.	Inspection and cleaning methods improved to prevent entry of contamination.
4/7/64 9395	13-03-00-00 D. Webb	Omniseal-Oxidizer R10105-015	Reid	MA	Oxidizer leak by sleeve seal. Seal deteriorates by normal wear and tear - 6000 secs. accumulative hot firing.	Used beyond expected life. No corrective action necessary.
4/27/64 9400	13-03-00-00 D. Webb	Omniseal Oxidizer R105J-.242A1Q	STL	MA	Oxidizer leak out propellant valve vent hole. Omniseal damaged (bottom seal on piston).	Balling up of microseal compound-contaminated and damaged the seal. Microseal processing to be changed to require burnishing and removal of excess, also ramp angle on sleeve changed to prevent installation damage. Re-opened due to subsequent failures (6-5-64)
5/6/64 9381	13-22-00-00 D. Webb	Piston 103947-3	STL 001-150A	CR	Ox leak from vent hole. Ox leak on start up and through test.	Design changes on 150A design-omniseals replaced with Bal-seals and microseal eliminated. New P/N's 106656-1 sleeve, 106657-1 piston, 106798-1 poppet. Parts are passivated per MIL STD 171.
5/18/64 9383	13-03-00-00 D. Webb	Omniseal R105J-.242 A1Q	Reid	CR	Ox leak from propellant valve vent, also valve was closing slow.	Same as above.

Severity Code

CR - Critical
MA - Major
MI - Minor

SURVEYOR VERNIER THRUST CHAMBER ASSEMBLY
FAILURE REPORT SUMMARY
SHUT-OFF VALVE - OXIDIZER (CONT'D)

Failure Date and Report No.	Unit I. D. Number and Responsible Engr.	Unit Part Name and Number	Unit Mfgr. and Serial No.	Sev.	Failure Description and Cause	Corrective Action Taken
5/25/64 9367	13-03-00-00 D. Webb.	Omniseal R105J-.242 A1Q	Reid	CR	Ox leak from shutoff valve vent hole.	Same as Failure Report No. 9381 dated 5/6/64.
6/24/64 8862	13-03-00-00 D. Webb	Omniseal R105J-.242 A1G	Reid	MA	Oxidizer leak from shutoff valve vent hole.	Same as above.
6/25/64 9370	13-03-00-00 D. Webb	Omniseal R105J-.242 A1G	Reid	MA	Ox leak from shutoff valve vent hole.	Same as above.
7/11/64 9358	13-21-00-00 R. D. Webb	Ox Shut-off Valve-Sleeve-103947 and Piston 106657	Adel	CR	Valve failed to close during attempted shutdown of engine. Ref. run CI-321 and CI-322. Adel valve used only because STL parts not available after hours.	Adel valve will not be used in final system. No action required.
10/9/64 10791	13-21-00-00 D. Webb	Oxidizer Shutoff Valve	STL 002	MI	Following Run C2-583, just as purges were applied, oxidizer fumes were emitted from the ox shutoff valve vent hole. Possible damage during assy. Possible defective seal when installed. Defective seals were found in stock.	Vendor will re-inspect seals in stock and replace defective items, if any. Assembly technicians to exercise greater care in examining and installing seals.

Severity Code

CR - Critical
MA - Major
MI - Minor

SURVEYOR VERNIER THRUST CHAMBER ASSEMBLY
FAILURE REPORT SUMMARY
FLOW CONTROL VALVE - FUEL

Failure Date and Report No.	Unit: I. D. Number and Responsible Engr.	Unit: Part Name and Number	Unit: Mfgr. and Serial No.	Sev.	Failure Description and Cause	Corrective Action Taken
1/3/64 8856	13-01-02-00 E. Fitzpatrick	Omniseal R10105-007	Reid	MI	Fuel leak at pintle of flow control valve. (See Rpt. 8857) both seals failed. Excessive wear or contamination of valve. Seal abraded.	Filter propellants and caution personnel on contamination of components during assembly and maintenance procedures.
1/3/64 8857	13-01-02-00 E. Fitzpatrick	Omniseal R10105-007	Reid	MI	Same as above.	Same as above.
1/16/64 9334	13-01-07-00 E. Fitzpatrick	Fuel Venturi (Pintle) 103954	STL	CR	Fuel venturi froze and resulted in breaking actuator flexure. Galling due to wearout, approx. 10,000 cycles on pintle.	Repair - pintle lapped and polished - sent out for microseal. No further corrective action anticipated.
3/19/64 9392	13-01-07-00 E. Fitzpatrick	Fuel Venturi (Pintle) 103954	STL	CR	Fuel venturi froze. Galling after 6000 secs. of hot firing. Wearout.	Unit repaired. No corrective action necessary.
4/2/64 9394	13-01-07-00 E. Fitzpatrick	Fuel Venturi (Pintle) 103954	STL	MI	Fuel flow varied from test to test due to contamination in valve.	Cleaned valve and replaced pintle. Filters added to propellant lines to remove contaminant from propellants.
10/15/64 10795	13-21-00-00 E. Fitzpatrick	Fuel, Flow Control Valve Assy. 105466	STL 005	MA	Fuel leak from fuel venturi seal during Run C2-594. $T_{ox}=100^{o}F, T_{f}=0^{o}F$.	Detailed analysis of onmiseal action indicates less clearance may be required. Still under investigation. (See Technical section)

Severity Code

CR - Critical
MA - Major
MI - Minor

SURVEYOR VERNIER THRUST CHAMBER ASSEMBLY
FAILURE REPORT SUMMARY
FLOW CONTROL VALVE - OXIDIZER

Failure Date and Report No.	Unit: I. D. Number and Reponsible Engr.	Unit: Part Name and Number	Unit: Mfgr. and Serial No.	Sev.	Failure Description and Cause	Corrective Action Taken
4/7/64 9388	13-01-06-00 E. Fitzpatrick	Oxidizer Venturi (Pintle) 103954-1	STL	CR	Oxidizer venturi pintle froze. Galling due to wearout.	Cycled beyond expected life. No corrective action necessary.
1/15/64 8893	13-01-02-00 E. Fitzpatrick	Venturi Valve (Omniseal) (Oxidizer) 103960	STL 005	MA	Leak at venturi pintle on pressure test replace omni-seals then satisfactory. (P/N R10105-007). Seals abraded by internal contam-ination in valve.	Contamination from installation procedures or from filtered propellants. No direct action required, caution personnel.

Severity Code

CR - Critical
MA - Major
MI - Minor

SURVEYOR VERNIER THRUST CHAMBER ASSEMBLY
FAILURE REPORT SUMMARY
ACTUATOR - ELECTROHYDRAULIC

Failure Date and Report No.	Unit: I. D. Number and Responsible Engr.	Unit: Part Name and Number	Unit: Mfgr. and Serial No.	Sev.	Failure Description and Cause	Corrective Action Taken
11/29/63 8855	13-25-00-00 D. Laine	Actuator-Servo C-104312	Hydraulic Research 003	MI	Fuel leak at static seal of output end of shaft- 1 drop/min. Assembly damage of "O" ring and subsequent leakage. Manufacturer assembly practice without proper care when installing "O" ring.	The "O" ring was replaced and the manufacturer notified of the fault. Greater care to be taken on assembly in future.
11/29/63 8818	13-25-00-00 D. Laine	Actuator-Servo C-104312	Hydraulic Research 003	CR	Unit failed to operate when signal was applied. Unit shorted out in connector plug (electrical). Small hair wire embedded in potting material in back of plug, shorting out two terminals.	Unit was disassembled at the manufacturer and trouble corrected there. Mfgr. will check all future units for this fault since it was determined that the unit was delivered in this condition.
12/6/63 8870	13-25-00-00 D. Laine	Actuator-Servo C-104312	Hydraulic Research 004	MA	Unit exhibits excessive overshoot on throttle change. Actuator sticking. Galling of 3rd stage output shaft.	Unit to be redesigned to preclude like hardness metals in contact and prevent entry of contamination at shafts.
12/17/63 8859	13-25-00-00 D. Laine	Actuator Servo C-104312	Hydraulic Research 002	MA	Same as above.	Same as above.
12/17/63 8815	13-25-00-00 D. Laine	Actuator-Servo C-104312	Hydraulic Research 005	MA	Same as above. Unit was found to be air bound and improper power was applied.	Same as above. Power source corrected and unit was bled to remove internal air, cycled and checked out o.k.
12/19/63 8868	13-25-00-00 D. Laine	Actuator-Servo C-104312	Hydraulic Research 003	MA	Unit exhibits excessive overshoot on throttle change. Actuator sticking. Galling of 3rd stage output shaft.	Unit to be redesigned to preclude like hardness metals in contact and prevent entry of contamination at shafts.
12/27/63 8876	13-25-00-00 D. Laine	Actuator Servo C-104312	Hydraulic Research 004	MA	Same as above.	Same as above.

Severity Code

CR - Critical
MA - Major
MI - Minor

SURVEYOR VERNIER THRUST CHAMBER ASSEMBLY
FAILURE REPORT SUMMARY
ACTUATOR - ELECTROHYDRAULIC (CONT'D)

Failure Date and Report No.	Unit: I. D. Number and Responsible Engr.	Unit: Part Name and Number	Unit: Mfgr. and Serial No.	Sev.	Failure Description and Cause	Corrective Action Taken
12/30/64 8858	13-25-00-00 D. Laine	Actuator-Servo 22003-3	Cadillac Gage 50666	MA	Same as Failure Report 8868. Internal contamination of Butyl "O" rings.	Redesigned to remove butyl "O" rings, place teflon slippers on all dynamic "O" rings, place dust catchers on output shaft and improve internal finishes of bores.
1/15/64 9331	13-25-00-00 D. Laine	Actuator-Servo C-104312	Hydraulic Research 004	MA	While item was being tested (step response) on engine test stand C-1, unit exhibited over shoot and underdamping when actuated and moved to different positions. Damping time averaged 2 secs. Overshoot varied from 65% to 45% (full thrust to min. thrust) and from 45% to 65% (min. thrust to max. thrust). Unknown at present.	Redesigned to preclude contact of like hardness metals and to prevent entry of contamination in output shaft. Failures occurred on acceptance test after units were returned from manufacturers.
1/15/64 9332	13-25-00-00 D. Laine	Actuator-Servo C-104312	Hydraulic Research 004	MA	Actuator jammed after 3 cycles during hysteresis test. Leakage was observed out of rear dynamic seal. Further inspection revealed that filter (fuel) was not installed upstream of actuator. Actuator jammed (test stand). See above report.	Redesigned to preclude contact of like hardness metals and to prevent entry of contamination in output shaft. Failure occurred on acceptance test after units were returned from mfgr.
1/15/64 9333	13-25-00-00 D. Laine	Actuator-Servo C-104312	Hydraulic Research 002	MA	Actuator was sticking during pre-firing checking while exercising the actuator with fuel at 700 psig. Contamination evidently caused jamming of the 2nd stage spool valve.	Redesigned to preclude contact of like hardness metals and to prevent entry of contamination in output shaft.

Failure Date and Report No.	Unit: I. D. Number and Responsible Engr.	Unit: Part Name and Number	Unit: Mfgr. and Serial No.	Sev.	Failure Description and Cause	Corrective Action Taken
1/28/64 9335	13-25-00-00 D. Laine	Actuator-Servo 32003-3	Cadillac Gage 50668	MA	Overshoot and drifting of position during step response operation. Internal "O" ring damage and deterioration, also internal contamination.	Unit will be redesigned to remove butyl "O" ring, place teflon slippers on all dynamic "O"rings, place dust catchers on output shaft and improve internal finishes of bores.
2/17/64 9398	13-25-00-00 D. Laine	Connector Servovalve 22003-3	Cadillac Gage 50669	MA	Electrical connector (Bendix PT1H-8-46) twisted out on servovalve case when inserting mating plug. Poor design and vibration testing.	Redesign by vendor.
9/5/64 9363	13-25-00-00 D. Laine	Servo Actuator C104312B	Cadillac C53752	MI	With fuel pressure applied (710 psig) and dump valve open, fuel leaked from actuator seals. With -80 ma applied actuator would not fully extend, with +50 ma applied actuator fully retracted. Particle imbedded in shaft seal; wrench flats too long rendering shaft wiper ineffective. Pressed in first stage nozzle shifted and leaked.	Wrench flats shortened and nozzle dimensions changed on new design. Ref. STL Spec. EQ 2-42 STL P/N C219217.
9/21/64 9364	13-25-00-00 D. Laine	Servo Actuator C104312B	Cadillac C53749	MI	With first try actuator would not operate. (First test since vibration). Actuator was then operated several times. After sitting overnight actuator was wet with fuel. Leak increased with pressure. Inadequate seal design.	All Phase III S/A have new seal design using E.P. O-ring Ref. STL Spec. EQ 2-42, STL P/N C219217.

Severity Code

CR - Critical
MA - Major
MI - Minor

SURVEYOR VERNIER THRUST CHAMBER ASSEMBLY
FAILURE REPORT SUMMARY
ACTUATOR - ELECTROHYDRAULIC (CONT'D)

Failure Date and Report No.	Unit: I. D. Number and Responsible Engr.	Unit: Part Name and Number	Unit: Mfgr. and Serial No.	Sev.	Failure Description and Cause	Corrective Action Taken
10/19/64 10797	13-25-00-00 D. Laine	Servo Actuator C104312B	Cadillac C53747	MA	Electrical short to ground for both coils. Fuel had leaked into torque motor. Leak path unknown. Ref. C2-600. Installed S/N 48. Torque motor static seal failure.	Redesigned seal on all Phase III actuators.
11/6/64 9354	13-25-00-00 D. Laine	Servo Actuator C104312B	Cadillac C53748	MA	Electrical short to ground for coil A-B (6000-ohms). Unable to obtain correct travel when calibrating instrumentation for Run C2-623C. Torque motor static seal failure.	Redesigned seal on all Phase III actuators.
11/10/64 9355	13-25-00-00 D. Laine	Servo Actuator C219217A	Cadillac 55390	MI	Null point shifted downward preventing entire from reaching max thrust position with 70 ma signal applied max position was achieved with +78 ma. Stop to stop -64 ma to 86 ma. Loose torque motor mounting screws (longlock type.)	Mounting screws to be lockwired on all Phase III actuators (also retrofit of new springs).
11/11/64 9374	13-25-00-00 D. Laine	Servo Actuator C104312-1	Cadillac C53750	CR	Sticking at the min thrust position.	Under investigation. (See Technical Section)
11/17/64 11193	13-25-00-00 D. Laine	Servo Actuator C219217A	Cadillac 55393	MI	Actuator appeared to be working satisfactorily, but was removed for a suspected design deficiency of this model actuators, Ref. F.R. 9355.	Return to vendor for retrofit of new springs and lockwire on torque motor mounting screws.

Severity Code

CR - Critical
MA - Major
MI - Minor

SURVEYOR VERNIER THRUST CHAMBER ASSEMBLY
FAILURE REPORT SUMMARY
SOLENOID VALVE - 3 WAY

Failure Date and Report No.	Unit: I. D. Number and Responsible Engr.	Unit: Part Name and Number	Unit: Mfgr. and Serial No.	Sev.	Failure Description and Cause	Corrective Action Taken
12/18/63 8820	11-00-00-00 H. Hoffman	Valve, Solenoid H_e Pilot BF 63-C-1	Eckel 002	CR	Valve ceased to operate with signal applied. Seizure due to oxidizer entering valve from leaking propellant valve (oxidizer) causing nylon poppet and guide to bind. When valve is de-energized it bleeds the shut-off valves. When leaking, it contaminates the unit.	Shut-off valve parts will be al. made of stainless steel which will stop the valve leakage and subsequent injection of contamination into this unit. (See Rpt. 8817 - oxidizer Shut-off valve)
2/10/64 9396	11-00-00-00 H. Hoffman	Valve, Solenoid H_e Pilot BF 63-C-1	Eckel 004	MA	Valve leaked when pressure was applied to upstream. Valve had operated properly for hot firings the preceeding evening. Oxidizer entered valve on vent cycle and caused contamination and corrosion and disintegrated vent poppet.	Nylon and aluminum parts replaced with teflon and stainless steel.
3/31/64 9391	11-00-00-00 D. Webb	Valve, Solenoid H_e Pilot 71135	Adel 7019X	MA	Nitrogen leak through case. Seal deterioration.	Adel valve superceded by Eckel valve.
5/25/64 8861	11-00-00-00 D. Webb	H_e Pilot Valve 71135	STL	MI	Engine did not shut down on signal, approximately 5 sec. time lag. Contamination of valve - sticking.	Valve replaced with superior design (Eckel valve). Valve used due to unavailability of approved design.
6/27/64 9389	11-00-00-00 D. Webb	H_e Solenoid Valve	Adel 7008X	MA	Solenoid failed to open propellant on-off valves during an attempted hot firing. Valve sticking due to contamination and excessive wear.	Replaced by improved design (Eckel valve). Used due to unavailability of approved design.

Severity Code

CR - Critical
MA - Major
MI - Minor

SURVEYOR VERNIER THRUST CHAMBER ASSEMBLY
FAILURE REPORT SUMMARY
SOLENOID VALVE - 3 WAY (CONT'D)

Failure Date and Report No.	Unit: I. D. Number and Responsible Engr.	Unit: Part Name and Number	Unit: Mfgr. and Serial No.	Sev.	Failure Description and Cause	Corrective Action Taken
6/29/64 9390	11-00-00-00 D. Webb	H_e Solenoid Valve-71135	Adel 7009X	MA	Solenoid failed to close propellant on-off valve during an engine run. Ref. Run No. C1-290. Excessive wear of internal parts and contamination.	Replaced with improved design (Eckel valve). Used due to unavailability of approved design.
7/25/64 9357	11-00-00-00	H_e Solenoid	Eckel	CR	Solenoid valve failed to close following run C2-432. Stuck open. Corrosion of soft iron parts due to rework by vendor and no subsequent plating.	None required. Part normally has electroless nickel plated on soft iron parts. Part was early configuration and was reworked. Plating was not possible at the time.
8/10/64 10036	11-00-00-00 R. D. Webb	H_e Pilot Valve EQZ-25C	Vinson	CR	Valve failed to operate when "open" signal was applied.	Redesign of Vinson valve to use stainless steel instead of plating.
8/21/64 9361	11-00-00-00 R. D. Webb	H_e Solenoid A-63198	Vinson	CR	Following test firing, H_e was leaking past seal between supply and vent. Tapping valve lightly decreased leakage. Ref. C2-522B.	Redesign of Vinson valve to use stainless steel instead of plating.
8/24/64 9362	11-00-00-00 D. Webb	H_e Solenoid Valve	Eckel 002	CR	0.56 seconds delay from initiation of signal and start of engine. After engine firing, removed valve. Would not fully open with 700 psi H_e applied. Yellow-brown contamination in valve bore and on outlet poppet/seat.	Valve cleaned and contamination given to Chemical Lab. for analysis. After cleaning, the valve was reassembled and functioned properly. (Valve parts were not corroded.)
9/11/64 10918	11-00-00-00 R. D. Webb	Solenoid Valve C104337-1	Eckel 013	MI	Helium leakage across vent poppet/seat when valve was energized. Leakage decreased with time.	Excessive contamination on seat due to inadequate cleanliness practices. Memo on cleanliness procedures sent to all responsible personnel (9730.4-64-9-30).

Severity Code

CR - Critical
MA - Major
MI - Minor

SURVEYOR VERNIER THRUST CHAMBER ASSEMBLY
FAILURE REPORT SUMMARY
SOLENOID VALVE - 3 WAY (CONT'D)

Failure Date and Report No.	Unit: I. D. Number and Responsible Engr.	Unit: Part Name and Number	Unit: Mfgr. and Serial No.	Sev.	Failure Description and Cause	Corrective Action Taken
10/1/64 10917	11-00-00-00 R. D. Webb	Solenoid Valve C104337-1	Eckel 004	MI	Helium leakage across vent poppet/seat when valve was energized. Leakage gradually decreased with time with solenoid power applied, i.e. as valve temp. increased.	Decrease in armature stroke caused by burr on peoppet shaft. Vendor Q.C. to exercise better inspection and care.
10/2/64 11526	11-00-00-00 R. D. Webb	Solenoid Valve C104337	Eckel 021	MA	With 850 psig helium pressure valve partially opens, unable to hold spec. tolerance of 10 CC per hour.	Seat (poppet) damage caused by excessive contamination. Possibly from environmental testing. Helium supply to be filtered and greater handling care to be exercised to avoid contamination.

APPENDIX I

PQT-011 - VIBRATION TEST DATA

No. of Pages: 18

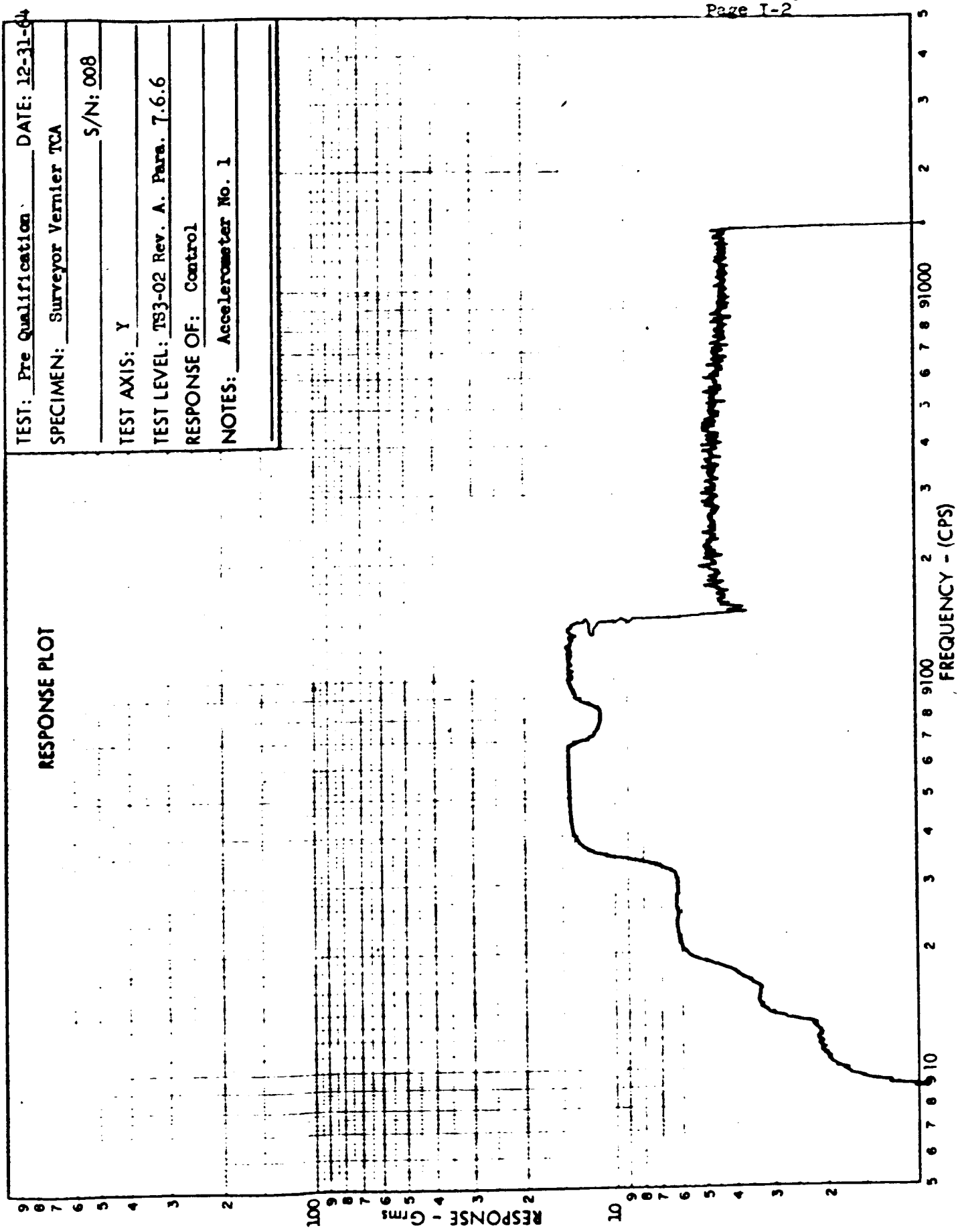
TEST: Pre Qualification DATE: 12-31-64
SPECIMEN: Surveyor Vernier TCA
S/N: 008
TEST AXIS: Y
TEST LEVEL: TS3-02 Rev. A. Para. 7.6.6
RESPONSE OF: Control
NOTES: Accelerometer No. 1
RESPONSE PLOT
RESPONSE - Grms
FREQUENCY - (CPS)

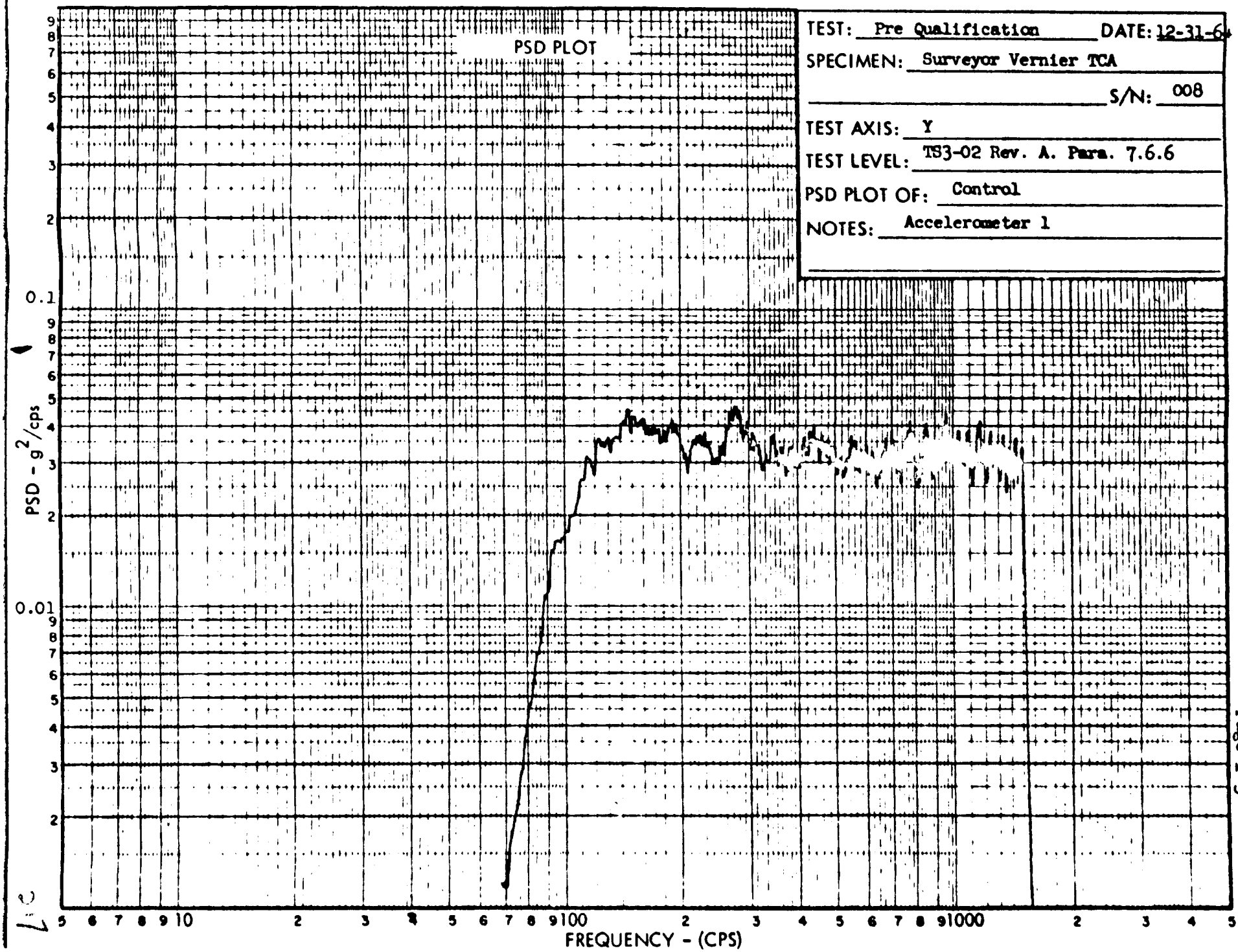
PSD PLOT
TEST: Pre Qualification DATE: 12-31-6
SPECIMEN: Surveyor Vernier TCA
S/N: 008
TEST AXIS: Y
TEST LEVEL: TS3-02 Rev. A. Para. 7.6.6
PSD PLOT OF: Control
NOTES: Accelerometer 1
PSD - g²/cps
FREQUENCY - (CPS)

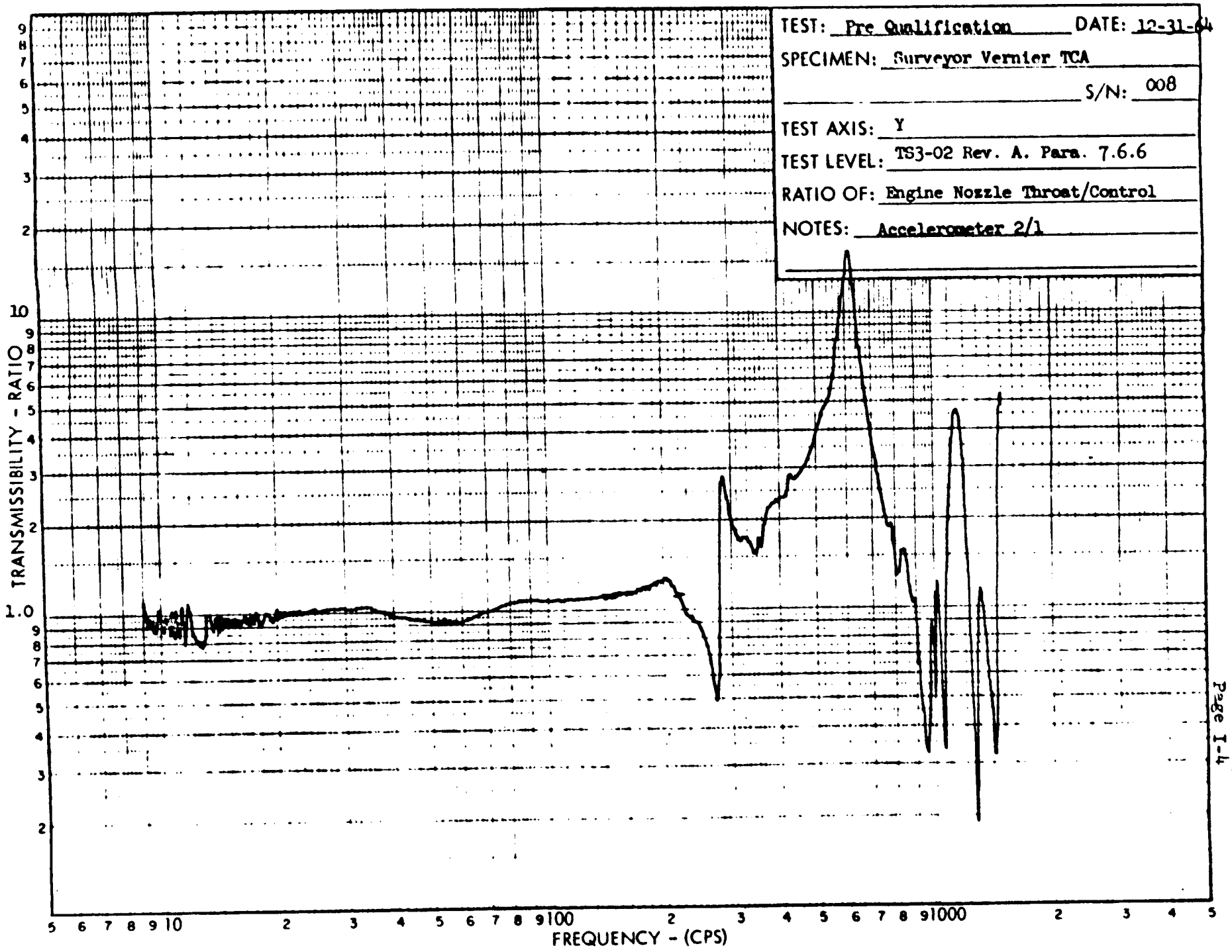
TEST: Pre Qualification DATE: 12-31-64
SPECIMEN: Surveyor Vernier TCA
S/N: 008
TEST AXIS: Y
TEST LEVEL: TS3-02 Rev. A. Para. 7.6.6
RATIO OF: Engine Nozzle Throat/Control
NOTES: Accelerometer 2/1
TRANSMISSIBILITY - RATIO
FREQUENCY - (CPS)
5 6 7 8 9 10 2 3 4 5 6 7 8 9 100 2 3 4 5 6 7 8 9 1000 2 3 4 5

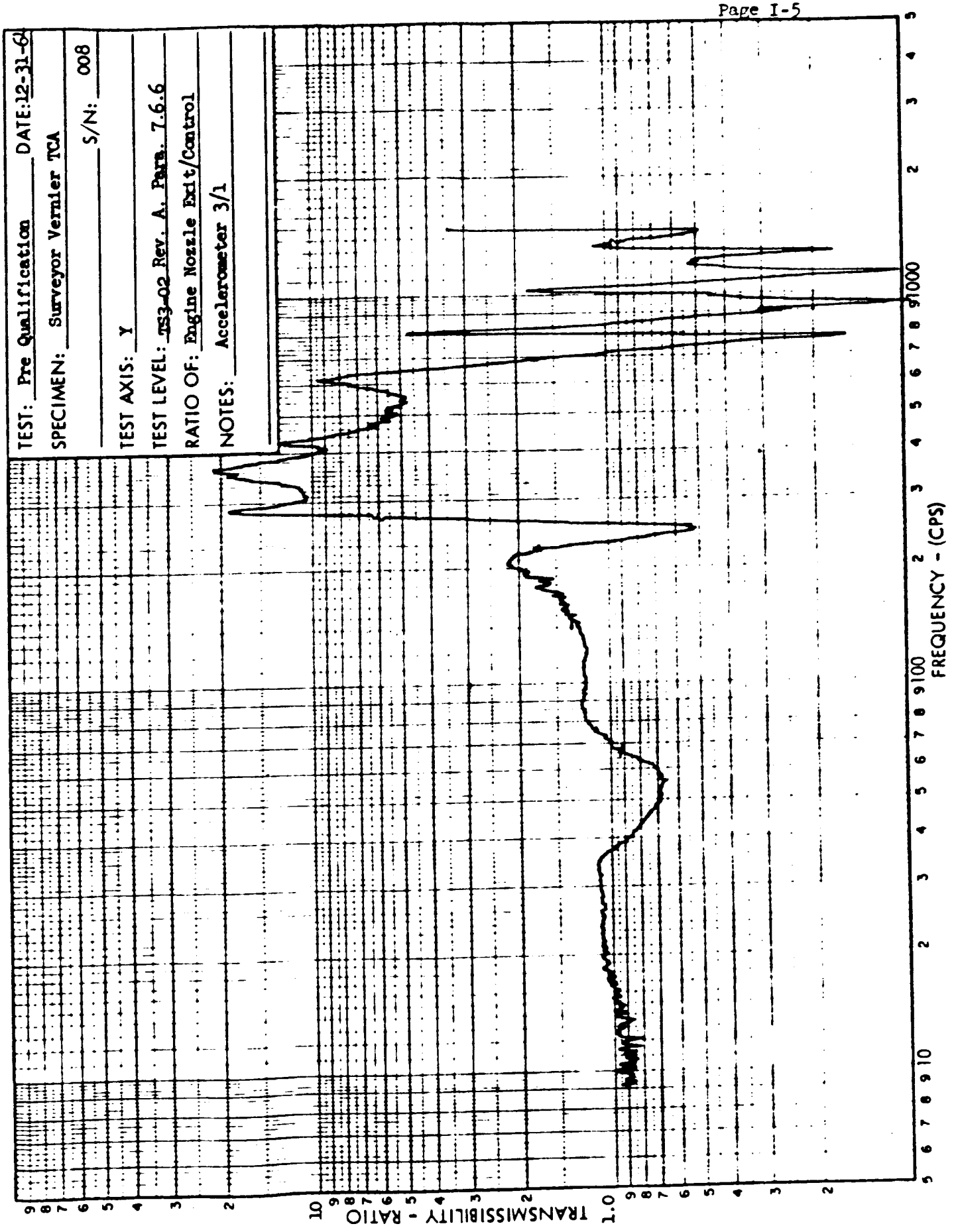
TEST: Pre Qualification DATE: 12-31-69
SPECIMEN: Surveyor Vernier TCA
S/N: 008
TEST AXIS: Y
TEST LEVEL: TS3-02 Rev. A, Para. 7.6.6
RATIO OF: Engine Nozzle Exit/Control
NOTES: Accelerometer 3/1
TRANSMISSIBILITY - RATIO
FREQUENCY - (CPS)

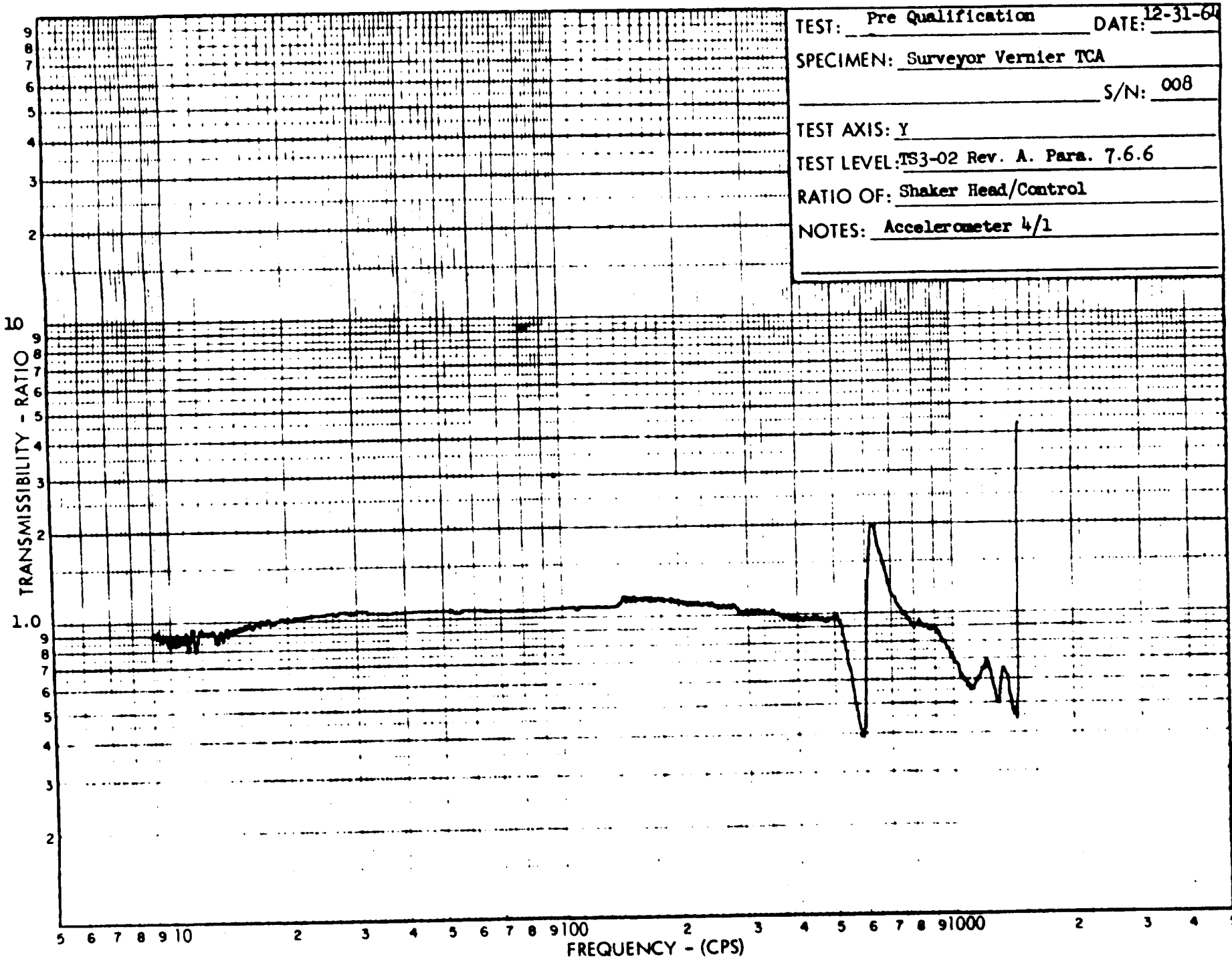
TEST: Pre Qualification DATE: 12-31-64
SPECIMEN: Surveyor Vernier TCA
S/N: 008
TEST AXIS: Y
TEST LEVEL: TS3-02 Rev. A. Para. 7.6.6
RATIO OF: Shaker Head/Control
NOTES: Accelerometer 4/1
TRANSMISSIBILITY - RATIO
FREQUENCY - (CPS)
5 6 7 8 9 10 2 3 4 5 6 7 8 9 100 2 3 4 5 6 7 8 9 1000 2 3 4 5

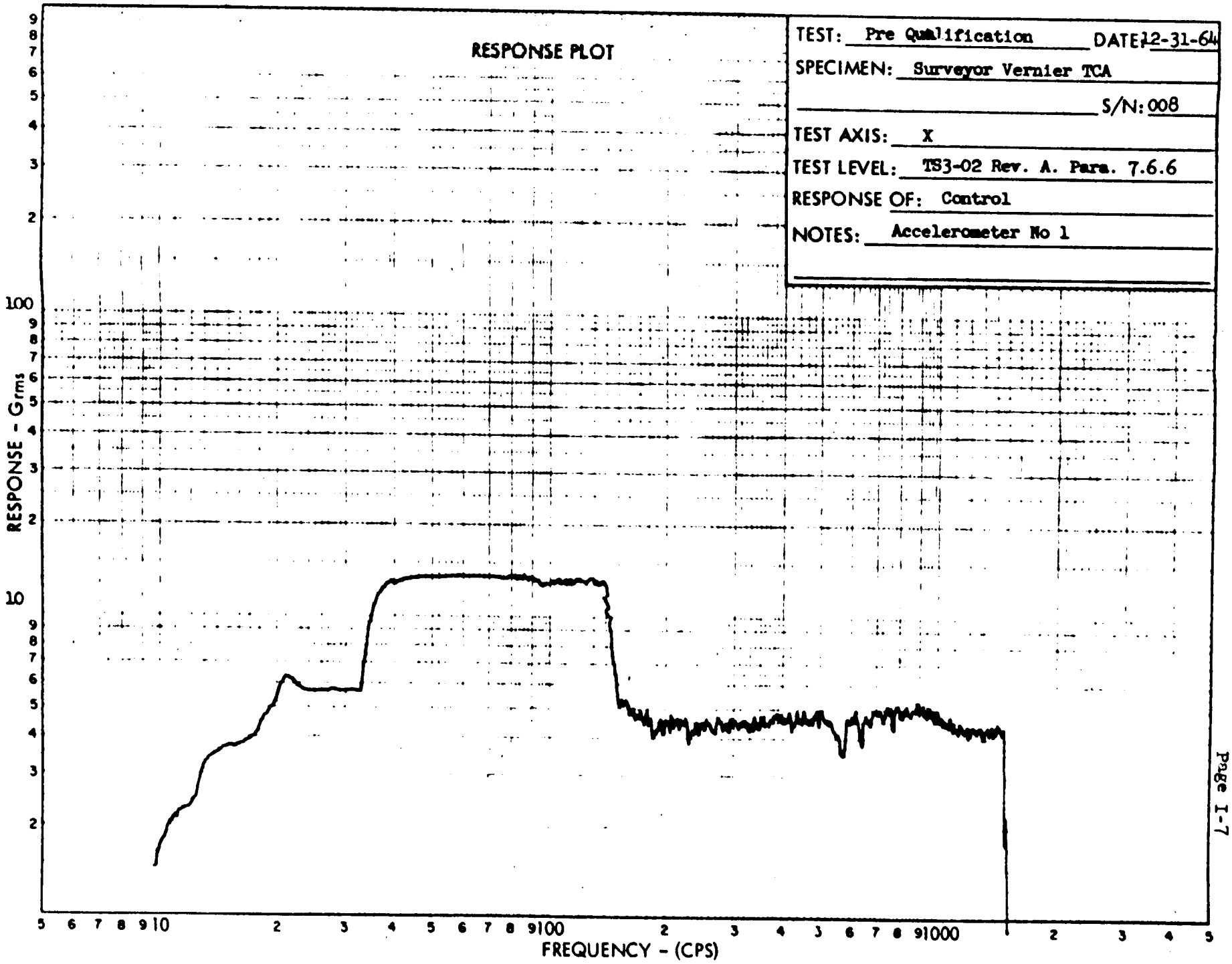
RESPONSE PLOT
TEST: Pre Qualification DATE: 12-31-64
SPECIMEN: Surveyor Vernier TCA
S/N: 008
TEST AXIS: X
TEST LEVEL: TS3-02 Rev. A. Para. 7.6.6
RESPONSE OF: Control
NOTES: Accelerometer No 1
RESPONSE - Grms
FREQUENCY - (CPS)
5 6 7 8 9 10 2 3 4 5 6 7 8 9 100 2 3 4 5 6 7 8 9 1000 2 3 4 5

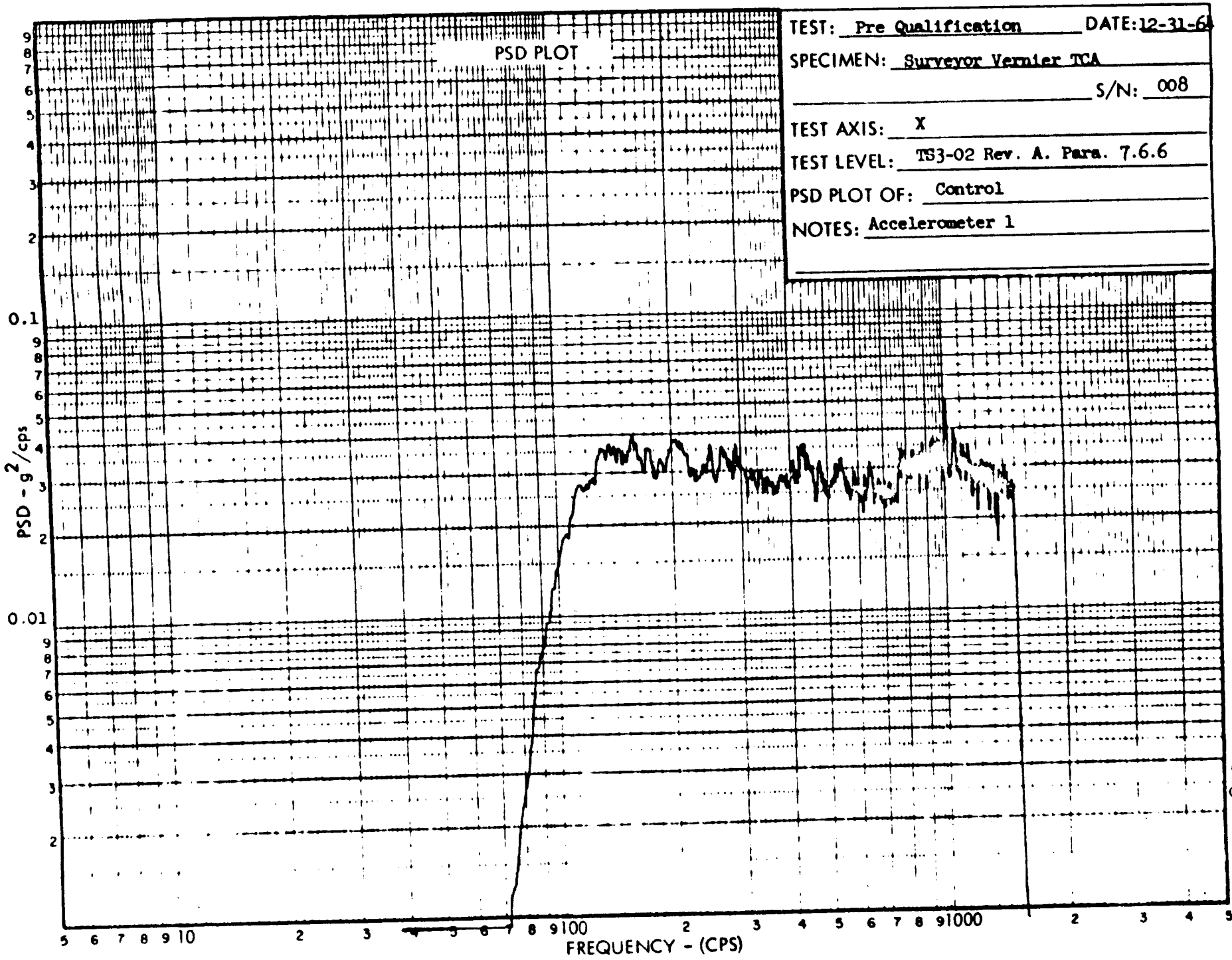
PSD PLOT
TEST: Pre Qualification
DATE: 12-31-6
SPECIMEN: Surveyor Vernier TCA
S/N: 008
TEST AXIS: X
TEST LEVEL: TS3-02 Rev. A. Para. 7.6.6
PSD PLOT OF: Control
NOTES: Accelerometer 1
PSD - g²/cps
FREQUENCY - (CPS)

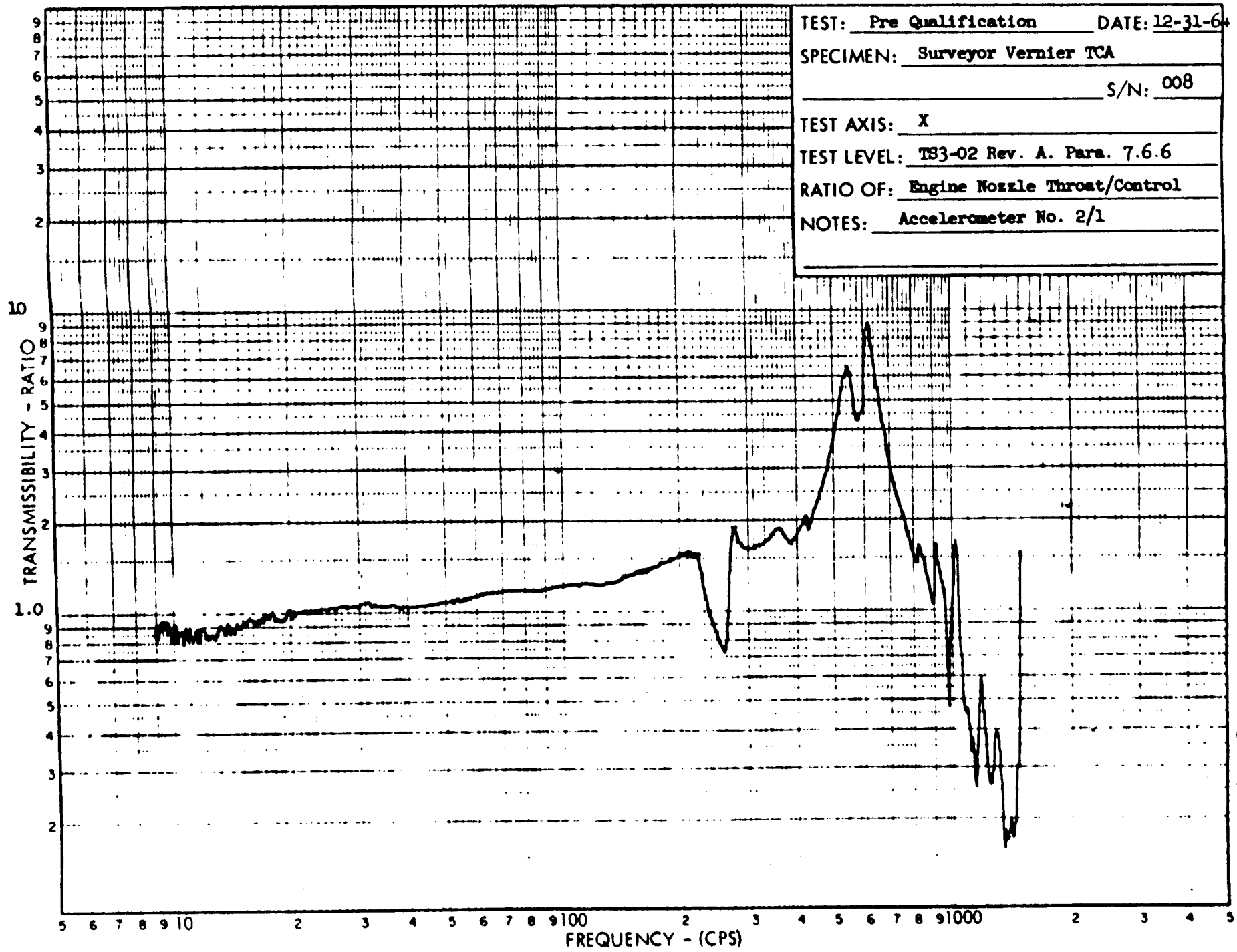
TEST: Pre Qualification DATE: 12-31-64
SPECIMEN: Surveyor Vernier TCA
S/N: 008
TEST AXIS: X
TEST LEVEL: TS3-02 Rev. A. Para. 7.6.6
RATIO OF: Engine Nozzle Throat/Control
NOTES: Accelerometer No. 2/1
TRANSMISSIBILITY - RATIO
10
1.0
FREQUENCY - (CPS)
5 6 7 8 9 10 2 3 4 5 6 7 8 9 100 2 3 4 5 6 7 8 9 1000 2 3 4 5

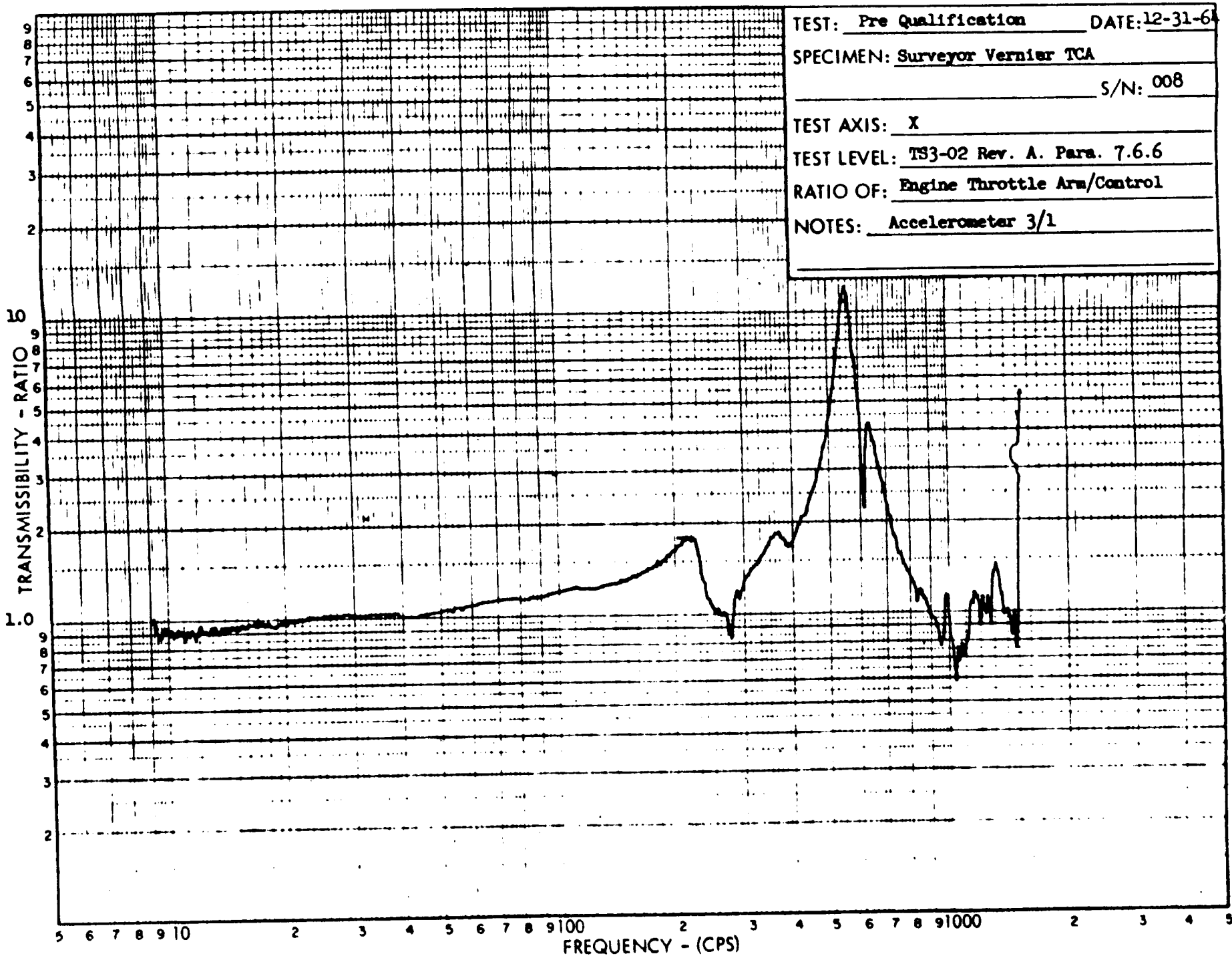
TEST: Pre Qualification DATE: 12-31-64
SPECIMEN: Surveyor Vernier TCA
S/N: 008
TEST AXIS: X
TEST LEVEL: TS3-02 Rev. A. Para. 7.6.6
RATIO OF: Engine Throttle Arm/Control
NOTES: Accelerometer 3/1
TRANSMISSIBILITY - RATIO
FREQUENCY - (CPS)

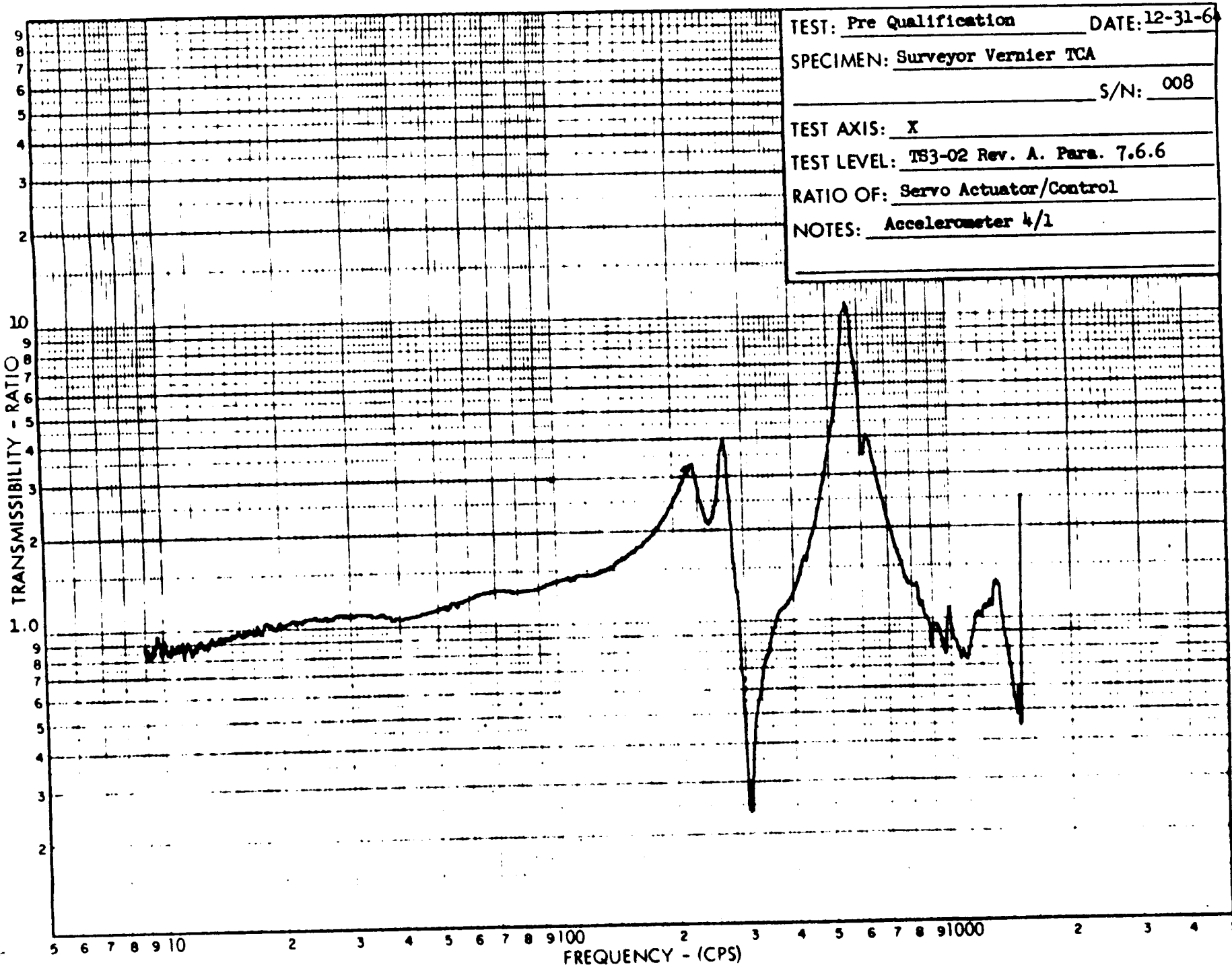
TEST: Pre Qualification
DATE: 12-31-6
SPECIMEN: Surveyor Vernier TCA
S/N: 008
TEST AXIS: X
TEST LEVEL: TS3-02 Rev. A. Para. 7.6.6
RATIO OF: Servo Actuator/Control
NOTES: Accelerometer 4/1
TRANSMISSIBILITY - RATIO
FREQUENCY - (CPS)

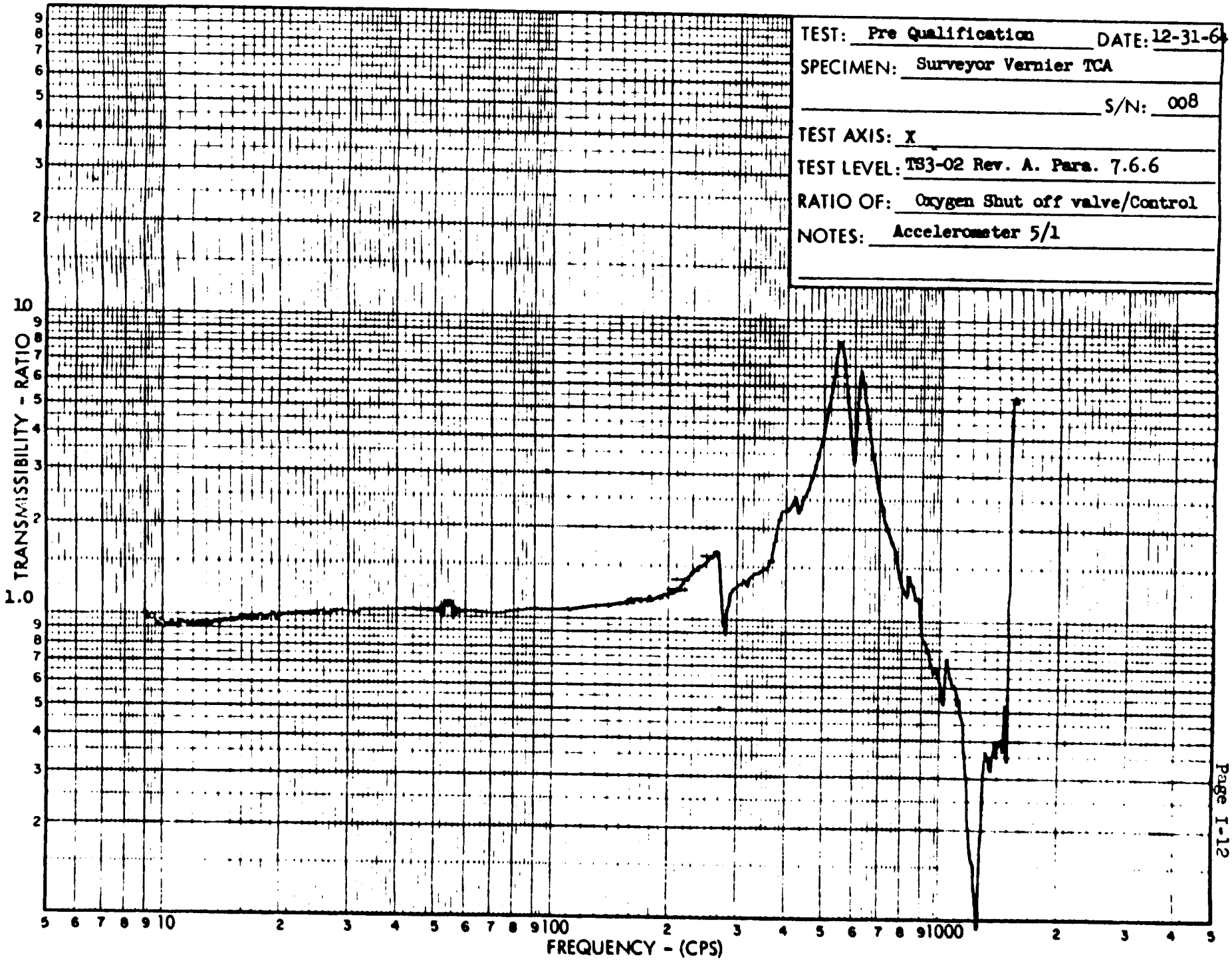
TEST: Pre Qualification DATE: 12-31-64
SPECIMEN: Surveyor Vernier TCA
S/N: 008
TEST AXIS: X
TEST LEVEL: TS3-02 Rev. A. Para. 7.6.6
RATIO OF: Oxygen Shut off valve/Control
NOTES: Accelerometer 5/1
TRANSMISSIBILITY - RATIO
1.0
10
FREQUENCY - (CPS)
5 6 7 8 9 10 2 3 4 5 6 7 8 9 100 2 3 4 5 6 7 8 9 1000 2 3 4 5

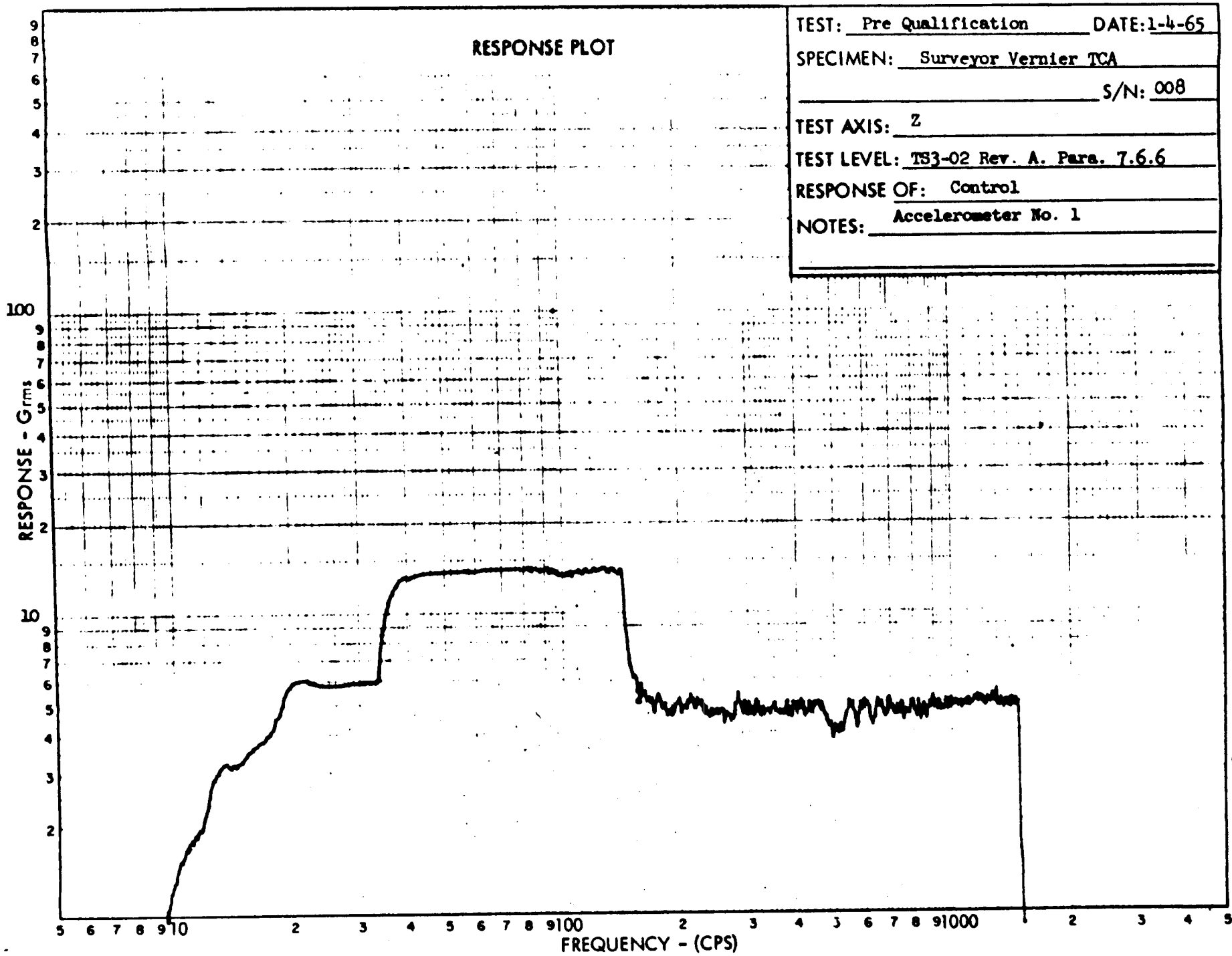
RESPONSE PLOT
TEST: Pre Qualification DATE: 1-4-65
SPECIMEN: Surveyor Vernier TCA
S/N: 008
TEST AXIS: Z
TEST LEVEL: TS3-02 Rev. A. Para. 7.6.6
RESPONSE OF: Control
NOTES: Accelerometer No. 1
RESPONSE - Grms
FREQUENCY - (CPS)
5 6 7 8 9 10 2 3 4 5 6 7 8 9 100 2 3 4 5 6 7 8 9 1000 2 3 4 5

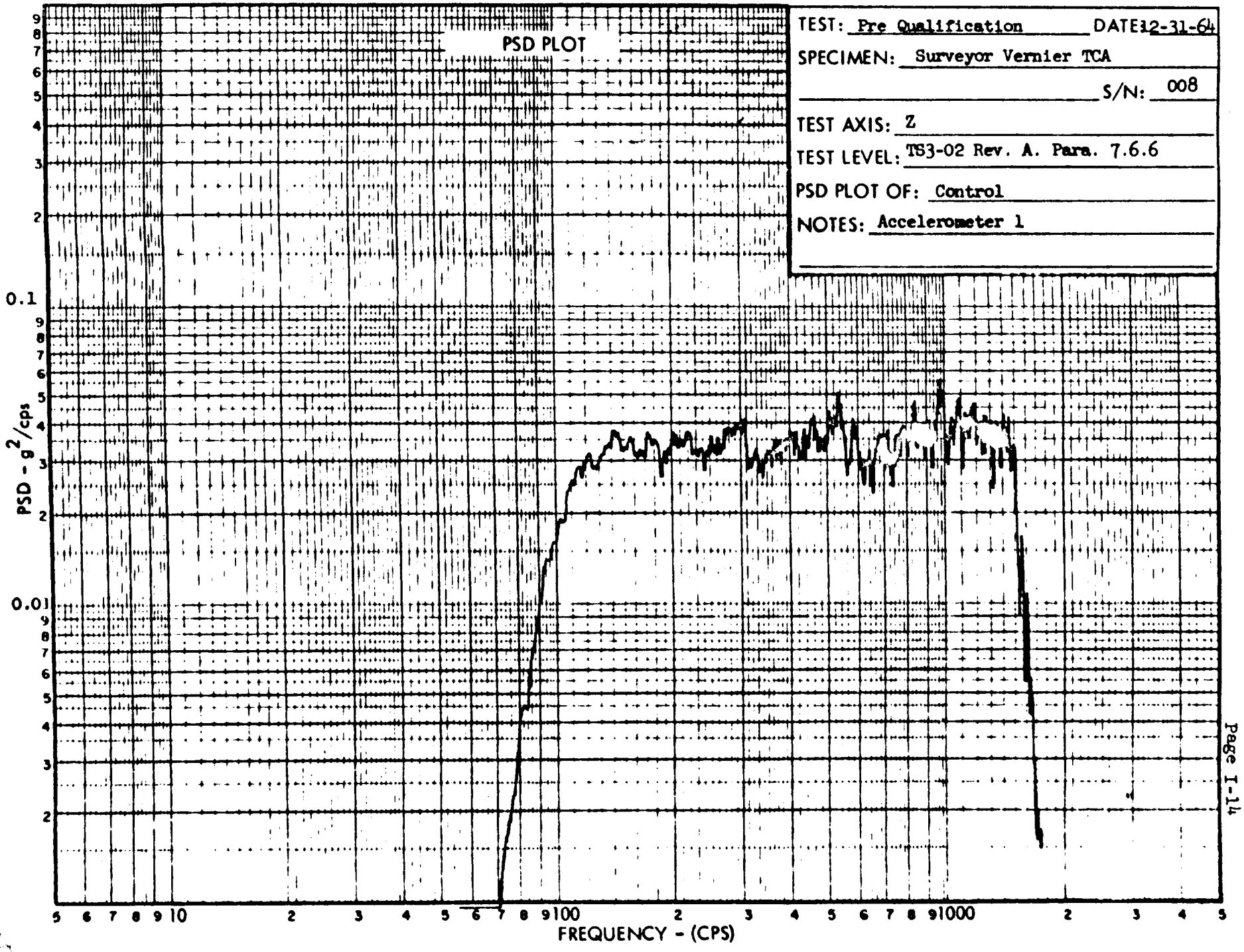
PSD PLOT
TEST: Pre Qualification DATE: 12-31-64
SPECIMEN: Surveyor Vernier TCA
S/N: 008
TEST AXIS: Z
TEST LEVEL: TS3-02 Rev. A. Para. 7.6.6
PSD PLOT OF: Control
NOTES: Accelerometer 1
PSD - g²/cps
FREQUENCY - (CPS)

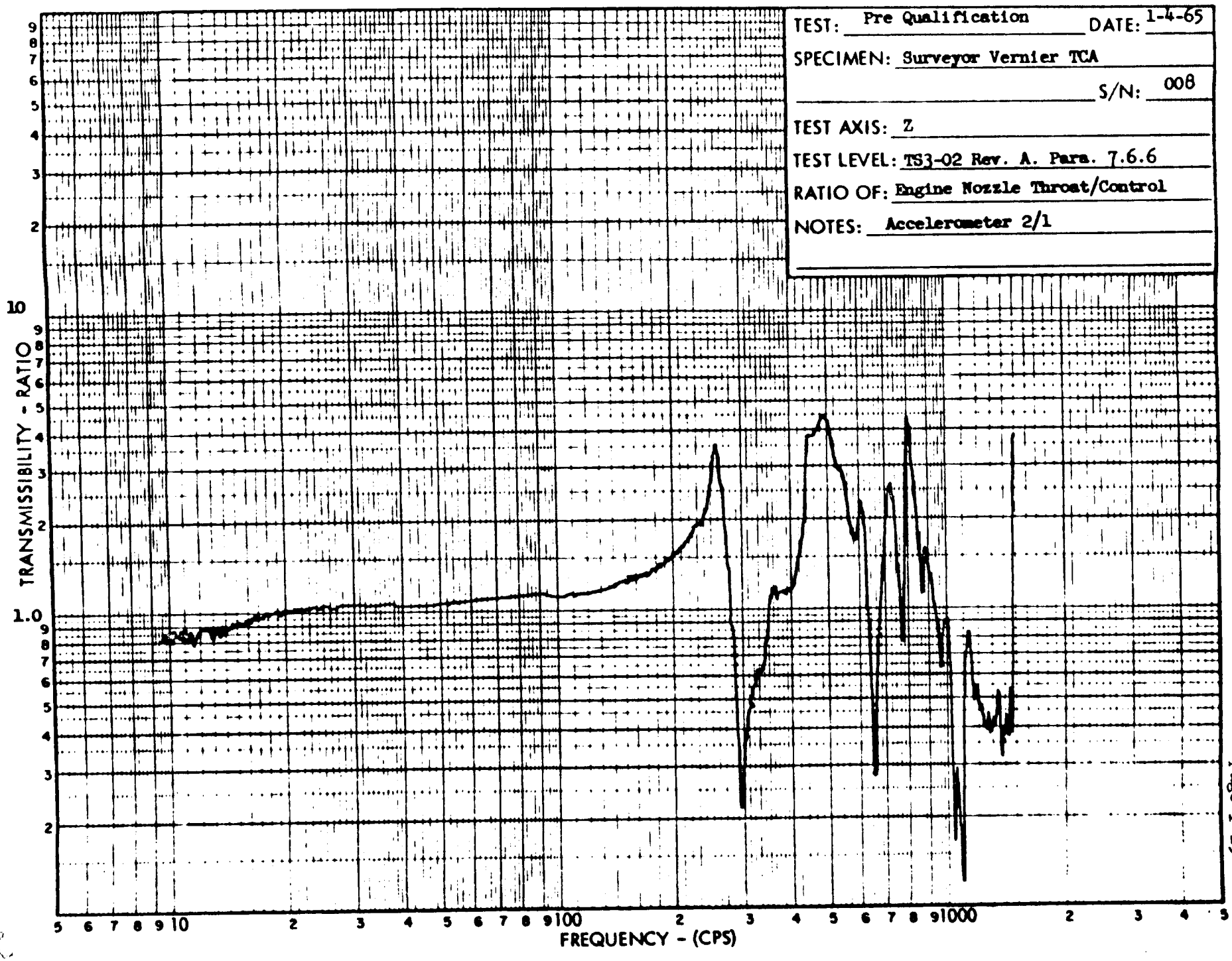
TEST: Pre Qualification DATE: 1-4-65
SPECIMEN: Surveyor Vernier TCA
S/N: 008
TEST AXIS: Z
TEST LEVEL: TS3-02 Rev. A. Para. 7.6.6
RATIO OF: Engine Nozzle Throat/Control
NOTES: Accelerometer 2/1
TRANSMISSIBILITY - RATIO
FREQUENCY - (CPS)

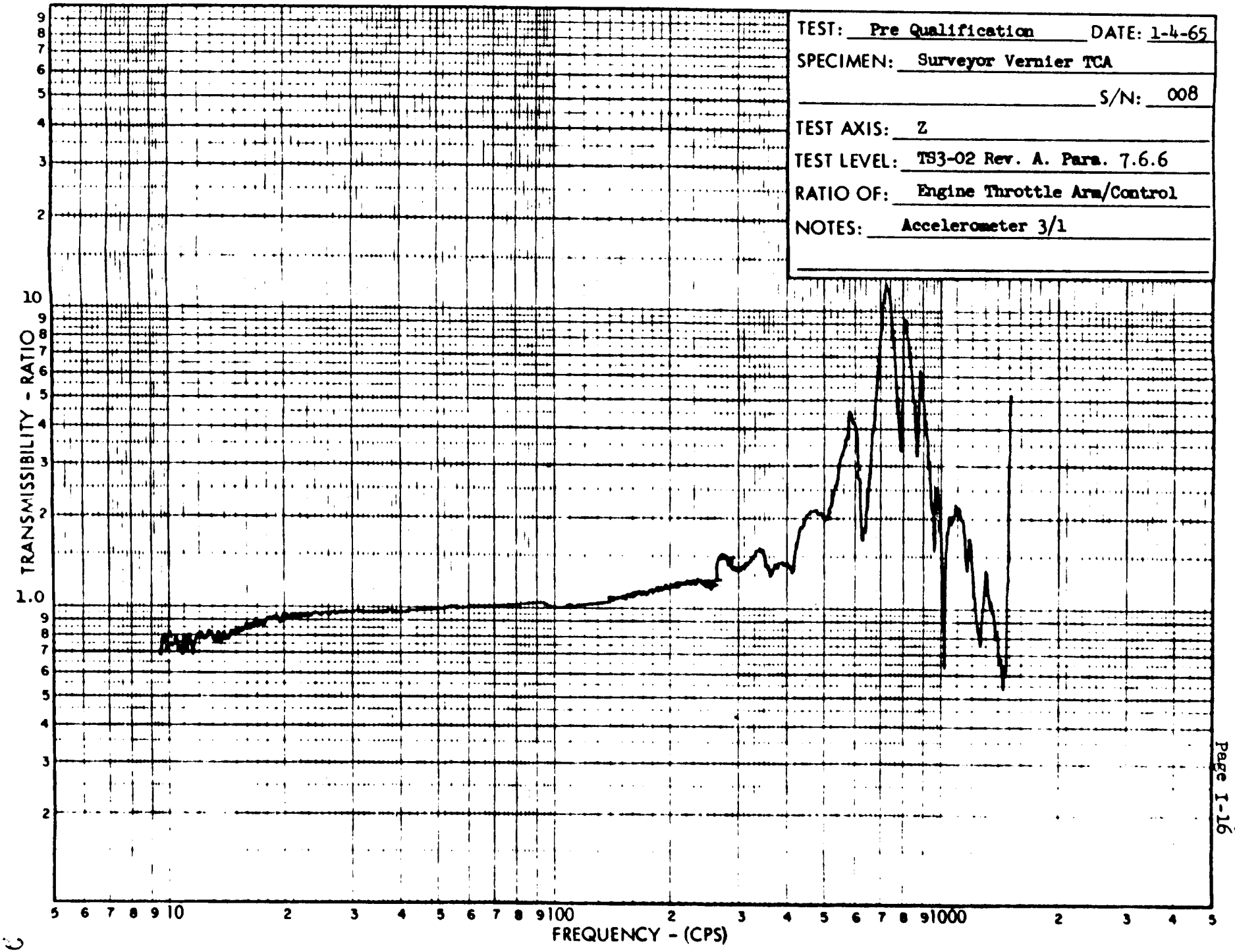
TEST: Pre Qualification DATE: 1-4-65
SPECIMEN: Surveyor Vernier TCA
S/N: 008
TEST AXIS: Z
TEST LEVEL: TS3-02 Rev. A. Para. 7.6.6
RATIO OF: Engine Throttle Arm/Control
NOTES: Accelerometer 3/1
TRANSMISSIBILITY - RATIO
FREQUENCY - (CPS)
5 6 7 8 9 10 2 3 4 5 6 7 8 9 100 2 3 4 5 6 7 8 9 1000 2 3 4 5

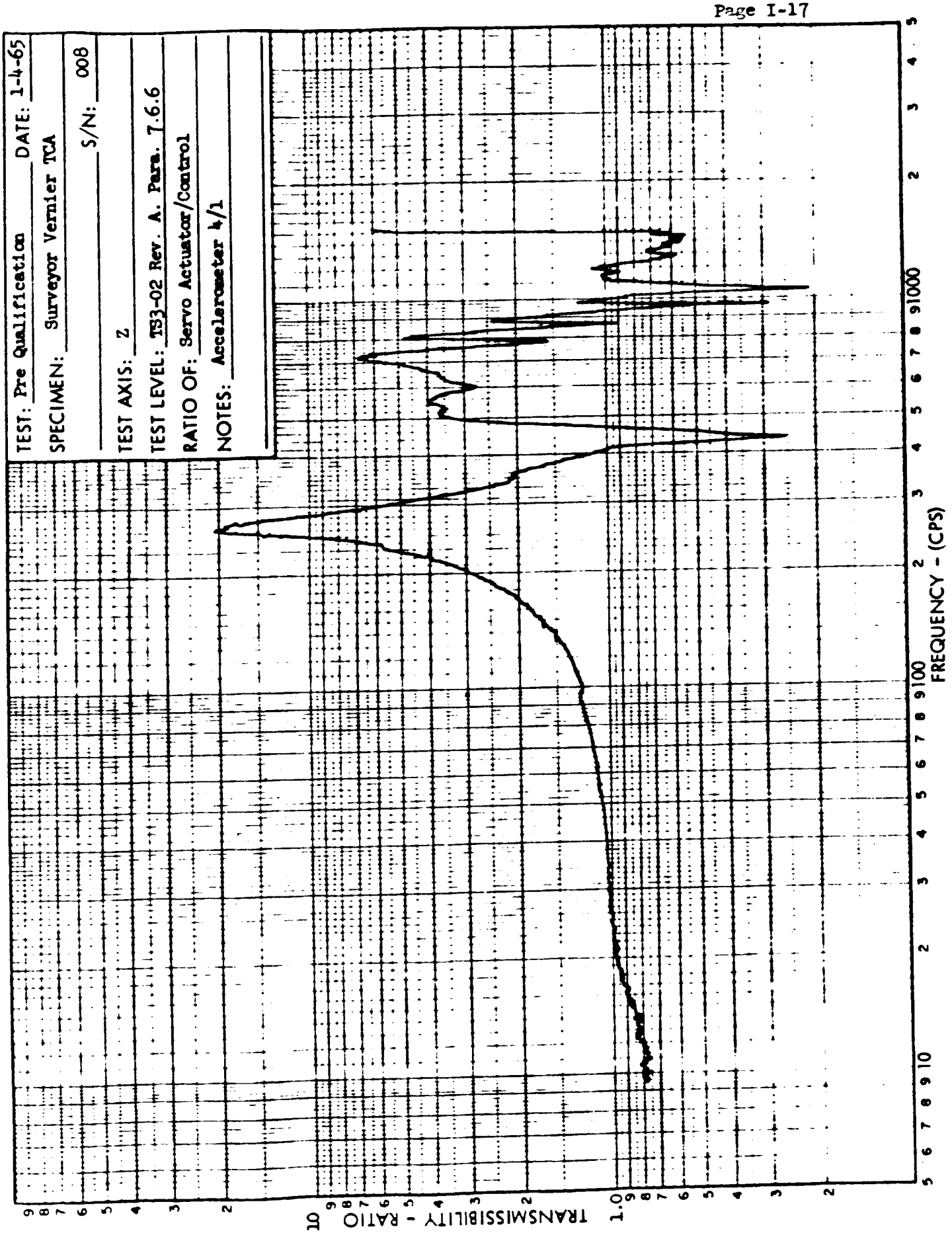
TEST: Pre Qualification DATE: 1-4-65
SPECIMEN: Surveyor Vernier TCA
S/N: 008
TEST AXIS: Z
TEST LEVEL: TS3-02 Rev. A. Para. 7.6.6
RATIO OF: Servo Actuator/Control
NOTES: Accelerometer 4/1
TRANSMISSIBILITY - RATIO Q
FREQUENCY - (CPS)

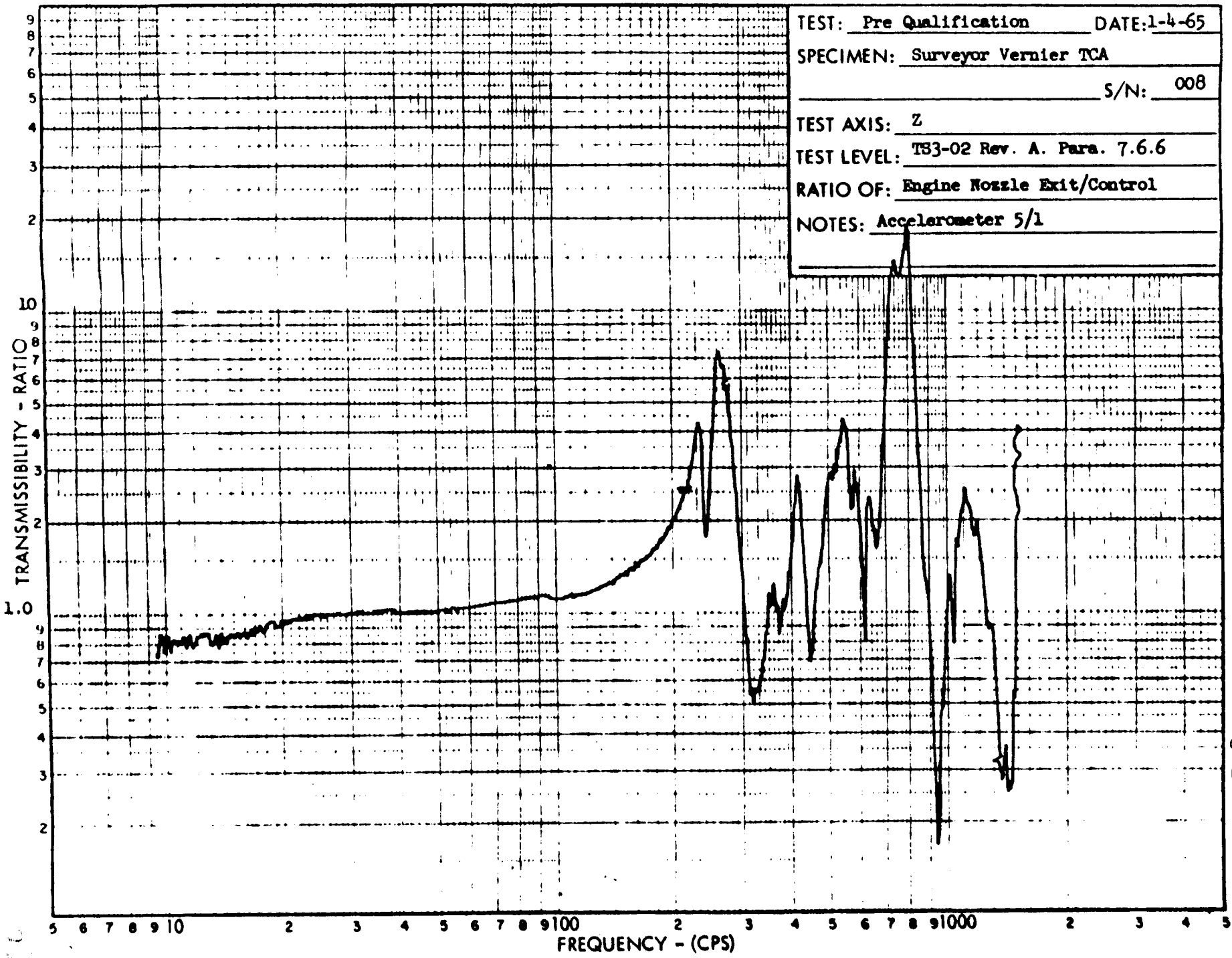
TEST: Pre Qualification DATE: 1-4-65
SPECIMEN: Surveyor Vernier TCA
S/N: 008
TEST AXIS: Z
TEST LEVEL: TS3-02 Rev. A. Para. 7.6.6
RATIO OF: Engine Nozzle Exit/Control
NOTES: Accelerometer 5/1
TRANSMISSIBILITY - RATIO
FREQUENCY - (CPS)

APPENDIX D

STATIC FIRING DATA

No. of Pages: 146

This work was performed for the Jet Propulsion Laboratory, California Institute of Technology, sponsored by the National Aeronautics and Space Administration under Contract NAS7-100.

APPENDIX D-1

JPL/ETS STATIC FIRING DATA

No. of Pages: 90

TABLE D-1-1. MIRA 150A STEADY-STATE PERFORMANCE
DATA FROM JPL/ETS TEST SITE

JPL/ETS Run No.	Development Plan or PQT Test No.	Test Date	HEA S/N	CC & NA Type	CC & NA S/N	Test Duration, sec.	Data Slice No.	Servo Command, ma	F_{vac}, lbs Site	F_{vac}, lbs Standard	Head-End P_c, psia Site	Head-End P_c, psia Standard	I_{sp} vac, sec. Site	I_{sp} vac, sec. Standard	M.R., o/f Site	M.R., o/f Standard	Total Flowrate, lbs/sec Site	Total Flowrate, lbs/sec Standard	Corrected C^* fps Site	Corrected C^* fps Standard	$C_{F_{vac}}$ Site	$C_{F_{vac}}$ Standard	Fuel Inlet Pr., psia	Ox. Inlet Pr., psia	Fuel Inlet Temp., °F	Ox. Inlet Temp., °F	Remarks
DY-18	5.2.8	9-11-[illegible]	004	Water-Cooled	106831	130	1	+ 35	Not Applicable; Sea level test.		87.7	89.0	Not Applicable; Sea level test.		1.517	1.523	0.4282	0.4320	5255	5256	Not Applicable; Sea Level Test		714	710	76	73	Sea level checkout firing with AT-1 acceptance test tape. Servoactuator dump valve not opened until fire signal.
							2	+ 70			106.1	108.0			1.550	1.557	0.5162	0.5228	5275	5276			708	703	75	72	
							3	+ 35			87.9	89.0			1.525	1.529	0.4290	0.4322	5254	5255			714	709	74	71	
							4	0			67.6	68.2			1.497	1.498	0.3308	0.3316	5240	5241			719	716	73	70	
							5	- 35			44.1	44.4			1.489	1.489	0.2203	0.2201	5135	5135			723	722	73	70	
							6	- 80			20.2	20.3			1.456	1.456	0.1039	0.1039	5048	5048			725	724	72	70	
							7	- 50			34.3	34.5			1.465	1.464	0.1743	0.1740	5052	5052			723	723	72	70	
							8	- 35			43.7	44.0			1.458	1.458	0.2212	0.2211	5065	5065			722	720	72	70	
							9	0			67.0	67.6			1.495	1.497	0.3277	0.3285	5240	5240			718	716	72	70	
DY-19	5.2.9	9-16-[illegible]	004	Water-Cooled	106831	45	1	+ 26.3	113.0	113.4	80.7	81.4	288.3	288.2	1.514	1.504	0.3921	0.3934	5272	5272	1.757	1.756	710	716	72	68	Altitude test with PQ-3 step thrust program tape. No injection pressure measurements.
							2	+ 51.9	133.0	133.7	94.8	95.8	288.6	288.5	1.529	1.519	0.4608	0.4636	5273	5273	1.759	1.758	706	712	72	67	
							3	+ 76.4	150.4	151.7	107.2	108.7	289.4	289.4	1.555	1.547	0.5196	0.5243	5290	5290	1.758	1.757	704	706	71	67	
							4	+ 1.6	93.7	93.7	67.2	67.5	286.8	286.7	1.497	1.486	0.3268	0.3268	5265	5265	1.750	1.745	714	720	71	67	
							5	- 23.1	70.1	69.9	50.5	50.7	281.5	281.4	1.509	1.498	0.2490	0.2485	5193	5194	1.743	1.743	717	722	71	66	
							6	- 48.8	46.6	46.4	33.9	33.9	267.9	267.8	1.491	1.478	0.1739	0.1732	4749	4749	1.726	1.725	721	727	71	66	
							7	- 73.2	27.5	27.3	20.0	20.0	253.8	253.7	1.477	1.465	0.1083	0.1078	4991	4991	1.727	1.726	720	726	71	66	
							8	- 11.3	82.6	82.5	59.3	59.5	286.0	286.9	1.498	1.486	0.2889	0.2885	5260	5260	1.748	1.747	716	721	71	66	
DY-20	5.2.11	9-18-[illegible]	004	Uncooled Altitude	002	52	1	+ 1.7	92.8	92.8	66.9	67.0	290.9	290.9	1.508	1.511	0.3190	0.3191	5271	5271	1.776	1.776	721	717	70	69	Altitude test with PQ-1 dynamic thrust program tape.
DY-21	5.2.11	9-18-[illegible]	004	Uncooled Altitude	002	70	1	- 28.5	62.8	62.7	46.2	46.2	286.5	286.5	1.488	1.495	0.2192	0.2189	5294	5294	1.741	1.741	725	718	69	69	Altitude test with PQ-1A dynamic thrust program tape.
							2	+ 74.7	145.8	147.3	105.3	106.4	290.9	291.0	1.532	1.545	0.5011	0.5061	5278	5279	1.773	1.774	712	700	69	69	
							3	- 71.2	27.1	27.0	20.0	19.9	252.5	252.5	1.535	1.543	0.1075	0.1070	4674	4673	1.738	1.738	730	721	69	69	
DY-22	5.2.11	9-21-[illegible]	004	Uncooled Altitude	002	40	1	+ 79.2	127.1	127.1	91.4	91.4	292.2	292.2	1.540	1.526	0.4351	0.4351	5276	5276	1.782	1.781	710	715	65	61	Altitude test with PQ-1B dynamic thrust program tape. Test aborted after 40 seconds due to facility feed system leak. Data questionable.
DY-23	5.2.11	9-21-[illegible]	004	Uncooled Altitude	002	115.8	1	+ 73.4	152.4	153.2	109.3	110.0	292.8	292.8	1.558	1.552	0.5203	0.5203	5278	5278	1.785	1.785	708	706	66	63	Altitude test with PQ-1B dynamic thrust program tape.
							2	+ 73.1	154.3	154.8	110.8	111.3	293.0	293.0	1.559	1.551	0.5265	0.5285	5287	5286	1.783	1.783	709	709	66	62	
							3	+ 73.3	153.7	154.2	110.4	110.8	292.6	292.6	1.560	1.550	0.5252	0.5270	5279	5279	1.784	1.783	708	710	66	62	
							4	- 70.0	30.9	30.6	22.7	22.5	262.6	262.5	1.484	1.470	0.1178	0.1165	4852	4852	1.741	1.741	726	732	66	63	
DY-24	5.2.11	9-21-[illegible]	004	Uncooled Altitude	002	70	1	- 29.0	68.0	68.0	49.8	49.4	286.7	286.6	1.525	1.518	0.2371	0.2353	5275	5275	1.749	1.748	725	723	65	62	Altitude test with PQ-1A dynamic thrust program tape.
							2	+ 72.5	150.5	150.9	108.4	108.7	291.7	291.7	1.559	1.555	0.5158	0.5172	5278	5278	1.778	1.778	712	707	65	61	
							3	- 71.2	28.8	28.5	21.3	21.1	262.9	262.8	1.466	1.457	0.1096	0.1083	4893	4893	1.728	1.728	730	730	65	61	

TABLE D-1-1. (Continued)

JPL/ETS Run No.	Development Plan or PQT Test No.	Test Date	HEA S/N	CC & NA Type	CC & NA S/N	Test Duration, sec.	Data Slice No.	Servo Command, ma	F_{vac}, lbs Site	F_{vac}, lbs Standard	Head-End P_c, psia Site	Head-End P_c, psia Standard	I_{sp} vac, sec. Site	I_{sp} vac, sec. Standard	M.R., o/f Site	M.R., o/f Standard	Total Flowrate, lbs/sec Site	Total Flowrate, lbs/sec Standard	Corrected C^* fps Site	Corrected C^* fps Standard	C_F vac Site	C_F vac Standard	Fuel Inlet Pr., psia	Ox. Inlet Pr., psia	Fuel Inlet Temp., °F	Ox. Inlet Temp., °F	Remarks
DY-25	PQT-001	10-[illegible]-64	001	Uncooled Altitude	003	45	1	+ 24.2	119.6	120.7	86.6	87.4	289.6	289.7	1.500	1.514	0.4130	0.4167	5299	5300	1.758	1.759	715	707	69	73	Altitude test with PQ-3 step thrust program tape. CC & NA S/N 003 replaced post-test due to leakage around ablative liner and retaining pins.
							2	+ 49.4	138.8	140.5	100.9	102.1	292.0	292.1	1.500	1.513	0.4754	0.4811	5360	5362	1.752	1.753	710	701	69	72	
							3	+ 73.5	154.4	157.1	111.6	113.6	292.1	292.3	1.516	1.534	0.5284	0.5374	5336	5337	1.761	1.762	706	692	68	71	
							4	+ 0.1	99.8	100.5	72.6	73.1	288.9	289.1	1.488	1.502	0.3456	0.3479	5309	5310	1.751	1.752	718	707	68	71	
							5	- 24.0	79.6	80.0	58.2	58.5	285.0	285.1	1.474	1.486	0.2795	0.2807	5259	5259	1.744	1.744	720	710	68	70	
							6	- 48.9	59.2	59.3	43.7	43.8	281.4	281.5	1.475	1.483	0.2104	0.2106	5251	5251	1.724	1.725	722	716	68	70	
							7	- 72.7	36.4	36.4	27.5	27.5	260.0	260.1	1.457	1.465	0.1401	0.1398	4966	4966	1.685	1.685	727	720	68	70	
							8	- 12.4	91.2	91.7	66.1	66.4	288.1	288.2	1.486	1.500	0.3166	0.3182	5269	5270	1.759	1.760	720	708	68	70	
DY-26	PQT-002	10-[illegible]-64	001	Uncooled Altitude	005	45	1	+ 24.2	117.9	120.3	86.5	88.0	287.5	288.7	1.420	1.525	0.4100	0.4168	5304	5312	1.744	1.749	758	660	69	70	Altitude test with PQ-4 step thrust program tape. Tank pressures adjusted to achieve 1.4 target mixture ratio.
							2	+ 49.5	136.3	139.7	100.1	102.2	288.7	290.0	1.419	1.528	0.4723	0.4816	5327	5336	1.744	1.749	755	654	68	69	
							3	+ 73.3	152.2	156.6	111.4	114.3	289.2	290.6	1.430	1.544	0.5262	0.5389	5323	5331	1.748	1.758	751	647	68	68	
							4	+ 0.3	98.6	100.2	72.5	73.5	286.6	287.8	1.410	1.512	0.3439	0.3483	5301	5308	1.740	1.744	762	663	68	68	
							5	- 23.9	78.4	79.5	57.8	58.4	283.3	284.7	1.379	1.476	0.2768	0.2793	5250	5258	1.736	1.742	765	668	68	68	
							6	- 48.8	57.1	57.7	42.3	42.7	274.9	276.0	1.390	1.485	0.2078	0.2091	5125	5130	1.726	1.731	767	672	68	68	
							7	- 72.6	35.7	35.9	27.0	27.1	260.1	260.9	1.399	1.495	0.1371	0.1378	4952	4952	1.690	1.695	770	674	68	68	
							8	+ 12.8	110.5	112.7	80.9	82.3	288.1	289.3	1.413	1.521	0.3834	0.3894	5305	5313	1.747	1.752	760	657	68	68	
DY-27	PQT-003	10-[illegible]-64	001	Uncooled Altitude	005	45	1	+ 25.2	122.5	123.5	89.8	90.7	290.4	290.0	1.629	1.521	0.4219	0.4259	5341	5345	1.749	1.746	650	745	68	70	Altitude test with PQ-5 step thrust program tape. Tank pressures adjusted to achieve 1.6 target mixture ratio.
							2	+ 50.5	141.2	142.8	103.4	104.9	291.7	291.3	1.633	1.528	0.4839	0.4903	5365	5368	1.750	1.746	646	737	68	69	
							3	+ 76.6	159.1	161.7	116.0	118.1	293.5	293.1	1.642	1.542	0.5421	0.5517	5369	5373	1.758	1.755	644	728	68	69	
							4	+ 1.2	102.8	103.4	75.3	75.9	290.7	290.3	1.614	1.508	0.3537	0.3562	5346	5350	1.749	1.746	653	746	68	69	
							5	- 22.8	82.2	82.4	60.4	60.7	286.3	285.8	1.594	1.490	0.2870	0.2883	5280	5284	1.745	1.740	657	750	68	69	
							6	- 47.9	60.7	60.5	45.2	45.1	276.8	276.5	1.607	1.490	0.2194	0.2187	5169	5177	1.722	1.719	660	766	68	69	
							7	- 71.8	39.6	39.5	30.0	30.0	266.3	266.4	1.615	1.507	0.1486	0.1485	5056	5066	1.695	1.692	663	760	68	69	
							8	- 35.2	73.0	73.2	53.8	54.1	281.7	281.3	1.595	1.493	0.2590	0.2600	5212	5217	1.739	1.735	659	751	68	70	
DY-28	PQT-004A	10-[illegible]-64	001	Uncooled Altitude	005	45	1	+ 23.5	120.4	121.2	88.2	88.8	288.4	288.5	1.517	1.528	0.4154	0.4180	5299	5300	1.751	1.752	715	704	66	68	Repeat of PQT-001.
							2	+ 48.5	138.9	140.3	101.9	103.0	289.8	289.9	1.518	1.532	0.4762	0.4809	5334	5335	1.748	1.748	712	698	65	67	
							3	+ 72.4	154.6	157.0	113.4	115.1	290.0	290.2	1.531	1.550	0.5290	0.5367	5334	5335	1.749	1.750	708	690	65	67	
							4	- 0.5	100.4	100.8	74.0	74.3	287.0	287.1	1.505	1.516	0.3488	0.3500	5303	5303	1.741	1.742	719	706	65	66	
							5	- 25.2	80.4	80.4	59.0	59.0	285.1	285.2	1.485	1.494	0.2814	0.2814	5245	5246	1.749	1.749	723	712	64	66	
							6	- 49.3	59.4	59.2	44.2	44.1	277.4	277.4	1.488	1.495	0.2138	0.2133	5184	5184	1.721	1.722	725	716	64	66	
							7	- 73.2	37.9	37.8	28.6	28.5	264.7	264.8	1.498	1.504	0.1430	0.1424	5020	5020	1.696	1.697	727	719	64	66	
							8	- 12.8	92.6	92.9	67.8	67.3	287.1	287.3	1.496	1.509	0.3214	0.3223	5274	5274	1.752	1.752	721	706	64	66	

TABLE D-1-1. (Continued)

JPL/ETS Run No.	Development Plan or PQT Test No.	Test Date	HEA S/N	CC & NA Type	CC & NA S/N	Test Duration sec.	Data Slice No.	Servo Command, ma	F_{vac}, lbs Site	F_{vac}, lbs Standard	Head-End $P_{c'}$ psia Site	Head-End $P_{c'}$ psia Standard	I_{sp} vac, sec. Site	I_{sp} vac, sec. Standard	M.R., o/f Site	M.R., o/f Standard	Total Flowrate, lbs/sec Site	Total Flowrate, lbs/sec Standard	Corrected C* fps Site	Corrected C* fps Standard	$C_{F_{vac}}$ Site	$C_{F_{vac}}$ Standard	Fuel Inlet Pr., psia	Ox. Inlet Pr., psia	Fuel Inlet Temp., °F	Ox. Inlet Temp., °F	Remarks
DY-29	PQT-004.5	10-22-64	001	Water Cooled	106831	45	1	+ 24.6	120.5	122.1	85.9	87.5	289.3	289.6	1.497	1.520	.4165	.4216	5295	5296	1.758	1.759	715	693	68	68	Altitude test with PQ-3 step thrust program tape. Water cooled CC & NA with radiation cooled extension used.
							2	+ 49.8	129.1	141.9	99.5	102.0	291.5	291.9	1.497	1.529	.4471	.4861	5350	5352	1.752	1.753	711	681	68	68	
							3	+ 74.0	154.8	158.8	110.4	113.8	291.6	292.1	1.500	1.539	.5309	.5438	5337	5340	1.758	1.759	707	671	68	68	
							4	+ 0.4	99.8	100.9	71.8	72.9	288.8	289.1	1.479	1.504	.3457	.3491	5320	5321	1.745	1.746	719	695	68	68	
							5	- 23.8	80.1	80.6	57.7	58.4	286.3	286.5	1.461	1.481	.2797	.2814	5295	5296	1.741	1.742	722	701	68	68	
							6	- 48.9	58.6	58.9	42.2	42.7	275.8	276.0	1.478	1.495	.2126	.2133	5095	5095	1.743	1.744	724	706	68	68	
							7	- 73.1	36.7	36.7	27.1	27.4	260.9	261.0	1.481	1.494	.1408	.1408	4940	4940	1.697	1.698	726	713	68	68	
							8	- 12.2	92.2	93.1	66.0	67.0	286.1	286.5	1.483	1.516	.3222	.3250	5250	5251	1.753	1.754	726	694	68	68	
DY-30	PQT-004.5	10-23-64	001	Water Cooled	106831	45	1	+ 25.2	119.3	120.8	85.0	87.1	287.3	288.4	1.429	1.527	.4153	.4189	5230	5237	1.750	1.754	764	673	67	70	Altitude test with PQ-4 step thrust program tape. Water cooled CC & NA with radiation cooled extension used. Tank pressures adjusted to achieve 1.4 target mixture ratio.
							2	+ 50.5	138.1	140.1	99.3	101.1	288.7	289.8	1.434	1.532	.4784	.4836	5316	5323	1.746	1.750	760	670	67	70	
							3	+ 75.5	155.2	157.9	111.3	113.5	288.9	290.0	1.448	1.545	.5372	.5446	5300	5306	1.751	1.755	756	666	67	69	
							4	+ 1.0	99.5	100.4	71.9	72.8	286.4	287.4	1.419	1.515	.3476	.3493	5292	5297	1.739	1.743	768	676	67	69	
							5	- 23.2	79.5	80.0	57.5	58.2	284.1	285.2	1.402	1.495	.2737	.2804	5268	5274	1.734	1.738	771	680	67	69	
							6	- 48.5	57.9	58.1	42.2	42.6	274.8	275.7	1.400	1.491	.2108	.2108	5128	5132	1.723	1.727	773	681	67	67	
							7	- 72.6	36.0	36.1	26.7	27.0	260.2	261.0	1.402	1.494	.1385	.1383	4955	4956	1.688	1.683	776	683	67	67	
							8	+ 13.6	115.5	112.6	80.3	81.5	287.0	288.0	1.426	1.522	.3885	.3911	5295	5301	1.743	1.747	766	674	67	69	
DY-31	PQT-004.5	10-26-64	001	Water Cooled	106831	45	1	+ 25.1	121.3	121.2	86.2	87.4	290.4	289.7	1.605	1.489	.4178	.4182	5320	5321	1.755	1.751	655	755	66	66	Altitude test with PQ-5 step thrust program tape. Water cooled CC & NA with radiation cooled extension used. Tank pressures adjusted to achieve 1.6 target mixture ratio.
							2	+ 50.5	140.5	140.7	100.6	101.4	292.2	291.5	1.612	1.496	.4809	.4827	5349	5349	1.756	1.752	651	751	66	66	
							3	+ 74.9	157.8	158.5	112.7	114.0	293.1	292.5	1.635	1.518	.5386	.5418	5353	5356	1.759	1.755	649	746	66	65	
							4	+ 0.9	101.8	101.4	73.1	73.4	289.3	288.7	1.605	1.488	.3519	.3511	5313	5317	1.750	1.746	658	760	66	65	
							5	- 23.3	815.	81.0	58.9	59.0	287.5	286.8	1.582	1.468	.2834	.2823	5313	5316	1.740	1.736	682	782	66	65	
							6	- 48.7	60.0	59.5	43.7	43.7	278.4	277.9	1.594	1.479	.2155	.2141	5173	5180	1.728	1.724	665	766	66	65	
							7	- 72.9	37.2	36.9	27.7	27.8	259.1	258.8	1.589	1.474	.1437	.1426	4940	4948	1.685	1.680	666	768	65	65	
							8	- 36.0	72.2	71.7	52.8	52.3	281.6	281.1	1.593	1.478	.2564	.2550	5207	5211	1.750	1.745	663	764	66	65	
DY-32	PQT-004.5	10-26-64	001	Water Cooled	106831	45	1	+ 24.8	122.5	122.9	87.6	88.4	289.5	289.5	1.538	1.540	.4232	.4246	5300	5300	1.756	1.756	715	709	65	65	Altitude test with PQ-3 step thrust program tape. Water cooled CC & NA with radiation cooled extension used.
							2	+ 50.1	141.5	142.5	101.3	102.5	291.0	291.0	1.589	1.531	.4864	.4895	5333	5334	1.755	1.755	710	705	66	65	
							3	+ 74.4	156.9	158.3	113.0	114.7	289.3	289.3	1.543	1.546	.5423	.5471	5340	5341	1.754	1.754	707	701	66	65	
							4	+ 0.6	101.6	101.6	73.1	73.5	287.7	287.7	1.516	1.516	.3532	.3532	5283	5283	1.748	1.748	718	714	65	65	
							5	- 23.8	81.2	81.0	58.7	58.9	284.7	284.7	1.494	1.493	.2851	.2843	5260	5260	1.739	1.739	721	718	65	65	
							6	- 49.0	59.3	59.0	43.2	43.2	275.3	275.3	1.508	1.505	.2154	.2142	5110	5110	1.729	1.729	724	722	65	65	
							7	- 73.1	37.2	37.0	27.6	27.7	260.5	260.5	1.502	1.501	.1427	.1418	4960	4960	1.689	1.689	726	723	65	66	
							8	- 12.0	93.4	93.3	67.4	67.7	287.0	287.0	1.509	1.510	.3255	.3251	5297	5301	1.741	1.741	721	716	65	66	
DY-33	PQT-004B	11-11-64		Uncooled	005	180	1	+ 73.4	147.9	150.0	109.1	110.7	291.7	291.4	1.542	1.511	.5071	.5114	5400	5400	1.738	1.735	654	652	-6	2	Altitude test with PQ-6 step thrust and dynamic thrust program tape. TCA and propellants conditioned to minimum specification temperatures. Facility propellant bleed valves left open during test resulting in flowrate and performance data accuracy degradation.
							2	+ 49.4	131.6	132.7	96.6	97.5	292.3	292.0	1.526	1.496	.4503	.4545	5388	5387	1.746	1.744	660	659	-7	1	
							3	+ 24.6	112.5	112.9	82.6	83.0	290.8	290.6	1.533	1.504	.3668	.3884	5365	5364	1.744	1.743	667	665	-7	2	
							4	+ 0.5	94.7	94.4	69.0	68.9	291.2	290.9	1.525	1.494	.3252	.3246	5327	5327	1.759	1.757	674	674	-7	2	
							5	- 23.2	74.8	74.3	55.1	54.8	286.8	286.8	1.523	1.494	.2607	.2592	5305	5306	1.739	1.738	681	679	-8	3	
							6	- 48.1	54.6	54.1	40.4	40.0	281.5	281.3	1.536	1.508	.1941	.1922	5224	5225	1.733	1.732	687	684	-8	3	
							7	- 72.1	33.7	33.2	25.2	24.9	244.2	244.4	1.748	1.715	.1380	.1360	4594	4600	1.710	1.710	692	691	-7	4	
							8	- 48.1	55.3	54.7	40.5	40.1	283.9	283.8	1.518	1.490	.1949	.1929	5224	5225	1.749	1.747	687	685	-7	4	
							9	- 23.2	75.3	74.8	55.5	55.2	284.3	284.1	1.514	1.486	.2648	.2634	5262	5262	1.738	1.737	680	679	-7	4	
							10	+ 0.4	95.9	95.8	70.3	70.3	292.5	292.3	1.511	1.483	.3279	.3278	5386	5386	1.747	1.746	674	673	-6	4	
							11	+ 24.5	115.0	115.4	84.3	84.7	294.0	293.7	1.516	1.486	.3913	.3930	5408	5407	1.749	1.748	667	667	-6	5	
							12	+ 49.6	131.9	133.0	96.4	97.4	292.1	291.8	1.511	1.482	.4514	.4557	5364	5363	1.752	1.751	661	660	-5	5	
							13	+ 73.5	146.4	148.4	106.8	108.3	290.3	290.1	1.542	1.513	.5044	.5117	5316	5315	1.757	1.756	655	654	-4	6	
							14	+ 49.6	130.9	132.3	95.7	96.8	292.7	292.5	1.517	1.496	.4503	.4555	5336	5335	1.753	1.752	660	658	-4	6	
							15	+ 24.5	113.3	113.9	82.8	83.2	294.2	294.0	1.515	1.489	.3852	.3873	5396	5396	1.754	1.753	669	666	-4	6	

TABLE D-1-1. (Continued)

JPL/ETS Run No.	Development Plan or PQT Test No.	Test Date	HEA S/N	CC & NA Type	CC & NA S/N	Test Duration sec.	Data Slice No.	Servo Command, ma	F_{vac}, lbs Site	F_{vac}, lbs Standard	Head-End P_c, psia Site	Head-End P_c, psia Standard	I_{sp} vac, sec. Site	I_{sp} vac, sec. Standard	M.R., o/f Site	M.R., o/f Standard	Total Flowrate, lbs/sec Site	Total Flowrate, lbs/sec Standard	Corrected C* fps Site	Corrected C* fps Standard	C_F vac Site	C_F vac Standard	Fuel Inlet Pr., psia	Ox. Inlet Pr., psia	Fuel Inlet Temp., °F	Ox. Inlet Temp., °F	Remarks
DY-34	None	11-1-64	001	Uncooled Sea Level	011	130	--	-----	---	-----	---	-----	---	-----	---	-----	---	-----	---	-----	---	-----	---	---	---	---	Sea level firing to obtain film coverage. Data not reduced.
DY-35	PQT-007	12-1-64	008	Uncooled Altitude	008	50	1	+ 68.0	152.5	156.1	110.2	113.1	291.7	290.5	1.565	1.439	.5227	.5372	5314	5309	1.766	1.760	629	777	100	100	Altitude test with PQ-7A fixed thrust program tape. TCA and propellants conditioned to maximum specification temperatures.
							2	+ 68.3	151.4	155.5	108.8	112.0	291.3	290.2	1.577	1.454	.5198	.5356	5277	5274	1.776	1.771	630	778	104	103	
DY-36	PQT-007	12-1-64	008	Uncooled Altitude	008	100	1	+ 68.3	144.0	148.2	104.1	107.6	291.6	290.5	1.625	1.450	.4938	.5103	5317	5316	1.765	1.758	600	779	99	97	Altitude test with PQ-7B fixed thrust program tape. TCA and propellants conditioned to maximum specification temperatures.
							2	+ 68.3	145.6	150.9	104.6	108.7	292.6	291.5	1.611	1.453	.4975	.5176	5298	5296	1.777	1.771	600	779	104	101	
							3	+ 68.7	144.6	150.1	104.1	108.4	291.2	290.2	1.608	1.454	.4966	.5175	5282	5280	1.774	1.768	600	780	103	106	
DY-37	PQT-007	12-2-64	008	Uncooled Altitude	008	150	1	+ 72.7	153.1	157.9	110.4	114.2	293.5	292.4	1.612	1.449	.5217	.5400	5335	5332	1.770	1.764	601	776	96	96	Altitude test with PQ-7C fixed thrust program tape. TCA and propellants conditioned to maximum specification temperatures
							2	+ 72.4	152.0	157.4	108.9	113.2	292.9	291.9	1.614	1.461	.5188	.5393	5294	5293	1.780	1.774	603	775	102	103	
							3	+ 72.5	151.9	157.6	109.0	113.5	292.0	290.9	1.601	1.449	.5202	.5418	5285	5282	1.778	1.772	602	776	104	105	
DY-38	PQT-008	12-4-64	008	Uncooled Altitude	001	160	1	- 71.6	29.5	31.2	22.3	23.6	245.5	246.1	1.702	1.535	.1203	.1270	4656	4680	1.697	1.692	580	742	96	97	Altitude test with PQ-8 fixed thrust program tape. CC & NA conditioned to minimum and propellants to maximum temperatures.
							2	- 75.5	32.2	34.0	23.9	25.3	257.9	258.7	1.728	1.559	.1249	.1316	4815	4843	1.723	1.719	582	744	98	97	
							3	- 76.3	32.4	34.2	23.8	25.2	260.7	261.5	1.725	1.556	.1242	.1308	4823	4850	1.739	1.735	583	746	99	98	
DY-39	PQT-008	12-7-64	008	Uncooled Altitude	001	160	1	- 73.1	30.6	33.5	22.9	25.1	249.6	249.8	1.570	1.527	.1224	.1339	4710	4717	1.705	1.704	594	667	100	102	Altitude test with PQ-8 fixed thrust program tape. Propellants conditioned to maximum temperature.
							2	- 74.1	32.0	35.0	23.8	26.0	259.1	259.3	1.574	1.529	.1235	.1348	4840	4848	1.722	1.721	596	671	100	102	
							3	- 74.7	31.6	34.5	23.4	25.6	260.4	260.6	1.554	1.509	.1215	.1325	4848	4855	1.728	1.727	596	674	102	103	
DY-40	PQT-008	12-7-64	008	Uncooled Altitude	001	160	1	- 70.0	31.9	34.4	23.5	25.5	255.3	255.2	1.532	1.451	.1248	.1349	4738	4745	1.734	1.730	589	685	98	96	Altitude test with PQ-8 fixed thrust program tape. Propellants conditioned to maximum temperature.
							2	- 70.0	32.2	34.8	23.7	25.7	258.0	257.8	1.546	1.463	.1250	.1348	4777	4784	1.737	1.734	590	690	99	97	
							3	- 70.0	32.0	34.5	23.5	25.4	259.9	259.6	1.523	1.441	.1231	.1328	4800	4804	1.742	1.739	591	692	99	98	

TABLE D-1-1. (Continued)

JPL/ETS Run No.	Development Plan or PQT Test No.	Test Date	HEA S/N	CC & NA Type	CC & NA S/N	Test Duration, sec.	Data Slice No.	Servo Command, ma	F_{vac}, lbs Site	F_{vac}, lbs Standard	Head-End P_c, psia Site	Head-End P_c, psia Standard	I_{sp} vac, sec. Site	I_{sp} vac, sec. Standard	M.R., o/f Site	M.R., o/f Standard	Total Flowrate, lbs/sec. Site	Total Flowrate, lbs/sec. Standard	Corrected C^*, fps Site	Corrected C^*, fps Standard	$C_{F_{vac}}$ Site	$C_{F_{vac}}$ Standard	Fuel Inlet Pr., psia	Ox. Inlet Pr., psia	Fuel Inlet Temp., °F	Ox. Inlet Temp., °F	Remarks
DY-41	PQT-010	12-10-64	004	Water cooled	106372	116	1	+ 73.2	154.8	157.6	110.5	113.3	291.6	291.7	1.526	1.528	0.5307	0.5404	5341	5342	1.757	1.757	697	703	75	76	Altitude firing with PQ1-C dynamic thrust program tape. Water-cooled CC & NA with radiation cooled extension used.
							2	+ 72.9	154.6	157.3	110.3	113.0	291.5	291.5	1.521	1.522	0.5304	0.5397	5336	5337	1.758	1.758	698	704	75	76	
							3	- 72.0	27.5	27.5	19.9	20.1	255.5	255.5	1.476	1.475	0.1075	0.1076	4752	4752	1.730	1.730	720	727	75	76	
DY-42	PQT-010	12-11-64	004	Water cooled	106372	52	1	+ 0.6	96.5	97.3	69.6	70.7	290.9	291.0	1.506	1.509	0.3318	0.3344	5378	5379	1.741	1.741	712	713	72	74	Altitude firing with PQ1-A dynamic thrust program tape. Water-cooled CC & NA with radiation cooled extension used.
DY-43	PQT-010	12-11-64	004	Water cooled	106372	70	1	- 29.4	67.4	67.8	48.9	49.5	285.6	285.6	1.535	1.535	0.2360	0.2374	5303	5304	1.733	1.733	713	714	73	71	Altitude firing with PQ1-B dynamic thrust program tape. Water-cooled CC & NA with radiation cooled extension used.
							2	+ 73.9	153.8	156.6	110.1	112.8	291.6	291.7	1.529	1.530	0.5272	0.5369	5353	5354	1.753	1.753	697	697	74	72	
							3	- 72.6	25.5	25.6	18.7	19.0	255.6	255.6	1.483	1.480	0.0999	0.1001	4815	4816	1.708	1.708	718	721	74	72	
DY-44	PQT-009.5	12-15-64	004	Water cooled	106372	52	1	+ 0.7	93.7	91.7	67.6	66.6	290.2	290.1	1.583	1.571	0.3228	0.3160	5347	5347	1.746	1.745	712	699	- 6	10	Altitude firing with PQ-1 dynamic thrust program tape. Water-cooled CC & NA with radiation cooled extension. Propellants and servoactuator conditioned to 0°F.
DY-45	PQT-009.5	12-16-64	004	Water cooled	106372	70	1	- 28.0	64.3	61.9	46.7	45.2	283.9	283.8	1.647	1.604	0.2267	0.2180	4750	4750	1.738	1.736	716	723	-18	- 4	Altitude firing with PQ-1A dynamic thrust program tape. Water-cooled CC & NA with radiation cooled extension. Propellants and servoactuator conditioned to 0°F.
							2	+ 69.6	153.7	149.9	110.0	107.9	293.1	293.0	1.615	1.579	0.5244	0.5116	5362	5363	1.759	1.758	699	700	-19	- 8	
							3	- 68.6	23.6	22.6	17.3	16.6	253.6	253.9	1.733	1.678	0.0931	0.0889	5255	5258	1.718	1.716	720	735	-18	- 7	
DY-46	PQT-009.5	12-16-64	004	Water cooled	106372	116	1	+ 69.3	153.0	149.4	109.7	107.7	293.2	293.1	1.622	1.581	0.5219	0.5097	5370	5371	1.757	1.756	698	698	-11	-10	Altitude firing with PQ-1B dynamic thrust program tape. Water-cooled CC & NA with radiation cooled extension. Propellants and servoactuator conditioned to 0°F.
							2	+ 69.3	153.4	149.8	109.9	108.0	292.4	292.4	1.621	1.583	0.5245	0.5125	5355	5356	1.757	1.756	699	696	- 9	-11	
							3	- 67.8	23.4	22.4	17.2	16.6	247.8	247.9	1.676	1.614	0.0946	0.0903	4652	4660	1.713	1.712	720	736	- 9	-10	
DY-47	PQT-005	12-18-64	010	Uncooled Altitude	010	45	1	0	81.9	81.4	60.3	59.9	279.6	279.4	1.472	1.455	0.2931	0.2912	5162	5161	1.743	1.742	711	714	50	51	Altitude firing with PQ-3 thrust program tape. Installed Phase III actuator prior to test.
							2	+ 24	103.6	103.2	75.9	75.9	280.9	280.7	1.503	1.486	0.3688	0.3676	5167	5167	1.749	1.748	707	711	51	52	
							3	+ 49.1	126.7	126.7	92.6	92.7	284.5	284.3	1.506	1.488	0.4452	0.4457	5222	5221	1.753	1.752	700	705	52	52	
							4	+ 73	145.1	145.6	105.9	106.3	283.4	283.2	1.490	1.474	0.5120	0.5141	5190	5189	1.757	1.756	698	702	53	54	
							5	+ 1.2	81.4	80.9	59.8	59.5	276.8	276.6	1.477	1.461	0.2939	0.2925	5104	5105	1.745	1.744	711	715	54	54	
							6	- 23.8	58.8	58.3	43.6	43.2	269.6	269.4	1.497	1.480	0.2180	0.2163	5014	5013	1.730	1.729	715	720	56	55	
							7	- 48.6	34.4	34.0	25.8	25.6	250.3	250.1	1.463	1.446	0.1374	0.1361	4716	4716	1.708	1.707	717	723	56	55	
							8	- 72.5	18.7	18.5	14.1	14.0	237.8	237.6	1.371	1.355	0.0788	0.0780	4505	4504	1.698	1.698	718	723	56	55	
							9	- 12.2	71.6	71.1	52.8	52.5	275.3	275.2	1.490	1.474	0.2600	0.2585	5093	5092	1.739	1.738	713	717	56	55	
DY-48A	PQT-005	12-18-64	010	Uncooled Altitude	010	45	1	+ 0.5	90.5	90.4	66.1	66.0	284.1	284.0	1.508	1.502	0.3185	0.3183	5206	5206	1.756	1.755	714	713	62	62	Altitude firing with PQ-4 thrust program tape. Adjusted throttle linkage to rains engine operating level.
							2	+ 24.7	113.2	113.4	82.4	82.6	286.5	286.4	1.539	1.531	0.3952	0.3960	5233	5233	1.761	1.761	710	711	63	62	
							3	+ 49.7	135.4	136.1	98.5	99.0	287.9	287.8	1.521	1.514	0.4702	0.4728	5255	5255	1.763	1.762	706	707	64	63	
							4	+ 73.6	154.6	156.1	112.2	113.4	290.2	290.2	1.509	1.503	0.5327	0.5381	5288	5288	1.766	1.766	700	702	65	64	
							5	+ 0.5	90.3	90.3	65.7	65.7	281.7	281.6	1.498	1.491	0.3205	0.3205	5145	5145	1.762	1.761	714	716	65	65	
							6	- 23.3	67.6	67.6	49.4	49.4	275.6	275.6	1.510	1.509	0.2453	0.2453	5050	5050	1.756	1.756	718	714	66	65	
							7	- 48.3	43.4	43.2	31.9	31.8	263.0	262.9	1.483	1.474	0.1651	0.1643	4856	4856	1.743	1.742	720	724	66	65	
							8	- 72.2	21.6	21.4	15.8	15.7	241.8	241.7	1.487	1.479	0.0891	0.0886	4445	4445	1.750	1.750	722	725	66	65	
							9	+ 13.0	103.7	103.8	75.2	72.3	284.8	284.7	1.505	1.497	0.3641	0.3645	5181	5181	1.768	1.768	712	716	66	65	

JPL/ETS Run No.	Development Plan or PQT Test No.	Test Date	HEA S/N	CC & NA Type	CC & NA S/N	Test Duration, sec.	Data Slice No.	Servo Command, ma	F_{vac}, lbs Site	F_{vac}, lbs Stand	Ox. Inlet Temp., °F	Remarks
DX-48B	PQT-005	12-18-64	010	Uncooled Altitude	010	45	1	+ 0.6	88.2	88.1	65	Altitude firing with PQ-5 thrust program tape.
							2	+ 24.6	110.6	110.8	66	
							3	+ 49.7	131.9	132.7	67	
							4	+ 73.7	149.6	151.2	68	
							5	+ 0.7	87.8	87.9	68	
							6	- 23.2	66.1	66.0	68	
							7	- 48.2	43.4	43.2	68	
							8	- 72.1	21.1	21.0	68	
							9	- 35.6	55.8	55.6	68	
DX-48C	PQT-005	12-18-64	010	Uncooled Altitude	010	45	1	+ 0.5	88.9	88.8	68	Altitude firing with PQ-3 thrust program tape.
							2	+ 24.5	110.8	111.2	68	
							3	+ 49.5	132.0	132.9	69	
							4	+ 73.5	149.4	151.0	70	
							5	+ 0.6	88.8	88.9	70	
							6	- 23.3	67.3	67.3	70	
							7	- 48.3	43.4	43.3	70	
							8	- 72.3	21.5	21.4	70	
							9	- 11.9	78.4	78.4	70	
DX-49	PQT-005	12-21-64	010	Water Cooled	106372	180	1	+ 74.2	146.3	147.5	62	Altitude firing with PQ-6 thrust program tape. Water-cooled chamber installed for this test for the purpose of verifying the altitude chamber performance.
							2	+ 50.0	129.4	130.1	61	
							3	+ 24.7	108.5	108.7	62	
							4	+ 0.1	87.2	87.1	62	
							5	- 23.3	65.1	64.9	62	
							6	- 48.3	42.8	42.6	62	
							7	- 72.2	22.4	22.3	63	
							8	- 48.5	43.4	43.1	63	
							9	- 23.5	66.1	62.8	63	
							10	0	87.7	87.6	63	
							11	+ 24.5	112.8	112.9	64	
							12	+ 49.7	135.5	136.3	65	
							13	+ 73.8	152.2	153.7	65	
							14	+ 49.6	134.8	135.6	66	
							15	+ 24.4	113.1	113.5	66	
							16	0	87.9	87.8	68	
							17	+ 73.7	148.1	149.7	68	
							18	- 79.2	22.8	22.7	69	
							19	+ 74.5	149.7	151.5		

NOTES:

1. Data at site conditions are corrected to 0 psia only.
2. Data at standard conditions are corrected to 0 psia, 70°F, and 720 psia inlet pressures.
3. Vacuum C_F computed from F_{vac} divided by 0.9928 x head-end P_c x throat area.
4. Characteristic velocity computed from 0.9928 x head-end P_c x throat area x standard gravity divided by total propellant weight flowrate.
5. Corrected characteristic velocity includes heat transfer and nozzle throat growth corrections for all water cooled combustion chamber firings.

FIGURE D-1-2. VACUUM SPECIFIC IMPULSE VS. THRUST AT 1.5 MIXTURE RATIO TEST DX-19 WITH TCA B/N 150A-004

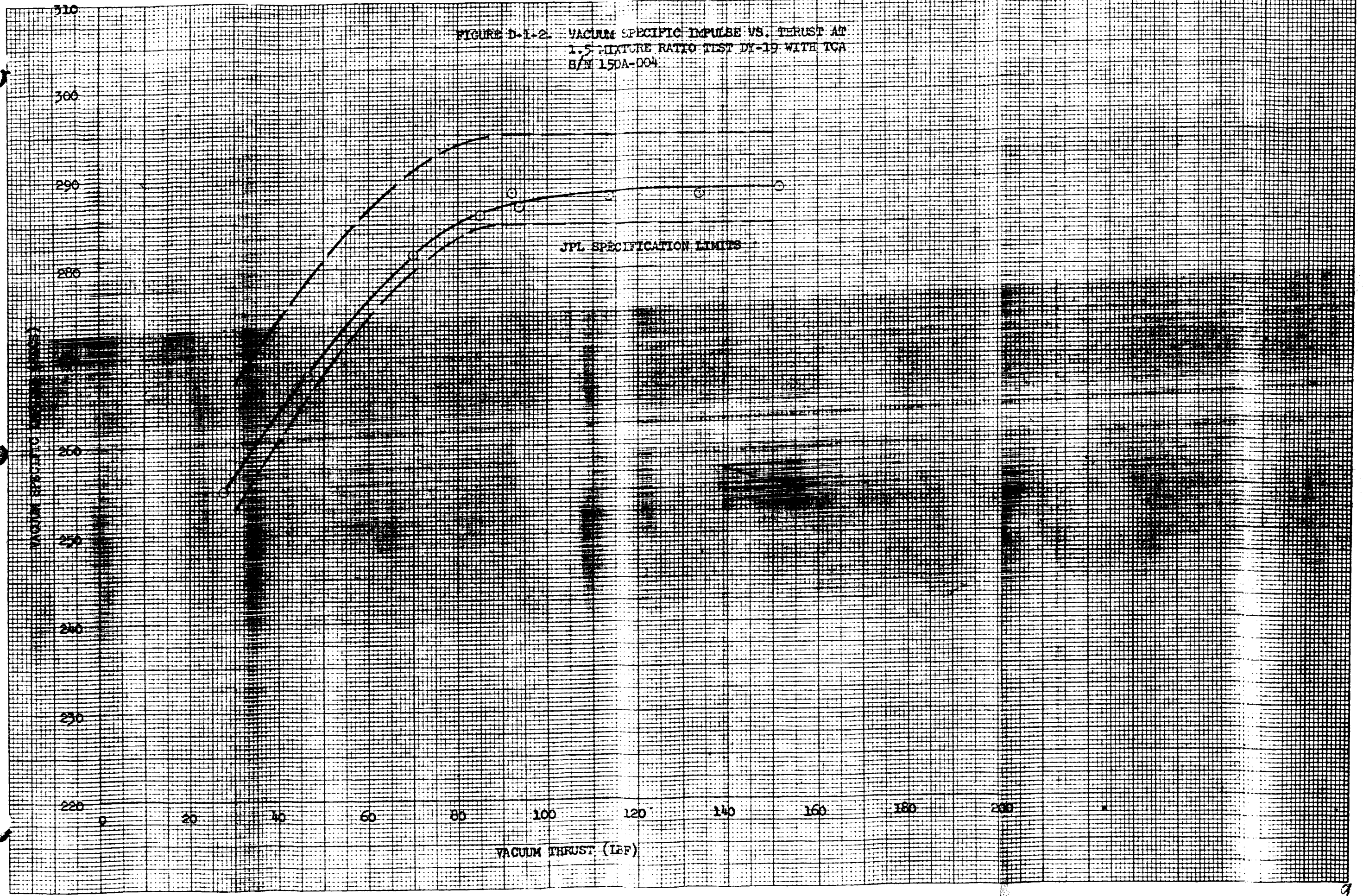

FIGURE D-1-3. CHARACTERISTIC EXHAUST VELOCITY VS. NOZZLE STAGNATION PRESSURE AT 1.5 MIXTURE RATIO FOR TEST DY-19 WITH LOX/B/[illegible]150A-004

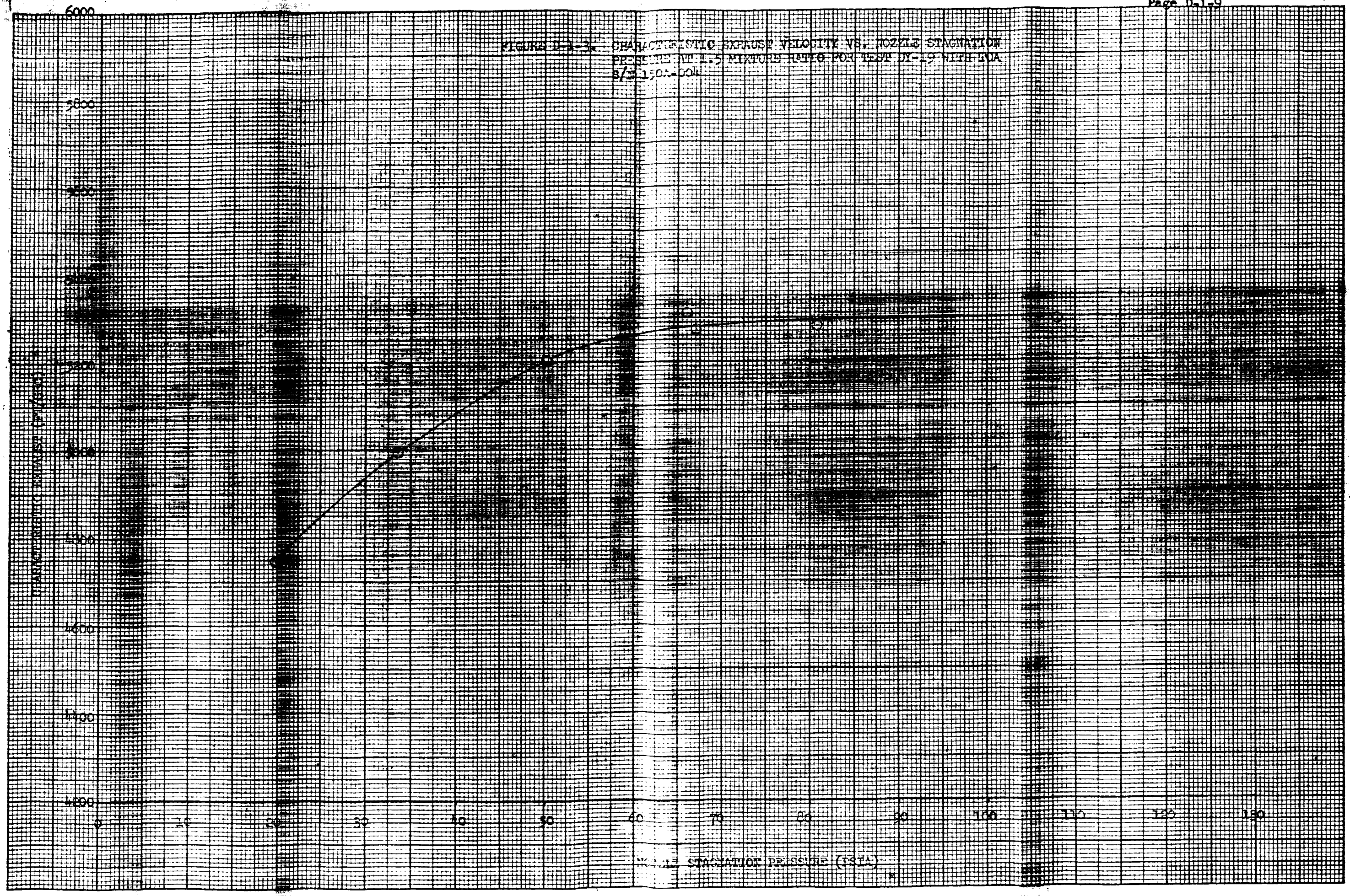

FIGURE D-1-4. VACUUM THRUST COEFFICIENT VS. NOZZLE STAGNATION PRESSURE AT 1.5 MIXTURE RATIO TEST DY-19 WITH TCA S/N 150A-004

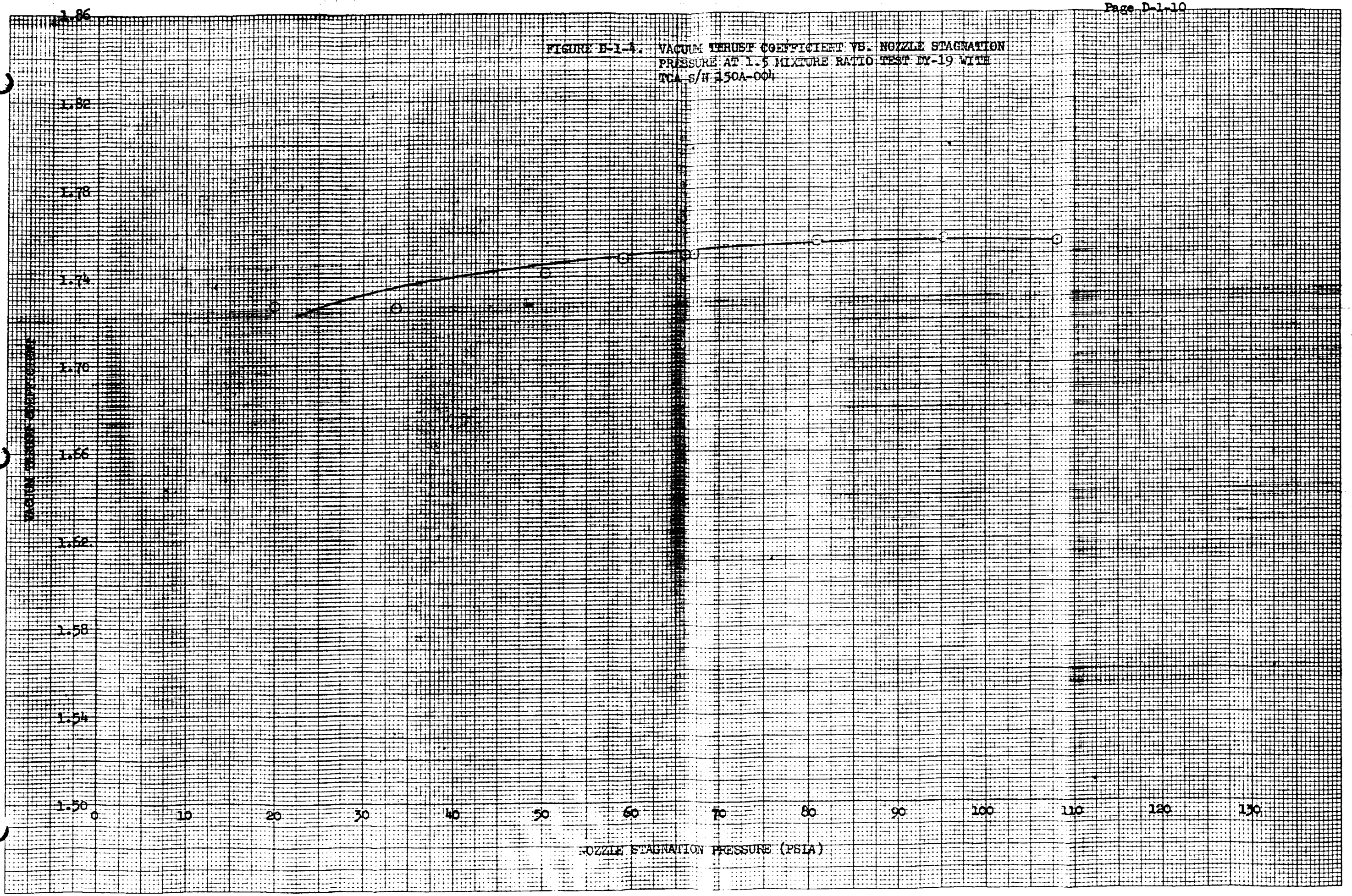

PIGURE D-1-5. MIXTURE RATIO VS. VACUUM THRUST AT STANDARD CONDITIONS FOR TEST DY-19 WITH TCA S/N 150A-004

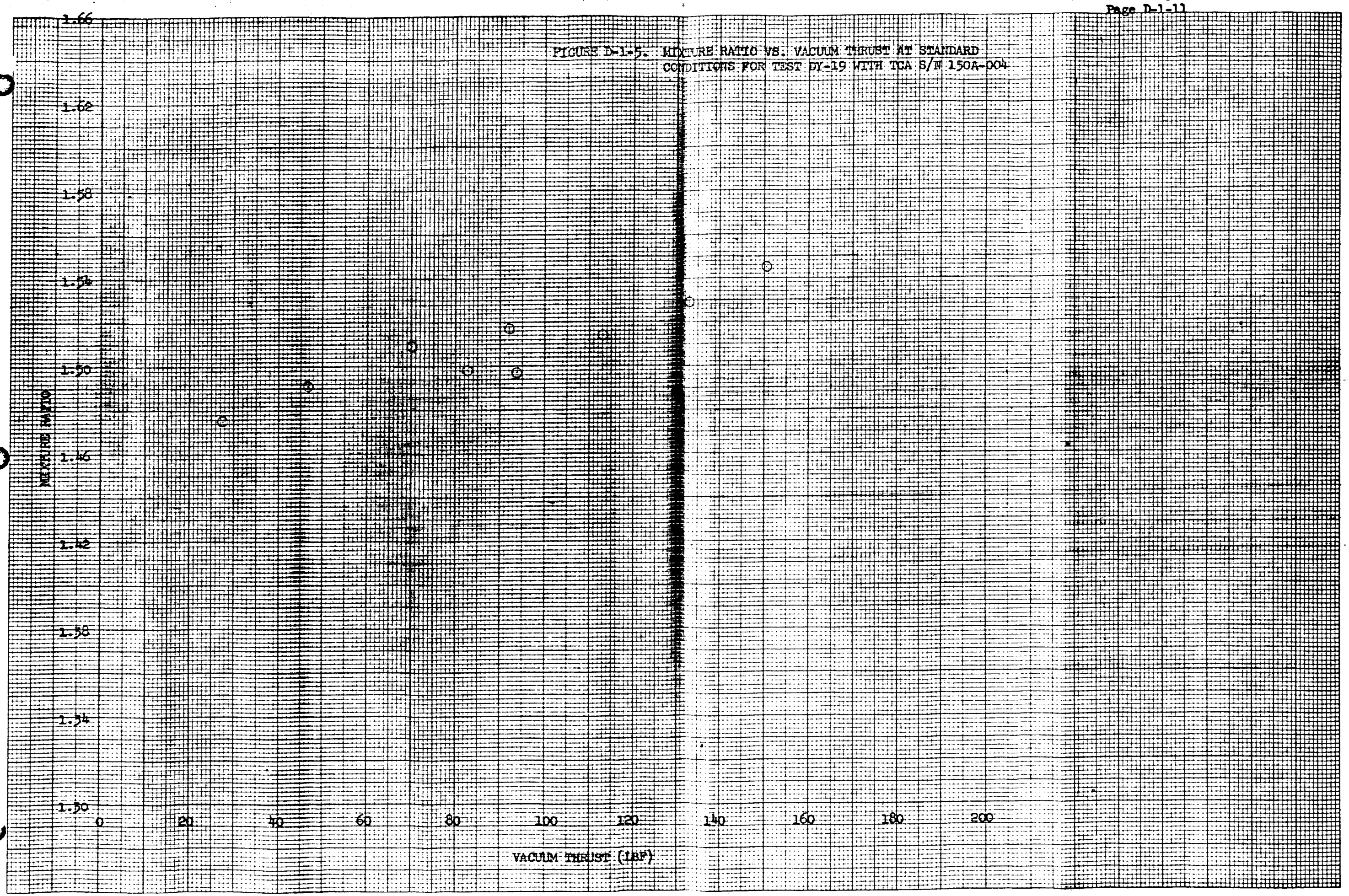

FIGURE D-1-6. VACUUM SPECIFIC IMPULSE VS. THRUST AT 1.5 MIXTURE RATIO FOR TESTS DY-20 THROUGH DY-24 WITH TCA S/N 150A-004

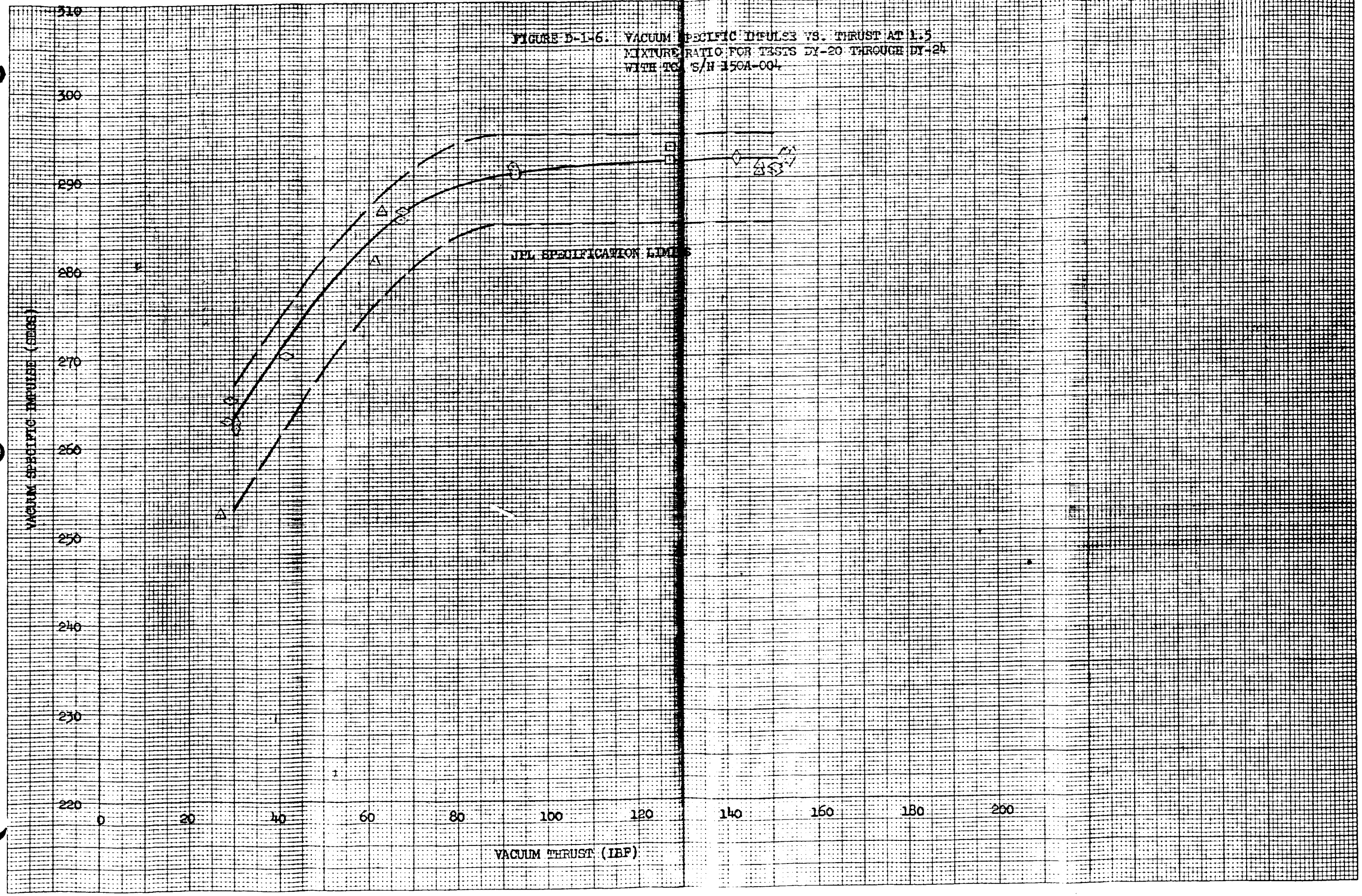

FIGURE D-1-7. CHARACTERISTIC EXHAUST VELOCITY VS. NOZZLE STAGNATION PRESSURE AT 1.5 MIXTURE RATIO FOR TESTS DY-20 THROUGH DY-24 WITH TCA 150A-004

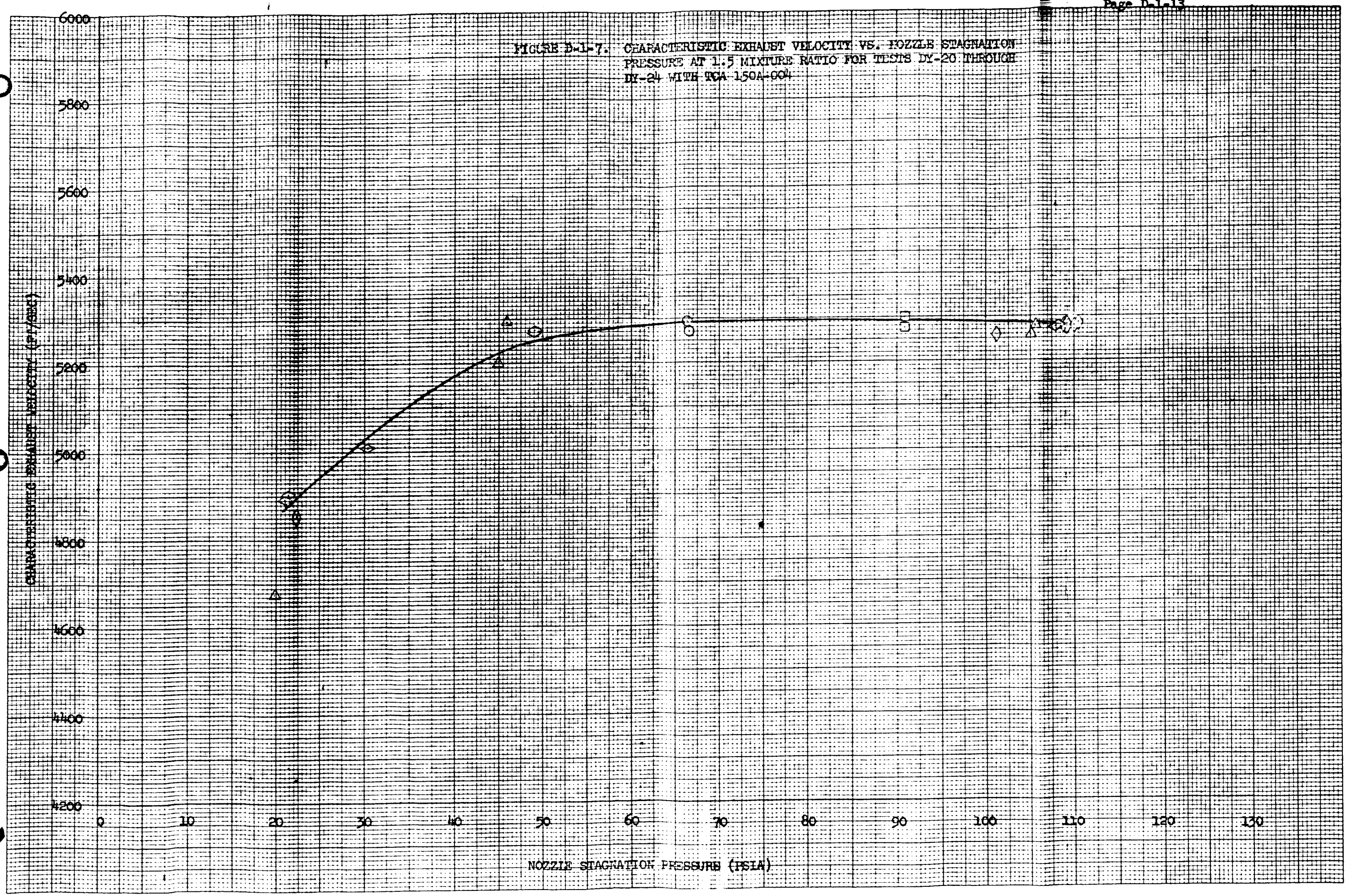

FIGURE D-1-9. MIXTURE RATIO VS. VACUUM THRUST AT STANDARD CONDITIONS FOR
[illegible] DY-20 THROUGH DY-21 WITH TCA S/N 150A-004

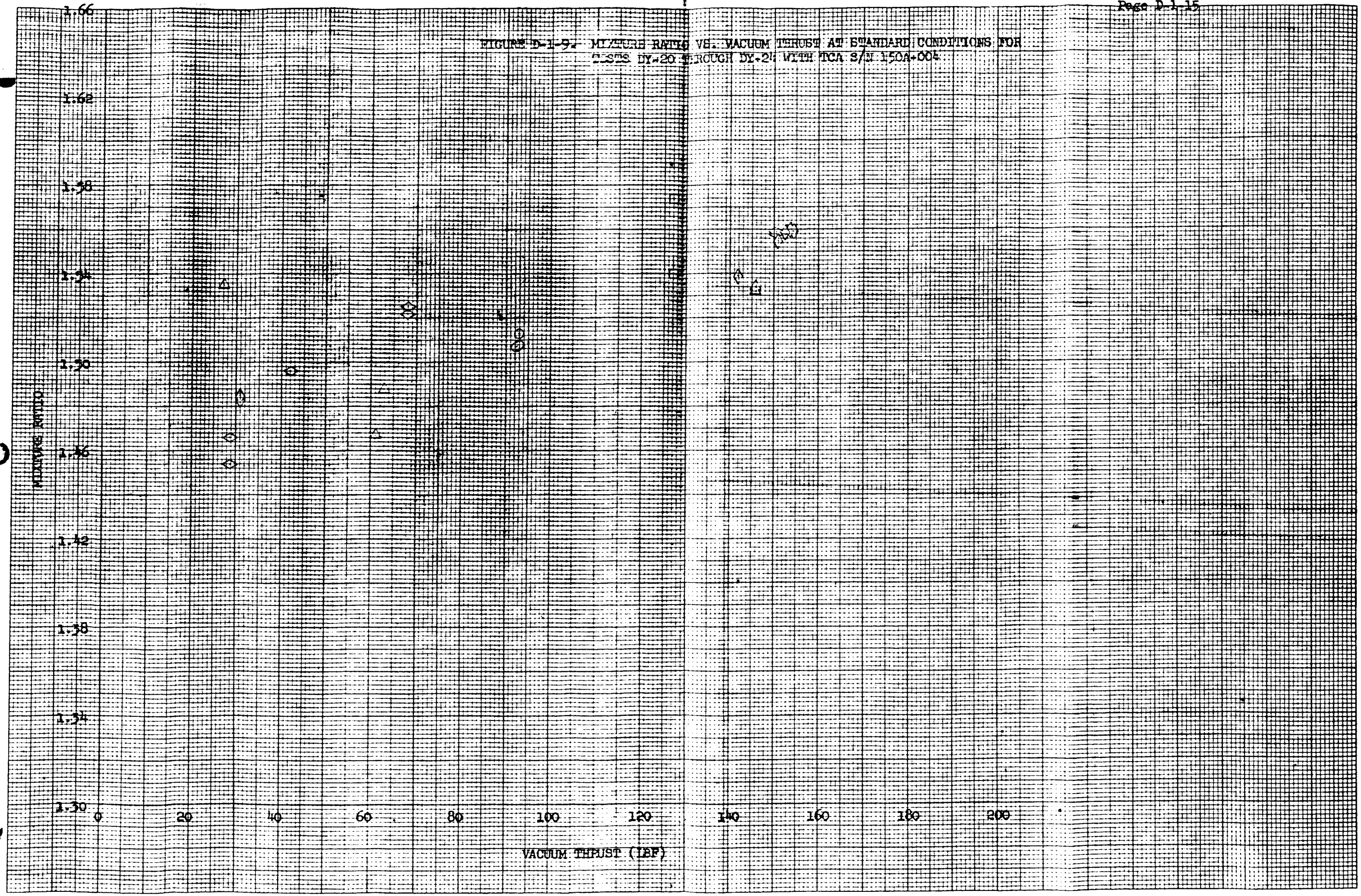

FIGURE D-1-8. VACUUM THRUST COEFFICIENT VS. NOZZLE STAGNATION PRESSURE AT 1.5 MIXTURE RATIO FOR TESTS DY-20 THROUGH DY-24 WITH TCA S/N 150A-004

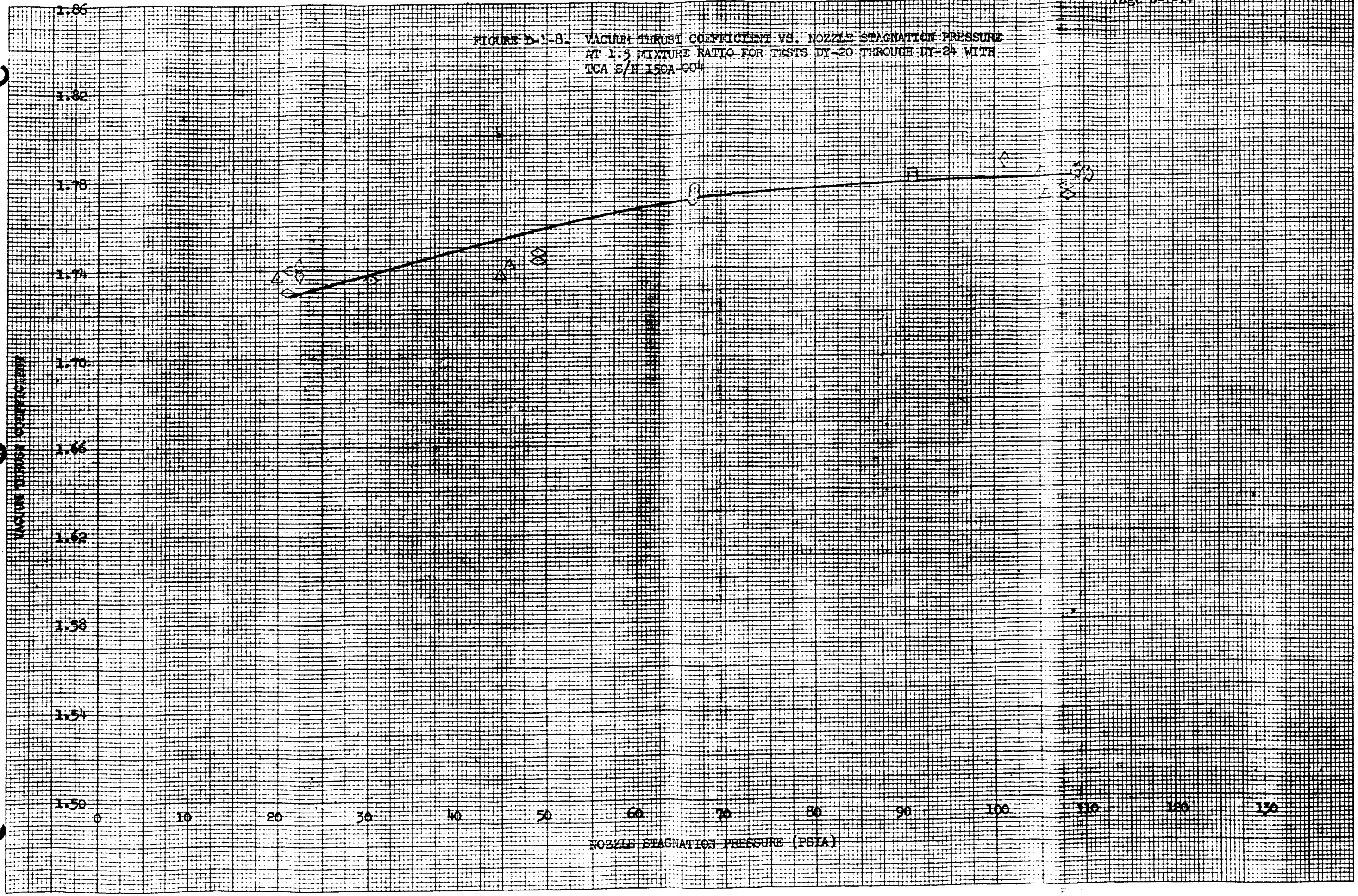

DX-25

FIGURE D-1-16. FIGURE TITLE: VALVE POSITION VS. DEMODULATOR COMMAND SIGNAL
AT 1.5 PRESSURE RATIO FOR TEST DX-25 VCEM 004.
R/N 150-001

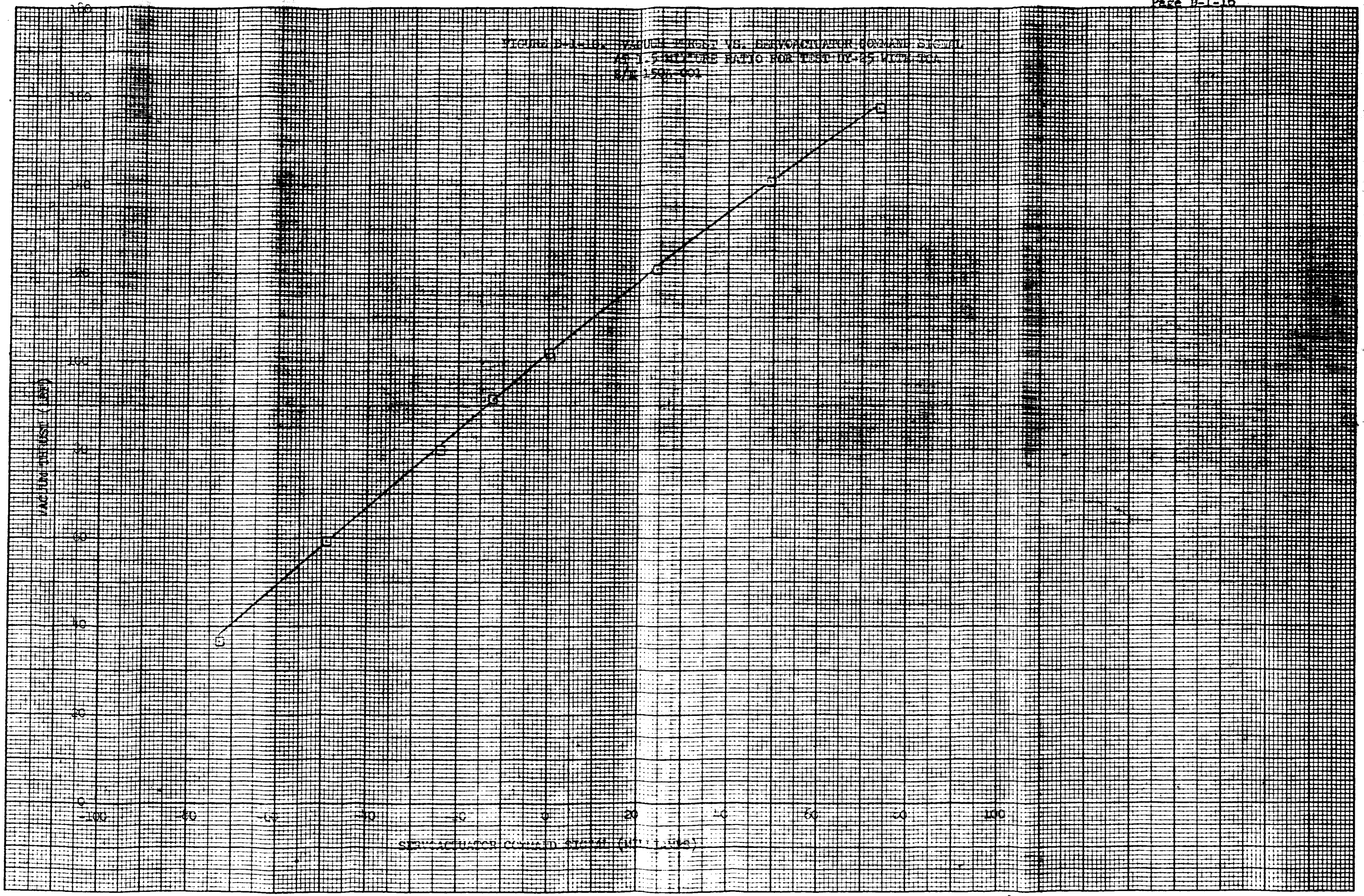

K&E 10 X 10 TO THE ½ INCH KEUFFEL & ESSER CO. 359-11L

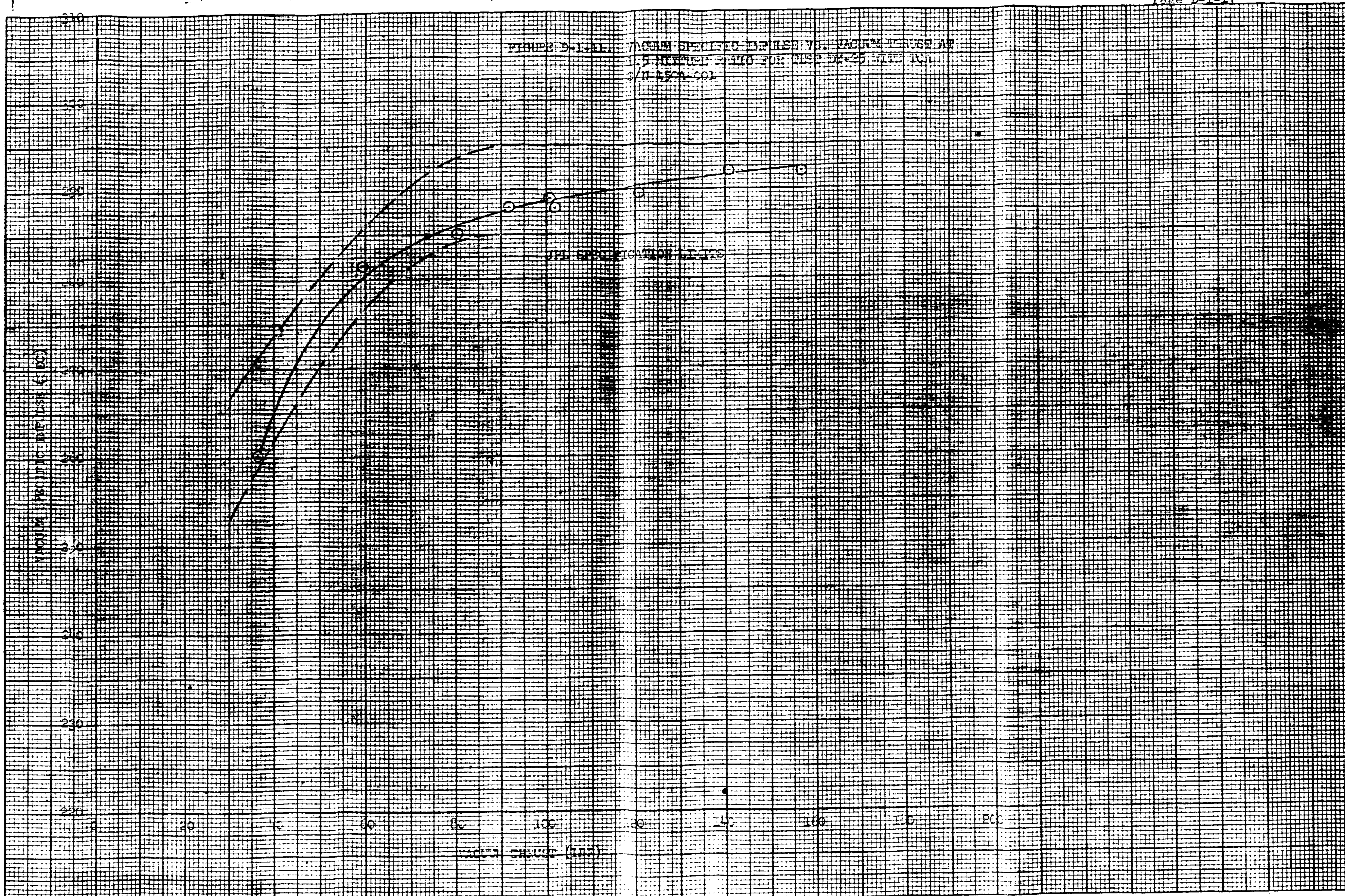

FIGURE D-1-11. VACUUM SPECIFIC IMPULSE VS. VACUUM THRUST AT 1.5 MIXTURE RATIO FOR ... S/N 4501-001

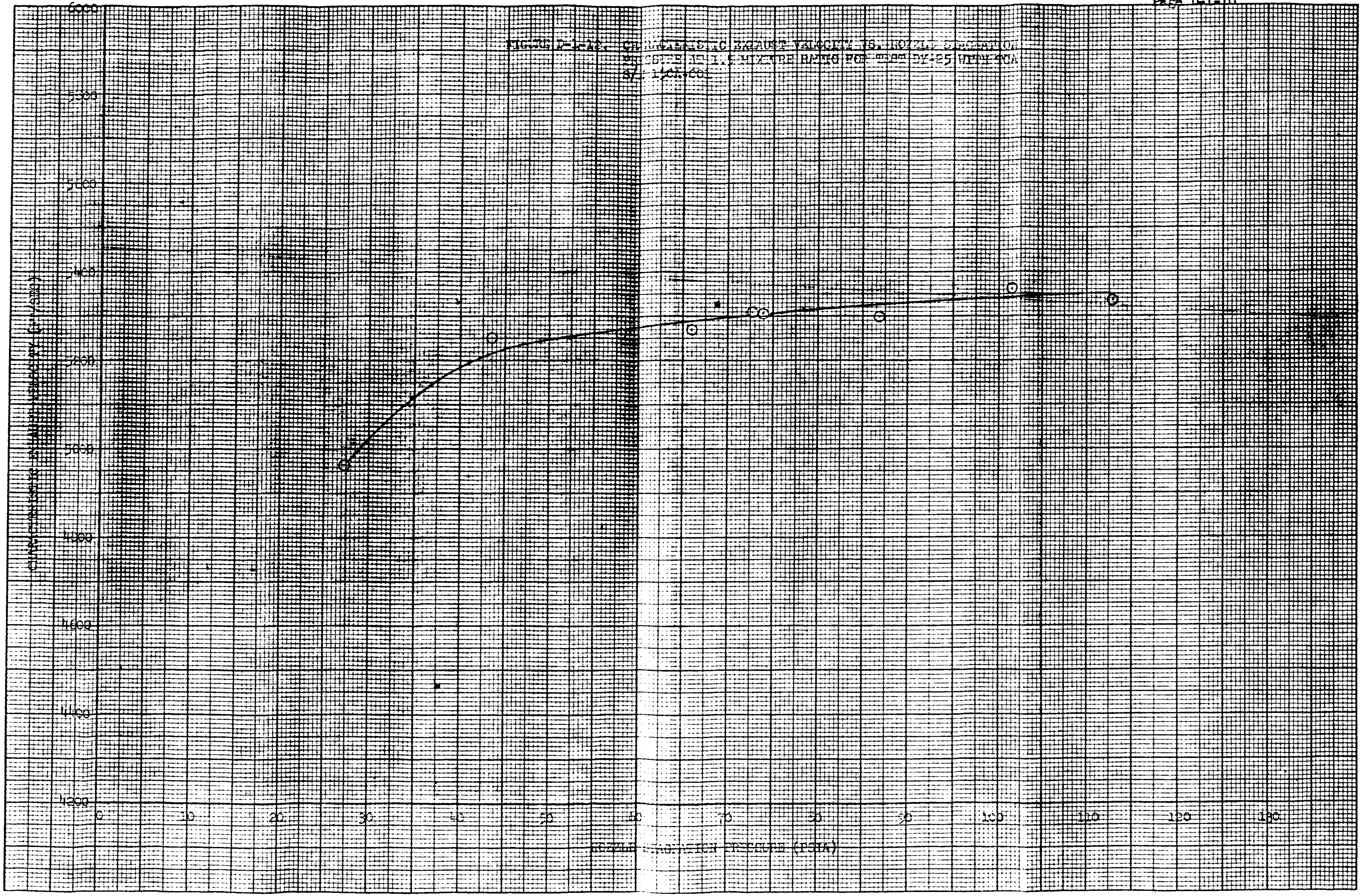

FIGURE D-1-12. CHARACTERISTIC EXHAUST VELOCITY VS. NOZZLE STAGNATION PRESSURE AT 1.5 MIXTURE RATIO FOR TEST DY-25 WITH TCA S/N 1/CH.601

DC-25

FIGURE D-1-13. TOTAL PRESSURE COEFFICIENT VS. NOZZLE STAGNATION PRESSURE AT 1.5 MIXTURE RATIO FOR TEST DC-25 WITH TCA S/N 1501-001

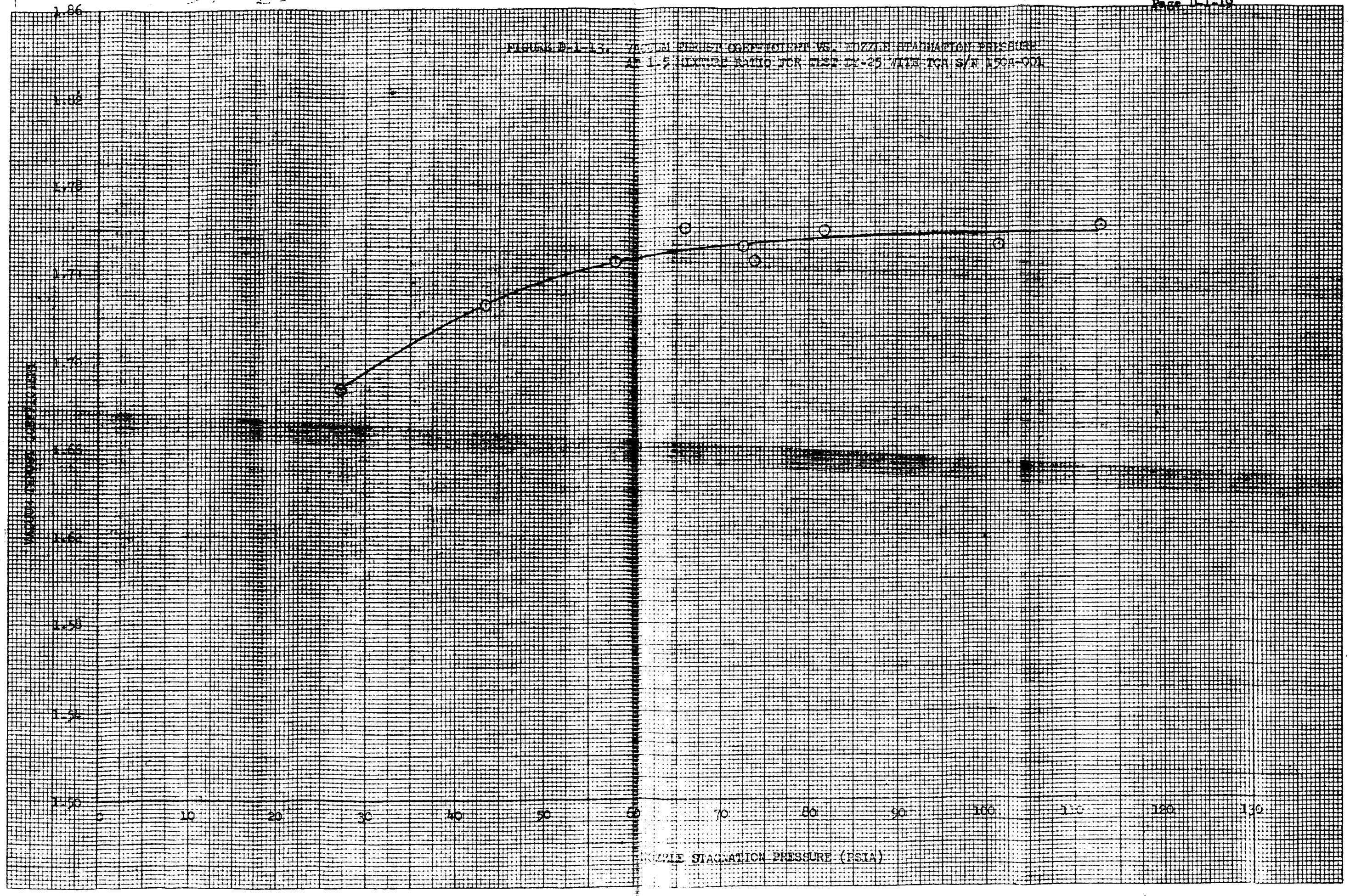

EUGENE DIETZGEN CO.
MADE IN U. S. A.

NO. 340DR-10½ DIETZGEN GRAPH PAPER
10 X 10 PER HALF INCH

FIGURE D-1-24. PROPELLANT FLOWRATES VS. SERVOACTUATOR POSITION AT 1.5 MIXTURE RATIO FOR DY-25 WITH TOA S/N 050A-001

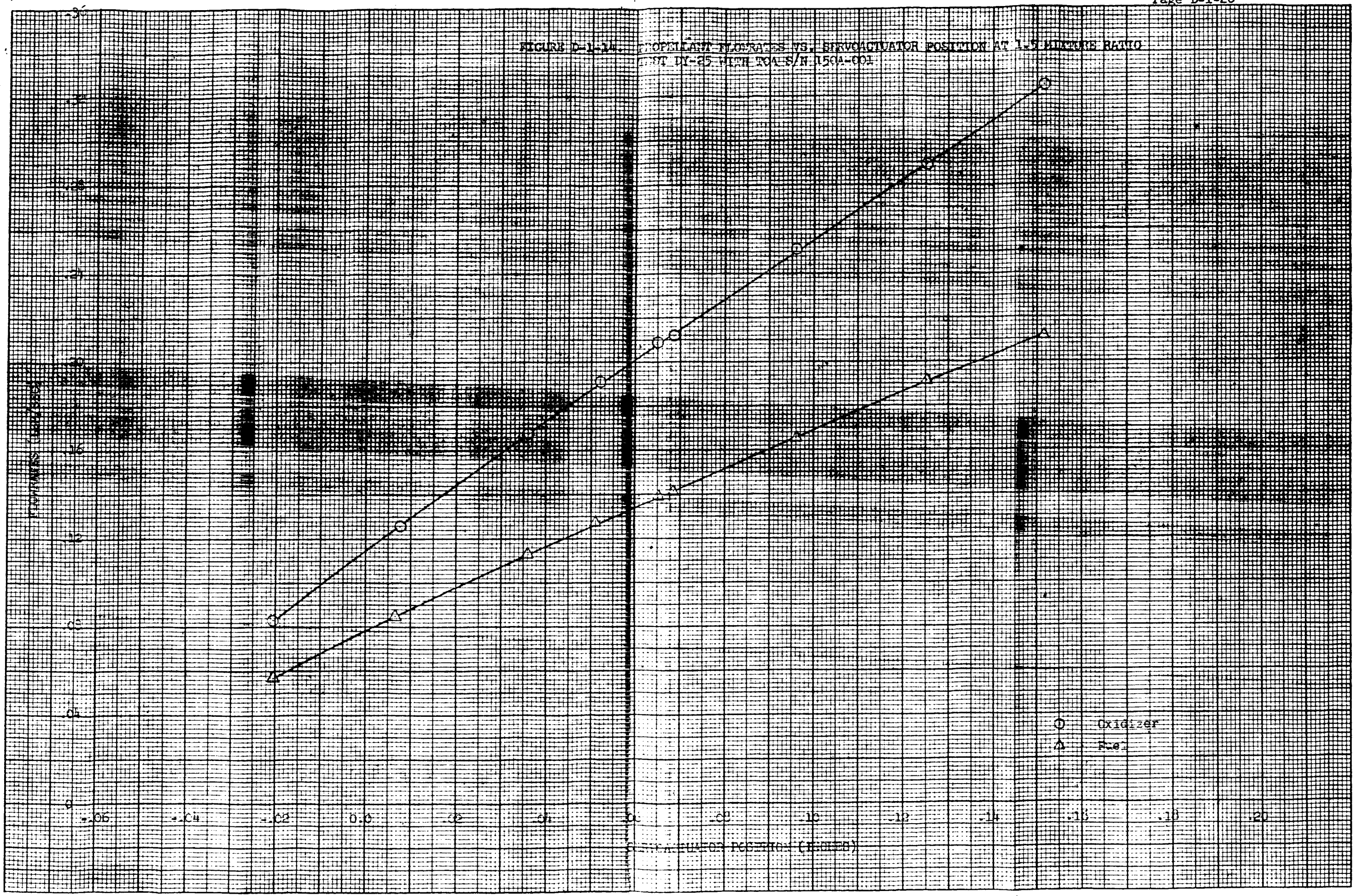

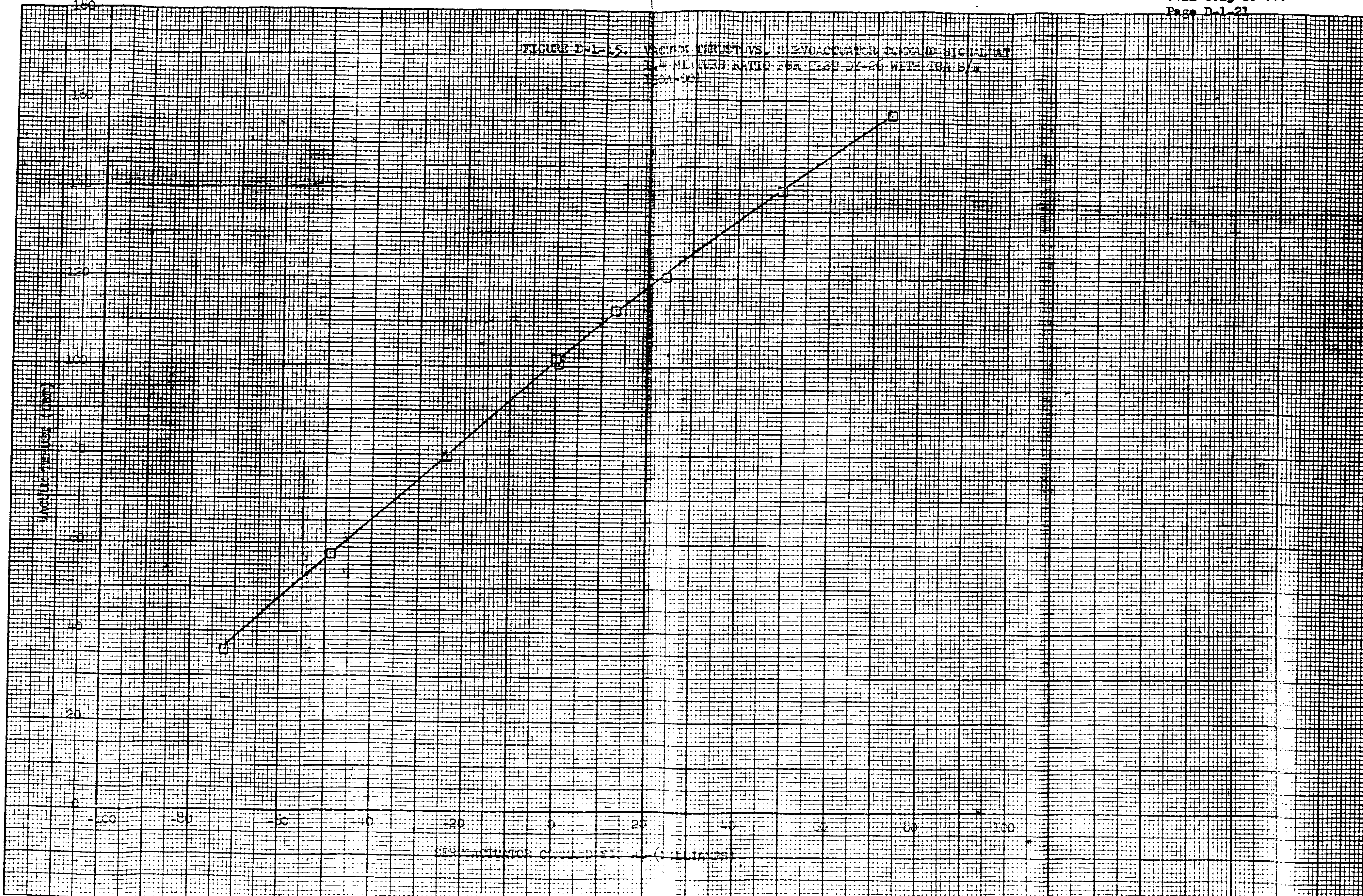

FIGURE D-1-15. VACUUM THRUST VS. SERVOACTUATOR COMMAND SIGNAL AT [illegible] MIXTURE RATIO FOR [illegible] WITH [illegible] S/N [illegible]

22

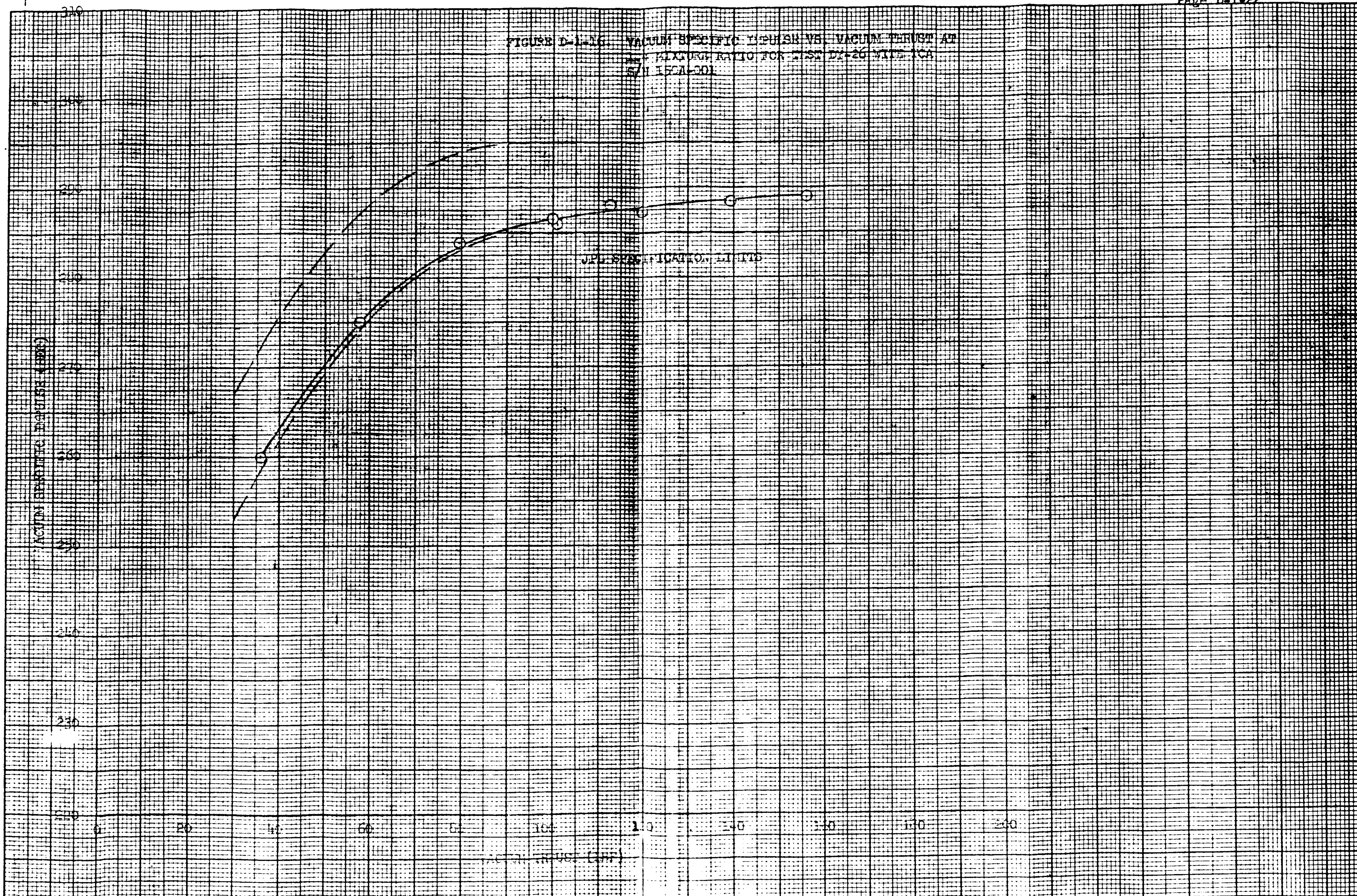

FIGURE D-1-16. VACUUM SPECIFIC IMPULSE VS. VACUUM THRUST AT [illegible] MIXTURE RATIO FOR TEST DV-26 WITH TCA S/N 15CA-201

FIGURE D-1-17. CHOPPER-STABILIZED BYEAUS PRESSURE VS. NOZZLE SEPARATION
PRESSURE AT 1.4 MIXTURE RATIO FOR TEST DY-26 WITH TCA
S/N 1301-001

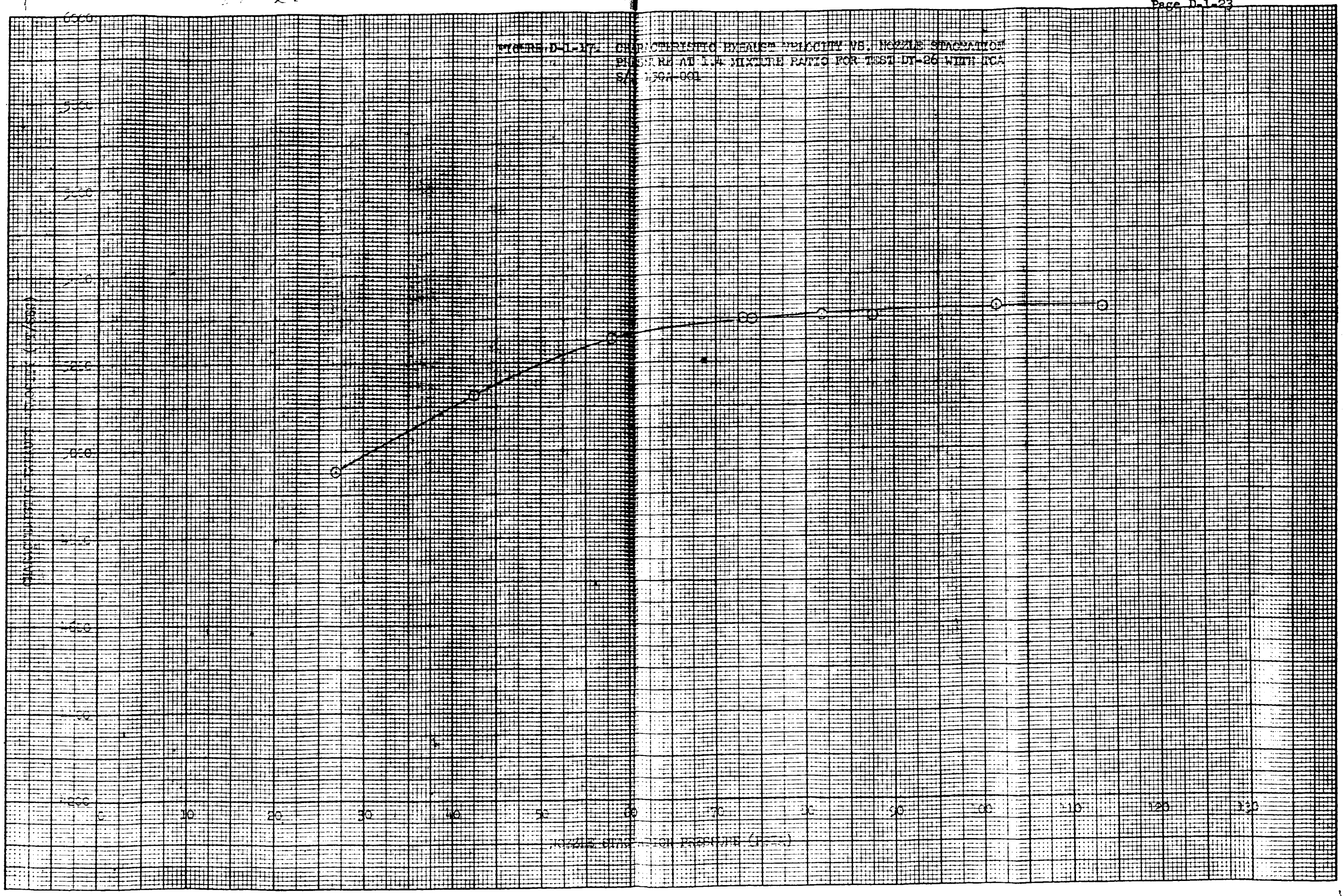

FIGURE 3-1-19. PROPELLANT FLOWRATE VS. SERVOACTUATOR POSITION AT MIXTURE RATIO FOR TEST DY-26 METHOD B/=

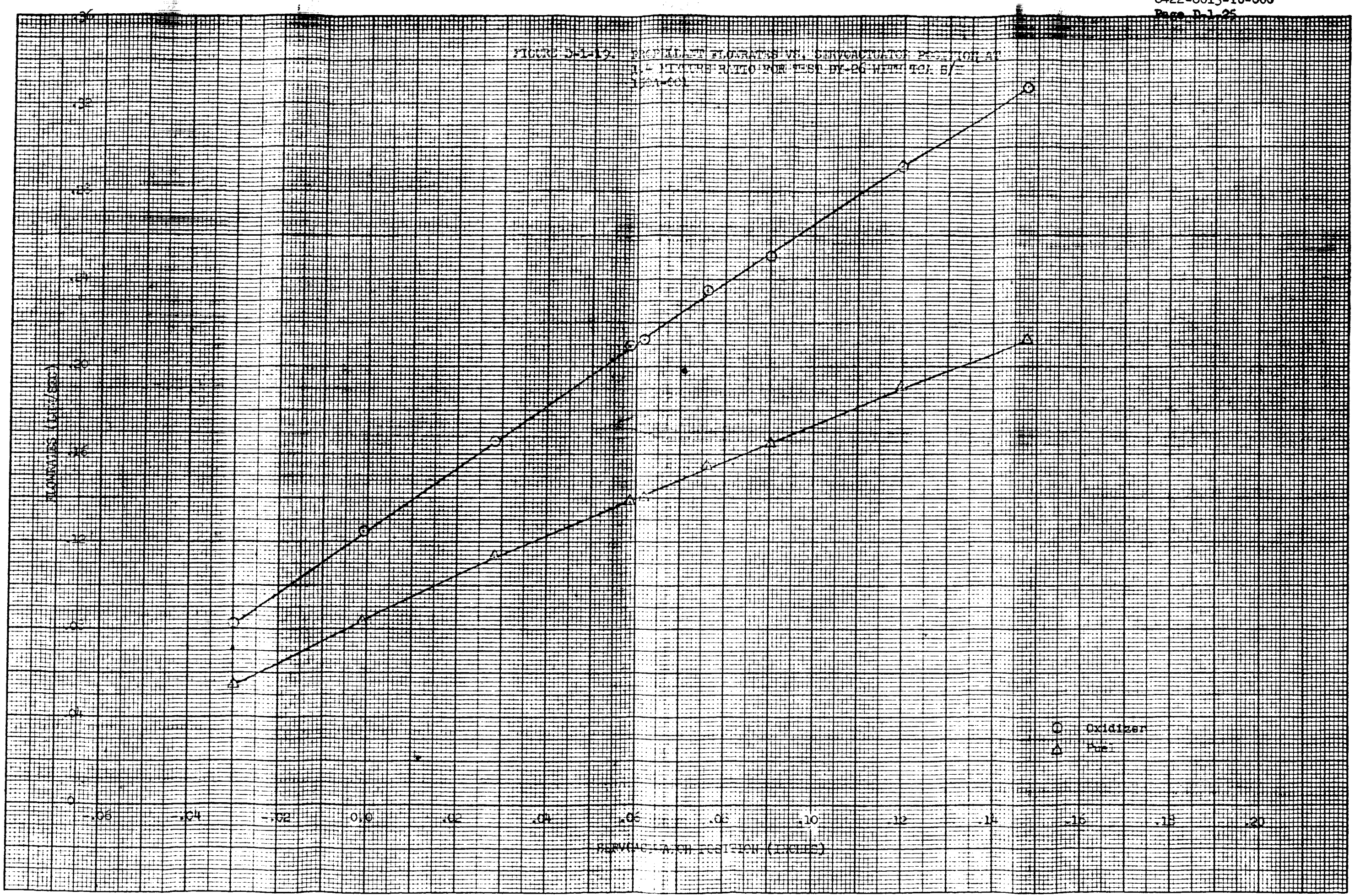

FIGURE D-1-20. VALID THRUST VS. SERVOACTUATOR COMMAND SIGNAL AT 1.6 MIXTURE RATIO FOR TEST FY-27 M1-3 ECA S/N 15[illegible]-001

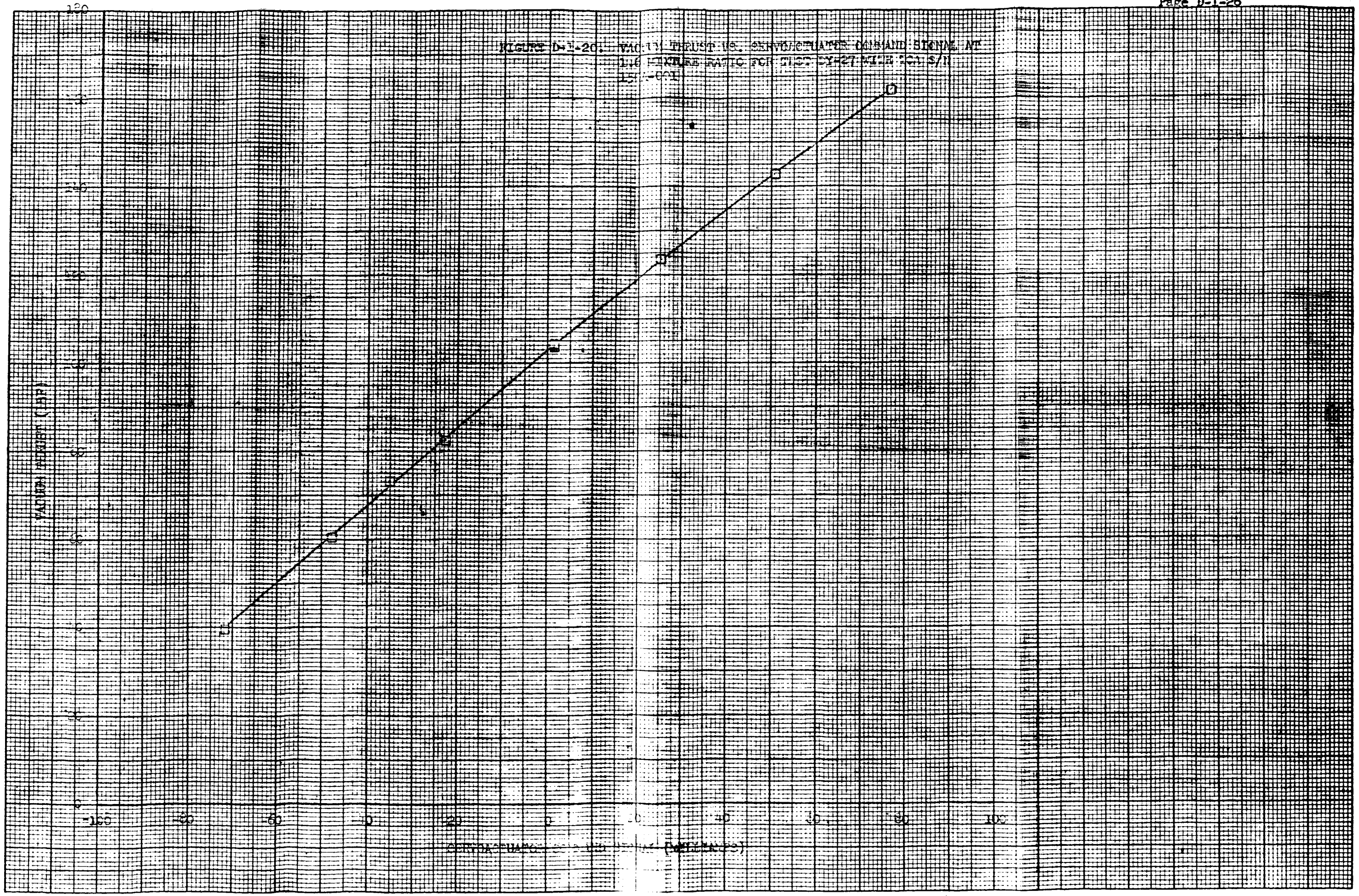

FIGURE D-1-01. VACUUM SPECIFIC IMPULSE VS. THRUST AT 1.6 MIXTURE RATIO FOR TEST DI-27 WITH ROCKETDYNE S/N 1456L-601

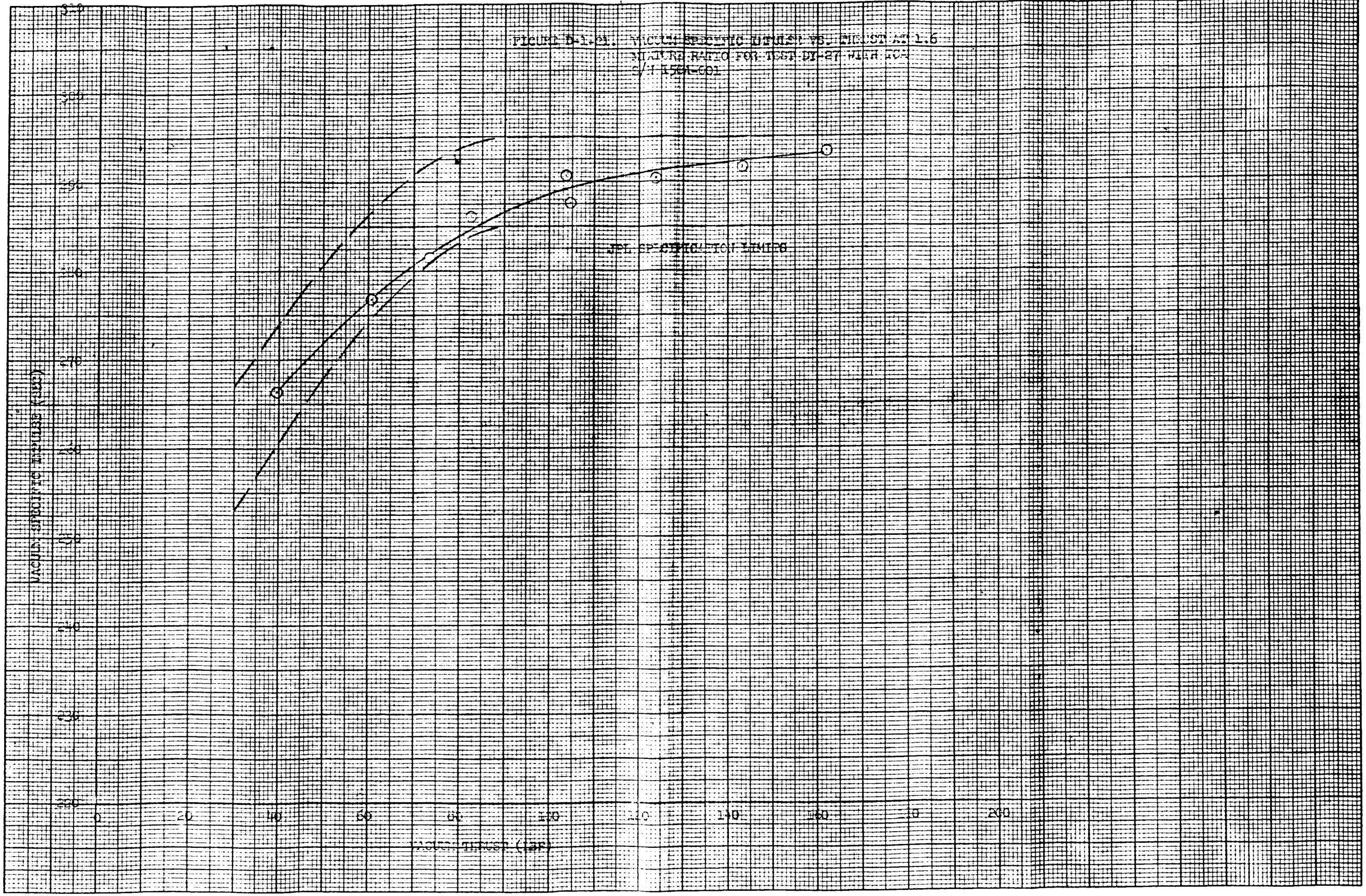

FIGURE D-1-2. PUMP FLOWRATE VS. SERVOACTUATOR POSITION AT [illegible] PRESSURE RATIO FOR [illegible] WITH JOA 5/[illegible]

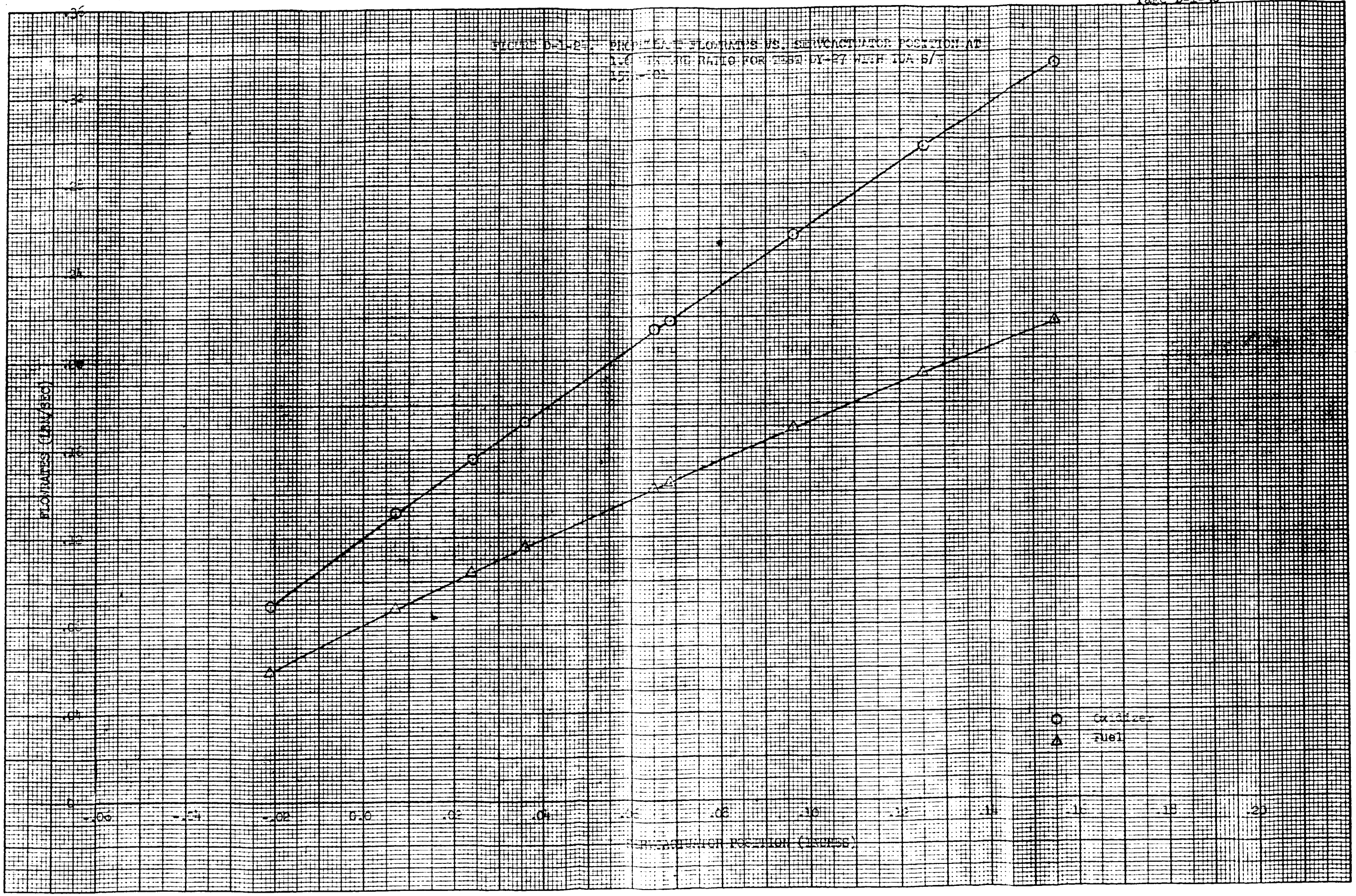

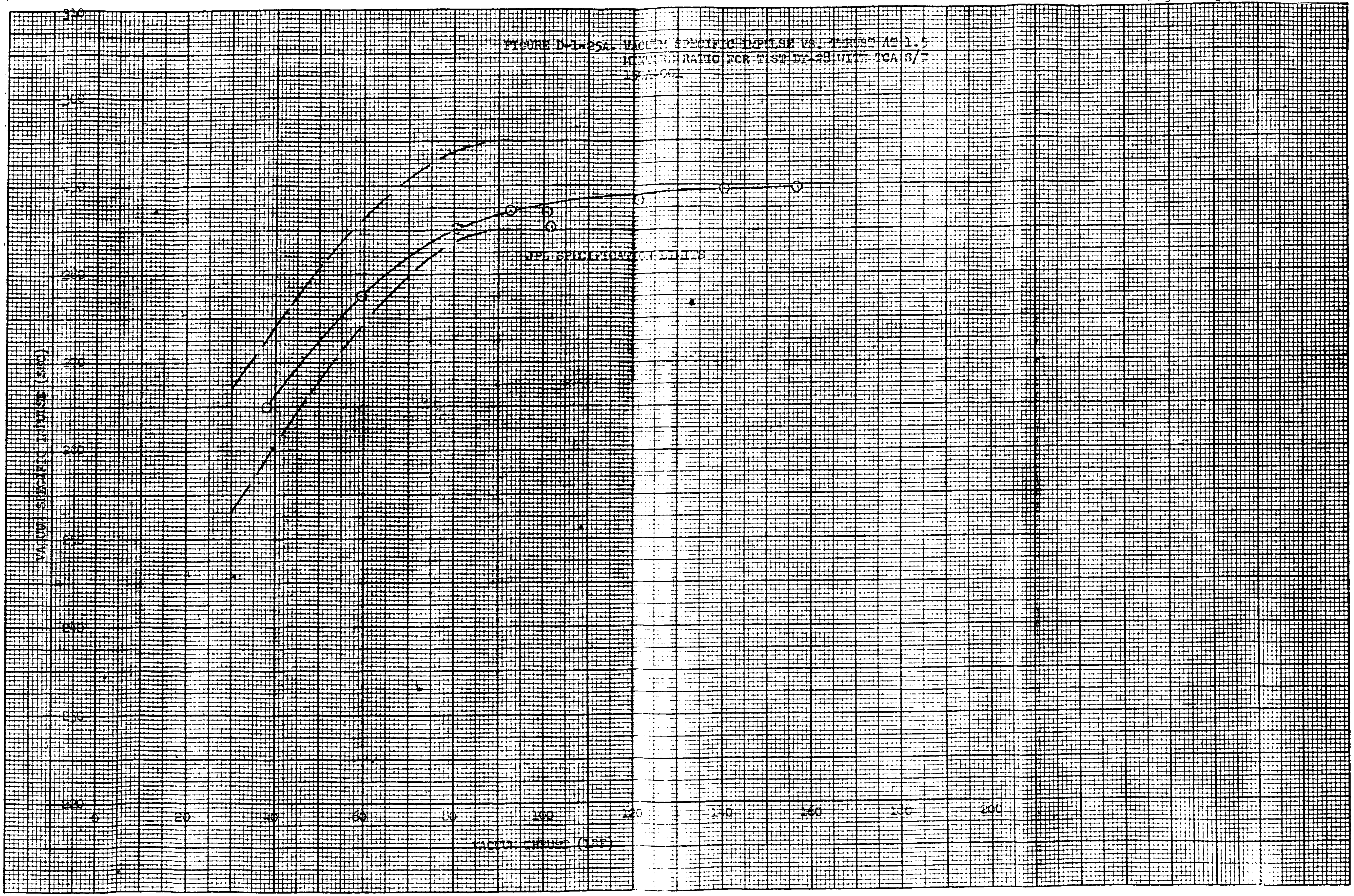

FIGURE D-1-25A. VACUUM SPECIFIC IMPULSE VS. THRUST AT 1.5 MIXTURE RATIO FOR TEST DT-28 WITH TCA S/N [illegible]

FIGURE D-1-25E. VACUUM THRUST VS. SERVOACTUATOR DEMAND STROKE AT 1.5 X TEMPERATURE RAMP TO FOR TEST DY-28 WITH PCA S/N 1201-001

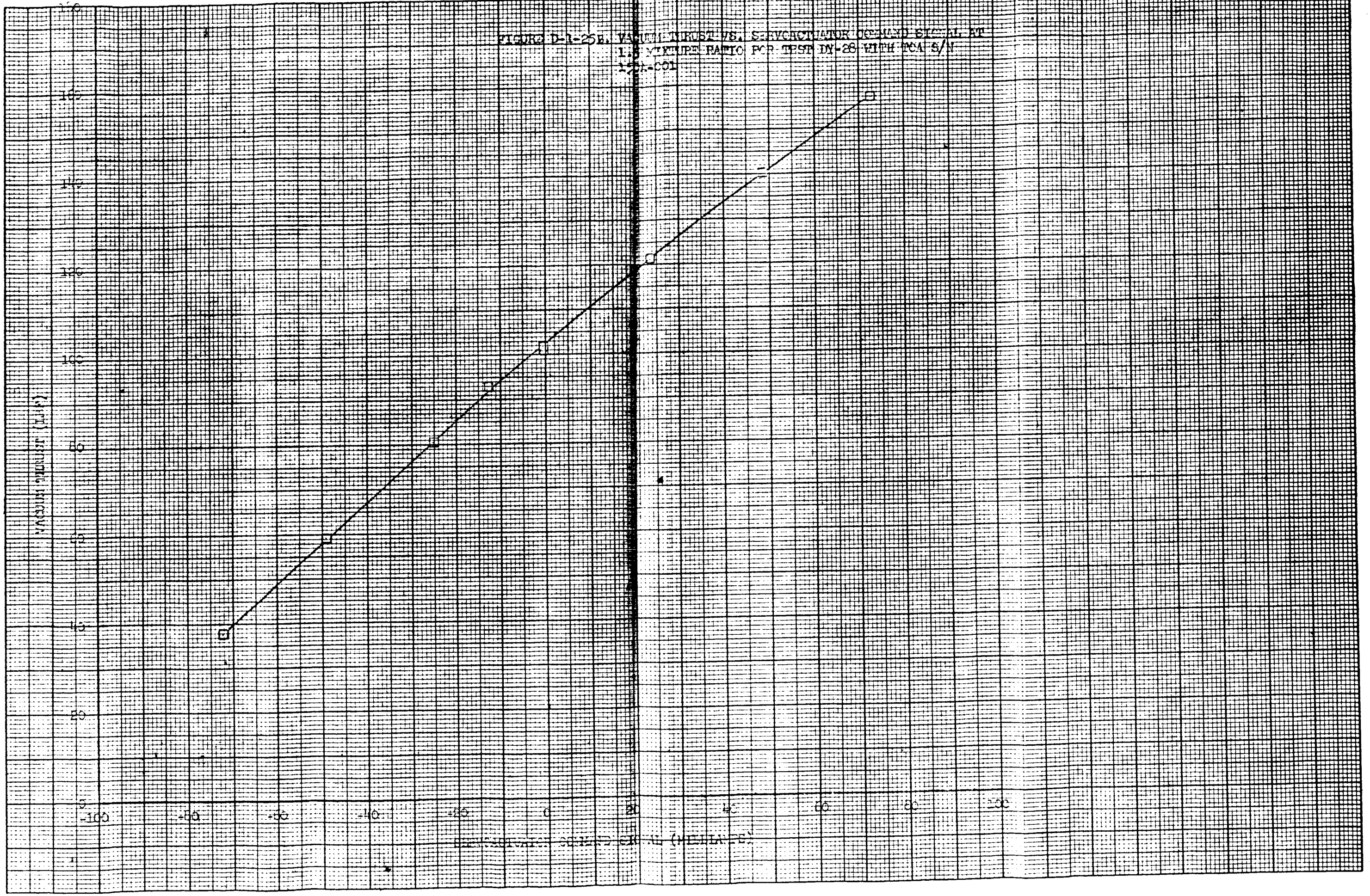

FIGURE D-1-26. CHARACTERISTIC HEAT RELEASE VS. NOZZLE STAGNATION PRESSURE AT 5.5 MIXTURE RATIO FOR TEST DY-26 WITH GCA S/N 1503-003

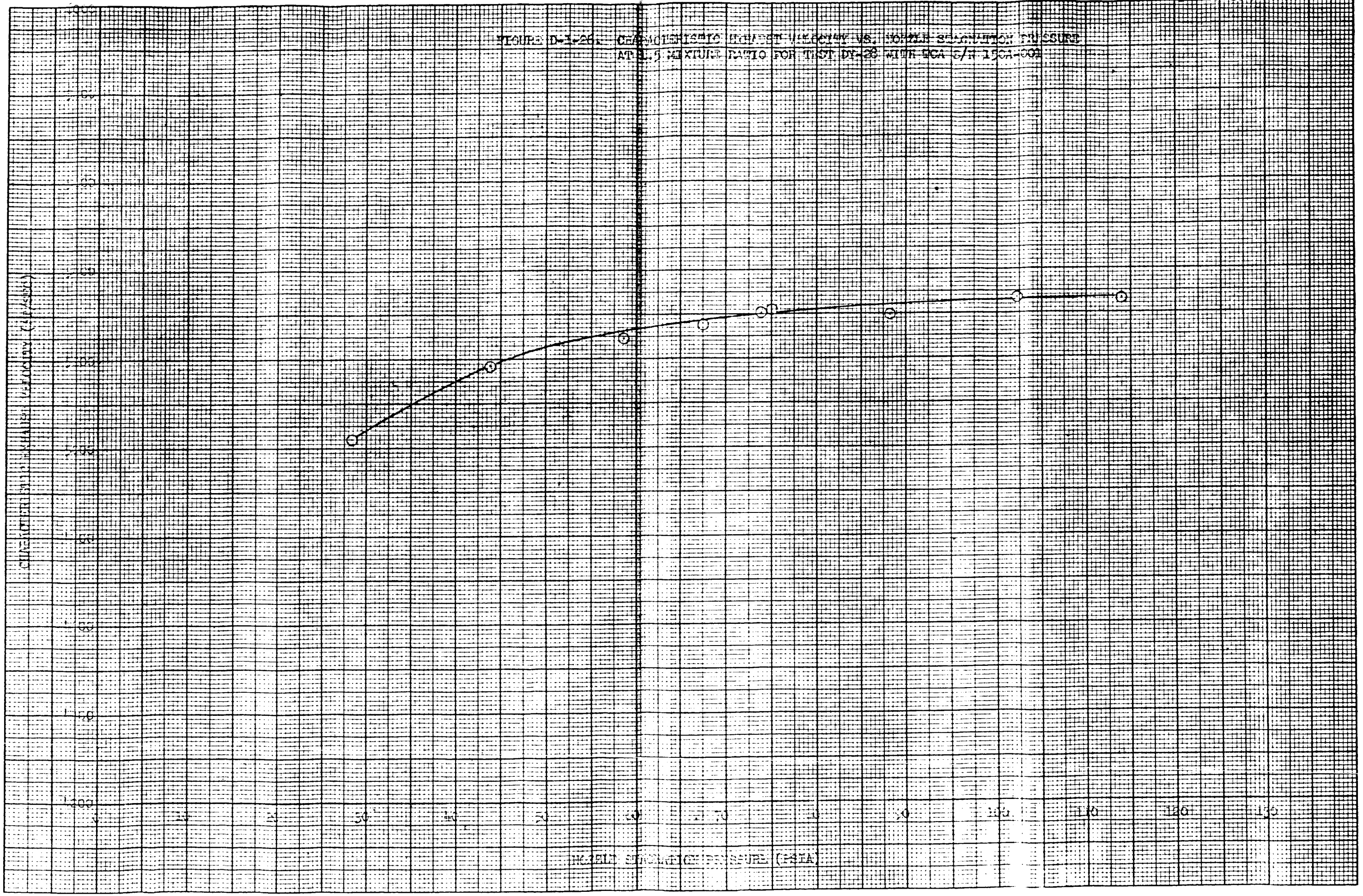

FIGURE D-1-27: VACUUM THRUST COEFFICIENT VS. NOZZLE STAGNATION PRESSURE AT 1.5 MIXTURE RATIO FOR TEST DY-23 WITH TCA S/N 1304-001

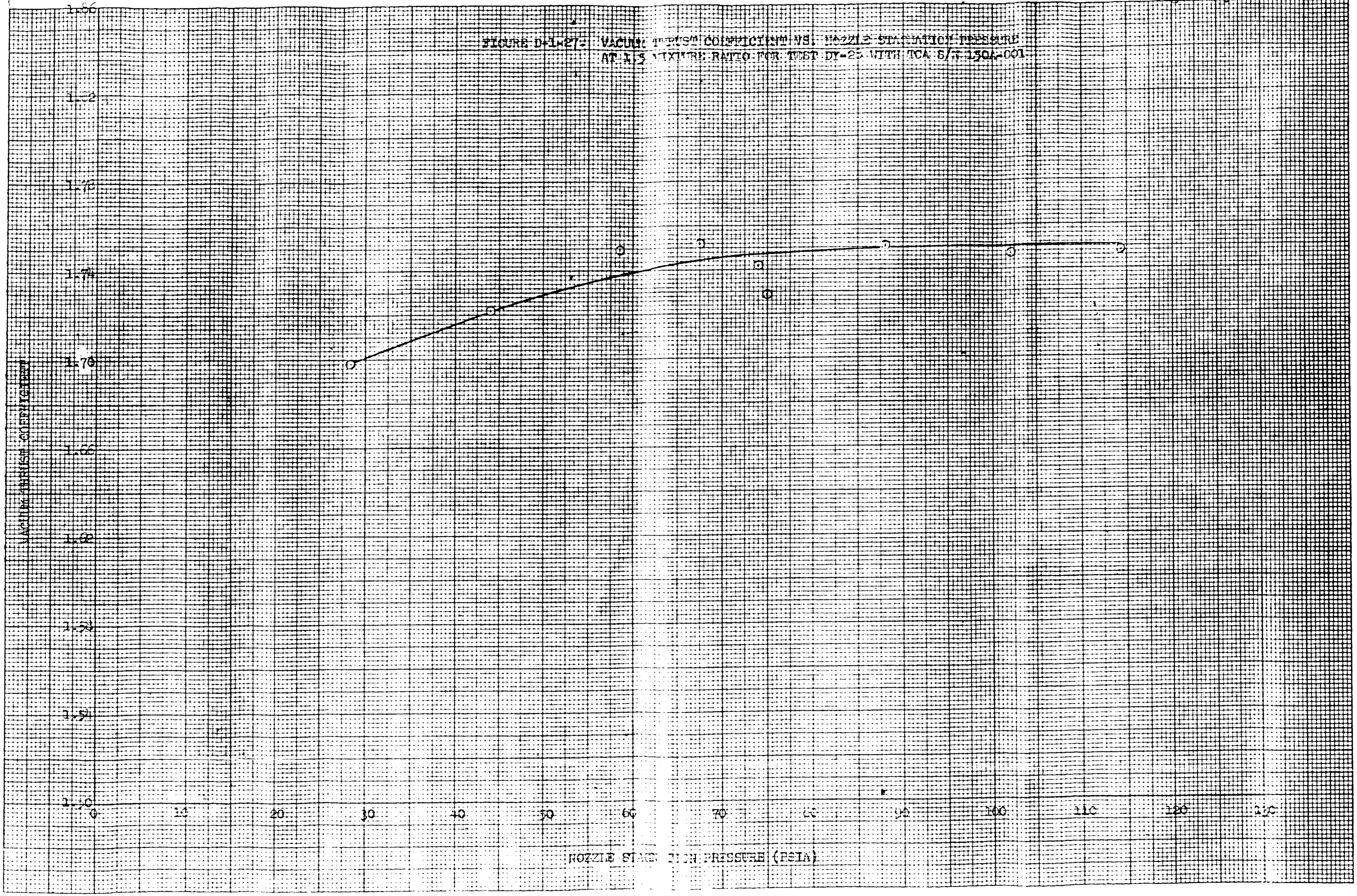

FIGURE D-1-23. [illegible] FLOWRATE VS. SERVOACTUATOR POSITION AT 145 PSIA TANK PRESSURE FOR TEST 7-20 WITH ICD S/N 1251-502

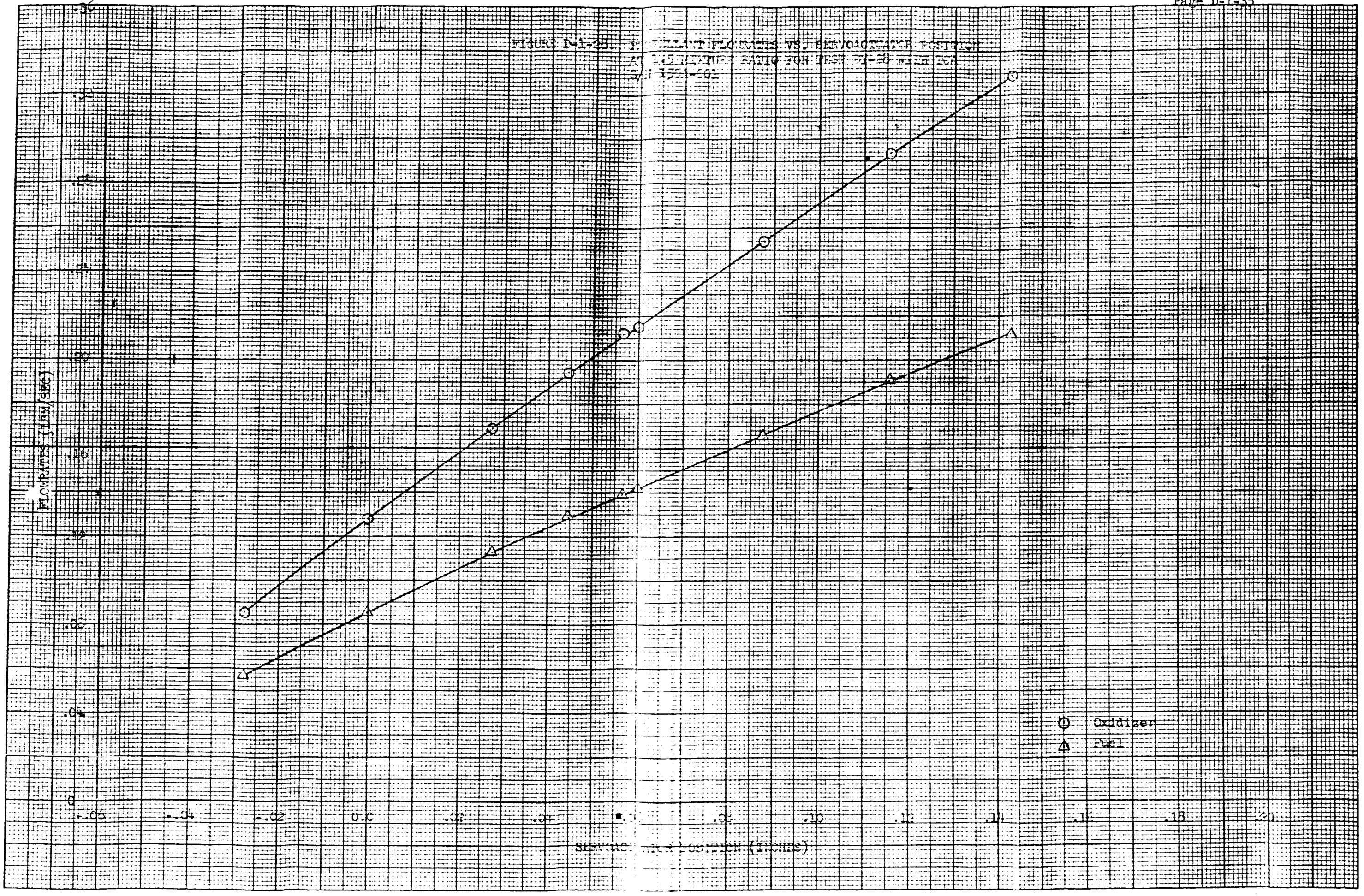

FIGURE D-1-29. VACUUM THRUST VS. BIMORPH/TORCH CONTROL SIGNAL
AT .5 MIXING RATIO FOR TEST D1-29 WITH TC4
S/N 1501-001

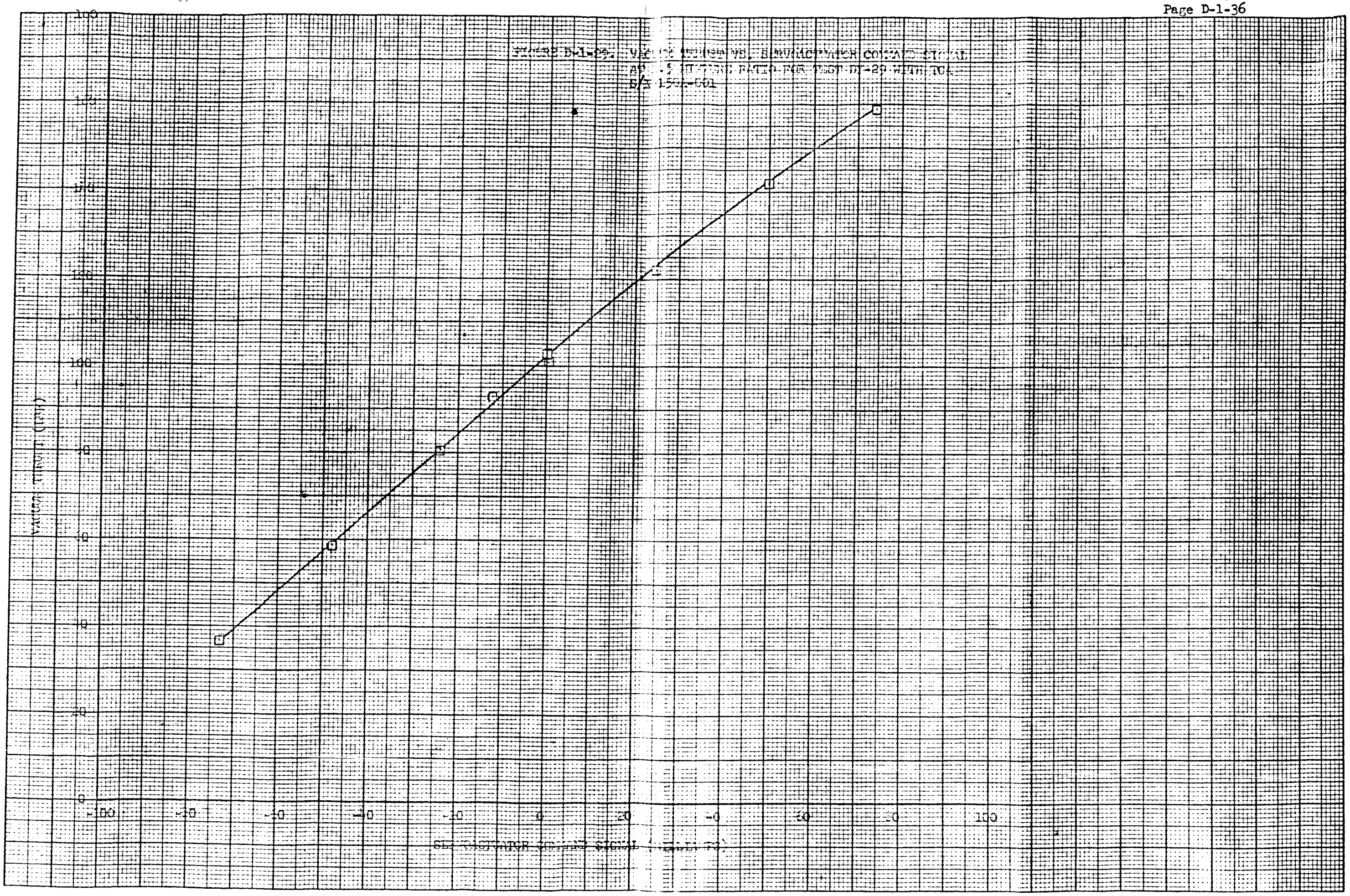

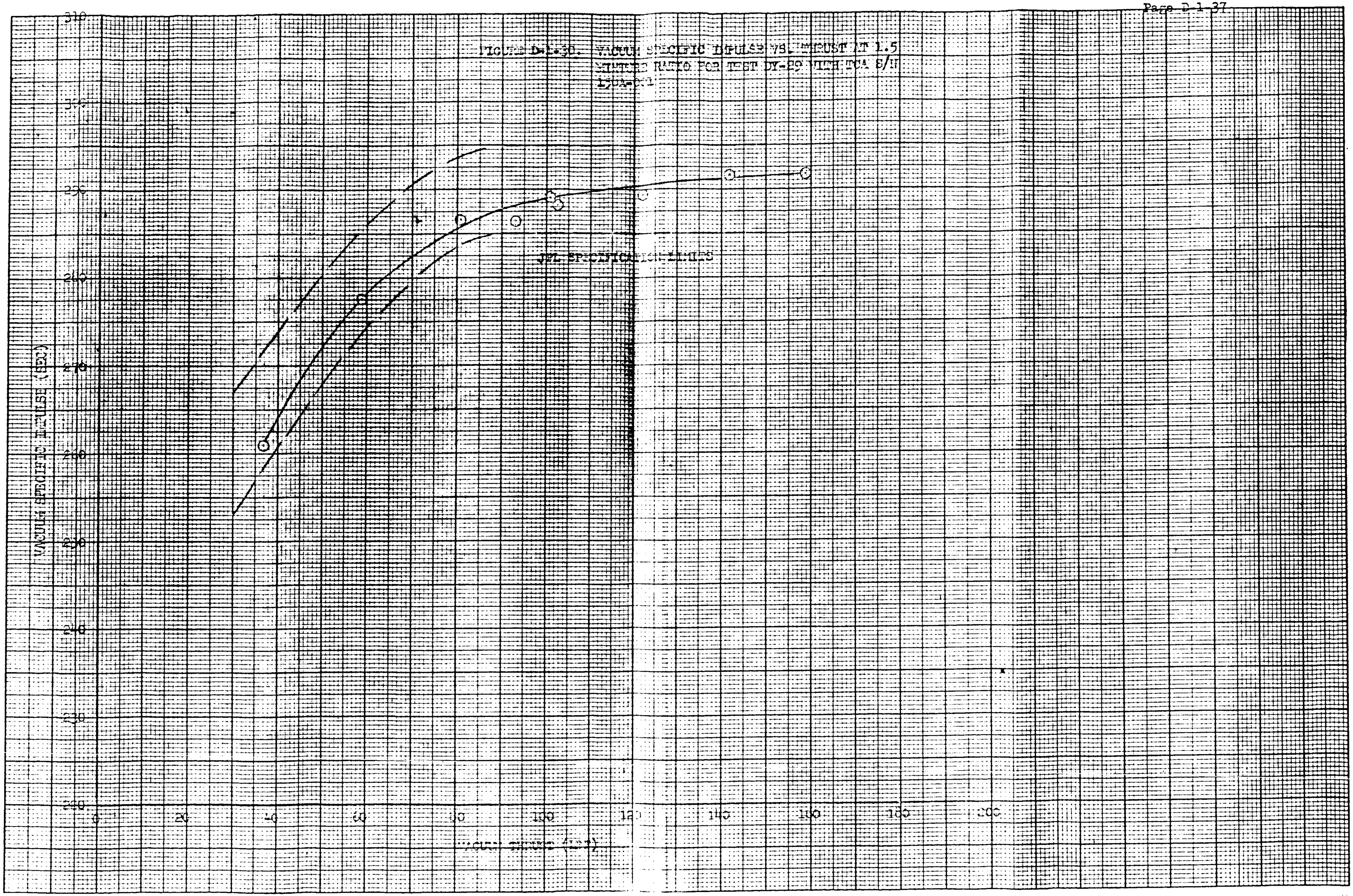

FIGURE D-1.30. VACUUM SPECIFIC IMPULSE VS. THRUST AT 1.5 MIXTURE RATIO FOR TEST DY-29 WITH TCA S/N 1/0A-001

FIGURE D-1-31. CHARACTERISTIC EXHAUST VELOCITY VS. NOZZLE STAGNATION PRESSURE AT 1.3 MIXTURE RATIO FOR TEST DI-20 WITH B/I 1,04A-001

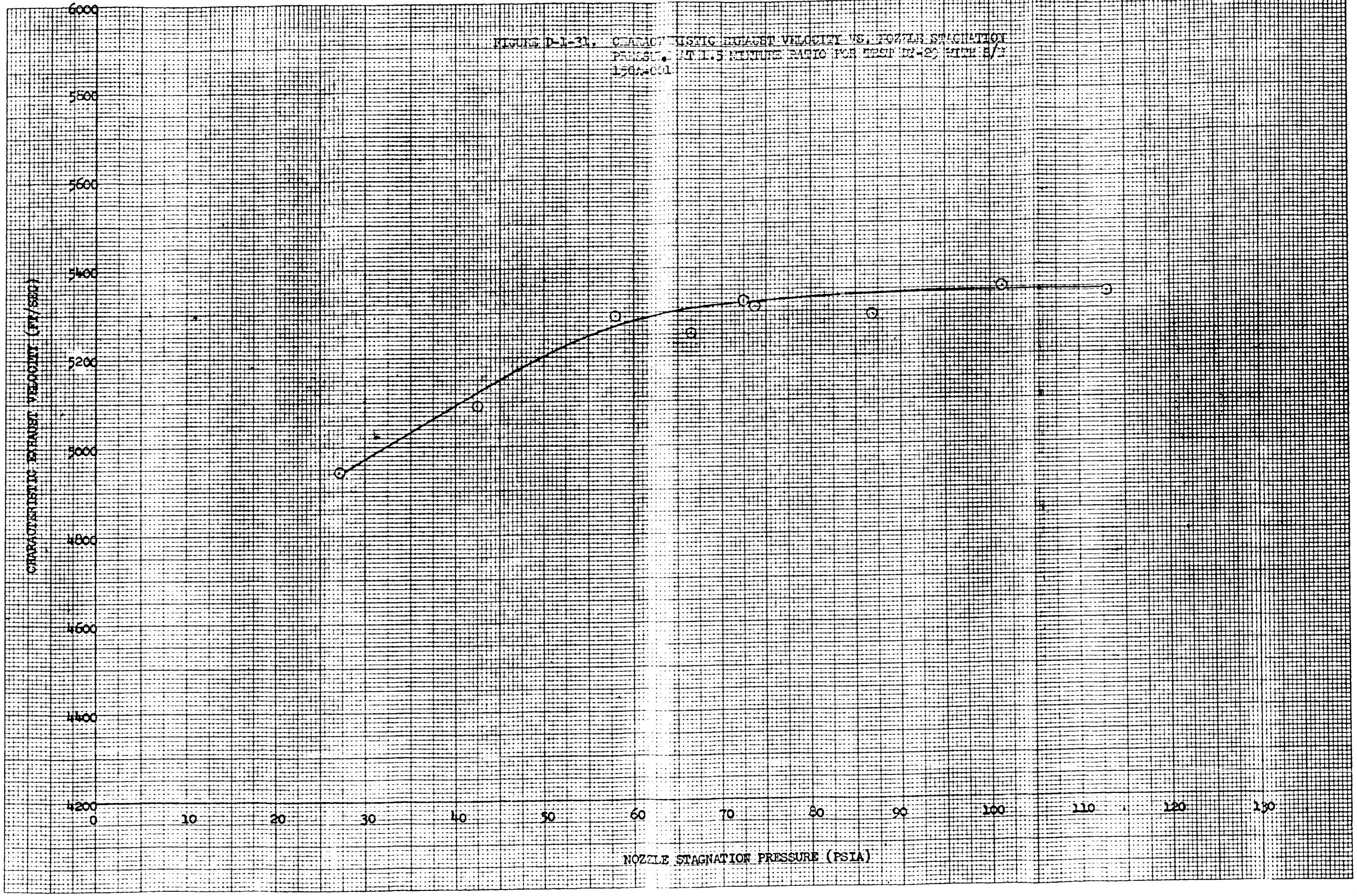

FIGURE D-1-32. VACUUM THRUST COEFFICIENT VS. NOZZLE STAGNATION PRESSURE AT 1.5 MIXTURE RATIO FOR TEST DV-29 WITH ECA S/N 1504-001

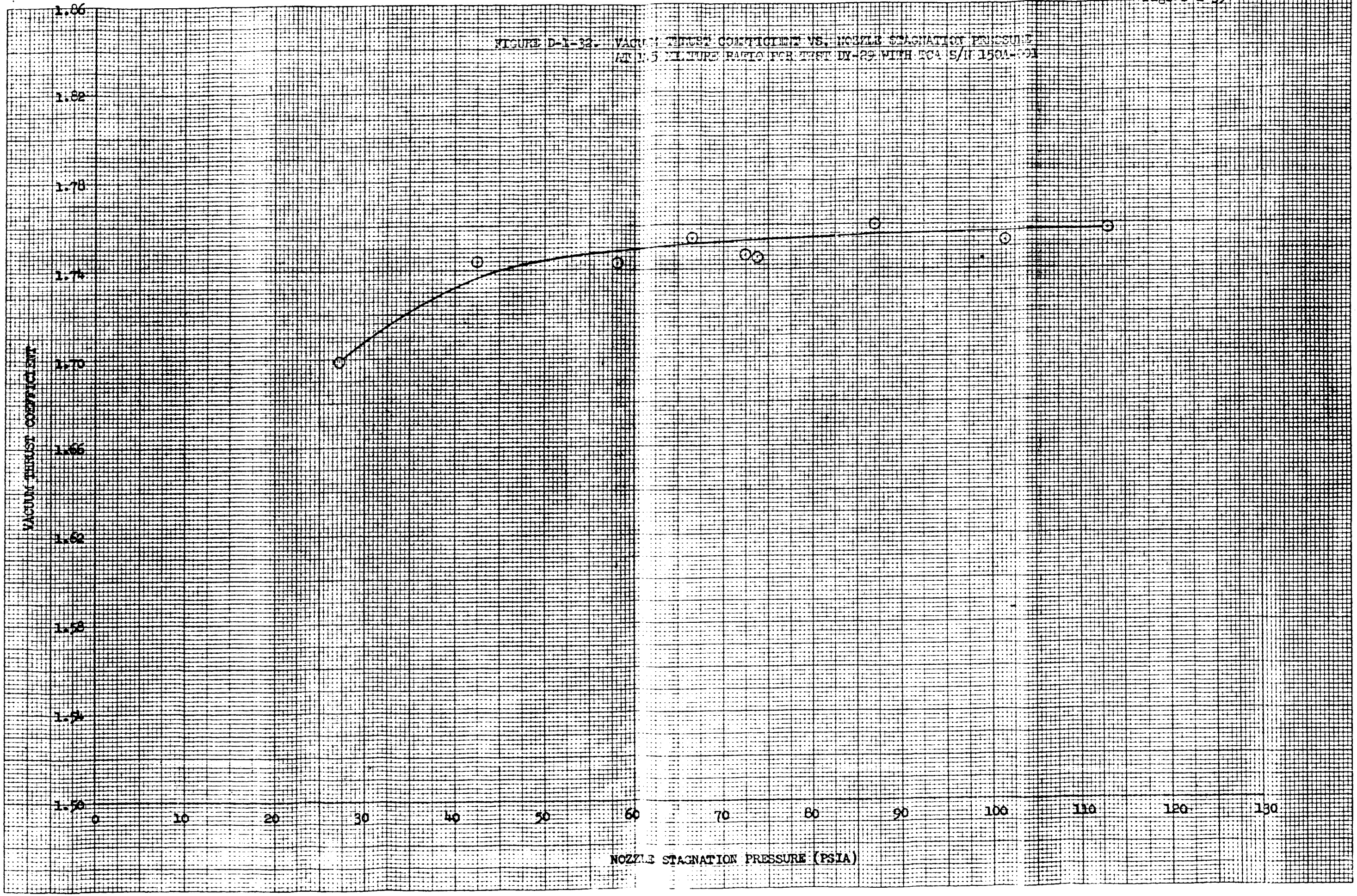

FIGURE D-1-38. PROPELLANT FLOWRATES VS. SERVOACTUATOR POSITION
45:1 PROPELLANT RATIO FOR 21.2 K-29 STT TCA S/N

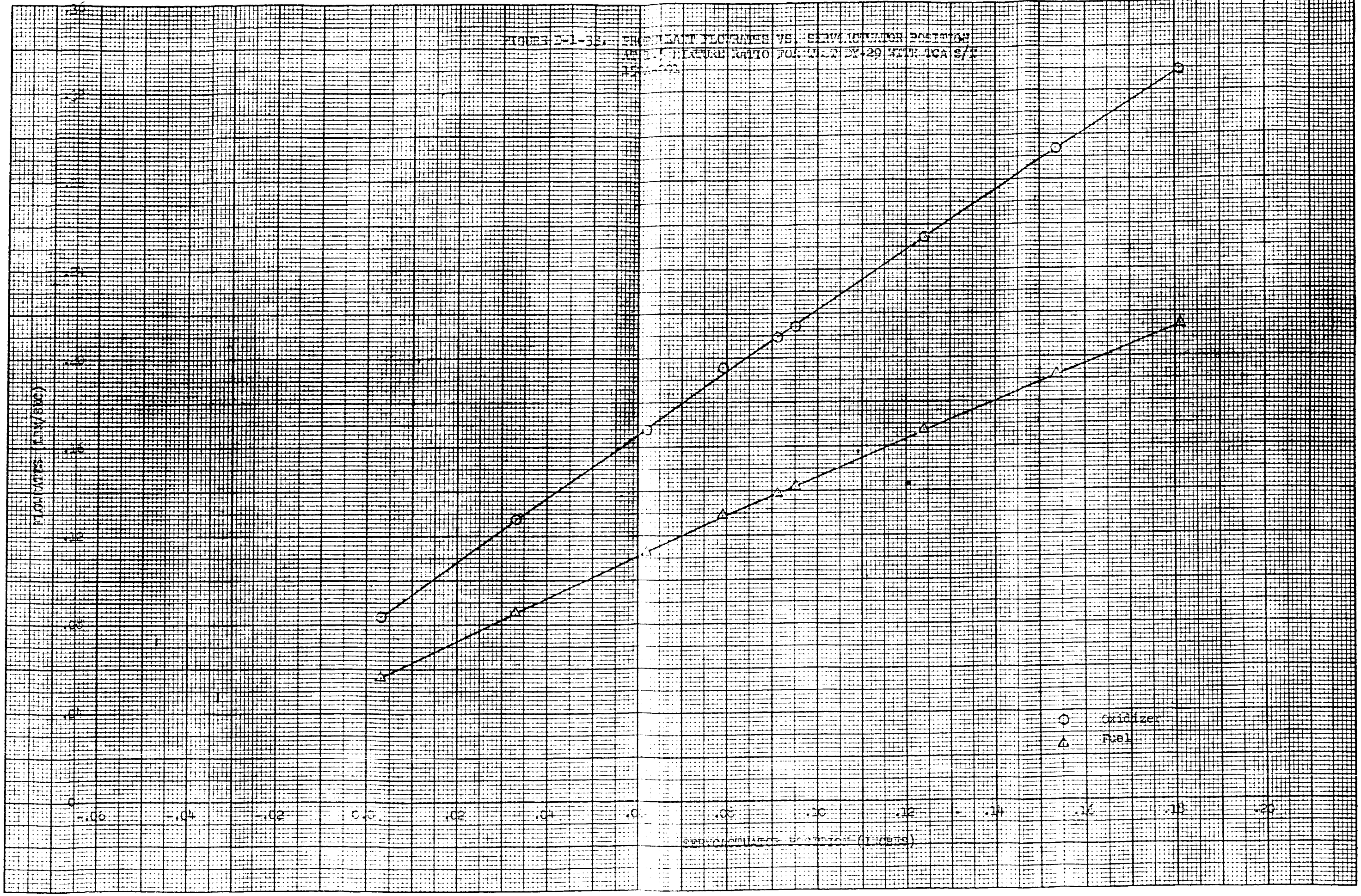

FIGURE D-1-14, [illegible] THRUST VS. [illegible] COMMAND [illegible] AT [illegible] RATIO FOR TEST [illegible]

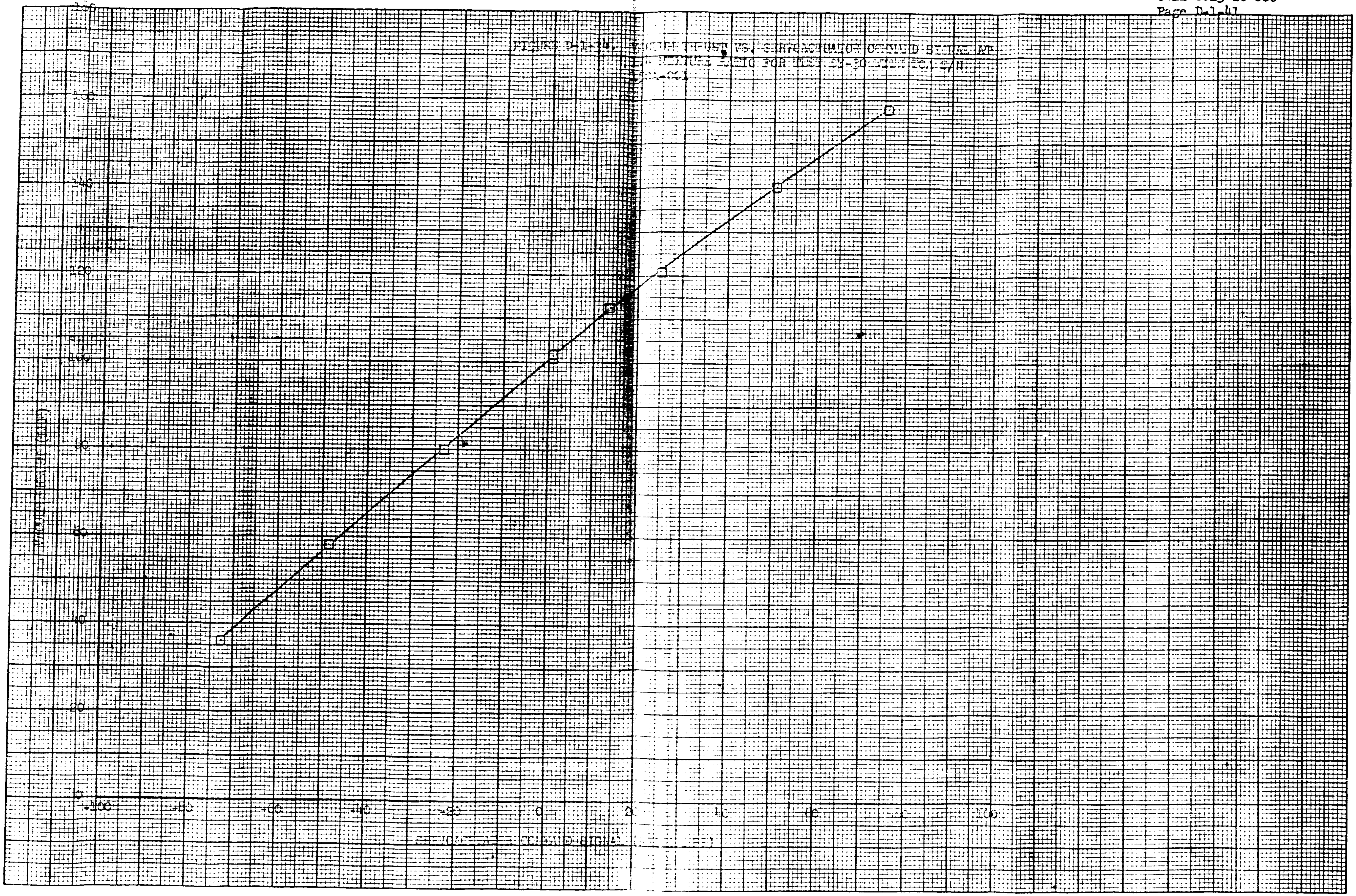

42

FIGURE D-2-35. VACUUM SPECIFIC IMPULSE VS. THRUST/CHAMBER PRESSURE RATIO FOR TEST DY-32 WITH TC-6/7 1,760 lbf

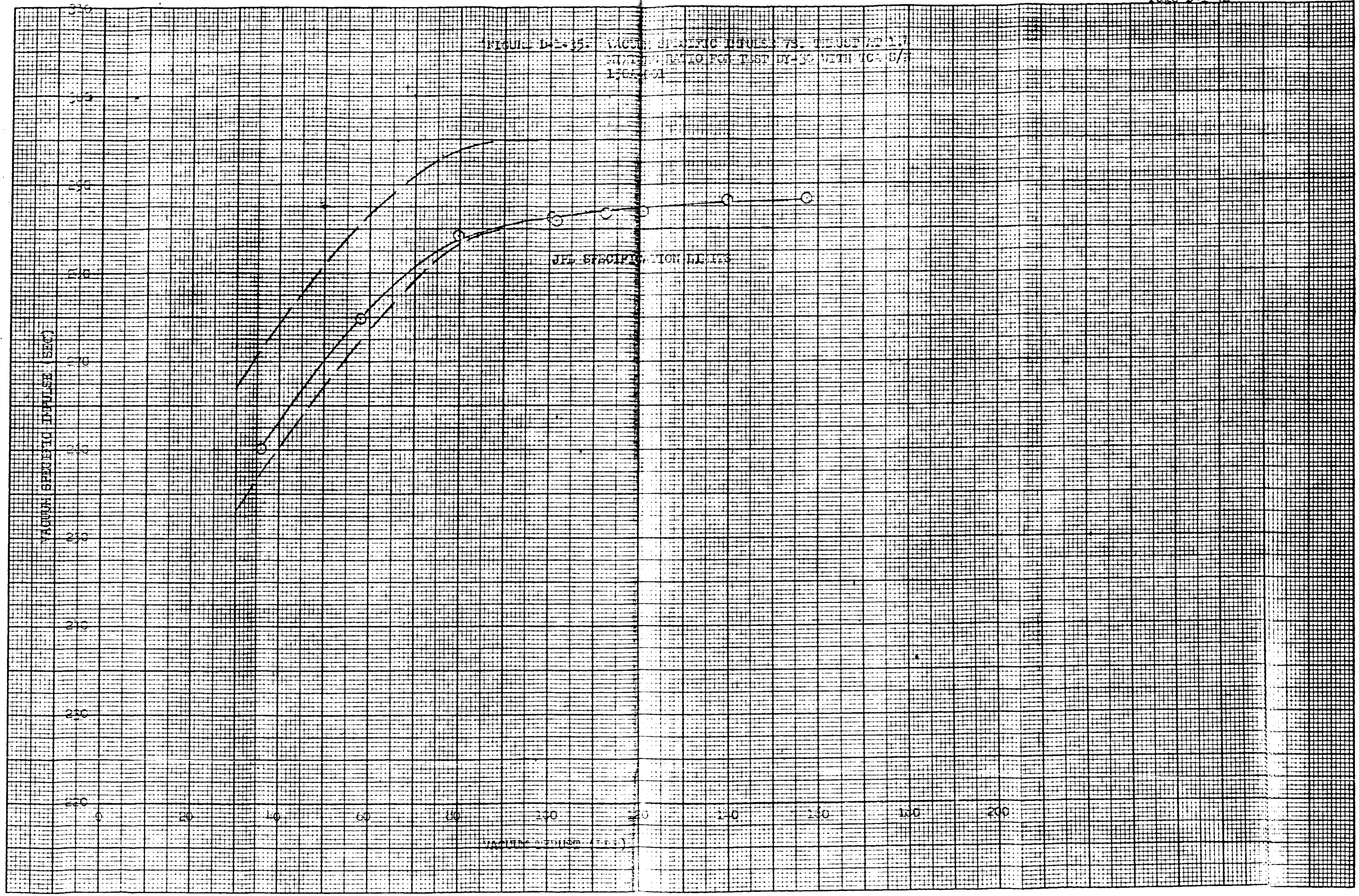

43

FIGURE D-1-36. CHARACTERISTIC EXHAUST VELOCITY VS. NOZZLE STAGNATION PRESSURE AT 1.4 MIXTURE RATIO FOR TEST IM-50 FIRE B/E 1584-001

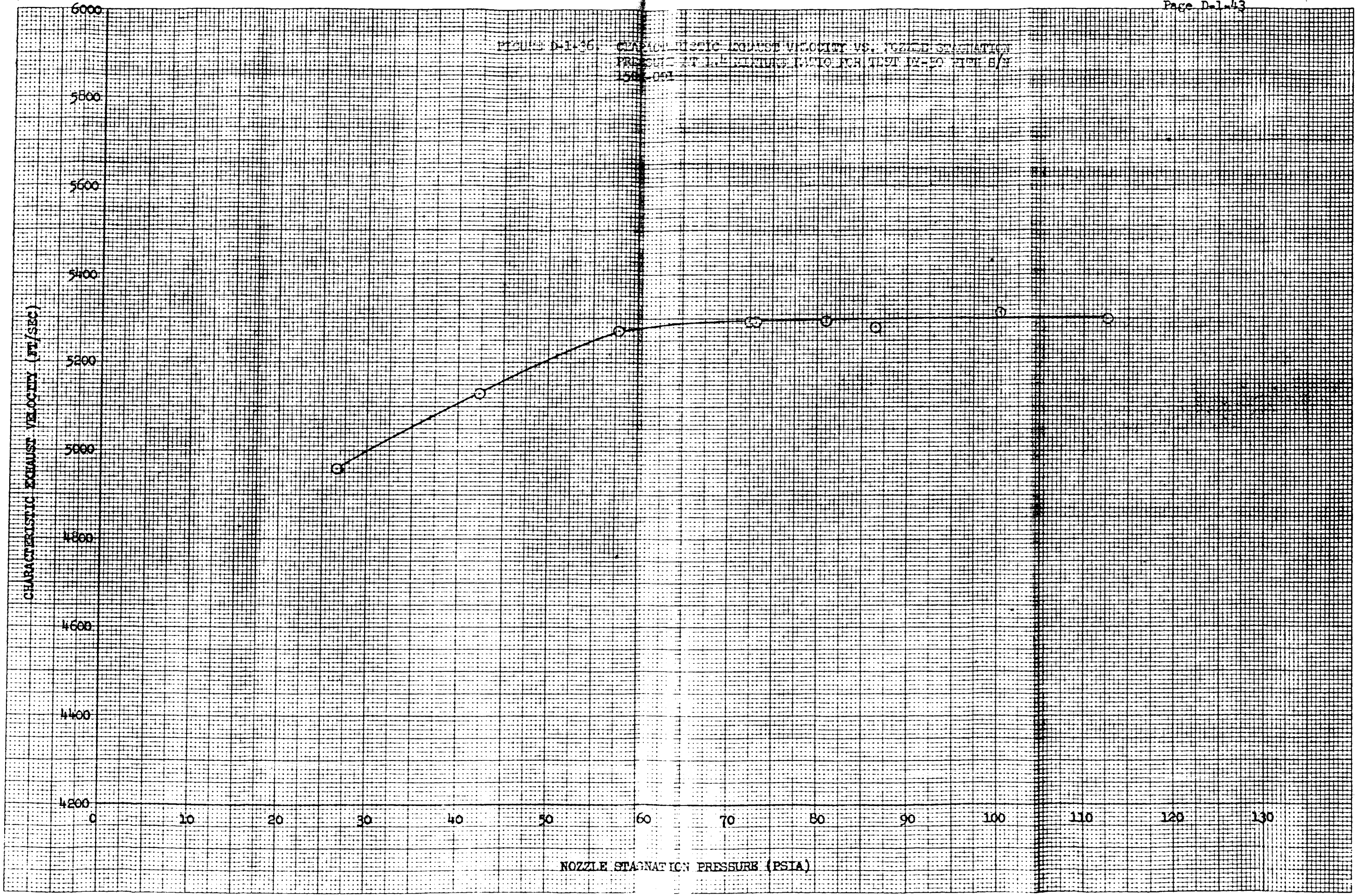

FIGURE D-1-37. VACUUM THRUST COEFFICIENT VS. NOZZLE STAGNATION PRESSURE FOR 5 AT 1.4 MIXTURE RATIO FOR TEST NO. 30 WITH S/N 156A-001

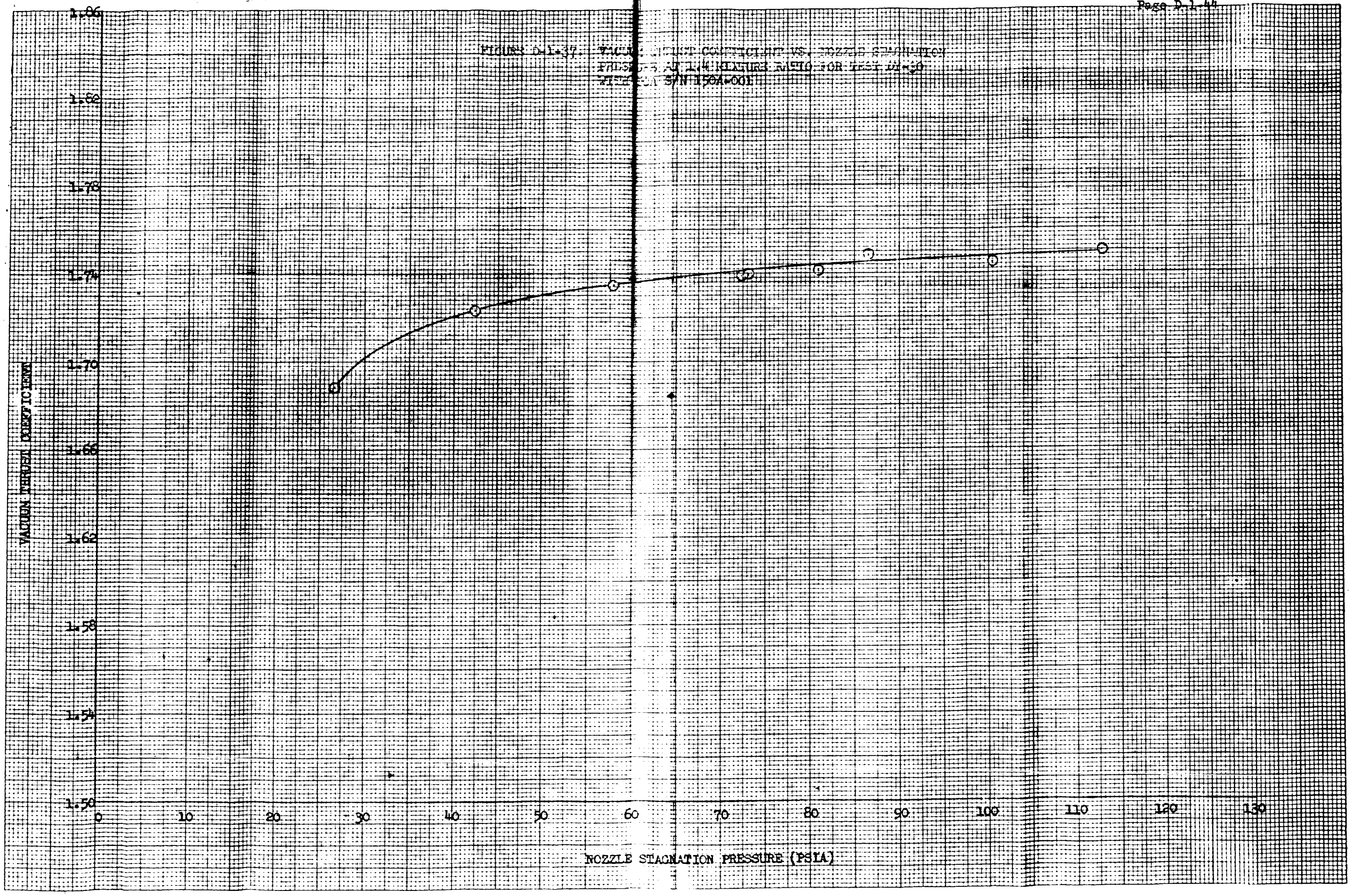

FIGURE D-1-8. THRUST COEFFICIENT VS. SEPARATION POSITION AT MIXTURE RATIO FOR TEST 2V-30 WITH TCA S/N 1001-001

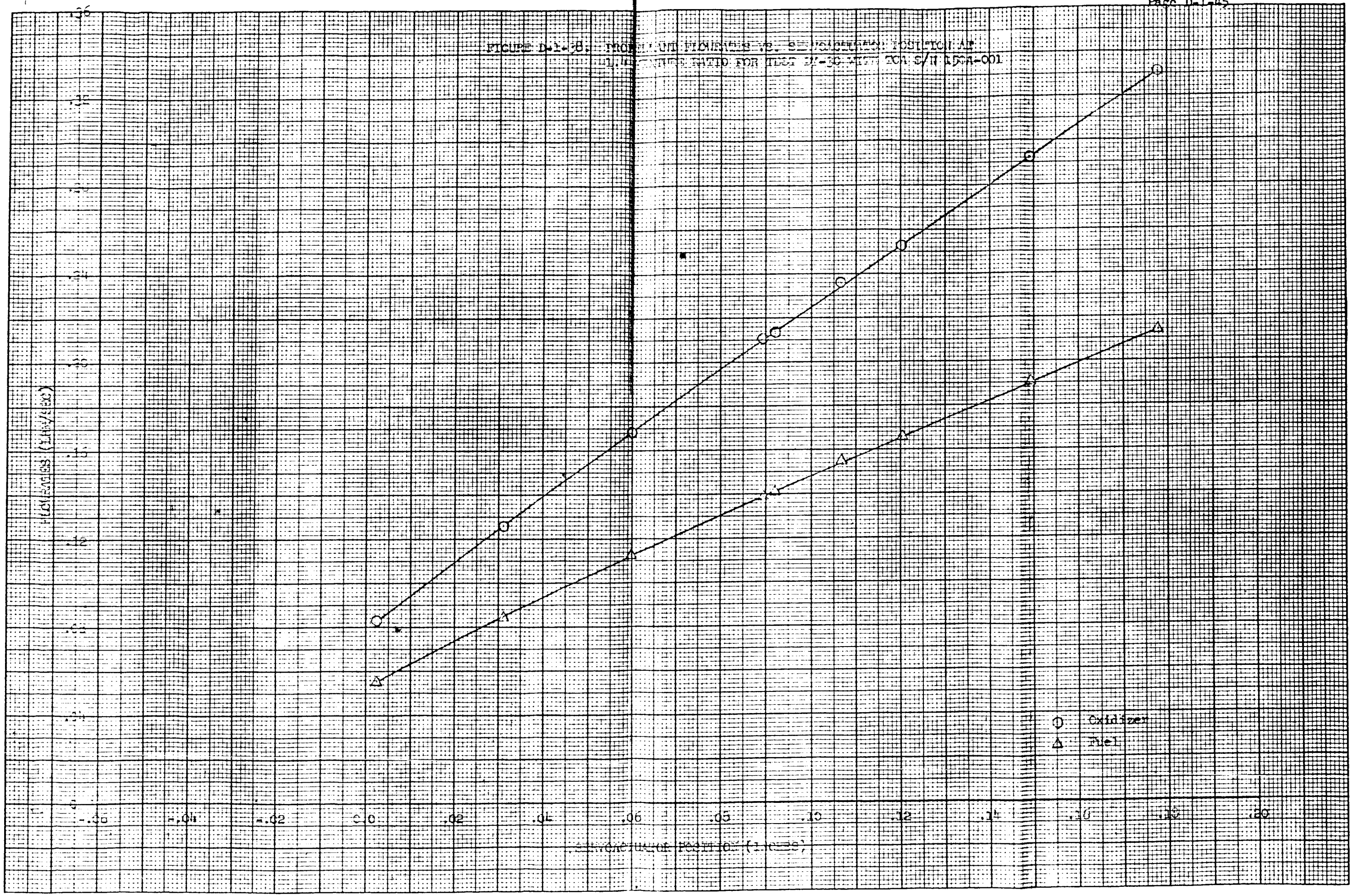

FIGURE D-1-39. VACUUM THRUST VS. SERVOACTUATOR CONTROL SIGNAL DUTY CYCLE RATIO FOR TEST DY-31 WITH TCA S/N 1504-001

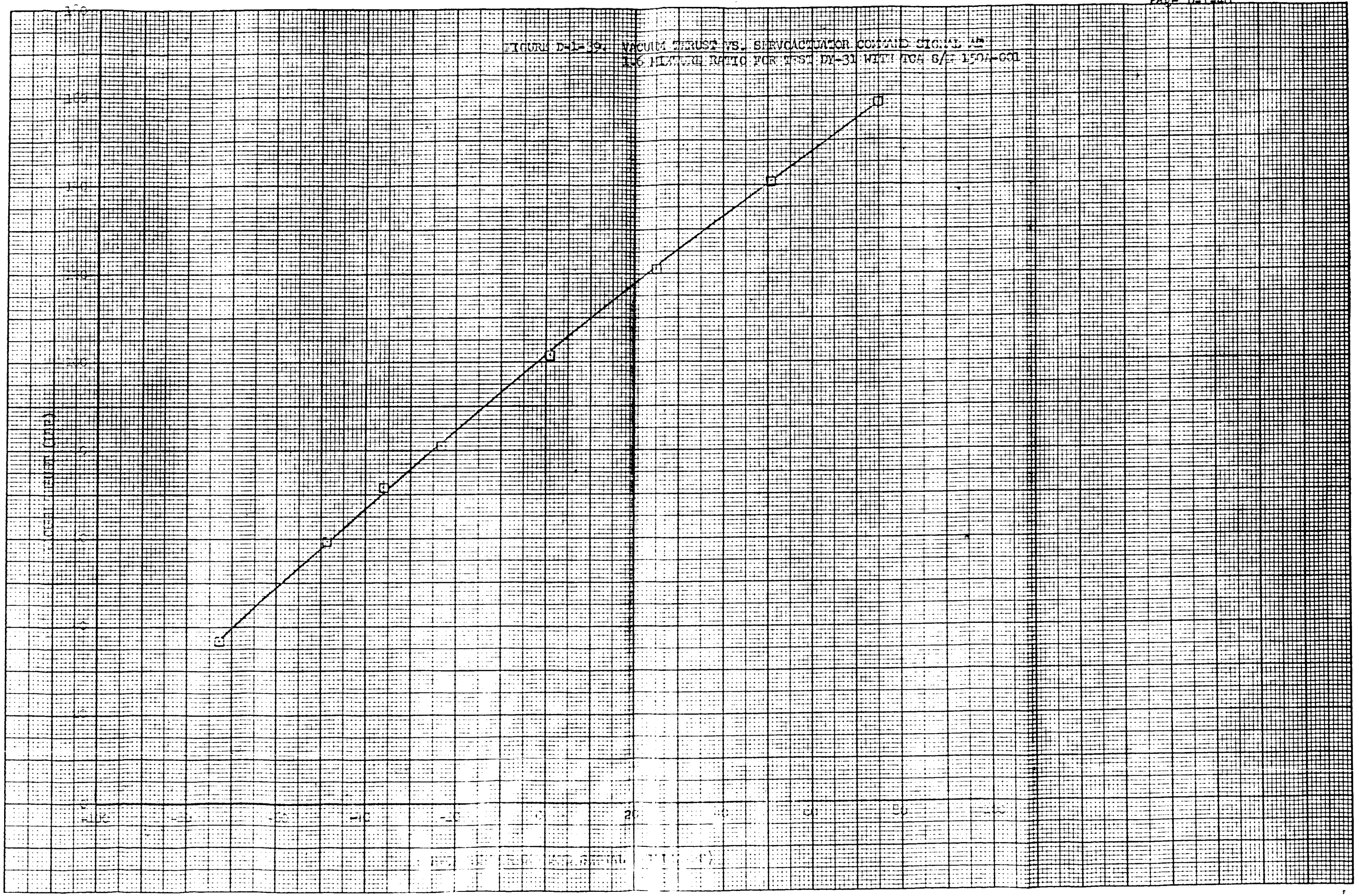

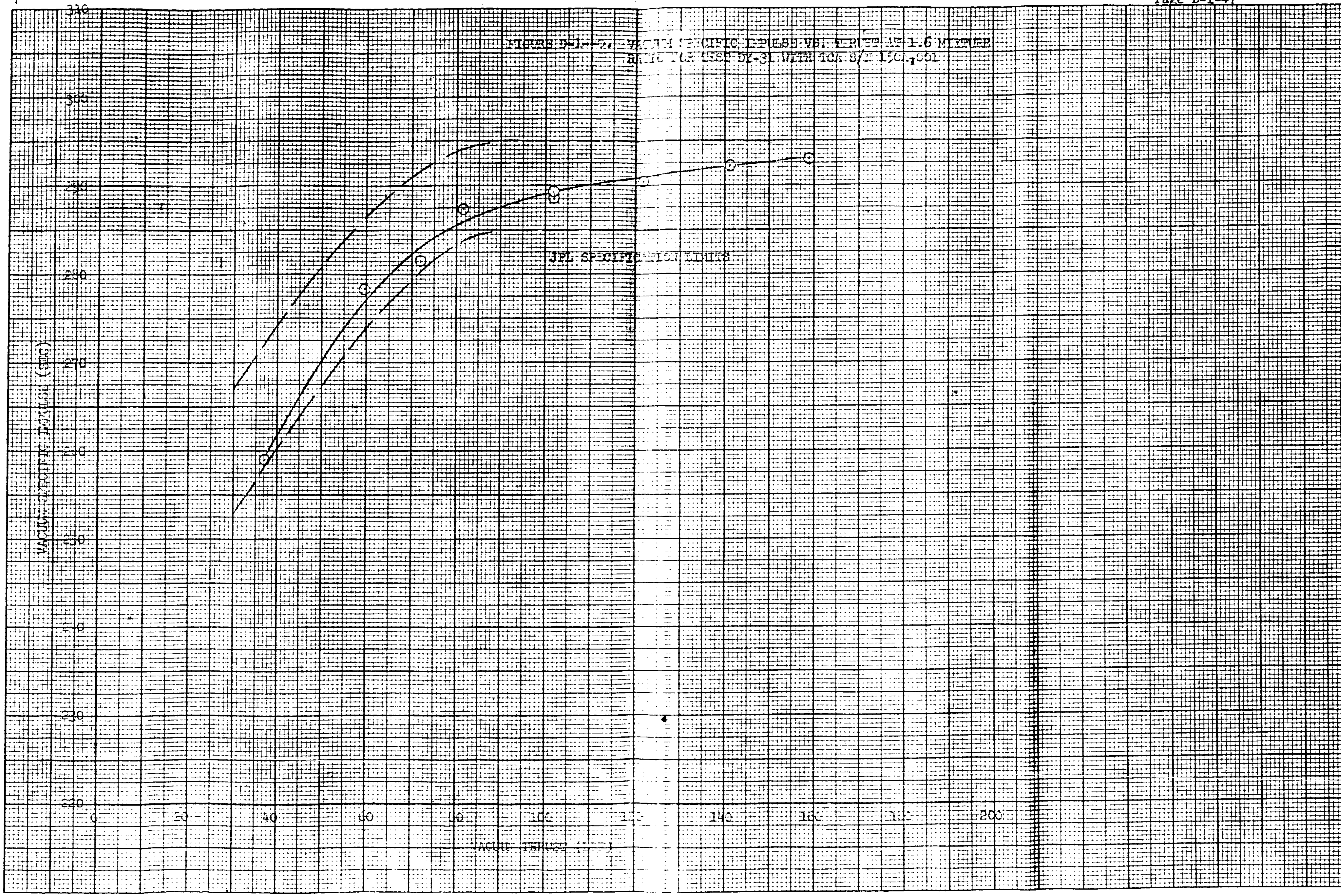
FIGURE D-1-47. VACUUM SPECIFIC IMPULSE VS. THRUST AT 1.6 MIXTURE RATIO FOR TEST DY-31 WITH TCA S/N 150,001
JPL SPECIFICATION LIMITS
VACUUM SPECIFIC IMPULSE (SEC)
VACUUM THRUST
310
300
290
280
270
260
250
240
230
220
0
20
40
60
80
100
140
200

FIGURE D-1-41. CHARACTERISTIC EXHAUST VELOCITY VS. NOZZLE STAGNATION PRESSURE AT 1.6 MIXTURE RATIO FOR TEST DY-31 WITH TCA S/N 150A-001

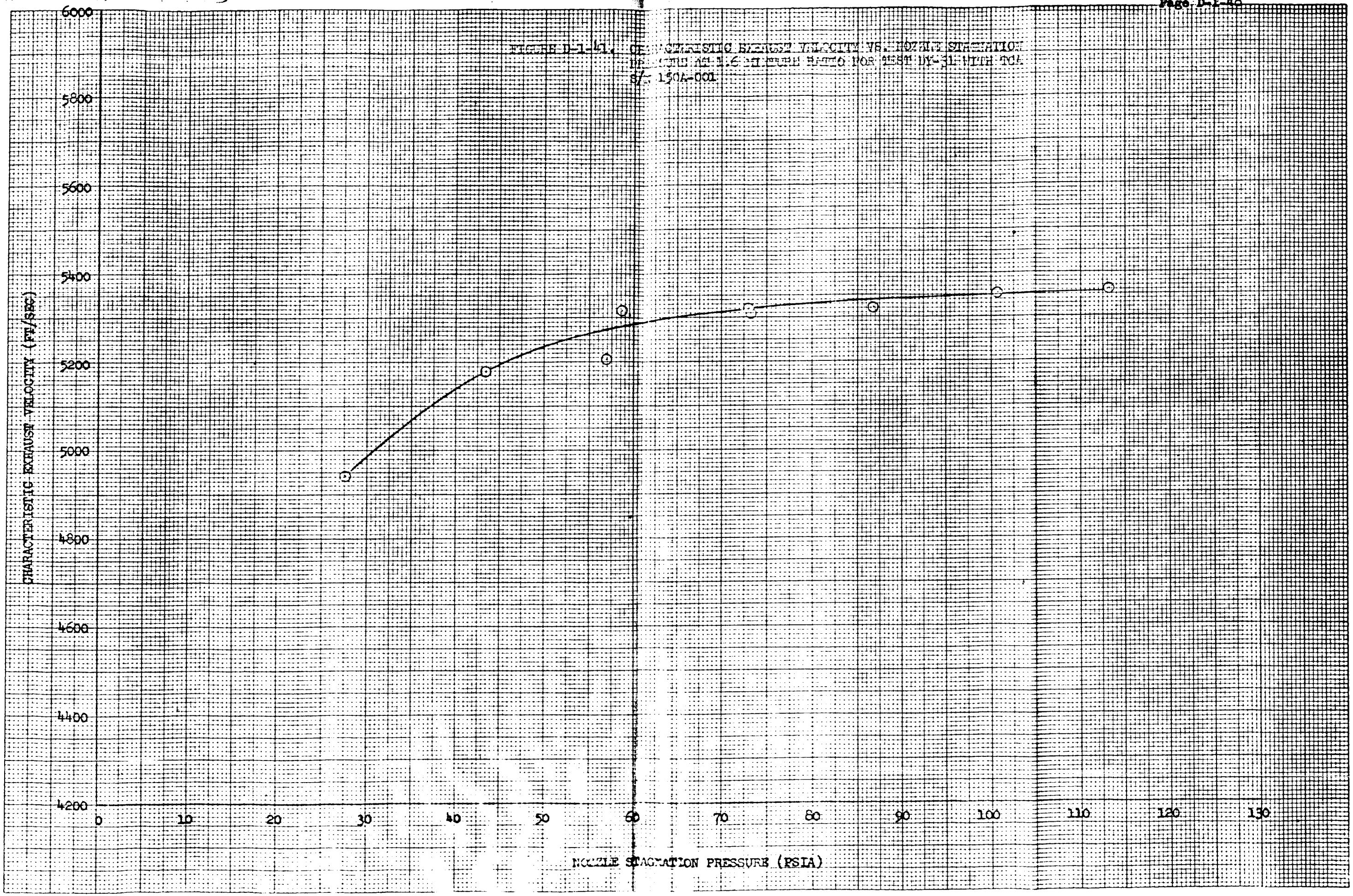

FIGURE D-1-42. [illegible] THRUST COEFFICIENT VS. THRUST AT 1.6 MIXTURE RATIO FOR [illegible] WITH TCA S/N [illegible]-001

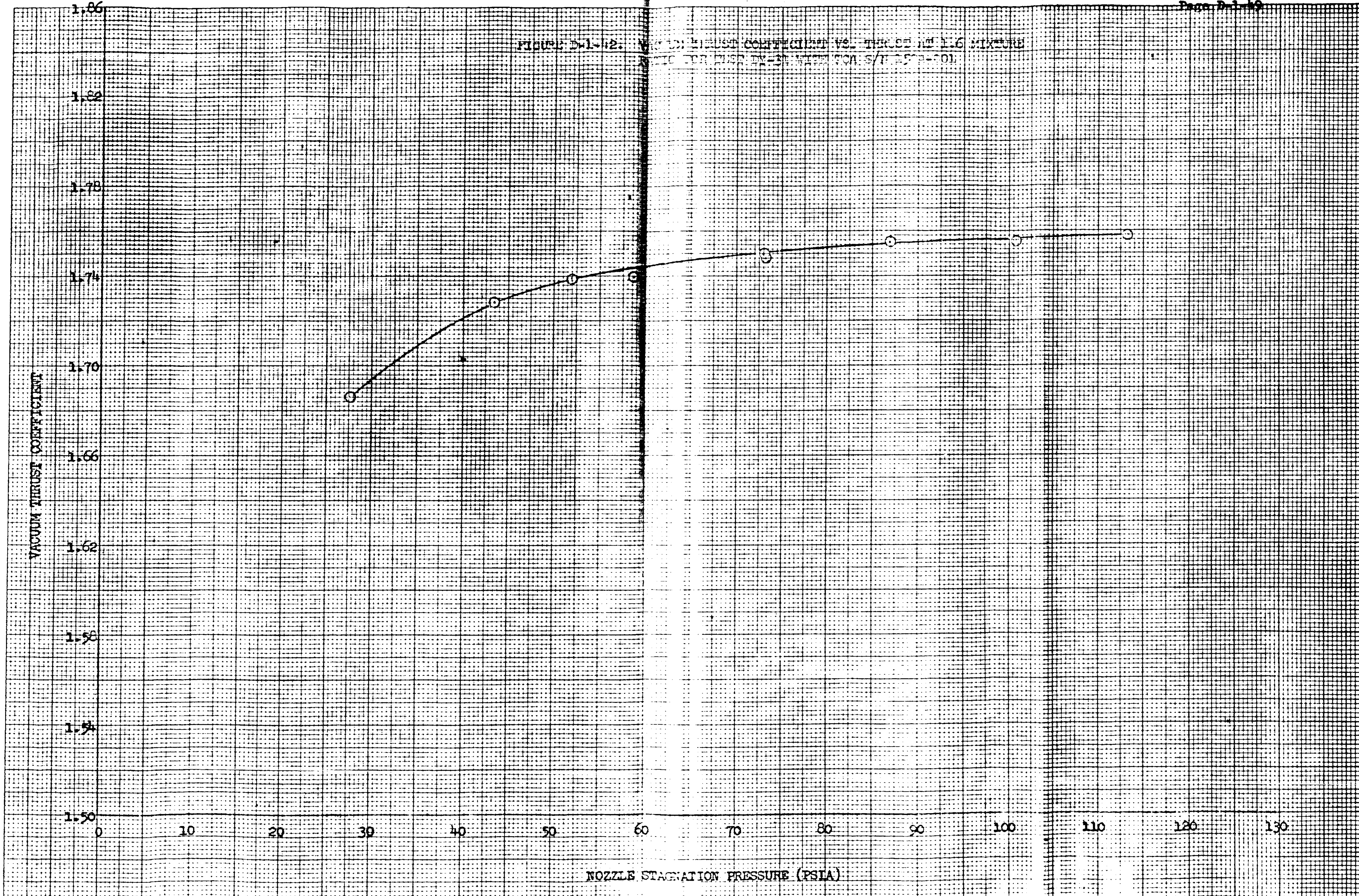

NO. 340DR-10½ DIETZGEN GRAPH PAPER
10 X 10 PER HALF INCH
EUGENE DIETZGEN CO.
MADE IN U. S. A.

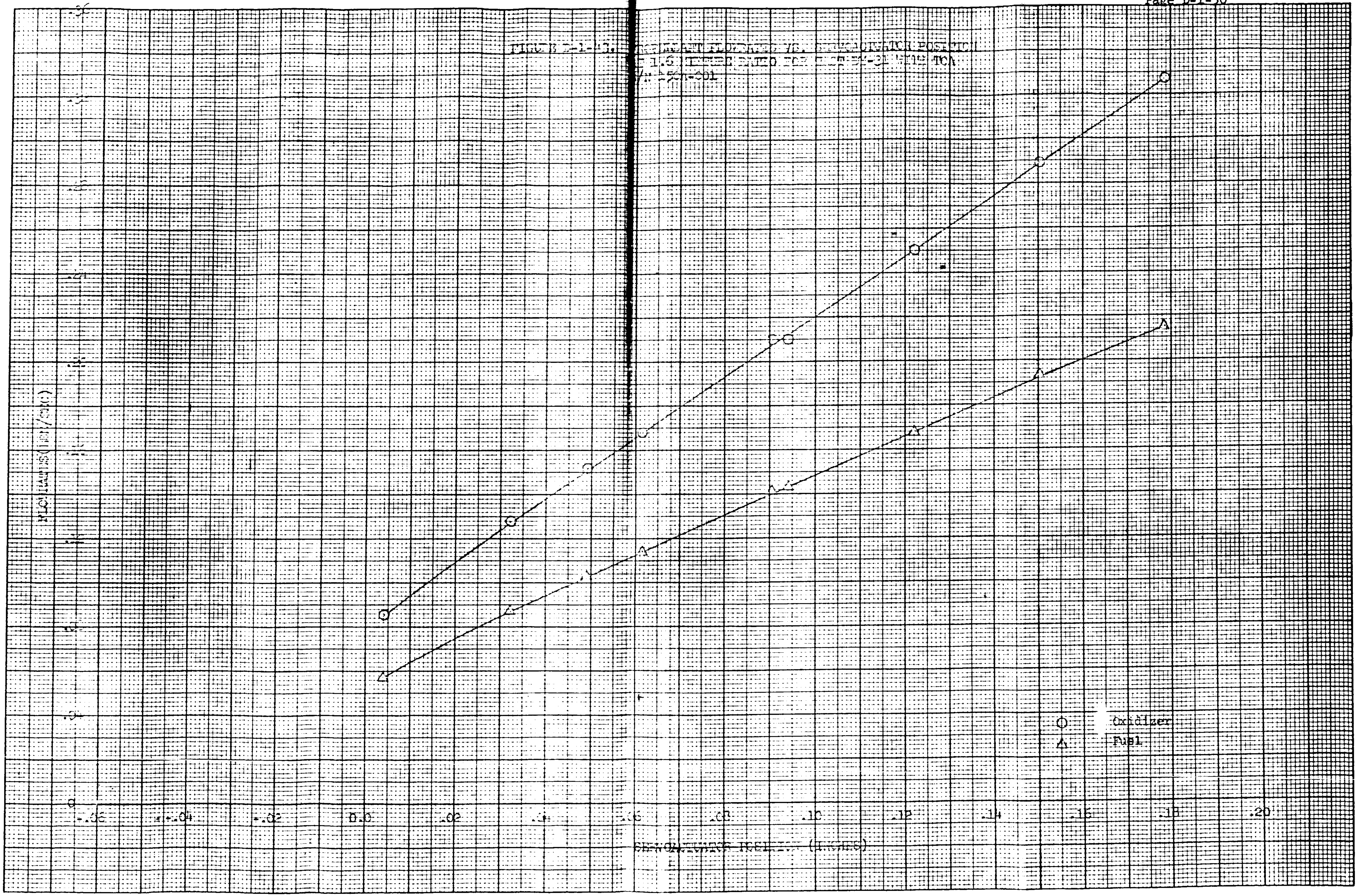
0.0
.02
.10
.12
.14
.16
.18
.20
Oxidizer
Fuel

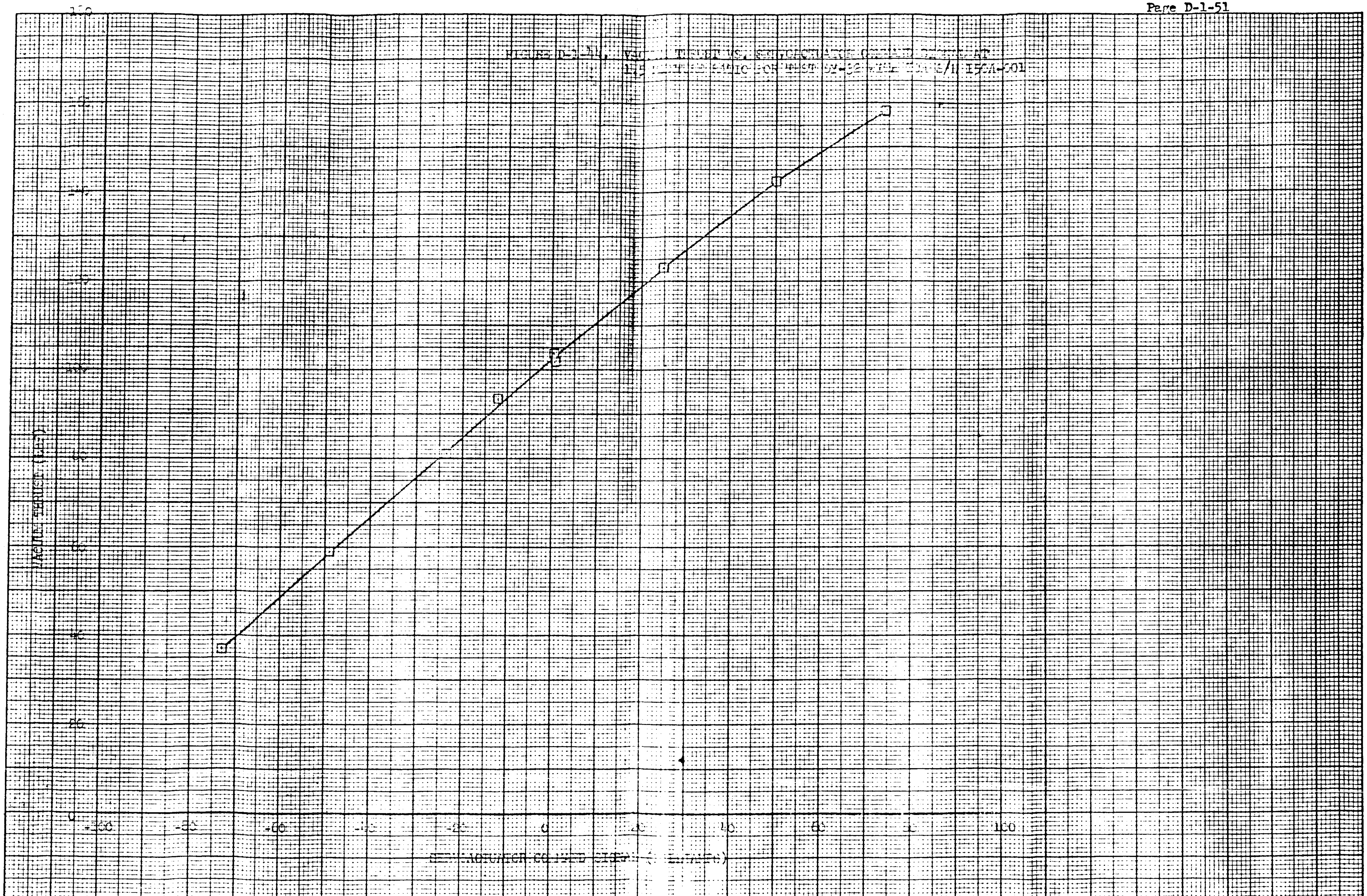
-100
-80
-60
-40
-20
0
20
40
60
80
100

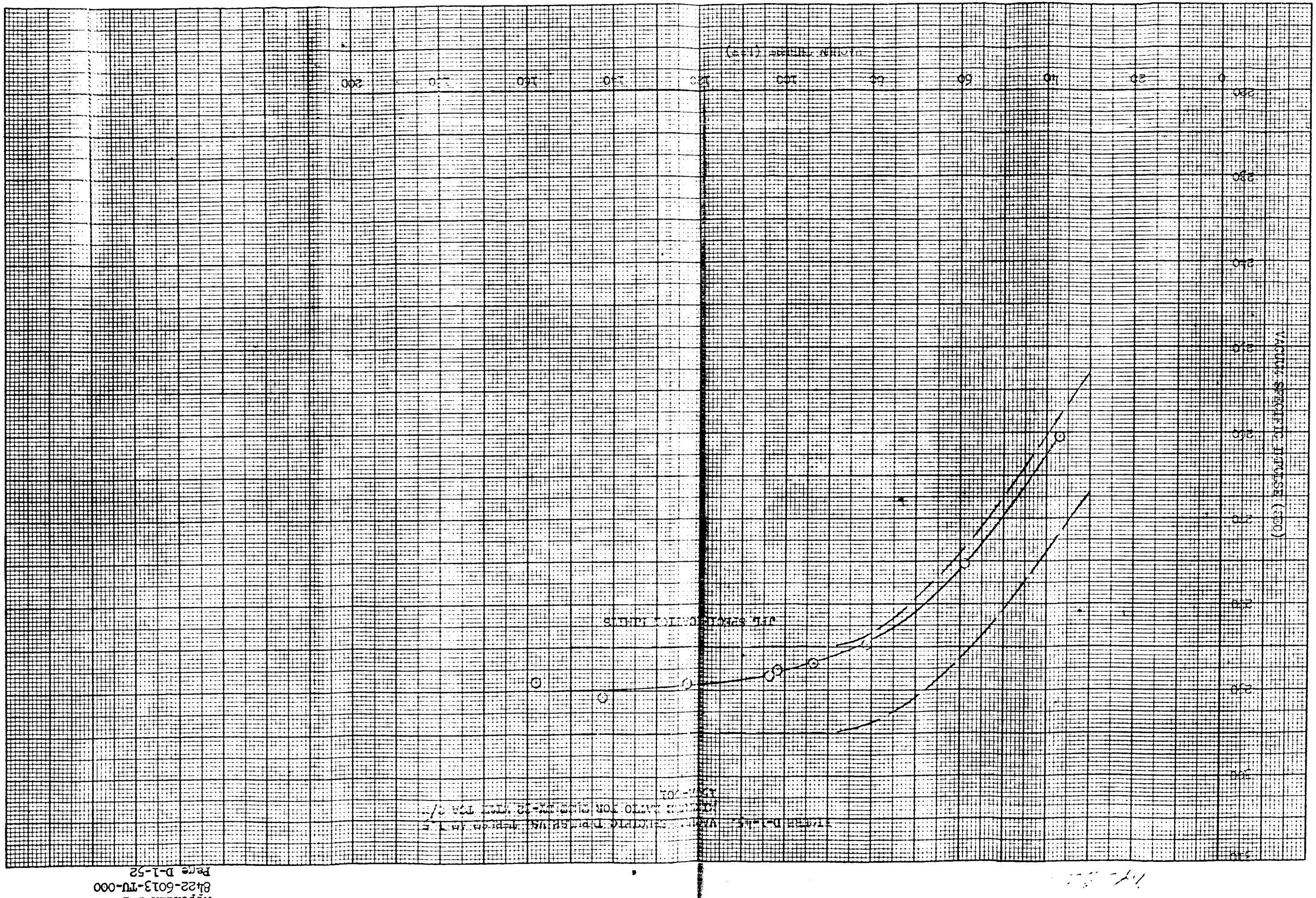
VACUUM SPECIFIC ENTHALPY (BTU/LBM)
JTL SPECIFIC TIC LINES

FIGURE D-1-45. CHARACTERISTIC EXHAUST VELOCITY VS. NOZZLE STAGNATION PRESSURE AT 1.5 MIXTURE RATIO FOR TEST DX-38 WITH TCA BL 1204-001

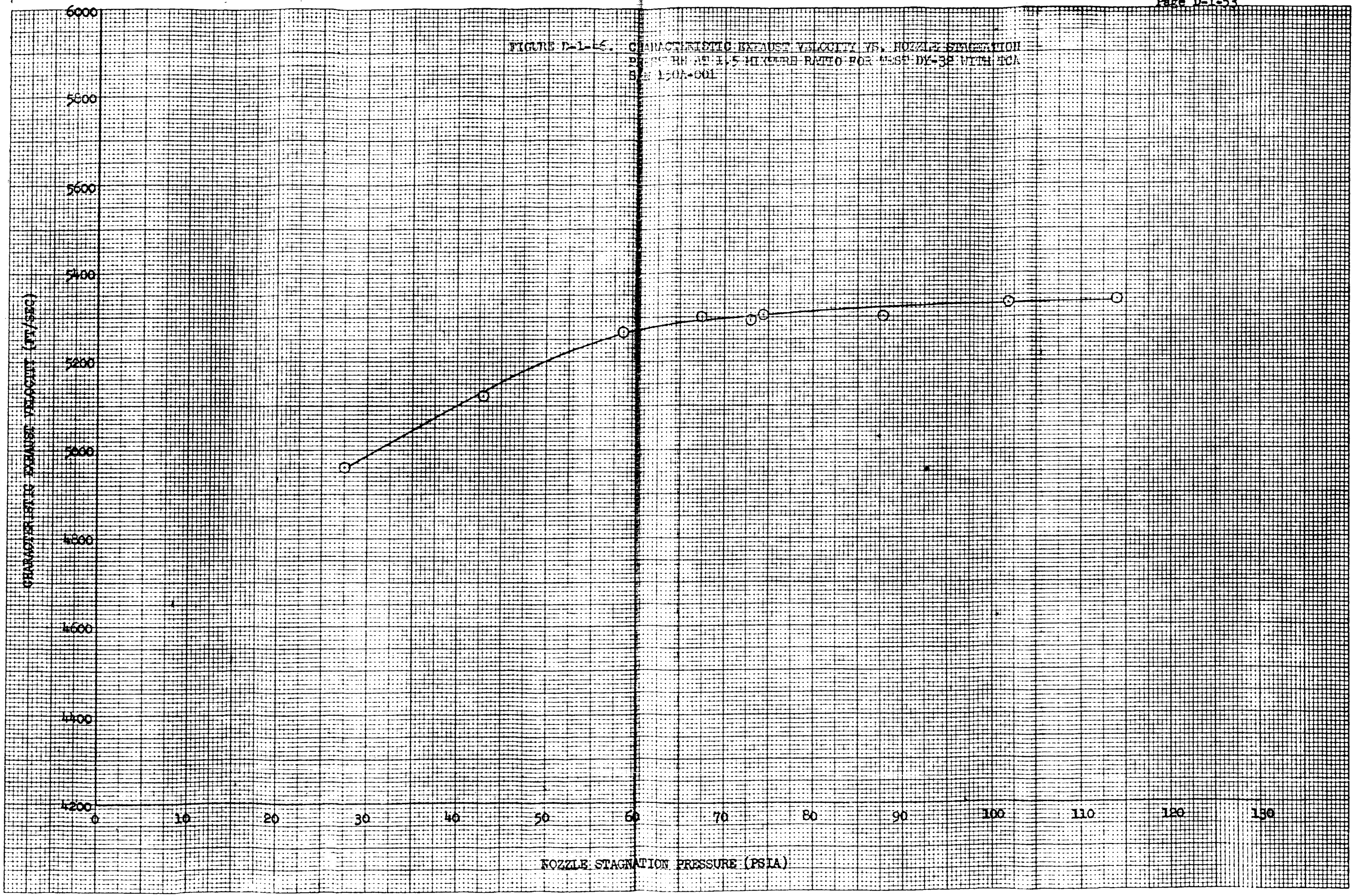

Figure D-1-47. VACUUM THRUST COEFFICIENT VS. NOZZLE STAGNATION PRESSURE AT 1.5 MIXTURE RATIO FOR 15BT HI-3C WITH TCA S/N 1504-001

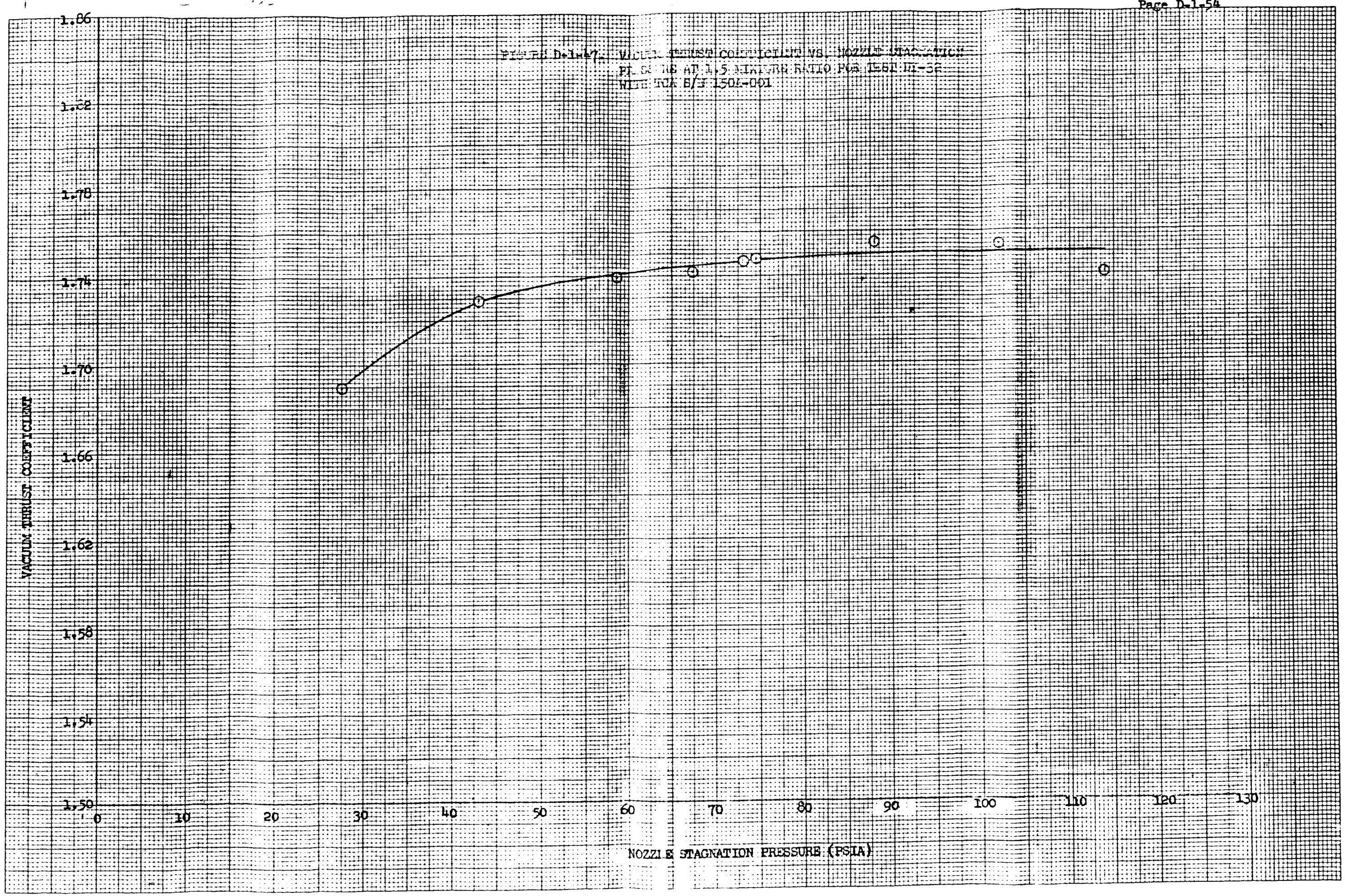

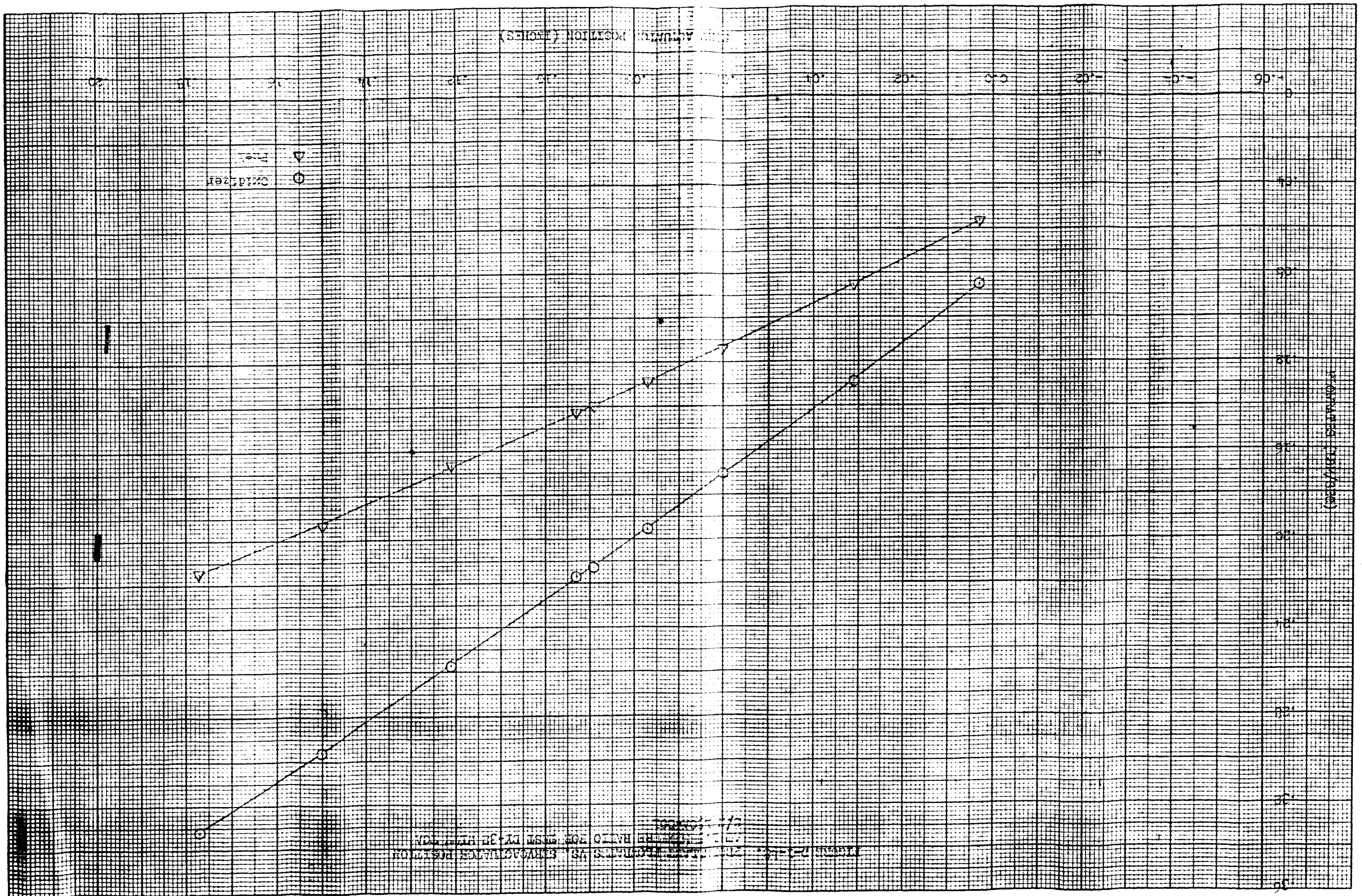
Actuator position (inches)
Oxidizer
Fuel

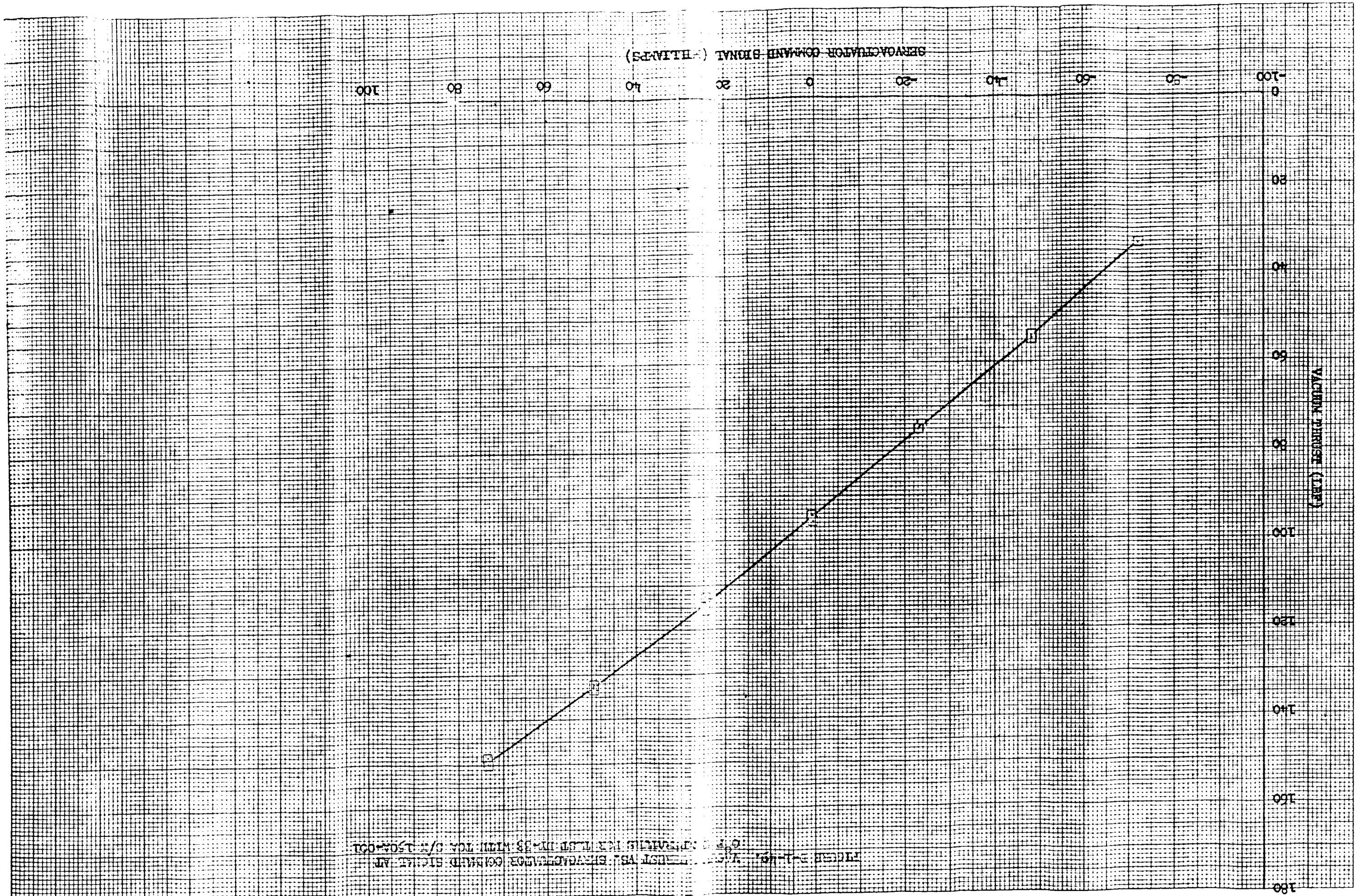

14-32

FIGURE D-1-50. VACUUM SPECIFIC IMPULSE VS. THRUST AT 6°F
AMBIENT TEMPERATURE POST DY-38 WITH TCA S/N 001

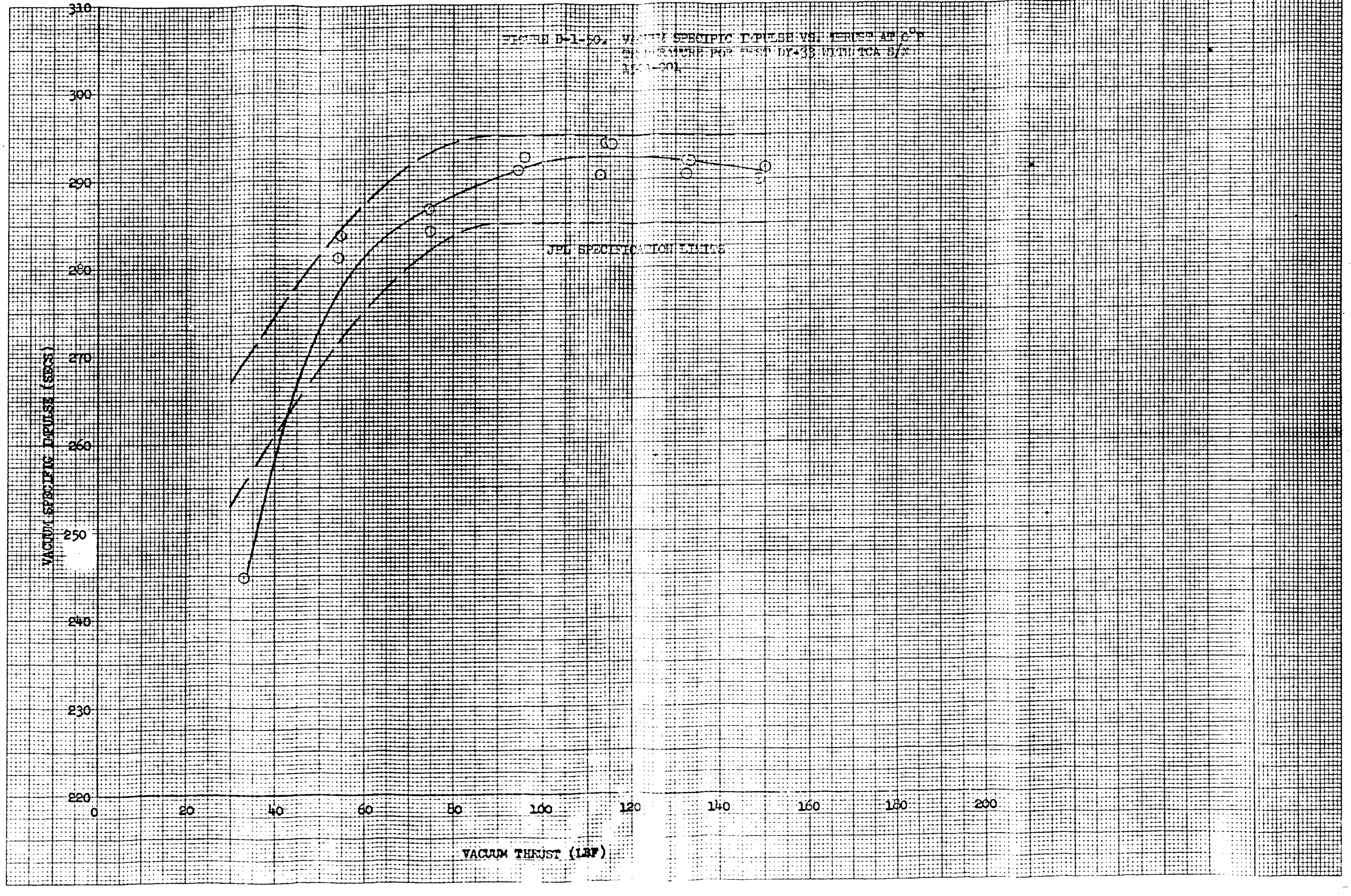

FIGURE D-1-51. CHARACTERISTIC EXHAUST VELOCITY VS. NOZZLE STAGNATION PRESSURE AT 0°F TEMPERATURE FOR TEST HT-33 WITH PCA B/E 1501-001

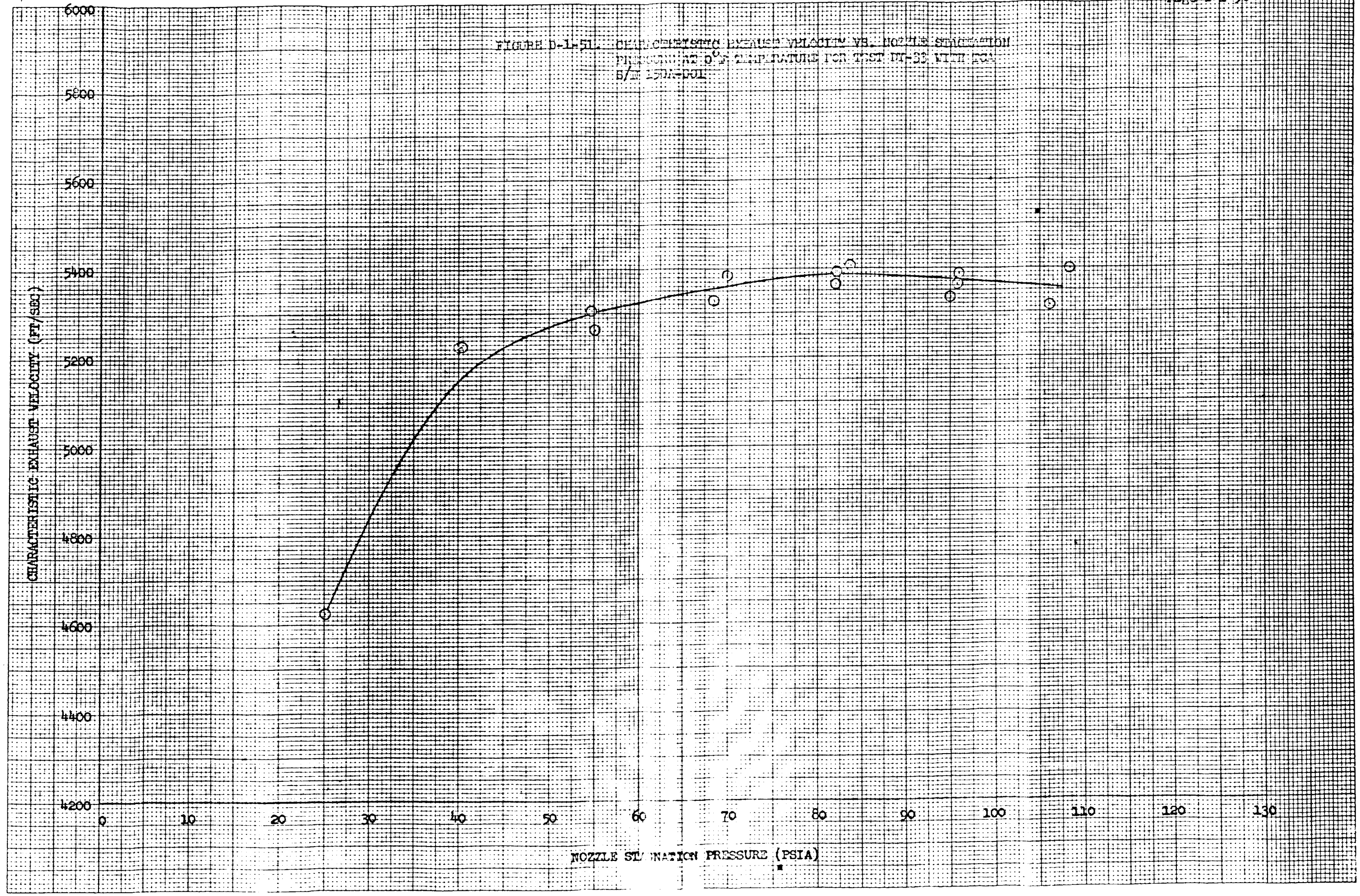

FIGURE D-1-52. VACUUM THRUST COEFFICIENT VS. NOZZLE STAGNATION PRESSURE AT 0° TEMPERATURE FOR TEST DX-33 WITH TCA S/N 1504-001

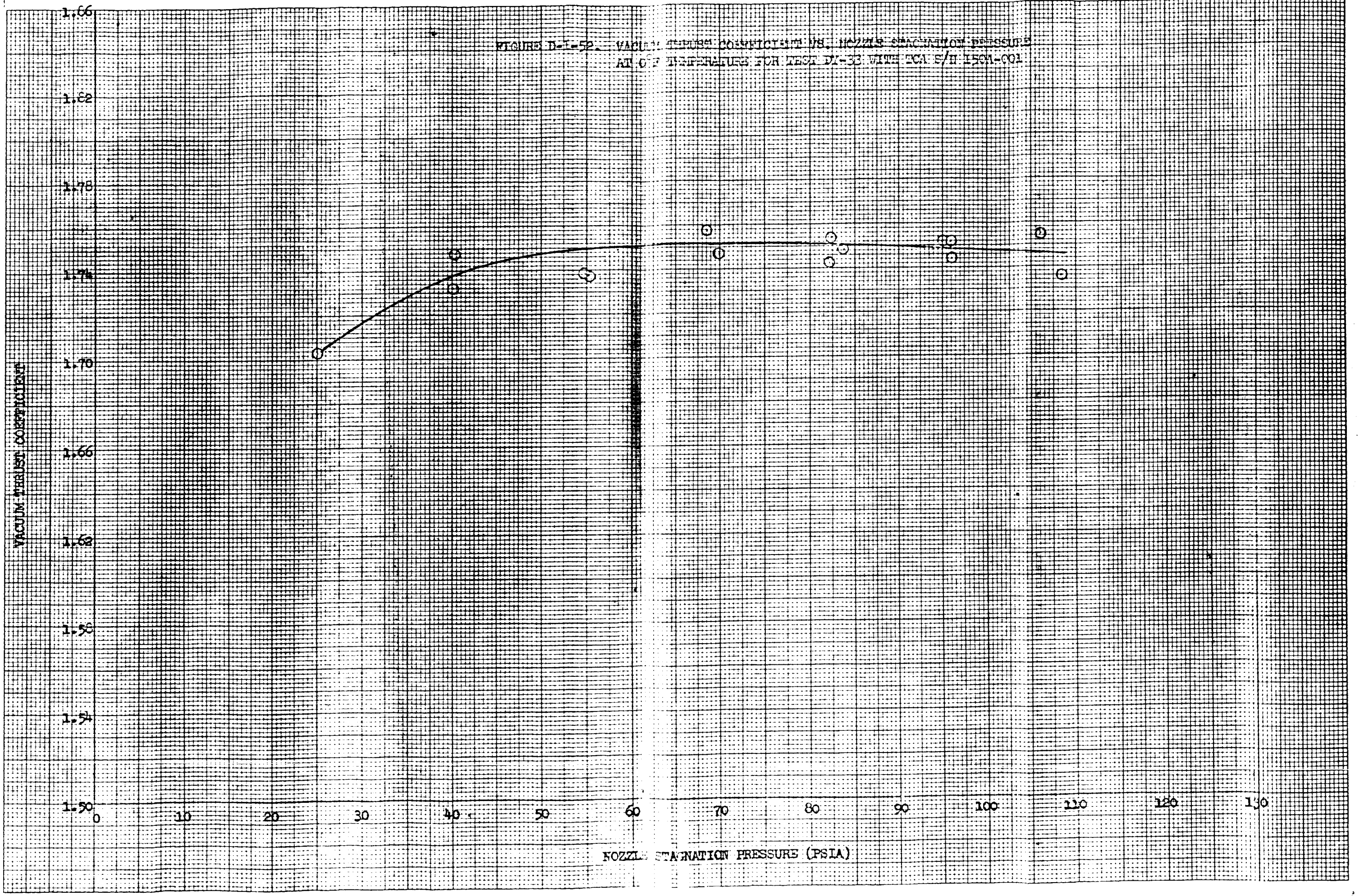

FIGURE D-1-53. PROPELLANT FLOWRATES VS. SERVOACTUATOR POSITION AT 0°F. AMBIENT TEMPERATURE FOR TEST DV-32 WITH SAC S/N 1204-001

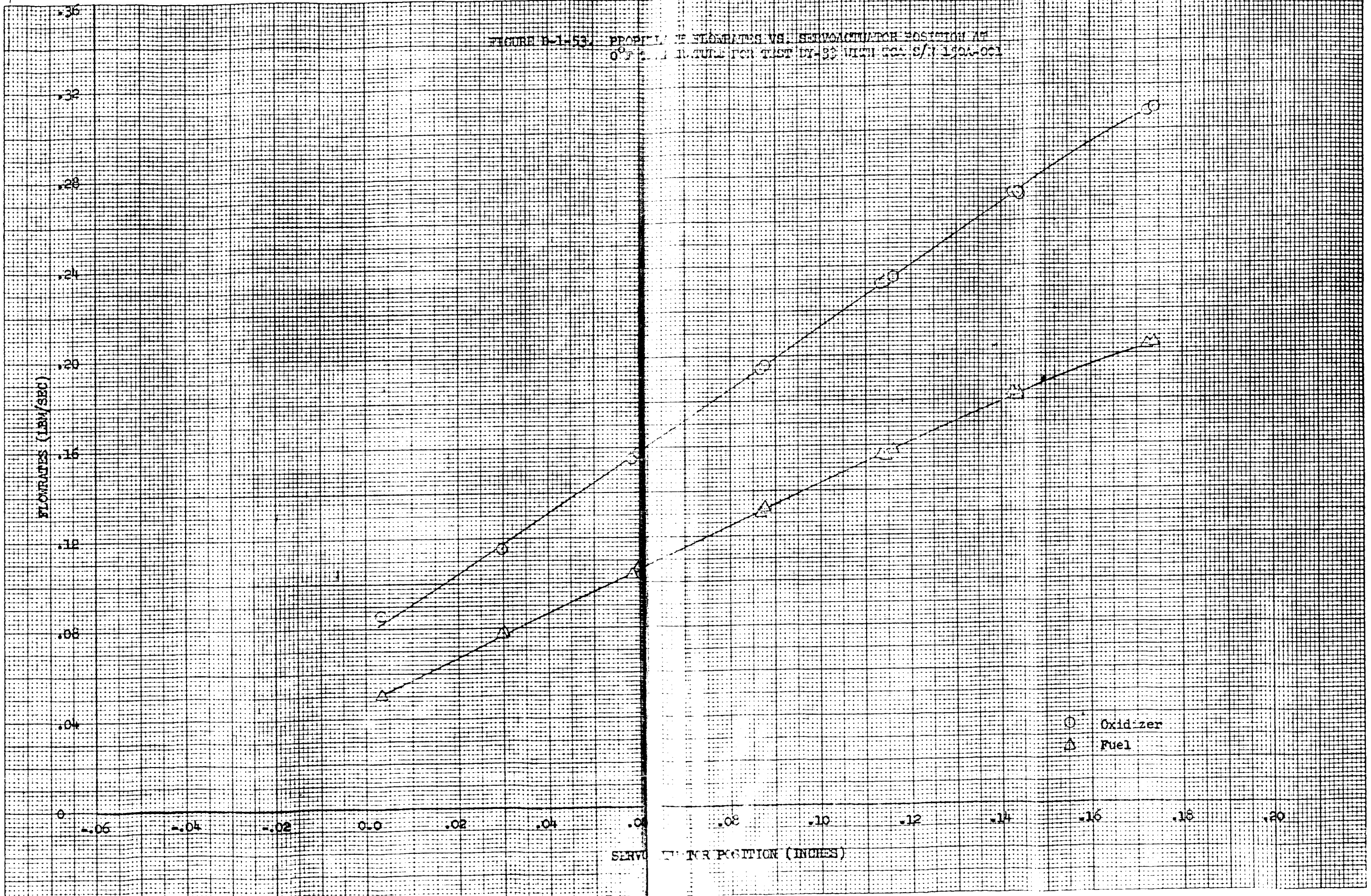

FIGURE D-1-54. VACUUM THRUST [redacted] VS. SERVOACTUATOR COMMAND SIGNAL AT 3.5 PERCENT RATIO FOR CASES DY-41 thru DY-43 HPH PQA S/N 1504-004

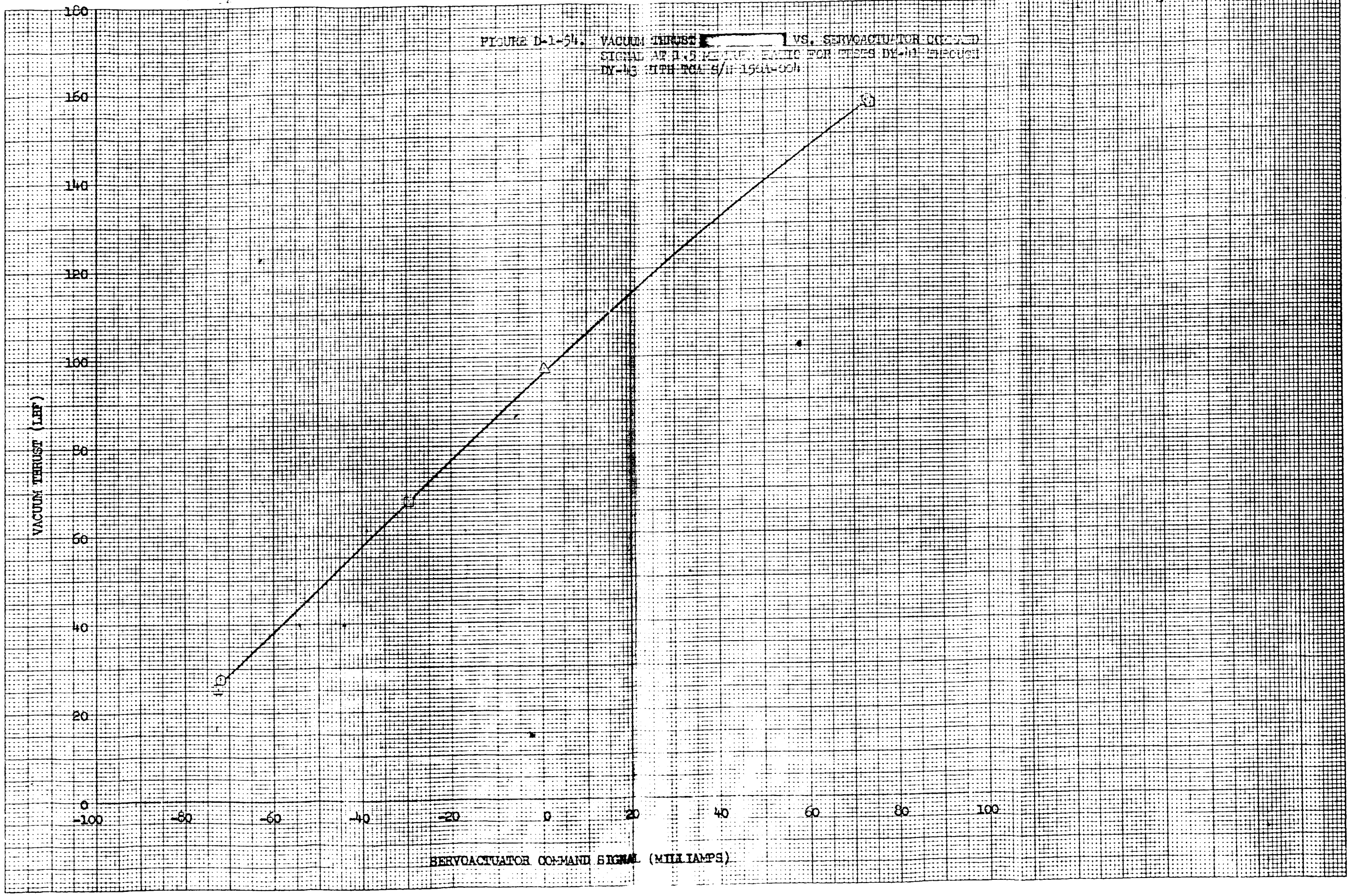

FIGURE D-1-55. VACUUM SPECIFIC IMPULSE VS. THRUST AT 1.6 MIXTURE RATIO FOR TESTS DY-41 THROUGH DY-43 WITH TCA S/N 1504-007

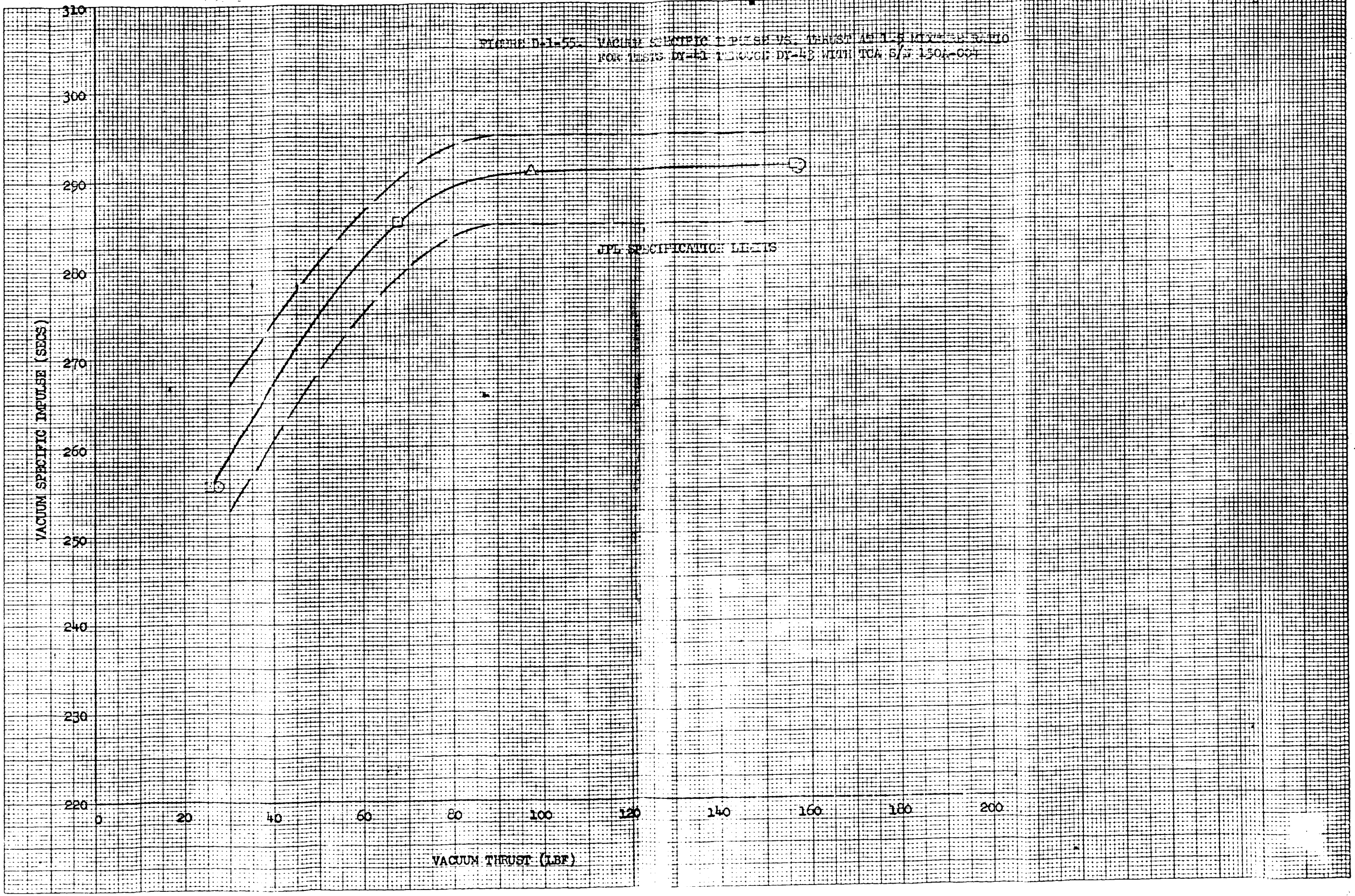

(Pages D-1-63 thru D-1-65
left intentionally blank)

FIGURE D-1-56. CHARACTERISTIC EXHAUST VELOCITY VS. NOZZLE STAGNATION PRESSURE AT 1.5 NOZZLE RATIO FOR TESTS DY-41 THROUGH DY-43 [illegible] ECA S/N 1 [illegible]

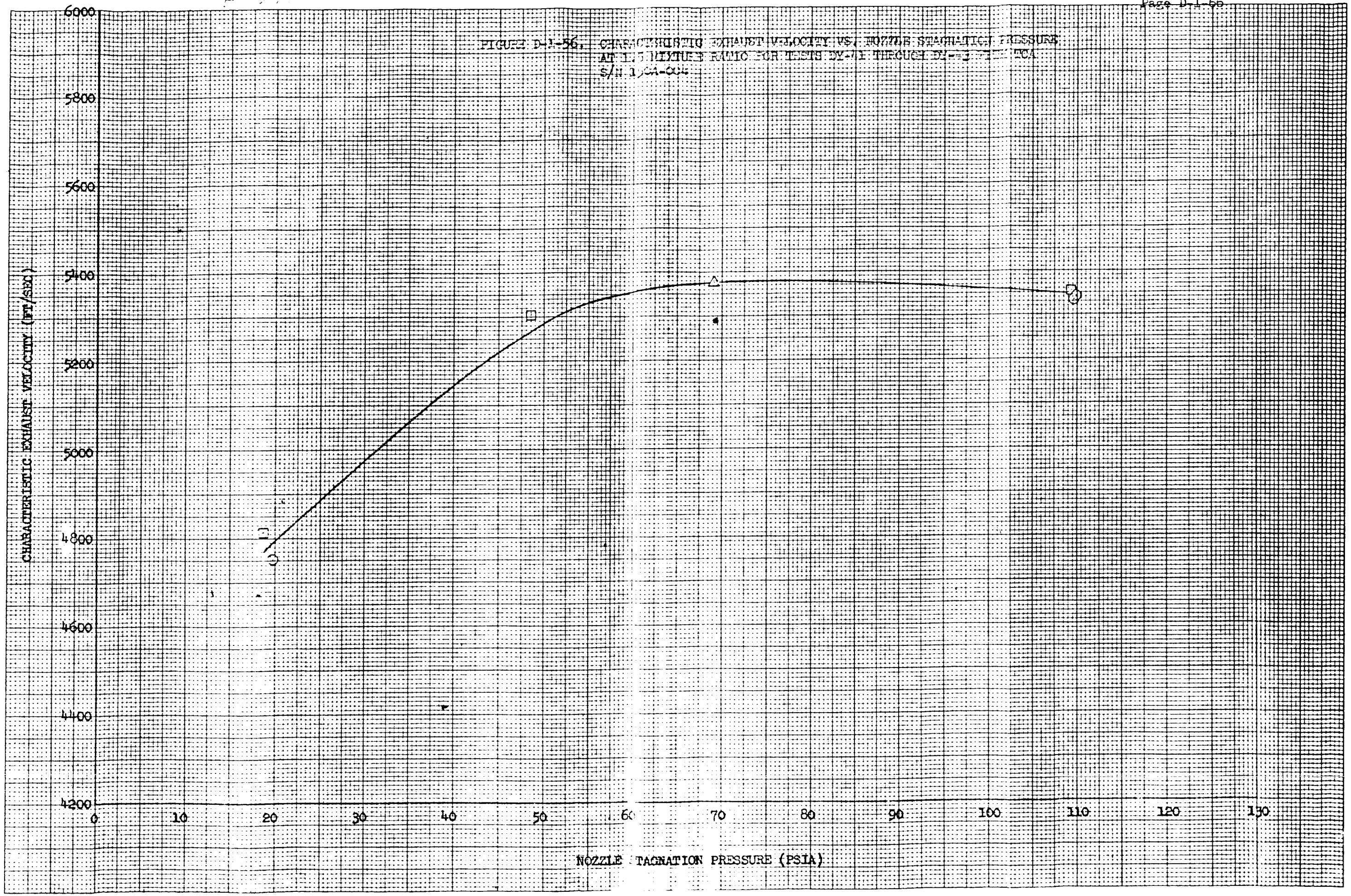

FIGURE D-1-57. VACUUM THRUST COEFFICIENT VS. NOZZLE STAGNATION PRESSURE AT 1.5 ... AREA RATIO FOR ... SLB DY-41 THROUGH DY-45, TCA S/N: 1501-004

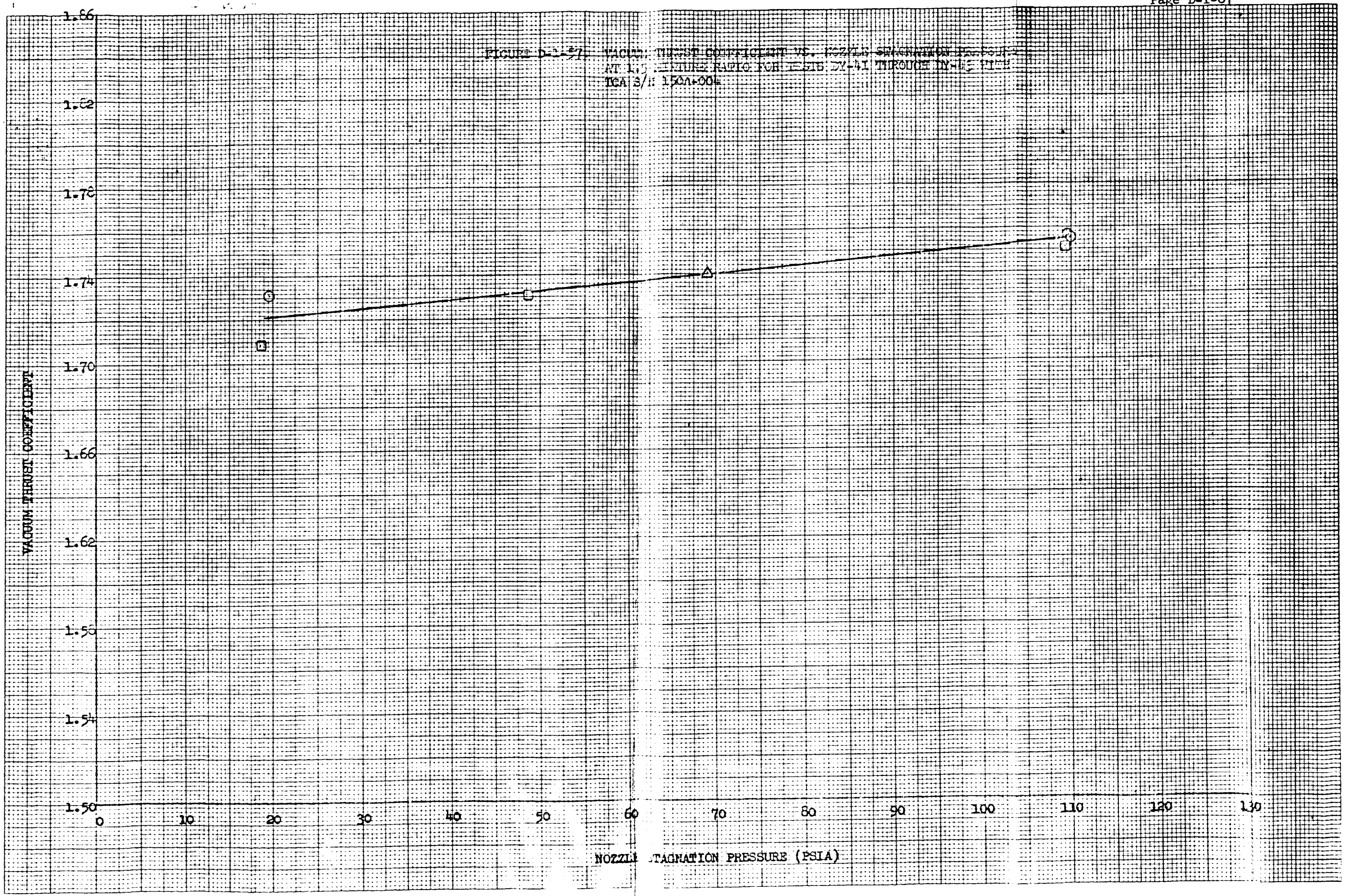

FIGURE D-1-58. PROPELLANT [illegible] VS. SERVOACTUATOR POSITION
AT 1.5 [illegible] RATIO FOR TESTS [illegible] THROUGH [illegible]
WITH [illegible] S/N [illegible]-C04

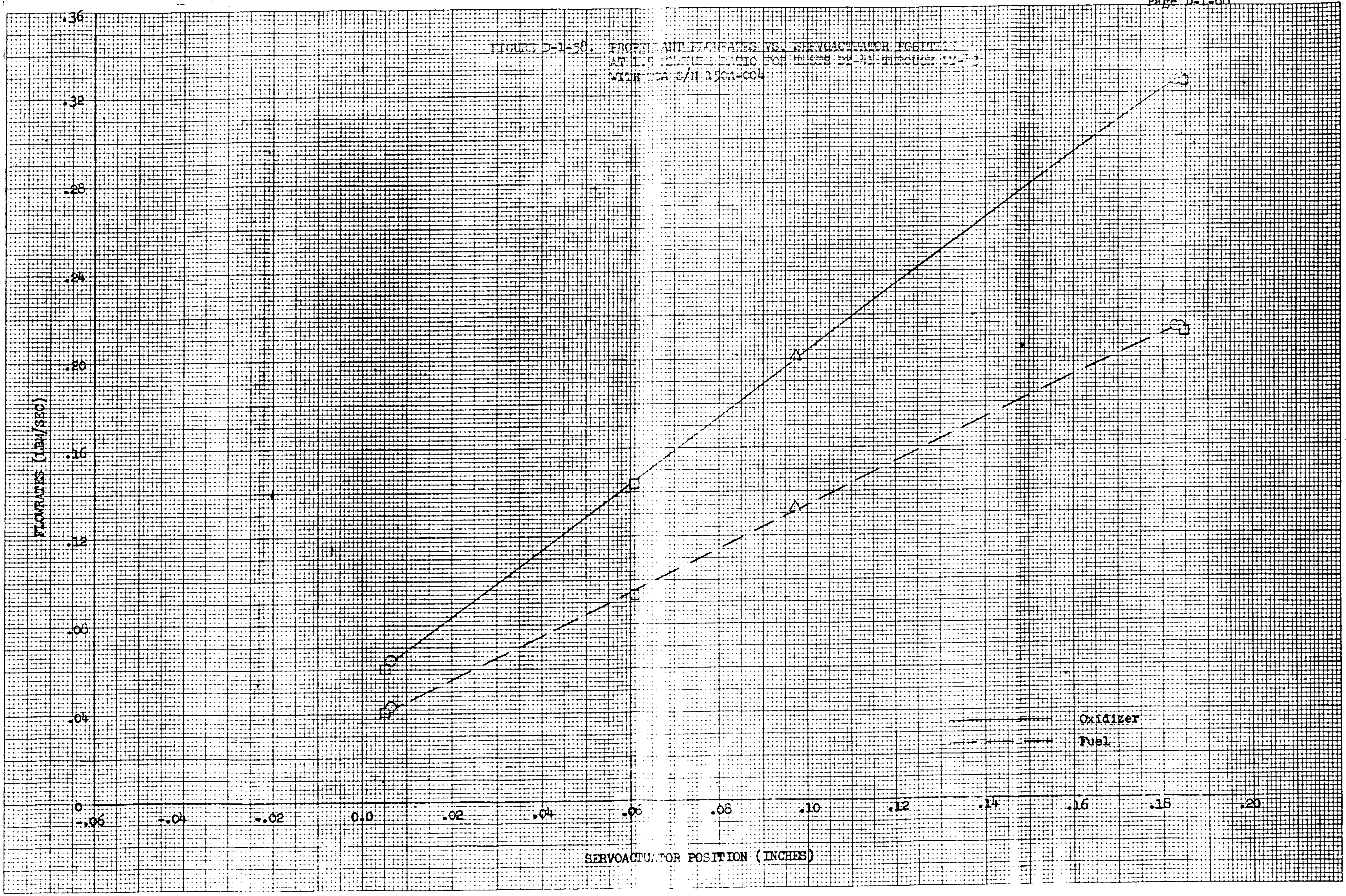

FIGURE D-1-59. MIXTURE RATIO VS. VACUUM THRUST AT STANDARD CONDITIONS FOR TESTS DY-41 THROUGH DY-46 WITH TCA S/N 150A-004

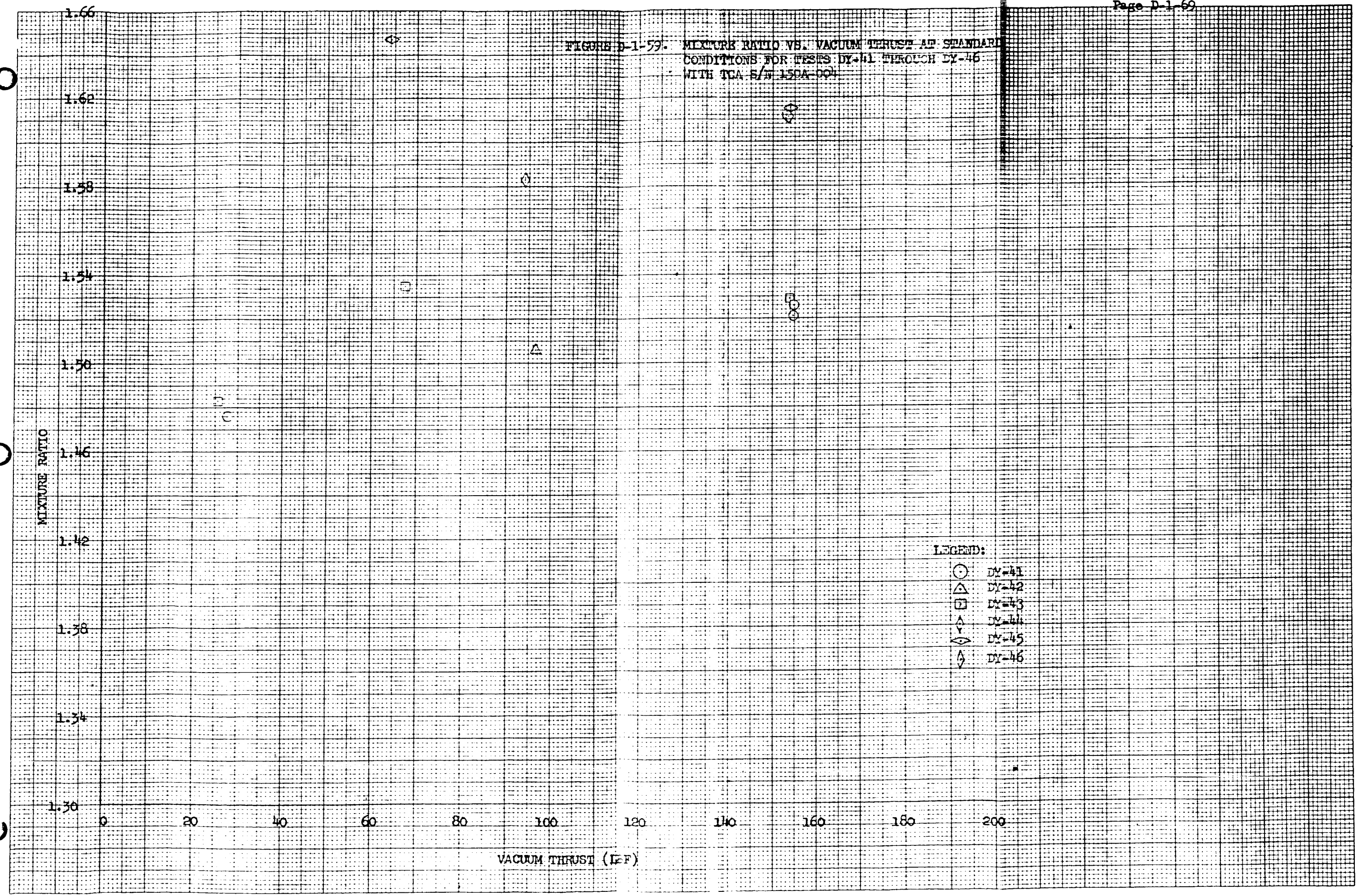

FIGURE D-1-60. VACUUM THRUST VS. SERVOACTUATOR COMMAND SIGNAL AT 0°F ELEVATION FOR TESTS EV-01 THROUGH EV-16 WITH RCA S/N 1501-005

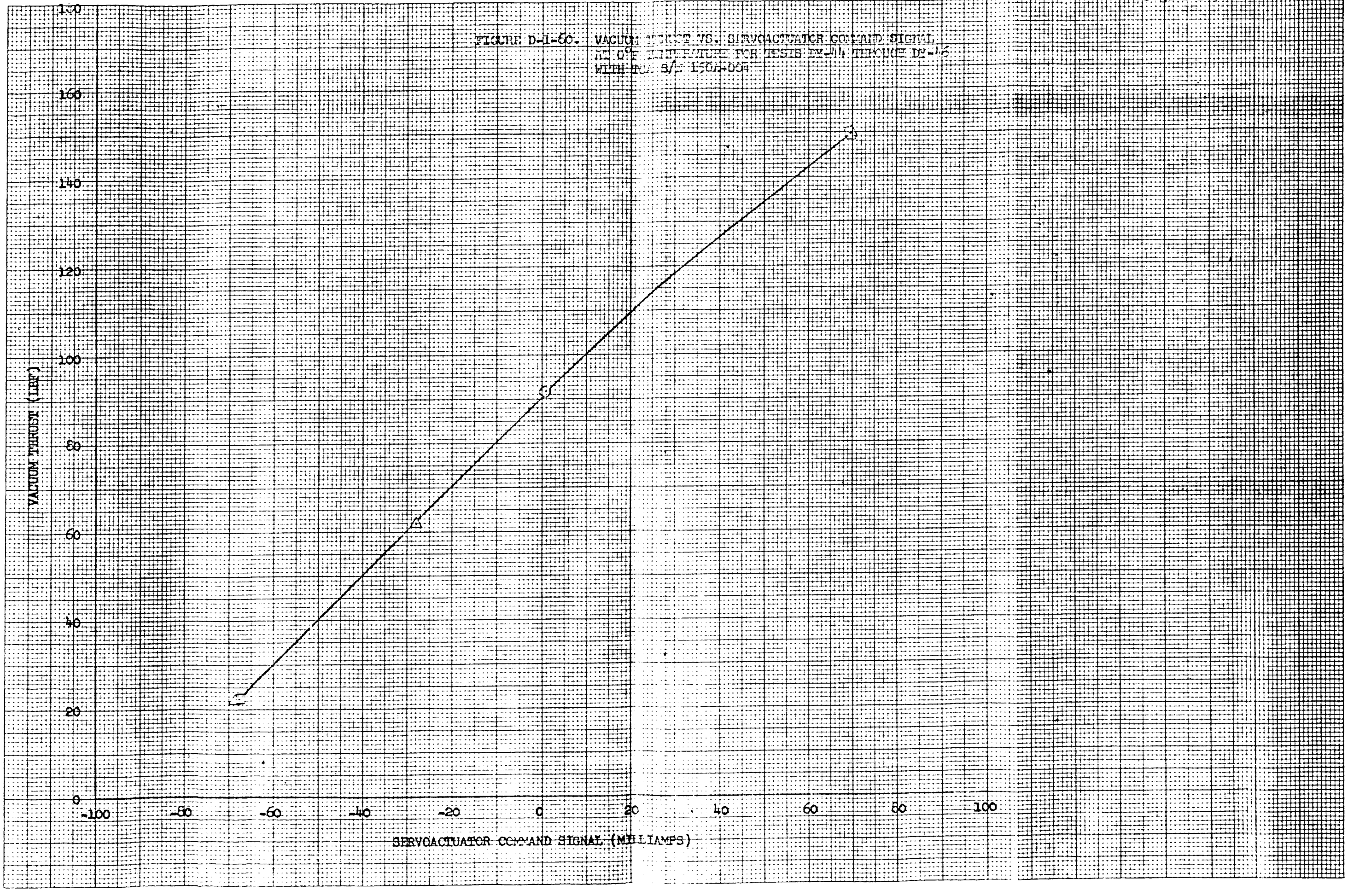

FIGURE D-1-21. VACUUM SPECIFIC IMPULSE VS. THRUST AT 60°F PROPELLANT TEMPERATURE
(2) 5 LBF THRUSTER DT-6 WITH TCA S/N 150A-004

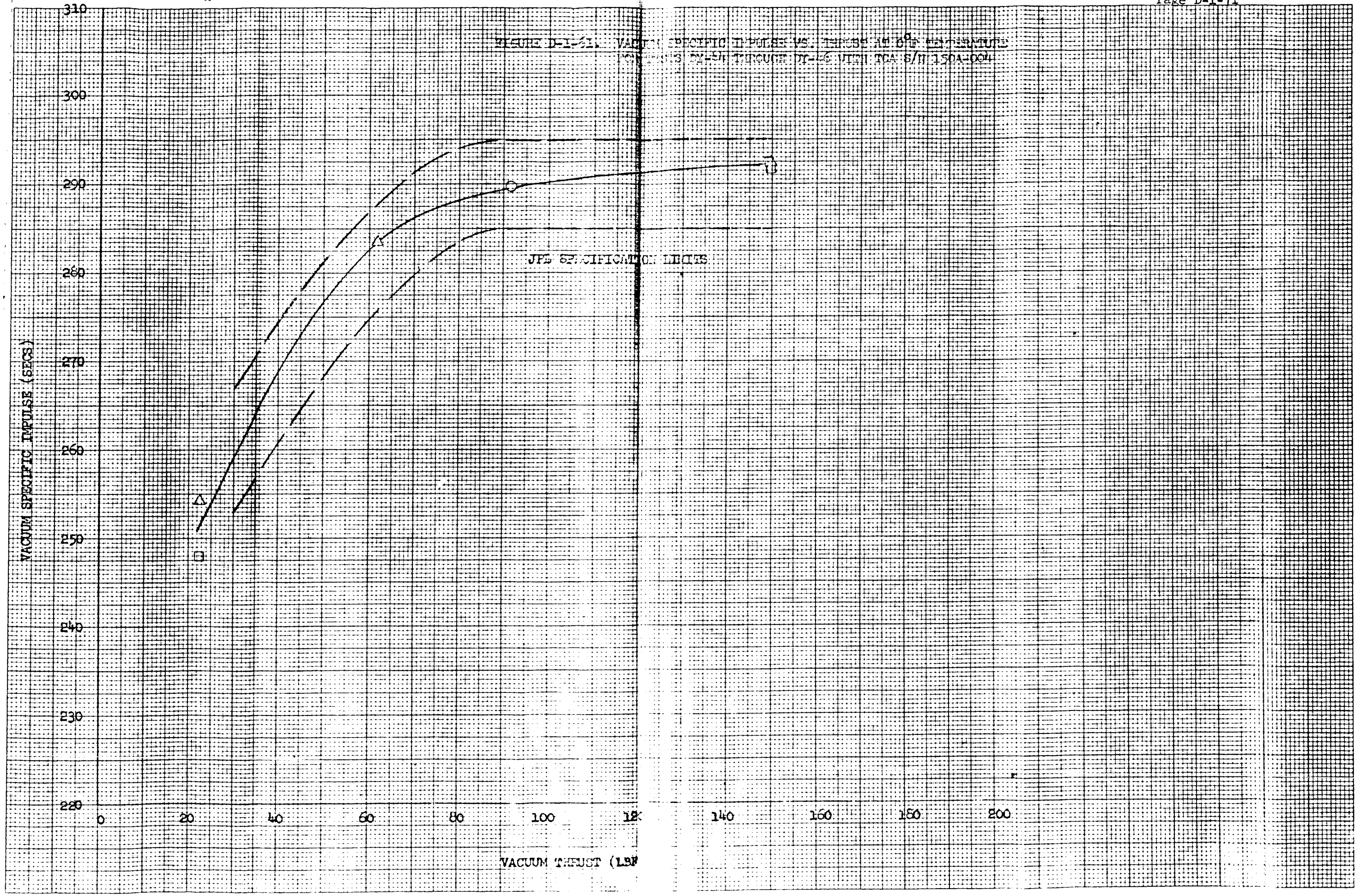

FIGURE D-1-68. CHARACTERISTIC EXHAUST VELOCITY VS. NOZZLE STAGNATION PRESSURE FOR USE ON THE PLATFORM FOR USES D1-1-4 THROUGH D1-1-6 WITH SCALE S/N 1504-004

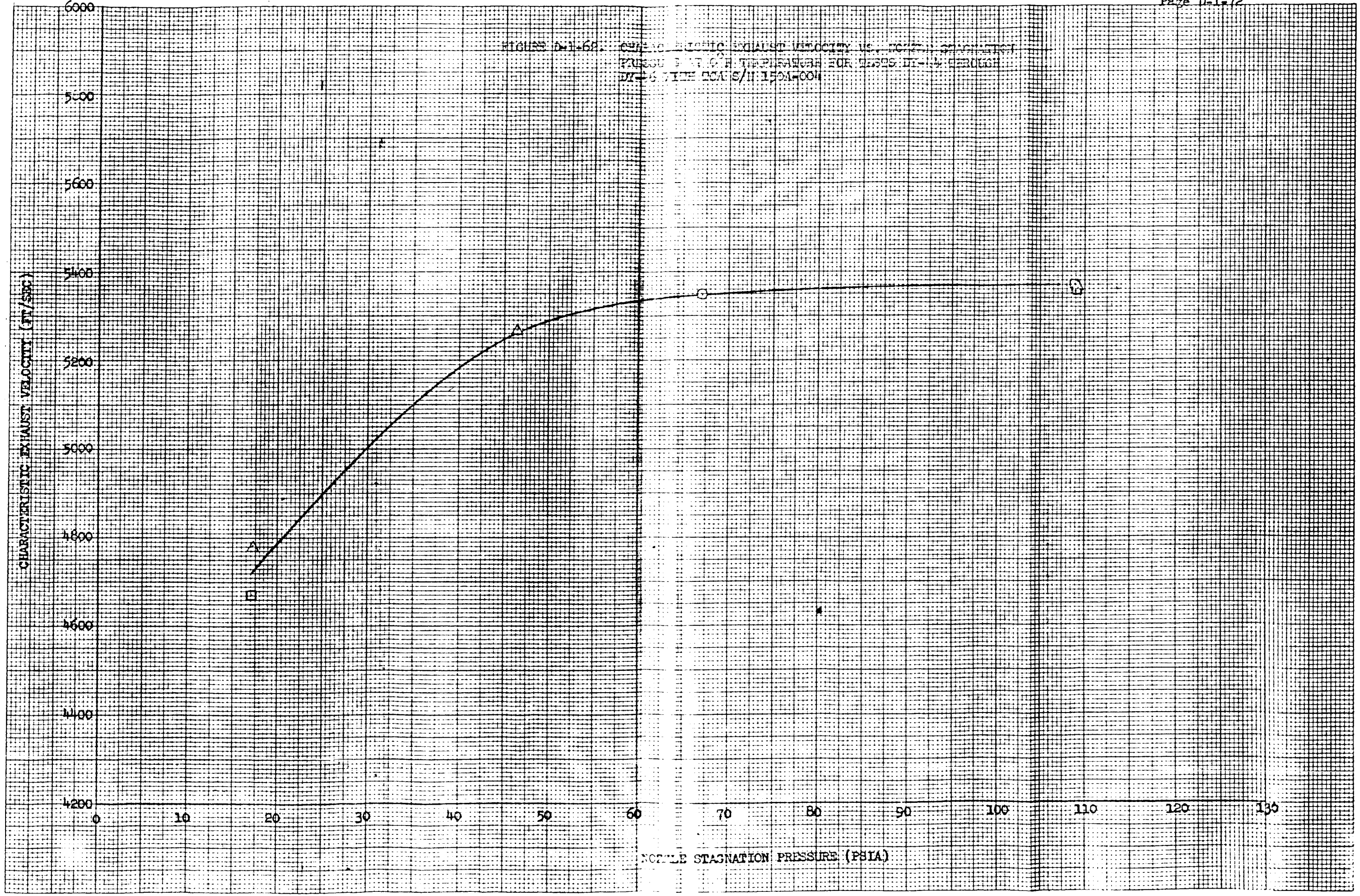

FIGURE D-1-63. VACUUM THRUST COEFFICIENT VS. NOZZLE STAGNATION PRESSURE AT 0°F TEMPERATURE FOR ENGINE DY-14 WITH NOZZLE DY-45 WITH TCA S/N 1SCA-004

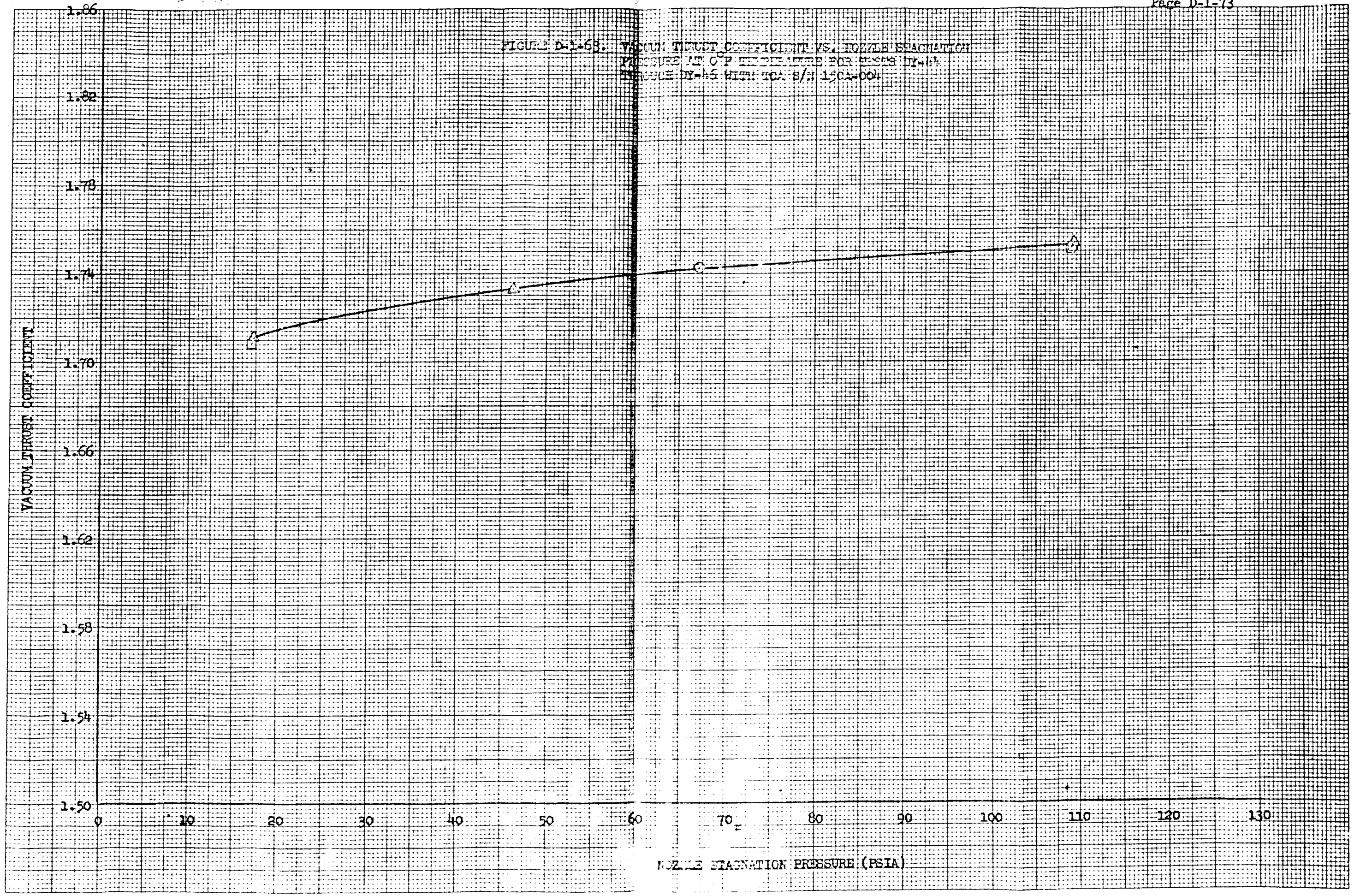

FIGURE D-1-64. PROPELLANT FLOWRATES VS. SERVOACTUATOR POSITION AT 0°F
TEMPERATURE FOR TESTS DX-14 THROUGH DX-46 FIRE TCA
S/N 1501-004

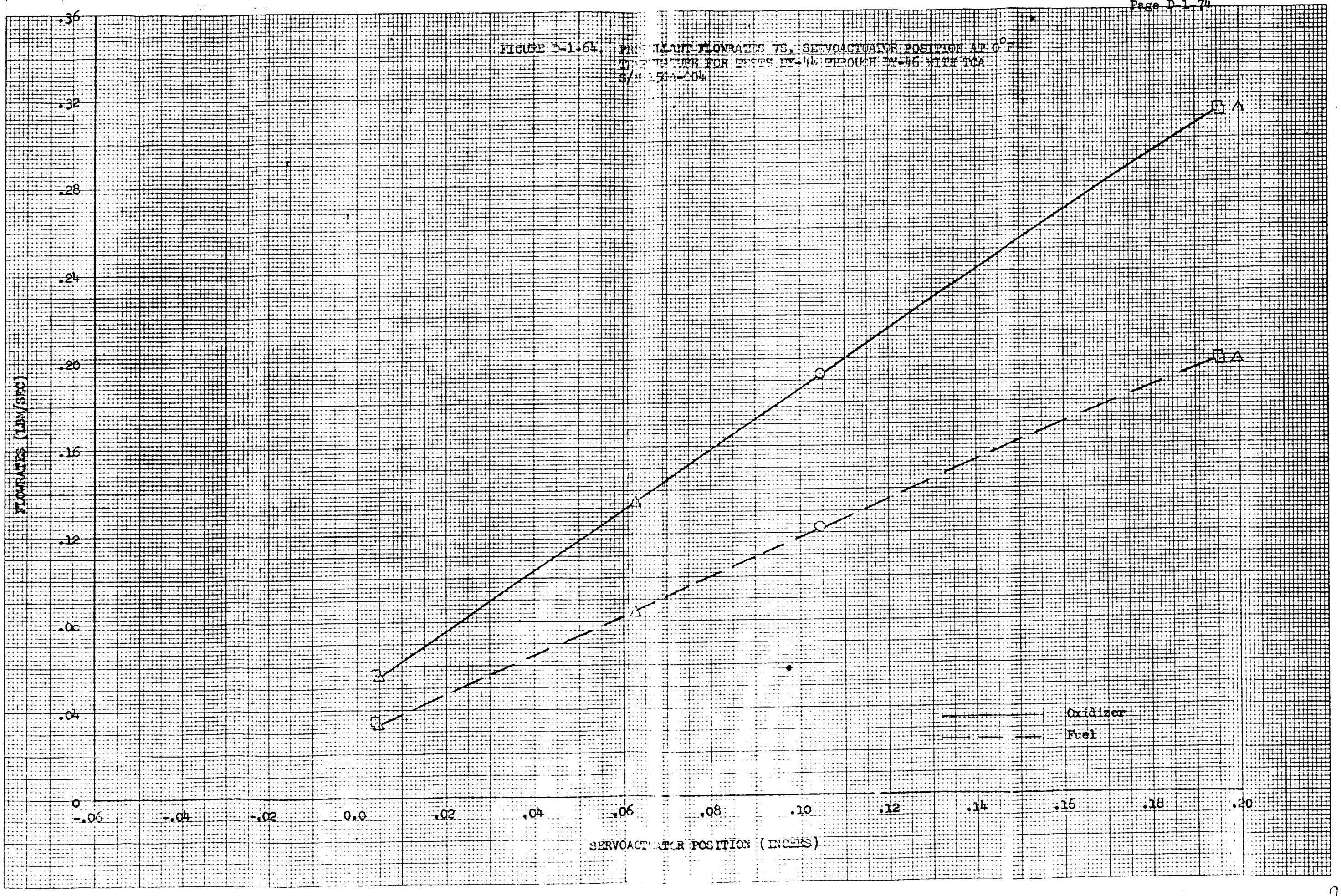

FIGURE D-1-65. VACUUM THRUST VS. SERVOACTUATOR COMMAND SIGNAL AT 1.15 THRUST RATIO FOR TESTS SV-7 AND SV-8 WITH TCA E/I

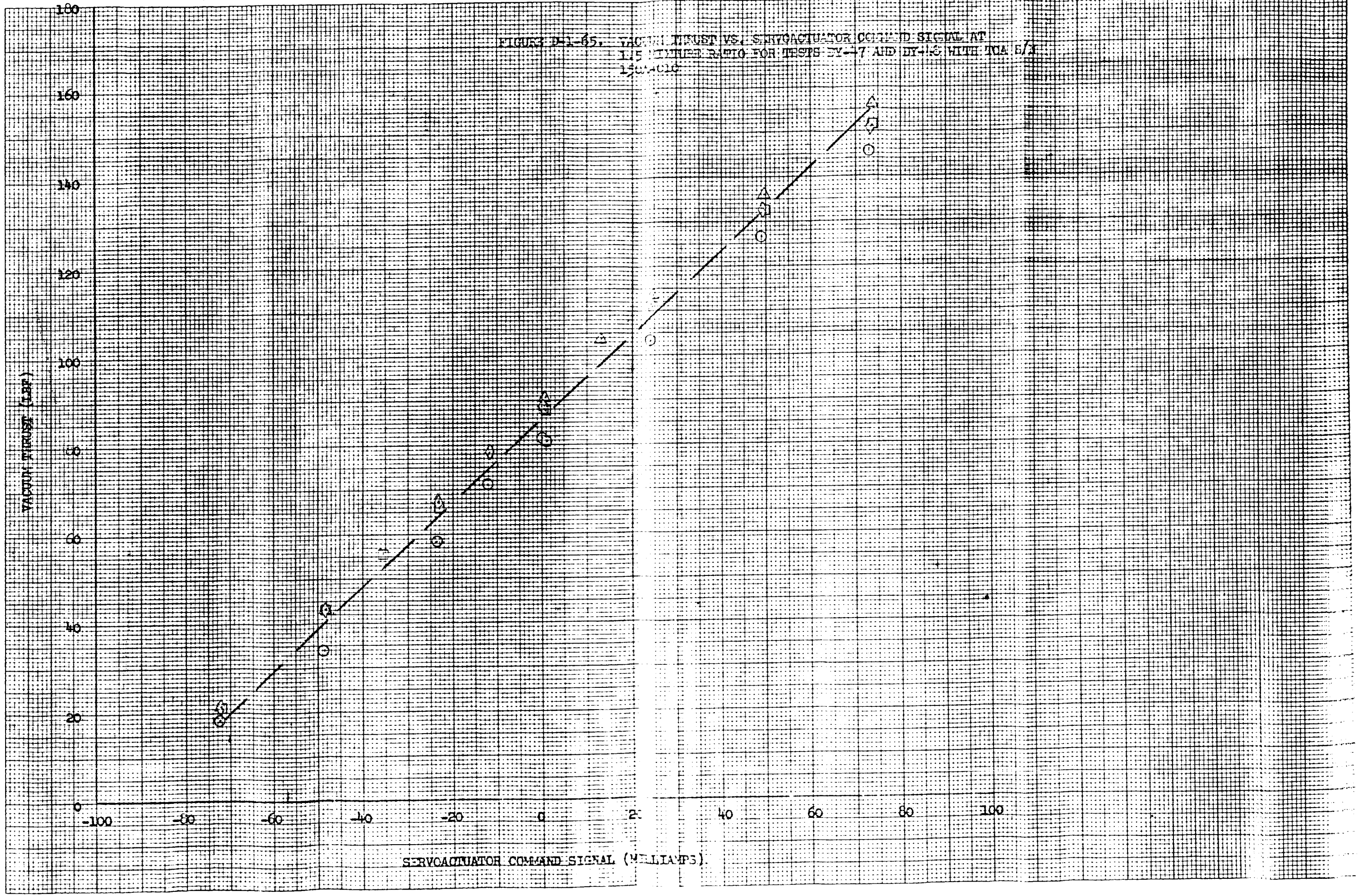

FIGURE D-1-66. VACUUM [illegible]CIFIC I[illegible]PULSE VS. THRUST AT 1.5 MIXTURE RATIO
FOR [illegible] DT-47 AND DT-48 [illegible] TCA S/N 1530-[illegible]

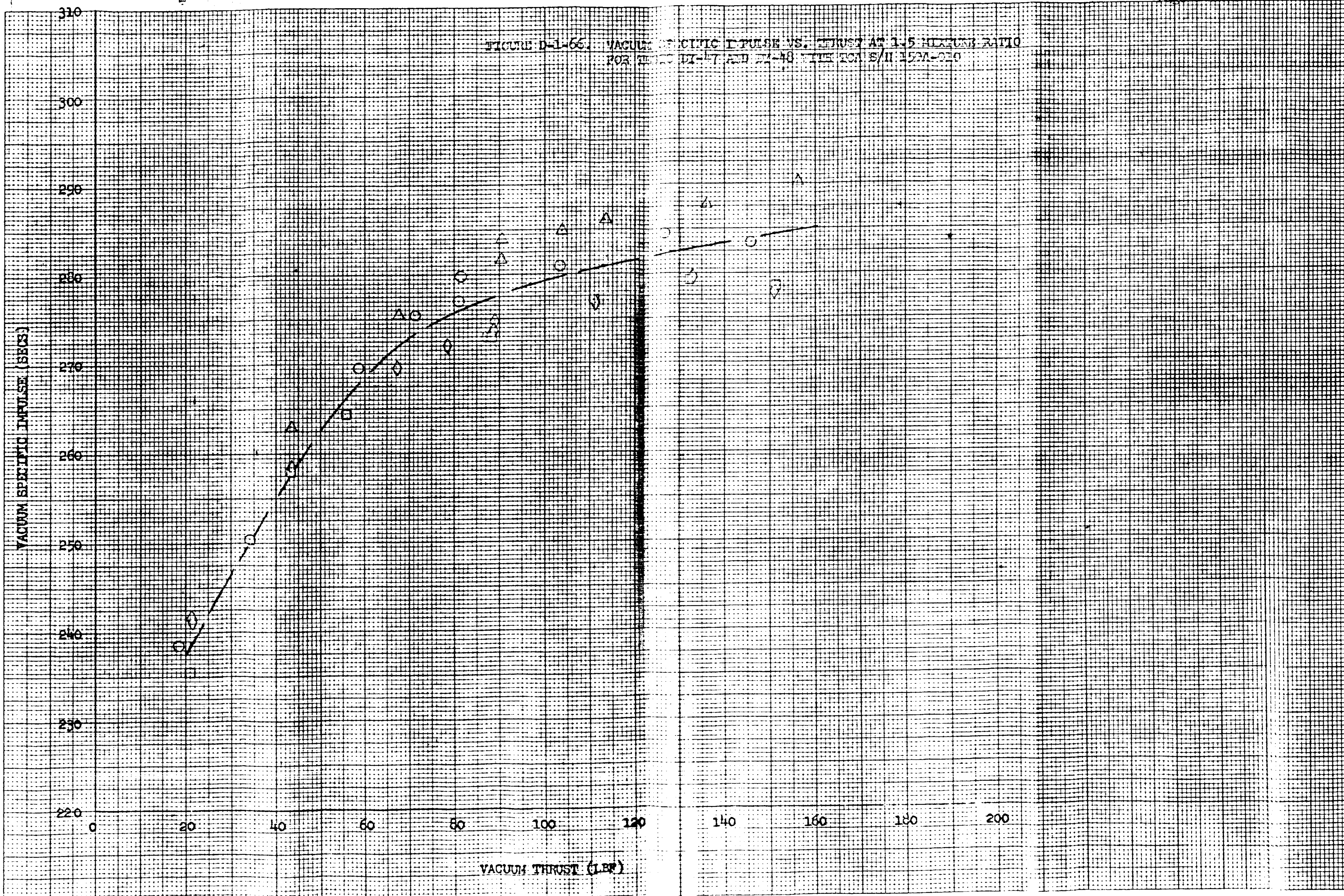

FIGURE D-1-67. CHARACTERISTIC EXHAUST VELOCITY VS. NOZZLE STAGNATION PRESSURE AT 1.5 MIXTURE RATIO FOR TESTS DX-47 AND DX-48 WITH TCA S/N 150A-010

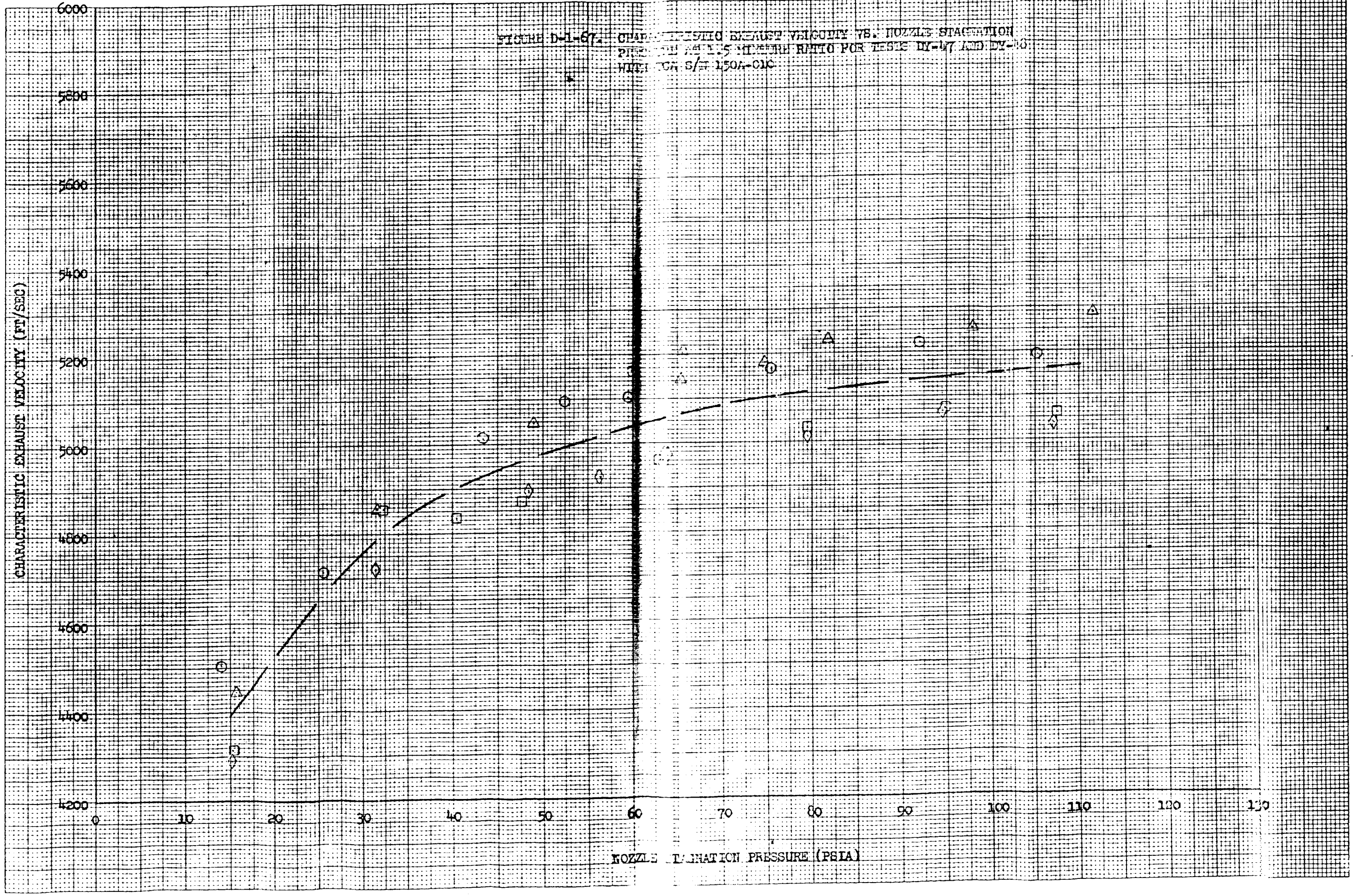

FIGURE D-1-68. VACUUM THRUST COEFFICIENT VS. NOZZLE STAGNATION PRESSURE AT 1.5 TEMPERATURE RATIO FOR TESTS SN-47 AND SN-48 WITH TCA S/N LWCA-010

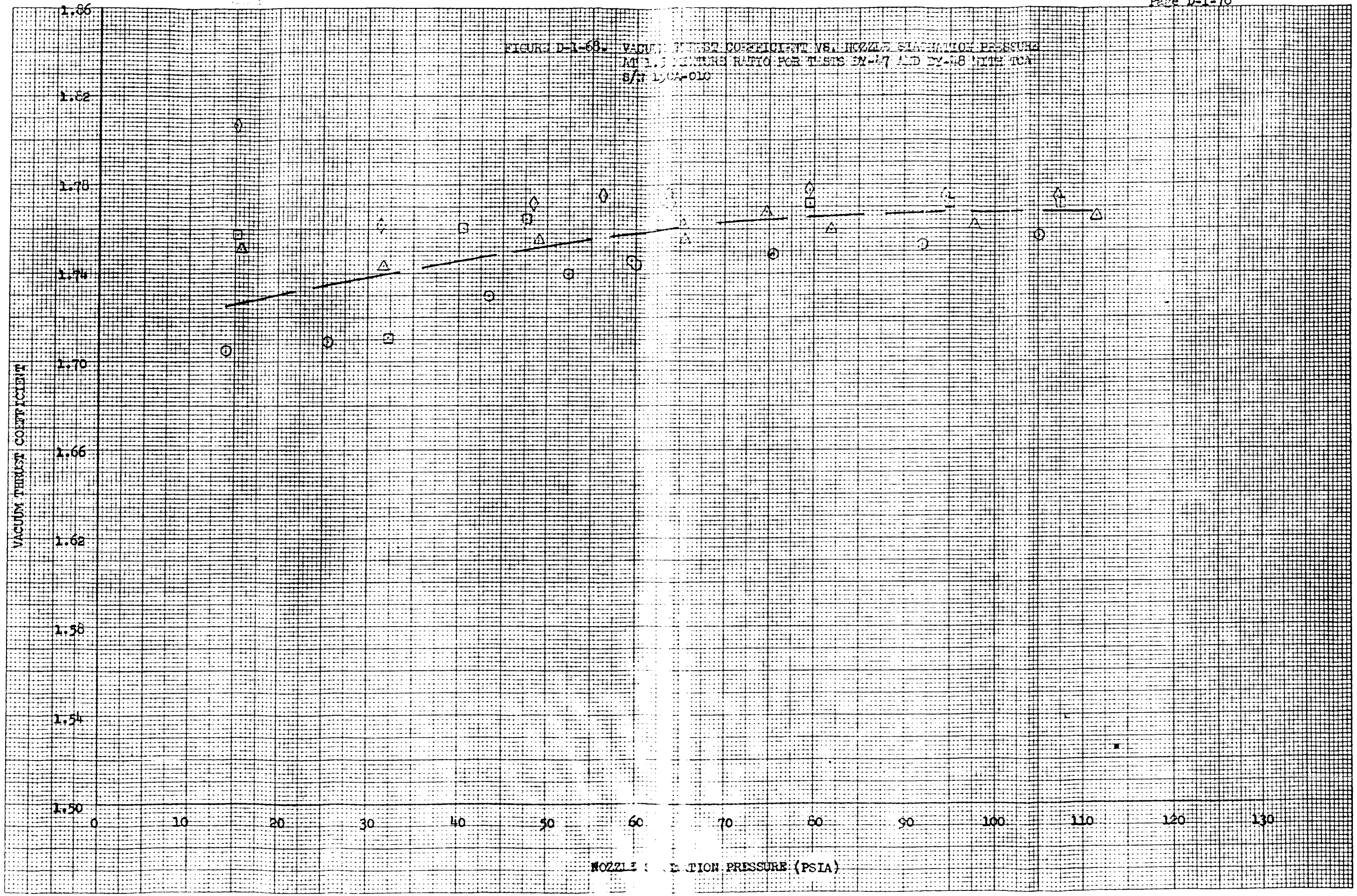

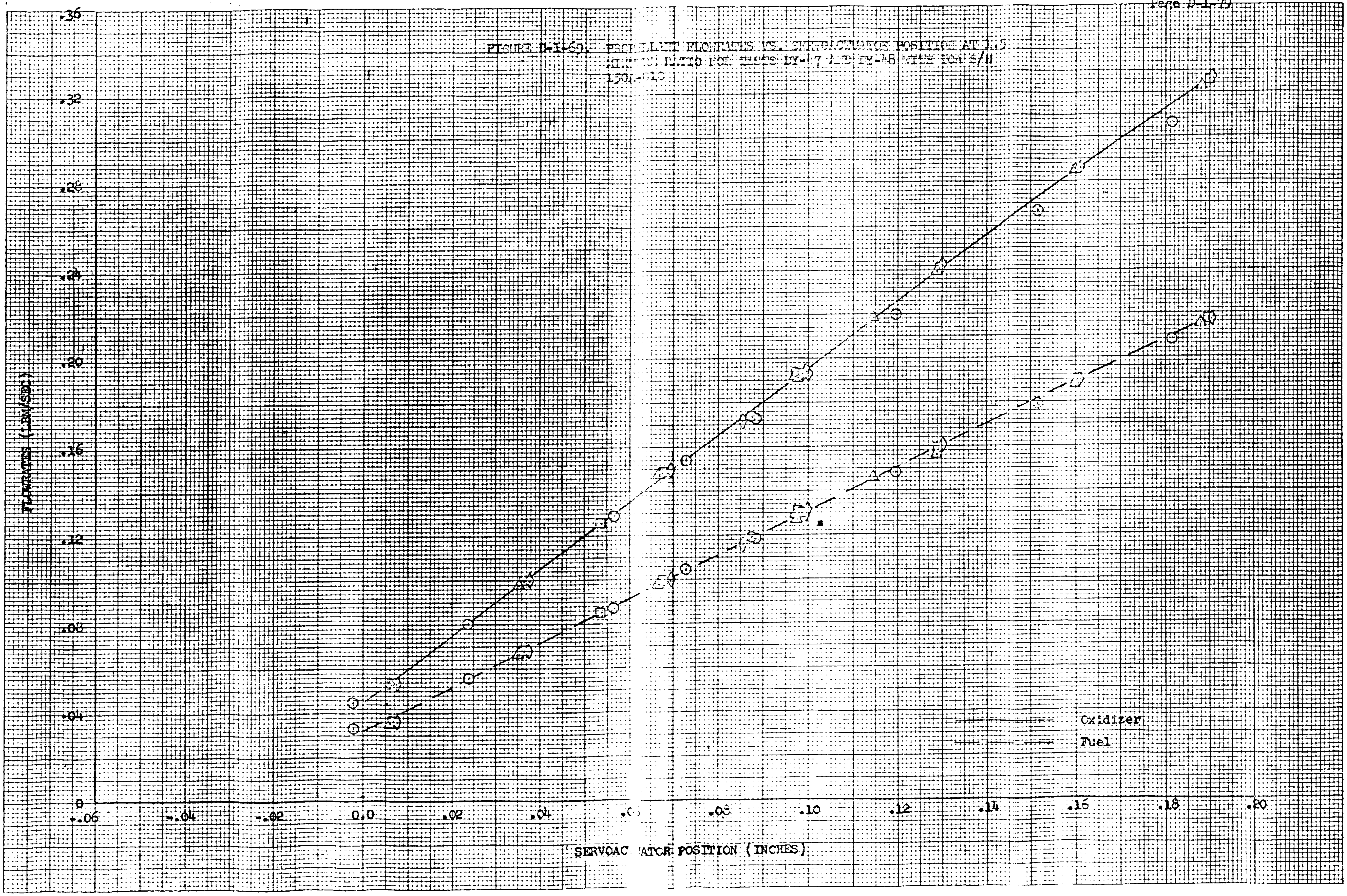

FIGURE D-1-69. PROPELLANT FLOWRATES VS. SERVOACTUATOR POSITION AT 1.5 MIXTURE RATIO FOR TESTS DY-17 AND DY-18 WITH FCA S/N 1501-010

FIGURE D-1-70. MIXTURE RATIO VS. VACUUM THRUST AT STANDARD CONDITIONS FOR ENGS DX-47 AND DX-48 WITH TCA S/N 150A-010

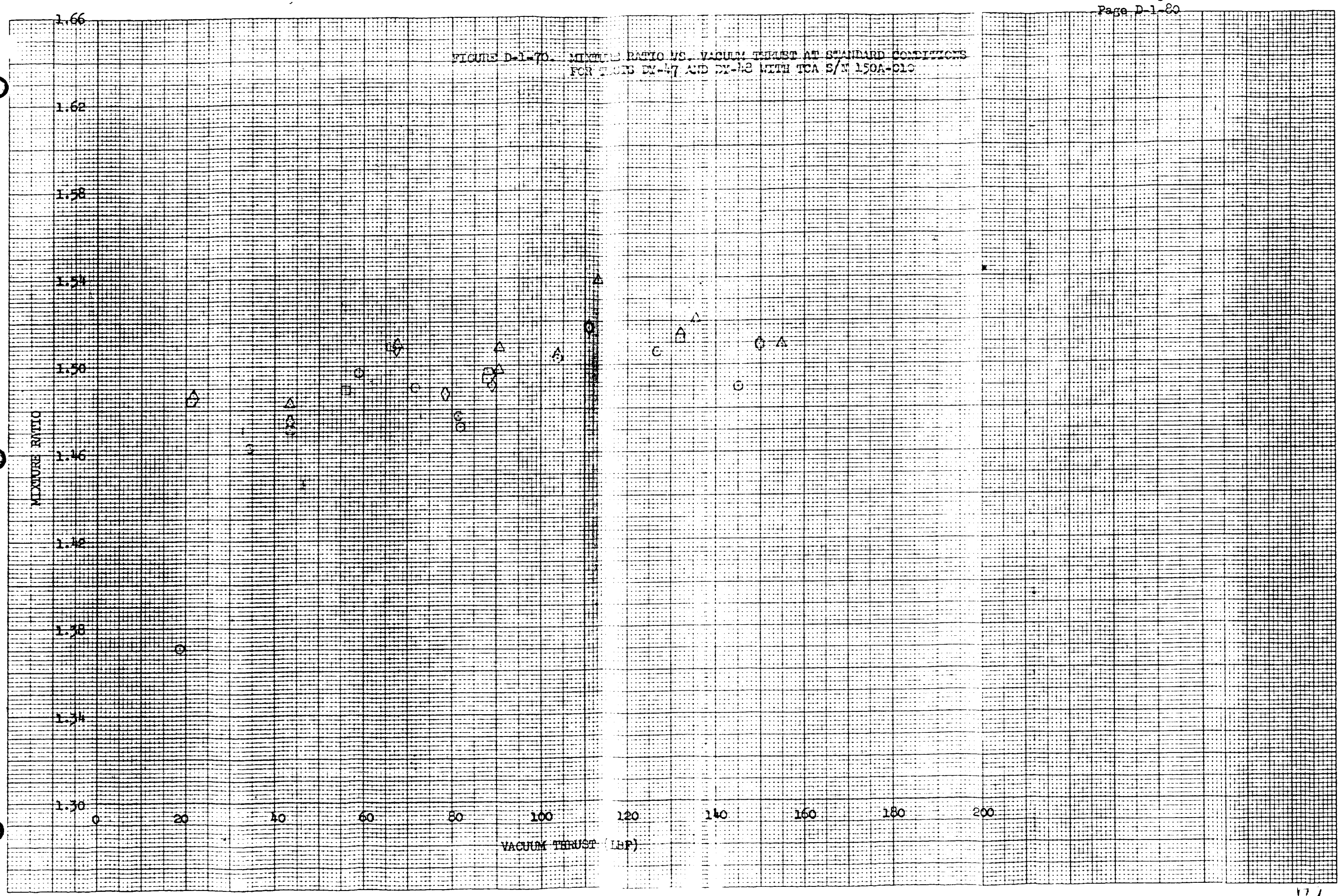

FIGURE D-1-71. VACUUM THRUST VS. SERVOACTUATOR COMMAND SIGNAL AT
1.5 [illegible] RATIO FOR TCS DV-49 WITH TCA S/N
150-000

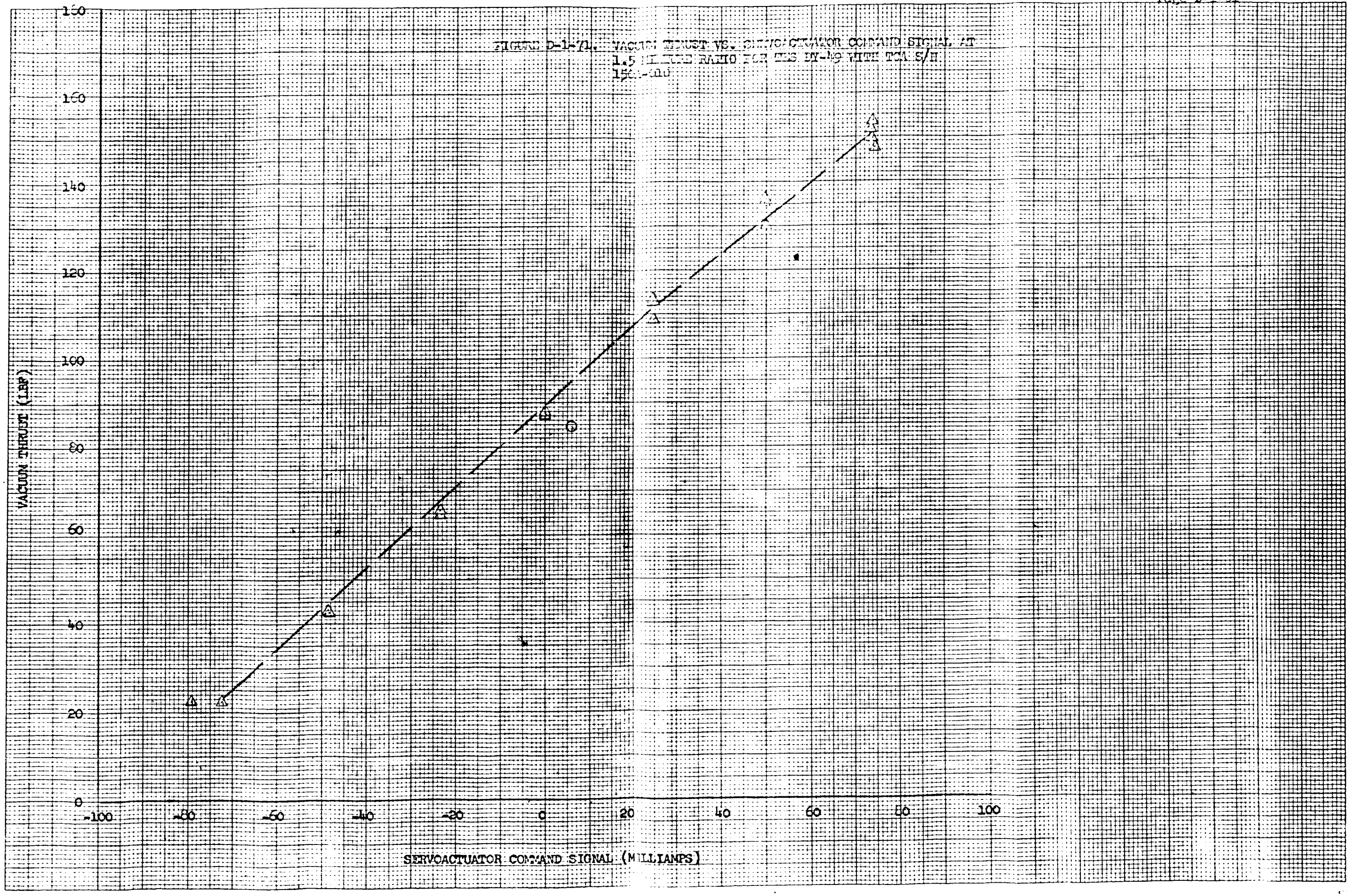

FIGURE D-1-72. VACUUM SPECIFIC IMPULSE VS. THRUST AT 1.5 MIXTURE RATIO FOR FLIGHT RV-59 WITH PCA S/N 1504-010

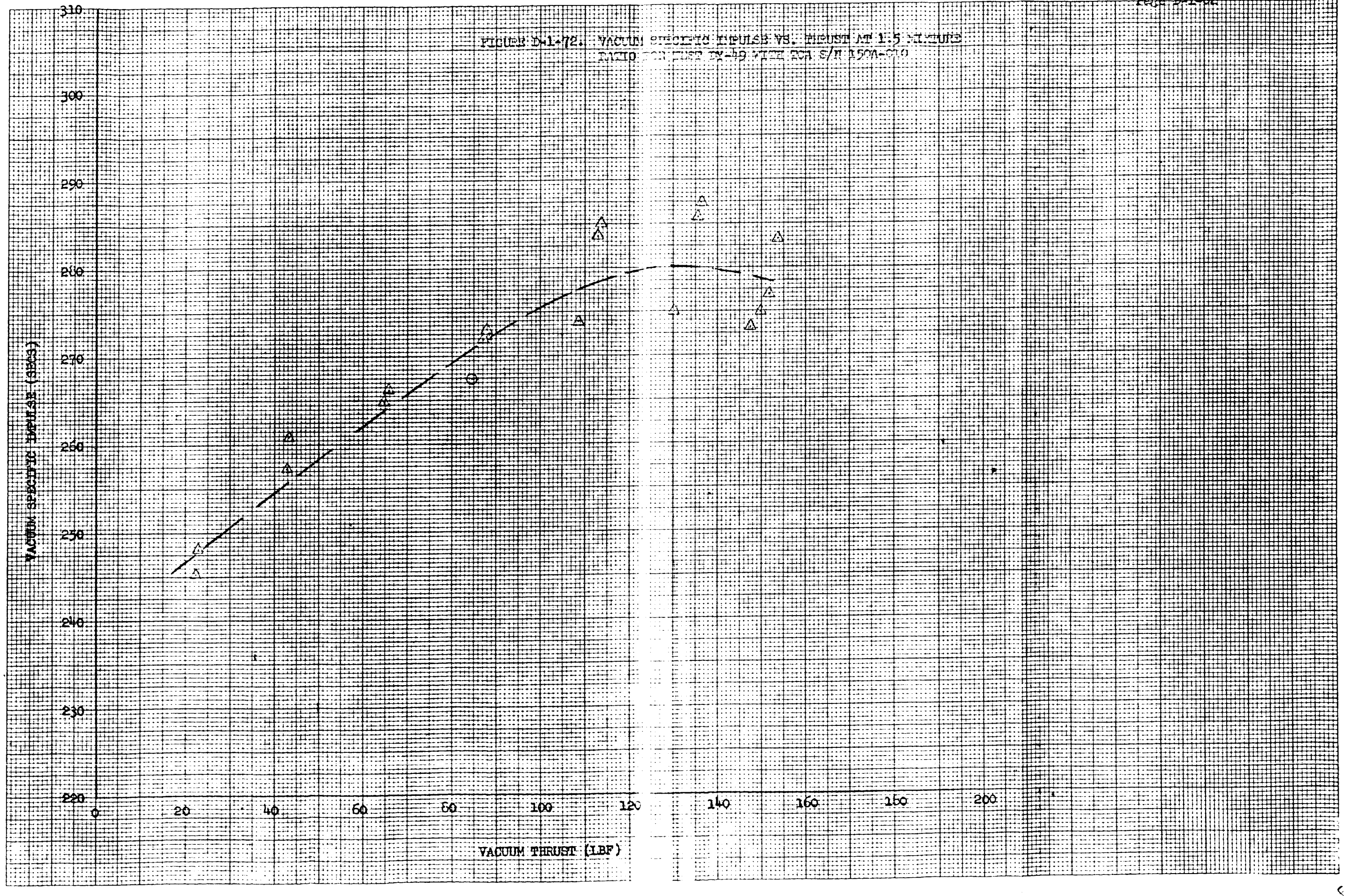

FIGURE D-1-73. CHARACTERISTIC EXHAUST VELOCITY VS. NOZZLE STAGNATION PRESSURE MIXTURE RATIO FOR TEST DY-47 WITH TCA S/N 100A-010

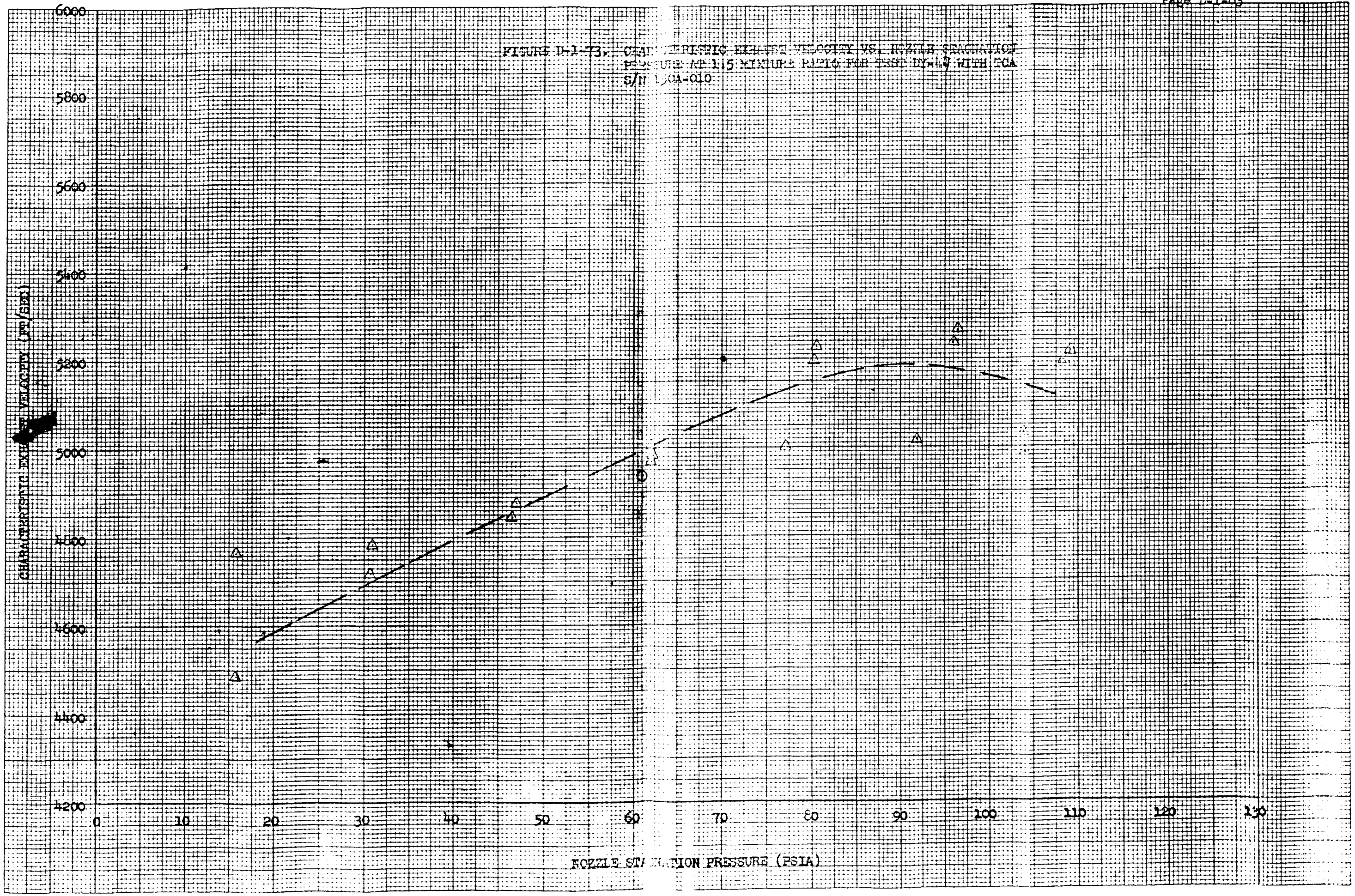

FIGURE D-1-74. VACUUM THRUST COEFFICIENT VS. NOZZLE STAGNATION PRESSURE AT 1.5 [illegible] PLASTIC FOR TEST IN-19 WITH TCA S/N 150A-010

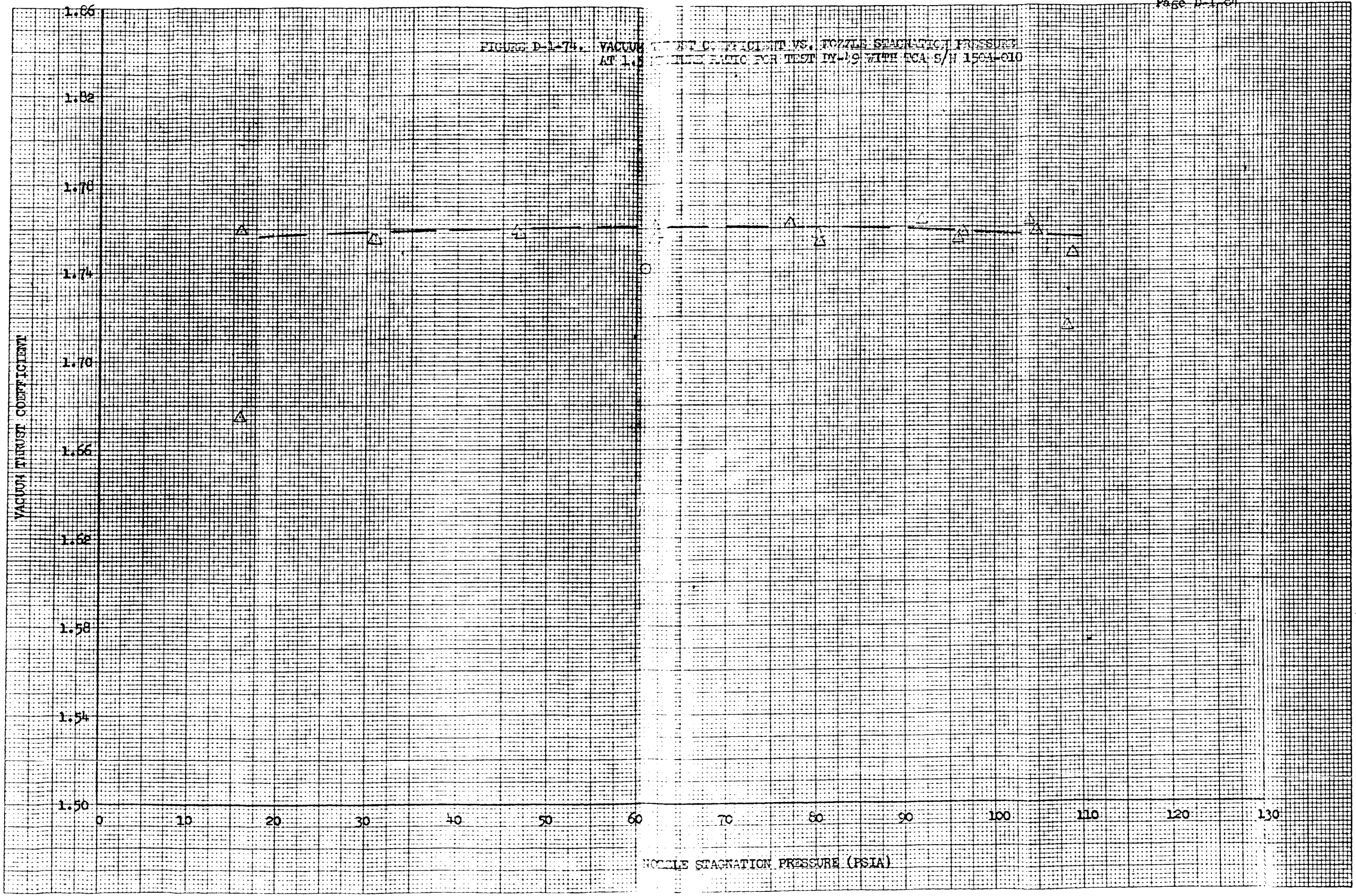

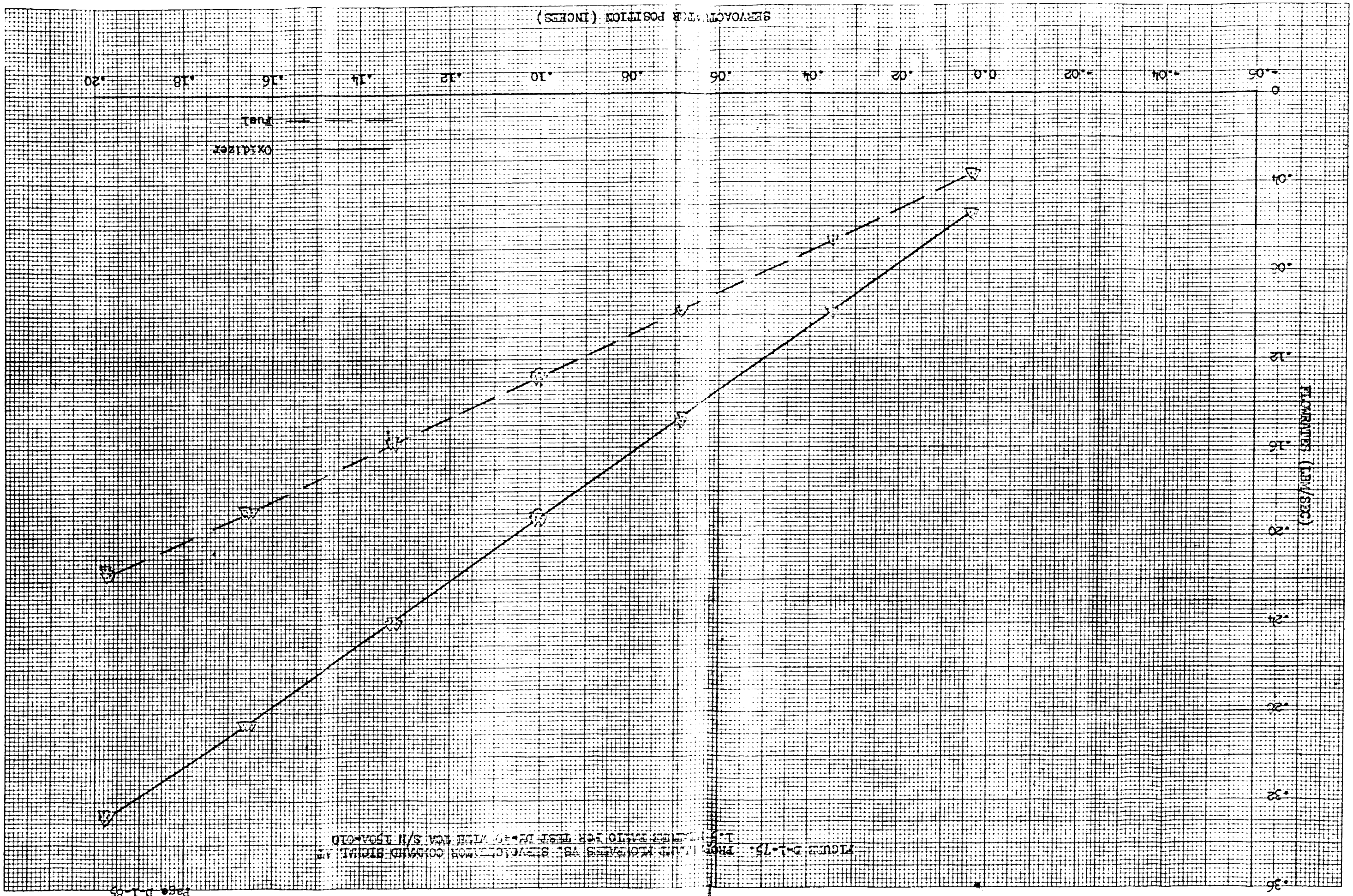

FIGURE D-1-75. PROPULSION MODULE SERVOACTUATOR COMMAND SIGNAL AT L.O.T. LIMIT RATIO FOR TEST DEMO/ATLE MCA S/N 1504-010

FIGURE D-1-76. MIXTURE RATIO VS. THRUST AT STANDARD CONDITIONS FOR TEST DY-49 WITH TCA S/N 150A-010

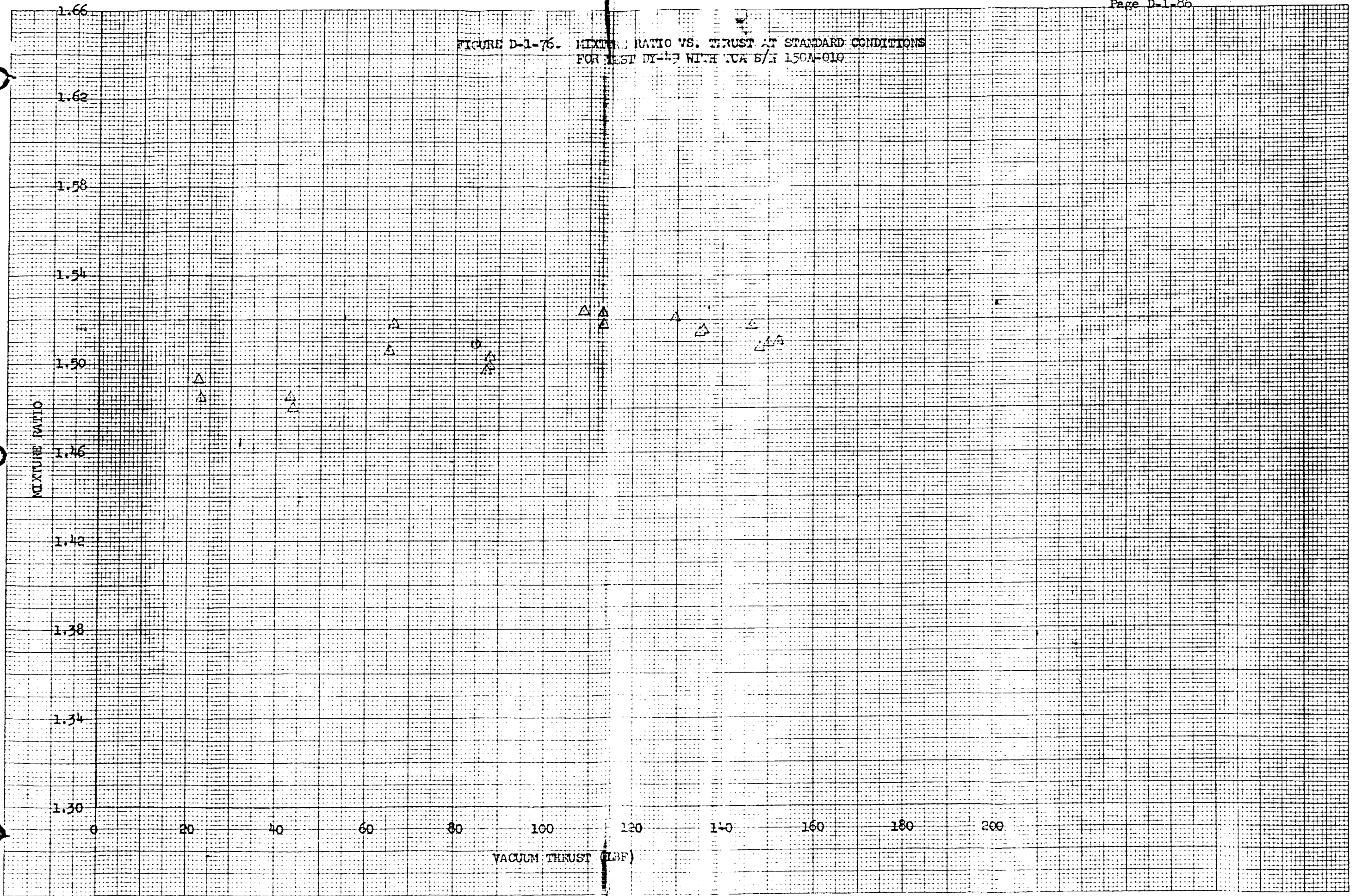

TABLE D-1-77. MIRA 150A TRANSIENT RESPONSE DATA FROM JPL/ETS TEST SITE

JPL/ETS Run No.	Development Plan or PQT Test No.	Test Date	HEA S/N	Servoactuator P/N	Servoactuator S/N	Helium Pilot Valve P/N	Helium Pilot Valve S/N	Propellants Bled Down to Shutoff Valves Pre-run	Startup Time sec. (1)	Startup Impulse lb-sec. (2)	Startup Thrust Level, lbs	Shutdown Time, sec. (3)	Shutdown Impulse, lb-sec. (4)	Shutdown Thrust Level, lbs	Servoactuator Step Response: Step Size, milliamps (5)	Step Time, seconds: Max.	Step Time, seconds: Mean	Remarks
DY-18	5.2.8	9-11-64	004	C104312B	C53748	C104337	004	No	0.297	(6)	86	0.107	(6)	86	+ 35 - 35 +120 -120	0.064 0.112 0.048 0.047	0.056 0.067 0.048 0.047	Sea level test with AT-1 tape. Response data based on Photocon P_c and current. Injection pressure taps used.
DY-19	5.2.9	9-16-64	004	C104312B	C53748	C104337	004	No	0.174	8.5	92	0.160	3.7	83	+ 24 - 70 - 24 + 58	0.014 0.021 0.014 0.034	0.013 0.021 0.013 0.034	Altitude test with PQ-3 tape. Response data based on Photocon P_c and current. Injection pressures removed on this run and all subsequent runs.
DY-20	5.2.11	9-18-64	004	C104312B	C53748	C104337	004	No	0.120 (7)	4.0 (7)	92	0.140 (7)	3.0 (7)	93	+ 7.5 - 15	0.027 0.025	0.026 0.025	Altitude test with PQ-1A tape. Response data based on thrust and current.
DY-21	5.2.11	9-18-64	004	C104312B	C53748	C104337	004	Yes	0.153 (7)	4.2 (7)	63	(6)	(6)	27	+ 7.5 - 15 -132	0.027 0.030 0.033	0.027 0.030 0.033	Altitude test with PQ-1B tape. Response data based on thrust and current.
DY-22	5.2.11	9-21-64	004	C104312B	C53748	C104337	004	Yes	0.080 (7)	3.4 (7)	142	0.170 (7)	2.2 (7)	127	(6)	(6)	(6)	Altitude test with PQ-1C tape. Response data based on thrust and current. Test aborted after 30 seconds.
DY-23	5.2.11	9-21-64	004	C104312B	C53748	C104337	004	Yes	0.082 (7)	3.6 (7)	142	0.130 (7)	1.6 (7)	31	+140 -140 +150 -150 + 7.5 - 15	0.042 0.035 0.047 0.054 0.018 0.018	0.041 0.034 0.047 0.054 0.017 0.018	Altitude test with PQ-1C tape. Tesponse data based on thrust and current.
DY-24	5.2.11	9-21-64	004	C104312B	C53748	C104337	004	Yes	0.230 (7)	7.7 (7)	68	1.30 (7)	2.4 (7)	29	+ 7.5 - 15 -132	0.022 0.017 0.034	0.022 0.017 0.034	Altitude test with PQ-1B tape. Response data based on thrust and current.
DY-25	PQT-001	10-12-64	001	C104312B	C53750	C104337	022	No	0.103 (7)	1.9	101	0.180 (7)	2.3 (7)	91	+ 24 - 70 - 24 + 58	0.023 0.016 0.023 0.039	0.022 0.016 0.017 0.039	Altitude test with PQ-3 tape. Response data based on thrust and current.
DY-26	PQT-002	10-15-64	001	C104312B	C53750	C104337	022	No	(6)	(6)	100	(6)	(6)	110	+ 24 - 70 - 24 + 82	0.020 0.018 0.019 0.050	0.020 0.018 0.017 0.050	Altitude test with PQ-4 tape. Response data based on thrust and current.
DY-27	PQT-003	10-16-64	001	C104312B	C53750	C104337	022	[illegible]	0.125 (7)	1.4 (7)	104	0.185 (7)	2.2 (7)	73	+ 24 - 70 - 24 + 35	0.025 0.021 0.014 0.031	0.023 0.021 0.014 0.031	Altitude test with PQ-5 tape. Response data based on thrust and current.

TABLE D-1-77. (Continued)

JPL/ETS Run No.	Development Plan or PQT Test No.	Test Date	HEA S/N	Servoactuator P/N	Servoactuator S/N	Helium Pilot Valve P/N	Helium Pilot Valve S/N	Propellants Bled Down to Shutoff Valves Pre-run	Startup Time sec. (1)	Startup Impulse lb-sec. (2)	Startup Thrust Level, lbs	Shutdown Time, sec. (3)	Shutdown Impulse, lb-sec. (4)	Shutdown Thrust Level, lbs	Servoactuator Step Response: Step Size, milliamps (5)	Step Time, seconds: Max.	Step Time, seconds: Mean	Remarks
DY-28	PQT-004A	10-20-64	001	C104312B	C53750	C104337	022	No	0.110 (7)	1.9 (7)	102	0.190 (7)	2.1 (7)	93	+ 24 - 70 - 24 + 58	0.022 0.018 0.021 0.040	0.022 0.018 0.015 0.040	Altitude test with PQ-3 tape. Response data based on thrust and current.
DY-29	PQT-004.5	10-22-64	001	C104312B	C53750	C104337	022	No	0.102	2.1	101	0.170	2.5	92	+ 24 - 70 - 24 + 58	0.035 0.019 0.020 0.042	0.026 0.019 0.014 0.042	Altitude test with PQ-3 tape. Response data based on Photocon P_c and current.
DY-30	PQT-004.5	10-23-64	001	C104312B	C53750	C104337	022	No	0.125	3.8	100	0.145	3.4	111	+ 24 - 70 - 24 + 82	0.021 0.018 0.025 0.053	0.019 0.018 0.016 0.053	Altitude test with PQ-4 tape. Response data based on Photocon P_c and current.
DY-31	PQT-004.5	10-26-64	001	C104312B	C53750	C104337	022	No	0.117	2.1	102	0.187	2.4	72	+ 24 - 70 - 24 + 35	0.023 0.017 0.012 0.031	0.023 0.017 0.012 0.031	Altitude test with PQ-5 tape. Response data based on Photocon P_c and current.
DY-32	PQT-004.5	10-26-64	001	C104312B	C53750	C104337	022	Yes	0.110	4.1	103	0.095	2.7	93	+ 24 - 70 - 24 + 58	0.020 0.016 0.012 0.040	0.019 0.016 0.012 0.040	Altitude test with PQ-3 tape. Response data based on Photocon P_c and current.
DY-33	PQT-004B	11-11-64	001	C104312B	C53750	C104337	022	No	0.082 (7)	4.2 (7)	147	0.047 (7)	2.8 (7)	84	+ 24 - 24 +150 -150 +160	0.116 0.021 0.081 0.030 0.158	0.032 0.015 0.081 0.030 0.158	Altitude test with PQ-6 tape. TCA and propellants conditioned to 0°F. Response data based on thrust and current.
DY-34	None	11-13-64	001	C104312B	C53750	C104337	022	No	(6)	(6)	(6)	(6)	(6)	(6)	+ 35 - 35 -120 +120 + 70	0.071 0.015 0.070 0.025 0.040	0.036 0.013 0.070 0.025 0.040	Sea level test with AT-1 tape. Response data based on thrust and current.
DY-35	PQT-007	12-1-64	008	C104312B	C53751	C104337	024	No	0.128 (7)	10.7 (7)	152	0.135 (7)	5.5 (7)	151	(6)	(6)	(6)	Altitude test with PQ-7 fixed thrust tape. TCA and propellants conditioned to 100°F. Data based on thrust and current.
DY-36	PQT-007	12-1-64	008	C104312B	C53751	C104337	024	Yes	0.073 (7)	1.6 (7)	144	0.104 (7)	5.4 (7)	145	(6)	(6)	(6)	Altitude test with PQ-7 fixed thrust tape. Data based on thrust and current TCA and propellants conditioned to 100°F.
DY-37	PQT-007	12-2-64	008	C104312B	C53751	C104337	024	No	0.105 (7)	7.6 (7)	153	0.130 (7)	6.0 (7)	152	(6)	(6)	(6)	Altitude test with PQ-7 fixed thrust tape. Data based on thrust and current TCA and propellants conditioned to 100°F.

TABLE D-1-77. (Continued)

JPL/ETS Run No.	Development Plan or PQT Test No.	Test Date	HEA S/N	Servoactuator P/N	Servoactuator S/N	Helium Pilot Valve P/N	Helium Pilot Valve S/N	Propellants Bled Down to Shutoff Valves Pre-run	Startup Time sec. (1)	Startup Impulse lb-sec. (2)	Startup Thrust Level, lbs	Shutdown Time, sec. (3)	Shutdown Impulse, lb-sec. (4)	Shutdown Thrust Level, lbs	Servoactuator Step Response: Step Size, milliamps (5)	Step Time, seconds: Max.	Step Time, seconds: Mean	Remarks
DY-38	PQT-008	12-4-64	008	C104312B	C53751	C104337	024	No	0.314 (7)	2.9 (7)	30	0.272 (7)	3.6 (7)	32	(6)	(6)	(6)	Altitude test with PQ-8 fixed thrust tape. TCA conditioned to subzero, propellants to 100°F. Data based on thrust and current.
DY-39	PQT-008	12-7-64	008	C104312B	C53751	C104337	024	Yes	0.261 (7)	1.9 (7)	31	0.217 (7)	3.1 (7)	32	(6)	(6)	(6)	Altitude test with PQ-8 fixed thrust tape. Propellants conditioned to 100°F. Data based on thrust and current.
DY-40	PQT-008	12-7-64	008	C104312B	C53751	C104337	024	Yes	0.290 (7)	4.8 (7)	32	0.242 (7)	3.3 (7)	32	(6)	(6)	(6)	Altitude test with PQ-8 fixed thrust tape. Propellants conditioned to 100°F. Data based on thrust and current.
DY-41	PQT-010	12-10-64	004	C219217	C55394	C104337	004	No	0.089	4.5	139	.060	4.6	26	-150 +150 -140 +140	.088 .085 .086 .066	.088 .085 .059 .055	Altitude test with PQ-1C tape. Response data based on current and Photocon data. Propellants and engine at ambient temperatures.
DY-42	PQT-010	12-11-64	004	C219217	C55394	C104337	004	Yes	.106	3.4	93	.168	4.2	94	- 15	.012	.012	Altitude test with PQ-1A tape. Response data based on current and Photocon. Propellants and engine at ambient temperatures.
DY-43	PQT-010	12-11-64	004	C219217	C55394	C104337	004	Yes	.156	3.2	67	.245	3.2	26	+ 70 -132.5	0.038 0.035	0.038 0.035	Altitude test with PQ-1B tape. Response data based on current and Photocon. Propellants and engine at ambient temperatures.
DY-44	PQT-009.5	12-15-64	004	C219217	C55394	C104337	004	No	0.099	2.67	88	0.127	3.1	91	- 15	.013	.013	Altitude test with PQ-1 tape. Response data based on current and Photocon. Actuator and propellants conditioned to 0°F.
DY-45	PQT-009.5	12-16-64	004	C219217	C55394	C104337	004	No	0.125	1.7	64	0.162	1.3	24	+ 70 -132.5	.027 .037	.027 .037	Altitude test with PQ-1A tapes. Response data based on current and Photocon. Actuator and propellants conditioned to 0°F.
DY-46	PQT-009.5	12-16-64	004	C219217	C55394	C104337	004	Yes	0.074	3.4	142	0.056	3.1	22	-150 +150 +140 -140	0.061 0.088 0.085 0.076	0.061 0.088 0.062 0.076	Altitude test with PQ-1B tape. Response data based on current and Photocon. Actuator and propellants conditioned to 0°F.
DY-47	PQT-005	12-18-64	010	C219217	C55394	C104337	004	No	.175 (7)	6.8 (7)	82	.200 (7)	3.7 (7)	72	+ 24 - 70 - 24 + 58	.020 .026 .030 .056	.019 .026 .022 .056	Altitude test with PQ-3 tape. Data based on thrust and servo current. Servoactuator replaced prior to this test.
DY-48A	PQT-005	12-18-64	010	C219217	C55394	C104337	004	No	.136 (7)	4.7 (7)	90	.174 (7)	4.6 (7)	104	+ 24 - 70 - 24 + 82	.018 .024 .016 .044	.017 .024 .014 .044	Altitude test with PQ-4 tape. Data based on thrust and servo current.

TABLE D-1-77. (Continued)

JPL/ETS Run No.	Development Plan or PQT Test No.	Test Date	HEA S/N	Servoactuator P/N	Servoactuator S/N	Helium Pilot Valve P/N	Helium Pilot Valve S/N	Propellants Bled Down to Shutoff Valves Pre-run	Startup Time sec. (1)	Startup Impulse lb-sec. (2)	Startup Thrust Level, lbs	Shutdown Time, sec. (3)	Shutdown Impulse, lb-sec. (4)	Shutdown Thrust Level, lbs	Servoactuator Step Response: Step Size, milliamps (5)	Step Time, seconds: Max.	Step Time, seconds: Mean	Remarks
DY-48B	PQT-005	12-18-64	010	C219217	C55394	C104337	004	Yes	.100 (7)	2.7 (7)	88	.320 (7)	3.9 (7)	56	+ 24	.018	.017	Altitude test with PQ-5 tape. Data based on thrust and servo current. Engine restarted 8 seconds after DY-48A shutdown.
															- 70	.025	.025	
															- 24	.016	.015	
															+ 35	.070	.070	
DY-48C	PQT-005	12-18-64	010	C219217	C55394	C104337	004	Yes	.107 (7)	3.2 (7)	89	.261 (7)	4.2 (7)	78	+ 24	.019	.018	Altitude test with PQ-3 tape. Data based on thrust and servo current. Engine restarted 10 seconds after DY-48B shutdown.
															- 70	.024	.024	
															- 24	.038	.023	
															- 58	.072	.072	
DY-49	PQT-005	12-21-64	010	C219217	C55394	C104337	004	Yes	.075	3.4	146	.247	4.2	73	- 24	.018	.015	Altitude test with PQ-6 tape. Data based on thrust and servo current. Water cooled chamber installed for this test.
															+ 24	.079	.027	
															- 62.5	.024	.024	
															+ 62.5	.032	.032	
															+ 7.5	.023	.023	
															-150	.038	.038	
															+150	.078	.078	
															-140	.038	.038	
															- 74.5	.019	.019	

NOTES: (1) Defined as the time from TCA receipt of startup signal to attainment of 95% commanded thrust level.
(2) The area under the thrust-time curve over the startup time interval.
(3) Defined as the time from TCA receipt of shutdown signal to accumulation of 95% of the total shutdown impulse.
(4) The area under the thrust-time curve over the time interval from TCA receipt of shutdown signal to attainment of zero thrust.
(5) Positive signs indicate increasing thrust steps; negative signs indicate decreasing thrust.
(6) Data not available because of test conditions or instrumentation malfunction.
(7) Values based on measured thrust and are not considered precise because of thrust stand oscillations during the transient.

APPENDIX D-2

IRTS STATIC FIRING DATA

No. of Pages: 53

TABLE D-2-1. MIRA 150A STEADY-STATE PERFORMANCE DATA SUMMARY FOR IRTS

IRTS Test No.	Development Plan or PQT Test No.	Test Date	HEA S/N	CC & NA Type	CC & NA Dwg. No or S/N	Total Duration sec.	Data Slice No.	Servo Command ra	Head-End P, psia Site	Head-End P, psia Standard	MR, o/f Site	MR, o/f Standard	Total Flowrate lbs/sec Site	Total Flowrate lbs/sec Standard	Corrected C* fps Site	Corrected C* fps Standard	Fuel Inlet Pressure psia	Oxidizer Inlet Pressure psia	Fuel Inlet Temperature °F	Oxidizer Inlet Temperature °F	Remarks
C2-591	None	10-15-64	005	Water Cooled	106372	19	1	+ 69.6	109.1	110.5	1.499	1.489	0.5163	0.5202	5327	5326	701	701	63	59	3 point manual step throttle run for performance checkout.
							2	- 0.6	74.1	74.5	1.489	1.477	0.3495	0.3498	5337	5336	709	711	63	59	
							3	- 70.4	23.1	23.2	1.471	1.459	0.1165	0.1160	4999	4999	716	718	63	59	
C2-592C	3.6.2.3	10-15-64	005	Water Cooled	106372	186	1	+ 69.6	107.6	108.9	1.513	1.504	0.5190	0.5230	5220	5220	701	700	62	59	Per Memo 9730.4-64-1-65 (28 September 1964).
							2	+ 51.6	99.6	100.7	1.499	1.490	0.4771	0.4802	5254	5254	702	702	62	59	
							3	+ 34.6	92.2	93.1	1.498	1.488	0.4383	0.4405	5294	5294	704	704	62	59	
							4	+ 17.2	84.5	85.2	1.504	1.493	0.3950	0.3960	5389	5389	708	708	62	59	
							5	- 0.6	74.9	75.4	1.494	1.484	0.3489	0.3494	5405	5405	709	709	62	59	
							6	- 18.0	61.7	62.0	1.506	1.495	0.2941	0.2940	5274	5274	711	712	62	59	
							7	- 35.4	49.0	49.2	1.525	1.514	0.2326	0.2322	5301	5302	713	714	62	59	
							8	- 52.8	36.4	36.5	1.528	1.517	0.1757	0.1751	5207	5208	716	716	62	59	
							9	- 70.0	23.1	23.2	1.534	1.522	0.1174	0.1168	4964	4965	717	718	62	59	
							10	- 52.8	36.0	36.0	1.532	1.521	0.1749	0.1742	5173	5174	716	717	62	59	
							11	+ 69.8	109.7	109.6	1.497	1.489	0.5243	0.5214	5271	5270	720	718	61	59	
							12	+ 52.4	101.3	101.0	1.491	1.482	0.4831	0.4795	5280	5280	722	721	61	59	
							13	+ 35.0	93.2	92.9	1.489	1.480	0.4425	0.4386	5307	5306	724	723	61	59	
							14	+ 17.4	85.6	85.1	1.492	1.482	0.3989	0.3944	5407	5406	727	727	61	59	
							15	- 0.4	75.8	75.3	1.486	1.476	0.3529	0.3487	5408	5408	728	728	61	59	
							16	- 17.6	62.7	62.2	1.498	1.488	0.2993	0.2951	5273	5273	731	731	61	59	
							17	- 35.4	50.1	49.6	1.519	1.508	0.2364	0.2327	5330	5330	733	733	61	59	
							18	- 52.4	37.4	37.0	1.517	1.506	0.1797	0.1767	5240	5240	735	735	61	59	
							19	- 69.6	23.6	23.2	1.533	1.521	0.1203	0.1180	4933	4934	737	738	61	59	
							20	- 52.4	36.8	36.3	1.525	1.509	0.1775	0.1741	5219	5219	735	740	61	59	
C2-596	None	10-16-64	005	Water Cooled	106372	19	1	+ 70.0	110.5	111.7	1.520	1.514	0.5201	0.5234	5352	5352	703	700	59	58	3 point manual step throttle run for performance checkout.
							2	- 0.2	74.7	75.0	1.492	1.486	0.3527	0.3525	5330	5330	713	709	58	58	
							3	- 69.8	23.7	23.7	1.529	1.523	0.1211	0.1202	4928	4928	721	718	58	58	
C2-618	None	11-2-64	007	Water Cooled	106372	91	1	+ 70.2	107.1	107.6	1.453	1.439	0.5223	0.5224	5165	5164	707	707	58	54	Manual step throttle performance checkout run.
							2	+ 0.2	66.5	66.5	1.466	1.453	0.3189	0.3173	5248	5248	715	714	58	54	
							3	- 69.8	21.0	21.1	1.452	1.439	0.1086	0.1077	4888	4888	719	718	58	54	
							4	- 0.8	67.1	67.1	1.488	1.473	0.3217	0.3199	5249	5249	715	714	59	53	
							5	+ 35.2	90.9	91.1	1.477	1.462	0.4296	0.4284	5330	5330	711	710	59	52	
							6	+ 17.6	79.6	79.7	1.491	1.476	0.3775	0.3759	5309	5309	713	712	59	52	
							7	0	68.3	68.1	1.487	1.474	0.3231	0.3213	5307	5306	716	713	59	52	
							8	- 17.6	56.4	56.3	1.473	1.459	0.2687	0.2669	5280	5279	717	715	59	52	
							9	- 35.4	43.7	43.6	1.514	1.498	0.2128	0.2111	5167	5168	718	717	59	52	
							10	- 52.6	31.1	31.1	1.494	1.480	0.1578	0.1564	4975	4975	720	718	59	52	

TABLE D-2-1. (Continued)

IRTS Test No.	Development Plan or PQT Test No.	Test Date	HEA S/N	CC & NA Type	CC & NA Dwg. No. or S/N	Test Duration	Data Slice No.	Servo Command ra	Head-End P, psia Site	Head-End P, psia Standard	MR, o/f Site	MR, o/f Standard	Total Flowrate lbs/sec Site	Total Flowrate lbs/sec Standard	Corrected C fps Site	Corrected C fps Standard	Fuel Inlet Pressure psia	Oxidizer Inlet Pressure psia	Fuel Inlet Temperature °F	Oxidizer Inlet Temperature °F	Remarks
C2-621	None	11-3-64	007	Water Cooled	106372	131	1	- 0.2	68.8	69.0	1.502	1.487	0.3259	0.3248	5315	5315	712	712	60	53	Acceptance test with AT-1 program tape.
							2	+ 35.0	91.2	91.6	1.488	1.471	0.4321	0.4317	5318	5317	708	708	61	53	
							3	+ 70.4	111.9	112.7	1.489	1.470	0.5283	0.5293	5338	5338	703	705	61	52	
							4	+ 35.2	91.1	91.5	1.491	1.474	0.4299	0.4295	5338	5337	708	708	61	52	
							5	+ 0.4	68.7	68.8	1.501	1.484	0.3231	0.3239	5320	5319	712	712	61	52	
							6	- 35.4	44.1	44.1	1.513	1.497	0.2143	0.2130	5180	5180	716	715	61	52	
							7	- 50.6	33.9	33.9	1.511	1.494	0.1699	0.1688	5026	5027	717	716	61	52	
							8	- 35.6	44.5	44.5	1.515	1.498	0.2167	0.2154	5164	5165	716	715	61	52	
							9	- 0.6	69.3	69.5	1.497	1.480	0.3273	0.3261	5335	5334	712	712	61	52	
							10	- 0.4	69.4	69.5	1.496	1.478	0.3274	0.3262	5338	5337	712	712	62	52	
							11	+ 70.6	113.0	113.8	1.487	1.466	0.5323	0.5336	5351	5350	702	705	62	52	
							12	+ 70.8	113.0	113.8	1.487	1.466	0.5323	0.5336	5351	5350	702	705	62	52	
C2-680	PQT-011	12-15-64	008	Water Cooled	106372	131	1	+ 0.4	70.1	70.1	1.511	1.497	0.3339	0.3319	5313	5313	715	715	56	53	Previbration firing with AT-1 program tape.
							2	+ 35.6	92.3	92.4	1.517	1.501	0.4352	0.4334	5368	5368	711	711	56	52	
							3	+ 71.0	111.6	111.9	1.499	1.482	0.5255	0.5245	5379	5378	707	708	56	51	
							4	+ 35.4	92.1	92.1	1.513	1.497	0.4334	0.4312	5382	5382	712	712	56	51	
							5	0	69.6	69.5	1.511	1.495	0.3295	0.3272	5346	5346	715	715	56	51	
							6	- 35.2	45.4	45.3	1.524	1.507	0.2207	0.2187	5209	5209	718	718	56	51	
							7	- 80.0	21.0	21.0	1.515	1.499	0.1081	0.1069	4937	4938	721	720	56	51	
							8	- 50.4	35.0	34.8	1.509	1.494	0.1742	0.1725	5077	5077	720	719	56	51	
							9	- 35.6	45.7	45.5	1.525	1.509	0.2225	0.2204	5192	5192	718	718	56	51	
							10	- 0.6	69.9	69.8	1.515	1.499	0.3317	0.3294	5333	5332	715	715	56	51	
							11	+ 78.6	115.8	115.8	1.488	1.470	0.5458	0.5448	5361	5359	707	708	56	51	
							12	- 2.6	67.9	67.8	1.509	1.492	0.3224	0.3201	5327	5327	715	715	56	51	
							13	+ 66.8	110.1	110.4	1.504	1.486	0.5202	0.5191	5360	5359	707	708	56	51	
C2-709A	PQT-011	1-7-65	008	Abl.	106546 S/N 007	15	1	+ 70.0	108.4	108.4	1.644	1.501	0.5131	0.5127	5356	5358	639	749	52	50	Post-vibration TCA durability test at maximum thrust and mixture ratio.
							2	+ 70.0	108.4	108.3	1.626	1.483	0.5155	0.5149	5331	5331	639	750	53	49	
C2-709B	PQT-011	1-7-65	008	Abl.	106546 S/N 007	50	3	+ 69.4	109.3	109.0	1.625	1.481	0.5215	0.5201	5311	5310	640	753	51	50	
							4	+ 69.4	108.6	108.2	1.627	1.483	0.5172	0.5151	5322	5322	642	753	51	48	
C2-709C	PQT-011	1-7-65	008	Abl.	106546 S/N 007	235	5	+ 70.4	109.2	109.0	1.607	1.471	0.5189	0.5185	5332	5330	642	752	54	54	
							6	+ 70.4	107.4	107.2	1.612	1.474	0.5122	0.5116	5313	5311	642	752	54	52	
C2-710	PQT-011	1-7-65	008	Water Cooled	106372	128	1	0	69.9	69.9	1.503	1.486	0.3316	0.3295	5389	5388	712	714	51	51	Post-vibration acceptance test with AT-1 tape program.
							2	+ 35.4	91.5	91.6	1.493	1.476	0.4330	0.4312	5403	5402	708	710	51	50	
							3	+ 70.8	110.4	110.8	1.479	1.458	0.5223	0.5213	5408	5407	703	708	51	49	
							4	+ 35.0	91.4	91.3	1.494	1.474	0.4313	0.4291	5415	5414	708	712	51	49	
							5	0	69.3	69.2	1.506	1.488	0.3293	0.3269	5381	5380	712	714	51	49	
							6	- 35.0	44.8	44.6	1.525	1.506	0.2192	0.2171	5218	5219	715	717	51	49	
							7	- 80.2	20.7	20.7	1.511	1.495	0.1071	0.1060	4952	4953	718	718	51	49	
							8	- 50.2	34.9	34.8	1.511	1.494	0.1738	0.1720	5136	5136	717	718	51	49	
							9	- 35.2	45.5	45.3	1.530	1.512	0.2219	0.2199	5231	5231	715	717	51	49	
							10	- 0.2	69.6	69.4	1.510	1.491	0.3315	0.3289	5361	5361	712	715	51	49	
							11	+ 80.0	114.7	115.0	1.476	1.456	0.5409	0.5401	5423	5422	703	707	51	49	
							12	- 0.8	68.8	68.5	1.506	1.488	0.3263	0.3229	5388	5387	717	718	51	49	
							13	+ 69.4	110.1	110.4	1.479	1.459	0.5206	0.5193	5410	5409	704	708	51	49	

TABLE D-2-1. (Continued)

IRTS Test No.	Development Plan or PQT Test No.	Test Date	HEA S/N	CC & NA Type	CC & NA S/N	Test Duration secs	Data Slice No.	Servo Command ma	Head-End P, psia Site	Head-End P, psia Standard	MR, o/f Site	MR, o/f Standard	Total Flowrate lbs/sec Site	Total Flowrate lbs/sec Standard	Corrected C* fps Site	Corrected C* fps Standard	Fuel Inlet Pressure psia	Oxidizer Inlet Pressure psia	Fuel Inlet Temperature °F	Oxidizer Inlet Temperature °F	Remarks
C2-682A	None	12-22-64	009	Water Cooled	106372	255	1	+ 52.4	103.6	104.8	1.497	1.478	0.4929	0.4919	5336	5335	705	708	53	50	Manual step throttle performance checkout firing prior to acceptance firing.
							2	+ 70.0	114.0	114.4	1.504	1.482	0.5391	0.5386	5322	5321	702	707	53	50	
							3	+ 52.6	104.1	104.3	1.518	1.498	0.4915	0.4904	5329	5328	705	708	53	50	
							4	+ 35.2	93.5	93.5	1.519	1.497	0.4419	0.4399	5323	5323	707	712	53	50	
							5	+ 17.8	82.1	82.0	1.524	1.503	0.3883	0.3861	5314	5314	709	713	53	50	
							6	+ 0.4	70.2	70.0	1.523	1.502	0.3327	0.3304	5300	5300	711	715	53	50	
							7	- 17.2	57.9	57.7	1.526	1.505	0.2756	0.2733	5277	5277	713	717	53	50	
							8	- 34.6	44.5	44.3	1.537	1.517	0.2172	0.2152	5144	5144	715	718	53	50	
							9	- 52.0	30.7	30.5	1.552	1.529	0.1580	0.1562	4880	4881	716	721	53	50	
							10	- 70.0	20.0	20.0	1.583	1.560	0.1040	0.1027	4848	4851	717	722	53	50	
							11	- 52.0	31.7	31.6	1.544	1.522	0.1619	0.1602	4924	4925	716	721	53	50	
							12	- 34.6	45.3	45.1	1.539	1.518	0.2207	0.2186	5155	5156	715	719	53	50	
							13	- 17.2	58.4	58.2	1.528	1.506	0.2780	0.2755	5279	5279	714	718	53	50	
							14	+ 0.4	70.6	70.4	1.518	1.497	0.3343	0.3318	5308	5308	712	716	53	50	
							15	+ 17.8	82.6	82.5	1.529	1.508	0.3914	0.3890	5305	5304	710	714	53	50	
							16	+ 35.2	93.8	93.8	1.524	1.502	0.4439	0.4415	5316	5315	708	713	53	49	
							17	+ 52.6	104.5	104.6	1.523	1.500	0.4935	0.4915	5330	5329	706	711	53	49	
							18	+ 70.0	114.6	115.0	1.511	1.489	0.5418	0.5409	5326	5324	703	708	53	49	
C2-683	None	12-22-64	009	Water Cooled	106372	131	1	+ 0.8	70.3	70.3	1.514	1.502	0.3347	0.3328	5280	5280	715	714	54	54	Acceptance test with AT-1 thrust program tape.
							2	+ 36.0	93.6	93.7	1.518	1.506	0.4448	0.4434	5290	5289	711	709	54	52	
							3	+ 71.4	114.6	115.0	1.501	1.486	0.5427	0.5420	5315	5314	707	706	54	51	
							4	+ 35.8	93.9	93.9	1.520	1.505	0.4453	0.4433	5304	5304	711	710	54	50	
							5	+ 0.8	70.3	70.1	1.521	1.498	0.3335	0.3309	5302	5301	716	714	54	50	
							6	- 34.4	44.5	44.4	1.537	1.521	0.2171	0.2150	5158	5159	718	717	54	50	
							7	- 79.4	19.9	19.9	1.566	1.554	0.1044	0.1032	4806	4807	722	718	54	50	
							8	- 49.6	32.6	32.4	1.537	1.524	0.1670	0.1652	4904	4904	721	718	54	50	
							9	- 34.4	44.6	44.5	1.537	1.522	0.2183	0.2162	5138	5139	718	717	54	50	
							10	+ 0.6	70.4	70.3	1.518	1.502	0.3342	0.3318	5300	5300	715	714	54	50	
							11	+ 81.4	117.4	117.8	1.515	1.496	0.5560	0.5550	5316	5314	705	707	54	50	
C2-685	None	12-23-64	010	Water Cooled	106372	142	1	+ 70.2	106.0	106.3	1.523	1.509	0.5366	0.5361	4968	4968	705	705	51	50	First performance checkout firing after DY-49 at JPL/ETS.
							2	+ 0.6	64.1	63.9	1.511	1.497	0.3217	0.3193	5007	5007	714	714	51	50	
							3	- 69.8	19.0	18.9	1.550	1.535	0.0939	0.0928	5088	5089	719	719	51	50	
							4	- 52.0	29.1	29.0	1.520	1.505	0.1527	0.1512	4785	4796	718	718	51	50	
							5	+ 70.2	106.7	106.9	1.524	1.507	0.5372	0.5362	4995	4994	705	707	51	50	
							6	+ 70.2	109.7	109.9	1.520	1.504	0.5406	0.5392	5105	5105	707	707	51	50	
							7	+ 70.4	109.9	110.1	1.520	1.504	0.5406	0.5386	5122	5121	707	707	51	50	
							8	+ 0.8	63.2	63.0	1.511	1.497	0.3235	0.3208	4907	4907	716	715	51	50	
							9	+ 70.4	104.9	105.0	1.519	1.504	0.5388	0.5374	4894	4894	707	707	51	51	
							10	+ 0.6	63.0	62.7	1.509	1.494	0.3212	0.3204	4895	4895	716	715	51	50	
							11	- 69.6	18.9	18.8	1.554	1.542	0.0945	0.0934	5031	5032	722	719	51	50	
							12	- 51.8	28.5	28.3	1.520	1.507	0.1536	0.1511	4659	4660	721	719	51	50	
							13	+ 70.6	109.5	109.6	1.521	1.507	0.5380	0.5364	5113	5118	708	707	51	50	
							14	+ 70.6	105.1	105.1	1.521	1.507	0.5382	0.5376	4898	4897	708	707	51	50	

TABLE D-2-1. (Continued)

IRTS Test No.	Development Plan or PQT Test No.	Test Date	HEA S/N	CC & NA Type	CC & NA S/N	Test Duration secs	Data Slice No.	Servo Command ma	Head-End P_c psia Site	Head-End P_c psia Standard	MR, o/f Site	MR, o/f Standard	Total Flowrate lbs/sec Site	Total Flowrate lbs/sec Standard	Corrected C* fps Site	Corrected C* fps Standard	Fuel Inlet Pressure psia	Oxidizer Inlet Pressure psia	Fuel Inlet Temperature °F	Oxidizer Inlet Temperature °F	Remarks
C2-686	None	12-28-64	010	Water Cooled	106372	75	1	+ 70.0	113.9	114.6	1.511	1.498	0.5333	0.5340	5378	5377	704	705	53	54	Performance checkout firing after removing metal chip from fuel injector.
							2	+ 0.2	66.3	66.2	1.495	1.482	0.3187	0.3170	5226	5225	713	714	53	54	
							3	- 69.8	19.2	19.1	1.542	1.530	0.0929	0.0920	5191	5192	719	719	53	54	
							4	- 52.4	27.9	27.8	1.501	1.489	0.1489	0.1477	4701	4701	718	718	53	54	
							5	+ 70.0	111.8	112.5	1.511	1.496	0.5339	0.5341	5275	5274	704	707	53	54	
							6	+ 70.0	114.5	115.1	1.514	1.499	0.5352	0.5354	5386	5386	704	707	53	54	
C2-689A	None	12-29-64	010	Water Cooled	106372	235	1	+ 70.2	110.0	109.8	1.460	1.441	0.5205	0.5171	5320	5318	708	711	46	46	ΔP shift studies with plugged Q.D.
							2	+ 52.6	100.0	99.7	1.457	1.439	0.4729	0.4693	5323	5321	710	712	46	46	
							3	+ 35.2	89.4	89.0	1.477	1.459	0.4224	0.4185	5326	5325	713	714	46	46	
							4	+ 17.6	77.9	77.5	1.468	1.450	0.3691	0.3653	5311	5310	714	716	46	46	
							5	+ 0.6	65.9	65.5	1.459	1.441	0.3118	0.3081	5317	5315	716	718	46	46	
							6	- 17.0	53.7	53.3	1.465	1.447	0.2545	0.2512	5303	5302	718	719	46	46	
							7	- 34.6	41.4	41.0	1.465	1.446	0.1985	0.1958	5237	5236	719	721	46	46	
							8	- 52.4	28.7	28.4	1.454	1.437	0.1420	0.1399	5077	5076	721	722	46	46	
							9	- 70.0	18.9	18.8	1.486	1.468	0.0883	0.0869	5393	5394	722	723	46	46	
							10	- 53.4	29.3	29.1	1.452	1.435	0.1446	0.1425	5104	5103	721	722	46	46	
							11	- 34.8	41.8	41.5	1.459	1.440	0.2007	0.1980	5236	5235	719	721	46	46	
							12	- 17.0	53.8	53.4	1.453	1.435	0.2560	0.2527	5287	5285	718	719	46	46	
							13	+ 0.4	66.3	65.8	1.452	1.435	0.3136	0.3099	5314	5312	717	718	46	46	
							14	+ 17.8	78.1	77.7	1.471	1.454	0.3701	0.3664	5306	5305	714	715	46	46	
							15	+ 35.2	89.5	89.1	1.478	1.460	0.4236	0.4197	5314	5313	713	714	46	46	
							16	+ 52.6	100.0	99.7	1.454	1.435	0.4739	0.4705	5310	5307	709	712	46	46	
							17	+ 70.2	110.5	110.3	1.463	1.443	0.5233	0.5202	5312	5310	707	710	46	46	
C2-676	None	12-14-64	011	Water Cooled	106372	160	1	+ 69.8	111.3	111.9	1.469	1.455	0.5255	0.5254	5333	5333	707	708	58	54	Manual step thrust performance checkout firing.
							2	+ 52.2	101.4	101.8	1.460	1.444	0.4781	0.4772	5342	5341	708	711	57	54	
							3	+ 34.8	91.9	92.1	1.476	1.461	0.4329	0.4313	5343	5343	711	713	57	54	
							4	+ 17.2	81.8	81.8	1.468	1.454	0.3850	0.3832	5344	5343	713	714	57	54	
							5	0.0	71.2	71.3	1.467	1.452	0.3356	0.3337	5341	5341	714	715	57	54	
							6	- 17.4	60.3	60.3	1.464	1.449	0.2857	0.2838	5313	5313	715	717	57	54	
							7	- 35.0	49.1	49.0	1.500	1.485	0.2365	0.2347	5217	5217	717	718	57	54	
							8	- 52.6	36.9	36.9	1.484	1.470	0.1835	0.1821	5055	5055	718	718	57	54	
							9	- 70.0	25.2	25.2	1.494	1.479	0.1320	0.1308	4810	4811	719	720	57	54	
							10	- 52.6	38.2	38.2	1.490	1.475	0.1894	0.1878	5076	5076	718	719	57	54	
							11	- 35.2	50.1	50.1	1.503	1.487	0.2406	0.2383	5237	5237	716	718	57	54	
							12	- 17.6	61.3	61.3	1.473	1.456	0.2900	0.2882	5318	5317	714	717	57	54	
							13	0.0	71.8	71.9	1.469	1.453	0.3392	0.3374	5328	5327	713	715	57	54	
							14	+ 17.2	82.4	82.5	1.470	1.454	0.3886	0.3868	5337	5337	712	714	57	54	
							15	+ 34.6	92.5	92.7	1.476	1.459	0.4356	0.4343	5345	5344	709	712	57	54	
							16	+ 52.0	102.3	102.7	1.466	1.448	0.4826	0.4816	5340	5339	707	711	57	54	
							17	+ 69.6	111.8	112.4	1.472	1.454	0.5280	0.5277	5334	5333	705	709	57	54	

FIGURE D-2-2. VACUUM THRUST VS. ACTUATOR SIGNAL AT 1.5 MIXTURE RATIO FOR MIRA 150A-005

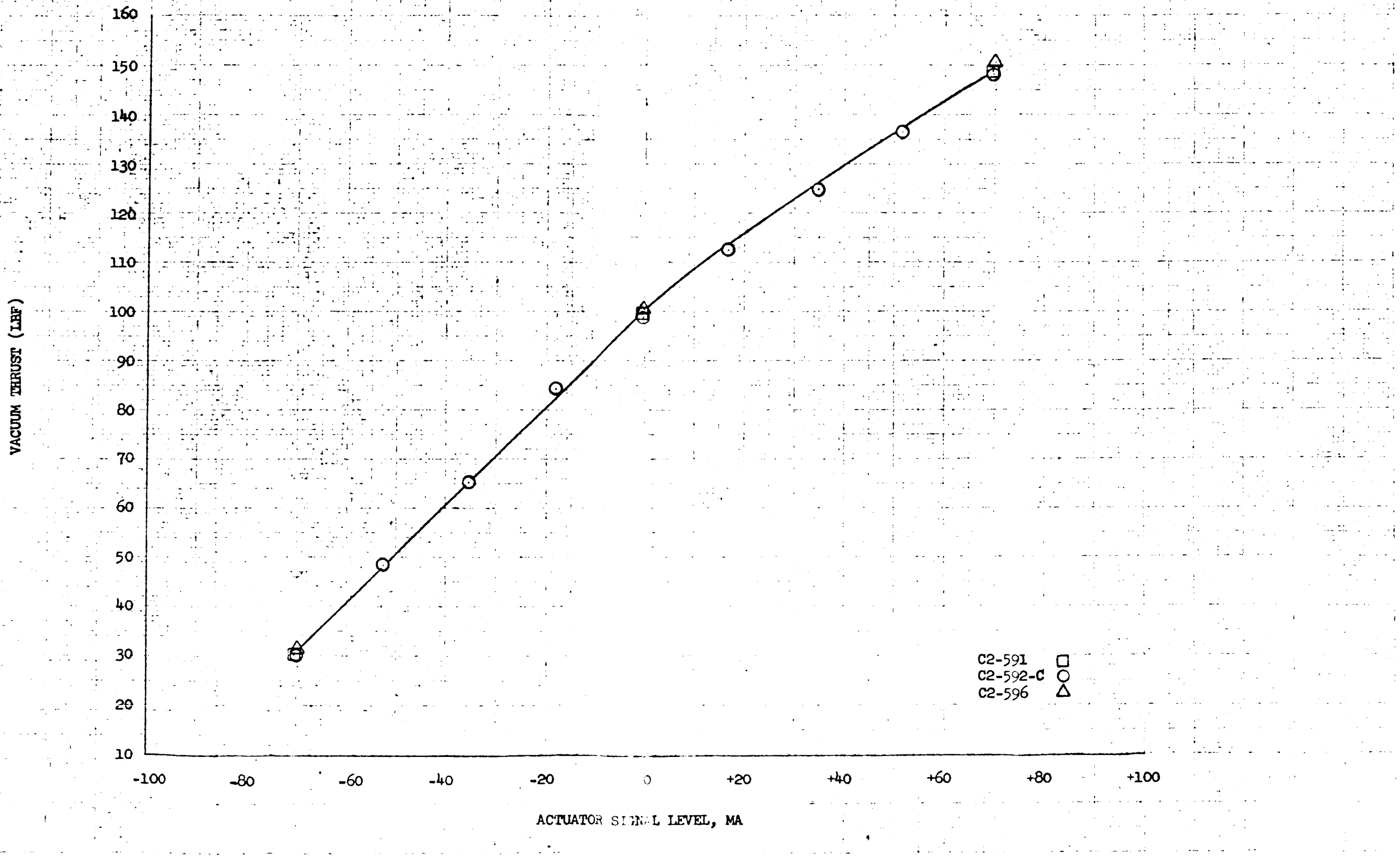

FIGURE D-2-3. CHARACTERISTIC EXHAUST VELOCITY VS. NOZZLE STAGNATION PRESSURE AT 1.5 MIXTURE RATIO FOR MIRA 150A-005

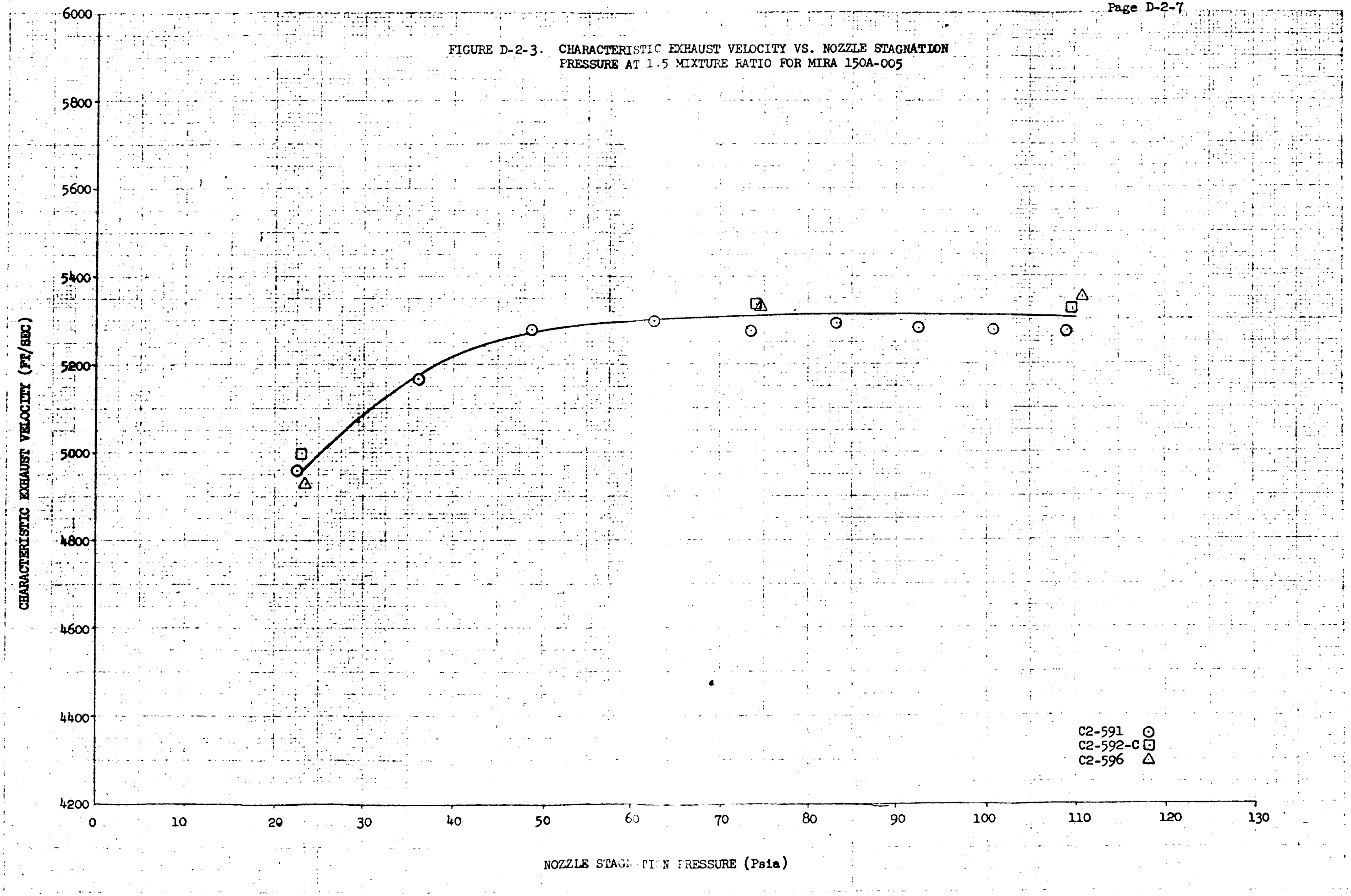

FIGURE D-2-4. MIXTURE RATIO VS. VACUUM THRUST AT STANDARD CONDITIONS FOR MIRA 150A-005

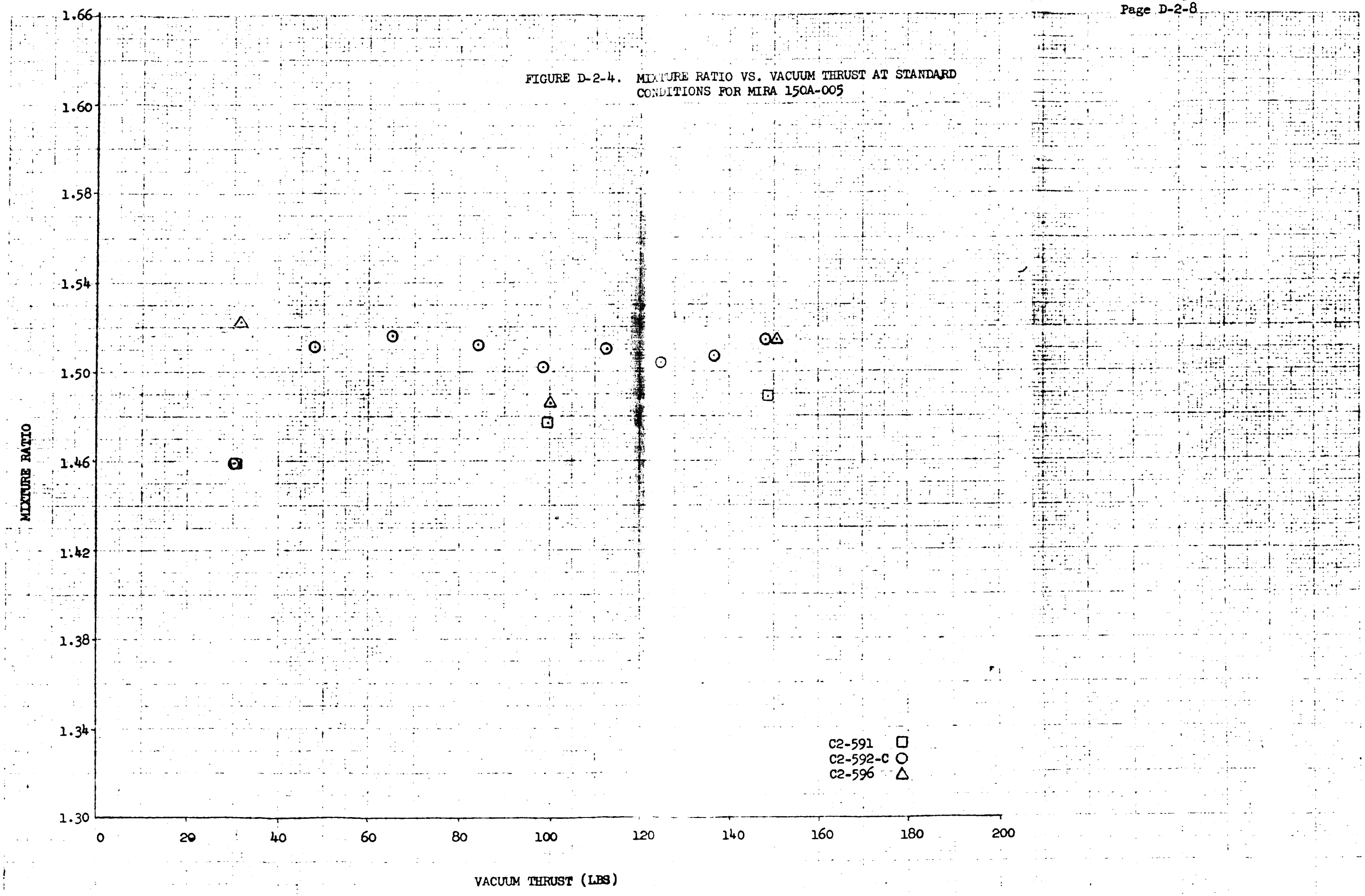

97

FIGURE D-2-5. VACUUM THRUST VS. ACTUATOR SIGNAL AT 1.5 MIXTURE RATIO FOR MIRA 150A-007

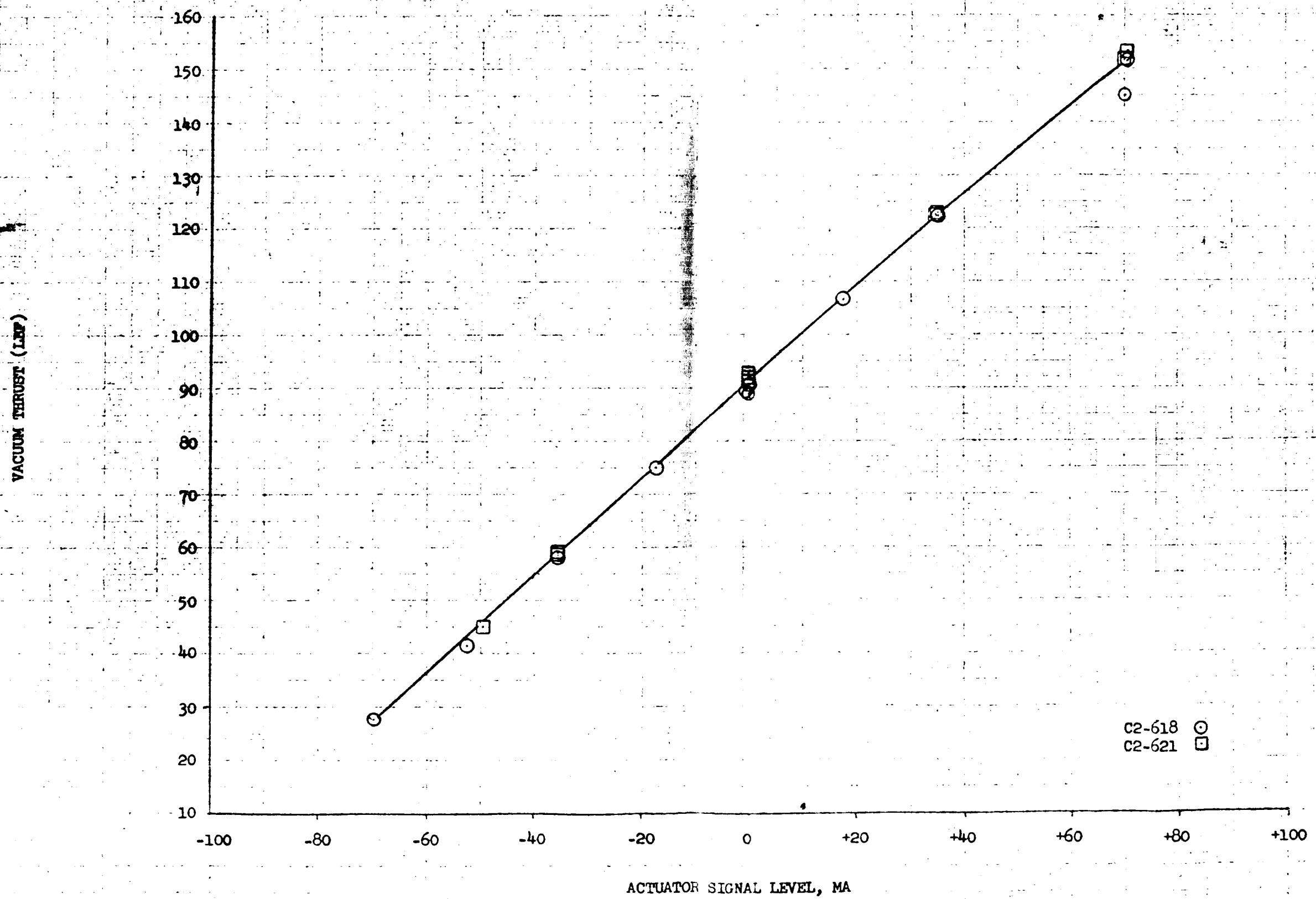

FIGURE D-2-6. CHARACTERISTIC EXHAUST VELOCITY VS. NOZZLE STAGNATION PRESSURE AT 1.5 MIXTURE RATIO FOR MIRA 150A-007

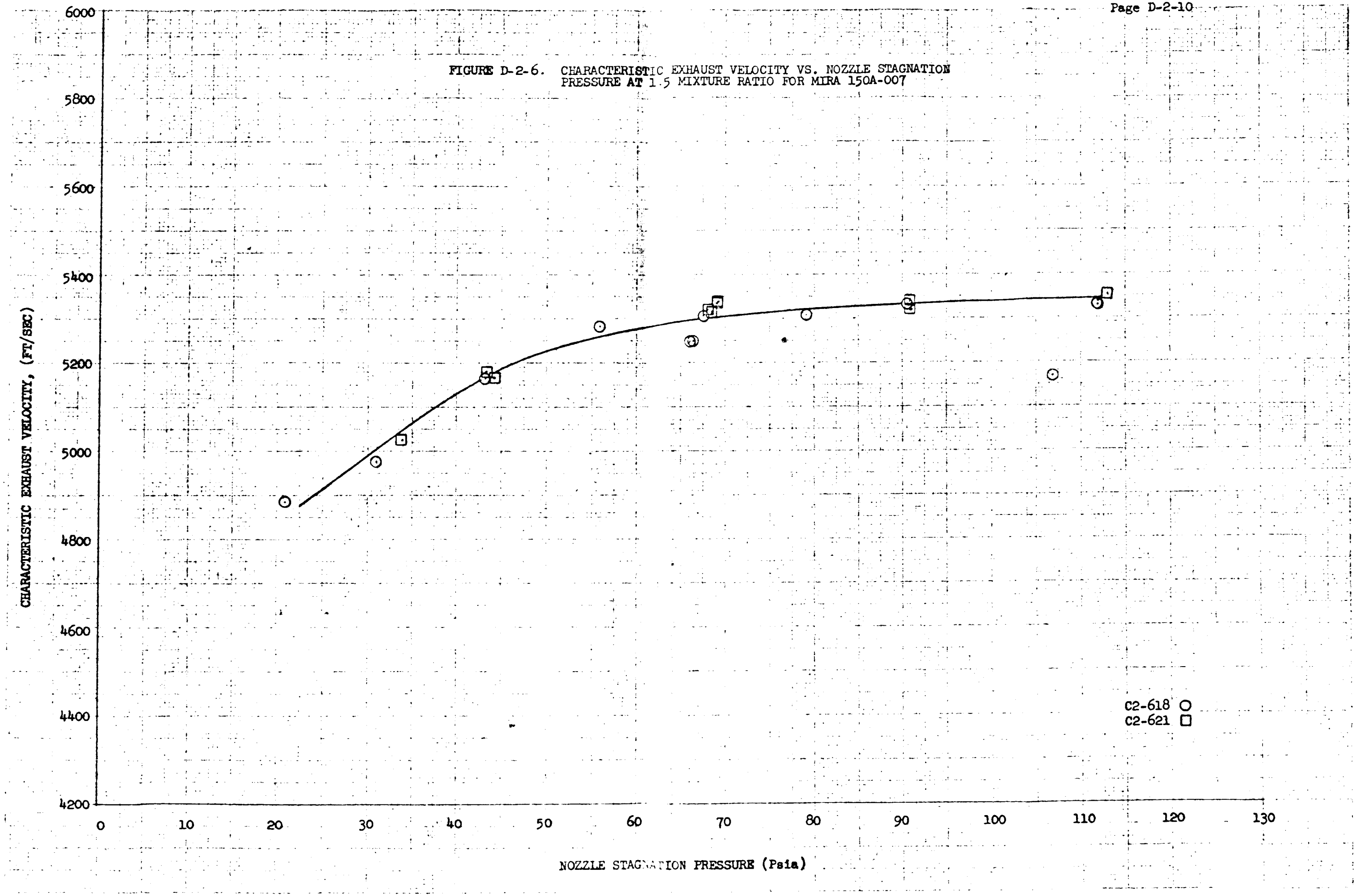

FIGURE D-2-7. MIXTURE RATIO VS. VACUUM THRUST AT STANDARD CONDITIONS FOR MIRA 150A-007

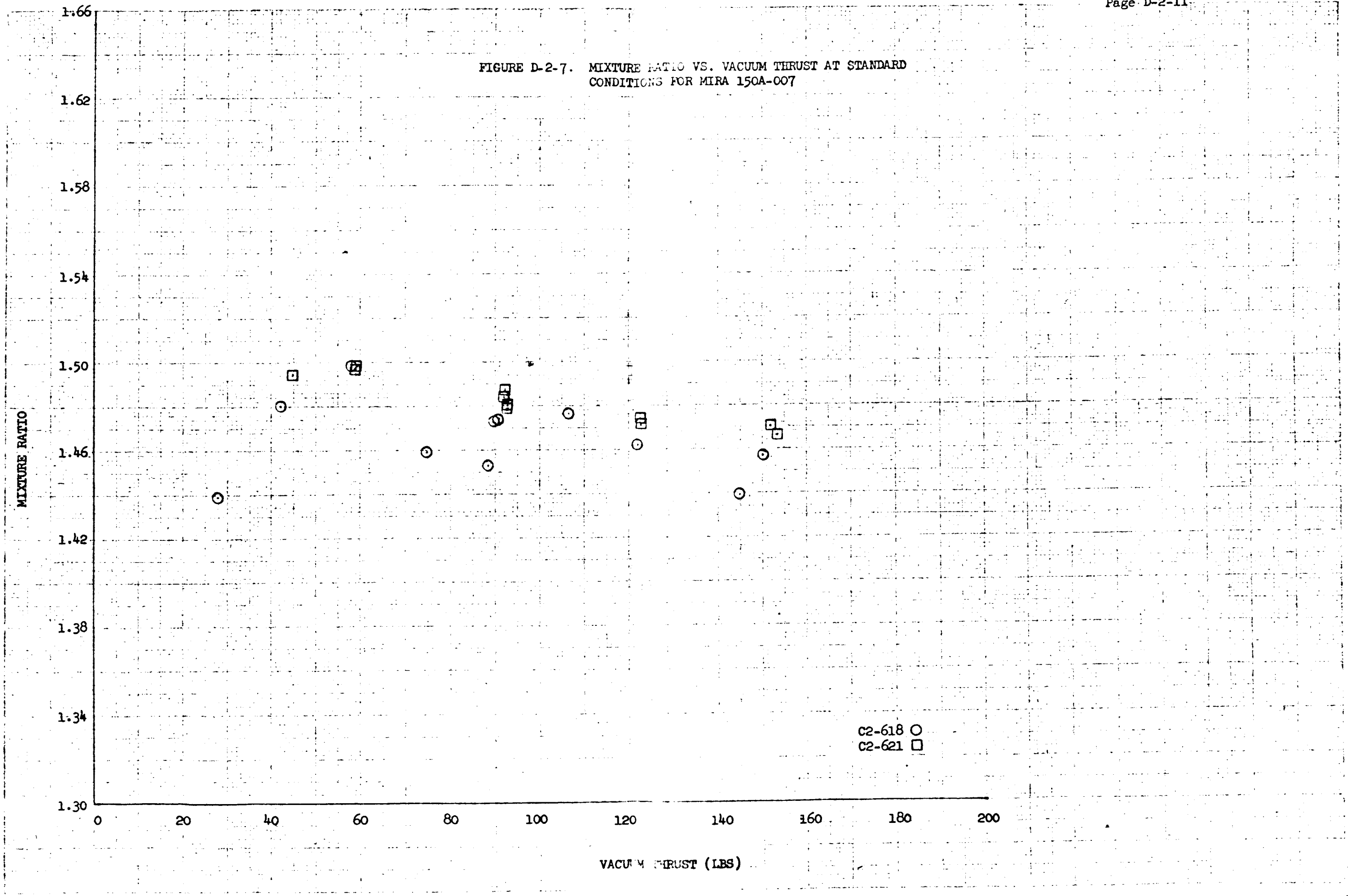

FIGURE D-2-8. VACUUM THRUST VS. ACTUATOR SIGNAL AT 1.6 MIXTURE RATIO FOR MIRA 150A-008

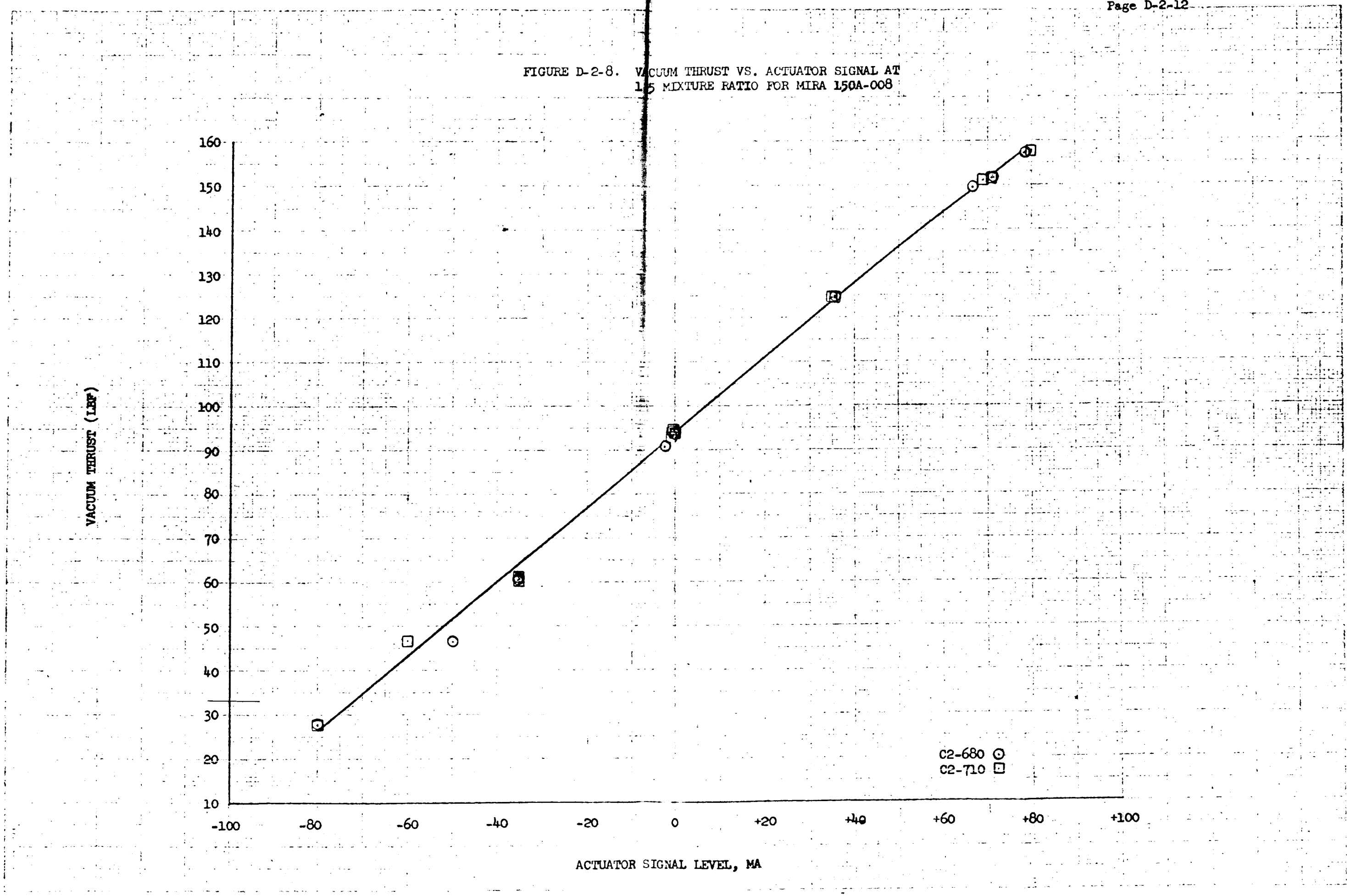

101

FIGURE D-2-9. CHARACTERISTIC EXHAUST VELOCITY VS. NOZZLE STAGNATION PRESSURE AT 1.5 MIXTURE RATIO FOR MIRA 150A-008

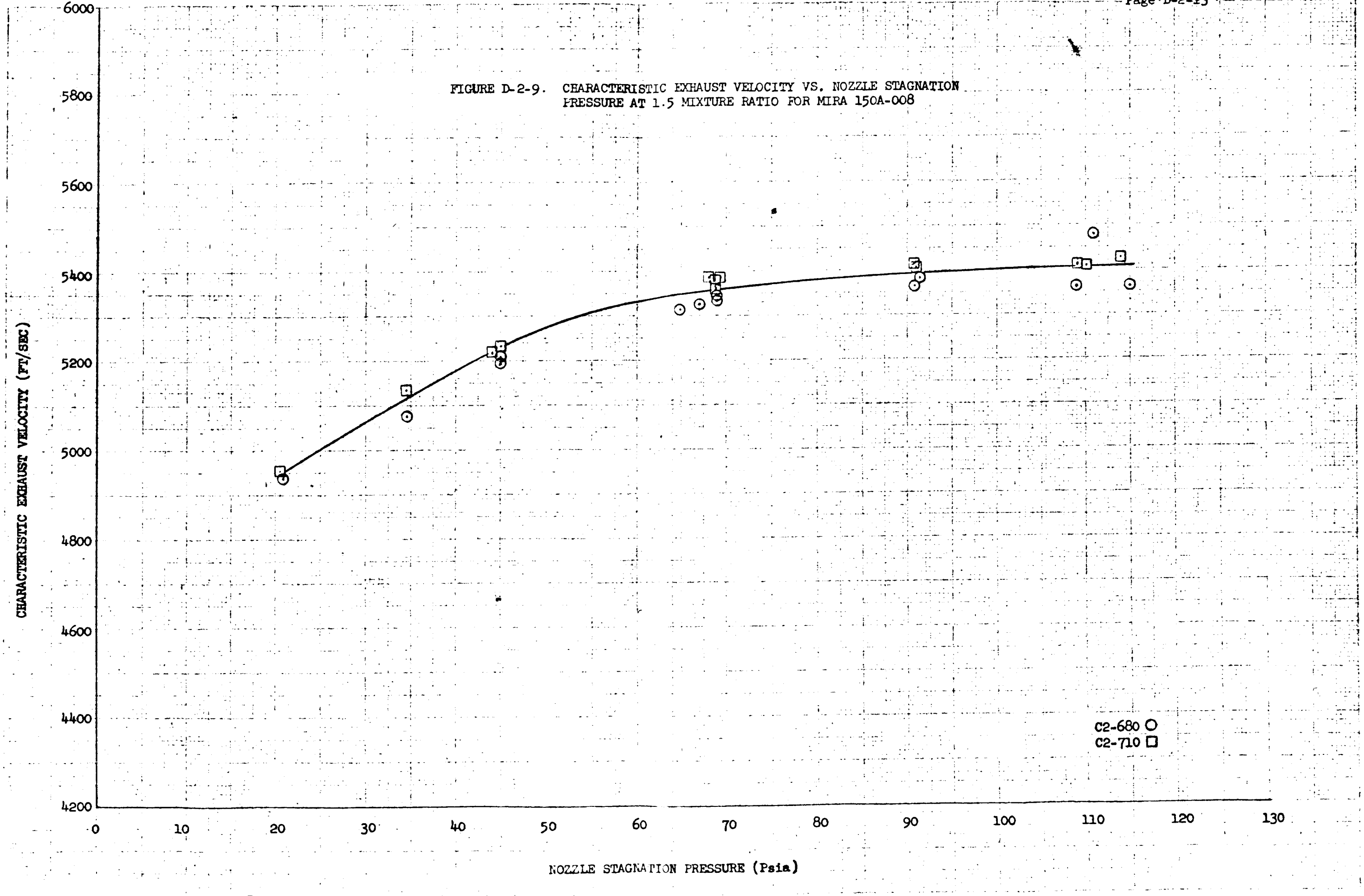

FIGURE D-2-10. MIXTURE RATIO VS. VACUUM THRUST AT STANDARD CONDITIONS FOR MIRA 150A-008

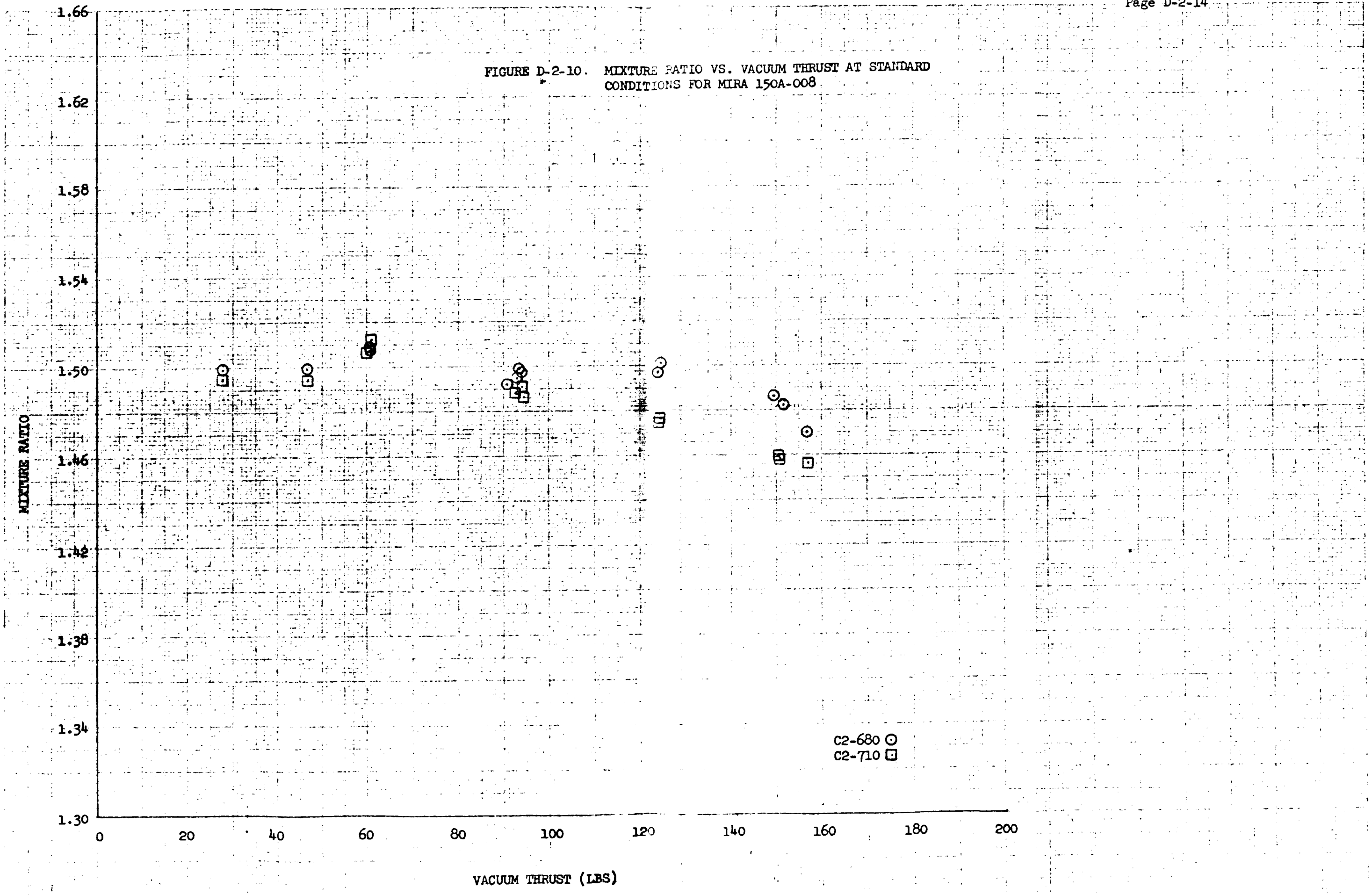

FIGURE D-2-11. VACUUM THRUST VS. ACTUATOR SIGNAT AT 1.5 MIXTURE RATIO FOR MIRA 150A-009

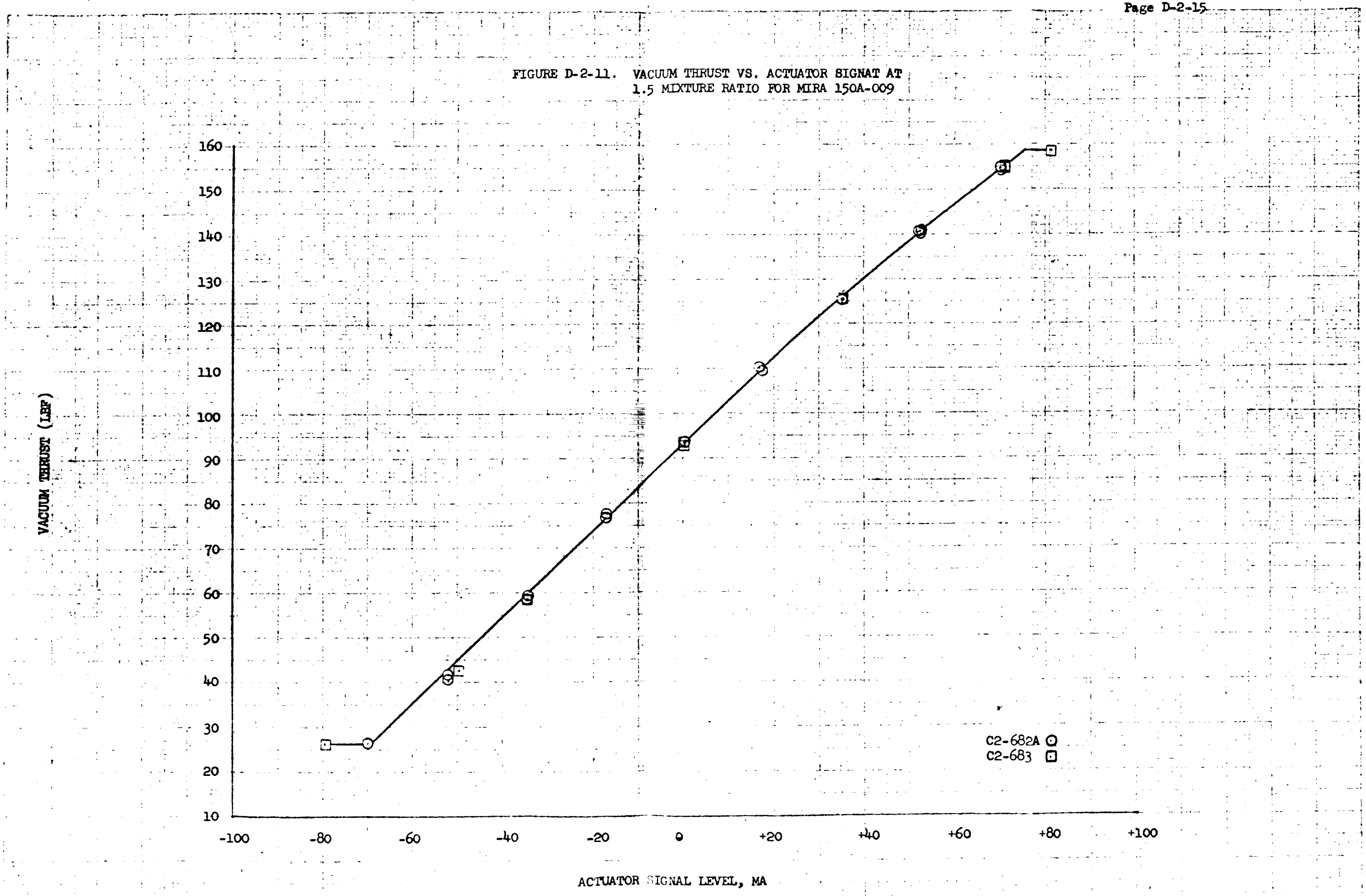

FIGURE D-2-12. CHARACTERISTIC EXHAUST VELOCITY VS. NOZZLE STAGNATION PRESSURE AT 1.5 MIXTURE RATIO FOR MIRA 150A-009

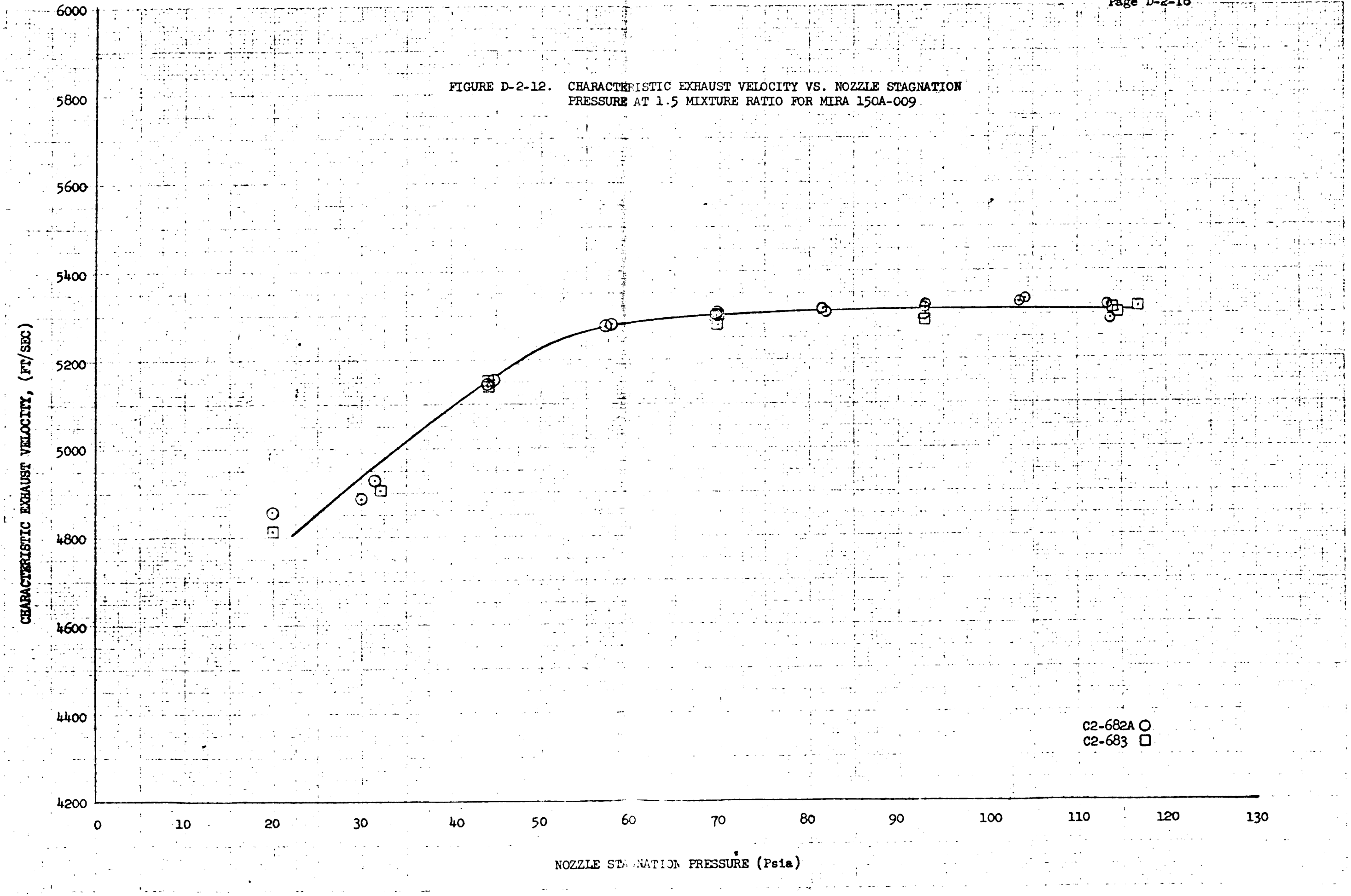

105

FIGURE D-2-13. MIXTURE RATIO VS. VACUUM THRUST AT STANDARD CONDITIONS FOR MIRA 150A-009

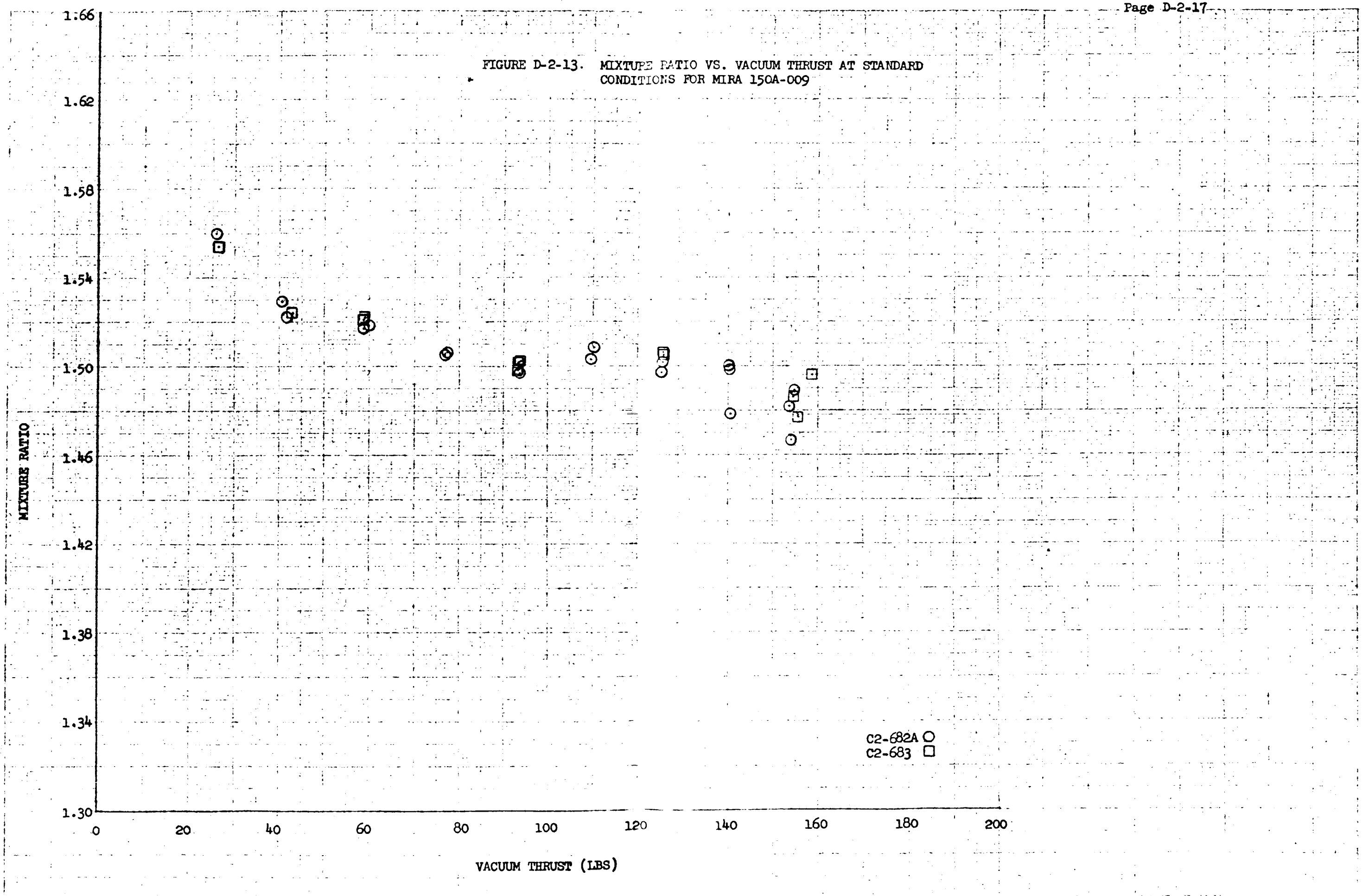

FIGURE D-2-14. VACUUM THRUST VS. ACTUATOR SIGNAL AT 1.5 MIXTURE RATIO FOR MIRA 150A-010

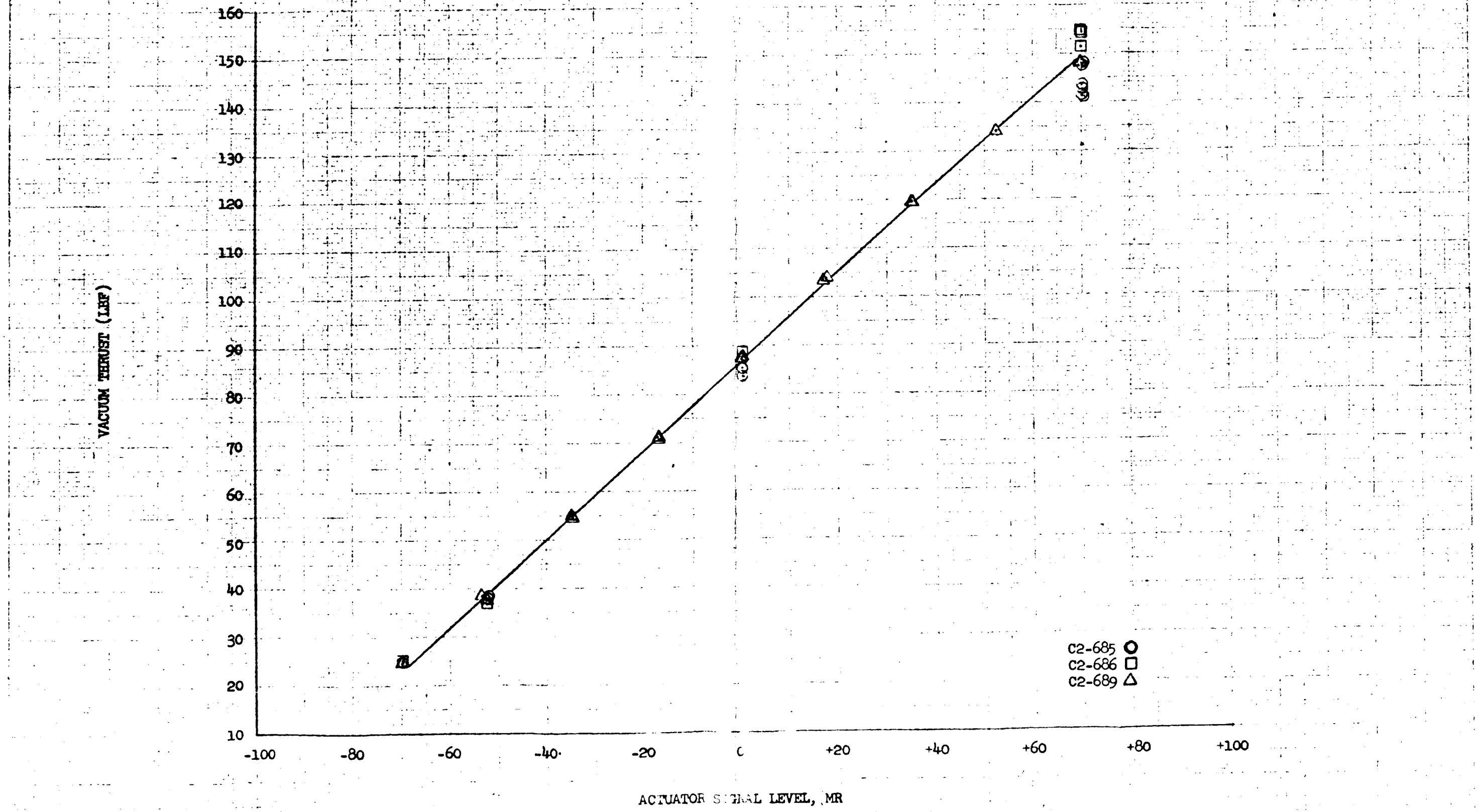

FIGURE D-2-15. CHARACTERISTIC EXHAUST VELOCITY VS. NOZZLE STAGNATION PRESSURE AT 1.5 MIXTURE RATIO FOR MIRA 150A-010

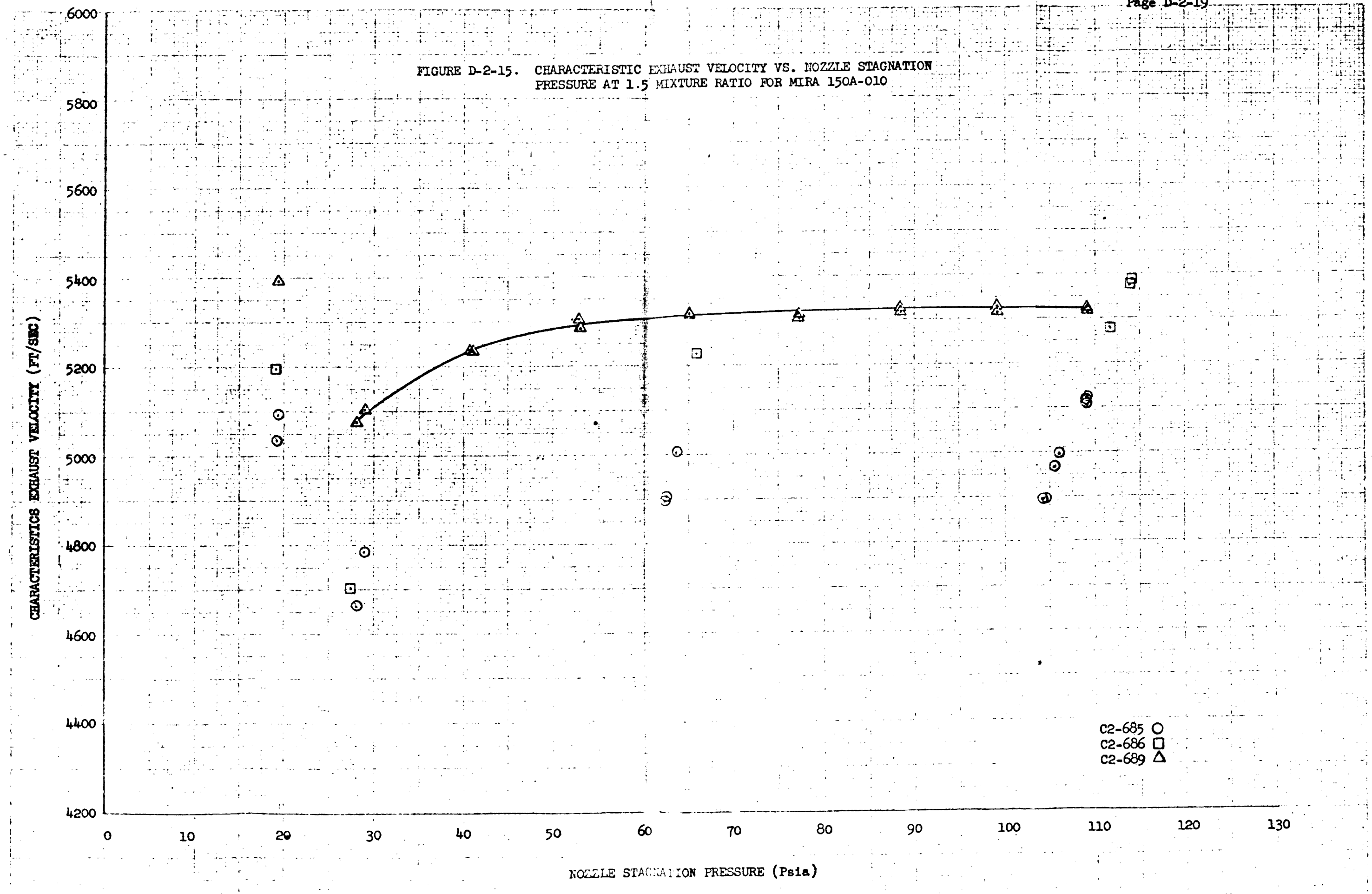

FIGURE D-2-16. MIXTURE RATIO VS. VACUUM THRUST AT STANDARD CONDITIONS FOR MIRA 150A-010

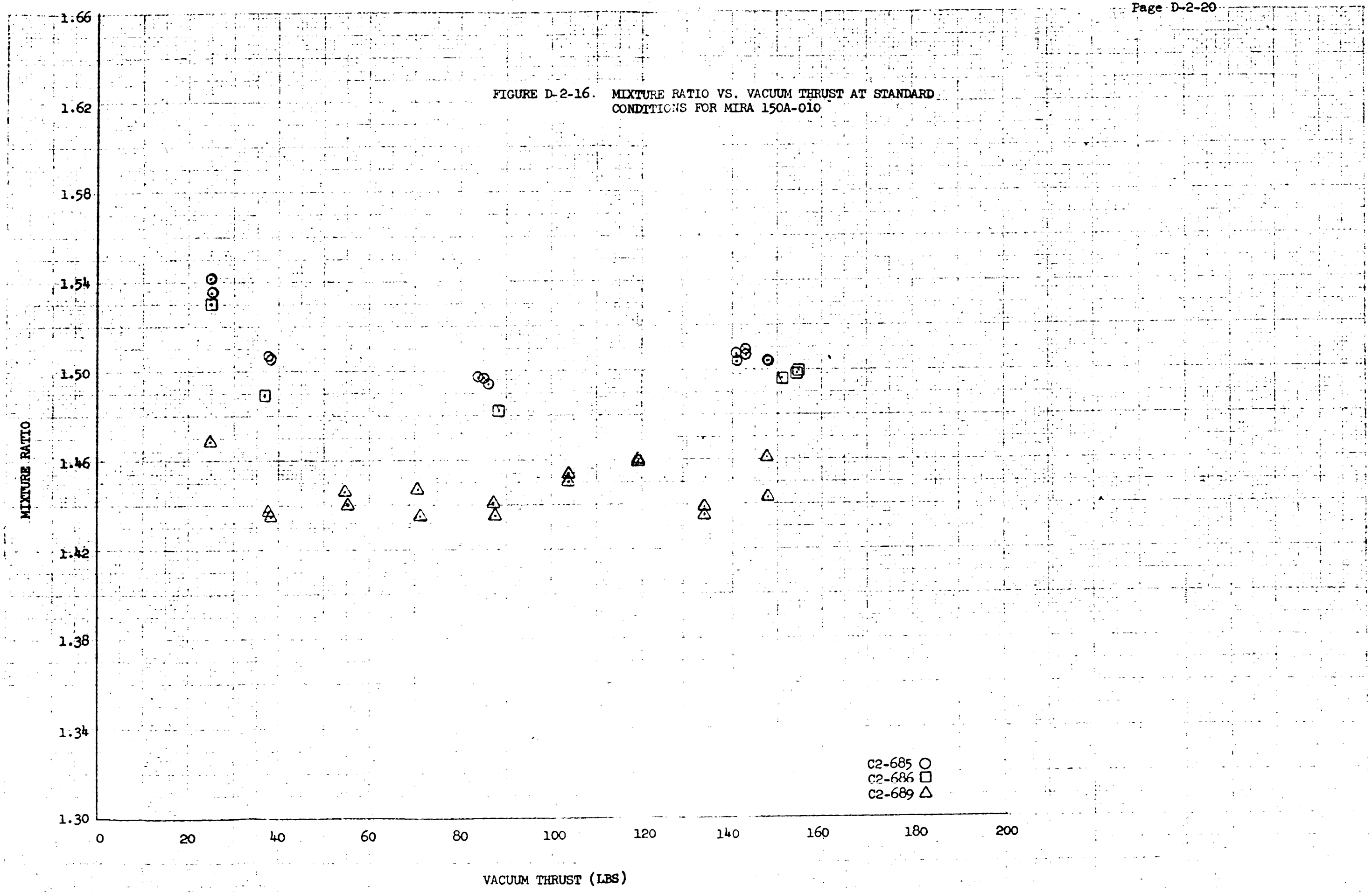

FIGURE D-2-17. VACUUM THRUST VS. ACTUATOR SIGNAL AT 1.5 MIXTURE RATIO FOR MIRA 150A-011

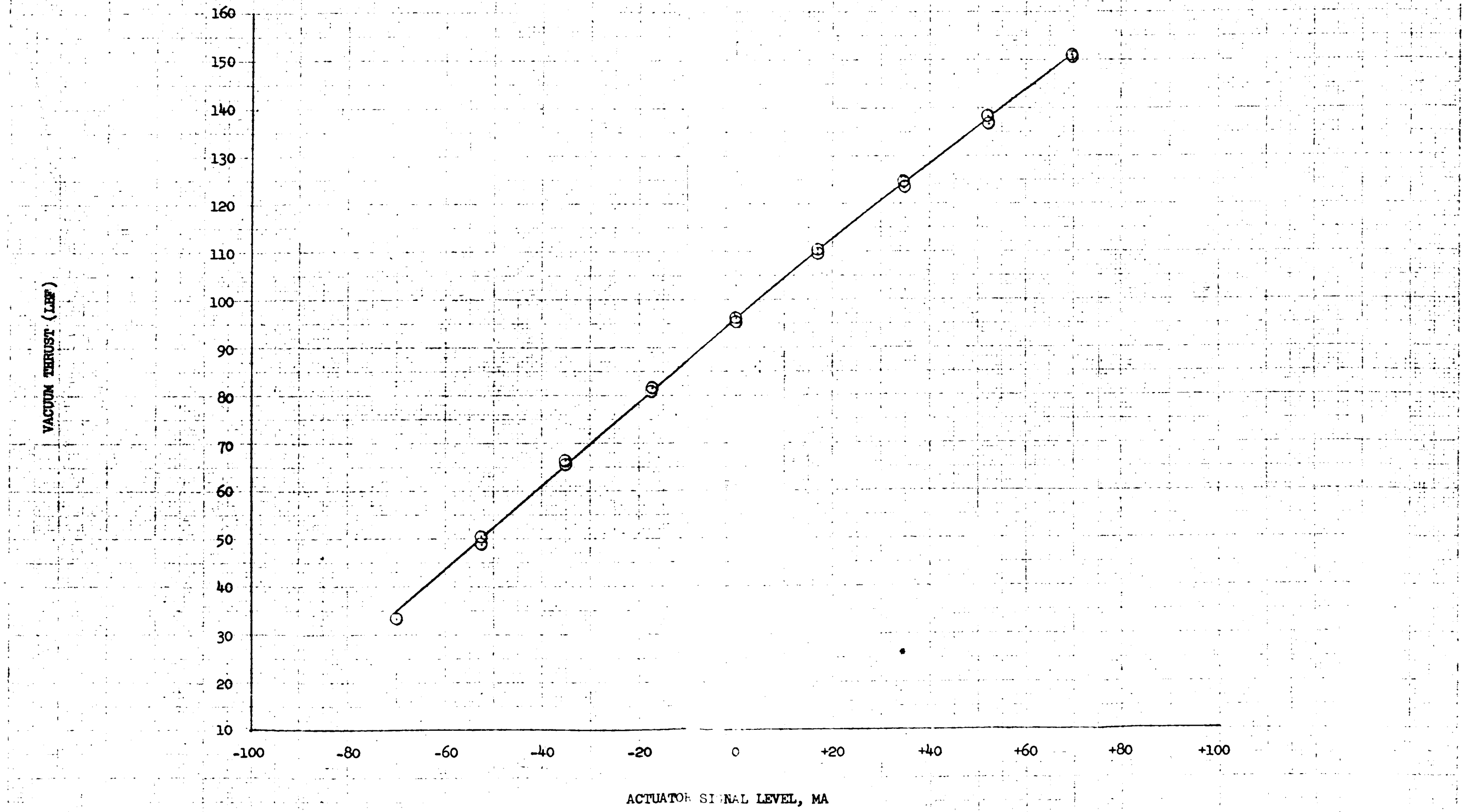

110

FIGURE D-2-18. CHARACTERISTIC VELOCITY VS. NOZZLE STAGNATION PRESSURE AT 1.5 MIXTURE RATIO FOR MIRA 150A-011

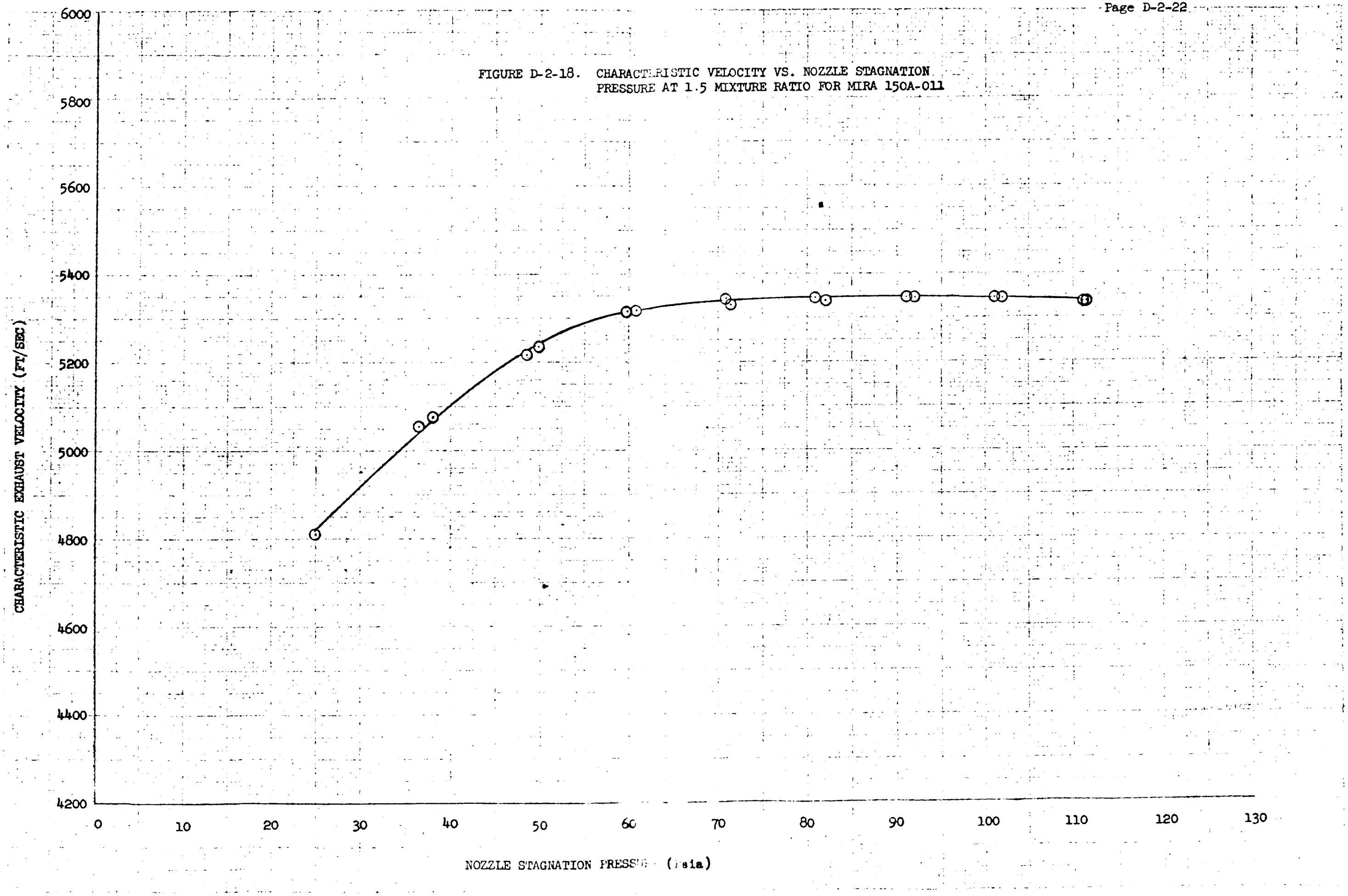

FIGURE D-2-19. MIXTURE RATIO VS. VACUUM THRUST AT STANDARD CONDITIONS FOR MIRA 150A-011

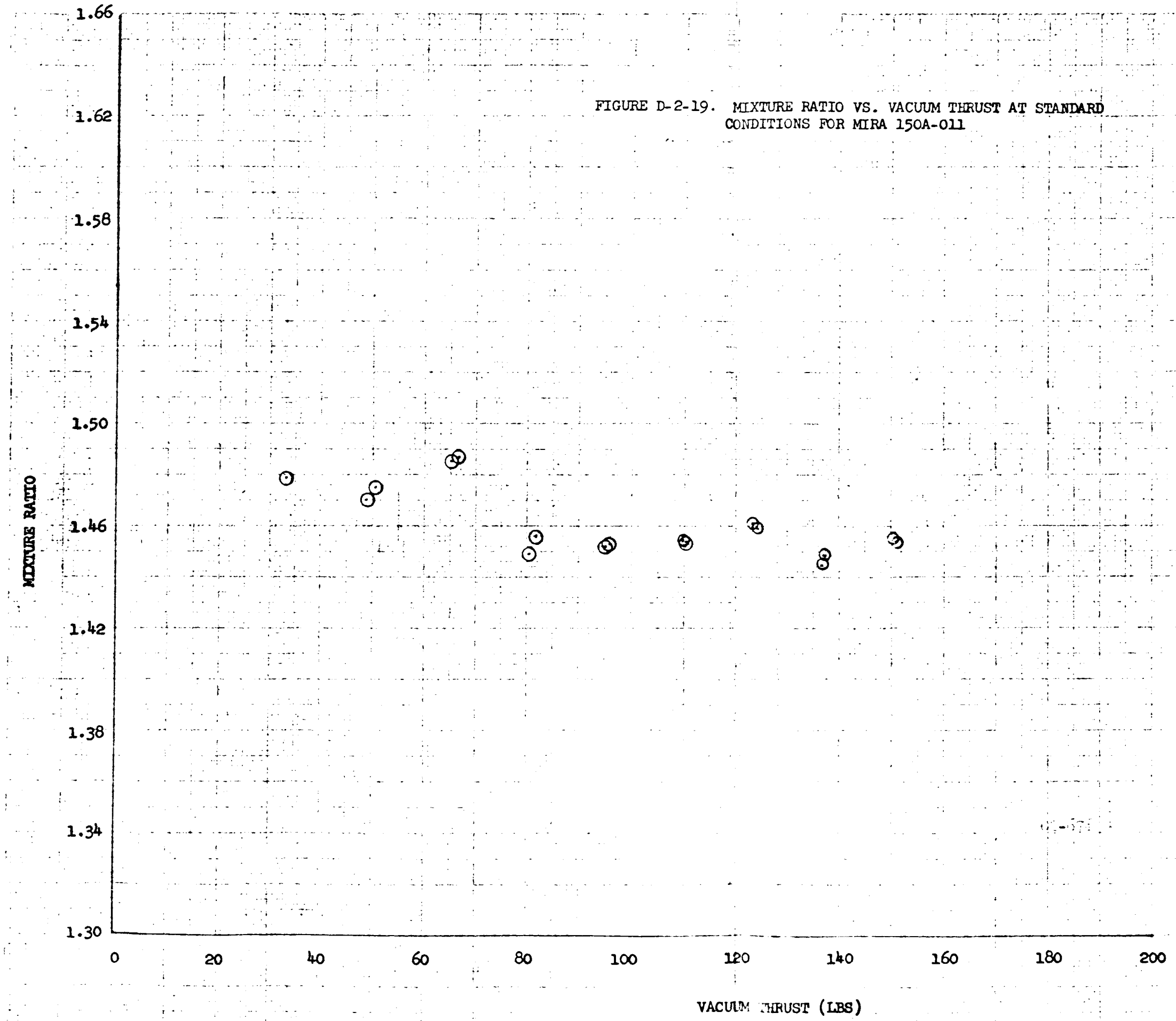

112

TABLE D-2-20. MIRA 150A TRANSIENT RESPONSE DATA FROM IRTS SEA LEVEL TESTS

IRTS Run No.	Development Plan or PQT Test No.	Test Date	HEA S/N	Servoactuator P/N	Servoactuator S/N	Helium Pilot Valve P/N	Helium Pilot Valve S/N	Propellant Bled Down to Shutoff Valve	Startup Time sec (1)	Startup Impulse lb/sec (2)	Startup Thrust Level lbs	Shutdown Time sec (3)	Shutdown Impulse lb/sec (4)	Shutdown Thrust Level lbs	Servoactuator Step Response: Step Size ma (5)	Servoactuator Step Response: Step Time sec Max	Servoactuator Step Response: Step Time sec Mean	Servoactuator 5 cps Response: Signal Amplitude ma	Servoactuator 5 cps Response: Phase Lag degrees	Large Ramp Loop Width ma	Large Ramp Gain lbs/ma	Remarks
C2-548	None	9-2-64	004	C104312	C53748	C104337	004	Yes	(6)	(6)	93	0.025	2.4	95	+110	0.038	0.038	-40 ± 7.5	14	3.9	0.71	HEA Acceptance Test with AT-1 thrust profile.
															-110	0.028	0.028	0 ± 7.5	13			
																		+62.5 ± 7.5	14			
C2-559	None	9-8-64	002	C104312	C53749	C104337	018	Yes	0.071	1.5	94	0.038	2.5	95				-40 ± 7.5	13	5.4	(6)	HEA Acceptance Test with AT-1 thrust profile.
															+110	0.023	0.023	0 ± 7.5	16			
															-110	0.023	0.023	+62.5 ± 7.5	15			
C2-564	None	9-11-64	001	C104312	C53750	C104337	010	Yes	0.082	2.6	93	(6)	(6)	94	+110	0.075	0.075	-40 ± 7.5	26	5.3	0.90	HEA Acceptance Test with AT-1 thrust profile.
															-110	0.022	0.022	0 ± 7.5	27			
																		+ 62.5 ± 7.5				
C2-568	None	9-18-64	005	C104312	C53747	C104337	019	Yes	0.066	1.9	95	0.154	16.4	94	+110	0.058	0.058	-40 ± 7.5	11	5.0	0.75	HEA Acceptance Test with AT-1 thrust profile.
															-110	0.071	0.071	0 ± 7.5	13			
																		+62.5 ± 7.5	13			
C2-571	None	9-24-64	002	C104312	C53751	C104337	018	Yes	0.044	3.4	92	0.020	2.3	93	+110	0.032	0.032	-40 ± 7.5	13	4.6	0.93	HEA Acceptance Test with AT-1 thrust profile.
															-110	0.023	0.023	0 ± 7.5	14			
																		+62.5 ± 7.5	10			
C2-621	None	11-3-64	007	C219217	C55390	C104337	023	Yes	0.076	2.0	92	0.048	4.6	92				-40 ± 7.5	15	2.3	1.0	HEA Acceptance Test with AT-1 thrust profile.
															+110	0.048	0.048	0 ± 7.5	16			
															-110	0.036	0.036	+62.5 ± 7.5	16			
C2-639	None	11-20-64	001	C104312	C53750	C104337	022	Yes	0.013	0.74	150	0.040	2.0	86	(6)	(6)	(6)	(6)	(6)	(6)	(6)	
C2-699	None	12-3-64	004	C219217	C55394	C104337-1	004	Yes	0.064	1.2	95	0.032	2.8	95	(6)	(6)	(6)	(6)	(6)	(6)	(6)	
C2-680	PQT-011	12-15-64	008	C219217	C55398	C104337	024	Yes	0.076	1.8	94	0.035	2.8	91	+140	0.056	0.056	(6)	(6)	(6)	(6)	HEA Acceptance Test with AT-1 thrust profile.
															-140	0.036	0.036					
C2-706B	None	1-5-65	010	C219217	C55394	C104337-1	026	Yes	0.039	0.94	148	0.029	4.0	149	(6)	(6)	(6)	(6)	(6)	(6)	(6)	Fixed thrust firing
C2-706C	None	1-5-65	010	C219217	C55394	C104337	026	Yes	0.038	0.86	150	0.029	3.9	150	(6)	(6)	(6)	(6)	(6)	(6)	(6)	Fixed thrust firing
C2-706D	None	1-5-65	010	C219217	C55394	C104337	026	Yes	0.013	0.94	149	0.028	3.8	150	(6)	(6)	(6)	(6)	(6)	(6)	(6)	Fixed thrust firing
C2-710	PQT-011	1-7-65	008	C219217	C55398	C104337-1	024	Yes	0.075	2.1	94	0.039	3.3	92	+140	0.046	0.046					
															-140	0.020	0.020					

NOTES: (1) The time from TCA receipt of startup signal to attainment of 95 percent of commanded thrust.
(2) The area under the derived thrust-time curve over the startup time interval.
(3) The time from TCA receipt of shutdown signal to attainment of 30 psia chamber pressure.
(4) The area under the derived thrust-time curve over the shutdown time interval.
(5) Positive signs indicate increasing thrust, and negative signs decreasing thrust steps.
(6) Data not available because of test conditions, instrumentation malfunctions, or data reduction errors.

TABLE D-2-21. MIRA 150 STEADY-STATE PERFORMANCE DATA
SUMMARY FOR IRTS FIXED AREA TESTING

IRTS Test No.	Development Plan or PQT Test No.	Test Date	HEA S/N	CC & NA Type	CC & NA S/N	Test Duration sec.	Data Slice No.	Servo Command ma	ΔP_{if} Stand	ΔP_{ox} Stand	Head-End P_c psia Site	Head-End P_c psia Stand	M.R. - Site	o/f Stand	Total Flowrate lbs/sec Site	Total Flowrate lbs/sec Stand	Corrected C* fps Site	Corrected C* fps Stand	Fuel Press. Actual	Oxidizer Press. Actual	Fuel Inlet Temperature Actual, °F	Oxidizer Inlet Temperature Actual, °F	ΔT_{H_2O} °F
C2-174	None	3-20-64	-002	MIRA 150	Water Cooled	44.0	1	None	182.7	192.4	80.5	Not	1.598	Not	0.321	Not	5373.2	Not	709.7	702.7	60	61	0
							2		149.3	161.3	72.9	Reduced	1.620	Deter-	0.291	Deter-	5353.1	Deter-	710.7	703.7	60	61	0
							3		113.9	130.7	64.3		1.638	mined	0.258	mined	5336.3	mined	711.7	704.7	60	61	0
							4		80.1	96.3	53.1		1.674		0.216		5243.1		712.7	706.7	60	61	0
							5		46.9	61.2	38.3		1.727		0.165		4953.1		715.7	708.7	60	61	0
							6		82.4	100.1	53.3		1.674		0.217		5226.1		712.7	706.7	60	61	0
							7		112.5	136.2	63.7		1.637		0.256		5314.6		711.7	704.7	60	61	0
							8		147.2	171.5	72.5		1.624		0.290		5341.0		710.7	702.7	60	61	0
							9		182.9	206.8	80.3		1.601		0.321		5364.0		709.7	701.7	60	61	0
							10		44.7	61.0	38.5		1.735		0.164		4955.5		716.7	709.7	60	61	0
							11		187.0	209.9	80.7		1.598		0.323		5337.7		709.7	701.7	60	61	0
C2-175		3-20-64	-002	MIRA 150	Water Cooled	44.0	1		221.3	220.8	86.5		1.591		0.346		5349.2		702.7	702.7	60	61	0
							2		164.8	172.9	75.8		1.620		0.303		5354.9		706.7	703.7	60	61	0
							3		113.6	129.6	64.0		1.648		0.257		5323.3		707.7	704.7	60	61	0
							4		71.1	86.7	49.3		1.680		0.204		5209.8		708.7	707.7	60	61	0
							5		31.7	44.2	30.6		1.725		0.136		4751.9		710.7	710.7	60	61	0
							6		72.6	89.6	48.8		1.681		0.204		5191.8		708.7	708.7	60	61	0
							7		112.2	136.7	63.4		1.648		0.257		5306.4		707.7	706.7	60	61	0
							8		159.9	184.0	75.2		1.620		0.302		5324.3		706.7	702.7	60	61	0
							9		215.9	233.5	85.9		1.593		0.344		5348.6		702.7	700.7	60	61	0
							10		28.5	43.0	28.8		1.895		0.120		5168.3		712.7	710.7	60	61	0
							11		218.2	232.8	86.1		1.597		0.344		5367.0		702.7	700.7	60	61	0
C2-181		3-21-64	-002	MIRA 150	"	45.0	1		85.6	84.6	83.4		1.523		0.328		5440.4		704.7	704.7	57	60	0
							2		64.1	64.6	71.3		1.539		0.282		5405.0		706.7	706.7	57	60	0
							3		44.7	45.7	57.2		1.553		0.233		5234.5		707.7	707.7	57	60	0
							4		25.2	28.2	40.1		1.570		0.176		4883.3		710.7	710.7	57	60	0
							5		9.2	12.2	24.1		1.769		0.103		4995.9		712.7	713.7	57	60	0
							6		27.1	29.6	40.7		1.560		0.178		4903.7		711.7	711.7	57	60	0
							7		46.3	47.3	57.1		1.547		0.232		5260.3		708.7	709.7	57	60	0
							8		63.7	69.3	71.2		1.543		0.282		5404.2		707.7	707.7	57	60	0
							9		87.4	92.9	83.6		1.520		0.330		5445.5		706.7	704.7	57	60	0
							10		8.2	11.2	22.5		1.827		0.093		5187.9		712.7	714.7	57	60	0
							11		88.8	94.3	84.2		1.525		0.332		5442.7		705.7	704.7	57	60	0
C2-182		"	-002	"	"	45.0	1		104.0	100.3	90.6		1.511		0.357		5476.5		702.7	699.7	57	60	0
							2		75.6	74.3	76.9		1.517		0.303		5470.3		706.7	702.7	57	60	0
							3		51.3	51.5	61.6		1.539		0.247		5377.8		708.7	705.7	57	60	0
							4		28.2	29.9	42.6		1.541		0.184		4989.5		710.7	708.7	57	60	0
							5		10.5	11.6	24.7		1.884		0.101		5268.8		712.7	710.7	57	60	0
							6		27.8	30.0	43.0		1.542		0.185		5017.6		710.7	708.7	57	60	0
							7		52.3	53.0	61.6		1.534		0.247		5380.9		708.7	706.7	57	60	0
							8		74.3	78.6	77.2		1.517		0.303		5484.6		706.7	701.7	57	60	0
							9		103.5	107.3	90.6		1.508		0.357		5484.6		702.7	698.7	57	60	0
							10		8.5	10.1	22.7		1.893		0.095		5086.7		712.7	709.7	57	60	0
							11		102.7	106.1	90.4		1.510		0.356		5486.1		702.7	698.7	57	60	0

114

TABLE D-2-22. DATA SUMMARY PROPELLANT TEMPERATURE AND PRESSURE EXTREMES TESTS

Run No.	Slice No.	Oxidizer Temperature, °F	Fuel Temperature, °F	Oxidizer Inlet Press, psia	Fuel Inlet Press, psia	Servo Command ma	MR, O/f Measured	MR, O/f Standard	Head End Chamber Press, psia	Vacuum Thrust, lbs Measured	Vacuum Thrust, lbs Standard	Corrected C*, fps
C2-592A	1	57.26	62.64	681.7	684.7	69.4	1.552	1.514	106.7	145.3	148.2	5272.6
	2	57.26	62.64	684.7	687.7	51.6	1.516	1.507	98.7	134.2	136.6	5277.6
	3	57.26	62.64	686.7	688.7	34.4	1.514	1.504	90.5	122.9	124.9	5281.1
	4	57.26	62.64	688.7	691.7	17.0	1.519	1.510	81.7	110.7	112.4	5291.0
	5	57.26	62.64	690.7	692.7	-0.6	1.512	1.502	72.1	97.6	98.9	5273.7
	6	57.26	62.64	692.7	696.7	-18.2	1.520	1.512	61.5	83.1	84.0	5297.9
	7	57.26	62.64	695.7	697.7	-35.6	1.526	1.516	48.0	64.6	65.2	5277.5
	8	57.26	62.64	697.7	699.7	-52.8	1.521	1.511	35.6	47.8	48.2	5166.6
	9	57.26	62.64	698.7	701.7	-70.0	1.468	1.459	22.2	29.8	30.1	4960.0
	10	57.26	62.64	697.7	699.7	-52.8	1.521	1.511	35.6	47.8	48.2	5166.6
C2-592B	1	58.98	62.22	681.7	682.7	69.6	1.510	1.502	106.4	144.9	147.9	5267.1
	2	58.98	62.22	683.7	684.7	51.6	1.502	1.494	98.4	133.8	136.5	5280.3
	3	58.98	62.22	686.7	687.7	34.6	1.499	1.490	90.9	123.4	125.6	5336.7
	4	58.98	62.22	688.7	689.7	17.2	1.493	1.484	83.1	112.8	114.6	5435.0
	5	58.98	62.22	690.7	691.7	-0.6	1.485	1.476	73.8	100.0	101.4	5457.8
	6	58.98	62.22	692.7	692.7	-18.0	1.497	1.487	61.3	82.8	83.8	5308.2
	7	58.98	62.22	695.7	696.7	-35.4	1.513	1.504	48.6	65.4	66.1	5349.4
	8	58.98	62.22	697.7	697.7	-53.0	1.513	1.503	36.1	48.5	48.9	5216.8
	9	58.98	62.22	698.7	698.7	-70.4	1.519	1.509	23.0	30.8	31.1	4988.2
	10	58.98	62.22	697.7	697.7	-53.0	1.521	1.511	35.5	47.7	48.1	5212.0
C2-592C	1	58.98	62.00	699.7	700.7	69.6	1.513	1.504	106.9	145.4	146.5	5219.9
	2	58.98	62.00	701.7	701.7	51.6	1.499	1.490	98.9	134.4	135.2	5254.4
	3	58.98	62.00	703.7	703.7	34.6	1.498	1.488	91.5	124.2	124.8	5293.5
	4	58.98	62.00	707.7	706.7	17.2	1.504	1.493	83.9	113.8	114.1	5388.9
	5	58.98	62.00	708.7	708.7	-0.6	1.494	1.484	74.4	100.7	100.8	5405.4
	6	58.98	62.00	711.7	710.7	-18.0	1.506	1.495	61.2	82.6	82.6	5274.3
	7	58.98	62.00	713.7	712.7	-35.4	1.525	1.514	48.7	65.5	65.4	5301.1
	8	58.98	62.00	715.7	715.7	-52.8	1.528	1.517	36.1	48.5	48.3	5207.3
	9	58.98	62.00	717.7	716.7	-70.0	1.534	1.522	23.0	30.8	30.7	4963.8
	10	58.98	62.00	716.7	715.7	-52.8	1.532	1.521	35.7	48.0	47.8	5173.3

115

TABLE D-2-22. (Continued)

Run No.	Slice No.	Oxidizer Temperature, °F	Fuel Temperature, °F	Oxidizer Inlet Press, psia	Fuel Inlet Press, psia	Servo Command ma	MR, o/f Measured	MR, o/f Standard	Head End Chamber Press, psia	Vacuum Thrust, lbs Measured	Vacuum Thrust, lbs Standard	Corrected C*, fps
C2-592D	1	58.98	61.37	717.7	719.7	69.8	1.497	1.489	108.9	148.4	147.5	5270.8
	2	58.98	61.37	720.7	721.7	52.4	1.491	1.482	100.6	136.8	135.7	5280.1
	3	58.98	61.37	722.7	723.7	35.0	1.489	1.480	92.6	125.8	124.6	5307.0
	4	58.98	61.37	726.7	726.7	17.4	1.492	1.482	85.0	115.3	114.0	5406.7
	5	58.98	61.37	727.7	727.7	-0.4	1.486	1.476	75.2	101.9	100.6	5408.3
	6	58.98	61.37	730.7	730.7	-17.6	1.498	1.488	62.3	84.1	82.9	5273.2
	7	58.98	61.37	732.7	732.7	-35.4	1.519	1.508	49.7	67.0	65.9	5330.4
	8	58.98	61.37	734.7	734.7	-52.4	1.517	1.506	37.2	49.9	49.1	5239.7
	9	58.98	61.37	737.7	736.7	-69.6	1.533	1.521	23.4	31.4	30.8	4933.4
	10	58.98	61.37	739.7	734.7	-52.4	1.525	1.509	36.6	49.1	48.2	5218.8
C2-593A	1	91.74	99.88	676.7	680.7	69.4	1.485	1.514	104.0	141.4	148.7	5241.3
	2	91.74	99.88	676.7	680.7	69.4	1.486	1.514	103.2	140.3	147.6	5195.0
	3	92.16	100.51	679.7	682.7	51.8	1.474	1.501	96.0	130.4	136.9	5217.1
	4	92.59	100.93	682.7	684.7	34.6	1.473	1.499	88.4	119.9	125.7	5231.5
	5	92.80	100.93	684.7	686.7	17.2	1.477	1.504	80.4	108.9	114.1	5270.9
	6	92.80	101.14	686.7	688.7	-0.6	1.457	1.483	72.4	98.0	102.5	5349.4
	7	94.91	101.56	689.7	690.7	-17.6	1.465	1.494	62.1	83.8	87.6	5392.5
	8	93.22	101.56	691.7	692.7	-35.4	1.475	1.501	48.9	65.9	68.7	5318.1
	9	93.22	101.56	693.7	694.7	-52.6	1.468	1.494	37.9	51.0	53.1	5359.0
	10	93.22	101.56	696.7	696.7	-69.6	1.462	1.486	24.6	33.0	34.3	5026.9
	11	93.22	101.56	692.7	694.7	-52.6	1.473	1.500	37.9	51.0	53.1	5347.5
C2-593B	1	91.32	99.88	694.7	698.7	69.6	1.488	1.514	103.8	141.2	146.4	5160.5
	2	91.32	99.88	694.7	698.7	69.6	1.488	1.514	103.8	141.2	146.4	5160.5
	3	91.53	100.09	697.7	700.7	52.0	1.479	1.504	96.3	130.7	135.3	5176.0
	4	91.74	100.30	700.7	702.7	34.6	1.475	1.499	88.5	120.0	124.0	5191.6
	5	92.16	100.51	702.7	705.7	17.2	1.478	1.504	80.6	109.1	112.6	5237.1
	6	92.16	100.51	704.7	707.7	-0.4	1.459	1.484	72.4	97.9	100.9	5297.8
	7	92.37	100.72	707.7	709.7	-17.4	1.467	1.491	62.5	84.4	86.8	5339.5
	8	92.37	100.72	711.7	711.7	-35.4	1.478	1.500	49.4	66.5	68.2	5283.2
	9	92.37	100.72	712.7	713.7	-52.6	1.467	1.490	38.1	51.1	52.4	5291.7
	10	92.37	100.72	714.7	715.7	-69.6	1.476	1.499	24.8	33.2	34.0	5019.3
	11	92.37	100.72	712.7	713.7	-52.6	1.477	1.500	38.3	51.4	52.7	5297.8

116

TABLE D-2-22. (Continued)

Run No.	Slice No.	Oxidizer Temperature, °F	Fuel Temperature, °F	Propellant Mass Flow, lb/sec Oxidizer Test	Oxidizer Standard	Fuel Test	Fuel Standard	Servo Command ra	MR o/f Measured	MR o/f Stand	Head End Chamber Pressure psia	Vacuum Thrust, lbs Measured	Vacuum Thrust, lbs Standard	Corrected C*, fps	Nozzle Stag. Press. psia
C2-594	1	99.25	-11.00	0.2974	0.3134	0.2036	0.2021	69.4	1.461	1.551	102.9	139.0	143.5	5172.1	102.2
	2	99.67	-12.00	0.2731	0.2873	0.1870	0.1854	51.8	1.461	1.550	95.3	128.5	132.5	5214.6	94.7
	3	100.09	-13.00	0.2498	0.2624	0.1706	0.1687	34.6	1.464	1.555	87.5	117.8	121.2	5236.9	86.9
	4	100.51	-13.00	0.2244	0.2356	0.1524	0.1504	17.2	1.472	1.567	77.3	103.8	106.6	5157.1	76.7
	5	100.93	-14.00	0.1976	0.2070	0.1341	0.1321	-0.6	1.473	1.567	68.4	91.8	94.1	5189.2	68.0
	6	101.14	-14.00	0.1683	0.1761	0.1126	0.1107	-17.8	1.494	1.590	58.2	77.9	79.7	5210.1	57.8
	7	101.14	-14.00	0.1317	0.1375	0.0870	0.0854	-35.6	1.514	1.610	45.6	60.9	62.1	5239.9	45.3
	8	101.56	-14.00	0.0998	0.1042	0.0653	0.0640	-52.8	1.528	1.628	33.5	44.7	45.5	5106.4	33.3
	9	101.35	-13.00	0.0577	0.0601	0.0025	0.0024	-70.0			14.9	19.7	26.0	6188.0	14.8
	10	101.35	-13.00	0.0999	0.1042	0.0655	0.0642	-52.8	1.524	1.624	33.7	45.0	45.8	5128.6	33.5
	11	102.41	- 1.00	0.2984	0.3157	0.2051	0.2041	69.6	1.455	1.547	104.3	140.8	145.9	5212.3	103.6
	12	102.62	- 1.00	0.2752	0.2907	0.1891	0.1877	51.8	1.455	1.549	96.3	129.8	134.2	5217.4	95.6
	13	102.83	- 1.00	0.2510	0.2647	0.1727	0.1711	34.6	1.453	1.547	88.7	119.4	123.2	5265.9	88.1
	14	103.04	- 1.00	0.2253	0.2371	0.1545	0.1527	17.0	1.458	1.553	78.3	105.1	108.3	5182.3	77.7
	15	103.04	- 1.00	0.1993	0.2093	0.1360	0.1343	-0.6	1.465	1.558	68.7	92.1	94.6	5149.6	68.2
	16	103.04	- 1.00	0.1676	0.1756	0.1133	0.1116	-18.2	1.479	1.573	58.5	78.2	80.2	5234.4	58.1
	17	103.04	- 1.00	0.1327	0.1389	0.0882	0.0867	-35.8	1.505	1.602	46.1	61.5	62.9	5242.6	45.8
	18	103.04	- 1.00	0.1013	0.1058	0.0664	0.0652	-53.2	1.526	1.623	34.3	45.7	46.6	5139.8	34.0
	19	103.04	- 1.00	0.0588	0.0613	0.0025	0.0024	-90.2			14.9	18.5	24.5	5721.5	14.8
	20	103.04	- 1.00	0.1006	0.1050	0.0662	0.0650	-53.0	1.520	1.617	34.1	45.4	46.3	5136.0	33.8
C2-595	1	85.75	14.00	0.3051	0.3156	0.2054	0.2053	70.0	1.486	1.537	106.9	144.4	147.6	5270.6	106.1
	2	89.97	14.00	0.2037	0.2102	0.1378	0.1367	-0.4	1.478	1.537	72.2	96.9	98.6	5317.6	71.7
	3	90.60	12.00	0.1729	0.1783	0.1154	0.1142	-17.6	1.499	1.561	60.7	81.3	82.6	5294.0	60.2
	4	91.66	11.00	0.1372	0.1413	0.0904	0.0893	-35.4	1.518	1.582	48.0	64.1	65.0	5203.9	47.6
	5	92.08	14.00	0.1046	0.1077	0.0681	0.0673	-52.6	1.534	1.599	35.3	47.0	47.7	5135.0	35.0
	6	92.08	11.00	0.0700	0.0720	0.0452	0.0445	-70.0	1.550	1.618	22.3	29.7	30.1	4878.0	22.2
	7	94.61	9.00	0.1968	0.2042	0.1337	0.1325	-0.4	1.472	1.542	69.5	93.3	95.3	5294.5	69.1
C2-597A	1	11.50	99.08	0.3190	0.3129	0.2012	0.2062	70.0	1.552	1.485	114.1	154.5	153.9	5443.2	113.3
	2	10.80	99.29	0.3203	0.3141	0.2016	0.2065	70.0	1.556	1.489	114.3	154.8	154.1	5434.0	113.5
	3	10.80	99.71	0.2948	0.2883	0.1880	0.1921	52.4	1.535	1.469	105.9	143.2	142.2	5444.1	105.2
	4	10.80	100.14	0.2709	2.2645	0.1732	0.1768	35.0	1.531	1.465	97.3	131.4	130.3	5439.2	96.7
	5	10.80	100.14	0.2444	0.2381	0.1560	0.1590	17.4	1.534	1.467	87.8	118.3	117.1	5439.0	87.2
	6	10.80	100.35	0.2157	0.2097	0.1395	0.1420	-0.4	1.514	1.445	78.0	104.9	103.7	5447.8	77.5
	7	10.80	100.56	0.1822	0.1767	0.1171	0.1190	-18.0	1.522	1.455	65.9	88.4	87.2	5457.7	65.4
	8	10.80	100.56	0.1462	0.1414	0.0933	0.0946	-35.6	1.533	1.463	52.1	69.8	68.7	5395.9	51.8
	9	10.80	100.77	0.1126	0.1088	0.0719	0.0728	-47.0	1.533	1.463	39.2	52.3	51.4	5263.1	38.9
	10	10.80	100.56	0.0766	0.0740	0.0494	0.0500	-35.2	1.519	1.450	24.2	32.3	31.7	4771.6	24.1
	11	10.80	100.35	0.1123	0.1084	0.0726	0.0735	-52.8	1.515	1.445	39.2	52.3	51.4	5255.3	38.9

117

TABLE D-2-22. (Continued)

Run No.	Slice No.	Oxidizer Temperature, °F	Fuel Temperature, °F	Propellant Mass Flow, lb/sec Oxidizer Test	Oxidizer Standard	Fuel Test	Fuel Standard	Servo Command ma	MR o/f Measured	MR o/f Stand	Head End Chamber Pressure psia	Vacuum Thrust, lbs Measured	Vacuum Thrust, lbs Standard	Corrected C*, fps	Nozzle Stag. Press. psia
C2-597B	1	12.10	100.77	0.3200	0.3140	0.1992	0.2038	70.0	1.572	1.508	111.9	151.4	150.8	5345.7	111.1
	2	10.80	101.19	0.3203	0.3141	0.2038	0.2085	70.0	1.539	1.475	112.7	152.5	151.8	5333.2	111.9
	3	10.80	101.40	0.2952	0.2886	0.1894	0.1936	52.4	1.526	1.460	103.9	140.4	139.4	5318.8	103.2
	4	10.80	101.40	0.2701	0.2637	0.1738	0.1773	35.0	1.521	1.457	95.6	128.9	127.7	5336.2	94.9
	5	10.80	101.40	0.2440	0.2377	0.1572	0.1602	37.4	1.519	1.453	36.2	116.0	114.8	5324.5	85.6
	6	10.80	101.62	0.2157	0.2097	0.1402	0.1425	-0.2	1.507	1.440	76.8	103.2	101.9	5350.2	76.3
	7	10.80	101.83	0.1848	0.1793	0.1197	0.1215	-18.0	1.513	1.445	65.9	88.3	87.1	5359.4	65.4
	8	10.80	101.83	0.1477	0.1429	0.0945	0.0958	-17.7	1.530	1.461	51.9	69.4	68.3	5309.2	51.6
	9	10.80	101.83	0.1141	0.1102	0.0730	0.0740	-26.5	1.530	1.460	38.8	51.7	50.8	5127.9	38.5
	10	10.80	101.83	0.0785	0.0758	0.0507	0.0513	-70.2	1.515	1.445	24.4	32.5	31.9	4680.2	24.3
	11	10.80	101.83	0.1134	0.1095	0.0722	0.0731	-55.0	1.538	1.466	38.4	51.1	50.3	5118.6	38.1
C2-598	1	35.59	25.65	0.3074	0.3128	0.2058	0.2068	70.0	1.494	1.513	109.2	147.7	149.7	5359.8	108.5
	2	36.22	36.23	0.3118	0.3103	0.2079	0.2062	70.0	1.499	1.505	110.4	149.3	148.4	5347.4	109.7
C2-599	1	11.52	-2.23	0.3107	0.3050	0.1997	0.1988	70.6	1.556	1.535	111.4	150.8	148.7	5498.3	110.6
	2	10.26	-2.86	0.3087	0.3024	0.1997	0.1987	70.6	1.546	1.522	111.0	150.3	148.0	5501.6	110.2
	3	10.26	-2.86	0.2860	0.2796	0.1834	0.1820	52.6	1.559	1.536	103.6	140.1	137.7	5563.2	102.9
	4	10.26	-2.86	0.2611	0.2552	0.1674	0.1659	35.4	1.562	1.538	95.6	129.1	126.7	5620.7	94.9
	5	10.26	-2.86	0.2356	0.2287	0.1500	0.1483	17.6	1.567	1.543	85.6	115.4	112.9	5602.1	85.0
	6	10.26	-2.86	0.2072	0.2011	0.1316	0.1300	0.0	1.574	1.547	73.6	98.9	96.6	5470.4	73.1
	7	10.26	-2.86	0.1757	0.1703	0.1105	0.1088	-17.4	1.590	1.565	62.1	83.2	81.1	5456.7	61.6
	8	10.26	-2.86	0.1391	0.1344	0.0854	0.0839	-35.4	1.629	1.601	48.1	64.3	62.5	5389.2	47.8
	9	10.26	-2.86	0.1049	0.1012	0.0639	0.0628	-52.6	1.641	1.613	35.1	46.8	45.5	5229.9	34.9
	10	10.26	-2.86	0.0682	0.0658	0.0416	0.0408	-70.0	1.642	1.613	21.7	28.9	28.0	4976.6	21.6
	11	10.26	-2.86	0.1037	0.1001	0.0630	0.0619	-52.6	1.646	1.617	34.7	46.3	44.9	5232.1	34.5
	12	11.31	-1.81	0.3178	0.3072	0.2039	0.2005	70.4	1.559	1.532	112.7	152.7	148.5	5446.5	111.9
	13	9.83	-2.86	0.3174	0.3066	0.2036	0.2000	70.4	1.559	1.533	112.5	152.4	148.1	5443.5	111.7
	14	9.83	-2.86	0.2912	0.2805	0.1877	0.1842	52.6	1.551	1.523	104.7	141.6	137.3	5511.5	104.0
	15	9.83	-2.86	0.2658	0.2557	0.1709	0.1674	35.4	1.555	1.528	96.7	130.6	126.3	5579.9	96.0
	16	9.83	-2.86	0.2390	0.2294	0.1531	0.1498	17.6	1.560	1.532	86.8	117.0	113.0	5579.4	86.2
	17	9.83	-2.86	0.2107	0.2017	0.1347	0.1315	-0.2	1.564	1.534	74.4	99.9	96.3	5418.7	73.9
	18	9.83	-2.86	0.1758	0.1678	0.1112	0.1083	-17.6	1.581	1.550	62.1	83.3	80.0	5448.2	61.7
	19	9.83	-2.86	0.1410	0.1343	0.0849	0.0825	-35.4	1.660	1.628	48.5	64.8	62.2	5395.7	48.1
	20	9.83	-2.86	0.1060	0.1009	0.0648	0.0629	-52.6	1.637	1.605	35.8	47.8	45.8	5273.1	35.6
	21	9.83	-2.86	0.0687	0.0652	0.0431	0.0418	-69.8	1.594	1.560	34.8	29.0	27.7	4901.1	21.6
	22	9.83	-2.86	0.1060	0.1009	0.646	0.0626	-52.6	1.643	1.610	35.8	47.8	45.8	5279.6	35.6
	23	11.31	3.47	0.3166	0.3068	0.2039	0.2008	70.0	1.552	1.528	113.8	154.1	150.1	5507.5	113.0
	24	12.16	3.05	0.2114	0.2031	0.1363	0.1332	-0.4	1.551	1.524	75.8	101.9	98.5	5490.2	75.3
	25	12.37	3.47	0.0726	0.0692	0.0451	0.0437	-70.0	1.611	1.581	23.7	31.6	30.3	5071.1	23.6
	26	13.00	3.47	0.1065	0.1016	0.0660	0.0642	-52.6	1.613	1.583	36.5	48.6	46.7	5314.2	36.2

TABLE D-2-22. (Continued)

Run No.	Slice No.	Oxidizer Temperature, °F	Fuel Temperature, °F	Propellant Mass Flow, lb/sec Oxidizer Test	Oxidizer Standard	Fuel Test	Fuel Standard	Servo Command ma	MR, o/f Measured	MR, o/f Stand	Head End Chamber Pressure psia	Vacuum Thrust, lbs Measured	Vacuum Thrust, lbs Standard	Corrected C^*, fps	Nozzle Stag. Press. psia
C2-600	1	85.12	91.80	0.1939	0.1959	0.1325	0.1324	- 1.0	1.464	1.479	69.6	92.8	93.4	5329.0	69.1
	2	85.33	92.85	0.2297	0.2327	0.1562	0.1565	22.2	1.470	1.487	82.2	109.8	110.9	5325.1	81.6
	3	87.23	94.54	0.2632	0.2679	0.1787	0.1795	46.0	1.473	1.492	94.0	125.9	127.6	5319.3	93.3
	4	88.92	95.39	0.2941	0.3010	0.1988	0.2002	68.8	1.479	1.504	104.8	140.7	143.2	5317.2	104.1
	5	90.18	95.81	0.1963	0.1996	0.1346	0.1346	- 0.8	1.459	1.483	70.4	93.9	94.9	5318.6	69.9
	6	90.81	96.02	0.1552	0.1574	0.1059	0.1057	-23.8	1.466	1.489	55.5	73.9	74.5	5320.1	55.2
	7	91.02	96.45	0.1101	0.1115	0.0749	0.0746	-47.4	1.469	1.493	36.9	48.9	49.3	4989.3	36.7
	8	91.66	96.66	0.0656	0.0664	0.0451	0.0448	-70.0	1.457	1.481	21.3	28.2	28.3	4808.6	21.1
	9	91.66	96.87	0.1716	0.1745	0.1173	0.1172	-12.6	1.462	1.489	61.3	81.7	82.6	5309.8	60.9
	10	91.23	88.21	0.1965	0.2000	0.1347	0.1350	0.0	1.458	1.482	70.3	93.8	94.9	5308.1	69.8
	11	91.45	89.26	0.2313	0.2364	0.1572	0.1580	23.0	1.472	1.497	82.5	110.3	112.1	5313.6	82.0
	12	91.66	90.11	0.2636	0.2703	0.1780	0.1793	47.0	1.481	1.507	93.6	125.3	127.8	5299.5	92.9
	13	92.71	91.16	0.2963	0.3052	0.1988	0.2009	69.8	1.490	1.519	104.0	139.6	142.8	5254.0	103.3
	14	93.55	91.59	0.1964	0.2009	0.1338	0.1342	- 0.2	1.468	1.497	70.5	94.0	95.5	5338.8	70.0
	15	93.76	91.80	0.1548	0.1579	0.1058	0.1058	-23.2	1.464	1.492	55.4	73.8	74.7	5321.2	55.1
	16	93.76	91.80	0.1102	0.1121	0.0750	0.0749	-47.2	1.468	1.497	37.6	49.8	50.4	5073.2	37.3
	17	94.40	91.80	0.0665	0.0676	0.0455	0.0454	-70.0	1.461	1.490	22.3	29.5	29.8	4977.5	22.2
	18	94.40	91.80	0.2110	0.2163	0.1452	0.1458	11.8	1.453	1.484	74.9	100.0	101.8	5260.6	75.4
C2-603A	1	92.31	90.19	0.2965	0.3042	0.2013	0.2030	70.0	1.473	1.499	104.0	139.5	142.4	5225.7	103.3
	2	94.42	93.36	0.2655	0.2724	0.1802	0.1815	46.8	1.473	1.501	92.6	124.0	126.4	5193.8	91.9
	3	95.48	93.36	0.2262	0.2316	0.1545	0.1549	22.8	1.464	1.495	79.3	106.0	107.7	5211.8	78.8
	4	97.60	95.48	0.1903	0.1949	0.1310	0.1313	-0.2	1.453	1.484	65.9	87.8	89.3	5128.6	65.4
	5	97.60	95.48	0.1496	0.1529	0.1023	0.1023	-22.8	1.462	1.495	52.8	70.3	71.3	5245.5	52.5
	6	98.65	95.48	0.1097	0.1120	0.0751	0.0749	-46.6	1.461	1.496	37.4	49.6	50.2	5062.9	37.1
	7	98.65	97.60	0.0719	0.0733	0.0495	0.0493	-69.0	1.453	1.487	23.8	31.4	31.8	4895.8	23.6
	8	99.71	97.60	0.1089	0.1113	0.0741	0.0740	-46.6	1.468	1.504	37.2	49.3	50.0	5083.7	36.9
	9	99.71	97.60	0.1479	0.1517	0.1037	0.1038	-22.8	1.426	1.461	53.5	71.1	72.3	5312.6	53.1
	10	99.71	97.60	0.1907	0.1959	0.1312	0.1317	- 0.2	1.453	1.488	66.9	89.2	90.9	5196.7	66.4
	11	100.77	97.60	0.2280	0.2351	0.1560	0.1569	23.0	1.461	1.499	79.9	106.8	109.2	5206.2	79.4
	12	101.83	97.60	0.2648	0.2746	0.1809	0.1824	47.0	1.464	1.506	93.6	125.3	128.7	5251.2	92.9
	13	101.83	97.60	0.2957	0.3078	0.2006	0.2028	69.6	1.474	1.518	104.6	140.4	144.7	5271.2	103.9
	14	102.89	99.71	0.2638	0.2740	0.1802	0.1818	47.0	1.464	1.507	93.6	125.3	128.9	5270.3	92.9
	15	102.89	99.71	0.2268	0.2347	0.1560	0.1570	23.0	1.454	1.495	80.1	107.1	109.7	5234.7	79.6
	16	102.89	99.71	0.1891	0.1951	0.1308	0.1314	0.0	1.445	1.485	67.3	89.7	91.7	5260.5	66.8
	17	103.94	99.71	0.2962	0.3093	0.2016	0.2040	70.0	1.469	1.516	104.6	140.4	145.0	5255.4	103.9
	18	103.94	99.71	0.0593	0.0610	0.0407	0.0405	-78.6	1.459	1.503	21.0	27.7	28.2	5241.2	20.8
	19	103.94	99.71	0.0716	0.0736	0.0498	0.0497	-69.0	1.436	1.480	24.2	32.0	32.5	4978.4	24.0
	20	103.94	101.83	0.3114	0.3255	0.2105	0.2134	80.0	1.480	1.525	110.0	147.8	152.9	5272.5	109.3
	21	103.94	101.83	0.2997	0.3128	0.2030	0.2056	70.0	1.476	1.522	105.6	141.7	146.4	5253.5	104.9
	22	103.94	101.83	0.0737	0.0757	0.0510	0.0509	-68.8	1.445	1.488	24.8	32.8	33.3	4968.7	24.6
	23	103.94	101.83	0.0744	0.0765	0.0516	0.0515	-68.8	1.441	1.483	25.2	33.3	33.9	4996.5	25.0
	24	103.94	101.83	0.3107	0.3245	0.2105	0.2136	79.6	1.476	1.519	110.0	147.8	152.8	5279.6	109.3
	25	103.94	101.83	0.2880	0.3002	0.1966	0.1989	62.6	1.465	1.509	102.0	136.8	141.1	5263.8	101.3
	26	103.94	101.83	0.1733	0.1789	0.1198	0.1203	-12.0	1.446	1.487	61.5	81.9	83.7	5246.0	61.0

TABLE D-2-22. (Continued)

Run No.	Slice No.	Oxidizer Temperature, °F	Fuel Temperature, °F	Propellant Mass Flow, lb/sec Oxidizer Test	Oxidizer Standard	Fuel Test	Fuel Standard	Servo Command ma	MR o/f Measured	MR o/f Stand	Head End Chamber Pressure psia	Vacuum Thrust, lbs Measured	Vacuum Thrust, lbs Standard	Corrected C*, fps	Nozzle Stag. Press. psia
C2-603B	1	90.19	91.25	0.1862	0.1889	0.1242	0.1243	- 1.2	1.499	1.520	65.5	87.4	88.2	5280.0	65.1
	2	90.19	93.36	0.2226	0.2265	0.1523	0.1527	22.0	1.461	1.483	79.6	106.3	107.7	5309.4	79.0
	3	93.36	93.36	0.2596	0.2660	0.1766	0.1776	45.6	1.470	1.498	92.0	123.2	125.5	5276.2	91.4
	4	93.36	95.48	0.2930	0.3013	0.1983	0.2000	68.6	1.477	1.507	103.1	138.3	141.3	5247.5	102.4
	5	96.75	95.48	0.1823	0.1865	0.1252	0.1252	- 1.0	1.456	1.490	65.7	87.6	88.9	5347.6	65.3
	6	95.48	97.17	0.1406	0.1433	0.0963	0.0963	-24.0	1.460	1.489	50.5	67.1	67.9	5328.3	50.1
	7	96.75	97.17	0.1046	0.1065	0.0712	0.0710	-47.6	1.468	1.500	35.4	47.0	47.5	5038.9	35.2
	8	96.75	97.17	0.0650	0.0662	0.0446	0.0444	-69.6	1.458	1.489	21.6	28.5	28.8	4921.5	21.4
	9	96.75	97.17	0.1629	0.1665	0.1122	0.1123	-13.0	1.452	1.483	58.3	77.6	78.7	5298.9	57.9
C2-604	1	88.84	96.63	0.1781	0.1863	0.1219	0.1259	- 0.2	1.461	1.480	62.9	83.8	87.3	5244.5	62.5
	2	93.28	94.09	0.1301	0.1366	0.0863	0.0890	-29.2	1.508	1.536	44.1	58.5	61.1	5093.8	43.8
	3	96.45	98.75	0.2878	0.3070	0.1939	0.2025	70.0	1.484	1.516	100.6	134.8	142.9	5220.8	99.9
	4	97.50	100.44	0.0667	0.0701	0.0457	0.0471	-69.8	1.459	1.490	22.2	29.3	30.6	4930.6	22.0
	5	100.04	101.29	0.2826	0.3036	0.1918	0.1997	69.4	1.474	1.520	99.3	133.1	141.5	5233.6	98.6
	6	101.73	101.93	0.2871	0.3088	0.1952	0.2034	69.4	1.470	1.519	100.9	135.3	144.0	5230.0	100.2
	7	101.73	101.93	0.2871	0.3083	0.1952	0.2034	69.4	1.471	1.516	101.3	135.8	144.4	5250.9	100.6
	8	101.73	101.93	0.0692	0.0732	0.0487	0.0500	-69.6	1.421	1.463	24.0	31.7	33.2	5085.3	23.8
	9	100.88	103.62	0.1755	0.1867	0.1203	0.1249	0.0	1.459	1.495	61.7	82.1	86.6	5211.6	61.2
	10	97.50	95.57	0.1343	0.1415	0.0906	0.0932	-29.0	1.481	1.517	76.1	61.1	63.9	5118.3	45.7
	11	98.14	98.75	0.2863	0.3057	0.1931	0.2011	70.0	1.482	1.521	100.3	134.4	142.3	5228.3	99.6
	12	99.62	99.81	0.0687	0.0723	0.0472	0.0484	-70.0	1.456	1.496	23.2	30.6	32.0	5000.1	23.0
C2-605	1	29.89	19.32	0.1922	0.1857	0.1239	0.1215	- 0.6	1.551	1.529	67.1	89.7	87.1	5321.9	66.6
	2	28.83	12.98	0.2325	0.2253	0.1507	0.1478	22.6	1.543	1.525	81.8	109.7	106.7	5354.4	81.2
	3	28.83	9.81	0.2717	0.2643	0.1746	0.1715	46.8	1.556	1.541	95.7	128.6	125.5	5379.8	95.1
	4	25.66	7.70	0.3063	0.2984	0.1988	0.1957	70.2	1.541	1.525	108.4	145.9	142.7	5381.4	107.6
	5	21.43	6.64	0.1921	0.1849	0.1266	0.1197	- 0.6	1.567	1.544	67.1	89.7	86.7	5346.1	66.6
	6	19.32	5.59	0.1507	0.1444	0.0943	0.0918	-24.0	1.599	1.573	51.6	68.7	66.2	5277.2	51.2
	7	17.63	5.59	0.1102	0.1053	0.0658	0.0640	-48.0	1.676	1.647	36.4	48.5	46.6	5193.3	36.2
	8	17.63	5.59	0.0697	0.0665	0.0427	0.0414	-70.8	1.634	1.606	21.7	28.8	27.6	4845.5	21.6
	9	21.43	16.15	0.3044	0.2950	0.1965	0.1939	72.4	1.549	1.522	108.5	146.2	142.5	5434.4	107.8
	10	17.21	2.42	0.3051	0.2959	0.1994	0.1958	69.0	1.530	1.511	108.6	146.3	142.5	5402.5	107.9
	11	9.81	7.70	0.0735	0.0698	0.0456	0.0442	-69.4	1.612	1.577	22.1	29.3	28.0	4645.1	21.9
	12	7.70	6.64	0.1537	0.1463	0.0966	0.0941	-23.4	1.591	1.555	50.2	66.9	64.2	5031.1	49.9
	13	6.64	6.64	0.1964	0.1873	0.1246	0.1217	- 0.4	1.576	1.540	65.3	87.4	84.0	5106.6	64.9
	14	4.53	4.53	0.2747	0.2636	0.1776	0.1741	46.4	1.547	1.514	94.0	126.3	122.1	5214.6	93.4
	15	2.42	4.53	0.3089	0.2971	0.1994	0.1960	69.4	1.549	1.516	105.1	141.5	137.1	5189.0	104.4
	16	0.31	4.53	0.3277	0.3154	0.2097	0.2053	79.4	1.567	1.529	114.0	153.6	149.1	5324.0	113.2

TABLE D-2-22. (Continued)

Run No.	Slice No.	Oxidizer Temperature, °F	Fuel Temperature, °F	Propellant Mass Flow, lb/sec Oxidizer Test	Oxidizer Standard	Fuel Test	Fuel Standard	Servo Command ma	MR o/f Measured	MR o/f Stand	Head End Chamber Pressure psia	Vacuum Thrust, lbs Measured	Vacuum Thrust, lbs Standard	Corrected C*, fps	Nozzle Stag. Press. psia
C2-606	1	18.25	18.27	0.1869	0.1848	0.1198	0.1208	- 0.6	1.560	1.530	64.7	86.2	85.9	5276.5	64.3
	2	19.30	15.10	0.2252	0.2238	0.1459	0.1470	22.4	1.544	1.523	79.2	105.8	105.6	5335.3	78.7
	3	20.36	11.93	0.2630	0.2628	0.1713	0.1731	46.4	1.535	1.519	92.8	124.2	124.6	5340.6	92.1
	4	16.13	9.81	0.2964	0.2967	0.1927	0.1952	69.2	1.538	1.520	104.5	140.2	140.9	5342.2	103.8
	5	14.01	8.76	0.1857	0.1835	0.1189	0.1195	- 0.4	1.561	1.536	64.9	86.5	86.0	5329.5	64.5
	6	11.90	7.70	0.1460	0.1437	0.0909	0.0912	-23.4	1.606	1.576	49.9	66.3	65.7	5264.1	49.5
	7	10.84	7.70	0.1070	0.1050	0.0659	0.0660	-47.0	1.625	1.592	35.3	46.8	46.3	5106.7	35.1
	8	9.78	7.70	0.0679	0.0663	0.0417	0.0417	-69.4	1.626	1.591	21.6	28.5	28.1	4916.6	21.4
	9	16.13	7.70	0.3007	0.2992	0.1948	0.1970	69.6	1.544	1.519	105.4	141.4	141.5	5319.4	104.7
	10	16.13	5.59	0.3010	0.3000	0.1950	0.1973	69.4	1.544	1.521	105.2	141.2	141.4	5304.4	104.5
	11	14.01	8.76	0.0717	0.0704	0.0451	0.0451	-69.2	1.590	1.561	21.7	28.7	28.3	4639.5	21.5
	12	11.90	6.64	0.1505	0.1479	0.0951	0.0952	-22.8	1.583	1.554	48.7	64.7	64.0	4957.7	48.4
	13	10.42	6.64	0.1904	0.1875	0.1224	0.1228	0.2	1.556	1.528	62.6	83.4	82.7	5004.5	62.2
	14	6.61	6.01	0.2691	0.2663	0.1734	0.1748	47.4	1.552	1.523	89.1	119.2	118.8	5035.8	88.5
	15	4.49	5.59	0.3021	0.2997	0.1952	0.1972	70.4	1.547	1.520	106.3	142.6	142.3	5341.5	105.5
	16	-0.59	4.53	0.3170	0.3137	0.2020	0.2043	80.2	1.569	1.535	111.4	149.5	149.1	5363.9	110.6
C2-608	1	55.70	59.51	0.3032	0.3035	0.1967	0.1987	69.6	1.541	1.528	106.2	143.6	144.2	5351.9	105.5
	2	55.70	59.51	0.1890	0.1878	0.1245	0.1250	- 0.4	1.517	1.503	67.1	90.0	89.8	5385.2	66.6
	3	55.70	59.51	0.0699	0.0692	0.0456	0.0455	-70.0	1.535	1.521	23.3	31.1	30.9	5089.5	23.2
	4	55.70	59.51	0.1018	0.1008	0.0660	0.0659	-52.6	1.543	1.529	34.3	45.7	45.4	5143.8	34.1
C2-609	1	99.71	99.62	0.3110	0.2961	0.1932	0.1957	69.6	1.610	1.513	107.4	145.2	141.3	5363.0	106.6
	2	99.71	99.62	0.2005	0.1892	0.1261	0.1270	- 0.4	1.589	1.490	68.9	92.5	89.3	5310.6	68.4
	3	99.71	99.62	0.0786	0.0737	0.0492	0.0493	-70.0	1.597	1.497	25.3	33.7	32.4	4979.5	25.1
C2-610	1	93.36	89.05	0.0993	0.0938	0.0601	0.0626	-52.0	1.653	1.499	30.7	40.7	40.0	4823.9	30.5
	2	100.77	97.50	0.1032	0.0985	0.0612	0.0640	-52.4	1.686	1.539	32.1	42.6	42.1	4886.3	31.9
	3	101.83	97.50	0.0985	0.0941	0.0604	0.0631	-52.4	1.631	1.491	31.9	42.3	41.9	5024.1	31.7
C2-611	1	94.42	93.78	0.3111	0.2983	0.1923	0.1976	70.4	1.618	1.509	105.4	142.1	139.7	5261.2	104.7
	2	103.94	102.79	0.3063	0.2970	0.1916	0.1972	70.4	1.599	1.506	103.9	140.0	138.6	5240.1	103.1
	3	91.25	91.16	0.3134	0.2990	0.1936	0.1984	70.0	1.619	1.507	106.1	143.0	140.0	5256.5	105.3
	4	103.94	102.79	0.3063	0.2970	0.1914	0.1970	70.0	1.600	1.508	105.1	141.7	140.3	5304.0	104.3
C2-612	1	95.33	99.62	0.3148	0.3017	0.1941	0.1998	71.0	1.622	1.510	106.6	143.4	141.1	5251.9	105.8
	2	97.44	97.50	0.3088	0.2974	0.1939	0.1989	70.6	1.593	1.495	105.6	142.1	139.9	5268.3	104.9
	3	103.77	103.00	0.3064	0.2976	0.1916	0.1969	70.4	1.599	1.512	104.8	141.0	139.7	5278.6	104.1
	4	97.44	97.50	0.3124	0.3001	0.1956	0.2007	70.2	1.597	1.495	107.6	144.9	142.4	5312.6	106.9
	5	105.88	103.42	0.3114	0.3026	0.1934	0.1988	70.0	1.610	1.522	105.8	142.4	141.2	5255.7	105.1

TABLE D-2-22. (Continued)

Run No.	Slice No.	Oxidizer Temperature, °F	Fuel Temperature °F	Propellant Mass Flow, lb/sec Oxidizer Test	Oxidizer Standard	Fuel Test	Fuel Standard	Servo Command ma	MR o/f Measured	MR o/f Stand	Head End Chamber Pressure psia	Vacuum Thrust, lbs Measured	Vacuum Thrust, lbs Standard	Corrected C*, fps	Nozzle Stag. Press. psia
C2-613	1	97.69	- 3.97	0.2918	0.3058	0.1967	0.1966	70.6	1.483	1.556	102.3	138.2	142.5	5273.3	101.6
	2	101.93	- 6.09	0.2907	0.3064	0.1969	0.1961	70.6	1.476	1.562	102.3	138.2	142.8	5283.0	101.6
	3	101.93	- 6.09	0.2665	0.2805	0.1799	0.1788	52.8	1.481	1.568	94.2	127.0	131.0	5312.5	93.5
	4	101.93	- 6.09	0.2402	0.2520	0.1614	0.1602	35.2	1.488	1.573	85.4	115.0	118.3	5353.2	84.8
	5	101.93	- 6.09	0.2127	0.2230	0.1432	0.1418	17.4	1.486	1.573	74.0	99.4	102.1	5230.3	73.5
	6	101.93	- 6.09	0.1835	0.1918	0.1224	0.1208	- 0.4	1.500	1.587	64.7	86.7	88.8	5321.3	64.2
	7	101.93	- 6.09	0.1554	0.1622	0.1024	0.1009	-18.4	1.518	1.607	50.7	67.7	69.2	4944.6	50.3
	8	101.93	- 6.09	0.1253	0.1304	0.0812	0.0798	-36.2	1.543	1.633	40.1	53.5	54.5	4882.4	39.8
	9	101.93	- 6.09	0.0973	0.1013	0.0627	0.0616	-53.8	1.552	1.645	30.7	40.8	41.5	4816.8	30.5
	10	101.93	- 6.09	0.0696	0.0722	0.0438	0.0429	-71.4	1.589	1.682	22.8	30.3	30.7	5050.4	22.6
	11	101.93	- 6.09	0.0973	0.1013	0.0632	0.0620	-54.0	1.542	1.633	33.1	43.8	44.8	5182.4	32.8
	12	99.81	- 3.97	0.2873	0.3014	0.1947	0.1937	71.0	1.476	1.556	101.2	136.6	140.7	5284.7	100.5
	13	101.93	- 6.09	0.2868	0.3018	0.1954	0.1943	71.0	1.468	1.553	100.9	136.1	140.5	5266.1	100.2
	14	101.93	- 6.09	0.2626	0.2755	0.1784	0.1770	53.0	1.472	1.556	92.9	125.2	128.8	5300.9	92.2
	15	101.93	- 6.09	0.2373	0.2488	0.1599	0.1583	35.2	1.485	1.572	84.2	113.3	116.4	5333.1	83.6
	16	101.93	- 6.09	0.2095	0.2190	0.1419	0.1401	17.4	1.477	1.563	73.4	98.5	100.9	5253.1	72.9
	17	101.93	- 6.09	0.1814	0.1891	0.1213	0.1196	- 0.4	1.496	1.582	63.9	85.6	87.5	5309.2	63.4
	18	101.93	- 6.09	0.1519	0.1581	0.1002	0.0985	-18.4	1.516	1.604	52.9	70.7	72.1	5277.7	52.5
	19	101.93	- 6.09	0.1221	0.1270	0.0790	0.0775	-36.4	1.546	1.638	41.4	55.2	56.2	5175.9	41.1
	20	101.93	- 6.09	0.0949	0.0985	0.0612	0.0600	-53.8	1.550	1.641	32.0	42.6	43.2	5150.2	31.7
	21	101.93	- 6.09	0.0671	0.0696	0.0425	0.0416	-71.4	1.579	1.673	22.1	29.3	29.7	5060.1	21.9
	22	101.93	- 6.09	0.0952	0.0989	0.0614	0.0602	-54.0	1.550	1.642	31.8	42.3	42.9	5098.0	31.5
C2-614	1	105.53	-18.78	0.2886	0.3068	0.1931	0.1931	70.4	1.494	1.589	100.9	136.2	141.8	5273.0	100.2
	2	106.16	-19.42	0.2895	0.3080	0.1957	0.1950	70.0	1.480	1.579	100.6	135.8	141.3	5219.1	99.9
	3	106.16	-19.42	0.2665	0.2827	0.1779	0.1769	52.4	1.498	1.598	91.9	123.7	128.4	5200.6	91.2
	4	106.16	-19.42	0.2406	0.2550	0.1597	0.1584	35.0	1.507	1.609	82.1	110.7	114.2	5158.3	81.5
	5	106.16	-19.42	0.2126	0.2246	0.1411	0.1397	17.4	1.507	1.608	73.5	98.7	101.9	5229.1	73.0
	6	106.16	-19.42	0.1835	0.1933	0.1208	0.1193	- 0.2	1.519	1.620	63.8	85.5	87.9	5270.3	63.3
	7	106.16	-19.42	0.1559	0.1639	0.1009	0.0994	-17.8	1.545	1.649	53.4	71.4	73.3	5232.2	53.0
	8	106.16	-19.42	0.1262	0.1325	0.0800	0.0786	-35.4	1.577	1.685	42.3	56.4	57.7	5154.0	42.0
	9	106.16	-19.42	0.0991	0.1039	0.0621	0.0609	-52.6	1.596	1.706	32.4	43.1	44.0	5052.4	32.2
	10	106.16	-19.42	0.0746	0.0781	0.0424	0.0415	-70.0	1.759	1.881	22.0	29.3	29.8	4731.8	21.9
	11	106.16	-19.42	0.0970	0.1017	0.0612	0.0600	-52.6	1.584	1.694	32.0	42.6	43.5	5084.0	31.8

TABLE D-2-23. MIRA 150A STEADY-STATE PERFORMANCE DATA
SUMMARY FOR EXTENDED RANGE THROTTLING TESTS

IRTS Test No.	Development Plan or PQT Test No.	Test Date	HEA S/N	CC & NA Type	CC & NA S/N	Test Duration secs.	Data Slice No.	Servo Command ma	ΔP_{if}	ΔP_{io}	Head-End P psia Site	Head-End P psia Standard	M.R. Site	o/f Stand	Total Flowrate lbs/sec Site	Total Flowrate lbs/sec Stand	Corrected C* fps Site	Corrected C* fps Stand	Fuel Inlet Pressure psia	Oxidizer Inlet Pressure psia	Fuel Inlet Temperature °F	Oxidizer Inlet Temperature °F	ΔT_{H_2O} °F
C2-714	20:180 lb/thrust	1-12-65	-004	Water Cooled	150A-004	203.0	1	+ 45.0	67.9	102.5	108.2	109.0	1.492	1.480	0.5098	0.5109	5341.0	5340.5	702.7	701.7	52	53	14.4
							2	+ 58.8	70.7	111.7	119.3	120.3	1.506	1.496	0.5609	0.5630	5354.4	5354.2	701.7	698.7	52	53	15.6
							3	+ 71.0	75.0	119.6	128.4	129.7	1.510	1.499	0.6043	0.6075	5351.7	5351.4	698.7	696.7	52	53	16.2
							4	+ 76.6	76.0	123.5	132.3	133.9	1.520	1.511	0.6234	0.6279	5345.1	5344.9	697.7	693.7	52	53	16.4
							5	+ 58.6	70.8	112.5	119.7	120.7	1.509	1.499	0.5616	0.5637	5365.8	5365.8	701.7	698.7	52	53	14.5
							6	+ 45.4	67.9	104.9	110.0	110.7	1.514	1.502	0.5155	0.5166	5368.7	5368.4	702.7	701.7	52	53	13.6
							7	+ 58.6	70.6	112.5	119.4	120.5	1.531	1.522	0.5585	0.5603	5381.9	5381.9	701.7	697.7	52	53	14.4
							8	+ 76.8	75.5	124.0	133.1	134.6	1.534	1.525	0.6224	0.6263	5383.5	5383.4	697.7	693.7	52	53	15.9
							9	+ 58.6	70.5	112.5	119.7	120.7	1.528	1.518	0.5601	0.5622	5379.3	5379.2	701.7	698.7	52	53	14.2
							10	+ 45.4	68.1	105.1	110.3	111.0	1.514	1.502	0.5155	0.5166	5382.6	5382.4	702.7	701.7	52	53	13.2
							11	+ 17.8	60.9	88.9	88.8	89.0	1.508	1.496	0.4186	0.4177	5335.3	5335.0	708.7	707.7	52	53	11.0
							12	+ 1.4	58.7	79.2	76.2	76.2	1.495	1.482	0.3604	0.3587	5316.8	5316.2	711.7	711.7	52	53	9.9
							13	- 37.2	50.5	54.1	43.8	43.7	1.490	1.475	0.2132	0.2113	5163.9	5163.7	716.7	717.7	52	53	6.4
							14	- 51.6	45.2	41.6	30.2	30.1	1.499	1.484	0.1536	0.1522	4933.0	4933.0	717.7	718.7	52	53	5.0
							15	- 61.4	43.8	32.5	21.8	21.7	1.480	1.466	0.1126	0.1115	4859.9	4860.2	719.7	719.7	52	53	4.4
							16	- 70.0	30.9	23.1	17.3	17.2	1.497	1.484	0.0780	0.0771	5566.5	5567.0	721.7	721.7	52	53	3.3
							17	- 62.0	45.0	32.5	21.8	21.7	1.466	1.454	0.1131	0.1119	4845.2	4845.5	720.7	719.7	52	53	4.9
							18	- 52.0	45.7	41.6	30.2	30.1	1.488	1.475	0.1541	0.1526	4923.1	4923.7	718.7	718.7	52	53	5.7
							19	- 37.0	50.5	53.4	43.8	43.7	1.498	1.483	0.2128	0.2109	5176.9	5176.7	716.7	717.7	52	53	7.0
							20	1.4	58.3	78.6	77.3	77.3	1.497	1.484	0.3640	0.3622	5338.5	5337.9	712.7	711.7	52	53	10.5
							21	17.8	60.1	87.8	89.7	89.9	1.513	1.502	0.4218	0.4204	5351.0	5350.8	710.7	708.7	52	53	11.8
							22	45.2	67.2	103.1	109.5	110.1	1.513	1.503	0.5131	0.5132	5371.4	5371.2	706.7	703.7	52	53	13.6
							23	58.6	70.2	111.0	118.7	119.5	1.527	1.516	0.5566	0.5580	5366.5	5366.3	702.7	700.7	52	53	14.4
							24	76.8	75.1	121.5	131.3	132.5	1.539	1.529	0.6156	0.6188	5368.4	5368.2	699.7	696.7	52	53	15.6

FIGURE D-2-24. EXTENDED RANGE THROTTLING TEST DATA

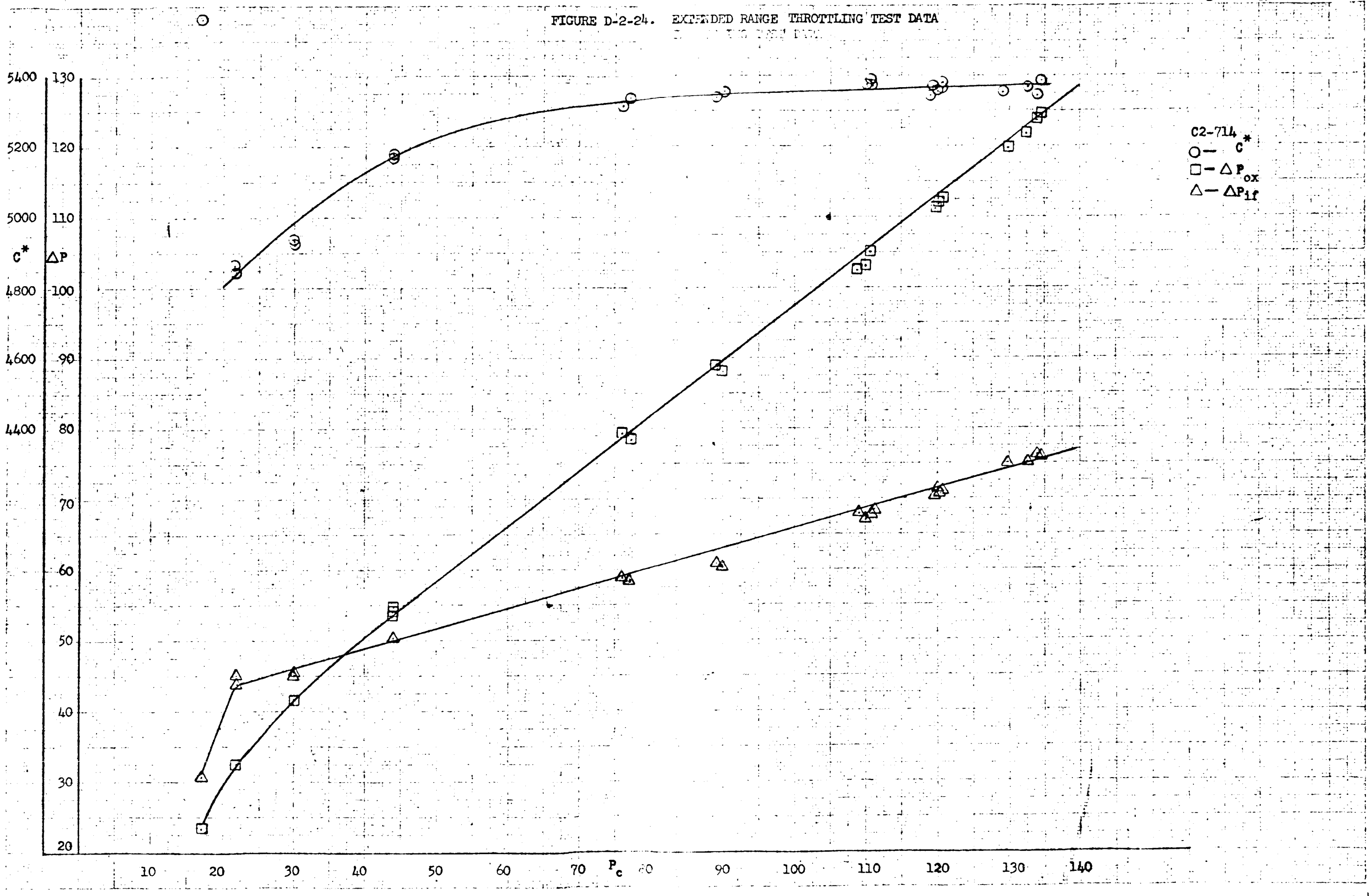

TABLE D-2-25. MIRA 150A PERFORMANCE SUMMARY - BISTABLE COMBUSTION INVESTIGATION

Scream (S)

Head End Assembly	Run No.	Date	Mod.	Water Cooled Unless Noted Chamber*	M.R.	C*unc	ΔP_{ox}	Normal ΔP_f	Bistable ΔP_f	ΔP_f Change	ΔT	$\dot{w}_{H_2O}$	Purge Volume	Empty Passages Downstream of SOV: Purges	Empty Passages Downstream of SOV: Empty Feed Lines	Partially Filled Passages: 5 min	Partially Filled Passages: 2 sec	Throttling	Remarks
150-003	C2-717a	1/12	103955		1.48	5350	80	68			32	64			X				103955 - No Shift
	C2-717b				1.48	5330	81	67			32	64				0/1	0/1		
	C2-717c				1.48	5350	80	69			32	64				0/1	0/1	0/1	
	C2-717d				1.48	5355	80	69			32	64					0/1		
	C2-718a	1/13			1.48	5380	76	65			31	64						0/3	
	C2-718b				1.48	5370	76	67			31	64				0/1		0/1	
	C2-718c				1.48	5400	75	66			31	64					0/1	0/1	
	C2-718d				1.48	5400	75	66			31	64				0/1		0/1	
	C2-719a	1/13			1.37	5300	71	71			30	64	OX			0/1		0/1	Low Mixture Ratio - High Fuel/Low Oxidizer
	C2-719b				1.37	5300	71	72			30	64	OX			0/1			
	C2-720a	1/13			1.62	5390	84	59			33	63	OX			0/1		0/1	High Mixture Ratio - Low Fuel/High Oxidizer
	C2-720b				1.62	5390	83	59			33	63	OX			0/1	0/1		
	C2-720c				1.62	5370	83	59			33	63	OX			0/1		0/1	
	C2-721a	1/13			1.63	5370	82	58			33	63		OX		0/1		0/1	High Mixture Ratio
	C2-721b				1.63	5420	81	58			32	63					0/1		
	C2-721c				1.62	5370	83	59			33	63				0/1			
	C2-722a	1/13			1.37	5290	70	71			30	64				0/1		0/1	Low Mixture Ratio - High Fuel/Low Oxidizer
	C2-722b				1.37	5295	70	71			30	64					0/1		
	C2-722c				1.37	5290	71	72			31	64				0/1			
	C2-722d				1.37	5295	72	71			31	64				0/1			
	C2-723	1/13		Streak	1.48	5385	77	65			13	65				0/1			SK - P_c Rise 13 psi, 200 sec
	C2-724	1/13		Streak	1.53	5540	57	49			13	65				0/1			SK @ Throat of .833 dia. (P_c rise 110→118)
150A-004 Phase II No Q.D.	C2-713a	1/11			1.50	5315	105	67			31	64			X			0/2	Phase II c/o on shift
	C2-713b				1.50	5315	105	69			31	64				0/1		0/4	
	C2-713c				1.51	5330	106	68			31	64					0/1	0/2	
	C2-713d				1.51	5450	106	68	90	22	38	64				1/1		0/4	
	C2-713e				1.51	5320	107	68			31	64					0/1	0/1	
	C2-714a	1/12			1.52	5320	119	73			35	64						0/2	20→180 lb Throttle Run
	C2-714b				1.52	5330	121	74	96	22	40	63				1/1		0/2	Value 132 P_c, wt = .622 lb/sec
	C2-714c				1.52	5330	121	(74)	96	22	39	63				1/1			
	C2-714d				1.52	5330	121	74			36	63					0/1		
	C2-714e				1.52	5330	121	74			36	63						0/1	
	C2-714f																	0/1	
	C2-715	1/12		Streak	1.55	5450	112	(72)	95	23	16	65				1/1			SK @ High ΔP - Bad Streak 112→102 psia P_c
	C2-716	1/12		Streak	1.57	5430	126	74	(96)	22	16	65				1/1		0/2	SK @ 180 lb Thrust - Low Good Streak 137→146 psia P_c

TABLE D-2-25. MIRA 150A PERFORMANCE SUMMARY - BISTABLE COMBUSTION INVESTIGATION

Scream (S)

Head End Assembly	Run No.	Date	Mod.	Water Cooled Unless Noted Chamber	M.R.	C*unc	Normal ΔP_{ox}	Bistable ΔP_f	Bistable ΔP_f Change	Bistable ΔT Change	$\dot{w}_{H_2O}$	Purge Volume	Empty Passages Downstream of SOV: Purges	Empty Passages Downstream of SOV: Empty Feed Lines	Partially Filled Passages: 5 min	Partially Filled Passages: 2 sec	Throttling	Remarks
150A-005	C2-599a	10/17			1.55	5355	97	72			29	64			0/1			*10 sec Cold Propellants
Phase II	C2-599b				1.55	5330	97	(72)	98	26	32	64				1/1*		
No Q.D.	C2-599c				1.56	5320	103	(75)	101	26	33	64			1/1			*10 sec
	C2-599d				1.56	5310	102	(74)	100	26	32	64				1/1*		
	C2-599e				1.55	5335	NR	NR			30	64			0/1			
150A-006	C2-512	8/12			1.63	5255	114	77			34	63			0/1			
Phase II	C2-513	8/12		Streak	1.64	5345	*123	77			15	64			0/1			*Helium Leak Possible
No. D.	C2-514	8/13			1.62	5225	120	(77)	85	8	34	63			1/1			
	C2-515a	8/13		009	1.61	5330	123	75							0/1			
	C2-515b			009	1.65	5330	126	75							0/1			
	C2-515c			009	1.65	5310	*134		NR						(1/1)*			*Helium Leak Possible High ΔP
150A-007	C2-615	10/31			1.52	5311	87	64			30	64		X				C/O
Q.D.s	C2-616	11/2		No Good F Flow			90	(65)	86	21	32	65			1/1			By Pass Open
Phase	C2-617	11/7		No Good F Flow			90	(65)	85	20	33	65			1/1			
III	C2-618	11/2			1.47	5250	91	67			31	65			0/1		0/1	
	C2-619	11/3			1.48	5240	90	68	86	20	33	63			1/1		0/1	4 Point Throttle
	C2-620	11/3		Streak	1.48	5390	91	(68)	85	17	19	66			1/1			Streak (Bad)
	C2-621	11/3			1.49	5260					31	66					0/1	AT-1
	C2-628	11/12		004	1.57	5365												Erosion High ΔP (P_c 109 ⟶ 99 psia)
	C2-629	11/13		004	1.43	5180	82	67			30	63			0/1		0/1	C/O W/C
	C2-630	11/16		004	1.40	5250	80	65			28	64			0/1		0/1	
150A-008	C2-631	11/17			1.48	5240	97	64			33	64		X			0/1	P_c 117 psia
Phase III	C2-632	11/17		Streak	1.49	5360	90	63			15	64			0/1			(Streak)
Q.D.	C2-633	11/17		002	1.61	5310	96								0/1			Good Chamber Test 235 sec
	C2-640	11/21			1.49	5315	97	63			31	64		X			0/1	C/O Following HEA Calib.
	C2-641	11/21			1.52	5215	99	63			31	64			0/1		0/1	
	C2-642	11/21			1.52	5215	94	63			32	64			0/1		0/1	
	C2-643	11/22		Streak	1.49	5380	94	63			12	66						Good Sk- Send to Edwards
	C2-669a	12/10			1.41	5100	81	59						X				C/O Actuator 103 P_c psia
	C2-669b				1.44	5260	88	60			31	64			0/1		0/1	
	C2-669c				1.44	5250	90	(60)	75	25	32	64			1/1			
	C2-669d				1.45	5320	94	(60)	79	29	34	64				1/1		
	C2-669e				1.45	5285	92	63			31	64				0/1		
	C2-670	12/10			1.46	5300	92	62									0/1	PQ3 Tape
	C2-678	12/15			1.50	5310	97	60			32	63		X			0/1	C/O - Pre Vib.
	C2-679	12/15			1.52	5300	95	60			31	64			0/1		0/1	17 Point Throttle
	C2-680	12/15			1.50	5280					31	65					0/1	AT-1 Tape

TABLE D-2-25. MIRA 150A PERFORMANCE SUMMARY - BISTABLE COMBUSTION INVESTIGATION

Head End Assembly	Run No.	Date	Mod.	Water Cooled Unless Noted Chamber	M.R.	C*unc	ΔP_{ox}	Nor-Bimal stable ΔP_f	ΔP_f	ΔP_f Change	ΔT	$\dot{w}_{H_2O}$	Purge Volume	Empty Passages Downstream of SOV: Purges	Empty Passages Downstream of SOV: Feed Lines	Partially Filled Passages: 5 min	Partially Filled Passages: 2 sec	Throttling	Remarks
150A-008 Phase III Q.D. (Continued)	C2-709a	1/6		007	1.64*	5350	91	51*							X				Post Vib. - Max F gas from Screws/ Flowing Bond Material
	C2-709b			007	1.62	5310	92	52								0/1			
	C2-709c			007	1.61	5330	92	53								0/1			
	C2-710	1/7			1.48	5280					31	64						0/1	AT-1 Tape
	C2-711a	1/7			1.47	5250	87	59			30	65				0/1		0/1	ΔP Investigation
	C2-711b				1.49	5280	87	59	74	15	32	65				1/1		0/1	
	C2-711c				1.49	5290	93	63	78	15	31	65					1/1	0/1	
	C2-711d				1.49	5310	96	66	82	16	31	65					1/1	0/1	
	C2-711e				1.49	5250	97	(66)	82	16	30	65				1/1			
	C2-711f				1.49	5270	95	66			29	65					0/1	0/1	
	C2-711g				1.49	5300	97	66	83	17	32	65					1/1	0/1	
150A-009 Phase III with Q.D.	C2-634	11/18			1.49	5290	97	63			32	64			X				4 Point C/O - Acceptance P_c-115 psia
	C2-635	11/19			1.46	5260	94	62			31	64				0/1			4 Point C/O P_c-110 psia
	C2-636	11/19			1.48	5310	95	61	80	19	32	65				1/1	0/1		
	C2-637	11/19		Streak	1.52	5440	94	(63)	76	13	15	66				1/1			Bad Streak
	C2-681a	12/22	Small Sleeve		1.49	5265	100	62			33	64			X			0/1	5 Point Thrust
	C2-681b				1.50	5270	102	66			33	64				0/1			
	C2-681c				1.50	5380	101	(66)	85	19	40	64					1/1		
	C2-681d				1.50	5360	97	65	83	18	39	64				1/1		2/3	
	C2-681e				1.50	5380	102	66	86	20	39	64					1/1	1/2	
	C2-682a	12/22			1.49	5415	98	62	81	19	39	64			X			0/2	Small Sleeve Tip
	C2-682b				1.51	5415	98	(64)	81	17	39	64					1/1		
	C2-682c				1.51	5410	98	64	83	19	40	64				1/1		0/1	
	C2-683	12/22			1.50	5280					33	64						0/5	AT-1 Tape
	C2-684	12/22		Streak	1.50	5500	97	62*	19	16	16	65				1/1		0/1	*Good Streak Low ΔP during 200 sec
150A-010	C2-644	11/23			1.512	5292	92	65			33	64			X				1st Firing on 010
	C2-645	11/23			1.520	5302	87	62			31	65				0/1			
	C2-646	11/23		Streak	1.535	5420	90	(62)	82	20	15	67			X	0/3			Bad Streak Test
	C2-649	11/30			1.533	5253	89	63			31	65			X	0/3			
	C2-650a	11/30			1.42	5330	85	(68)	90	22	30	65				1/1			S Low MR
	C2-650b				1.65	5315	93	56			29	65				0/1*			High MR*
	C2-651a	11/30			1.52	5273	95	66			31	65				0/1*			High Momentum
	C2-651b				1.55	5315	88	(62)	74	22	35	65				1/1			S Low Mom.
	C2-652	12/1		Streak	1.43	5370	84	(66)	72	16	12	65				0/1			Low MR - Ox Filter
	C2-653a	12/1			1.52	5260	95	66			28	66				0/1			High Mom.
	C2-653b				1.53	5200	97	67			26	66				0/1			High Mom.
	C2-654	12/1		Streak	1.53	5410	99	(67)	90	23	13	67			X				C/O

TABLE D-2-25. MIRA 150A PERFORMANCE SUMMARY
BISTABLE COMBUSTION INVESTIGATION

Scream Ⓢ

Head End Assembly	Run No.	Date.	Mod.	Water Cooled Unless Noted Chamber	M.R.	C*unc	Normal ΔP_{ox}	Normal ΔP_f	Bi-stable ΔP_f	Bi-stable ΔP_f Change	ΔT	$\dot{w}_{H_2O}$	Purge Volume	Empty Passages Downstream of SOV: Purges	Empty Passages Downstream of SOV: Empty Feed Lines	Partially Filled Passages: 5 min	Partially Filled Passages: 2 sec	Throttling	Remarks
150A-010	C2-661	12/8			1.52	5270	84	59			29	63			X				C/O
	C2-662a	12/8			1.52	5266	90	62			32	65				0/1			Normal Mom.
	C2-662b	12/8			1.52	5338	91	(62)	80	18	37	65				1/1			Ⓢ Normal Mom.
	C2-663a	12/8			1.52	5275	99	72			31	64				0/1			High Mom.
	C2-663b				1.52	5322	99	72			31	64				0/1			High Mom.
	C2-663c				1.52	5322	100	(72)	92	20	35	64				1/1			Ⓢ High Mom.
	C2-664a	12/8			1.51	5325	109	(80)	100	20	34	65				1/1			Ⓢ High Mom.
	C2-664b				1.51	5315	111	(80)	105	25	34	65				1/1			Ⓢ High Mom.
	C2-664c				1.51	5295	111	(80)	105	25	33	65				1/1			Ⓢ High Mom.
	C2-665a	12/9	Rough		1.47	5225	84	63			29	65				0/1			Normal
	C2-665b		Sleeve		1.47	5255	85	(63)	78	15	31	65				1/1			Ⓢ
	C2-666a	12/9	Installed &		1.48	5205	101	(61)	75	14	32	65				1/1			Ⓢ
	C2-666b		Left in		1.48	5245	99	(61)	74	13	32	65				1/1			Ⓢ
	C2-666c				1.48	5220	103	(61)	76	15	32	65				1/1			Ⓢ
	C2-666d				1.48	5230	103	61			30	65					0/1		
	C2-666e				1.48	5225	105	(61)	78	17	32	65				1/1			Ⓢ
	C2-667a	12/9			1.49	5240	86	62			29	65	F	F		0/1			
	C2-667b				1.49	5260	86	62			29	65	F			0/1			
	C2-667c				1.49	5250	86	62			29	65	F				0/1		
	C2-667d				1.49	5275	88	(62)	79	17	31	65	F			1/1			Ⓢ
	C2-667e				1.49	5250	87	62			29	65	F	F		0/1			
	C2-667f				1.49	5240	87	62			29	65	F	F		0/1			
	C2-667g				1.49	5230	86	62			29	65	F	F		0/1			
	C2-667h				1.49	5230	87	62			29	65	F			0/1			
	C2-667i				1.49	5260	85	61			29	65	O&F	O&F		0/1			
	C2-667j				1.49	5270	85	61			29	65	O	O&F			0/1		
	C2-668a	12/9		Streak	1.48	5351	85	62			12/13	66		O&F					200 sec. Purge Line removed
	C2-668b			Streak	1.48		86	(62)	79	17	13/15	66				1/1			15 sec
	C2-671	12/11			1.52	5275	89	60			30	65			X			0/1	5 Point Thrust Run
	C2-672				1.52	5185	89	60			31	65						0/1	PQ-3 Tape
	C2-673	12/11		Streak	1.52	5375	87	60			13	66		F					Good Streak
	C2-685a	12/23			1.53	4940	86	66			25	65			X				Engine with chip from
	C2-685b				1.53	5075	88	(66)	84	18	28	65				1/1			Edwards: Low C*(Chip
	C2-685c				1.53	5106	90	(67)	85	18	28	65					1/1*	1/1*	in Fuel Gap)
	C2-686	12/28			1.51	5330	85	37*			33*	64			X			0/1	
	C2-687a	12/28			1.52	5280	86	64								0/1		0/1	
	C2-687b				1.52	5265	88	(68)	82	14						1/1		0/1	
	C2-687c				1.52	5265	90	(68)	85	17						1/1			
	C2-687d				1.52	5360	89	68									0/1		
	C2-687e				1.52	5270	89	68									0/1		
	C2-688a	12/28	Plugged Q.D.		1.53	5280	93	70			31	65			X			0/1	*Quick D. Plugged (Teflon)

TABLE D-2-25. MIRA 150A PERFORMANCE SUMMARY
BISTABLE COMBUSTION INVESTIGATION

Scream (S)

Head End Assembly	Run No.	Date	Mod.	Water Cooled Unless Noted Chamber	M.R.	C*unc	Normal Bistable ΔP_{ox}	ΔP_f	ΔP_f Change	ΔT	$\dot{W}_{H_2O}$	Purge Volume	Empty Passages Downstream of SOV: Purges	Empty Feed Lines	Partially Filled Passages: 5 min	2 sec	Throttling	Remarks
150A-010	C2-688b	12/28	Plugged		1.53	5265	90	68		31	65				0/1*			
	C2-688c		Q.D.		1.53	5268	90	68	91 23	33	65					0/1	2/2	
	C2-688d				1.53	5265	90	68		30	65					0/1		
	C2-688e				1.52	5280	93	(68)	91 23	33	65				1/1		3/3	
	C2-688f				1.53	5300	91	(69)	91 22	33	65				0/1*		1/1	
	C2-688g				1.53	5275	90	68		30	65					0/1	0/2	
	C2-688h		Plugged Q.D.		1.53	5270	90	68		30	65					0/1		
	C2-689a	12/29			1.46	5270	86	69		30	64				0/1*		0/3	*Quick D. Plugged(Teflon)
	C2-689b				1.47	5283	90	(69)	89 20	31	64				1/1		0/1	
	C2-689c				1.48	5281	86	68		30	64					0/1	0/1	
	C2-690a	12/29			1.53	5290	91	71	93 22	33	64			X			1/1	Std.Conf.
	C2-690b				1.53	5270	90	70	92 22	33	64					0/1	1/2	
	C2-690c				1.53	5250	90	70		30	64					0/1		
	C2-691a	12/29			1.62*	5280	93	63	82* 19	36	64				0/1		2/3	Std.Conf. @ 1.6 M.R.
	C2-691b				1.62*	5310	93	63	82* 19	36	64					0/1	1/2	
	C2-692	12/29		Streak	1.52	5355	90	69	92 23	14	65				0/1		1/1	Bad Streak, Dirt
	C2-693	12/29		Streak	1.52	5400	90	(69)	86 17	14	65				1/1			Dirt Removed Between Runs
	C2-694a	12/30		CC 014	1.61	5398	94	(63)	79 16						0/1		1/1	Hole in Side of Chamber at
	C2-694b			CC 014	1.61	5380	92	(63)	77 14						1/1		1/1	265 seconds/300
	C2-694c			CC 014	1.61	5370	94	(63)	80 17						0/1		1/3	
	C2-695	12/31		Streak	1.61	5440	95	(61)	79 18	14	66				0/1	0/1	1/13	Bad - Streak
	C2-696a	12/31	80°		1.52	5260	90	75	79 4	32	64				0/1		1/1	*80° Pintle
	C2-696b		Pintle		1.52	5270	91	76		31	64				0/1			
	C2-696c				1.52	5328	92	76	81 5	33	64				0/1	0/1	2/3	
	C2-697a	12/31			1.53	5300	91	78		30	64				0/1		0/2	80°Pintle
	C2-697b				1.52	5280	93	78		30	64					0/1		
	C2-698	12/31		Streak	1.50	5410	88	77		12	66				0/1*			
	C2-699a	1/4	Phase		1.52	5275	89	66		30	64			X			0/1	006 Pintle
	C2-699b		II 006		1.53	5280	90	66	84 18	34	64				0/1		1/1	
	C2-699c		Pintle		1.53	5280	90	67	87 20	34	64					0/1	3/3	
	C2-700a	1/4	P.Q.D.		1.52	5320	90	67	86 19	34	64			X			1/1	Plugged Q.D.
	C2-700b				1.52	5280	92	(67)	83 16	33	64				1/1			
	C2-700c				1.52	5300	94	(68)	87 19	34	64					0/1	1/1	
	C2-701a	1/4	P.Q.P.		1.53	5260				34	64				0/1		1/1	S Plugged* Q.D. & Pinj
	C2-701b		Pinj		1.53	5260				34	64				0/1		1/1	S "
	C2-701c				1.53	5260				34	64					1/1	0/3	S "
	C2-701d				1.53	5260				34	64				0/1		0/2	S "
	C2-701e				1.53	5260				34	64					1/1	0/1	S "
	C2-702a	1/5			1.50	5240	88	65		30	64			X			0/3	Original Configuration
	C2-702b				1.50	5250	88	66		30	64				0/1		0/1	
	C2-702c				1.52	5310	93	66	86 20	33	65					0/1	3/3	
	C2-702d				1.52	5300	94	67	89 22	33	65					0/1	1/1	

TABLE D-2-25. MIRA 150A PERFORMANCE SUMMARY
BISTABLE COMBUSTION INVESTIGATION

Scream ©

Head End Assembly	Run No.	Date	Mod.	Water Cooled Unless Noted Chamber	M.R.	C*unc	Normal Bistable ΔP_{ox}	ΔP_f	ΔP_f Change	ΔT	$\dot{w}_{H_2O}$	Purge Volume	Empty Passages Downstream of SOV: Purges	Empty Feed Lines	Partially Filled Passages: 5 min	2 sec	Throttling	Remarks
150A-010	C2-703a	1/5	QDB		1.52	5280	92	68		31	64				0/1		0/2	*Q.D.S. Bled
	C2-703b				1.52	5280	92	68		31	64					0/1	0/5	"
	C2-703c				1.52	5340	94	68	87 19	34	64				0/1*		1/1	"
	C2-703d				1.52	5315	94	67	87 20	34	64					0/1	1/1	"
	C2-703e				1.52	5200	95	(68)	95 27	31	64				1/1			"
	C2-703f				1.52	5310	94	68	87 19	35	63					0/1	1/1	"
	C2-703g				1.52	5310	94	67	87 20	35	63					0/1	1/1	"
	C2-704a	1/5			1.52	5280				33	65				0/1*		1/2	*Q.D.S. Bled, P_f, P_{ox} Removed
	C2-704b				1.52	5320				34	65					1/1	1/1	"
	C2-704c				1.52	5340				33	65					0/1	1/1	"
	C2-704d				1.52	5320				35	64				0/1*		2/2	"
	C2-704e				1.52	5330				35	64					0/1	1/1	"
	C2-705a	1/5			1.52	5340				34	65			X			1/1	Q.D.S. Plugged Inj. Ports
	C2-705b				1.52	5330				35	64					0/1	1/1	
	C2-706a	1/5	QDP		1.52	5280				30	64				0/1		0/3	Q.D.S. Pinj Plugged
	C2-706b				1.52	5310				34	64					0/1	1/1	
	C2-706c				1.52	5320				34	64					0/1	1/1	
	C2-706d				1.52	5310				34	65					0/1	1/1	
	C2-706e				1.52	5310				34	64				1/1		1/1	
	C2-706f				1.52	5310				34	64					0/1	7/8	
	C2-707a	1/5		Streak	1.52	5390				14	66				1/1		3/3	Streak Lost Propellant @ 165
	C2-708	1/6		Streak	1.63	5420				15	66				2/2		2/2	Bad Streak
150A-011	C2-674a	12/14			1.47	5300	92	69*		32	64			X				*Dirt Int ΔP_f @ 117 P_c
	C2-674b				1.47	5100	101	(69*)	89 20	31	64				1/1			
	C2-674c				1.49	5065	103	(69*)	90 21	31	64					1/1		
	C2-674d				1.49	5035	103	(69*)	91 22	31	64					1/1		
	C2-675a	12/14			1.47	5120	85	62	76 14	29*	64				1/1		0/1	*5 sec High Engine Cleaned itself
	C2-676	12/14			1.47	5285	81	59		328	64				0/1		0/1	Heat Flux decreased when ΔP shifted. C2-675.
	C2-677	12/15		Streak	1.46	5365	79	59		13	66				0/1			

FIGURE D-2-26. BISTABLE COMBUSTION INVESTIGATION DATA - HEA 150-003

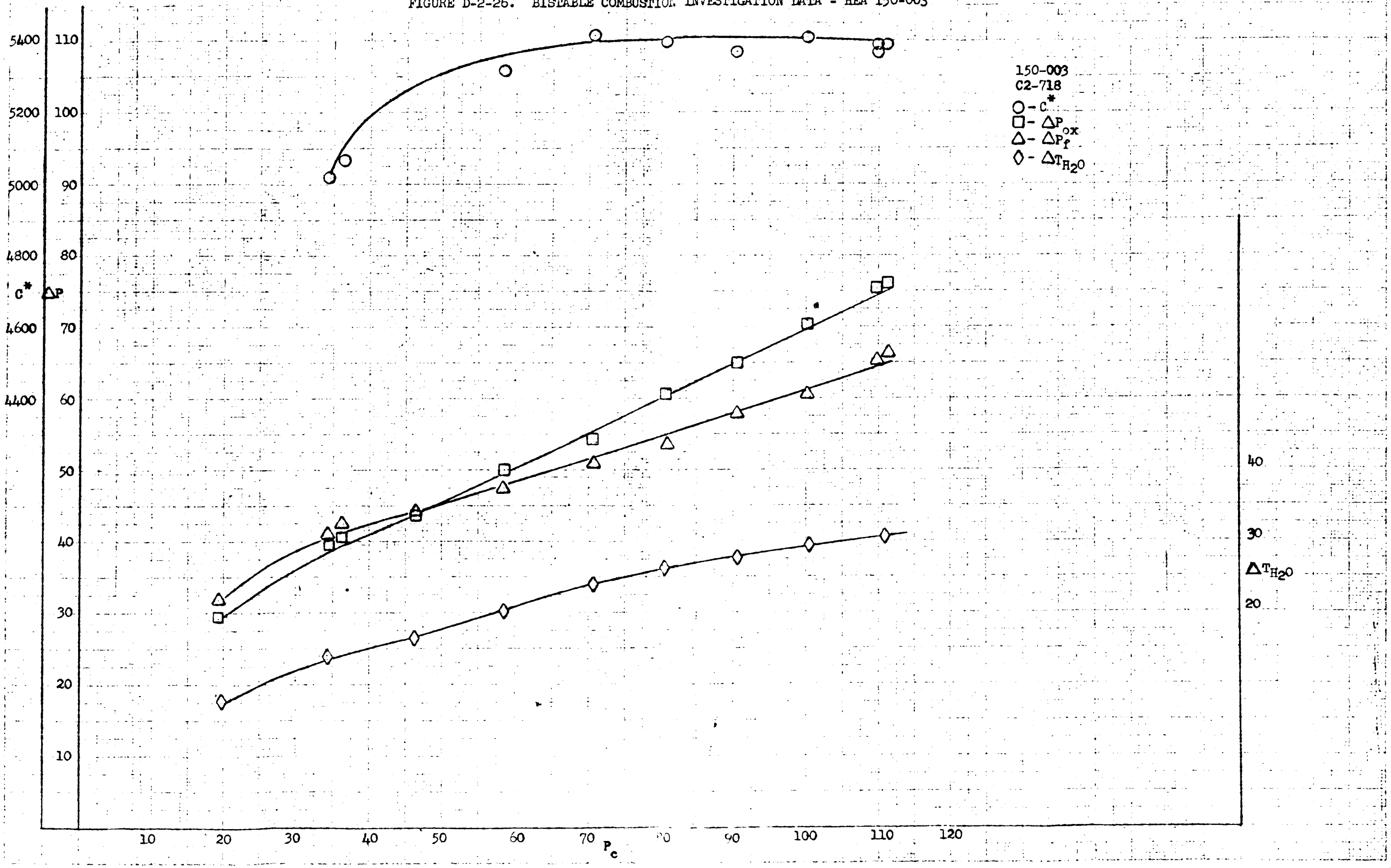

FIGURE D-2-27. BISTABLE COMBUSTION INVESTIGATION DATA - HEA 150A-040

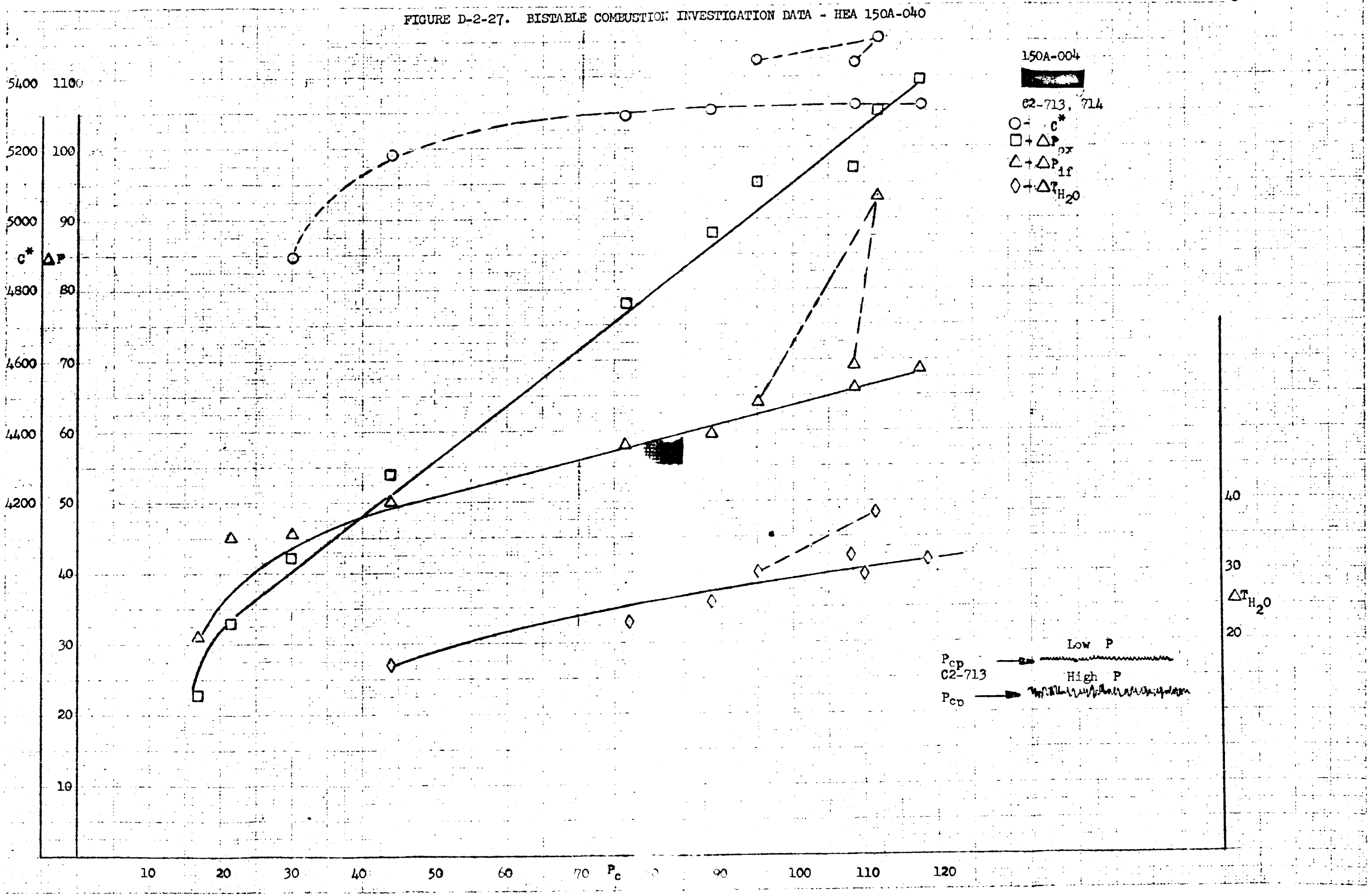

FIGURE D-2-28. BISTABLE COMBUSTION INVESTIGATION DATA - HEA 150A-005

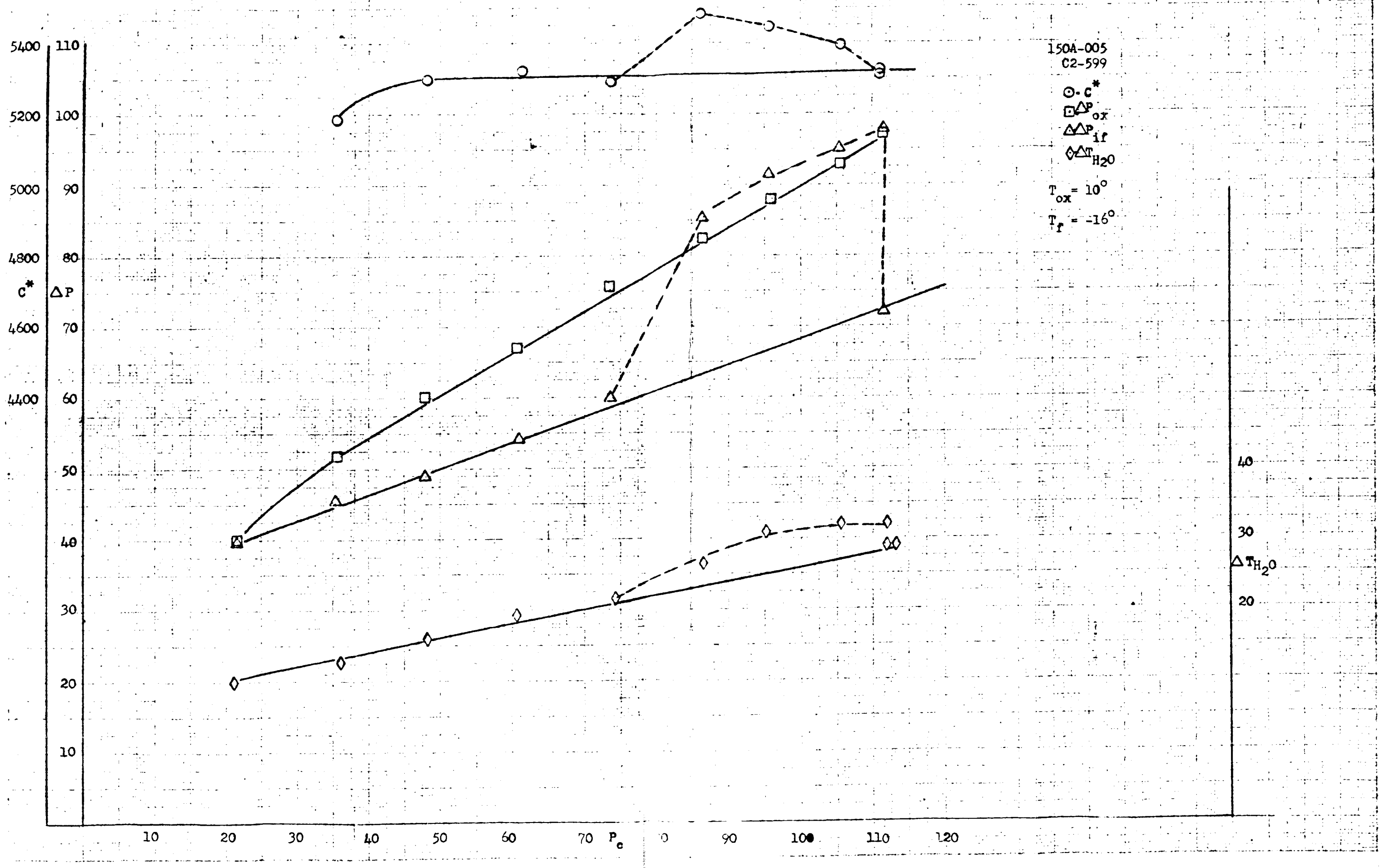

FIGURE D-2-29. BISTABLE COMBUSTION INVESTIGATION DATA - HEA 150A-006

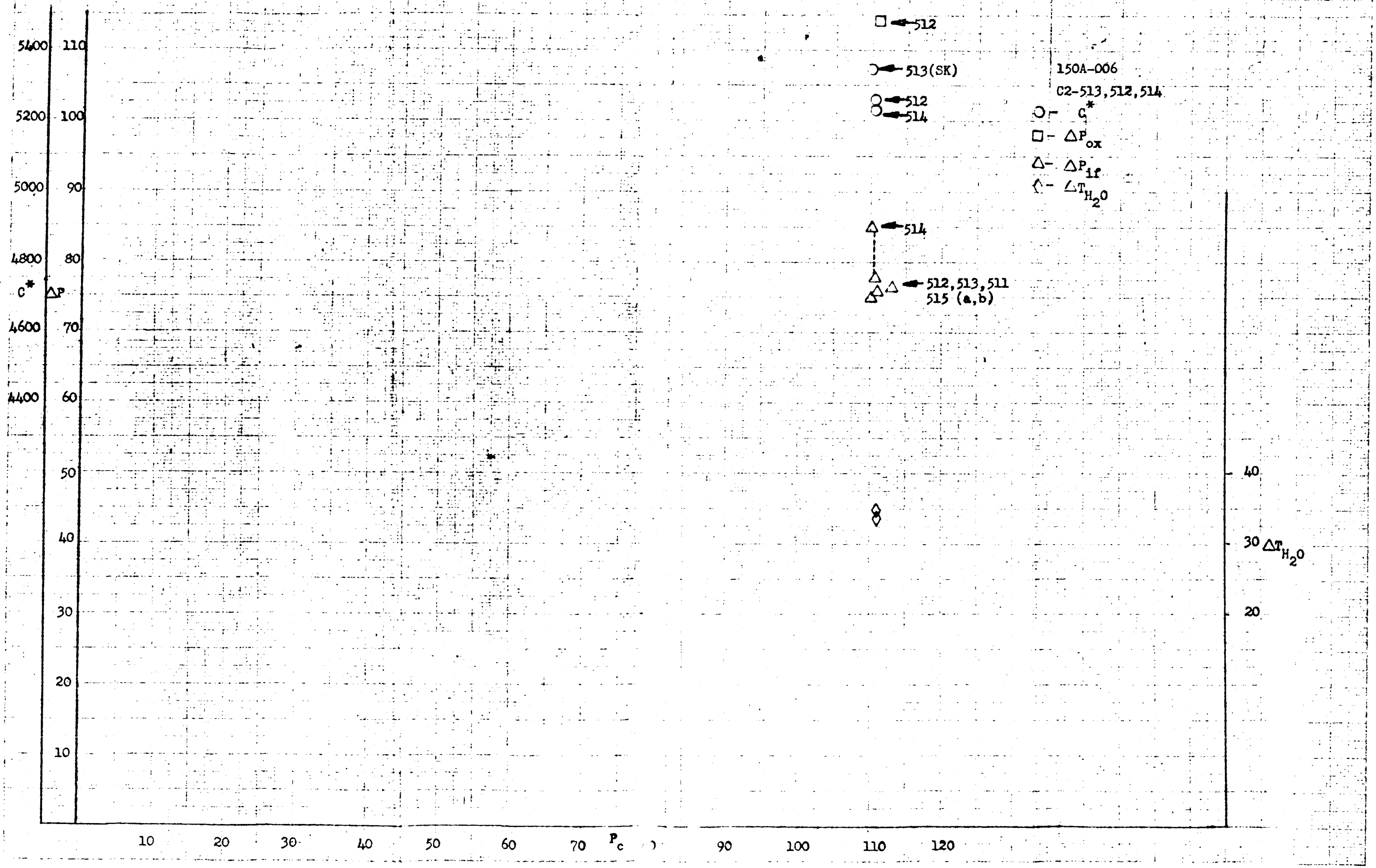

FIGURE D-2-31. BISTABLE COMBUSTION INVESTIGATION DATA - HEA 150A-008

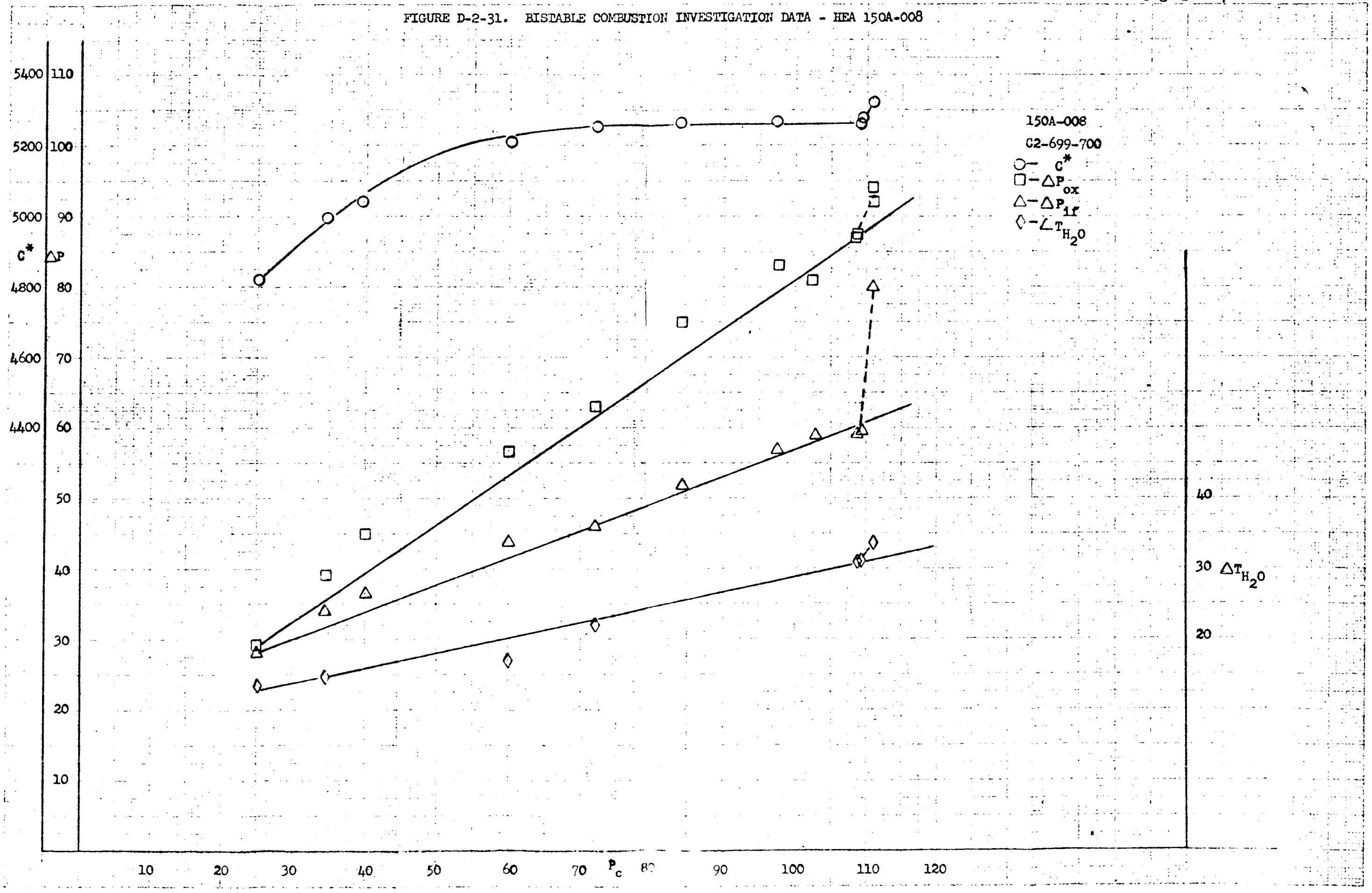

FIGURE D-2-32. BISTABLE COMBUSTION INVESTIGATION DATA - HEA 150A-009

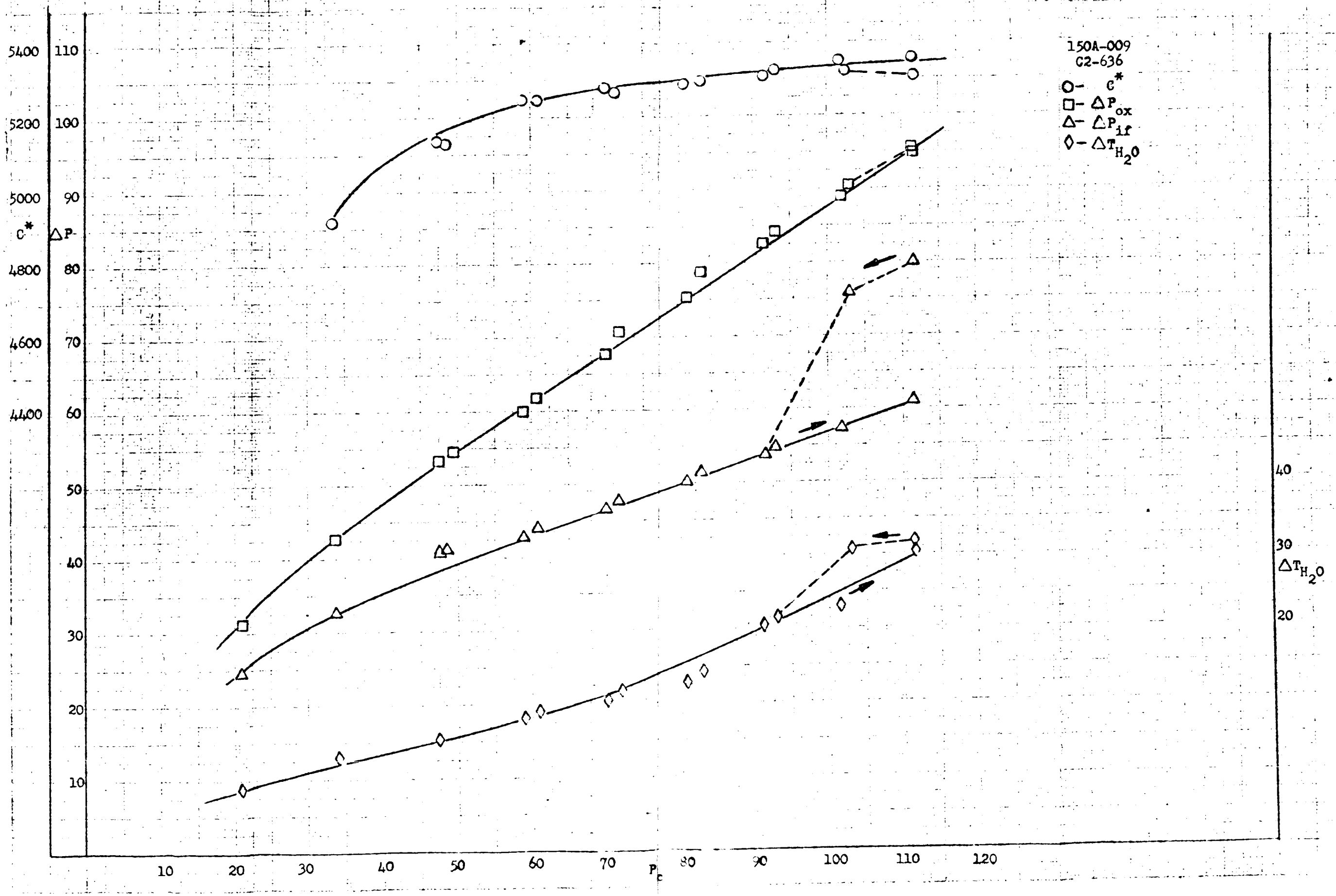

FIGURE D-2-33. BISTABLE COMBUSTION INVESTIGATION DATA - HEA 150A-009 WITH SMALL SLEEVE

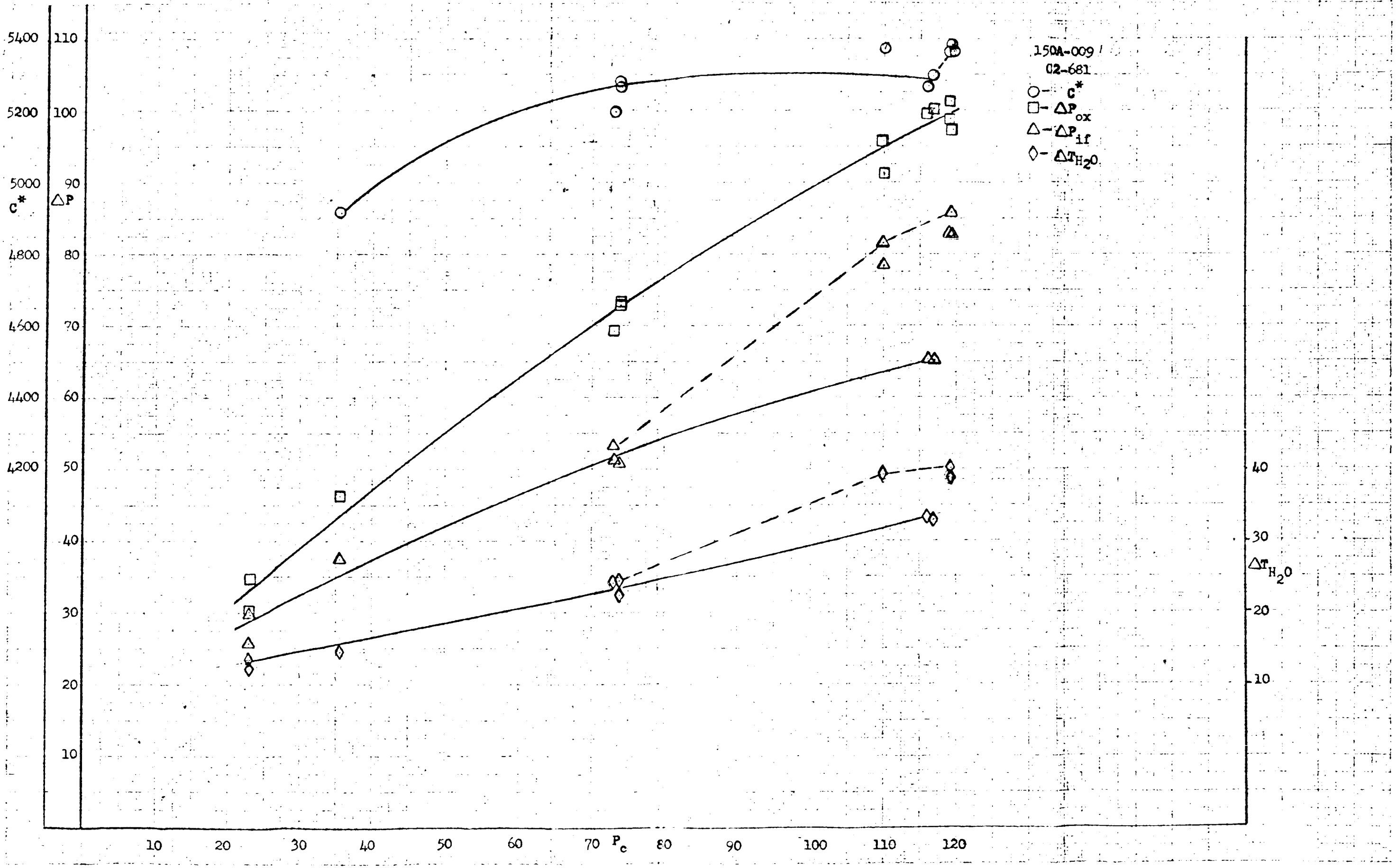

FIGURE D-2-34. BISTABLE COMBUSTION INVESTIGATION DATA - HEA 150A-010

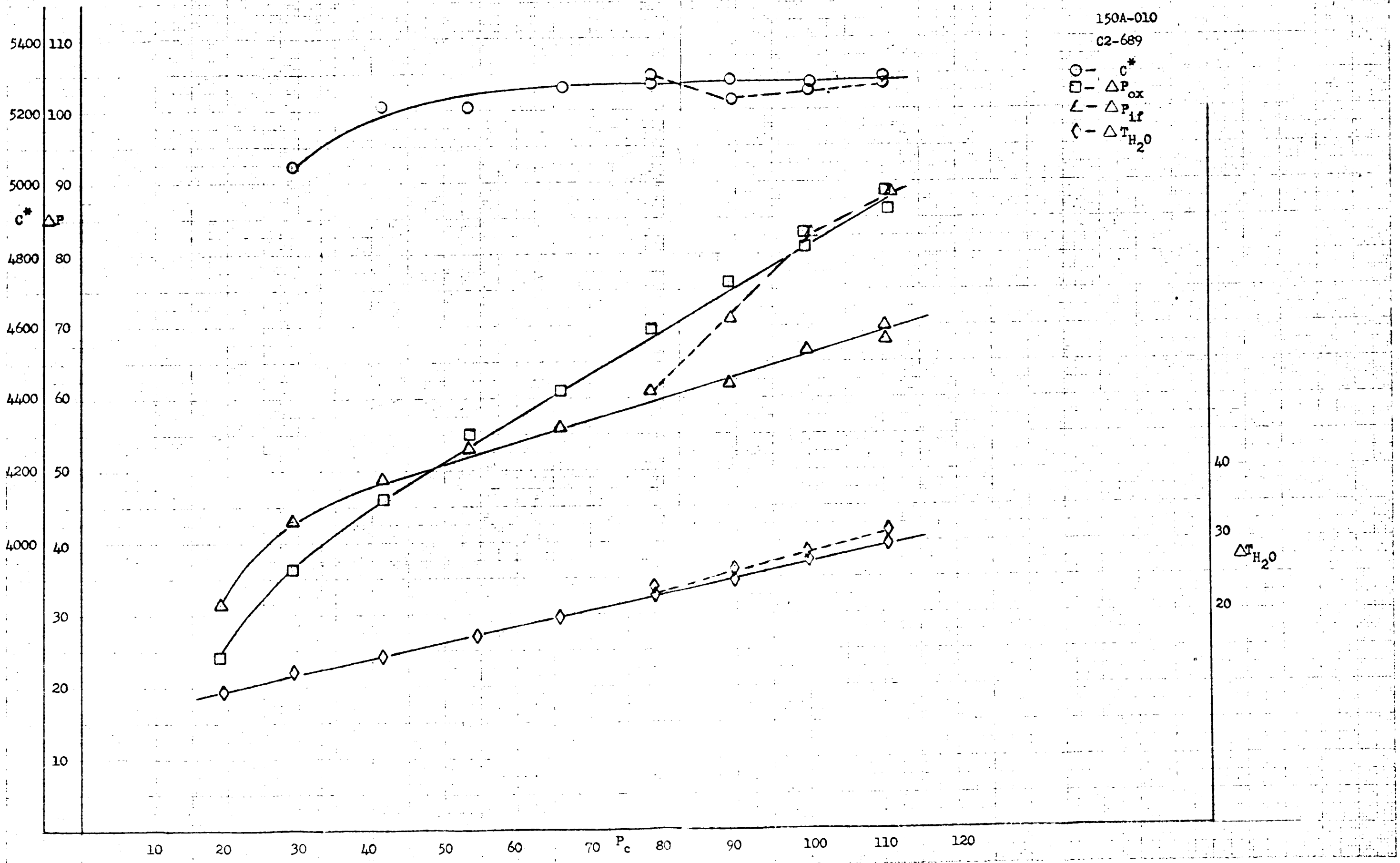

FIGURE D-2-35. BISTABLE COMBUSTION INVESTIGATION DATA - HEA 150A-010 WITH EXCHANGED PINTLE

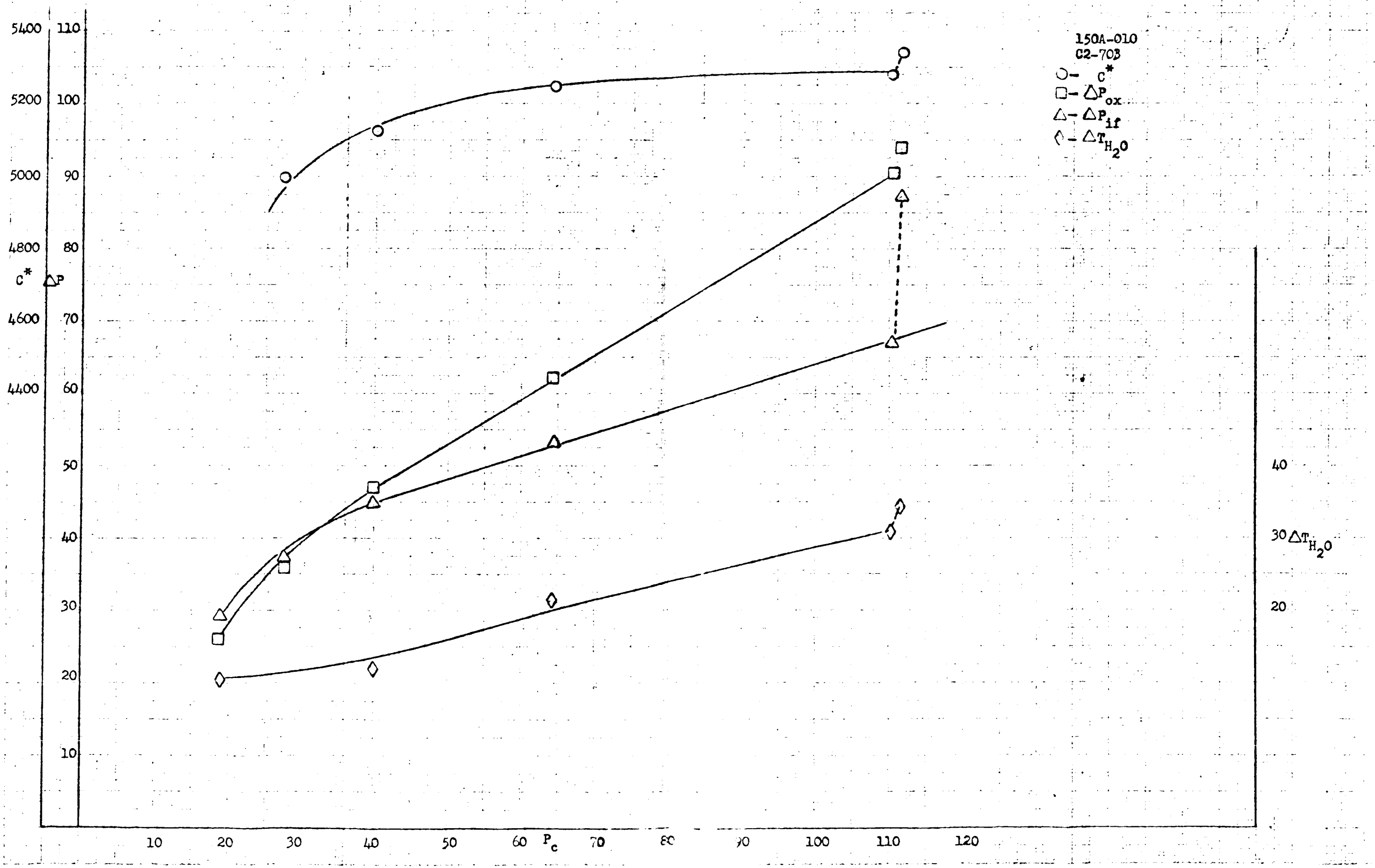

140

FIGURE D-2-36. BISTABLE COMBUSTION INVESTIGATION DATA - HEA 150A-010 WITH 80° PINTLE

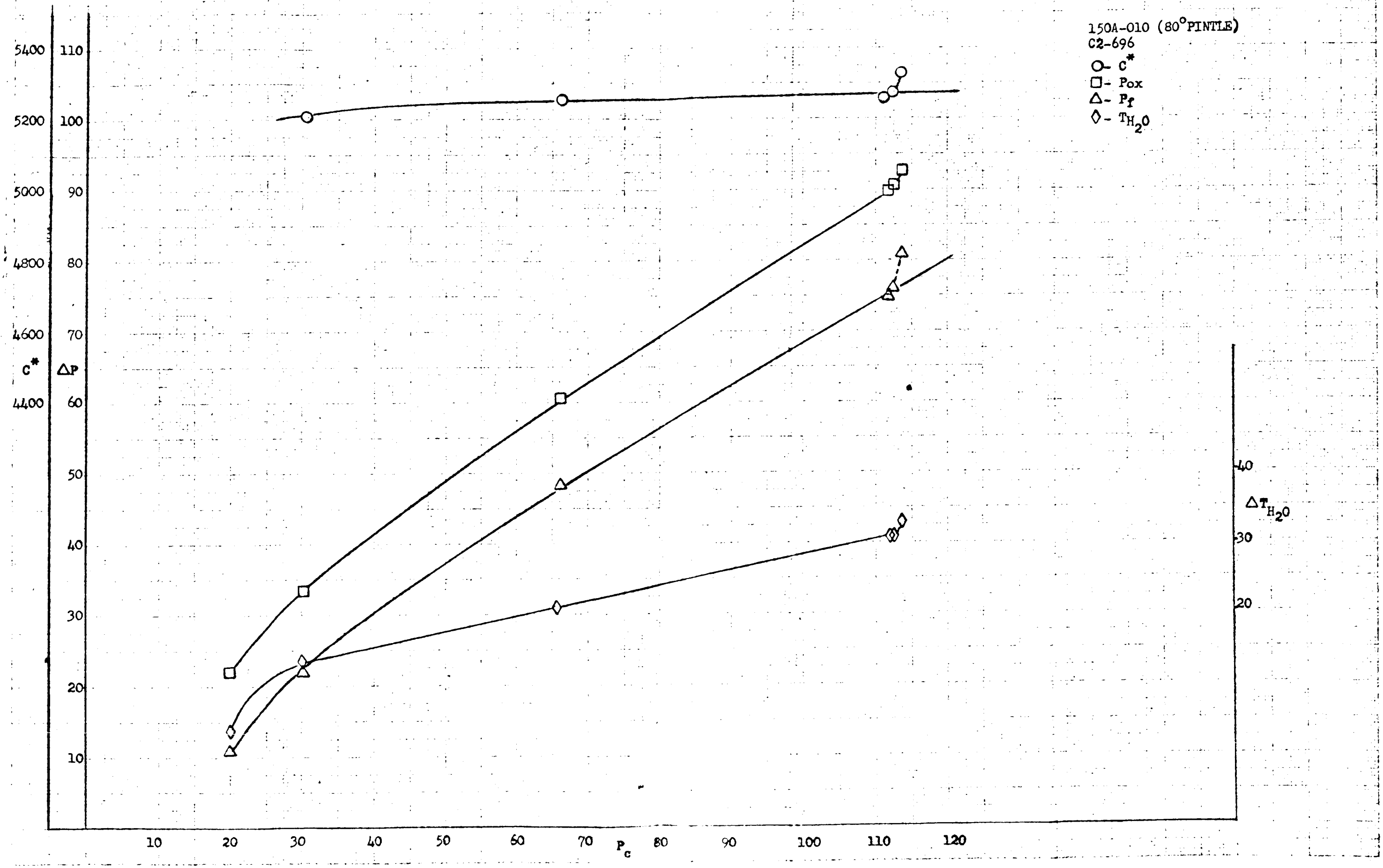

FIGURE D-2-37. BISTABLE COMBUSTION INVESTIGATION DATA - HEA 150A-011

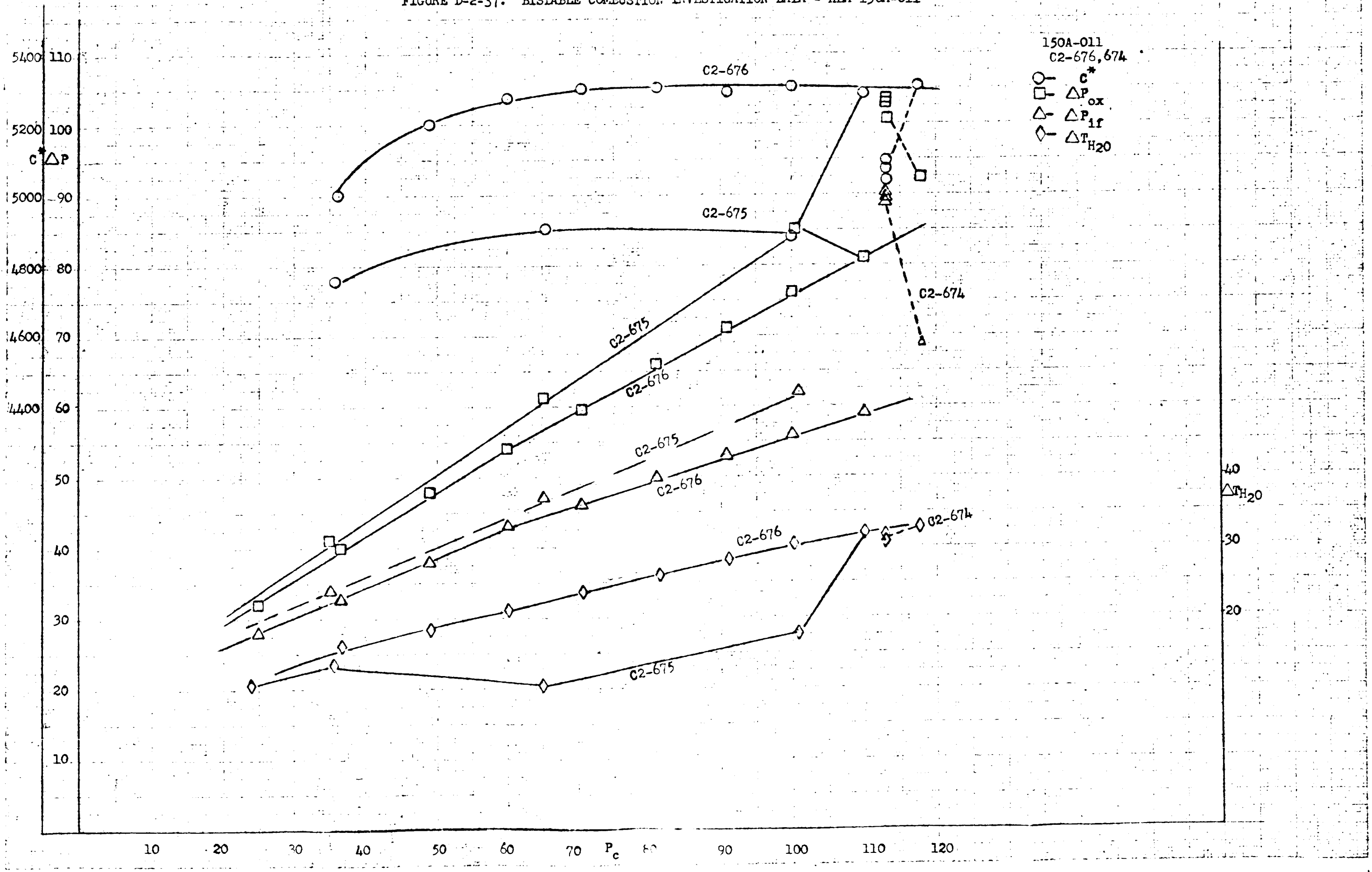

APPENDIX D-3

CAPISTRANO STATIC FIRING DATA

No. of Pages: 3

TABLE D-3-1. MIRA 150A STEADY-STATE PERFORMANCE, CAPISTRANO TEST SITE (HEPS) - CENTRIFUGE TESTS

IRTS Test No.	Development Plan or PQT Test No.	Test Date	HEA S/N	CC ≠ NA Type	CC ≠ NA S/N	Test Duration sec.	Data Slice No.	Servo Command ma	ΔP_{if} Stand	ΔP_{ox} Stand	Head-End P_c psia Site	Stand	M.R. - o/f Site	Stand	Total Flowrate lbs/sec Site	Stand	Corrected C^* fps Site	Stand	Fuel Inlet Press, psia Actual	Oxidizer Inlet Press, psia Actual	Fuel Inlet Temp, °F	Oxidizer Inlet Temp, °F
HEPS-001	None	11-27-64	001	Abl	006	130.0	1	Lost	46.6	60.0	67.8	70.2	1.534	1.504	.3287	.3403	5175.1	5177.2	649.5	664.5	52	53
							2	Instru-	53.5	75.9	88.0	92.7	1.571	1.513	.4222	.4445	5231.9	5234.3	615.5	652.5	53	55
							3	mentation	60.2	89.1	105.2	112.5	1.619	1.536	.4994	.5339	5285.0	5289.3	586.5	641.5	54	56
							4		53.4	75.1	87.2	92.0	1.604	1.510	.4183	.4410	5231.0	5234.8	597.5	663.5	55	56
							5		46.4	60.7	68.2	71.1	1.605	1.503	.3294	.3432	5192.1	5198.0	607.5	682.5	55	57
							6		36.2	44.8	47.2	48.8	1.610	1.503	.2350	.2436	5016.6	5025.5	616.5	696.5	55	57
							7		24.1	26.7	25.5	27.2	0.010	0.009	.0519	.0555			625.5	706.5	55	57
							8		31.6	33.9	34.4	37.0	0.008	0.007	.0687	.0740			614.5	699.5	55	57
							9		37.8	45.0	47.2	49.5	1.615	1.502	.2363	.2471	5016.8	5027.0	598.5	681.5	55	57
							10		47.7	61.8	68.5	73.0	1.638	1.503	.3321	.3529	5178.7	5188.6	570.5	666.5	55	57
							11		62.2	90.7	107.3	119.4	1.807	1.535	.5047	.5583	5334.0	5368.5	477.5	651.5	56	59
							12		47.2	57.7	65.7	72.5	1.830	1.510	.3173	.3469	5194.8	5243.4	471.5	681.5	56	59
							13		60.0	85.3	101.4	114.3	1.898	1.533	.4775	.5324	5327.0	5385.9	440.5	664.5	56	60
							14		60.6	84.9	99.9	115.0	1.915	1.529	.4697	.5342	5339.0	5403.6	417.5	644.5	65	60
HEPS-002	None	11-27-64	001	Abl	006	110.0	1		44.6	58.1	64.7	66.0	1.499	1.499	.3195	.3259	5081.9	5083.0	684.5	669.5	48	50
							2		51.0	72.3	85.2	88.6	1.540	1.511	.4102	.4263	5214.9	5216.3	644.5	656.5	50	52
							3		57.9	84.6	102.4	107.6	1.550	1.519	.4898	.5145	5246.6	5247.3	630.5	644.5	51	52
							4		50.6	70.5	84.7	86.5	1.528	1.506	.4092	.4179	5195.3	5195.9	671.5	678.5	51	52
							5		43.7	58.5	65.4	66.0	1.505	1.483	.3175	.3205	5168.6	5168.6	687.5	694.5	52	53
							6		34.6	48.9	43.8	43.7	1.493	1.478	.2204	.2200	4986.5	4986.3	707.5	707.5	52	54
							7		25.3	37.2	26.5	26.4	.009	.009	.0567	.0564			718.5	717.5	52	54
							8		28.2	40.3	29.0	29.1	.008	.008	.0626	.0628			708.5	714.5	53	54
							9		35.5	49.6	43.3	43.8	1.715	1.691	.2370	.2399	4581.6	4586.1	684.5	691.5	53	54
							10		44.3	59.9	66.0	67.8	1.500	1.483	.3199	.3285	5176.1	5177.0	667.5	671.5	53	54
							11		58.5	85.7	109.6	114.2	1.581	1.528	.5148	.5362	5342.9	5344.3	631.5	684.5	53	55
							12		43.3	57.9	65.5	66.1	1.494	1.474	.3173	.3198	5183.6	5183.4	691.5	697.5	54	56
							13		56.4	80.5	104.8	107.8	1.553	1.510	.4961	.5103	5301.2	5300.8	652.5	678.5	54	56
							14		57.5	81.0	102.9	108.3	1.553	1.510	.4883	.5139	5286.1	5286.6	623.5	648.5	54	56

FIGURE D-3-3. MIRA 150A STEADY-STATE PERFORMANCE, CAPISTRANO TEST SITE (HEPS) - CENTRIFUGE TESTS

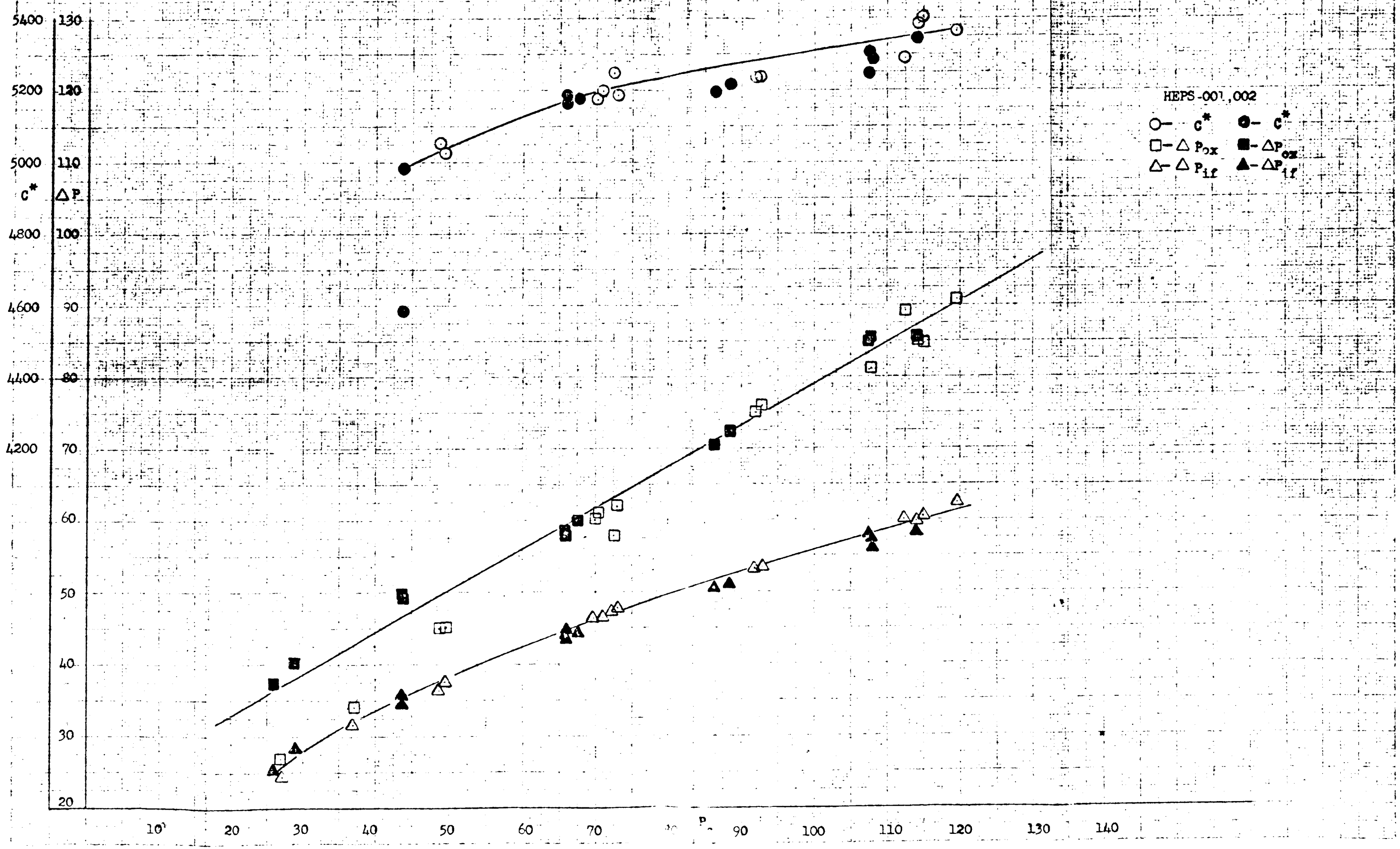

145

APPENDIX E

HEA CALIBRATION DATA

No. of Pages: 9

FIGURE E-1. 150A-001

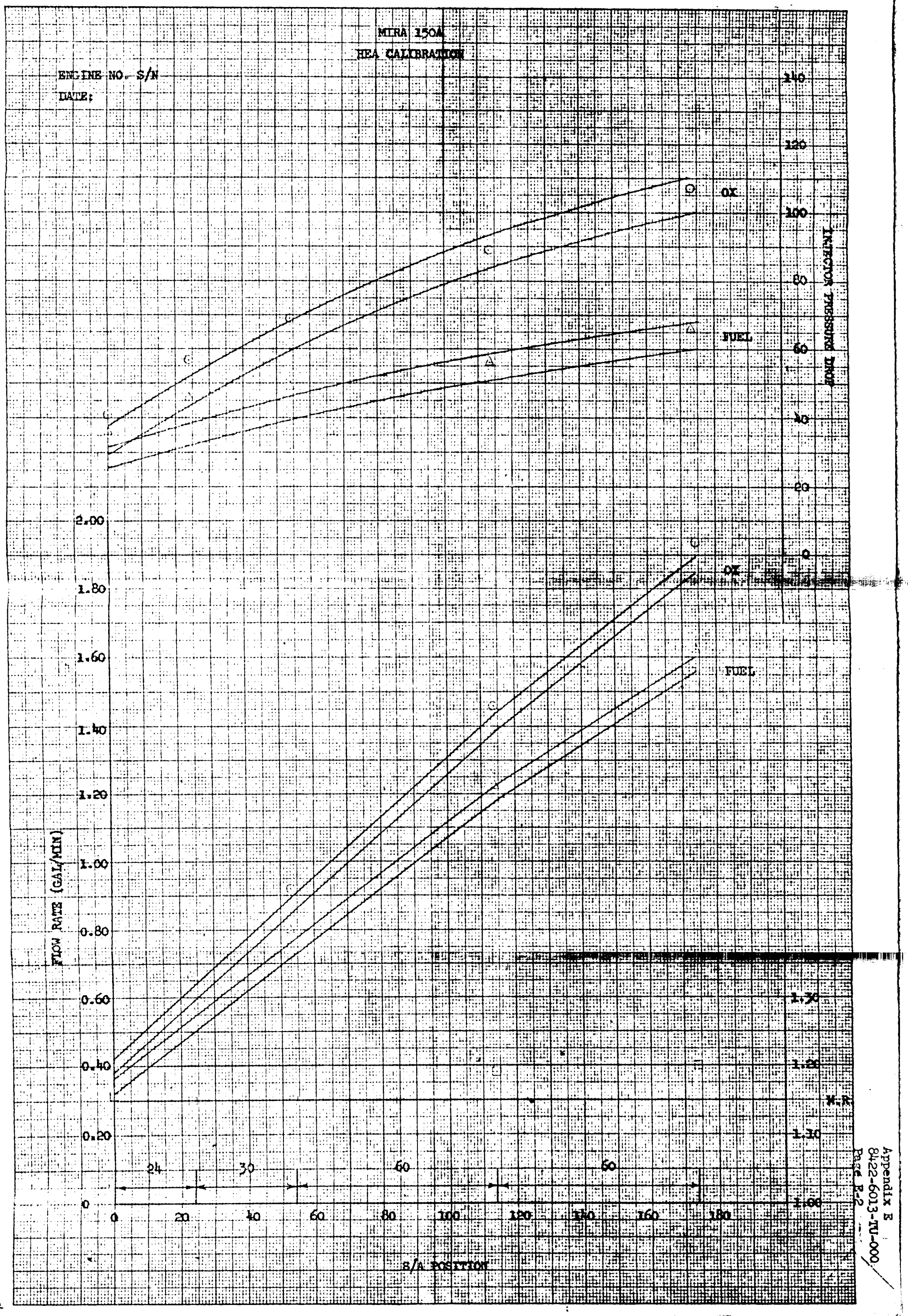

FIGUER E-2. 150A-002

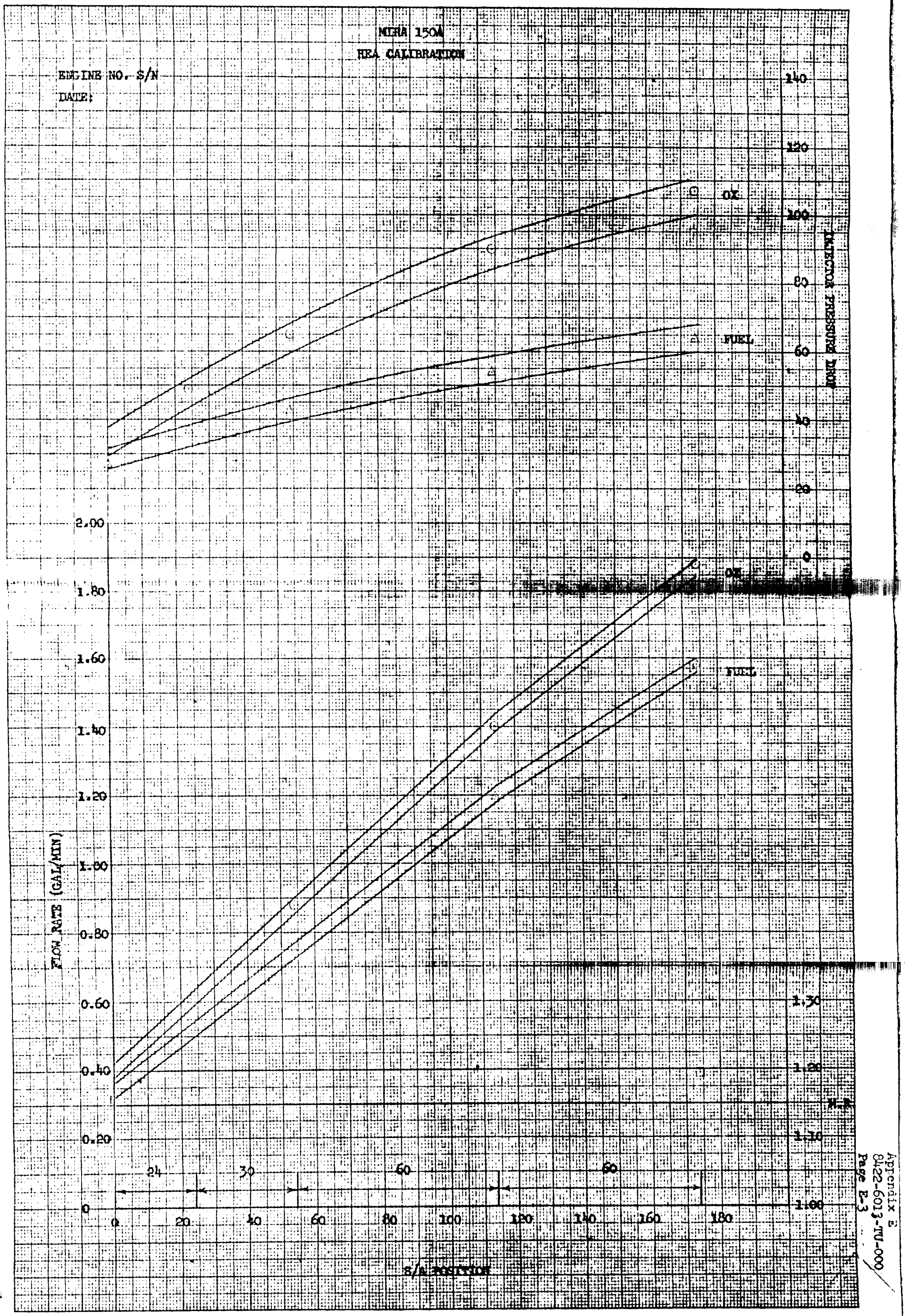

FIGURE E-3. 150A-004

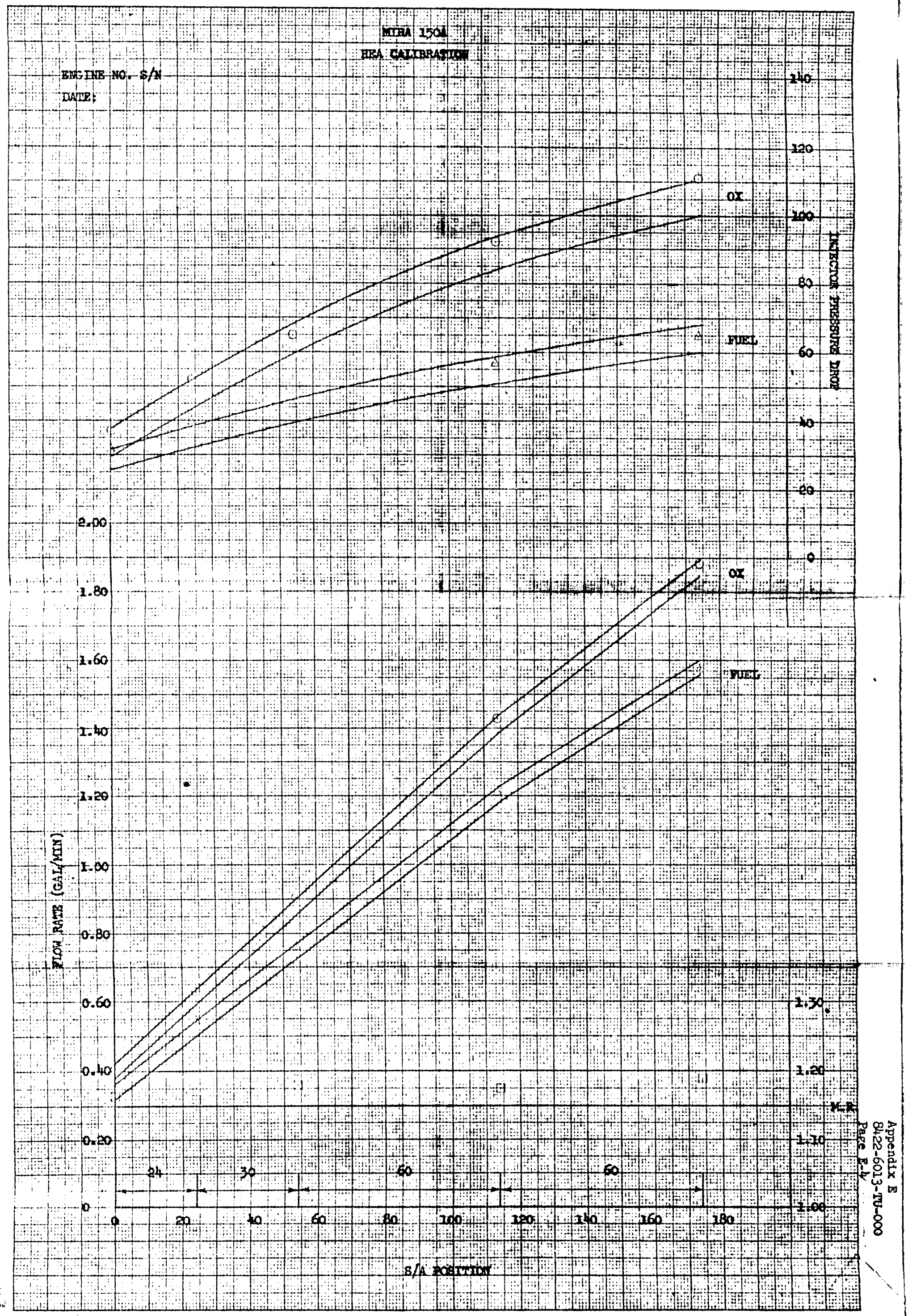

FIGURE E-4. 150A-005

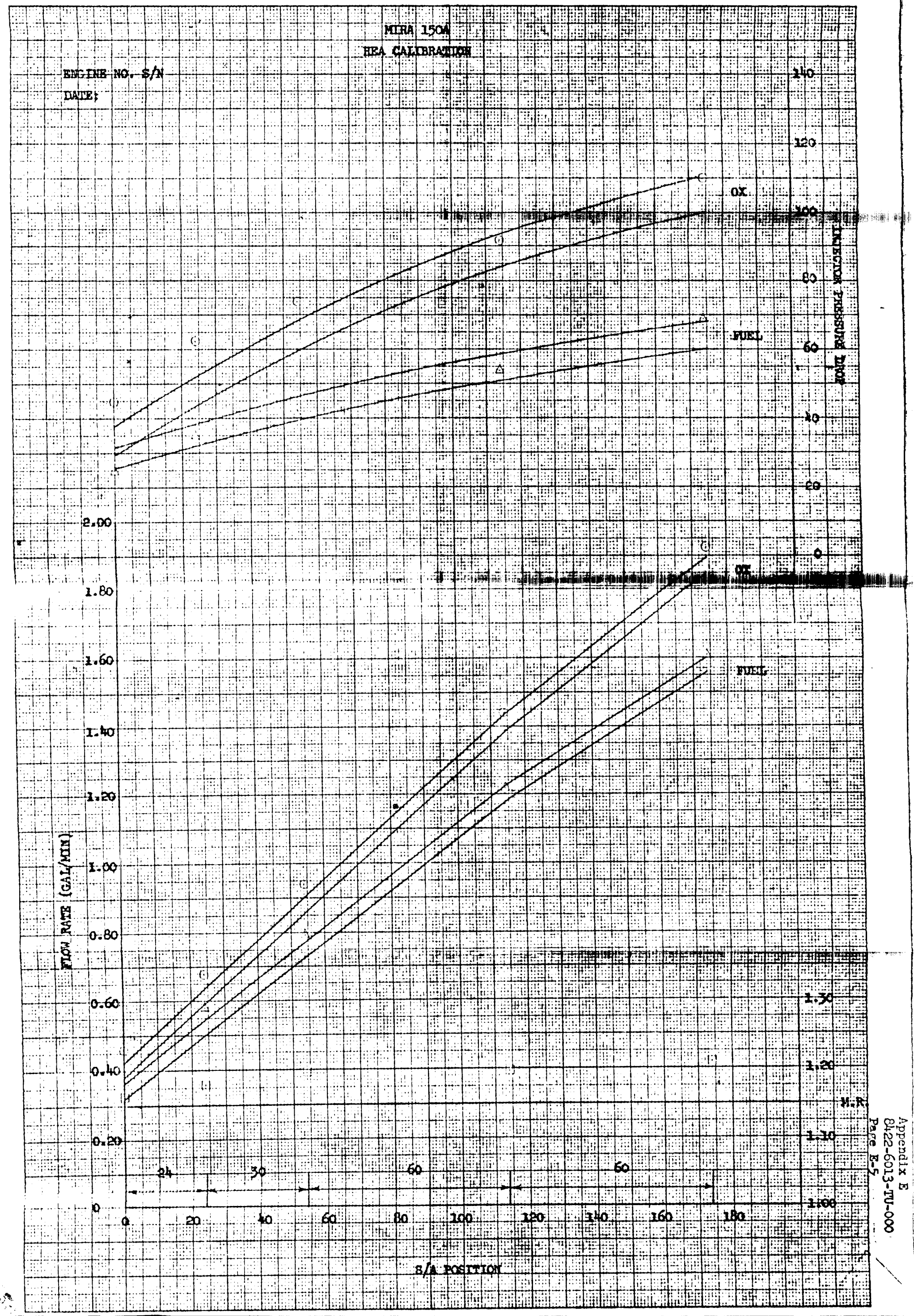

FIGURE E-5. 150A-006

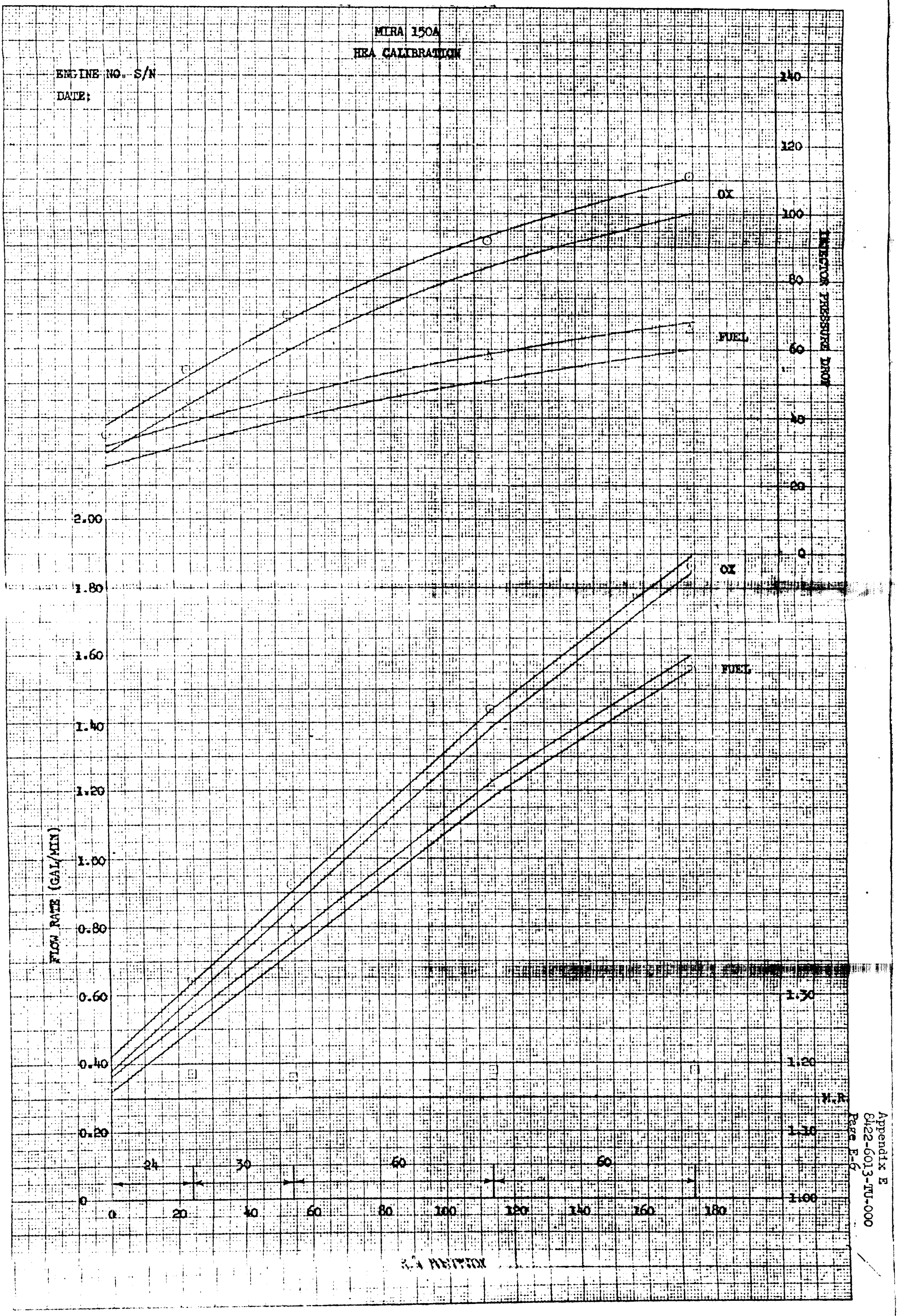

FIGURE E-6. 150A-007

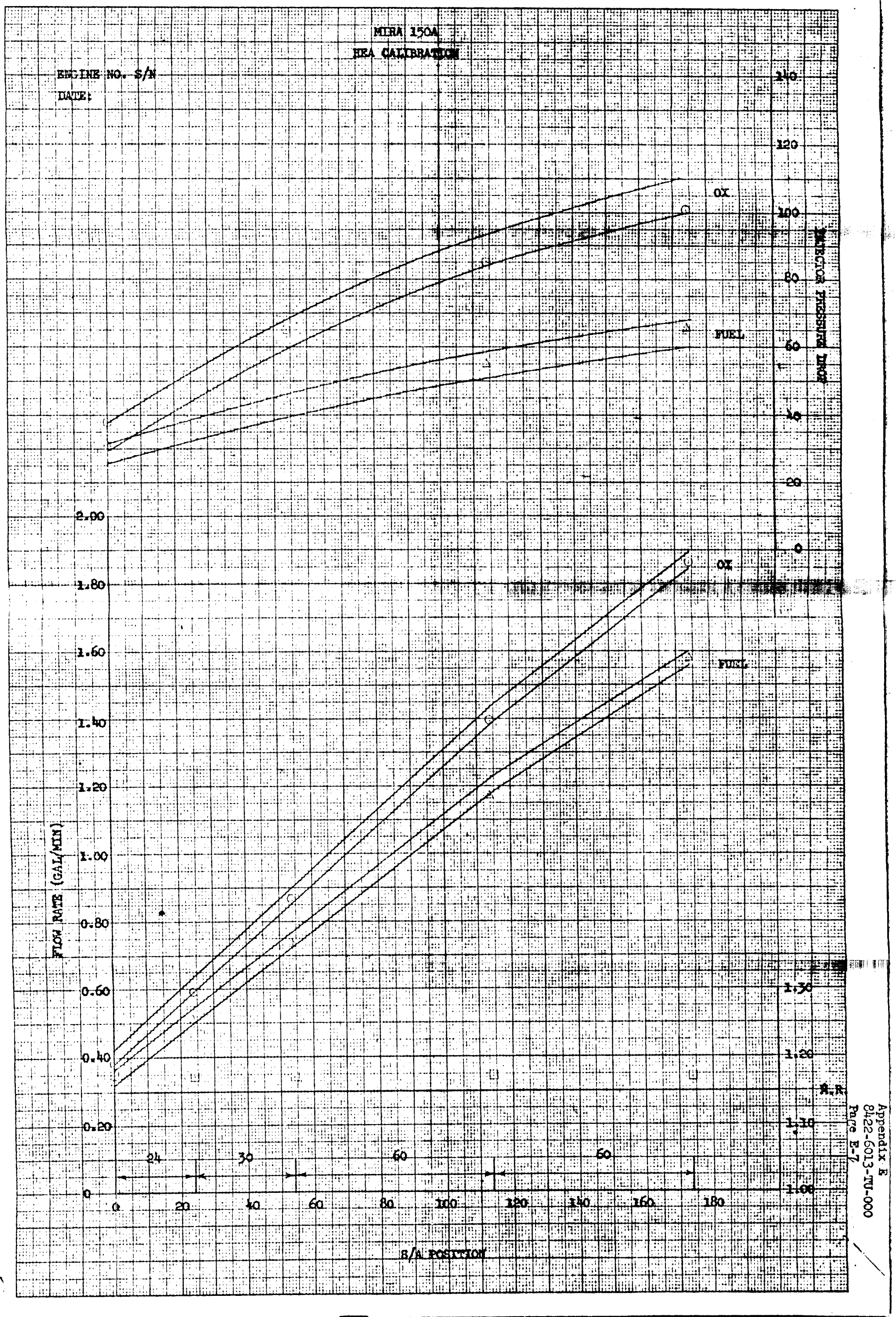

FIGURE E-7. 150A-008

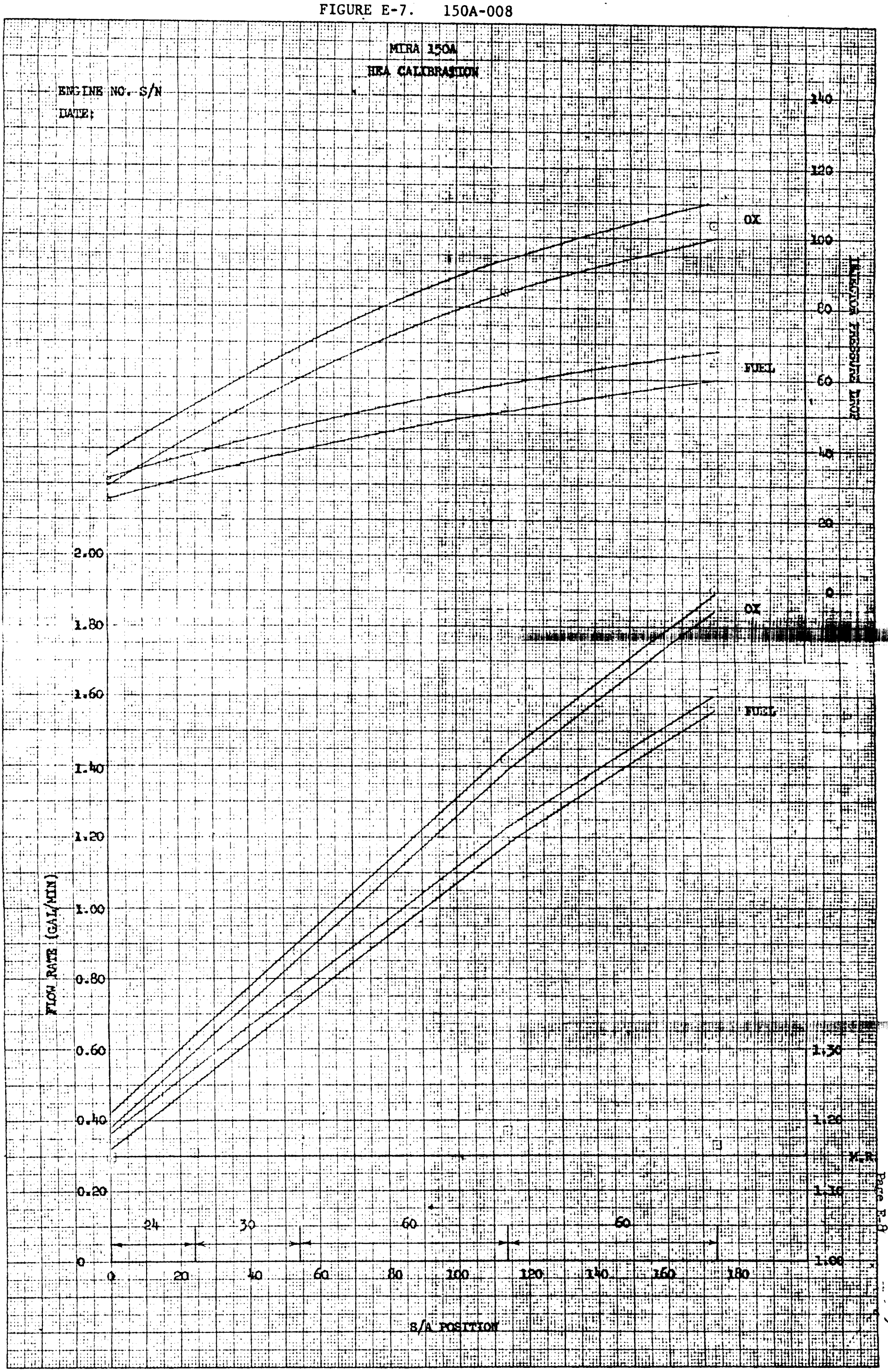

FIGURE E-8. 150A-009

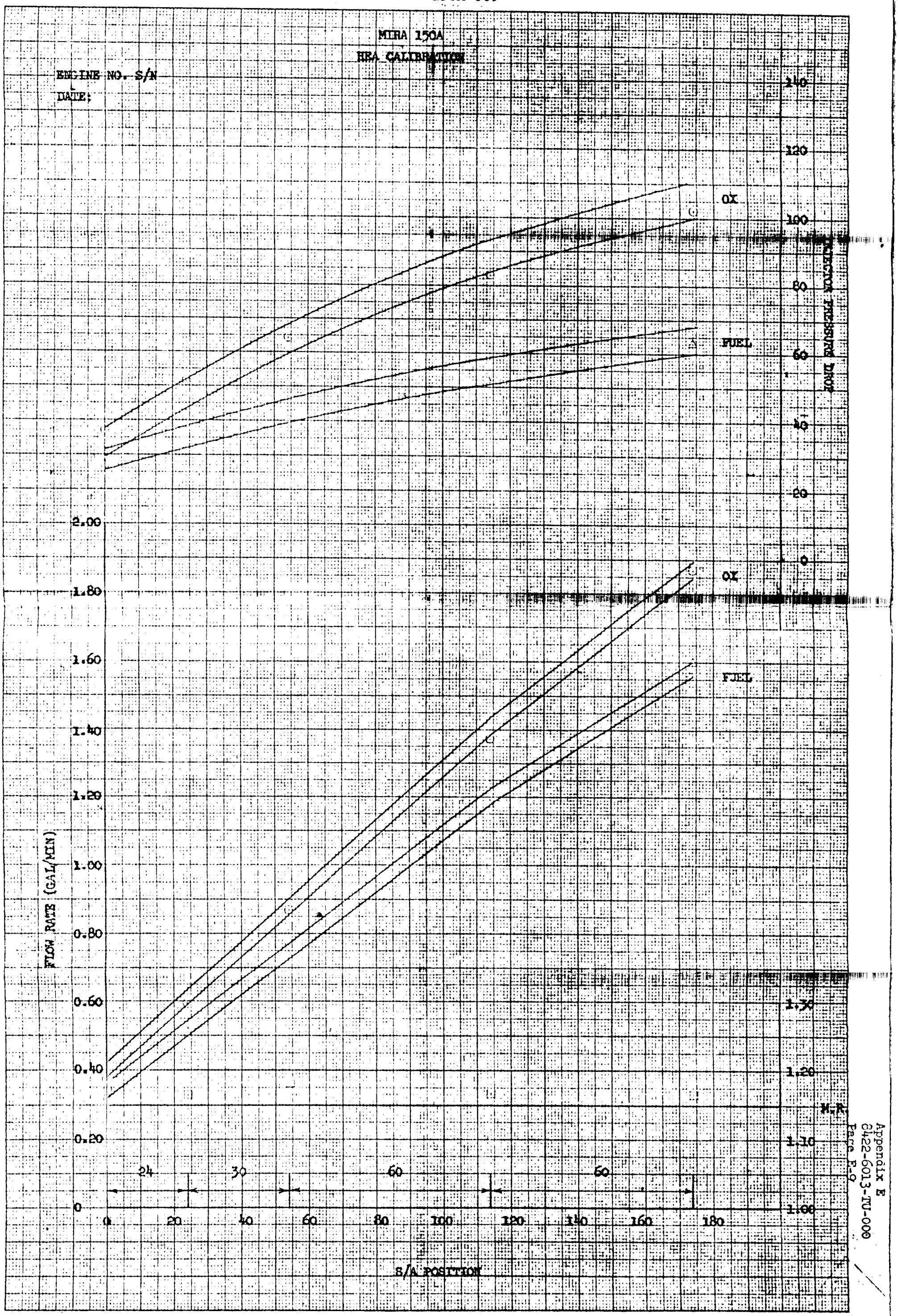

APPENDIX G

SURVEYOR SPECIAL TEST EQUIPMENT SCHEMATICS

No. of Pages: 9

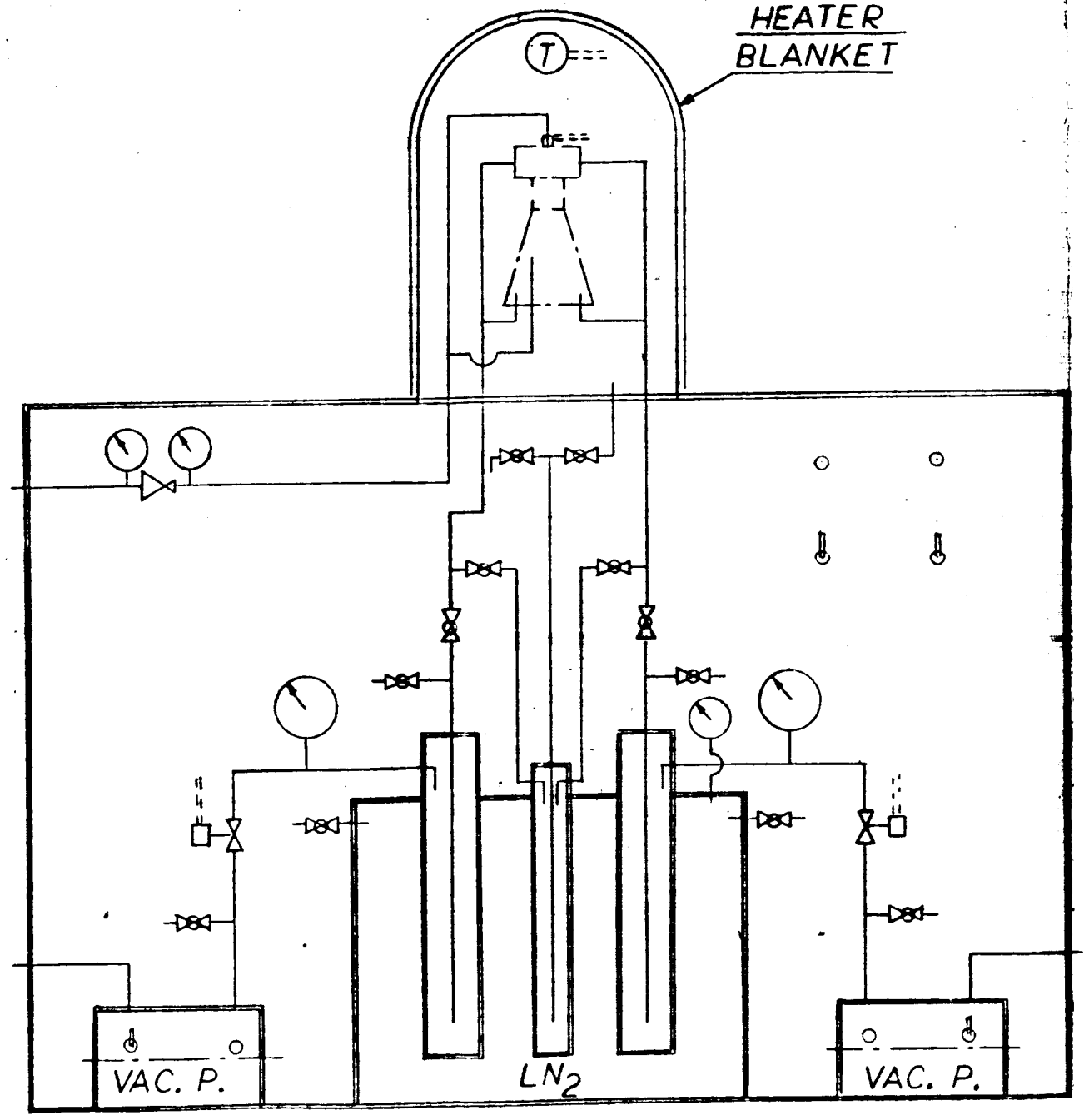

SYSTEM SCHEMATIC

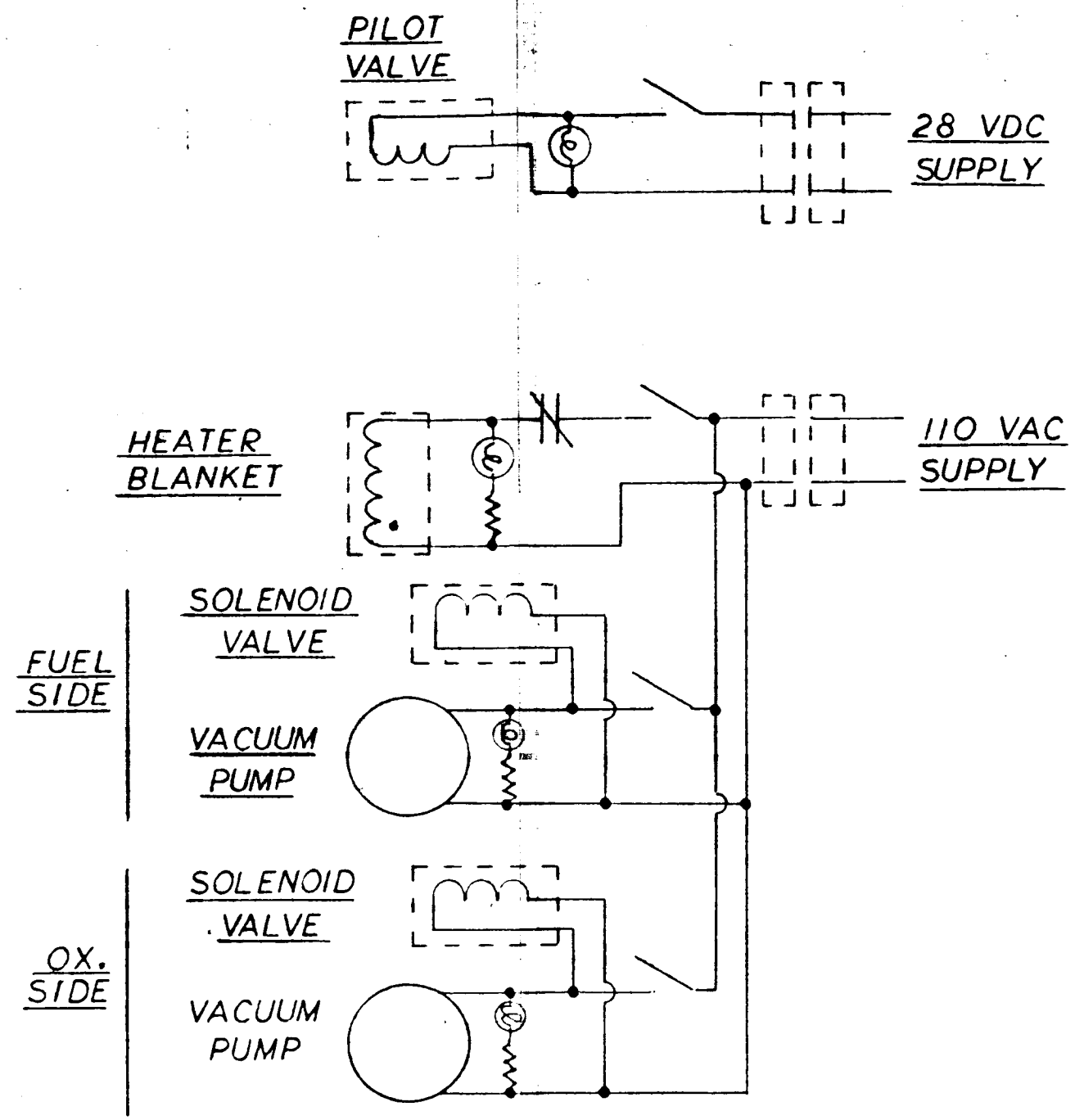

ELECTRICAL SCHEMATIC

ORIGINATOR J. Schwartzberg	DATE 12-11-64	TITLE ENGINE CLEANING CONSOLE SCHEMATIC	ENGINEERING SKETCH SPACE TECHNOLOGY LABORATORIES, INC. LOS ANGELES, CALIFORNIA
R. J. Ishman	12-11-64		SK-108166
MJO 8422-04			SHEET 1 OF 1

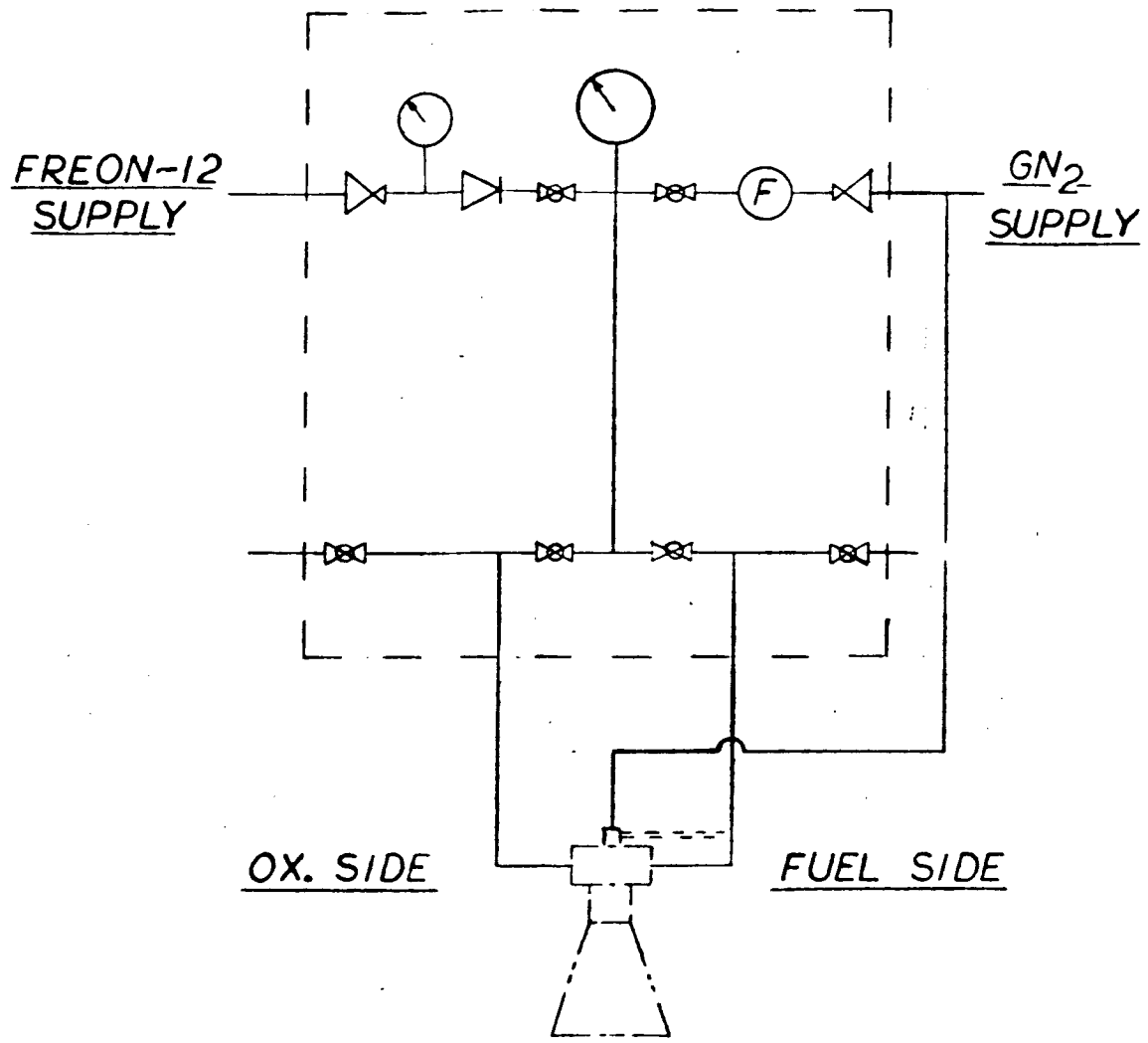

SYSTEM SCHEMATIC

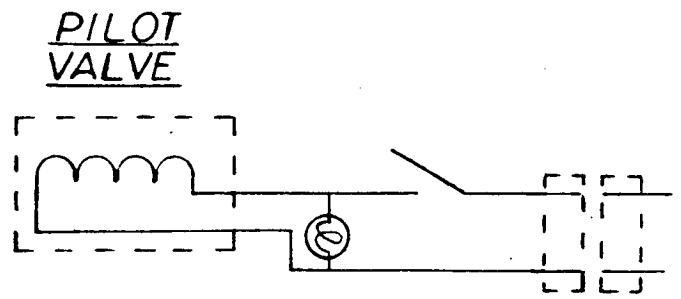

ELECTRICAL SCHEMATIC

ORIGINATOR A Zimmerman	DATE 12.14.64	TITLE ENGINE LEAK TEST CONSOLE SCHEMATIC	ENGINEERING SKETCH SPACE TECHNOLOGY LABORATORIES, INC. LOS ANGELES, CALIFORNIA
R J Johnson	12.14.64		SK-108155
			SHEET 1 OF 1
MJO 8422-04			

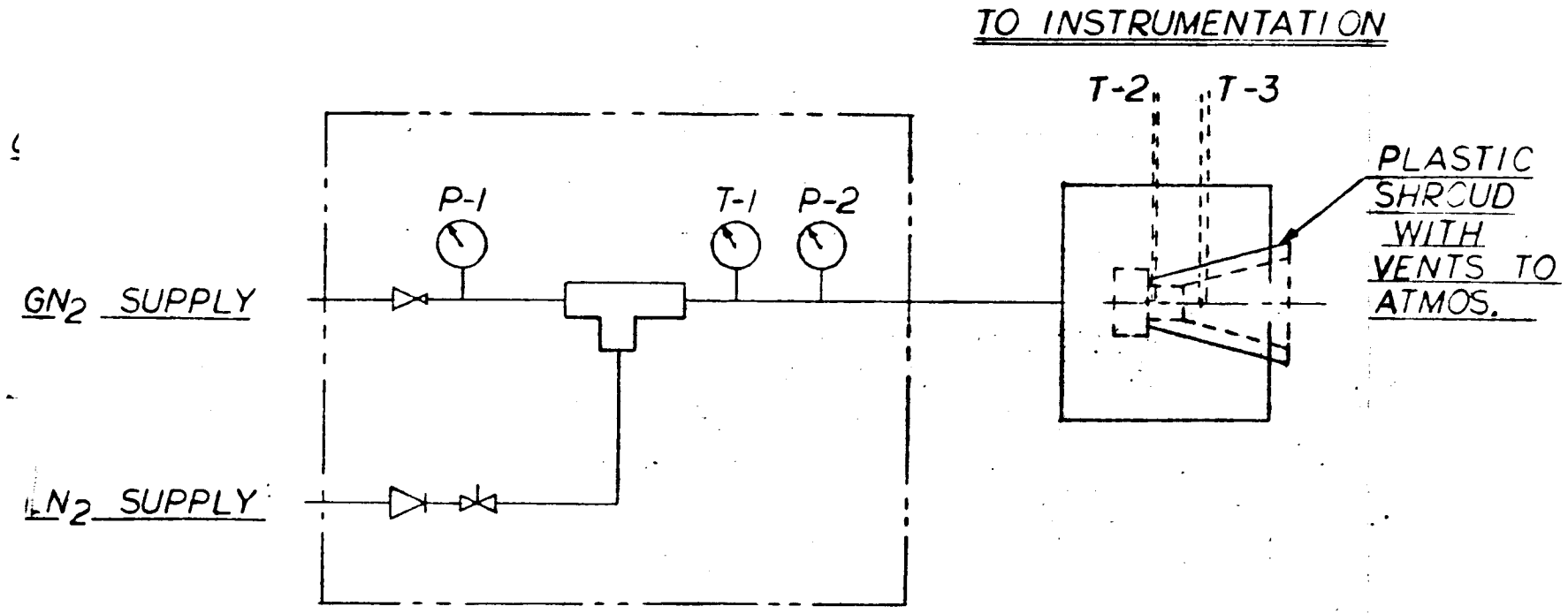

COOLING CYCLE

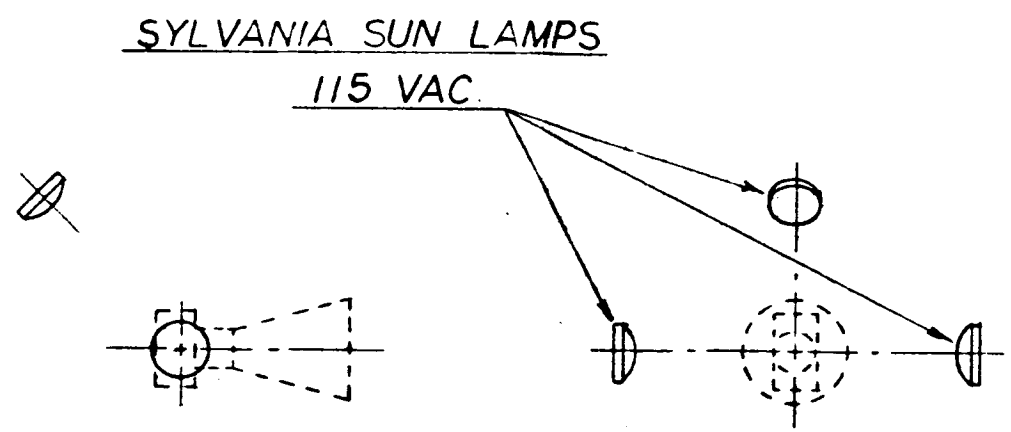

HEATING CYCLE

ORIGINATOR A Lumentarsky / R J Johnson	DATE 12-10-64 / 12-11-64	TITLE ENGINE THERMAL CONDITIONER SCHEMATIC	ENGINEERING SKETCH TRW SPACE TECHNOLOGY LABORATORIES SK-108120
MJO 8422-04			SHEET / OF /

STL Form 523B (Rev. 12 63)

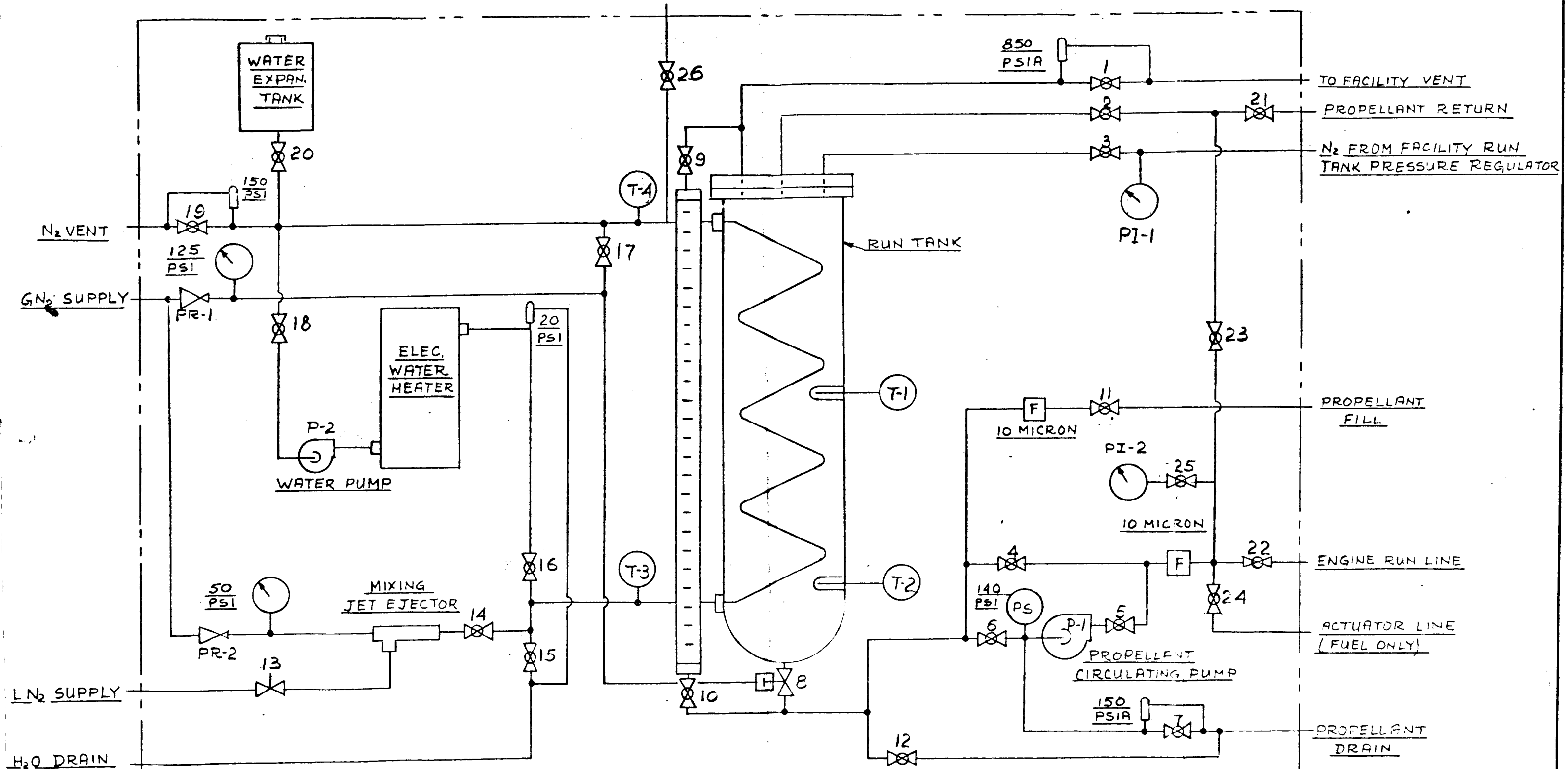

ORIGINATOR PEG BROWN	DATE 8-12-64	TITLE PROPELLANT CONDITIONER SYSTEM SCHEMATIC	ENGINEERING SKETCH SPACE TECHNOLOGY LABORATORIES, INC. LOS ANGELES, CALIFORNIA
APPROVED W. A. TOWER	8-13-64		SK-108168
REDRAWN	10-26-64		SHEET 1 OF 2
MJO 8422-04			

STL Form 523B (Rev. 2-59)

TO WATER HEATER
220 VAC

FROM POWER PANEL
220 V
3 ϕ
4 WIRE

A
B
C
D

PROPELLANT PUMP P-1

M

HEATER

SOLENOID VALVE
STL-8

M

WATER PUMP
P-2

4 PIN

A B C D

A B C D

HEATER

7 PIN

CIRC. PUMP

6 PIN

EMERG. SHUT OFF VALVE

WATER PUMP

24 V DC.

110 VAC
POWER

ORIGINATOR A Sementovsky	DATE 10/27/64	TITLE PROPELLANT CONDITIONER ELECTRICAL SCHEMATIC	ENGINEERING SKETCH SPACE TECHNOLOGY LABORATORIES, INC. LOS ANGELES, CALIFORNIA
APPROVED R J Johnson	10/27/64		SK-108168
MJO 8422-01			SHEET 2 OF 2

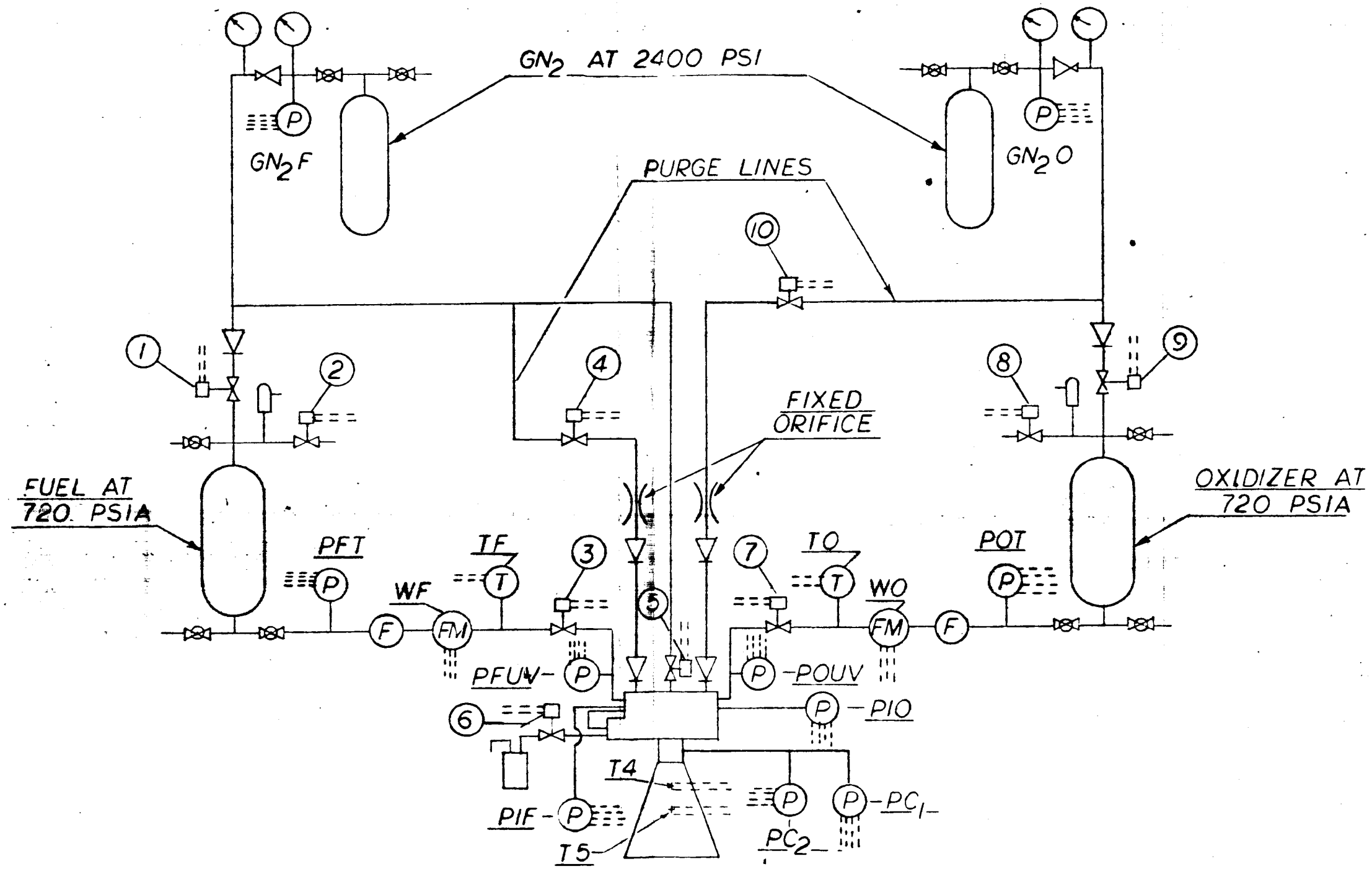

ORIGINATOR G Demetrovsky	DATE 5-1-64	TITLE CENTRIFUGE SYSTEM SCHEMATIC	ENGINEERING SKETCH TRW SPACE TECHNOLOGY LABORATORIES THOMPSON RAMO WOOLDRIDGE INC ONE SPACE PARK — REDONDO BEACH CALIFORNIA
R J Johnson	5-1-64		SK-108167
MJO 8422-04			SHEET 1 OF 3

STL Form 523B (Rev. 12 63)

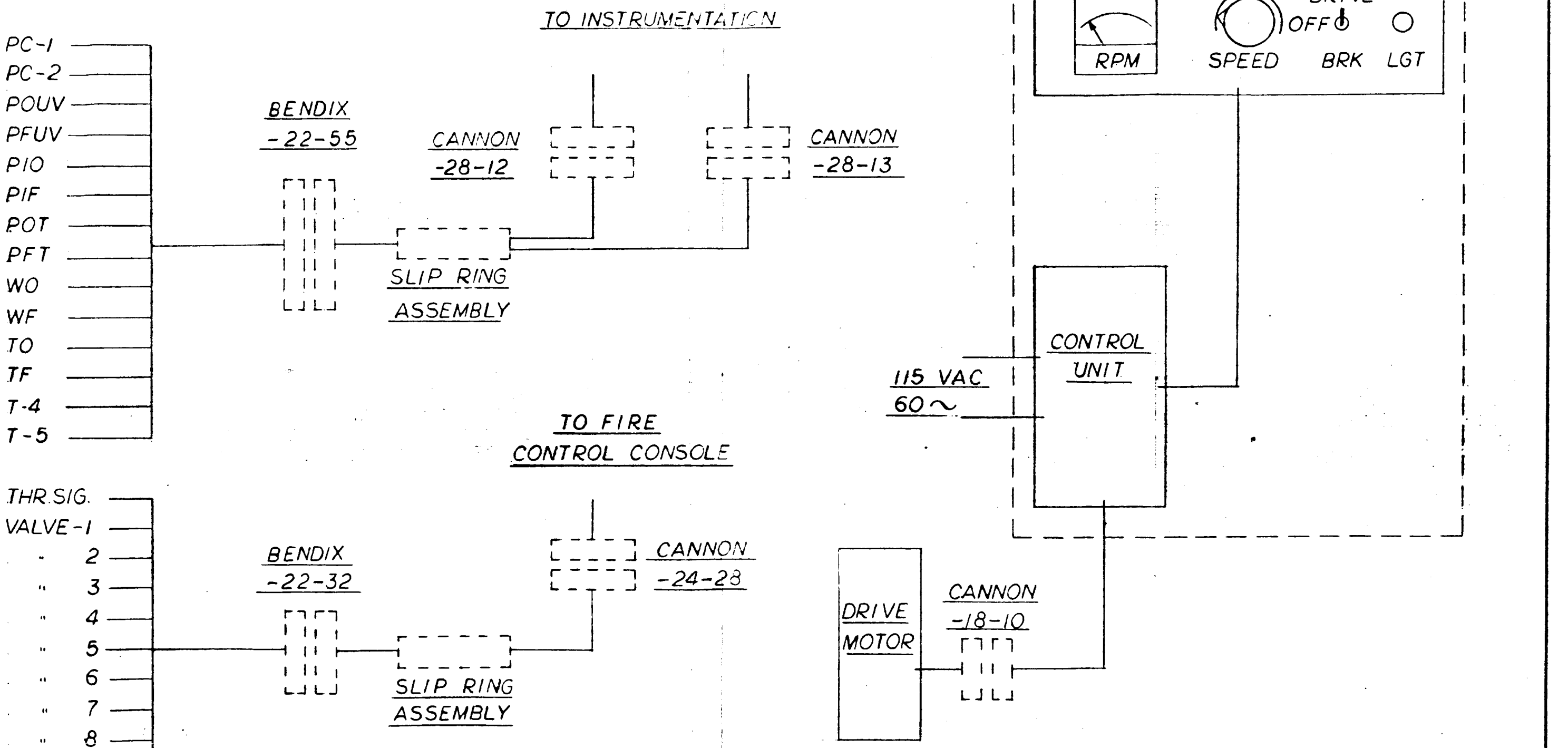

ORIGINATOR	DATE	TITLE	ENGINEERING SKETCH
R Dimentovsky	5-1-64	CENTRIFUGE ELECTRICAL SHEMATIC	TRW SPACE TECHNOLOGY LABORATORIES THOMPSON RAMO WOOLDRIDGE INC ONE SPACE PARK · REDONDO BEACH · CALIFORNIA
MJO			SK-108167 SHEET 2 OF 3

	BENDIX -22-55	CANNON -28-12
	A	A
PC-1	B	B
	V	C
	W	D
	U	R
PC-2	T	P
	S	N
	n	M
	X	S
POUV	C	T
	Y	a
	D	b
	p	U
PFUV	q	V
	AA	E
	BB	F
	k	Z
PIO	m	Y
	R	L
	z	K
	P	W
PIF	j	d
	i	x
	y	H
Spares	L	G
	J	J

	BENDIX -22-55	CANNON -28-13
	FF	A
WO	EE	B
	DD	C
	t	R
WF	b	P
	F	N
	s	S
POT	Z	T
	a	a
	E	b
	v	d
PFT	u	W
	x	M
	w	Z
TO	GG	L
	HH	Y
TF	CC	G
	r	F
T4	N	U
	M	D
T5	g	V
	f	E
Spares	K	K
	H	X

	BENDIX -22-32	CANNON -24-28
	A	A
Throttle	P	B
Signal	N	C
Valve	R	D
1 & 9	B	J
Valve	L	G
2	a	H
Valve	S	M
3	C	N
Valve	T	U
4	D	V
Valve	Z	P
5	g	Q
Valve	E	W
6	F	X
Valve	h	K
7	c	L
Valve	M	E
8	b	F
Valve	J	R
10	d	S
Spares	j	Y

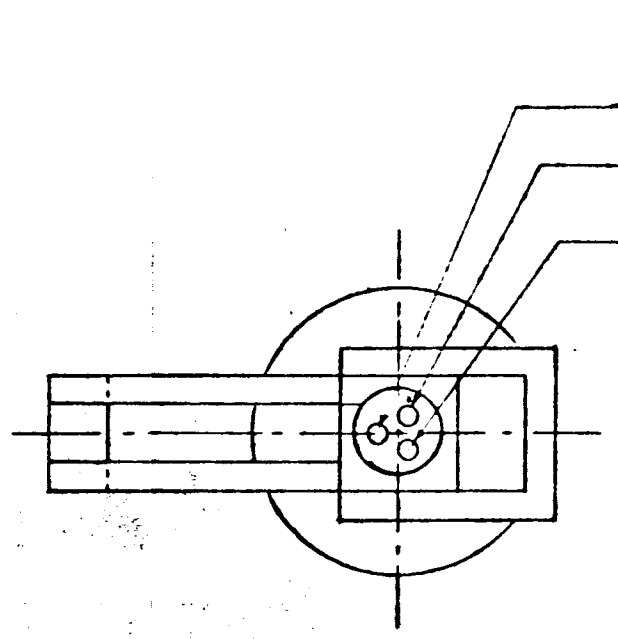

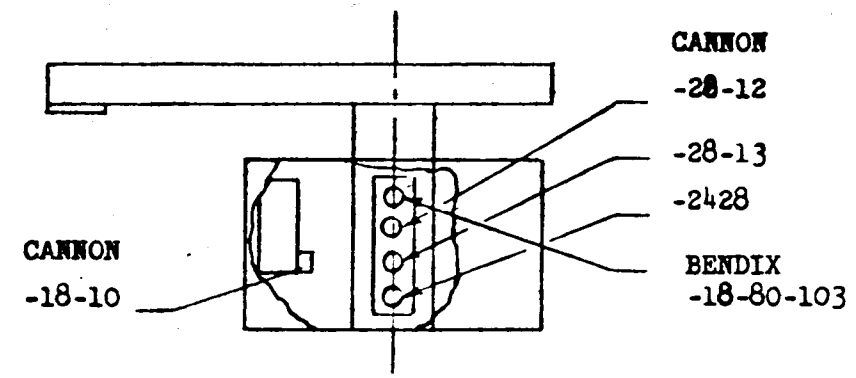

Co Ax Connectors Bendix -18-80-103

		Rotor	Base
1	Center	C	C
	Shield	C	C
2	Center	G	G
	Shield	G	G

MOTOR	CANNON -18-10
1	A
2	B
3	C
4	D

ORIGINATOR	DATE	TITLE	ENGINEERING SKETCH
W Siemontowicz	5-1-64	CENTRIFUGE CONNECTOR PIN ASSIGNEMENT	TRW SPACE TECHNOLOGY LABORATORIES (THOMPSON RAMO WOOLDRIDGE INC, ONE SPACE PARK, REDONDO BEACH, CALIFORNIA)
			SK 703767
MJO			SHEET 3 OF 3